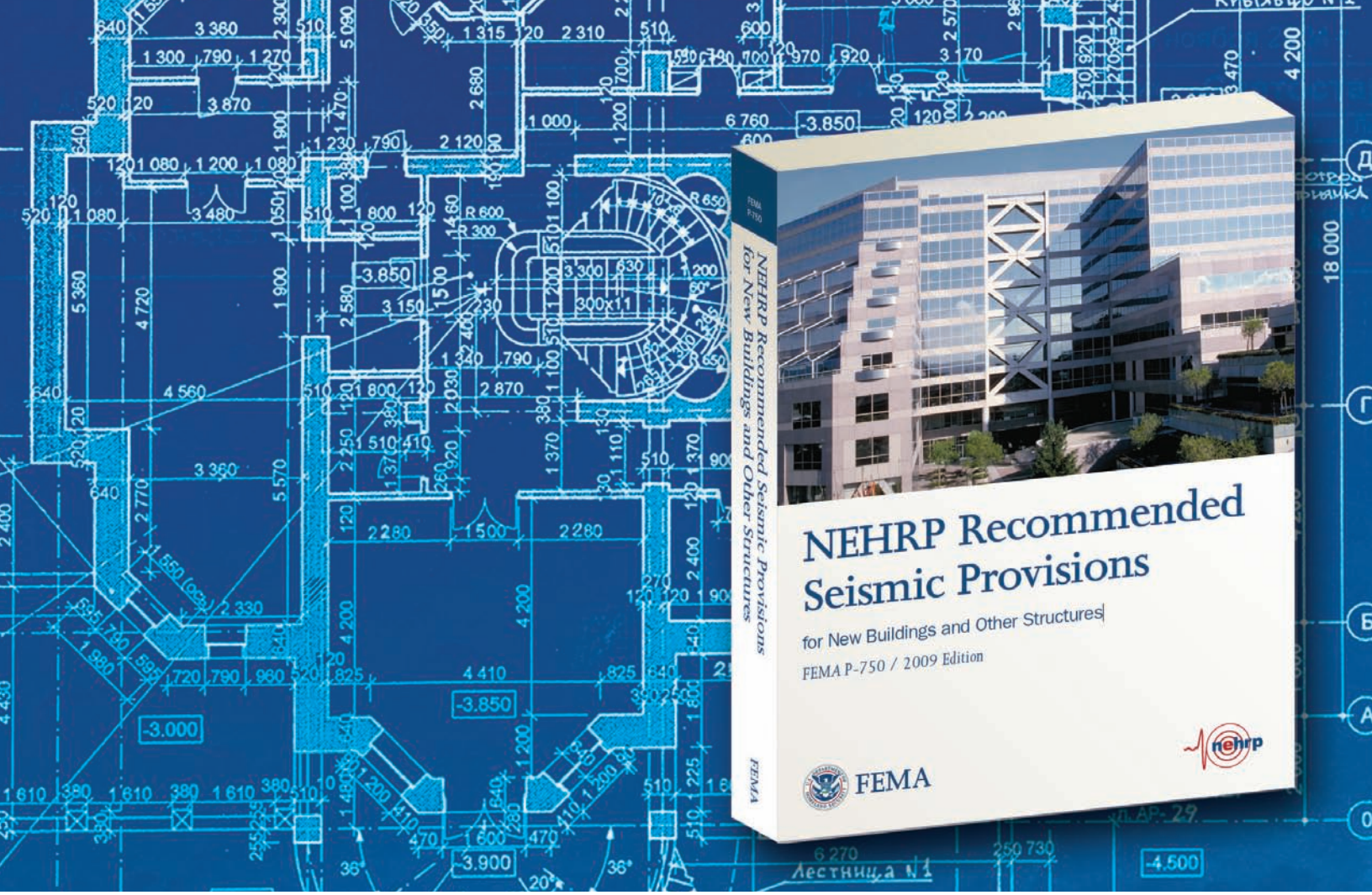

2009 NEHRP Recommended Seismic Provisions: Design Examples

FEMA P-751 / September 2012

FEMA

nehrp

2009 NEHRP Recommended Seismic Provisions: Design Examples

FEMA P-751 - September 2012

Prepared by the
National Institute of Building Sciences
Building Seismic Safety Council

For the
Federal Emergency Management Agency
of the Department of Homeland Security

NOTICE: Any opinions, findings, conclusions, or recommendations expressed in this publication do not necessarily reflect the views of the Federal Emergency Management Agency. Additionally, neither FEMA nor any of its employees make any warranty, expressed or implied, nor assume any legal liability or responsibility for the accuracy, completeness, or usefulness of any information, product or process included in this publication.

The opinions expressed herein regarding the requirements of the International Residential Code do not necessarily reflect the official opinion of the International Code Council. The building official in a jurisdiction has the authority to render interpretation of the code.

This report was prepared under Contract HSFEHQ-09-R-0147 between the Federal Emergency Management Agency and the National Institute of Building Sciences.

For further information on the Building Seismic Safety Council, see the Council's website — www.bssconline.org — or contact the Building Seismic Safety Council, 1090 Vermont, Avenue, N.W., Suite 700, Washington, D.C. 20005; phone 202-289-7800; fax 202-289-1092; e-mail bssc@nibs.org.

FOREWORD

One of the goals of the Department of Homeland Security's Federal Emergency Management Agency (FEMA) and the National Earthquake Hazards Reduction Program (NEHRP) is to encourage design and building practices that address the earthquake hazard and minimize the resulting risk of damage and injury. The 2009 edition of the *NEHRP Recommended Seismic Provisions for New Buildings and Other Structures* (FEMA P-750) affirmed FEMA's ongoing support to improve the seismic safety of construction in this country. The *NEHRP Provisions* serves as a key resource for the seismic requirements in the ASCE/SEI 7 Standard *Minimum Design Loads for Buildings and Other Structures* as well as the national model building codes, the *International Building Code (IBC), International Residential Code (IRC) and NFPA 5000 Building Construction Safety Code.* FEMA welcomes the opportunity to provide this material and to work with these codes and standards organizations.

This product provides a series of design examples that will assist the users of the 2009 *NEHRP Provisions* and the ASCE/SEI 7 standard the *Provisions* adopted by reference.

FEMA wishes to express its gratitude to the authors listed elsewhere for their significant efforts in preparing this material and to the BSSC Board of Direction and staff who made this possible. Their hard work has resulted in a guidance product that will provide important assistance to a significant number of users of the nation's seismic building codes and their reference documents.

Department of Homeland Security/
Federal Emergency Management Agency

PREFACE

This volume of design examples is intended for those experienced structural designers who are relatively new to the field of earthquake-resistant design and to the *2009 NEHRP (National Earthquake Hazards Reduction Program) Recommended Seismic Provisions for New Buildings and Other Structures.* By extension, it also applies to use of the current model codes and standards because the *Provisions* is the key resource for updating seismic design requirements in most of those documents including ASCE 7 Standard, *Minimum Design Loads for Buildings and Other Structures;* and the *International Building Code* (IBC). Furthermore, the *2009 NEHRP Provisions* (FEMA P-750) adopted ASCE7-05 by reference and the 2012 *International Building Code* adopted ASCE7-10 by reference; therefore, seismic design requirements are essentially equivalent across the *Provisions,* ASCE7 and the national model code.

The design examples, updated in this edition, reflect the technical changes in the *2009 NEHRP Recommended Provisions.* The original design examples were developed from an expanded version of an earlier document (entitled *Guide to Application of the NEHRP Recommended Provisions,* FEMA 140) which reflected the expansion in coverage of the *Provisions* and the expanding application of the *Provisions* concepts in codes and standards. The widespread use of the *NEHRP Recommended Provisions* in the past and the essential equivalency of ASCE7, the *Provisions* and the national model codes at present attested to the success of the NEHRP at the Federal Emergency Management Agency and the efforts of the Building Seismic Safety Council to ensure that the nation's building codes and standards reflect the state of the art of earthquake-resistant design.

In developing this set of design examples, the BSSC initially decided on the types of structures; types of construction and materials; and specific structural elements that needed to be included to provide the reader with at least a beginning grasp of the new requirements and critical issues frequently encountered when addressing seismic design problems. Many of the examples are from the previous edition of the design examples but updated by the authors to illustrate issues or design requirements not covered or that have changed from the past edition. Because it obviously is not possible to present, in a volume of this type, complete building designs for all the situations and features that were selected, only portions of designs have been used.

All users of the *Design Examples* are recommended to obtain and familiarize themselves with the 2003 and 2009 *NEHRP Recommended Provisions* (FEMA 450 and FEMA P-750) or ASCE7, Copies of the *Provisions* are available free of charge from FEMA by calling 1-800-480-2520 (order by FEMA Publication Number). Currently available are the 2003 and 2009 editions as follows:

NEHRP (National Earthquake Hazards Reduction Program) Recommended Seismic Provisions for New Buildings and Other Structures, 2009 Edition, FEMA P-750, 1 volume with maps (issued as paper document with a CD attached)

NEHRP (National Earthquake Hazards Reduction Program) Recommended Provisions for Seismic Regulations for New Buildings and Other Structures, 2003 Edition, 2 volumes and maps, FEMA 450 (issued as a paper document).The 2003 and 2009 edition of the *Provisions* can also be downloaded from the BSSC website at www.nibs.org/bssc. Also see the website for information regarding BSSC projects

and publications or write to the BSSC at bssc@nibs.org or at the National Institute of Building Sciences, 1090 Vermont Avenue, NW, Suite 700, Washington, DC 20005 (telephone 202-289-7800).

Updated education/training materials to supplement this set of design examples will be published as a separate FEMA product, *2009 NEHRP Recommended Seismic Provisions: Training Material*, FEMA P-752.

The BSSC is grateful to all those individuals and organizations whose assistance made the 2012 edition of the design examples a reality:

- Michael T. Valley, Magnusson Klemencic Associates, Seattle, Washington, who served as project manager and managing technical editor for the update.

- Ozgur Atlayan, Robert Bachman, Finley A. Charney, Brian Dean, Susan Dowty, John Gillengerten, James Robert Harris, Charles A. Kircher, Suzanne Dow Nakaki, Clinton O. Rex, Frederic R. Rutz, Rafael A. Sabelli, Peter W. Somers, Greg Soules, Adrian Tola Tola and Michael T. Valley for editing the original chapters to prepare this update of the 2006 Edition.

- Robert Pekelnicky for preparing a new Introduction; and Nicolas Luco, Michael Valley and C.B. Crouse for preparing a new chapter on Earthquake Ground Motions for this edition.

- Lawrence A. Burkett, Kelly Cobeen, Finley Charney, Ned Cleland, Dan Dolan, Jeffrey J. Dragovich, Jay Harris, Robert D. Hanson, Neil Hawkins, Joe Maffei, Greg Soules, and Mai Tong for their reviews of the edited, updated and expanded material.

And finally, the BSSC Board is grateful to FEMA Project Officer Mai Tong for his support and guidance and to Deke Smith, Roger Grant and Pamela Towns of the NIBS staff for their efforts preparing the 2012 volume for publication and issuance as an e-document available for download and on CD-ROM.

Jim. W. Sealy, Chairman
BSSC Board of Direction

Table of Contents

FOREWORD iii
PREFACE iv

1 INTRODUCTION
1.1 EVOLUTION OF EARTHQUAKE ENGINEERING 1-3
1.2 HISTORY AND ROLE OF THE NEHRP PROVISIONS 1-6
1.3 THE NEHRP DESIGN EXAMPLES 1-8
1.4 GUIDE TO USE OF THE PROVISIONS 11-1
1.5 REFERENCES 1-38

2 FUNDAMENTALS
2.1 EARTHQUAKE PHENOMENA 2-3
2.2 STRUCTURAL RESPONSE TO GROUND SHAKING 2-5
2.2.1 Response Spectra 2-5
2.2.2 Inelastic Response 2-11
2.2.3 Building Materials 2-14
2.2.4 Building Systems 2-16
2.2.5 Supplementary Elements Added to Improve Structural Performance 2-17
2.3 ENGINEERING PHILOSOPHY 2-18
2.4 STRUCTURAL ANALYSIS 2-19
2.5 NONSTRUCTURAL ELEMENTS OF BUILDINGS 2-22
2.6 QUALITY ASSURANCE 2-23

3 EARTHQUAKE GROUND MOTION
3.1 BASIS OF EARTHQUAKE GROUND MOTION MAPS 3-2
3.1.1 ASCE 7-05 Seismic Maps 3-2

3.1.2 MCE_R Ground Motions in the Provisions and in ASCE 7-10 3-3
3.1.3 PGA Maps in the Provisions and in ASCE 7-10 3-7
3.1.4 Basis of Vertical Ground Motions in the Provisions and in ASCE 7-10 3-7
3.1.5 Summary 3-7
3.1.6 References 3-8
3.2 DETERMINATION OF GROUND MOTION VALUES AND SPECTRA 3-9
3.2.1 ASCE 7-05 Ground Motion Values 3-9
3.2.2 2009 Provisions Ground Motion Values 3-10
3.2.3 ASCE 7-10 Ground Motion Values 3-11
3.2.4 Horizontal Response Spectra 3-12
3.2.5 Vertical Response Spectra 3-13
3.2.6 Peak Ground Accelerations 3-14
3.3 SELECTION AND SCALING OF GROUND MOTION RECORDS 3-14
3.3.1 Approach to Ground Motion Selection and Scaling 3-15
3.3.2 Two-Component Records for Three Dimensional Analysis 3-24
3.3.3 One-Component Records for Two-Dimensional Analysis 3-27
3.3.4 References 3-28

4 STRUCTURAL ANALYSIS

4.1 IRREGULAR 12-STORY STEEL FRAME BUILDING, STOCKTON, CALIFORNIA 4-3
4.1.1 Introduction 4-3
4.1.2 Description of Building and Structure 4-3
4.1.3 Seismic Ground Motion Parameters 4-4
4.1.4 Dynamic Properties 4-8
4.1.5 Equivalent Lateral Force Analysis 4-11
4.1.6 Modal Response Spectrum Analysis 4-29
4.1.7 Modal Response History Analysis 4-39
4.1.8 Comparison of Results from Various Methods of Analysis 4-50
4.1.9 Consideration of Higher Modes in Analysis 4-53
4.1.10 Commentary on the ASCE 7 Requirements for Analysis 4-56
4.2 SIX-STORY STEEL FRAME BUILDING, SEATTLE, WASHINGTON 4-57
4.2.1 Description of Structure 4-57
4.2.2 Loads 4-60
4.2.3 Preliminaries to Main Structural Analysis 4-64
4.2.4 Description of Model Used for Detailed Structural Analysis 4-72
4.2.5 Nonlinear Static Analysis 4-94

4.2.6 Response History Analysis 4-109
4.2.7 Summary and Conclusions 4-134

5 FOUNDATION ANALYSIS AND DESIGN

5.1 SHALLOW FOUNDATIONS FOR A SEVEN-STORY OFFICE BUILDING, LOS ANGELES, CALIFORNIA 5-3
5.1.1 Basic Information 5-3
5.1.2 Design for Gravity Loads 5-8
5.1.3 Design for Moment-Resisting Frame System 5-11
5.1.4 Design for Concentrically Braced Frame System 5-16
5.1.5 Cost Comparison 5-24
5.2 DEEP FOUNDATIONS FOR A 12-STORY BUILDING, SEISMIC DESIGN CATEGORY D 5-25
5.2.1 Basic Information 5-25
5.2.2 Pile Analysis, Design and Detailing 5-33
5.2.3 Other Considerations 5-47

6 STRUCTURAL STEEL DESIGN

6.1 INDUSTRIAL HIGH-CLEARANCE BUILDING, ASTORIA, OREGON 6-3
6.1.1 Building Description 6-3
6.1.2 Design Parameters 6-6
6.1.3 Structural Design Criteria 6-7
6.1.4 Analysis 6-10
6.1.5 Proportioning and Details 6-16
6.2 SEVEN-STORY OFFICE BUILDING, LOS ANGELES, CALIFORNIA 6-40
6.2.1 Building Description 6-40
6.2.2 Basic Requirements 6-42
6.2.3 Structural Design Criteria 6-44
6.2.4 Analysis and Design of Alternative A: SMF 6-46
6.2.5 Analysis and Design of Alternative B: SCBF 6-60
6.2.6 Cost Comparison 6-72
6.3 TEN-STORY HOSPITAL, SEATTLE, WASHINGTON 6-72
6.3.1 Building Description 6-72
6.3.2 Basic Requirements 6-76
6.3.3 Structural Design Criteria 6-78
6.3.4 Elastic Analysis 6-80

6.3.5 Initial Proportioning and Details 6-86
6.3.6 Nonlinear Response History Analysis 6-93

7 REINFORCED CONCRETE

7.1 SEISMIC DESIGN REQUIREMENTS 7-7
7.1.1 Seismic Response Parameters 7-7
7.1.2 Seismic Design Category 7-8
7.1.3 Structural Systems 7-8
7.1.4 Structural Configuration 7-9
7.1.5 Load Combinations 7-9
7.1.6 Material Properties 7-10
7.2 DETERMINATION OF SEISMIC FORCES 7-11
7.2.1 Modeling Criteria 7-11
7.2.2 Building Mass 7-12
7.2.3 Analysis Procedures 7-13
7.2.4 Development of Equivalent Lateral Forces 7-13
7.2.5 Direction of Loading 7-19
7.2.6 Modal Analysis Procedure 7-20
7.3 DRIFT AND P-DELTA EFFECTS 7-21
7.3.1 Torsion Irregularity Check for the Berkeley Building 7-21
7.3.2 Drift Check for the Berkeley Building 7-23
7.3.3 P-delta Check for the Berkeley Building 7-27
7.3.4 Torsion Irregularity Check for the Honolulu Building 7-29
7.3.5 Drift Check for the Honolulu Building 7-29
7.3.6 P-Delta Check for the Honolulu Building 7-31
7.4 STRUCTURAL DESIGN OF THE BERKELEY BUILDING 7-32
7.4.1 Analysis of Frame-Only Structure for 25 Percent of Lateral Load 7-33
7.4.2 Design of Moment Frame Members for the Berkeley Building 7-37
7.4.3 Design of Frame 3 Shear Wall 7-60
7.5 STRUCTURAL DESIGN OF THE HONOLULU BUILDING 7-66
7.5.1 Compare Seismic Versus Wind Loading 7-66
7.5.2 Design and Detailing of Members of Frame 1 7-69

8 PRECAST CONCRETE DESIGN

8.1 HORIZONTAL DIAPHRAGMS 8-4
8.1.1 Untopped Precast Concrete Units for Five-Story Masonry Buildings Located in Birmingham, Alabama and New York, New York 8-4

8.1.2 Topped Precast Concrete Units for Five-Story Masonry Building Located in Los Angeles, California (see Sec. 10.2) 8-18
8.2 THREE-STORY OFFICE BUILDING WITH INTERMEDIATE PRECAST CONCRETE SHEAR WALLS 8-26
8.2.1 Building Description 8-27
8.2.2 Design Requirements 8-28
8.2.3 Load Combinations 8-29
8.2.4 Seismic Force Analysis 8-30
8.2.5 Proportioning and Detailing 8-33
8.3 ONE-STORY PRECAST SHEAR WALL BUILDING 8-45
8.3.1 Building Description 8-45
8.3.2 Design Requirements 8-48
8.3.3 Load Combinations 8-49
8.3.4 Seismic Force Analysis 8-50
8.3.5 Proportioning and Detailing 8-52
8.4 SPECIAL MOMENT FRAMES CONSTRUCTED USING PRECAST CONCRETE 8-65
8.4.1 Ductile Connections 8-65
8.4.2 Strong Connections 8-67

9 COMPOSITE STEEL AND CONCRETE

9.1 BUILDING DESCRIPTION 9-3
9.2 PARTIALLY RESTRAINED COMPOSITE CONNECTIONS 9-7
9.2.1 Connection Details 9-7
9.2.2 Connection Moment-Rotation Curves 10
9.2.3 Connection Design 9-13
9.3 LOADS AND LOAD COMBINATIONS 9-17
9.3.1 Gravity Loads and Seismic Weight 9-17
9.3.2 Seismic Loads 9-18
9.3.3 Wind Loads 9-19
9.3.4 Notional Loads 9-19
9.3.5 Load Combinations 20
9.4 DESIGN OF C-PRMF SYSTEM 9-21
9.4.1 Preliminary Design 9-21
9.4.2 Application of Loading 9-22
9.4.3 Beam and Column Moment of Inertia 9-23
9.4.4 Connection Behavior Modeling 9-24
9.4.5 Building Drift and P-delta Checks 9-24

9.4.6 Beam Design 9-26
9.4.7 Column Design 9-27
9.4.8 Connection Design 9-28
9.4.9 Column Splices 9-29
9.4.10 Column Base Design 9-29

10 MASONRY

10.1 WAREHOUSE WITH MASONRY WALLS AND WOOD ROOF, LOS ANGELES, CALIFORNIA 10-3
10.1.1 Building Description 10-3
10.1.2 Design Requirements 10-4
10.1.3 Load Combinations 10-6
10.1.4 Seismic Forces 10-8
10.1.5 Side Walls 10-9
10.1.6 End Walls 10-25
10.1.7 In-Plane Deflection – End Walls 10-44
10.1.8 Bond Beam – Side Walls (and End Walls) 10-45
10.2 FIVE-STORY MASONRY RESIDENTIAL BUILDINGS IN BIRMINGHAM, ALABAMA; ALBUQUERQUE, NEW MEXICO; AND SAN RAFAEL, CALIFORNIA 10-45
10.2.1 Building Description 10-45
10.2.2 Design Requirements 10-48
10.2.3 Load Combinations 10-50
10.2.4 Seismic Design for Birmingham 1 10-51
10.2.5 Seismic Design for Albuquerque 10-69
10.2.6 Birmingham 2 Seismic Design 10-81
10.2.7 Seismic Design for San Rafael 10-89
10.2.8 Summary of Wall D Design for All Four Locations 10-101

11 WOOD DESIGN

11.1 THREE-STORY WOOD APARTMENT BUILDING, SEATTLE, WASHINGTON 11-3
11.1.1 Building Description 11-3
11.1.2 Basic Requirements 11-6
11.1.3 Seismic Force Analysis 11-9
11.1.4 Basic Proportioning 11-11
11.2 WAREHOUSE WITH MASONRY WALLS AND WOOD ROOF, LOS ANGELES, CALIFORNIA 11-30
11.2.1 Building Description 11-30

11.2.2 Basic Requirements....11-31
11.2.3 Seismic Force Analysis....11-33
11.2.4 Basic Proportioning of Diaphragm Elements....11-34

12 SEISMICALLY ISOLATED STRUCTURES
12.1 BACKGROUND AND BASIC CONCEPTS.... 12-4
12.1.1 Types of Isolation Systems.... 12-4
12.1.2 Definition of Elements of an Isolated Structure.... 12-5
12.1.3 Design Approach.... 12-6
12.1.4 Effective Stiffness and Effective Damping.... 12-7
12.2 CRITERIA SELECTION.... 12-7
12.3 EQUIVALENT LATERAL FORCE PROCEDURE.... 12-9
12.3.1 Isolation System Displacement.... 12-9
12.3.2 Design Forces....11
12.4 DYNAMIC LATERAL RESPONSE PROCEDURE.... 12-15
12.4.1 Minimum Design Criteria.... 12-15
12.4.2 Modeling Requirements.... 12-16
12.4.3 Response Spectrum Analysis.... 12-18
12.4.4 Response History Analysis.... 12-18
12.5 EMERGENCY OPERATIONS CENTER USING DOUBLE-CONCAVE FRICTION PENDULUM BEARINGS, OAKLAND, CALIFORNIA.... 12-21
12.5.1 System Description.... 12-22
12.5.2 Basic Requirements.... 12-25
12.5.3 Seismic Force Analysis.... 12-34
12.5.4 Preliminary Design Based on the ELF Procedure.... 12-36
12.5.5 Design Verification Using Nonlinear Response History Analysis.... 12-51
12.5.6 Design and Testing Criteria for Isolator Units.... 12-61

13 NONBUILDING STRUCTURE DESIGN
13.1 NONBUILDING STRUCTURES VERSUS NONSTRUCTURAL COMPONENTS.... 13-4
13.1.1 Nonbuilding Structure.... 13-5
13.1.2 Nonstructural Component.... 13-6
13.2 PIPE RACK, OXFORD, MISSISSIPPI.... 13-6
13.2.1 Description.... 13-7
13.2.2 Provisions Parameters.... 13-7
13.2.3 Design in the Transverse Direction.... 13- 8
13.2.4 Design in the Longitudinal Direction....13-11

13.3 STEEL STORAGE RACK, OXFORD, MISSISSIPPI 13-13
13.3.1 Description 13-13
13.3.2 Provisions Parameters 13-14
13.3.3 Design of the System 13-15
13.4 ELECTRIC GENERATING POWER PLANT, MERNA, WYOMING 13-17
13.4.1 Description 13-17
13.4.2 Provisions Parameters 13-19
13.4.3 Design in the North-South Direction 13-20
13.4.4 Design in the East-West Direction 13-21
13.5 PIER/WHARF DESIGN, LONG BEACH, CALIFORNIA 13-21
13.5.1 Description 13-21
13.5.2 Provisions Parameters 13-22
13.5.3 Design of the System 13-23
13.6 TANKS AND VESSELS, EVERETT, WASHINGTON 13-24
13.6.1 Flat-Bottom Water Storage Tank 13-25
13.6.2 Flat-Bottom Gasoline Tank 13-28
13.7 VERTICAL VESSEL, ASHPORT, TENNESSEE 13-31
13.7.1 Description 13-31
13.7.2 Provisions Parameters 13-32
13.7.3 Design of the System 13-33

14 DESIGN FOR NONSTRUCTURAL COMPONENTS

14.1 DEVELOPMENT AND BACKGROUND OF THE REQUIREMENTS FOR NONSTRUCTURAL COMPONENTS 14-3
14.1.1 Approach to Nonstructural Components 14-3
14.1.2 Force Equations 14-4
14.1.3 Load Combinations and Acceptance Criteria 14-5
14.1.4 Component Amplification Factor 14-6
14.1.5 Seismic Coefficient at Grade 14-7
14.1.6 Relative Location Factor 14-7
14.1.7 Component Response Modification Factor 14-7
14.1.8 Component Importance Factor 14-7
14.1.9 Accommodation of Seismic Relative Displacements 14-8
14.1.10 Component Anchorage Factors and Acceptance Criteria 14-9
14.1.11 Construction Documents 14-9
14.2 ARCHITECTURAL CONCRETE WALL PANEL 14-10

14.2.1 Example Description 14-10
14.2.2 Design Requirements 14-12
14.2.3 Spandrel Panel 14-12
14.2.4 Column Cover 14-19
14.2.5 Additional Design Considerations 14-20
14.3 HVAC FAN UNIT SUPPORT 14-21
14.3.1 Example Description 14-21
14.3.2 Design Requirements 14-22
14.3.3 Direct Attachment to Structure 14-23
14.3.4 Support on Vibration Isolation Springs 14-26
14.3.5 Additional Considerations for Support on Vibration Isolators 14-31
14.4 ANALYSIS OF PIPING SYSTEMS 14-33
14.4.1 ASME Code Allowable Stress Approach 14-33
14.4.2 Allowable Stress Load Combinations 14-34
14.4.3 Application of the Standard 14-36
14.5 PIPING SYSTEM SEISMIC DESIGN 14-38
14.5.1 Example Description 14-38
14.5.2 Design Requirements. 14-43
14.5.3 Piping System Design 14-45
14.5.4 Pipe Supports and Bracing 14-48
14.5.5 Design for Displacements 14-53
14.6 ELEVATED VESSEL SEISMIC DESIGN 14-55
14.6.1 Example Description 14-55
14.6.2 Design Requirements 14-58
14.6.3 Load Combinations 14-60
14.6.4 Forces in Vessel Supports 14-60
14.6.5 Vessel Support and Attachment 14-62
14.6.6 Supporting Frame 14-65
14.6.7 Design Considerations for the Vertical Load-Carrying System 14-69

A THE BUILDING SEISMIC SAFETY COUNCIL

1

Introduction

Robert G. Pekelnicky, P.E., S.E. and Michael Valley, S.E.

Contents

1.1 EVOLUTION OF EARTHQUAKE ENGINEERING 3
1.2 HISTORY AND ROLE OF THE NEHRP PROVISIONS 6
1.3 THE NEHRP DESIGN EXAMPLES 8
1.4 GUIDE TO USE OF THE PROVISIONS 11
1.5 REFERENCES 38

The *NEHRP Recommended Provisions: Design Examples* are written to illustrate and explain the applications of the *2009 NEHRP Recommended Seismic Provisions for Buildings and Other Structures,* ASCE 7-10 *Minimum Design Loads for Buildings and Other Structures* and the material design standards referenced therein and to provide explanations to help understand them. Designing structures to be resistant to major earthquake is complex and daunting to someone unfamiliar with the philosophy and history of earthquake engineering. The target audience for the Design Examples is broad. College students learning about earthquake engineering, engineers studying for their licensing exam, or those who find themselves presented with the challenge of designing in regions of moderate and high seismicity for the first time should all find this document's explanation of earthquake engineering and the *Provisions* helpful.

Fortunately, major earthquakes are a rare occurrence, significantly rarer than the other hazards, such as damaging wind and snow storms that one must typically consider in structural design. However, past experiences have shown that the destructive power of a major earthquake can be so great that its effect on the built environment can be underestimated. This presents a challenge since one cannot typically design a practical and economical structure to withstand a major earthquake elastically in the same manner traditionally done for other hazards.

Since elastic design is not an economically feasible option for most structures where major earthquakes can occur, there must be a way to design a structure to be damaged but still safe. Unlike designing for strong winds, where the structural elements that resist lateral forces can be proportioned to elastically resist the pressures generated by the wind, in an earthquake the lateral force resisting elements must be proportioned to deform beyond their elastic range in a

controlled manner. In addition to deforming beyond their elastic range, the lateral force resisting system must be robust enough to provide sufficient stability so the building is not at risk of collapse.

While typical structures are designed to be robust enough to have a minimal risk of collapse in major earthquakes, there are other structures whose function or type of occupants warrants higher performance designs. Structures, like hospitals, fire stations and emergency operation centers need to be designed to maintain their function immediately after or returned to function shortly after the earthquake. Structures like schools and places where large numbers of people assemble have been deemed important enough to require a greater margin of safety against collapse than typical buildings. Additionally, earthquake resistant requirements are needed for the design and anchorage of architectural elements and mechanical, electrical and plumbing systems to prevent falling hazards and in some cases loss of system function.

Current building standards, specifically the American Society of Civil Engineers (ASCE) 7 *Minimum Design Loads for Buildings and Other Structures* and the various material design standards published by the American Concrete Institute (ACI), the American Institute of Steel Construction (AISC), the American Iron and Steel Institute (AISI), the American Forest & Paper Association (AF&PA) and The Masonry Society (TMS) provide a means by which an engineer can achieve these design targets. These standards represent the most recent developments in earthquake resistant design. The majority of the information contained in ASCE 7 comes directly from the *NEHRP Recommended Seismic Provisions for New Buildings and Other Structures*. The stated intent of the *NEHRP Provisions* is to provide reasonable assurance of seismic performance that will:

1. Avoid serious injury and life loss,
2. Avoid loss of function in critical facilities, and
3. Minimize structural and nonstructural repair costs where practical to do so.

The *Provisions* have explicit requirements to provide life safety for buildings and other structures though the design forces and detailing requirements. The current provisions have adopted a target risk of collapse of 1% over a 50 year lifespan for a structure designed to the *Provisions.* The *Provisions* provide prevention of loss of function in critical facilities and minimized repair costs in a more implicit manner though prescriptive requirements.

Having good building codes and design standards is only one action necessary to make a community's buildings resilient to a major earthquake. A community also needs engineers who can carry out designs in accordance with the requirements of the codes and standards and contractors who can construct the designs in accordance with properly prepared construction documents. The first item is what the *NEHRP Recommended Provisions: Design Examples* seeks to foster. The second item is discussed briefly later in this document in Chapter 1, Section 1.6 Quality Assurance.

The purpose of this introduction is to offer general guidance for users of the design examples and to provide an overview. Before introducing the design examples, a brief history of earthquake engineering is presented. That is followed by a history of the *NEHRP Provisions* and its role in

setting standards for earthquake resistant design. This is done to give the reader a perspective of the evolution of the *Provisions* and some background for understanding the design examples. Following that is a brief summary of each chapter.

1.1 EVOLUTION OF EARTHQUAKE ENGINEERING

It is helpful to understand the evolution of the earthquake design standards and the evolution of the field of earthquake engineering in general. Much of what is contained within the standards is based on lessons learned from earthquake damage and the ensuing research.

Prior to 1900 there was little consideration of earthquakes in the design of buildings. Major earthquakes were experienced in the United States, notably the 1755 Cap Ann Earthquake around Boston, the 1811 and 1812 New Madrid Earthquakes, the 1868 Hayward California Earthquake and the 1886 Charleston Earthquake. However, none of these earthquakes led to substantial changes in the way buildings were constructed.

Many things changed with the Great 1906 San Francisco Earthquake. The earthquake and ensuing fire destroyed much of San Francisco and was responsible for approximately 3,000 deaths. To date it is the most deadly earthquake the United States has ever experienced. While there was significant destruction to the built environment, there were some important lessons learned from those buildings that performed well and did not collapse. Most notable was the exemplary performance of steel framed buildings which consisted of riveted wind frames and brick infill, built in the Chicago style.

The recently formed San Francisco Section of the American Society of Civil Engineers (ASCE) studied the effects of the earthquake in great detail. An observation was that “a building designed with a proper system of bracing wind pressure at 30 lbs. per square foot will resist safely the stresses caused by a shock of the intensity of the recent earthquake.” (ASCE, 1907) That one statement became the first U.S. guideline on how to provide an earthquake resistant design.

The earthquakes in Tokyo in 1923 and Santa Barbara in 1925 spurred major research efforts. Those efforts led to the development of the first seismic recording instruments, shake tables to investigate earthquake effects on buildings, and committees dedicated to creating code provisions for earthquake resistant design. Shortly after these earthquakes, the 1927 *Uniform Building Code* (UBC) was published (ICBO, 1927). It was the first model building code to contain provisions for earthquake resistant design, albeit in an appendix. In addition to that, a committee began working on what would become California’s first state-wide seismic code in 1939.

Another earthquake struck Southern California in Long Beach in 1933. The most significant aspect, of that earthquake was the damage done to school buildings. Fortunately the earthquake occurred after school hours, but it did cause concern over the vulnerabilities of these buildings. That concern led to the Field Act, which set forth standards and regulations for earthquake

resistance of school buildings. This was the first instance of what has become a philosophy engrained in the earthquake design standards of requiring higher levels of safety and performance for certain buildings society deems more important that a typical building. In addition to the Field Act, the Long Beach earthquake led to a ban on unreinforced masonry construction in California, which in later years was extended to all areas of moderate and high seismic risk.

Following the 1933 Long Beach Earthquake there was significant activity both in Northern and Southern California, with the local Structural Engineers Associations of each region drafting seismic design provisions for Los Angeles in 1943 and San Francisco in 1948. Development of these codes was facilitated greatly by observations from the 1940 El Centro Earthquake. Additionally, that earthquake was the first major earthquake for which the strong ground motion shaking was recorded with an accelerograph.

A joint committee of the San Francisco Section of ASCE and the Structural Engineers Association of Northern California began work on seismic design provisions which were published in 1951 as ASCE *Proceedings-Separate No. 66. Separate 66, as it is commonly referred to as,* was a landmark document which set forth earthquake design provisions which formed the basis of US building codes for almost 40 years. Many concepts and recommendations put forth in *Separate 66,* such as the a period dependent design spectrum, different design forces based on the ductility of a structure and design provisions for architectural components are still found in today's standards.

Following *Separate 66*, the Structural Engineers Association of California (SEAOC) formed a Seismology committee and in 1959 put forth the first edition of the *Recommended Lateral Force Requirements*, commonly referred to as the "The SEAOC Blue Book." The Blue Book became the base document for updating and expanding the seismic design provisions of the Uniform Building Code (UBC), the model code adopted by most western states including California. SEAOC regularly updated the Blue Book from 1959 until 1999, with the changes made and new recommendations in each new edition of the Blue Book being incorporated in to the subsequent edition of the UBC.

The 1964 Anchorage Earthquake and the 1971 San Fernando Earthquake both were significant events. Both earthquakes exposed significant issues with the way reinforced concrete structures would behave if not detailed for ductility. There were failures of large concrete buildings which had been designed to recent standards and those buildings had to be torn down. To most engineers and the public this was unacceptable performance.

Following the 1971 San Fernando Earthquake, the National Science Foundation gave the Applied Technology Council (ATC) a grant to develop more advanced earthquake design provisions. That project engaged over 200 preeminent experts in the field of earthquake engineering. The landmark report they produced in 1978, ATC 3-06, *Tentative Provisions for the Development of Seismic Regulations for Buildings* (1978), has become the basis for the current earthquake design standards. The *NEHRP Provisions* trace back to ATC 3-06, as will be discussed in more detail in the following section.

There have been additional earthquakes since the 1971 San Fernando Earthquake which have had significant influence on seismic design. Table 1 provides a summary of major North American earthquakes and changes to the building codes that resulted from them through the 1997 UBC. Of specific note are the 1985 Mexico City, 1989 Loma Prieta and 1994 Northridge Earthquakes.

Earthquake	**UBC Edition**	**Enhancement**
1971 San Fernando	1973	Direct positive anchorage of masonry and concrete walls to diaphragms
	1976	Seismic Zone 4, with increased base shear requirements
		Occupancy Importance Factor *I* for certain buildings
		Interconnection of individual column foundations
		Special Inspection requirements
1979 Imperial Valley	1985	Diaphragm continuity ties
1985 Mexico City	1988	Requirements for column supporting discontinuous walls
		Separation of buildings to avoid pounding
		Design of steel columns for maximum axial forces
		Restrictions for irregular structures
		Ductile detailing of perimeter frames
1987 Whittier Narrows	1991	Revisions to site coefficients
		Revisions to spectral shape
		Increased wall anchorage forces for flexible diaphragm buildings
1989 Loma Prieta	1991	Increased restrictions on chevron-braced frames
		Limitations on b/t ratios for braced frames
	1994	Ductile detailing of piles
1994 Northridge	1997	Restrictions on use of battered piles
		Requirements to consider liquefaction
		Near-fault zones and corresponding base shear requirements
		Revised base shear equations using 1/T spectral shape
		Redundancy requirements
		Design of collectors for overstrength
		Increase in wall anchorage requirements
		More realistic evaluation of design drift
		Steel moment connection verification by test

Table 1: Recent North American Earthquakes and Subsequent Code Changes (from SEOAC, 2009)

The 1985 Mexico City Earthquake was extremely devastating. Over 10,000 people were killed and there was three to four billion dollars of damage. The most significant aspect of this earthquake was that while the epicenter was located over 200 miles away from Mexico City. The unique geologic nature, that Mexico City was sited on an old (ancient?) lake bed of silt and clay, generated ground shaking with a much longer period and larger amplitudes than would be expected from typical earthquakes. This long period shaking was much more damaging to mid-rise and larger structures because these buildings were in resonance with the ground motions. In current design practice site factors based on the underlying soil are used to modify the seismic hazard parameters.

The 1989 Loma Prieta Earthquake caused an estimated $6 billion in damage, although it was far less deadly than other major earthquakes throughout history. Only sixty-three people lost their lives, a testament to the over 40 years of awareness and consideration of earthquakes in the design of structures. A majority of those deaths, 42, resulted from the collapse of the Cyprus Street Viaduct, a nonductile concrete elevated freeway. In this earthquake the greatest damage occurred in Oakland, parts of Santa Cruz and the Marina District in San Francisco where the soil was soft or poorly compacted fill. As with the Mexico City experience, this indicates the importance of subsurface conditions on the amplification of earthquake shaking. The earthquake also highlighted the vulnerability of soft and weak story buildings because a significant number of the collapsed buildings in the Marina District were wood framed apartment buildings with weak first stories consisting of garages with door openings that greatly reduced the wall area at the first story.

Five years later the 1994 Northridge earthquake struck California near Los Angeles. Fifty seven people lost their lives and the damage was estimated at around $20 billion. The high cost of damage repair emphasized the need for engineers to consider overall building performance, in addition to building collapse, and spurred the movement toward Performance-Based design. As with the 1989 Loma Prieta earthquake, there was a disproportionate number of collapses of soft/weak first story wood framed apartment buildings.

The 1994 Northridge Earthquake was most significant for the unanticipated damage to steel moment frames that was discovered. Steel moment frames had generally been thought of as the best seismic force resisting system. However, many moment frames experienced fractures of the welds that connected the beam flange to the column flange. This led to a multi-year, FEMA funded problem-focused study to assess and improve the seismic performance of steel moment frames. It also led to requirements for the number of frames in a structure, and penalties for having a lateral force resisting system that does not have sufficient redundancy.

1.2 HISTORY AND ROLE OF THE NEHRP PROVISIONS

Following the completion of the ATC 3 project in 1978, there was desire to make the ATC 3-06 approach the basis for new regulatory provisions and to update them periodically. FEMA, as the lead agency of the National Earthquake Hazard Reduction Program (NEHRP) at the time, contracted with the then newly formed Building Seismic Safety Council (BSSC) to perform trial designs based on ATC 3-06 to exercise the proposed new provisions. The BSSC put together a

group of experts consisting of consulting engineers, academics, representatives from various building industries and building officials. The result of that effort was the first (1985) edition of the *NEHRP Recommended Provisions for the Development of Seismic Regulations for New Buildings*.

Since the publication of the first edition through the 2003 edition, the *NEHRP Provisions* were updated every three years. Each update incorporated recent advances in earthquake engineering research and lessons learned from previous earthquakes. The intended purpose of the *Provisions* was to serve as a code resource document. While the SEAOC Blue Book continued to serve as the basis for the earthquake design provisions in the *Uniform Building Code*, the *BOCA National Building Code* and the *Standard Building Code* both adopted the 1991 *NEHRP Provisions* in their 1993 and 1994 editions respectively. The 1993 version of the ASCE 7 standard *Minimum Design Loads for Buildings and Other Structures* (which had formerly been American National Standards Institute (ANSI) Standard A58.1) also utilized the 1991 *NEHRP Provisions*.

In the late 1990's the three major code organizations, ICBO (publisher of the UBC), BOCA, and SBC decided to merge their three codes into one national model code. When doing so they chose to incorporate the 1997 *NEHRP Provisions* as the seismic design requirements for the inaugural 2000 edition of the *International Building Code* (IBC). Thus, the SEAOC Blue Book was no longer the base document for the UBC/IBC. The 1997 *NEHRP Provisions* had a number of major changes. Most significant was the switch from the older seismic maps of ATC 3-06 to new, uniform hazard spectral value maps produced by USGS in accordance with BSSC Provisions Update Committee (PUC) Project 97. The 1998 edition of ASCE 7 was also based on the 1997 *NEHRP Provisions*.

ASCE 7 continued to incorporate the 2000 and 2003 editions of the *Provisions* for its 2002 and 2005 editions, respectively. However, the 2000 IBC adopted the 1997 NEHRP Provisions by directly transferring the text from the provisions into the code. In the 2003 IBC the provisions from the 2000 IBC were retained and there was also language, for the first time, which pointed the user to ASCE 7-02 for seismic provisions instead of adopting the 2000 *NEHRP Provisions* directly. The 2006 IBC explicitly referenced ASCE 7 for the earthquake design provisions, as did the 2009 and 2012 editions.

With the shift in the IBC from directly incorporating the NEHRP Provision for their earthquake design requirements to simply referencing the provisions in ASCE 7, the BSSC Provisions Update Committee decided to move the NEHRP Provisions in a new direction. Instead of providing all the seismic design provisions within the NEHRP Provisions, which would essentially be repeating the provisions in ASCE 7, and then modifying them, the PUC chose to adopt ASCE 7-05 by reference and then provide recommendations to modify it as necessary. Therefore, Part 1 of the 2009 NEHRP Provisions contains major technical modifications to ASCE 7-05 which, along with other recommendations from the ASCE 7 Seismic Subcommittee, were the basis for proposed changes that were incorporated into ASCE 7-10 and included associated commentary on those changes. The PUC also developed a detailed commentary to the seismic provisions of ASCE 7-05, which became Part 2 of the 2009 NEHRP Provisions.

In addition to Part 1 and Part 2 in the 2009 *NEHRP Provisions*, a new section was introduced – Part 3. The intent of this new portion was to showcase new research and emerging methods, which the PUC did not feel was ready for adoption into national design standards but was important enough to be disseminated to the profession. This new three part format marks a change in the *Provisions* from a code-language resource document to the key knowledge-based resource for improving the national seismic design standards and codes.

The most significant technical change to Part 1 of the 2009 *Provisions* was the adoption of a "Risk-Targeted" approach to determine the Maximum Considered Earthquake hazard parameters. This was a switch from the Uniform Hazard approach in the 1997, 2000, and 2003 editions. In the "Risk Targeted" approach, the ground motion parameters are adjusted such that they provide a uniform 1% risk of collapse in a 50 year period for a generic building, as opposed to a uniform return period for the seismic hazard. A detailed discussion of this can be found in the commentary in Part 1 of the 2009 Provisions.

Today, someone needing to design a seismically resilient building in the U.S. would first go to the local building code which has generally adopted the IBC with or without modifications by the local jurisdiction. For seismic design requirements, the IBC then points to relevant Chapters of ASCE 7. Those chapters of ASCE 7 set forth the seismic hazard, design forces and system detailing requirements. The seismic forces in ASCE 7 are dependent upon the type of detailing and specific requirements of the lateral force resisting system elements. ASCE 7 then points to material specific requirements found in the material design standards published by ACI, AISC, AISI, AF&PA and TMS for those detailing requirements. Within this structure, the NEHRP Provisions serves as a consensus evaluation of the design standards and a vehicle to transfer new knowledge to ASCE 7 and the material design standards.

1.3 *THE NEHRP DESIGN EXAMPLES*

Design examples were first prepared for the 1985 *NEHRP Provisions* in a publication entitled *Guide to Application of the NEHRP Recommended Provisions*, FEMA 140. These design examples were based on real buildings. The intent was the same as it is now, to show people who are not familiar with seismic design of how to apply the *Provisions*, the standards referenced by the *Provisions* and the concepts behind the *Provisions*.

Because of the expanded role that the *Provisions* were having as the basis for the seismic design requirements for the model codes and standards, it was felt that there should be an update and expansion of the original design examples. Following the publication of the 2003 NEHRP Provisions, FEMA commissioned a project to update and expand the design examples. This resulted in *NEHRP Recommended Provisions: Design Examples*, FEMA 451. Many of the design problems drew heavily on the examples presented in FEMA 140, but were completely redesigned based on first the 2000 and then the 2003 *NEHRP Provisions* and the materials standards referenced therein. Additional examples were created to reflect the myriad of structures now covered under the *Provisions*.

This volume is an update of the design examples in FEMA 451 to reflect the *2009 NEHRP Provisions* and the updated standards referenced therein. Many of the design examples are the same as presented in FEMA 451, with only changes made due to changes in the provisions.

The *Design Examples* not only covers the application of ASCE 7, the material design standards and the *NEHRP Provisions*, it also illustrates the use of analysis methods and earthquake engineering knowledge and judgment in situations which would be encountered in real designs. The authors of the design examples are subject matter experts in the specific area covered by the chapter they authored. Furthermore, the companion *NEHRP Recommend Provisions: Training Materials* provides greater background information and knowledge, which augment the design examples.

It is hoped that with the Part 2 Expanded Commentary in the *2009 NEHRP Provisions*, the Design Examples and the Training Materials, an engineer will be able to understand not just how to use the Provisions, but also the philosophical and technical basis behind the provisions. Through this understanding of the intent of the seismic design requirements found in ASCE 7, the material design standards and the 2009 NEHRP Provisions, it is hoped that more engineers will find the application of those standards less daunting and thereby utilize the standards more effectively in creating innovative and safe designs.

Chapter 1 – This preceding introduction and the Guide to Use of the *Provisions* which follows provides background and presents a series of flow charts to walk an engineer through the use of the provisions.

Chapter 2 – Fundamentals presents a brief but thorough introduction to the fundamentals of earthquake engineering. While this section does not present any specific applications of the *Provisions,* it provides the reader with the essential philosophical background to what is contained within the *Provisions*. The concepts of idealizing a seismic dynamic load as an equivalent static load and providing ductility instead of pure elastic strength are explained.

Chapter 3 - Earthquake Ground Motion is new to this edition of the *Design Examples.* This chapter explains the basis for determining seismic hazard parameters used for design in the *Provisions*. It discusses the seismic hazard maps in ASCE 7-05 and the new Risk Targeted maps found in the 2009 *NEHRP Provisions* and ASCE 7-10. The chapter also discusses probabilistic seismic hazard assessment, the maximum direction response parameters and selection and scaling of ground motion histories for use in linear and nonlinear response history analysis.

Chapter 4 – Structural Analysis presents the analysis of two different buildings, a 12-story steel moment frame and a 6-story steel moment frame structure. The 12-story structure is irregular and is analyzed using the three linear procedures referenced in ASCE 7 – Equivalent Lateral Force, Modal Response Spectrum, and Linear Response History. The 6-story structure is analyzed using three methods referenced in ASCE 7 - Equivalent Lateral Force, Modal Response Spectrum and Nonlinear Response History – and two methods which are referenced in other documents – Plastic Strength (Virtual Work) and Nonlinear Static Pushover. The intent of this chapter is to show the variations in predicted response based on the chosen analysis method.

Some of the examples have been updated based on advances in the state of the practice with respect to seismic analysis.

Chapter 5 – Foundation Analysis and Design presents design examples for both shallow and deep foundations. First, a spread footing foundation for a 7-story steel framed building is presented. Second the design of a pile foundation for a 12-story concrete moment frame building is presented. Designs of the steel and concrete structures whose foundations are designed in this chapter are presented in Chapters 6 and 7 respectively.

Chapter 6 – Structural Steel Design presents the design of three different types of steel buildings. The first building is a high-bay industrial warehouse which uses an ordinary concentric braced frame in one direction and an intermediate steel moment frame in the other direction. The second example is a 7-story office building which is designed using two alternate framing systems, special steel moment frames and special concentric braced frames. The third example is new to this edition of the design examples. It is a 10-story hospital using buckling restrained braced frames (BRBF). This replaces an example using eccentrically braced frames (EBF) in the previous edition of the design examples because the profession has moved toward favoring the BRBF system over the EBF system.

Chapter 7 – Reinforced Concrete presents the designs of a 12-story office building located in moderate and high seismicity. The same building configuration is used in both cases, but in the moderate seismicity region “Intermediate” member frames are used while “Special” moment frames are used in the high seismicity region. Also in the high seismicity region, special concrete walls are needed in one direction and their design is presented.

Chapter 8 – Precast Concrete Design presents examples of four common cases where precast concrete elements are a component of a seismic force resisting system. The first example presents the design of precast concrete panels being used as horizontal diaphragms both with and without a concrete topping slab. The second example presents the design of 3-story office building using intermediate precast concrete shear walls in a region of low or moderate seismicity The third example presents the design of a one-story tilt-up concrete industrial building in a region of high seismicity. The last example, which is new to this edition of the design examples, presents the design of a precast Special Moment Frame.

Chapter 9 – Composite Steel and Concrete presents the design of a 4-story medical office building in a region of moderate seismicity. The building uses composite partially restrained moment frames in both directions as the lateral force resisting system.

Chapter 10 – Masonry presents the design of two common types of buildings using reinforced masonry walls as their lateral force resisting system. The first example is a single-story masonry warehouse building with tall, slender walls. The second example is a five-story masonry hotel building with a bearing wall system designed in areas with different seismicity.

Chapter 11 – Wood Design presents the design of a variety of wood elements in common seismic force resisting applications. The first example is a three-story, wood-frame apartment

building. The second example illustrates the design of the roof diaphragm and wall-to-roof anchorage for the masonry building featured in the first example of Chapter 10.

Chapter 12 – Seismically Isolated Structures presents both the basic concepts of seismic isolation and then the design of an essential facility using a seismic isolation system. The example building has a special concentrically braced frame superstructure and uses double-concave friction pendulum isolators, which have become the most common type of isolator used in regions of high seismicity. In the previous edition of the design examples, high-damping rubber isolators were used.

Chapter 13 – Nonbuilding Structure Design presents the design of various types of structures other than buildings that are covered by the *Provisions*. First there is a brief discussion about the difference between a nonbuilding structure and a nonstructural component. The first example is the design of a pipe rack. The second example is of an industrial storage rack. The third example is a power generating plant with significant mass irregularities. The third example is a pier. The fourth examples are flat-bottomed storage tanks, which also illustrates how the *Provisions* are used in conjunction with industry design standards. The last example is of a tall, slender vertical storage vessel containing hazardous materials, which replaces an example of an elevated transformer.

Chapter 14 – Design for Nonstructural Components presents a discussion on the design of nonstructural components and their anchorage plus several design examples. The examples are of an architectural concrete wall panel, the supports for a large rooftop fan unit, the analysis and bracing of a piping system (which is greatly expanded from FEMA 451) and an elevated vessel (which is new).

1.4 GUIDE TO USE OF THE PROVISIONS

The flow charts that follow are provided to assist the user of the *NEHRP Recommended Provisions* and, by extension, the seismic provisions of ASCE 7, *Minimum Design Loads for Buildings and Other Structures*; and the *International Building Code*. The flow charts provide an overview of the complete process for satisfying the *Provisions*, including the content of all technical chapters.

Part 1 of the 2009 *NEHRP Recommended Seismic Provisions for New Buildings and Other Structures* (the *Provisions*) adopts by reference the national consensus design loads standard, ASCE/SEI 7-05, *Minimum Design Loads for Buildings and Other Structures* (the *Standard*), including Supplements 1 and 2, and makes modifications to the seismic requirements in the *Standard*. Part 2 of the *Provisions* contains an up-to-date, user friendly commentary on the seismic design requirements of the *Standard*. Part 3 of the *Provisions* consists of a series of resource papers that clarify aspects of the *Provisions* and present new seismic design concepts and procedures.

The flow charts in this chapter are expected to be of most use to those who are unfamiliar with the scope of the *NEHRP Recommended Provisions*, but they cannot substitute for a careful reading of the *Provisions*. The level of detail shown varies, being greater where questions of applicability of the *Provisions* are pertinent and less where a standard process of structural analysis or detailing is all that is required. The details contained in the many standards referenced in the *Provisions* are not included;

therefore, the actual flow of information when proportioning structural members for the seismic load effects specified in the *Provisions* will be considerably more complex.

Cited section numbers (such as Sec. 11.1.2) refer to sections of the *Standard*. Where reference is to a *Provisions* Part 1 modification to the *Standard*, the citation indicates that (such as *Provisions* Sec. 11.1.2). In a few rare instances, the Provisions Update Committee deferred to the ASCE 7 committee to make needed technical changes; in those cases reference is made specifically to ASCE 7-10 (such as ASCE 7-10 Sec. 12.12.3).

On each chart the flow generally is from a heavy-weight box at the top-left to a medium-weight box at the bottom-right. User decisions are identified by six-sided cells. Optional items and modified flow are indicated by dashed lines.

Chart 1.1 provides an overall summary of the process which begins with consideration of the Scope of Coverage and ends with Quality Assurance Requirements. Additions to, changes of use in and alterations of existing structures are covered by the *Provisions* (see Chart 1.3), but evaluation and rehabilitation of existing structures is not. Nearly two decades of FEMA-sponsored development of technical information to improve seismic safety in existing buildings has culminated in a comprehensive set of codes, standards and guidelines. The *International Existing Building Code* references the ASCE 31 Standard, *Seismic Evaluation of Existing Buildings*; and the ASCE 41 Standard, *Seismic Rehabilitation of Existing Buildings*.

Chart 1.1
Overall Summary of Flow

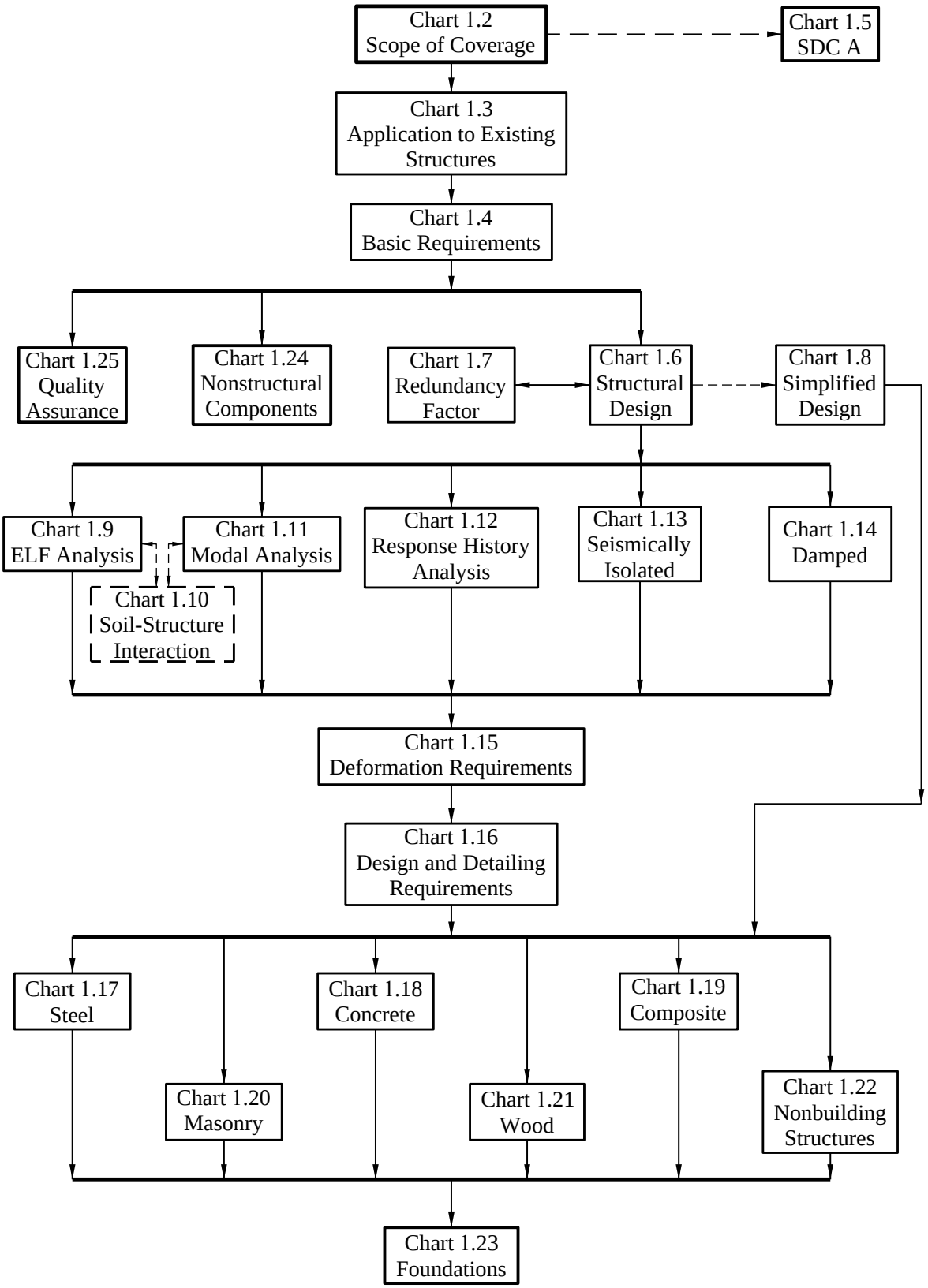

Chart 1.2
Scope of Coverage

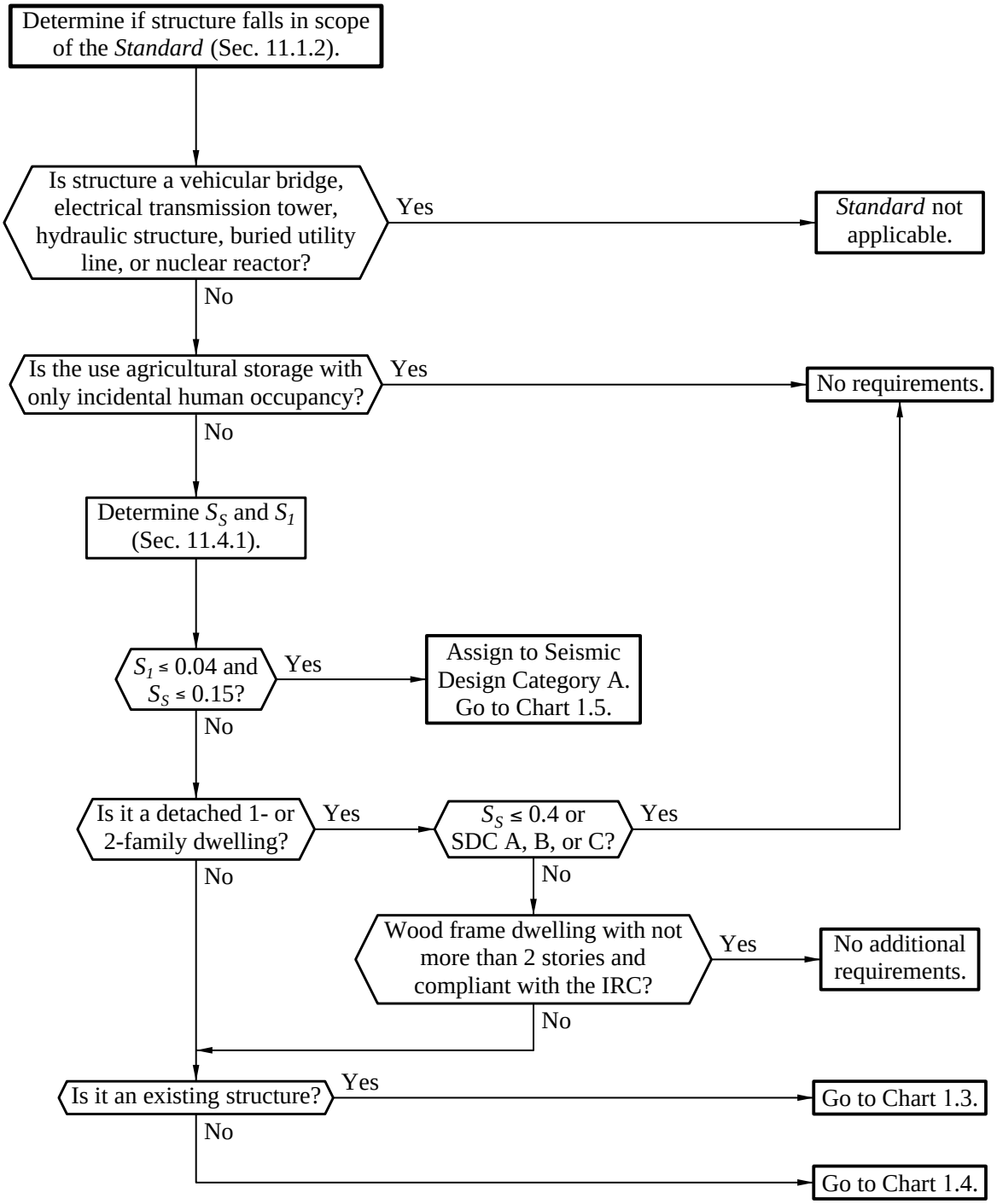

Chart 1.3
Application to Existing Structures

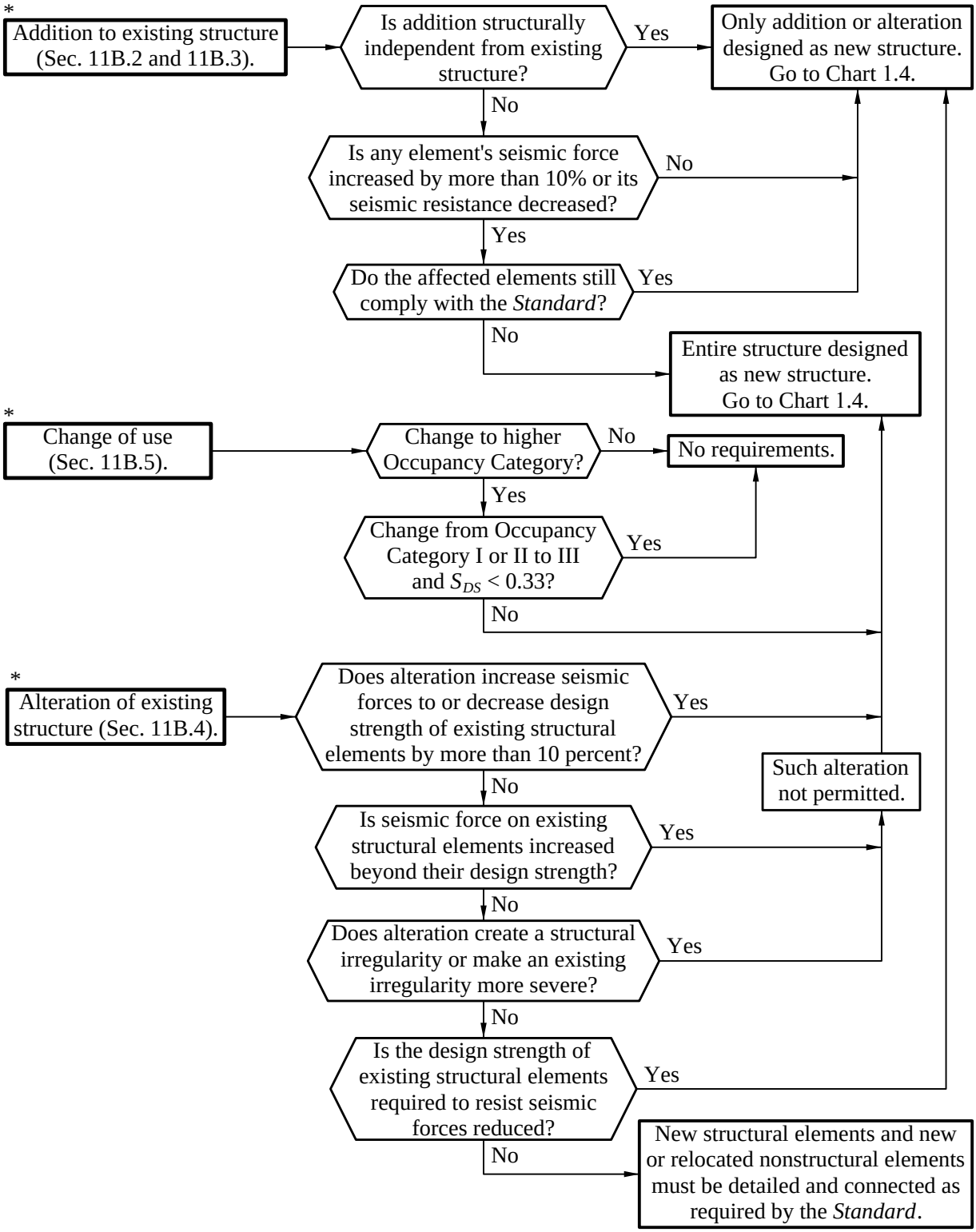

* The *Standard* applies to existing structures only in the cases of additions to, changes of use in, and alterations of such structures.

Chart 1.4
Basic Requirements

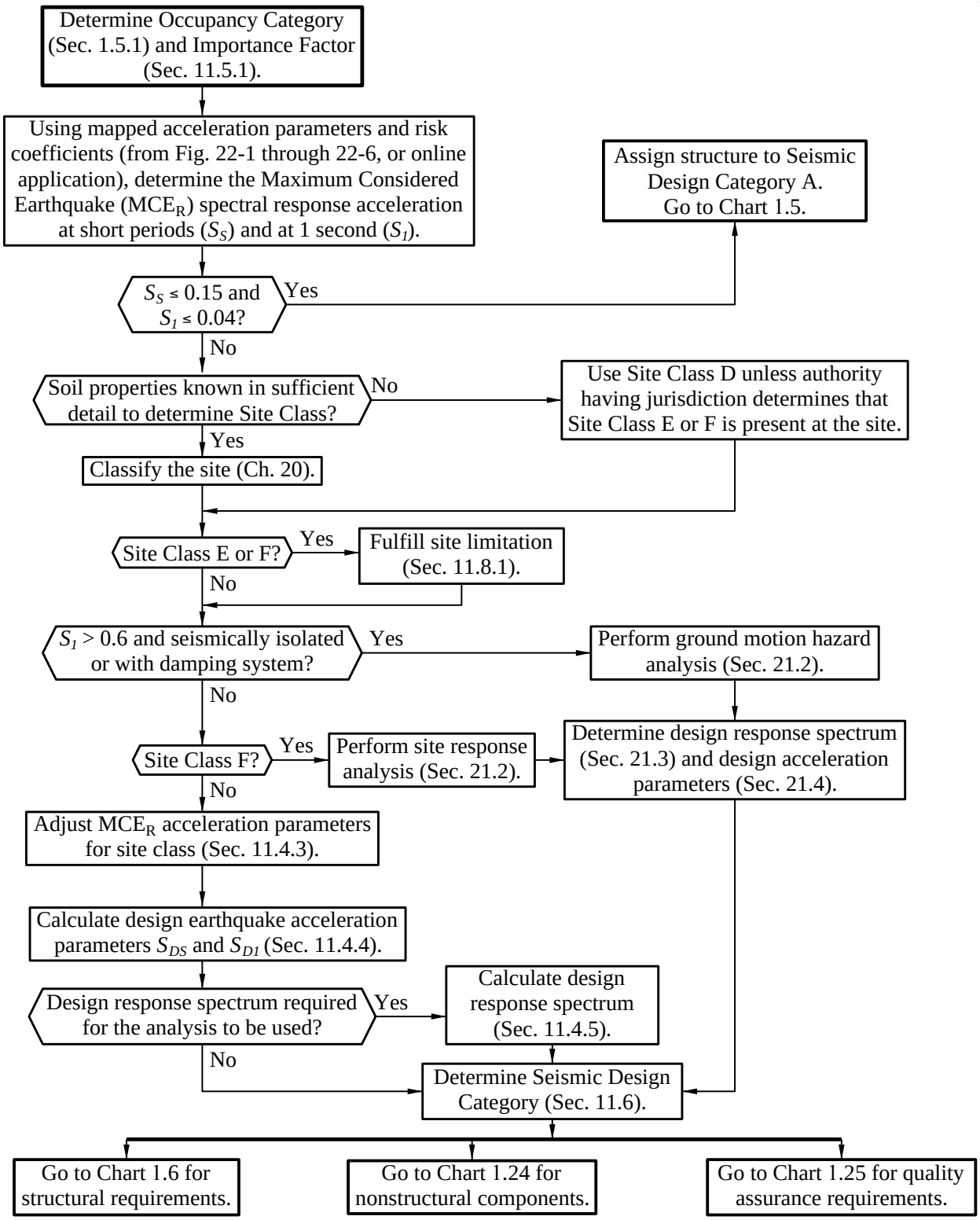

Chart 1.5
Seismic Design Category A

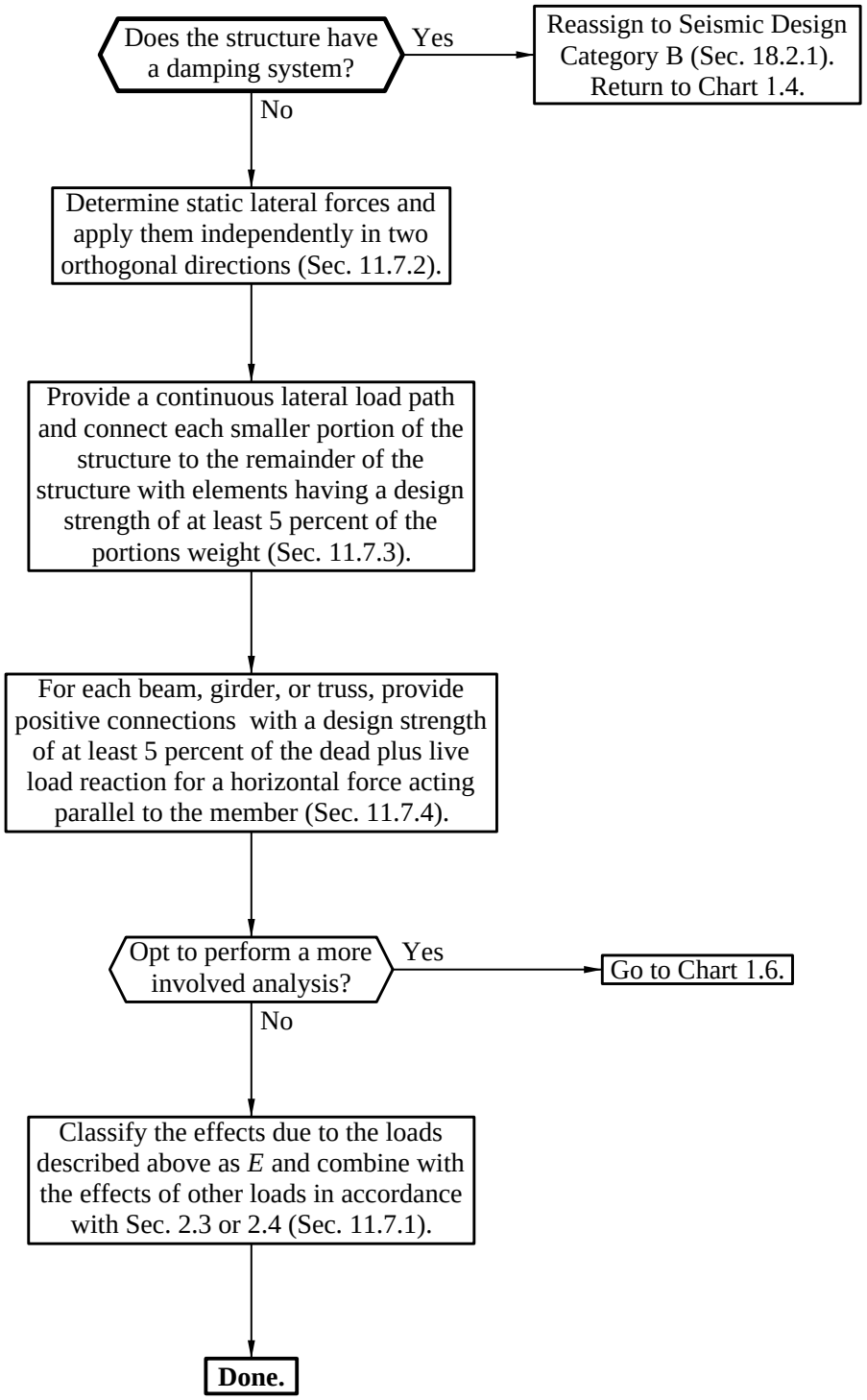

***** The requirement to reclassify Seismic Design Category A structures to Seismic Design Category B has been declared editorially erroneous and will be removed via errata for ASCE 7-13.

Chart 1.6
Structural Design

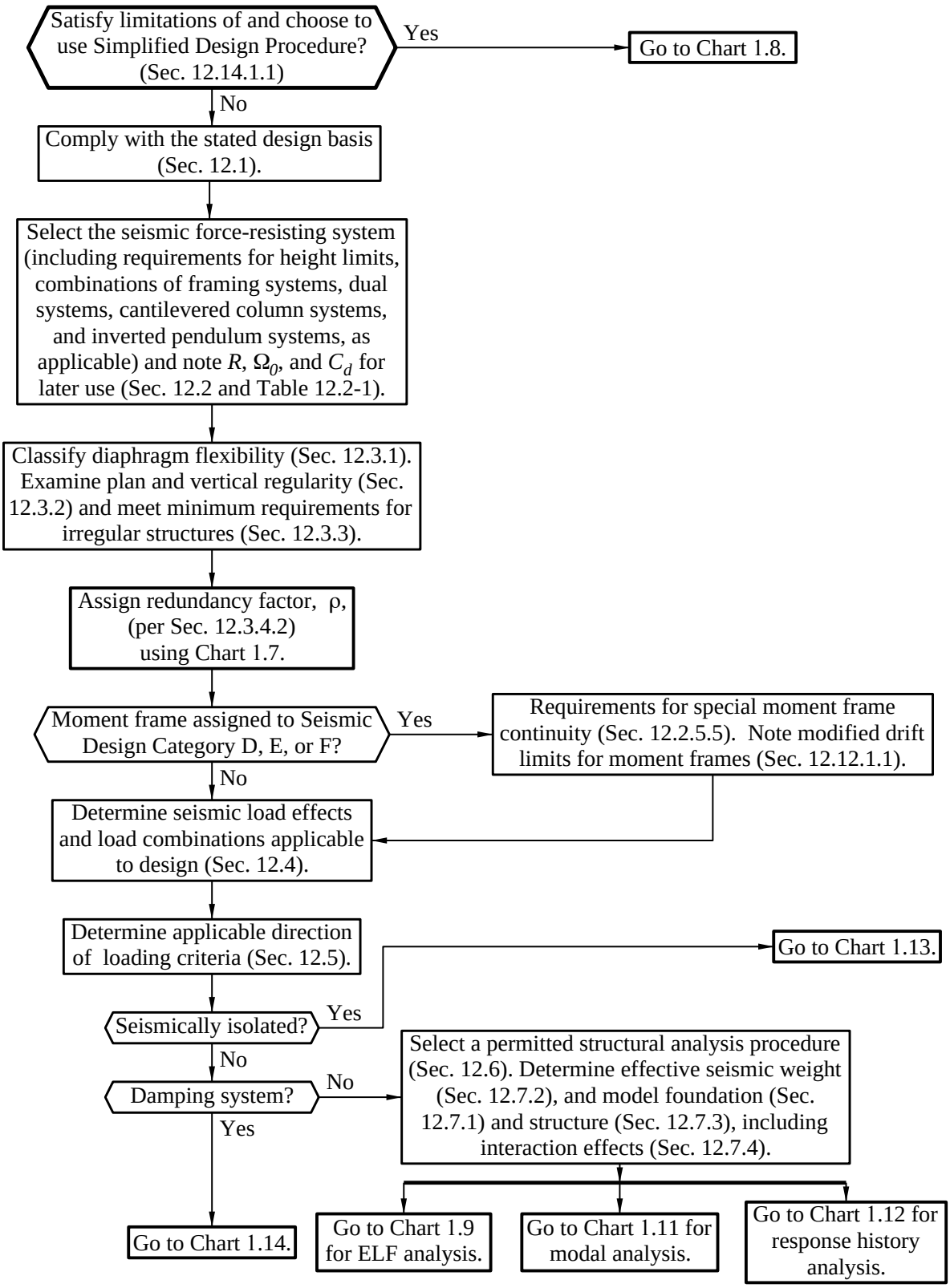

Chart.7
Redundancy Factor

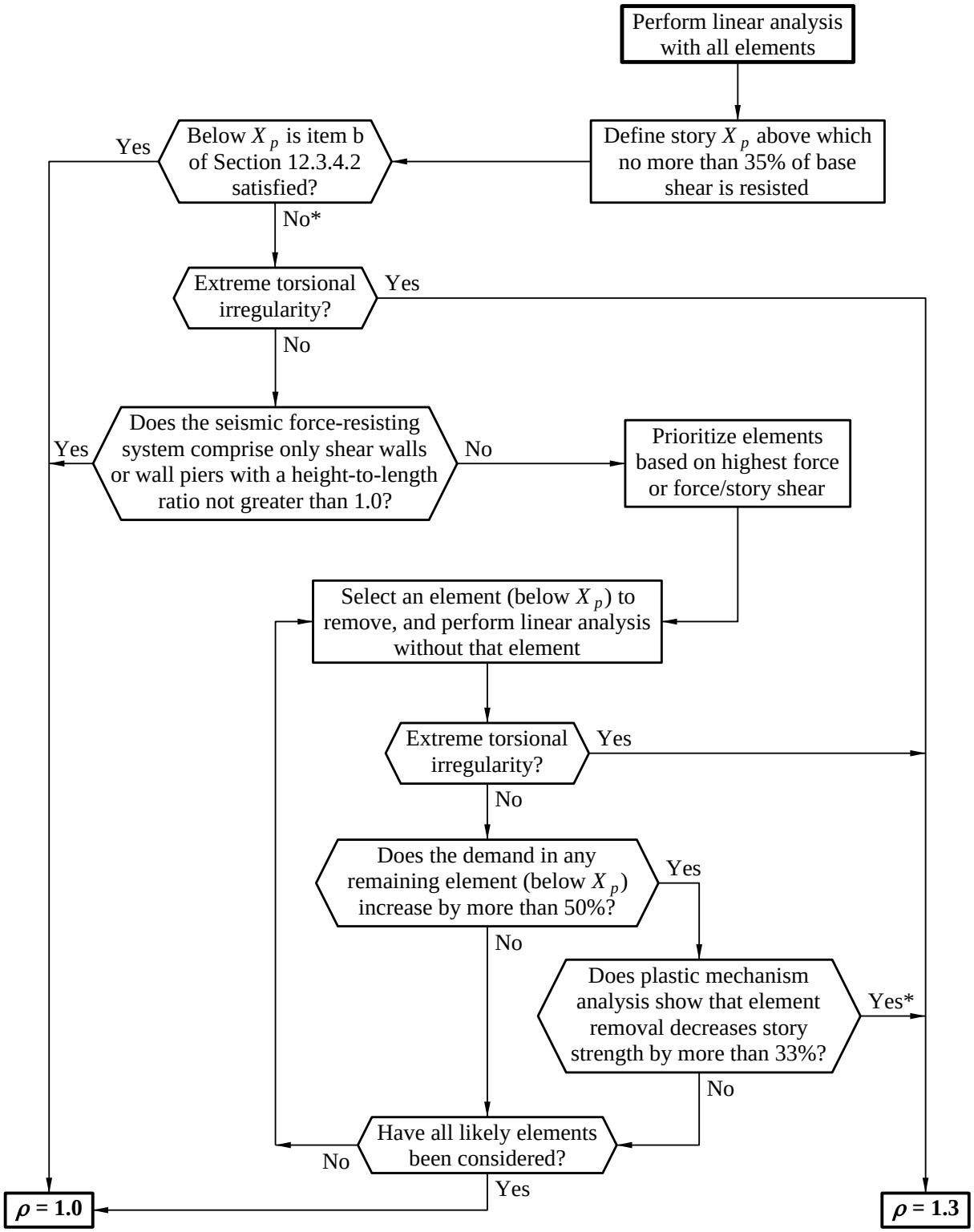

* or not considered

Chart 1.8
Simplified Design Procedure

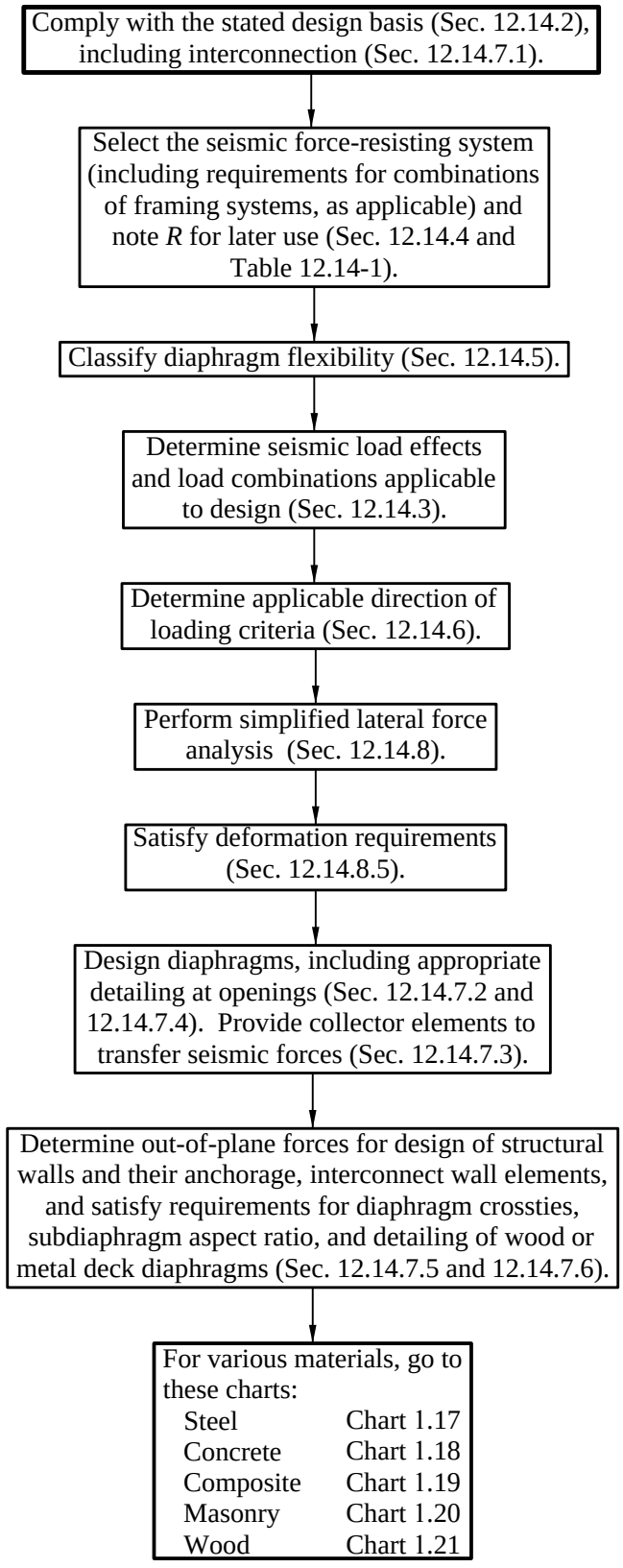

Chart 1.9
Equivalent Lateral Force (ELF) Analysis

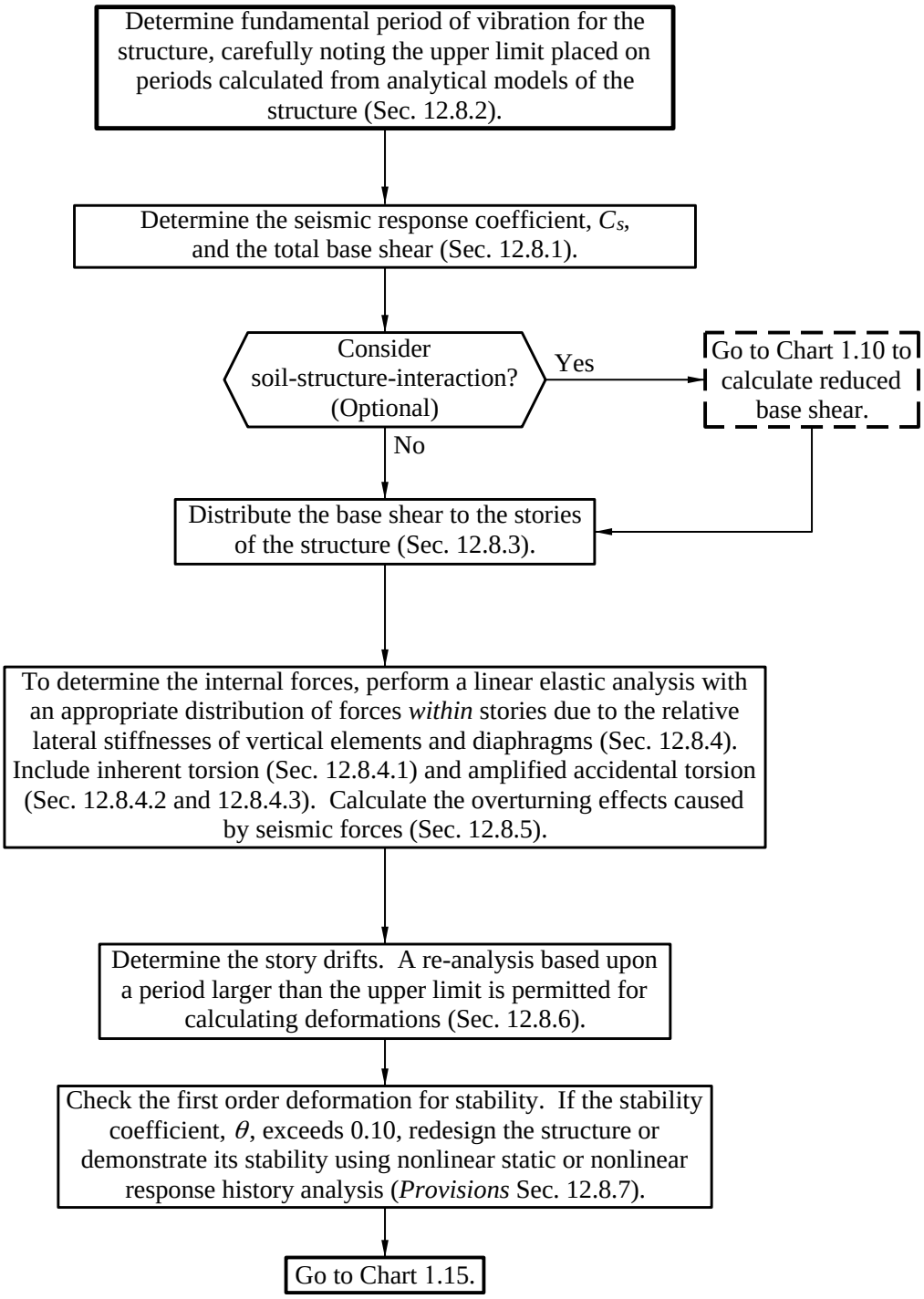

Chart 1.10
Soil-Structure Interaction (SSI)

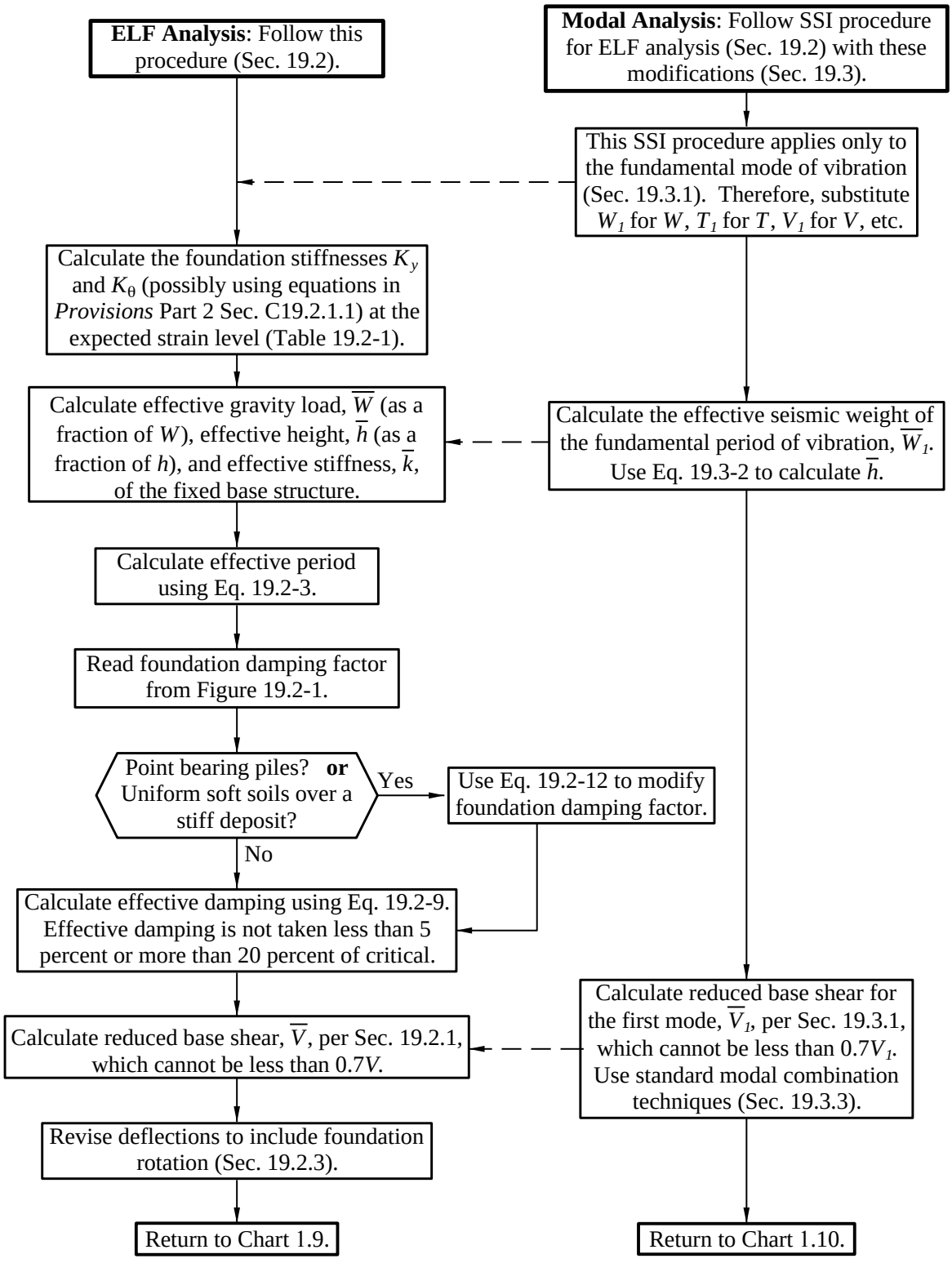

Chart 1.11
Modal Response Spectrum Analysis

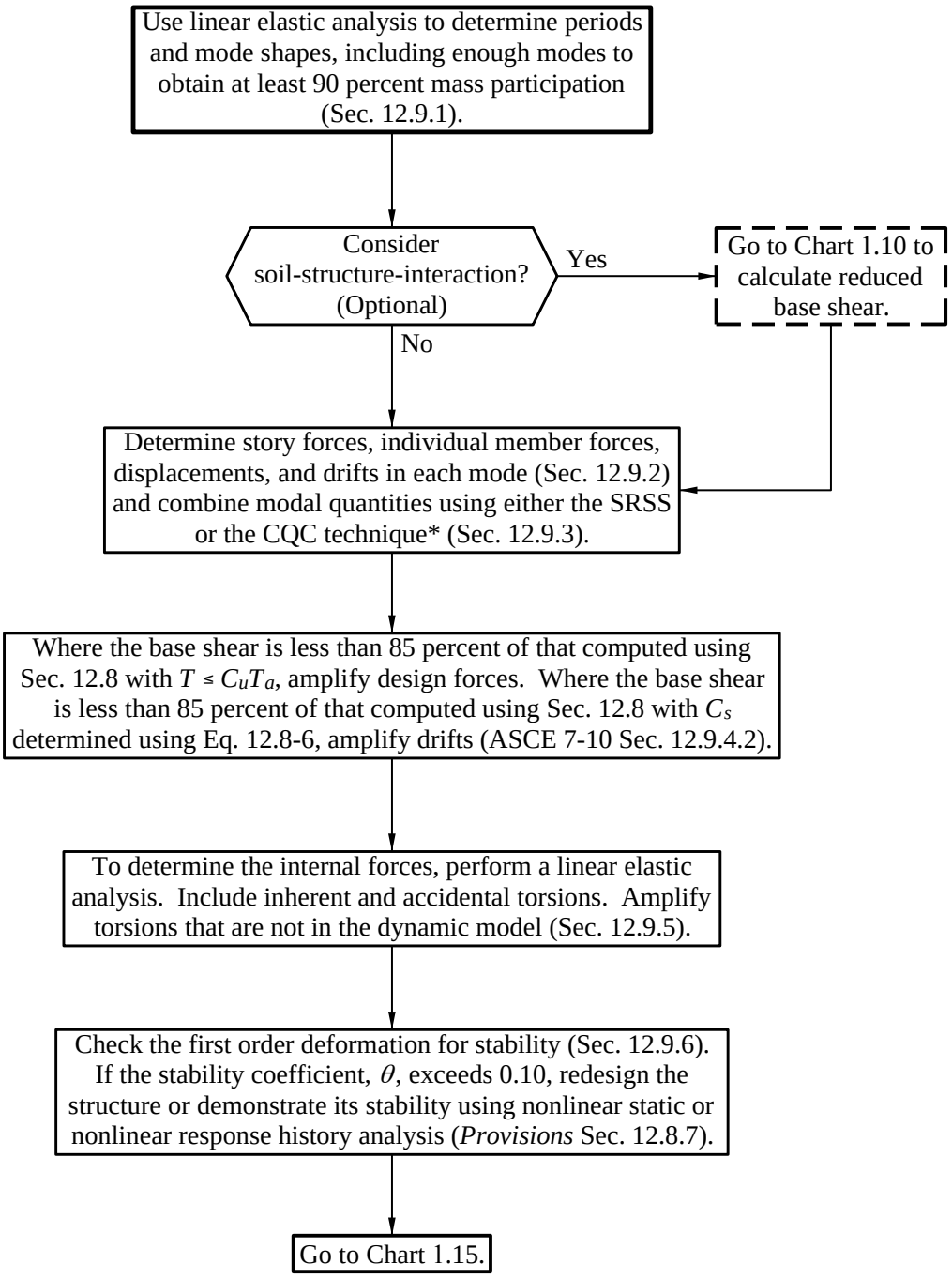

*As indicated in the text, use of the CQC technique is required where closely spaced periods in the translational and torsional modes will result in cross-correlation of the modes.

Chart 1.12
Response History Analysis

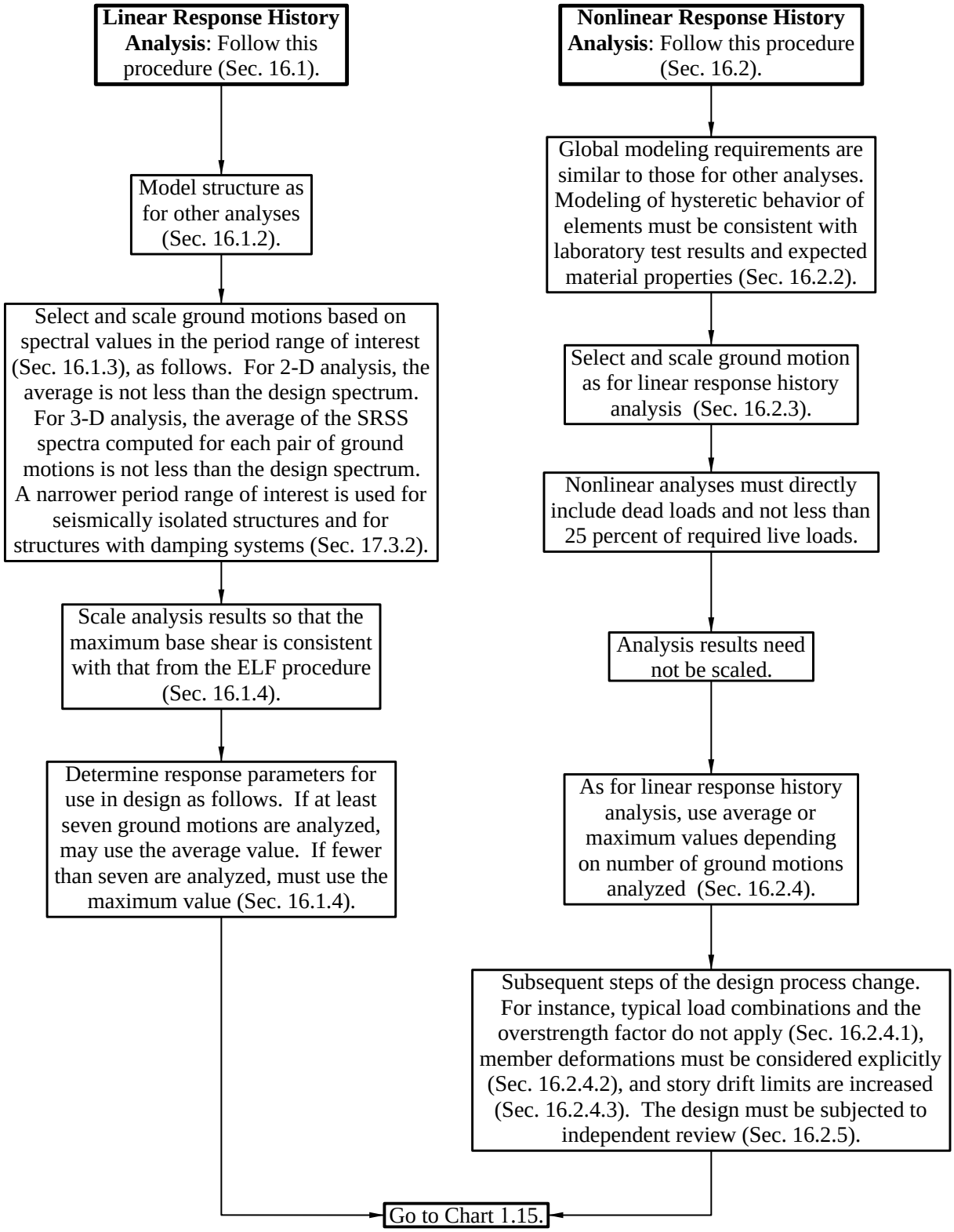

Chart 1.13
Seismically Isolated Structures

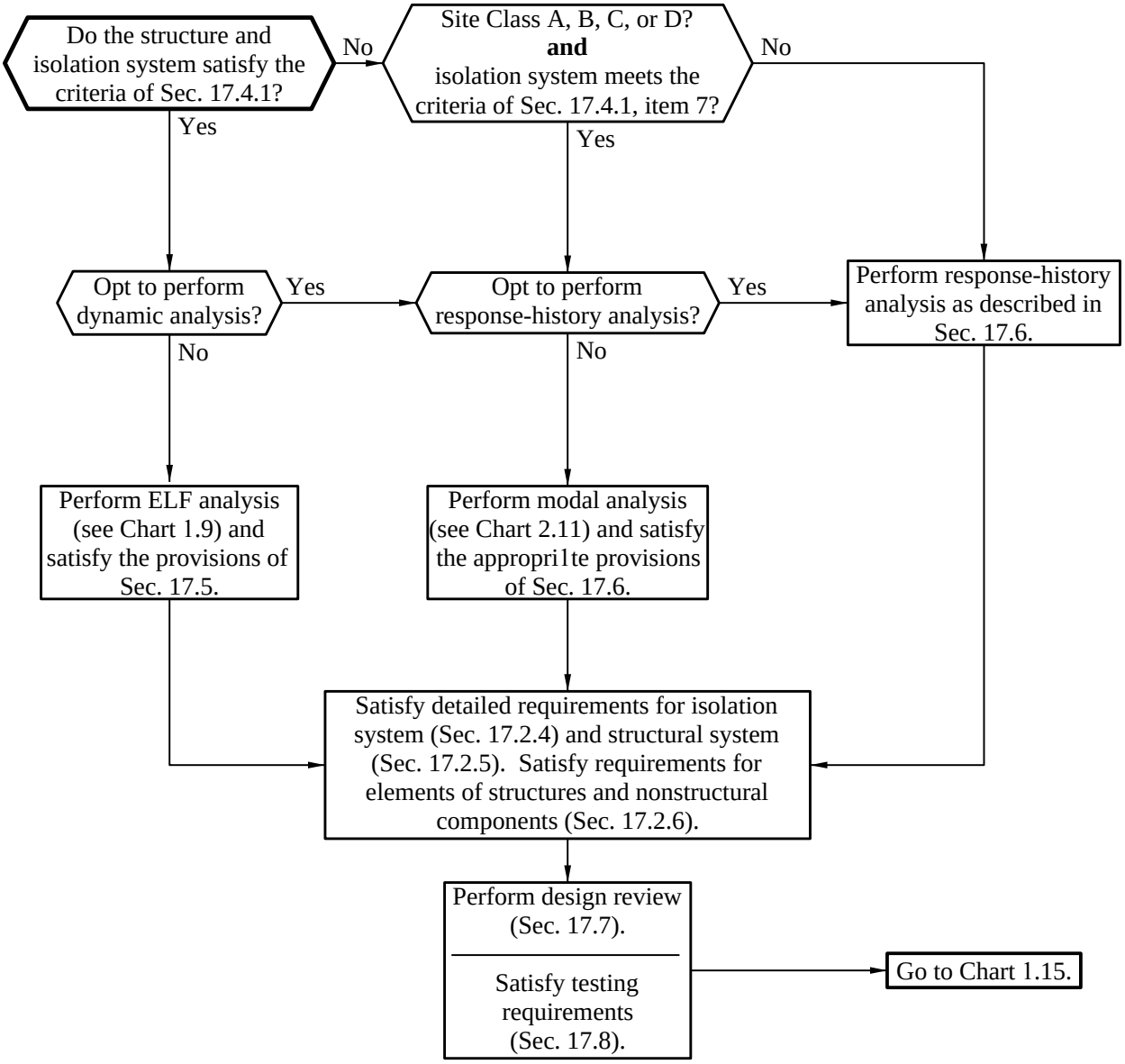

Chart 1.14
Structures with Damping Systems

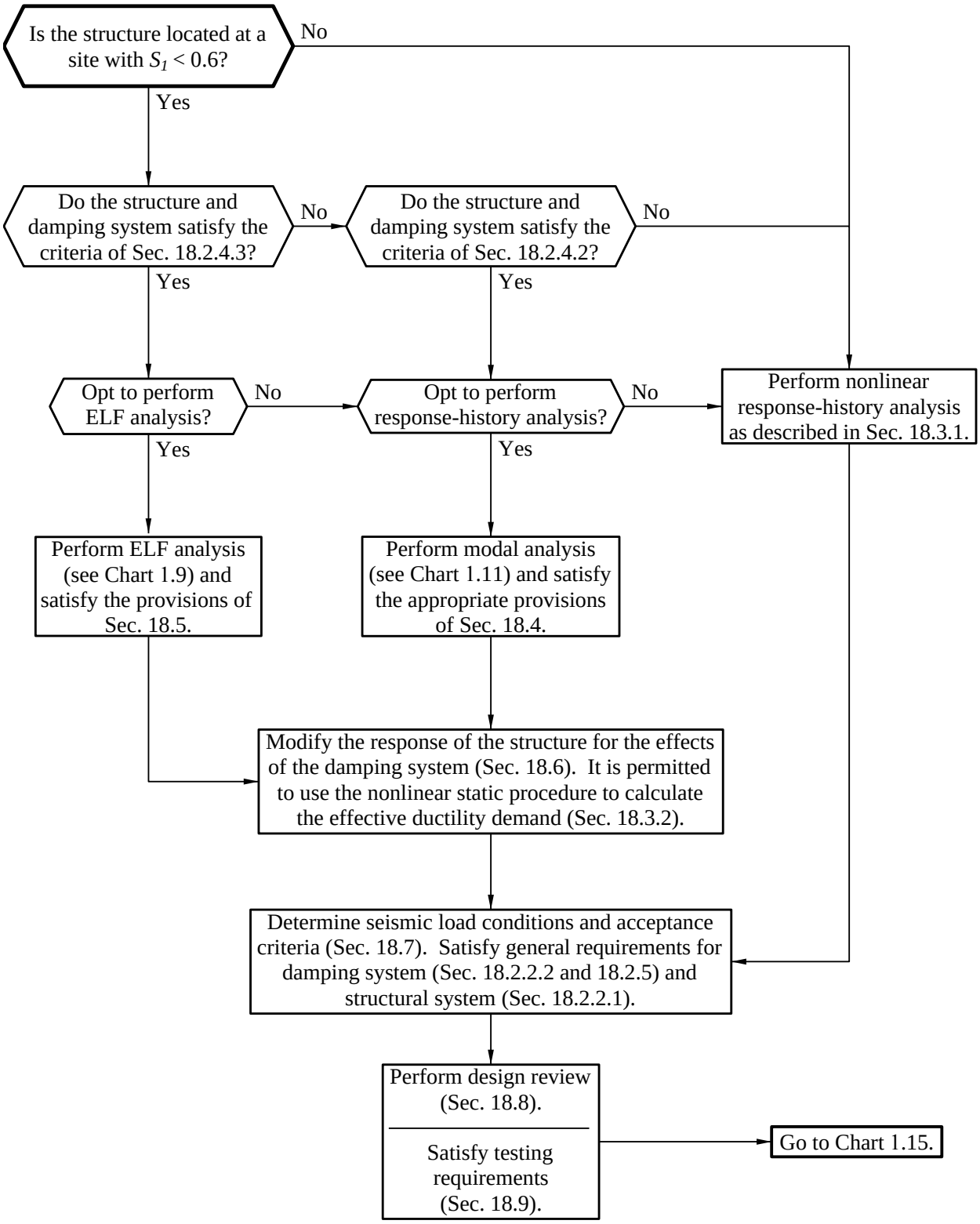

Chart 1.15
Deformation Requirements

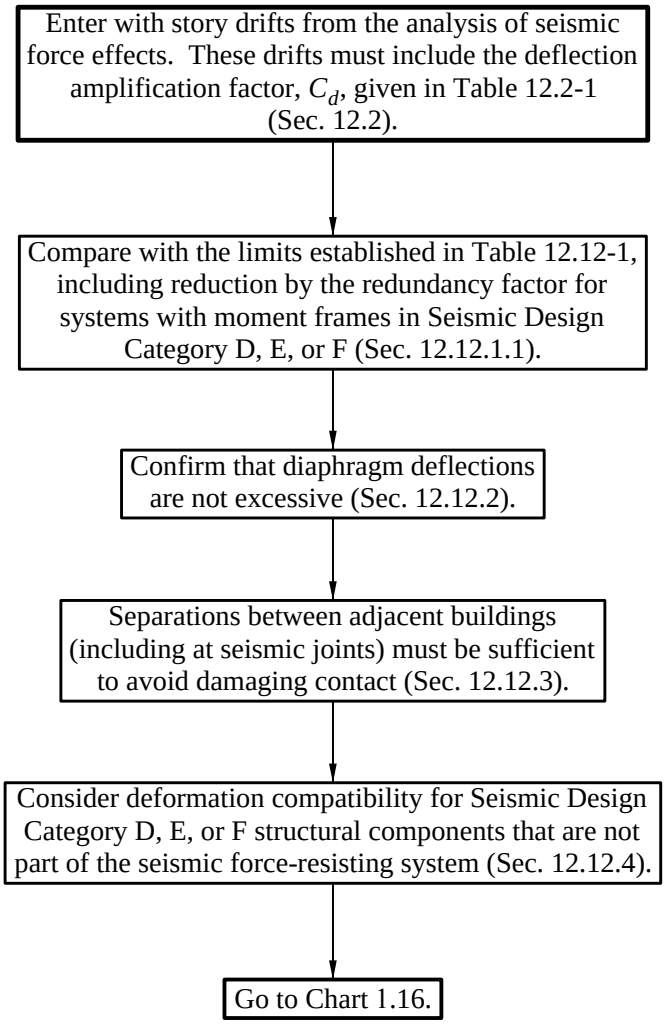

Chart 1.16
Design and Detailing Requirements

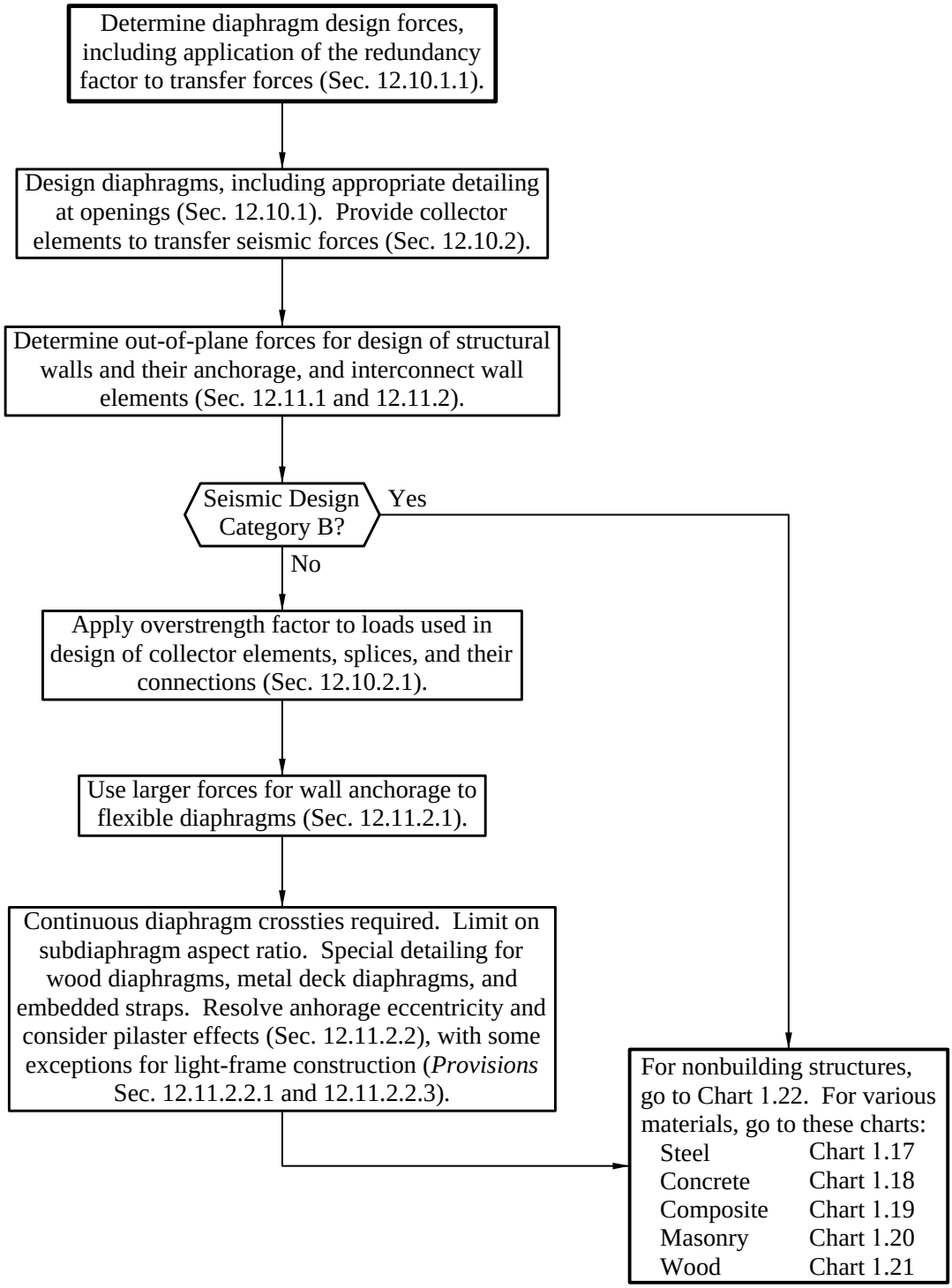

Chart 1.17
Steel Structures

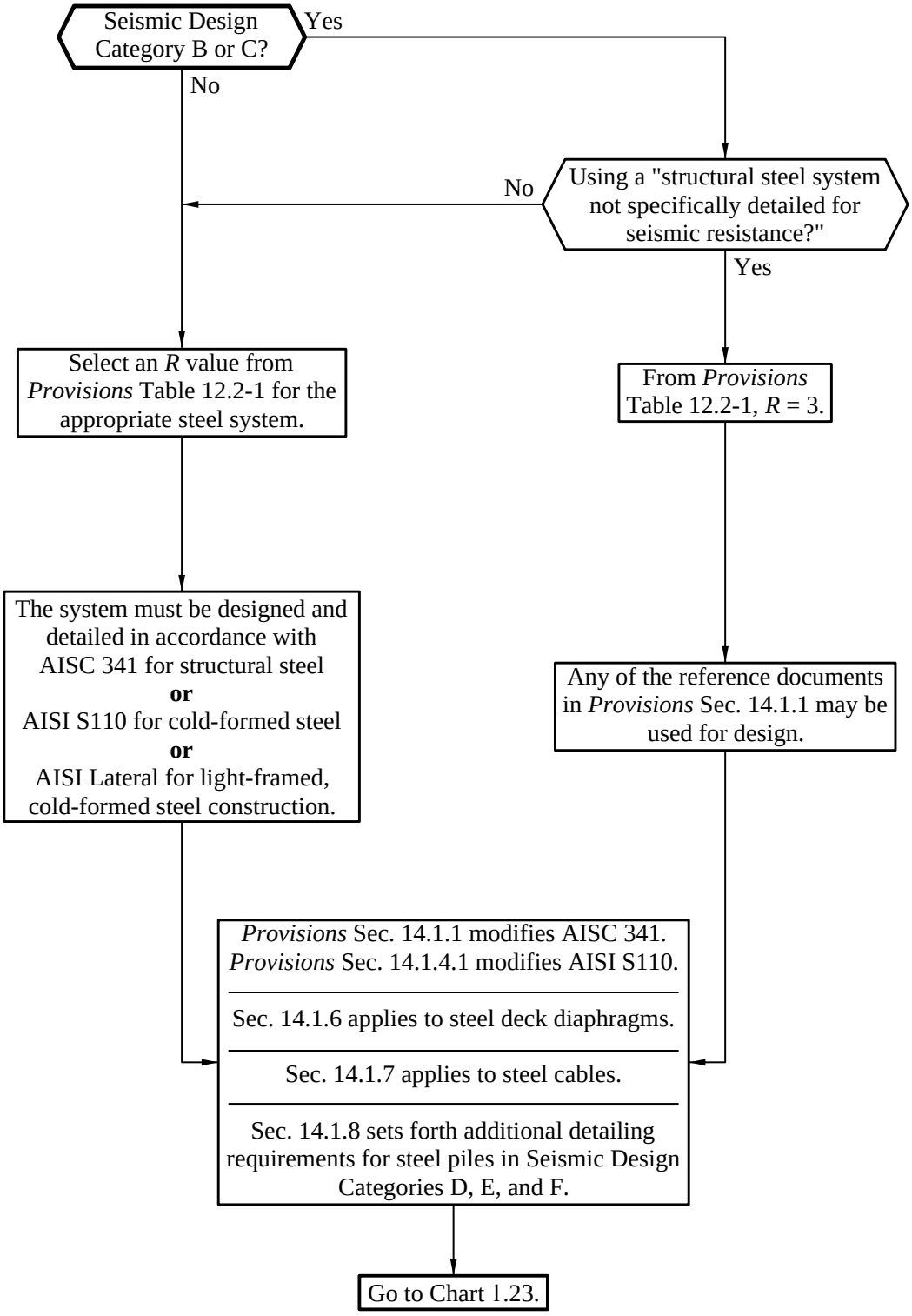

Chart 1.18
Concrete Structures

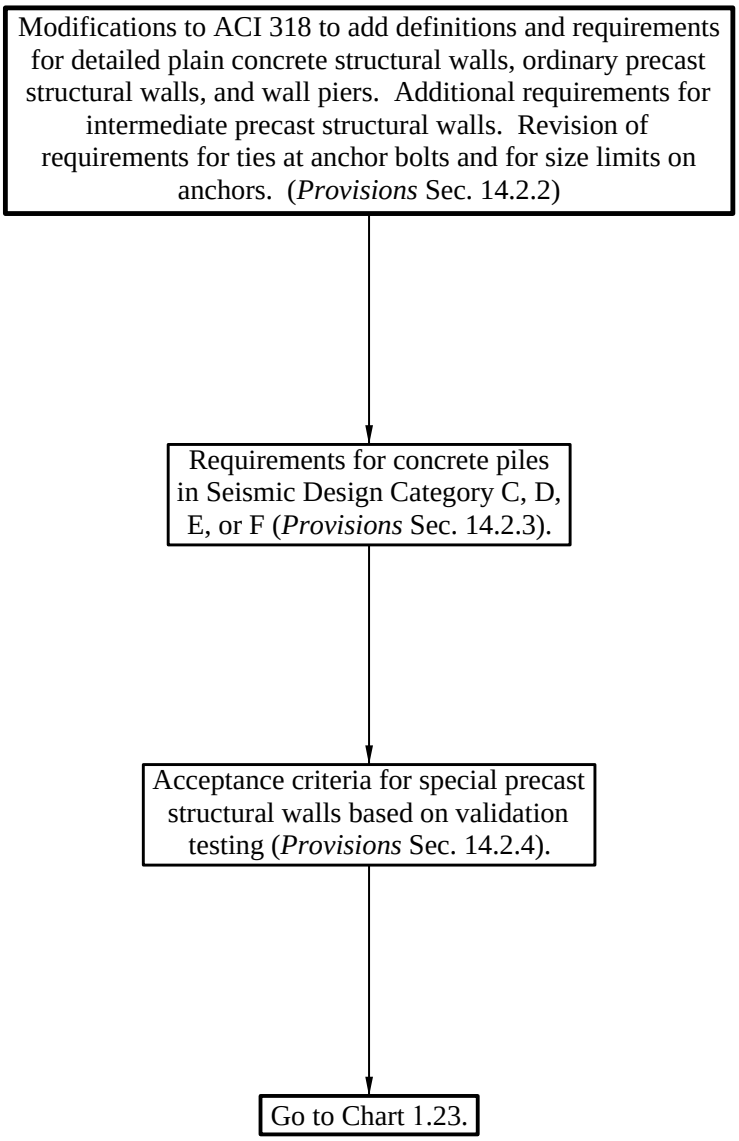

Chart 1.19
Composite Steel and Concrete Structures

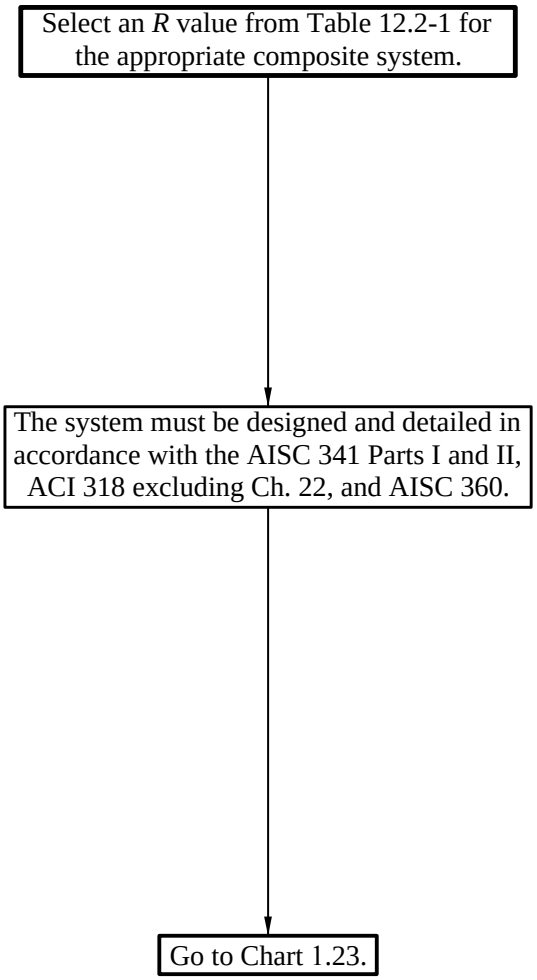

Chart 2.20
Masonry Structures

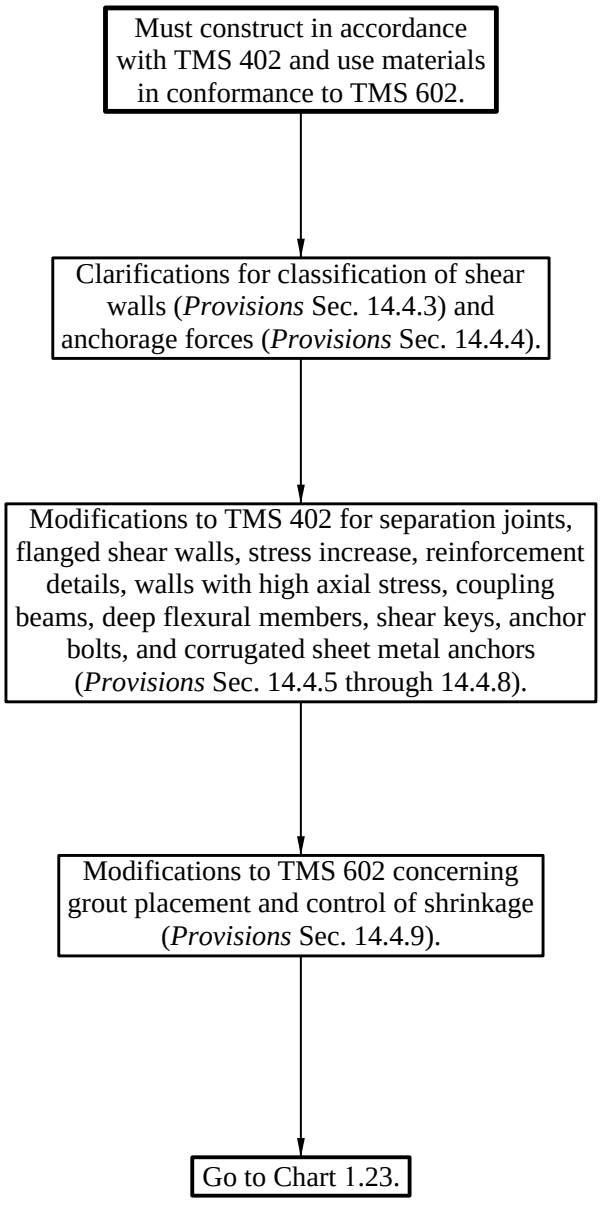

Chart 1.21
Wood Structures

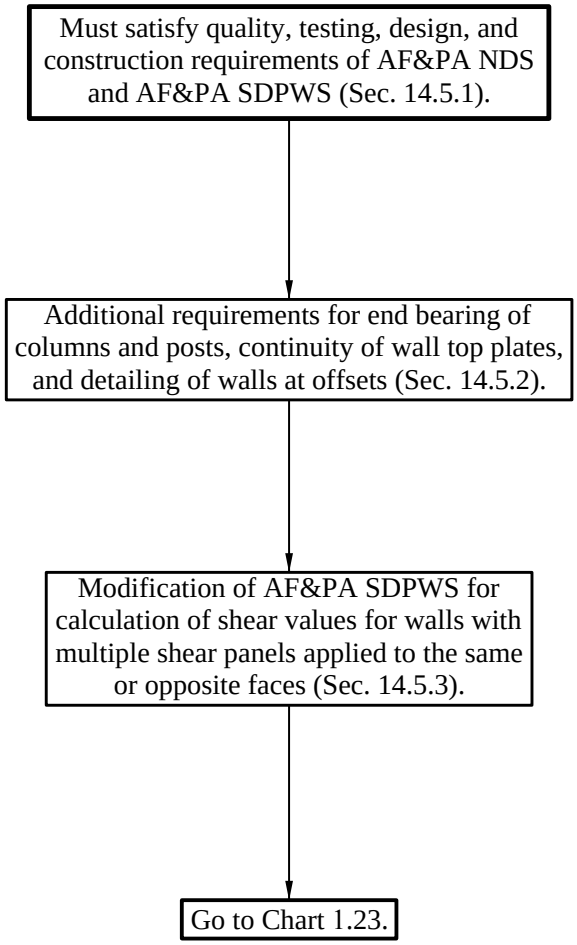

Chart 1.22
Non-building Structures

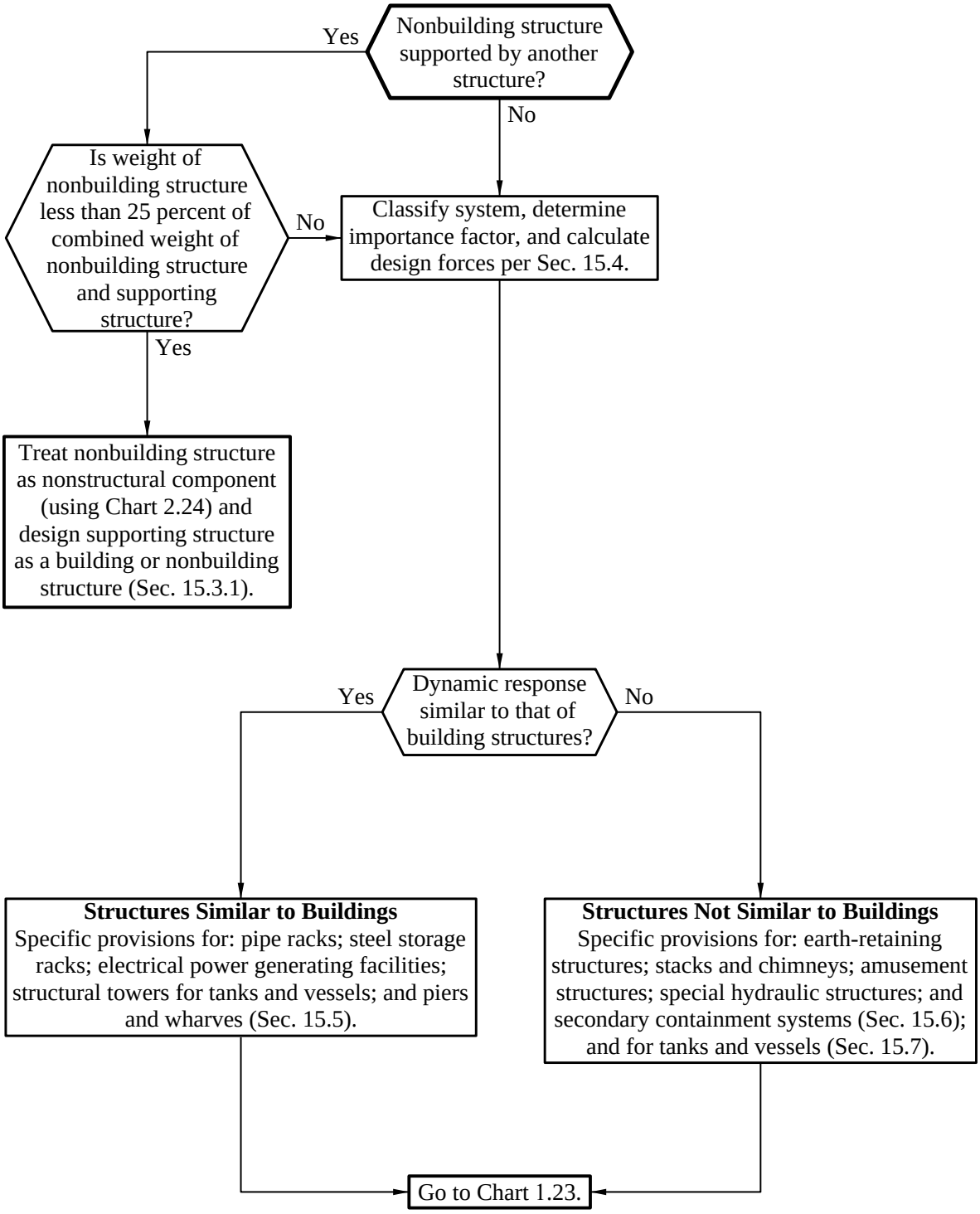

Chart 1.23
Foundations

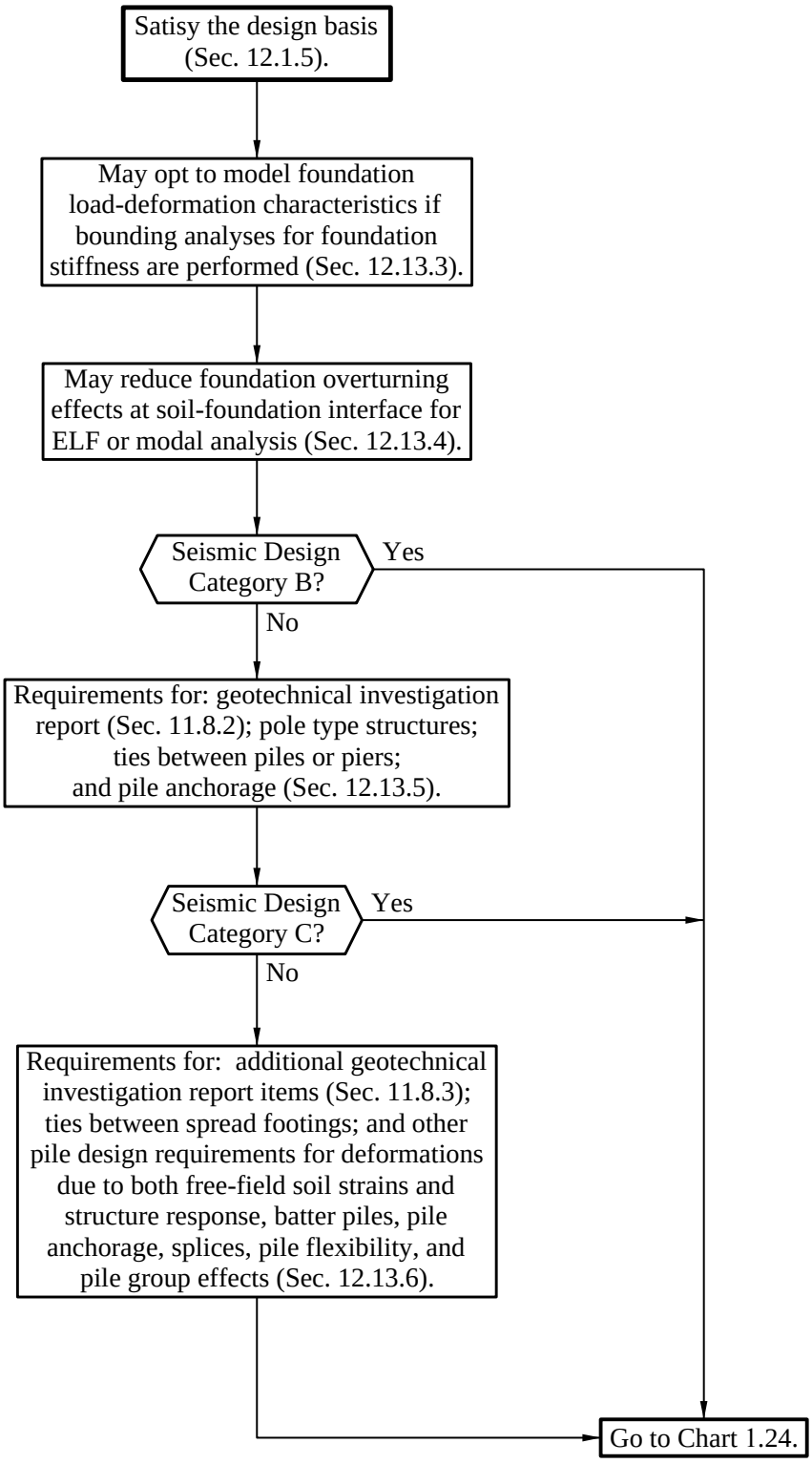

Chart 1.24
Nonstructural Components

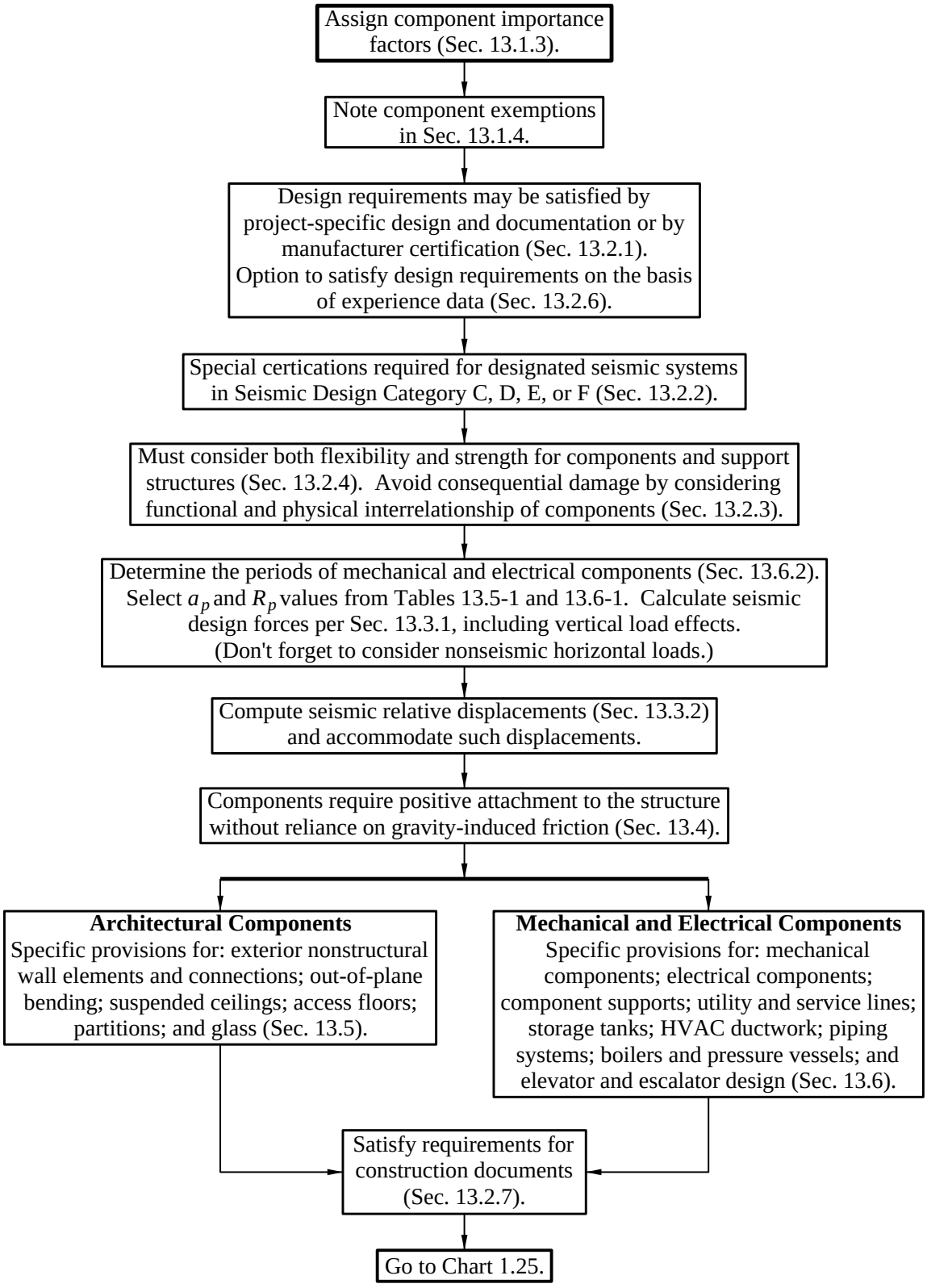

Chart 1.25
Quality Assurance

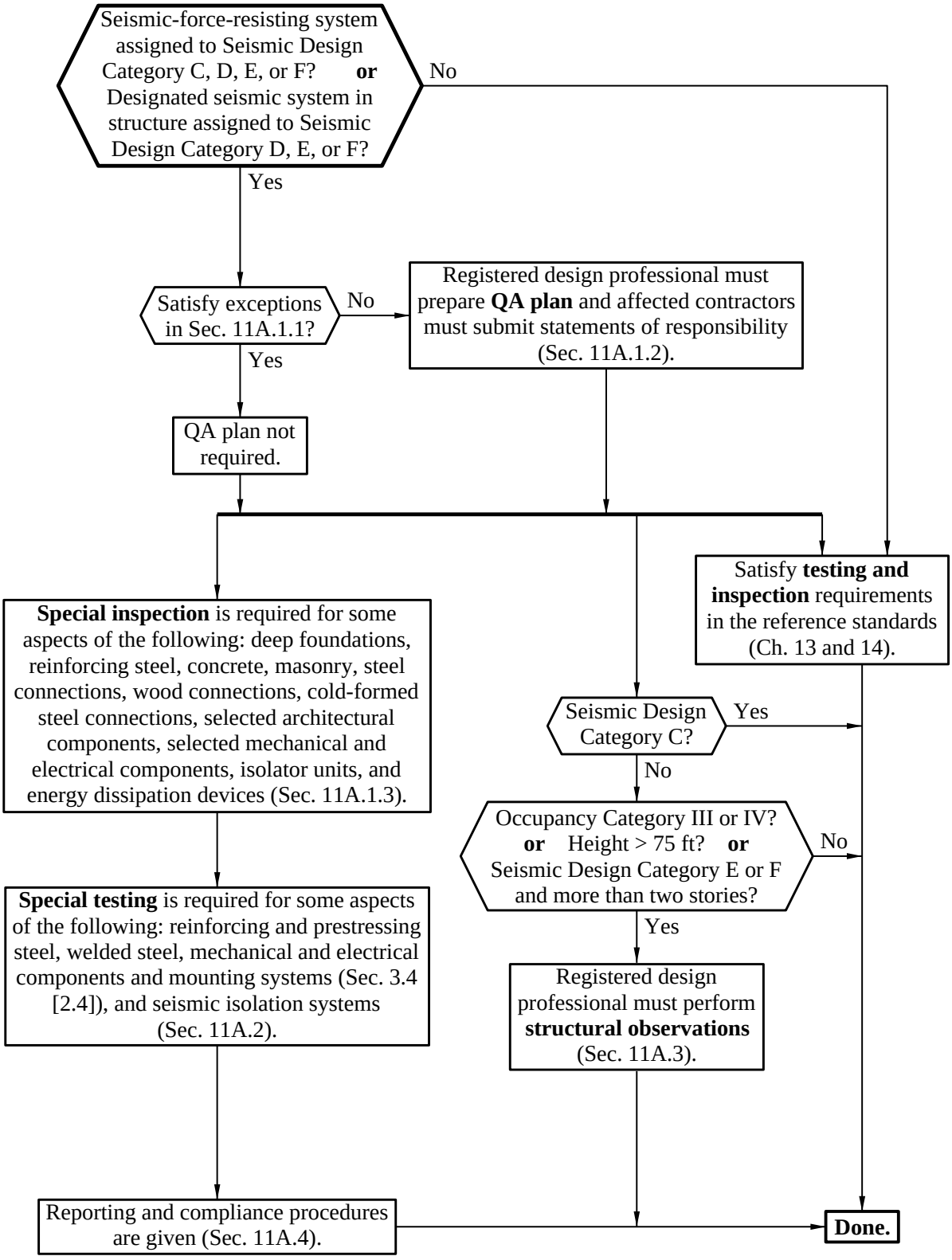

1.5 REFERENCES

American Society of Civil Engineers, 1907, *The Effects of the San Francisco Earthquake of April 18, 1906.*, New York, NY.

American Society of Civil Engineers, 1951, *Proceedings-Separate No. 66.*, New York, NY.

American Society of Civil Engineers, 2010, ASCE 7-10: *Minimum Design Loads for Buildings and Other Structures*, Reston, VA.

Applied Technology Council, 1978, ATC 3-06: *Tentative Provisions for the Development of Seismic Regulations for Buildings*, Redwood City, California.

Building Seismic Safety Council, 2009, 2009 NEHRP Recommended Seismic Provisions for Buildings and Other Structures, prepared for the Federal Emergency Management Agency, Washington, DC.

International Conference of Building Officials, 1927, *Uniform Building Code.* Whittier, CA.

Structural Engineers Association of California, *SEAOC Blue Book: Seismic Design Recommendations*, Sacramento, CA.

2

Fundamentals

James Robert Harris, P.E., PhD

Contents

2.1 EARTHQUAKE PHENOMENA 3
2.2 STRUCTURAL RESPONSE TO GROUND SHAKING 5
2.2.1 Response Spectra 5
2.2.2 Inelastic Response 11
2.2.3 Building Materials 14
2.2.4 Building Systems 16
2.2.5 Supplementary Elements Added to Improve Structural Performance 17
2.3 ENGINEERING PHILOSOPHY 18
2.4 STRUCTURAL ANALYSIS 19
2.5 NONSTRUCTURAL ELEMENTS OF BUILDINGS 22
2.6 QUALITY ASSURANCE 23

In introducing their classic text, *Fundamentals of Earthquake Engineering*, Newmark and Rosenblueth (1971) comment:

> In dealing with earthquakes, we must contend with appreciable probabilities that failure will occur in the near future. Otherwise, all the wealth of the world would prove insufficient to fill our needs: the most modest structures would be fortresses. We must also face uncertainty on a large scale, for it is our task to design engineering systems – about whose pertinent properties we know little – to resist future earthquakes and tidal waves – about whose characteristics we know even less. . . . In a way, earthquake engineering is a cartoon. . . . Earthquake effects on structures systematically bring out the mistakes made in design and construction, even the minutest mistakes.

Several points essential to an understanding of the theories and practices of earthquake-resistant design bear restating:

1. Ordinarily, a large earthquake produces the most severe loading that a building is expected to survive. The probability that ***failure*** will occur is very real and is greater than for other loading phenomena. Also, in the case of earthquakes, the definition of ***failure*** is altered to permit certain types of behavior and damage that are considered unacceptable in relation to the effects of other phenomena.

2. The levels of uncertainty are much greater than those encountered in the design of structures to resist other phenomena. This is in spite of the tremendous strides made since the Federal government began strongly supporting research in earthquake engineering and seismology following the 1964 Prince William Sound and 1971 San Fernando earthquakes. The high uncertainty applies both to knowledge of the loading function and to the resistance properties of the materials, members and systems.

3. The details of construction are very important because flaws of no apparent consequence often will cause systematic and unacceptable damage simply because the earthquake loading is so severe and an extended range of behavior is permitted.

The remainder of this chapter is devoted to a very abbreviated discussion of fundamentals that reflect the concepts on which earthquake-resistant design are based. When appropriate, important aspects of the *NEHRP Recommended Seismic Provisions for New Buildings and Other Structures* are mentioned and reference is made to particularly relevant portions of that document or the standards that are incorporated by reference. The *2009 Provisions* is composed of three parts: 1) “Provisions”, 2) “Commentary on ASCE/SEI 7-2005” and 3) “Resource Papers on Special Topics in Seismic Design”. Part 1 states the intent and then cites ASCE/SEI 7-2005 *Minimum Design Loads for Buildings and Other Structures* as the primary reference. The remainder of Part 1 contains recommended changes to update ASCE/SEI 7-2005; the recommended changes include

commentary on each specific recommendation. All three parts are referred to herein as the *Provisions*, but where pertinent the specific part is referenced and ASCE/SEI 7-2005 is referred to as the *Standard*. ASCE/SEI 7-2005 itself refers to several other standards for the seismic design of structures composed of specific materials and those standards are essential elements to achieve the intent of the *Provisions*.

2.1 EARTHQUAKE PHENOMENA

According to the most widely held scientific belief, most earthquakes occur when two segments of the earth's crust suddenly move in relation to one another. The surface along which movement occurs is known as a fault. The sudden movement releases strain energy and causes seismic waves to propagate through the crust surrounding the fault. These waves cause the surface of the ground to shake violently, and it is this ground shaking that is the principal concern of structural engineering to resist earthquakes.

Earthquakes have many effects in addition to ground shaking. For various reasons, the other effects generally are not major considerations in the design of buildings and similar structures. For example, seismic sea waves or tsunamis can cause very forceful flood waves in coastal regions, and seiches (long-period sloshing) in lakes and inland seas can have similar effects along shorelines. These are outside the scope of the *Provisions*. This is not to say, however, that they should not be considered during site exploration and analysis. Designing structures to resist such hydrodynamic forces is a very specialized topic, and it is common to avoid constructing buildings and similar structures where such phenomena are likely to occur. Long-period sloshing of the liquid contents of tanks is addressed by the *Provisions*.

Abrupt ground displacements occur where a fault intersects the ground surface. (This commonly occurs in California earthquakes but apparently did not occur in the historic Charleston, South Carolina, earthquake or the very large New Madrid, Missouri, earthquakes of the nineteenth century.) Mass soil failures such as landslides, liquefaction and gross settlement are the result of ground shaking on susceptible soil formations. Once again, design for such events is specialized, and it is common to locate structures so that mass soil failures and fault breakage are of no major consequence to their performance. Modification of soil properties to protect against liquefaction is one important exception; large portions of a few metropolitan areas with the potential for significant ground shaking are susceptible to liquefaction. Lifelines that cross faults require special design beyond the scope of the *Provisions*. The structural loads specified in the *Provisions* are based solely on ground shaking; they do not provide for ground failure. Resource Paper 12 ("Evaluation of Geologic Hazards and Determination of Seismic Lateral Earth Pressures") in Part 3 of the *Provisions* includes a description of current procedures for prediction of seismic-induced slope instability, liquefaction and surface fault rupture.

Nearly all large earthquakes are *tectonic* in origin – that is, they are associated with movements of and strains in large segments of the earth's crust, called *plates*, and virtually all such earthquakes occur at or near the boundaries of these plates. This is the

case with earthquakes in the far western portion of the United States where two very large plates, the North American continent and the Pacific basin, come together. In the central and eastern United States, however, earthquakes are not associated with such a plate boundary, and their causes are not as completely understood. This factor, combined with the smaller amount of data about central and eastern earthquakes (because of their infrequency), means that the uncertainty associated with earthquake loadings is higher in the central and eastern portions of the nation than in the West. Even in the West, the uncertainty (when considered as a fraction of the predicted level) about the hazard level is probably greater in areas where the mapped hazard is low than in areas where the mapped hazard is high.

The amplitude of earthquake ground shaking diminishes with distance from the source, and the rate of attenuation is less for lower frequencies of motion than for higher frequencies. This effect is captured, to an extent, by the fact that the *Provisions* use three parameters to define the hazard of seismic ground shaking for structures. Two are based on statistical analysis of the database of seismological information: the S_S values are pertinent for higher frequency motion, and the S_1 values are pertinent for other middle frequencies. The third value, T_L, defines an important transition point for long period (low frequency) behavior; it is not based upon as robust an analysis as the other two parameters.

Two basic data sources are used in establishing the likelihood of earthquake ground shaking, or seismicity, at a given location. The first is the historical record of earthquake effects and the second is the geological record of earthquake effects. Given the infrequency of major earthquakes, there is no place in the United States where the historical record is long enough to be used as a reliable basis for earthquake prediction – certainly not as reliable as with other phenomena such as wind and snow. Even on the eastern seaboard, the historical record is too short to justify sole reliance on the historical record. Thus, the geological record is essential. Such data require very careful interpretation, but they are used widely to improve knowledge of seismicity. Geological data have been developed for many locations as part of the nuclear power plant design process. On the whole, there is more geological data available for the far western United States than for other regions of the country. Both sets of data have been taken into account in the *Provisions* seismic ground shaking maps.

The *Commentary* provides a more thorough discussion of the development of the maps, their probabilistic basis, the necessarily crude lumping of parameters and other related issues. Prior to its 1997 edition, the basis of the *Provisions* was to "provide *life safety* at the design earthquake motion," which was defined as having a 10 percent probability of being exceeded in a 50-year reference period. As of the 1997 edition, the basis became to "avoid *structural collapse* at the maximum considered earthquake (MCE) ground motion," which is defined as having a 2 percent probability of being exceeded in a 50-year reference period. In the 2009 edition of the *Provisions* the design basis has been refined to target a 1% probability of structural collapse for ordinary buildings in a 50 year period. The MCE ground motion has been adjusted to deliver this level of risk combined with a 10% probability of collapse should the MCE ground motion occur. This new

approach incorporates a fuller consideration of the nature of the seismic hazard at a location than was possible with the earlier definitions of ground shaking hazard, which were tied to a single level of probability of ground shaking occurrence.

2.2 STRUCTURAL RESPONSE TO GROUND SHAKING

The first important difference between structural response to an earthquake and response to most other loadings is that the earthquake response is *dynamic*, not *static*. For most structures, even the response to wind is essentially static. Forces within the structure are due almost entirely to the pressure loading rather than the acceleration of the mass of the structure. But with earthquake ground shaking, the aboveground portion of a structure is not subjected to any applied force. The stresses and strains within the superstructure are created entirely by its dynamic response to the movement of its base, the ground. Even though the most used design procedure resorts to the use of a concept called the equivalent static force for actual calculations, some knowledge of the theory of vibrations of structures is essential.

2.2.1 Response Spectra

Figure 2.2-1 shows accelerograms, records of the acceleration at one point along one axis, for several representative earthquakes. Note the erratic nature of the ground shaking and the different characteristics of the different accelerograms. Precise analysis of the elastic response of an ideal structure to such a pattern of ground motion is possible; however, it is not commonly done for ordinary structures. The increasing power and declining cost of computational aids are making such analyses more common but, at this time, only a small minority of structures designed across the country, are analyzed for specific response to a specific ground motion.

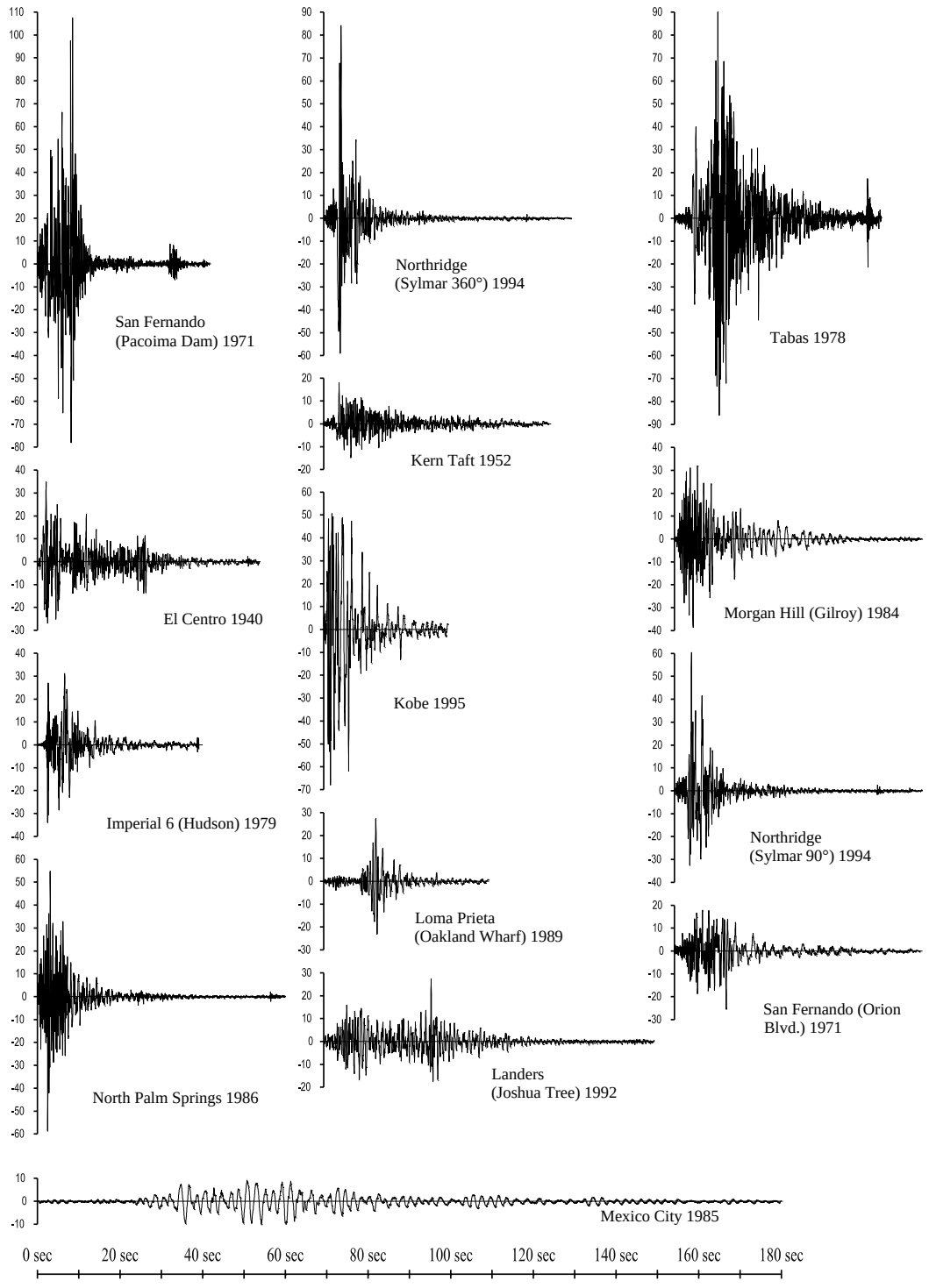

Figure 2.2-1 Earthquake Ground Acceleration in Epicentral Regions (all accelerograms are plotted to the same scale for time and acceleration – the vertical axis is % gravity). Great earthquakes extend for much longer periods of time.

Figure 2.2-2 shows further detail developed from an accelerogram. Part (a) shows the ground acceleration along with the ground velocity and ground displacement derived from it. Part (b) shows the acceleration, velocity and displacement for the same event at

the roof of the building located where the ground motion was recorded. Note that the peak values are larger in the diagrams of Figure 2.2-2(b) (the vertical scales are essentially the same). This increase in response of the structure at the roof level over the motion of the ground itself is known as dynamic amplification. It depends very much on the vibrational characteristics of the structure and the characteristic frequencies of the ground shaking at the site.

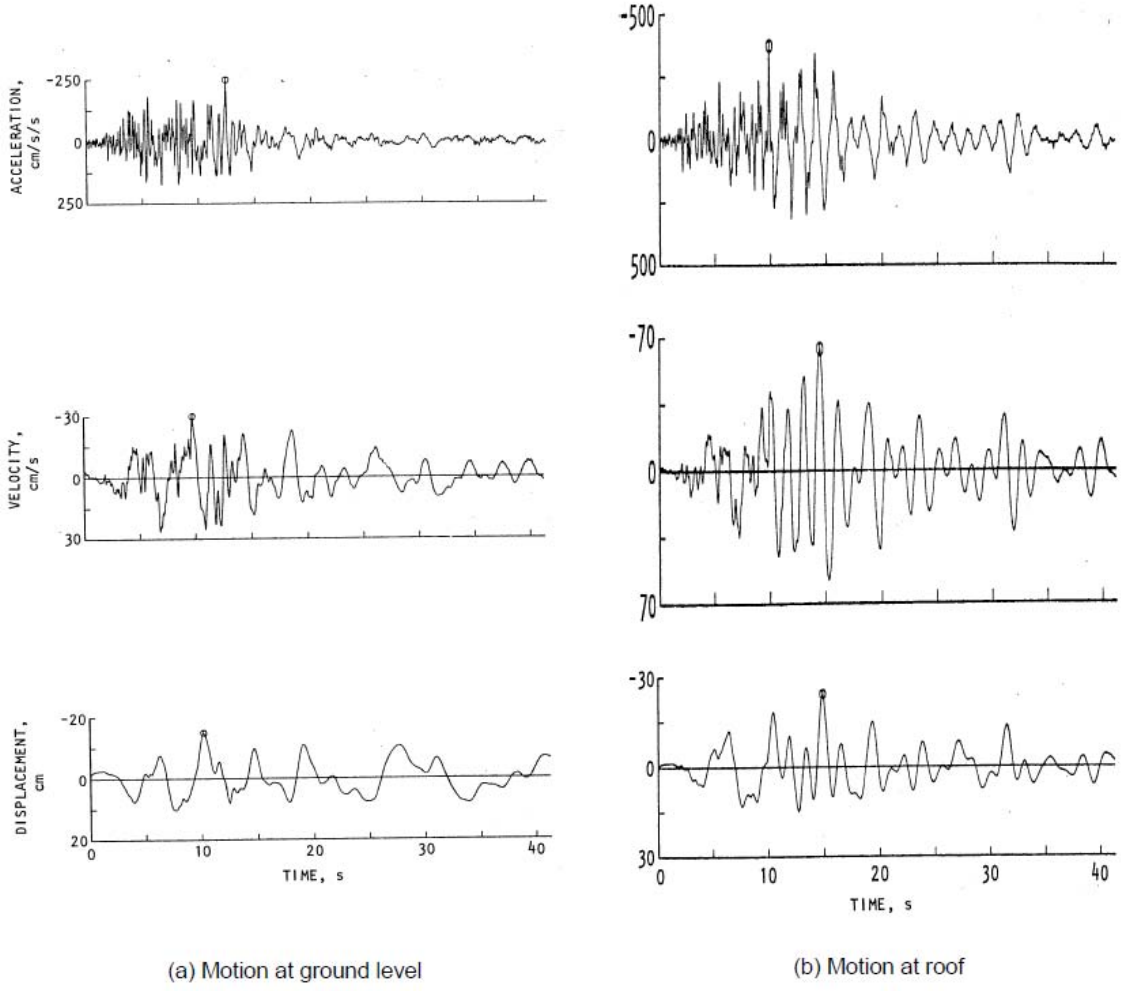

Figure 2.2-2 Holiday Inn Ground and Building Roof Motion During the M6.4 1971 San Fernando Earthquake: (a) north-south ground acceleration, velocity and displacement and (b) north-south roof acceleration, velocity and displacement (Housner and Jennings, 1982). The Holiday Inn, a 7-story, reinforced concrete frame building, was approximately 5 miles from the closest portion of the causative fault. The recorded building motions enabled an analysis to be made of the stresses and strains in the structure during the earthquake.

In design, the response of a specific structure to an earthquake is ordinarily estimated from a design response spectrum such as is specified in the *Provisions*. The first step in creating a design response spectrum is to determine the maximum response of a given structure to a specific ground motion (see Figure 2.2-2). The underlying theory is based entirely on the response of a single-degree-of-freedom oscillator such as a simple one-story frame with the mass concentrated at the roof. The vibrational characteristics of

such a simple oscillator may be reduced to two: the natural period[1] and the amount of damping. By recalculating the record of response versus time to a specific ground motion for a wide range of natural periods and for each of a set of common amounts of damping, the family of response spectra for one ground motion may be determined. It is simply the plot of the maximum value of response for each combination of period and damping.

Figure 2.2-3 shows such a result for the ground motion of Figure 2.2-2(a) and illustrates that the erratic nature of ground shaking leads to a response that is very erratic in that a slight change in the natural period of vibration brings about a very large change in response. The figure also illustrates the significance of damping. Different earthquake ground motions lead to response spectra with peaks and valleys at different points with respect to the natural period. Thus, computing response spectra for several different ground motions and then averaging them, based on some normalization for different amplitudes of shaking, will lead to a smoother set of spectra. Such smoothed spectra are an important step in developing a design spectrum.

[1] Much of the literature on dynamic response is written in terms of frequency rather than period. The cyclic frequency (cycles per second, or Hz) is the inverse of period. Mathematically it is often convenient to use the angular frequency expressed as radians per second rather than Hz. The conventional symbols used in earthquake engineering for these quantities are $\boldsymbol{T}$ for period (seconds per cycle), $\boldsymbol{f}$ for cyclic frequency (Hz) and $\boldsymbol{\omega}$ for angular frequency (radians per second). The word frequency is often used with no modifier; be careful with the units.

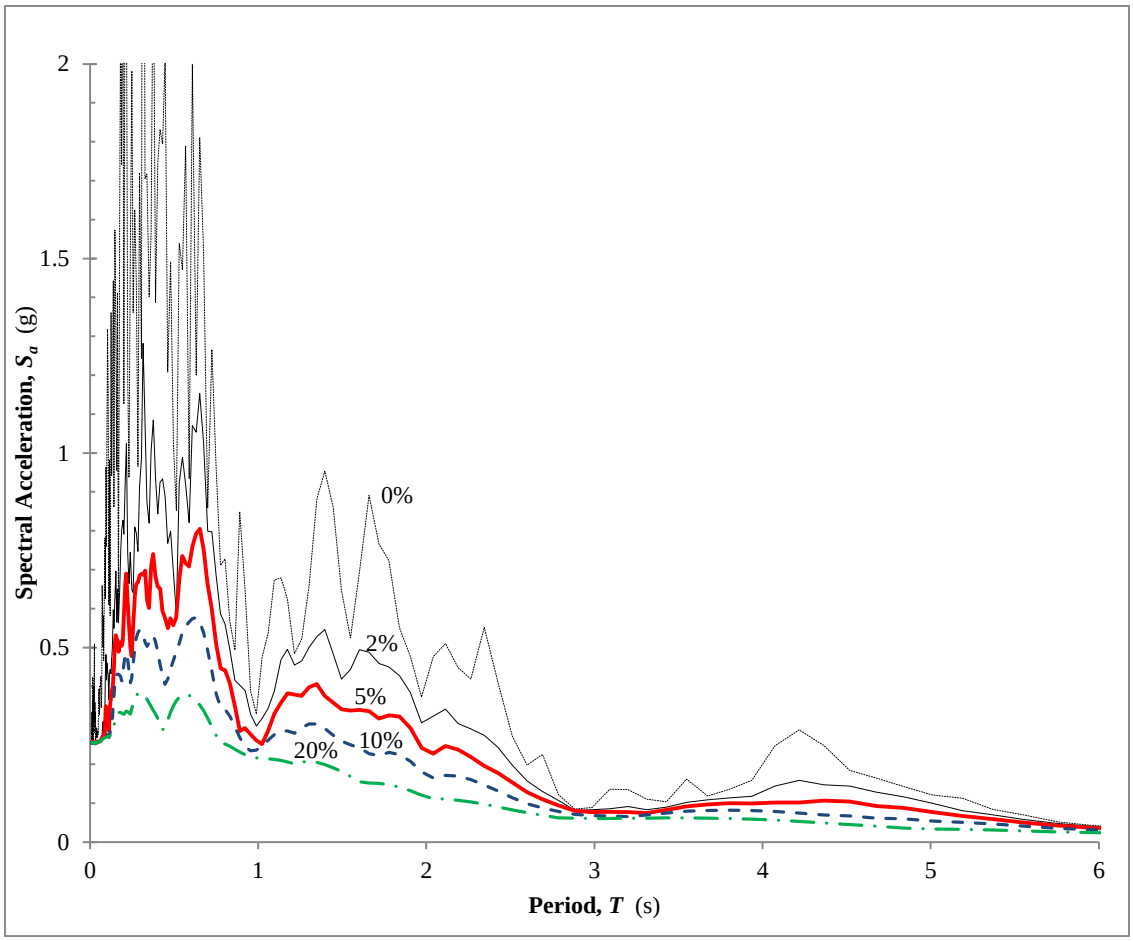

Figure 2.2-3 Response spectrum of north-south ground acceleration (0%, 2%, 5%, 10%, 20% of critical damping) recorded at the Holiday Inn, approximately 5 miles from the causative fault in the 1971 San Fernando earthquake.

Figure 2.2-4 is an example of an averaged spectrum. Note that acceleration, velocity, or displacement may be obtained from Figure 2.2-3 or 1.2-4 for a structure with known period and damping.

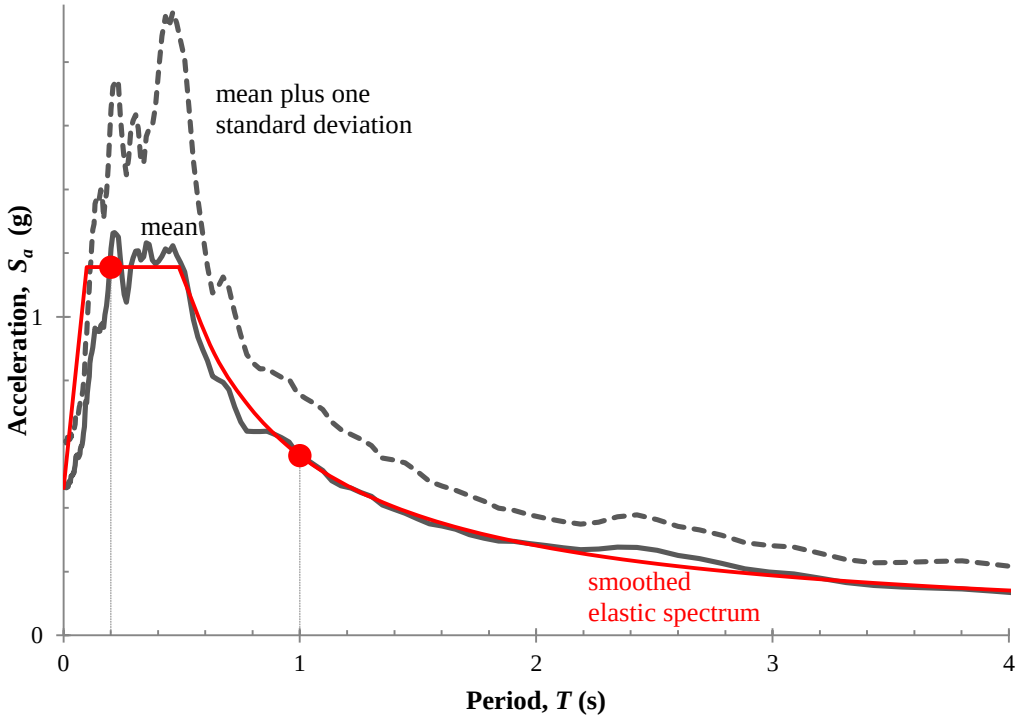

Figure 2.2-4 Averaged Spectrum(In this case, the statistics are for seven ground motions representative of the de-aggregated hazard at a particular site.)

Prior to the 1997 edition of the *Provisions*, the maps that characterized the ground shaking hazard were plotted in terms of peak ground acceleration (at period, T, = 0), and design response spectra were created using expressions that amplified (or de-amplified) the ground acceleration as a function of period and damping. With the introduction of the new maps in the 1997 edition, this procedure changed. Now the maps present spectral response accelerations at two periods of vibration, 0.2 and 1.0 second, and the design response spectrum is computed more directly, as implied by the smooth line in Figure 2.2-4. This has removed a portion of the uncertainty in predicting response accelerations.

Few structures are so simple as to actually vibrate as a single-degree-of-freedom system. The principles of dynamic modal analysis, however, allow a reasonable approximation of the maximum response of a multi-degree-of-freedom oscillator, such as a multistory building, if many specific conditions are met. The procedure involves dividing the total response into a number of natural modes, modeling each mode as an equivalent single-degree-of-freedom oscillator, determining the maximum response for each mode from a single-degree-of-freedom response spectrum and then estimating the maximum total response by statistically summing the responses of the individual modes. The *Provisions* does not require consideration of all possible modes of vibration for most buildings because the contribution of the higher modes (lower periods) to the total response is relatively minor.

The soil at a site has a significant effect on the characteristics of the ground motion and, therefore, on the structure's response. Especially at low amplitudes of motion and at longer periods of vibration, soft soils amplify the motion at the surface with respect to

bedrock motions. This amplification is diminished somewhat, especially at shorter periods as the amplitude of basic ground motion increases, due to yielding in the soil. The *Provisions* accounts for this effect by providing amplifiers that are to be applied to the 0.2 and 1.0 second spectral accelerations for various classes of soils. (The ground motion maps in the *Provisions* are drawn for sites on rock.) Thus, very different design response spectra are specified depending on the type of soil(s) beneath the structure. The *Commentary* (Part 2) contains a thorough explanation of this feature.

2.2.2 Inelastic Response

The preceding discussion assumes elastic behavior of the structure. The principal extension beyond ordinary behavior referenced at the beginning of this chapter is that structures are permitted to strain beyond the elastic limit in responding to earthquake ground shaking. This is dramatically different from the case of design for other types of loads in which stresses and therefore strains, are not permitted to approach the elastic limit. The reason is economic. Figure 2.2-3 shows a peak acceleration response of about 1.0 g (the acceleration due to gravity) for a structure with moderately low damping – for only a moderately large earthquake! Even structures that resist lateral forces well will have a static lateral strength of only 20 to 40 percent of gravity.

The dynamic nature of earthquake ground shaking means that a large portion of the shaking energy can be dissipated by inelastic deformations if the structure is ductile and some damage to the structure is accepted. Figure 2.2-5 will be used to illustrate the significant difference between wind and seismic effects. Figure 2.2-5(1) would represent a cantilever beam if the load W were small and a column if W were large. Wind pressures create a force on the structure, which in turn produces a displacement. The force is the independent variable and the displacement is the dependent result. Earthquake ground motion creates displacement between the base and the mass, which in turn produces an internal force. The displacement is the independent variable, and the force is the dependent result. Two graphs are plotted with the independent variables on the horizontal axis and the dependent response on the vertical axis. Thus, part (b) of the figure is characteristic of the response to forces such as wind pressure (or gravity weight), while part (c) is characteristic of induced displacements such as earthquake ground shaking (or foundation settlement).

Note that the ultimate resistance (H_u) in a force-controlled system is marginally larger than the yield resistance (H_y), while the ultimate displacement (Δ_u) in a displacement-controlled system is much larger than the yield displacement (Δ_y). The point being made with the figures is that ductile structures have the ability to resist displacements much larger than those that first cause yield.

The degree to which a member or structure may deform beyond the elastic limit is referred to as ductility. Different materials and different arrangements of structural members lead to different ductilities. Response spectra may be calculated for oscillators with different levels of ductility. At the risk of gross oversimplification, the following conclusions may be drawn:

1. For structures with very long natural periods, the acceleration response is reduced by a factor equivalent to the ductility ratio (the ratio of maximum usable displacement to effective yield displacement – note that this is displacement and not strain).

2. For structures with very short natural periods, the acceleration response of the ductile structure is essentially the same as that of the elastic structure, but the displacement is increased.

3. For intermediate periods (which applies to nearly all buildings), the acceleration response is reduced, but the displacement response is generally about the same for the ductile structure as for the elastic structure strong enough to respond without yielding.

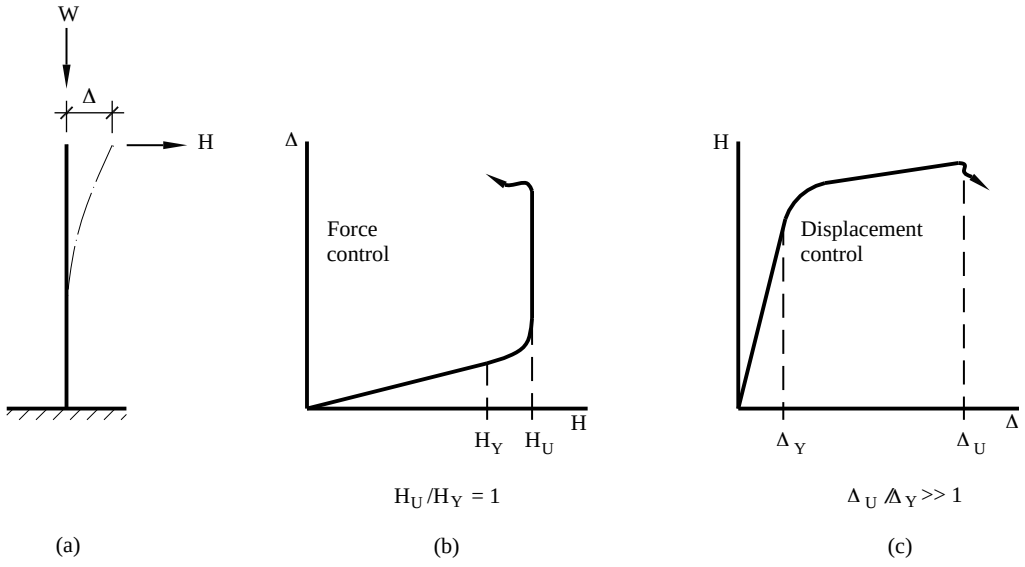

Figure 2.2-5 Force Controlled Resistance Versus Displacement Controlled Resistance (after Housner and Jennings 1982). In part (b) the force *H* is the independent variable. As *H* is increased, the displacement increases until the yield point stress is reached. If *H* is given an additional increment (about 15 percent) a plastic hinge forms, giving large displacements. For this kind of system, the force producing the yield point stress is close to the force producing collapse. The ductility does not produce a large increase in load capacity, although in highly redundant structures the increase is more than illustrated for this very simple structure. In part (c) the displacement is the independent variable. As the displacement is increased, the base moment increases until the yield point is reached. As the displacement increases still more, the resistance (*H*) increases only a small amount. For a highly ductile element, the displacement can be increased 10 to 20 times the yield point displacement before the system collapses under the weight *W*. (As *W* increases, this ductility is decreased dramatically.) During an earthquake, the oscillator is excited into vibrations by the ground motion and it behaves essentially as a displacement-controlled system and can survive displacements much beyond the yield point. This explains why ductile structures can survive ground shaking that produces displacements much greater than yield point displacement.

Inelastic response is quite complex. Earthquake ground motions involve a significant number of reversals and repetitions of the strains. Therefore, observation of the inelastic

properties of a material, member, or system under a monotonically increasing load until failure can be very misleading. Cycling the deformation can cause degradation of strength, stiffness, or both. Systems that have a proven capacity to maintain a stable resistance to a large number of cycles of inelastic deformation are allowed to exercise a greater portion of their ultimate ductility in designing for earthquake resistance. This property is often referred to as toughness, but this is not the same as the classic definition used in mechanics of materials.

Most structures are designed for seismic response using a linear elastic analysis with the strength of the structure limited by the strength at its critical location. Most structures possess enough complexity so that the peak strength of a ductile structure is not accurately captured by such an analysis. Figure 2.2-6 shows the load versus displacement relation for a simple frame. Yield must develop at four locations before the peak resistance is achieved. The margin from the first yield to the peak strength is referred to as overstrength, and it plays a significant role in resisting strong ground motion. Note that a few key design standards (for example, American Concrete Institute (ACI) 318 for the design of concrete structures) do allow for some redistribution of internal forces from the critical locations based upon ductility; however, the redistributions allowed therein are minor compared to what occurs in response to strong ground motion.

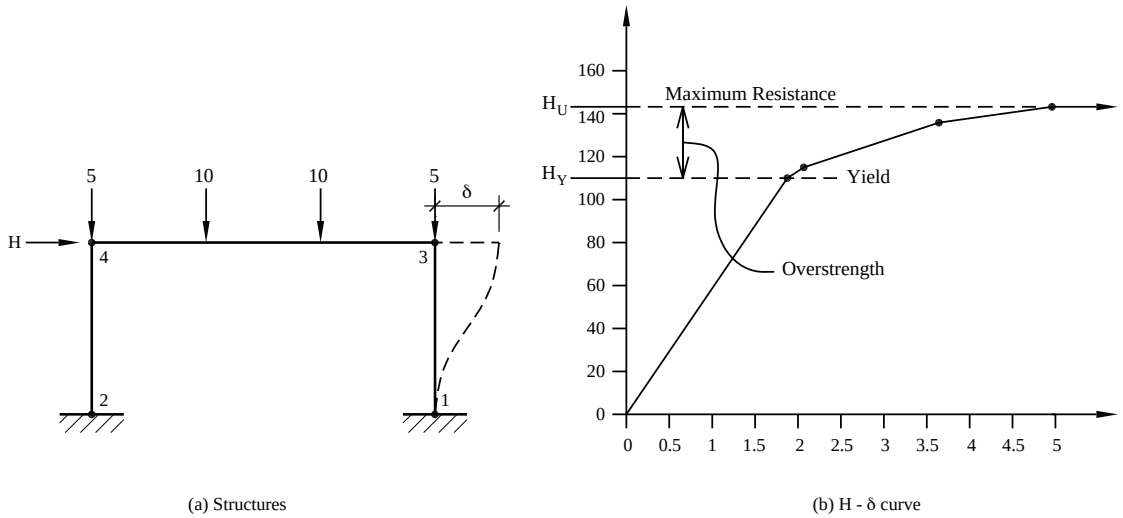

Figure 2.2-6 Initial Yield Load and Failure for a Ductile Portal Frame
(The margin from initial yield to failure (mechanism in this case) is known as overstrength.)

To summarize, the characteristics important in determining a building's seismic response are natural period, damping, ductility, stability of resistance under repeated reversals of inelastic deformation and overstrength. The natural frequency is dependent on the mass and stiffness of the building. Using the *Provisions* the designer calculates, or at least approximates, the natural period of vibration (the inverse of natural frequency). Damping, ductility, toughness and overstrength depend primarily on the type of building system, but not the building's size or shape. Three coefficients – R, C_d and Ω_0 – are

provided to encompass damping, ductility, stability of resistance and overstrength. R is intended to be a conservatively low estimate of the reduction of acceleration response in a ductile system from that for an elastic oscillator with a certain level of damping. It is used to compute a required strength. Computations of displacement based upon ground motion reduced by the factor R will underestimate the actual displacements. C_d is intended to be a reasonable mean for the amplification necessary to convert the elastic displacement response computed for the reduced ground motion to actual displacements. Ω_0 is intended to deliver a reasonably high estimate of the peak force that would develop in the structure. Sets of R, C_d and Ω_0 are specified in the *Provisions* for the most common structural materials and systems.

2.2.3 Building Materials

The following brief comments about building materials and systems are included as general guidelines only, not for specific application.

2.2.3.1 Wood

Timber structures nearly always resist earthquakes very well, even though wood is a brittle material as far as tension and flexure are concerned. It has some ductility in compression (generally monotonic), and its strength increases significantly for brief loadings, such as earthquake. Conventional timber structures (plywood, oriented strand board, or board sheathing on wood framing) possess much more ductility than the basic material primarily because the nails, and other steel connection devices yield, and the wood compresses against the connector. These structures also possess a much higher degree of damping than the damping that is assumed in developing the basic design spectrum. Much of this damping is caused by slip at the connections. The increased strength, connection ductility, and high damping combine to give timber structures a large reduction from elastic response to design level. This large reduction should not be used if the strength of the structure is actually controlled by bending or tension of the gross timber cross sections. The large reduction in acceleration combined with the light weight timber structures make them very efficient with regard to earthquake ground shaking when they are properly connected. This is confirmed by their generally good performance in earthquakes. Capacities and design and detailing rules for wood elements of seismic force-resisting systems are now found in the *Special Design Provisions for Wind and Seismic* supplement to the *National Design Specification for Wood Construction*.

2.2.3.2 Steel

Steel is the most ductile of the common building materials. The moderate-to-large reduction from elastic response to design response allowed for steel structures is primarily a reflection of this ductility and the stability of the resistance of steel. Members subject to buckling (such as bracing) and connections subject to brittle fracture (such as

partial penetration welds under tension) are much less ductile and are addressed in the *Provisions* in various ways. Defects, such as stress concentrations and flaws in welds, also affect earthquake resistance as demonstrated in the Northridge earthquake. The basic and applied research program that grew out of that experience has greatly increased knowledge of how to avoid low ductility details in steel construction. Capacities and design and detailing rules for seismic design of hot-rolled structural steel are found in the *Seismic Provisions for Structural Steel Building*s (American Institute of Steel Construction (AISC) Standard 341) and similar provisions for cold-formed steel are found in the "Lateral Design" supplement to the *North American Specification for the Design of Cold-Formed Steel Structures* published by AISI (American Iron and Steel Institute).

2.2.3.3 Reinforced Concrete

Reinforced concrete achieves ductility through careful limits on steel in tension and concrete in compression. Reinforced concrete beams with common proportions can possess ductility under monotonic loading even greater than common steel beams; in which local buckling is usually a limiting factor. Providing stability of the resistance to reversed inelastic strains, however, requires special detailing. Thus, there is a wide range of reduction factors from elastic response to design response depending on the detailing for stable and assured resistance. The *Commentary* and the commentary with the ACI 318 standard *Building Code Requirements for Structural Concrete* explain how to design to control premature shear failures in members and joints, buckling of compression bars, concrete compression failures (through confinement with transverse reinforcement), the sequence of plastification and other factors, which can lead to large reductions from the elastic response.

2.2.3.4 Masonry

Masonry is a more complex material than those mentioned above and less is known about its inelastic response characteristics. For certain types of members (such as pure cantilever shear walls), reinforced masonry behaves in a fashion similar to reinforced concrete. The nature of masonry construction, however, makes it difficult, if not impossible, to take some of the steps (e.g., confinement of compression members) used with reinforced concrete to increase ductility, and stability. Further, the discrete differences between mortar, grout and the masonry unit create additional failure phenomena. Thus, the response reduction factors for design of reinforced masonry are not quite as large as those for reinforced concrete. Unreinforced masonry possesses little ductility or stability, except for rocking of masonry piers on a firm base and very little reduction from the elastic response is permitted. Capacities and design and detailing rules for seismic design of masonry elements are contained within The Masonry Society (TMS) 402 standard *Building Code Requirements for Masonry Structures*.

2.2.3.5 Precast Concrete

Precast concrete obviously can behave quite similarly to reinforced concrete but it also can behave quite differently. The connections between pieces of precast concrete commonly are not as strong as the members being connected. Clever arrangements of connections can create systems in which yielding under earthquake motions occurs away from the connections, in which case the similarity to reinforced concrete is very real. Some carefully detailed connections also can mimic the behavior of reinforced concrete. Many common connection schemes, however, will not do so. Successful performance of such systems requires that the connections perform in a ductile manner. This requires some extra effort in design but it can deliver successful performance. As a point of reference, the most common wood seismic resisting systems perform well yet have connections (nails) that are significantly weaker than the connected elements (structural wood panels). The *Provisions* includes guidance, some only for trial use and comment (Part 3), for seismic design of precast structures. ACI 318 also includes provisions for precast concrete elements resisting seismic forces, and there are also supplemental ACI standards for specialized seismic force-resisting systems of precast concrete.

2.2.3.6 Composite Steel and Concrete

Reinforced concrete is a composite material. In the context of the *Provisions*, *composite* is a term reserved for structures with elements consisting of structural steel and reinforced concrete acting in a composite manner. These structures generally are an attempt to combine the most beneficial aspects of each material. Capacities and design and detailing rules are found in the *Seismic Provisions for Structural Steel Buildings* (AISC Standard 341).

2.2.4 Building Systems

Three basic lateral-load-resisting elements – walls, braced frames and unbraced frames (moment resisting frames) – are used to build a classification of structural types in the *Provisions*. Unbraced frames generally are allowed greater reductions from elastic response than walls and braced frames. In part, this is because frames are more redundant, having several different locations with approximately the same stress levels and common beam-column joints frequently exhibit an ability to maintain a stable response through many cycles of reversed inelastic deformations. Systems using connection details that have not exhibited good ductility and toughness, such as unconfined concrete and the welded steel joint used before the Northridge earthquake, are penalized: the R factors permit less reduction from elastic response.

Connection details often make development of ductility difficult in braced frames, and buckling of compression members also limits their inelastic response. The actual failure of steel bracing often occurs because local buckling associated with overall member

buckling frequently leads to locally high strains that then lead to brittle fracture when the member subsequently approaches yield in tension. Eccentrically braced steel frames and new proportioning and detailing rules for concentrically braced frames have been developed to overcome these shortcomings. But the newer and potentially more popular bracing system is the buckling-restrained braced frame. This new system has the advantages of a special steel concentrically braced frame, but with performance that is superior as brace buckling is controlled to preserve ductility. Design provisions appear in the *Seismic Provisions for Structural Steel Buildings* (AISC Standard 341).

Shear walls that do not bear gravity load are allowed a greater reduction than walls that are load bearing. Redundancy is one reason; another is that axial compression generally reduces the flexural ductility of concrete and masonry elements (although small amounts of axial compression usually improve the performance of materials weak in tension, such as masonry and concrete). The 2010 earthquake in Chile is expected to lead to improvements in understanding and design of reinforced concrete shear wall systems because of the large number of significant concrete shear wall buildings subjected to strong shaking in that earthquake. Systems that combine different types of elements are generally allowed greater reductions from elastic response because of redundancy.

Redundancy is frequently cited as a desirable attribute for seismic resistance. A quantitative measure of redundancy is included in the *Provisions* in an attempt to prevent use of large reductions from elastic response in structures that actually possess very little redundancy. Only two values of the redundancy factor, ρ, are defined: 1.0 and 1.3. The penalty factor of 1.3 is placed upon systems that do not possess some elementary measures of redundancy based on explicit consideration of the consequence of failure of a single element of the seismic force-resisting system. A simple, deemed-to-comply exception is provided for certain structures.

2.2.5 Supplementary Elements Added to Improve Structural Performance

The *Standard* includes provisions for the design of two systems to significantly alter the response of the structure to ground shaking. Both have specialized rules for response analysis and design detailing.

Seismic isolation involves placement of specialized bearings with low lateral stiffness and large lateral displacement capacity between the foundation and the superstructure. It is used to substantially increase the natural period of vibration and thereby decrease the acceleration response of the structures. (Recall the shape of the response spectrum in Figure 2.2-4; the acceleration response beyond a threshold period is roughly proportional to the inverse of the period). Seismic isolation is becoming increasingly common for structures in which superior performance is necessary, such as major hospitals and emergency response centers. Such structures are frequently designed with a stiff superstructure to control story drift, and isolation makes it feasible to design such structures for lower total lateral force. The design of such systems requires a conservative estimate of the likely deformation of the isolator. The early provisions for

that factor were a precursor of the changes in ground motion mapping implemented in the 1997 *Provisions*.

Added damping involves placement of specialized energy dissipation devices within stories of the structure. The devices can be similar to a large shock absorber, but other technologies are also available. Added damping is used to reduce the structural response, and the effectiveness of increased damping can be seen in Figure 2.2-3. It is possible to reach effective damping levels of 20 to 30 percent of critical damping, which can reduce response by factors of 2 or 3. The damping does not have to be added in all stories; in fact, it is common to add damping at the isolator level of seismically isolated buildings.

Isolation and damping elements require extra procedures for analysis of seismic response. Both also require considerations beyond common building construction to assure quality and durability.

2.3 ENGINEERING PHILOSOPHY

The *Commentary*, under "Intent," states:

> "The primary intent of the *NEHRP Recommended Seismic Provisions* for normal buildings and structures is to prevent serious injury and life loss caused by damage from earthquake ground shaking. Most earthquake injuries and deaths are caused by structural collapse. Thus, the main thrust of the *Provisions* is to prevent collapse for very rare and intense ground motion, termed the maximum considered earthquake (MCE) motion…Falling exterior walls and cladding, and falling ceilings, light fixtures, pipes, equipment and other nonstructural components also cause deaths and injuries."

The *Provisions* states:

> "The degree to which these goals can be achieved depends on a number of factors including structural framing type, building configuration, materials, as-built details and overall quality of design. In addition, large uncertainties as to the intensity and duration of shaking and the possibility of unfavorable response of a small subset of buildings or other structures may prevent full realization of the intent."

At this point it is worth recalling the criteria mentioned earlier in describing the risk-targeted ground motions used for design. The probability of structural collapse due to ground shaking is not zero. One percent in 50 years is actually a higher failure rate than is currently considered acceptable for buildings subject to other natural loads, such as wind and snow. The reason is as stated in the quote at the beginning of this chapter "…all the wealth of the world would prove insufficient…" Damage is to be expected when an earthquake equivalent to the design earthquake occurs. (The "design earthquake" is currently taken as two-thirds of the MCE ground motion). Some collapse

is to be expected when and where ground motion equivalent to the MCE ground motion occurs.

The basic structural criteria are strength, stability and distortion. The yield-level strength provided must be at least that required by the design spectrum (which is reduced from the elastic spectrum as described previously). Structural elements that cannot be expected to perform in a ductile manner are to have greater strength, which is achieved by applying the Ω_0 amplifier to the design spectral response. The stability criterion is imposed by amplifying the effects of lateral forces for the destabilizing effect of lateral translation of the gravity weight (the P-delta effect). The distortion criterion is a limit on story drift and is calculated by amplifying the linear response to the (reduced) design spectrum by the factor C_d to account for inelastic behavior.

Yield-level strengths for steel and concrete structures are easily obtained from common design standards. The most common design standards for timber and masonry are based on allowable stress concepts that are not consistent with the basis of the reduced design spectrum. Although strength-based standards for both materials have been introduced in recent years, the engineering profession has not yet embraced these new methods. In the past, the *Provisions* stipulated adjustments to common reference standards for timber and masonry to arrive at a strength level equivalent to yield, and compatible with the basis of the design spectrum. Most of these adjustments were simple factors to be applied to conventional allowable stresses. With the deletion of these methods from the *Provisions*, other methods have been introduced into model building codes, and the ASCE standard *Minimum Design Loads for Buildings and Other Structures* to factor downward the seismic load effects based on the *Provisions* for use with allowable stress design methods.

The *Provisions* recognizes that the risk presented by a particular building is a combination of the seismic hazard at the site and the consequence of failure, due to any cause, of the building. Thus, a classification system is established based on the use and size of the building. This classification is called the Occupancy Category (Risk Category in the *Standard*). A combined classification called the Seismic Design Category (SDC) incorporates both the seismic hazard and the Occupancy Category. The SDC is used throughout the *Provisions* for decisions regarding the application of various specific requirements. The flow charts in Chapter 2 illustrate how these classifications are used to control application of various portions of the *Provisions*.

2.4 STRUCTURAL ANALYSIS

The *Provisions* sets forth several procedures for determining the force effect of ground shaking. Analytical procedures are classified by two facets: linear versus nonlinear and dynamic versus equivalent static. The two most fully constrained and frequently used are both linear methods: an equivalent static force procedure and a dynamic modal response spectrum analysis procedure. A third linear method, a full history of dynamic response (previously referred to as a time-history analysis, now referred to as a response-history analysis), and a nonlinear method are also permitted, subject to certain limitations. These

methods use real or synthetic ground motions as input but require them to be scaled to the basic response spectrum at the site for the range of periods of interest for the structure in question. Nonlinear analyses are very sensitive to assumptions about structural behavior made in the analysis and to the ground motions used as input, and a peer review is required. A nonlinear static method, also known as a pushover analysis, is described in Part 3 of the *Provisions*, but it is not included in the *Standard*. The *Provisions* also reference ASCE 41, *Seismic Rehabilitation of Existing Buildings*, for the pushover method. The method is instructive for understanding the development of mechanisms but there is professional disagreement over its utility for validating a structural design.

The two most common linear methods make use of the same design spectrum. The reduction from the elastic spectrum to design spectrum is accomplished by dividing the elastic spectrum by the coefficient ***R***, which ranges from 1-1/4 to 8. Because the design computations are carried out with a design spectrum that is two-thirds the MCE spectrum that means the full reduction from elastic response ranges from 1.9 to 12. The specified elastic spectrum is based on a damping level at 5 percent of critical damping, and a part of the ***R*** factor accomplishes adjustments in the damping level. Ductility and overstrength make up the larger part of the reduction. The *Provisions* define the total effect of earthquake actions as a combination of the response to horizontal motions (or forces for the equivalent static force method) with response to vertical ground acceleration. The response to vertical ground motion is roughly estimated as a factor (positive or negative) on the dead load force effect. The resulting internal forces are combined with the effects of gravity loads and then compared to the full strength of the members, reduced by a resistance factor, but not by a factor of safety.

With the equivalent static force procedure, the level of the design spectrum is set by determining the appropriate values of basic seismic acceleration, the appropriate soil profile type and the value for ***R***. The particular acceleration for the building is determined from this spectrum by selecting a value for the natural period of vibration. Equations that require only the height and type of structural system are given to approximate the natural period for various building types. (The area and length of shear walls come into play with an optional set of equations.) Calculation of a period based on an analytical model of the structure is encouraged, but limits are placed on the results of such calculations. These limits prevent the use of a very flexible model in order to obtain a large period and correspondingly low acceleration. Once the overall response acceleration is found, the base shear is obtained by multiplying it by the total effective mass of the building, which is generally the total permanent load.

Once the total lateral force is determined, the equivalent static force procedure specifies how this force is to be distributed along the height of the building. This distribution is based on the results of dynamic studies of relatively uniform buildings and is intended to give an envelope of shear force at each level that is consistent with these studies. This set of forces will produce, particularly in tall buildings, an envelope of gross overturning moment that is larger than many dynamic studies indicate is necessary. Dynamic analysis is encouraged, and the modal procedure is required for structures with large periods (essentially this means tall structures) in the higher seismic design categories.

With one exception, the remainder of the equivalent static force analysis is basically a standard structural analysis. That exception accounts for uncertainties in the location of the center of mass, uncertainties in the strength and stiffness of the structural elements and rotational components in the basic ground shaking. This concept is referred to as horizontal torsion. The *Provisions* requires that the center of force be displaced from the calculated center of mass by an arbitrary amount in either direction (this torsion is referred to as accidental torsion). The twist produced by real and accidental torsion is then compared to a threshold and if the threshold is exceeded, the accidental torsion must be amplified.

In many respects, the modal analysis procedure is very similar to the equivalent static force procedure. The primary difference is that the natural period and corresponding deflected shape must be known for several of the natural modes of vibration. These are calculated from a mathematical model of the structure. The procedure requires inclusion of enough modes so that the dynamic response of the analytical model captures at least 90 percent of the mass in the structure that can vibrate. The base shear for each mode is determined from a design spectrum that is essentially the same as that for the static procedure. The distribution of displacements and accelerations (forces) and the resulting story shears, overturning moments and story drifts are determined for each mode directly from the procedure. Total values for subsequent analysis and design are determined by taking the square root of the sum of the squares for each mode. This summation gives a statistical estimate of maximum response when the participation of the various modes is random. If two or more of the modes have very similar periods, more advanced techniques for summing the values are required; these procedures must account for coupling in the response of close modes. The sum of the absolute values for each mode is always conservative.

A lower limit to the base shear determined from the modal analysis procedure is specified based on the static procedure, and the approximate periods specified in the static procedure. When this limit is violated, which is common, all results are scaled up in direct proportion. The consideration of horizontal torsion is the same as for the static procedure. Because the equivalent static forces applied at each floor, the story shears and the overturning moments are separately obtained from the summing procedure, the results are not statically compatible (that is, the moment calculated from the summed floor forces will not match the moment from the summation of moments). Early recognition of this will avoid considerable problems in later analysis and checking.

For structures that are very uniform in a vertical sense, the two procedures give very similar results. The modal analysis method is better for buildings having unequal story heights, stiffnesses, or masses. The modal procedure is required for such structures in higher seismic design categories. Both methods are based on purely elastic behavior, and, thus, neither will give a particularly accurate picture of behavior in an earthquake approaching the design event. Yielding of one component leads to redistribution of the forces within the structural system; while this may be very significant, none of the linear methods can account for it.

Both of the common methods require consideration of the stability of the building as a whole. The technique is based on elastic amplification of horizontal displacements created by the action of gravity on the displaced masses. A simple factor is calculated and the amplification is provided for in designing member strengths when the amplification exceeds about 10 percent. The technique is referred to as the P-delta analysis and is only an approximation of stability at inelastic response levels.

2.5 NONSTRUCTURAL ELEMENTS OF BUILDINGS

Severe ground shaking often results in considerable damage to the nonstructural elements of buildings. Damage to nonstructural elements can pose a hazard to life in and of itself, as in the case of heavy partitions or facades, or it can create a hazard if the nonstructural element ceases to function, as in the case of a fire suppression system. Some buildings, such as hospitals and fire stations, need to be functional immediately following an earthquake; therefore, many of their nonstructural elements must remain undamaged.

The *Provisions* treats damage to and from nonstructural elements in three ways. First, indirect protection is provided by an overall limit on structural distortion; the limits specified, however, may not offer enough protection to brittle elements that are rigidly bound by the structure. More restrictive limits are placed upon those Occupancy Categories (Risk Categories in the *Standard*) for which better performance is desired given the occurrence of strong ground shaking. Second, many components must be anchored for an equivalent static force. Third, the explicit design of some elements (the elements themselves, not just their anchorage) to accommodate specific structural deformations or seismic forces is required.

The dynamic response of the structure provides the dynamic input to the nonstructural component. Some components are rigid with respect to the structure (light weights, and small dimensions often lead to fundamental periods of vibration that are very short). Application of the response spectrum concept would indicate that the response history of motion of a building roof to which mechanical equipment is attached looks like a ground motion to the equipment. The response of the component is often amplified above the response of the supporting structure. Response spectra developed from the history of motion of a point on a structure undergoing ground shaking are called floor spectra, and are useful in understanding the demands upon nonstructural components.

The *Provisions* simplifies the concept greatly. The force for which components are checked depends on:

1. The component mass;

2. An estimate of component acceleration that depends on the structural response acceleration for short period structures, the relative height of the component within the structure and a crude approximation of the flexibility of the component or its anchorage;

3. The available ductility of the component or its anchorage; and

4. The function or importance of the component or the building.

Also included in the *Provisions* is a quantitative measure for the deformation imposed upon nonstructural components. The inertial force demands tend to control the seismic design for isolated or heavy components whereas the imposed deformations are important for the seismic design for elements that are continuous through multiple levels of a structure or across expansion joints between adjacent structures, such as cladding or piping.

2.6 QUALITY ASSURANCE

Since strong ground shaking has tended to reveal hidden flaws or *weak links* in buildings, detailed requirements for assuring quality during construction are contained in the *Provisions* by reference to the *Standard*, where they are located in an appendix. The actively implemented provisions for quality control are actually contained in the model building codes, such as the *International Building Code*, and the material design standards, such as *Seismic Provisions for Structural Steel Buildings*. Loads experienced during construction provide a significant test of the likely performance of ordinary buildings under gravity loads. Tragically, mistakes occasionally will pass this test only to cause failure later, but it is fairly rare. No comparable proof test exists for horizontal loads, and experience has shown that flaws in construction show up in a disappointingly large number of buildings as distress and failure due to earthquakes. This is coupled with the seismic design approach based on excursions into inelastic straining, which is not the case for response to other loads.

The quality assurance provisions require a systematic approach with an emphasis on documentation and communication. The designer who conceives the systems to resist the effects of earthquake forces must identify the elements that are critical for successful performance as well as specify the testing and inspection necessary to confirm that those elements are actually built to perform as intended. Minimum levels of testing and inspection are specified in the *Provisions* for various types of systems and components.

The *Provisions* also requires that the contractor and building official be aware of the requirements specified by the designer. Furthermore, those individuals who carry out the necessary inspection and testing must be technically qualified, and must communicate the results of their work to all concerned parties. In the final analysis, there is no substitute for a sound design, soundly executed.

3

Earthquake Ground Motion

Nicolas Luco[1], Ph.D., P.E., Michael Valley[2], S.E., C.B. Crouse[3], P.E., Ph.D.

Contents

3.1 BASIS OFEARTHQUAKE GROUND MOTION MAPS....2
3.1.1 ASCE 7-05 Seismic Maps....2
3.1.2 MCE_R Ground Motions in the *Provisions* and in ASCE 7-10....3
3.1.3 PGA Maps in the *Provisions* and in ASCE 7-10....7
3.1.4 Basis of Vertical Ground Motions in the *Provisions* and in ASCE 7-10....7
3.1.5 Summary....7
3.1.6 References....8
3.2 DETERMINATION OF GROUND MOTION VALUES AND SPECTRA....9
3.2.1 ASCE 7-05 Ground Motion Values....9
3.2.2 2009 *Provisions* Ground Motion Values....10
3.2.3 ASCE 7-10 Ground Motion Values....11
3.2.4 Horizontal Response Spectra....12
3.2.5 Vertical Response Spectra....13
3.2.6 Peak Ground Accelerations....14
3.3 SELECTION AND SCALING OF GROUND MOTION RECORDS....14
3.3.1 Approach to Ground Motion Selection and Scaling....15
3.3.2 Two-Component Records for Three Dimensional Analysis....24
3.3.3 One-Component Records for Two-Dimensional Analysis....27
3.3.4 References....28

[1] Author of Section 3.1.
[2] Author of Sections 3.2 and 3.3.
[3] Reviewing author.

Most of the effort in seismic design of buildings and other structures is focused on structural design. This chapter addresses another key aspect of the design process—characterization of earthquake ground motion. Section 3.1 describes the basis of the earthquake ground motion maps in the *Provisions* and in ASCE 7. Section 3.2 has examples for the determination of ground motion parameters and spectra for use in design. Section 3.3 discusses and provides an example for the selection and scaling of ground motion records for use in response history analysis.

3.1 BASIS OFEARTHQUAKE GROUND MOTION MAPS

This section explains the basis of the new Risk-Targeted Maximum Considered Earthquake (MCE_R) ground motions specified in the 2009 *Provisions* and mapped in ASCE 7-10. In doing so, it also explains the basis for the uniform-hazard ground motion (S_{SUH} and S_{1UH}) maps, risk coefficient (C_{RS} and C_{R1}) maps and deterministic ground motion (S_{SD} and S_{1D}) maps in the 2009 *Provisions.* These three sets of maps are combined to form the Site Class B MCE_R ground motion (S_S and S_1) maps in ASCE 7-10. The use of S_S and S_1 ground motions in the 2009 *Provision*s and ASCE 7-10 to derive a design response spectrum remains the same as it is in ASCE 7-05.

This section also explains the basis for the new Peak Ground Acceleration (PGA) maps in the 2009 *Provisions* and ASCE 7-10 and the new equations for vertical ground motions. The basis for the long-period transition (T_L) maps in the 2009 *Provisions* and ASCE 7-10, which are identical to those in ASCE 7-05, is also reviewed. In fact, we start with a review of these maps and the Maximum Considered Earthquake (MCE) ground motion maps in ASCE 7-05.

3.1.1 ASCE 7-05 Seismic Maps

The bases for the seismic ground motion (MCE) and long-period transition (T_L) maps in Chapter 22 of ASCE 7-05 were established by, respectively, the Building Seismic Safety Council (BSSC) Seismic Design Procedures Group, also referred to as Project ’97, and Technical Subcommittee 1 (TS-1) of the 2003 Provisions Update Committee. They are reviewed briefly in the following two subsections.

3.1.1.1 Maximum Considered Earthquake (MCE) Ground Motion Maps

The MCE ground motion maps in ASCE 7-05 can be described as applications of its site-specific ground motion hazard analysis procedure in Chapter 21 (Section 21.2), using ground motion values computed by the USGS National Seismic Hazard Mapping Project (in Golden, CO) for a grid of locations and/or polygons that covers the US. In particular, the 1996 USGS update of the ground motion values was used for ASCE 7-98 and ASCE 7-02; the 2002 USGS update was used for ASCE 7-05. The site-specific procedure in all three editions calculates the MCE ground motion as the lesser of a probabilistic and a deterministic ground motion. Hence, the USGS computed both types of ground motions, whereas otherwise it would have only computed probabilistic ground motions. Brief reviews of how the USGS computed the probabilistic and deterministic ground motions are provided in the next few paragraphs. For additional information, see Leyendecker et al. (2000).

The USGS computation of the probabilistic ground motions that are part of the basis of the MCE ground motion maps in ASCE 7-05 is explained in detail in Frankel et al. (2002). In short, the USGS combines research on potential sources of earthquakes (e.g., faults and locations of past earthquakes), the potential magnitudes of earthquakes from these sources and their frequencies of occurrence, and the potential ground motions generated by these earthquakes. Uncertainty and randomness in each of these components is accounted for in the computation via contemporary Probabilistic Seismic Hazard Analysis (PSHA), which was originally conceived by Cornell (1968). The primary output of PSHA computations are so-called hazard curves, for locations on a grid covering the US in the case of the USGS computation.

Each hazard curve provides mean annual frequencies of exceeding various user-specified ground motions amplitudes. From these hazard curves, the ground motion amplitudes for a user-specified mean annual frequency can be interpolated and then mapped. The results are known as uniform-hazard ground motion maps, since the mean annual frequency (or corresponding probability) is uniform geographically.

For ASCE 7-05 (as well as ASCE 7-02 and ASCE 7-98), a mean annual exceedance frequency of 1/2475 per year, corresponding to 2% probability of exceedance in 50 years, was specified by the aforementioned BSSC Project '97. That project also specified that the ground motion parameters be spectral response accelerations at vibration periods of 0.2 seconds and 1 second, for 5% of critical damping. For the average shear wave velocity at small shear strains in the upper 100 feet (30 m) of subsurface below each location ($v_{S,30}$), the USGS decided on a reference value of 760 m/s. The BSSC subsequently decided to regard this reference value, which is at the boundary of Site Classes B and C, as corresponding to Site Class B. Justifications for the decisions summarized in this paragraph are provided in the *Commentary* of FEMA 303, FEMA 369 and FEMA 450.

The USGS computation of the deterministic ground motions for ASCE 7-05 is detailed in the FEMA 303 *Commentary*. As defined by Project '97 and subsequently specified in the site-specific procedure of ASCE 7-05 (Section 21.2.2), each deterministic ground motion is calculated as 150% of the median spectral response acceleration for a characteristic earthquake on a known active fault within the region. The specific characteristic earthquake is that which generates the largest median spectral response acceleration at the given location. As for the probabilistic ground motions, the spectral response accelerations are at vibration periods of 0.2 seconds and 1 second, for 5% of critical damping. The same reference site class (see preceding paragraph) is used as well. Though not applied to probabilistic ground motions, lower limits of 1.5g and 0.6g are applied to the deterministic ground motions.

As mentioned at the beginning of this section, the lesser of the probabilistic and deterministic ground motions described above yields the MCE ground motions mapped in ASCE 7-05. Thus, the MCE spectral response accelerations at 0.2 seconds and 1 second are equal to the corresponding probabilistic ground motions wherever they are less than the lower limits of the deterministic ground motions (1.5g and 0.6g, respectively). Where the probabilistic ground motions are greater than the lower limits, the deterministic ground motions sometimes govern, but only if they are less than their probabilistic counterparts. On the MCE ground motion maps in ASCE 7-05, the deterministic ground motions govern mainly near major faults in California (like the San Andreas), in Reno and in parts of the New Madrid Seismic Zone. The deterministic ground motions that govern are as small as 40% of their probabilistic counterparts.

3.1.1.2 Long-Period Transition Period (T_L) Maps

The details of the procedure and rationale used in developing the T_L maps in ASCE 7-05; and now in ASCE 7-10 and the 2009 *Provisions*, are found in Crouse et al. (2006). In short, the procedure consisted of two steps. First, a relationship between T_L and earthquake magnitude was established. Second, the modal magnitude from deaggregation of the USGS 2% in 50-year ground motion hazard at a 2-second period (1 second for Hawaii) was mapped. The long-period transition period (T_L) maps that combined these two steps delimit the transition of the design response spectrum from a constant velocity ($1/T$) to a constant displacement ($1/T^2$) shape.

3.1.2 MCE_R Ground Motions in the *Provisions* and in ASCE 7-10

Like the MCE ground motion maps in ASCE 7-05 reviewed in the preceding section, the new Risk-Targeted Maximum Considered Earthquake (MCE_R) ground motions in the 2009 *Provisions* and ASCE 7-10 can be described as applications of the site-specific ground motion hazard analysis procedure in Chapter 21 (Section 21.2) of both documents. For the MCE_R ground motions, however, the USGS values (for a grid of site and/or polygons covering the US) that are used in the procedure are from its 2008 update. Still, the site-specific procedure of the *Provisions* and ASCE 7-10 calculates the MCE_R ground

motion as the lesser of a probabilistic and a deterministic ground motion. The definitions of the probabilistic and deterministic ground motions in ASCE 7-10, however, are different than in ASCE 7-05. The definitions were revised for the 2009 ***Provisions*** and ASCE 7-10 by the BSSC Seismic Design Procedures Reassessment Group (SDPRG), also referred to as Project '07. Three revisions were made:

1) The probabilistic ground motions are redefined as so-called risk-targeted ground motions, in lieu of the uniform-hazard (2% in 50-year) ground motions that underlie the ASCE 7-05 MCE ground motion maps,

2) the deterministic ground motions are redefined as 84^{th}-percentile ground motions, in lieu of median ground motions multiplied by 1.5; and

3) the probabilistic and deterministic ground motions are redefined as maximum-direction ground motions, in lieu of geometric mean ground motions.

In addition to these three BSSC redefinitions of probabilistic and deterministic ground motions, there is a fourth difference in the ground motion values computed by the USGS for the 2009 ***Provisions*** and ASCE 7-10 versus ASCE 7-05:

4) The probabilistic and deterministic ground motions were recomputed using updated earthquake source and ground motion propagation models, e.g., the Unified California Earthquake Rupture Forecast (UCERF, Version 2; Field et al., 2008) and the Next Generation Attenuation (NGA) ground motion models[4].

Each of the above four differences between the basis of the MCE ground motions (in ASCE 7-05) and that of the MCE_R ground motions (in the 2009 ***Provisions*** and ASCE 7-10) is explained in more detail below. Also explained are the differences in the presentation of MCE_R ground motions between the 2009 ***Provisions*** and ASCE 7-10; the numerical values of the MCE_R ground motions in the two documents are otherwise identical.

3.1.2.1 Risk-Targeted Probabilistic Ground Motions

For the MCE ground motion maps in ASCE 7-05, recall (from Section 3.1.1) that the underlying probabilistic ground motions are specified to be uniform-hazard ground motions that have a 2% probability of being exceeded in 50 years. It has long been recognized, though, that "it really is the probability of structural failure with resultant casualties that is of concern; and the geographical distribution of that probability is not necessarily the same as the distribution of the probability of exceeding some ground motion" (p. 296 of ATC 3-06, 1978). The primary reason that the distributions of the two probabilities are not the same is that there are geographic differences in the shape of the hazard curves from which uniform-hazard ground motions are read. The ***Commentary*** of FEMA 303 (p. 289) reports that "because of these differences, questions were raised concerning whether definition of the ground motion based on a constant probability for the entire United States would result in similar levels of seismic safety for all structures".

The changeover to risk-targeted probabilistic ground motions for the 2009 ***Provisions*** and ASCE 7-10 takes into account the differences in the shape of hazard curves across the US. Where used in design, the risk-targeted ground motions are expected to result in buildings with a geographically uniform mean annual frequency of collapse, or uniform risk. The BSSC, via Project '07, decided on a target risk level corresponding to 1% probability of collapse in 50 years. This target is based on the average of the mean annual frequencies of collapse across the Western US (WUS) expected to result from design for the

[4] See the February 2008 *Earthquake Spectra* "Special Issue on the Next Generation Attenuation Project," Volume 24, Number 1.

probabilistic ground motions in ASCE 7-05. Consequently, in the WUS the risk-targeted ground motions in the 2009 *Provisions* and ASCE 7-10 are generally within 15% of the corresponding uniform-hazard (2% in 50-year) ground motions. In the Central and Eastern US, where the shapes of hazard curves are known to differ from those in the WUS, the risk-targeted ground motions generally are smaller. For instance, in the New Madrid Seismic Zone and near Charleston, South Carolina ratios of risk-targeted to uniform-hazard ground motions are as small as 0.7.

The computation of risk-targeted probabilistic ground motions for the MCE_R ground motions in the 2009 *Provisions* and ASCE 7-10 is detailed in *Provisions* Part 1 Sections 21.2.1.2 and C21.2.1 and in Luco et al. (2007). While the computation of the risk-targeted ground motions is different than that of the uniform-hazard ground motions specified for the MCE ground motions in ASCE 7-05, both begin with USGS computations of hazard curves. As explained in Section 3.1.1, the uniform-hazard ground motions simply interpolate the hazard curves for a 2% probability of exceedance in 50 years. In contrast, the risk-targeted ground motions make use of entire hazard curves. In either case, the end results are probabilistic spectral response accelerations at 0.2 seconds and 1 second, for 5% of critical damping and the reference site class.

3.1.2.2 84th-Percentile Deterministic Ground Motions

For the MCE ground motion maps in ASCE 7-05, recall (from Section 3.1.1) that the underlying deterministic ground motions are defined as 150% of median spectral response accelerations. As explained in the FEMA 303 *Commentary* (p. 296),

> *Increasing the median ground motion estimates by 50 percent [was] deemed to provide an appropriate margin and is similar to some deterministic estimates for a large magnitude characteristic earthquake using ground motion attenuation functions with one standard deviation. Estimated standard deviations for some active fault sources have been determined to be higher than 50 percent, but this increase in the median ground motions was considered reasonable for defining the maximum considered earthquake ground motions for use in design.*

For the MCE_R ground motions in the 2009 *Provisions* and ASCE 7-10, however, the BSSC decided to define directly the underlying deterministic ground motions as those at the level of one standard deviation. More specifically, they are defined as 84th-percentile ground motions (since it has been widely observed that ground motions follow lognormal probability distributions). The remainder of the definition of the deterministic ground motions remains the same as that used for the MCE ground motions maps in ASCE 7-05. For example, the lower limits of 1.5g and 0.6g described in Section 3.1.1 are retained.

The USGS applied a simplification specified by the BSSC in computing the 84th-percentile deterministic ground motions for the 2009 *Provisions* and ASCE 7-10. The 84th-percentile spectral response accelerations were approximated as 180% of median values. This approximation corresponds to a logarithmic ground motion standard deviation of approximately 0.6, as demonstrated in the *Provisions* Part 1 Section C21.2.2. The computation of deterministic ground motions is further described in *Provisions* Part 2 Section C21.2.2.

3.1.2.3 Maximum-Direction Probabilistic and Deterministic Ground Motions

Due to the ground motion attenuation models used by the USGS in computing them[5], overall the MCE spectral response accelerations in ASCE 7-05 represent the geometric mean of two horizontal components of ground motion. Most users of ASCE 7-05 are unaware of this fact, particularly since the discussion notes on the MCE ground motion maps incorrectly state that they represent "the random horizontal component of ground motion." For the 2009 *Provisions* and ASCE 7-10, the BSSC decided that it would

[5] See the January/February 1997 *Seismological Research Letters* "Special Issue on Ground Motion Attenuation Relations," Volume 68, Number 1.

be an improvement if the MCE_R ground motions represented the maximum direction of horizontal spectral response acceleration. Reasons for this decision are explained in ***Provisions*** Part 1 Section C21.2.

Since the attenuation models used in computing the 2008 update of the USGS ground motions also represent (overall) "geomean" spectral response accelerations, for the 2009 ***Provisions*** and ASCE 7-10 the BSSC provided factors to convert approximately to "maximum-direction" ground motions. Based on research by Huang et al. (2008) and others, the factors are 1.1 and 1.3 for the spectral response accelerations at 0.2 seconds and 1.0 second, respectively. The basis for these factors is elaborated upon in the ***Provisions*** Part 1 Section C21.2. They are applied to both the USGS probabilistic hazard curves from which the risk-targeted ground motions (described in Section 3.1.2.1) are derived and the USGS deterministic ground motions (described in Section 3.1.2.2).

3.1.2.4 Updated Ground Motions from USGS (2008)

For the MCE ground motion maps in ASCE 7-05, recall (from Section 3.1.1) that the underlying probabilistic and deterministic ground motions are from the 2002 USGS update. As mentioned above, the MCE_R ground motions in the 2009 ***Provisions*** and ASCE 7-10 are instead based on the 2008 update of the USGS ground motion values. This update is documented in Petersen et al. (2008) and supersedes the 1996 and 2002 USGS ground motions values. It involved interactions with hundreds of scientists and engineers at regional and topical workshops, including advice from working groups, expert panels, state geological surveys, other federal agencies and hazard experts from industry and academia. Based in large part on new published studies, the 2008 update incorporated changes in both earthquake source models (including magnitudes and occurrence frequencies) and models of ground motion propagation. The UCERF and NGA models mentioned above are just two examples of such changes. The end results are updated ground motions that represent the "best available science" as determined by the USGS from an extensive information-gathering and review process.

It is important to note that the 2008 USGS hazard curves and uniform-hazard maps (posted at http://earthquake.usgs.gov/hazards/products/conterminous/2008/), like their 2002 counterparts, represent the "geomean" ground motions discussed in the preceding subsection. Only the MCE_R ground motions and their underlying probabilistic and deterministic ground motions represent the maximum direction of horizontal spectral response acceleration.

3.1.2.5 Differing Presentation of MCE_R Ground Motions in the Provisions *and in ASCE 7-10*

Though their numerical values are identical, the MCE_R ground motions specified in the ***Provisions*** and in ASCE 7-10 are presented differently. As replacements to the MCE ground motion maps in ASCE 7-05, ASCE 7-10 presents (in Chapter 22) contour maps of the MCE_R ground motions for Site Class B, which are still denoted S_S and S_1 for the 0.2- and 1.0-second spectral response accelerations, respectively. Like the MCE ground motions in ASCE 7-05, the MCE_R ground motions mapped in ASCE 7-10 are accessible electronically via a USGS web application (see http://earthquake.usgs.gov/designmaps/).

In contrast, ***Provisions*** Section 11.4 presents equations to calculate MCE_R ground motions (S_S and S_1) for Site Class B using maps (in Chapter 22) of uniform-hazard 2% in 50-year ground motions (denoted S_{SUH} and S_{1UH}), so-called risk coefficients (denoted C_{RS} and C_{R1}); and deterministic ground motions (denoted S_{SD} and S_{1D}, not to be confused with the design ground motions S_{DS} and S_{D1}). The risk coefficient maps show the ratio of the risk-targeted probabilistic ground motions (described in Section 3.1.2.1) to corresponding 2% in 50-year ground motions like those used to derive the MCE ground motion maps in ASCE 7-05. The intent of the equations and three sets of maps presented in the ***Provisions*** is transparency in the derivation of the MCE_R ground motions. The mapped values of the uniform-hazard ground motions, risk coefficients and deterministic ground motions are all accessible electronically via http://earthquake.usgs.gov/designmaps/.

3.1.3 PGA Maps in the *Provisions* and in ASCE 7-10

The basis of the Peak Ground Acceleration (PGA) maps in the *Provisions* and in ASCE 7-10 nearly parallels that of the MCE ground motion maps in ASCE 7-05 described in Section 3.1.1.1. More specifically, the mapped PGA values for Site Class B are calculated as the lesser of uniform-hazard (2% in 50-year) probabilistic and deterministic PGA values that represent the geometric mean of two horizontal components of ground motion. Unlike in ASCE 7-05, though, the deterministic values are defined as 84th-percentile ground motions rather than 150% of median ground motions. This definition of deterministic ground motions parallels that which is described above for the MCE_R ground motions in the 2009 *Provisions* and ASCE 7-10. The deterministic PGA values, though, are stipulated to be no lower than 0.5g, as opposed to 1.5g and 0.6g (respectively) for the MCE_R 0.2- and 1.0-second spectral response accelerations. All of these details of the basis of the PGA maps are provided in ASCE 7-10 Section 21.5; the *Provisions* do not contain a site-specific procedure for PGA values.

The USGS-computed PGA values for $v_{S,30}$ = 760m/s that are mapped, like their MCE_R ground motion counterparts in the *Provisions* and in ASCE 7-10, are from the 2008 USGS update. Also like their MCE_R ground motion counterparts, the 84th-percentile PGA values have been approximated as median values multiplied by 1.8.

While the values on and format of the PGA maps in the *Provisions* and in ASCE 7-10 are identical, the terminology used to label the maps (and values) is different in the two documents. In the *Provisions*, they are referred to as "MCE Geometric Mean PGA" maps. In ASCE 7-10, they are labeled "Maximum Considered Earthquake Geometric Mean (MCE_G) PGA" maps. The MCE_G abbreviation is intended to remind users of the differences between the basis of the PGA maps and the MCE_R maps also in ASCE 7-10, namely that the PGA values represent the geometric mean of two horizontal components of ground motion, not the maximum direction; and that the probabilistic PGA values are not risk-targeted ground motions, but rather uniform-hazard (2% in 50-year) ground motions.

3.1.4 Basis of Vertical Ground Motions in the *Provisions* and in ASCE 7-10

Whereas ASCE 7-05 determines vertical seismic load effects via a single constant fraction of the horizontal short-period spectral response acceleration S_{DS}, the 2009 *Provisions* and ASCE 7-10 determine a vertical design response spectrum, S_{av}, that is analogous to the horizontal design response spectrum, S_a. The S_{av} values are determined via functions (for four different ranges of vertical period of vibration) that each depend on S_{DS} and a coefficient C_v representing the ratio of vertical to horizontal spectral response acceleration. This is in contrast to determination of S_a via mapped horizontal spectral response accelerations. The coefficient C_v, in turn, depends on the amplitude of spectral response acceleration (by way of S_S) and site class. These dependencies, as well as the period dependence of the equations for S_{av}, are based on studies by Bozorgnia and Campbell (2004) and others. Those studies observed that the ratio of vertical to horizontal spectral response acceleration is sensitive to period of vibration, site class, earthquake magnitude (for relatively soft sites) and distance to the earthquake. The sensitivity to the latter two characteristics is captured by the dependence of C_v on S_S.

The basis of the equations for vertical response spectra in the *Provisions* and in ASCE 7-10 is explained in more detail in the commentary to Chapter 23 of each document. Note that for vertical periods of vibration greater than 2 seconds, Chapter 23 stipulates that the vertical spectral response accelerations be determined via a site-specific procedure. A site-specific study also may be performed for periods less than 2 seconds, in lieu of using the equations for vertical response spectra.

3.1.5 Summary

While the new Risk-Targeted Maximum Considered Earthquake (MCE_R) ground motions in the *Provisions* and in ASCE 7-10 are similar to the MCE ground motions in ASCE 7-05, in that they both represent the lesser of probabilistic and deterministic ground motions, there are many differences in their

development. The definitions of the probabilistic and deterministic ground motions that underlie the MCE_R ground motions were revised by the BSSC Seismic Design Procedures Reassessment Group (SDPRG, or Project '07); and the hazard modeling upon which these ground motions are based was updated by the USGS (in 2008). In particular, the underlying probabilistic ground motions were redefined as so-called risk-targeted ground motions, which led to the new "MCE_R ground motion" terminology.

The basis of the new Peak Ground Acceleration (PGA) maps in the *Provisions* and in ASCE 7-10 nearly parallels that of the 0.2- and 1.0-second MCE spectral response accelerations in ASCE 7-05 (with one important exception); new equations for vertical ground motion spectra are based on recent studies of the ratio of vertical to horizontal ground motions. The long-period transition (T_L) maps in the new documents are the same as those in ASCE 7-05.

3.1.6 References

American Society of Civil Engineers. 1998. *Minimum Design Loads for Buildings and Other Structures*, ASCE/SEI 7-98. ASCE, Reston, Virginia.

American Society of Civil Engineers. 2002. *Minimum Design Loads for Buildings and Other Structures*, ASCE/SEI 7-02. ASCE, Reston, Virginia.

American Society of Civil Engineers. 2006. *Minimum Design Loads for Buildings and Other Structures*, ASCE/SEI 7-05. ASCE, Reston, Virginia.

American Society of Civil Engineers. 2010. *Minimum Design Loads for Buildings and Other Structures*, ASCE/SEI 7-10. ASCE, Reston, Virginia.

Applied Technology Council. 1978. *Tentative Provisions for the Development of Seismic Regulations for Buildings*, ATC 3-06. ATC, Palo Alto, California.

Bozorgnia, Y. and K.W. Campbell. 2004. "The Vertical-to-Horizontal Response Spectral Ratio and Tentative Procedures for Developing Simplified V/H and Vertical Design Spectra," *Journal of Earthquake Engineering*, 8:175-207.

Building Seismic Safety Council. 1997. *NEHRP Recommended Provisions for Seismic Regulations for New Buildings and Other Structures, Part 2: Commentary*, FEMA 303. FEMA, Washington, D.C.

Building Seismic Safety Council. 2000. *NEHRP Recommended Provisions for Seismic Regulations for New Buildings and Other Structures, Part 2: Commentary*, FEMA 369. FEMA, Washington, D.C.

Building Seismic Safety Council. 2003. *NEHRP Recommended Provisions and Commentary for Seismic Regulations for New Buildings and Other Structures*, FEMA 450. FEMA, Washington, D.C.

Building Seismic Safety Council. 2009. *NEHRP Recommended Seismic Provisions for New Buildings and Other Structures*, FEMA P-750. FEMA, Washington, D.C.

Cornell, C.A. 1968. "Engineering Seismic Risk Analysis," *Bulletin of the Seismological Society of America*, 58(5):1583-1606.

Crouse C.B., E.V. Leyendecker, P.G. Somerville, M. Power and W.J. Silva. 2006. "Development of Seismic Ground-Motion Criteria for the ASCE 7 Standard," in *Proceedings of the 8th US National Conference on Earthquake Engineering*. Earthquake Engineering Research Institute, Oakland, California.

Field, E.H., T.E. Dawson, K.R. Felzer, A.D. Frankel, V. Gupta, T.H. Jordan, T. Parsons, M.D. Petersen, R.S. Stein, R.J. Weldon and C.J. Wills. 2008. *The Uniform California Earthquake Rupture Forecast, Version 2 (UCERF 2)*, USGS Open File Report 2007-1437 (http://pubs.usgs.gov/of/2007/1437/). USGS, Golden, Colorado.

Frankel, A.D., M.D. Petersen, C.S. Mueller, K.M. Haller, R.L. Wheeler, E.V. Leyendecker, R.L. Wesson, S.C. Harmsen, C.H. Cramer, D.M. Perkins and K.S. Rukstales. 2002. *Documentation for the 2002 Update of the United States National Seismic Hazard Maps*, USGS Open File Report 02-420 (http://pubs.usgs.gov/of/2002/ofr-02-420/). USGS, Golden, Colorado.

Huang, Y.-N., A.S. Whittaker and N. Luco, 2008. "Maximum Spectral Demands in the Near-Fault Region," *Earthquake Spectra*, 24(1):319-341.

Leyendecker, E.V., R.J. Hunt, A.D. Frankel and K.S. Rukstales. 2000. "Development of Maximum Considered Earthquake Ground Motion Maps," *Earthquake Spectra*, 16(1):21-40.

Luco, N. B.R. Ellingwood, R.O. Hamburger, J.D. Hooper, J.K. Kimball and C.A. Kircher. 2007. "Risk-Targeted versus Current Seismic Design Maps for the Conterminous United States," in *Proceedings of the SEAOC 76th Annual Convention*. Structural Engineers Association of California, Sacramento, California.

Petersen, M.D., A.D. Frankel, S.C. Harmsen, C.S. Mueller, K.M. Haller, R.L. Wheeler, R.L. Wesson, Y. Zeng, O.S. Boyd, D.M. Perkins, N. Luco, E.H. Field, C.J. Wills and K.S. Rukstales. 2008. *Documentation for the 2008 Update of the United States National Seismic Hazard Maps*, USGS Open File Report 2008-1128 (http://pubs.usgs.gov/of/2008/1128/). USGS, Golden, Colorado.

3.2 DETERMINATION OF GROUND MOTION VALUES AND SPECTRA

This example illustrates the determination of seismic design parameters for a site in Seattle, Washington. The site is located at 47.65ºN latitude, 122.3ºW longitude. Using the results of a site-specific geotechnical investigation and the procedure specified in *Standard* Chapter 20, the site is classified as Site Class C. (This is the same site used in Design Example 6.3.)

In the sections that follow design ground motion parameters are determined using ASCE 7-05, the 2009 *Provisions* and ASCE 7-10. Using the 2009 *Provisions*, horizontal response spectra, vertical response spectra and peak ground accelerations are computed for both design and maximum considered earthquake ground motions.

3.2.1 ASCE 7-05 Ground Motion Values

ASCE 7-05 Section 11.4.1 requires that spectral response acceleration parameters S_S and S_1 be determined using the maps in Chapter 22. Those maps are too small to permit reading values to a sufficient degree of precision for most sites, so in practice the mapped parameters are determined using a software application available at www.earthquake.usgs.gov/designmaps. That application requires that longitude be entered in degrees east of the prime meridian; negative values are used for degrees west. Given the site location, the following values may be determined using the online application (or read from Figures 22-1 and 22-2).

$S_S = 1.306$
$S_1 = 0.444$

Using these mapped spectral response acceleration values and the site class, site coefficients F_a and F_v are determined in accordance with Section 11.4.3 using Tables 11.4-1 and 11.4-2. Using Table 11.4-1, for $S_S = 1.306 > 1.25$, $F_a = 1.0$ for Site Class C. Using Table 11.4-2, read $F_v = 1.4$ for $S_1 = 0.4$ and $F_v = 1.3$ for $S_1 \geq 0.5$ for Site Class C. Using linear interpolation for $S_1 = 0.444$,

$$F_v = 1.4 + \frac{0.444 - 0.4}{0.5 - 0.4}(1.3 - 1.4) = 1.356$$

Using Equations 11.4-1 and 11.4-2 to determine the adjusted maximum considered earthquake spectral response acceleration parameters,

$$S_{MS} = F_a S_S = 1.0(1.306) = 1.306$$
$$S_{M1} = F_v S_1 = 1.356(0.444) = 0.602$$

Using Equations 11.4-3 and 11.4-4 to determine the design earthquake spectral response acceleration parameters,

$$S_{DS} = \frac{2}{3} S_{MS} = \frac{2}{3}(1.306) = 0.870$$
$$S_{D1} = \frac{2}{3} S_{M1} = \frac{2}{3}(0.602) = 0.401$$

Given the site location read Figure 22-15 for the long-period transition period, T_L = 6 seconds.

3.2.2 2009 *Provisions* Ground Motion Values

Part 1 of the 2009 *Provisions* modifies Chapter 11 of ASCE 7-05 to update the seismic design ground motion parameters and procedures as described in Section 3.1.2 above. Given the site location, the following values may be determined using the online application (or read from *Provisions* Figures 22-1 through 22-6).

S_{SUH} = 1.305
S_{1UH} = 0.522
C_{RS} = 0.988
C_{R1} = 0.955
S_{SD} = 1.5
S_{1D} = 0.6

"UH" and "D" appear, respectively, in the subscripts to indicate uniform hazard and deterministic values of the spectral response acceleration parameters at short periods and at a period of 1 second, S_S and S_1. C_{RS} and C_{R1} are the mapped risk coefficients at short periods and at a period of 1 second. S_{1D} should not be confused with S_{D1}, which is computed below.

The spectral response acceleration parameter at short periods, S_S, is taken as the lesser of the values computed using *Provisions* Equations 11.4-1 and 11.4-2.

$S_S = C_{RS}\, S_{SUH}$ = 0.988(1.305) = 1.289
$S_S = S_{SD}$ = 1.5

Therefore, S_S = 1.289.

The spectral response acceleration parameter at a period of 1 second, S_1, is taken as the lesser of the values computed using *Provisions* Equations 11.4-3 and 11.4-4.

$S_1 = C_{R1}\, S_{1UH} = 0.955(0.522) = 0.498$
$S_1 = S_{1D} = 0.6$

Therefore, $S_1 = 0.498$.

Using these spectral response acceleration values and the site class, site coefficients F_a and F_v are determined in accordance with Section 11.4.3 using Tables 11.4-1 and 11.4-2 (which are identical to the Tables in ASCE 7-05). Using Table 11.4-1, for $S_S = 1.289 > 1.25$, $F_a = 1.0$ for Site Class C. Using Table 11.4-2, read $F_v = 1.4$ for $S_1 = 0.4$ and $F_v = 1.3$ for $S_1 \geq 0.5$ for Site Class C. Using linear interpolation for $S_1 = 0.498$,

$$F_v = 1.4 + \frac{0.498 - 0.4}{0.5 - 0.4}(1.3 - 1.4) = 1.302$$

Using *Provisions* Equations 11.4-5 and 11.4-6 to determine the MCE_R spectral response acceleration parameters,

$$S_{MS} = F_a S_S = 1.0(1.289) = 1.289$$
$$S_{M1} = F_v S_1 = 1.302(0.498) = 0.649$$

Using *Provisions* Equations 11.4-7 and 11.4-8 to determine the design earthquake spectral response acceleration parameters,

$$S_{DS} = \frac{2}{3} S_{MS} = \frac{2}{3}(1.289) = 0.859$$
$$S_{D1} = \frac{2}{3} S_{M1} = \frac{2}{3}(0.649) = 0.433$$

Given the site location read *Provisions* Figure 22-7 for the long-period transition period, $T_L = 6$ seconds.

3.2.3 ASCE 7-10 Ground Motion Values

The seismic design ground motion parameters and procedures in Chapter 11 of ASCE 7-10 are consistent with those in the 2009 *Provisions*. Given the site location, the following values may be determined using the online application (or read from ASCE 7-10 Figures 22-1 and 22-2).

$S_S = 1.289$
$S_1 = 0.498$

Using these spectral response acceleration values and the site class, site coefficients F_a and F_v are determined in accordance with Section 11.4.3 using Tables 11.4-1 and 11.4-2 (which are identical to the Tables in ASCE 7-05 and in the 2009 *Provisions*). Using Table 11.4-1, for $S_S = 1.289 > 1.25$, $F_a = 1.0$ for Site Class C. Using Table 11.4-2, read $F_v = 1.4$ for $S_1 = 0.4$ and $F_v = 1.3$ for $S_1 \geq 0.5$ for Site Class C. Using linear interpolation for $S_1 = 0.498$,

$$F_v = 1.4 + \frac{0.498 - 0.4}{0.5 - 0.4}(1.3 - 1.4) = 1.302$$

Using Equations 11.4-1 and 11.4-2 to determine the MCE_R spectral response acceleration parameters,

$$S_{MS} = F_a S_S = 1.0(1.289) = 1.289$$
$$S_{M1} = F_v S_1 = 1.302(0.498) = 0.649$$

Using Equations 11.4-3 and 11.4-4 to determine the design earthquake spectral response acceleration parameters,

$$S_{DS} = \frac{2}{3} S_{MS} = \frac{2}{3}(1.289) = 0.859$$
$$S_{D1} = \frac{2}{3} S_{M1} = \frac{2}{3}(0.649) = 0.433$$

Given the site location read ASCE 7-10 Figure 22-12 for the long-period transition period, T_L = 6 seconds.

The procedure specified in ASCE 7-10 produces seismic design ground motion parameters that are identical to those produced using the 2009 *Provisions*—but in fewer steps.

3.2.4 Horizontal Response Spectra

The design spectrum is constructed in accordance with *Provisions* Section 11.4.5 using *Provisions* Figure 11.4-1 and *Provisions* Equations 11.4-9, 11.4-10 and 11.4-11. The design spectral response acceleration ordinates, S_a, may be divided into four regions based on period, T, as described below.

From T = 0 to $T_0 = 0.2\frac{S_{D1}}{S_{DS}} = 0.2\left(\frac{0.433}{0.859}\right) = 0.101$ seconds, S_a varies linearly from $0.4S_{DS}$ to S_{DS}.

From T_0 to $T_S = \frac{S_{D1}}{S_{DS}} = \frac{0.433}{0.859} = 0.504$ seconds, S_a is constant at S_{DS}.

From T_S to T_L, S_a is inversely proportional to T, being anchored to S_{D1} at T = 1 second.

At periods greater than T_L, S_a is inversely proportional to the square of T, being anchored to $\frac{S_{D1}}{T_L}$ at T_L.

As prescribed in *Provisions* Section 11.4.6, the MCE_R response spectrum is determined by multiplying the design response spectrum ordinates by 1.5. Figure 3-1 shows the design and MCE_R response spectra determined using the ground motion parameters computed in Section 3.2.3.

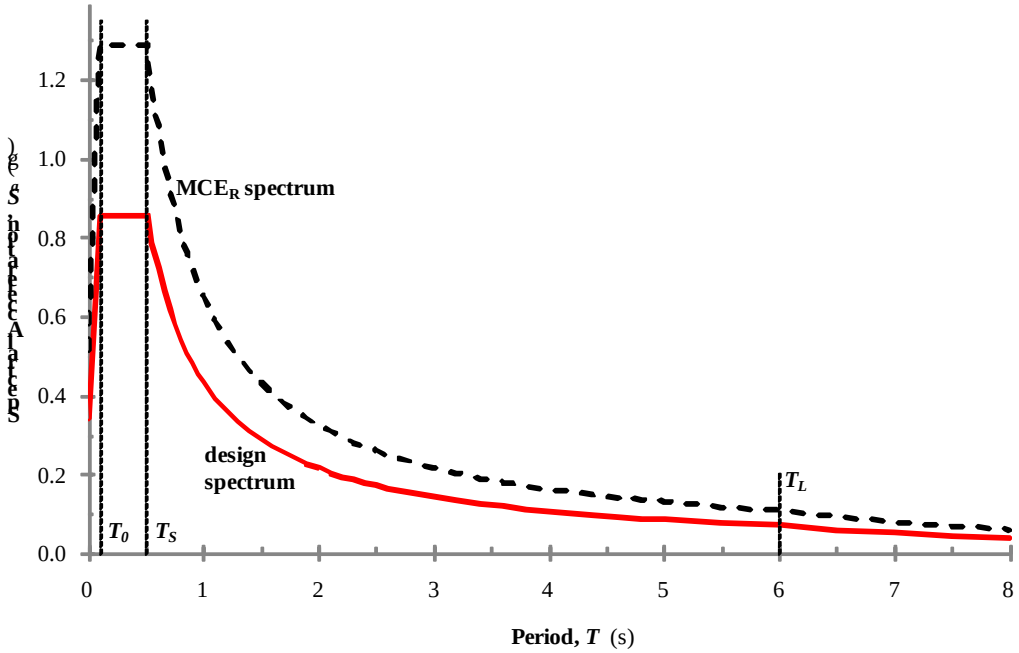

Figure 3-1 Horizontal Response Spectra for Design and MCE$_R$ Ground Motions

3.2.5 Vertical Response Spectra

Part 1 of the 2009 *Provisions* adds a new chapter (Chapter 23) to ASCE 7-05 to define vertical ground motions for seismic design. The design vertical response spectrum is constructed in accordance with *Provisions* Section 23.1 using *Provisions* Equations 23.1-1, 23.1-2, 23.1-3 and 23.1-4. Vertical ground motion values are related to horizontal ground motion values by a vertical coefficient, C_v, which is determined as a function of site class and the MCE$_R$ spectral response parameter at short periods, S_S. The design vertical spectral response acceleration ordinates, S_{av}, may be divided into four regions based on vertical period, T_v, as described below.

Using *Provisions* Table 23.1-1, read $C_v = 1.3$ for $S_S \geq 2.0$ and $C_v = 1.1$ for $S_S = 1.0$ for Site Class C. Using linear interpolation for $S_S = 1.289$,

$$C_v = 1.1 + \frac{1.289 - 1}{2 - 1}(1.3 - 1.1) = 1.158$$

From $T_v = 0$ to 0.025 seconds, S_{av} is constant at $0.3C_vS_{DS} = 0.3(1.158)(0.859) = 0.298$. From $T_v = 0.025$ to 0.05 seconds, S_{av} varies linearly from $0.3C_vS_{DS} = 0.298$ to $0.8C_vS_{DS} = 0.8(1.158)(0.859) = 0.796$. From $T_v = 0.05$ to 0.15 seconds, S_{av} is constant at $0.8C_vS_{DS} = 0.796$. From $T_v = 0.15$ to 2.0 seconds, S_{av} is inversely proportional to $T_v^{0.75}$, being anchored to $0.8C_vS_{DS} = 0.796$ at $T_v = 0.15$ seconds. For vertical periods greater than 2.0 seconds, the vertical response spectral acceleration must be determined using site-specific procedures.

As prescribed in *Provisions* Section 23.2, the MCE$_R$ vertical response spectrum is determined by multiplying the design vertical response spectrum ordinates by 1.5. Figure 3-2 shows the design and MCE$_R$ vertical response spectra determined using the ground motion parameters computed in Section 3.2.3.

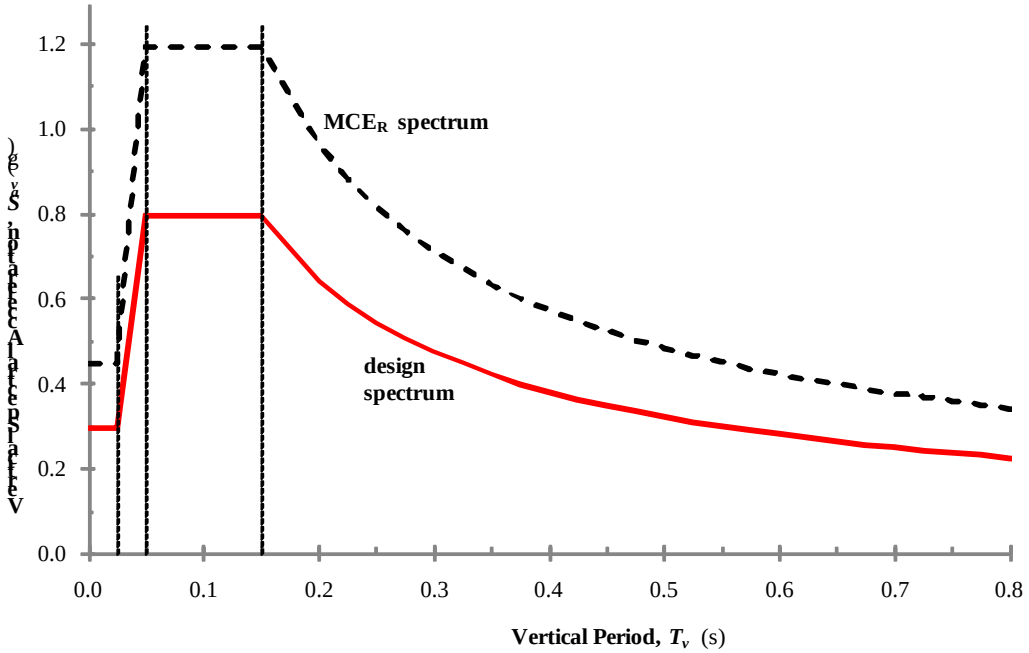

Figure 3-2 Vertical Response Spectra for Design and MCE$_R$ Ground Motions

3.2.6 Peak Ground Accelerations

Part 1 of the 2009 *Provisions* modifies Section 11.8.3 of the ASCE 7-05 to update the calculation of peak ground accelerations used for assessment of the potential for liquefaction and soil strength loss and for determination of lateral earth pressures for design of basement and retaining walls. Given the site location, the following value of maximum considered earthquake geometric mean peak ground acceleration may be determined using the online application (or read from *Provisions* Figure 22-8).

$PGA = 0.521$ g

Using this mapped peak ground acceleration value and the site class, site coefficient F_{PGA} is determined in accordance with Section 11.8.3 using Table 11.8-1. Using Table 11.8-1, for $PGA = 0.521 > 0.5$, $F_{PGA} = 1.0$ for Site Class C. Using *Provisions* Equation 11.8-1 to determine the maximum considered earthquake geometric mean peak ground acceleration adjusted for site class effects,

$PGA_M = F_{PGA}\, PGA = 1.0(0.521) = 0.521$ g

This value is used directly to assess the potential for liquefaction or for soil strength loss. The design peak ground acceleration used to determine dynamic seismic lateral earth pressures for design of basement and retaining walls is computed as $\frac{2}{3} PGA_M = \frac{2}{3}(0.521) = 0.347$ g.

3.3 SELECTION AND SCALING OF GROUND MOTION RECORDS

Response history analysis (whether linear or nonlinear) consists of the step-wise application of time-varying ground accelerations to a mathematical model of the subject structure. The selection and scaling of appropriate horizontal ground motion acceleration time histories is essential to produce meaningful

results. For two-dimensional or three-dimensional structural analysis, single-component or two-component records are used, respectively. The sections that follow discuss the approach to selection and scaling of ground motion records as prescribed in the *Provisions* (and ASCE 7), illustrate the selection and scaling of two-component ground motions for the structure analyzed in Design Example 6.3 located at the site considered in Section 3.2 and discuss differences in the process for single-component ground motions.

3.3.1 Approach to Ground Motion Selection and Scaling

In the simplest terms the goal of ground motion selection and scaling is to produce acceleration histories that are consistent with the ground shaking hazard anticipated for the subject structure at the site in question. As difficult as it is to forecast the occurrence of an earthquake, it is even more difficult to predict the precise waveform and phasing of the resulting accelerations at a given site. Instead it is necessary to approximate (somewhat crudely) what ground motions can be expected based on past observations (and, possibly, geologic modeling). *Provisions* Section 16.1.3 prescribes the most commonly applied approach to this process. While some aspects of the process are quite prescriptive, others permit considerable latitude in application.

The Pacific Earthquake Engineering Research Center makes available a database of ground motions (at http://peer.berkeley.edu/peer_ground_motion_database/) and a web application for the selection and scaling of ground motions (PEER, 2010). As useful as that data and application are, they do not provide a comprehensive solution to the challenge of ground motion selection and scaling in accordance with the *Provisions* for all U.S. sites. Pertinent limitations include the following.

- The database is limited to shallow crustal earthquakes recorded in "active tectonic regimes," like parts of the western U.S. It does not include records from subduction zone earthquakes, deep intraplate events, or events in less active tectonic regimes (such as the central and eastern U.S.).

- The web application allows use of a code design spectrum (from the *Provisions* or ASCE 7) as a target and includes powerful selection and scaling methods. However, the set of selected and scaled records produced would still require minor adjustment (scaling up) to satisfy the requirements in *Provisions* Section 16.1.3 over the period range of interest.

3.3.1.1 Number of ground motions. In recognition of the impossibility of predicting the actual ground motion history that should be expected, Section 16.1.3 requires the use of at least three ground motions in any response history analysis. Where at least seven ground motions are used, Sections 16.1.4 and 16.2.4 permit the use of average response quantities for design. The difference is not one of statistical significance; in either case mean response is approximated, but an incentive is given for the use of more records, which could identify a potential sensitivity in the response. The objective of the response history analyses is not to evaluate the response of the building for each record (since none of the records used will actually occur), but to determine the expected (average) response quantities for use in design calculations. If the analysis predicts collapse for one or more ground motions, the average cannot be computed; the structure is deemed inadequate and must be redesigned.

3.3.1.2 Recorded or synthetic ground motions. Horizontal ground motion acceleration records should be selected as single components (for two-dimensional analysis) or as orthogonal pairs (for three-dimensional analysis) from actual recorded events. Where the number of appropriate recorded ground motions is insufficient, use of "simulated" records is permitted. While generation of completely artificial records is not directly prohibited, the intent (as expressed in *Provisions* Section C16.1.3) is that such simulation is limited to modification for site distance and soil conditions.

3.3.1.3 "Appropriate" ground motions. The measure of "appropriate" applied to ground motions by the *Provisions* is consistency with the magnitude, fault distance and source mechanism that control the maximum considered earthquake. (Other characteristics of ground motion, such as duration, may influence response, but are not addressed by the *Provisions*.) While it is good practice to select ground motions with these characteristics in mind, the available data are quite limited. And even where the available records are very carefully binned and match the target characteristics quite closely, they are far from homogeneous.

As discussed in Section 3.1 the mapped ground motion parameters reflect the likelihood that a certain level of spectral acceleration will be exceeded in a selected period, considering numerous sources of earthquake ground shaking. While the mapping process does not sum accelerations from various sources it does aggregate the probabilities of occurrence from those sources. As a result, it is impossible to determine the controlling source characteristics using only the mapped acceleration parameters. In order to identify the magnitude, fault distance and source mechanism that control the maximum considered earthquake at a specific spectral period, it is necessary to "deaggregate" the hazard, which requires reviewing the underlying calculations to note the relative contribution of each source. The USGS provides tools to deaggregate hazard, providing results in three formats: a text tabulation, a graphic presentation binned by distance and magnitude and a graphic presentation projected on a map. Figure 3-3 shows the two graphic formats for the 2-second period spectral acceleration with a 2% probability of exceedance in 50 years (the maximum considered earthquake) at the site considered in Section 3.2.

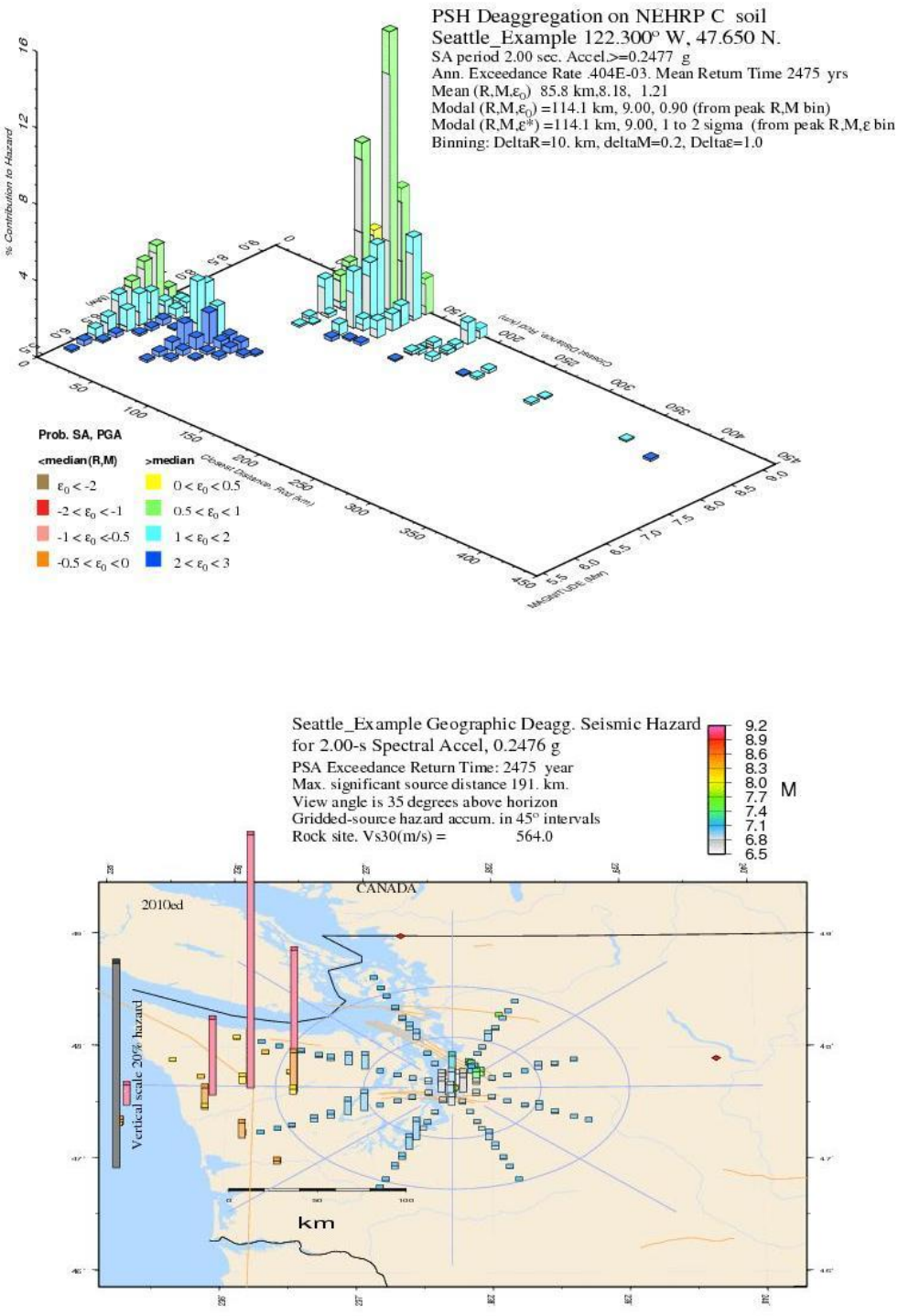

Figure 3-3 Graphic results of deaggregation

At most sites deaggregation of hazard reveals that a single source controls the maximum considered earthquake ground motions for all spectral periods. However, at some sites different sources control the maximum considered earthquake ground motions at different spectral periods. Figure 3-4 shows, for one such site, the maximum considered earthquake response spectrum generated from mapped ground motion

parameters as well as median acceleration response spectra for two of the contributing sources. Since the shape of the uniform hazard spectrum, upon which the design spectrum is based, is artificial (arising from the probabilistic seismic hazard analysis rather than the characteristics of recorded ground motions), there may be conservatisms involved in providing an aggregate match for design purposes (PEER, 2010). However, that aggregate match is exactly what the *Provisions* requires, so it is prudent to consider how that conservatism may best be balanced.

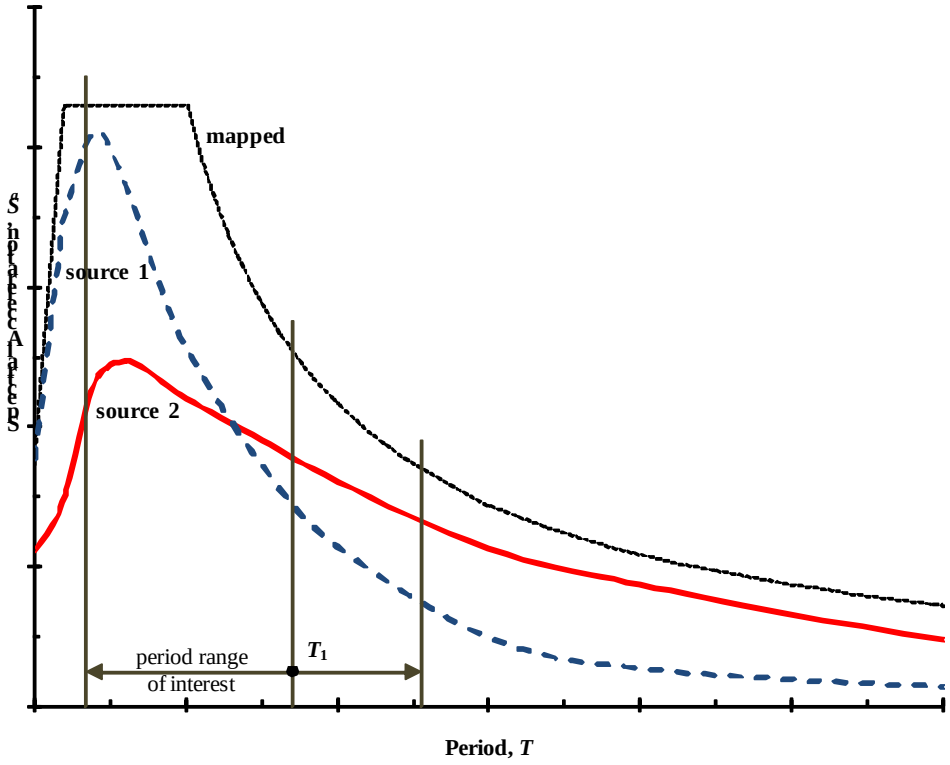

Figure 3-4 Response spectra for a site with multiple controlling sources

In this example, source 1 can generate moderate magnitude events close to the site; Source 2 can generate very large magnitude events far from the site. Due to differing source and attenuation characteristics, each source can control a portion of the MCE_R response spectrum. The response of short period structures or very long period structures will be governed by source 1 or source 2, respectively. However, the "controlling" source is less clear for a structure with a fundamental period shown as T_1 in the figure. Source 2 appears to control at period T_1, but as discussed in Section 3.3.1.5, the *Provisions* defines a wider period range of interest over which the selected ground motions must be "appropriate." As outlined below, three approaches are readily apparent.

- First (and arguably most technically correct), select two full sets of (seven or more) ground motion records conditionally—one set for each source, enveloping the MCE_R spectrum for the **portion** of the period range of interest controlled by that source. Since the corresponding portions of the actual and target spectral shapes would be similar, scale factors would be modest. In this case, an independent series of analyses would be performed for each set of ground motion records. Mean response parameters of interest could be computed for each set of analyses and the more conservative of the two mean values for each response parameter could be used for design verification. Although this approach has technical appeal, the *Provisions* do not outline such a

procedure that makes use of two sets of ground motions, instead requiring use of a single set that on average envelops the entire period range of interest of the target spectrum.

- Second, select a full set of ground motions consistent with Source 2 and then scale the set to envelop the much differently shaped MCE_R spectrum over the specified period range of interest. While permitted by the *Provisions*, this approach would require large scale factors that unrealistically exaggerate the long period response. It may seem that this set of ground motions has a desired degree of homogeneity, but that comes at the expense of a very poor fit for the average.

- Third, select a set with some ground motions for each controlling source type. Select individual scale factors so that the average of their linear elastic spectra envelops the target spectrum (as required by the *Provisions*) and is shaped similarly to the target. As a result of this process, records consistent with Source 1 will control short periods and those consistent with Source 2 will control long periods. The scale factors will be somewhat larger than those required by the first (conditional) approach, but not excessively large like those in the second approach. Although the record set is less homogeneous than that used in the second approach, the average is much closer to the target. Where used for linear response history analysis, this approach will produce average response quantities consistent with the average linear response spectrum used in the scaling process. Where used for nonlinear response history analysis, this approach (which uses scale factors that are larger than those for the conditional approach) will bias the average response quantities to be slightly more conservative and may increase the prediction of response extremes (collapse). This third method is commonly employed by seismological consultants where multiple source types may govern.

3.3.1.4 Scale factors. The most commonly employed ground motion scaling method involves multiplying all of the acceleration values of the time-acceleration pairs by a scalar value. This time-domain scaling modifies the amplitude of the accelerations (to approximate changes in source magnitude and/or distance) without affecting frequency content or phasing. Although not limited by the *Provisions*, the scale factors applied to recorded ground motions should be modest (usually falling between 1/3 and 3); if very small or very large scale factors are needed, some aspect of the event that produced the source motion likely is inconsistent with the maximum considered earthquake being modeled. An identical scale factor is applied to both components of a given ground motion to avoid unrealistically biasing one direction of response. Since the response spectra for time-domain scaled ground motions retain their natural jaggedness, the acceptance criterion compares their average to the target spectrum, without imposing limits on the scaling of individual ground motions. That means that there is no single set of scale factors that may be applied to the selected ground motions (as discussed further in *Provisions* Part 2 Section C16.1.3.2)

Another ground motion scaling method involves transforming the time-acceleration data into the frequency domain (such as by means of the fast Fourier transform), making adjustments (to match exactly the target spectrum at multiple, specific frequencies) and transforming back into the time domain. This method affects amplitude, frequency content and phasing (and tends to increase the total input energy). This method makes it possible to estimate mean response with fewer ground motions, but may obscure somewhat the potential variability of response. Use of this method is permitted by the *Provisions*, but the same number of records is required as for time-domain scaling. Given the jaggedness of individual response spectra, the process of spectral matching (which produces smoother spectra) requires scale factors that can be considerably smaller or larger than those used in time-domain scaling. Since this method applies numerous scale factors to differing frequencies of each ground motion component in order to match spectral ordinates, there is no requirement that the two components be scaled identically. As the spectral ordinates of frequency-domain scaled records may fall below the target spectrum at frequencies

other than those used for matching, a second round of (minor) scaling is needed to satisfy the *Provisions* requirements.

Where single-component records are being selected for two-dimensional analysis the design response spectrum is used as a target; and *Provisions* Section 16.1.3.1 requires that the average of the response spectra not fall below the target over the period range of interest. A different approach is needed where two-component records are being selected for three-dimensional analysis. The code writers selected the square root of the sum of the squares (SRSS) of the response spectra for the two components as a measure of the ground motion amplitude for each record. However, the SRSS of two spectra is always larger than the average (and larger than the maximum). In practical terms for ground motion, it is reasonable to expect that the SRSS is larger than the average by a factor of 1.4 to 1.5 and is larger than the maximum (resultant) by a factor of about 1.2.

The code writers decided that it is sufficiently conservative to scale two-component records such that the average of the SRSS spectra does not fall below the target over the period range of interest. Given the relationship between SRSS and average, that means that scale factors for ground motions used in three-dimensional analysis are only 2/3 of those for ground motions used in two-dimensional analysis. The rationale is that a three-dimensional analysis (using two-component ground motions) subjects the structure to the maximum (resultant) acceleration in **some** direction due to the interaction of ground motion components, while that is not possible in two-dimensional analysis. Considering other conservative criteria, such as fitting over the entire period range of interest, code writers accepted that the resultant acceleration could be about 20 percent less than the design acceleration at some periods. Note that *Provisions* Section 16.1.3.2 erroneously requires that the average of the SRSS spectra not fall below the MCE_R spectrum over the period range of interest. ASCE 7-10 corrects this error by requiring that the average of the SRSS spectra be compared to "the response spectrum used in the design" (rather than to the MCE_R response spectrum).

For the special case described in Section 3.3.1.7 below, both ASCE 7-10 and the *Provisions* require scaling so that the maximum acceleration exceeds the MCE_R response spectrum. Apparently, this is an error carried forward from the *Provisions* to ASCE 7-10. Like the rest of Section 16.1.3.2, the target spectrum used for scaling should be "the response spectrum used in the design" rather than the MCE_R response spectrum (which is 1.5 times the design response spectrum).

3.3.1.5 Period range of interest. The smooth spectral acceleration response spectrum constructed using mapped acceleration parameters (and site response coefficients) is a location-specific estimate of the ground shaking hazard. No matter how carefully recorded ground motions are selected and scaled, it is unrealistic to expect a close match to the smooth target spectrum over all periods. On the other hand, selecting and scaling ground motions to match the target spectrum at the natural period for the fundamental mode of vibration of a structure is not enough to produce reasonable estimates of response; important aspects of structural response (including collapse) are affected by both higher modes of response and period elongation due to yielding. To balance these realities, code writers have established a period range of interest (with respect to the fundamental period, T) that extends from $0.2T$ (to capture higher mode effects) to $1.5T$ (to include period elongation). Although yielding and period elongation cannot occur in linear response history analysis, for simplicity of application ground motions are selected and scaled considering the same period range of interest as for nonlinear response history analysis.

3.3.1.6 Orientation of ground motion components. Accelerometers record earthquake ground shaking along the vertical axis and two horizontal (orthogonal) instrument axes. Acceleration records can be used in the as-recorded orientation, but orientation in the directions normal to and parallel to the strike of the causative fault (termed the fault-normal and fault-parallel directions, respectively) by means of a simple trigonometric transformation permits greater seismological insights, since some ground motions recorded

very close to the causative fault contain rupture directivity effects. The differences may be meaningful for selection and scaling, application in analysis, or both. Since the orientation of instrument axes is arbitrary and reorientation along the fault-normal and fault-parallel directions can provide additional insight, it has become common (but not universal) to reorient all horizontal ground motion records in that manner.

In the very common condition where a site is not within several miles of the controlling source, the orientation of ground shaking is inconsequential, so the *Provisions* contain no general requirement to consider orientation. As discussed in Section 3.3.1.7 below, there is a selection and scaling orientation requirement (but no application orientation requirement) for sites close to active controlling faults.

Figure 3-5 shows the time series of two components of ground acceleration. Component 1 is fault-normal; component 2 is fault-parallel. What is not apparent in such traces is the interaction of the components. Figure 3-6 shows an orbit plot of ground acceleration pairs (effectively zero-period response) for the same recording. The maximum resultant acceleration occurs along a diagonal direction.

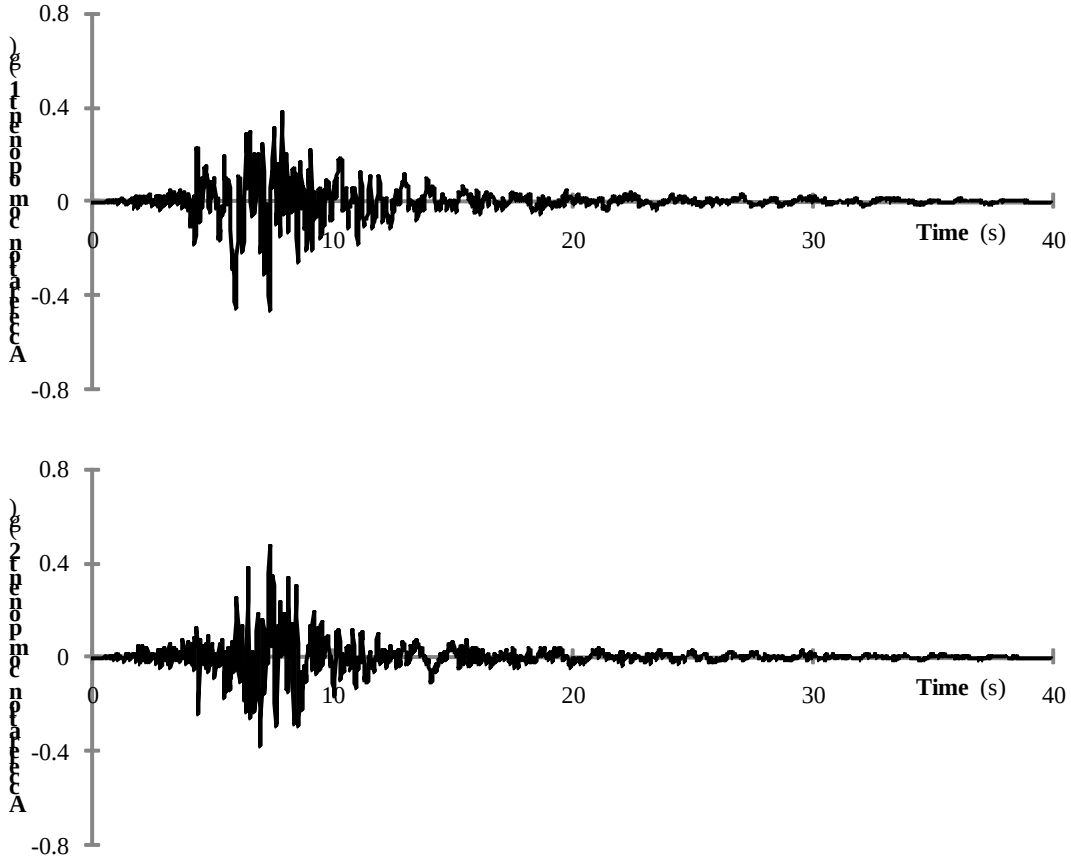

Figure 3-5 Horizontal acceleration components for the 1989 Loma Prieta earthquake (Saratoga – Aloha Avenue recording station)

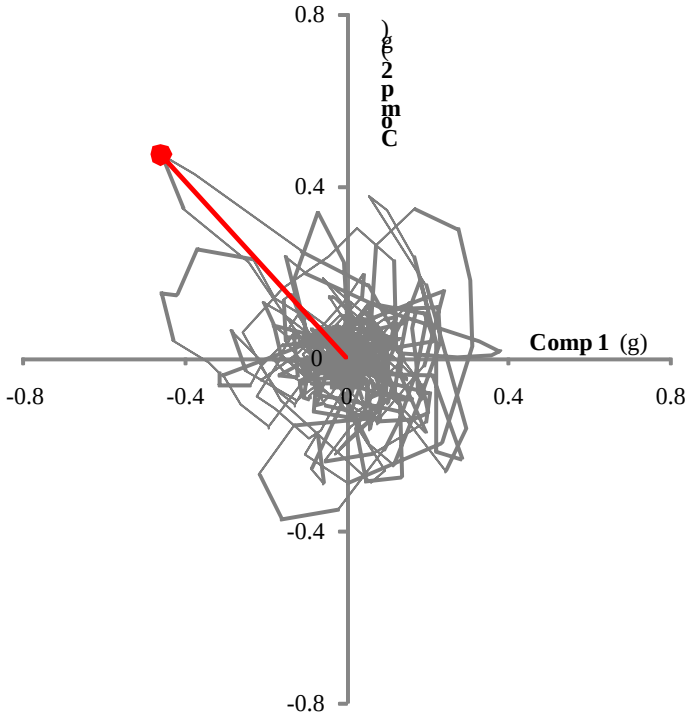

Figure 3-6 Horizontal acceleration orbit plot for the 1989 Loma Prieta earthquake (Saratoga – Aloha Avenue recording station)

Unfortunately, the direction of maximum ground acceleration may or may not correspond to the direction of maximum acceleration response at any other period and the direction of maximum response generally differs at various periods. If bilinear oscillators with various fundamental periods are subjected to the two-component acceleration record, response spectra like those in Figure 3-7 result. The uniaxial response spectra in that figure are identified by component. The "resultant" response spectrum indicates the maximum acceleration along any direction. The SRSS response spectrum is obtained by taking the square root of the sum of the squares of the corresponding component response spectrum ordinates. The case illustrated reflects a possible near-source condition: for long periods, the fault-normal component (component 1) is much larger than the fault-parallel component and is very close to the maximum (resultant) response.

The *Provisions* do not require application of ground motions in multiple possible orientations. Whether using three, seven, or more pairs, it is acceptable to consider a single, arbitrary orientation of a given two-component pair. For example, analysis can be performed with "Component 1" applied in the +X direction without considering the implications of applying that component in the -X, +Y, -Y, or other directions. Since the objective of the analyses is to estimate "average" response quantities, it may be advisable (but is not required) to consider whether there is an unwanted directional bias in the selected and scaled ground motions. For instance, in the common case where the controlling source should not produce strongly directional response, records could be oriented when applied so that the average of the component 1 spectra is similar to the average of the component 2 spectra. The much-less-common case, where strongly directional response is expected, is discussed in Section 3.3.1.7. Section 12.4.4 of these *Design Examples* outlines a more involved approach that is recommended for seismically isolated structures.

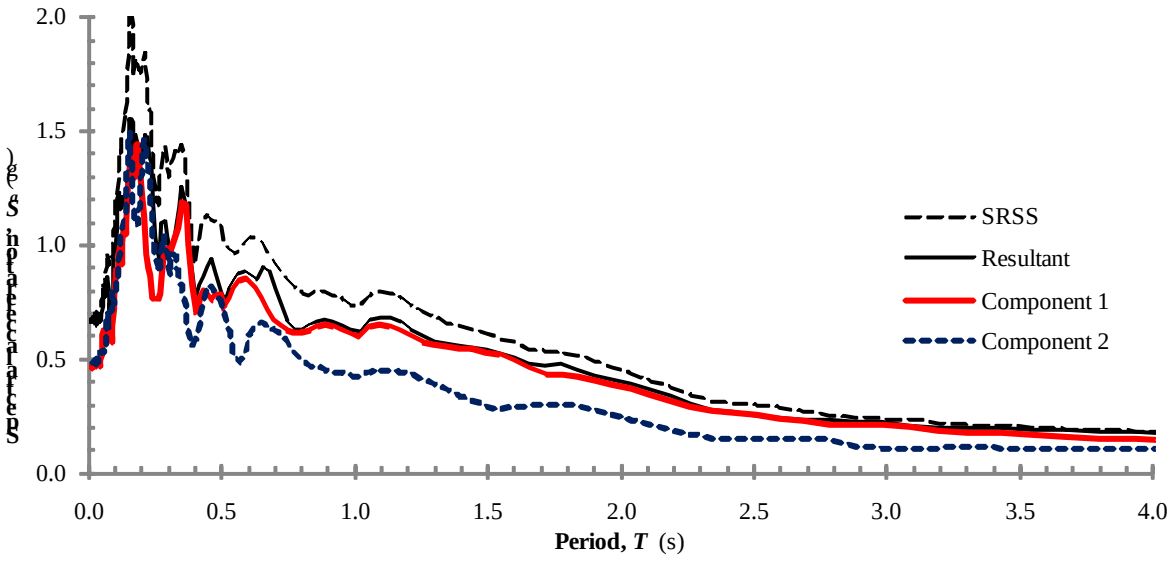

Figure 3-7 Horizontal acceleration response spectra for the 1989 Loma Prieta earthquake (Saratoga – Aloha Avenue recording station)

3.3.1.7 Sites close to controlling active faults. Ground motions at sites close to a causative fault can be strongly directional. At such sites, the maximum long period ground motion often occurs in the fault-normal direction. The last paragraph of *Provisions* Section 16.1.3.2 addresses this case, where code writers have judged that scaling should be more conservative than that achieved using the SRSS-based method. Although this requirement is well intentioned, the specific language provides a degree of additional conservatism that can vary greatly. The intent is that the maximum spectral acceleration for the scaled motions exceeds the target response spectrum.

While it is often true that the fault-normal component is dominant at long periods, some near-field ground motions show no directional bias and some are dominant in the fault-parallel direction. For instance, of the 3182 records in the PEER Ground Motion Database (for shallow crustal earthquakes), only 109 have pulse-like directional effects. Of those, 60 have pulses only in the fault-normal direction, 19 have pulses only in the fault-parallel direction, and 30 have pulses in both directions. As discussed above, it is acceptable to reorient all horizontal ground motion records to the fault-normal and fault-parallel directions. However, that does not assure that the fault-normal component will coincide with the maximum. Figure 3-8 shows response spectra for a ground motion where the fault-parallel direction (component 2) dominates for long periods. Scaling such that the fault-normal component exceeds the target response spectrum, as required in the last paragraph of Section 16.1.3.2, would force the maximum well above the target response spectrum. To obtain the intended result, ground motions should "be scaled so that the average of the ~~fault-normal~~ dominant components is not less than the ~~MCE$_R$~~ response spectrum used in the design for the period range from 0.2*T* to 1.5*T*." (Section 3.3.1.4 above explains why all of Section 16.1.3.2 should refer to the response spectrum used in the design rather than to the MCE$_R$ response spectrum.)

While the *Provisions* set forth orientation requirements for the selection and scaling of ground motions at sites close to controlling active faults, the orientation of ground motion components as applied in analysis is not prescribed. After going to the effort of orienting records in the fault-normal and fault-parallel directions and applying special rules for scaling in recognition of near-source effects, it would be prudent

(but not required) to apply the records in the analyses consistent with the fault-normal and fault-parallel directions at the actual site.

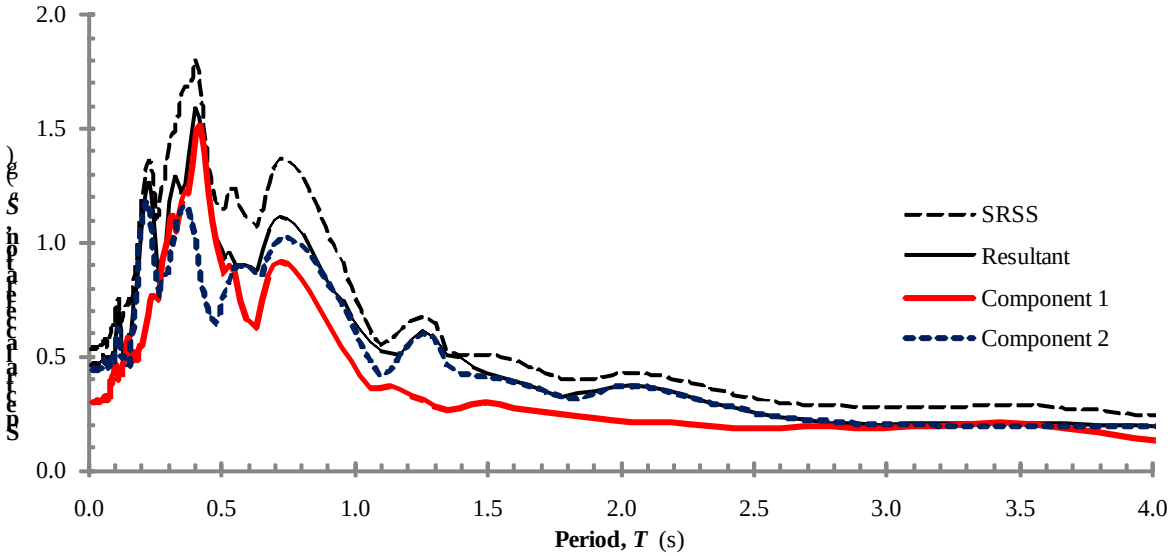

Figure 3-8 Horizontal acceleration response spectra for 1999 Duzce, Turkey earthquake (Duzce recording station)

3.3.2 Two-Component Records for Three Dimensional Analysis

Design Example 6.3 is a buckling restrained braced frame structure located at the Seattle, Washington site considered in Section 3.2. Some aspects of the design are based on results from three-dimensional nonlinear response history analysis performed in accordance with *Provisions* Section 16.2. This section illustrates application of the procedures described in Section 3.3.1 for the selection and scaling of two-component ground motion records. Pertinent information from Sections 3.2 and 6.3.6.1 is summarized as follows.

- Location: 47.65ºN, 122.3ºW
- Site Class C
- S_{MS} = 1.289
- S_{M1} = 0.649
- T_L = 6 seconds
- $T_x = T_y$ = 2.3 seconds

The period range of interest is from 0.2 × 2.3 = 0.46 seconds to 1.5 × 2.3 = 3.45 seconds. If the two fundamental translational periods differed, the period range of interest would extend from 0.2 times the shorter period to 1.5 times the longer period.

The next step is to deaggregate the hazard, as discussed in Section 3.3.1.3, over the period range of interest. Figure 3-9 shows the MCE_R (target) response spectrum and the relative contributions of three important sources to spectral acceleration at periods between 0 and 4 seconds. For periods greater than about 1.5 seconds, ground shaking hazard is controlled by very large, but distant, subduction zone events. At shorter periods, hazard is controlled by deep intraplate events, with substantial contributions from shallow crustal events. It is necessary to identify not only the magnitude of the controlling event, but also

the distance and source type. Short and intermediate period response may be more important than long period response (depending on the period of the structure).

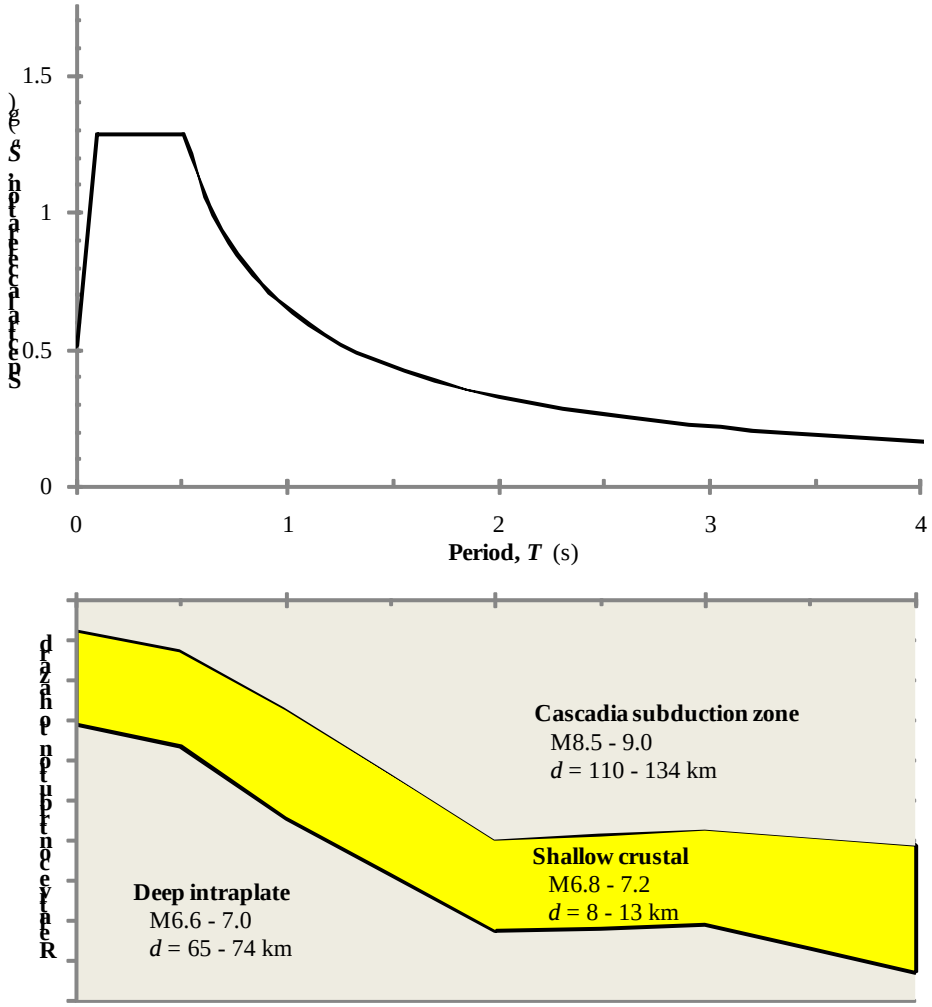

Figure 3-9 MCE_R response spectrum and corresponding hazard contributions

Since the MCE_R response spectrum over the period range of interest is controlled by multiple sources with substantially different spectral shapes, the procedure recommended in Section 3.3.1.3 is used. Table 3-1 provides key information for the selected ground motion records. Few large magnitude subduction zone records are available. Records 1, 2 and 3 are for slightly smaller events than those that control the long period hazard, but at closer distances. These differences are partially offsetting so the required scale factors are acceptable. Record 4 is nearly a perfect match for the hazard that controls short period response; and it is from a past occurrence of a similar event in the same region. Records 5, 6 and 7 are from shallow crustal events with magnitude and distance appropriate for this site. Two of those records include near-source velocity pulses. In a manner similar to that illustrated in Figure 3-4, the actual spectra for the selected ground motion records control different periods of response. Figure 3-10 shows the SRSS spectra for Records 1 and 4, along with the target (MCE_R) spectrum. The subduction zone event (Record No. 1) dominates long period response; the deep intraplate event (Record No. 4) dominates short period response.

Table 3-1 Selected and Scaled Ground Motions for Example Site

Record No.	Year	Earthquake name	M	Source type	Recording station	Distance (km)	Scale factor
1	2003	Tokachi-oki, Japan	8.3	Subduction zone	HKA 094	67	2.99
2	2003	Tokachi-oki, Japan	8.3	Subduction zone	HKD 092	46	0.96
3	1968	Tokachi-oki, Japan	8.2	Subduction zone	Hachinohe (S-252)	71	1.28
4	1949	Western Washington	7.1	Deep intraplate	Olympia	75	1.92
5	1989	Loma Prieta	6.9	Shallow crustal	Saratoga -- Aloha Ave	9	1.28
6	1999	Duzce, Turkey	7.1	Shallow crustal	Duzce	7	0.85
7	1995	Kobe, Japan	6.9	Shallow crustal	Nishi-Akashi	7	1.18

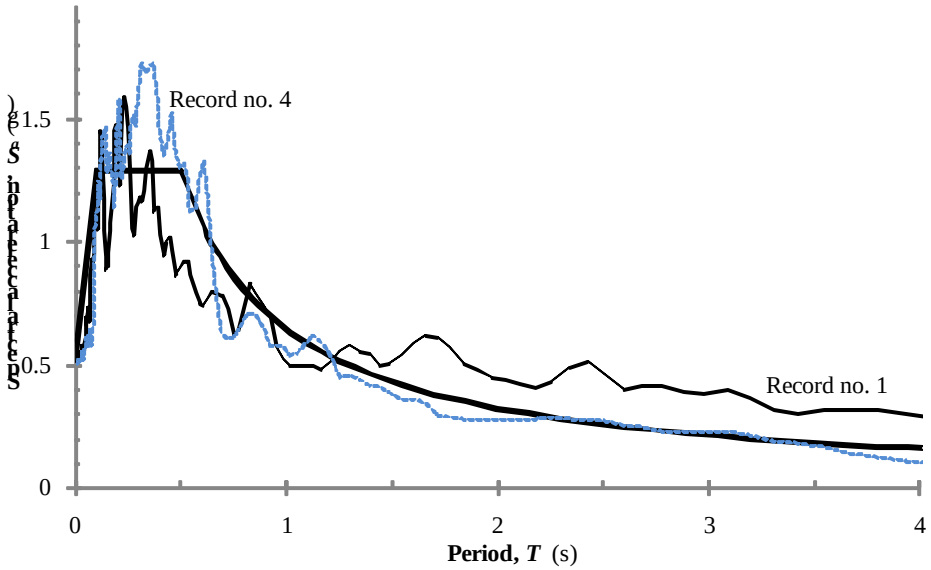

Figure 3-10 SRSS response spectra from different source types

Figure 3-11 compares the average of the SRSS spectra for the selected ground motions with the target (MCE_R) response spectrum. It also shows the period range of interest for ground motion selection for this structure. In an average sense the suite of ground motions provides a very good fit to the target. Since seven records are used, average response quantities may be used in design. This suite so well matches the target spectrum that it could be used with no modification for periods from 0.18 to 4.95 seconds, a range much wider than the period range of interest defined in *Provisions* Section 16.1.3.2. Since this suite of ground motions has been selected and scaled to match the MCE_R response spectrum, an additional scale factor of 2/3 must be applied when the records are used in an analysis to represent design-level conditions.

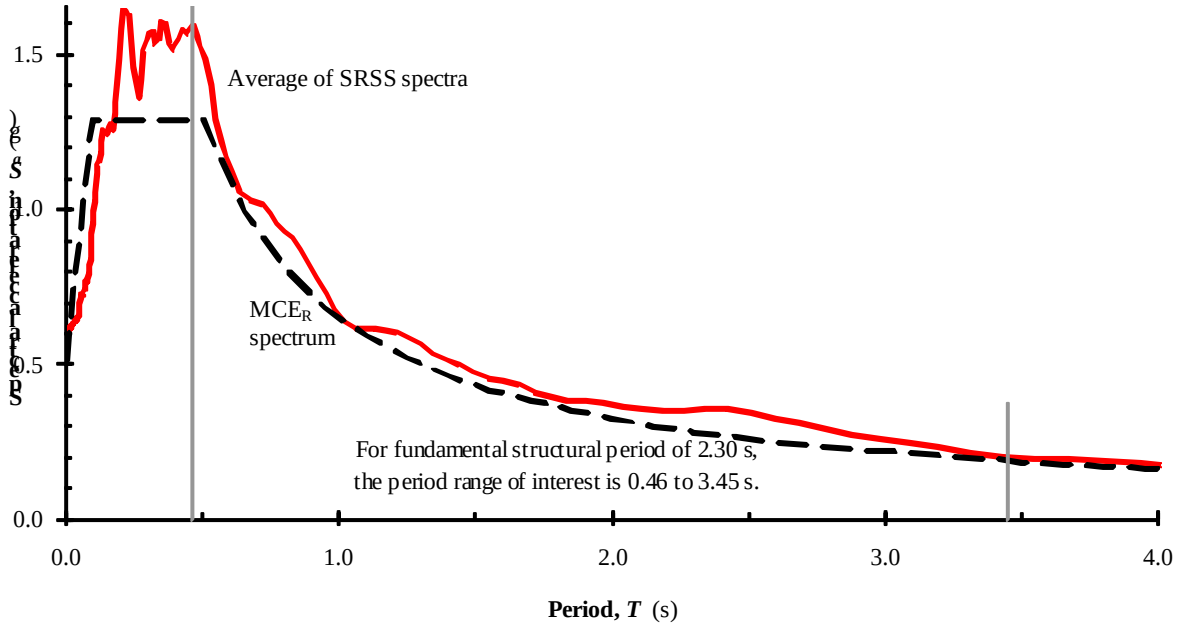

Figure 3-11 Fit of the selected suite of ground motion records to the target spectrum (for three-dimensional analysis)

3.3.3 One-Component Records for Two-Dimensional Analysis

As discussed in Section 3.3.1.4, one-component records (for use in two-dimensional analysis) are selected and scaled such that their **average** fits the design response spectrum, which is two-thirds of the MCE_R response spectrum. Figure 3-12 compares the average of the 14 component spectra (for the records selected and scaled in Section 3.3.2) to the design response spectrum. These records provide an excellent fit to the target spectrum. The suite of 14 records could be used without modification. If a subset of seven records were selected, some minor adjustment to scale factors might be required. Figure 3-12 also shows the average of the SRSS spectra for those 14 scaled records. As observed in Section 3.3.1.4, the average of the SRSS spectra is about 1.5 times the average of the component spectra. Therefore, if the same suite of records was used for three-dimensional analysis, the scale factors required would be about 2/3 of those required for two-dimensional analysis, due to the difference between average and SRSS spectra (and not due to the purely coincidental 2/3 relationship between design and MCE_R response spectra).

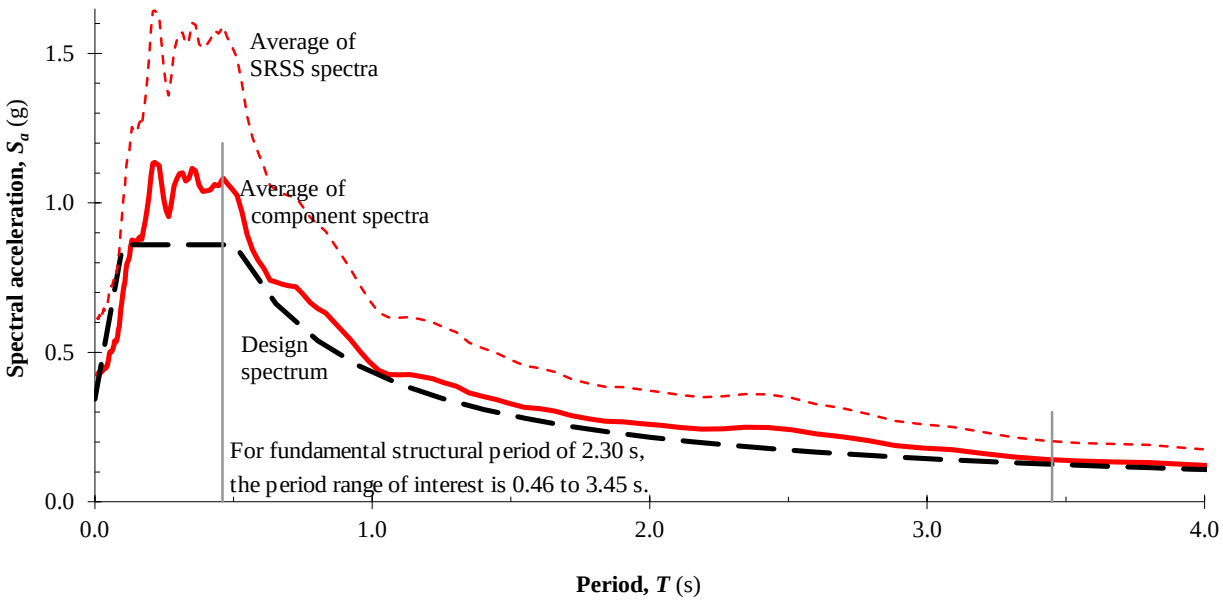

Figure 3-12 Fit of the selected suite of ground motion records to the target spectrum (for two-dimensional analysis)

3.3.4 References

PEER. 2010. *Technical Report for the PEER Ground Motion Database Web Application*, Pacific Earthquake Engineering Research Center, Berkeley, California.

4

Structural Analysis

Finley Charney, Adrian Tola Tola and Ozgur Atlayan

Contents

4.1 IRREGULAR 12-STORY STEEL FRAME BUILDING, STOCKTON, CALIFORNIA 3
4.1.1 Introduction.....3
4.1.2 Description of Building and Structure.....3
4.1.3 Seismic Ground Motion Parameters.....4
4.1.4 Dynamic Properties 8
4.1.5 Equivalent Lateral Force Analysis.....11
4.1.6 Modal Response Spectrum Analysis 29
4.1.7 Modal Response History Analysis.....39
4.1.8 Comparison of Results from Various Methods of Analysis.....50
4.1.9 Consideration of Higher Modes in Analysis 53
4.1.10 Commentary on the ASCE 7 Requirements for Analysis 56
4.2 SIX-STORY STEEL FRAME BUILDING, SEATTLE, WASHINGTON.....57
4.2.1 Description of Structure.....57
4.2.2 Loads.....60
4.2.3 Preliminaries to Main Structural Analysis.....64
4.2.4 Description of Model Used for Detailed Structural Analysis.....72
4.2.5 Nonlinear Static Analysis 94
4.2.6 Response History Analysis.....109
4.2.7 Summary and Conclusions 134

This chapter presents two examples that focus on the dynamic analysis of steel frame structures:

1. A 12-story steel frame building in Stockton, California. The highly irregular structure is analyzed using three techniques: equivalent lateral force analysis, modal response spectrum analysis and modal response history analysis. In each case, the structure is modeled in three dimensions and only linear elastic response is considered. The results from each of the analyses are compared and the accuracy and relative merits of the different analytical approaches are discussed.

2. A six-story steel frame building in Seattle, Washington. This regular structure is analyzed using both linear and nonlinear techniques. Due to the regular configuration of the structural system, the analyses are performed for only two dimensions. For the nonlinear analysis, two approaches are used: static pushover analysis and nonlinear response history analysis. The relative merits of pushover analysis versus response history analysis are discussed.

   Although the Seattle building, as originally designed, responds reasonably well under the design ground motions, a second set of response history analyses is presented for the structure augmented with added viscous fluid damping devices. As shown, the devices have the desired effect of reducing the deformation demands in the critical regions of the structure.

In addition to the *Standard*, the following documents are referenced:

AISC 341	American Institute of Steel Construction. 2005. *Seismic Provisions for Structural Steel Buildings*.
AISC 358	American Institute of Steel Construction. 2005. *Prequalified Connections for Special and Intermediate Steel Moment Frames for Seismic Applications*.
AISC 360	American Institute of Steel Construction. 2005. *Specification for Structural Steel Buildings*.
AISC Manual	American Institute of Steel Construction. 2005. *Manual of Steel Construction*, 13th Edition.
AISC SDM	American Institute of Steel Construction. 2006. *Seismic Design Manual*.
ASCE 41	American Society of Civil Engineers. 2006. *Seismic Rehabilitation of Existing Buildings*.
ASCE 7-10	American Society of Civil Engineers. 2010. *Minimum Design Loads for Buildings and Other Structures*
Charney & Marshall	Charney, F. A. and Marshall, J. D., 2006, "A comparison of the Krawinkler and Scissors models for including beam-column joint deformations in the analysis of steel frames," *Engineering Journal*, 43(1), 31-48.
Charney (2008)	Charney, F. A., 2008, "Unintended consequences of modeling damping in structures," *Journal of Structural Engineering*, 134(4), 581-592.
Clough & Penzien	Ray W. Clough and Joseph Penzien, *Dynamics of Structures*, 2nd Edition.

FEMA 440 — Federal Emergency Management Agency. 2005. *Improvement of Nonlinear Static Seismic Analysis Procedures*

FEMA P-750 — Federal Emergency Management Agency. 2010. *2009 NEHRP Recommended Seismic Provisions for Buildings and Other Structures*

Prakash et al. (1993) — Prakash, V., Powell, G.H. and Campbell, S., 1993, *Drain 2DX Base Program Description and User's Guide*, University of California, Berkeley, CA.

Uang & Bertero — Uang C.M. and Bertero V.V., 1990, "Evaluation of Seismic Energy in Structures", *Earthquake Engineering and Structural Dynamics*, 19, 77-90.

4.1 IRREGULAR 12-STORY STEEL FRAME BUILDING, STOCKTON, CALIFORNIA

4.1.1 Introduction

This example presents the analysis of a 12-story steel frame building under seismic effects acting alone. Gravity forces due to dead and live load are not computed. For this reason, member stress checks, member design and detailing are not discussed. Load combinations that include gravity effects are considered, however. For detailed examples of the seismic-resistant design of structural steel buildings, see Chapter 6 of this volume of design examples.

The analysis of the structure, shown in Figures 4.1-1 through 4.1-3, is performed using three methods:

1. The Equivalent Lateral Force (ELF) procedure based on the requirements of *Standard* Section 12.8,

2. The modal response spectrum procedure based on the requirements of *Standard* Section 12.9 and

3. The modal response history procedure based on the requirements of Chapter 16 of ASCE 7-10. (The 2010 version of the *Standard* is used for this part of the example because it eliminates several omissions and inconsistencies that were present in Chapter 16 of ASCE 7-05.)

In each case, special attention is given to applying the *Standard'* rules for direction of loading and for accidental torsion. All analyses were performed in three dimensions using the finite element analysis program SAP2000 (developed by Computers and Structures, Inc., Berkeley, California).

4.1.2 Description of Building and Structure

The building has 12 stories above grade and a one-story basement below grade and is laid out on a rectangular grid with a maximum of seven 30-foot-wide bays in the X direction and seven 25-foot bays in the Y direction. Both the plan and elevation of the structure are irregular with setbacks occurring at Levels 5 and 9. All stories have a height of 12.5 feet except for the first story which is 18 feet high and the basement which extends 18 feet below grade. Reinforced 1-foot-thick concrete walls form the perimeter of the basement. The total height of the building above grade is 155.5 feet.

Gravity loads are resisted by composite beams and girders that support a normal-weight concrete slab on metal deck. The slab has an average thickness of 4.0 inches at all levels except Levels G, 5 and 9. The slabs on Levels 5 and 9 have an average thickness of 6.0 inches for more effective shear transfer through the diaphragm. The slab at Level G is 6.0 inches thick to minimize pedestrian-induced vibrations and to support heavy floor loads. The low roofs at Levels 5 and 9 are used as outdoor patios and support heavier live loads than do the upper roofs or typical floors.

At the perimeter of the base of the building, the columns are embedded into pilasters cast into the basement walls, with the walls supported on reinforced concrete tie beams over drilled piers. Interior columns are supported by concrete caps over drilled piers. A grid of reinforced concrete grade beams connects all tie beams and pier caps.

The lateral load-resisting system consists of special steel moment frames at the perimeter of the building and along Grids C and F. For the frames on Grids C and F, the columns extend down to the foundation, but the lateral load-resisting girders terminate at Level 5 for Grid C and Level 9 for Grid F. Girders below these levels are simply connected. Since the moment-resisting girders terminate in Frames C and F, much of the Y direction seismic shears below Level 9 are transferred through the diaphragms to the frames on Grids A and H. Overturning moments developed in the upper levels of these frames are transferred down to the foundation by axial forces in the columns. Columns in the moment-resisting frame range in size from W24x146 at the roof to W24x229 at Level G. Girders in the moment frames vary from W30x108 at the roof to W30x132 at Level G. Members of the moment-resisting frames have a nominal yield strength of 36 ksi and floor members and interior columns that are sized strictly for gravity forces have a nominal yield strength of 50 ksi.

4.1.3 Seismic Ground Motion Parameters

For this example the relevant seismic ground motion parameters are as follows:

- $S_S = 1.25$
- $S_1 = 0.40$
- Site Class C

From *Standard* Tables 11.4-1 and 11.4-2:

- $F_a = 1.0$
- $F_v = 1.4$

Using *Standard* Equations 11.4-1 through 11.4-4:

- $S_{MS} = F_a S_s = 1.0(1.25) = 1.25$
- $S_{M1} = F_v S_1 = 1.4(0.4) = 0.56$
- $S_{DS} = \frac{2}{3} S_{MS} = \frac{2}{3}(1.25) = 0.833$
- $S_{D1} = \frac{2}{3} S_{M1} = \frac{2}{3}(0.56) = 0.373$

As the primary occupancy of the building is business offices, the Occupancy Category is II (*Standard* Table 1-1) and the Importance Factor (*I*) is 1.0 (*Standard* Table 11.5-1). According to *Standard* Tables 11.6-1 and 11.6-2, the Seismic Design Category (SDC) for this building is D.

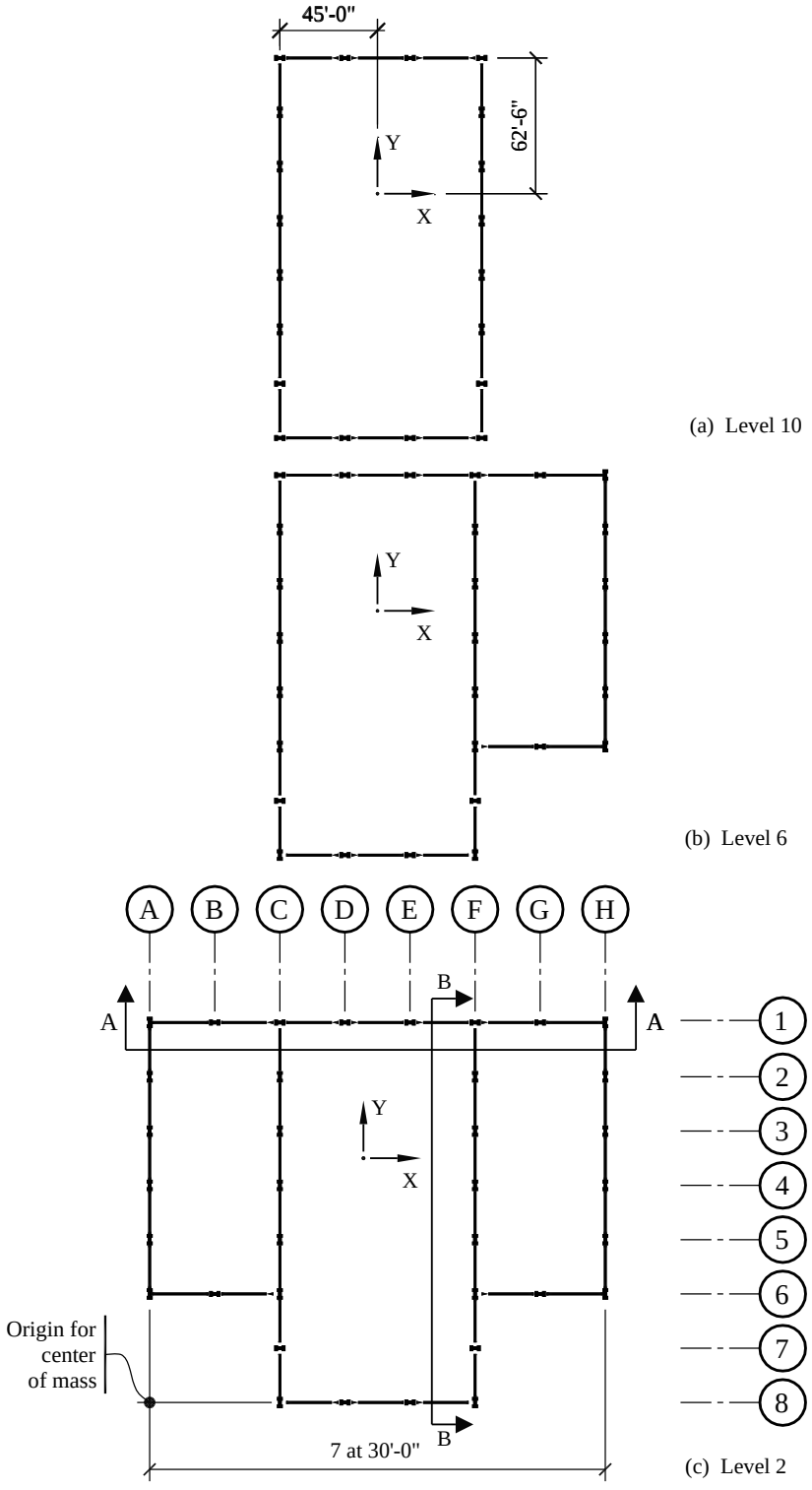

Figure 4.1-1 Various floor plans of 12-story Stockton building

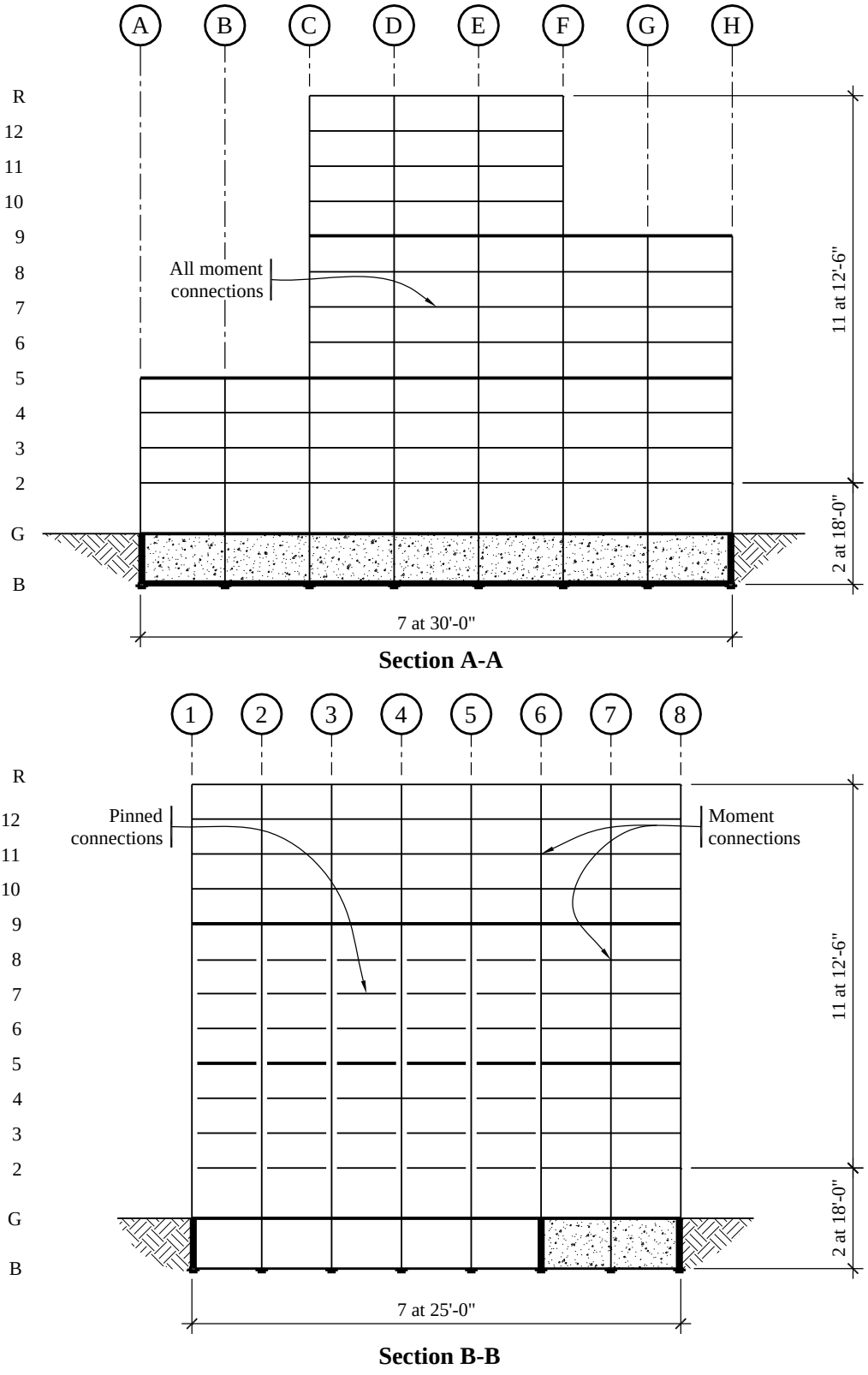

Figure 4.1-2 Sections through Stockton building

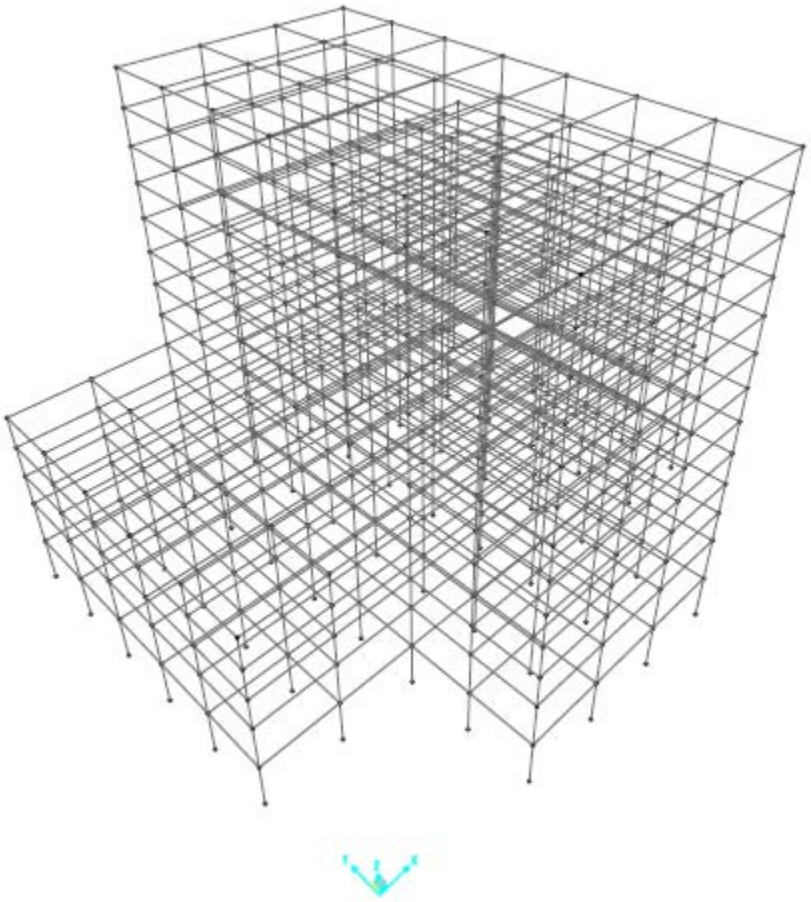

Figure 4.1-3 Three-dimensional wire-frame model of Stockton building

The lateral load-resisting system of the building is a special moment-resisting frame of structural steel. For this type of system, *Standard* Table 12.2-1 has a response modification coefficient (R) of 8 and a deflection amplification coefficient (C_d) of 5.5. There is no height limit for special moment frames. Section 12.2.5.5 of the standard requires that special moment frames in SDC D, where required by Table 12.1-1, be continuous to the foundation. While the girders of the interior moment frames are not present at the lower levels of the interior frames, the frames are continuous to the foundation and the columns are detailed as required for special moment frames. Additionally, there are no other structural system types below the moment frames. Therefore, in the opinion of the author, the requirement is met.

Standard Table 12.6-1 is used to determine the minimum level of analysis. Because of the setbacks, the structure clearly has a weight irregularity (Irregularity Type 2 in *Standard* Table 12.3-2). Thus, the minimum level of analysis required for the SDC D building is modal response spectrum analysis. However, the determination of torsional irregularities, the application of accidental torsion effects and the assessment of P-delta effects are based on ELF analysis procedures. For this reason and for comparison purposes, a complete ELF analysis is carried out and described herein.

4.1.4 Dynamic Properties

Before any analysis can be carried out, it is necessary to determine the dynamic properties of the structure. These properties include stiffness, mass and damping. The stiffness of the structure is numerically represented by the system stiffness matrix, which is computed automatically by SAP2000. The terms in this matrix are a function of several modeling choices that are made. These aspects of the analysis are described later in the example. The computer can also determine the mass properties automatically, but for this analysis they are developed by hand and are explicitly included in the computer model. Damping is represented in different ways for the different methods of analysis, as described in Section 4.1.4.2.

4.1.4.1 Seismic Weight. In the past it was often advantageous to model floor plates as rigid diaphragms because this allowed for a reduction in the total number of degrees of freedom used in the analysis and a significant reduction in analysis time. Given the speed and capacity of most personal computers, the use of rigid diaphragms is no longer necessary and the floor plates may be modeled using 4-node shell elements. The use of such elements provides an added benefit of improved accuracy because the true "semi-rigid" behavior of the diaphragms is modeled directly. Where it is not necessary to recover diaphragm stresses, a very coarse element mesh may be used for modeling the diaphragm.

Where the diaphragm is modeled using finite elements, the diaphragm mass, including contributions from structural dead weight and superimposed dead weight, is automatically represented by entering the proper density and thickness of the diaphragm elements. The density may be adjusted to represent superimposed dead loads (but the thickness and modulus are "true" values). Line mass, such as window walls and exterior cladding, are modeled with frame element line masses. While complete building masses are easily represented in this manner, the SAP2000 program does not automatically compute the locations of the centers of mass, so these must be computed separately. Center of mass locations are required for the purpose of applying lateral forces in the ELF method and for determining story drift.

Due to the various sizes and shapes of the floor plates and to the different dead weights associated with areas within the same floor plate, the computation of mass properties is not easily carried out by hand. For this reason, a special purpose computer program was used. The basic input for the program consists of the shape of the floor plate, its mass density and definitions of auxiliary masses such as line, rectangular and concentrated mass.

The uniform area and line masses (in weight units) associated with the various floor plates are given in Tables 4.1-1 and 4.1-2. The line masses are based on a cladding weight of 15.0 psf, story heights of 12.5 or 18.0 feet and parapets 4.0 feet high bordering each roof region. Figure 4.1-4 shows where each mass type occurs. The total computed floor mass, mass moment of inertia and locations of center of mass are shown in Table 4.1-3. Note that the mass moments of inertia are not required for the analysis but are provided in the table for completeness. The reference point for center of mass location is the intersection of Grids A and 8.

Table 4.1-3 includes a mass computed for Level G of the building. This mass is associated with an extremely stiff story (the basement level) and is dynamically excited by the earthquake in very high frequency modes of response. As shown later, this mass is not included in equivalent lateral force computations.

Table 4.1-1 Area Weights Contributing to Masses on Floor Diaphragms

Mass Type	Area Weight Designation				
	A	B	C	D	E
Slab and Deck (psf)	50	75	50	75	75
Structure (psf)	20	20	20	20	50
Ceiling and Mechanical (psf)	15	15	15	15	15
Partition (psf)	10	10	0	0	10
Roofing (psf)	0	0	15	15	0
Special (psf)	0	0	0	60	25
Total (psf)	95	120	100	185	175

See Figure 4.1-4 for mass location.
1.0 psf = 47.9 N/m^2.

Table 4.1-2 Line Weights Contributing to Masses on Floor Diaphragms

Mass Type	Line Weight Designation				
	1	2	3	4	5
From Story Above (plf)	60.0	93.8	93.8	93.8	135.0
From Story Below (plf)	93.8	93.8	0.0	135.0	1,350.0
Total (plf)	153.8	187.6	93.8	228.8	1,485.0

See Figure 4.1-4 for mass location.
1.0 plf = 14.6 N/m.

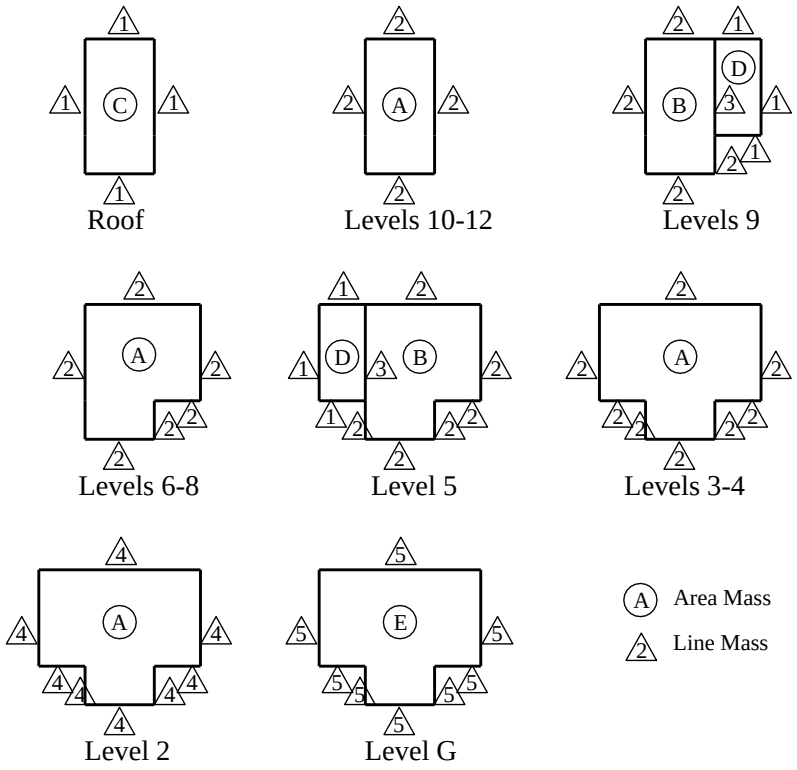

Figure 4.1-4 Key diagram for computation of floor weights

Table 4.1-3 Floor Weight, Floor Mass, Mass Moment of Inertia and Center of Mass Locations

Level	Weight (kips)	Mass (kip-sec$^{2/}$in.)	Mass Moment of Inertia (in.-kip-sec$^{2/}$/radian)	X Distance to C.M. (in.)	Y Distance to C.M. (in.)
R	1,657	4.287	2.072×10^6	1,260	1,050
12	1,596	4.130	2.017×10^6	1,260	1,050
11	1,596	4.130	2.017×10^6	1,260	1,050
10	1,596	4.130	2.017×10^6	1,260	1,050
9	3,403	8.807	5.309×10^6	1,638	1,175
8	2,331	6.032	3.703×10^6	1,553	1,145
7	2,331	6.032	3.703×10^6	1,553	1,145
6	2,331	6.032	3.703×10^6	1,553	1,145
5	4,320	11.19	9.091×10^6	1,160	1,206
4	3,066	7.935	6.356×10^6	1,261	1,184
3	3,066	7.935	6.356×10^6	1,261	1,184
2	3,097	8.015	6.437×10^6	1,262	1,181
G	6,525	16.89	1.503×10^7	1,265	1,149
Σ	36,912				

1.0 in. = 25.4 mm, 1.0 kip = 4.45 kN.

4.1.4.2 Damping. Where an equivalent lateral force analysis or a modal response spectrum analysis is performed, the structure's damping, assumed to be 5 percent of critical, is included in the development of the spectral accelerations S_S and S_1. An equivalent viscous damping ratio of 0.05 is appropriate for linear analysis of lightly damaged steel structures.

Where recombining the individual modal responses in modal response spectrum analysis, the square root of the sum of the squares (SRSS) technique has generally been replaced in practice by the complete quadratic combination (CQC) approach. Indeed, *Standard* Section 12.9.3 requires that the CQC approach be used where the modes are closely spaced. Where using the CQC approach, the analyst must correctly specify a damping factor. This factor, which is entered into the SAP2000 program, must match that used in developing the response spectrum. It should be noted that if zero damping is used in CQC, the results are the same as those for SRSS.

For modal response history analysis, SAP2000 allows an explicit damping ratio to be used in each mode. For this structure, a damping of 5 percent of critical was specified in each mode.

4.1.5 Equivalent Lateral Force Analysis

Prior to performing modal response spectrum or response history analysis, it is necessary to perform an ELF analysis of the structure. This analysis is used for preliminary design, for evaluating torsional regularity, for computing torsional amplification factors (where needed), for application of accidental torsion, for evaluation of P-delta effects and for development of redundancy factors.

The first step in the ELF analysis is to determine the period of vibration of the building. This period can be "accurately" computed from a three-dimensional computer model of the structure. However, it is first necessary to estimate the period using empirical relationships provided by the *Standard*.

Standard Equation 12.8-7 is used to estimate the building period:

$$T_a = C_t h_n^x$$

where, from *Standard* Table 12.8-2, $C_t = 0.028$ and $x = 0.8$ for a steel moment frame. Using h_n = the total building height (above grade) = 155.5 ft, $T_a = 0.028(155.5)^{0.8} = 1.59$ seconds[1].

Even where the period is accurately computed from a properly substantiated structural analysis (such as an eigenvalue or Rayleigh analysis), the *Standard* requires that the period used for ELF base shear calculations not exceed $C_u T_a$ where $C_u = 1.4$ (from *Standard* Table 12.8-1 using $S_{D1} = 0.373$). For the structure under consideration, $C_u T_a = 1.4(1.59) = 2.23$ seconds.

Note that where the accurately computed period is less than $C_u T_a$, the computed period should be used. In no case, however, is it necessary to use a period less than $T = T_a = 1.59$ seconds. The use of the Rayleigh method and the eigenvalue method of determining accurate periods of vibration are illustrated in a later part of this example.

In anticipation of the accurately computed period of the building being greater than 2.23 seconds, the ELF analysis is based on a period of vibration equal to $C_u T_a = 2.23$ seconds[2]. For the ELF analysis, it is

[1] The proper computational units for period of vibration are theoretically "seconds/cycle". However, it is traditional to use units of "seconds," and this is done in the remainder of this example.
[2] As shown later in this example, the computed period is indeed greater than $C_u T_a$.

assumed that the structure is "fixed" at grade level. Hence, the total effective weight of the structure (see Table 4.1-3) is the total weight minus the grade level weight, or 36,920 – 6,526 = 30,394 kips.

4.1.5.1 Base shear and vertical distribution of force. Using *Standard* Equation 12.8-1, the total seismic base shear is:

$$V = C_s W$$

where W is the total weight of the structure. From *Standard* Equation 12.8-2, the maximum (constant acceleration region) spectral acceleration is:

$$C_{S_{max}} = \frac{S_{DS}}{(R/I)} = \frac{0.833}{8/1} = 0.104$$

Standard Equation 12.8-3 controls in the constant velocity region:

$$C_S = \frac{S_{D1}}{T(R/I)} = \frac{0.373}{2.23(8/1)} = 0.021$$

However, the acceleration must not be less than that given by *Standard* Equation 12.8-5:

$$C_{S_{min}} = 0.044 I S_{DS} \geq 0.01 = 0.044(1)(0.833) = 0.037$$

The C_s value determined from Equation 12.8-5 controls the seismic base shear for this building. Using W = 30,394 kips, V = 0.037(30,394) = 1,124 kips. The acceleration response spectrum given by the above equations is plotted in Figure 4.1-5.

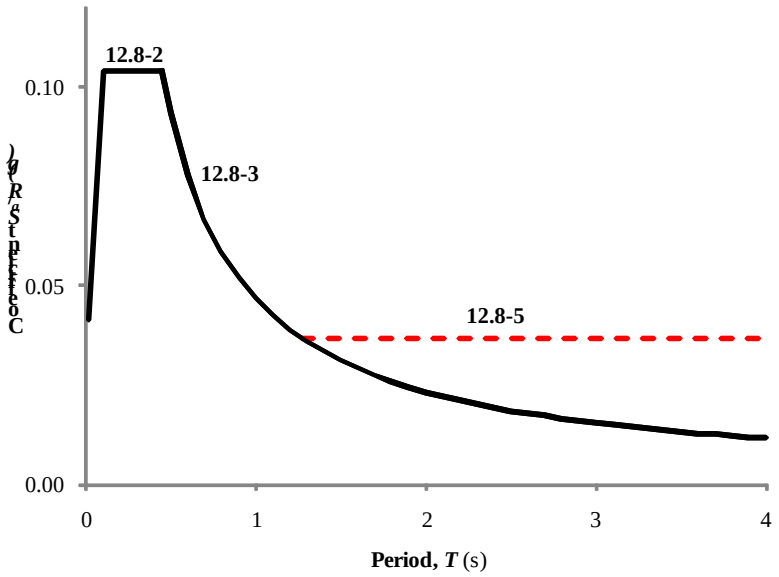

Figure 4.1-5 Computed ELF total acceleration response spectrum

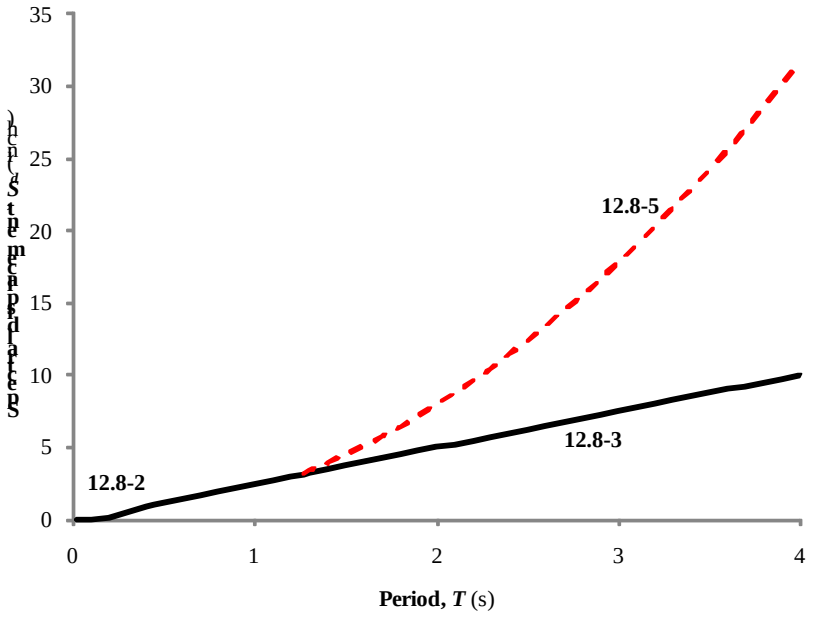

Figure 4.1-6 Computed ELF relative displacement response spectrum

While it is reasonable to use Equation 12.8-5 to establish a minimum base shear, the equation should not be used as a basis determining lateral forces used in displacement computations. The effect of using Equation 12.8-5 for displacements is shown in Figure 4.1-6, which represents Equations 12.8-2, 12.8-3 and 12.8-5 in the form of a displacement spectrum. It can be seen from this figure that the dotted line, representing Equation 12.8-5, will predict significantly larger displacements than Equation 12.8-3. The problem with the line represented by Equation 12.8-5 is that it gives an exponentially increasing displacement up to unlimited periods, whereas it is expected that the true spectral displacements will converge towards a constant displacement (the maximum ground displacement) at large periods. In other words, Equation 12.8-5 should not be considered as a branch of the response spectrum—it is simply used to represent the lower bound on design base shear. The *Standard* does not directly recognize this problem. However, Section 12.8.6.2 allows the deflection analysis of the seismic force-resisting system to be based on the accurately computed fundamental period of vibration, without the $C_u T_a$ upper limit on period. It is the 'authors' opinion that this clause may be used to justify drift calculations with forces based on Equation 12.8-3 even when Equation 12.8-5 controls the design base shear. ASCE 7-10 has clarified this issue, by providing an exception that specifically states that Equation 12.8-5 need not be considered for computing drift.

It is important to note, however, that where Equation 12.8-6 controls the design base shear, drifts must be based on lateral forces consistent with Equation 12.8-6. This is due to the fact that Equation 12.8-6 is an approximation of the long period acceleration spectrum for "near field" ground motions (where S_1 is likely to be greater than 0.6 g.)

In this example, all ELF analysis is performed using the forces obtained from Equation 12.8-5, but for the purposes of computing drift, the story deflections are computed using the forces from Equation 12.8-3. When using Equation 12.8-3, the upper bound period $C_u T_a$ was used in lieu of the computed period. This allows for a simple "conversion" of displacements where displacements computed from forces based on Equation 12.8-5 are multiplied by the factor (0.021/0.037 = 0.568) to obtain displacements that would be

generated from forces based on Equation 12.8-3 and the $C_u T_a$ limit. If it is found that the factored computed drifts violate the drift limits (which is not the case in this example), it might be advantageous to re-compute the drifts on the basis of Equation 12.8-3 and the computed period *T*.

The seismic base shear computed according to *Standard* Equation 12.8-1 is distributed along the height of the building using *Standard* Equations 12.8-11 and 12.8-12:

$$F_x = C_{vx} V$$

and

$$C_{vx} = \frac{w_x h^k}{\sum_{i=1}^{n} w_i h_i^k}$$

where $k = 0.75 + 0.5T = 0.75 + 0.5(2.23) = 1.865$. The story forces, story shears and story overturning moments are summarized in Table 4.1-4.

Table 4.1-4 Equivalent Lateral Forces for Building Response in X and Y Directions

Level x	w_x (kips)	h_x (ft)	$w_x h_x^k$	C_{vx}	F_x (kips)	V_x (kips)	M_x (ft-kips)
R	1,657	155.5	20,272,144	0.1662	186.9	186.9	2,336
12	1,596	143.0	16,700,697	0.1370	154.0	340.9	6,597
11	1,596	130.5	14,081,412	0.1155	129.9	470.8	12,482
10	1,596	118.0	11,670,590	0.0957	107.6	578.4	19,712
9	3,403	105.5	20,194,253	0.1656	186.3	764.7	29,271
8	2,331	93.0	10,933,595	0.0897	100.8	865.5	40,090
7	2,331	80.5	8,353,175	0.0685	77.0	942.5	51,871
6	2,331	68.0	6,097,775	0.0500	56.2	998.8	64,356
5	4,324	55.5	7,744,477	0.0635	71.4	1,070.2	77,733
4	3,066	43.0	3,411,857	0.0280	31.5	1,101.7	91,505
3	3,066	30.5	1,798,007	0.0147	16.6	1,118.2	103,372
2	3,097	18.0	679,242	0.0056	6.3	1,124.5	120,694
Σ	30,394	-	121,937,234	1.00	1124.5		

Values in column 4 based on exponent k=1.865.
1.0 ft = 0.3048 m, 1.0 kip = 4.45 kN.

4.1.5.2 Accidental torsion and orthogonal loading effects. Where using the ELF method as the basis for structural design, two effects must be added to the direct lateral forces shown in Table 4.1-4. The first of these effects accounts for the fact that an earthquake can produce inertial forces that act in any direction. For SDC D, E and F buildings, *Standard* Section 12.5 requires that the structure be investigated for forces that act in the direction that causes the "critical load effects." Since this direction is not easily defined, the *Standard* allows the analyst to load the structure with 100 percent of the seismic

force in one direction (along the X axis, for example) simultaneous with the application of 30 percent of the force acting in the orthogonal direction (along the Y axis).

The other requirement is that the structure be modeled with additional forces to account for uncertainties in the location of center of mass and center of rigidity, uneven yielding of vertical systems and the possibility of torsional components of ground motion. For torsionally regular buildings, this requirement, given in *Standard* Section 12.8.4.2, can be satisfied by applying the equivalent lateral force at an "accidental" eccentricity, where the eccentricity is equal to 5 percent of the overall dimension of the structure in the direction perpendicular to the line of the application of force. For torsionally irregular structures in SDC C, D, E, or F, *Standard* Section 12.8.4.3 requires that the accidental eccentricity be amplified (although the amplification factor may be 1.0).

According to *Standard* Table 12.3-1, a torsional irregularity exists if:

$$\frac{\Delta_{max}}{\Delta_{avg}} \geq 1.2$$

where δ_{max} is the maximum story drift at the edge of the floor diaphragm and Δ_{avg} is the average drift at the center of the diaphragm (see *Standard* Figure 12.8-1). If the ratio of drifts is greater than 1.4, the torsional irregularity is referred to as "extreme." In computing the drifts, the structure must be loaded with the basic equivalent lateral forces applied at a 5 percent eccentricity.

For main loads acting in the X direction, displacements and drifts were determined on Grid Line D. For the main loads acting in the Y direction, the story displacements on Grid Line 1 were used. Because of the architectural setbacks, the locations for determining displacements associated with Δ_{min} and Δ_{max} are not always vertically aligned. This situation is shown in Figure 4.1-7, where it is seen that three displacement monitoring stations are required at Levels 5 and 9. The numerical values shown in Figure 4.1-7 are discussed later in relation to Table 4.1-5b.

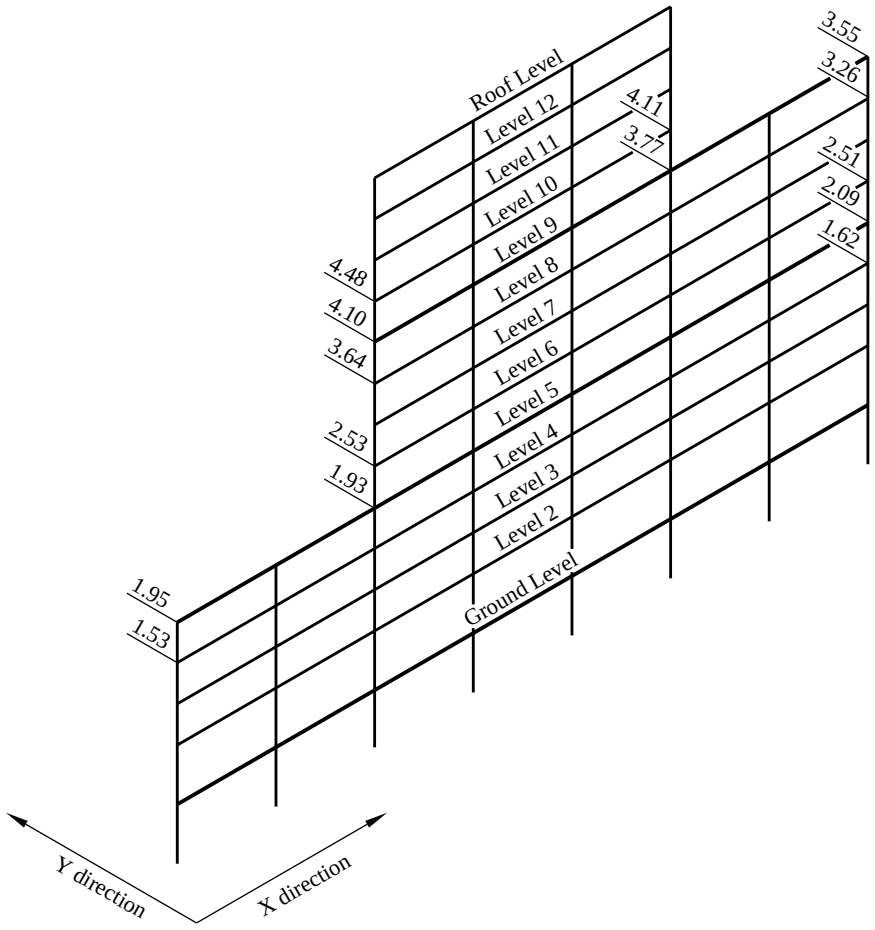

Figure 4.1-7 Drift monitoring stations for determination of torsional irregularity and torsional amplification (deflections in inches, 1.0 in. = 25.4 mm)

The analysis of the structure for accidental torsion was performed using SAP2000. The same model was used for ELF, modal response spectrum and modal response history analysis. The following approach was used for the mathematical model of the structure:

1. The floor diaphragm was modeled with shell elements, providing nearly rigid behavior in-plane.

2. Flexural, shear, axial and torsional deformations were included in all columns and beams.

3. Beam-column joints were modeled using centerline dimensions. This approximately accounts for deformations in the panel zone.

4. Section properties for the girders were based on bare steel, ignoring composite action. This is a reasonable assumption since most of the girders are on the perimeter of the building and are under reverse curvature.

5. Except for those lateral load-resisting columns that terminate at Levels 5 and 9, all columns were assumed to be fixed at their base.

6. The basement walls and grade level slab were explicitly modeled using 4-node shell elements. This was necessary to allow the interior columns to continue through the basement level. No additional lateral restraint was applied at the grade level; thus, the basement level acts as a very stiff first floor of the structure. This basement level was not relevant for the ELF analysis, but it did influence the modal response spectrum and modal response history analyses as described in later sections of this example

7. P-delta effects were not included in the mathematical model. These effects are evaluated separately using the procedures provided in ***Standard*** Section 12.8.7.

The results of the accidental torsion analysis are shown in Tables 4.1-5a and 4.1-5b. For loading in the X direction, there is no torsional irregularity because all drift ratios ($\Delta_{max}/\Delta_{avg}$) are less than 1.2. For loading in the Y direction, the largest ratio of maximum to average story drift is 1.24 at Level 9 of the building. Hence, this structure has a Type 1 torsional irregularity, but only marginally so. See Figure 4.1-7 for the source of the dual displacement values shown for Levels 9 and 5 in Table 4.1-5b.

Even though the torsional irregularity is marginal, Section 12.8.4.3 of the ***Standard*** requires that torsional amplification factors be determined for this SDC D building. The results for these calculations, which are based on story displacement, not drift, are presented in Tables 4.1-6a and 4.1-6b for the main load applied in the X and Y directions, respectively. As may be observed, the calculated amplification factors are significantly less than 1.0 at all levels for both directions of loading.

Table 4.1-5a Computation for Torsional Irregularity with ELF Loads Acting in X Direction and Torsional Moment Applied Counterclockwise

Level	δ_1 (in.)	δ_2 (in.)	Δ_1 (in.)	Δ_2 (in.)	Δ_{avg} (in.)	Δ_{max} (in.)	$\Delta_{max}/\Delta_{avg}$	Irregularity
R	7.27	6.15	0.34	0.29	0.31	0.34	1.08	None
12	6.93	5.87	0.48	0.42	0.45	0.48	1.07	None
11	6.44	5.45	0.60	0.51	0.55	0.60	1.07	None
10	5.85	4.93	0.66	0.56	0.61	0.66	1.08	None
9	5.19	4.37	0.65	0.54	0.59	0.65	1.10	None
8	4.54	3.84	0.69	0.58	0.64	0.69	1.09	None
7	3.84	3.26	0.70	0.59	0.65	0.70	1.09	None
6	3.14	2.67	0.69	0.58	0.63	0.69	1.09	None
5	2.46	2.09	0.60	0.50	0.55	0.60	1.09	None
4	1.86	1.60	0.59	0.50	0.55	0.59	1.08	None
3	1.27	1.10	0.58	0.49	0.53	0.58	1.08	None
2	0.69	0.61	0.69	0.61	0.65	0.69	1.06	None

1.0 in. = 25.4 mm.

Table 4.1-5b Computation for Torsional Irregularity with ELF Loads Acting in Y Direction and Torsional Moment Applied Clockwise

Level	δ_1 (in.)	δ_2 (in.)	Δ_1 (in.)	Δ_2 (in.)	Δ_{avg} (in.)	Δ_{max} (in.)	$\Delta_{max}/\Delta_{avg}$	Irregularity
R	5.19	4.77	0.15	0.14	0.15	0.15	1.03	None
12	5.03	4.63	0.25	0.23	0.24	0.25	1.03	None
11	4.79	4.40	0.31	0.29	0.30	0.31	1.04	None
10	4.48	4.11	0.38	0.34	0.36	0.38	1.06	None
9	4.10	3.77, 3.55	0.46	0.28	0.37	0.46	1.24	Irregularity
8	3.64	3.26	0.54	0.36	0.45	0.54	1.20	None
7	3.09	2.90	0.56	0.39	0.47	0.56	1.18	None
6	2.53	2.51	0.60	0.42	0.51	0.60	1.18	None
5	1.93, 1.95	2.09	0.41	0.47	0.44	0.47	1.06	None
4	1.53	1.62	0.47	0.50	0.48	0.50	1.03	None
3	1.07	1.12	0.47	0.50	0.48	0.50	1.03	None
2	0.60	0.63	0.60	0.63	0.61	0.63	1.03	None

1.0 in. = 25.4 mm.

Table 4.1-6a Amplification Factor A_x for Accidental Torsional Moment Loads Acting in the X Direction and Torsional Moment Applied Counterclockwise

Level	δ_1 (in.)	δ_2 (in.)	δ_{avg} (in.)	δ_{max} (in.)	A_x calculated	A_x used
R	7.27	6.15	6.71	7.27	0.81	1.00
12	6.93	5.87	6.40	6.93	0.81	1.00
11	6.44	5.45	5.95	6.44	0.82	1.00
10	5.85	4.93	5.39	5.85	0.82	1.00
9	5.19	4.37	4.78	5.19	0.82	1.00
8	4.54	3.84	4.19	4.54	0.82	1.00
7	3.84	3.26	3.55	3.84	0.81	1.00
6	3.14	2.67	2.90	3.14	0.81	1.00
5	2.46	2.09	2.27	2.46	0.81	1.00
4	1.86	1.60	1.73	1.86	0.80	1.00
3	1.27	1.10	1.18	1.27	0.80	1.00
2	0.69	0.61	0.65	0.69	0.79	1.00

1.0 in. = 25.4 mm.

Table 4.1-6b Amplification Factor A_x for Accidental Torsional Moment Loads Acting in the Y Direction and Torsional Moment applied Clockwise

Level	δ_1 (in.)	δ_2 (in.)	δ_{avg} (in.)	δ_{max} (in.)	A_x calculated	A_x used
R	5.19	4.77	4.98	5.19	0.75	1.00
12	5.03	4.63	4.83	5.03	0.75	1.00
11	4.79	4.40	4.59	4.79	0.76	1.00
10	4.48	4.11	4.29	4.48	0.76	1.00
9	4.10	3.55	3.82	4.10	0.80	1.00
8	3.64	3.26	3.45	3.64	0.77	1.00
7	3.09	2.90	3.00	3.09	0.74	1.00
6	2.53	2.51	2.52	2.53	0.70	1.00
5	1.95	2.09	2.02	2.09	0.74	1.00
4	1.53	1.62	1.58	1.62	0.73	1.00
3	1.07	1.12	1.10	1.12	0.73	1.00
2	0.60	0.63	0.61	0.63	0.73	1.00

1.0 in. = 25.4 mm.

4.1.5.3 Drift and P-delta effects. Using the basic structural configuration shown in Figure 4.1-1 and the equivalent lateral forces shown in Table 4.1-4, the total story deflections were computed as described in the previous section. In this section, story drifts are computed and compared to the allowable drifts specified by the *Standard*.

For structures with "significant torsional effects", *Standard* Section 12.12.1 requires that the maximum drifts include torsional effects, meaning that the accidental torsion, amplified as appropriate, must be included in the drift analysis. The same section of the *Standard* requires that deflections used to compute drift should be taken at the edges of the structure if the structure is torsionally irregular. For torsionally regular buildings, the drifts may be based on deflections at the center of mass of adjacent levels.

As the structure under consideration is only marginally irregular in torsion, the lateral loads were placed at the center of mass and total drifts are based on center of mass deflections and not deflections at the edges of the floor plate. Using the centers of mass of the floor plates to compute story drift is awkward where the centers of mass of the upper and lower floor plates are not aligned vertically. For this reason, the story drift is computed as the difference between displacements of the center of mass of the upper level diaphragm and the displacement at a point on the lower diaphragm which is located directly below the center of mass of the upper level diaphragm. Note that computation of drift in this manner has been adopted in ASCE 7-10 Section 12.8-6.

The values in Column 1 of Tables 4.1-7 and 4.1-8 are the total story displacements (δ) at the center of mass of the story as reported by SAP2000 and the values in Column 2 are the story drifts (Δ) computed from these numbers in the manner described earlier. The true elastic "amplified" story drift, which by assumption is equal to C_d (= 5.5) times the SAP2000 drift, is shown in Column 3. As discussed above in Section 4.1.5.1, the values in Column 4 are multiplied by 0.568 to scale the results to the base shear computed using *Standard* Equation 12.8-3.

The allowable story drift of 2.0 percent of the story height per *Standard* Table 12.12-1 is shown in Column 5. (Recall that this building is assigned to Occupancy Category II.) It is clear from Tables 4.1-7 and 4.1-8 that the allowable drift is not exceeded at any level. It is also evident that the allowable drifts

would not have been exceeded even if accidental torsion effects were included in the drift calculations, with the drift determined at the edge of the building.

Table 4.1-7 ELF Drift for Building Responding in X Direction

Level	1 Total drift from SAP2000 (in.)	2 Story drift from SAP2000 (in.)	3 Amplified story drift (in.)	4 Amplified drift times 0.568 (in.)	5 Allowable drift (in.)
R	6.67	0.32	1.74	0.99	3.00
12	6.35	0.45	2.48	1.41	3.00
11	5.90	0.56	3.07	1.75	3.00
10	5.34	0.62	3.39	1.92	3.00
9	4.73	0.58	3.20	1.82	3.00
8	4.15	0.63	3.47	1.97	3.00
7	3.52	0.64	3.54	2.01	3.00
6	2.87	0.63	3.47	1.97	3.00
5	2.24	0.54	2.95	1.67	3.00
4	1.71	0.54	2.97	1.69	3.00
3	1.17	0.53	2.90	1.65	3.00
2	0.64	0.64	3.51	2.00	4.32

Column 4 adjusts for *Standard* Eq. 12.8-3 (for drift) vs 12.8-5 (for strength).
1.0 in. = 25.4 mm.

Table 4.1-8 ELF Drift for Building Responding in Y Direction

Level	1 Total drift from SAP2000 (in.)	2 Story drift from SAP2000 (in.)	3 Amplified story drift (in.)	4 Amplified drift times 0.568 (in.)	5 Allowable drift (in.)
R	4.86	0.15	0.81	0.46	3.00
12	4.71	0.24	1.30	0.74	3.00
11	4.47	0.30	1.64	0.93	3.00
10	4.17	0.36	1.96	1.11	3.00
9	3.82	0.37	2.05	1.16	3.00
8	3.44	0.46	2.54	1.44	3.00
7	2.98	0.48	2.64	1.50	3.00
6	2.50	0.48	2.62	1.49	3.00
5	2.03	0.45	2.49	1.42	3.00
4	1.57	0.48	2.66	1.51	3.00
3	1.09	0.48	2.64	1.50	3.00
2	0.61	0.61	3.35	1.90	4.32

Column 4 adjusts for *Standard* Eq. 12.8-3 (for drift) versus Eq. 12.8-5 (for strength).
1.0 in. = 25.4 mm.

4.1.5.3.1 Using ELF forces and drift to compute accurate period. Before continuing with the example, it is advisable to use the computed drifts to more accurately estimate the fundamental periods of vibration of the building. This will serve as a check on the "exact" periods computed by eigenvalue extraction in SAP2000. A Rayleigh analysis will be used to estimate the periods. This procedure, which usually is very accurate, is derived as follows:

The exact frequency of vibration ω (a scalar), in units of radians/second, is found from the following eigenvalue equation:

$$K\phi = \omega^2 M\phi$$

where K is the structure stiffness matrix, M is the (diagonal) mass matrix and ϕ is a vector containing the components of the mode shape associated with ω.

If an approximate mode shape δ is used instead of ϕ, where δ is the deflected shape under the equivalent lateral forces F, the frequency ω can be closely approximated. Making the substitution of δ for ϕ, premultiplying both sides of the above equation by δ^T (the transpose of the displacement vector), noting that $F = K\delta$ and $M = W/g$, the following is obtained:

$$\delta^T F = \omega^2 \delta^T M \delta = \frac{\omega^2}{g} \delta^T W \delta$$

where W is a vector containing the story weights and g is the acceleration due to gravity (a scalar). After rearranging terms, this gives:

$$\omega = \sqrt{g \frac{\delta^T F}{\delta^T W \delta}}$$

Using the relationship between period and frequency, $T = \frac{2\pi}{\omega}$

Using F from Table 4.1-4 and δ from Column 1 of Tables 4.1-7 and 4.1-8, the periods of vibration are computed as shown in Tables 4.1-9 and 4.1-10 for the structure loaded in the X and Y directions, respectively. As may be seen from the tables, the X direction period of 2.85 seconds and the Y-direction period of 2.56 seconds are significantly greater than the approximate period of T_a = 1.59 seconds and also exceed the upper limit on period of $C_u T_a$ = 2.23 seconds.

Table 4.1-9 Rayleigh Analysis for X Direction Period of Vibration

Level	Drift, δ (in.)	Force, F (kips)	Weight, W (kips)	δF (in.-kips)	$\delta W/g$ (in.-kips-sec^2)
R	6.67	186.9	1,657	1,247	191
12	6.35	154.0	1,596	979	167
11	5.90	129.9	1,596	767	144
10	5.34	107.6	1,596	575	118
9	4.73	186.3	3,403	881	197
8	4.15	100.8	2,331	418	104

Table 4.1-9 Rayleigh Analysis for X Direction Period of Vibration

Level	Drift, δ (in.)	Force, F (kips)	Weight, W (kips)	δF (in.-kips)	$\delta W/g$ (in.-kips-sec^2)
7	3.52	77.0	2,331	271	75
6	2.87	56.2	2,331	162	50
5	2.24	71.4	4,324	160	56
4	1.71	31.5	3,066	54	23
3	1.17	16.6	3,066	19	11
2	0.64	6.3	3,097	4	3
Σ				5,536	1,138

$\omega = (5{,}536/1{,}138)^{0.5} = 2.21$ rad/sec. $T = 2\pi/\omega = 2.85$ sec.
1.0 in. = 25.4 mm, 1.0 kip = 4.45 kN.

Table 4.1-10 Rayleigh Analysis for Y Direction Period of Vibration

Level	Drift, δ (in.)	Force, F (kips)	Weight, W (kips)	δF	$\delta W/g$
R	4.86	186.9	1,657	908	101
12	4.71	154.0	1,596	725	92
11	4.47	129.9	1,596	581	83
10	4.17	107.6	1,596	449	72
9	3.82	186.3	3,403	711	128
8	3.44	100.8	2,331	347	72
7	2.98	77.0	2,331	230	54
6	2.50	56.2	2,331	141	38
5	2.03	71.4	4,324	145	46
4	1.57	31.5	3,066	49	20
3	1.09	16.6	3,066	18	9
2	0.61	6.3	3,097	4	3
Σ				4,307	716

$\omega = (4{,}307/716)^{0.5} = 2.45$ rad/sec. $T = 2\pi/\omega = 2.56$ sec.
1.0 in. = 25.4 mm, 1.0 kip = 4.45 kN.

4.1.5.3.2 P-delta effects. P-delta effects are computed for the X direction response in Table 4.1-11. The last column of the table shows the story stability ratio computed according to *Standard* Equation 12.8-16[3]:

$$\theta = \frac{P_x \Delta I}{V_x h_{sx} C_d}$$

[3] Note that the *I* in the numerator of Equation 12.8-16 was inadvertently omitted in early printings of the *Standard*.

Standard Equation 12.8-17 places an upper limit on θ:

$$\theta_{\max} = \frac{0.5}{\beta C_d}$$

where β is the ratio of shear demand to shear capacity for the story. Conservatively taking $\beta = 1.0$ and using $C_d = 5.5$, $\theta_{max} = 0.091$.

The Δ terms in Table 4.1-11 are taken from the fourth column of Table 4.1-7 because these are consistent with the ELF story shears of Table 4.1-4 and thereby represent the true lateral stiffness of the system. (If 0.568 times the story drifts were used, then 0.568 times the story shears also would need to be used. Hence, the 0.568 factor would cancel out since it would appear in both the numerator and denominator.) The deflections used in P-delta stability ratio calculations must include the deflection amplifier C_d.

The live load P_L in Table 4.1-11 is based on a 20 psf uniform live load over 100 percent of the floor and roof area. This live load is somewhat conservative because Section 12.8.7 of the *Standard* states that the gravity load should be the "total vertical design load". For a 50 psf live load for office buildings, a live load reduction factor of 0.4 would be applicable for each level (see *Standard* Sec. 4.8), producing a reduced live load of 20 psf at the floor levels. This could be further reduced by a factor of 0.5 as allowed by Section 2.3.2, bringing the effective live load to 10 psf. This value is close to the mean survey live load of 10.9 psf for office buildings, as listed in Table C4.2 of the *Standard*. Several publications, including ASCE 41 include 25 percent of the *unreduced* live load in P-delta calculations. This would result in a 12.5 psf live load for the current example.

Table 4.1-11 Computation of P-delta Effects for X Direction Response

Level	h_{sx} (in.)	Δ (in.)	P_D (kips)	P_L (kips)	P_T (kips)	P_X (kips)	V_X (kips)	θ_X
R	150	1.74	1,656.5	315.0	1,971.5	1,971.5	186.9	0.022
12	150	2.48	1,595.8	315.0	1,910.8	3,882.3	340.9	0.034
11	150	3.07	1,595.8	315.0	1,910.8	5,793.1	470.8	0.046
10	150	3.39	1,595.8	315.0	1,910.8	7,703.9	578.4	0.055
9	150	3.20	3,403.0	465.0	3,868.0	11,571.9	764.7	0.059
8	150	3.47	2,330.8	465.0	2,795.8	14,367.7	865.8	0.070
7	150	3.54	2,330.8	465.0	2,795.8	17,163.5	942.5	0.078
6	150	3.47	2,330.8	465.0	2,795.8	19,959.3	998.8	0.084
5	150	2.95	4,323.8	615.0	4,938.8	24,898.1	1,070.2	0.083
4	150	2.97	3,066.1	615.0	3,681.1	28,579.2	1,101.7	0.093
3	150	2.90	3,066.1	615.0	3,681.1	32,260.3	1,118.2	0.101
2	216	3.51	3,097.0	615.0	3,712.0	35,972.3	1,124.5	0.095

1.0 in. = 25.4 mm, 1.0 kip = 4.45 kN.

The stability ratio just exceeds 0.091 at Levels 2 through 4. However, the live loads were somewhat conservative and β was very conservatively taken as 1.0. Because a more refined analysis would provide somewhat lower live loads and a lower value of β, we will proceed assuming that P-delta effects are not a

problem for this structure. Calculations for P-delta effects under Y direction loading gave no story stability ratios greater than 0.091 and for brevity, those results are not included herein.

It is important to note that for this structure, P-delta effects are a potential issue even though drift limits were easily satisfied. This is often the case when drift limits are based on lateral loads that have been computed using the computed period of vibration (without the $C_u T_a$ limit, or without the use of Equation 12.8.5). It is the authors' experience that this is a typical situation in the analysis of steel special steel moment frame systems.

Part 1 of the *Provisions* recommends that a significant change be made to the current P-delta approach. In the recommended approach, Equation 12.8-16 is still used to determine the magnitude of P-delta effects. However, if the stability ratio at any level is greater than 0.1, the designer must either redesign the building such that the stability ratio is less than 0.1, or must perform a static pushover analysis and demonstrate that the slope of the pushover curve of the structure is continuously positive up to the "target displacement" computed in accordance with the requirements of ASCE 41.

4.1.5.4 Computation of member forces. Before member forces may be computed, the proper load cases and combinations of load must be identified such that all critical seismic effects are captured in the analysis.

4.1.5.4.1 Orthogonal loading effects and accidental torsion. For SDC D structures with a Type 5 horizontal structural irregularity, Section 12.5.3 of the *Standard* requires that orthogonal load effects be considered. For the purposes of this example, it is assumed that such an irregularity does exist because the layout of the frames is not symmetric. (ASCE 7-10 has eliminated non-symmetry as a trigger for invoking the nonparallel system horizontal irregularity. However, as the structural system under consideration has several intersecting frames, it would be advisable to perform the orthogonal load analysis as required under Section 12.5.4 of both the 2005 and 2010 versions of the *Standard*.)

When orthogonal load effects are included in the analysis, four directions of seismic force (+X, -X, +Y, -Y) must be considered and for each direction of force, there are two possible directions in which the accidental eccentricity can apply (causing positive or negative torsion). This requires a total of eight possible combinations of direct force plus accidental torsion. Where the 30 percent orthogonal loading rule is applied (see *Standard* Sec. 12.5.3 Item "a"), the number of load combinations increases to 16 because, for each direct application of load, a positive or negative orthogonal loading can exist. Orthogonal loads are applied without accidental eccentricity.

Figure 4.1-8 illustrates the basic possibilities of application of load. Although this figure shows 16 different load conditions, it may be observed that eight of these conditions—7, 8, 5, 6, 15, 16, 13 and 14—are negatives (opposite signs throughout) of conditions 1, 2, 3, 4, 9, 10, 11 and 12, respectively.

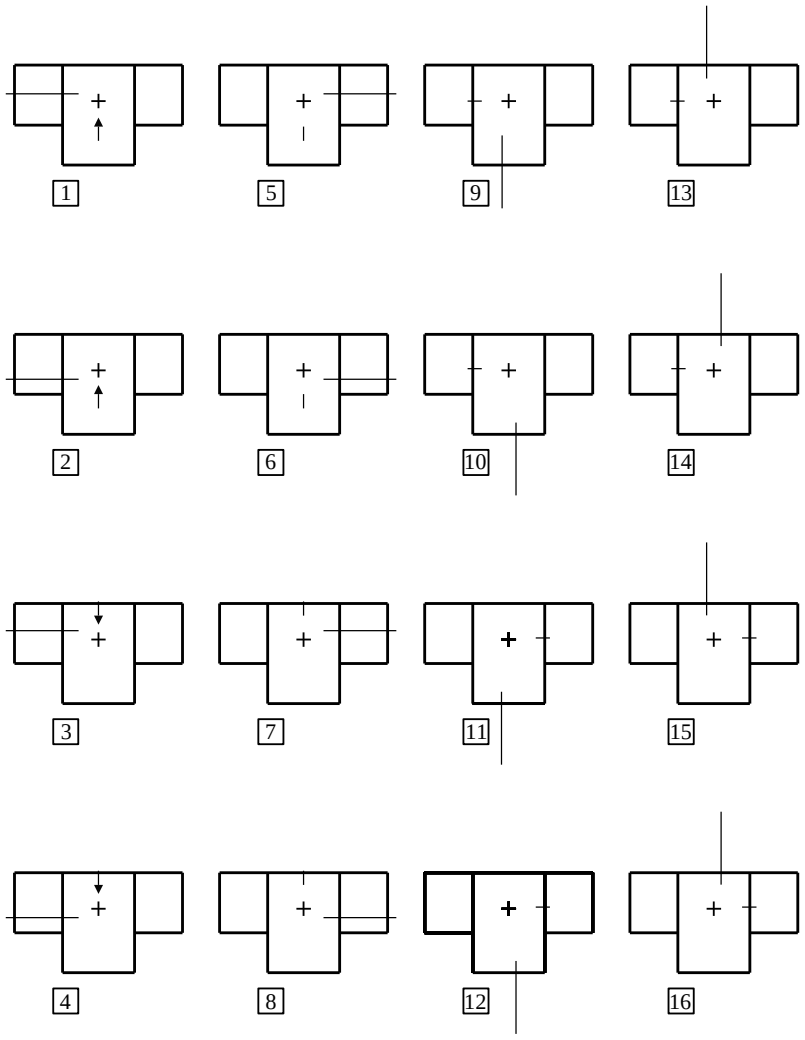

Figure 4.1-8 Basic load conditions used in ELF analysis

4.1.5.4.2 Load combinations. The basic load combinations for this structure are designated in Chapter 2 of the *Standard*. Two sets of combinations are provided: one for strength design and the other for allowable stress design. The strength-based combinations that are related to seismic effects are the following:

$1.2D + 1.0E + 1.0L + 0.2S$

$0.9D + 1.0E + 1.6H$

The factor on live load, *L*, may be reduced to 0.5 if the nominal live load is less than 100 psf. The load due to lateral earth pressure, *H*, may need to be considered when designing the basement walls.

Section 12.4 of the *Standard* divides the earthquake load, E, into two components, E_h and E_v, where the subscripts h and v represent horizontal and vertical seismic effects, respectively. These components are defined as follows:

$$E_h = \rho Q_E$$

$$E_v = 0.2 S_{DS} D$$

where Q_E is the earthquake load effect and ρ is a redundancy factor, described later.

When the above components are substituted into the basic load combinations, the load combinations for strength design with a factor of 0.5 used for live load and with the H load removed are as follows:

$$(1.2 + 0.2 S_{DS}) D + \rho Q_E + 0.5 L + 0.2 S$$

$$(0.9 - 0.2 S_{DS}) D + \rho Q_E$$

Using $S_{DS} = 0.833$ and assuming the snow load is negligible in Stockton, California, the basic load combinations for strength design become:

$$1.37 D + 0.5 L + \rho Q_E$$

$$0.73 D + \rho Q_E$$

The redundancy factor, ρ, is determined in accordance with *Standard* Section 12.3.4. This factor will take a value of 1.0 or 1.3, with the value depending on a variety of conditional tests. None of the conditions specified in Section 12.3.4.1 are applicable, so ρ may not be automatically taken as 1.0, and the more detailed evaluation specified in Section 12.3.4.2 is required. Subparagraph "b" of Section 12.3.4.2 applies to this building (because of the plan irregularities) and therefore, the evaluation described in the second row of Table 12.3-3 must be performed. It can be seen from inspection that the removal of a single beam from the perimeter moment frames will not cause a reduction in strength of 33 percent, nor will an extreme torsional irregularly result from the removal of the beam. Hence, the redundancy factor may be taken as 1.0 for this structure.

Hence, the final load conditions to be used for design are as follows:

$$1.37 D + 0.5 L + 1.0 Q_E$$

$$0.73 D + 1.0 Q_E$$

The first load condition will produce the maximum negative moments (tension on the top) at the face of the supports in the girders and maximum compressive forces in columns. The second load condition will produce the maximum positive moments (or minimum negative moment) at the face of the supports of the girders and maximum tension (or minimum compression) in the columns. In addition to the above load condition, the gravity-only load combinations as specified in the *Standard* also must be checked. Due to the relatively short spans in the moment frames, however, it is not expected that the non-seismic load combinations will control.

4.1.5.4.3 Setting up the load combinations in SAP2000. The load combinations required for the analysis are shown in Table 4.1-12.

It should be noted that 32 different load combinations are required only if one wants to maintain the signs in the member force output, thereby providing complete design envelopes for all members. As mentioned later, these signs are lost in response spectrum analysis and as a result, it is possible to capture the effects of dead load plus live load plus-or-minus earthquake load in a single SAP2000 run containing only four load combinations.

Table 4.1-12 Seismic and Gravity Load Combinations as Run on SAP2000

Run	Combination	Lateral*		Gravity	
		A	B	1 (Dead)	2 (Live)
One	1	[1]		1.37	0.5
	2	[1]		0.73	0.0
	3	[7]		1.37	0.5
	4	[7]		0.73	0.0
	5		[2]	1.37	0.5
	6		[2]	0.73	0.0
	7		[8]	1.37	0.5
	8		[8]	0.73	0.0
Two	1	[3]		1. 37	0.5
	2	[3]		0.73	0.0
	3		[4]	1. 37	0.5
	4		[4]	0.73	0.0
	5	[5]		1. 37	0.5
	6	[5]		0.73	0.0
	7		[6]	1. 37	0.5
	8		[6]	0.73	0.0
Three	1	[9]		1. 37	0.5
	2	[9]		0.73	0.0
	3		[10]	1. 37	0.5
	4		[10]	0.73	0.0
	5	[15]		1. 37	0.5
	6	[15]		0.73	0.0
	7		[16]	1. 37	0.5
	8		[16]	0.73	0.0
Four	1	[11]		1. 37	0.5
	2	[11]		0.73	0.0
	3		[12]	1. 37	0.5
	4		[12]	0.73	0.0
	5	[13]		1. 37	0.5
	6	[13]		0.73	0.0
	7		[14]	1. 37	0.5
	8		[14]	0.73	0.0

*Numbers in brackets [ ] in represent load cases shown in Figure 4.1-8.

4.1.5.4.4 Member forces. For this portion of the analysis, the earthquake shears in the girders along Gridline 1 are computed. This analysis considers 100 percent of the X direction forces applied in combination with 30 percent of the (positive or negative) Y direction forces. The accidental torsion is not included and will be considered separately. The results of the member force analysis are shown in Figure 4.1-9a. In a later part of this example, the girder shears are compared to those obtained from modal response spectrum and modal response history analyses.

Beam shears in the same frame, due to accidental torsion *only*, are shown in Figure 4.1-9b. The eccentricity was set to produce clockwise torsions (when viewed from above) on the floor plates. These shears would be added to the shears shown in Figure 4.1-9a to produce the total seismic beam shears in the frame. The same torsional shears (from Table 4.1-9b) will be used in the modal response spectrum and modal response history analyses.

R-12			8.99 17.3	10.3 18.9	10.3 19.0		
12-11			27.7	28.1	29.5		
11-10			33.4	33.1	35.7		
10-9			34.8	34.7	32.2	30.3	13.2
9-8			36.4	35.9	33.9	37.8	23.7
8-7			41.2	40.1	38.4	41.3	25.8
7-6			43.0	40.6	39.3	41.7	26.4
6-5	14.1	33.1	33.8	36.5	35.5	37.2	24.9
5-4	24.1	37.9	32.0	34.6	33.9	34.9	23.9
4-3	24.1	37.0	33.3	35.1	34.6	35.4	24.6
3-2	22.9	36.9	34.1	35.3	34.9	35.9	23.3
2 - G							

Figure 4.1-9a Seismic shears (kips) in girders on Frame Line 1 as computed using ELF analysis (analysis includes orthogonal loading but excludes accidental torsion)

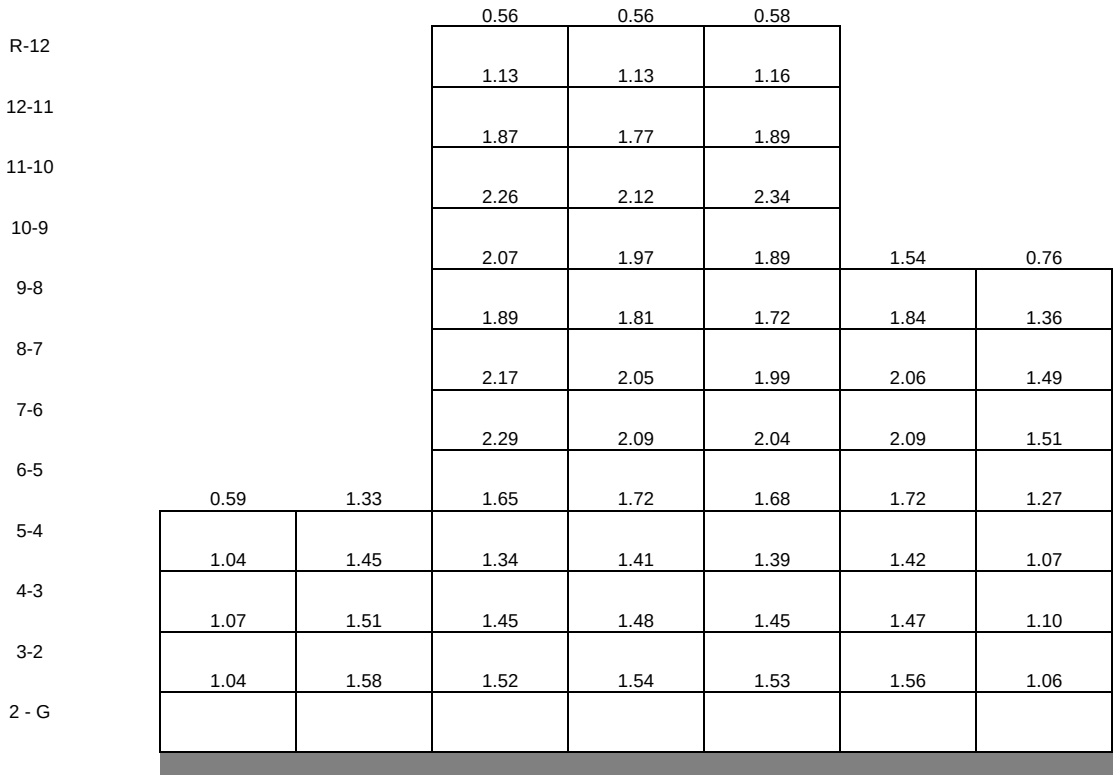

Figure 4.1-9b Seismic shears in girders (kips) from clockwise torsion only

4.1.6 Modal Response Spectrum Analysis

The first step in the modal response spectrum analysis is the computation of the natural mode shapes and associated periods of vibration. Using the structural masses from Table 4.1-4 and the same mathematical model as used for the ELF and the Rayleigh analyses, the mode shapes and frequencies are automatically computed by SAP2000. This mathematical model included the basement as a separate level. (See Section 4.1.5.2 of this example for a description of the mathematical model used in the analysis). The basement walls were fixed at the base but were unrestrained at grade level. Thus, the basement level is treated as a separate story in the analysis. However, the lateral stiffness of the basement level is significantly greater than that of the upper levels and this causes complications when interpreting the requirements of *Standard* Section 12.9.1. As shown later, the explicit modeling of the basement can also lead to some unexpected results in the modal response history analysis of the structure.

The periods of vibration for the first 12 modes, computed from an eigenvalue analysis, are summarized in the second column of Table 4.1-13. The first eight mode shapes are shown in Figure 4.1-10. The first mode period, 2.87 seconds, corresponds to vibration primarily in the X direction and the second period, 2.60 seconds, corresponds to vibration in the Y direction. The third mode, with a period of 1.57 seconds, is almost purely torsion. The directionality of the modes may be inferred from the effective mass values shown in Columns 3 through 5 of the tables, as well as from the mode shapes. There is very little lateral-torsional coupling in any of the first 12 modes, which is somewhat surprising because of the shifted centers of mass associated with the plan offsets.

The X- and Y-translation periods of 2.87 and 2.60 seconds, respectively, are somewhat longer than the upper limit on the approximate period, $C_u T_a$, of 2.23 seconds.

The first and second mode periods are virtually identical to the periods compute by Rayleigh analysis (2.85 and 2.56 seconds in the X and Y directions, respectively). The closeness of the Rayleigh and eigenvalue periods for this building arises from the fact that the first and second modes of vibration act primarily along the orthogonal axes. Had the first and second modes not acted along the orthogonal axes, the Rayleigh periods (based on loads and displacements in the X and Y directions) would have been somewhat less accurate.

Standard Section 12.9.1 specifies that "the analysis shall include a sufficient number of modes to obtain a combined modal mass participation of at least 90 percent of the total mass in each of the orthogonal horizontal directions of response considered by the model". Usually, this is a straightforward requirement and the first twelve modes would be sufficient for a 12-story building. For this building, however, twelve modes capture only about 82 percent of the X and Y direction mass. (The effective mass as a fraction of total mass is shown in brackets [ ] in Columns 3 through 5 of Tables 4.1-13 and 4.1-14.) Most of the remaining effective mass is in the grade-level slab and in the basement walls. This mass does not show up until Mode 112 in the Y direction and Mode 118 in the X direction. This is shown in Table 12.1-14, which provides the periods and effective modal masses in Modes 108 through 119. The intermediate modes (13 through 107) represent primarily vertical vibration of various portions of the floor diaphragms.

Analyzing the system with 120 or more modes might provide useful information on the response of the basement level, including shears through the basement and total system base shears at the base of the basement. However, there would be some difficulty in interpreting the results because the model did not include sub-grade soil that would be in contact with the basement walls and which would absorb part of the base shear. Additionally, the computed response of the upper 12 levels of the building, which is the main focus of this analysis, is virtually identical for the 12 and the 120 mode analyses. For this reason, the modal response spectrum analysis discussed in this example was run with only the first 12 modes listed in Table 4.1-13.

Mode 1: T = 2.87 sec

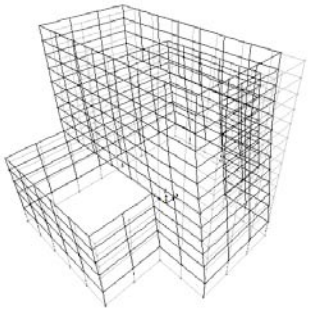

Mode 2: T = 2.60 sec

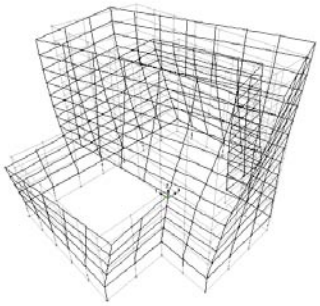

Mode 3: T = 1.57 sec

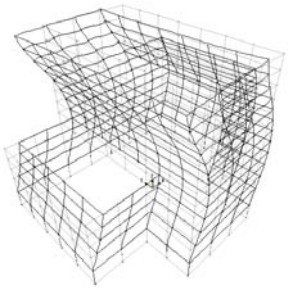

Mode 4: T = 1.15 sec

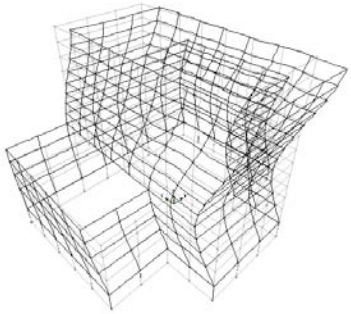

Mode 5: T = 0.98 sec

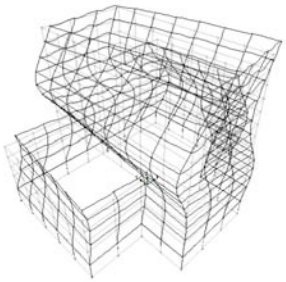

Mode 6: T = 0.71 sec

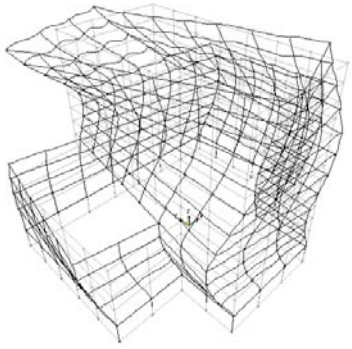

Mode 7: T = 0.68 sec

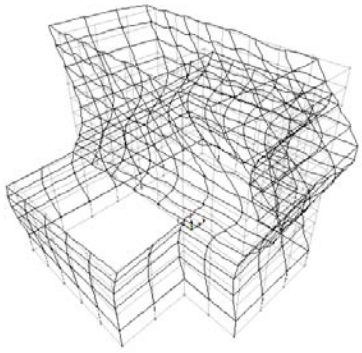

Mode 8: T = 0.57 sec

Figure 4.1-10 First eight mode shapes

Table 4.1-13 Computed Periods and Effective Mass Factors (Lower Modes)

Mode	Period (sec.)	Effective Mass Factor [Accum Mass Factor]		
		X Translation	Y Translation	Z Rotation
1	2.87	0.6446 [0.64]	0.0003 [0.00]	0.0028 [0.00]
2	2.60	0.0003 [0.65]	0.6804 [0.68]	0.0162 [0.02]
3	1.57	0.0035 [0.65]	0.0005 [0.68]	0.5806 [0.60]
4	1.15	0.1085 [0.76]	0.0000 [0.68]	0.0000 [0.60]
5	0.975	0.0000 [0.76]	0.0939 [0.78]	0.0180 [0.62]
6	0.705	0.0263 [0.78]	0.0000 [0.78]	0.0271 [0.64]
7	0.682	0.0056 [0.79]	0.0006 [0.79]	0.0687 [0.71]
8	0.573	0.0000 [0.79]	0.0188 [0.79]	0.0123 [0.73]

Table 4.1-13 Computed Periods and Effective Mass Factors (Lower Modes)

Mode	Period (sec.)	Effective Mass Factor [Accum Mass Factor]		
		X Translation	Y Translation	Z Rotation
9	0.434	0.0129 [0.80]	0.0000 [0.79]	0.0084 [0.73]
10	0.387	0.0048 [0.81]	0.0000 [0.79]	0.0191 [0.75]
11	0.339	0.0000 [0.81]	0.0193 [0.81]	0.0010 [0.75]
12	0.300	0.0089 [0.82]	0.0000 [0.81]	0.0003 [0.75]

Table 4.1-14 Computed Periods and Effective Mass Factors (Higher Modes)

Mode	Period (sec.)	Effective Mass Factor [Accum Effective Mass]		
		X Translation	Y Translation	Z Rotation
108	0.0693	0.0000 [0.83]	0.0000 [0.83]	0.0000 [0.79]
109	0.0673	0.0000 [0.83]	0.0000 [0.83]	0.0000 [0.79]
110	0.0671	0.0000 [0.83]	0.0354 [0.86]	0.0000 [0.79]
111	0.0671	0.0000 [0.83]	0.0044 [0.87]	0.0000 [0.79]
112	0.0669	0.0000 [0.83]	0.1045 [0.97]	0.0000 [0.79]
113	0.0663	0.0000 [0.83]	0.0000 [0.97]	0.0000 [0.79]
114	0.0646	0.0000 [0.83]	0.0000 [0.97]	0.0000 [0.79]
115	0.0629	0.0000 [0.83]	0.0000 [0.97]	0.0000 [0.79]
116	0.0621	0.0008 [0.83]	0.0010 [0.97]	0.0000 [0.79]
117	0.0609	0.0014 [0.83]	0.0009 [0.97]	0.0000 [0.79]
118	0.0575	0.1474 [0.98]	0.0000 [0.97]	0.0035 [0.80]
119	0.0566	0.0000 [0.98]	0.0000 [0.97]	0.0000 [0.80]

4.1.6.1 Response spectrum coordinates and computation of modal forces. The coordinates of the response spectrum are based on *Standard* Section 11.4.5. This spectrum consists of three parts (for periods less than T_L = 8.0 seconds) as follows:

- For periods less than T_0:

$$S_a = 0.6\frac{S_{DS}}{T_0}T + 0.4S_{DS}$$

- For periods between T_0 and T_S:

$$S_a = S_{DS}$$

- For periods greater than T_S:

$$S_a = \frac{S_{D1}}{T}$$

where $T_0 = 0.2S_{D1}/S_{DS}$ and $T_S = S_{D1}/S_{DS}$.

Using S_{DS} = 0.833 and S_{D1} = 0.373, T_S = 0.448 seconds and T_0 = 0.089 seconds. The computed response spectrum coordinates for several period values are shown in Table 4.1-15 and the response spectrum, shown with and without the I/R = 1/8 modification, is plotted in Figure 4.1-11. The spectrum does not include the high period limit on C_s ($0.044IS_{DS}$), which controlled the ELF base shear for this structure and which ultimately will control the scaling of the results from the response spectrum analysis. (Recall that if the computed base shear falls below 85 percent of the ELF base shear, the computed response must be scaled up such that the computed base shear equals 85 percent of the ELF base shear.)

Table 4.1-15 Response Spectrum Coordinates

T_m (sec.)	S_a	$S_a(I/R)$
0.000	0.333	0.0416
0.089 (T_0)	0.833	0.104
0.448 (T_S)	0.833	0.104
1.000	0.373	0.0446
1.500	0.249	0.0311
2.000	0.186	0.0235
2.500	0.149	0.0186
3.000	0.124	0.0155

I = 1, R = 8.0.

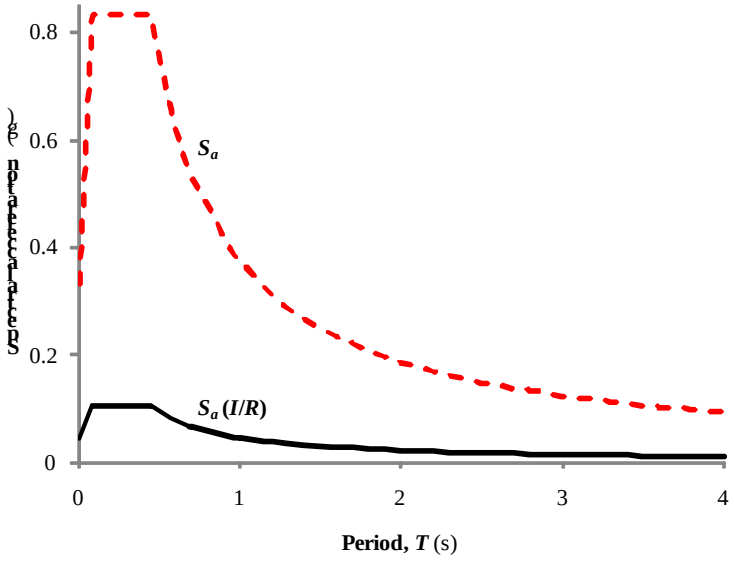

Figure 4.1-11 Total acceleration response spectrum used in analysis

Using the response spectrum coordinates listed in Column 3 of Table 4.1-15, the response spectrum analysis was carried out using SAP2000. As mentioned above, the first 12 modes of response were computed and superimposed using the CQC approach. A modal damping ratio of 5 percent of critical was used in the CQC calculations.

Two analyses were carried out. The first directed the seismic motion along the X axis of the structure and the second directed the motion along the Y axis. Combinations of these two loadings plus accidental torsion are discussed later.

4.1.6.1.1 Dynamic base shear. After specifying member groups, SAP2000 automatically computes the CQC story shears. Groups were defined such that total shears would be obtained for each story of the structure. The shears at the base of the first story above grade are reported as follows:

- X direction base shear = 438.1 kips
- Y direction base shear = 492.8 kips

These values are much lower that the ELF base shear of 1,124 kips. Recall that the ELF base shear was controlled by *Standard* Equation 12.8-5. The modal response spectrum shears are less than the ELF shears because the fundamental periods of the structure used in the response spectrum analysis (2.87 seconds and 2.6 seconds in the X and Y directions, respectively) are greater than the upper limit empirical period, $C_u T_a$, of 2.23 seconds and because the response spectrum of Figure 4.1-11 does not include the minimum base shear limit imposed by *Standard* Equation 12.8-5.

According to *Standard* Section 12.9.4, the base shears from the modal response spectrum analysis must not be less than 85 percent of that computed from the ELF analysis. If the response spectrum shears are lower than the ELF shear, then the computed shears must be scaled up such that the response spectrum base shear is 85 percent of that computed from the ELF analysis.

Hence, the required scale factors are as follows:

- X direction scale factor = 0.85(1124)/438.1 = 2.18
- Y direction scale factor = 0.85(1124)/492.8 = 1.94

The computed and scaled story shears are as shown in Table 4.1-16. Since the base shears for the ELF and the modal analysis are different (due to the 0.85 factor), direct comparisons cannot be made between Table 4.1-16 and Table 4.1-4. However, it is clear that the vertical distribution of forces is somewhat similar where computed by ELF and modal response spectrum.

Table 4.1-16 Story Shears from Modal Response Spectrum Analysis

Story	X Direction (SF = 2.18)		Y Direction (SF = 1.94)	
	Unscaled Shear (kips)	Scaled Shear (kips)	Unscaled Shear (kips)	Scaled Shear (kips)
R-12	82.7	180	77.2	150
12-11	130.9	286	132.0	256
11-10	163.8	357	170.4	330
10-9	191.4	418	201.9	392
9-8	240.1	524	265.1	514
8-7	268.9	587	301.4	585
7-6	292.9	639	328.9	638
6-5	316.1	690	353.9	686
5-4	359.5	784	405.1	786

Table 4.1-16 Story Shears from Modal Response Spectrum Analysis

Story	X Direction (SF = 2.18)		Y Direction (SF = 1.94)	
	Unscaled Shear (kips)	Scaled Shear (kips)	Unscaled Shear (kips)	Scaled Shear (kips)
4-3	384.8	840	435.5	845
3-2	401.4	895	462.8	898
2-G	438.1	956	492.8	956

1.0 kip = 4.45 kN.

4.1.6.2 Drift and P-delta effects. According to *Standard* Section 12.9.4, the computed displacements and drift (as based on the response spectrum of Figure 4.1-11) need not be scaled by the base shear factors (SF) of 2.18 and 1.94 for the structure loaded in the X and Y directions, respectively. This provides consistency with Section 12.8.6.2, which allows drift from an ELF analysis to be based on the computed period without the upper limit $C_u T_a$.

Section 12.9.4.2 of ASCE 7-10 requires that drifts from a response spectrum analysis be scaled only if Equation 12.8-6 controls the value of C_S. In this example, Equation 12.8-5 controlled the base shear, so drifts need not be scaled in ASCE 7-10.

In Tables 4.1-17 and 4.1-18, the story displacement from the response spectrum analysis, the story drift, the amplified story drift (as multiplied by C_d = 5.5) and the allowable story drift are listed. As before the story drifts represent the differences in the displacement at the center of mass of one level, and the displacement at vertical projection of that point at the level below. These values were determined in each mode and then combined using CQC. As may be observed from the tables, the allowable drift is not exceeded at any level.

Table 4.1-17 Response Spectrum Drift for Building Responding in X Direction

Level	Total Drift from R.S. Analysis (in.)	Story Drift (in.)	Story Drift × C_d (in.)	Allowable Story Drift (in.)
R	2.23	0.12	0.66	3.00
12	2.10	0.16	0.89	3.00
11	1.94	0.19	1.03	3.00
10	1.76	0.20	1.08	3.00
9	1.56	0.18	0.98	3.00
8	1.38	0.19	1.06	3.00
7	1.19	0.20	1.08	3.00
6	0.99	0.20	1.08	3.00
5	0.80	0.18	0.97	3.00
4	0.62	0.19	1.02	3.00
3	0.43	0.19	1.05	3.00
2	0.24	0.24	1.34	4.32

1.0 in. = 25.4 mm.

Table 4.1-18 Response Spectrum Drift for Building Responding in Y Direction

Level	Total Drift from R.S. Analysis (in.)	Story Drift (in.)	Story Drift × C_d (in.)	Allowable Story Drift (in.)
R	1.81	0.06	0.32	3.00
12	1.76	0.09	0.49	3.00
11	1.67	0.11	0.58	3.00
10	1.56	0.12	0.67	3.00
9	1.44	0.13	0.70	3.00
8	1.31	0.16	0.87	3.00
7	1.15	0.17	0.91	3.00
6	0.99	0.17	0.92	3.00
5	0.92	0.17	0.93	3.00
4	0.65	0.19	1.04	3.00
3	0.46	0.20	1.08	3.00
2	0.26	0.26	1.44	4.32

1.0 in. = 25.4 mm.

According to *Standard* Section 12.9.6, P-delta effects should be checked using the ELF method. This implies that such effects should *not* be determined using the results from the modal response spectrum analysis. Thus, the results already shown and discussed in Table 4.1-11 of this example are applicable.

Nevertheless, P-delta effects can be assessed using the results of the modal response spectrum analysis if the displacements, drifts and story shears are used as computed from the response spectrum analysis, *without the base shear scale factors*. However, when computing the stability ratio, the drifts must include the amplifier C_d (because of the presence of C_d in the denominator of Standard Equation 12.8-16). Using this approach, P-delta effects were computed for the X direction response as shown in Table 4.1-19. Note that the stability factors are very similar to those given in Table 4.1-11. As with Table 4.1-11, the stability factors from Table 4.1-19 exceed the limit ($\theta_{max} = 0.091$) only at the bottom three levels of the structure and are only marginally above the limit. Since the β factor was conservatively set at 1.0 inch for computing the limit, it is likely that a refined analysis for β would indicate that P-delta effects are not of particular concern for this structure.

Table 4.1-19 Computation of P-delta Effects for X Direction Response

Level	h_{sx} (in.)	Δ (in.)	P_D (kips)	P_L (kips)	P_T (kips)	P_X (kips)	V_X (kips)	θ_X
R	150	0.66	1,656.5	315.0	1,971.5	1,971.5	82.7	0.019
12	150	0.89	1,595.8	315.0	1,910.8	3,882.3	130.9	0.032
11	150	1.03	1,595.8	315.0	1,910.8	5,793.1	163.8	0.044
10	150	1.08	1,595.8	315.0	1,910.8	7,703.9	191.4	0.053
9	150	0.98	3,403.0	465.0	3,868.0	11,571.9	240.1	0.057
8	150	1.06	2,330.8	465.0	2,795.8	14,367.7	268.9	0.069
7	150	1.08	2,330.8	465.0	2,795.8	17,163.5	292.9	0.077
6	150	1.08	2,330.8	465.0	2,795.8	19,959.3	316.1	0.083
5	150	0.97	4,323.8	615.0	4,938.8	24,898.1	359.5	0.081

Table 4.1-19 Computation of P-delta Effects for X Direction Response

Level	h_{sx} (in.)	Δ (in.)	P_D (kips)	P_L (kips)	P_T (kips)	P_X (kips)	V_X (kips)	θ_X
4	150	1.02	3,066.1	615.0	3,681.1	28,579.2	384.8	0.092
3	150	1.05	3,066.1	615.0	3,681.1	32,260.3	401.9	0.102
2	216	1.34	3,097.0	615.0	3,712.0	35,972.3	438.1	0.093

1.0 in. = 25.4 mm, 1.0 kip = 4.45 kN.

4.1.6.3 Torsion, orthogonal loading and load combinations. To determine member design forces, it is necessary to add the effects of accidental torsion and orthogonal loading into the analysis. When including accidental torsion in modal response spectrum analysis, there are generally two approaches that can be taken:

- Displace the center of mass of the floor plate plus or minus 5 percent of the plate dimension perpendicular to the direction of the applied response spectrum. As there are four possible mass locations, this will require four separate modal analyses for torsion with each analysis using a different set of mode shapes and frequencies.

- Compute the effects of accidental torsion by creating a load condition with the accidental story torques applied as static forces. Member forces created by the accidental torsion are then added directly to the results of the response spectrum analysis. As with the displaced mass method, there are four possible ways to apply the accidental torsion: plus and minus torsion for primary loads in the X and Y directions. Where scaling of the modal response spectrum design forces is required, the torsional loading used for accidental torsion analysis should be multiplied by 0.85.

Each of the above approaches has advantages and disadvantages. The primary disadvantage of the first approach is a practical one: most computer programs do not allow for the extraction of member force maxima from more than one run where the different runs incorporate a different set of mode shapes and frequencies. An advantage of the approach stipulated in *Standard* Section 12.9.5 is that accidental torsion need not be amplified (when otherwise required by *Standard* Section 12.8.4.3) because the accidental torsion effect is amplified within the dynamic analysis.

For structures that are torsionally regular and which will not require amplification of torsion, the second approach may be preferred. A disadvantage of the approach is the difficulty of combining member forces from a CQC analysis (all results positive), and a separate static torsion analysis (member forces have positive and negative signs as appropriate).

In the analysis that follows, the second approach has been used because the structure has excellent torsional rigidity, and amplification of accidental torsion is not required (all amplification factors = 1.0).

There are two possible methods for applying the orthogonal loading rule:

- Run two separate response spectrum analyses, one in the X direction and one in the Y direction, with CQC being used for modal combinations in each analysis. Using a direct sum, combine 100 percent of the scaled X direction results with 30 percent of the scaled Y direction results. Perform a similar analysis using 100 percent of the scaled Y direction forces and 30 percent of the scaled X direction forces. All seismic effects can be considered in only two dynamic load cases (one response spectrum analysis in each direction) and two torsion cases (resulting from loads applied at a 5 percent eccentricity in each direction). These are shown in Figure 4.1-12.

- Run two separate response spectrum analyses, one in the X direction and one in the Y direction, with CQC being used for modal combinations in each analysis. Using SRSS, combine 100 percent of the scaled X direction results with 100 percent of the scaled Y direction results (Wilson, 2004).

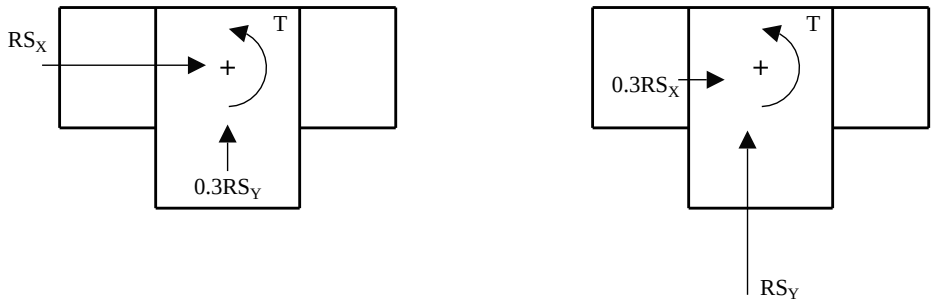

Figure 4.1-12 Load combinations for response spectrum analysis

4.1.6.4 Member design forces. Earthquake shear forces in the beams of Frame 1 are given in Figure 4.1-13. These member forces are based on 2.18 times the spectrum applied in the X direction and 1.94 times of the spectrum applied independently in the Y direction. Individual member forces from the X and Y directions are obtained by CQC for that analysis and these forces are combined by SRSS. To account of accidental torsion, the forces in Figure 4.1-13 should be added to 0.85 times the forces shown in Figure 4.1-9b.

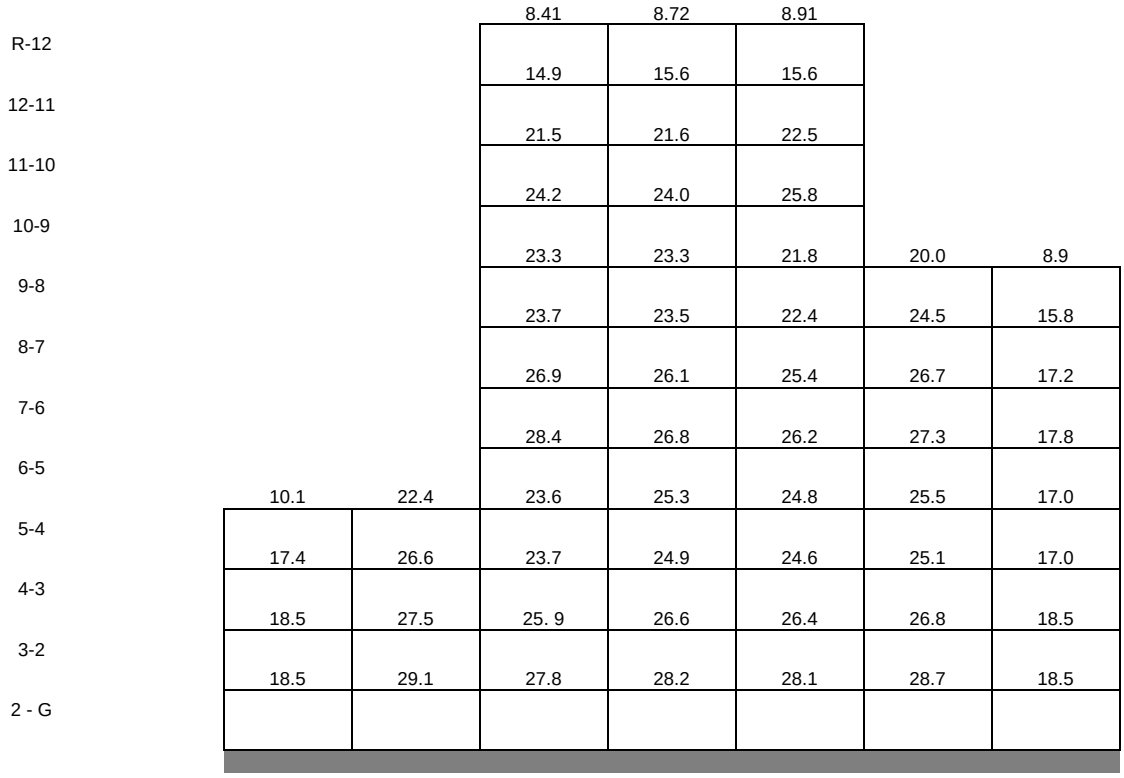

Figure 4.1-13 Seismic shears in girders (kips) as computed using response spectrum analysis (analysis includes orthogonal loading but excludes accidental torsion)

4.1.7 Modal Response History Analysis

Before beginning this section, it is important to note that the analysis performed here is based on the requirements of Chapter 16 of ASCE 7-10. This version contains several important updates that removed inconstancies and omissions that were present in Chapter 16 of ASCE 7-05.

In modal response history analysis, the original set of coupled equations of motion is transformed into a set of uncoupled "modal" equations, an explicit displacement history is computed for each mode, the modal histories are transformed back into the original coordinate system, and these responses are added together to produce the response history of the displacements at each of the original degrees of freedom. These displacement histories may then be used to determine histories of story drift, member forces, or story shears.

Requirements for response history analysis are provided in Chapter 16 of ASCE 7-10. The same mathematical model of the structure used for the ELF and response spectrum analysis is used for the response history analysis. Five percent damping was used in each mode and as with the response spectrum method, 12 modes were used in the analysis. These 12 modes captured more than 90 percent of the mass of the structure above grade. Several issues related to a reanalysis of the structure with 120 modes are described later.

As allowed by ASCE 7-10 Section 16.1, the structure is analyzed using three different pairs of ground acceleration histories. The development of a proper suite of ground motions is one of the most critical

and difficult aspects of response history approaches. The motions should be characteristic of the site and should be from real (or simulated) ground motions that have a magnitude, distance and source mechanism consistent with those that control the maximum considered earthquake (MCE).

For the purposes of this example, however, the emphasis is on the *implementation* of the response history approach rather than on selection of realistic ground motions. For this reason, the motion suite developed for Example 4.2 is also used for the present example.[5] The structure for Example 4.2 is situated in Seattle, Washington and uses three pairs of motions developed specifically for the site. The use of the Seattle motions for a Stockton building analysis is, of course, not strictly consistent with the requirements of the *Standard*. However, a realistic comparison may still be made between the ELF, response spectrum and response history approaches.

4.1.7.1 The Seattle ground motion suite. It is beneficial to provide some basic information on the Seattle motion suites in Table 4.1-20a below. Refer to Figures 4.2-40 through 4.2-42 for additional information, including plots of the ground acceleration histories and 5-percent damped response spectra for each component of each motion.

The acceleration histories for each source motion were downloaded from the PEER NGA Strong Ground Motion Database:

http://peer.berkeley.edu/products/strong_ground_motion_db.html

The PEER NGA record number is provided in the first column of the table. Note that the magnitude, epicenter distance and site class were obtained from the NGA Flatfile (a large Excel file that contains information about each NGA record).

Table 4.1-20a Suite of Ground Motions Used for Response History Analysis

NGA Record Number	Magnitude [Epicenter Distance, km]	Site Class	Number of Points and Digitization Increment	Component Source Motion	PGA (g)	Record Name (This Example)
0879	7.28 [44]	C	9625 @ 0.005 sec	Landers/LCN260*	0.727	A00
				Landers/LCN345*	0.789	A90
0725	6.54 [11.2]	D	2230 @ 0.01 sec	SUPERST/B-POE270	0.446	B00
				SUPERST/B-POE360	0.300	B90
0139	7.35 [21]	C	1192 @ 0.02 sec	TABAS/DAY-LN	0.328	C00
				TABAS/DAY-TR	0.406	C90

*Note that the two components of motion for the Landers earthquake are apparently separated by an 85 degree angle, not 90 degrees as is traditional. It is not known whether these are true orientations or whether there is an error in the descriptions provided in the NGA database.

Before the ground motions may be used in the response history analysis, they must be scaled for compatibility with the design spectrum. The scaling procedures for three-dimensional dynamic analysis are provided in Section 16.1.3.2 of ASCE 7-10. These requirements are provided verbatim as follows:

[5] See Sec. 3.2.6.2 of this volume of design examples for a detailed discussion of the selection and scaling of ground motions.

> "For each pair of horizontal ground motion components a square root of the sum of the squares (SRSS) spectrum shall be constructed by taking the SRSS of the 5-percent damped response spectra for the scaled components (where an identical scale factor is applied to both components of a pair). Each pair of motions shall be scaled such that for each period in the range from $0.2T$ to $1.5T$, the average of the SRSS spectra from all horizontal component pairs does not fall below the corresponding ordinate of the design response spectrum, determined in accordance with Section 11.4.5 or 11.4.7."

ASCE 7-10 does not provide clear guidance as to which fundamental period, T, should be used for determining $0.2T$ and $1.5T$ when the periods of vibration are different in the two orthogonal directions of analysis. This issue is resolved herein by taking T as the average of the computed periods in the two principal directions. For this example, the average period, referred to a T_{Avg}, is 0.5(2.87 + 2.60) = 2.74 seconds. (Another possibility would be to use the shorter of the two fundamental periods for computing $0.2T$ and the longer of the two fundamental periods for computing $1.5T$.)

It is also noted that the scaling procedure provided by ASCE 7-10 does not provide a unique set of scale factors for each set of ground motions. This "degree of freedom" in the scaling process may be eliminated[4] by providing a six-step procedure, as described below:

1. Compute the 5 percent damped pseudo-acceleration spectrum for each unscaled component of each pair of ground motions in the set and produce the SRSS spectrum for each pair of motions within the set.

2. Using the same period values used to compute the ground motion spectra, compute the design spectrum following the procedures in ***Standard*** Section 11.4.5. This spectrum is designated as the "target spectrum".

3. Scale each SRSS spectrum such that the spectral ordinate of the scaled spectrum at T_{Avg} is equal to the spectral ordinate of the design spectrum at the same period. Each SRSS spectrum will have a unique scale factor, $S1_i$, where i is the number of the pair (i ranges from 1 to 3 for the current example).

4. Create a new spectrum that is the average of the S1 scaled SRSS spectra. This spectrum is designated as the "average S1 scaled SRSS spectrum" and should have the same spectral ordinate as the target spectrum at the period T_{Avg}.

5. For each spectral ordinate in the period range $0.2T_{Avg}$ to $1.5T_{Avg}$, divide the ordinate of the target spectrum by the corresponding ordinate of the average S1 scaled SRSS spectrum, producing a set of spectral ratios over the range $0.2T_{Avg}$ to $1.5T_{Avg}$. The ***largest*** value among these ratios is designated as S2.

6. Multiply the factor $S1_i$ determined in Step 3 for each pair in the set by the factor S2 determined in Step 5. This product, $SS_i = S1_i \times S2$ is the scale factor that should be applied to each component of ground motion in pair i of the set.

The results of the scaling process are summarized in Table 4.1-20b and in Figures 4.1-14 through 4.1-18.

[4] Elimination of the degree of freedom results in consistent scale factors for all persons using the process. This consistency is not required by ASCE 7 and experienced analysts may wish to use the "degree of freedom" to reduce or increase the influence of a given ground motion.

Table 4.1-20b Result of 3D Scaling Process

Set Number	Designation	SRSS Ordinate at $T = T_{Avg}$ (g)	Target Ordinate at $T = T_{Avg}$ (g)	S1	S2	SS
1	A00 & A90	0.335	0.136	0.407	1.184	0.482
2	B00 & B90	0.191	0.136	0.712	1.184	0.843
3	C00 & C90	0.104	0.136	1.310	1.184	1.551

Figure 4.1-14 shows the unscaled SRSS spectra for each component pair, together with the target spectrum. Figure 4.1-15 shows the average S1 scaled SRSS spectrum and the target spectrum, where it may be seen that both spectra have a common ordinate at the average period of 2.74 seconds. Figure 4.1-16 is a plot of the spectral ratios computed in Step 5. Figure 4.1-17 is a plot of the SS scaled average SRSS spectrum, together with the target spectrum. From this plot it may be seen that all ordinates of the SS scaled average SRSS spectrum are greater than or equal to the ordinate of the target spectrum over the period range $0.2T_{Avg}$ to $1.5T_{Avg}$. The "controlling" period at which the two spectra in Figure 4.1-17 have exactly the same ordinate is approximately 1.6 seconds.

Figure 4.1-18a shows the SS scaled spectra for the "00" components of each earthquake, together with the target spectrum. Figure 4.-18b is similar, but shows the "90" components of the ground motions. Also shown in these plots are vertical lines that represent the first 12 periods of vibration for the structure under consideration. Two additional vertical lines are shown that represent the periods for Modes 112 and 118, at which the basement walls and grade-level slab become dynamically effective. Three important points are noted from Figures 4.1-18:

The match for the lower few modes ($T > 1.0$ sec) is good for the "00" components, but not as good for the "90" components. In particular, the ground motion coordinates for motions A90 and B90 are considerably less than those for the target spectrum.

- Higher mode responses ($T < 1.0$ sec) will be significantly greater in Earthquake C than in Earthquake A or B. In Modes 10 through 12, the response for Earthquake A is several times greater than for Earthquake B.

- In Modes 112 and 118, the response for Earthquake A is approximately three times that for the code spectrum.

The impact of these points on the computed response of the structure will be discussed in some detail later in this example.

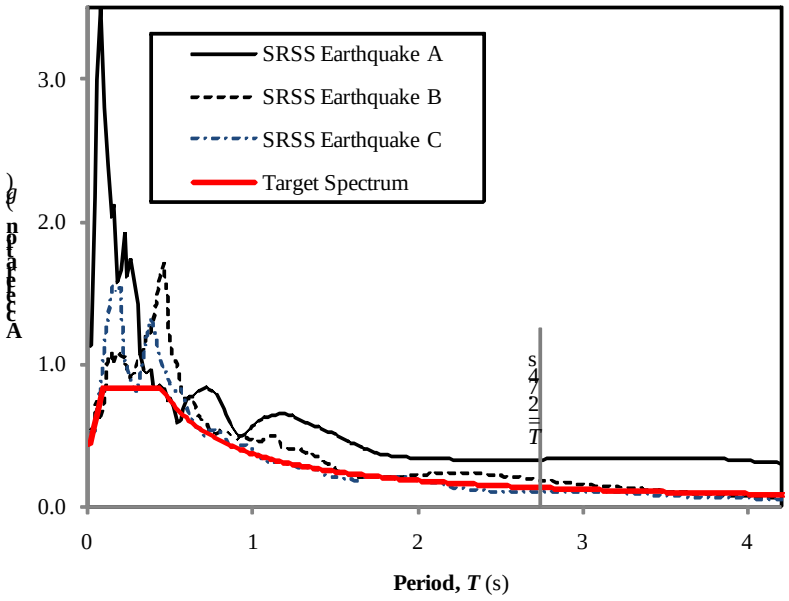

Figure 4.1-14 Unscaled SRSS spectra and target spectrum

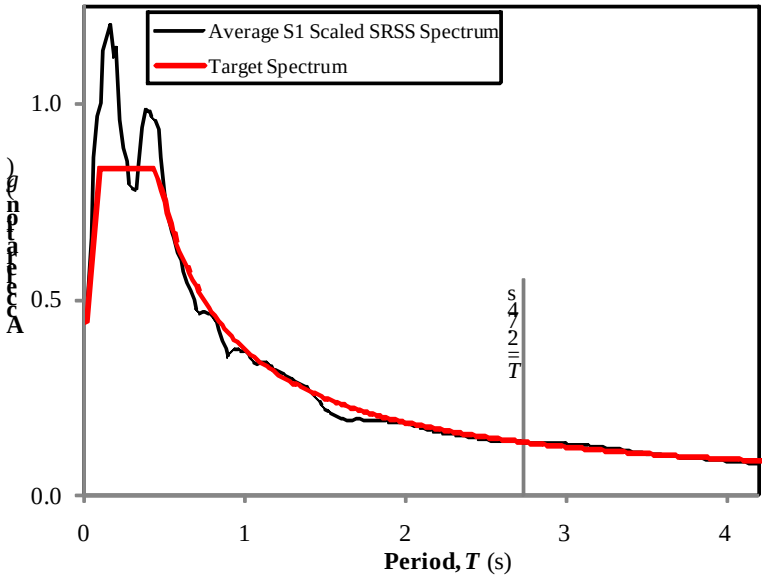

Figure 4.1-15 Average S1 scaled SRSS spectrum and target spectrum

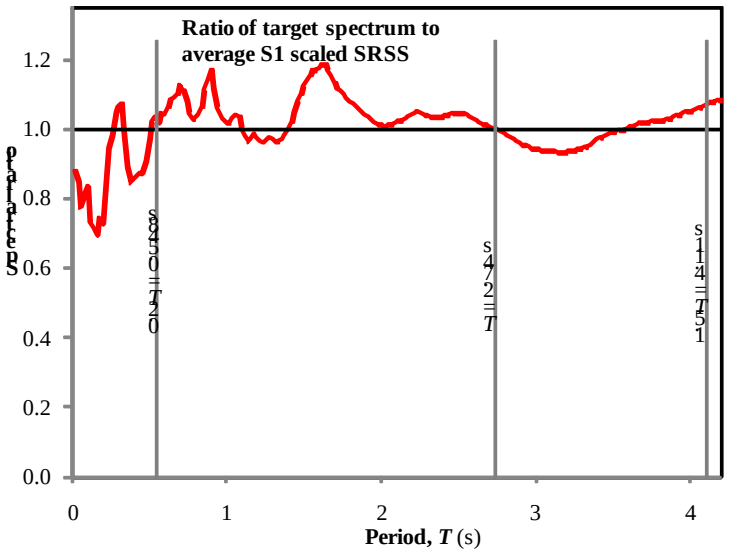

Figure 4.1-16 Ratio of target spectrum to average S1 scaled SRSS spectrum

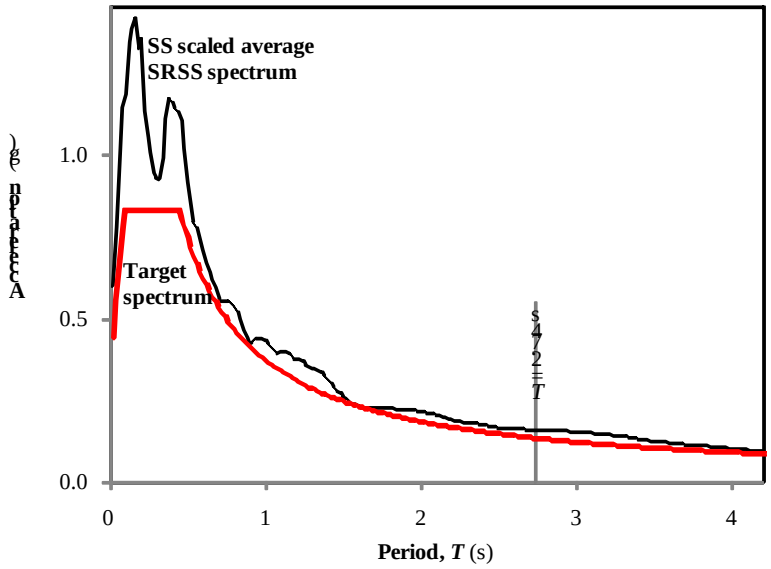

Figure 4.1-17 SS scaled average SRSS spectrum and target spectrum

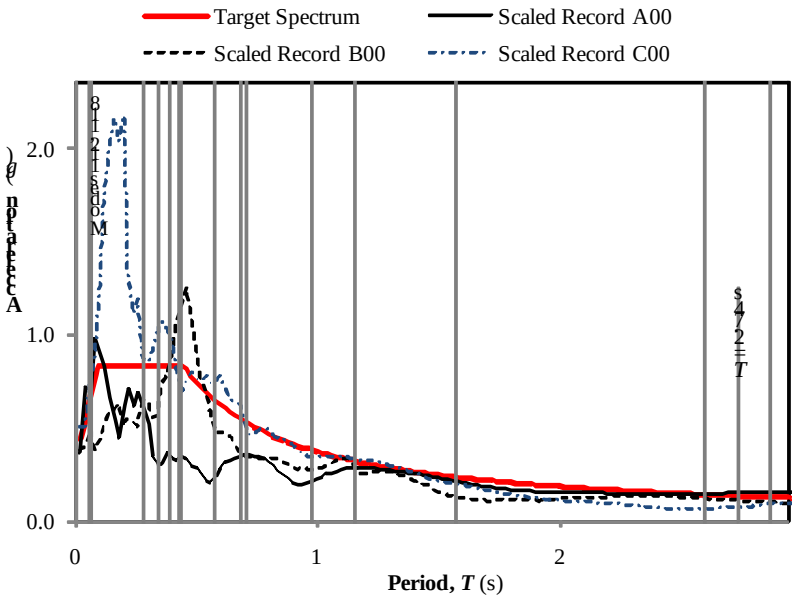

(a) 00 Components

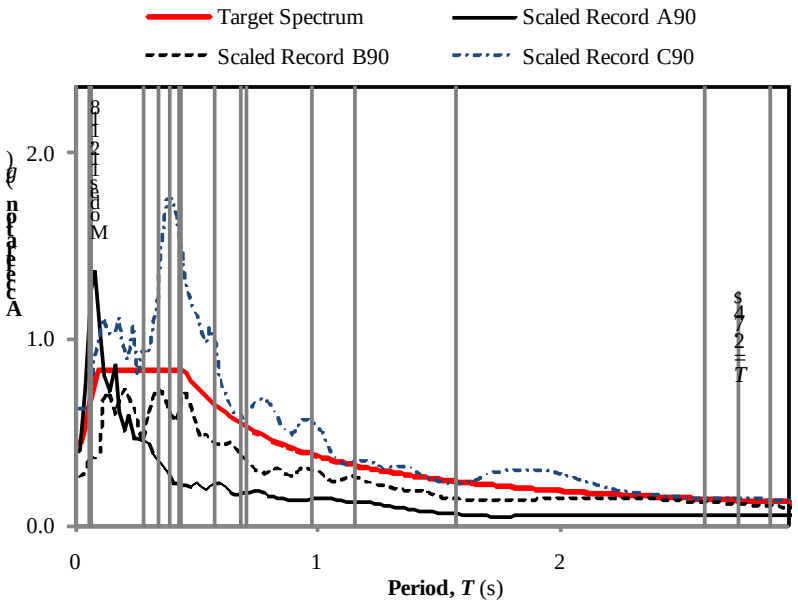

(b) 90 Components

Figure 4.1-18 SS scaled individual spectra and target spectrum

Another detail not directly specified by Chapter 16 of ASCE 7-10 is how ground motions should be oriented when applied. In the analysis presented herein, 12 dynamic analyses were performed with scaled ground motions applied only in one direction, as follows:

- A00-X: SS scaled component A00 applied in X direction
- A00-Y: SS scaled component A00 applied in Y direction

- A90-X: SS scaled component A90 applied in X direction
- A90-Y: SS scaled component A90 applied in Y direction

- B00-X: SS scaled component B00 applied in X direction
- B00-Y: SS scaled component B00 applied in Y direction
- B90-X: SS scaled component B90 applied in X direction
- B90-Y: SS scaled component B90 applied in Y direction

- C00-X: SS scaled component C00 applied in X direction
- C00-Y: SS scaled component C00 applied in Y direction
- C90-X: SS scaled component C90 applied in X direction
- C90-Y: SS scaled component C90 applied in Y direction

The scaled motions, without the (I/R) factor, were applied at the base of the basement walls. Accidental torsion effects are included in a separate static analysis, as described later. All 12 individual response history analyses were carried out using SAP2000. As with the response spectrum analysis, 12 modes were used in the analysis. Five percent of critical damping was used in each mode. The integration time-step used in all analyses was equal to the digitization interval of the ground motion used (see Table 4.1-20a). The results from the analyses are summarized Tables 4.1-21.

A summary of base shear and roof displacement results from the analyses using the SS scaled ground motions is provided in Table 4.1-21. As may be observed, the base shears range from a low of 1,392 kips for analysis A90-Y to a high of 5,075 kips for analysis C90-Y. Roof displacements range from a low of 5.16 inches for analysis A90-Y to a high of 20.28 inches for analysis A00-X. This is a remarkable range of behavior when one considers that the ground motions were scaled for consistency with the design spectrum.

Table 4.1-21 Result Maxima from Response History Analysis Using SS Scaled Ground Motions

Analysis	Maximum base shear (kips)	Time of maximum shear (sec.)	Maximum roof displacement (in.)	Time of maximum displacement (sec.)
A00-X	3507	11.29	20.28	11.38
A00-Y	3573	11.27	14.25	11.28
A90-X	1588	12.22	7.32	12.70
A90-Y	1392	13.56	5.16	10.80
B00-X	3009	8.28	12.85	9.39
B00-Y	3130	9.37	11.20	10.49
B90-X	2919	8.85	11.99	7.11
B90-Y	3460	7.06	11.12	8.20
C00-X	3130	13.5	9.77	13.54
C00-Y	2407	4.64	6.76	8.58
C90-X	3229	6.92	15.61	6.98
C90-Y	5075	6.88	14.31	7.80

1.0 in. = 25.4 mm, 1.0 kip = 4.45 kN.

The analysis was performed without the (I/R) factor, so in conformance with Section 16.1.4 of ASCE 7-10, all force quantities produced from the analysis were multiplied by this factor. All displacements from the analysis were multiplied by the factor C_d/R.

Additionally, the 2010 version of the ***Standard*** requires that forces be scaled by the factor $0.85V/V_i$ where the base shears from the response history analysis, V_i, are less than 0.85 times the base shears, V, produced by the ELF method when either Equation 12.8-5 or 12.8-6 controls the seismic base shear. The displacements must be scaled by the same factor only if Equation 12.8-6 controls when computing the seismic base shear. (It is noted that these requirements are similar to the scaling requirements provided for modal response spectrum analysis [Sections 12.9.4.1 and 12.9.4.2] except that forces from modal response spectrum analysis would be scaled if the shear from the response spectrum analysis is less than $0.85V$, regardless of the C_s equation which controls V.)

The base shears from the SS scaled motions with the I/R = 1/8 scaling are provided in the first column of Table 4.1-22. These forces are all significantly less than 0.85 times the ELF base shear, which is 0.85(112.5) = 956 kips. The required scale factors to bring the base shears up to the 85 percent requirement are shown in Column 2 of Table 4.2-22.

Before proceeding, it is important to remind the reader that three separate sets of scale factors apply to the response history analysis of this structure when member design forces are being obtained:

1. The ground motion SS scale factors

2. The I/R scale factor

3. The $0.85V/V_i$ factor because the base shear from modal response history analysis (including scale factors 1 and 2 above) is less than 85 percent of that determined from ELF when ELF is governed by Equation 12.8-5 or 12.8-6.

Table 4.1-22 I/R Scaled Shears and Required 85% Rule Scale Factors

Analysis	(I/R) times maximum base shear from analysis (kips)	Required additional scale factor for $V = 0.85V_{ELF}$ = 956 kips
A00-X	438.4	2.18
A00-Y	446.7	2.14
A90-X	198.5	4.81
A90-Y	173.9	5.49
B00-X	376.1	2.54
B00-Y	391.2	2.44
B90-X	364.8	2.62
B90-Y	432.5	2.21
C00-X	391.2	2.44
C00-Y	300.9	3.18
C90-X	403.6	2.37
C90-Y	634.4	1.51

1.0 kip = 4.45 kN

4.1.7.2 Drift and P-delta effects. Only two scale factors are required for displacement and drift because Equation 12.8-6 did not control the base shear for this structure:

- The ground motion scale factors SS
- The C_d/R scale factor

Drift is checked for each individual component of motion acting in the X direction and the envelope values of drift are taken as the design drift values. The procedure is repeated for motions applied in the Y direction. As with the ELF and Modal Response Spectrum analyses, drifts are taken as the difference between the displacement at the center of mass of one level and the displacement at the projection of this point on the level below. The results of the analysis, shown in Table 4.1-23 for the X direction only, indicate that the allowable drift is not exceeded at any level of the structure. Similar results were obtained for Y direction loading.

Table 4.1-23 Response History Drift for Building Responding in X Direction for All of the Ground Motions in the X Directions

Level	Envelope of drift (in.) for each ground motion						Envelope of drift for all the ground motions	Envelope of drift $\times C_d/R$	Allowable drift (in.)
	A00-X	A90-X	B00-X	B90-X	C00-X	C90-X			
R	1.17	0.49	0.95	0.81	0.91	1.23	1.23	0.85	3.00
12	1.64	0.66	1.22	0.95	1.16	1.27	1.64	1.13	3.00
11	1.97	0.78	1.32	0.99	1.25	1.52	1.97	1.35	3.00
10	2.05	0.86	1.42	1.04	1.20	1.68	2.05	1.41	3.00
9	1.79	0.82	1.26	1.25	0.99	1.41	1.79	1.23	3.00
8	1.83	0.87	1.22	1.42	1.23	1.50	1.83	1.26	3.00
7	1.82	0.83	1.27	1.36	1.21	1.67	1.82	1.25	3.00
6	1.77	0.74	1.36	1.35	1.06	1.94	1.94	1.33	3.00
5	1.50	0.59	1.19	1.21	1.09	1.81	1.81	1.24	3.00
4	1.55	0.62	1.22	1.32	1.23	1.76	1.76	1.21	3.00
3	1.56	0.64	1.24	1.30	1.33	1.60	1.60	1.10	3.00
2	1.97	0.86	1.64	1.58	1.73	1.85	1.97	1.35	4.32

1.0 in. = 25.4 mm.

ASCE 7-10 does not provide information on how P-delta effects should be addressed in response history analysis. It would appear reasonable to use the same procedure as specified for ASCE 7-05 and ASCE 7-10 for Modal Response Spectrum Analysis (Sec. 12.9.6), where it is stated that the Equivalent Lateral Force method of analysis be used. Such an analysis was performed in Section 4.1.5.3.2 of this example, with results provided in Table 4.1-11. These results indicate that allowable stability ratios are marginally exceeded at Levels 2, 3 and 4, but that rigorous analysis with β less than 1.0 would show that the allowable stability ratios are not exceeded.

4.1.7.3 Torsion, orthogonal loading and member design forces. As with ELF or response spectrum analysis, it is necessary to add the effects of accidental torsion and orthogonal loading into the analysis.

Accidental torsion is applied separately with a static analysis in exactly the same manner as done for the response spectrum approach. Member shears for this torsion-only analysis are shown separately in Figure 4.1-9b. These shears must be multiplied by 0.85 before adding to the scaled shears produced by the dynamic response history analysis.

Orthogonal loading is automatically accounted for by applying the 100 percent of the ground motions in the X and Y direction simultaneously. For each ground motion pair, these forces are applied in the orientations shown in Figure 4.1-19. The figure also shows the scale factor that was used in each analysis.

Load Combination for Response History Analysis

Earthquake	Load Combination	Loading X Direction		Loading Y Direction	
		Record	Scale Factor	Record	Scale Factor
A	1	A00-X	2.18	A00-Y	5.49
	2	A90-X	-4.81	A90-Y	2.14
	3	A00-X	-2.18	A00-Y	-5.49
	4	A90-X	4.81	A90-Y	-2.14
B	5	B00-X	2.54	B00-Y	2.21
	6	B90-X	-2.62	B90-Y	2.44
	7	B00-X	-2.54	B00-Y	-2.21
	8	B90-X	2.62	B90-Y	-2.44
C	9	C00-X	2.44	C00-y	1.50
	10	C90-X	-2.36	C90-Y	3.18
	11	C00-X	-2.44	C00-Y	-1.50
	12	C90-X	2.36	C90-Y	-3.18

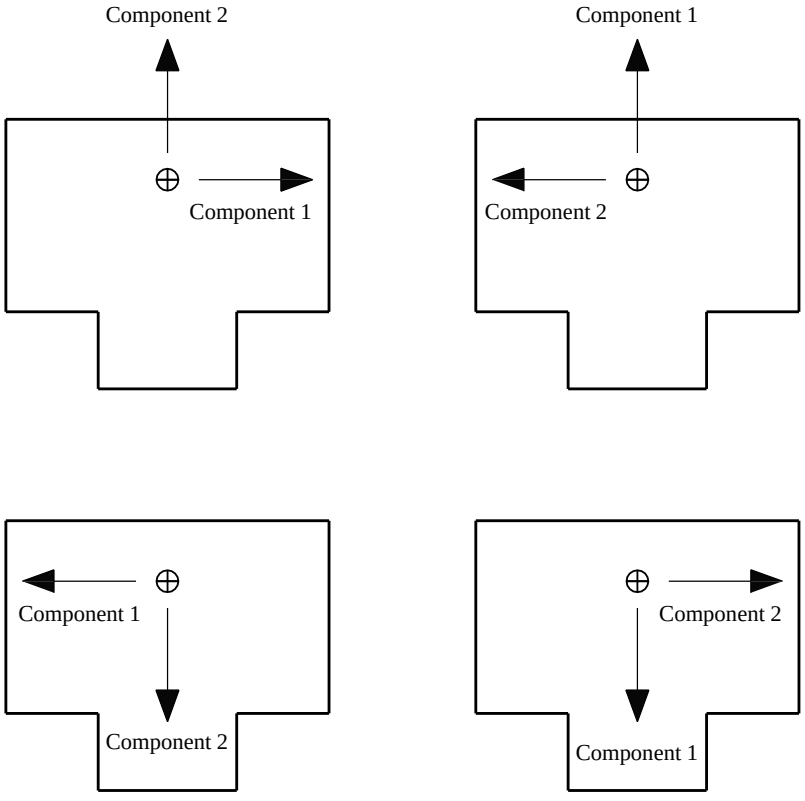

Figure 4.1-19 Orthogonal Loading in Response History Analysis

Using the load combinations described above, the individual beam shear maxima developed in Frame 1 were computed for each load combination. Envelope values from all combinations are shown in Figure 4.1-20.

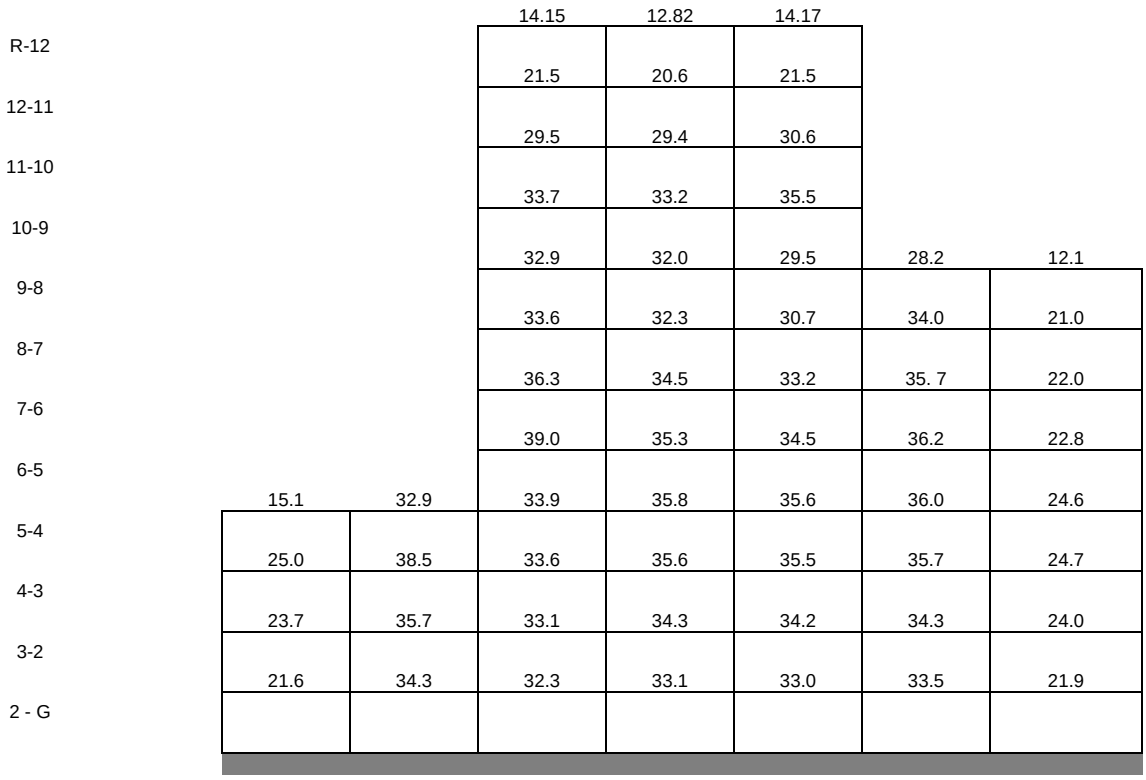

Figure 4.1-20 Envelope of seismic shears in girders (kips) as computed using response history analysis (analysis includes orthogonal loading but excludes accidental torsion)

4.1.8 Comparison of Results from Various Methods of Analysis

A summary of the results from all of the analyses is provided in Tables 4.1-24 through 4.1-28.

4.1.8.1 Comparison of base shear and story shear. The maximum story shears are shown in Table 4.1-24. For the response history analysis, the shears are the envelope values of story shears for all twelve individual analyses. Note that the modal response spectrum and modal response history shears for the lowest level are both equal to 956 kips, which is 0.85 times the ELF base shear.

The story shear is basically of the same character—lower values in upper stories, larger values in lower stories. It appears, however, that the maximum shears from the modal response history analysis occur at stories 2, 3 and 4. This must be due to the amplified energy in the higher modes in the actual ground motions (when compared to the design spectrum).

4.1.8.2 Comparison of drift. Table 4.1-25 summarizes the drifts computed from each of the analyses. The modal response history drifts are the envelopes among all analyses. The ELF drifts are significantly greater than those determined using modal response spectrum analysis. The drifts from the modal response history analysis are slightly greater than those from the response spectrum analysis.

4.1.8.3 Comparison member forces. The shears developed in Bay D-E of Frame 1 are compared in Table 4.1-26. The shears from the response history analysis are envelope values among all analyses, including torsion and orthogonal load effects. The response history approach produced beam shears similar to those from ELF analysis and somewhat greater than those produced by response spectrum analysis.

Table 4.1-24 Summary of Results of Various Methods of Analysis: Story Shear

Level	ELF	Modal response spectrum	Modal response history
R	187	180	295
12	341	286	349
11	471	357	462
10	578	418	537
9	765	524	672
8	866	587	741
7	943	639	753
6	999	690	943
5	1,070	784	1,135
4	1,102	840	1,099
3	1,118	895	1,008
2	1,124	956	956

Table 4.1-25 Summary of Results from Various Methods of Analysis: Story Drifts

Level	X Direction Drift (in.)		
	ELF	Modal response spectrum	Modal response history
R	0.99	0.66	0.85
12	1.41	0.89	1.13
11	1.75	1.03	1.35
10	1.92	1.08	1.41
9	1.82	0.98	1.23
8	1.97	1.06	1.26
7	2.01	1.08	1.25
6	1.97	1.08	1.33
5	1.67	0.97	1.24

Table 4.1-25 Summary of Results from Various Methods of Analysis: Story Drifts

Level	X Direction Drift (in.)		
	ELF	Modal response spectrum	Modal response history
4	1.69	1.02	1.21
3	1.65	1.05	1.10
2	2.00	1.34	1.35

1.0 in. = 25.4 mm.

Table 4.1-26 Summary of Results from Various Methods of Analysis: Beam Shear

Level	Beam Shear Force in Bay D-E of Frame 1 (kips)		
	ELF	Modal response spectrum	Modal response history
R	10.27	8.72	12.82
12	18.91	15.61	20.61
11	28.12	21.61	29.45
10	33.15	24.02	33.22
9	34.69	23.32	32.02
8	35.92	23.47	32.30
7	40.10	26.15	34.53
6	40.58	26.76	35.29
5	36.52	25.29	35.82
4	34.58	24.93	35.65
3	35.08	26.60	34.27
2	35.28	28.25	33.07

1.0 kip = 4.45 kN.

4.1.8.4 Which analysis method is best? In this example, an analysis of an irregular steel moment frame was performed using three different techniques: equivalent lateral force analysis, modal response spectrum analysis and modal response history analysis. Each analysis was performed using a linear elastic model of the structure even though it is recognized that the structure will repeatedly yield during the earthquake. Hence, each analysis has significant shortcomings with respect to providing a reliable prediction of the actual response of the structure during an earthquake.

The purpose of analysis, however, is not to predict response but rather to provide information that an engineer can use to proportion members and to estimate whether or not the structure has sufficient stiffness to limit deformations and avoid overall instability. In short, the analysis only has to be "good enough for design." If, on the basis of any of the above analyses, the elements are properly designed for strength, the stiffness requirements are met and the elements and connections of the structure are detailed for inelastic response according to the requirements of ASCE 7 and AISC 341, the structure will likely survive an earthquake consistent with the MCE ground motion. The exception would be if a highly

irregular structure were analyzed using the ELF procedure. Fortunately, ASCE 7 safeguards against this by requiring three-dimensional dynamic analysis for highly irregular structures.

For the structure analyzed in this example, the irregularities were probably not so extreme such that the ELF procedure would produce a "bad design." However, where computer programs that can perform modal response spectrum analysis with only marginally increased effort over that required for ELF are available (e.g., SAP2000 and ETABS), the modal analysis should always be used for final design in lieu of ELF (even if ELF is allowed by the *Provisions*). As mentioned in the example, this does not negate the need for or importance of ELF analysis because such an analysis is useful for preliminary design and several components of the ELF analysis are necessary for application of accidental torsion.

Modal response history analysis is of limited practical use where applied to a linear elastic model of the structure. The amount of additional effort required to select and scale the ground motions, perform the modal response history analysis, scale the results and determine envelope values for use in design simply is not warranted where compared to the effort required for modal response spectrum analysis. This might change in the future where "standard" suites of ground motions are developed and are made available to the earthquake engineering community. Also, significant improvement is needed in the software available for the preprocessing and, particularly, for the post-processing of the huge amounts of information that produced by the analysis.

Scaling the ground motions used for modal response history analysis is also an issue. The *Standard* requires that the selected motions be consistent with the magnitude, distance and source mechanism of the MCE expected at the site. If the ground motions satisfy this criterion, then why scale at all? Distant earthquakes may have a lower peak acceleration but contain a frequency content that is more significant. Near-source earthquakes may display single damaging pulses. Scaling these two earthquakes to the *Standard* design spectrum seems to eliminate some of the most important characteristics of the ground motions. The fact that there is a degree of freedom in the ASCE 7 scaling requirements compensates for this effect, but only for very knowledgeable users.

The main benefit of modal response history analysis is in the nonlinear dynamic analysis of structures or in the analysis of non-proportionally damped linear systems. This type of analysis is the subject of Example 4.2.

4.1.9 Consideration of Higher Modes in Analysis

All of the computed results for the modal response spectrum and modal response history methods of analysis were based on the first 12 modes of the model with the basement level explicitly modeled. Recall that the basement walls were modeled with 1.0-foot shell elements, that the grade-level diaphragm was modeled using 6.0-inch-thick shell elements and that the grade level was not laterally restrained. The weight associated with the basement-level walls and grade-level slab is 6,526 kips, which is approximately 15 percent of the total weight of the structure (see Table 4.1-3).

The accumulated effective modal mass for the first 12 modes (see Table 4.1-14a) is in the neighborhood of 82 percent of the total mass of the structure, which is less than the 90 percent required by Section 12.9-1 of the *Standard.* However, the first 12 modes capture more than 90 percent of the mass above grade, so it was deemed sufficient to run the analysis with only 12 modes. If the requirement of Section 12.9-1 were satisfied for the structure as modeled, it would have taken 119 modes to capture more than 90 percent of the effective mass of the entire system (see Table 4.1-14b).

In the analysis presented so far, all of the seismic base shears were computed at the base of the first story above grade, not the base of the entire structure (the base of the basement walls). It is of some interest to

examine how the results of the analysis would change if 120 modes were to be used in the analysis. This would definitely satisfy the requirements of Section 12.9-1 for the full structure.

4.1.9.1 Modal response spectrum analysis with higher modes. Table 4.1-27a provides the seismic shears through the basement level and through the first floor above grade for the analysis run with 12, 18, 120 and 200 modes. In this part of the table, the "modes" are the natural mode shapes from an eigenvalue analysis. As may be seen, the shear through the first story above grade is unchanged as the number of modes increases above 12 modes. However, the shears though the basement level are substantially increased when 120 or more modes are used. In the X direction, for example, the ratio of the basement-level shear for 120 modes to that for 12 modes is 630/439 = 1.44. Thus, in terms of the shear at the base of the structure, the activation of the higher modes increases the shears 44 percent, while the added weight associated with the basement level is only 15 percent.

This increase in shear was rather unexpected, so the analysis was re-run using Ritz vectors in lieu of the natural mode shapes. Ritz vectors automatically include the "static corrections" that are sometimes needed for very high frequency modes. As may be seen from Table 4.1-27b, the results using Ritz Vectors are virtually identical to those obtained using the natural mode shapes.

4.1.9.2 Modal response history analysis with higher modes. The comparison of shears using modal response history analysis with 12, 18, 120 and 200 modes are presented in Table 4.1-28. The results are based on the use of natural mode shapes. For brevity, results are given only for motions A00, B00 and C00 applied in the X and Y directions. The analyses include SS ground motion scaling, I/R scaling, but not the 85 percent scaling.

As may be observed from Table 4.1-27, the use of the higher modes produces virtually no change in the shears through the first level above grade. However, very significant increases in shear are developed through the basement. The most extreme increase in shears is for ground motion A00, wherein the shears in the basement increase from 439 kips to 744 kips for loading in the X direction and increase from 440 kips to 862 kips for loading in the Y direction. These increases in shear are not unexpected because of the spectral amplitudes of the ground motions at periods associated with modes 112 and 118 (see Figure 4.1-18).

4.1.9.3 Discussion on use of higher modes. Many structures have stiff lower stories or have one or more levels of basement. If the basement is modeled explicitly and if full lateral restraint is not provided at the top of the basement or at subgrade slab levels, the phenomena described herein will likely result.

Based on the results presented above, there is some question as to which results should be used for the 85 percent scaling requirements of *Standard* Section 12.9.4. If the basement level were included in the ELF analysis, the *computed* period would not significantly change, and the base shear would increase 15 percent to accommodate the added weight associated with the basement walls and grade-level slab. However, the scale factors required to bring the modal response spectrum or modal response history shears up to 85 percent of the ELF shears (with 15 percent increase) could be *significantly less* than those obtained when the basement level is not included in the model. The net result would be significantly reduced for design shears in the upper levels of the structure.

Given these results, it is recommended that scaling always be based on the shears determined at the first level above grade. The question of how many modes to use in the analysis is not as easy to answer. Certainly, a sufficient number of modes must be used to capture at least 90 percent of the above-grade mass. In cases where it is desired to explicitly determine the shears at the base of unrestrained basements, enough modes should be used to capture 90 percent of the mass of the entire structure.

Table 4.1-27 Comparison of Modal Response Spectrum Shears Using 12, 18, 120 and 200 Modes

(a) Using Natural Mode Shapes
(values from SAP2000 without 85% scaling)

Shear Location	Load Case	Shear (kips) for number of modes =			
		12	18	120	200
Base of 1st story	Code spectrum X direction	438	438	439	439
Base of structure	Code spectrum X direction	439	439	630	631
Base of 1st story	Code spectrum Y direction	492	493	493	493
Base of structure	Code spectrum Y direction	493	493	686	686

(b) Using Ritz Vectors
(values from SAP2000 without 85% scaling)

Shear Location	Load Case	Shear (kips) for number of modes =			
		12	18	120	200
Base of 1st story	Code spectrum X direction	435	439	439	439
Base of structure	Code spectrum X direction	435	439	467	630
Base of 1st story	Code spectrum Y direction	485	494	494	494
Base of structure	Code spectrum Y direction	485	494	497	686

Table 4.1-28 Comparison of Modal Response History Shears Using 12, 18, 120 and 200 Modes

Using Natural Mode Shapes
(values from SAP2000 without 85% scaling)

Shear Location	Load Case	Shear (kips) for number of modes=			
		12	18	120	200
Base of 1st story	A00 in X direction	438	438	445	445
Base of structure	A00 in X direction	439	439	744	744
Base of 1st story	B00 in X direction	376	376	377	490
Base of structure	B00 in X direction	377	377	529	530
Base of 1st story	C00 in X direction	391	391	392	391
Base of structure	C00 in X direction	392	392	438	440
Base of 1st Story	A00 in Y direction	447	447	452	452
Base of Structure	A00 in Y direction	440	447	861	862
Base of 1st Story	B00 in Y direction	391	391	395	395
Base of Structure	B00 in Y direction	397	392	508	508
Base of 1st Story	C00 in Y direction	301	301	301	301
Base of Structure	C00 in Y direction	307	302	561	562

4.1.10 Commentary on the ASCE 7 Requirements for Analysis

As mentioned in this example, ASCE 7-05 contained several inconsistencies in scaling requirements for modal response spectrum analysis and for modal response history analysis. The main source of problems was in Chapter 16 of ASCE 7-05 and fortunately, most of these problems have been eliminated in ASCE 7-10.

There are still a few issues that need to be clarified. Some of these are listed below:

- Accidental torsion: The *Standard* needs to be more specific on how accidental torsion should be applied where used with modal response spectrum and modal response history analyses. The method suggested herein, to apply such torsions as part of a static loading, is easy to implement. However, "automatic" methods based on shifting center of mass need to be explored and, if effective, standardized.

- Amplification of accidental torsion: Currently, accidental torsion need be amplified only for torsionally irregular structures in SDC C and higher (Sec. 12.8.4.3). However, the torsion need not be amplified if a "dynamic" analysis is performed (Sec. 12.9.5). This implies that the amplification of torsion is a dynamic phenomenon, but the author has found no published technical basis for such amplification. Indeed, most references to amplification are based on problems associated with uneven yielding of lateral load-resisting components. This issue needs to be clarified and resolved.

- P-Delta effects: It appears that the most efficient method for handling P-delta effects is to perform the analysis without such effects, use a separate ELF analysis to determine if such effects are significant and if so, magnify forces and displacements to include such effects. It would be much more reasonable to include such effects in the analysis directly and establish procedures to determine if such effects are excessive. Comparison of analysis results with and without P-delta effects included is an effective means to assess the significance of the effects.

- Computing drift: When three-dimensional analysis is performed, drift should be checked at the corners of the building, not the center of mass. Consideration should be given to eliminating the use of story drift in favor of computing shear strain in damageable components. Such calculations can be easily automated.

- Scaling ground motions for linear response history analysis: The need to scale ground motions over a period range of $0.2T$ to $1.5T$ is not appropriate for elastic analysis because the effective period in any mode will never exceed $1.0T$. Additionally, placing equal weight on scaling spectral ordinates at higher modes does not seem rational. In some cases a high mode that is only barely contributing to response can dominate the scaling process.

- Development of standard ground motion histories: The requirement that analysts scan through thousands of ground motion records to find appropriate suites for analysis is unnecessarily burdensome. The *Standard* should provide tables of ground motion suites that are appropriate to simple parameters such as magnitude, site class and distance.

Finally, it is suggested that requirements for linear response history analysis be removed from Chapter 16 and placed in Chapter 12 (as Section 12.10, for example). Requirements for performing such analysis should be as consistent as possible with those of modal response spectrum analysis.

4.2 SIX-STORY STEEL FRAME BUILDING, SEATTLE, WASHINGTON

In this example, the behavior of a simple, six-story structural steel moment-resisting frame is investigated using a variety of analytical techniques. The structure was initially proportioned using a preliminary analysis and it is this preliminary design that is investigated. The analysis will show that the structure falls short of several performance expectations. In an attempt to improve performance, viscous fluid dampers are considered for use in the structural system. Analysis associated with the added dampers is performed in a very preliminary manner.

The following analytical techniques are employed:

- Linear static analysis
- Plastic strength analysis (using virtual work)
- Nonlinear static (pushover) analysis
- Linear dynamic (response history) analysis
- Nonlinear dynamic (response history) analysis

The primary purpose of this example is to highlight some of the more advanced analytical techniques; hence, more detail is provided on these methods. It is also noted that the linear dynamic analysis was performed only as a precursor and check on the analytical model used for nonlinear dynamic analysis and is not discussed in the example.

The 2005 and 2010 versions of the *Standard* do not provide any guidance on pushover analysis because it is not a permitted method of analysis in Table 12.6-1. Some guidance for pushover analysis is provided in Resource Paper 2 in Part 3 of the *Provisions*. More detailed information on pushover analysis is provided in FEMA 440 and in ASCE 41. The procedures outlined in ASCE 41 are used in this example.

Chapter 16 of the *Standard* provides some guidance and requirements for linear and nonlinear response history analysis. Certain aspects of these requirements are clarified in ASCE 7-10, but the basic methodology is unchanged. More detailed requirements for response history analysis are provided in Resource Paper 3 of the *Provisions*. This example follows the recommendations in Resource Paper 3, with certain exceptions, which are noted as the example proceeds.

4.2.1 Description of Structure

The structure analyzed for this example is a six-story office building in Seattle, Washington. According to the descriptions in *Standard* Table 1-1, the building is assigned to Occupancy Category II. From *Standard* Table 11.5-1, the importance factor (I) is 1.0. A plan and elevation of the building are shown in Figures 4.2-1 and 4.2-2, respectively. The lateral load-resisting system consists of steel moment-resisting frames on the perimeter of the building. There are five bays at 28 feet on center in the north-south (N-S) direction and six bays at 30 feet on center in the east-west (E-W) direction. The typical story height is 12 feet-6 inches with the exception of the first story, which has a height of 15 feet. There is a 5-foot-tall perimeter parapet at the roof and one basement level that extends 15 feet below grade. For this example, it is assumed that the columns of the moment-resisting frames are embedded into pilasters formed into the reinforced concrete basement wall.

For the moment-resisting frames in the N-S direction (Frames A and G), all of the columns bend about their strong axes and the girders are attached with fully welded moment-resisting connections. The expected plastic hinge regions of the girders have reduced flange sections, detailed in accordance with AISC 341.

For the frames in the E-W direction (Frames 1 and 6), moment-resisting connections are used only at the interior columns. At the exterior bays, the E-W girders are connected to the weak axis of the exterior (corner) columns using non-moment-resisting connections. All interior columns are gravity columns and are not intended to resist lateral loads. A few of these columns, however, would be engaged as part of the added damping system described in the last part of this example. With minor exceptions, all of the analyses in this example are for lateral loads acting in the N-S direction. Analysis for lateral loads acting in the E-W direction would be performed in a similar manner.

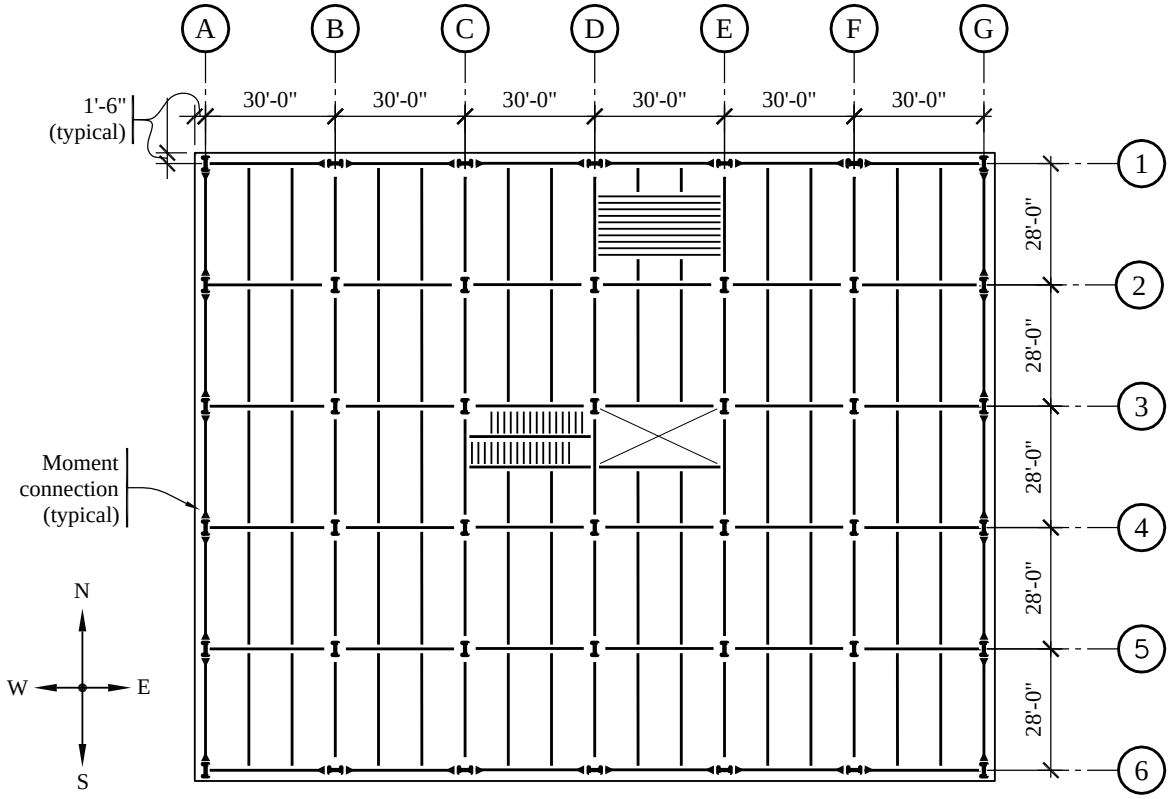

Figure 4.2-1 Plan of structural system

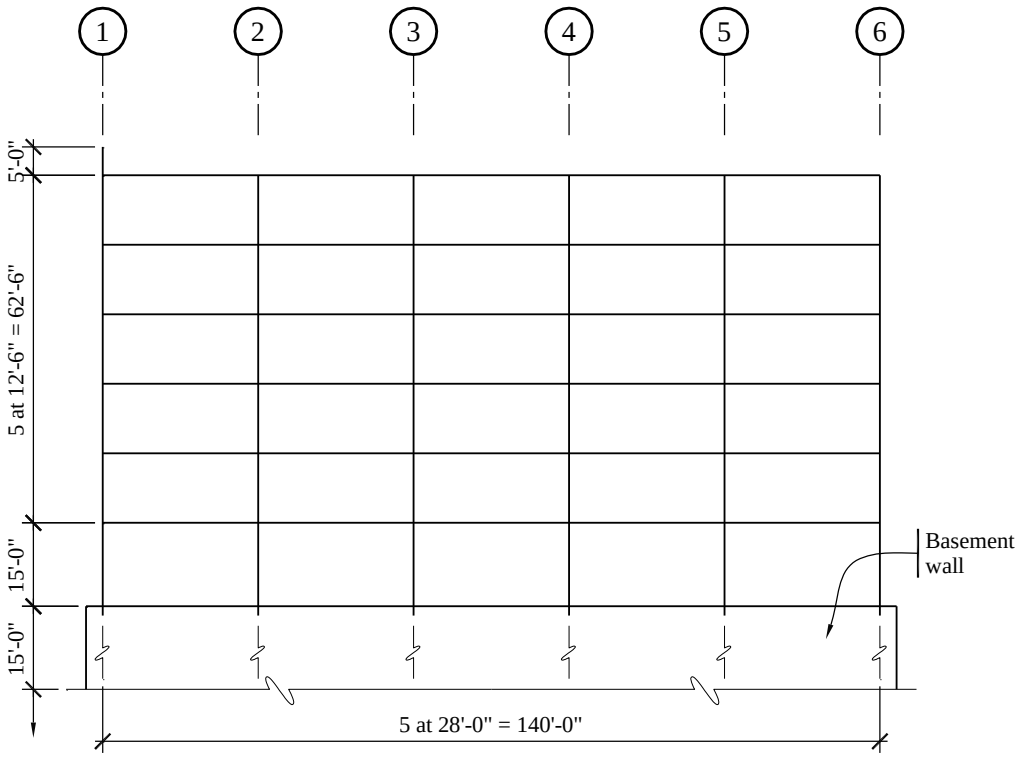

Figure 4.2-2 Elevation of structural system

Prior to analyzing the structure, a preliminary design was performed in accordance with AISC 341. All members, including miscellaneous plates, were designed using steel with a nominal yield stress of 50 ksi and expected yield strength of 55 ksi**.** Detailed calculations for the design are beyond the scope of this example. Table 4.2-1 summarizes the members selected for the preliminary design.[1]

Table 4.2-1 Member Sizes Used in N-S Moment Frames

Member supporting level	Column	Girder	Doubler plate thickness (in.)
R	W21x122	W24x84	1.00
6	W21x122	W24x84	1.00
5	W21x147	W27x94	1.00
4	W21x147	W27x94	1.00
3	W21x201	W27x94	0.875
2	W21x201	W27x94	0.875

[1]The term *Level* is used in this example to designate a horizontal plane at the same elevation as the centerline of a girder. The top level, Level R, is at the roof elevation; Level 2 is the first level above grade; and Level 1 is at grade. The term *Story* represents the distance between adjacent levels. The story designation is the same as the designation of the level at the bottom of the story. Hence, Story 1 is the lowest story (between Levels 2 and 1) and Story 6 is the uppermost story (between Levels R and 6).

The sections shown in Table 4.2-1 meet the width-to-thickness requirements for special moment frames and the size of the column relative to the girders should ensure that plastic hinges initially will form in the girders. Due to strain hardening, plastic hinges will eventually form in the columns. However, these form under lateral displacements that are in excess of those allowed under the Design Basis Earthquake (DBE). Doubler plates of 0.875 inch thick are used at each of the interior columns at Levels 2 and 3 and 1.00 inch thick plates are used at the interior columns at Levels 4, 5, 6 and R. Doubler plates were not used in the exterior columns.

4.2.2 Loads

4.2.2.1 Gravity loads. It is assumed that the floor system of the building consists of a normal-weight composite concrete slab formed on metal deck. The slab is supported by floor beams that span in the N-S direction. These floor beams have a span of 28 feet and are spaced 10 feet on center.

The dead weight of the structural floor system is estimated at 70 psf. Adding 15 psf for ceiling and mechanical units, 10 psf for partitions at Levels 2 through 6 and 10 psf for roofing at Level R, the total dead load at each level is 95 psf. The cladding system is assumed to weigh 15 psf.

A basic live load of 50 psf is used at Levels 2 through 6. The roof live load is 20 psf and (based on calculations not shown here) the roof snow load is 25 psf. The reduced floor loads are taken as 0.4(50), or 20 psf. Only half of this load is required in seismic load combinations (see *Standard* Section 2.3), so the design live loads for the floor is 0.5(20) = 10 psf. The roof live load is not reducible, but never appears in seismic load combinations. The snow load for seismic load combinations is 0.2(25) = 5 psf, which is half of the floor live load.

Based on these loads, the total dead load, live or snow load and dead plus live or snow load applied to each level of the entire building are given in Table 4.2-2. The slight difference in dead loads at Levels R and 2 is due to the parapet and the tall first story, respectively.

Tributary areas for columns and girders as well as individual element gravity loads used in the analysis are illustrated in Figure 4.2-3. These loads are based on a total dead load of 95 psf, a cladding weight of 15 psf and a live load of 10 psf.

Table 4.2-2 Gravity Loads on Seattle Building*

	Dead load (kips)		Reduced live or snow load (kips)		Total load (kips)	
Level	Story	Accumulated	Story	Accumulated	Story	Accumulated
R	2,596	2,596	131	131	2,727	2,727
6	2,608	5,204	262	393	2,739	5,597
5	2,608	7,813	262	655	2,739	8,468
4	2,608	10,421	262	917	2,739	11,338
3	2,608	13,029	262	1,179	2,739	14,208
2	2,621	15,650	262	1,441	2,752	17,091

*Loads are for the entire building.

4.2.2.2 Equivalent static earthquake loads. Although the main analysis in this example is nonlinear, equivalent static forces are computed in accordance with *Standard* Section 12.8. These forces are used in a preliminary static analysis to determine whether the structure, as designed, conforms to the drift requirements limitations imposed by *Standard* Section 12.2.

The structure is situated in Seattle, Washington. The short period and the 1-second mapped spectral acceleration parameters for the site are as follows:

- $S_S = 1.63$
- $S_1 = 0.57$

The structure is situated on Site Class C materials. From *Standard* Tables 11.4-1 and 11.4-2:

- $F_a = 1.00$
- $F_v = 1.30$

From *Standard* Equations 11.4-1 and 11.4-2, the maximum considered spectral acceleration parameters are as follows:

$S_{MS} = F_a S_S = 1.00(1.63) = 1.63$

$S_{M1} = F_v S_1 = 1.30(0.57) = 0.741$

And from *Standard* Equations 11.4-3 and 11.4-4, the design acceleration parameters are as follows:

$S_{DS} = (2/3)S_{M1} = (2/3)1.63 = 1.09$

$S_{D1} = (2/3)S_{M1} = (2/3)0.741 = 0.494$

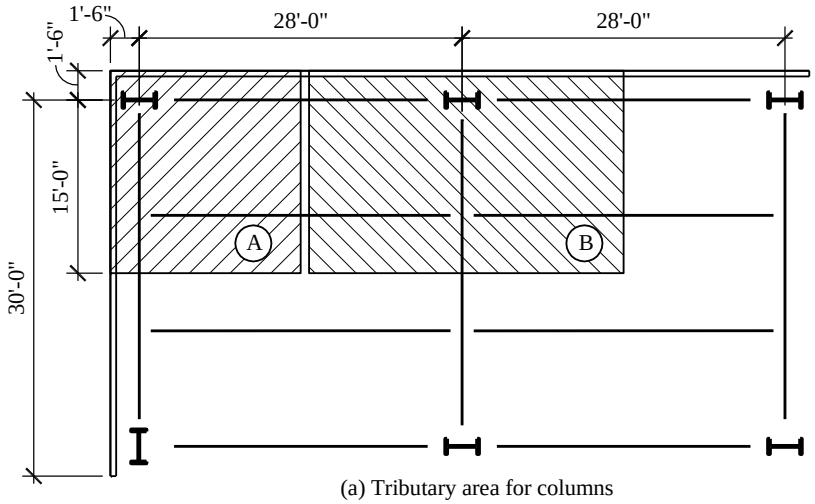

(a) Tributary area for columns

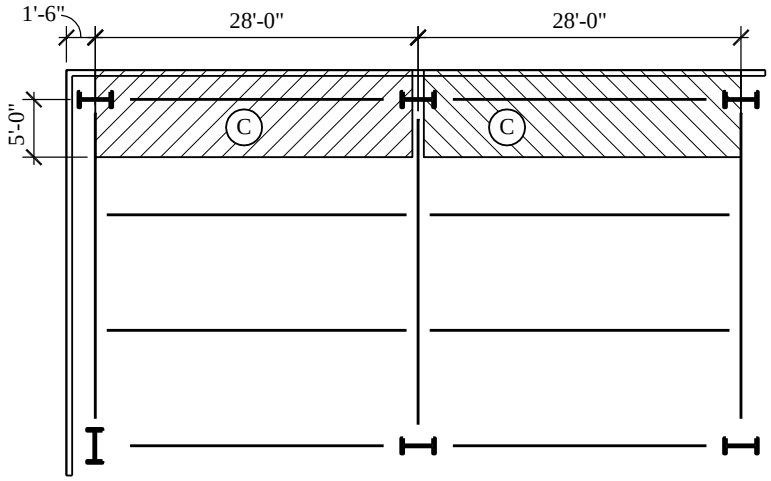

(b) Tributary area for girders

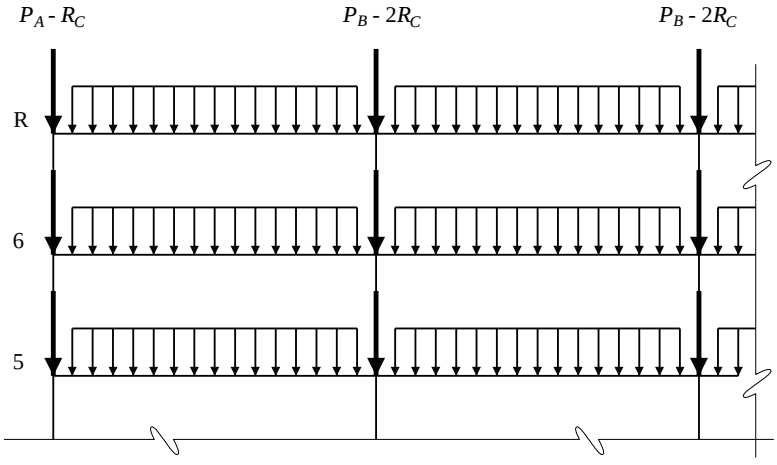

(c) Element and nodal loads

Figure 4.2-3 Element loads used in analysis

Based on the above coefficients and on *Standard* Tables 11.6-1 and 11.6-2, the structure is assigned to Seismic Design Category D. For the purpose of analysis, it is assumed that the structure complies with the requirements for a special moment frame, which, according to *Standard* Table 12.2-1, has the following design values:

- $R = 8$
- $C_d = 5.5$
- $\Omega_0 = 3.0$

Note that the overstrength factor, Ω_0, is not needed for the analysis presented herein.

4.2.2.2.1 Approximate period of vibration. *Standard* Equation 12.8-7 is used to estimate the building period:

$$T_a = C_t h_n^x$$

where, from *Standard* Table 12.8-2, $C_t = 0.028$ and $x = 0.8$ for a steel moment frame. Using h_n (the total building height above grade) = 77.5 feet, $T_a = 0.028(77.5)^{0.8} = 0.91$ sec/cycle[5].

Where the period is determined from a properly substantiated analysis, the *Standard* requires that the period used for computing base shear not exceed $C_u T_a$ where, from *Standard* Table 12.8-1 (using $S_{D1} = 0.494$), $C_u = 1.4$. For the structure under consideration, $C_u T_a = 1.4(0.91) = 1.27$ seconds. This period is used for base shear calculation as it is expected that the period computed for the actual structure will be greater than 1.27 seconds.

4.2.2.2.2 Computation of base shear. Using *Standard* Equation 12.8-1, the total seismic base shear is:

$$V = C_S W$$

where W is the total seismic weight of the structure. From *Standard* Equation 12.8-2, the maximum (constant acceleration region) seismic response coefficient is:

$$C_{S_{\max}} = \frac{S_{DS}}{(R/I)} = \frac{1.09}{(8/1)} = 0.136$$

Equation 12.8-3 controls in the constant velocity region:

$$C_S = \frac{S_{D1}}{T(R/I)} = \frac{0.494}{1.27(8/1)} = 0.0485$$

The seismic response coefficient, however, must not be less than that given by Equation 12.8-5:

$$C_{S_{\min}} = 0.044 I S_{DS} = 0.044(1)(1.09) = 0.0480$$

[5] The correct computational units for period of vibration is "seconds per cycle". However, the traditional units of "seconds" are used in the remainder of this example.

Thus, the value from Equation 12.8-3 controls for this building. Using W = 15,650 kips, V = 0.0485(15,650) = 759 kips.

4.2.2.2.2 Vertical distribution of forces. The seismic base shear is distributed along the height of the building using *Standard* Equations 12.8-11 and 12.8-12:

$$F_x = C_{vx}V \text{ and } C_{vx} = \frac{w_x h^k}{\sum_{i=1}^{n} w_i h_i^k}$$

where k = 0.75 + 0.5T = 0.75 + 0.5(1.27) = 1.385. The lateral forces acting at each level and the story shears acting at the bottom of the story below the indicated level are summarized in Table 4.2-3. These are the forces acting on the whole building. For analysis of a single frame, one-half of the tabulated values are used.

Table 4.2-3 Equivalent Lateral Forces for Building Responding in N-S Direction

Level x	w_x (kips)	h_x (ft)	$w_x h_x^k$	C_{vx}	F_x (kips)	V_x (kips)
R	2,596	77.5	1,080,327	0.321	243.6	243.6
6	2,608	65.0	850,539	0.253	191.8	435.4
5	2,608	52.5	632,564	0.188	142.6	578.0
4	2,608	40.0	433,888	0.129	97.8	675.9
3	2,608	27.5	258,095	0.077	58.2	734.1
2	2,621	15.0	111,909	0.033	25.2	759.3
Σ	15,650		3,367,323	1.000	759.3	

4.2.3 Preliminaries to Main Structural Analysis

Performing a nonlinear analysis of a structure is an incremental process. The analyst should first perform a linear analysis to obtain some basic information on expected behavior and to serve later as a form of verification for the more advanced analysis. Once the linear behavior is understood (and extrapolated to expected nonlinear behavior), the anticipated nonlinearities are introduced. If more than one type of nonlinear behavior is expected to be of significance, it is advisable to perform a preliminary analysis with each nonlinearity considered separately and then to perform the final analysis with all nonlinearities considered. This is the approach employed in this example.

4.2.3.1 The computer programs NONLIN-Pro and DRAIN 2Dx

The computer program NONLIN-Pro was used for all of the analyses described in this example. This program is basically a pre- and post-processor to DRAIN 2Dx (Prakash et al., 1993). While DRAIN is not the most robust program currently available for performing nonlinear response history analysis, it was used because many of the details of the analysis (e.g., panel zone modeling) must be done explicitly. This detail provides insight into the modeling process which is not available when using the automated features of the more robust software. Note that a full version of NONLIN-Pro, as well as input files used for this example, is provided on the CD.

DRAIN has several shortcomings that are related specifically to the example at hand. These shortcomings are listed below. Also provided is a brief explanation of the influence the shortcoming may have on the analysis.

- It is not possible to model strength loss when using the ASCE 41 model for girder plastic hinges. However, as discussed later in the example, this loss of strength generally occurs at plastic hinge rotations well beyond the rotational demands produced under the DBE ground motions. Maximum plastic rotation angles of plastic hinges were checked with the values in Table 5-6 of ASCE 41-06.

- The DRAIN model for axial-flexural interaction in columns is not particularly accurate. This is of some concern in this example because hinges form at the base of the columns in all of the analyses and in some of the upper columns during analysis with MCE level ground motions.

- Only two-dimensional analysis may be performed. Such an analysis is reasonable for the structure considered in this example because of its regular shape and because full moment connections are provided only in the N-S direction for the corner columns (see Fig. 4.2-1).

As with any finite element analysis program, DRAIN models the structure as an assembly of nodes and elements. While a variety of element types is available, only three element types were used in the analysis:

- Type 1 inelastic bar (truss) element

- Type 2 beam-column element

- Type 4 connection element

Two models of the structure were prepared for DRAIN. The first model, used for preliminary analysis and for verification of the second (more advanced) model, consisted only of Type 2 elements for the main structure and Type 1 elements for modeling P-delta effects. All analyses carried out using this model were linear.

For the second, more detailed model, Type 1 elements were used for modeling P-delta effects and the dampers in the damped system. It was assumed that these elements would remain linear elastic throughout the response. Type 2 elements were used to model the beams, the columns and the braces in the damped system, as well as the rigid links associated with the panel zones. Plastic hinges were allowed to form in all columns. The column hinges form through the mechanism provided in DRAIN's Type 2 element. Plastic behavior in girders and in the panel zone region of the structure was modeled explicitly through the use of Type 4 connection elements. Girder yielding was forced to occur in the Type 4 elements (in lieu of the main span represented by the Type 2 elements) to provide more control in hinge location and modeling. A complete description of the implementation of these elements is provided later.

4.2.3.2 Description of preliminary model and summary of preliminary results

The *preliminary* DRAIN model is shown in Figure 4.2-4. Important characteristics of the model are as follows:

- Only a single frame (Frame A or G) is modeled. Hence one-half of the loads shown in Tables 4.2-2 and 4.2-3 are applied.

- Columns are fixed at their base (at grade level; the basement is not modeled).

- Each beam or column element is modeled using a Type 2 element. For the columns, axial, flexural and shear deformations are included. For the girders, flexural and shear deformations are included but, because of diaphragm slaving, axial deformation is not included. Composite action in the floor slab is ignored for all analysis.

- All members are modeled using centerline dimensions without rigid end offsets. This approach allows for the effects of panel zone deformation to be included in an approximate but reasonably accurate manner. Note that this model does not provide any increase in beam-column joint stiffness due to the presence of doubler plates. The stiffness of the girders was decreased by 7 percent (in preliminary analyses) to account for the reduced flange sections. Moment rotation properties of the reduced flange sections are used in the detailed analyses.

P-delta effects are modeled using the leaner "ghost" column shown in Figure 4.2-4 at the right of the main frame. This column is modeled with an axially rigid truss element. P-delta effects are activated for this column only (P-delta effects are turned off for the columns of the main frame). The lateral degree of freedom at each level of the P-delta column is slaved to the floor diaphragm at the matching elevation. Where P-delta effects are included in the analysis, a special initial load case was created and executed. This special load case consists of a vertical force equal to one-half of the total story weight (dead load plus 50 percent of the fully reduced live load) applied to the appropriate node of the P-delta column. When P-delta effects are included, modal analysis should be performed after the P-delta load case is applied so that stiffness modification of P-delta effects will increase the period of the structure. P-delta effects are modeled in this manner to provide true column axial forces for assessing strength.

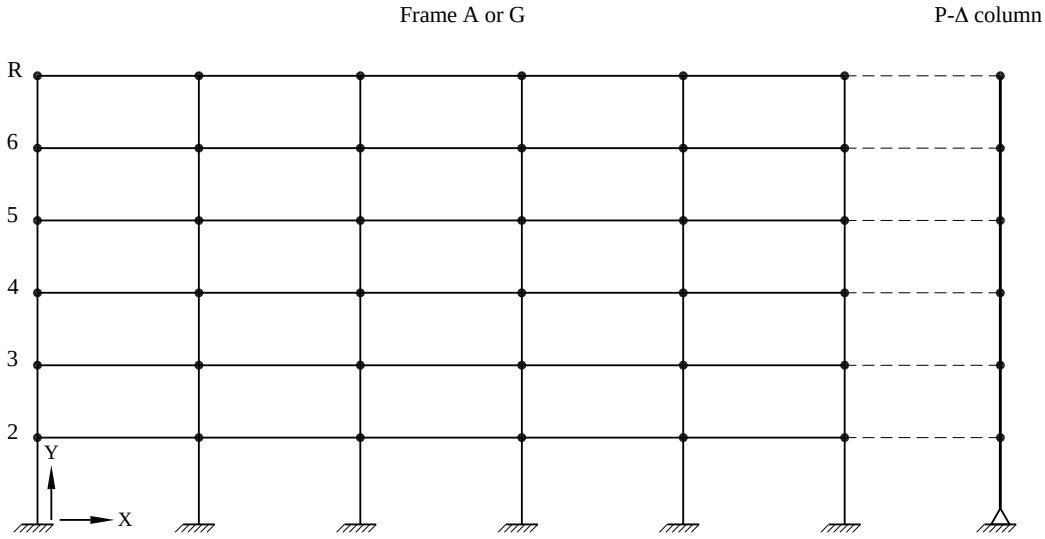

Figure 4.2-4 Simple wire frame model used for preliminary analysis

4.2.3.2.1 Results of preliminary analysis: period of vibration and drift. The computed periods for the first three natural modes of vibration are shown in Table 4.2-4. As expected, the period including P-delta effects is slightly larger than that produced by the analysis without such effects. More significant is the fact that the first mode period is considerably longer than that predicted from *Standard*

Equation 12.8-7. Recall from previous calculations that this period (T_a) is 0.91 seconds and the upper limit on the computed period $C_u T_a$ is 1.4(0.91) = 1.27 seconds. Where doubler plate effects are included in the detailed analysis, the period will decrease slightly, but it remains obvious that the structure is quite flexible.

Table 4.2-4 Periods of Vibration From Preliminary Analysis (sec/cycle)

Mode	P-delta excluded	P-delta included
1	2.054	2.130
2	0.682	0.698
3	0.373	0.379

The results of the preliminary analysis for drift are shown in Tables 4.2-5 and 4.2-6 for the computations excluding and including P-delta effects, respectively. In each table, the deflection amplification factor (C_d) equals 5.5 and the acceptable story drift (story drift limit) is taken as 2 percent of the story height, which is the limit provided by ***Standard*** Table 12.12-1. In the ***Standard*** it is permitted to determine the elastic drifts using seismic design forces based on the computed fundamental period of the structure without the upper limit $C_u T_a$. Thus a new set of lateral loads based on the computed period of the actual structure is applied to the structure to calculate the elastic drifts.

Where P-delta effects are not included, the computed story drift is less than the allowable story drift at each level of the structure. The largest magnified story drift, including C_d = 5.5, is 2.26 inches in Stories 2 and 3. As a preliminary estimate of the importance of P-delta effects, story stability coefficients, θ, were computed in accordance with ***Standard*** Section 12.8-7. These are shown in the last column of Table 4.2-5. At Story 2, the stability coefficient is 0.0862. According to the ***Standard***, P-delta effects may be ignored where the stability coefficient is less than 0.10. For this example, however, analyses are performed with and without P-delta effects.

When P-delta effects are included (Table 4.2-6), the drifts can also be estimated as the drifts without P-delta times the quantity $1/(1-\theta)$, where θ is the stability coefficient for the story. As can be seen in Table 4.2-6, drifts calculated in this manner are consistent with the results obtained by running the analyses with P-delta effects. The difference is always less than 2 percent.

Table 4.2-5 Results of Preliminary Analysis Excluding P-delta Effects

Story	Total drift (in.)	Story drift (in.)	Magnified story drift (in.)	Drift limit (in.)	Story stability ratio, θ
6	2.08	0.22	1.21	3.00	0.0278
5	1.86	0.32	1.76	3.00	0.0453
4	1.54	0.38	2.09	3.00	0.0608
3	1.16	0.41	2.26	3.00	0.0749
2	0.75	0.41	2.26	3.00	0.0862
1	0.34	0.34	1.87	3.60	0.0691

Table 4.2-6 Results of Preliminary Analysis Including P-delta Effects

Story	Total drift (in.)	Story drift (in.)	Magnified story drift (in.)	Drift from θ (in.)	Drift limit (in.)
6	2.23	0.23	1.27	1.24	3.00
5	2.00	0.34	1.87	1.84	3.00
4	1.66	0.40	2.20	2.23	3.00
3	1.26	0.45	2.48	2.44	3.00
2	0.81	0.45	2.48	2.47	3.00
1	0.36	0.36	1.98	2.01	3.60

4.2.3.2.2 Results of preliminary analysis: demand-to-capacity ratios. To determine the likelihood and possible order of yielding, demand-to-capacity ratios (DCR) are computed for each element. The results are shown in Figure 4.2-5. For this analysis, the structure is subjected to full dead load plus 0.5 times the fully reduced live load, followed by equivalent lateral forces computed without the *R* factor. P-delta effects are included. Figure 4.2-5(a) displays the DCR of columns and girders and Figure 4.2-5(b) displays the DCR of panel zones with and without doubler plates. In Figure 4.2-5b, the values in parentheses represent the DCRs without doubler plates. Since the DCRs in Figure 4.2-5 are found from preliminary analyses, in which the centerline model is used, doubler plates aren't added into the model. Thus, the demand values of Figure 4.2-5(b) are the same with and without doubler plates. However, since the capacity of the panel zone increases with added doubler plates, the DCRs decrease at the interior beam column joints as the doubler plates are used only at the interior joints. As may be seen in Figure 4.2-5(b), the DCR at the exterior joints are the same with and without doubler plates added.

For girders, the DCR is simply the maximum moment in the member divided by the member's plastic moment capacity where the plastic capacity is $Z_e F_{ye}$. Z_e is the plastic section modulus at center of reduced beam section and F_{ye} is the expected yield strength. For columns, the ratio is similar except that the plastic flexural capacity is estimated to be $Z_{col}(F_{ye}-P_u/A_{col})$ where P_u is the total axial force in the column. The ratios are computed at the center of the reduced section for beams and at the face of the girder for columns.

To find the shear demand at the panel zones, the total moment in the girders (at the left and right sides of the joint) is divided by the effective beam depth to produce the panel shear due to beam flange forces. Then the column shear at above or below the panel zone joint was subtracted from the beam flange shears and the panel zone shear force is obtained. This force is divided by the shear strength capacity, R_v (which is discussed in Section 4.2.4.2) to determine the DCR of the panel zones.

Several observations are made regarding the likely inelastic behavior of the frame:

- The structure has considerable overstrength, particularly at the upper levels.
- The sequence of yielding will progress from the lower-level girders to the upper-level girders. Because of relatively low live load, the DCRs in the girders are almost uniform at each level. Hence, all the hinges in the girders in a level will form almost simultaneously.
- With the possible exception of the first level, the girders should yield before the columns. While not shown in the table, the DCRs for the lower-story columns are controlled by the moment at the base of the column. It is usually very difficult to prevent yielding of the base of the first-story

columns in moment frames and this frame is no exception. The column on the leeward (right) side of the building will yield first because of the additional axial compressive force arising from the seismic effects.

- The maximum DCR of the columns and girders is 3.475, while the maximum DCR for the panel zones without doubler plates is 4.339. Thus, if doubler plates aren't used, the first yield in the structure is in the panel zones. However, with doubler plates added, the first yield is at the girders as the maximum DCR of the panel zones reduces to 2.405.

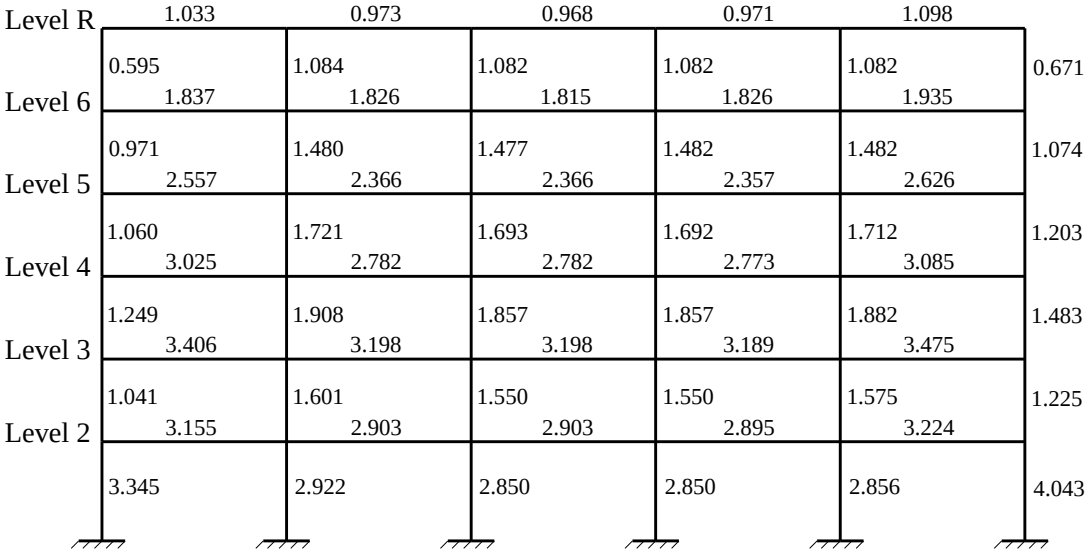

(a) DCRs of columns and girders

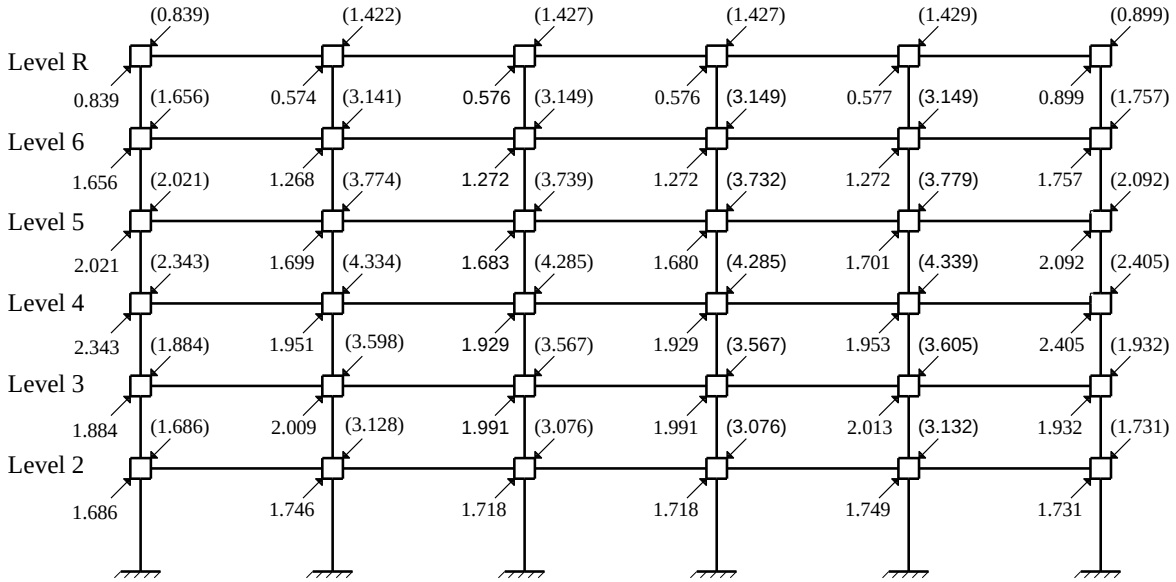

(b) DCRs of panel zones with and without doubler plates
(DCR values in parentheses are without doubler plates)

Figure 4.2-5 DCRs for elements from preliminary analysis with P-delta effects included

4.2.3.2.3 Results of preliminary analysis: overall system strength. The last step in the preliminary analysis is to estimate the total lateral strength (collapse load) of the frame using virtual work. In the analysis, it is assumed that plastic hinges are perfectly plastic. Girders hinge at a value $Z_e F_{ye}$ and the hinges form at the center of the reduced section (approximately 15 inches from the face of the column).

Columns hinge only at the base and the plastic moment capacity is assumed to be $Z_{col}(F_{ye}\text{-}P_u/A_{col})$. The fully plastic mechanism for the system is illustrated in Figure 4.2-6. The inset to the figure shows how the angle modification term, σ, was computed. The strength, V, for the **total structure** is computed from the following relationships (see Figure 4.2-6 for nomenclature):

- Internal Work = External Work
- Internal Work = $2[20\sigma\theta M_{PA} + 40\sigma\theta M_{PB} + \theta(M_{PC} + 4M_{PD} + M_{PE})]$
- External Work = $V\theta \sum_{i=1}^{nLevels} F_i H_i$ where $\sum_{i=1}^{nLevels} F_i = 1$

Three lateral force patterns are used: uniform, upper triangular and *Standard* (where the *Standard* pattern is consistent with the vertical force distribution of Table 4.2-3 in this volume of design examples). The results of the analysis are shown in Table 4.2-7. As expected, the strength under uniform load is significantly greater than under triangular or *Standard* load. The closeness of the *Standard* and triangular load strengths results from the vertical-load-distributing parameter (k = 1.385) being close to 1.0.

The ELF base shear, 759 kips (see Table 4.2-3), when divided by the *Standard* pattern capacity, 2,616 kips, is 0.29. This is reasonably consistent with the DCRs shown in Figure 4.2-5.

Table 4.2-7 Lateral Strength on Basis of Rigid-Plastic Mechanism

Lateral Load Pattern	Lateral strength for entire structure (kips)	Lateral strength single frame (kips)
Uniform	3,332	1,666
Upper Triangular	2,747	1,373
Standard	2,616	1,308

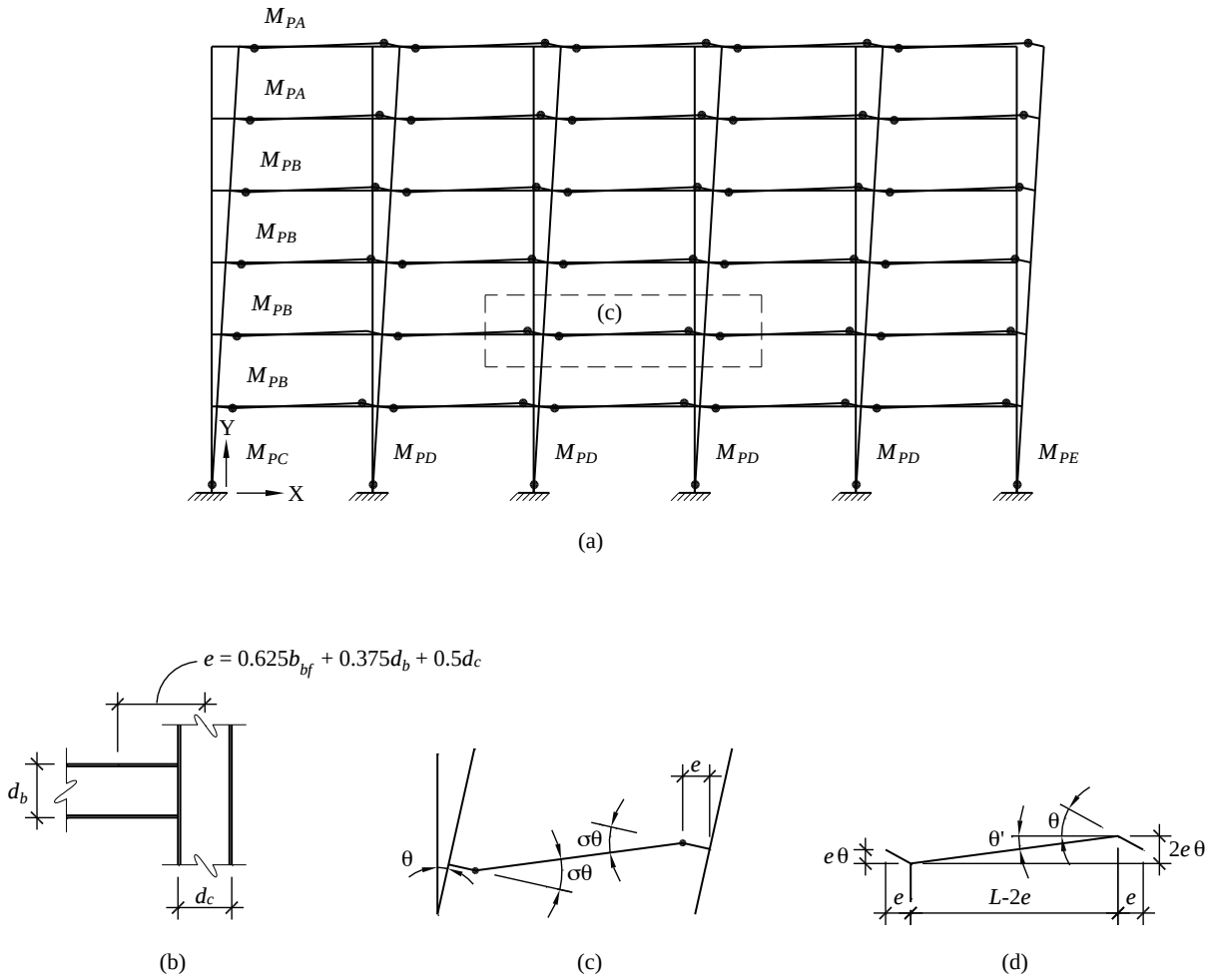

Figure 4.2-6 Plastic mechanism for computing lateral strength

Three important points concerning the virtual work analysis are as follows:

- The rigid-plastic analysis does not include strain hardening, which is an additional source of overstrength.
- The rigid-plastic analysis does not consider the true behavior of the panel zone region of the beam-column joint. Yielding in this area can have a significant effect on system strength.
- Slightly more than 15 percent of the system strength comes from plastic hinges that form in the columns. If the strength of the column is taken simply as M_p (without the influence of axial force), the difference in total strength is less than 2 percent.

4.2.4 Description of Model Used for Detailed Structural Analysis

Nonlinear static and nonlinear dynamic analyses require a much more detailed model than was used in the linear analysis. The primary reason for the difference is the need to explicitly represent yielding in the girders, columns and panel zone region of the beam-column joints.

The DRAIN model used for the nonlinear analysis is shown in Figure 4.2-7. A detail of a girder and its connection to two interior columns is shown in Figure 4.2-8. The detail illustrates the two main features of the model: an explicit representation of the panel zone region and the use of concentrated plastic hinges in the girders.

In Figure 4.2-7, the column shown to the right of the structure is used to represent P-delta effects. See Section 4.2.3.2 for details.

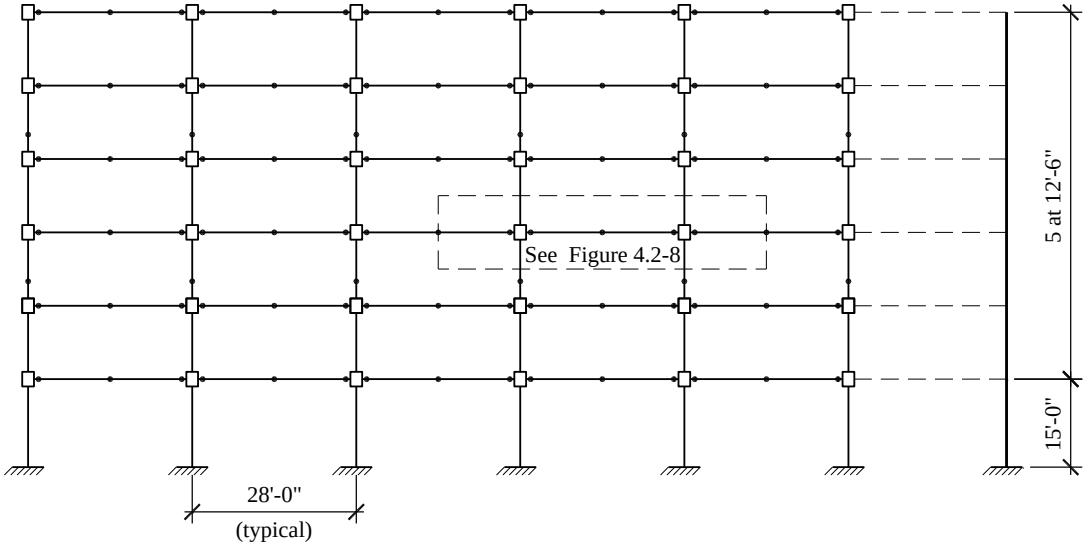

Figure 4.2-7 Detailed analytical model of six-story frame

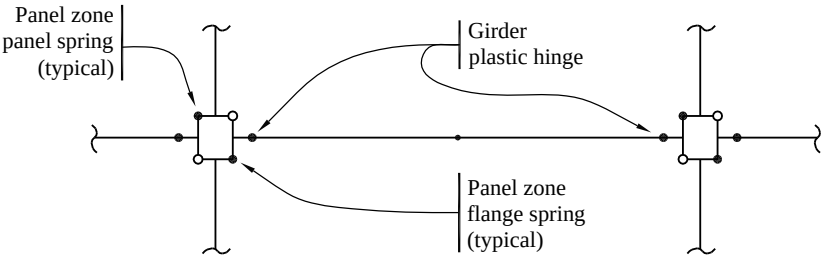

Figure 4.2-8 Model of girder and panel zone region

The development of the numerical properties used for panel zone and girder hinge modeling is not straightforward. For this reason, the following theoretical development is provided before proceeding with the example.

4.2.4.1 Plastic hinge modeling and compound nodes. In the analysis described below, much use is made of compound nodes. These nodes are used to model plastic hinges in girders and deformations in the panel zone region of beam-column joints.

A compound node typically consists of a pair of single nodes with each node sharing the same point in space. The X and Y degrees of freedom of the first node of the pair (the slave node) are constrained to be equal to the X and Y degrees of freedom of the second node of the pair (the master node), respectively. Hence, the compound node has four degrees of freedom: an X displacement, a Y displacement and two independent rotations.

In most cases, one or more rotational spring connection elements (DRAIN element Type 4) are placed between the two single nodes of the compound node and these springs develop bending moment in resistance to the relative rotation between the two single nodes. If no spring elements are placed between the two single nodes, the compound node acts as a moment-free hinge. A typical compound node with a single rotational spring is shown in Figure 4.2-9. The figure also shows the assumed bilinear, inelastic moment-rotation behavior for the spring.

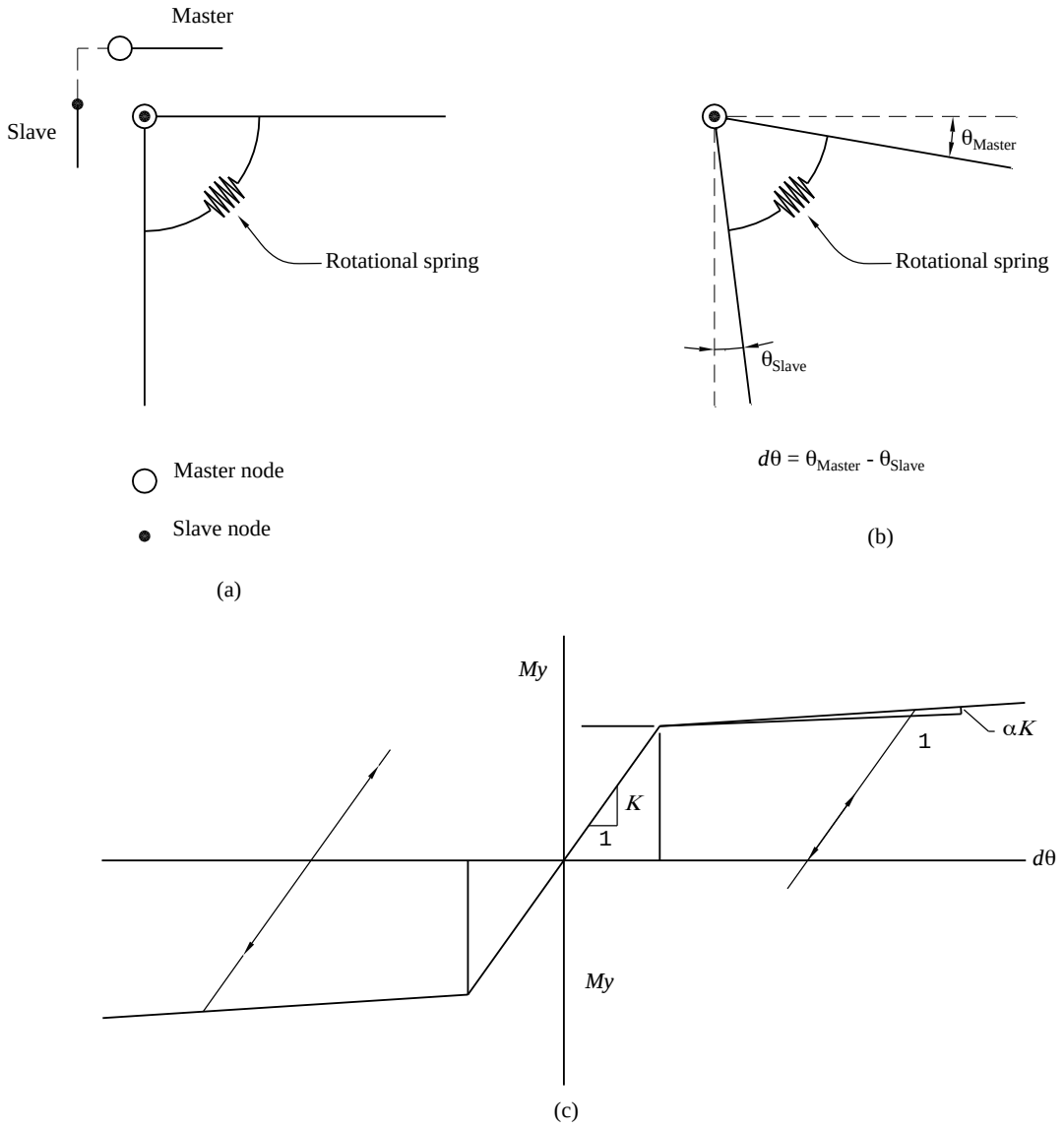

Figure 4.2-9 A compound node and attached spring

4.2.4.2 Modeling of beam-column joint regions. A very significant portion of the total story drift of a moment-resisting frame is due to deformations that occur in the panel zone region of the beam-column joint. In this example, panel zones are modeled explicitly using an approach developed by Krawinkler (1978) and described in more detail in Charney and Marshall (2006). Only a brief overview is presented here.

This model, illustrated in Figure 4.2-10, represents the panel zone stiffness and strength by an assemblage of four rigid links and two rotational springs. The links form the boundary of the panel and the springs are used to provide the desired inelastic behavior. The model has the advantage of being conceptually

simple, yet robust. The disadvantage of the model is that the number of degrees of freedom required to model a structure is significantly increased.[4]

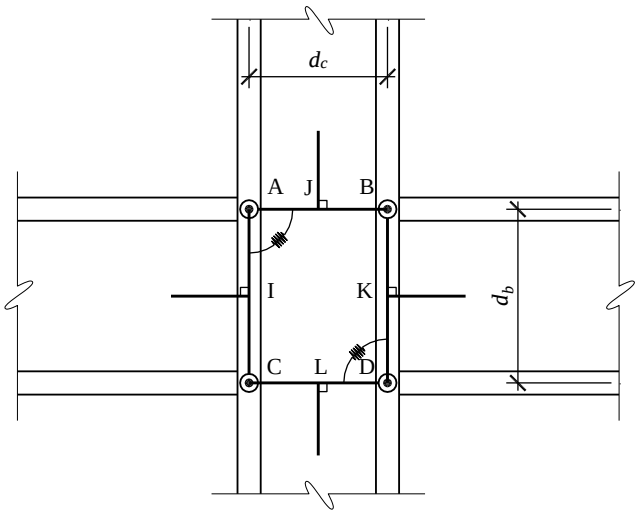

Figure 4.2-10 Krawinkler beam-column joint model

The Krawinkler model assumes that the panel zone has two resistance mechanisms acting in parallel:

- Shear resistance of the web of the column, including doubler plates
- Flexural resistance of the flanges of the column

These two resistance mechanisms, apparent in AISC 360 Section J10-11, are used for determining panel zone shear strength:

$$R_v = 0.6F_y d_c t_p \left[1 + \frac{3b_{cf} t_{cf}^2}{d_b d_c t_p}\right]$$

The equation can be rewritten as:

$$R_v = 0.6F_y d_c t_p + 1.8\frac{F_y b_{cf} t_{cf}^2}{d_b} = V_{Panel} + 1.8V_{Flanges}$$

In ASCE 41, the first term of the above equation is taken as $0.55F_{ye} d_c t_p$ and the second term is neglected conservatively. In this study, the following equation—in which the first term is taken as the same as in

[4] The numbers of degrees of freedom in the Krawinkler model may be reduced to only four if the rigid links around the perimeter of the model are represented by mathematical constraints instead of stiff elements. Most commercial programs employ this approach for the Krawinkler model.

ASCE 41 and the second term is taken from AISC 360, with the exception of replacing nominal yield stress with expected yield strength (for consistency)—is used to calculate the panel zone shear strength:

$$R_v = 0.55F_{ye}d_c t_p + 1.8\frac{F_{ye}b_{cf}t_{cf}^2}{d_b} = V_{Panel} + 1.8V_{Flanges}$$

where the first term is the panel shear resistance and the second term is the plastic flexural resistance of the column flange. The terms in the equations are defined as follows:

F_{ye} = expected yield strength of the column and the doubler plate

d_c = total depth of column

t_p = thickness of panel zone region = column web thickness plus doubler plate thickness

b_{cf} = width of column flange

t_{cf} = thickness of column flange

d_b = total depth of girder

Additional terms used in the subsequent discussion are:

t_{bf} = girder flange thickness

G = shear modulus of steel

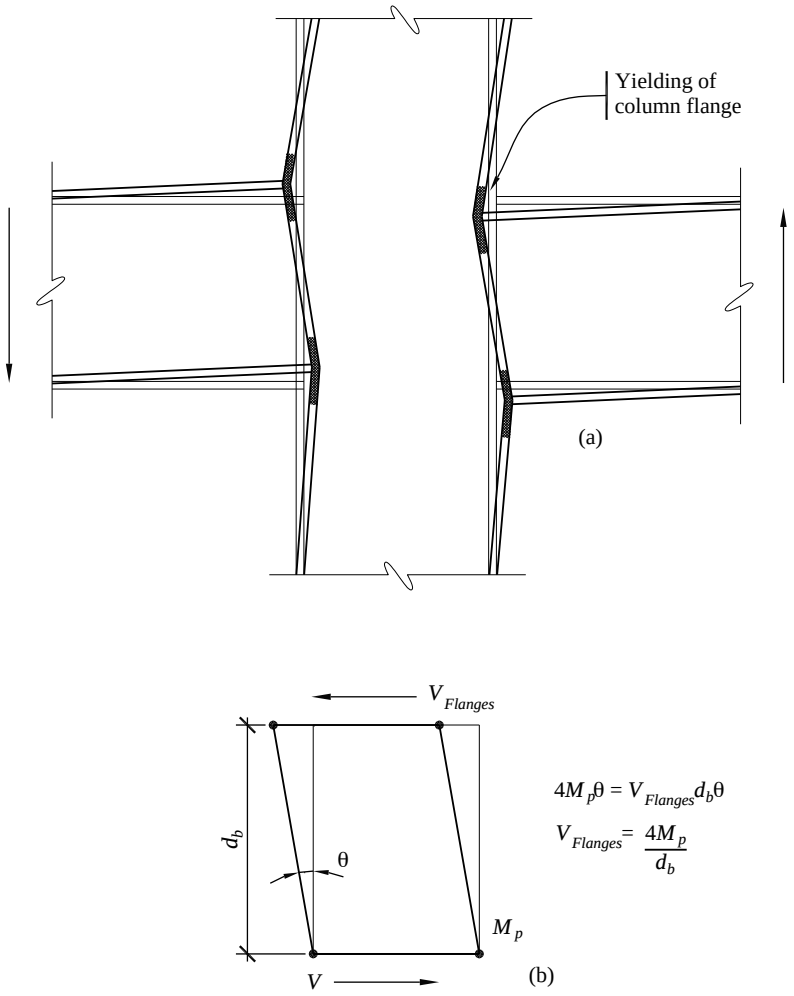

Figure 4.2-11 Column flange component of panel zone resistance

The panel zone shear resistance, V_{Panel}, is simply the effective shear area of the panel, $d_c t_p$, multiplied by the yield stress in shear, assumed as $0.55F_{ye}$. (The 0.55 factor is a simplification of the Von Mises yield criterion that gives the yield stress in shear as $1/\sqrt{3} = 0.577$ times the strength in tension.) The additional plastic flexural resistance provided by yielding in the column flange is neglected in ASCE 41-06 but is included herein.

The second term, $1.8V_{Flanges}$, is based on experimental observation. Testing of simple beam-column subassemblies show that a "kink" forms in the column flanges as shown in Figure 4.2-11(a). If it can be assumed that the kink is represented by a plastic hinge with a plastic moment capacity of $M_p = F_{ye}Z = F_{ye}b_{cf}t_{cf}^2/4$, it follows from virtual work (see Figure 4.2-11b) that the equivalent shear strength of the column flanges is:

$$V_{Flanges} = \frac{4M_p}{d_b}$$

and by simple substitution for M_p:

$$V_{Flanges} = \frac{F_{ye} b_{cf} t_{cf}^2}{d_b}$$

This value does not include the 1.8 multiplier that appears in the AISC equation. This multiplier is based on calibration of experimental results. It should be noted that the flange component of strength is small compared to the panel component unless the column has very thick flanges.

The shear stiffness of the panel is derived as shown in Figure 4.2-12:

$$K_{Panel,\gamma} = \frac{V_{Panel}}{\gamma} = \frac{V_{Panel}}{\delta / d_b}$$

noting that the displacement δ can be written as follows:

$$\delta = \frac{V_{Panel} d_b}{G t_p d_c}$$

$$K_{Panel,\gamma} = \frac{V_{Panel}}{\left(\frac{V_{Panel} d_b}{G t_p d_c} \right) \frac{1}{d_b}} = G t_p d_c$$

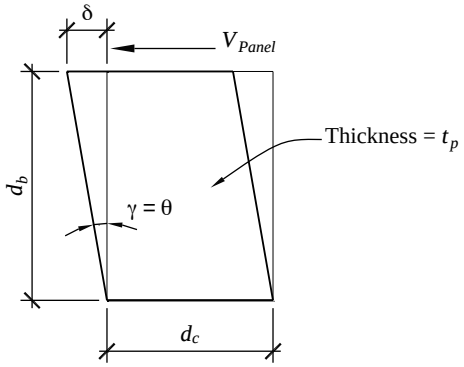

Figure 4.2-12 Column web component of panel zone resistance

Krawinkler assumes that the column flange component yields at four times the yield deformation of the panel component, where the panel yield deformation is:

$$\gamma_y = \frac{V_{Panel}}{K_{Panel,\gamma}} = \frac{0.55 F_{ye} d_c t_p}{G d_c t_p} = \frac{0.55 F_{ye}}{G}$$

At this deformation, the panel zone strength is V_{Panel} + 0.25 $_{Vflanges}$; at four times this deformation, the strength is V_{Panel} + $V_{Flanges}$. The inelastic force-deformation behavior of the panel is illustrated in

Figure 4.2-13. This figure applies also to exterior joints (girder on one side only), roof joints (girders on both sides, column below only) and corner joints (girder on one side only, column below only).

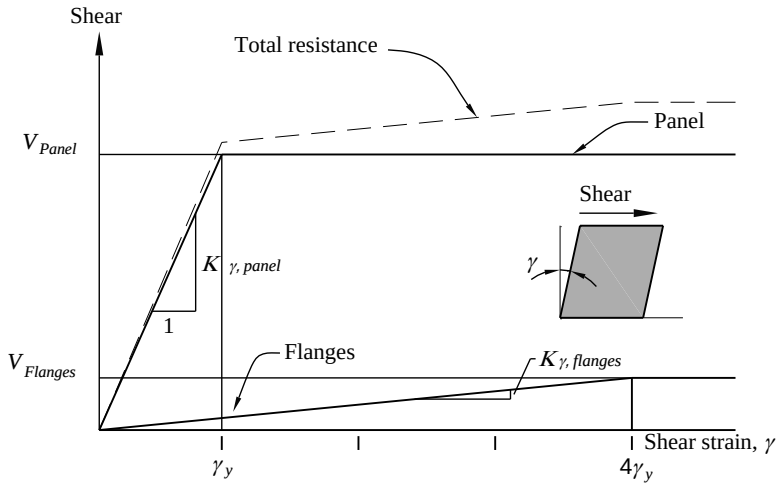

Figure 4.2-13 Force-deformation behavior of panel zone region

The actual Krawinkler model is shown in Figure 4.2-10. This model consists of four rigid links, connected at the corners by compound nodes. The columns and girders frame into the links at right angles at Points I through L. These are moment-resisting connections. Rotational springs are used at the upper left (Point A) and lower right (Point D) compound nodes. These springs are used to represent the panel resistance mechanisms described earlier. The upper right and lower left corners (Points B and C), without rotational springs, act as real hinges.

The finite element model of the joint requires 12 individual nodes: one node each at Points I through L and two nodes (compound node pairs) at Points A through D. It is left to the reader to verify that the total number of degrees of freedom in the model is 28 (if the only constraints are associated with the corner compound nodes).

The rotational spring properties are related to the panel shear resistance mechanisms by a simple transformation, as shown in Figure 4.2-14. From the figure it may be seen that the moment in the rotational spring is equal to the applied shear times the beam depth. Using this transformation, the properties of the rotational spring representing the panel shear component of resistance are as follows:

$$M_{Panel} = V_{Panel} d_b = 0.55 F_{ye} d_c d_b t_p$$

$$K_{Panel,\theta} = K_{Panel,\gamma} d_b = G d_c d_b t_p$$

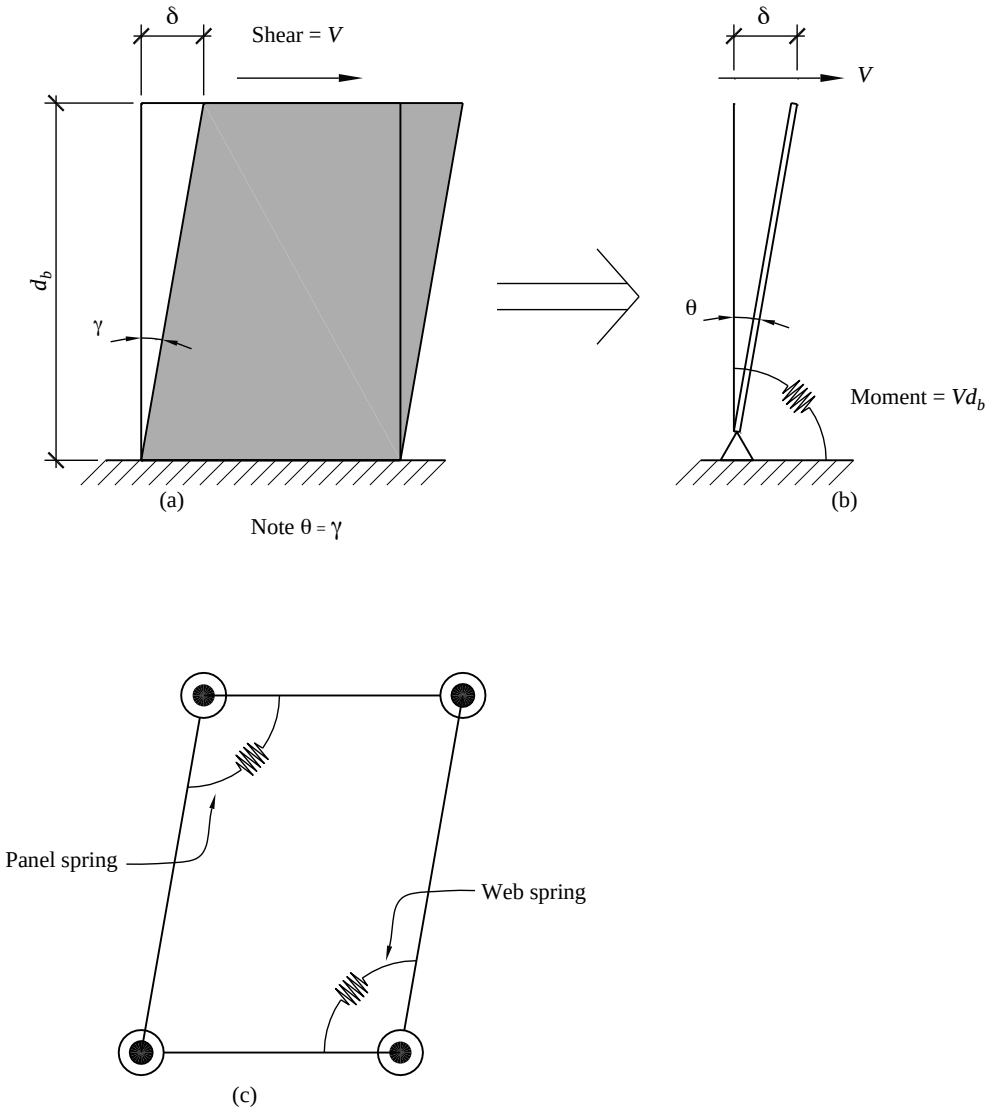

Figure 4.2-14 Transforming shear deformation to rotational deformation in the Krawinkler model

It is interesting to note that the shear strength in terms of the rotation spring is simply $0.55F_{ye}$ times the volume of the panel and the shear stiffness in terms of the rotational spring is equal to G times the panel volume.

The flange component of strength in terms of the rotational spring is determined in a similar manner:

$$M_{Flanges} = 1.8V_{Flanges}d_b = 1.8F_{ye}b_{cf}t_{cf}^2$$

Because of the equivalence of rotation and shear deformation, the yield rotation of the panel is the same as the yield strain in shear:

$$\theta_y = \gamma_y = \frac{M_{Panel}}{K_{Panel,\theta}} = \frac{0.55F_{ye}}{G}$$

To determine the initial stiffness of the flange spring, it is assumed that this spring yields at four times the yield deformation of the panel spring. Hence:

$$K_{Flanges,\theta} = \frac{M_{Flanges}}{4\theta_y} = 0.82Gb_{cf}t_{cf}^2$$

The complete resistance mechanism, in terms of rotational spring properties, is shown in Figure 4.2-13. This trilinear behavior is represented by two elastic-perfectly plastic springs at the opposing corners of the joint assemblage.

If desired, strain-hardening may be added to the system. ASCE 41 suggests use of a strain hardening stiffness equal to 6 percent of the initial stiffness of the joint. In this analysis, the strain-hardening component was simply added to both the panel and the flange components:

$$K_{SH,\theta} = 0.06(K_{Panel,\theta} + K_{Flanges,\theta})$$

Before continuing, one minor adjustment is made to the above derivations. Instead of using the nominal total beam and girder depths in the calculations, the distance between the center of the flanges was used as the effective depth. Hence:

$$d_c \equiv d_{c,nom} - t_{cf}$$

where the *nom* part of the subscript indicates the property listed as the total depth in the AISC Manual.

The Krawinkler properties are now computed for a typical interior subassembly of the six-story frame. A summary of the properties used for all connections is shown in Table 4.2-8.

Table 4.2-8 Properties for the Krawinkler Beam-Column Joint Model

Connection	Girder	Column	Doubler plate (in.)	$M_{panel,\theta}$ (in.-k)	$K_{panel,\theta}$ (in.-k/rad)	$M_{flanges,\theta}$ (in.-k)	$K_{flanges,\theta}$ (in.-k/rad)
A	W24x84	W21x122	–	8,782	3,251,567	1,131	104,721
B	W24x84	W21x122	1.00	23,419	8,670,846	1,131	104,721
C	W27x94	W21x147	–	11,934	4,418,647	1,637	151,486
D	**W27x94**	**W21x147**	**1.00**	**28,510**	**10,555,656**	**1,637**	**151,486**
E	W27x94	W21x201	–	15,386	5,696,639	3,314	306,771
F	W27x94	W21x201	0.875	30,180	11,174,176	3,314	306,771

Example calculations shown for row in **bold** type.

The sample calculations below are for Connection D in Table 4.2-8.

- Material Properties:

F_{ye} = 55.0 ksi (girder, column and doubler plate)

G = 11,200 ksi

- Girder:

  W27x94

  $d_{b,nom}$ = 26.90 in.

  t_{bf} = 0.745 in.

  d_b = 26.16 in.

- Column:

  W21x147

  $d_{c,nom}$ = 22.10 in.

  t_w = 0.72 in.

  t_{cf} = 1.150 in.

  d_c = 20.95 in.

  b_{cf} = 12.50 in.

- Doubler plate: 1.00 in.

  Total panel zone thickness = t_p = 0.72 + 1.00 = 1.72 in.

  $V_{Panel} = 0.55F_{ye}d_c t_p = 0.55(55)(20.95)(1.72)$ = 1,090 kips

  $V_{Flanges} = 1.8\frac{F_{ye}b_{cf}t_{cf}^2}{d_b} = 1.8\frac{55(12.50)(1.15^2)}{26.16}$ = 62.6 kips

  $K_{Panel,\gamma} = Gt_p d_c = 11,200(1.72)(20.95)$ = 403,581 kips/unit shear strain

  $\gamma_y = \theta_y = \frac{0.55F_{ye}}{G} = \frac{0.55(55)}{11,200}$ = 0.0027

  $M_{Panel} = V_{Panel}d_b = 1,090(26.16)$ = 28,510 in.-kips

  $K_{Panel,\theta} = K_{Panel,\gamma}d_b = 403,581(26.16)$ = 10,555,656 in.-kips/radian

$$M_{Flanges} = V_{Flanges} d_b = 62.6(26.16) = 1{,}637 \text{ in.-kips}$$

$$K_{Flanges,\theta} = \frac{M_{Flanges}}{4\gamma_y} = \frac{1{,}637}{4(0.0027)} = 151{,}486 \text{ in.-kips/radian}$$

4.2.4.3 Modeling girders. Because this structure is designed in accordance with the strong-column/weak-beam principle, it is anticipated that the girders will yield in flexure. Although DRAIN provides special yielding beam elements (Type 2 elements), more control over behavior is obtained through the use of the Type 4 connection element.

The modeling of a typical girder is shown in Figure 4.2-8. This figure shows an interior girder, together with the panel zones at the ends. The portion of the girder between the panel zones is modeled as four segments with one simple node at mid-span and one compound node near each end. The mid-span node is used to enhance the deflected shape of the structure.[5] The compound nodes are used to represent inelastic behavior in the hinging region.

The following information is required to model each plastic hinge:

- The initial stiffness (moment per unit rotation)
- The effective yield moment
- The secondary stiffness
- The location of the hinge with respect to the face of the column

AISC SDM recommends design practices to force the plastic hinge forming in the beam away from the face of the column. There are two methods used to move the plastic hinges of the beam away from the column face. The first one aims to reduce the cross-sectional properties of the beam at a specific location away from the column, and the second one focuses on special detailing of the beam-column connection to provide adequate strength and toughness in the connection so that inelasticity will be forced into the beam adjacent to the column face. In this study the reduced beam section (RBS) was used.

A side view of the reduced beam sections is shown in Figure 4.2-15. The distance between the column face and the edge of the reduced beam section was chosen as $a = 0.625 b_f$ and the reduced section length was assumed as $b = 0.75 d_b$. Both of these values are just at the middle of the limits stated in AISC 358. Plastic hinges of the beams are modeled at the center of the reduced section length.

[5] A graphic post-processor was used to display the deflected shape of the structure. The program represents each element as a straight line. Although the computational results are unaffected, a better graphical representation is obtained by subdividing the member.

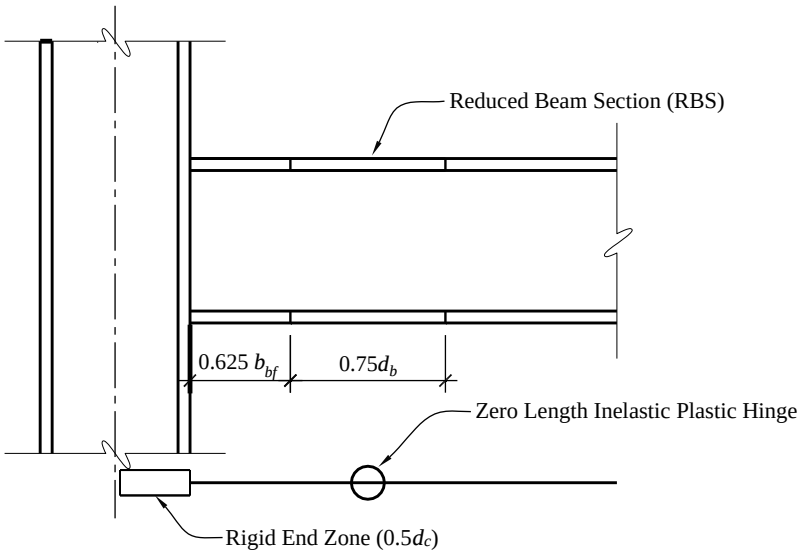

Figure 4.2-15 Side view of beam element and beam modeling

To determine the plastic hinge capacities of the girder cross section, a moment-curvature analysis, which is dependent on the stress-strain curve of the steel, was implemented. The idealized stress-strain curve is shown in Figure 4.2-16. This curve does not display a yield plateau, which is consistent with the assumption that the section has yielded in previous cycles, with the Bauschinger effect eliminating any trace of the yield plateau. The strain hardening ratio is taken as 3 percent of the initial stiffness and the curvature ductility limit used is 20.

To compute the moment-curvature relationship, the girder is divided into 50 slices through it's depth, with 10 slices in each flange and 30 slices at the web. By gradually increasing the rotation, fiber strains, fiber stresses, fiber forces and then the resisting moment are found consecutively. Figure 4.2-17 shows the top view of the assumed reduced beam section in this study. The reduced beam length is divided into seven equal sections and flange widths of each section are calculated using the radius of the cut. The radius of the cut, *R*, is calculated using the formulas in AISC 358.

$$R = \frac{(4c^2 + b^2)}{8c}$$

$$c = 0.175 b_f$$

$$b = 0.75 d_b$$

$$a = 0.625 b_f$$

where:

c = depth of cut at center of the RBS, in.

b_f = width of beam flange, in.

b = length of RBS cut, in.

d_b = beam depth, in.

a = distance from face of the column to start of RBS cut, in.

R = radius of cut, in.

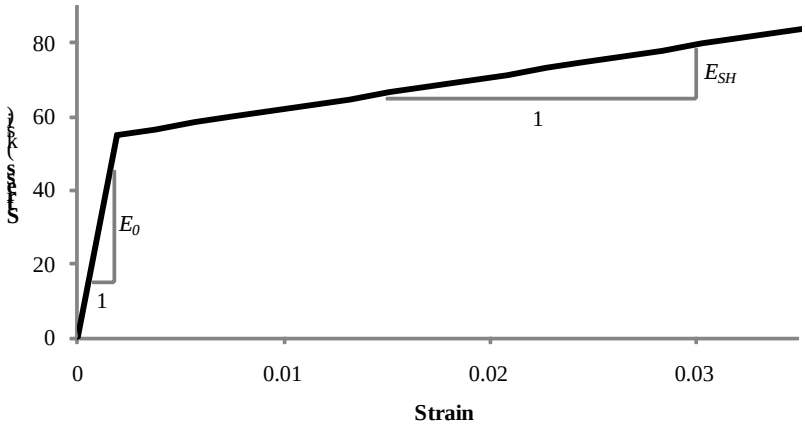

Figure 4.2-16 Assumed stress-strain curve for modeling girders

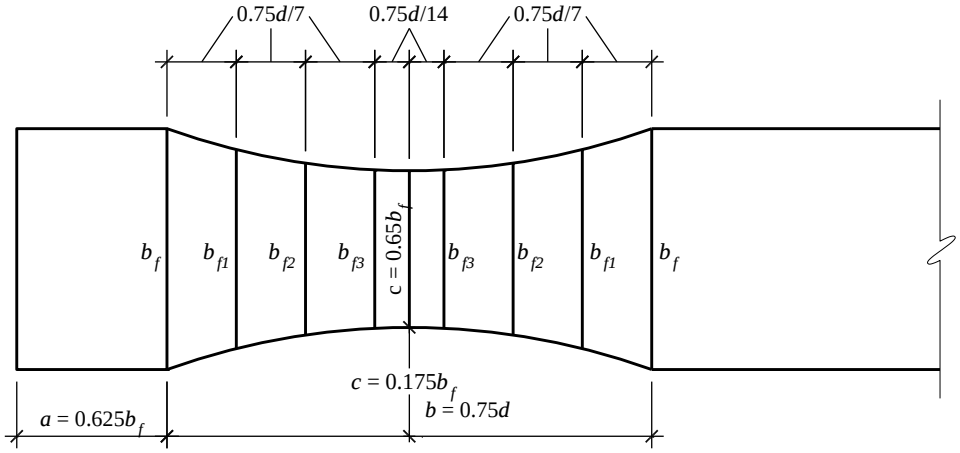

Figure 4.2-17 Top view of RBS

Figure 4.2-18 shows the moment-curvature diagram for the W27x94 girder. As may be seen in the figure, the moment-curvature relationship is different at each segment of the reduced length. The locations of the different reduced beam sections used in Figure 4.2-18, named as "b_{f1}", "b_{f2}" and "b_{f3}", can be seen in

Figure 4.2-17. Because of the closely adjacent locations chosen for "0.65b_f" and "b_{f3}" (see Figure 4.2-17), their moment-curvature plots are nearly indistinguishable from each other in Figure 4.2-18.

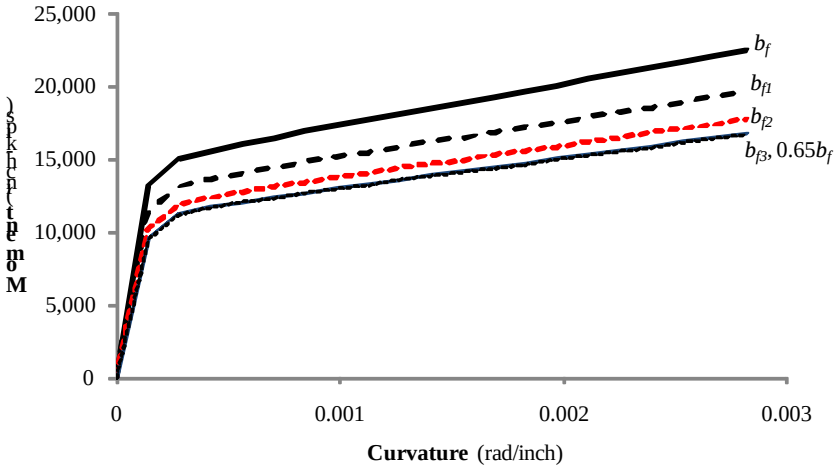

Figure 4.2-18 Moment-curvature diagram for W27x94 girder

A tip loaded cantilever beam analysis using half of the clear span length is used to generate the moment-rotation relationship for the inelastic hinges. For regular beams, where a cantilever beam is tip loaded, the moment diagram is linear and the curvature diagram is also linear as long as the moment along the beam remains in the elastic region (see Figure 4.2-19). If the moment along the beam exceeds the yield moment, the curvature along the beam will be as shown in Figure 4.2-20.

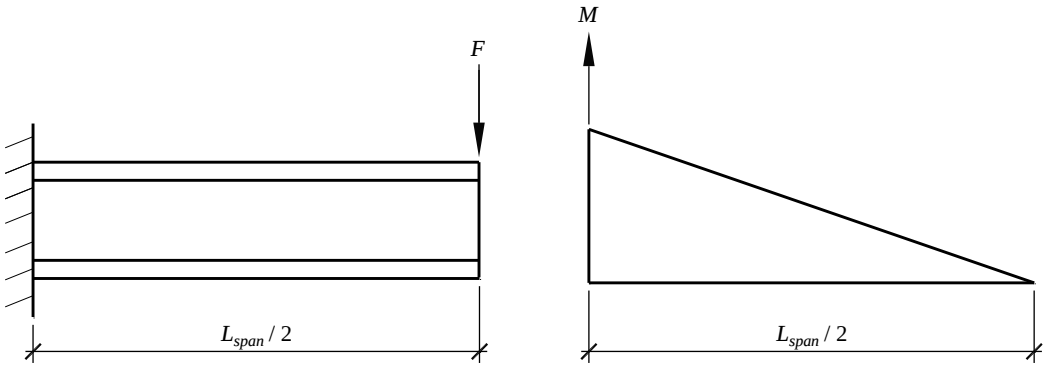

Figure 4.2-19 Tip loaded cantilever beam and moment diagram for cantilever beam

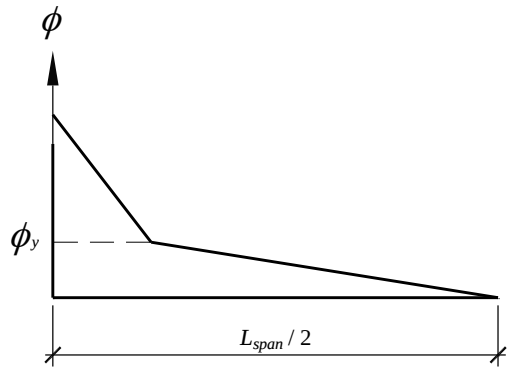

Figure 4.2-20 Curvature diagram for cantilever beam

Because a RBS is used in this study, the curvature diagrams are different from those for regular beams. As may be seen in Figure 4.2-21, the curvatures in the reduced flange region of the beam have a distinctive "bump". Because the moment diagram of the tip loaded cantilever beam is always linear, the moment values can be found easily at the different sections of the reduced flange, and then the corresponding curvature values can be assigned from the moment curvature diagram (Figure 4.2-18) to the curvature diagram along half of the clear span length (Figure 4.2-21).

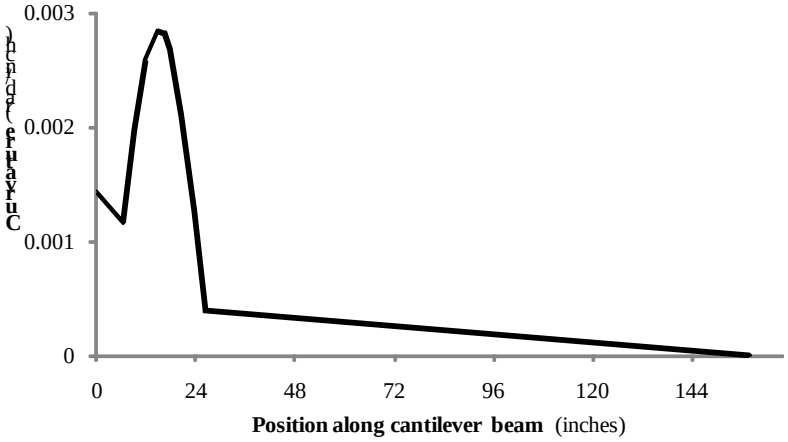

Figure 4.2-21 Curvature diagram for cantilever beam with reduced beam section

Figure 4.2-21 shows the curvature diagram when the curvature ductility reaches 20. The curvature difference (the bump at the center of RBS in Figure 4.2-21) section is less prominent when the ductility is smaller. Given the curvature distribution along the cantilever beam length, the deflections at the point of load (tip deflections) can be found using the moment area method. Figure 4.2-22 illustrates the force-displacement relationship at the end of the half span cantilever for the W27x94 with the reduced flange section.

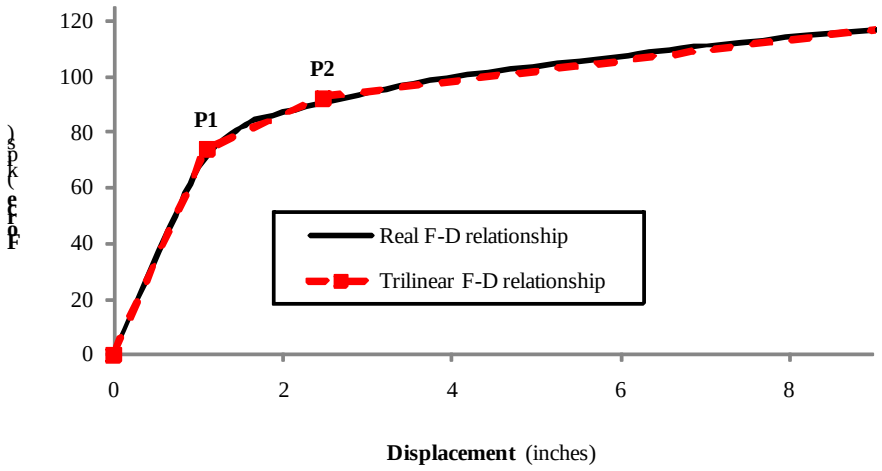

Figure 4.2-22 Force displacement diagram for W27x94 with RBS

To convert the force-tip displacement diagram into moment-rotation of the plastic hinge, the following procedure is followed:

1. Using the trilinear force displacement relationship shown in Figure 4.2-22, find the moment at the plastic hinge for P_1, P_2 and P_3 load levels and name them M_1, M_2 and M_3. To find the moments, the tip forces (P_1, P_2 and P_3) are multiplied by the distance from the center of the reduced section to the tip of the cantilever.

2. Calculate the change in moment for each added load (for example: $dM_1 = M_2 - M_1$).

3. Find the flexural rigidity (EI) of the beam given a tip displacement of 1 inch under the first load (P_1 in Figure 4.2-22).

4. Calculate the required rotational stiffnesse of the hinge between M_1 and M_2 and then M_2 and M_3.

5. Calculate the change in rotation from M_1 to M_2 and from M_2 to M_3, by dividing the change in moment found at Step 2 by the required rotational stiffness values calculated at Step 4.

6. Find the specific rotations at M_1, M_2 and M_3 using the change in rotation values found in Step 5. Note that the rotation is zero at M_1.

7. Plot a moment-rotation diagram of the plastic hinge using the values calculated at Step 1 and Step 6.

Figure 4.2-23 shows the moment-rotation diagrams for the plastic hinges of both of the girders used in the models. Note that two bilinear springs (Components 1 and 2) are needed to represent the trilinear behavior shown in the figure.

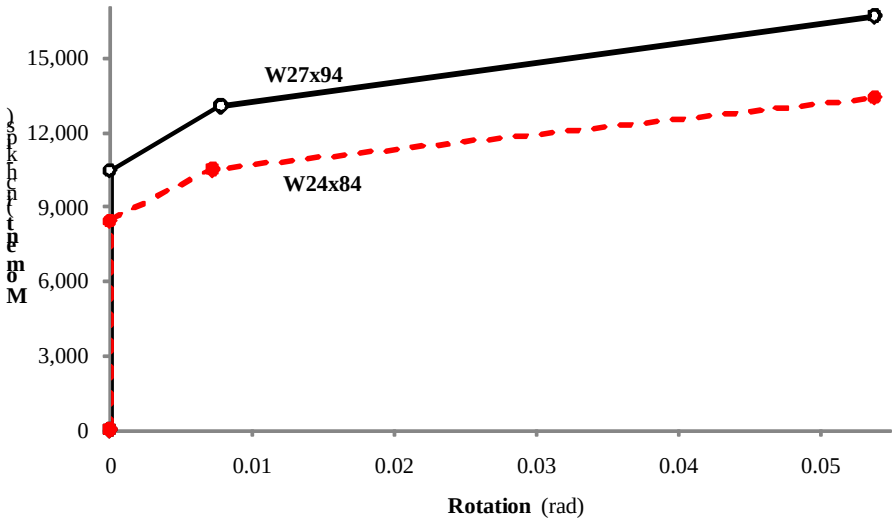

Figure 4.2-23 Moment-rotation diagram for girder hinges with RBS

The properties for the W24x84 and W27x94 girder are shown in Table 4.2-9. Note that the first yield of the model is the yield moment from Component 1.
s

Table 4.2-9 Girder Properties as Modeled in DRAIN

	Property	Section	
		W24x84	W27x94
Elastic Properties	Moment of Inertia (in.^{4})	2,370	3,270
	Shear Area (in.^{2})	11.3	13.2
Inelastic Component 1	Yield Moment (in.-kip)	8,422	10,458
	Initial Stiffness (in.-kip/radian)	1×10^{10}	1×10^{10}
	S.H. Ratio	0.0	0.0
Inelastic Component 2	Yield Moment (in.-kip)	2,075	2,615
	Initial Stiffness (in.-kip/radian)	287,550	337,020
	S.H. Ratio	0.217	0.232
Comparative Property	Plastic Moment = Z_eF_{ye}	9,200	11,539

4.2.4.4 Modeling columns. All columns in the analysis are modeled in DRAIN with Type-2 elements. Preliminary analysis indicated that columns should not yield, except at the base of the first story. Subsequent analysis shows that the columns will yield in the upper portion of the structure as well. For this reason, column yielding must be activated in all of the Type-2 column elements. The columns are modeled using the built-in yielding functionality of the DRAIN program, wherein the yield moment is a function of the axial force in the column. The yield surfaces used by DRAIN for all the columns in the model are shown in Figure 4.2-24.

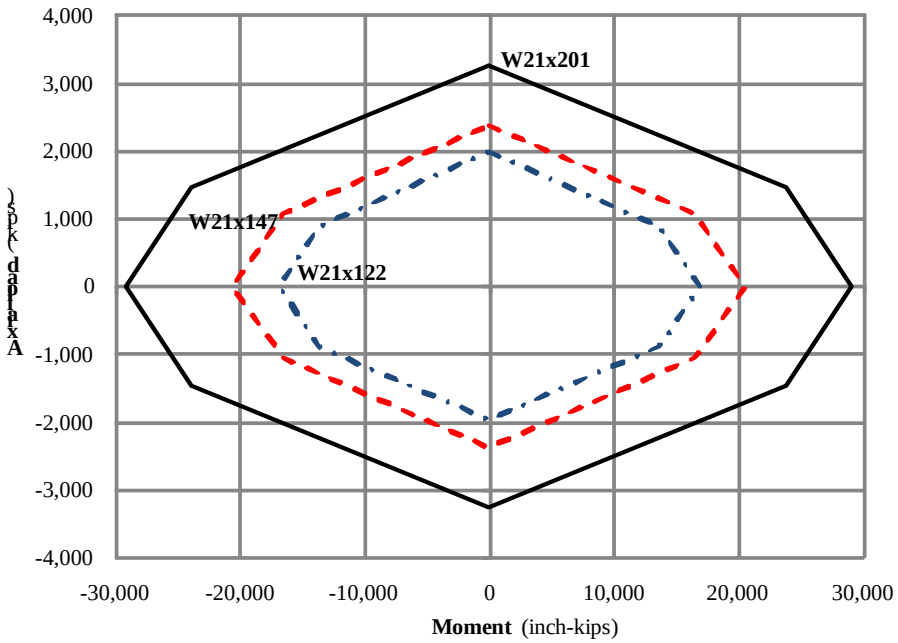

Figure 4.2-24 Yield surface used for modeling columns

The rules employed by DRAIN to model column yielding are adequate for event-to-event nonlinear static pushover analysis, but leave much to be desired where dynamic analysis is performed. The greatest difficulty in the dynamic analysis is adequate treatment of the column when unloading and reloading. An assessment of the effect of these potential problems is beyond the scope of this example.

4.2.4.5 Results of detailed analysis.

4.2.4.5.1 Period of vibration. Table 4.2-10 tabulates the first three natural modes of vibration for models with and without doubler plates. While the P-delta effects increase the period, the doubler plates decrease the period because the model becomes stiffer with doubler plates. As may be seen, different period values are obtained from preliminary and detailed analyses (see Table 4.2-4). The detailed model results in a slightly stiffer structure than the preliminary model especially when doubler plates are added.

Table 4.2-10 Periods of Vibration From Detailed Analysis (sec/cycle)

Model	Mode	P-delta excluded	P-delta included
Strong Panel with Doubler Plates	1	1.912	1.973
	2	0.627	0.639
	3	0.334	0.339
Weak Panel without Doubler Plates	1	2.000	2.069
	2	0.654	0.668
	3	0.344	0.349

4.2.4.5.2 Demand-to-capacity ratios. DCRs are found for the detailed analyses with the same load combination used for the preliminary analyses. The main reason for repeating the DCR for the detailed

model is to make a comparison with the DCR of the preliminary model. The detailed analyses include the advanced panel zone, girder and column modeling discussed in Section 4.2.4. Figures 4.2-25(a) and 4.2-25(b) illustrate the DCR of the beams with columns and panel zones of the detailed model respectively. In both figures, the values in the parentheses represent the DCR with no doubler plates added to the structure.

The DCR values of the detailed analyses are similar to those of the preliminary analysis displayed in Figure 4.2-5. The girders of the first and fifth bays at the third level have the maximum DCR in both the preliminary and detailed analyses. Similar trends are also observed for the DCR of the columns in both analyses. Note that the flexural stiffness of the girders is decreased by 7 percent in the preliminary analyses to compensate for the effect of reduced beam sections (with 35 percent flange reduction) which are included in the detailed analyses.

Similar to the preliminary DCR, the panel zone DCR increases significantly when doubler plates aren't used. Since the doubler plates are used only at the interior columns, that is where the difference of the DCRs changes significantly with and without doubler plates. See Figure 4.2-5(b) and Figure 4.2-25 (b).

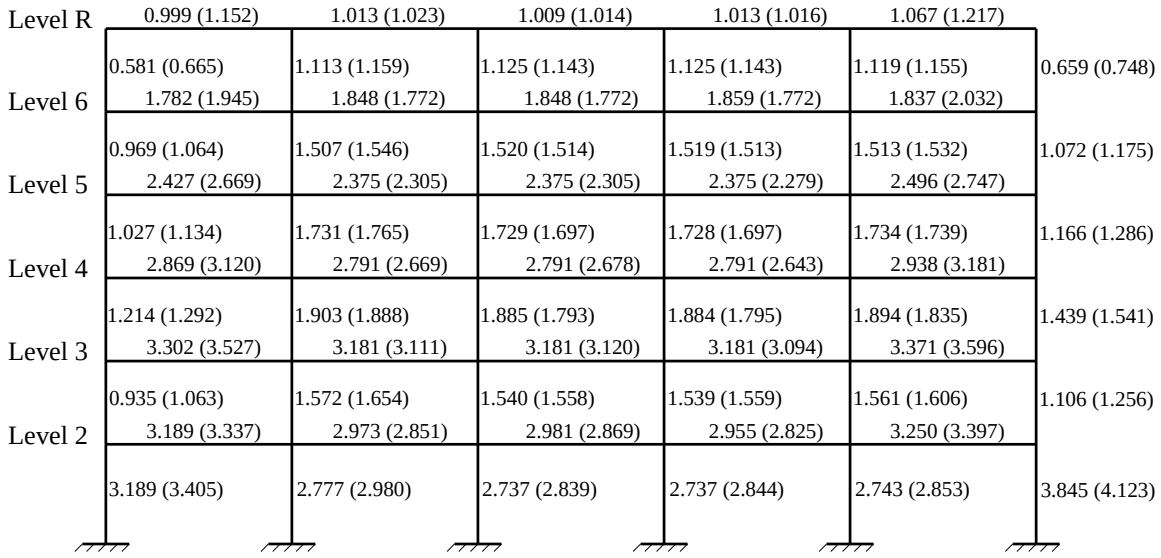

(a) DCRs of columns and girders with and without doubler plates
(DCR values in parentheses are for without doubler plates)

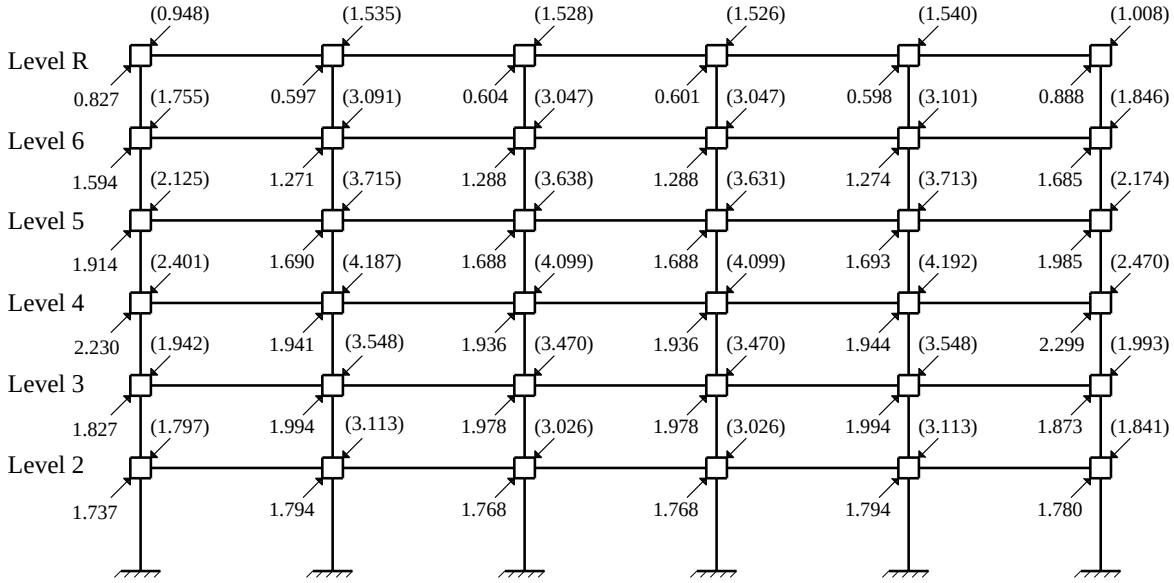

(b) DCRs of panel zones with and without doubler plates
(DCR values in parentheses are for without doubler plates)

Figure 4.2-25 DCRs for elements from detailed analysis with P-delta effects included

4.2.5 Nonlinear Static Analysis

As mentioned in the introduction to this example, nonlinear static (pushover) analysis is not an allowed analysis procedure in the *Standard*, nor does it appear in ASCE 7-10. The method is allowed in analysis related to rehabilitation of existing buildings and guidance for that use is provided in ASCE 41.

The *Provisions* makes at least two references to pushover analysis. In Section 12.8.7 of Part 1 pushover analysis is used to determine if structures with stability ratios (see Equation 12.8-16) greater than 0.1 are allowed. Such systems have a potential for dynamic instability and the pushover curve is used to determine if the slope of the pushover curve is continuously positive up to the target displacement. If the slope is positive, the system is deemed acceptable. If not, it must be redesigned such that either the stability ratio is less than 0.1, or the slope stays positive. The analysis carried out for this purpose must be performed according to the requirements of ASCE 41.

Pushover analysis is also mentioned in *Provisions* Part 3 Resource Paper 2. The intent of the procedure outlined there is to "determine whether lateral strength is nominally less than that required by the ELF procedure." The use of nonlinear static analysis for this purpose is limited to structures with a height of less than 40 feet. The building under consideration has a height of 77.5 feet and violates this limit.

In this example, pushover analysis is used simply to establish an estimate of the inelastic behavior of the structure under gravity and lateral loads. Of particular interest is the sequence of yielding in the beams, columns and panel zones; the lateral strength of the structure; the expected inelastic displacement; and the basic shape of the pushover curve. In the authors' opinion, such analysis should *always* be used as a precursor to nonlinear response history analysis. Without pushover analysis as a precursor, it is difficult to determine if the response history analysis is producing reasonable results.

The nonlinear static analysis illustrated in this example follows the recommendations of ASCE 41. The reader is also referred to FEMA 440.

The pushover curve obtained from a nonlinear static analysis is a function of both modeling and load application. For this example, the structure is subjected to the full dead load plus 50 percent of the fully reduced live load, followed by the lateral loads.

The *Provisions* states that the lateral load pattern should follow the shape of the first mode. In this example, three different load patterns are initially considered:

- UL = uniform load (equal force at each level)
- ML = modal load (lateral loads proportional to first mode shape)
- BL = *Provisions* load distribution (using the forces indicated in Table 4.2-3)

Relative values of these load patterns are summarized in Table 4.2-11. The loads have been normalized to a value of 15 kips at Level 2.

DRAIN analyses are run with P-delta effects included and, for comparison purposes, with such effects excluded. This effect is represented through linearized geometric stiffness, which is the basis of the outrigger column shown in Figure 4.2-4. Consistent geometric stiffness, which may be used to represent the influence of axial forces on the flexural flexibility of individual columns, may not be used directly in

DRAIN. Such effects may be approximated in DRAIN by subdividing columns into several segments and activating the linearized geometric stiffness on a column-by-column basis.[6]

Table 4.2-11 Lateral Load Patterns Used in Nonlinear Static Analysis

Level	Uniform load, UL (kips)	Modal load, ML (kips)	*Provisions* load, BL (kips)
R	15.0	85.1	144.8
6	15.0	77.3	114.0
5	15.0	64.8	84.8
4	15.0	49.5	58.2
3	15.0	32.2	34.6
2	15.0	15.0	15.0

As described later, the pushover analysis indicates most of the yielding in the structure occurs in the clear span of the girders and columns. Panel zone hinging occurs only at the exterior columns where doubler plates weren't used. To see the effect of doubler plates, the ML analysis is repeated for a structure without doubler plates. These structures are referred to as the strong panel (SP) and weak panel (WP) structures, respectively.

The analyses are carried out using the DRAIN-2Dx computer program. Using DRAIN, an analysis may be performed under "load control" or under "displacement control." Under load control, the structure is subjected to gradually increasing lateral loads. If, at any load step, the tangent stiffness matrix of the structure has a negative on the diagonal, the analysis is terminated. Consequently, loss of strength due to P-delta effects cannot be tracked. Using displacement control, one particular point of the structure (the control point) is forced to undergo a monotonically increasing lateral displacement, and the lateral forces are constrained to follow the desired pattern. In this type of analysis, the structure can display loss of strength because the displacement control algorithm adds artificial stiffness along the diagonal to overcome the stability problem. This approach is meaningful because structures subjected to dynamic loading can display strength loss and remain stable incrementally. It is for this reason that the post-strength-loss realm of the pushover response is of interest.

Where performing a displacement controlled pushover analysis in DRAIN with P-delta effects included, one must be careful to recover the base-shear forces properly.[7] At any displacement step in the analysis, the true base shear in the system consists of two parts:

$$V = \sum_{i=1}^{n} V_{C,i} - \frac{P_1 \Delta_1}{h_1}$$

where the first term represents the sum of all the column shears in the first story, and the second term represents the destabilizing P-delta shear in the first story. The P-delta effects for this structure are

[6] DRAIN uses the axial forces at the end of the gravity load analysis to set geometric stiffness for the structure. This is reasonably accurate where consistent geometric stiffness is used, but is questionable where linearized geometric stiffness is used.

[7] If P-delta effects have been included, this procedure needs to be used where recovering base shear from column shear forces. This is true for displacement controlled static analysis, force controlled static analysis and dynamic response history analysis.

included through the use of the outrigger column shown at the right of Figure 4.2-4. Figure 4.2-26 plots two base shear components of the pushover response for the SP structure subjected to the ML loading. Also shown is the total response. The kink in the line representing P-delta forces occurs because these forces are based on first-story displacement, which, for an inelastic system, generally will not be proportional to the roof displacement.

For all of the pushover analyses reported in this example, the structure is pushed to a displacement of 37.5 inches at the roof level. This value is approximately 4 percent of the total height.

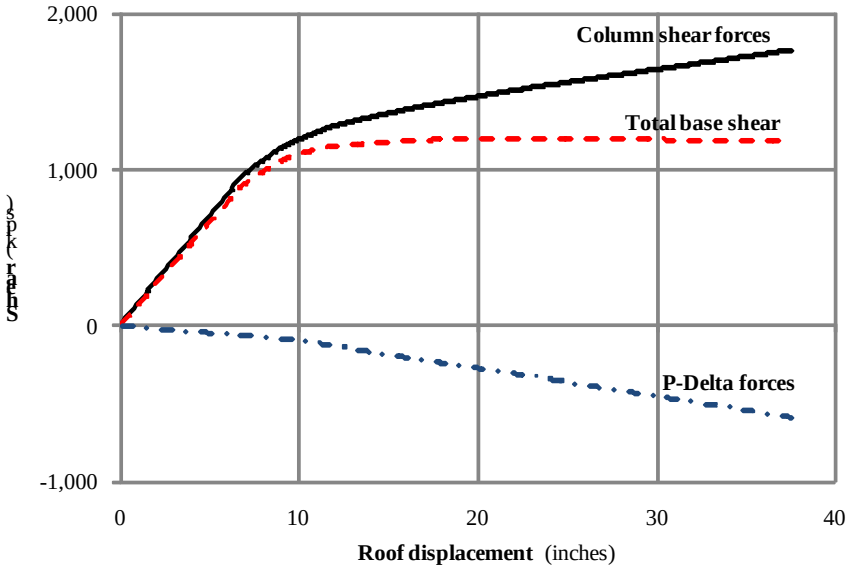

Figure 4.2-26 Two base shear components of pushover response

4.2.5.1 Pushover response of strong panel structure. Figure 4.2-27 shows the pushover response of the SP structure to all three lateral load patterns where P-delta effects are excluded. In each case, gravity loads are applied first, and then the lateral loads are applied using the displacement control algorithm. Figure 4.2-28 shows the response curves if P-delta effects are included. In Figure 4.2-29, the response of the structure under ML loading with and without P-delta effects is illustrated. Clearly, P-delta effects are an extremely important aspect of the response of this structure and the influence grows in significance after yielding. This is particularly interesting in the light of the *Standard*, which ignores P-delta effects in elastic analysis if the maximum stability ratio is less than 0.10 (see Sec. 12.8-7). For this structure, the maximum computed stability ratio is 0.0862 (see Table 4.2-5), which is less than 0.10 and is also less than the upper limit of 0.0909. The upper limit is computed according to *Standard* Equation 12.8-17 and is based on the very conservative assumption that $\beta = 1.0$. While the *Standard* allows the analyst to exclude P-delta effects in an elastic analysis, this clearly should not be done in the pushover analysis (or in response history analysis). (In the *Provisions* the upper limit for the stability ratio is eliminated. Where the calculated θ is greater than 0.10, a pushover analysis must be performed in accordance with ASCE 41, and it must be shown that that the slope of the pushover curve is positive up to the target displacement. The pushover analysis must be based on the MCE spectral acceleration and must include P-delta effects [and loss of strength, as appropriate]. If the slope of the pushover curve is negative at displacements less than the target displacement, the structure must be redesigned such that θ is less than 0.10 or the pushover slope is positive up to the target displacement.)

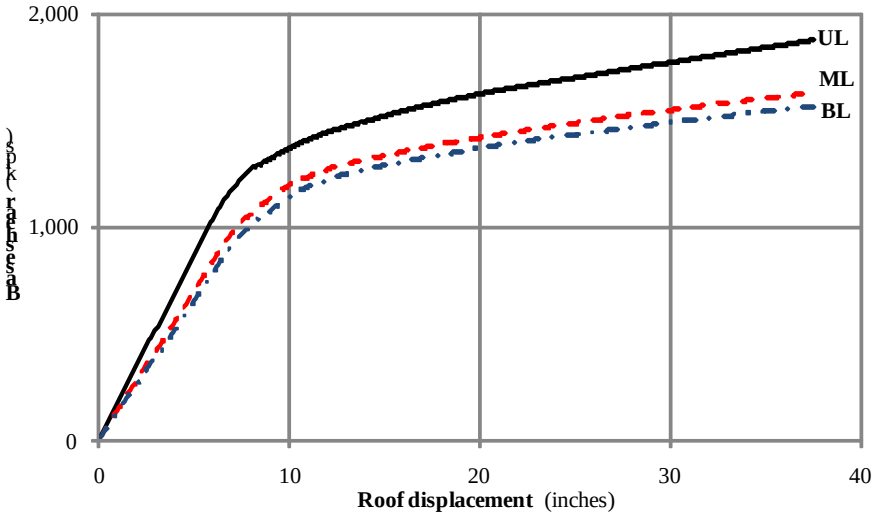

Figure 4.2-27 Response of strong panel model to three load patterns, excluding P-delta effects

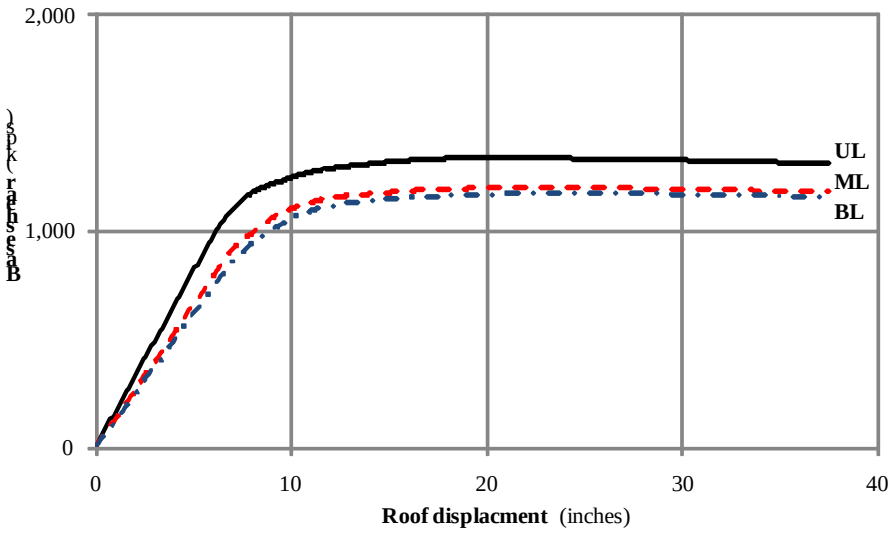

Figure 4.2-28 Response of strong panel model to three load patterns, including P-delta effects

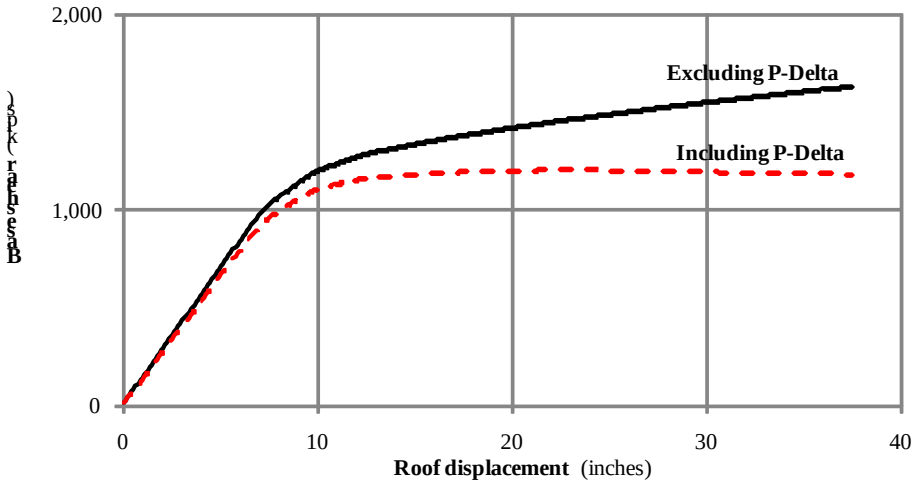

Figure 4.2-29 Response of strong panel model to ML loads, with and without P-delta effects

In Figure 4.2-30, a plot of the tangent stiffness versus roof displacement is shown for the SP structure with ML loading and with P-delta effects excluded or included. This plot, which represents the slope of the pushover curve at each displacement value, is more effective than the pushover plot in determining when yielding occurs. As Figure 4.2-30 illustrates, the first significant yield occurs at a roof displacement of approximately 6.5 inches and that most of the structure's original stiffness is exhausted by the time the roof displacement reaches 13 inches.

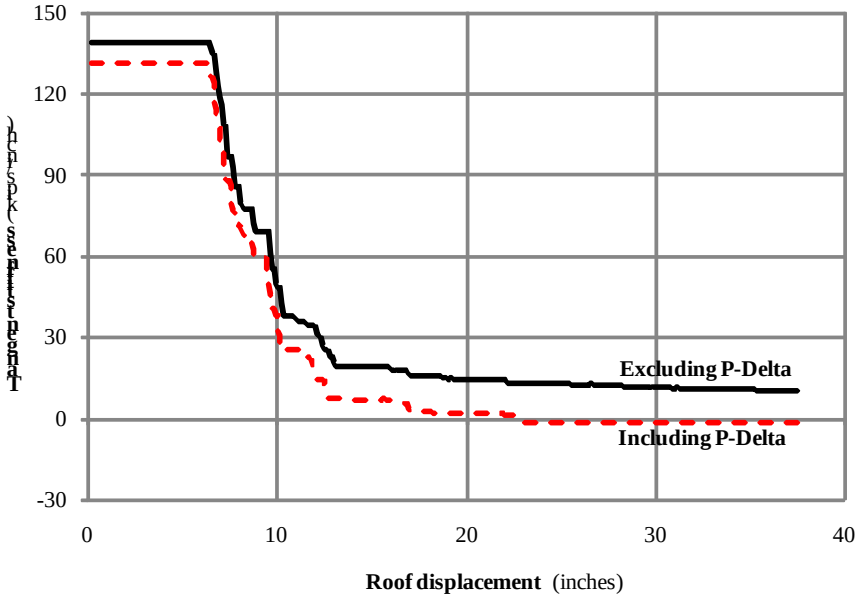

Figure 4.2-30 Tangent stiffness history for structure under ML loads, with and without P-delta effects

For the case with P-delta effects excluded, the final tangent stiffness shown in Figure 4.2-30 is approximately 10.2 kips/in., compared to an original value of 139 kips/in. Hence, the strain-hardening stiffness of the structure is 0.073 times the initial stiffness. This is somewhat greater than the 0.03 (3.0 percent) strain hardening ratio used in the development of the model because the entire structure does not yield simultaneously.

Where P-delta effects are included, the final tangent stiffness is -1.6 kips per inch. The structure attains this negative tangent stiffness at a displacement of approximately 23 inches.

4.2.5.1.1 Sequence and pattern of plastic hinging. The sequence of yielding in the structure with ML loading and with P-delta effects included is shown in Figure 4.2-31. Part (a) of the figure shows an elevation of the structure with numbers that indicate the sequence of plastic hinge formation. For example, the numeral "1" indicates that this was the first hinge to form. Part (b) of the figure shows a pushover curve with several hinge formation events indicated. These events correspond to numbers shown in Part (a) of the figure. The pushover curve only shows selected events because an illustration showing all events would be difficult to read. Comparing Figure 4.2-31(a) with Figures 4.2-5 and 4.2-25, it can be seen how the DCRs indicate the plastic hinge formation sequence. The highest ratios in Figure 4.2-5 are observed at the girders of the third and the second levels beginning from the bays at the leeward (right) side. As may be seen from Figure 4.2-31(a), first plastic hinges form at the same locations of the building. Similarly, the first panel zone hinge forms at the beam-column joint of the sixth column at the fourth level, and this is where the highest DCR values are obtained for the panel zones in both preliminary and detailed DCR analyses.

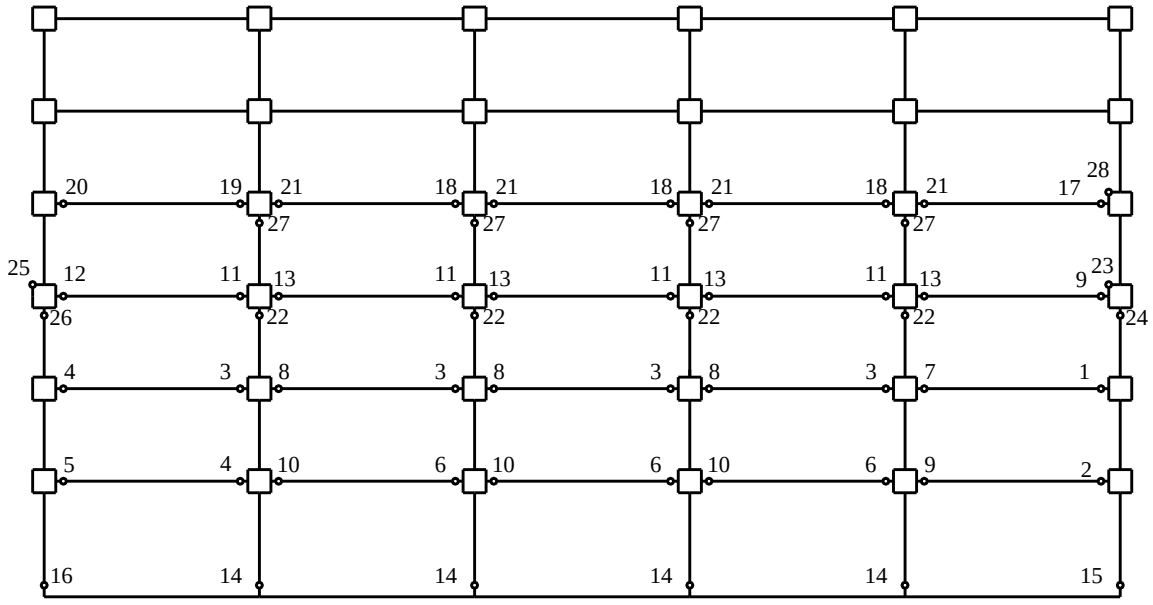

(a)

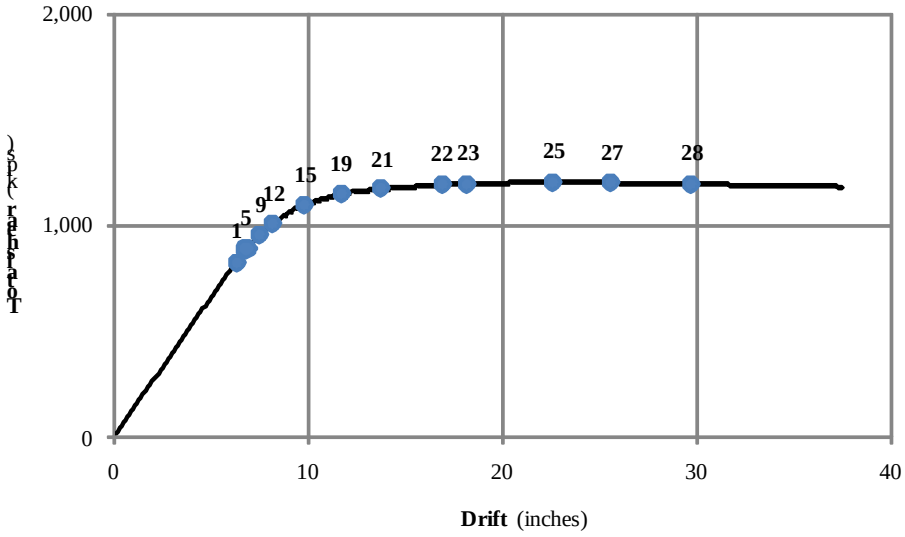

(b)

Figure 4.2-31 Patterns of plastic hinge formation: SP model under ML load, including P-delta effects

Several important observations are made from Figure 4.2-31:

- There is no hinging in Levels 6 and R.
- There is panel zone hinging only at the exterior columns at Levels 4 and 5. Panel zone hinges do not form at the interior joints where doubler plates are used.
- Hinges form at the base of all the Level 1 columns.
- Plastic hinges form in all columns on Level 3 and all the interior columns on Level 4.
- Both ends of all the girders at Levels 2 through 5 yield.

It appears the structure is somewhat weak in the middle two stories and is relatively strong at the upper stories. The doubler plates added to the interior columns prevent panel zone yielding.

The presence of column hinging at Levels 3 and 4 is a bit troublesome because the structure is designed as a strong-column/weak-beam system. This design philosophy, however, is intended to prevent the formation of complete story mechanisms, not to prevent individual column hinging. While hinges do form at the top of each column in the third story, hinges do not form at the bottom of these columns and a complete story mechanism is avoided.

Even though the pattern of hinging is interesting and useful as an evaluation tool, the performance of the structure in the context of various acceptance criteria cannot be assessed until the expected inelastic displacement can be determined. This is done below in Section 4.2.5.3.

4.2.5.1.2 Comparison with strength from plastic analysis. It is interesting to compare the strength of the structure from pushover analysis with that obtained from the rigid-collapse analysis performed using virtual work. These values are summarized in Table 4.2-12. The strength from the case with P-delta excluded was estimated from the curves shown in Figure 4.2-27 and is taken as the strength at the principal bend in the curve (the estimated yield from a bilinear representation of the pushover curve). Consistent with the upper bound theorem of plastic analysis, the strength from virtual work is greater than that from pushover analysis. The reason for the difference in predicted strengths is related to the pattern of yielding that actually formed in the structure, compared to that assumed in the rigid-plastic analysis.

Table 4.2-12 Strength Comparisons: Pushover versus Rigid Plastic

Pattern	Lateral Strength (kips)		
	P-delta Excluded	P-delta Included	Rigid-Plastic
Uniform	1,340	1,270	1,666
Modal (Triangular)	1,200	1,130	1,373
BSSC	1,170	1,105	1,308

4.2.5.2 Pushover response of weak panel structure. Before continuing, the structure should be re-analyzed without panel zone reinforcing, and the behavior compared with that determined from the analysis described above. For this exercise, only the modal load pattern is considered, but the analysis is performed with and without P-delta effects.

The pushover curves for the structure under modal loading and with weak panels are shown in Figure 4.2-32. Curves for the analyses run with and without P-delta effects are included. Figures 4.2-33 and 4.2-34 are more informative because they compare the response of the structures with and without panel zone reinforcement. Figure 4.2-35 shows the tangent stiffness history comparison for the structures with and without doubler plates. In both cases P-delta effects have been included.

Figures 4.2-32 through 4.2-35 show that the doubler plates, which represent approximately 2.0 percent of the volume of the structure, increase the strength and initial stiffness by approximately 10 percent.

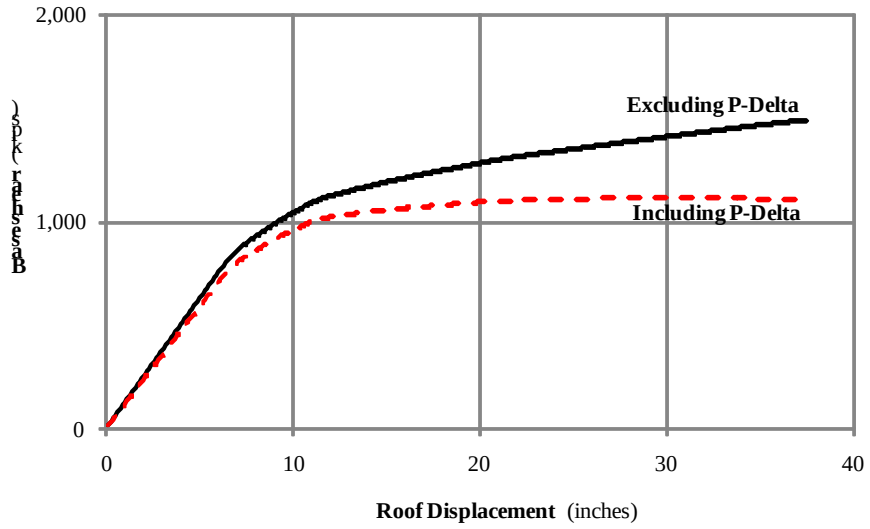

Figure 4.2-32 Weak panel zone model under ML load

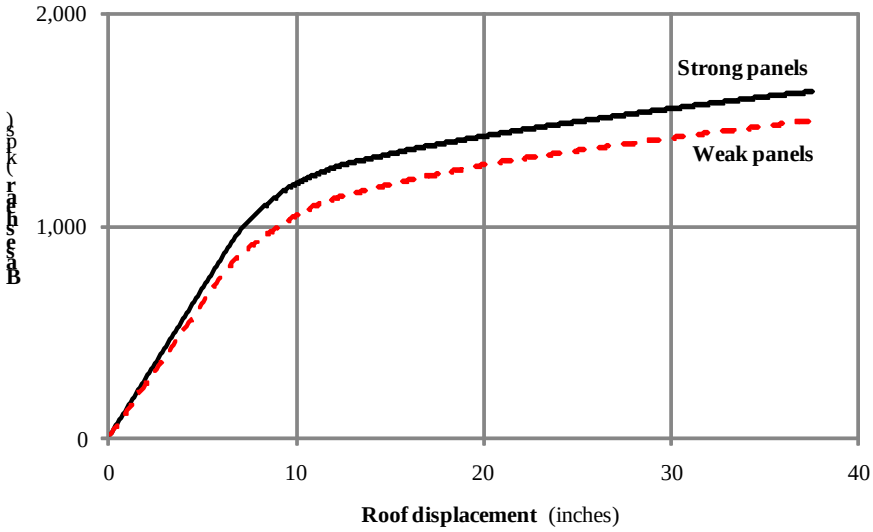

Figure 4.2-33 Comparison of weak panel zone model with strong panel zone model, excluding P-delta effects

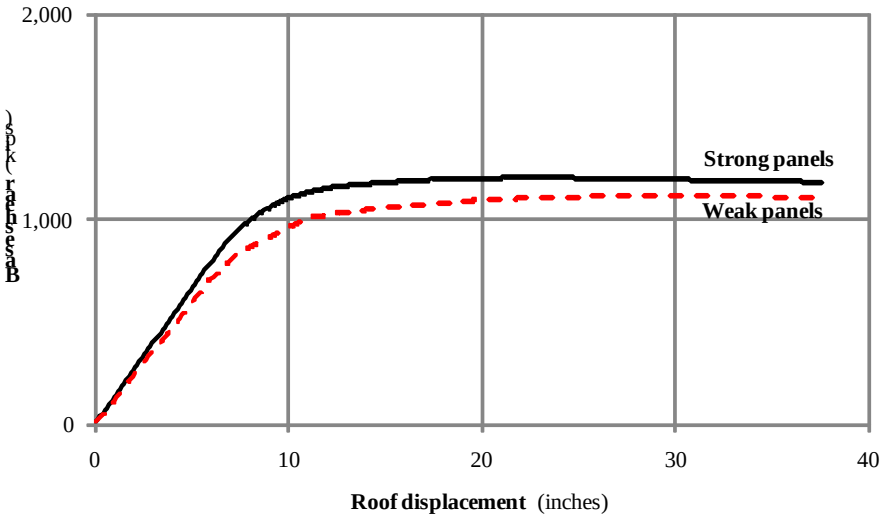

Figure 4.2-34 Comparison of weak panel zone model with strong panel zone model, including P-delta effects

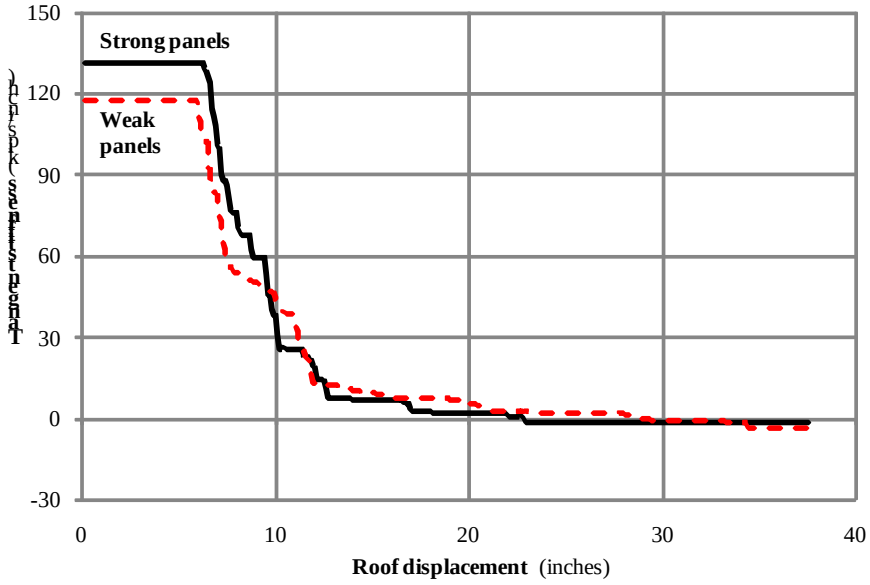

Figure 4.2-35 Tangent stiffness history for structure under ML loads, strong versus weak panels, including P-delta effects

The difference between the behavior of the structures with and without doubler plates is attributed to the yielding of the panel zones in the structure without panel zone reinforcement. The sequence of hinging is illustrated in Figure 4.2-36. Part (a) of this figure indicates that panel zone yielding occurs early. (Panel zone yielding is indicated by a numeric sequence label in the corner of the panel zone.) In fact, the first yielding in the structure is due to yielding of a panel zone at the fourth level of the structure, which is consistent with panel zone DCR calculated before where no doubler plates were added to the structure.

Under very large displacements the flange component of the panel zone yields. Girder and column hinging also occurs, but the column hinging appears relatively late in the response. It is also significant that the upper two levels of the structure display yielding in several of the panel zones.

Aside from the relatively marginal loss in stiffness and strength due to removal of the doubler plates, it appears that the structure without panel zone reinforcement behaves adequately. Of course, actual performance cannot be evaluated without predicting the maximum inelastic panel shear strain and assessing the stability of the panel zones under these strains.

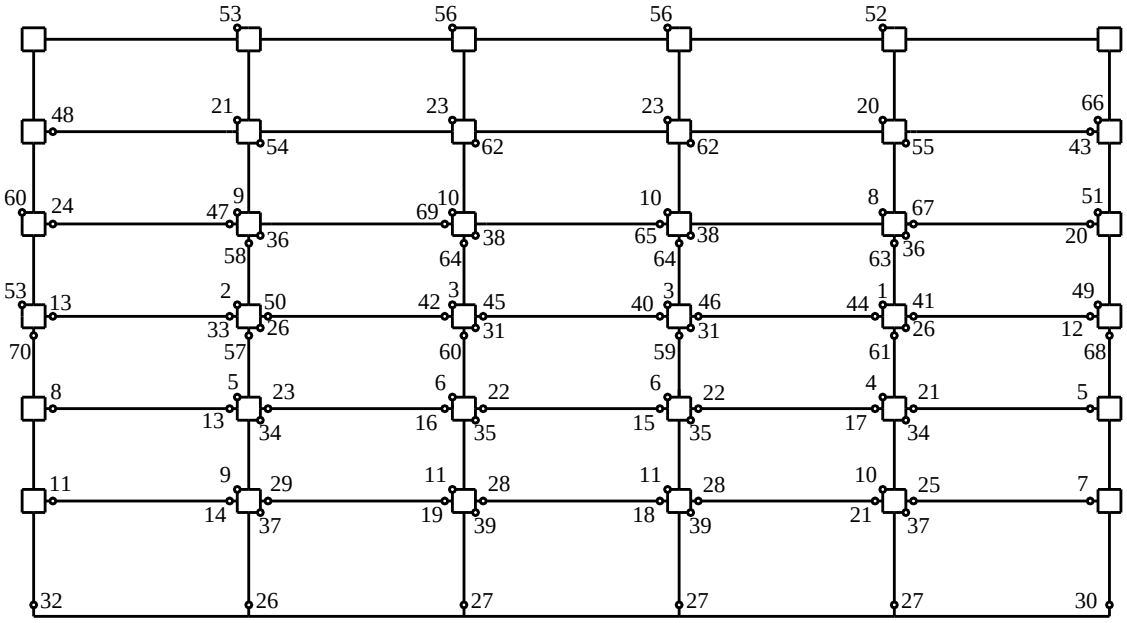

(a)

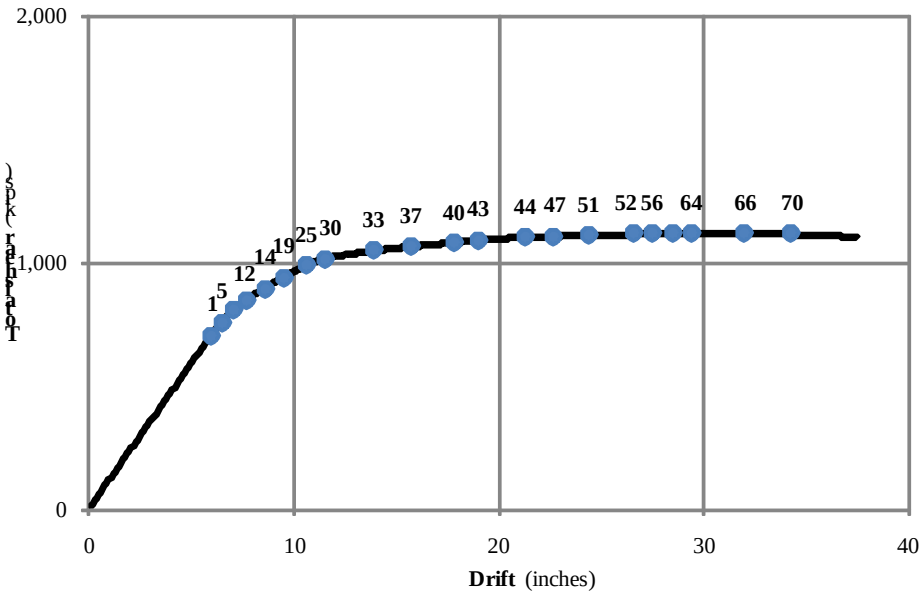

(b)

Figure 4.2-36 Patterns of plastic hinge formation: weak panel zone model under ML load, including P-delta effects

4.2.5.3 Target displacement. In this section, the only loading pattern considered is the modal load pattern discussed earlier. This is consistent with the requirements of ASCE 41 and FEMA 440. The structures with strong and weak panel zones are analyzed including P-delta effects.

ASCE 41 uses the coefficient method for calculating target displacement. The target displacement is computed as follows:

$$\delta_t = C_0 C_1 C_2 S_a \frac{T_e^2}{4\pi^2} g$$

where:

$C_0 = \phi_{1,r}\Gamma_1$ = modification factor to relate roof displacement of a multiple degree of freedom building system to the spectral displacement of an equivalent single degree of freedom system

$\phi_{1,r}$ = the ordinate of mode shape 1 at the roof (control node)

Γ_1 = the first mode participation factor

C_1 = modification factor to relate expected maximum inelastic displacements to displacements calculated for linear elastic response

C_2 = modification factor to represent the effect of pinched hysteresis shape, cyclic stiffness degradation and strength deterioration on maximum displacement response

S_a = response spectrum acceleration, at the effective fundamental period and damping ratio of the building in the direction under consideration

$T_e = T_i\sqrt{\frac{K_i}{K_e}}$ = effective fundamental period of the building in the direction under consideration

T_i = elastic fundamental period in the direction under consideration calculated by elastic dynamic analysis

K_i = elastic lateral stiffness of the building in the direction under consideration

K_e = effective lateral stiffness of the building in the direction under consideration

g = acceleration due to gravity

To find the coefficient S_a, the general horizontal response spectrum defined in ASCE 41 Section 1.6.1.5 is used. The damping of the spectrum is chosen as 2 percent for this study. The same damping ratio is used in the dynamic analysis. The parameters S_{XS} and S_{X1} are chosen as the same values as S_{MS} and S_{M1} which are defined in Section 4.2.2.2 of this study. Note that these are the MCE spectral acceleration parameters. Figure 4.2-37 shows the horizontal response spectrum obtained from ASCE 41. The parameters of this spectrum are discussed further with the dynamic analyses. This spectrum is for the Basic Safety Earthquake 2 (BSE-2) hazard level which has a 2 percent probability of exceedance in 50 years.

Coefficient C_0 is found using the first mode shape of the model with the mass matrix. For both strong and weak panel models, the C_0 coefficient is found a bit higher than 1.3, which is the value provided in Table 3.2 of ASCE41 for the shear buildings with triangular load pattern.

C_1 and C_2 are equal to 1.0 for periods greater than 1.0 second and 0.7 second respectively. Since the first mode periods of the strong and weak panel models are both approximately 2 seconds, these coefficients are taken as 1.0.

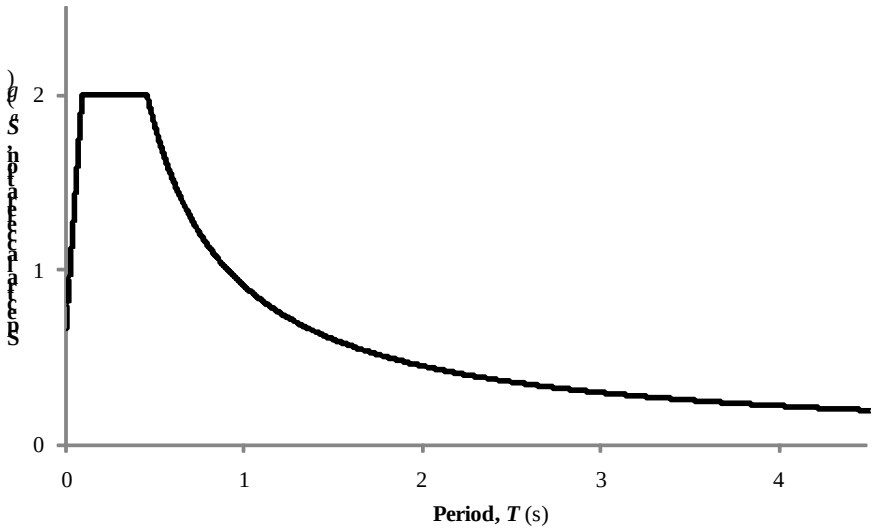

Figure 4.2-37 Two percent damped horizontal response spectrum from ASCE 41

To find the target displacement, the procedure described in ASCE 41 is followed. The nonlinear force-displacement relationship between the base shear and displacement of the control node are replaced with an idealized force-displacement curve. The effective lateral stiffness and the effective period depend on the idealized force-displacement curve. The idealized force-displacement curve is developed using an iterative graphical procedure where the areas below the actual and idealized curves are balanced approximately up to a displacement value of Δ_d. Δ_d is the displacement at the end of second line segment of the idealized curve and V_d is the base shear at the same displacement. (Δ_d, V_d) should be a point on the actual force displacement curve either at the calculated target displacement or at the displacement corresponding to the maximum base shear, whichever is the least. The first line segment of the idealized force-displacement curve should begin at the origin and finish at (Δ_y, V_y), where V_y is the effective yield strength and Δ_y is the yield displacement of idealized curve. The slope of the first line segment is equal to the effective lateral stiffness, K_e, which should be taken as the secant stiffness calculated at a base shear force equal to 60 percent of the effective yield strength of the structure. See Figures 4.2-38 and 4.2-39 for the actual and idealized force-displacement curves of strong and weak panel models which are under ML loading and both include P-delta effects.

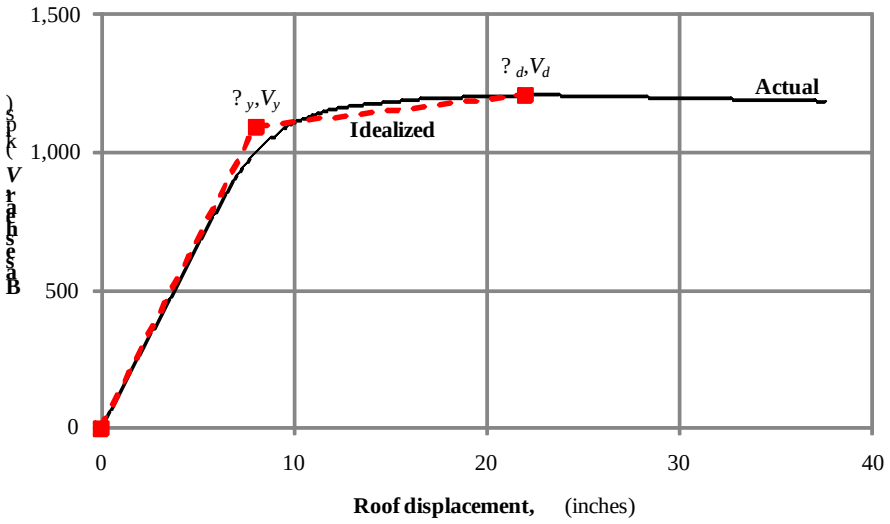

Figure 4.2-38 Actual and idealized force displacement curves for strong panel model, under ML load, including P-delta effects

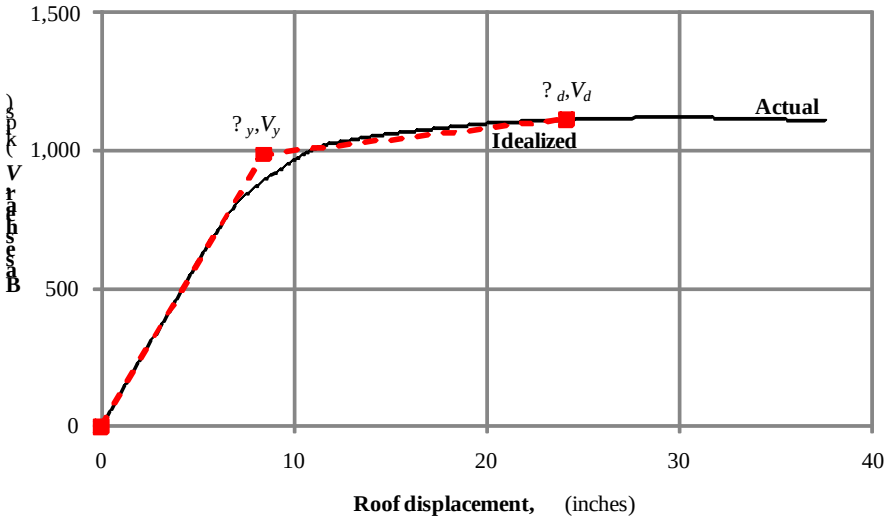

Figure 4.2-39 Actual and idealized force displacement curves for weak panel model, under ML load, including P-delta effects

Table 4.2-13 shows the target displacement values of SP and WP models. Story drifts are also shown at the load level of target displacement for both models.

Table 4.2-13 Target Displacement for Strong and Weak Panel Models

	Strong Panel	Weak Panel
C_0	1.303	1.310
C_1	1.000	1.000

Table 4.2-13 Target Displacement for Strong and Weak Panel Models

	Strong Panel	Weak Panel
C_2	1.000	1.000
S_a (g)	0.461	0.439
T_e (sec)	1.973	2.069
δ_t (in.) at Roof Level	**22.9**	**24.1**
Drift R-6 (in.)	0.96	1.46
Drift 6-5 (in.)	1.76	2.59
Drift 5-4 (in.)	2.87	3.73
Drift 4-3 (in.)	4.84	4.84
Drift 3-2 (in.)	5.74	5.35
Drift 2-1 (in.)	6.73	6.12

Negative tangent stiffness starts at 22.9 inches and 29.3 inches for strong and weak panel models, respectively. Thus negative tangent stiffness starts after target displacements for both models. Again note that these displacements are computed from the 2 percent-damped MCE horizontal response spectrum of ASCE 41.

4.2.6 Response History Analysis

The response history analysis method, with three ground motions, is used to estimate the inelastic deformation demands for the structure. While an analysis with seven or more ground motions generally is preferable, that was not done here due to time and space limitations.

The analysis did consider a number of parameters, as follows:

- Scaling of ground motions to the DBE and MCE level
- Analysis with and without P-delta effects
- Two percent and five percent inherent damping
- Added linear viscous damping

All of the models analyzed have “Strong Panels” (with doubler plates included in the interior beam-column joints).

4.2.6.1 Modeling and analysis procedure.

The DRAIN-2Dx program is used for each of the response history analyses. With the exception of requirements for including inherent damping, the structural model is identical to that used in the nonlinear static analysis. Second-order effects are included through the use of the leaning column element shown to the right of the actual frame in Figure 4.2-4. Only one-half of the building (a single frame in the N-S direction) is modeled.

Inelastic hysteretic behavior is represented through the use of a bilinear model. This model exhibits neither a loss of stiffness nor a loss of strength and for this reason, it will generally have the effect of overestimating the hysteretic energy dissipation in the yielding elements. Fortunately, the error produced by such a model will not be of great concern for this structure because the hysteretic behavior of panel

zones and flexural plastic hinges should be very robust where inelastic rotations are less than about 0.03 radians.

Rayleigh proportional damping was used to represent viscous energy dissipation in the structure. The mass and stiffness proportional damping factors are set initially to produce 2.0 percent damping in the first and third modes. It is generally recognized that this level of damping (in lieu of the 5 percent damping that is traditionally used in elastic analysis) is appropriate for nonlinear response history analysis. Two percent damping is also consistent with that used in the pushover analysis (see Section 4.2.5 of this example).

In Rayleigh proportional damping, the damping matrix, *C*, is a linear combination of the mass matrix, *M and* the *initial* stiffness matrix, *K*:

$$C = \alpha M + \beta K$$

where α and β are mass and stiffness proportionality factors, respectively. If the first and third mode frequencies, ω_1 and ω_3, are known, the proportionality factors may be computed from the following expression (Clough & Penzien):

$$\begin{Bmatrix} \alpha \\ \beta \end{Bmatrix} = \frac{2\xi}{w_1 + w_3} \begin{Bmatrix} w_1 w_3 \\ 1 \end{Bmatrix}$$

Note that α and β are directly proportional to ξ. To increase the target damping from 2 percent to 5 percent of critical, all that is required is a multiplying factor of 2.5 on α and β.

The targeted structural frequencies and the resulting damping proportionality factors are shown in Table 4.2-14. The frequencies shown in the table are computed from the detailed model shown in Figure 4.2-7.

Table 4.2-14 Structural frequencies and damping factors used in response history analysis (damping factors that produce 2 percent damping in modes 1 and 3)

Model/Damping Parameters	ω_1 (rad/sec)	ω_3 (rad/sec)	α	β
Strong Panel with P-delta	3.184	18.55	0.109	0.00184
Strong Panel without P-delta	3.285	18.81	0.112	0.00181

The stiffness proportional damping factor must *not* be included in the Type 4 elements used to represent rotational plastic hinges in the structure. These hinges, particularly those in the girders, have a very high initial stiffness. Before the hinge yields, there is virtually no rotational velocity in the hinge. After yielding, the rotational velocity is significant. If a stiffness proportional damping factor is used for the hinge, a viscous moment will develop in the hinge. This artificial viscous moment—the product of the rotational velocity, the initial rotational stiffness of the hinge and the stiffness proportional damping factor—can be quite large. In fact, the viscous moment may even exceed the intended plastic capacity of the hinge. These viscous moments occur in phase with the plastic rotation; hence, the plastic moment and the viscous moments are additive. These large moments transfer to the rest of the structure, affecting the sequence of hinging in the rest of the structure and produce artificially high base shears. The use of

stiffness proportional damping in discrete plastic hinges can produce a totally inaccurate analysis result. See Charney (2008) for details.

The structure is subjected to dead load and half of the fully reduced live load, followed by ground acceleration. The incremental differential equations of motion are solved in a step-by-step manner using the Newmark constant average acceleration approach. Time steps and other integration parameters are carefully controlled to minimize errors. The minimum time step used for analysis is as small as 0.0005 second for the first earthquake and 0.001 second for the second and third earthquakes. A smaller integration time step is required for the first earthquake because of its impulsive nature.

4.2.6.2 Development of ground motion records. The ground motion acceleration histories used in the analysis are developed specifically for the site. Basic information for the records is shown in Table 4.1-20a.

Ground acceleration histories and 2- and 5-percent-damped pseudoacceleration spectra for each of the motions are shown in Figures 4.2-40 through 4.2-42. For these two-dimensional analyses performed using DRAIN, single ground motion components areapplied one at a time. For this example, the component that produces the larger spectral acceleration at the structure's fundamental period (A00, B90 and C90) is used. A complete analysis would require consideration of both components of ground motions and possibly of a rotated set of components.

When analyzing structures in two dimensions, Section 16.1.3.1 of the *Standard* (as well as ASCE 7-10) gives the following instructions for scaling:

> The ground motions shall be scaled such that the average value of the 5 percent damped response spectra for the suite of motions is not less than the design response spectrum for the site for periods ranging from 0.2T to 1.5T where T is the natural period of the structure in the fundamental mode for the direction of response being analyzed.

The scaling requirements in *Provisions* Part 3 Resource Paper 3are similar, except that the target spectrum for scaling is the MCE_R spectrum. In this example, the only adjustment is made for scaling when the inherent damping is taken as 2 percent of critical. In this case, the ground motion spectra are based on 2 percent damping and the DBE or MCE spectrum is adjusted from 5 percent damping to 2 percent damping using the modification factors given in ASCE 41.

The scaling procedure described above has a "degree of freedom" in that there are an infinite number of scaling factors that can fit the criterion. To avoid this, a two-step scaling process is used wherein each spectrum is initially scaled to match the target spectrum at the structure's fundamental period and then the average of the scaled spectra are re-scaled such that no ordinate of the scaled average spectrum falls below the target spectrum in the range of periods between 0.2T and 1.5T. The final scale factor for each motion consists of the product of the initial scale factor and the second scale factor.

The initial scale factors, referred to as $S1_i$ (for each ground motion, i), are different for the three ground motions. The second scale factor, S2, is the same for each ground motion. The scale factors used in the response history analyses are shown in Table 4.2-15. Factors are determined for 2 percent and 5 percent damping and for the DBE and MCE motions. The 2 percent damped target MCE spectrum corresponds to ASCE 41-06 spectrum used in the pushover analysis. If a scale factor of 1.367 is used for the structure with 2 percent damping, Figure 4.2-43 indicates that the scaling criteria specified by the *Standard* are met for all periods in the range 0.2(1.973) = 0.4 second to 1.5(1.973) = 3.0 seconds. 1.973 seconds is the period of the SP model with P-delta effects included (See Table 4.2-10).

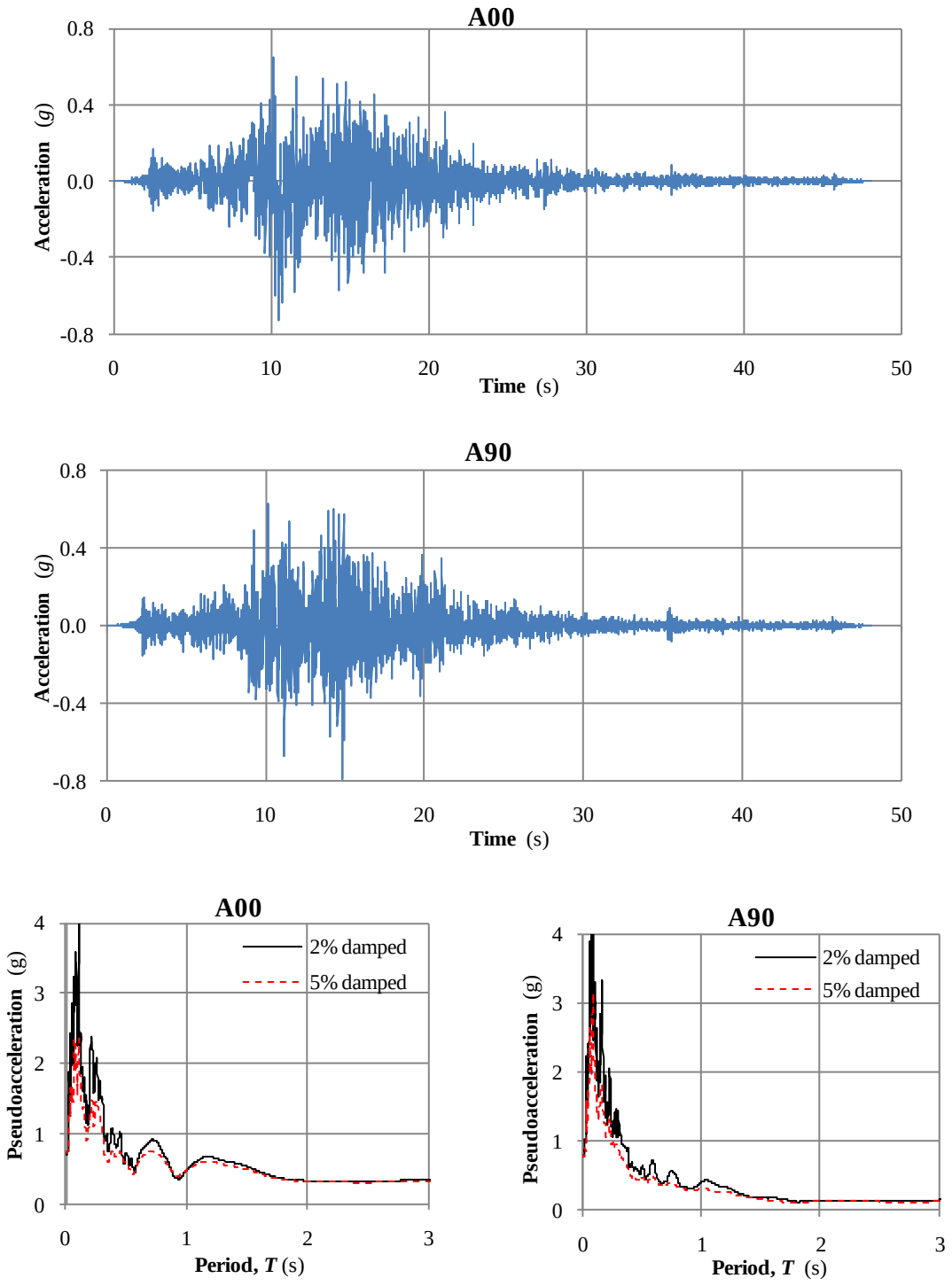

Figure 4.2-40 Ground acceleration histories and response spectra for Record A

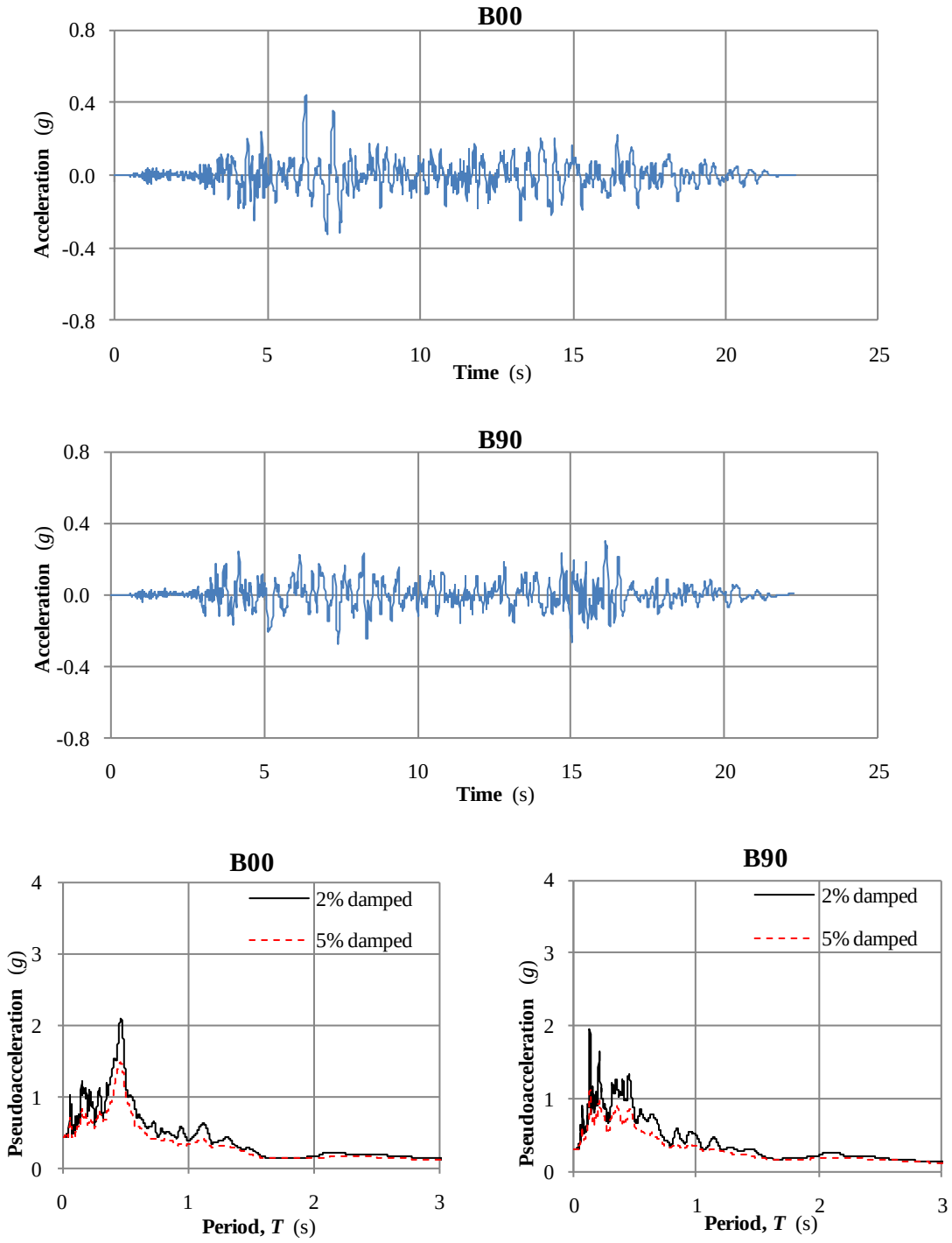

Figure 4.2-41 Ground acceleration histories and response spectra for Record B

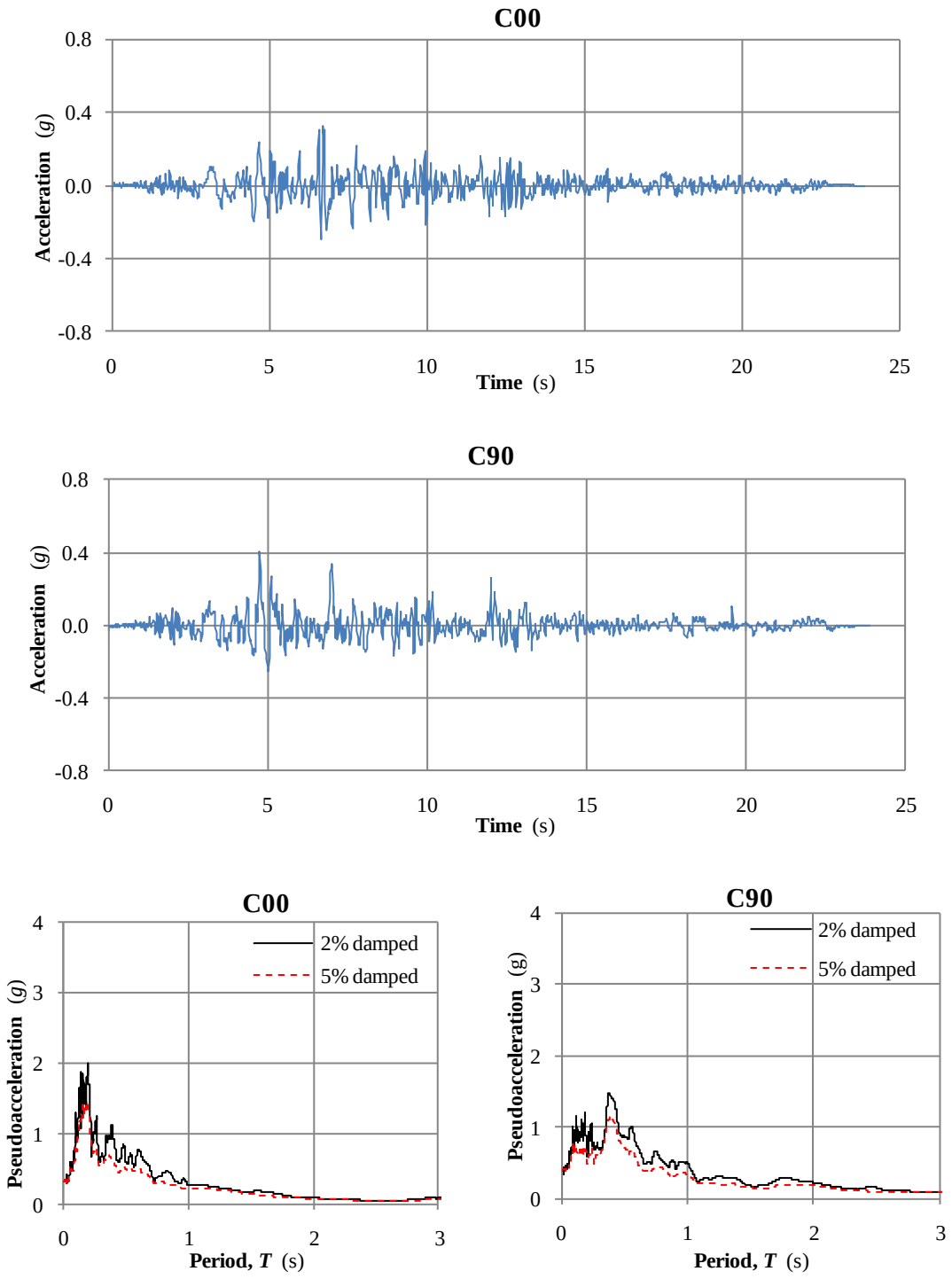

Figure 4.2-42 Ground acceleration histories and response spectra for Record C

Table 4.2-15 Ground Motion Scale Factors Used in the Analyses

	Scale Factor	2% Damped DBE	2% Damped MCE	5%Damped DBE	5% Damped MCE
Motion A00	S1	0.919	1.380	0.765	1.147
	S2	1.367	1.367	1.428	1.428
	SS	**1.257**	**1.886**	**1.092**	**1.638**
Motion B90	S1	1.495	2.245	1.439	2.159
	S2	1.367	1.367	1.428	1.428
	SS	**2.045**	**3.068**	**2.056**	**3.084**
Motion C90	S1	1.332	2.000	1.359	2.039
	S2	1.367	1.367	1.428	1.428
	SS	**1.822**	**2.734**	**1.941**	**2.911**

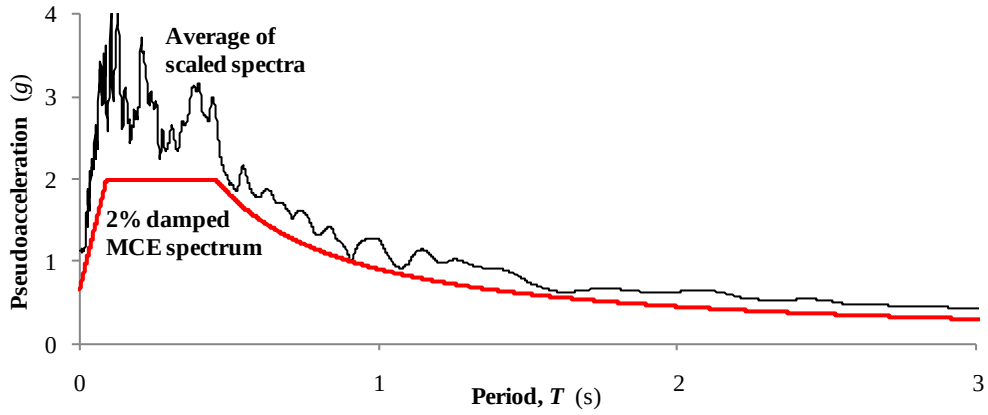

(a) Comparison of average of scaled spectra and target spectrum (SF = 1.367)

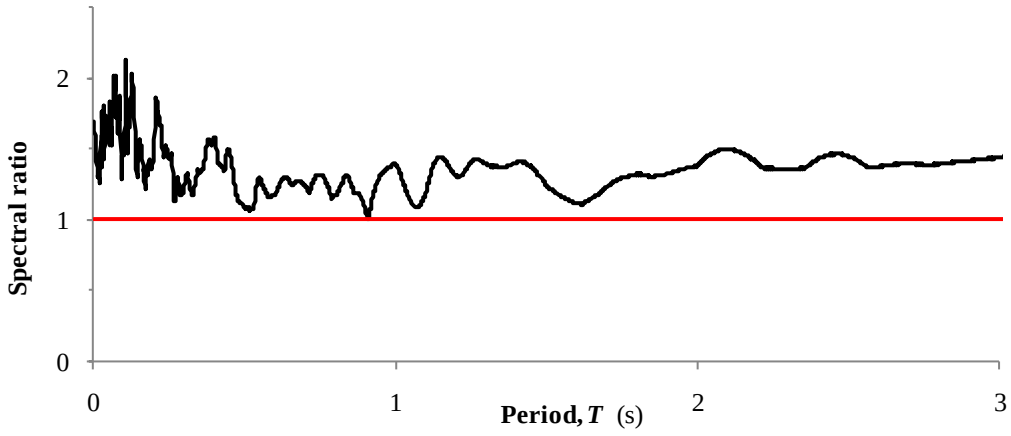

(b) Ratio of average of scaled spectra to target spectrum (SF = 1.367)

Figure 4.2-43 Ground motion scaling parameters

4.2.6.3 Results of response history analysis. The following parameters are varied to determine the sensitivity of the response to that parameter:

- Analyses are run with and without P-delta effects for all three ground motions.
- Analyses are run with 2 percent and 5 percent inherent damping. The ground motion scale factors are correlated with the corresponding inherent damping of the structure.
- Added dampers are used for the structure with 2 percent inherent damping. Various added damper configurations are used. These analyses are performed to assess the potential benefit of added viscous fluid damping devices. The SP model with P-delta effects included is used for this analysis and only Ground Motions A00 and B90 are used.

The results from the first series of analyses, all run with 2 or 5 percent of critical damping with and without P-delta effects, are summarized in Tables 4.2-16 through 4.2-23. Selected time history traces are shown in Figures 4.2-44 through 4.2-48.

The tabulated shears in the tables are for the single frame analyzed and should be doubled to obtain the total shear in the structure. The tables of story shear also provide two values for each ground motion. The first value is the maximum total elastic column story shear, including P-delta effects if applicable. The second value represents the maximum total inertial force for the structure. The inertial base shear, which is not necessarily concurrent with the column shears, was obtained as a sum of the products of the total horizontal accelerations and nodal mass of each joint. For a system with no damping, the story shears obtained from the two methods should be identical. For a system with damping, the base shear obtained from column forces generally will be less than the shear from inertial forces because the viscous component of column shear is not included. Additionally, the force absorbed by the mass proportional component of damping will be lost (as this is not directly recoverable in DRAIN).

The total roof displacement and the story drifts listed in the tables are peak (envelope) values and are not necessarily concurrent.

4.2.6.3.1 Response of structure with 2 and 5 percent of critical damping. Tables 4.2-16 and 4.2-17 summarize the results of the DBE analyses with 2 percent inherent damping, including and excluding P-delta effects. Part (a) of each table provides the maximum base shears, computed either as the sum of column forces (including P-delta effects as applicable), or as the sum of the products of the total acceleration and mass at each level. In each case, the shears computed using the two methods are similar, which serves as a check on the accuracy of the analysis. Had the analysis been run without damping, the shears computed by the two methods should be identical. As expected base shears decrease when P-delta effects are included.

The maximum story drifts are shown in the (b) parts of each table. The drift limits in the table, equal to 2 percent of the story height, are the same as provided in *Standard* Table 12.12-1. *Standard* Section 16.2.4.3 provides for the allowable drift to be increased by25 percent where nonlinear response history analysis is used; these limits are shown in the tables in parentheses. *Provisions* Part 2 states that the increase in drift limit is attributed to “the more accurate analysis and the fact that drifts are computed explicitly.” Drifts that exceed the increased limits are shown in bold text in the tables.

When a SP frame with 2 percent inherent damping is analyzed under MCE spectrum scaled motions excluding P-delta effects, earthquake A00 results in 62.40-inch displacement at the roof level and approximately between 15- to 20-inch drifts at the first three stories of the structure. These story drifts are well above the limits. When P-delta effects are included with the same level of motion, roof

displacement increases to 101.69 inches with approximately 20- to 40-inch displacement at the first three stories.

It is clear from Part (b) of Tables 4.2-16 and 4.2-17 that Ground Motion A00 is much more demanding with respect to drift than are the other two motions. The drifts produced by Ground Motion A00 are particularly large at the lower levels, with the more liberal drift limits being exceeded in the lower four stories of the building. When P-delta effects are included, the drifts produced by Ground Motion A00 increase significantly;drifts produced by Ground Motions B90 and C90 change only slightly.

Tables 4.2-18 and 4.2-19 provide result summaries for the structure analyzed with the MCE ground motions. Damping is still set at 2 percent of critical and analysis is run with and without P-delta effects. The drift limits listed in the (b) parts of Tables 4.2-18 and 4.2-19 are based on *Provisions* Part 3 Resource Paper 3 Section 16.4.5. These limits are 1.5 times those allowed by *Standard* Section 12.2.1. The 50 percent increase in drift limits is consistent with the increase in ground motion intensity when moving from DBE to MCE ground motions. If all of the increase in drift limit is attributed to the DBE-MCE scaling, there is no apparent adjustment related to "the more accurate analysis and explicit computation of drift".

When P-delta effects are included maximum story shears decrease and the drifts in lower stories increase for all motions. The drifts predicted for Ground Motion A00 (as much as 40 inches) indicate probable collapse of the structure. Loss of strength associated with such large drifts is not included in the analytical model (since DRAIN does not provide a mechanism for decreasing moment capacity under large plastic rotations). It is highly likely, however, that collapse would be predicted by more accurate modeling.

Similar trends in response are produced when the inherent damping is increased from 2 percent critical to 5 percent. The results for the 5 percent damped analysis are provided in Tables 4.2-20 through 4.2-23. The first two of these tables, Tables 4.1-20 and 4.1-21, are for the analysis using the DBE ground motions. When compared to the results using 2 percent damping, it is seen that both the base shears and the story drifts decrease significantly. DBE-level drifts at lower stories due to Ground Motion A00 exceed the drift limit but may not indicate collapse. MCE-level drifts produced by the A00 ground motion indicate likely collapse.

Table 4.2-16 DBE Results for 2% Damped Strong Panel Model with P- Delta Excluded

(a) Maximum Base Shear (kips)

Level	Motion A00	Motion B90	Motion C90
Column forces	1,780	1,649	1,543
Inertial forces	1,848	1,650	1,540

(b) Maximum Displacment and Story Drift (in.)

Level	Motion A00	Motion B90	Motion C90	Limit*
Roof displacement	26.80	14.57	13.55	NA
Drift R-6	1.85	1.92	1.71	3.00 (3.75)
Drift 6-5	2.51	2.60	2.33	3.00 (3.75)
Drift 5-4	**3.75**	3.08	3.03	3.00 (3.75)

(b) Maximum Displacment and Story Drift (in.)

Level	Motion A00	Motion B90	Motion C90	Limit*
Drift 4-3	**5.62**	2.98	3.03	3.00 (3.75)
Drift 3-2	**6.61**	3.58	2.82	3.00 (3.75)
Drift 2-G	**8.09**	**4.68**	3.29	3.60 (4.50)

*Values in ( ) reflect increased drift limits provided by ***Standard*** Sec. 16.2.4.3.

Table 4.2-17 DBE Results for 2% Damped Strong Panel Model with P-Delta Included

(a) Maximum Base Shear (kips)

Level	Motion A00	Motion B90	Motion C90
Column forces	1,467	1,458	1,417
Inertial forces	1,558	1,481	1,419

(b) Maximum Displacement and Story Drift (in.)

Level	Motion A00	Motion B90	Motion C90	Limit*
Roof displacement	32.65	14.50	14.75	NA
Drift R-6	1.86	1.82	1.70	3.00 (3.75)
Drift 6-5	2.64	2.50	2.41	3.00 (3.75)
Drift 5-4	**4.08**	2.81	3.19	3.00 (3.75)
Drift 4-3	**6.87**	3.21	3.33	3.00 (3.75)
Drift 3-2	**8.19**	3.40	2.90	3.00 (3.75)
Drift 2-G	**10.40**	**4.69**	3.44	3.60 (4.50)

*Values in ( ) reflect increased drift limits provided by ***Standard*** Sec. 16.2.4.3.

Table 4.2-18 MCE Results for 2% Damped Strong Panel Model with P-Delta Excluded

(a) Maximum Base Shear (kips)

Level	Motion A00	Motion B90	Motion C90
Column forces	2,181	1,851	1,723
Inertial forces	2,261	1,893	1,725

(b) Maximum Displacement and Story Drift (in.)

Level	Motion A00	Motion B90	Motion C90	Limit
Roof displacement	62.40	22.45	20.41	NA
Drift R-6	1.98	2.30	3.05	4.5
Drift 6-5	3.57	2.77	3.69	4.5
Drift 5-4	**7.36**	3.33	4.43	4.5
Drift 4-3	**14.61**	**4.61**	4.45	4.5
Drift 3-2	**16.29**	**5.21**	3.97	4.5
Drift 2-G	**19.76**	**6.60**	5.11	5.4

Table 4.2-19 MCE Results for 2% Damped Strong Panel Model with P-Delta Included

(a) Maximum Base Shear (kips)

Level	Motion A00	Motion B90	Motion C90
Column Forces	1,675	1,584	1,507
Inertial Forces	1,854	1,633	1,515

(b) Maximum Story Drifts (in.)

Level	Motion A00	Motion B90	Motion C90	Limit
Total Roof	101.69	26.10	20.50	NA
R-6	1.95	2.32	2.93	4.5
6-5	2.97	2.60	3.49	4.5
5-4	**6.41**	3.62	4.32	4.5
4-3	**20.69**	**5.61**	**4.63**	4.5
3-2	**31.65**	**6.32**	4.18	4.5
2-G	**40.13**	**7.03**	5.11	5.4

Table 4.2-20 DBE Results for 5% Damped Strong Panel Model with P-Delta Excluded

(a) Maximum Base Shear (kips)

Level	Motion A00	Motion B90	Motion C90
Column Forces	1,622	1,568	1,483
Inertial Forces	1,773	1,576	1,482

(b) Maximum Story Drifts (in.)

Level	Motion A00	Motion B90	Motion C90	*Limit
Total Roof	19.17	14.09	13.14	NA
R-6	1.33	1.73	1.77	3.00 (3.75)
6-5	2.18	2.52	2.32	3.00 (3.75)
5-4	3.06	2.98	2.89	3.00 (3.75)
4-3	**3.97**	2.86	2.78	3.00 (3.75)
3-2	**5.02**	3.19	2.72	3.00 (3.75)
2-G	**6.13**	4.05	3.01	3.60 (4.50)

*Values in ( ) reflect increased drift limits provided by ***Standard*** Sec. 16.2.4.3.

Table 4.2-21 DBE Results for 5% Damped Strong Panel Model with P-Delta Included

(a) Maximum Base Shear (kips

Level	Motion A00	Motion B90	Motion C90
Column forces	1,374	1,419	1,355
Inertial forces	1,524	1,448	1,361

(b) Maximum Displacement and Story Drift (in.)

Level	Motion A00	Motion B90	Motion C90	*Limit
Roof displacement	21.76	14.07	14.16	NA
Drift R-6	1.40	1.56	1.73	3.00 (3.75)
Drift 6-5	2.25	2.42	2.33	3.00 (3.75)
Drift 5-4	3.23	2.80	3.00	3.00 (3.75)
Drift 4-3	**4.38**	3.04	3.09	3.00 (3.75)
Drift 3-2	**5.60**	3.28	2.77	3.00 (3.75)
Drift 2-G	**7.12**	4.33	3.15	3.60 (4.50)

*Values in ( ) reflect increased drift limits provided by ***Standard*** Sec. 16.2.4.3.

Table 4.2-22 MCE Results for 5% Damped Strong Panel Model with P-Delta Excluded

(a) Maximum Base Shear (kips)

Level	Motion A00	Motion B90	Motion C90
Column forces	1,918	1,760	1,630
Inertial forces	2,139	1,861	1,633

(b) Maximum Displacement and Story Drift (in.)

Level	Motion A00	Motion B90	Motion C90	Limit
oof displacement	40.84	20.17	21.10	NA
Drift R-6	1.68	1.94	2.97	4.5
Drift 6-5	2.91	2.61	3.75	4.5
Drift 5-4	**4.86**	3.12	**4.50**	4.5
Drift 4-3	**9.04**	4.18	4.43	4.5
Drift 3-2	**10.48**	**4.77**	3.98	4.5
Drift 2-G	**13.04**	**6.09**	4.93	5.4

Table 4.2-23 MCE Results for 5% Damped Strong Panel Model with P-Delta Included

(a) Maximum Base Shear (kips)

Level	Motion A00	Motion B90	Motion C90
Column forces	1,451	1,486	1,413
Inertial forces	1,798	1,607	1,419

(b) Maximum Displacement and Story Drift (in.)

Level	Motion A00	Motion B90	Motion C90	Limit
Roof displacement	54.33	23.12	21.83	NA
Drift R-6	1.66	2.01	2.88	4.5
Drift 6-5	2.65	2.38	3.64	4.5
Drift 5-4	**4.88**	3.31	4.49	4.5
Drift 4-3	**12.63**	**5.09**	**4.72**	4.5
Drift 3-2	**15.27**	**5.66**	4.28	4.5
Drift 2-G	**19.31**	**6.14**	5.07	5.4

4.2.6.3.2 Discussion of response history analyses. The computed structural response to Ground Motion A00 is clearly quite different from that for Ground Motions B90 and C90. This difference in behavior occurs even though the records are all scaled to produce exactly the same spectral acceleration at the structure's fundamental period. A casual inspection of the ground acceleration histories and response spectra (Figures 4.2-40 through 4.2-42) does not reveal the underlying reason for this difference in behavior.

Figure 4.2-44 shows response histories of roof displacement and first story drift for the 2 percent damped SP model subjected to the DBE-scaled A00 ground motion. Two trends are readily apparent. First, the vast majority of the roof displacement results in residual deformation in the first story. Second, the P-delta effect increases residual deformations by about 50 percent. Such extreme differences in behavior do not appear in plots of base shear, as provided in Figure 4.2-45.

The residual deformations shown in Figure 4.2-44 may be real (due to actual system behavior) or may reflect accumulated numerical errors in the analysis. Numerical errors are unlikely because the shears computed from member forces and from inertial forces are similar. The energy response history can provide further validation.. Figure 4.2-46 shows the energy response history for the 2 percent damped DBE analysis with P-delta effects included. If the analysis is accurate, the input energy will coincide with the total energy (sum of kinetic, damping and structural energy). DRAIN 2D produces individual energy values as well as the input energy. See the article by Uang and Bertero for background on computing energy curves.

As evident from Figure 4.2-46, the total and input energy curves coincide, so the analysis is numerically accurate. Where this accuracy is in doubt, the analysis should be re-run using a smaller integration time step. A time step of 0.0005 second is required to produce the energy balance shown in Figure 4.2-46. A time step of 0.001 second is sufficient for analyses with Ground Motions B90 and C90.

The trends observed for the DBE analysis are even more extreme when the MCE ground motion is used. Figure 4.2-47 shows the displacement histories for the 2 percent damped structure under the MCE scaled A00 ground motion. As may be seen, residual deformations again dominate and in this case the total residual roof displacement with P-delta effects included is five times that without P-delta effects. This behavior indicates dynamic instability and eventual collapse.

It is interesting to compare the response computed for Ground Motion B90 with that obtained for ground motion A00. Displacements occurring for the 2 percent damped model under the MCE-scaled B90 ground motions are shown in Figure 4.2-48. While there is some small residual deformation in this

system, it is not extreme, and it appears that the structure is not in danger of collapse. (The corresponding plastic rotations are less than those that would be associated with significant strength loss.)

The characteristic of the ground motion that produces the residual deformations shown in Figures 4.2-44 and 4.2-48 (the DBE and MCE scaled A00 ground motions, respectively) is not evident from the ground acceleration history or from the acceleration response spectrum. The source of the behavior is quite obvious from plots of the ground velocity and ground displacement histories, shown in Figure 4.2-49(a) and (b), respectively. The ground velocity history shows that a very large velocity pulse occurs approximately 10 seconds into the earthquake. This leads to a surge in ground displacement, also occurring approximately 10 seconds into the response. The surge in ground displacement is more than *8 feet*, which is somewhat unusual. Recall from Table 4.1-20(a) that the distance between the epicenter and the recording site for this ground motion is 44 kilometers; so, the motion would not be considered as near-field. The unusual characteristics of Ground Motion A00 may be seen in Figure 4.2-49 (c), which is a tripartite spectrum.

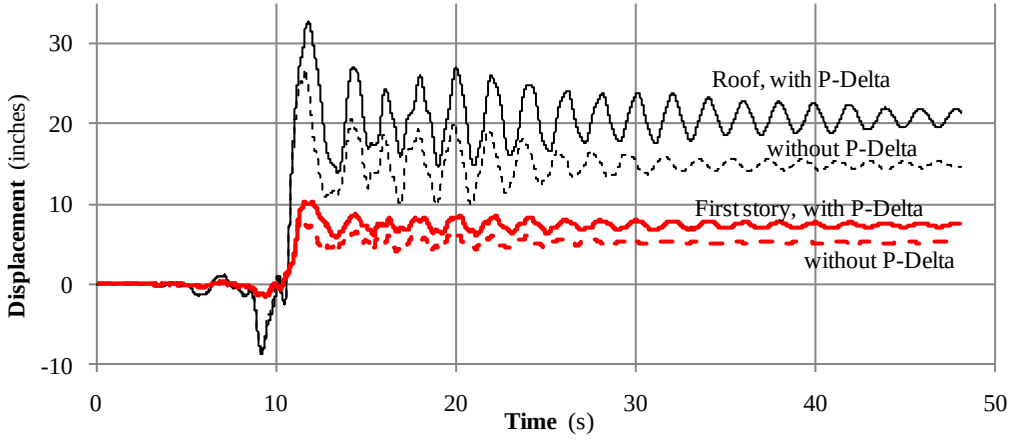

Figure 4.2-44 Response history of roof and first-story displacement, Ground Motion A00 (DBE)

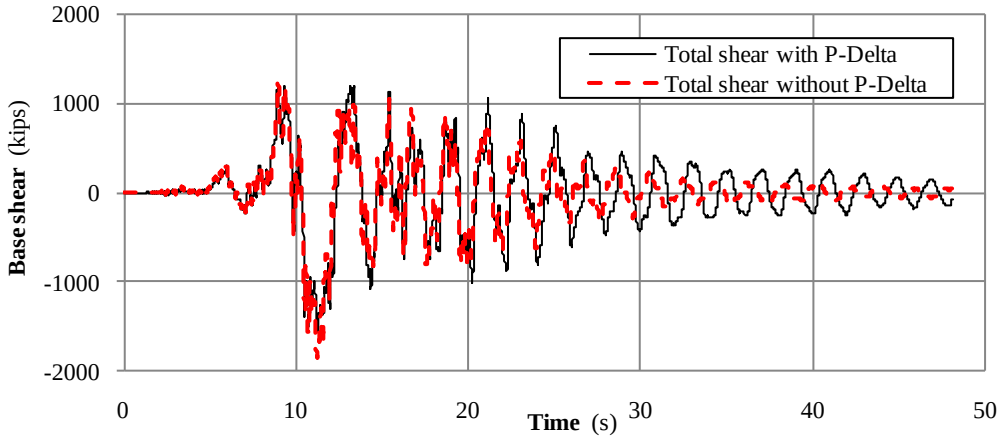

Figure 4.2-45 Response history of total base shear, Ground Motion A00 (DBE)

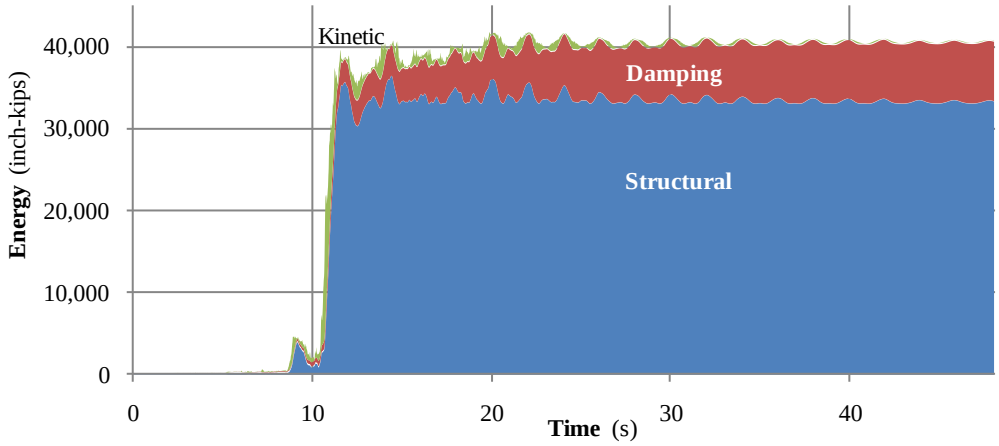

Figure 4.2-46 Energy response history, Ground Motion A00 (DBE), including P-delta effects

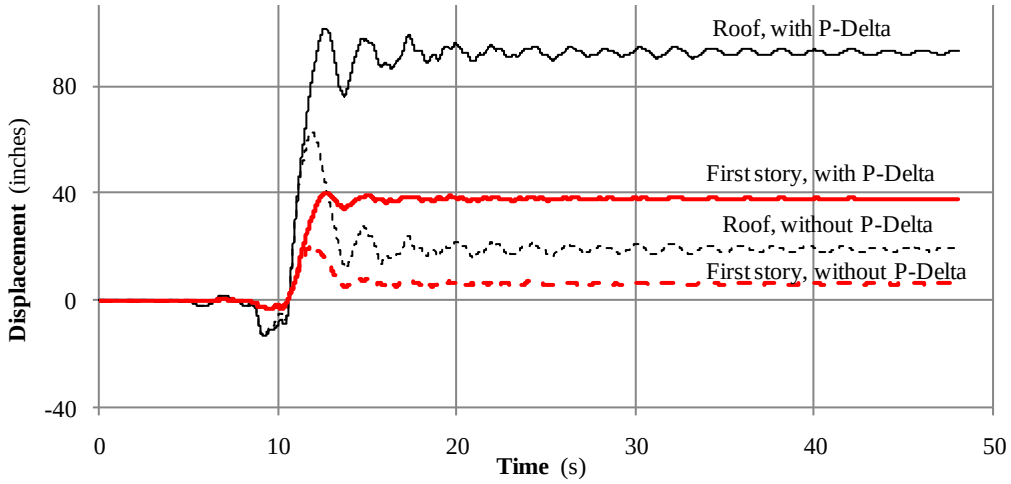

Figure 4.2-47 Response history of roof and first-story displacement, Ground Motion A00 (MCE)

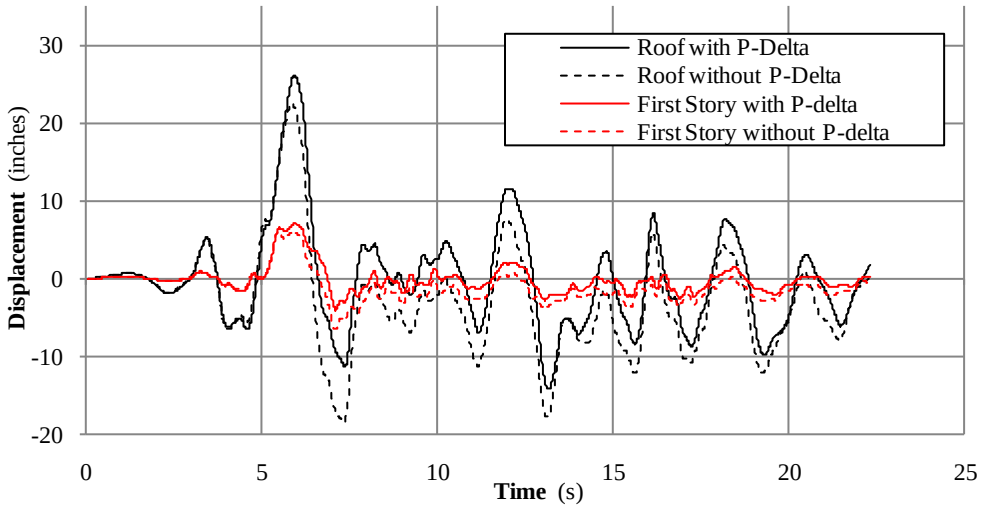

Figure 4.2-48 Response history of roof and first-story displacement, Ground Motion B90 (MCE)

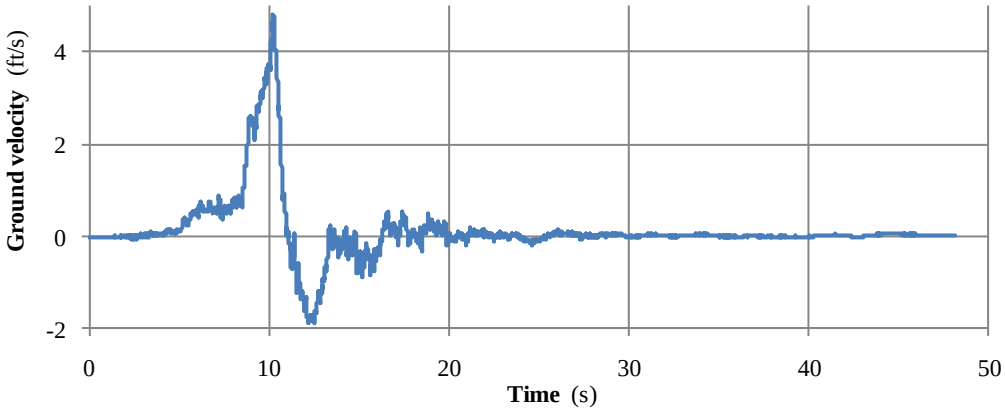

(a) Ground velocity history

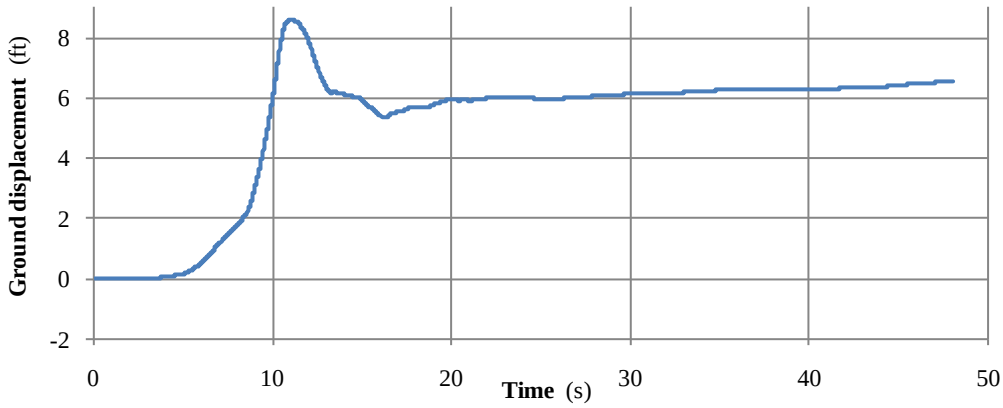

(b) Ground displacement history

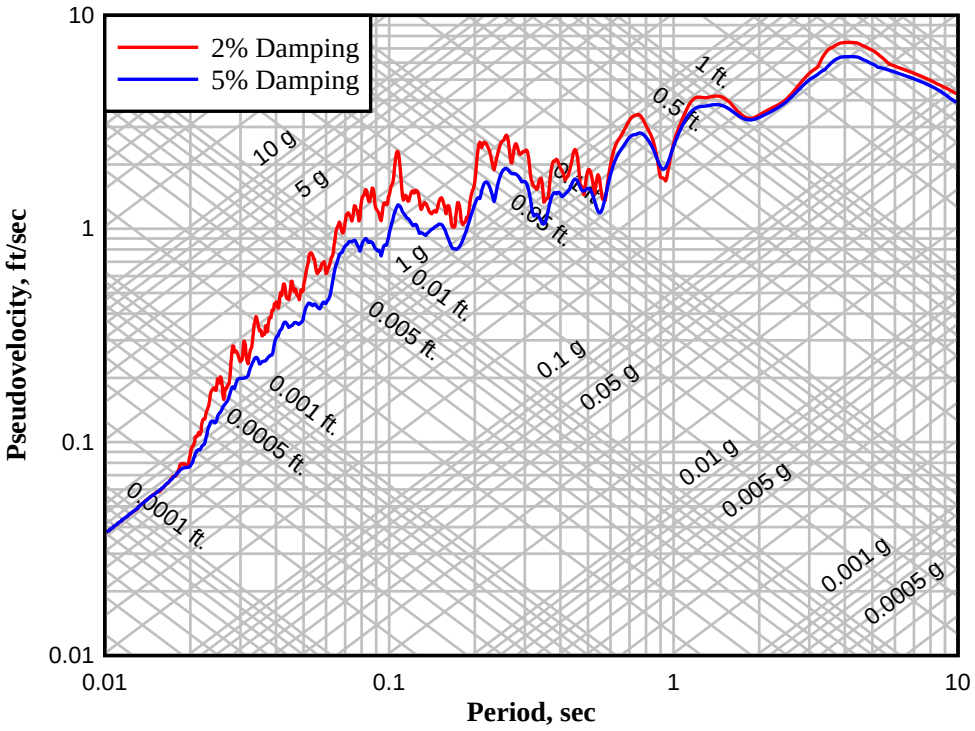

(c) Tripartite spectrum

Figure 4.2-49 Ground velocity and displacement histories and tripartite spectrum of Ground Motion A00 (unscaled)

Figure 4.2-50 shows the pattern of yielding in the structure subjected to a 2 percent damped MCE-scaled Ground Motion B90 including P-delta effects. Recall that the model incorporates panel zone reinforcement at the interior beam-column joints. The circles on the figure represent yielding at any time during the response; consequently, yielding does not necessarily occur at all locations simultaneously. The circles shown at the upper left corner of the beam-column joint region indicate yielding in the rotational spring, which represents the web component of panel zone behavior. There is no yielding in the flange component of the panel zones, as seen in Figure 4.2-50.

Yielding patterns for the other ground motions and for analyses run with and without P-delta effects are similar but are not shown here. As expected, there is more yielding in the columns when the structure is subjected to the A00 ground motion.

Figure 4.2-50 shows that yielding occurs at both ends of each of the girders at Levels 2, 3, 4 and 5. Yielding occurs at the bottom of all the first-story columns as well as at the top of the interior columns at the third and fourth stories and at bottom of the fifth-story interior columns. The panel zones at the exterior joints of Levels 4 and 5 also yield. The maximum plastic hinge rotations are shown where they occur for the columns, girders and panel zones; values are shown in Table 4.2-24. The maximum plastic shear strain in the web of the panel zone is identical to the computed hinge rotation in the panel zone spring. For the DBE-scaled B90 ground motion, the maximum rotations occurring at the plastic hinges are less than 0.02 radians.

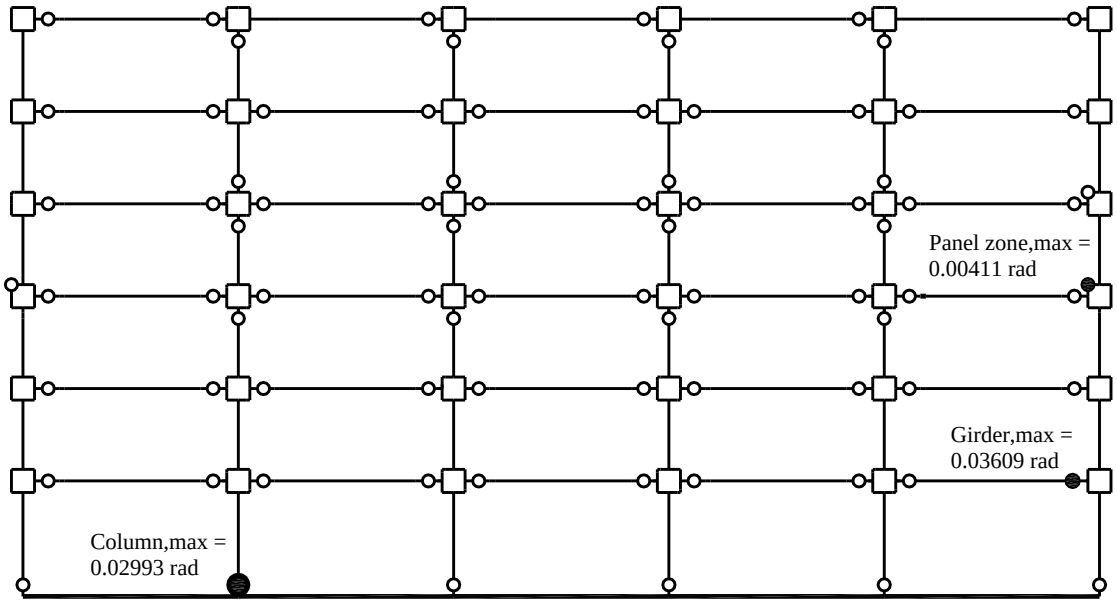

Figure 4.2-50 Yielding locations for structure with strong panels subjected to MCE-scaled B90 motion, including P-delta effects

4.2.6.3.3 Comparison with results from other analyses. Table 4.2-24 compares the results from the response history analysis with those from the ELF and the nonlinear static analyses. Base shears in the table are half of the total shear. The nonlinear static analysis results are for the 2 percent damped MCE target displacement so, for consistency, the tabulated dynamic analysis results are for the 2 percent damped MCE-scaled B90 ground motion. In addition, the lateral forces used to find the ELF drifts in Table 4.2-6 are multiplied by 1.5 forconsistency with MCE-level shaking; the ELF analysis drift values include the deflection amplification factor of 5.5. The results show some similarities and some striking differences, as follows:

- The base shear from nonlinear dynamic analysis is approximately three times the value from ELF analysis. The predicted displacements and story drifts are similar at the top three stories but are significantly different at the bottom three stories. Due to the highly empirical nature of the ELF approach, it is difficult to explain these differences. The ELF method also has no mechanism to include the overstrength that will occur in the structure, although it is represented explicitly in the static and dynamic nonlinear analyses.

- The nonlinear static analysis predicts base shears and story displacements that are less than those obtained from response history analysis. Excessive drift occurred at the bottom three stories as a result of both pushover and response history analyses.

Table 4.2-24 Summary of All Analyses for Strong Panel Structure, Including P-delta Effects

Response Quantity	Analysis Method		
	Equivalent Lateral Forces	Nonlinear Static Pushover	Nonlinear Dynamic
Base shear (kips)	569	1,208	1,633
Roof disp. (in.)	18.4	22.9	26.1
Drift R-6 (in.)	1.86	0.96	2.32
Drift 6-5 (in.)	2.78	1.76	2.60
Drift 5-4 (in.)	3.34	2.87	3.62
Drift 4-3 (in.)	3.73	4.84	5.61
Drift 3-2 (in.)	3.67	5.74	6.32
Drift 2-1 (in.)	2.98	6.73	7.03
Girder hinge rot. (rad)	NA	0.03304	0.03609
Column hinge rot. (rad)	NA	0.02875	0.02993
Panel hinge rot. (rad)	NA	0.00335	0.00411
Panel plastic shear strain	NA	0.00335	0.00411

Note: Shears are for half of total structure.

Some of the difference between pushover and nonlinear response history results is due to the scale factor (1.367) used to satisfy ground motion scaling requirements for the nonlinear response history analysis, but most of the difference is due to higher mode effects. Figure 4.2-51 shows the inertial forces from the nonlinear response history analyses at the time of peak base shear and the loads applied to the nonlinear static analysis model at the target displacement. The higher mode effects apparent in Figure 4.2-51 likely are the cause of the different hinging patterns and certainly are the reason for the very high base shear developed in the response history analysis. (If the inertial forces were constrained to follow the first mode response, the maximum base shear that could be developed in the system would be in the range of 1200 kips. See, for example, Figure 4.2-28.)

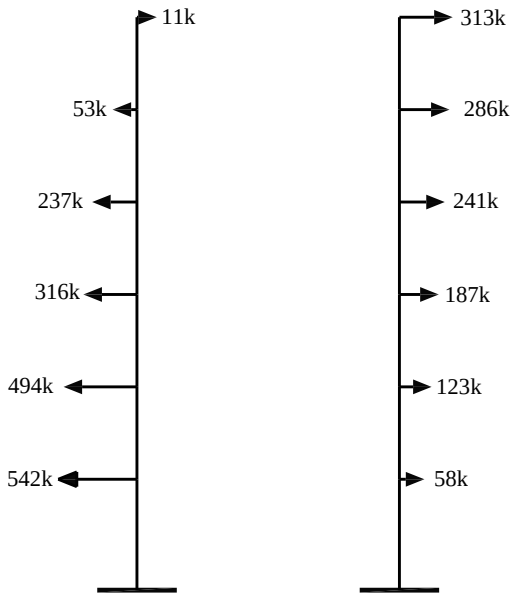

Figure 4.2-51 Comparison of inertial force patterns

4.2.6.3.4 Effect of increased damping on response. The nonlinear response history analysis of the structure with panel zone reinforcement indicates first story drifts in excess of the allowable limits. The most cost-effective measure to enhance the performance of the structure probably would be to provide additional strength and/or stiffness at this story. However, added damping is also a viable approach.

To investigate the viability of added damping, additional analysis that treats individual dampers explicitly is required. Linear viscous damping can be modeled in DRAIN using the stiffness proportional component of Rayleigh damping. Base shear increases with added damping, so in practice added damping systems usually employ viscous fluid devices with a "softening" nonlinear relationship between the deformational velocity in the device and the force in the device, to limit base shears when deformational velocities become large.

A linear viscous fluid damping device (Figure 4.2-52) in a selected story can be modeled using a Type 1 (truss bar) element. A damping constant for the device, C_{device}, is obtained as follows:

The elastic stiffness of the damper element is simply as follows:

$$k_{device} = \frac{A_{device} E_{device}}{L_{device}}$$

where:

A_{device} = the cross sectional area

E_{device} = the modulus of elasticity

L_{device} = the length of the Type 1 damper element

As stiffness proportional damping is used, the damping constant for the element is:

$$C_{device} = \beta_{device} k_{device}$$

The damper elastic stiffness should be negligible, so consider k_{device} = 0.001 kips/in. Thus:

$$\beta_{device} = \frac{C_{device}}{0.001} = 1000 C_{device}$$

Where modeling added dampers in this manner, it is convenient to consider E_{device} = 0.001 and A_{device} = the damper length L_{device}.

This value of β_{device} is for the added damper element *only*. Different dampers may require different values. Also, a different (global) value of β is required to model the stiffness proportional component of damping in the remaining nondamper elements.

Modeling the dynamic response using Type 1 elements is exact within the typical limitations of finite element analysis. Using the modal strain energy approach, DRAIN reports a damping value in each mode. These modal damping values are approximate and may be poor estimates of actual modal damping, particularly where there is excessive flexibility in the mechanism that connects the damper to the structure.

To determine the effect of added damping on the behavior of the structure, dampers are added to the SP frame with 2 percent inherent damping, and the structure is subjected to the DBE-scaled A00 and B90 ground motions. P-delta effects are included in the analyses. Table 4.2-25 shows the base shear and story drifts of the SP frame with 2 percent inherent damping when it is subjected to DBE-scaled A00 and B90 ground motions. The results summarized in this table can also be found in the tables of Section 4.2.6.3.1.

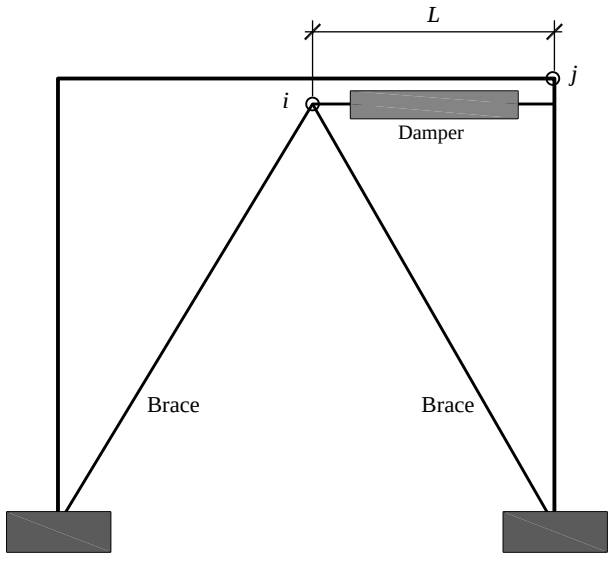

Figure 4.2-52 Modeling a simple damper

Table 4.2-25 Maximum Story Drifts (in.) and Base Shear (kips) when SP Model with 2% Inherent Damping is Subjected to DBE Scaled A00 and B90 Ground Motions, including P-delta Effects

Level	Motion A00	Motion B90	Limit
Roof displacement	32.65	14.50	NA
Drift R-6	1.86	1.82	3.75
Drift 6-5	2.64	2.50	3.75
Drift 5-4	**4.08**	2.81	3.75
Drift 4-3	**6.87**	3.21	3.75
Drift 3-2	**8.19**	3.40	3.75
Drift 2-G	**10.40**	**4.69**	4.50
Column forces	1467	1458	NA
Inertial forces	1558	1481	NA

As can be seen in Table 4.2-25, drift limits are exceeded at the bottom four stories for the A00 ground motion and only for the bottom story for the B90 ground motion.

Four different added damper configurations are used to assess their effect on story drifts and base shear, as summarized in Tables 4.2-26 and 4.2-27.

Table 4.2-26 Effect of Different Added Damper Configurations when SP Model is Subjected to DBE-Scaled A00 Ground Motion, including P-delta Effects

Level	First Config		Second Config		Third Config		Fourth Config		Drift Limit (in.)
	Damper Coeff. (kip-sec/in.)	Drift (in.)	Damper Coeff. (kip-sec/in.)	Drift (in.)	Damper Coeff. (kip-sec/in.)	Drift (in.)	Damper Coeff. (kip-sec/in.)	Drift (in.)	
R-6	10.5	1.10	60	1.03	-	1.82	-	1.47	3.75
6-5	33.7	1.90	60	1.84	-	3.56	-	2.41	3.75
5-4	38.4	2.99	70	2.88	-	**4.86**	56.25	3.46	3.75
4-3	32.1	**5.46**	70	**4.42**	-	**5.24**	56.25	**4.47**	3.75
3-2	36.5	**6.69**	80	**5.15**	160	**4.64**	112.5	**4.76**	3.75
2-G	25.6	**8.39**	80	**5.87**	160	4.40	112.5	**4.96**	4.50
Column base shear (kips)	1,629		2,170		2,134		2,267		
Inertial base shear (kips)	1,728		2,268		2,215		2,350		
Total damping (%)	10.1		20.4		20.2		20.4		

Table 4.2-27 Effect of Different Added Damper Configurations when SP Model is Subjected to DBE-Scaled B90 Ground Motion, including P-delta Effects

Level	First Config		Second Config		Third Config		Fourth Config		Drift Limit (in.)
	Damper Coeff. (kip-sec/in.)	Drift (in.)	Damper Coeff. (kip-sec/in.)	Drift (in.)	Damper Coeff. (kip-sec/in.)	Drift (in.)	Damper Coeff. (kip-sec/in.)	Drift (in.)	
R-6	10.5	1.11	60	0.86	-	1.53	-	1.31	3.75
6-5	33.7	1.76	60	1.35	-	2.11	-	1.83	3.75
5-4	38.4	2.33	70	1.75	-	2.51	56.25	2.07	3.75
4-3	32.1	2.67	70	2.11	-	2.37	56.25	2.16	3.75
3-2	36.5	2.99	80	2.25	160	2.09	112.5	2.13	3.75
2-G	25.6	3.49	80	1.96	160	1.87	112.5	1.82	4.50
Column base shear (kips)	1,481		1,485		1,697		1,637		
Inertial base shear (kips)	1,531		1,527		1,739		1,680		
Total damping (%)	10.1		20.4		20.2		20.4		

These configurations increase total damping of the structure from 2 percent (inherent) to 10 and 20 percent. In the first configuration added dampers are distributed proportionally to approximate story stiffnesses. In the second configuration, dampers are added at all six stories, with larger dampers in lower stories. Since the structure seems to be weak at the bottom stories (where it exceeds drift limits), dampers are concentrated at the bottom stories in the last two configurations. Added dampers are used only at the first and second stories in the third configuration and at the bottom four stories in the fourth configuration.

Based on this supplemental damper study, it appears to be impossible to decrease the story drifts for the A00 ground motion below the limits. This is because of the incremental velocity of Ground Motion A00 causes such significant structural damage. The drift limits could be satisfied if the total damping ratio is increased to 33.5 percent, but since that is impractical the results are not reported here. The third configuration of added dampers reduces the first-story drift from 10.40 inches to 4.40 inches

All of the configurations easily satisfy drift limits for the B90 ground motion.While the system with 10 percent total damping is sufficient for drift limits, systems with 20 percent damping further improve performance. Although configurations 3 and 4 have the same amount of total damping as configuration 2, story drifts are higher at the top stories since dampers are added only at lower stories.

Figures 4.2-53 through 4.2-55 show the effect of added damping of roof displacement, inertial base shear and energy history for the A00 ground motion. As Figure 4.2-53 shows added dampers reduce roof displacement significantly but do not prevent residual displacement. Figure 4.2-54 shows how added damping increases peak base shear. Figure 4.2-55 is an energy response history for the structure with damping configuration 4. It should be compared to Figure 4.2-46, which is the energy history for the structure with 2 percent inherent damping but with no added damping. As should be expected, adding discrete damping reduces the hysteretic energy demand in the structure (designated as structural energy in Figure 4.2-55). A reduction in hysteretic energy demand for the system with added damping corresponds to a reduction in structural damage.

Figures 4.2-56 through 4.2-58 display the same response plots for Ground Motion B90. As for Ground Motion A00 roof displacement decreases with added damping, peak base shear increases and hysteretic energy demand (which is related to structural damage) decreases.

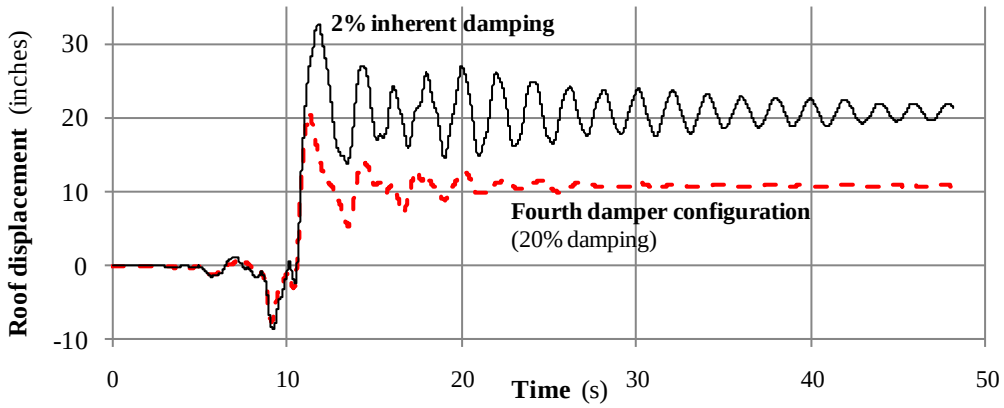

Figure 4.2-53 Roof displacement response histories with added damping (20% total) and inherent damping (2%) for Ground Motion A00

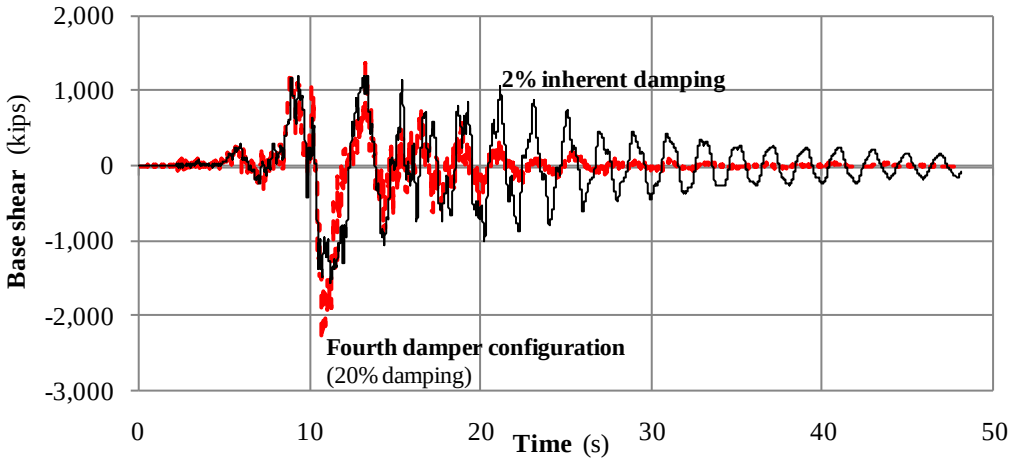

Figure 4.2-54 Inertial base shear response histories with added damping (20% total) and inherent damping (2%) for Ground Motion A00

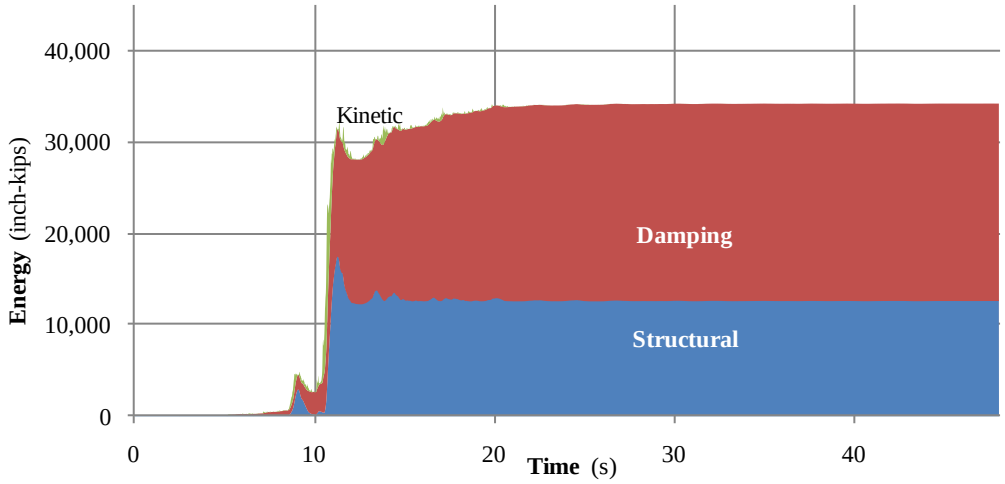

Figure 4.2-55 Energy response history with added damping of fourth configuration (20% total damping) for Ground Motion A00

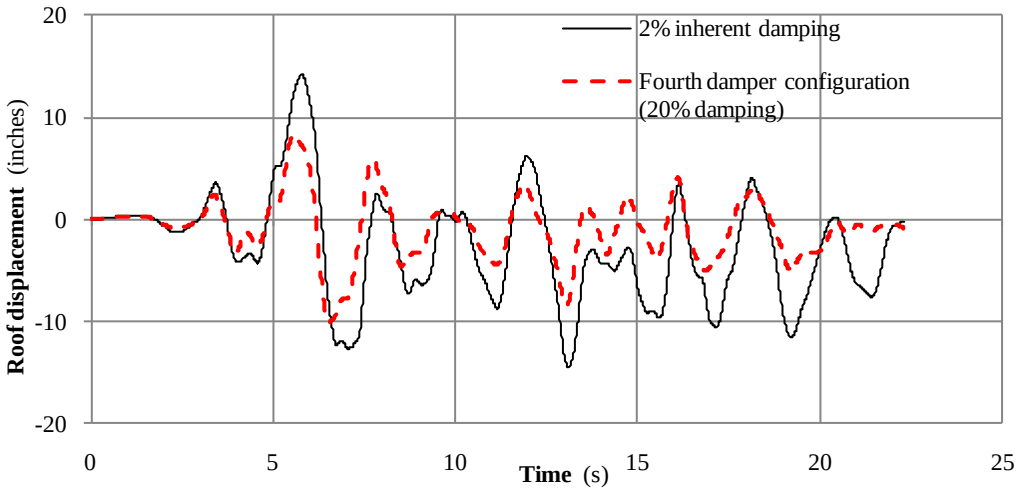

Figure 4.2-56 Roof displacement response histories with added damping (20% total) and inherent damping (2%) for Ground Motion B90

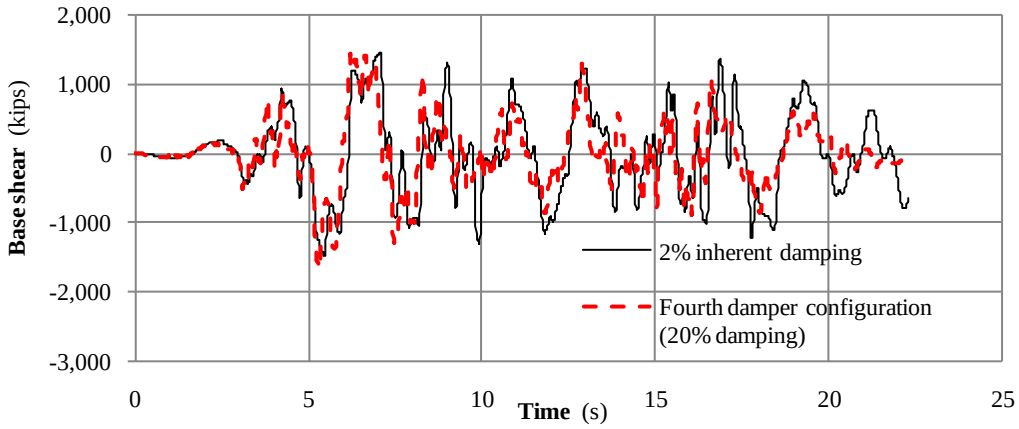

Figure 4.2-57 Inertial base shear response histories with added damping (20% total) and inherent damping (2%) for Ground Motion B90

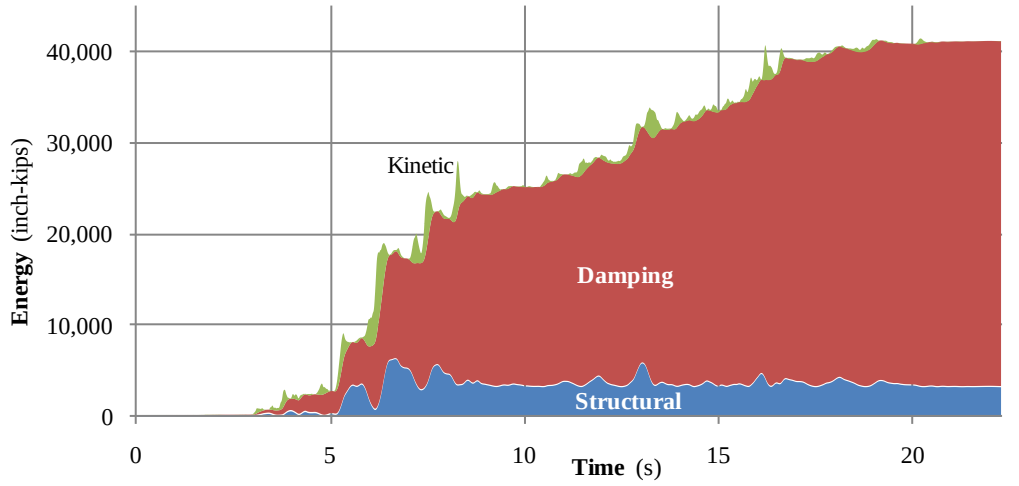

Figure 4.2-58 Energy response history with added damping of fourth configuration (20% total damping) for Ground Motion B90

4.2.7 Summary and Conclusions

In this example, five different analytical approaches are used to estimate the deformation demands in a simple structural steel moment-resisting frame structure:

1. Linear static analysis (the equivalent lateral force method)
2. Plastic strength analysis (using virtual work)
3. Nonlinear static (pushover) analysis
4. Linear dynamic (modal response history) analysis

5. Nonlinear dynamic (response history) analysis

The nonlinear structural model includes careful representation of possible inelastic behavior in the panel-zone regions of the beam-column joints.

The results obtained from the three different analytical approaches 1, 3 and 5 are quite dissimilar. Except for preliminary design, the ELF approach should not be used in explicit performance evaluation since it cannot reflect the location and extent of yielding in the structure. Due to higher mode effects, pushover analysis, where used alone, is inadequate.

This leaves nonlinear response history analysis as the most viable approach. Given the speed and memory capacity of personal computers, nonlinear response history analysis is increasingly common in the seismic analysis of buildings. However, significant shortcomings, limitations and uncertainties in response history analysis still exist.

Among the most pressing problems is the need for a suitable suite of ground motions. All ground motions must adequately reflect site conditions and where applicable, the suite must include near-field effects. Through future research and the efforts of code writing bodies, it may be possible to develop standard suites of ground motions that could be published together with selection tools and scaling methodologies. The scaling techniques currently recommended in the ***Standard*** are a start but need improvement.

Systematic methods need to be developed for identifying uncertainties in the modeling of the structure and for quantifying the effect of such uncertainties on the response. While probabilistic methods for dealing with such uncertainties seem like a natural extension of the analytical approach, the authors believe that deterministic methods should not be abandoned entirely.

In the context of performance-based design, improved methods for assessing the effect of inelastic response and acceptance criteria based on such measures need to be developed. Methods based on explicit quantification of damage should be considered seriously.

The ideas presented above certainly are not original. They have been presented by many academics and practicing engineers. What is still lacking is a comprehensive approach to seismic-resistant design based on these principles.

5

Foundation Analysis and Design

Michael Valley, S.E.

Contents

5.1 SHALLOW FOUNDATIONS FOR A SEVEN-STORY OFFICE BUILDING, LOS ANGELES, CALIFORNIA....3
5.1.1 Basic Information....3
5.1.2 Design for Gravity Loads....8
5.1.3 Design for Moment-Resisting Frame System....11
5.1.4 Design for Concentrically Braced Frame System....16
5.1.5 Cost Comparison....24
5.2 DEEP FOUNDATIONS FOR A 12-STORY BUILDING, SEISMIC DESIGN CATEGORY D....25
5.2.1 Basic Information....25
5.2.2 Pile Analysis, Design and Detailing....33
5.2.3 Other Considerations....47

This chapter illustrates application of the 2009 Edition of the *NEHRP Recommended Provisions* to the design of foundation elements. Example 5.1 completes the analysis and design of shallow foundations for two of the alternative framing arrangements considered for the building featured in Example 6.2. Example 5.2 illustrates the analysis and design of deep foundations for a building similar to the one highlighted in Chapter 7 of this volume of design examples. In both cases, only those portions of the designs necessary to illustrate specific points are included.

The force-displacement response of soil to loading is highly nonlinear and strongly time dependent. Control of settlement is generally the most important aspect of soil response to gravity loads. However, the strength of the soil may control foundation design where large amplitude transient loads, such as those occurring during an earthquake, are anticipated.

Foundation elements are most commonly constructed of reinforced concrete. As compared to design of concrete elements that form the superstructure of a building, additional consideration must be given to concrete foundation elements due to permanent exposure to potentially deleterious materials, less precise construction tolerances and even the possibility of unintentional mixing with soil.

Although the application of advanced analysis techniques to foundation design is becoming increasingly common (and is illustrated in this chapter), analysis should not be the primary focus of foundation design. Good foundation design for seismic resistance requires familiarity with basic soil behavior and common geotechnical parameters, the ability to proportion concrete elements correctly, an understanding of how such elements should be detailed to produce ductile response and careful attention to practical considerations of construction.

In addition to the *Standard* and the *Provisions* and *Commentary*, the following documents are either referenced directly or provide useful information for the analysis and design of foundations for seismic resistance:

ACI 318	American Concrete Institute. 2008. *Building Code Requirements and Commentary for Structural Concrete*.
Bowles	Bowles, J. E. 1988. *Foundation Analysis and Design*. McGraw-Hill.
CRSI	Concrete Reinforcing Steel Institute. 2008. *CRSI Design Handbook*. Concrete Reinforcing Steel Institute.
ASCE 41	ASCE. 2006. *Seismic Rehabilitation of Existing Buildings.*
Kramer	Kramer, S. L. 1996. *Geotechnical Earthquake Engineering*. Prentice Hall.
LPILE	Reese, L. C. and S. T. Wang. 2009. *Technical Manual for LPILE Plus 5.0 for Windows*. Ensoft.
Rollins et al. (a)	Rollins, K. M., Olsen, R. J., Egbert, J. J., Jensen, D. H., Olsen, K. G.and Garrett, B. H. (2006). "Pile Spacing Effects on Lateral Pile Group Behavior: Load Tests." *Journal of Geotechnical and Geoenvironmental Engineering*, ASCE, Vol. 132, No. 10, p. 1262-1271.
Rollins et al. (b)	Rollins, K. M., Olsen, K. G., Jensen, D. H, Garrett, B. H., Olsen, R. J.and Egbert, J. J. (2006). "Pile Spacing Effects on Lateral Pile Group Behavior: Analysis."

Journal of Geotechnical and Geoenvironmental Engineering, ASCE, Vol. 132, No. 10, p. 1272-1283.

Wang & Salmon — Wang, C.-K. and C. G. Salmon. 1992. *Reinforced Concrete Design* . HarperCollins.

Several commercially available programs were used to perform the calculations described in this chapter. SAP2000 is used to determine the shears and moments in a concrete mat foundation; LPILE, in the analysis of laterally loaded single piles; and spColumn, to determine concrete pile section capacities.

5.1 SHALLOW FOUNDATIONS FOR A SEVEN-STORY OFFICE BUILDING, LOS ANGELES, CALIFORNIA

This example features the analysis and design of shallow foundations for two of the three framing arrangements for the seven-story steel office building described in Section 6.2 of this volume of design examples. Refer to that example for more detailed building information and for the design of the superstructure.

5.1.1 Basic Information

5.1.1.1 Description. The framing plan in Figure 5.1-1 shows the gravity load-resisting system for a representative level of the building. The site soils, consisting of medium dense sands, are suitable for shallow foundations. Table 5.1-1 shows the design parameters provided by a geotechnical consultant. Note the distinction made between *bearing pressure* and *bearing capacity*. If the long-term, service-level loads applied to foundations do not exceed the noted bearing pressure, differential and total settlements are expected to be within acceptable limits. Settlements are more pronounced where large areas are loaded, so the bearing pressure limits are a function of the size of the loaded area. The values identified as bearing capacity are related to gross failure of the soil mass in the vicinity of loading. Where loads are applied over smaller areas, punching into the soil is more likely.

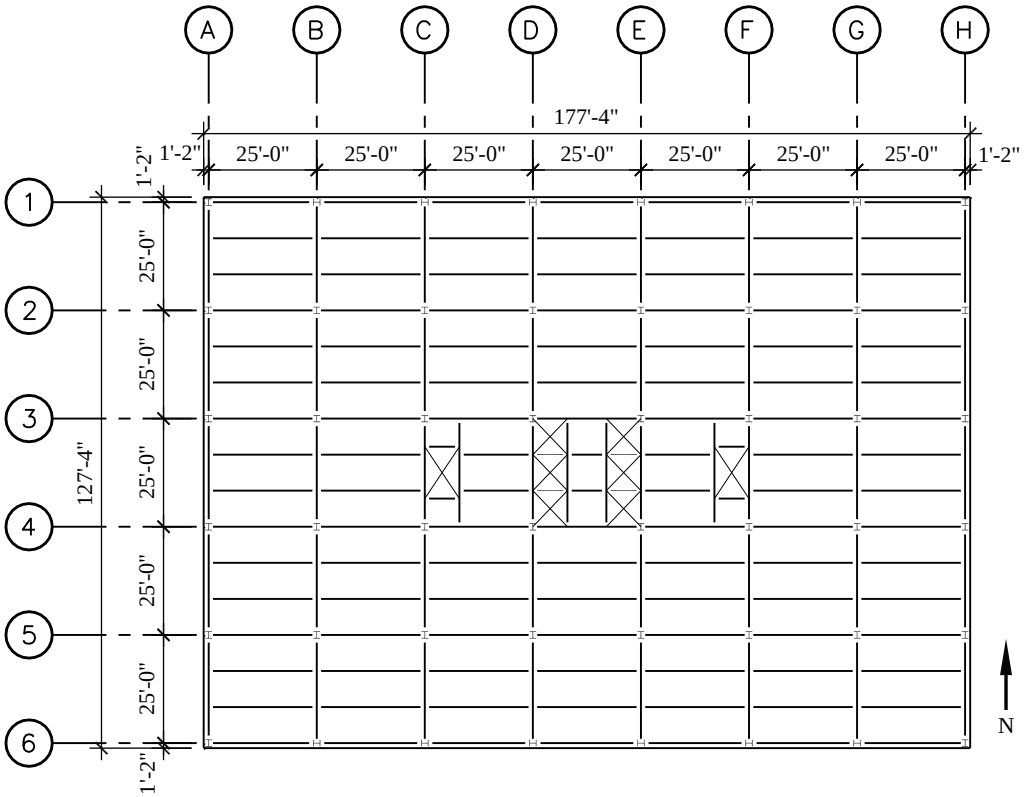

Figure 5.1-1 Typical framing plan

Because bearing capacities are generally expressed as a function of the minimum dimension of the loaded area and are applied as limits on the maximum pressure, foundations with significantly non-square loaded areas (tending toward strip footings) and those with significant differences between average pressure and maximum pressure (as for eccentrically loaded footings) have higher calculated bearing capacities. The recommended values are consistent with these expectations.

Table 5.1-1 Geotechnical Parameters

Parameter	Value
Basic soil properties	Medium dense sand (SPT) N = 20 γ = 125 pcf Angle of internal friction = 33 degrees

Table 5.1-1 Geotechnical Parameters

Parameter	Value
Net bearing pressure (to control settlement due to sustained loads)	≤ 4,000 psf for $B \leq 20$ feet ≤ 2,000 psf for $B \geq 40$ feet (may interpolate for intermediate dimensions)
Bearing capacity (for plastic equilibrium strength checks with factored loads)	2,000B psf for concentrically loaded square footings 3,000B' psf for eccentrically loaded footings where B and B' are in feet, B is the footing width and B' is an average width for the compressed area. Resistance factor, $\phi = 0.7$ [This ϕ factor for cohesionless soil is specified in *Provisions* Part 3 Resource Paper 4; the value is set at 0.7 for vertical, lateral and rocking resistance.]
Lateral properties	Earth pressure coefficients: ▪ Active, $K_A = 0.3$ ▪ At-rest, $K_0 = 0.46$ ▪ Passive, $K_P = 3.3$ "Ultimate" friction coefficient at base of footing = 0.65 Resistance factor, $\phi = 0.7$

The structural material properties assumed for this example are as follows:

- f'_c = 4,000 psi
- f_y = 60,000 psi

5.1.1.2 Seismic Parameters. The complete set of parameters used in applying the *Provisions* to design of the superstructure is described in Section 6.2.2.1 of this volume of design examples. The following parameters, which are used during foundation design, are duplicated here.

- Site Class = D
- S_{DS} = 1.0
- Seismic Design Category = D

5.1.1.3 Design Approach.

5.1.1.3.1 Selecting Footing Size and Reinforcement. Most foundation failures are related to excessive movement rather than loss of load-carrying capacity. In recognition of this fact, settlement control should be the first issue addressed. Once service loads have been calculated, foundation plan dimensions should be selected to limit bearing pressures to those that are expected to provide adequate settlement performance. Maintaining a reasonably consistent level of service load-bearing pressures for all of the individual footings is encouraged since it will tend to reduce differential settlements, which are usually of more concern than are total settlements.

Once a preliminary footing size that satisfies serviceability criteria has been selected, bearing capacity can be checked. It would be rare for bearing capacity to govern the size of footings subjected to sustained loads. However, where large transient loads are anticipated, consideration of bearing capacity may become important.

The thickness of footings is selected for ease of construction and to provide adequate shear capacity for the concrete section. The common design approach is to increase footing thickness as necessary to avoid the need for shear reinforcement, which is uncommon in shallow foundations.

Design requirements for concrete footings are found in Chapters 15 and 21 of ACI 318. Chapter 15 provides direction for the calculation of demands and includes detailing requirements. Section capacities are calculated in accordance with Chapters 10 (for flexure) and 11 (for shear). Figure 5.1-2 illustrates the critical sections (dashed lines) and areas (hatched) over which loads are tributary to the critical sections. For elements that are very thick with respect to the plan dimensions (as at pile caps), these critical section definitions become less meaningful and other approaches (such as strut-and-tie modeling) should be employed. Chapter 21 provides the minimum requirements for concrete foundations in Seismic Design Categories D, E and F, which are similar to those provided in prior editions of the *Provisions*.

For shallow foundations, reinforcement is designed to satisfy flexural demands. ACI 318 Section 15.4 defines how flexural reinforcement is to be distributed for footings of various shapes.

Section 10.5 of ACI 318 prescribes the minimum reinforcement for flexural members where tensile reinforcement is required by analysis. Provision of the minimum reinforcement assures that the strength of the cracked section is not less than that of the corresponding unreinforced concrete section, thus preventing sudden, brittle failures. Less reinforcement may be used as long as "the area of tensile reinforcement provided is at least one-third greater than that required by analysis." Section 10.5.4 relaxes the minimum reinforcement requirement for footings of uniform thickness. Such elements need only satisfy the shrinkage reinforcement requirements of Section 7.12. Section 10.5.4 also imposes limits on the maximum spacing of bars.

5.1.1.3.2 Additional Considerations for Eccentric Loads. The design of eccentrically loaded footings follows the approach outlined above with one significant addition: consideration of overturning stability. Stability calculations are sensitive to the characterization of soil behavior. For sustained eccentric loads, a linear distribution of elastic soil stresses is generally assumed and uplift is usually avoided. If the structure is expected to remain elastic when subjected to short-term eccentric loads (as for wind loading), uplift over a portion of the footing is acceptable to most designers. Where foundations will be subjected to short-term loads and inelastic response is acceptable (as for earthquake loading), plastic soil stresses may be considered. It is most common to consider stability effects on the basis of statically applied loads even where the loading is actually dynamic; that approach simplifies the calculations at the expense of increased conservatism. Figure 5.1-3 illustrates the distribution of soil stresses for the various assumptions. Most textbooks on foundation design provide simple equations to describe the conditions

shown in Parts b, c and d of the figure; finite element models of those conditions are easy to develop. Simple hand calculations can be performed for the case shown in Part f. Practical consideration of the case shown in Part e would require modeling with inelastic elements, but that offers no advantage over direct consideration of the plastic limit. (All of the discussion in this section focuses on the common case in which foundation elements may be assumed to be rigid with respect to the supporting soil. For the interested reader, Chapter 4 of ASCE 41 provides a useful discussion of foundation compliance, rocking and other advanced considerations.)

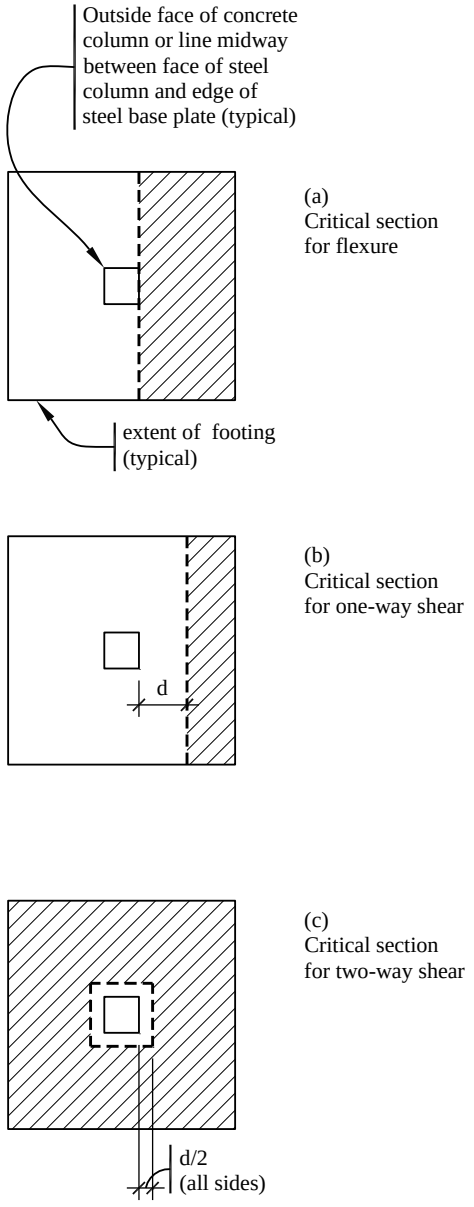

Figure 5.1-2 Critical sections for isolated footings

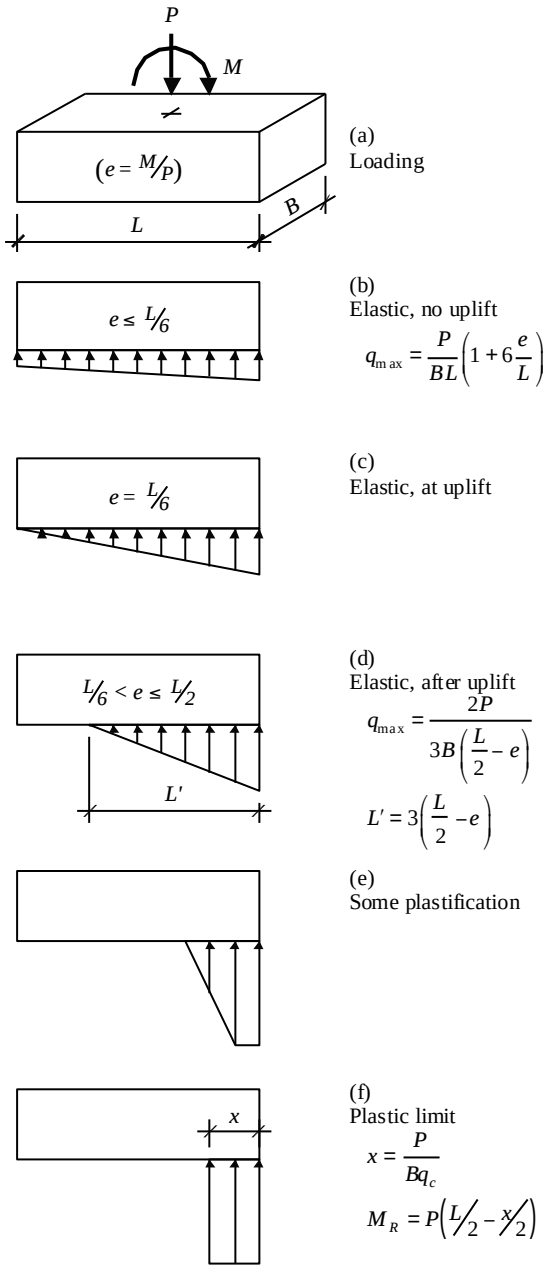

Figure 5.1-3 Soil pressure distributions

5.1.2 Design for Gravity Loads

Although most of the examples in this volume do not provide detailed design for gravity loads, it is provided in this section for two reasons. First, most of the calculation procedures used in designing shallow foundations for seismic loads are identical to those used for gravity design. Second, a complete gravity design is needed to make the cost comparisons shown in Section 5.1.5 below meaningful.

Detailed calculations are shown for a typical interior footing. The results for all three footing types are summarized in Section 5.1.2.5.

5.1.2.1 Demands. Dead and live load reactions are determined as part of the three-dimensional analysis described in Section 6.2 of this volume of design examples. Although there are slight variations in the calculated reactions, the foundations are lumped into three groups (interior, perimeter and corner) for gravity load design and the maximum computed reactions are applied to all members of the group, as follows:

- Interior: D = 387 kips
L = 98 kips
- Perimeter: D = 206 kips
L = 45 kips
- Corner: D = 104 kips
L = 23 kips

The service load combination for consideration of settlement is $D + L$. Considering the load combinations for strength design defined in Section 2.3.2 of the *Standard*, the controlling gravity load combination is $1.2D + 1.6L$.

5.1.2.2 Footing Size. The preliminary size of the footing is determined considering settlement. The service load on a typical interior footing is calculated as:

$P = D + L$ = 387 kips + 98 kips = 485 kips

Since the footing dimensions will be less than 20 feet, the allowable bearing pressure (see Table 5.1-1) is 4,000 psf. Therefore, the required footing area is 487,000 lb/4,000 psf = 121.25 ft^2.

Check a footing that is 11'-0" by 11'-0":

P_{allow} = 11 ft(11 ft)(4,000 psf) = 484,000 lb = 484 kips ≈ 485 kips (demand) OK

The strength demand is:

P_u = 1.2(387 kips) + 1.6(98 kips) = 621 kips

As indicated in Table 5.1-1, the bearing capacity (q_c) is 2,000B = 2,000 × 11 = 22,000 psf = 22 ksf.

The design capacity for the foundation is:

$\phi P_n = \phi q_c B^2$ = 0.7(22 ksf)(11 ft)^2 = 1,863 kips > 621 kips OK

For use in subsequent calculations, the factored bearing pressure q_u = 621 kips/(11 ft)^2 = 5.13 ksf.

5.1.2.3 Footing Thickness. Once the plan dimensions of the footing are selected, the thickness is determined such that the section satisfies the one-way and two-way shear demands without the addition of shear reinforcement. Demands are calculated at critical sections, shown in Figure 5.1-2, which depend on the footing thickness.

Check a footing that is 26 inches thick:

For the W14 columns used in this building, the side dimensions of the loaded area (taken halfway between the face of the column and the edge of the base plate) are approximately 16 inches. Accounting for cover and expected bar sizes, d = 26 - (3 + 1.5(1)) = 21.5 in.

One-way shear:

$$V_u = 11\left(\frac{11-\frac{16}{12}}{2}-\frac{21.5}{12}\right)(5.13) = 172 \text{ kips}$$

$$\phi V_n = \phi V_c = (0.75)2\sqrt{4{,}000}\,(11\times 12)(21.5)\left(\tfrac{1}{1{,}000}\right) = 269 \text{ kips} > 172 \text{ kips} \quad \text{OK}$$

Two-way shear:

$$V_u = 621-\left(\tfrac{16+21.5}{12}\right)^2(5.13) = 571 \text{ kips}$$

$$\phi V_n = \phi V_c = (0.75)4\sqrt{4{,}000}\left[4\times(16+21.5)\right](21.5)\left(\tfrac{1}{1{,}000}\right) = 612 \text{ kips} > 571 \text{ kips} \quad \text{OK}$$

5.1.2.4 Footing Reinforcement. Footing reinforcement is selected considering both flexural demands and minimum reinforcement requirements. The following calculations treat flexure first because it usually controls:

$$M_u = \frac{1}{2}(11)\left(\frac{11-\frac{16}{12}}{2}\right)^2(5.13) = 659 \text{ ft-kips}$$

Try nine #8 bars each way. The distance from the extreme compression fiber to the center of the top layer of reinforcement, $d = t$ - cover - $1.5d_b$ = 26 - 3 - 1.5(1) = 21.5 in.

$T = A_s f_y$ = 9(0.79)(60) = 427 kips

Noting that $C = T$ and solving the expression $C = 0.85\, f'_c\, b\, a$ for a produces a = 0.951 in.

$$\phi M_n = \phi T\left(d-\tfrac{a}{2}\right) = 0.90(427)\left(21.5-\tfrac{0.951}{2}\right)\left(\tfrac{1}{12}\right) = 673 \text{ ft-kips} > 659 \text{ ft-kips} \quad \text{OK}$$

The ratio of reinforcement provided is ρ = 9(0.79)/[(11)(12)(26)] = 0.00207. The distance between bars spaced uniformly across the width of the footing is s = [(11)(12)-2(3+0.5)]/(9-1) = 15.6 in.

According to ACI 318 Section 7.12, the minimum reinforcement ratio = 0.0018 < 0.00207 OK

and the maximum spacing is the lesser of 5 × 26 in. and 18 = 18 in. > 15.6 in. OK

5.1.2.5 Design Results. The calculations performed in Sections 5.1.2.2 through 5.1.2.4 are repeated for typical perimeter and corner footings. The footing design for gravity loads is summarized in Table 5.1-2; Figure 5.1-4 depicts the resulting foundation plan.

Table 5.1-2 Footing Design for Gravity Loads

Location	Loads	Footing Size and Reinforcement; Soil Capacity	Critical Section Demands and Design Strengths	
Interior	D = 387 kip L = 98 kip	11'-0" × 11'-0" × 2'-2" deep 9-#8 bars each way	One-way shear: Two-way shear:	V_u = 172 kip ϕV_n = 269 kip V_u = 571 kip ϕV_n = 612 kip
	P = 485 kip P_u = 621 kip	P_{allow} = 484 kip ϕP_n = 1863 kip	Flexure:	M_u = 659 ft-kip ϕM_n = 673 ft-kip
Perimeter	D = 206 kip L = 45 kip	8'-0" × 8'-0" × 1'-6" deep 9-#6 bars each way	One-way shear: Two-way shear:	V_u = 88.1 kip ϕV_n = 123 kip V_u = 289 kip ϕV_n = 302 kip
	P = 251 kip P_u = 319 kip	P_{allow} = 256 kip ϕP_n = 716 kip	Flexure:	M_u = 222 ft-kip ϕM_n = 234 ft-kip
Corner	D = 104 kip L = 23 kip	6'-0" × 6'-0" × 1'-2" deep 6-#5 bars each way	One-way shear: Two-way shear:	V_u = 41.5 kip ϕV_n = 64.9 kip V_u = 141 kip ϕV_n = 184 kip
	P = 127 kip P_u = 162 kip	P_{allow} = 144 kip ϕP_n = 302 kip	Flexure:	M_u = 73.3 ft-kip ϕM_n = 75.2 ft-kip

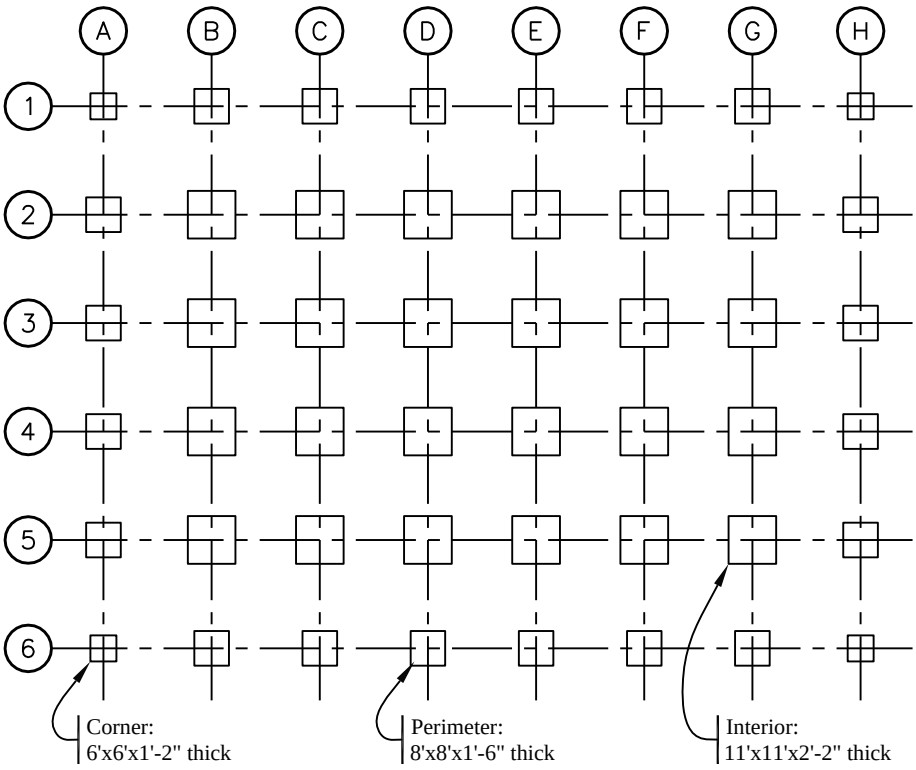

Figure 5.1-4 Foundation plan

5.1.3 Design for Moment-Resisting Frame System

Framing Alternate A in Section 6.2 of this volume of design examples includes a perimeter moment-resisting frame as the seismic force-resisting system. A framing plan for the system is shown in Figure 5.1-5. Detailed calculations are provided in this section for a combined footing at the corner and focus on overturning and sliding checks for the eccentrically loaded footing; settlement checks and design of concrete sections would be similar to the calculations shown in Section 5.1.2. The results for all footing types are summarized in Section 5.1.3.4.

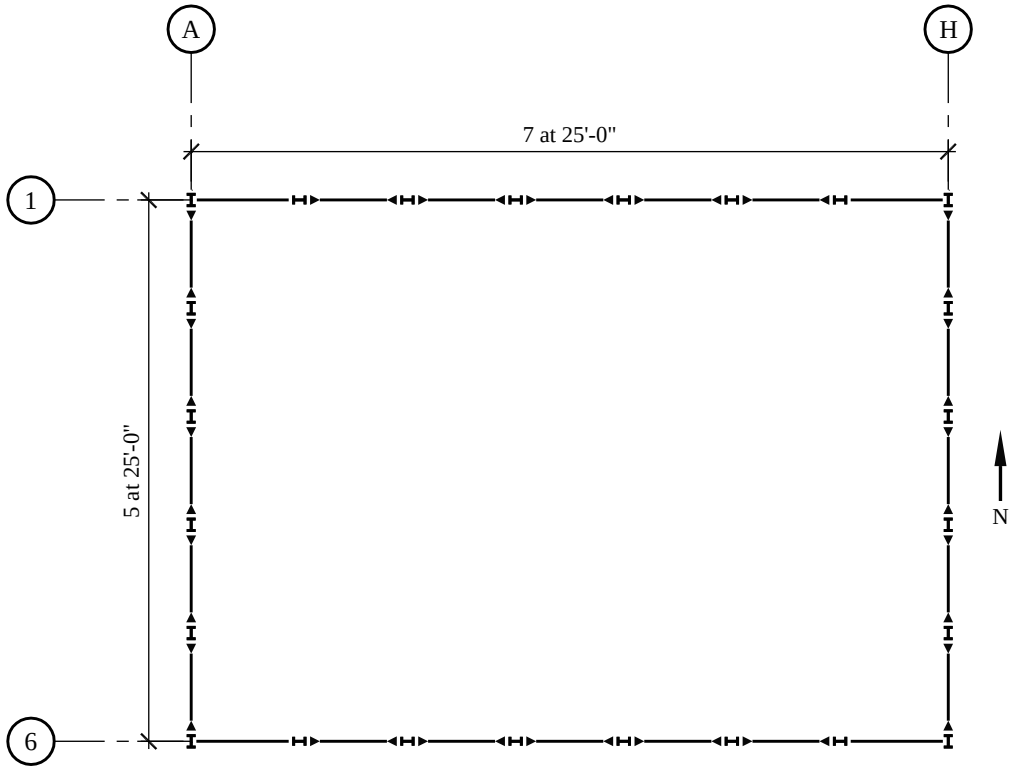

Figure 5.1-5 Framing plan for moment-resisting frame system

5.1.3.1 Demands. A three-dimensional analysis of the superstructure, in accordance with the requirements for the equivalent lateral force (ELF) procedure, is performed using the ETABS program. Foundation reactions at selected grids are reported in Table 5.1-3.

Table 5.1-3 Demands from Moment-Resisting Frame System

Location	Load	*Fx*	*Fy*	*Fz*	*Mxx*	*Myy*
A-5	*D*			-203.8		
	L			-43.8		
	Ex	-13.8	4.6	3.8	53.6	-243.1
	Ey	0.5	-85.1	-21.3	-1011.5	8.1
A-6	*D*			-103.5		
	L			-22.3		
	Ex	-14.1	3.7	51.8	47.7	-246.9
	Ey	0.8	-68.2	281.0	-891.0	13.4

Note: Units are kips and feet. Load *Ex* is for loads applied toward the east, including appropriately amplified counter-clockwise accidental torsion. Load *Ey* is for loads applied toward the north, including appropriately amplified clockwise accidental torsion.

Section 6.2.3.5 of this volume of design examples outlines the design load combinations, which include the redundancy factor as appropriate. A large number of load cases result from considering two senses of accidental torsion for loading in each direction and including orthogonal effects . The detailed calculations presented here are limited to two primary conditions, both for a combined foundation for columns at Grids A-5 and A-6: the downward case (1.4*D* + 0.5*L* + 0.3*Ex* + 1.0*Ey*) and the upward case (0.7*D* + 0.3*Ex* + 1.0*Ey*).

Before loads can be computed, attention must be given to ***Standard*** Section 12.13.4. That Section states that "overturning effects at the soil-foundation interface are permitted to be reduced by 25 percent" where the ELF procedure is used and by 10 percent where modal response spectrum analysis is used. Because the overturning effect in question relates to the global overturning moment for the *system*, judgment must be used in determining which design actions may be reduced. If the seismic force-resisting system consists of isolated shear walls, the shear wall overturning moment at the base best fits that description. For a perimeter moment-resisting frame, most of the global overturning resistance is related to axial loads in columns. Therefore, in this example column axial loads (*Fz*) from load cases *Ex* and *Ey* are multiplied by 0.75 and all other load effects remain unreduced.

5.1.3.2 Downward Case (1.4*D* + 0.5*L* + 0.3*Ex* + 1.0*Ey*). In order to perform the overturning checks, a footing size must be assumed. Preliminary checks (not shown here) confirmed that isolated footings under single columns were untenable. Check overturning for a footing that is 9 feet wide by 40 feet long by 5 feet thick. Furthermore, assume that the top of the footing is 2 feet below grade (the overlying soil contributes to the resisting moment). (In these calculations the $0.2S_{DS}D$ modifier for vertical accelerations is used for the dead loads ***applied to*** the foundation but not for the weight of the foundation and soil. This is the author's interpretation of the ***Standard***. The footing and soil overburden are not subject to the same potential for dynamic amplification as the dead load of the superstructure and it is not common practice to include the vertical acceleration on the weight of the footing and the overburden. Furthermore, for footings that resist significant overturning, this issue makes a significant difference in design.) Combining the loads from columns at Grids A-5 and A-6 and including the weight of the foundation and overlying soil produces the following loads at the foundation-soil interface:

P = applied loads + weight of foundation and soil
= 1.4(-203.8 - 103.5) + 0.5(-43.8 - 22.3) +0.75[0.3(3.8 + 51.8) + 1.0(-21.3 + 281)]
- 1.2[9(40)(5)(0.15) + 9(40)(2)(0.125)]
= -688 kips.

M_{xx} = direct moments + moment due to eccentricity of applied axial loads
= 0.3(53.6 + 47.7) + 1.0(-1011.5 - 891.0)
+ [1.4(-203.8) + 0.5(-43.8) + 0.75(0.3)(3.8) + 0.75(1.0)(-21.3)](12.5)
+ [1.4(-103.5) + 0.5(-22.3) + 0.75(0.3)(51.8) + 0.75(1.0)(281)](-12.5)
= -6,717 ft-kips.

M_{yy} = 0.3(-243.1 - 246.9) + 1.0(8.1 + 13.4)
= -126 ft-kips. (The resulting eccentricity is small enough to neglect here, which simplifies the problem considerably.)

V_x = 0.3(-13.8 - 14.1) + 1.0(0.5 + 0.8)
= -7.11 kips.

V_y = 0.3(4.6 + 3.7) + 1.0(-85.1 -68.2)
= -149.2 kips.

Note that the above load combination does not yield the maximum downward load. Reversing the direction of the seismic load results in P = -1,103 kips and M_{xx} = 2,964 ft-kips. This larger axial load does not control the design because the moment is so much less that the resultant is within the kern and no uplift occurs.

The following soil calculations use a different sign convention than that in the analysis results noted above; compression is positive for the soil calculations. The eccentricity is as follows:

$e = |M/P| = 6{,}717/688 = 9.76$ ft

Figure 5.1-3 shows the elastic and plastic design conditions and their corresponding equations. Where e is less than $L/2$, a solution to the overturning problem exists; however, as e approaches $L/2$, the bearing pressures increase without bound. Since e is greater than $L/6 = 40/6 = 6.67$ feet, uplift occurs and the maximum bearing pressure is:

$$q_{\max} = \frac{2P}{3B\left(\frac{L}{2} - e\right)} = \frac{2(688)}{3(9)\left(\frac{40}{2} - 9.76\right)} = 4.98 \text{ ksf}$$

and the length of the footing in contact with the soil is:

$$L' = 3\left(\frac{L}{2} - e\right) = 3\left(\frac{40}{2} - 9.76\right) = 30.7 \text{ ft}$$

The bearing capacity $q_c = 3{,}000B' = 3{,}000 \times \min(B, L'/2) = 3{,}000 \times \min(9, 30.7/2) = 27{,}000$ psf = 27 ksf. ($L'/2$ is used as an adjustment to account for the gradient in the bearing pressure in that dimension.)

The design bearing capacity $\phi q_c = 0.7(27 \text{ ksf}) = 18.9 \text{ ksf} > 4.98 \text{ ksf}$ OK

The foundation satisfies overturning and bearing capacity checks. The upward case, which follows, will control the sliding check.

5.1.3.3 Upward Case (0.7*D* + 0.3*Ex* + 1.0*Ey*). For the upward case the loads are:

P = -332 kips

M_{xx} = -5,712 ft-kips

M_{yy} = -126 ft-kips (negligible)

V_x = -7.1 kips

V_y = -149 kips

The eccentricity is:

$e = |M/P| = 5{,}712/332 = 17.2$ feet

Again, e is greater than $L/6$, so uplift occurs and the maximum bearing pressure is:

$$q_{max} = \frac{2(332)}{3(10)\left(\frac{40}{2} - 17.2\right)} = 8.82 \text{ ksf}$$

and the length of the footing in contact with the soil is:

$$L' = 3\left(\frac{40}{2} - 17.2\right) = 8.4 \text{ ft}$$

The bearing capacity q_c = 3,000 × min(9, 8.4/2) = 12,500 psf = 12.5 ksf.

The design bearing capacity ϕq_c = 0.7(12.5 ksf) = 8.78 ksf < 8.82 ksf. NG

Using an elastic distribution of soil pressures, the foundation fails the bearing capacity check (although stability is satisfied). Try the plastic distribution. Using this approach, the bearing pressure over the entire contact area is assumed to be equal to the design bearing capacity. In order to satisfy vertical equilibrium, the contact area times the design bearing capacity must equal the applied vertical load P. Because the bearing capacity used in this example is a function of the contact area and the value of P changes with the size, the most convenient calculation is iterative.

By iteration, the length of contact area is L' = 4.19 feet.

The bearing capacity q_c = 3,000 × min(10, 4.19) = 12,570 psf = 12.57 ksf. (No adjustment to L' is needed as the pressure is uniform.)

The design bearing capacity ϕq_c = 0.7(12.6 ksf) = 8.80 ksf.

(8.80)(4.19)(9) = 332 kips = 332 kips, so equilibrium is satisfied.

The resisting moment, $M_R = P\ (L/2\text{-}L'/2)$ = 33 (40/2 - 4.19/2) = 5,944 ft-kip > 5,712 ft-kip. OK

Therefore, using a plastic distribution of soil pressures, the foundation satisfies overturning and bearing capacity checks.

The calculation of demands on concrete sections for strength checks should use the same soil stress distribution as the overturning check. Using a plastic distribution of soil stresses defines the upper limit of static loads for which the foundation remains stable, but the extreme concentration of soil bearing tends to drive up shear and flexural demands on the concrete section. It should be noted that the foundation may remain stable for larger loads if they are applied dynamically; even in that case, the strength demands on the concrete section will not exceed those computed on the basis of the plastic distribution.

For the sliding check, initially consider base traction only. The sliding demand is:

$$V = \sqrt{V_x^2 + V_y^2} = \sqrt{(-7.11)^2 + (-149.2)^2} = 149.4 \text{ kips}$$

As calculated previously, the total compression force at the bottom of the foundation is 332 kips. The design sliding resistance is:

$\phi V_c = \phi \times$ friction coefficient $\times P$ = 0.7(0.65)(332 kips) = 151 kips > 149.4 kips OK

If base traction alone had been insufficient, resistance due to passive pressure on the leading face could be included. Section 5.2.2.2 below illustrates passive pressure calculations for a pile cap.

5.1.3.4 Design Results. The calculations performed in Sections 5.1.3.2 and 5.1.3.3 are repeated for combined footings at middle and side locations. Figure 5.1-6 shows the results.

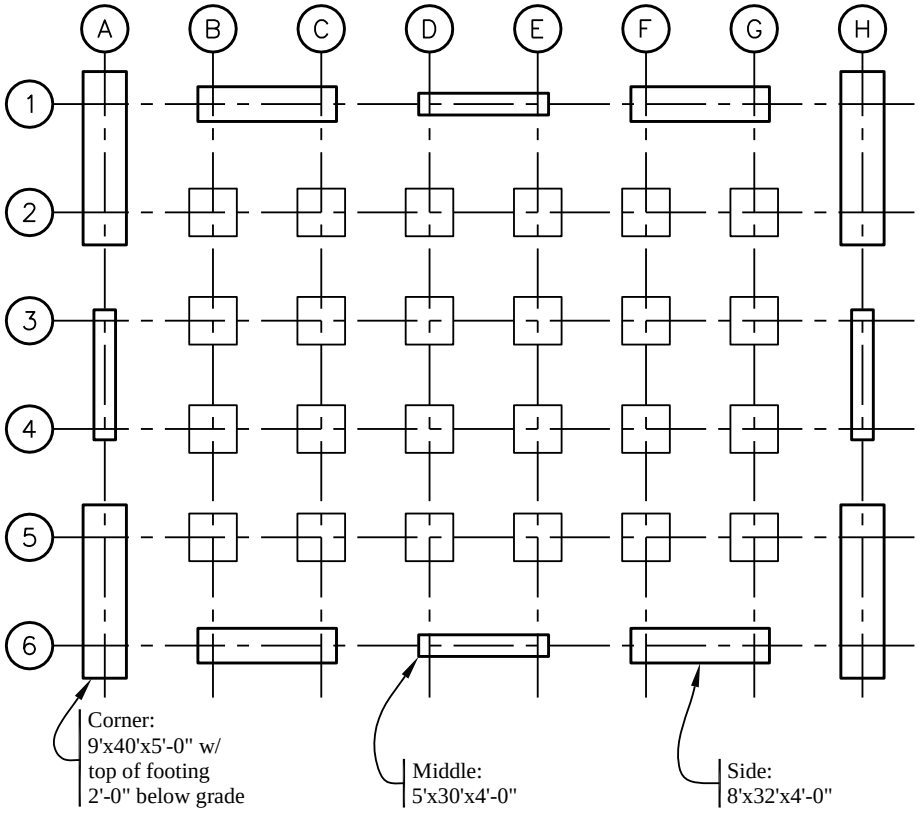

Figure 5.1-6 Foundation plan for moment-resisting frame system

One last check of interest is to compare the flexural stiffness of the footing with that of the steel column, which is needed because the steel frame design was based upon flexural restraint at the base of the columns. Using an effective moment of inertia of 50 percent of the gross moment of inertia and also using the distance between columns as the effective span, the ratio of *EI/L* for the smallest of the combined footings is more than five times the *EI/h* for the steel column. This is satisfactory for the design assumption.

5.1.4 Design for Concentrically Braced Frame System

Framing Alternate B in Section 6.2 of this volume of design examples employs a concentrically braced frame system at a central core to provide resistance to seismic loads. A framing plan for the system is shown in Figure 5.1-7.

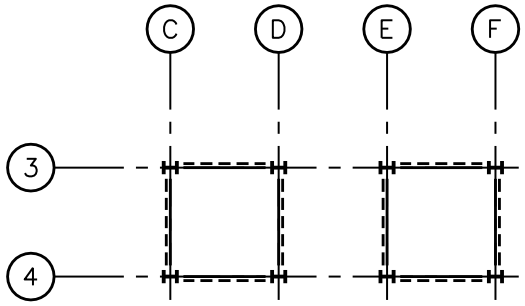

Figure 5.1-7 Framing plan for concentrically braced frame system

5.1.4.1 Check Mat Size for Overturning. Uplift demands at individual columns are so large that the only practical shallow foundation is one that ties together the entire core. The controlling load combination for overturning has minimum vertical loads (which help to resist overturning), primary overturning effects (M_{xx}) due to loads applied parallel to the short side of the core and smaller moments about a perpendicular axis (M_{yy}) due to orthogonal effects. Assume mat dimensions of 45 feet by 95 feet by 7 feet thick, with the top of the mat 3'-6" below grade. Combining the factored loads applied to the mat by all eight columns and including the weight of the foundation and overlying soil produces the following loads at the foundation-soil interface:

- P = -7,849 kips
- M_{xx} = -148,439 ft-kips
- M_{yy} = -42,544 ft-kips
- V_x = -765 kips
- V_y = -2,670 kips

Figure 5.1-8 shows the soil pressures that result from application in this controlling case, depending on the soil distribution assumed. In both cases the computed uplift is significant. In Part a of the figure, the contact area is shaded. The elastic solution shown in Part b was computed by modeling the mat in SAP2000 with compression only soil springs (with the stiffness of edge springs doubled as recommended by Bowles). For the elastic solution, the average width of the contact area is 11.1 feet and the maximum soil pressure is 16.9 ksf.

The bearing capacity q_c = 3,000 × min(95, 11.1/2) = 16,650 psf = 16.7 ksf.

The design bearing capacity ϕq_c = 0.7(16.7 ksf) = 11.7 ksf < 16.9 ksf. NG

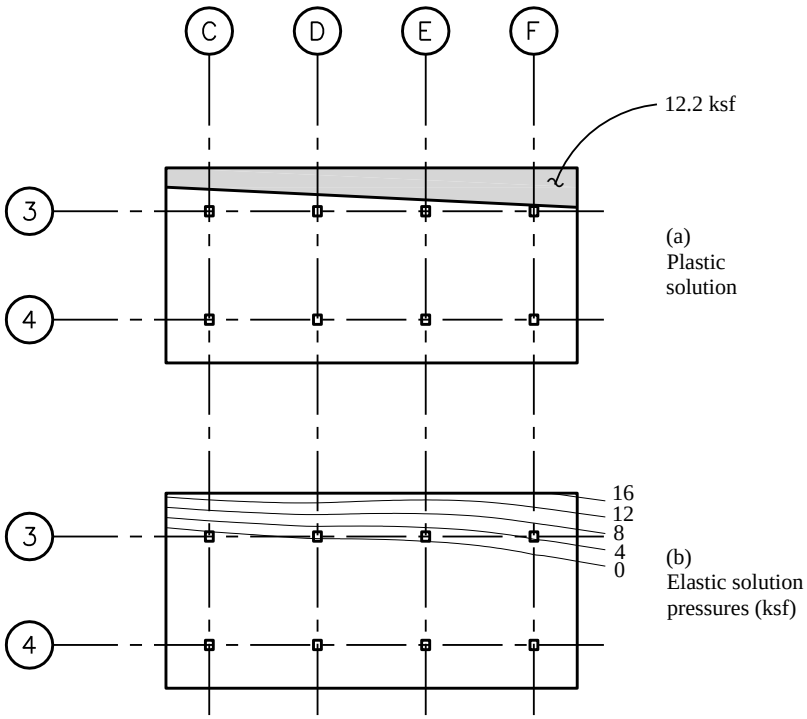

Figure 5.1-8 Soil pressures for controlling bidirectional case

As was done in Section 5.1.3.3 above, try the plastic distribution. The present solution has an additional complication as the off-axis moment is not negligible. The bearing pressure over the entire contact area is assumed to be equal to the design bearing capacity. In order to satisfy vertical equilibrium, the contact area times the design bearing capacity must equal the applied vertical load *P*. The shape of the contact area is determined by satisfying equilibrium for the off-axis moment. Again the calculations are iterative.

Given the above constraints, the contact area shown in Figure 5.1-8 is determined. The length of the contact area is 4.13 feet at the left side and 8.43 feet at the right side. The average contact length, for use in determining the bearing capacity, is (4.13 + 8.43)/2 = 6.27 feet. The distances from the center of the mat to the centroid of the contact area are as follows:

$\bar{x} = 5.42$ ft

$\bar{y} = 19.24$ ft

The bearing capacity is q_c = 3,000 × min(95, 6.27) = 18,810 psf = 18.81 ksf.

The design bearing capacity is ϕq_c = 0.7(18.8 ksf) = 13.2 ksf.

(13.2)(6.27)(95) = 7,863 kips ≈ 7,849 kips, confirming equilibrium for vertical loads.

(7,849)(5.42) = 42,542 ft-kips ≈ 42,544 ft-kips, confirming equilibrium for off-axis moment.

The resisting moment, $M_{R,xx} = P\bar{y} = 7{,}849(19.24) = 151{,}015$ ft-kips > 148,439 ft-kips. OK

So, the checks of stability and bearing capacity are satisfied. The mat dimensions are shown in Figure 5.1-9.

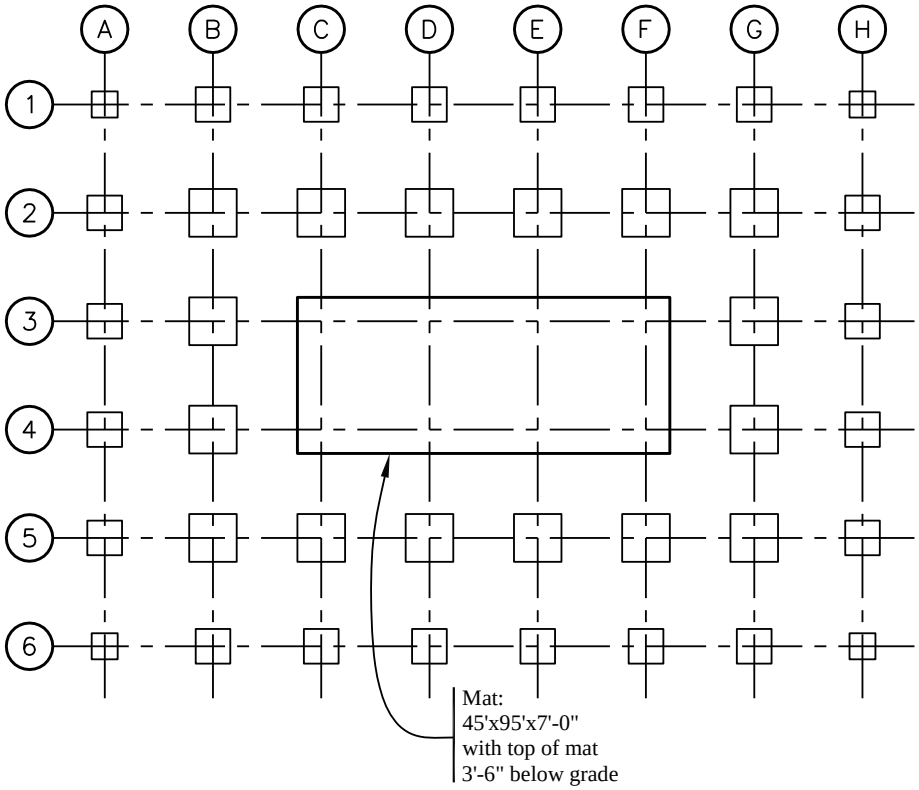

Figure 5.1-9 Foundation plan for concentrically braced frame system

5.1.4.2 Design Mat for Strength Demands. As was previously discussed, the computation of strength demands for the concrete section should use the same soil pressure distribution as was used to satisfy stability and bearing capacity. Because dozens of load combinations were considered and hand calculations were used for the plastic distribution checks, the effort required would be considerable. The same analysis used to determine elastic bearing pressures yields the corresponding section demands directly. One approach to this dilemma would be to compute an additional factor that must be applied to selected elastic cases to produce section demands that are consistent with the plastic solution. Rather than provide such calculations here, design of the concrete section will proceed using the results of the elastic analysis. This is conservative for the demand on the concrete for the same reason that it was unsatisfactory for the soil: the edge soil pressures are high (that is, we are designing the concrete for a peak soil pressure of 16.9 ksf, even though the plastic solution gives 13.2 ksf).

Standard Section 12.13.3 requires consideration of parametric variation for soil properties where foundations are modeled explicitly. This example does not illustrate such calculations.

Concrete mats often have multiple layers of reinforcement in each direction at the top and bottom of their thickness. Use of a uniform spacing for the reinforcement provided in a given direction greatly increases the ease of construction. The minimum reinforcement requirements defined in Section 10.5 of ACI 318 were discussed in Section 5.1.1.3 above. Although all of the reinforcement provided to satisfy

Section 7.12 of ACI 318 may be provided near one face, for thick mats it is best to compute and provide the amount of required reinforcement separately for the top and bottom halves of the section. Using a bar spacing of 10 inches for this 7-foot-thick mat and assuming one or two layers of bars, the section capacities indicated in Table 5.1-4 (presented in order of decreasing strength) may be precomputed for use in design. The amount of reinforcement provided for Marks B, C and D are less than the basic minimum for flexural members, so the demands should not exceed three-quarters of the design strength where those reinforcement patterns are used. The amount of steel provided for Mark D is the minimum that satisfies ACI 318 Section 7.12.

Table 5.1-4 Mat Foundation Section Capacities

Mark	Reinforcement	A_s (in.^{2} per ft)	ϕM_n (ft-kip/ft)	3/4ϕM_n (ft-kip/ft)
A	2 layers of #10 bars at 10 in. o.c.	3.05	1,012	Not used
B	2 layers of #9 bars at 10 in. o.c.	2.40	Not used	601
C	2 layers of #8 bars at 10 in. o.c.	1.90	Not used	477
D	#8 bars at 10 in. o.c.	0.95	Not used	254

Note: Where the area of steel provided is less than the minimum reinforcement for flexural members as indicated in ACI 318 Sec. 10.5.1, demands are compared to 3/4 of ϕM_n as permitted in Sec. 10.5.3.

To facilitate rapid design, the analysis results are processed in two additional ways. First, the flexural and shear demands computed for the various load combinations are enveloped. Then the enveloped results are presented (see Figure 5.1-10) using contours that correspond to the capacities shown for the reinforcement patterns noted in Table 5.1-4.

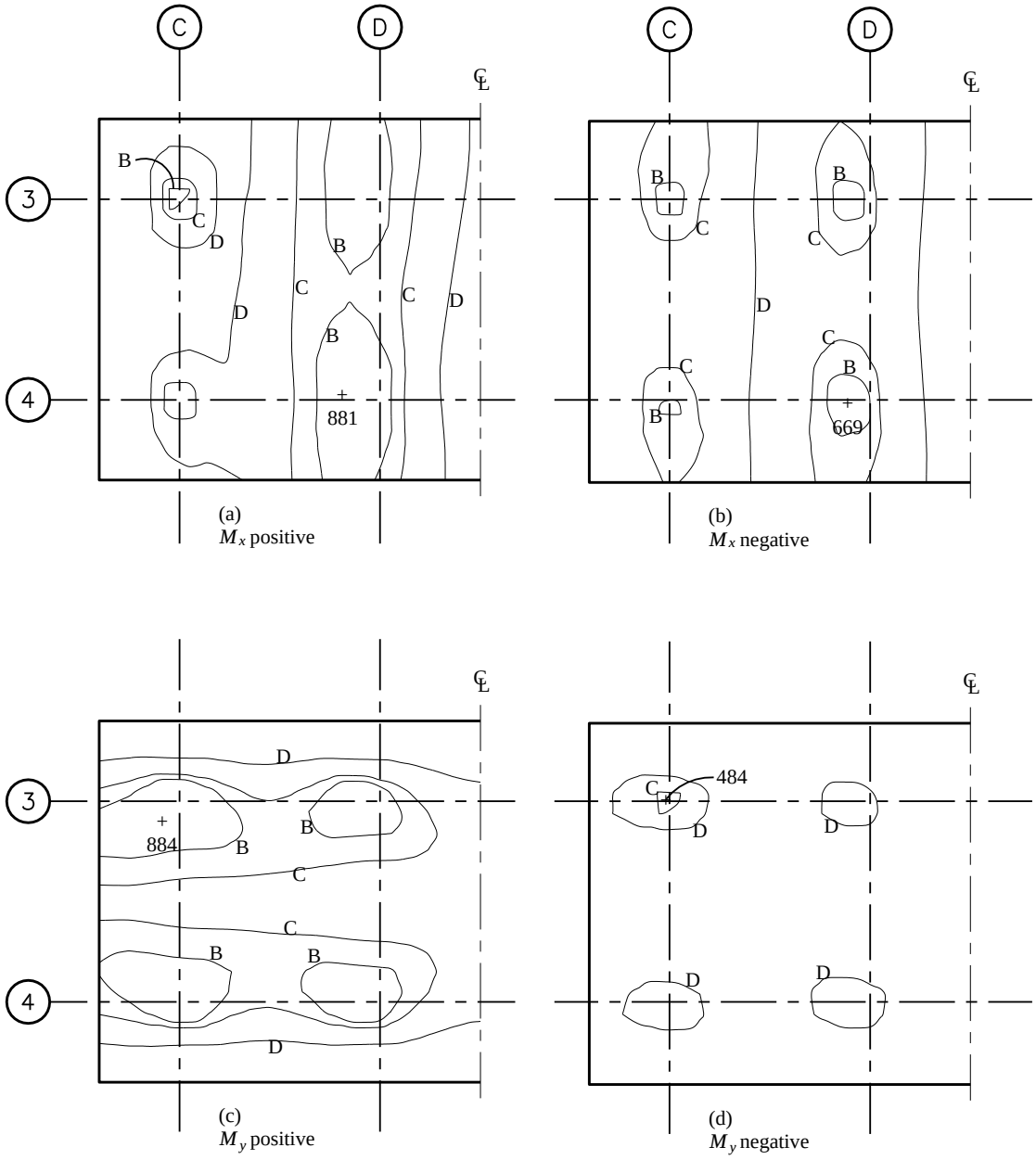

Figure 5.1-10 Envelope of mat foundation flexural demands

Using the noted contours permits direct selection of reinforcement. The reinforcement provided within a contour for a given mark must be that indicated for the next higher mark. For instance, all areas within Contour B must have two layers of #10 bars. Note that the reinforcement provided will be symmetric about the centerline of the mat in both directions. Where the results of finite element analysis are used in the design of reinforced concrete elements, averaging of demands over short areas is appropriate. In Figure 5.1-11, the selected reinforcement is superimposed on the demand contours. Figure 5.1-12 shows a section of the mat along Gridline C.

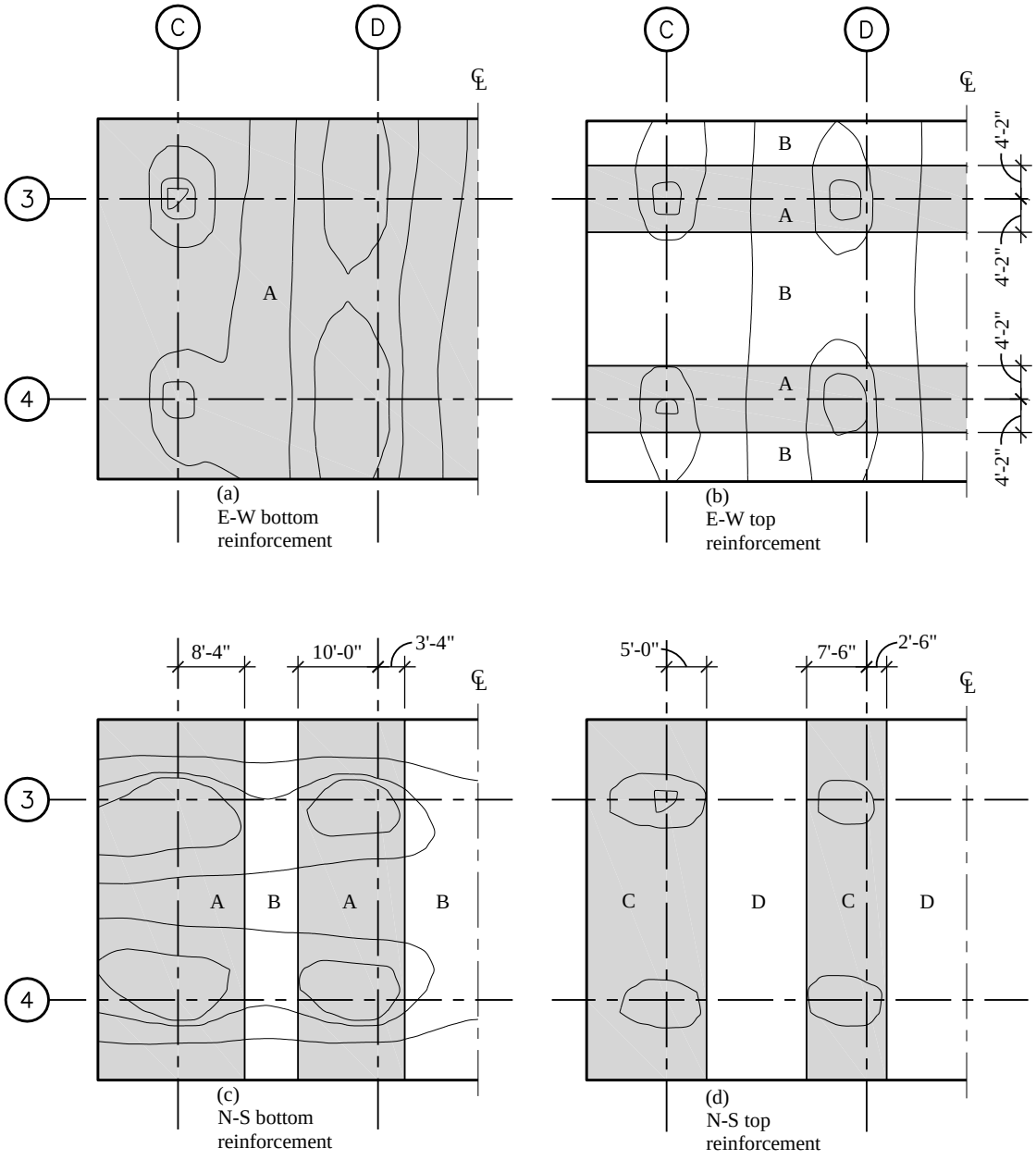

Figure 5.1-11 Mat foundation flexural reinforcement

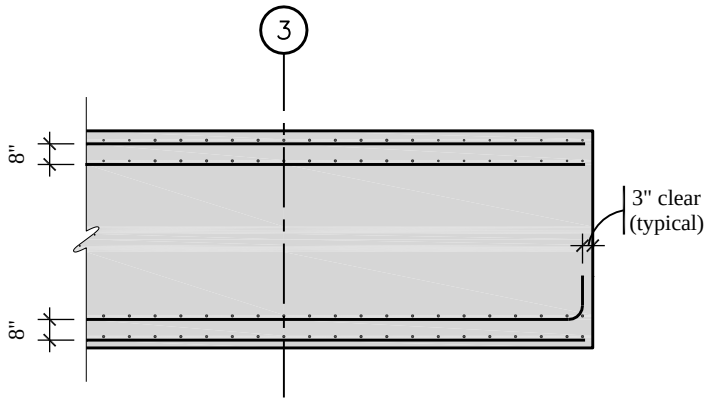

Figure 5.1-12 Section of mat foundation

Figure 5.1-13 presents the envelope of shear demands. The contours used correspond to the design strengths computed assuming $V_s = 0$ for one-way and two-way shear. In the hatched areas the shear stress exceeds $\phi 4\sqrt{f_c'}$ and in the shaded areas it exceeds $\phi 2\sqrt{f_c'}$. The critical sections for two-way shear (as discussed in Section 5.1.1.3) also are shown. The only areas that need more careful attention (to determine whether they require shear reinforcement) are those where the hatched or shaded areas are outside the critical sections. At the columns on Gridline D, the hatched area falls outside the critical section, so closer inspection is needed. Because the perimeter of the hatched area is substantially smaller than the perimeter of the critical section for punching shear, the design requirements of ACI 318 are satisfied.

One-way shears at the edges of the mat exceed the $\phi 2\sqrt{f_c'}$ criterion. Note that the high shear stresses are not produced by loads that create high bearing pressures at the edge. Rather, they are produced by loads that create large bending stresses parallel to the edge. The distribution of bending moments and shears is not uniform across the width (or breadth) of the mat, primarily due to the torsion in the seismic loads and the orthogonal combination. It is also influenced by the doubled spring stiffnesses used to model the soil condition. However, when the shears are averaged over a width equal to the effective depth (d), the demands are less than the design strength.

In this design, reinforcement for punching or beam shear is not required. If shear reinforcement cannot be avoided, standee bars may be used both to chair the upper decks of reinforcement and to provide resistance to shear in which case they may be bent thus: ⩘.

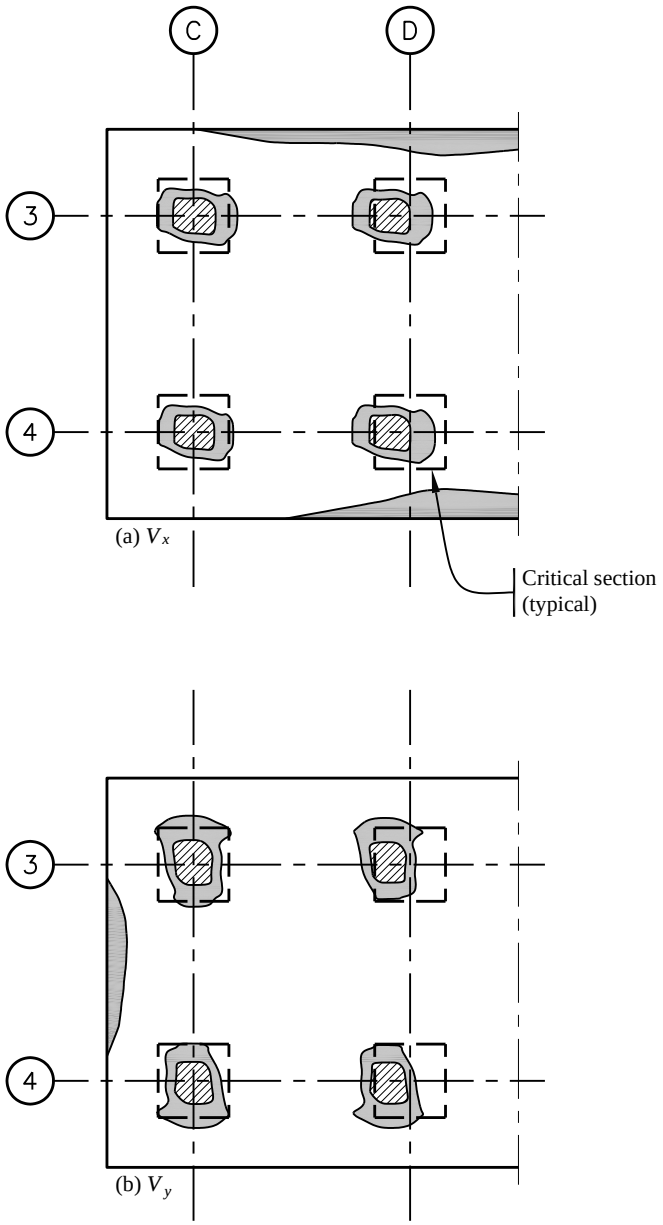

Figure 5.1-13 Critical sections for shear and envelope of mat foundation shear demands

5.1.5 Cost Comparison

Table 5.1-5 provides a summary of the material quantities used for all of the foundations required for the various conditions considered. Corresponding preliminary costs are assigned. The gravity-only condition does not represent a realistic case because design for wind loads would require changes to the foundations; it is provided here for discussion. It is obvious that design for lateral loads adds cost as compared to a design that neglects such loads. However, it is also worth noting that braced frame systems usually have substantially more expensive foundation systems than do moment frame systems. This condition occurs for two reasons. First, braced frame systems are stiffer, which produces shorter periods

and higher design forces. Second, braced frame systems tend to concentrate spatially the demands on the foundations. In this case the added cost amounts to approximately $0.80/ft^2, which is an increase of perhaps 4 or 5 percent to the cost of the structural system.

Table 5.1-5 Summary of Material Quantities and Cost Comparison

Design Condition	Concrete at Gravity Foundations	Concrete at Lateral Foundations	Total Excavation	Total Cost
Gravity only (see Figure 5.1-4)	310 cy at $350/cy = $108,600		310 cy at $30/cy = $9,300	$117,900
Moment frame (see Figure 5.1-6)	233 cy at $350/cy = $81,600	507 cy at $400/cy = $202,900	770 cy at $30/cy = $23,100	$307,600
Braced frame (see Figure 5.1-9)	233 cy at $350/cy = $81,600	1,108 cy at $400/cy = $443,300	1895 cy at $30/cy = $56,800	$581,700

5.2 DEEP FOUNDATIONS FOR A 12-STORY BUILDING, SEISMIC DESIGN CATEGORY D

This example features the analysis and design of deep foundations for a 12-story reinforced concrete moment-resisting frame building similar to that described in Chapter 7 of this volume of design examples.

5.2.1 Basic Information

5.2.1.1 Description. Figure 5.2-1 shows the basic design condition considered in this example. A 2×2 pile group is designed for four conditions: for loads delivered by a corner and a side column of a moment-resisting frame system for Site Classes C and E. Geotechnical parameters for the two sites are given in Table 5.2-1.

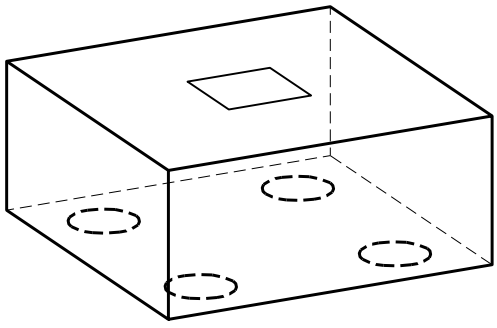

Figure 5.2-1 Design condition: Column of concrete moment-resisting frame supported by pile cap and cast-in-place piles

Table 5.2-1 Geotechnical Parameters

Depth	Class E Site	Class C Site
0 to 3 feet	Loose sand/fill γ = 110 pcf Angle of internal friction = 28 degrees Soil modulus parameter, k = 25 pci Neglect skin friction Neglect end bearing	Loose sand/fill γ = 110 pcf Angle of internal friction = 30 degrees Soil modulus parameter, k = 50 pci Neglect skin friction Neglect end bearing
3 to 30 feet	Soft clay γ = 110 pcf Undrained shear strength = 430 psf Soil modulus parameter, k = 25 pci Strain at 50 percent of maximum stress, ε_{50} = 0.01 Skin friction (ksf) = 0.3 Neglect end bearing	Dense sand (one layer: 3- to 100-foot depth) γ = 130 pcf Angle of internal friction = 42 degrees Soil modulus parameter, k = 125 pci Skin friction (ksf)* = 0.3 + 0.03/ft ≤ 2 End bearing (ksf)* = 65 + 0.6/ft ≤ 150
30 to 100 feet	Medium dense sand γ = 120 pcf Angle of internal friction = 36 degrees Soil modulus parameter, k = 50 pci Skin friction (ksf)* = 0.9 + 0.025/ft ≤ 2 End bearing (ksf)* = 40 + 0.5/ft ≤ 100	
Pile cap resistance	300 pcf, ultimate passive pressure	575 pcf, ultimate passive pressure
Resistance factor, ϕ	0.8 for vertical, lateral and rocking resistance of cohesive soil	0.7 for vertical, lateral and rocking resistance of cohesionless soil
Safety factor for settlement	2.5	2.5

*Skin friction and end bearing values increase (up to the maximum value noted) for each additional foot of depth below the top of the layer. (The values noted assume a minimum pile length of 20 ft.)

The structural material properties assumed for this example are as follows:

- f'_c = 3,000 psi
- f_y = 60,000 psi

5.2.1.2 Seismic Parameters.

- Site Class = C and E (both conditions considered in this example)
- S_{DS} = 1.1
- Seismic Design Category = D (for both conditions)

5.2.1.3 Demands. The unfactored demands from the moment frame system are shown in Table 5.2-2.

Table 5.2-2 Gravity and Seismic Demands

Location	Load	*Vx*	*Vy*	*P*	*Mxx*	*Myy*
Corner	*D*			-460.0		
	L			-77.0		
	Vx	55.5	0.6	193.2	4.3	624.8
	Vy	0.4	16.5	307.5	189.8	3.5
	ATx	1.4	3.1	26.7	34.1	15.7
	ATy	4.2	9.4	77.0	103.5	47.8
Side	*D*			-702.0		
	L			-72.0		
	Vx	72.2	0.0	0.0	0.0	723.8
	Vy	0.0	13.9	181.6	161.2	1.2
	ATx	0.4	1.8	2.9	18.1	4.2
	ATy	1.2	5.3	8.3	54.9	12.6

Note: Units are kips and feet. Load *Vy* is for loads applied toward the east. *ATx* is the corresponding accidental torsion case. Load *Vx* is for loads applied toward the north. *ATy* is the corresponding accidental torsion case.

Using Load Combinations 5 and 7 from Section 12.4.2.3 of the ***Standard*** (with $0.2S_{DS}D = 0.22D$ and taking $\rho = 1.0$), considering orthogonal effects as required for Seismic Design Category D and including accidental torsion, the following 32 load conditions must be considered.

$1.42D + 0.5L \pm 1.0Vx \pm 0.3Vy \pm \max(1.0ATx, 0.3ATy)$

$1.42D + 0.5L \pm 0.3Vx \pm 1.0Vy \pm \max(0.3ATx, 1.0ATy)$

$0.68D \pm 1.0Vx \pm 0.3Vy \pm \max(1.0ATx, 0.3ATy)$

$0.68D \pm 0.3Vx \pm 1.0Vy \pm \max(0.3ATx, 1.0ATy)$

5.2.1.4 Design Approach. For typical deep foundation systems, resistance to lateral loads is provided by both the piles and the pile cap. Figure 5.2-2 shows a simple idealization of this condition. The relative contributions of these piles and pile cap depend on the particular design conditions, but often both effects

are significant. Resistance to vertical loads is assumed to be provided by the piles alone regardless of whether their axial capacity is primarily due to end bearing, skin friction, or both. Although the behavior of foundation and superstructure are closely related, they typically are modeled independently. Earthquake loads are applied to a model of the superstructure, which is assumed to have fixed supports. Then the support reactions are seen as demands on the foundation system. A similar substructure technique is usually applied to the foundation system itself, whereby the behavior of pile cap and piles are considered separately. This section describes that typical approach.

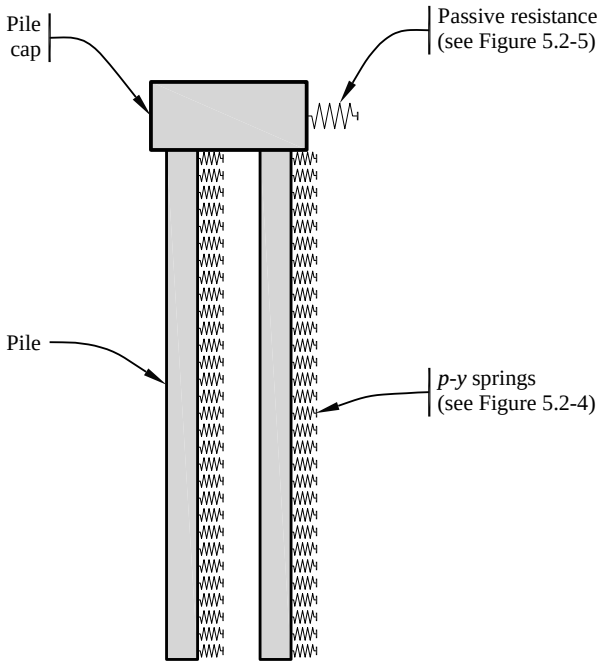

Figure 5.2-2 Schematic model of deep foundation system

5.2.1.4.1 Pile Group Mechanics. With reference to the free body diagram (of a 2×2 pile group) shown in Figure 5.2-3, demands on individual piles as a result of loads applied to the group may be determined as follows:

$V = \frac{V_{group} - V_{passive}}{4}$ and $M = V \times \ell$, where ℓ is a characteristic length determined from analysis of a laterally loaded single pile.

$P_{ot} = \frac{V_{group}h + M_{group} + 4M - h_p V_{passive}}{2s}$, where s is the pile spacing, h is the height of the pile cap and h_p is the height of $V_{passive}$ above Point O.

$P_p = \frac{P_{group}}{4}$ and $P = P_{ot} + P_p$

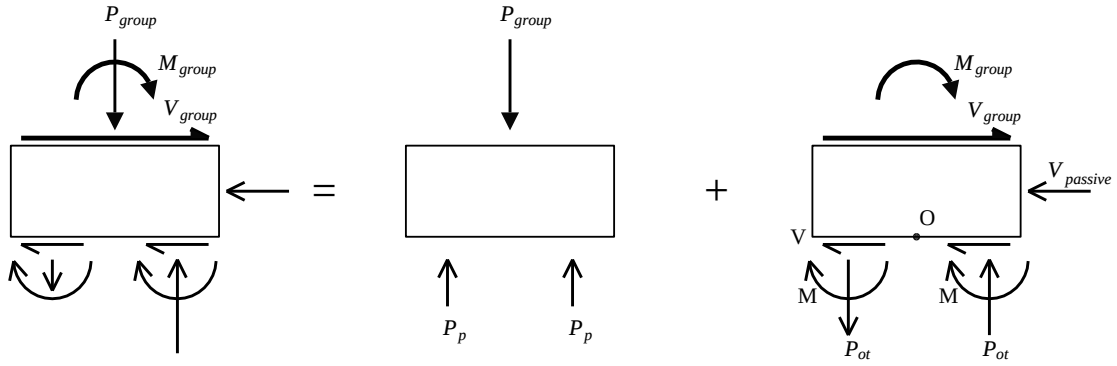

Figure 5.2-3 Pile cap free body diagram

5.2.1.4.2 Contribution of Piles. The response of individual piles to lateral loads is highly nonlinear. In recent years it has become increasingly common to consider that nonlinearity directly. Based on extensive testing of full-scale specimens and small-scale models for a wide variety of soil conditions, researchers have developed empirical relationships for the nonlinear *p-y* response of piles that are suitable for use in design. Representative *p-y* curves (computed for a 22-inch-diameter pile) are shown in Figure 5.2-4. The stiffness of the soil changes by an order of magnitude for the expected range of displacements (the vertical axis uses a logarithmic scale). The *p-y* response is sensitive to pile size (an effect not apparent in the figure, which is based on a single pile size); soil type and properties; and, in the case of sands, vertical stress, which increases with depth. Pile response to lateral loads, like the *p-y* curves on which the calculations are based, is usually computed using computer programs like LPILE.

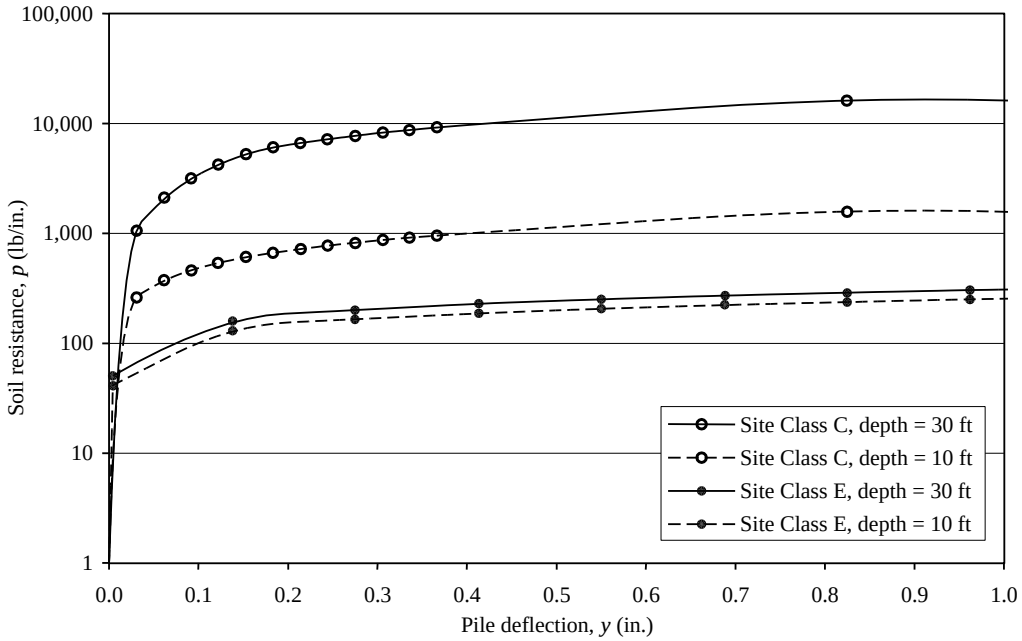

Figure 5.2-4 Representative *p-y* curves
(note that a logarithmic scale is used on the vertical axis)

5.2.1.4.3 Contribution of Pile Cap. Pile caps contribute to the lateral resistance of a pile group in two important ways: directly as a result of passive pressure on the face of the cap that is being pushed into the soil mass and indirectly by producing a fixed head condition for the piles, which can significantly reduce displacements for a given applied lateral load. Like the *p-y* response of piles, the passive pressure resistance of the cap is nonlinear. Figure 5.2-5 shows how the passive pressure resistance (expressed as a fraction of the ultimate passive pressure) is related to the imposed displacement (expressed as a fraction of the minimum dimension of the face being pushed into the soil mass).

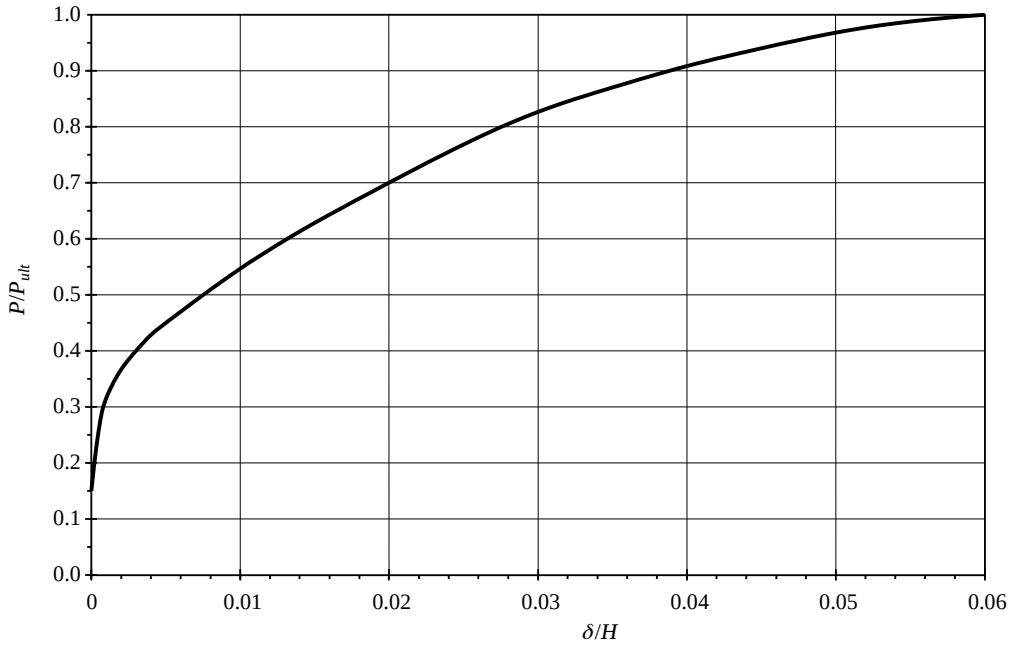

Figure 5.2-5 Passive pressure mobilization curve (after ASCE 41)

5.2.1.4.4 Group Effect Factors. The response of a group of piles to lateral loading will differ from that of a single pile due to pile-soil-pile interaction. (Group effect factors for axial loading of very closely spaced piles may also be developed but are beyond the scope of the present discussion.)

Full-size and model tests show that the lateral capacity of a pile in a pile group versus that of a single pile (termed "efficiency") is reduced as the pile spacing is reduced. The observed group effects are associated with shadowing effects. Various researchers have found that leading piles are loaded more heavily than trailing piles when all piles are loaded to the same deflection. The lateral resistance is primarily a function of row location within the group, rather than pile location within a row. Researchers recommend that these effects may be approximated by adjusting the resistance value on the single pile *p*-*y* curves (that is, by applying a *p*-multiplier).

Based on full-scale testing and subsequent analysis, Rollins et al. recommend the following *p*-multipliers (f_m), where D is the pile diameter or width and s is the center-to-center spacing between rows of piles in the direction of loading.

First (leading) row piles: $f_m = 0.26 \ln\left(s/D\right) + 0.5 \le 1.0$

Second row piles: $f_m = 0.52 \ln\left(s/D\right) \le 1.0$

Third or higher row piles: $f_m = 0.60 \ln\left(s/D\right) - 0.25 \le 1.0$

Because the direction of loading varies during an earthquake and the overall efficiency of the group is the primary point of interest, the average efficiency factor is commonly used for all members of a group in the analysis of any given member. In that case, the average *p*-reduction factor is as follows:

$$\bar{f}_m = \frac{1}{n}\sum_{i=1}^{n} f_{mi}$$

For a 2×2 pile group thus 

with $s = 3D$, the group effect factor is calculated as follows:

For piles 1 and 2, in the leading row, $f_m = 0.26\ln(3) + 0.5 = 0.79$.

For piles 3 and 4, in the second row, $f_m = 0.52\ln(3) = 0.57$.

So, the group effect factor (average *p*-multiplier) is $\bar{f}_m = \dfrac{0.79 + 0.79 + 0.57 + 0.57}{4} = 0.68$.

Figure 5.2-6 shows the group effect factors that are calculated for pile groups of various sizes with piles at several different spacings.

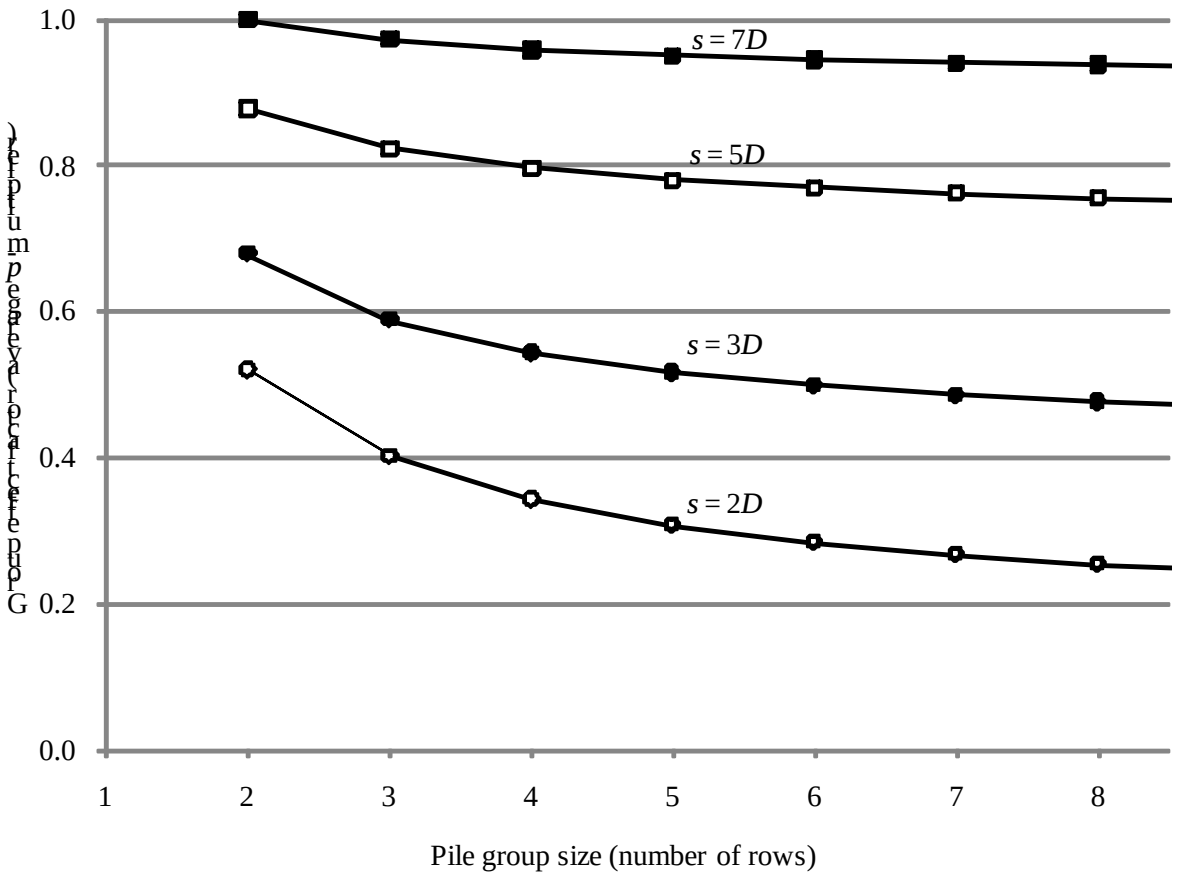

Figure 5.2-6 Calculated group effect factors

5.2.2 Pile Analysis, Design and Detailing

5.2.2.1 Pile Analysis. For this design example, it is assumed that all piles will be fixed-head, 22-inch-diameter, cast-in-place piles arranged in 2×2 pile groups with piles spaced at 66 inches center-to-center. The computer program LPILE Plus 5.0 is used to analyze single piles for both soil conditions shown in Table 5.2-1 assuming a length of 50 feet. Pile flexural stiffness is modeled using one-half of the gross moment of inertia because of expected flexural cracking. The response to lateral loads is affected to some degree by the coincident axial load. The full range of expected axial loads was considered in developing this example, but in this case the lateral displacements, moments and shears were not strongly affected; the plots in this section are for zero axial load. A *p*-multiplier of 0.68 for group effects (as computed at the end of Section 5.2.1.4) is used in all cases. Figures 5.2-7, 5.2-8 and 5.2-9 show the variation of shear, moment and displacement with depth (within the top 30 feet) for an applied lateral load of 15 kips on a single pile with the group reduction factor. It is apparent that the extension of piles to depths beyond 30 feet for the Class E site (or approximately 25 feet for the Class C site) does not provide additional resistance to lateral loading; piles shorter than those lengths would have reduced lateral resistance. The trends in the figures are those that should be expected. The shear and displacement are maxima at the pile head. Because a fixed-head condition is assumed, moments are also largest at the top of the pile. Moments and displacements are larger for the soft soil condition than for the firm soil condition.

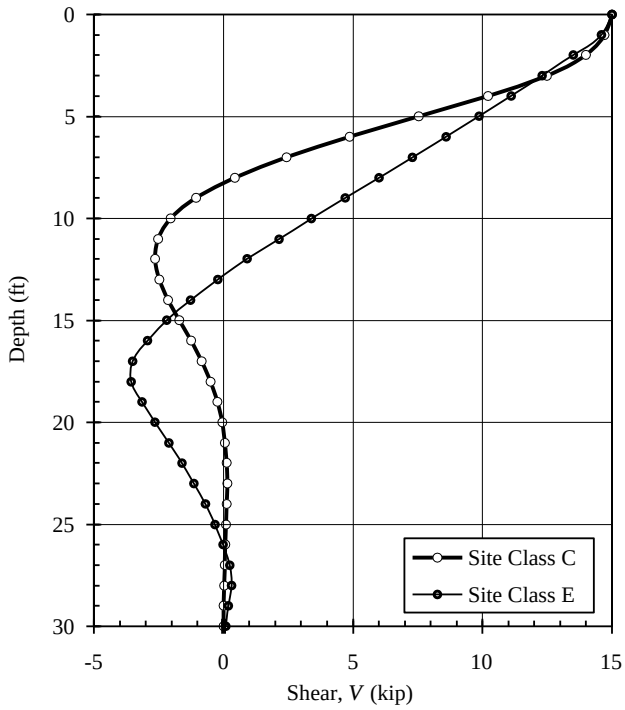

Figure 5.2-7 Results of pile analysis-shear versus depth (applied lateral load is 15 kips)

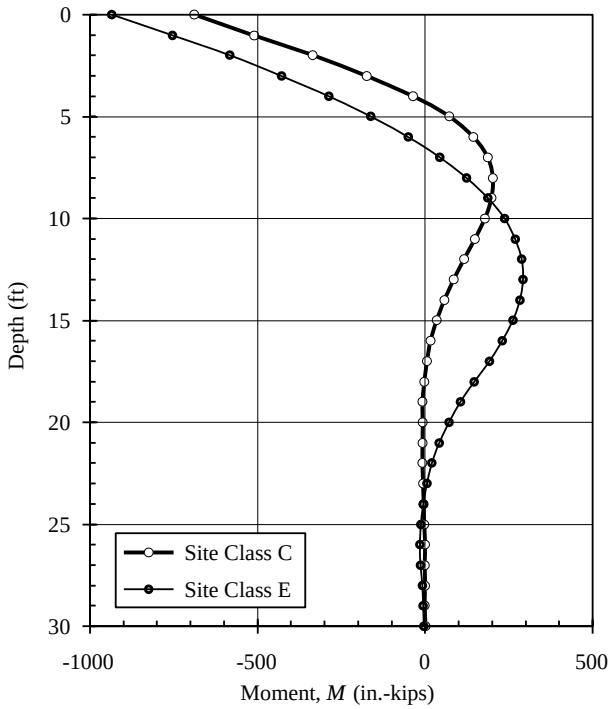

Figure 5.2-8 Results of pile analysis-moment versus depth (applied lateral load is 15 kips)

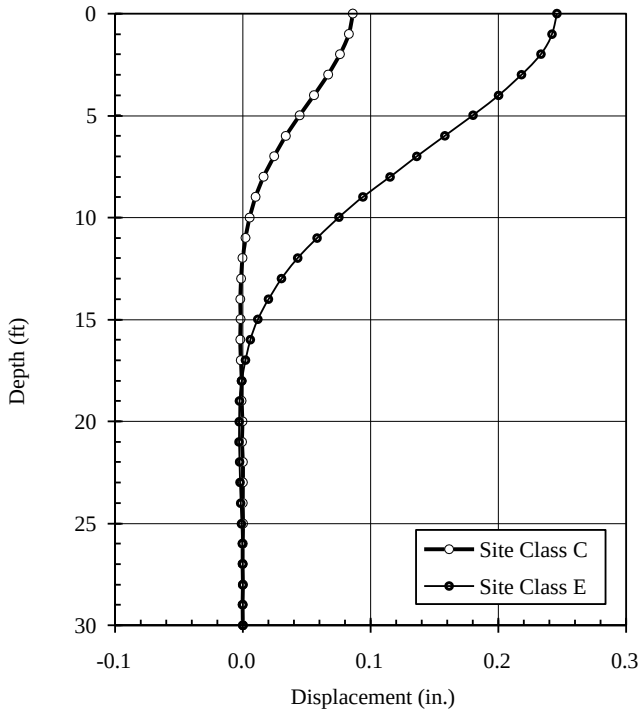

Figure 5.2-9 Results of pile analysis-displacement versus depth (applied lateral load is 15 kips)

The analyses performed to develop Figures 5.2-7 through 5.2-9 are repeated for different levels of applied lateral load. Figures 5.2-10 and 5.2-11 show how the moment and displacement at the head of the pile are related to the applied lateral load. It may be seen from Figure 5.2-10 that the head moment is related to the applied lateral load in a nearly linear manner; this is a key observation. Based on the results shown, the slope of the line may be taken as a characteristic length that relates head moment to applied load. Doing so produces the following:

- ℓ = 46 in. for the Class C site
- ℓ = 70 in. for the Class E site

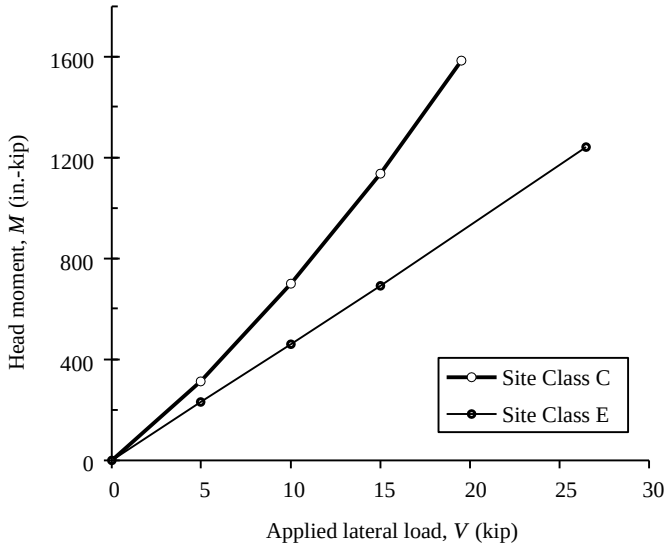

Figure 5.2-10 Results of pile analysis – applied lateral load versus head moment

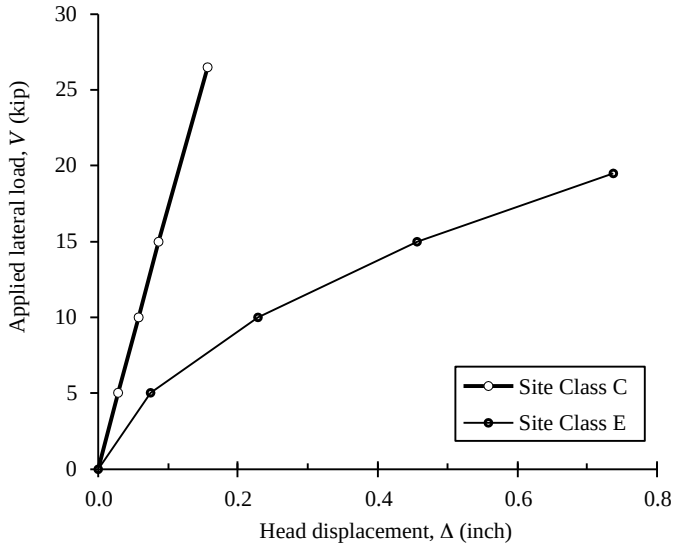

Figure 5.2-11 Results of pile analysis – head displacement versus applied lateral load

A similar examination of Figure 5.2-11 leads to another meaningful insight. The load-displacement response of the pile in Site Class C soil is essentially linear. The response of the pile in Site Class E soil is somewhat nonlinear, but for most of the range of response a linear approximation is reasonable (and useful). Thus, the effective stiffness of each individual pile is:

- k = 175 kip/in. for the Class C site
- k = 40 kip/in. for the Class E site

5.2.2.2 Pile Group Analysis. The combined response of the piles and pile cap and the resulting strength demands for piles are computed using the procedure outlined in Section 5.2.1.4 for each of the 32 load combinations discussed in Section 5.2.1.3. Assume that each 2×2 pile group has a 9'-2" × 9'-2" × 4'-0" thick pile cap that is placed 1'-6" below grade.

Check the Maximum Compression Case under a Side Column in Site Class C

Using the sign convention shown in Figure 5.2-3, the demands on the group are as follows:

- P = 1,224 kip
- M_{yy} = 222 ft-kips
- V_x = 20 kips
- M_{yy} = 732 ft-kips
- V_y = 73 kips

From preliminary checks, assume that the displacements in the x and y directions are sufficient to mobilize 30 percent and 35 percent, respectively, of the ultimate passive pressure:

$$V_{passive,x} = 0.30(575)\left(\frac{18}{12} + \frac{48}{2(12)}\right)\left(\frac{48}{12}\right)\left(\frac{110}{12}\right)\left(\tfrac{1}{1000}\right) = 22.1 \text{ kips}$$

and

$$V_{passive,y} = 0.35(575)\left(\frac{18}{12} + \frac{48}{2(12)}\right)\left(\frac{48}{12}\right)\left(\frac{110}{12}\right)\left(\tfrac{1}{1000}\right) = 25.8 \text{ kips}$$

and conservatively take $h_p = h/3 = 16$ inches.

Since $V_{passive,x} > V_x$, passive resistance alone is sufficient for this case in the x direction. However, in order to illustrate the full complexity of the calculations, reduce $V_{passive,x}$ to 4 kips and assign a shear of 4.0 kips to each pile in the x direction. In the y direction, the shear in each pile is as follows:

$$V = \frac{73 - 25.8}{4} = 11.8 \text{ kips}$$

The corresponding pile moments are:

$M = 4.0(46) = 186$ in.-kips for x-direction loading

and

$M = 11.8(46) = 543$ in.-kips for y-direction loading

The maximum axial load due to overturning for x-direction loading is:

$$P_{ot} = \frac{20(48) + 222(12) + 4(184) - 16(4)}{2(66)} = 32.5 \text{ kips}$$

and for y-direction loading (determined similarly), $P_{ot} = 106.4$ kips.

The axial load due to direct loading is $P_p = 1224/4 = 306$ kips.

Therefore, the maximum load effects on the most heavily loaded pile are the following:

$P_u = 32.5 + 106.4 + 306 = 445$ kips

$$M_u = \sqrt{(184)^2 + (543)^2} = 573 \text{ in.-kips}$$

The expected displacement in the y direction is computed as follows:

$\delta = V/k = 11.8/175 = 0.067$ in., which is 0.14 percent of the pile cap height (h)

Reading Figure 5.2-5 with $\delta/H = 0.0014$, $P/P_{ult} \approx 0.34$, so the assumption that 35 percent of P_{ult} would be mobilized was reasonable.

5.2.2.3 Design of Pile Section. The calculations shown in Section 5.2.2.2 are repeated for each of the 32 load combinations under each of the four design conditions. The results are shown in Figures 5.2-12 and 5.2-13. In these figures, circles indicate demands on piles under side columns and squares indicate demands on piles under corner columns. Also plotted are the ϕP-ϕM design strengths for the 22-inch-diameter pile sections with various amounts of reinforcement (as noted in the legends). The appropriate reinforcement pattern for each design condition may be selected by noting the innermost capacity curve that envelops the corresponding demand points. The required reinforcement is summarized in Table 5.2-4, following calculation of the required pile length.

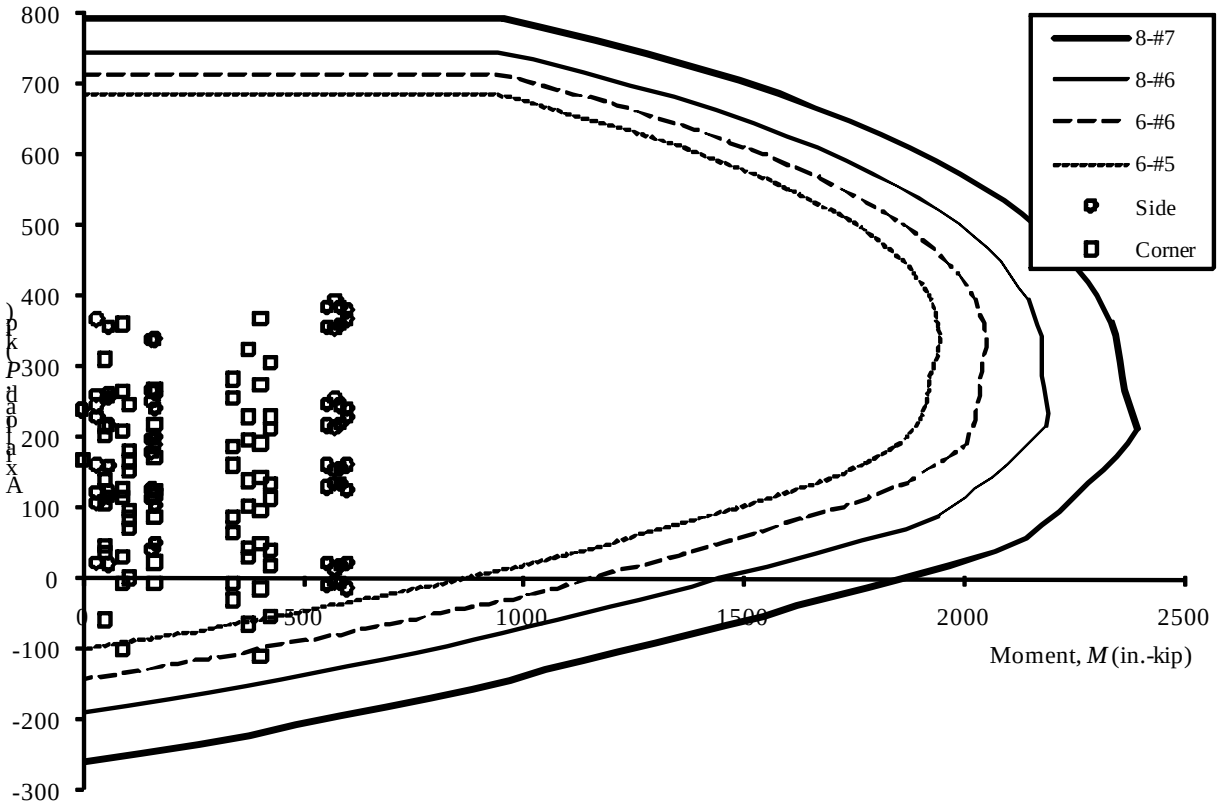

Figure 5.2-12 P-M interaction diagram for Site Class C

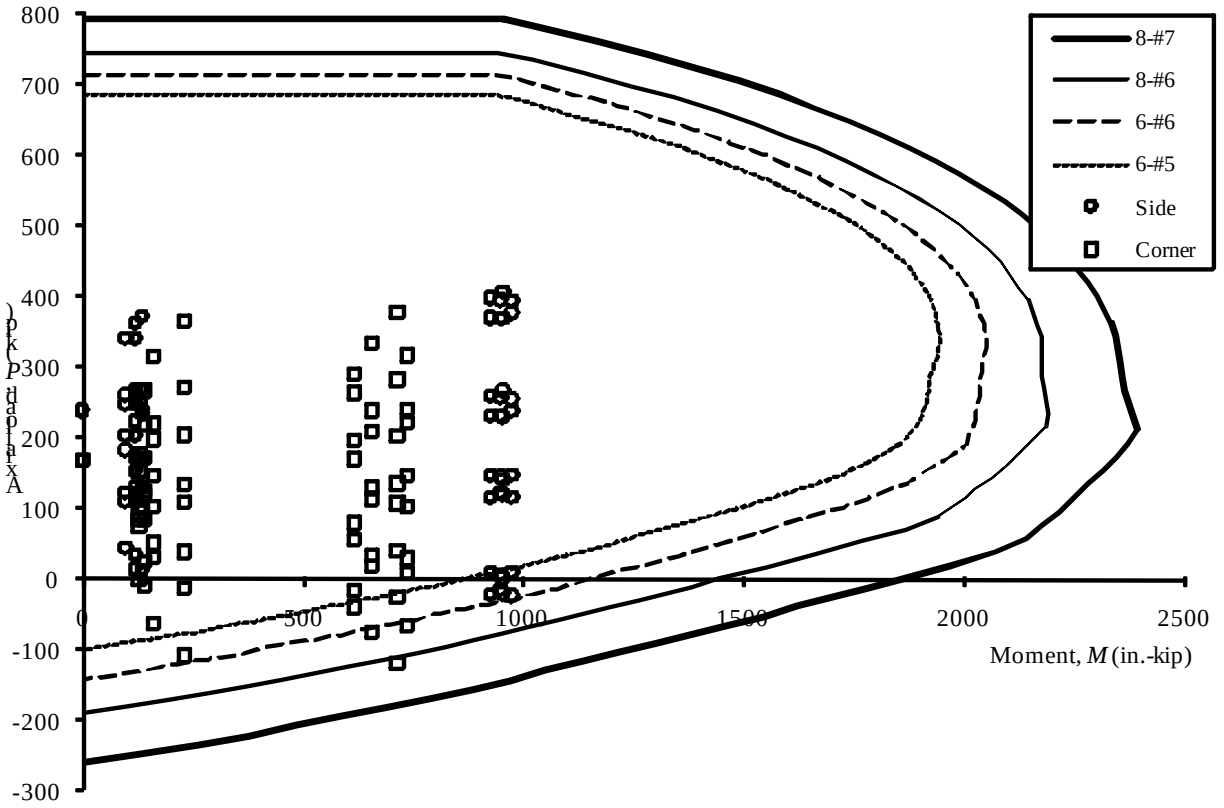

Figure 5.2-13 P-M interaction diagram for Site Class E

5.2.2.4 Pile Length for Axial Loads. For the calculations that follow, recall that skin friction and end bearing are neglected for the top 3 feet in this example. The design is based on having 1'-6" of soil over a 4'-0" deep pile cap.

5.2.2.4.1 Length for Settlement. Service loads per pile are calculated as $P = (P_D + P_L)/4$.

Check the pile group under the side column in Site Class C, assuming L = 52.5 feet – 5.5 feet = 47 feet:

P = (752 + 114)/4 = 217 kips.

P_{skin} = average friction capacity × pile perimeter × pile length for friction
= 0.5[0.3 + 2.5(0.03) + 0.3 + 49.5(0.03)]π(22/12)(44) = 292 kips

P_{end} = end bearing capacity at depth × end bearing area
= [65 + 49.5(0.6)](π/4)(22/12)^2 = 250 kips

$P_{allow} = (P_{skin} + P_{end})$/S.F. = (292 + 250)/2.5 = 217 kips = 217 kips (demand) OK

Check the pile group under the corner column in Site Class E, assuming L = 49 feet:

P = (460 + 77)/4 = 134 kips

P_{skin} = [friction capacity in first layer + average friction capacity in second layer] × pile perimeter
= [24.5(0.3) + (24.5/2)(0.9 + 0.9 + 24.5[0.025])]π(22/12) = 212 kips

P_{end} = [40 + 24.5(0.5)](π/4)(22/12)^2 = 138 kips

P_{allow} = (212 + 138)/2.5 = 140 kips > 134 kips OK

5.2.2.4.2 Length for Compression Capacity. All of the strength-level load combinations (discussed in Section 5.2.1.3) must be considered.

Check the pile group under the side column in Site Class C, assuming L = 49 feet:

As seen in Figure 5.1-12, the maximum compression demand for this condition is P_u = 394 kips.

P_{skin} = 0.5[0.3 + 0.3 + 47(0.03)]π(22/12)(47) = 272 kips

P_{end} = [65 + 47(0.6)](π/4)(22/12)^2 = 246 kips

$\phi P_n = \phi(P_{skin} + P_{end})$ = 0.75(272 + 246) = 389 kips ≈ 390 kips OK

Check the pile group under the corner column in Site Class E, assuming L = 64 feet:

As seen in Figure 5.2-13, the maximum compression demand for this condition is P_u = 340 kips.

P_{skin} = [27(0.3) + (34/2)(0.9 + 0.9 + 34[0.025])]π(22/12) = 306 kips

P_{end} = [40 + 34(0.5)](π/4)(22/12)^2 = 150 kips

$\phi P_n = \phi(P_{skin} + P_{end})$ = 0.75(306 + 150) = 342 kips > 340 kips OK

5.2.2.4.3 Length for Uplift Capacity. Again, all of the strength-level load combinations (discussed in Section 5.2.1.3) must be considered.

Check the pile group under side column in Site Class C, assuming L = 5 feet:

As seen in Figure 5.2-12, the maximum tension demand for this condition is P_u = -1.9 kips.

P_{skin} = 0.5[0.3 + 0.3 + 2(0.03)]π(22/12)(2) = 3.8 kips

$\phi P_n = \phi(P_{skin})$ = 0.75(3.8) = 2.9 kips > 1.9 kips OK

Check the pile group under the corner column in Site Class E, assuming L = 52 feet:

As seen in Figure 5.2-13, the maximum tension demand for this condition is P_u = -144 kips.

P_{skin} = [27(0.3) + (22/2)(0.9 + 0.9 + 22[0.025])]π(22/12) = 196 kips

$\phi P_n = \phi(P_{skin})$ = 0.75(196) = 147 kips > 144 kips OK

5.2.2.4.4 Graphical Method of Selecting Pile Length. In the calculations shown above, the adequacy of the soil-pile interface to resist applied loads is checked once a pile length is assumed. It would be possible to generate mathematical expressions of pile capacity as a function of pile length and then solve such expressions for the demand conditions. However, a more practical design approach is to pre-calculate the capacity for piles for the full range of practical lengths and then select the length needed to satisfy the demands. This method lends itself to graphical expression as shown in Figures 5.2-14 and 5.2-15.

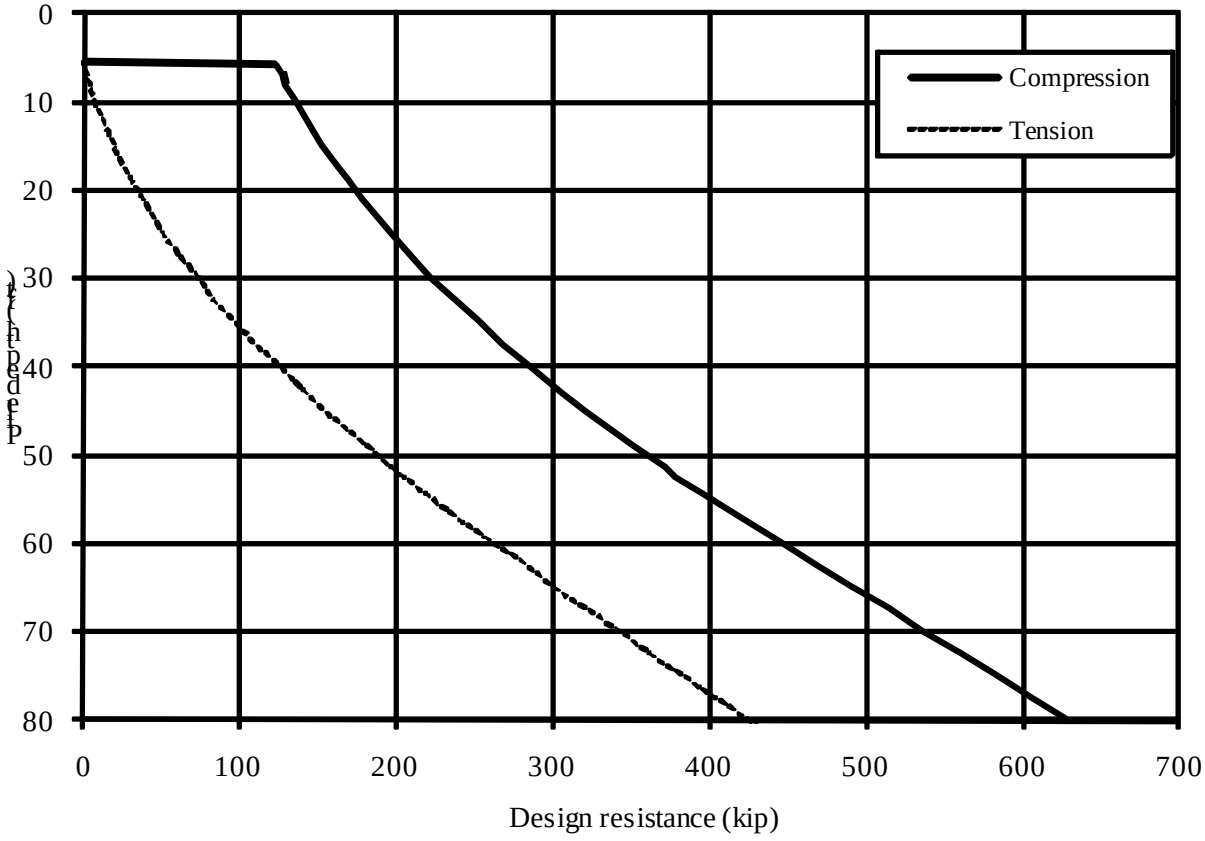

Figure 5.2-14 Pile axial capacity as a function of length for Site Class C

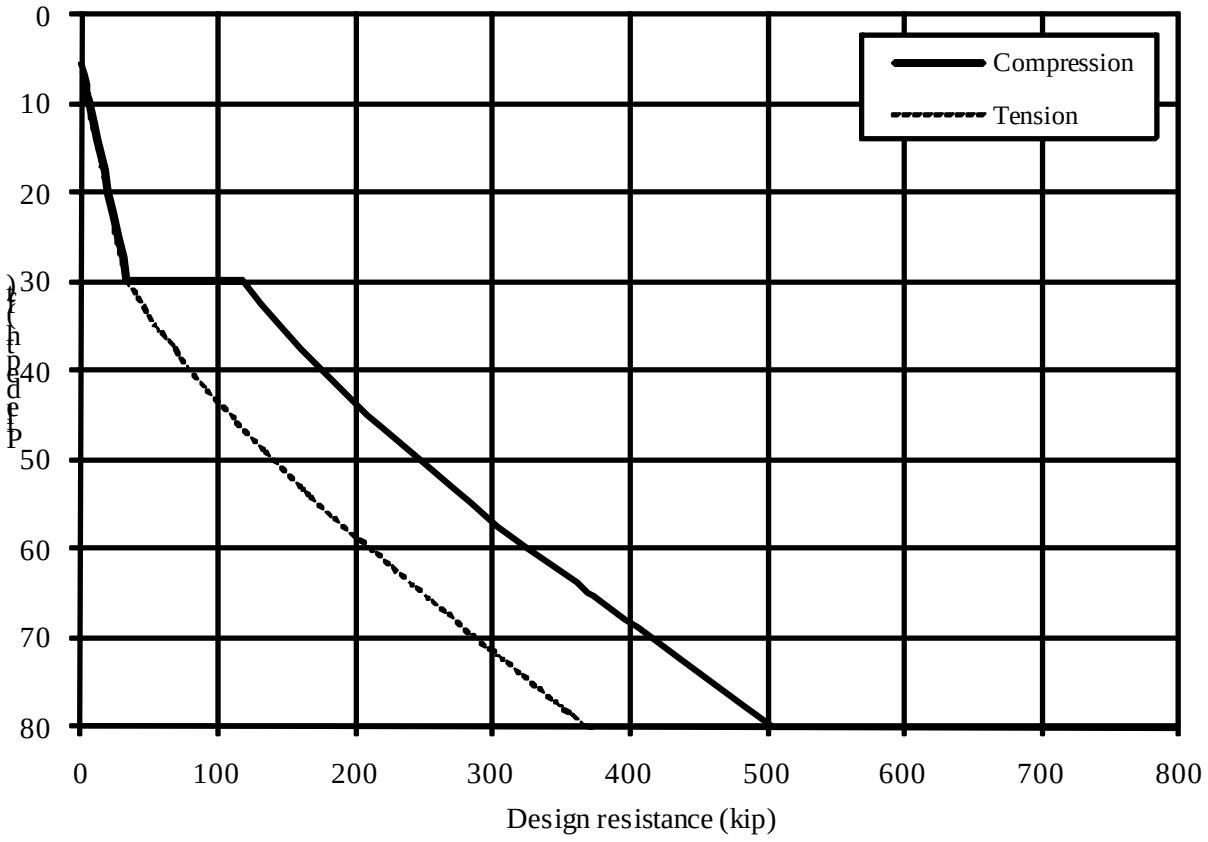

Figure 5.2-15 Pile axial capacity as a function of length for Site Class E

5.2.2.4.5 Results of Pile Length Calculations. Detailed calculations for the required pile lengths are provided above for two of the design conditions. Table 5.2-3 summarizes the lengths required to satisfy strength and serviceability requirements for all four design conditions.

Table 5.2-3 Pile Lengths Required for Axial Loads

	Piles Under Corner Column			Piles Under Side Column		
Site Class	Condition	Load	Min Length	Condition	Load	Min Length
Site Class C	**Compression**	**369 kip**	**46 ft**	**Compression**	**394 kip**	**49 ft**
	Uplift	108 kip	32 ft	Uplift	13.9 kip	8 ft
	Settlement	134 kip	27 ft	Settlement	217 kip	47 ft
Site Class E	**Compression**	**378 kip**	**61 ft**	Compression	406 kip	64 ft
	Uplift	119 kip	42 ft	Uplift	23.6 kip	17 ft
	Settlement	134 kip	48 ft	**Settlement**	**217 kip**	**67 ft**

5.2.2.5 Design Results. The design results for all four pile conditions are shown in Table 5.2-4. The amount of longitudinal reinforcement indicated in the table is that required at the pile-pile cap interface and may be reduced at depth as discussed in the following section.

Table 5.2-4 Summary of Pile Size, Length and Longitudinal Reinforcement

Site Class	Piles Under Corner Column	Piles Under Side Column
Site Class C	22 in. diameter by 46 ft long 8-#6 bars	22 in. diameter by 49 ft long 6-#5 bars
Site Class E	22 in. diameter by 61 ft long 8-#7 bars	22 in. diameter by 67 ft long 6-#6 bars

5.2.2.6 Pile Detailing. *Standard* Sections 12.13.5, 12.13.6, 14.2.3.1 and 14.2.3.2 contain special pile requirements for structures assigned to Seismic Design Category C or higher and D or higher. In this section, those general requirements and the specific requirements for uncased concrete piles that apply to this example are discussed. Although the specifics are affected by the soil properties and assigned site class, the detailing of the piles designed in this example focuses on consideration of the following fundamental items:

- All pile reinforcement must be developed in the pile cap (*Standard* Sec. 12.13.6.5).
- In areas of the pile where yielding might be expected or demands are large, longitudinal and transverse reinforcement must satisfy specific requirements related to minimum amount and maximum spacing.
- Continuous longitudinal reinforcement must be provided over the entire length resisting design tension forces (ACI 318 Sec. 21.12.4.2).

The discussion that follows refers to the detailing shown in Figures 5.2-16 and 5.2-17.

5.2.2.6.1 Development at the Pile Cap. Where neither uplift nor flexural restraint are required, the development length is the full development length for compression. Where the design relies on head fixity or where resistance to uplift forces is required (both of which are true in this example), pile reinforcement must be fully developed in tension unless the section satisfies the overstrength load condition or demands are limited by the uplift capacity of the soil-pile interface (*Standard* Sec. 12.13.6.5). For both site classes considered in this example, the pile longitudinal reinforcement is extended straight into the pile cap a distance that is sufficient to fully develop the tensile capacity of the bars. In addition to satisfying the requirements of the *Standard*, this approach offers two advantages. By avoiding lap splices to field-placed dowels where yielding is expected near the pile head (although such would be permitted by the *Standard*), more desirable inelastic performance would be expected. Straight development, while it may require a thicker pile cap, permits easier placement of the pile cap's bottom reinforcement followed by the addition of the spiral reinforcement within the pile cap. Note that embedment of the entire pile in the pile cap facilitates direct transfer of shear from pile cap to pile but is not a requirement of the *Standard*. (Section 1810.3.11 of the 2009 *International Building Code* requires that piles be embedded at least 3 inches into pile caps.)

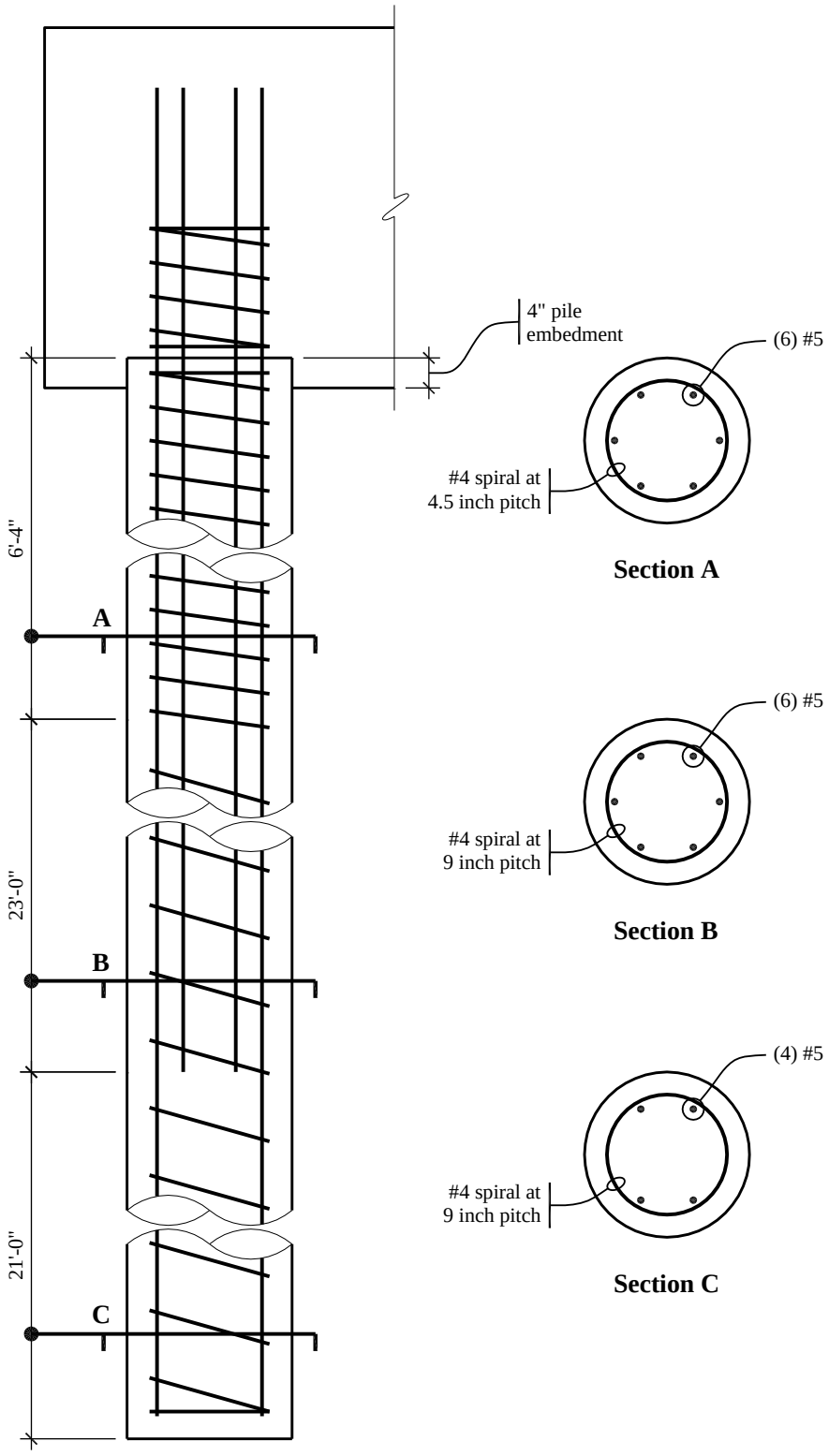

Figure 5.2-16 Pile detailing for Site Class C (under side column)

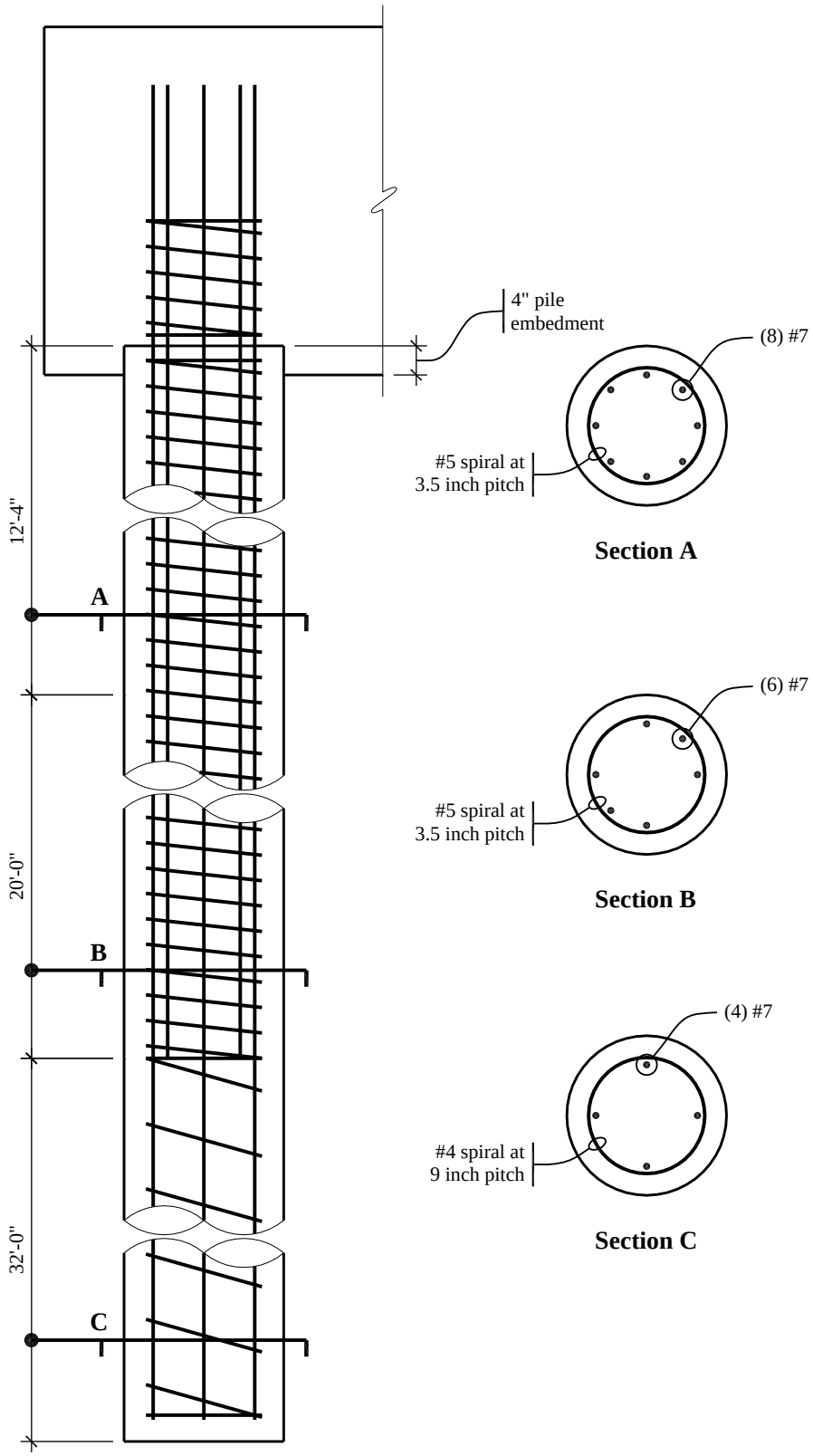

Figure 5.2-17 Pile detailing for Site Class E (under corner column)

5.2.2.6.2 Longitudinal and Transverse Reinforcement Where Demands Are Large. Requirements for longitudinal and transverse reinforcement apply over the entire length of pile where demands are large. For uncased concrete piles in Seismic Design Category D, at least four longitudinal bars (with a minimum reinforcement ratio of 0.005) must be provided over the largest region defined as follows: the top one-half of the pile length, the top 10 feet below the ground, or the flexural length of the pile. The flexural length is taken as the length of pile from the cap to the lowest point where 0.4 times the concrete section cracking moment (see ACI 318 Section 9.5.2.3) exceeds the calculated flexural demand at that point. For the piles used in this example, one-half of the pile length governs. (Note that "providing" a given reinforcement ratio means that the reinforcement in question must be developed at that point. Bar development and cutoff are discussed in more detail in Chapter 7 of this volume of design examples.) Transverse reinforcement must be provided over the same length for which minimum longitudinal reinforcement requirements apply. Because the piles designed in this example are larger than 20 inches in diameter, the transverse reinforcement may not be smaller than 0.5 inch diameter. For the piles shown in Figures 5.2-16 and 5.2-17, the spacing of the transverse reinforcement in the top half of the pile length may not exceed the least of the following: $12d_b$ (7.5 in. for #5 longitudinal bars and 10.5 in. for #7 longitudinal bars), 22/2 = 11 in., or 12 in.

Where yielding may be expected, even more stringent detailing is required. For the Class C site, yielding can be expected within three diameters of the bottom of the pile cap ($3D = 3 \times 22 = 66$ in.). Spiral reinforcement in that region must not be less than one-half of that required in Section 21.4.4.1(a) of ACI 318 (since the site is not Class E, Class F, or liquefiable) and the requirements of Sections 21.4.4.2 and 21.4.4.3 must be satisfied. Note that Section 21.4.4.1(a) refers to Equation 10-5, which often will govern. In this case, the minimum volumetric ratio of spiral reinforcement is one-half that determined using ACI 318 Equation 10-5. In order to provide a reinforcement ratio of 0.01 for this pile section, a #4 spiral must have a pitch of no more than 4.8 inches, but the maximum spacing permitted by Section 21.4.4.2 is 22/4 = 5.5 inches or $6d_b$ = 3.75 inches, so a #4 spiral at 3.75-inch pitch is used. (Section 1810.3.2.1.2 of the 2009 *International Building Code* clarifies that ACI 318 Equation 10-5 need not be applied to piles.)

For the Class E site, the more stringent detailing must be provided "within seven diameters of the pile cap and of the interfaces between strata that are hard or stiff and strata that are liquefiable or are composed of soft to medium-stiff clay" (*Standard* Sec. 14.2.3.2.1). The author interprets "within seven diameters of ... the interface" as applying in the direction into the softer material, which is consistent with the expected location of yielding. Using that interpretation, the *Standard* does not indicate the extent of such detailing into the firmer material. Taking into account the soil layering shown in Table 5.2-1 and the pile cap depth and thickness, the tightly spaced transverse reinforcement shown in Figure 5.2-17 is provided within $7D$ of the bottom of pile cap and top of firm soil and is extended a little more than $3D$ into the firm soil. Because the site is Class E, the full amount of reinforcement indicated in ACI 318 Section 21.6.4 must be provided. In order to provide a reinforcement ratio of 0.02 for this pile section, a #5 spiral must have a pitch of no more than 3.7 inches. The maximum spacing permitted by Section 21.6.4.3 is 22/4 = 5.5 inches or $6d_b$ = 5.25 inches, so a #5 spiral at 3.5-inch pitch is used.

5.2.2.6.3 Continuous Longitudinal Reinforcement for Tension. Table 5.2-3 shows the pile lengths required for resistance to uplift demands. For the Site Class E condition under a corner column (Figure 5.2-17), longitudinal reinforcement must resist tension for at least the top 42 feet (being developed at that point). Extending four longitudinal bars for the full length and providing widely spaced spirals at such bars is practical for placement, but it is not a specific requirement of the *Standard*. For the Site Class C condition under a side column (Figure5.2-16), design tension due to uplift extends only approximately 5 feet below the bottom of the pile cap. Therefore, a design with Section C of

Figure 5.2-16 being unreinforced would satisfy the *Provisions* requirements, but the author has decided to extend very light longitudinal and nominal transverse reinforcement for the full length of the pile.

5.2.3 Other Considerations

5.2.3.1 Foundation Tie Design and Detailing. *Standard* Section 12.13.5.2 requires that individual pile caps be connected by ties. Such ties are often grade beams, but the *Standard* would permit use of a slab (thickened or not) or calculations that demonstrate that the site soils (assigned to Site Class A, B, or C) provide equivalent restraint. For this example, a tie beam between the pile caps under a corner column and a side column is designed. The resulting section is shown in Figure 5.2-18.

For pile caps with an assumed center-to-center spacing of 32 feet in each direction and given P_{group} = 1,224 kips under a side column and P_{group} = 1,142 kips under a corner column, the tie is designed as follows.

As indicated in *Standard* Section 12.13.5.2, the minimum tie force in tension or compression equals the product of the larger column load times S_{DS} divided by 10 = 1224(1.1)/10 = 135 kips.

The design strength for six #6 bars is as follows

$\phi A_s f_y$ = 0.9(6)(0.44)(60) = 143 kips > 135 kips OK

According to ACI 318 Section 21.12.3.2, the smallest cross-sectional dimension of the tie beam must not be less than the clear spacing between pile caps divided by 20 = (32'-0" - 9'-2")/20 = 13.7 inches. Use a tie beam that is 14 inches wide and 16 inches deep. ACI 318 Section 21.12.3.2 further indicates that closed ties must be provided at a spacing of not more than one-half the minimum dimension, which is 14/2 = 7 inches.

Assuming that the surrounding soil provides restraint against buckling, the design strength of the tie beam concentrically loaded in compression is as follows:

$\phi P_n = 0.8\phi[0.85f'_c(A_g - A_{st}) + f_y A_{st}]$

= 0.8(0.65)[0.85(3){(16)(14) – 6(0.44)}+ 60(6)(0.44)] = 376 kips > 135 kips OK

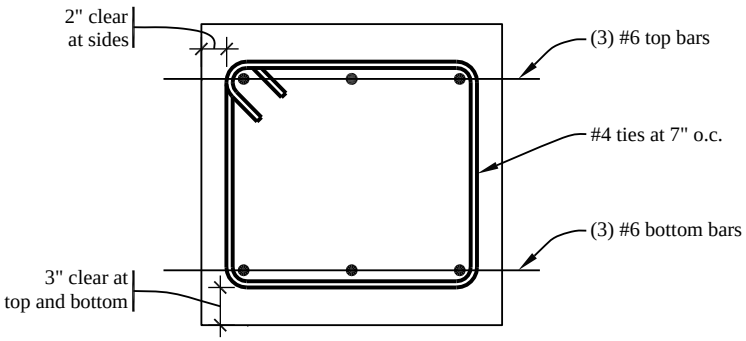

Figure 5.2-18 Foundation tie section

5.2.3.2 Liquefaction. For Seismic Design Categories C, D, E and F, *Standard* Section 11.8.2 requires that the geotechnical report address potential hazards due to liquefaction. For Seismic Design Categories D, E and F, *Standard* Section 11.8.3 further requires that the geotechnical report describe the likelihood and potential consequences of liquefaction and soil strength loss (including estimates of differential settlement, lateral movement, lateral loads on foundations, reduction in foundation soil-bearing capacity, increases in lateral pressures on retaining walls and flotation of buried structures) and discuss mitigation measures. During the design of the structure, such measures (which can include ground stabilization, selection of appropriate foundation type and depths and selection of appropriate structural systems to accommodate anticipated displacements and forces) must be considered. *Provisions* Part 3, Resource Paper 12 contains a calculation procedure that can be used to evaluate the liquefaction hazard.

5.2.3.3 Kinematic Interaction. Piles are subjected to curvature demands as a result of two different types of behavior: inertial interaction and kinematic interaction. The term *inertial interaction* is used to describe the coupled response of the soil-foundation-structure system that arises as a consequence of the mass properties of those components of the overall system. The structural engineer's consideration of inertial interaction is usually focused on how the structure *loads* the foundation and how such loads are transmitted to the soil (as shown in the pile design calculations that are the subject of most of this example) but also includes assessment of the resulting foundation movement. The term *kinematic interaction* is used to describe the manner in which the stiffness of the foundation system impedes development of free-field ground motion. Consideration of kinematic interaction by the structural engineer is usually focused on assessing the strength and ductility demands imposed directly on piles by movement of the soil. Although it is rarely done in practice, *Standard* Section 12.13.6.3 requires consideration of kinematic interaction for foundations of structures assigned to Seismic Design Category D, E, or F. Kramer discusses kinematic and inertial interaction and the methods of analysis employed in consideration of those effects and demonstrates "that the solution to the entire soil-structure interaction problem is equal to the sum of the solutions of the kinematic and inertial interaction analyses."

One approach that would satisfy the requirements of the *Standard* would be as follows:

- The geotechnical consultant performs appropriate kinematic interaction analyses considering free-field ground motions and the stiffness of the piles to be used in design.

- The resulting pile demands, which generally are greatest at the interface between stiff and soft strata, are reported to the structural engineer.

- The structural engineer designs piles for the sum of the demands imposed by the vibrating superstructure and the demands imposed by soil movement.

A more practical, but less rigorous, approach is to provide appropriate detailing in regions of the pile where curvature demands imposed directly by earthquake ground motions are expected to be significant. Where such a judgment-based approach is used, one must decide whether to provide only additional transverse reinforcement in areas of concern to improve ductility or whether additional longitudinal reinforcement should also be provided to increase strength. Section 18.10.2.4.1 of the 2009 *International Building Code* permits application of such deemed-to-comply detailing in lieu of explicit calculations and prescribes a minimum longitudinal reinforcement ratio of 0.005.

5.2.3.4 Design of Pile Cap. Design of pile caps for large pile loads is a very specialized topic for which detailed treatment is beyond the scope of this volume of design examples. CRSI notes that "most pile caps are designed in practice by various short-cut rule-of-thumb procedures using what are hoped to be conservative allowable stresses." Wang & Salmon indicates that "pile caps frequently must be designed for shear considering the member as a deep beam. In other words, when piles are located inside the critical sections *d* (for one-way action) or *d*/2 (for two-way action) from the face of column, the shear cannot be neglected." They go on to note that "there is no agreement about the proper procedure to use." Direct application of the special provisions for deep flexural members as found in ACI 318 is not possible since the design conditions are somewhat different. CRSI provides a detailed outline of a design procedure and tabulated solutions, but the procedure is developed for pile caps subjected to concentric vertical loads only (without applied overturning moments or pile head moments). Strut-and-tie models (as described in Appendix A of ACI 318) may be employed, but their application to elements with important three-dimensional characteristics (such as pile caps for groups larger than 2×1) is so involved as to preclude hand calculations.

5.2.3.5 Foundation Flexibility and Its Impact on Performance

5.2.3.5.1 Discussion. Most engineers routinely use fixed-base models. Nothing in the *Provisions* or *Standard* prohibits that common practice; the consideration of foundation flexibility and of soil-structure interaction effects (*Standard* Section 12.13.3 and Chapter 19) is "permitted" but not required. Such fixed-base models can lead to erroneous results, but engineers have long assumed that the errors are usually conservative. There are two obvious exceptions to that assumption: soft soil site-resonance conditions (e.g., as in the 1985 Mexico City earthquake) and excessive damage or even instability due to increased displacement response.

Site resonance can result in significant amplification of ground motion in the period range of interest. For sites with a fairly long predominant period, the result is spectral accelerations that increase as the structural period approaches the site period. However, the shape of the general design spectrum used in the *Standard* does not capture that effect; for periods larger than T_0, accelerations remain the same or decrease with increasing period. Therefore, increased system period (as a result of foundation flexibility) always leads to lower design forces where the general design spectrum is used. Site-specific spectra may reflect long-period site-resonance effects, but the use of such spectra is required only for Class F sites.

Clearly, an increase in displacements, caused by foundation flexibility, does change the performance of a structure and its contents—raising concerns regarding both stability and damage. Earthquake-induced instability of buildings has been exceedingly rare. The analysis and acceptance criteria in the *Standard* are not adequate to the task of predicting real stability problems; calculations based on linear, static behavior cannot be used to predict instability of an inelastic system subjected to dynamic loading. While *Provisions* Part 2 Section 12.12 indicates that structural stability was considered in arriving at the "consensus judgment" reflected in the drift limits, such considerations were qualitative. In point of fact, the values selected for the drift limits were selected considering damage to nonstructural systems (and, perhaps in some cases, control of structural ductility demands). For most buildings, application of the *Standard* is intended to satisfy performance objectives related to life safety and collapse prevention, not damage control or post-earthquake occupancy. Larger design forces and more stringent drift limits are applied to structures assigned to Occupancy Category III or IV in the hope that those measures will improve performance without requiring explicit consideration of such performance. Although foundation flexibility can affect structural performance significantly, since all consideration of performance in the context of the *Standard* is approximate and judgment-based, it is difficult to define how such changes in performance should be characterized. Explicit consideration of performance measures also tends to increase engineering effort substantially, so mandatory performance checks often are resisted by the user community.

The engineering framework established in ASCE 41 is more conducive to explicit use of performance measures. In that document (Sections 4.4.3.2.1 and 4.4.3.3.1), the use of fixed-based structural models is prohibited for "buildings being rehabilitated for the Immediate Occupancy Performance Level that are sensitive to base rotations or other types of foundation movement." In this case the focus is on damage control rather than structural stability.

5.2.3.5.2 Example Calculations. To assess the significance of foundation flexibility, one may compare the dynamic characteristics of a fixed-base model to those of a model in which foundation effects are included. The effects of foundation flexibility become more pronounced as foundation period and structural period approach the same value. For this portion of the example, use the Site Class E pile design results from Section 5.2.2.1 and consider the north-south response of the concrete moment frame building located in Berkeley (Section 7.2) as representative for this building.

5.2.3.5.2.1 Stiffness of the Structure. Calculations of the effect of foundation flexibility on the dynamic response of a structure should reflect the overall stiffness of the structure (e.g., that associated with the fundamental mode of vibration) rather than the stiffness of any particular story. Table 7-2 shows that the total weight of the structure is 43,919 kips. Table 7-3 shows that the calculated period of the fixed-base structure is 2.02 seconds and Table 7-7 indicates that 83.6 percent of the mass participates in that mode. Using the equation for the undamped period of vibration of a single-degree-of-freedom oscillator, the effective stiffness of the structure is as follows:

$$K = \frac{4\pi^2 M}{T^2} = \frac{4\pi^2\left((0.836)43{,}919/386.1\right)}{2.02^2} = 920 \text{ kip/in.}$$

5.2.3.5.2.2 Foundation Stiffness. As seen in Figure 7-1, there are 36 moment frame columns. Assume that a 2×2 pile group supports each column. As shown in Section 5.2.2.1, the stiffness of each pile is 40 kip/in. Neglecting both the stiffness contribution from passive pressure resistance and the flexibility of the beam-slab system that ties the pile caps, the stiffness of each pile group is 4 × 40 = 160 kip/in. and the stiffness of the entire foundation system is 36 × 160 = 5,760 kip/in.

5.2.3.5.2.3 Effect of Foundation Flexibility. Because the foundation stiffness is much greater than the structural stiffness, period elongation is expected to be minimal. To confirm this expectation, the period of the combined system is computed. The total stiffness for the system (springs in series) is as follows:

$$K_{combined} = \frac{1}{\frac{1}{K_{structure}} + \frac{1}{K_{fdn}}} = \frac{1}{\frac{1}{920} + \frac{1}{5760}} = 793 \text{ kip/in.}$$

Assume that the weight of the foundation system is 4,000 kips and that 100 percent of the corresponding mass participates in the new fundamental mode of vibration. The period of the combined system is as follows:

$$T = 2\pi\sqrt{\frac{M}{K}} = 2\pi\sqrt{\frac{\left[(0.836)(43{,}919) + (1.0)(4000)\right]/386.1}{793}} = 2.29 \text{ sec}$$

which is an increase of 13 percent over that predicted by the fixed-base model. For systems responding in the constant-velocity portion of the spectrum, accelerations (and thus forces) are a function of $1/T$ and relative displacements are a function of T. Therefore, with respect to the fixed-based model, the

combined system would have forces that are 12 percent smaller and displacements that are 13 percent larger. In the context of earthquake engineering, those differences are not significant.

6

Structural Steel Design

Rafael Sabelli, S.E. and Brian Dean, P.E.

Originally developed by
James R. Harris, P.E., PhD, Frederick R. Rutz, P.E., PhD and Teymour Manouri, P.E., PhD

Contents

6.1 INDUSTRIAL HIGH-CLEARANCE BUILDING, ASTORIA, OREGON 3
6.1.1 Building Description 3
6.1.2 Design Parameters 6
6.1.3 Structural Design Criteria 7
6.1.4 Analysis 10
6.1.5 Proportioning and Details 16
6.2 SEVEN-STORY OFFICE BUILDING, LOS ANGELES, CALIFORNIA 40
6.2.1 Building Description 40
6.2.2 Basic Requirements 42
6.2.3 Structural Design Criteria 44
6.2.4 Analysis and Design of Alternative A: SMF 46
6.2.5 Analysis and Design of Alternative B: SCBF 60
6.2.6 Cost Comparison 72
6.3 TEN-STORY HOSPITAL, SEATTLE, WASHINGTON 72
6.3.1 Building Description 72
6.3.2 Basic Requirements 76
6.3.3 Structural Design Criteria 78
6.3.4 Elastic Analysis 80
6.3.5 Initial Proportioning and Details 86
6.3.6 Nonlinear Response History Analysis 93

This chapter illustrates how the 2009 *NEHRP Recommended Provisions* (the *Provisions*) is applied to the design of steel framed buildings. The following three examples are presented:

1. An industrial warehouse structure in Astoria, Oregon
2. A multistory office building in Los Angeles, California
3. A mid-rise hospital in Seattle, Washington

The discussion examines the following types of structural framing for resisting horizontal forces:

- Ordinary concentrically braced frames (OCBF)
- Special concentrically braced frames
- Intermediate moment frames
- Special moment frames
- Buckling-restrained braced frames, with moment-resisting beam-column connections

The examples cover design for seismic forces in combination with gravity they are presented to illustrate only specific aspects of seismic analysis and design—such as lateral force analysis, design of concentric and eccentric bracing, design of moment resisting frames, drift calculations, member proportioning detailing.

All structures are analyzed using three-dimensional static or dynamic methods. ETABS (Computers & Structures, Inc., Berkeley, California, v.9.5.0, 2008) is used in Examples 6.1 and 6.2.

In addition to the 2009 *NEHRP Recommended Provisions*, the following documents are referenced:

- AISC 341 — American Institute of Steel Construction. 2005. *Seismic Provisions for Structural Steel Buildings*, including Supplement No. 1.
- AISC 358 — American Institute of Steel Construction. 2005. *Prequalified Connections for Special and Intermediate Steel Moment Frames for Seismic Applications*.
- AISC 360 — American Institute of Steel Construction. 2005. *Specification for Structural Steel Buildings.*
- AISC Manual — American Institute of Steel Construction. 2005. *Manual of Steel Construction*, 13th Edition.
- AISC SDM — American Institute of Steel Construction. 2006. *Seismic Design Manual.*
- IBC — International Code Council, Inc. 2006. *2006 International Building Code*.
- AISC SDGS-4 — AISC Steel Design Guide Series 4. Second Edition. 2003. *Extended End-Plate Moment Connections*, 2003.

- SDI — Luttrell, Larry D. 1981. S*teel Deck Institute Diaphragm Design Manual*. Steel Deck Institute.

The symbols used in this chapter are from Chapter 11 of the *Standard*, the above referenced documents, or are as defined in the text. U.S. Customary units are used.

6.1 INDUSTRIAL HIGH-CLEARANCE BUILDING, ASTORIA, OREGON

This example utilizes a transverse intermediate steel moment frame and a longitudinal ordinary concentric steel braced frame. The following features of seismic design of steel buildings are illustrated:

- Seismic design parameters
- Equivalent lateral force analysis
- Three-dimensional analysis
- Drift check
- Check of compactness and spacing for moment frame bracing
- Moment frame connection design
- Proportioning of concentric diagonal bracing

6.1.1 Building Description

This building has plan dimensions of 180 feet by 90 feet and a clear height of approximately 30 feet. It includes a 12-foot-high, 40-foot-wide mezzanine area at the east end of the building. The structure consists of 10 gable frames spanning 90 feet in the transverse (north-south) direction. Spaced at 20 feet on center, these frames are braced in the longitudinal (east-west) direction in two bays at the east end. The building is enclosed by nonstructural insulated concrete wall panels and is roofed with steel decking covered with insulation and roofing. Columns are supported on spread footings.

The elevation and transverse sections of the structure are shown in Figure 6.1-1. Longitudinal struts at the eaves and at the mezzanine level run the full length of the building and therefore act as collectors for the distribution of forces resisted by the diagonally braced bays and as weak-axis stability bracing for the moment frame columns.

The roof and mezzanine framing plans are shown in Figure 6.1-2. The framing consists of a steel roof deck supported by joists between transverse gable frames. The mezzanine represents both an additional load and additional strength and stiffness. Because all the frames resist lateral loading, the steel deck functions as a diaphragm for distribution of the effects of eccentric loading caused by the mezzanine floor when the building is subjected to loads acting in the transverse direction.

The mezzanine floor at the east end of the building is designed to accommodate a live load of 125 psf. Its structural system is composed of a concrete slab over steel decking supported by floor beams spaced at 10 feet on center. The floor beams are supported on girders continuous over two intermediate columns spaced approximately 30 feet apart and are attached to the gable frames at each end.

The member sizes in the main frame are controlled by serviceability considerations. Vertical deflections due to snow were limited to 3.5 inches and lateral sway due to wind was limited to 2 inches.

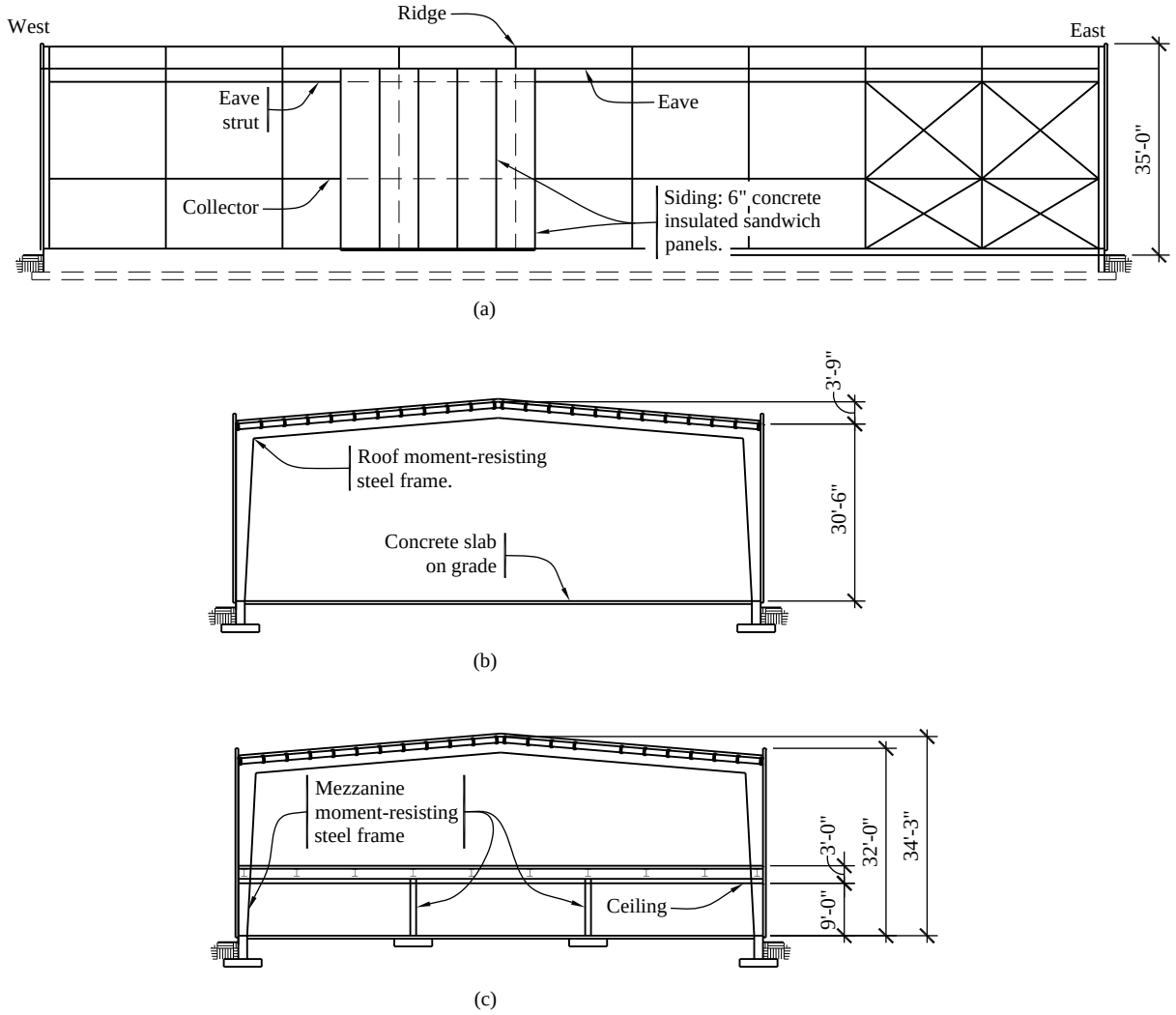

Figure 6.1-1 Framing elevation and sections
(1.0 ft = 0.3048 m; 1.0 in. = 25.4 mm)

Earthquake rather than wind governs the lateral design due to the mass of the insulated concrete panels. The panels are attached with long pins perpendicular to the concrete surface. These slender, flexible pins isolate the panels from acting as shear walls.

The building is supported on spread footings based on moderately deep alluvial deposits (i.e., medium dense sands). The foundation plan is shown in Figure 6.1-3. Transverse ties are placed between the footings of the two columns of each moment frame to provide restraint against horizontal thrust from the moment frames. Grade beams carrying the enclosing panels serve as ties in the longitudinal direction as well as across the end walls. The design of footings and columns in the braced bays requires consideration of combined seismic loadings. The design of foundations is not included here.

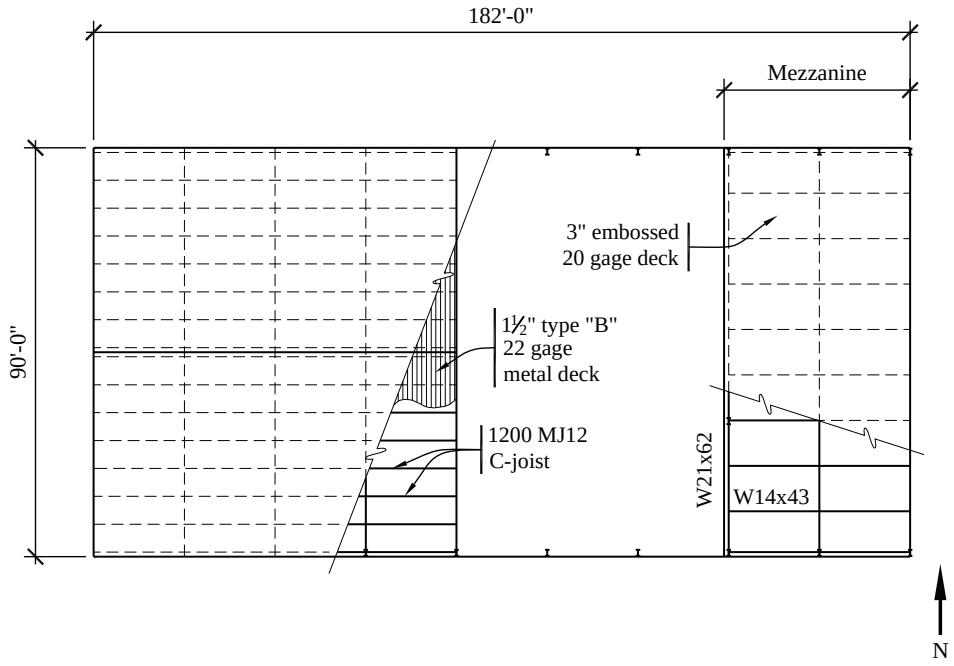

Figure 6.1-2 Roof framing and mezzanine framing plan
(1.0 ft = 0.3048 m; 1.0 in. = 25.4 mm)

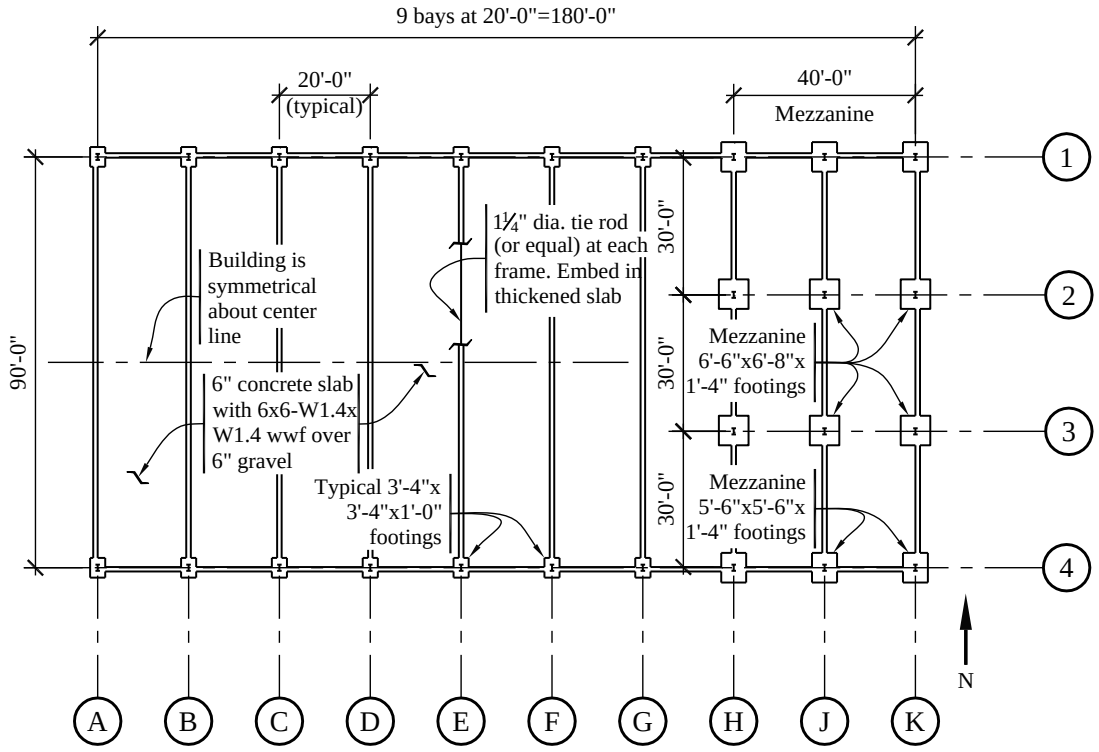

Figure 6.1-3 Foundation plan
(1.0 ft = 0.3048 m; 1.0 in. = 25.4 mm)

6.1.2 Design Parameters

6.1.2.1 Ground motion and system parameters. See Section 3.2 for an example illustrating the determination of design ground motion parameters. For this example the parameters are as follows.

- S_{DS} = 1.0
- S_{D1} = 0.6
- Occupancy Category II
- Seismic Design Category D

Note that *Standard* Section 12.2.5.6 permits an ordinary steel moment frame for buildings that do not exceed one story and 65 feet tall with a roof dead load not exceeding 20 psf. Intermediate steel moment frames with stiffened bolted end plates and ordinary steel concentrically braced frames are used in this example.

- North-south (N-S) direction:

  Moment-resisting frame system = intermediate steel moment frame (*Standard* Table 12.2-1)
  R = 4.5

$\Omega_0 = 3$
$C_d = 4$

- East-west (E-W) direction:

  Braced frame system = ordinary steel concentrically braced frame (*Standard* Table 12.2-1)
  $R = 3.25$
  $\Omega_0 = 2$
  $C_d = 3.25$

6.1.2.2 Loads

- Roof live load (L), snow = 25 psf
- Roof dead load (D) = 15 psf
- Mezzanine live load, storage = 125 psf
- Mezzanine slab and deck dead load = 69 psf
- Weight of wall panels = 75 psf

Roof dead load includes roofing, insulation, metal roof deck, purlins, mechanical and electrical equipment that portion of the main frames that is tributary to the roof under lateral load. For determination of the seismic weights, the weight of the mezzanine will include the dead load plus 25 percent of the storage load (125 psf) in accordance with *Standard* Section 12.7.2. Therefore, the mezzanine seismic weight is 69 + 0.25(125) = 100 psf.

6.1.2.3 Materials

- Concrete for footings: f_c' = 2.5 ksi
- Slabs-on-grade: f_c' = 4.5 ksi
- Mezzanine concrete on metal deck: f_c' = 3.0 ksi
- Reinforcing bars: ASTM A615, Grade 60
- Structural steel (wide flange sections): ASTM A992, Grade 50
- Plates (except continuity plates): ASTM A36
- Bolts: ASTM A325
- Continuity Plates: ASTM A572, Grade 50

6.1.3 Structural Design Criteria

6.1.3.1 Building configuration. Because there is a mezzanine at one end, vertical weight irregularities might be considered to apply (*Standard* Sec. 12.3.2.2). However, the upper level is a roof and the

Standard exempts roofs from weight irregularities. There also are no plan irregularities in this building (*Standard* Sec. 12.3.2.1).

6.1.3.2 Redundancy. In the N-S direction, the moment frames do not meet the requirements of *Standard* Section 12.3.4.2b since the frames are only one bay long. Thus, *Standard* Section 12.3.4.2a must be checked. A copy of the three-dimensional model is made, with the moment frame beam at Gridline A pinned. The structure is checked to make sure that an extreme torsional irregularity (*Standard* Table 12.3-1) does not occur:

$$1.4\left(\frac{\Delta_K + \Delta_A}{2}\right) \geq \Delta_A$$

$$1.4\left(\frac{4.17\,\text{in.} + 6.1\,\text{in.}}{2}\right) = 7.19\,\text{in.} \geq 6.1\,\text{in.}$$

where:

Δ_A = maximum displacement at knee along Gridline A, in.

Δ_K = maximum displacement at knee along gridline K, in.

Thus, the structure does not have an extreme torsional irregularity when a frame loses moment resistance.

Additionally, the structure must be checked in the N-S direction to ensure that the loss of moment resistance at Beam A has not resulted in more than a 33 percent reduction in story strength. This can be checked using elastic methods (based on first yield) as shown below, or using strength methods. The original model is run with the N-S load combinations to determine the member with the highest demand-capacity ratio. This demand-capacity ratio, along with the applied base shear, is used to calculate the base shear at first yield:

$$V_{yield} = \left(\frac{1}{(D/C)_{max}}\right) V_{base}$$

$$V_{yield} = \left(\frac{1}{0.89}\right)(223\,\text{kips}) = 250.5\,\text{kips}$$

where:

V_{base} = base shear from Equivalent Lateral Force (ELF) analysis

A similar analysis can be made using the model with no moment resistance at Frame A:

$$V_{yield,MFremoved} = \left(\frac{1}{0.951}\right)(223\,\text{kips}) = 234.5\,\text{kips}$$

$$\frac{V_{yield,MFremoved}}{V_{yield}} = \frac{234.5\,\text{kips}}{250.5\,\text{kips}} = 0.94$$

Thus, the loss of resistance at both ends of a single beam only results in a 6 percent reduction in story strength. The moment frames can be assigned a value of $\rho = 1.0$.

In the E-W direction, the OCBF system meets the prescriptive requirements of *Standard* Section 12.3.4.2a. As a result, no further calculations are needed and this system can be assigned a value of $\rho = 1.0$.

6.1.3.3 Orthogonal load effects. A combination of 100 percent seismic forces in one direction plus 30 percent seismic forces in the orthogonal direction must be applied to the columns of this structure in Seismic Design Category D (*Standard* Sec. 12.5.4).

6.1.3.4 Structural component load effects. The effect of seismic load (*Standard* Sec. 12.4.2) is:

$$E = \rho Q_E \pm 0.2 S_{DS} D$$

$S_{DS} = 1.0$ for this example. The seismic load is combined with the gravity loads as shown in *Standard* Sec. 12.4.2.3, resulting in the following:

$$1.4D + 1.0L + 0.2S + \rho Q_E$$

$$0.7D + \rho Q_E$$

Note that $1.0L$ is for the storage load on the mezzanine; the coefficient on L is 0.5 for many common live loads.

6.1.3.5 Drift limits. For a building assigned to Occupancy Category II, the allowable story drift (*Standard* Table 12.12-1) is:

- $\Delta_a = 0.025 h_{sx}$ in the E-W direction
- $\Delta_a/\rho = 0.025 h_{sx}/1.0$ in the N-S direction

At the roof ridge, h_{sx} = 34 ft-3 in. and Δ_a = 10.28 in.

At the knee (column-roof intersection), h_{sx} = 30 ft-6 in. and Δ_a = 9.15 in.

At the mezzanine floor, h_{sx} = 12 ft and Δ_a = 3.60 in.

Footnote c in *Standard* Table 12.12-1 permits unlimited drift for single-story buildings with interior walls, partitions, etc., that have been designed to accommodate the story drifts. See Section 6.1.4.3 for further discussion. The main frame of the building can be considered to be a one-story building for this purpose, given that there are no interior partitions except below the mezzanine. (The definition of a story in building codes generally does not require that a mezzanine be considered a story unless its area exceeds one-third the area of the room or space in which it is placed; this mezzanine is less than one-third of the footprint of the building.)

6.1.3.6 Seismic weight. The weights that contribute to seismic forces are:

	E-W direction	N-S direction
Roof D = (0.015)(90)(180) =	243 kips	243 kips
Panels at sides = (2)(0.075)(32)(180)/2 =	0 kips	437 kips
Panels at ends = (2)(0.075)(35)(90)/2 =	224 kips	0 kips
Mezzanine slab and 25% LL =	360 kips	360 kips
Mezzanine framing =	35 kips	35 kips
Main frames =	27 kips	27 kips
Seismic weight =	889 kips	1,102 kips

The weight associated with the main frames accounts for only the main columns, because the weight associated with the remainder of the main frames is included in the roof dead load above. The computed seismic weight is based on the assumption that the wall panels offer no shear resistance for the structure but are self-supporting when the load is parallel to the wall of which the panels are a part. Additionally, snow load does not need to be included in the seismic weight per *Standard* Section 12.7.2 because it does not exceed 30 psf.

6.1.4 Analysis

Base shear will be determined using an ELF analysis.

6.1.4.1 Equivalent Lateral Force procedure. In the longitudinal direction where stiffness is provided only by the diagonal bracing, the approximate period is computed using *Standard* Equation 12.8-7:

$$T_a = C_r h_n^x = (0.02)\left(34.25^{0.75}\right) = 0.28\,\text{sec}$$

where h_n is the height of the building, taken as 34.25 feet at the mid-height of the roof. In accordance with *Standard* Section 12.8.2, the computed period of the structure must not exceed the following:

$$T_{max} = C_u T_a = (1.4)(0.28) = 0.39\,\text{sec}$$

The subsequent three-dimensional modal analysis finds the computed period to be 0.54 seconds. For purposes of determining the required base shear strength, T_{max} will be used in accordance with the *Standard*; drift will be calculated using the period from the model.

In the transverse direction where stiffness is provided by moment-resisting frames (*Standard* Eq. 12.8-7):

$$T_a = C_r h_n^x = (0.028)\left(34.25^{0.8}\right) = 0.47\,\text{sec}$$

and

$$T_{max} = C_u T_a = (1.4)(0.47) = 0.66\,\text{sec}$$

Also note that the dynamic analysis finds a computed period of 1.03 seconds. As in the longitudinal direction, T_{max} will be used for determining the required base shear strength.

The seismic response coefficient (C_s) is computed in accordance with *Standard* Section 12.8.1.1. In the longitudinal direction:

$$C_S = \frac{S_{DS}}{R/I} = \frac{1.0}{3.25/1.0} = 0.308$$

but need not exceed:

$$C_S = \frac{S_{D1}}{T\left(\frac{R}{I}\right)} = \frac{0.6}{0.39\left(\frac{3.25}{1.0}\right)} = 0.473$$

Therefore, use C_s = 0.308 for the longitudinal direction.

In the transverse direction:

$$C_S = \frac{S_{DS}}{R/I} = \frac{1.0}{4.5/1} = 0.222$$

but need not exceed:

$$C_S = \frac{S_{DS}}{T(R/I)} = \frac{0.6}{(0.66)(4.5/1)} = 0.202$$

Therefore, use C_s = 0.202 for the transverse direction.

In both directions the value of C_s exceeds the minimum value (*Standard* Eq. 12.8-5) computed as:

$$C_S = 0.044IS_{DS} \geq 0.01 = (0.044)(1)(1.0) = 0.044$$

The seismic base shear in the longitudinal direction (*Standard* Eq. 12.8-1) is:

$$V = C_S W = (0.308)(889\,\text{kips}) = 274\,\text{kips}$$

The seismic base shear in the transverse direction is:

$$V = C_S W = (0.202)(1102\,\text{kips}) = 223\,\text{kips}$$

Standard Section 12.8.3 prescribes the vertical distribution of lateral force in a multilevel structure. Even though the building is considered to be one story for some purposes, it is clearly a two-level structure. Using the data in Section 6.1.3.6 of this example and interpolating the exponent *k* as 1.08 for the period of 0.66 second, the distribution of forces for the N-S analysis is shown in Table 6.1-1.

Table 6.1-1 ELF Vertical Distribution for N-S Analysis

Level	Weight (w_x) (kips)	Height (h_x) (ft)	$w_x h_x^{\,k}$	$C_{vx} = \frac{w_x h_x^k}{\sum_{i=1}^{n} w_{ih_x^k}}$	$F_x = C_{vx} V$ (kips)
Roof	707	32.375	30,231	0.84	187

Table 6.1-1 ELF Vertical Distribution for N-S Analysis

Level	Weight (w_x) (kips)	Height (h_x) (ft)	$w_x h_x^k$	$C_{vx} = \frac{w_x h_x^k}{\sum_{i=1}^{n} w_{ih_x^k}}$	$F_x = C_{vx} V$ (kips)
Mezzanine	395	12	5,782	0.16	36
Total	1,102		36,013		223

It is not immediately clear whether the roof (a 22-gauge steel deck with conventional roofing over it) will behave as a flexible, semi-rigid, or rigid diaphragm. For this example, a three-dimensional model was created in ETABS including frame and diaphragm stiffness.

6.1.4.2 Three-dimensional ELF analysis. The three-dimensional analysis is performed for this example to account for the following:

- The differing stiffness of the gable frames with and without the mezzanine level
- The different centers of mass for the roof and the mezzanine
- The flexibility of the roof deck
- The significance of braced frames in controlling torsion due to N-S ground motions

The gabled moment frames, the tension bracing, the moment frames supporting the mezzanine and the diaphragm chord members are explicitly modeled using three-dimensional beam-column elements. The tapered members are approximated as short, discretized prismatic segments. Thus, combined axial bending checks are performed on a prismatic element, as required by AISC 360 Chapter H. The collector at the knee level is included, as are those at the mezzanine level in the two east bays. The mezzanine diaphragm is modeled using planar shell elements with their in-plane rigidity being based on actual properties and dimensions of the slab. The roof diaphragm also is modeled using planar shell elements, but their in-plane rigidity is based on a reduced thickness that accounts for compression buckling phenomena and for the fact that the edges of the roof diaphragm panels are not connected to the wall panels. SDI's *Diaphragm Design Manual* is used for guidance in assessing the stiffness of the roof deck. The analytical model includes elements with one-tenth the stiffness of a plane plate of 22 gauge steel.

The ELF analysis of the three-dimensional model in the transverse direction yields an important result: the roof diaphragm behaves as a rigid diaphragm. Accidental torsion is applied at the center of the roof as a moment whose magnitude is the roof lateral force multiplied by 5 percent of 180 feet (9 feet). A moment is also applied to the mezzanine level in a similar fashion. The resulting displacements are shown in Table 6.1-2.

Table 6.1-2 ELF Analysis Displacements in N-S Direction

Grid	Roof Displacement (in.)
A	4.98
B	4.92

Table 6.1-2 ELF Analysis Displacements in N-S Direction

Grid	Roof Displacement (in.)
C	4.82
D	4.68
E	4.56
F	4.46
G	4.34
H	4.19
J	4.05
K	3.92

The average of the extreme displacements is 4.45 inches. The displacement at the centroid of the roof is 4.51 inches. Thus, the deviation of the diaphragm from a straight line is 0.06 inch, whereas the average frame displacement is approximately 75 times that. Clearly, then, the diaphragm flexibility is negligible and the deck behaves as a rigid diaphragm. The ratio of maximum to average displacement is 1.1, which does not exceed the 1.2 limit given in *Standard* Table 12.3-1 and torsional irregularity is not triggered.

The same process needs to be repeated for the E-W direction.

Table 6.1-3 ELF Analysis Displacements in N-S Direction

Grid	Roof Displacement (in.)
1	0.88
2/3	0.82
4	0.75

The ratio of the maximum to average displacement is 1.07, well under the torsional irregularity threshold ratio of 1.2.

The demands from the three-dimensional ELF analysis are combined to meet the orthogonal combination requirement of *Standard* Section 12.5.3 for the columns:

- E-W: (1.0)(E-W direction spectrum) + (0.3)(N-S direction spectrum)
- N-S: (0.3)(E-W direction spectrum) + (1.0)(N-S direction spectrum)

6.1.4.3 Drift. The lateral deflection cited previously must be multiplied by $C_d = 4$ to find the transverse drift:

$$\delta_x = \frac{C_d \delta_e}{I} = \frac{(4)(4.51)}{1.0} = 18 \text{ in.}$$

This exceeds the limit of 10.28 inches computed previously. However, there is no story drift limit for single-story structures with interior wall, partitions, ceilings and exterior wall systems that have been designed to accommodate the story drifts. Detailing for this type of design may be problematic.

In the longitudinal direction, the lateral deflection is much smaller and is within the limits of *Standard* Section 12.12.1. The deflection computations do not include the redundancy factor.

6.1.4.4 P-delta effects. The P-delta effects on the structure may be neglected in analysis if the provisions of *Standard* Section 12.8.7 are followed. First, the stability coefficient maximum should be determined using *Standard* Equation 12.8-17. β may be assumed to be 1.0.

$$\theta_{max} = \frac{0.5}{\beta C_d} \le 0.25$$

$$\theta_{max,N-S} = \frac{0.5}{(1.0)(4)} = 0.125$$

$$\theta_{max,E-W} = \frac{0.5}{(1.0)(3.25)} = 0.154$$

Next, the stability coefficient is calculated using *Standard* Equation 12.8-16. The stability coefficient is calculated at both the roof and mezzanine levels in both orthogonal directions. For purposes of illustration, the roof level check in the N-S direction will be shown as:

$$\theta = \frac{P_x \Delta I}{V_x h_{sx} C_d} \qquad \Delta = \frac{C_d (\delta_{e2} - \delta_{e1})}{I}$$

$$\theta = \frac{P_x (\delta_{e2} - \delta_{e1}) C_d I}{V_x h_{sx} C_d I} = \frac{P_x (\delta_{e2} - \delta_{e1})}{V_x h_{sx}}$$

$$P_{roof} = \text{Roof LL} + \text{Roof DL} + \text{Panels} + \text{Frames}$$

$$P_{roof} = (180\,\text{ft} \times 90\,\text{ft})(15\,\text{psf} + 25\,\text{psf}) + 437\,\text{kips} + 224\,\text{kips} + 27\,\text{kips}$$

$$P_{roof} = 1336\,\text{kips}$$

$$\theta = \frac{(1{,}336\,\text{kips})(4.51\,\text{in.})}{(187\,\text{kips})(32.375\,\text{ft})} = 0.083 < 0.1$$

The three other stability coefficients were all determined to be less than θ_{max}, thus allowing P-delta effects to be excluded from the analysis.

6.1.4.5 Force summary. The maximum moments and axial forces caused by dead, live and earthquake loads on the gable frames are listed in Tables 6.1-3 and 6.1-4. The frames are symmetrical about their

ridge and the loads are either symmetrical or can be applied on either side on the frame because the forces are given for only half of the frame extending from the ridge to the ground. The moments are given in Table 6.1-4 and the axial forces are given in Table 6.1-5. The moment diagram for the combined load condition is shown in Figure 6.1-4. The load combination is $1.4D + L + 0.2S + \rho Q_E$, which is used throughout the remainder of calculations in this section, unless specifically noted otherwise.

The size of the members is controlled by gravity loads, not seismic loads. The design of connections will be controlled by the seismic loads.

Forces in the design of the braces are discussed in Section 6.1.5.5.

Table 6.1-4 Moments in Gable Frame Members

Location	D (ft-kips)	L (ft-kips)	S (ft-kips)	Q_E (ft-kips)	Combined* (ft-kips)
1 - Ridge	61	0	128	0	112 (279)
2 - Knee	161	0	333	162	447 (726)
3 - Mezzanine	95	83	92	137	79
4 - Base	0	0	0	0	0

* Combined Load = $1.4D + L + 0.2S + \rho Q_E$ (or $1.2D + 1.6S$). Individual maxima are not necessarily on the same frame; combined load values are maximum for any frame.
1.0 ft = 0.3048 m, 1.0 kip = 1.36 kN-m.

Table 6.1-5 Axial Forces in Gable Frame Members

Location	D (ft-kips)	L (ft-kips)	S (ft-kips)	ρQ_E (ft-kips)	Combined* (ft-kips)
1 - Ridge	14	3.5	25	0.8	39
2 - Knee	16	4.5	27	7.0	37
3 - Mezzanine	39	39	23	26	127
4 - Base	39	39	23	26	127

* Combined Load = $1.4D + L + 0.2S + \rho Q_E$. Individual maxima are not necessarily on the same frame; combined load values are maximum for any frame.
1.0 ft = 0.3048 m, 1.0 kip = 1.36 kN-m.

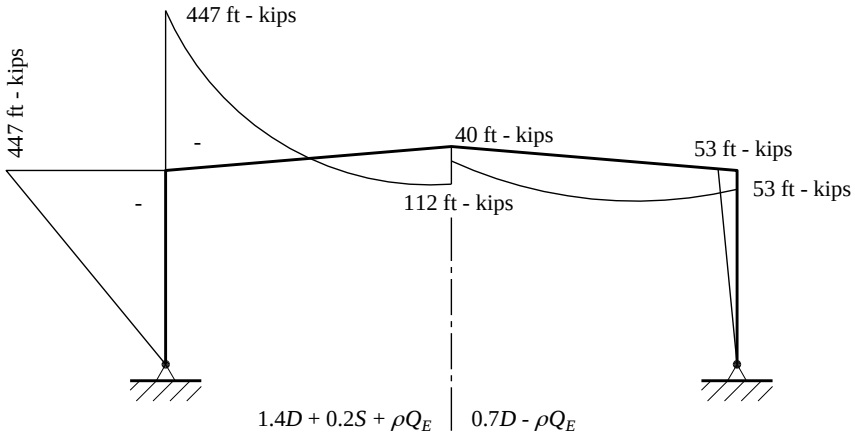

Figure 6.1-4 Moment diagram for seismic load combinations
(1.0 ft-kip = 1.36 kN-m)

6.1.5 Proportioning and Details

The gable frame is shown schematically in Figure 6.1-5. Using the load combinations presented in Section 6.1.3.4 and the loads from Tables 6.1-4 and 6.1-5, the proportions of the frame are checked at the roof beams and the variable-depth columns (at the knee). The mezzanine framing, also shown in Figure 6.1-1, was proportioned similarly. The diagonal bracing, shown in Figure 6.1-1 at the east end of the building, is proportioned using tension forces determined from the three-dimensional ELF analysis.

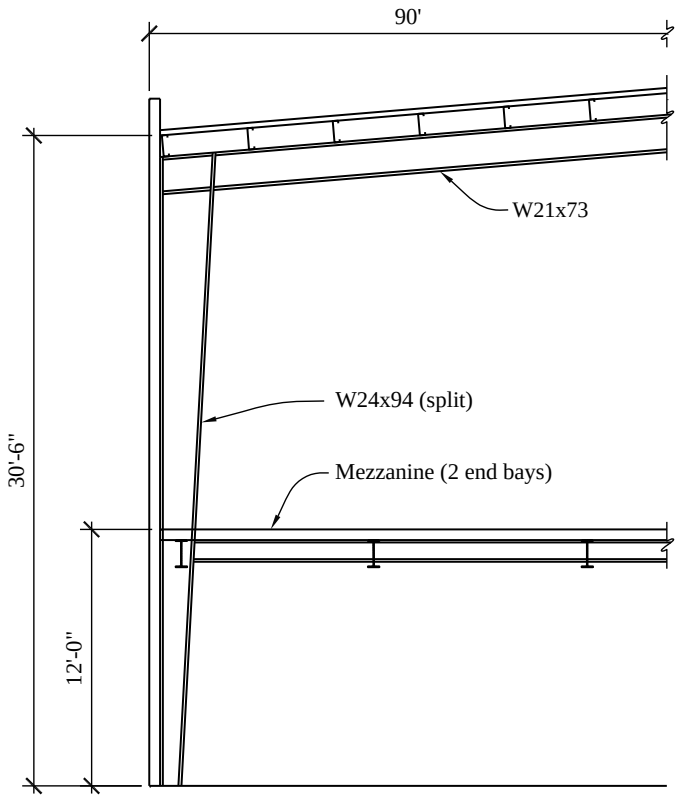

Figure 6.1-5 Gable frame schematic: Column tapers from 12 in. at base to 36 in. at knee; roof beam tapers from 36 in. at knee to 18 in. at ridge; plate sizes are given in Figure 6.1-7
(1.0 in. = 25.4 mm)

Additionally, the bolted, stiffened, extended end-plate connections must be sized correctly to conform to the pre-qualification standards. AISC 358 Table 6.1 provides parametric limits on the beam and connection sizes. Table 6.1-6 shows these limits as well as the values used for design.

Table 6.1-6 Parametric Limits for Moment Frame Connection

Parameter	Minimum (in.)	As Designed (in.)	Maximum (in.)
t_p	3/4	1 1/4	2 1/2
b_p	9	9	15
g	5	5	6
p_{fi}, p_{fo}	1 3/4	1 3/4	2
p_b	3 1/2	3 1/2	3 3/4
d	18 1/2	36	36
t_{bf}	19/32	5/8	1
b_{bf}	7 3/4	8	12 1/4

6.1.5.1 Frame compactness and brace spacing. According to *Standard* Section 14.1.3, steel structures assigned to Seismic Design Category D, E, or F must be designed and detailed per AISC 341. For an intermediate moment frame (IMF), AISC 341, Part I, Section 1, "Scope," stipulates that those requirements are to be applied in conjunction with AISC 360. Part I, Section 10 of AISC 341 itemizes a few additional items from AISC 360 for intermediate moment frames, but otherwise the intermediate moment frames are to be designed per AISC 360.

AISC 341 requires IMFs to have compact width-thickness ratios per AISC 360, Table B4.1.

All width-thickness ratios are less than the limiting λ_p from AISC 360, Table B4.1. All P-M ratios (combined compression and flexure) are less than 1.00. This is based on proper spacing of lateral bracing.

Lateral bracing is provided by the roof joists. The maximum spacing of lateral bracing is determined using beam properties at the ends and AISC 341, Section 10.8:

$$L_{b,max} \le 0.17 r_y \frac{E}{F_y}$$

$$L_{b,max} \le 0.17(1.46\text{in.})\left(\frac{29000\,\text{ksi}}{50\,\text{ksi}}\right) = 148 \text{ in.}$$

L_b is 48 inches; therefore, the spacing is OK.

Also, the required brace strength and stiffness are calculated per AISC 360, Equations A-6-7 and A-6-8:

$$P_{br} = \frac{0.02 M_r C_d}{h_o}$$

$$\beta_{br} = \frac{1}{\phi}\left(\frac{10 M_r C_d}{L_b h_o}\right)$$

where:

$$M_r = R_y Z F_y$$

$$C_d = 1.0$$

h_o = distance between flange centroids, in.

L_b = distance between braces or L_p (from AISC 360 Eq. F2-5), whichever is greater, in.

$$M_r = (1.1)\left(309 \text{ in.}^3\right)(50 \text{ ksi}) = 16{,}992 \text{ in.-kip} = 1{,}416 \text{ ft-kip}$$

$$P_{br} = \frac{0.02(16{,}992 \text{ in.-kip})(1.0)}{(36 \text{ in.} - 5/8 \text{ in.})}$$

$$P_{br} = 9.61 \text{ kips}$$

$$L_p = 1.76 r_y \sqrt{\frac{E}{F_y}}$$

$$L_p = 1.76(1.46 \text{ in.})\sqrt{\frac{29{,}000 \text{ ksi}}{50 \text{ ksi}}} = 62 \text{ in.}$$

$$\beta_{br} = \frac{1}{(0.75)}\left(\frac{10(16{,}992 \text{ in.-kip})(1.0)}{(62 \text{ in.})(35.375 \text{ in.})}\right)$$

$$\beta_{br} = 104 \text{ kips/in.}$$

Adjacent to the plastic hinge regions, lateral bracing must have additional strength as defined in AISC 341 10.8

$$P_u = \frac{0.06 M_u}{h_o}$$

$$P_u = \frac{0.06(16992 \text{in -kip})}{(35.375 \text{in.})}$$

$$P_u = 28.8 \text{kips}$$

The C-joists used in this structure likely are not adequate to brace the moment frames. Instead, tube brace members will be used, but they are not analyzed in this example.

At the negative moment regions near the knee, lateral bracing is necessary on the bottom flange of the beams and inside the flanges of the columns (Figure 6.1-6).

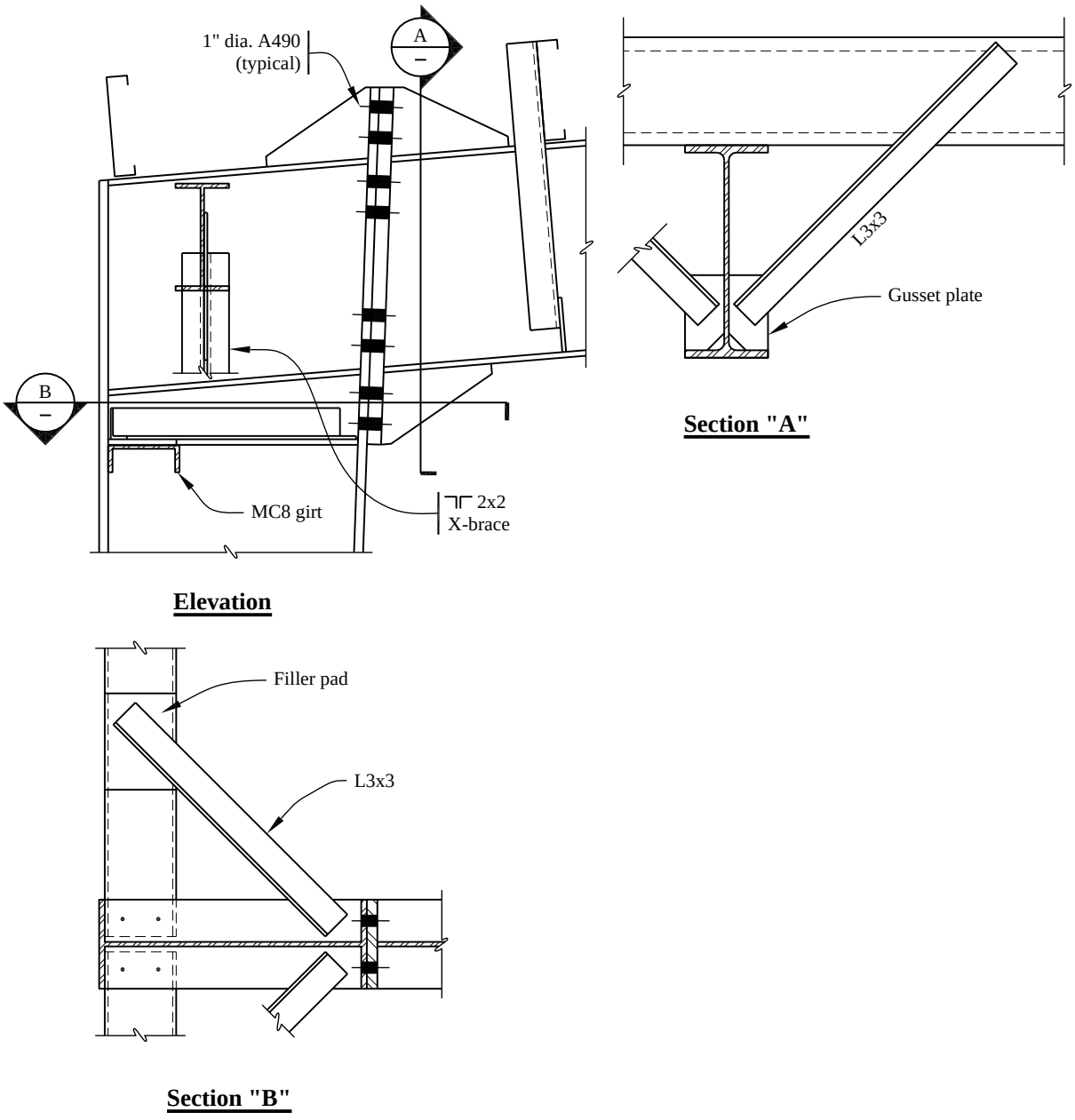

Figure 6.1-6 Arrangement at knee
(1.0 in. = 25.4 mm)

6.1.5.2 Knee of the frame. The knee detail is shown in Figures 6.1-6 and 6.1-7. The vertical plate shown near the upper left corner in Figure 6.1-6 is a gusset providing connection for X-bracing in the longitudinal direction. The beam-to-column connection requires special consideration. The method of AISC 358 for bolted, stiffened end plate connections is used. Refer to Figure 6.1-8 for the configuration. Highlights from this method are shown for this portion of the example. Refer to AISC 358 for a discussion of the entire procedure.

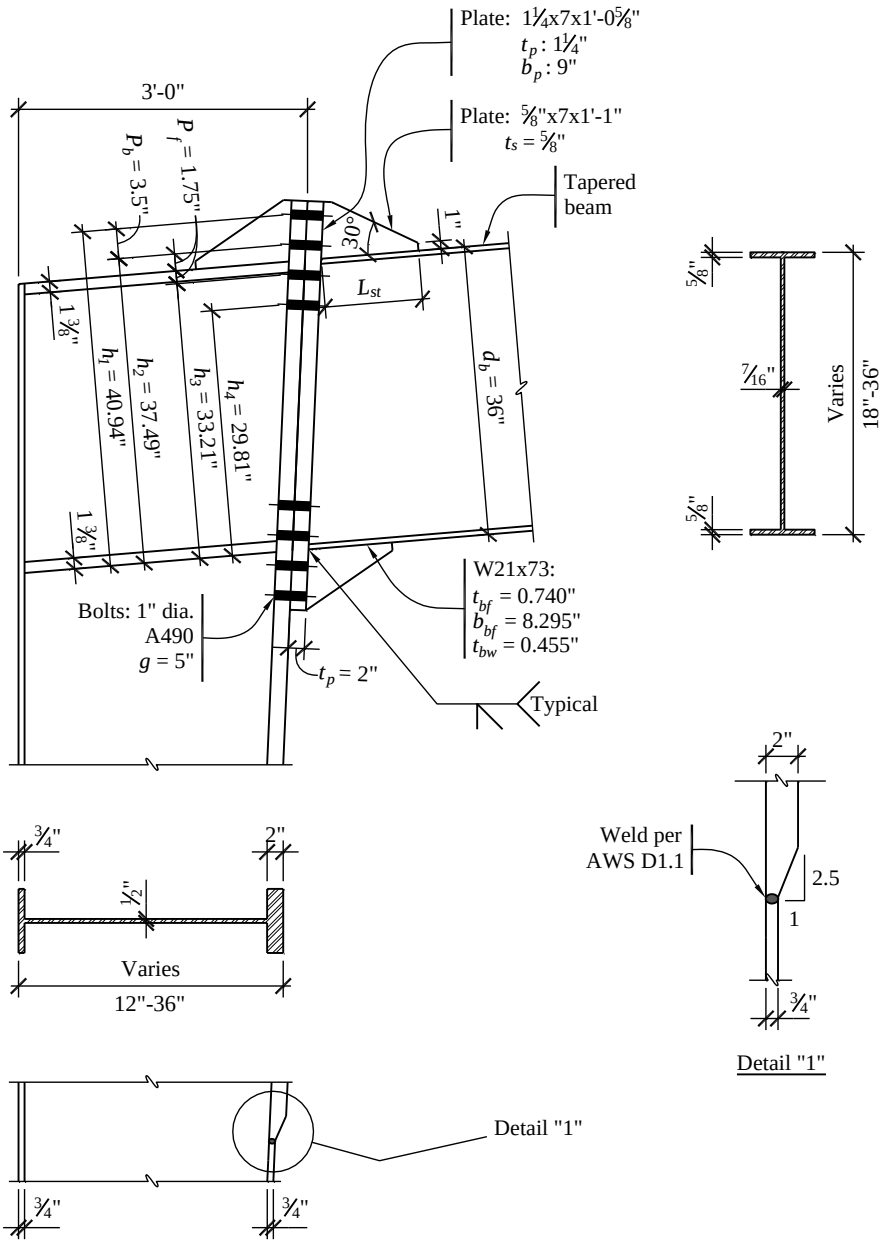

Figure 6.1-7 Bolted stiffened connection at knee
(1.0 in. = 25.4 mm)

The AISC 358 method for bolted stiffened end plate connection requires the determination of the maximum moment that can be developed by the beam. The steps in AISC 358 for bolted stiffened end plates follow:

Step 1. Determine the maximum moment at the plastic hinge location. The end plate stiffeners at the top and bottom flanges increase the local moment of inertia of the beam, forcing the plastic hinge to occur away from the welds at the end of beam/face of column. The stiffeners should be long enough to force the plastic hinge to at least $d/2$ away from the end of the beam. With

the taper of the section, the depth will be slightly less than 36 inches at the location of the hinge, but that reduction will be ignored here. The probable maximum moment, M_{pe}, at the plastic hinge is computed using AISC 358 Equation 6.9-2 as follows:

$$M_{pe} = C_{pr} R_y F_y Z_x$$

Where, per AISC 358 Equation 2.4.3-2:

$$C_{pr} = \frac{F_y + F_u}{2F_y} \le 1.2$$

$$C_{pr} = \frac{50 + 65}{2(50)}$$

$$C_{pr} = 1.15$$

where:

R_y = 1.1 from AISC 341 Table I-6-1

Z_e = 309 in.^{3}

F_y = 50 ksi

Therefore:

$$M_{pe} = (1.15)(1.1)(50 \text{ ksi})(309 \text{ in.}^3) = 19{,}541 \text{ in.-kip} = 1{,}628 \text{ ft-kip}$$

The moment at the column flange, M_f, which drives the connection design, is determined from AISC 358 Equation 6.9-2 as follows:

$$M_f = M_{pe} + V_u S_h$$

where:

V_u = shear at location of plastic hinge

L' = distance between plastic hinges

S_h = distance from the face of the column to the plastic hinge, ft.

$$S_h = L_{st} + t_p$$

where:

L_{st} = length of end-plate stiffener, as shown in AISC 358 Figure 6.2.

t_p = thickness of end plate, in.

$$L_{st} \geq \frac{h_{st}}{\tan 30°}$$

where:

h_{st} = height of the end-plate from the outside face of the beam flange to the end of the end-plate

$$L_{st} \geq \frac{(7\text{ in.})}{\tan 30°}$$

$$L_{st} \geq 12.1\text{ in.}$$

Use L_{st} = 13 in.

$$S_h = 13\text{ in.} + 1.25\text{ in.} = 14.3\text{ in.}$$

$$L' = L_{out} - 2d_c - 2S_h$$

$$L' = (90\text{ ft}) - 2(36\text{ in.}) - 2(14.3\text{ in.}) = 81.63\text{ ft}$$

$$V_u = \frac{2M_{pe}}{L'} + V_{gravity}$$

$$V_u = \frac{2(1628\text{ ft-kip})}{81.63\text{ ft}} + 18.9\text{ kips} = 58.8\text{ kips}$$

$$M_f = 19{,}541\text{ in.-kip} + (58.8\text{ kips})(14.3\text{ in.})$$

$$M_f = 1{,}698\text{ ft-kip} = 20{,}379\text{ in.-kip}$$

Step 2. Find bolt size for end plates. For a connection with two rows of two bolts inside and outside the flange, AISC 358 Equation 6.9-7 indicates the following:

$$d_{b\,req'd} = \sqrt{\frac{2M_f}{\pi\phi_n F_{nt}(h_1 + h_2 + h_3 + h_4)}}$$

where:

F_{nt} = nominal tensile stress of bolt, ksi

h_i = distance from the centerline of the beam compression flange to the centerline of the i^{th} tension bolt row, in.

Try A490 bolts. See Figure 6.1-7 for bolt geometry.

$$d_{b\,req'd} = \sqrt{\frac{2(20{,}379\text{ in.-kip})}{\pi(0.9)(113\text{ ksi})(29.81\text{ in.} + 33.31\text{ in.} + 37.44\text{ in.} + 40.94\text{ in.})}} = 0.95\text{ in.}$$

Use 1 in. diameter A490N bolts.

Step 3. Determine the minimum end-plate thickness from AISC 358 Equation 6.9-8.

$$t_{p\,req'd} = \sqrt{\frac{1.11M_f}{\phi_d F_{yp} Y_p}}$$

where:

F_{yp} = specified minimum yield stress of the end plate material, ksi

Y_p = the end-plate yield line mechanism parameter from AISC 358 Table 6.4

ϕ_d = resistance factor for ductile limit states, taken as 1.0

From AISC 358 Table 6.4:

$$s = \frac{1}{2}\sqrt{b_p g}$$

where:

b_p = width of the end plate, in.

g = horizontal distance between bolts on the end plate, in.

$$s = \frac{1}{2}\sqrt{(9\text{ in.})(5\text{ in.})} = 3.35\text{in.}$$

d_e = 7 in. (see Figure 6.1-7)

Use Case 1 from AISC 358 Table 6.4, since $d_e > s$

$$Y_p = \frac{b_p}{2}\left[h_1\left(\frac{1}{2d_e}\right) + h_2\left(\frac{1}{p_{fo}}\right) + h_3\left(\frac{1}{p_{fi}}\right) + h_4\left(\frac{1}{s}\right)\right]$$
$$+ \frac{2}{g}\left[h_1\left(d_e + \frac{p_b}{4}\right) + h_2\left(p_{fo} + \frac{3p_b}{4}\right) + h_3\left(p_{fi} + \frac{p_b}{4}\right) + h_4\left(s + \frac{3p_b}{4}\right) + p_b^2\right] + g$$

where:

p_{fo} = vertical distance between beam flange and the nearest outer row of bolts, in.

p_{fi} = vertical distance between beam flange and the nearest inner row of volts, in.

p_b = distance between the inner and our row of bolts, in.

$$Y_p = \frac{(9\text{ in.})}{2}\left[(40.94\text{ in.})\left(\frac{1}{3.35\text{ in.}}\right)+(37.44\text{ in.})\left(\frac{1}{1.75\text{ in.}}\right)+(33.31\text{ in.})\left(\frac{1}{1.75\text{ in.}}\right)+(29.81\text{ in.})\left(\frac{1}{3.35\text{ in.}}\right)\right]$$
$$+\frac{2}{(5\text{ in.})}\left[(40.94\text{ in.})\left(3.35\text{ in.}+\frac{(3.5\text{ in.})}{4}\right)+(37.44\text{ in.})\left(1.75\text{ in.}+\frac{3(3.5\text{ in.})}{4}\right)+(33.31\text{ in.})\left(1.75\text{ in.}+\frac{3.5\text{ in.}}{4}\right)+(29.81\text{ in.})\left(3.35\text{ in.}+\frac{3(3.5\text{ in.})}{4}\right)+(3.5\text{ in.})^2\right]$$
$$+(5\text{ in.})$$

$$Y_p = 499\text{ in.}$$

$$t_{p\,req'd} = \sqrt{\frac{1.11(20{,}379\text{ in.-kip})}{(1.0)(36\text{ ksi})(499\text{ in.})}} = 1.12\text{ in.}$$

Use 1.25-inch thick end-plates.

Step 4. Calculate the factored beam flange force from AISC 358 Equation 6.9-9.

$$F_{fu} = \frac{M_f}{d - t_{bf}}$$

where:

d = depth of the beam, in.

t_{bf} = thickness of beam flange, in.

$$F_{fu} = \frac{20{,}379\text{ in.-kip}}{36\text{ in.} - 5/8\text{ in.}} = 576\text{ kips}$$

Step 5. Determine the end-plate stiffener thickness from AISC 358 Equation 6.9-13.

$$t_s \geq t_{bw}\left(\frac{F_{yb}}{F_{ys}}\right)$$

where:

t_{bw} = thickness of the beam web, in.

F_{yb} = specified minimum yield stress of beam material, ksi

F_{ys} = specified minimum yield stress of stiffener material, ksi

$$t_s \geq (7/16 \text{ in.})\left(\frac{50 \text{ ksi}}{36 \text{ ksi}}\right) = 0.61 \text{ in.}$$

Use 5/8-inch plates.

The stiffener width-thickness ratio must also comply with AISC 358 Equation 6.9-14.

$$\frac{h_{st}}{t_s} \leq 0.56\sqrt{\frac{E}{F_{ys}}}$$

$$h_{st} \leq 0.56\sqrt{\frac{(29000 \text{ ksi})}{(36 \text{ ksi})}}(5/8 \text{ in.})$$

$$h_{st} \leq 9.93 \text{in.}$$

h_{st} = 7 in. OK

Step 6. Check bolt shear rupture strength at the compression flange by AISC 358 Equation 6.9-15.

$$V_u < \phi_n R_n = \phi_n (n_b) F_v A_b$$

where:

ϕ_n = resistance factor for non-ductile limit states, taken as 0.9

n_b = number of bolts at compression flange

F_v = nominal shear stress of bolts from AISC 360 Table J3.2, ksi

A_b = nominal bolt area, in.

$$\phi_n R_n = (0.9)(8)(60)\left(\pi\frac{1^2}{4}\right) = 339 \text{ kips} > 58.8 \text{ kips}$$ OK

Step 7. Check bolt bearing/tear-out of the end-plate and column flange by AISC 358 Equation 6.9-17.

$$V_u < \phi_n R_n = \phi_n (n_i) r_{ni} + \phi_n (n_o) r_{no}$$

where:

n_i = number of inner bolts

n_o = number of outer bolts

$r_{ni} = 1.2L_c tF_u < 2.4d_b tF_u$ for each inner bolt

$r_{no} = 1.2L_c tF_u < 2.4d_b tF_u$ for each outer bolt

L_c = clear distance, in the direction of force, between the edge of the hole and the edge of the adjacent hole or edge of the material, in.

t = end-plate or column flange thickness, in.

F_u = specified minimum tensile strength of end-plate or column flange material, ksi

d_b = diameter of bolt, in.

$$L_{ci} = p_b - d_e$$

$$L_{co} = L_e - \frac{d_e}{2}$$

where:

d_e = effective area of bolt hole, in.

L_e = edge spacing of the bolts, in.

$$L_{ci} = 3.5 \text{ in.} - 1\tfrac{1}{8} \text{ in.} = 2.38 \text{ in.}$$

$$L_{co} = 1.75 \text{ in.} - \frac{1\tfrac{1}{8} \text{ in.}}{2} = 1.19 \text{ in.}$$

$$r_{ni} = 1.2(2.38 \text{ in.})(1.25 \text{ in.})(58 \text{ ksi}) < 2.4(1 \text{ in.})(1.25 \text{ in.})(58 \text{ ksi})$$

$$r_{ni} = 207 \text{ kips} < 174 \text{ kips}$$

$$r_{ni} = 174 \text{ kips}$$

$$r_{no} = 1.2L_c tF_u < 2.4d_b tF_u$$

$$r_{no} = 1.2(1.19 \text{ in.})(1.25 \text{ in.})(58 \text{ ksi}) < 2.4(1 \text{ in.})(1.25 \text{ in.})(58 \text{ ksi})$$

$$r_{no} = 103 \text{ kips} < 174 \text{ kips}$$

$$r_{no} = 103 \text{ kips}$$

$$V_u < \phi_n R_n = (1)(4)(174 \text{ kips}) + (1)(4)(103 \text{ kips})$$

$$\phi_n R_n = 998 \text{ kips} > 58.8 \text{ kips}$$ OK

Step 8. Check the column flange for flexural yielding by AISC 358 Equation 6.9-20.

$$t_{cf\ req'd} = \sqrt{\frac{1.11 M_f}{\phi_d F_{yc} Y_c}} \le t_{cf}$$

where:

F_{yc} = specified minimum yield stress of column flange material, ksi

Y_c = stiffened column flange yield line from AISC 358 Table 6.6

t_{cf} = column flange thickness, in.

$$Y_c = \frac{b_{cf}}{2}\left[h_1\left(\frac{1}{s}\right) + h_2\left(\frac{1}{p_{so}}\right) + h_3\left(\frac{1}{p_{si}}\right) + h_4\left(\frac{1}{s}\right)\right] + \frac{2}{g}\left[h_1\left(s + \frac{p_b}{4}\right) + h_2\left(p_{so} + \frac{3p_b}{4}\right) + h_3\left(p_{si} + \frac{p_b}{4}\right) + h_4\left(s + \frac{3p_b}{4}\right) + p_b^2\right] + g$$

where:

b_{cf} = column flange width, in.

p_{si} = distance from column stiffener to inner bolts, in.

p_{so} = distance from column stiffener to outer bolts, in.

$$s = \frac{1}{2}\sqrt{b_{cf}\, g}$$

$$s = \frac{1}{2}\sqrt{(8 \text{ in.})(5 \text{ in.})} = 3.16 \text{ in.}$$

$$Y_c = \frac{(8\text{ in.})}{2}\left[(40.94\text{ in.})\left(\frac{1}{3.16\text{ in.}}\right)+(37.44\text{ in.})\left(\frac{1}{1.75\text{ in.}}\right)\right.$$
$$\left.+(33.31\text{ in.})\left(\frac{1}{1.75\text{ in.}}\right)+(29.81\text{ in.})\left(\frac{1}{3.16\text{ in.}}\right)\right]$$
$$+\frac{2}{(5\text{ in.})}\left[(40.94\text{ in.})\left(3.16\text{ in.}+\frac{(3.5\text{ in.})}{4}\right)+(37.44\text{ in.})\left(1.75\text{ in.}+\frac{3(3.5\text{ in.})}{4}\right)\right.$$
$$\left.+(33.31\text{ in.})\left(1.75\text{ in.}+\frac{3.5\text{ in.}}{4}\right)+(29.81\text{ in.})\left(3.16\text{ in.}+\frac{3(3.5\text{ in.})}{4}\right)+(3.5\text{ in.})^2\right]$$
$$+(5\text{ in.})$$

$$Y_c = 497\text{ in.}$$

$$t_{cf\ req'd} = \sqrt{\frac{1.11(20{,}379\text{ in.-kip})}{(1)(50\text{ ksi})(497\text{ in.})}} \le 2\text{ in.}$$

$$t_{cf\ req'd} = 0.95\text{ in.} \le 2\text{ in.}$$

Column flange of 2 inches is OK.

Step 9. Determine the required stiffener force by AISC 358 Equation 6.9-21.

$$\phi_d M_{cf} = \phi_d F_{yc} Y_c t_{cf}^2$$

$$\phi_d M_{cf} = (1)(50\text{ ksi})(497\text{ in.})(2\text{ in.})^2 = 99{,}344\text{ in.-kip}$$

The equivalent column flange design force used for stiffener design by AISC 358 Equation 6.9-22.

$$\phi_d R_n = \frac{\phi_d M_{cf}}{(d - t_{bf})}$$

$$\phi_d R_n = \frac{(99{,}690\text{ in.-kip})}{(36\text{ in.}) - (5/8\text{ in.})} = 2{,}808\text{ kips}$$

2,808 kips > 576 kips OK

Step 10. Check local column web yielding strength of the unstiffened column web at the beam flanges by AISC 358 Equations 6.9-23 and 6.9-24.

$$\phi_d R_n \ge F_{fu}$$

$$\phi_d R_n = \phi_d C_t \left(6k_c + t_{bf} + 2t_p\right) F_{yc} t_{cw}$$

where:

C_t = 0.5 if the distance from the column top to the top of the beam flange is less than the depth of the column: otherwise 1.0

k_c = distance from outer face of the column flange to web toe of fillet weld, in.

t_p = end-plate thickness, in.

F_{yc} = specified yield stress of the column web material, ksi

t_{cw} = column web thickness, in.

t_{bf} = beam flange thickness, in.

$$\phi_d R_n = (1.0)(0.5)\left(6\left(2 \text{ in.} + \tfrac{5}{16} \text{ in.}\right) + (0.5 \text{ in.}) + 2(1.25 \text{ in.})\right)(50 \text{ ksi})(0.5 \text{ in.})$$

$$\phi_d R_n = 212 \text{ kips} \le 576 \text{ kips}$$

The design is not acceptable. Column stiffeners need to be provided.

Step 11. Check the unstiffened column web buckling strength at the beam compression flange by AISC 358 Equations 6.9-25 and 6.9-27.

$$\phi R_n \ge F_{fu}$$

$$\phi R_n = \phi \frac{12 t_{cw}^3 \sqrt{E F_{yc}}}{h}$$

where:

h = clear distance between flanges when welds are used for built-up shapes, in.

$$\phi R_n = (0.75)\frac{12(0.5 \text{ in.})^3 \sqrt{(29{,}000 \text{ ksi})(50 \text{ ksi})}}{(36 \text{ in.} - 2 \text{ in.} - 0.75 \text{ in.})} = 42 \text{ kips}$$

42 kips < 576 kips NOT OK

Step 12. Check the unstiffened column web crippling strength at the beam compression flange by AISC 358 Equation 6-30.

$$\phi R_n \ge F_{fu}$$

$$\phi R_n = \phi 0.40 t_{cw}^2 \left[1 + 3\left(\frac{N}{d_c}\right)\left(\frac{t_{cw}}{t_{cf}}\right)^{1.5}\right]\sqrt{\frac{EF_{yc}t_{cf}}{t_{cw}}}$$

where:

N = thickness of beam flange plus 2 times the groove weld reinforcement leg size, in.

d_c = overall depth of the column, in.

$$R_n = (0.75)(0.80)(0.5\text{ in.})^2\left[1 + 3\left(\frac{3(\frac{5}{8}\text{ in.})}{36\text{ in.}}\right)\left(\frac{0.5\text{ in.}}{2\text{ in.}}\right)^{1.5}\right]\sqrt{\frac{(29{,}000\text{ ksi})(50\text{ ksi})(2\text{ in.})}{0.5\text{ in.}}}$$

$$R_n = 184\text{ kips}$$

184 kips < 576 kips NOT OK

Step 13. Check the required strength of the stiffener plates by AISC 358 Equation 6-32.

$$F_{su} = F_{fu} - \min\phi R_n = 576\text{ kips} - 42\text{ kips} = 534\text{ kips}$$

where:

$\min\phi R_n$ = the minimum design strength value from column flange bending check, column web yielding, column web buckling and column web crippling check

Although AISC 358 says to use this value of 534 kips to design the continuity plate, a different approach will be used in this example. In compression, the continuity plate will be designed to take the full force delivered by the beam flange, F_{su}. In tension, however, the compressive limit states (web buckling and web yielding) are not applicable and column web yielding will control the design instead. The tension design force can be taken as follows:

$$F_{su} = F_{fu} - \phi R_{n,web\ yielding} = 576\text{ kips} - 212\text{ kips} = 364\text{ kips}$$

Step 14. Design the continuity plate for required strength by AISC 360 Section J10.

Find the cross-sectional area required by the continuity plate acting in tension:

$$A_{s,reqd} = \frac{F_{su}}{\phi F_y}$$

$$A_{s,reqd} = \frac{364\text{ kips}}{(0.9)(50\text{ ksi})} = 8.1\text{ in.}^2$$

$$t_{s,reqd} = \frac{A_{s,reqd}}{b_{st}}$$

$$t_{s,reqd} = \frac{8.1 \text{ in.}^2}{8 \text{ in.}} = 1.01 \text{ in.}$$

Use a 1-3/8-inch continuity plate. As it will be shown later, net section rupture (not gross yielding) will control the design of this plate.

From AISC Section J10.8, calculate member properties using an effective length of 0.75*h* and a column web length of $12t_w$ = 6 in.:

$$I_x = \frac{t_{cw}12t_{cw}^3}{12} + \frac{\left(b_{st} - t_{cw}\right)t_{st}^3}{12}$$

$$I_x = \frac{\left(0.5 \text{ in.}\right)\left(6 \text{ in.}\right)^3}{12} + \frac{\left(8 \text{ in.} - 0.5 \text{ in.}\right)\left(1.375 \text{ in.}\right)^3}{12} = 10.6 \text{ in.}^4$$

$$I_y = \frac{t_{st}b_{st}^3}{12} + \frac{\left(12t_{cw} - t_{st}\right)t_{cw}^3}{12}$$

$$I_y = \frac{\left(1.375 \text{ in.}\right)\left(8 \text{ in.}\right)^3}{12} + \frac{\left(6 \text{ in.} - 1.375 \text{ in.}\right)\left(0.5 \text{ in.}\right)^3}{12} = 58.7 \text{ in.}^4$$

$$J \cong \frac{b_{st}t_{st}^3}{3} + \frac{\left(12t_{cw} - t_{st}\right)t_{cw}^3}{3}$$

$$J \cong \frac{\left(8 \text{ in.}\right)\left(1.375 \text{ in.}\right)^3}{3} + \frac{\left(6 \text{ in.} - 1.375 \text{ in.}\right)\left(0.5 \text{ in.}\right)^3}{3} = 7.13 \text{ in.}^4$$

$$A = b_{st}t_{st} + \left(12t_{cw} - t_{st}\right)t_{cw}$$

$$A = \left(8 \text{ in.}\right)\left(1.375 \text{ in.}\right) + \left(6 \text{ in.} - 1.375 \text{ in.}\right)\left(0.5 \text{ in.}\right) = 13.3 \text{ in.}^2$$

$$r_y = \sqrt{\frac{I_y}{A}}$$

$$r_y = \sqrt{\frac{58.7 \text{ in.}^4}{13.3 \text{ in.}^2}} = 2.1 \text{ in.}$$

$$L = 0.75h = 0.75\left(d_c - t_{f1} - t_{f2} - 2t_{weld}\right)$$

$$L = 0.75\left(36 \text{ in.} - 2 \text{ in.} - 0.75 \text{ in.} - 2\left(5/16 \text{ in.}\right)\right) = 24.5 \text{ in.}$$

Check the continuity plate in compression from AISC 360 Equation J4.4:

$$\frac{KL}{r_y} = \frac{(1.0)(24.5 \text{ in.})}{2.1 \text{ in.}} = 11.65 \le 25$$

Strength in the other direction does not need to be checked because the cruciform section will not buckle in the plane of the column web.

Since *KL*/*r* is less than 25, use AISC 360 Equation J4-6 to determine compression strength:

$$\phi P_n = \phi F_y A_g$$

$$\phi P_n = (0.9)(50 \text{ ksi})(13.3 \text{ in.}^2) = 599 \text{ kips}$$

However, torsional buckling may control. Therefore, check flexural-torsional buckling using AISC 360 Equation E4-4:

$$F_e = \frac{GJ}{I_x + I_y}$$

$$F_e = \frac{(11{,}200 \text{ ksi})(7.13 \text{ in.}^4)}{10.6 \text{ in.}^4 + 58.7 \text{ in.}^4} = 1{,}150 \text{ ksi}$$

$$F_{cr} = \left[0.658^{\frac{F_y}{F_e}} \right] F_y$$

$$F_{cr} = \left[0.658^{\frac{50 \text{ ksi}}{1{,}150 \text{ ksi}}} \right] (50 \text{ ksi}) = 49.1 \text{ ksi}$$

$$\phi P_n = (0.9)(49.1 \text{ ksi})(13.3 \text{ in.}^2) = 588 \text{ kips}$$

Check the continuity plate in tension. The continuity plate had been previously sized for adequacy to tensile yielding of the gross section. Now tensile rupture of the net section must be checked using AISC 360 Section D2-2. The critical section will be analyzed where the continuity plates are clipped adjacent to the k-region of the column.

$$A_e = (t_{st})(b_{st} - 2(t_{weld} + \text{clip}))$$

$$A_e = (1.375 \text{ in.})(8 \text{ in.} - 2(5/16 \text{ in.} + 0.5 \text{ in.})) = 8.77 \text{ in.}^2$$

$$\phi_t P_n = \phi_t F_u A_e = 381 \text{ kips} > 364 \text{ kips}$$ OK

Step 15. Check the panel zone for required strength per AISC 341 Equation J10-9.

$$P_c = F_y A$$

where:

A = column cross sectional area, in^2.

$$P_c = (50 \text{ ksi})(38.6 \text{ in.}) = 1{,}931 \text{ kips}$$

$$P_r = F_{fu} = 576 \text{ kips}$$

$$\frac{P_r}{P_c} = \frac{576 \text{ kips}}{1{,}931 \text{ kips}} = 0.3 < 0.75$$

Therefore, use AISC 360 Equation J10-111. Note that panel zone flexibility was accounted for in the ETABS model.

$$\phi R_n = \phi 0.60 F_y d_c t_{cw} \left(1 + \frac{3 b_{cf} t_{cf}^2}{d_b d_c t_{cw}}\right)$$

$$\phi R_n = (0.9)(0.60)(50 \text{ ksi})(36 \text{ in.})(0.5 \text{ in.}) \left(1 + \frac{3(8 \text{ in.})(2 \text{ in.})^2}{(36 \text{ in.})(36 \text{ in.})(0.5 \text{ in.})}\right)$$

$$\phi R_n = 558 \text{ kips} < 576 \text{ kips}$$ NOT OK

The column web is not sufficient to resist the panel zone shear. Although doubler plates can be added to the panel zone to increase strength, this may be an expensive solution. A more economical solution would be to simply upsize the column web to a sufficient thickness, such as 5/8 inch.

$$\phi R_n = \phi 0.60 F_y d_c t_{cw} \left(1 + \frac{3 b_{cf} t_{cf}^2}{d_b d_c t_{cw}}\right)$$

$$\phi R_n = (0.9)(0.60)(50 \text{ ksi})(36 \text{ in.})(5/8 \text{ in.}) \left(1 + \frac{3(8 \text{ in.})(2 \text{ in.})^2}{(36 \text{ in.})(36 \text{ in.})(5/8 \text{ in.})}\right)$$

$$\phi R_n = 680 \text{ kips} > 576 \text{ kips}$$

Note that changing the column member properties might affect the analysis results. In this example, this is not the case, although the slight difference in web thickness would result in

marginally different values for some of the end-plate connection calculations. For simplicity, these changes are not undertaken in this example.

6.1.5.3 Frame at the ridge. The ridge joint detail is shown in Figure 6.1-8. An unstiffened bolted connection plate is selected.

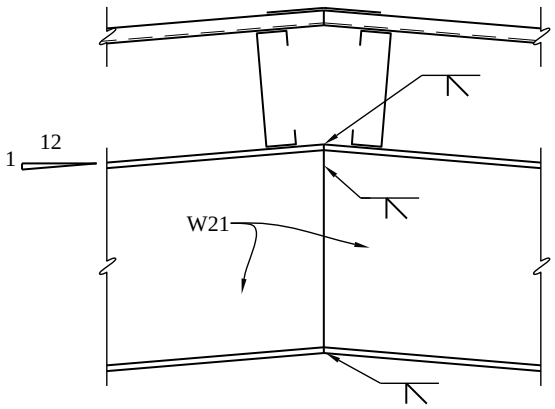

Figure 6.1-8 End plate connection at ridge

This is an AISC 360 designed connection, not an AISC 358 designed connection because there should not be a plastic hinge forming in this vicinity. Lateral seismic forces produce no moment at the ridge until yielding takes place at one of the knees. Vertical accelerations on the dead load do produce a moment at this point; however, the value is small compared to all other moments and does not appear to be a concern. Once seismic loads produce a plastic hinge at one knee, further lateral displacement produces positive moment at the ridge. Under the condition on which the AISC 358 design is based (a full plastic moment is produced at each knee), the moment at the ridge will simply be the static moment from the gravity loads less the horizontal thrust times the rise from knee to ridge. Analyzing this frame under the gravity load case $1.2D + 0.2S$, the static moment is 406 ft-kip and the reduction for the thrust is 128 ft-kip, leaving a net positive moment of 278 ft-kip, coincidentally close to the design moment for the factored gravity loads.

6.1.5.4 Design of mezzanine framing. The design of the framing for the mezzanine floor at the east end of the building is controlled by gravity loads. The concrete-filled 3-inch, 20-gauge steel deck of the mezzanine floor is supported on steel beams spaced at 10 feet and spanning 20 feet (Figure 6.1-2). The steel beams rest on three-span girders connected at each end to the portal frames and supported on two intermediate columns (Figure 6.1-1). The girder spans are approximately 30 feet each. Those lateral forces that are received by the mezzanine are distributed to the frames and diagonal bracing via the floor diaphragm. A typical beam-column connection at the mezzanine level is provided in Figure 6.1-9. The design of the end plate connection is similar to that at the knee, but simpler because the beam is horizontal and not tapered. Also note that demands on the end-plate connection will be less because this connection is not at the end of the column.

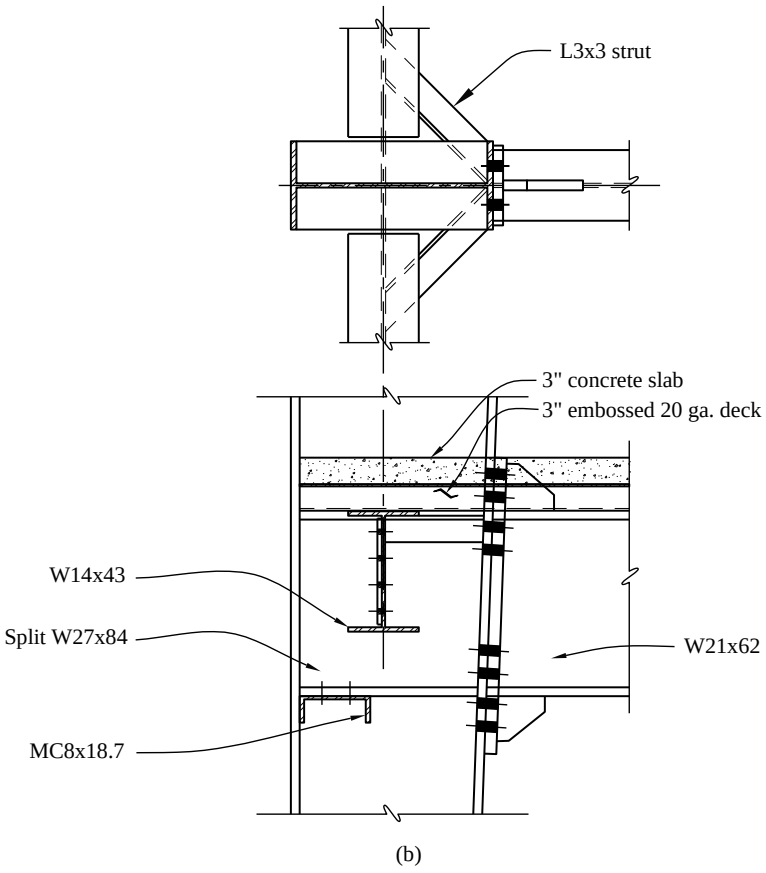

Figure 6.1-9 Mezzanine framing (1.0 in. = 25.4 mm)

6.1.5.5 Braced frame diagonal bracing

Although the force in the diagonal X-braces can be either tension or compression, only the tensile value is considered because it is assumed that the diagonal braces are capable of resisting only tensile forces.

See AISC 341 Section 14.2 for requirements on braces for OCBFs. The strength of the members and connections, including the columns in this area but excluding the brace connections, must be based on *Standard* Section 12.4.2.3:

$$1.4D + 1.0L + 0.2S + \rho Q_E$$

$$0.7D + \rho Q_E$$

Recall that a 1.0 factor is applied to L when the live load is greater than 100 psf (*Standard* Sec. 2.3.2). For the case discussed here, the "tension only" brace does not carry any live or dead load, so the load factor does not matter.

For simplicity, we can assume that the lateral force is equally divided among the roof level braces and is slightly amplified to account for torsional effects. Thus the brace force can be approximated using the following equation:

$$P_u = 0.55V \times \tfrac{1}{2} \times \frac{1}{\cos\theta}$$

$$P_u = 0.55(211 \text{ kips}) \times \tfrac{1}{2} \times \frac{1}{\cos 47°} = 85 \text{ kips}$$

All braces at this level will have the same design. Choose a brace member based on tensile yielding of the gross section by AISC 360 Equation D2-1:

$$\phi_t P_n = \phi_t F_y A_g$$

$$A_{g,reqd} = \frac{85 \text{ kips}}{(0.9)(36 \text{ ksi})} = 2.62 \text{ in.}^2$$

This also needs to be checked for tensile rupture of the net section. Demand will be taken as either the expected yield strength of the brace or the amplified seismic load. Try a 2L3½x3x 7/16, which is the smallest seismically compact angle shape available.

$A_g = 5.34 \text{ in.}^2$

The *Kl/r* requirement of AISC 341 Section 14.2 does not apply because this is not a V or an inverted V configuration.

Check net rupture by AISC 360 Equation D2-2 and D3-1:

$$\phi_t P_n = \phi_t F_u A_e$$

$$A_e = A_n U$$

Determine the shear lag factor, *U,* from AISC 360, Table D3.1, Case 2. In ordered to calculate *U*, the weld length along the double angles needs to be determined.

$$U = 1 - \bar{x}/L$$

Brace connection demand is given as the expected yield strength of the brace in tension per AISC 341 Section 14.4.

$$R_y F_y A_g = (1.5)(36 \text{ ksi})(5.34 \text{ in.}^2) = 288 \text{ kips}$$

Expected yield strength of the brace is 288 kips. However, AISC 341 Section 14.4b limits the brace connection design force to the amplified seismic load.

$$\Omega_0 P_{QE} = (2)(85 \text{ kips}) = 170 \text{ kips}$$

Use four fillet welds, two on each angle. Try 1/4-inch welds using AISC 360 Equation J2-3:

$$\phi R_n = \phi F_w A_w$$

$$\phi R_n = \phi\left(0.60F_{EXX}\right)\left(0.707t_w\right)\left(L\right)$$

$$L = \frac{170 \text{ kips}}{4\left(0.75\right)\left(0.6\right)(70 \text{ ksi})(0.707)(0.25 \text{ in.})} = 7.63 \text{ in.}$$

Use four 1/4-inch fillet welds 8 inches long.

Check the base metal:

$$\phi R_n = \phi F_{BM} A_{BM}$$

Shear yielding from AISC 360 Equation J4-3:

$$\phi R_n = \phi 0.6 F_y A_g$$

$$\phi R_n = \left(1.0\right)\left(0.6\right)\left(36 \text{ ksi}\right)\left(0.25 \text{ in.}\right)(8 \text{ in.}) = 173 \text{kips}$$ OK

Shear rupture from AISC 360 Equation J4-4:

$$\phi R_n = \phi 0.6 F_u A_{nv}$$

$$\phi R_n = \left(0.75\right)\left(0.6\right)\left(58 \text{ ksi}\right)\left(0.25 \text{ in.}\right)(8 \text{ in.})$$ OK

Calculate the shear lag factor and the effective net area:

$$U = 1 - {(0.846 \text{ in.})}/{(9 \text{ in.})} = 0.89$$

$$A_e = \left(5.34 \text{ in.}^2\right)\left(0.89\right) = 4.78 \text{ in.}^2$$

Calculate the tensile rupture strength:

$$\phi_t P_n = \left(0.9\right)\left(58 \text{ ksi}\right)\left(6.1 \text{in.}^2\right) = 207 \text{ kips} > 170 \text{ kips}$$ OK

Additionally, the capacity of the eave strut at the roof must be checked. The eave strut, part of the braced frame, also acts as a collector element and must be designed using the overstrength factor per ***Standard*** Section 12.10.2.1.

6.1.5.6 Roof deck diaphragm. Figure 6.1-10 shows the in-plane shear force in the roof deck diaphragm for both seismic loading conditions. There are deviations from simple approximations in both directions. In the E-W direction, the base shear is 274 kips (Section 6.1.4.2) with 77 percent or 211 kips at the roof. Torsion is not significant, so a simple approximation is to take half the force to each side and divide by

the length of the building, which yields (211,000/2)/180 feet = 586 plf. The plot shows that the shear in the edge of the diaphragm is significantly higher in the two braced bays. This is a shear lag effect; the eave strut in the three-dimensional model is a HSS 6x6x1/4. In the N-S direction, the shear is generally highest in the bay between the mezzanine frame and the first frame without the mezzanine. This is expected given the significant change in stiffness. There is no simple approximation to estimate the shear here without a three-dimensional model. The shear is also high at the longitudinal braced bays because they tend to resist the horizontal torsion. However, the shear at the braced bays is lower than observed for the E-W motion.

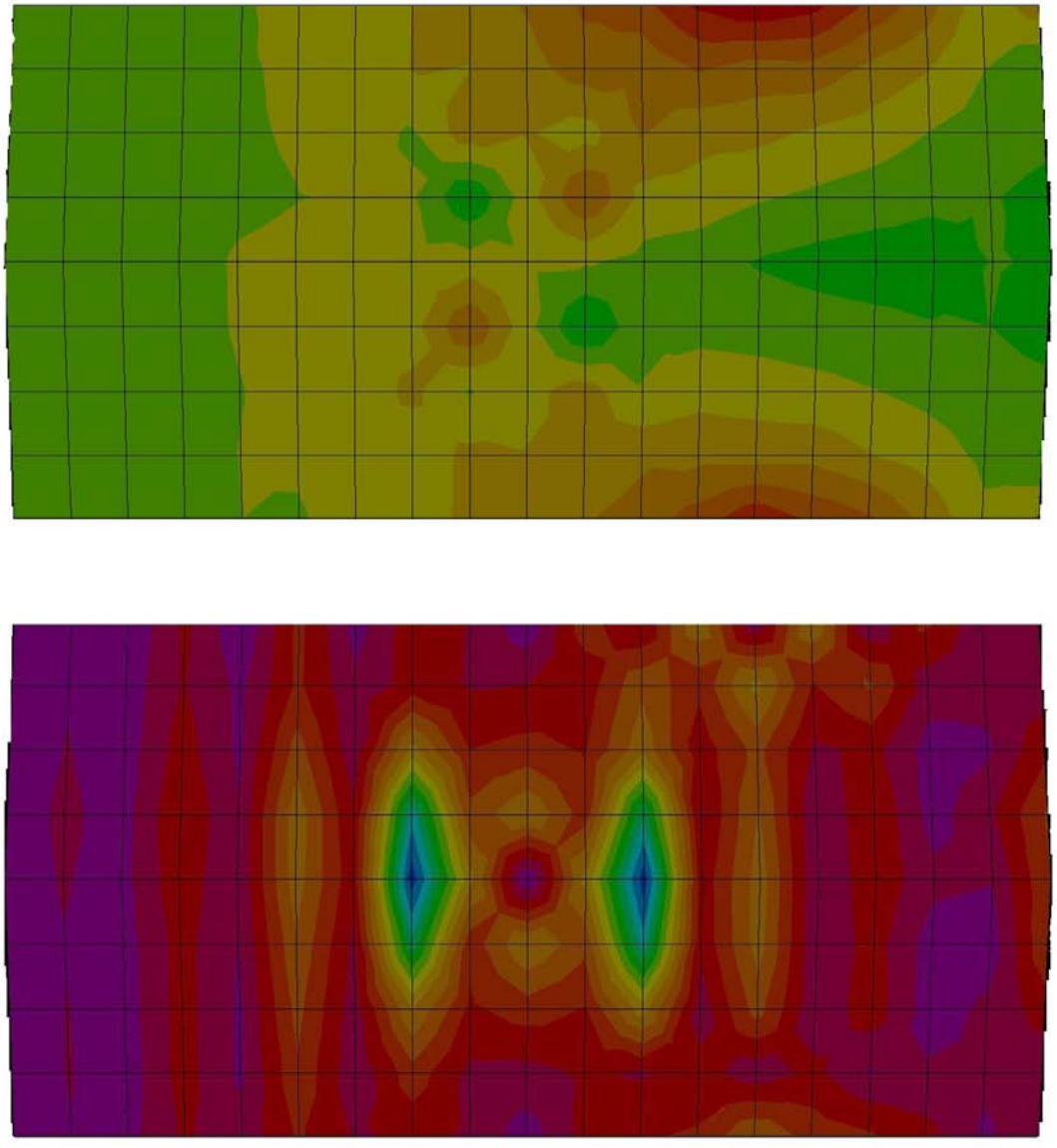

Figure 6.1-10 Shear force in roof deck diaphragm;
upper diagram is for E-W motion and lower is for N-S motion

6.2 SEVEN-STORY OFFICE BUILDING, LOS ANGELES, CALIFORNIA

Two alternative framing arrangements for a seven-story office building are illustrated.

6.2.1 Building Description

6.2.1.1 General description. This seven-story office building of rectangular plan configuration is 177 feet, 4 inches long in the E-W direction and 127 feet, 4 inches wide in the N-S direction (Figure 6.2-1). The building has a penthouse. It is framed in structural steel with 25-foot bays in each direction. The typical story height is 13 feet, 4 inches; the first story is 22 feet, 4 inches high. The penthouse extends 16 feet above the roof level of the building and covers the area bounded by Gridlines C, F, 2 5 in Figure 6.2-1. Floors consist of 3-1/4-inch lightweight concrete over composite metal deck. The elevators and stairs are located in the central three bays.

6.2.1.2 Alternatives. This example includes two alternatives—a steel moment-resisting frame and a concentrically braced frame:

- Alternative A: Seismic force resistance is provided by special moment frames (SMF) with prequalified Reduced Beam Section (RBS) connections located on the perimeter of the building (on Gridlines A, H, 1 6 in Figure 6.2-1, also illustrated in Figure 6.2-2). There are five bays of moment frames on each line.

- Alternative B: Seismic force resistance is provided by four special concentrically braced frames (SCBF) in each direction. They are located in the elevator core walls between Columns 3C and 3D, 3E and 3F, 4C and 4D 4E and 4F in the E-W direction and between Columns 3C and 4C, 3D and 4D, 3E and 4E 3F and 4F in the N-S direction (Figure 6.2-1). The braced frames are in a two-story X configuration. The frames are identical in brace size and configuration, but there are some minor differences in beam and column sizes. Braced frame elevations are shown in Figures 6.2-10 through 6.2-12.

6.2.1.3 Scope. The example covers:

- Seismic design parameters (Sec. 6.2.2.1)
- Analysis of perimeter moment frames (Sec. 6.2.4.1)
- Beam and column proportioning (Sec. 6.2.4.2.3)
- Moment frame connection design (Sec. 6.2.4.2.5)
- Analysis of concentrically braced frames (Sec. 6.2.5.1)
- Proportioning of braces (Sec. 6.2.5.2.1)
- Braced frame connection design (Sec. 6.2.5.2.5)

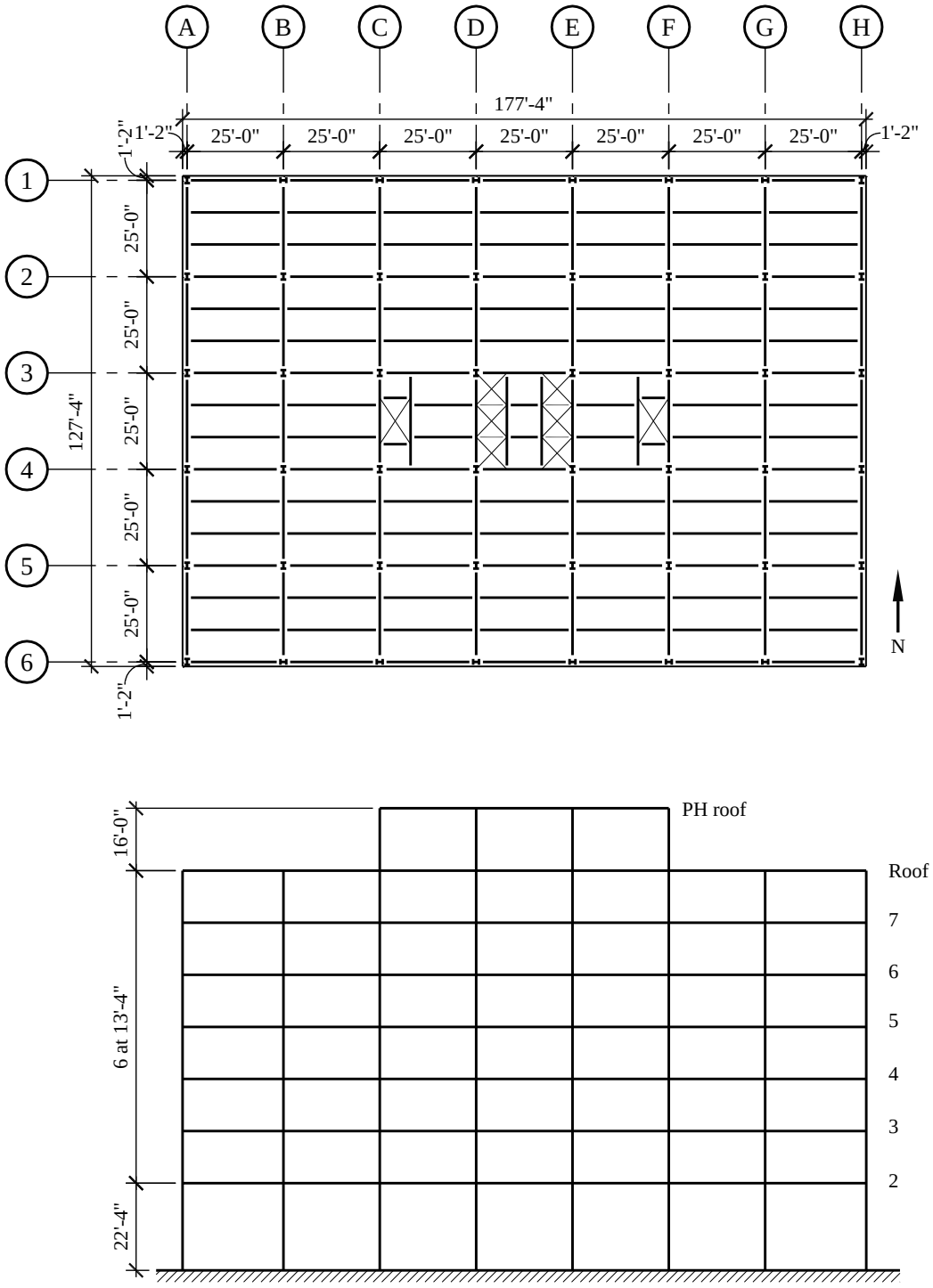

Figure 6.2-1 Typical floor framing plan and building section
(1.0 in. = 25.4 mm, 1.0 ft = 0.3048 m)

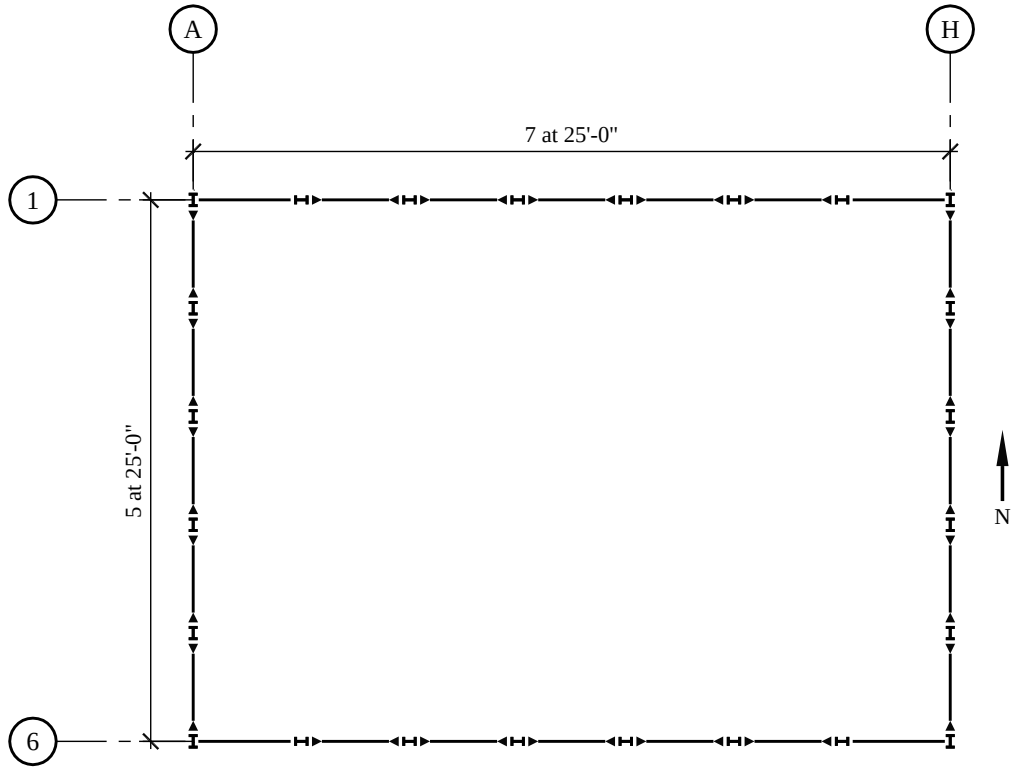

Figure 6.2-2 Framing plan for special moment frame
(1.0 in. = 25.4 mm, 1.0 ft = 0.3048 m)

6.2.2 Basic Requirements

6.2.2.1 *Provisions* parameters. See Section 3.2 for an example illustrating the determination of design ground motion parameters. For this example, the parameters are as follows

- S_{DS} = 1.0
- S_{D1} = 0.6
- Occupancy Category II
- Seismic Design Category D

For Alternative A, Special Steel Moment Frame (*Standard* Table 12.2-1)

- R = 8
- Ω_0 = 3
- C_d = 5.5

For Alternative B, Special Steel Concentrically Braced Frame (*Standard* Table 12.2-1):

- $R = 6$
- $\Omega_0 = 2$
- $C_d = 5$

6.2.2.2 Loads.

- Roof live load (*L*): 25 psf
- Penthouse roof dead load (*D*): 25 psf
- Exterior walls of penthouse: 25 psf of wall
- Roof *DL* (roofing, insulation, deck beams, girders, fireproofing, ceiling, mechanical, electrical plumbing): 55 psf
- Exterior wall cladding: 25 psf of wall
- Penthouse floor *D*: 65 psf
- Penthouse Equipment: 39 psf
- Floor *L*: 50 psf
- Floor *D* (deck, beams, girders, fireproofing, ceiling, mechanical electrical, plumbing, partitions): 68 psf
- Floor *L* reductions: per the IBC

6.2.2.3 Basic gravity loads.

- Penthouse roof:

Roof slab = (0.025 ksf)(25 ft)(75 ft)	=	47 kips
Walls = (0.025 ksf)(8 ft)(200 ft)	=	40 kips
Columns = (0.110 ksf)(8 ft)(8 ft)	=	7 kips
Total	=	94 kips

- Lower roof:

Roof slab = (0.055 ksf)[(127.33 ft)(177.33 ft) - (25 ft)(75 ft)	=	1139 kips
Penthouse floor = (0.065 ksf)(25 ft)(75 ft)	=	122 kips
Walls = 40 kips + (0.025 ksf)(609 ft)(6.67 ft)	=	142 kips
Columns = 7 kips + (0.170 ksf)(6.67 ft)(48 ft)	=	61 kips
Equipment = (0.039 ksf)(25 ft)(75 ft)	=	73 kips
Total	=	1,537 kips

- Typical floor:

Floor = (0.068 ksf)(127.33 ft)(177.33 ft)	= 1,535 kips
Walls = (0.025 ksf)(609 ft)(13.33 ft)	= 203 kips
Columns = (0.285 ksf)(13.33 ft)(48 ft)	= 182 kips
Total	= 1,920 kips

Total weight of building = 94 kips + 1,537 kips + 6 (1,920 kips) = 13,156 kips

6.2.2.4 Materials

- Concrete for floors: f_c' = 3 ksi, lightweight (LW)
- All other concrete: f_c' = 4 ksi, normal weight (NW)
- Structural steel:
  Wide flange sections: ASTM A992, Grade 50
  HSS: ASTM A500, Grade B
  Plates: ASTM A36

6.2.3 Structural Design Criteria

6.2.3.1 Building configuration. The building has no vertical irregularities despite the relatively tall height of the first story. The exception of *Standard* Section 12.3.2.2 is taken, in which the drift ratio of adjacent stories are compared rather than the stiffness of the stories. In the three-dimensional analysis, the first story drift ratio is less than 130 percent of that for the story above. Because the building is symmetrical in plan, plan irregularities would not be expected. Analysis reveals that Alternative B is torsionally irregular, which is not uncommon for core-braced buildings.

6.2.3.2 Orthogonal load effects. A combination of 100 percent of the seismic forces in one direction with 30 percent of the seismic forces in the orthogonal direction is required for structures in Seismic Design Category D for certain elements—namely, the shared columns in the SCBF (*Standard* Sec. 12.5.4). In using modal response spectrum analysis (MRSA), the bidirectional case is handled by using the square root of the sum of the squares (SRSS) of the orthogonal spectra.

6.2.3.3 Structural component load effects. The effect of seismic load is defined by *Standard* Section 12.4.2 as:

$$E = \rho Q_E + 0.2 S_{DS} D$$

Using *Standard* Section 12.3.4.2, ρ is 1.0 for Alternative A and 1.3 for Alternative B. (For simplicity, ρ is taken as 1.3; the design does not comply with the prescriptive requirements of *Standard* Sec. 12.3.4.2. It is assumed that the design would fail the calculation-based requirements of *Standard* Sec. 12.3.4.2.) Substitute for ρ (and for S_{DS} = 1.0).

- For Alternative A:

  $E = Q_E \pm 0.2D$

- Alternative B:

$E = 1.3Q_E \pm 0.2D$

6.2.3.4 Load combinations

Load combinations from ASCE 7-05 are as follows:

- $1.4D$
- $1.2D + 1.6L + 0.5L_r$
- $1.2D + L + 1.6L_r$
- $(1.2 + 0.2S_{DS})D + 0.5L + \rho Q_E$
- $(0.9 – 0.2\ S_{DS})D + \rho Q_E$

For each of these load combinations, substitute E as determined above, showing the maximum additive and minimum subtractive. Q_E acts both east and west (or north and south):

- Alternative A:

  $1.4D$
  $1.2D + 1.6L + 0.5L_r$
  $1.2D + L + 1.6L_r$
  $1.4D + 0.5L + Q_E$
  $0.7D + Q_E$

- Alternative B"

  $1.4D$
  $1.2D + 1.6L + 0.5L_r$
  $1.2D + L + 1.6L_r$
  $1.4D + 0.5L + 1.3Q_E$
  $0.7D + 1.3Q_E$

For both cases, six scaled response spectrum cases are used:

1) Spectrum in X direction
2) Spectrum in X direction with 5 percent eccentricity
3) Spectrum in Y direction
4) Spectrum in Y direction with 5 percent eccentricity
5) SRSS combined spectra in X and Y directions
6) SRSS combined spectra in X and Y directions with 5 percent eccentricity.

6.2.3.5 Drift limits. The allowable story drift per *Standard* Section 12.12.1 is $\Delta_a = 0.02h_{sx}$.

The allowable story drift for the first floor is Δ_a = (0.02)(22.33 ft)(12 in./ft) = 5.36 in.

The allowable story drift for a typical story is Δ_a = (0.02)(13.33 ft)(12 in./ft) = 3.20 in.

Adjust calculated story drifts by the appropriate C_d factor from *Standard* Table 12.2-1.

6.2.4 Analysis and Design of Alternative A: SMF

6.2.4.1 Modal Response Spectrum Analysis. Determine the building period (T) per *Standard* Equation 12.8-7:

$$T_a = C_t h_n^x = (0.028)(102.3)^{0.8} = 1.14\,\text{sec}$$

where h_n, the height to the main roof, is conservatively taken as 102.3 feet. The height of the penthouse will be neglected since its seismic mass is negligible. $C_u T_a$, the upper limit on the building period, is determined per *Standard* Table 12.8-1:

$$T = C_u T_a = (1.4)(1.14) = 1.596\ \text{sec}$$

It is assumed that the calculated period will exceed $C_u T_a$; this is verified after member selection. The seismic response coefficient (C_s) is determined from *Standard* Equation 12.8-2 as follows:

$$C_s = \frac{S_{DS}}{R/I} = \frac{1}{8/1} = 0.125$$

However, *Standard* Equation 12.8-3 indicates that the value for C_s need not exceed:

$$C_s = \frac{S_{D1}}{T(R/I)} = \frac{0.6}{(1.596\,\text{sec})(8/1)} = 0.047$$

and the minimum value for C_s per *Standard* Equation 12.8-5 is:

$$C_s = 0.044 I S_{DS} \geq 0.01 = (0.044)(1)(1) = 0.044$$

Therefore, use C_s = 0.047.

Seismic base shear is computed per *Standard* Equation 12.8-1 as:

$$V = C_S W = (0.047)(13{,}156\,\text{kips}) = 618\,\text{kips}$$

where W is the seismic mass of the building as determined above.

In evaluating the building in ETABS, twelve modes are analyzed, resulting in a total modal mass participation of 97 percent. The code requires at least 90 percent participation for strength. A scaling factor is used to take the response spectrum to 85 percent of the base shear, with a minimum scale factor for strength calculations of I/R. Typical software utilizes a spectrum presented as a coefficient of g, thus

requiring scaling by g, thus the scaling factor used here is $g/(R/I)$ = 386/(8/1) = 48.3. For drift, results are scaled by $C_d/(R/I)$; for a spectrum using a coefficient times g, this factor is $gC_d/(R/I)$.

6.2.4.2 Size members. The method used is as follows:

1. Select preliminary member sizes
2. Check deflection and drift (*Standard* Sec. 12.12)
3. Check the column-beam moment ratio rule (AISC 341 Sec. 9.6)
4. Check beam strength
5. Check connection design (AISC 341 Sec. 9.7)
6. Check shear requirement at panel-zone (AISC 341 Sec. 9.3; AISC 358 Sec. 5.4)

After the weight and stiffness have been modified by changing member sizes, the response spectrum must be rescaled for strength. The most significant criteria for the design are drift limits, relative strengths of columns and beams the panel-zone shear. Member strength must be checked but rarely governs for this system.

1. Select Preliminary Member Sizes: The preliminary member sizes are shown for the moment frame in the X-direction in Figure 6.2-3 and in the Y direction in Figure 6.2-4. These sections are selected from AISC SDM Table 1-2, ensuring that they are seismically compact. Members are sized to meet the prequalification limits of AISC 358 Section 5.3 for span-depth ratios, weight flange thickness. Members are also sized for drift limitations and to satisfy strong column–weak beam requirements by using a target ratio of:

$$\frac{\sum Z_c}{\sum Z_b} \geq 1.25$$

This proportioning does not guarantee compliance with AISC 341 Section 9.6, but is a useful target that makes conformance likely. Using a ratio of 2.0 may save on detailing costs, such as continuity plates, doublers bracing.

The software used accounts explicitly for the increase in beam flexibility due to the RBS cuts. For every beam, RBS parameters were chosen as follows:

$$a = 0.625 b_f \quad b = 0.75 d_b \quad c = 0.20 b_f$$

In accordance with AISC 341 Table I-8-1, beam flange slenderness ratios are limited to $0.3\sqrt{E/F_y}$ (7.22 for F_y = 50 ksi) beam web height-to-thickness ratios are limited to $2.45\sqrt{E/F_y}$ (59.0 for F_y = 50 ksi). Since all members selected are seismically compact per AISC SDM Table 1-2, they conform to these limits.

For columns in special steel moment frames such as this example, AISC 341 Table I-8-1 Footnote b requires that where the ratio of column moment strength to beam moment strength is less than or

equal to 2.0, the more stringent λ_p requirements apply for b/t (given above) when $P_u/\phi_b P_y$ is greater than or equal to 0.125, the more stringent h/t requirements apply.

Per AISC 341 Table I-8-1, consider the W14x132 column at Gridline B:

$$h / t_w \le 1.49\sqrt{E / F_y} \quad = 22.8 \le 35.9$$

Therefore, the column is seismically compact.

Strength checks are performed using ETABS; all members are satisfactory for strength

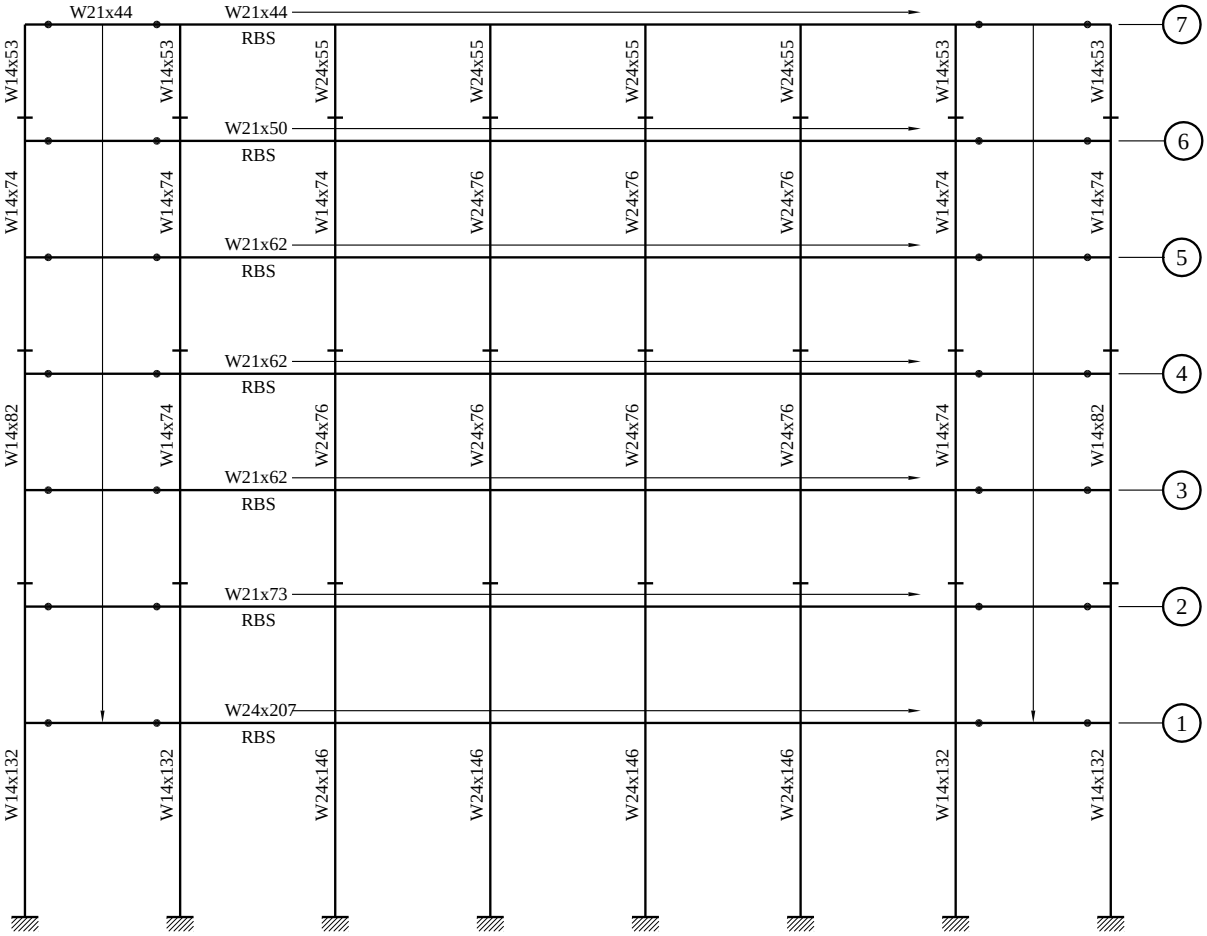

Figure 6.2-3 SMRF frame in E-W direction (penthouse not shown)

2. Check Drift: Check drift is in accordance with *Standard* Section 12.12.1. The building is modeled in three dimensions using ETABS. Displacements at the building corners under the 5 percent accidental torsion load cases are used here. Calculated story drifts, response spectrum scaling factors C_d amplification factors are summarized in Table 6.2-1 below. P-delta effects are included.

All story drifts are within the allowable story drift limit of $0.020h_{sx}$ per *Standard* Section 12.12 and Section 6.2.3.6 of this chapter.

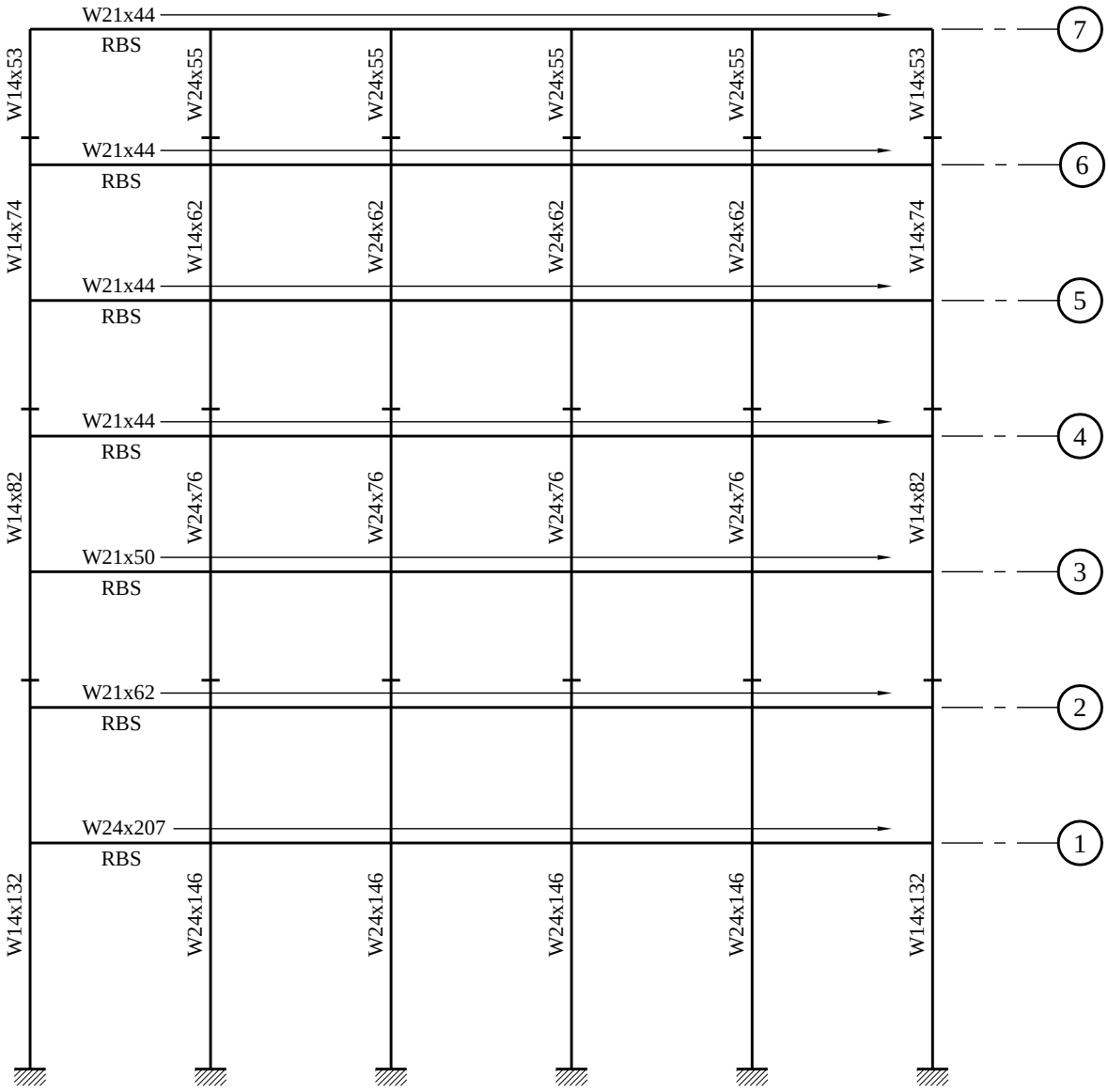

Figure 6.2-4 SMRF frame in N-S direction (penthouse not shown)

Table 6.2-1 Alternative A (Moment Frame) Story Drifts under Seismic Loads

	Elastic Displacement at Building Corner, From Analysis		Expected Displacement ($=\delta_e C_d$)		Design Story Drift Ratio		Allowable Story Drift Ratio
Level	δ_eE-W (in.)	δ_eN-S (in.)	δ E-W (in.)	δ N-S (in.)	Δ E-W/h (%)	Δ N-S/h (%)	Δ/h (%)
Level 7	2.92	3.18	16.0	17.5	1.2	1.2	2.0
Level 6	2.66	2.89	14.7	15.9	1.4	1.7	2.0
Level 5	2.33	2.47	12.8	13.6	1.6	2.0	2.0
Level 4	1.91	1.95	10.5	10.7	1.9	2.0	2.0
Level 3	1.41	1.40	7.76	7.70	1.8	1.8	2.0
Level 2	0.90	0.88	4.96	4.85	1.2	1.2	2.0
Level 1	0.55	0.52	3.04	2.89	1.1	1.1	2.0

1.0 in. = 25.4 mm.

3. Check the Column-Beam Moment Ratio: Check the column-beam moment ratio per AISC 341 Section 9.6. The expected moment strength of the beams is projected from the plastic hinge location to the column centerline per the requirements of AISC 341 Section 9.6. This is illustrated in Figure 6.2-5. For the columns, the moments at the location of the beam flanges are projected to the column-beam intersection as shown in Figure 6.2-6.

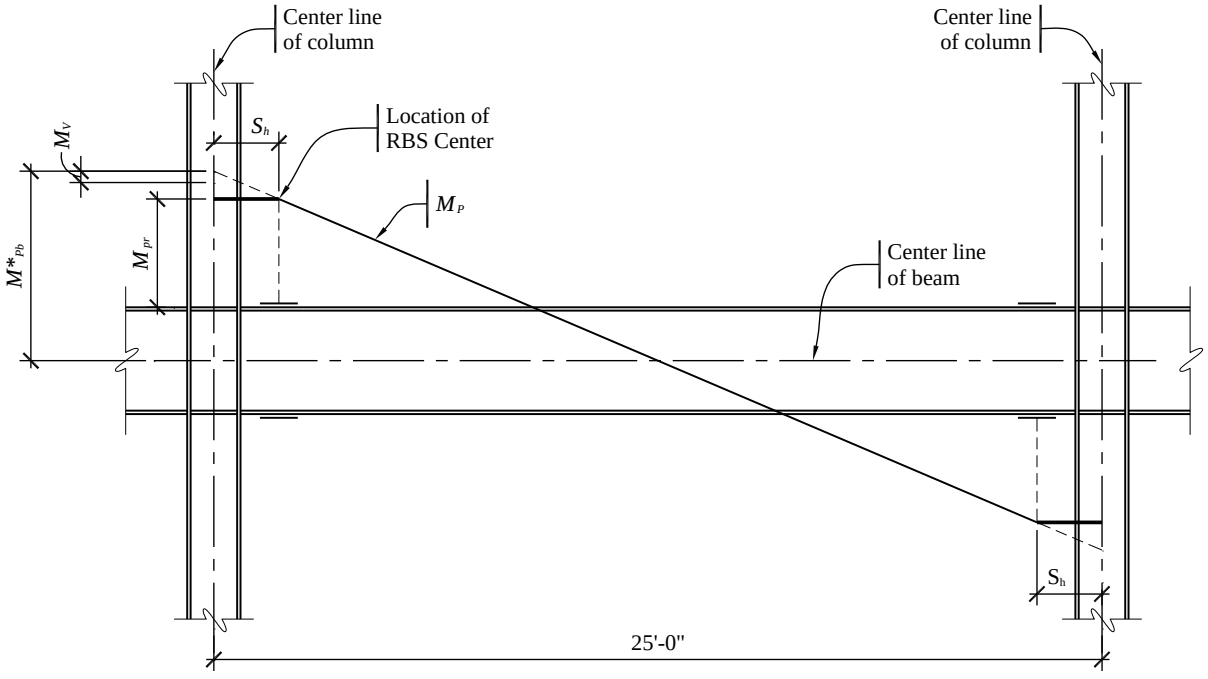

Figure 6.2-5 Projection of expected moment strength of beam
(1.0 in. = 25.4 mm, 1.0 ft = 0.3048 m)

The column-beam strength ratio calculation is illustrated for the lower level in the E-W direction, Level 2, at Gridline D (W24x146 column and W21x73 beam).

For the beams:

$$M^{\bullet}_{pb} = M_{pr} + V_e\left(S_h + \frac{d_c}{2}\right) \pm V_g\left(S_h + \frac{d_c}{2}\right)$$

where:

$M_{pr} = C_{pr}R_yF_y\,Z_e$ = (1.15)(1.1)(50) (122) = 7,361 in.-kips

R_y = 1.1 for Grade 50 steel

$Z_e = Z_x - 2ct_{bf}(d - t_{bf})$ = 172 – 2(1.659)(0.74)(21.24-0.74) = 122 in.^{3}

S_h = Distance from column face to centerline of plastic hinge (see Figure 6.2-9) = $a + b/2$ = 13.2 in. for the RBS

$$V_e = 2M_{pr} / L' \quad V_g = w_u L' / 2$$

L' = Distance between plastic hinges = 248.8 in.

w_u = Factored uniform gravity load along beam
= 1.4D + 0.5L = 1.4[(0.068 ksf)(12.5 ft)+(0.025)(13.3 ft)] + 0.5(0.050 ksf)(12.5 ft)
= 2.42 klf

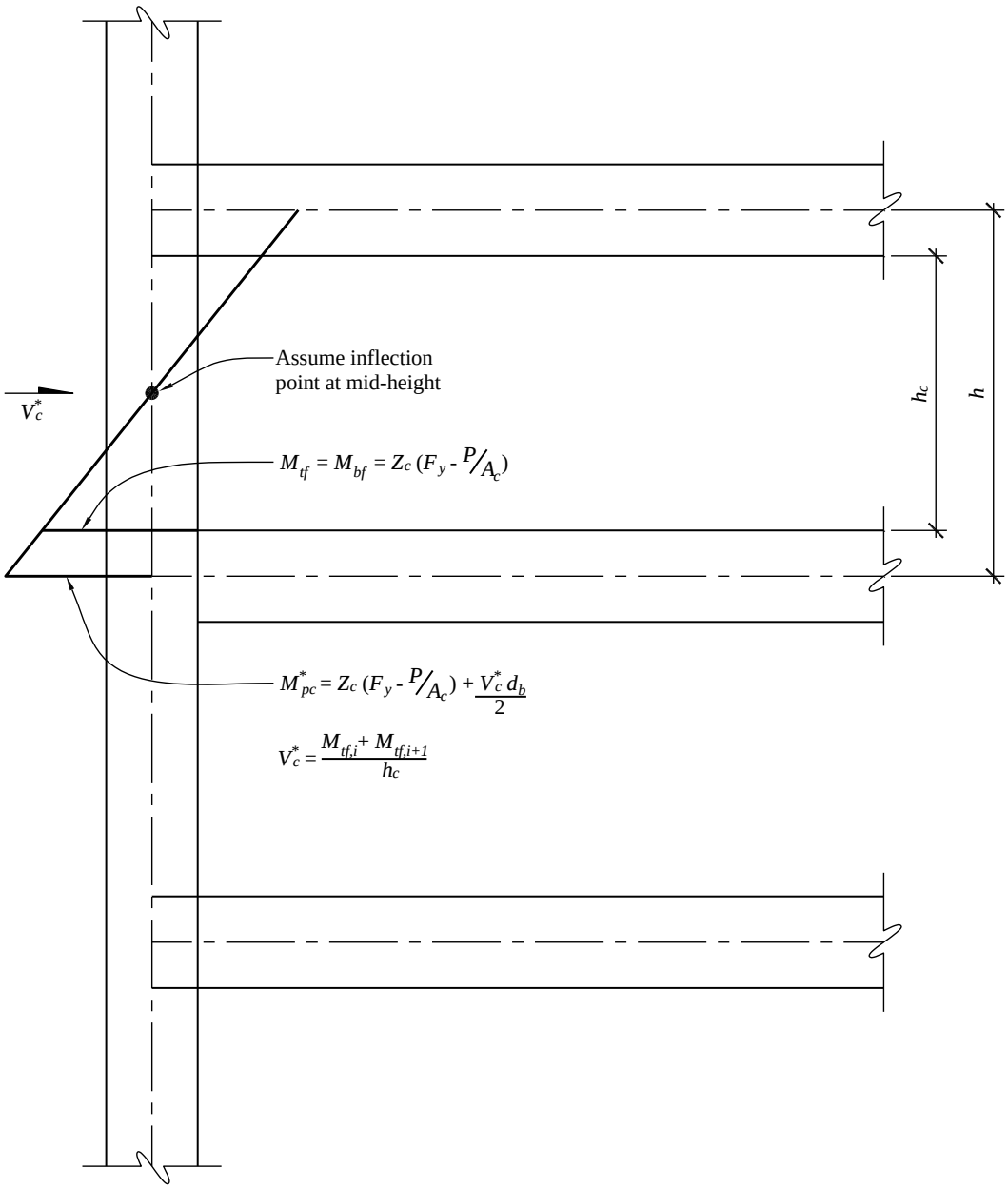

Figure 6.2-6 Moment in the column

The shear at the plastic hinge (Figure 6.2-7) is computed as:

$$V_p = V_e + V_g$$

where:

V_p = Shear at plastic hinge location

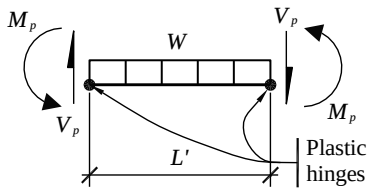

Figure 6.2-7 Free body diagram bounded by plastic hinges

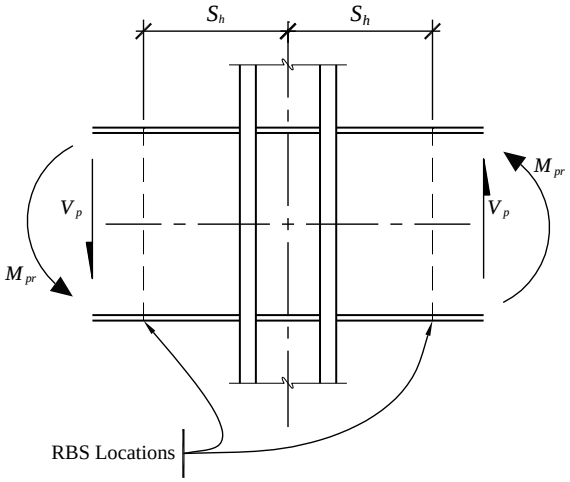

Figure 6.2-8 Forces at beam-column connection

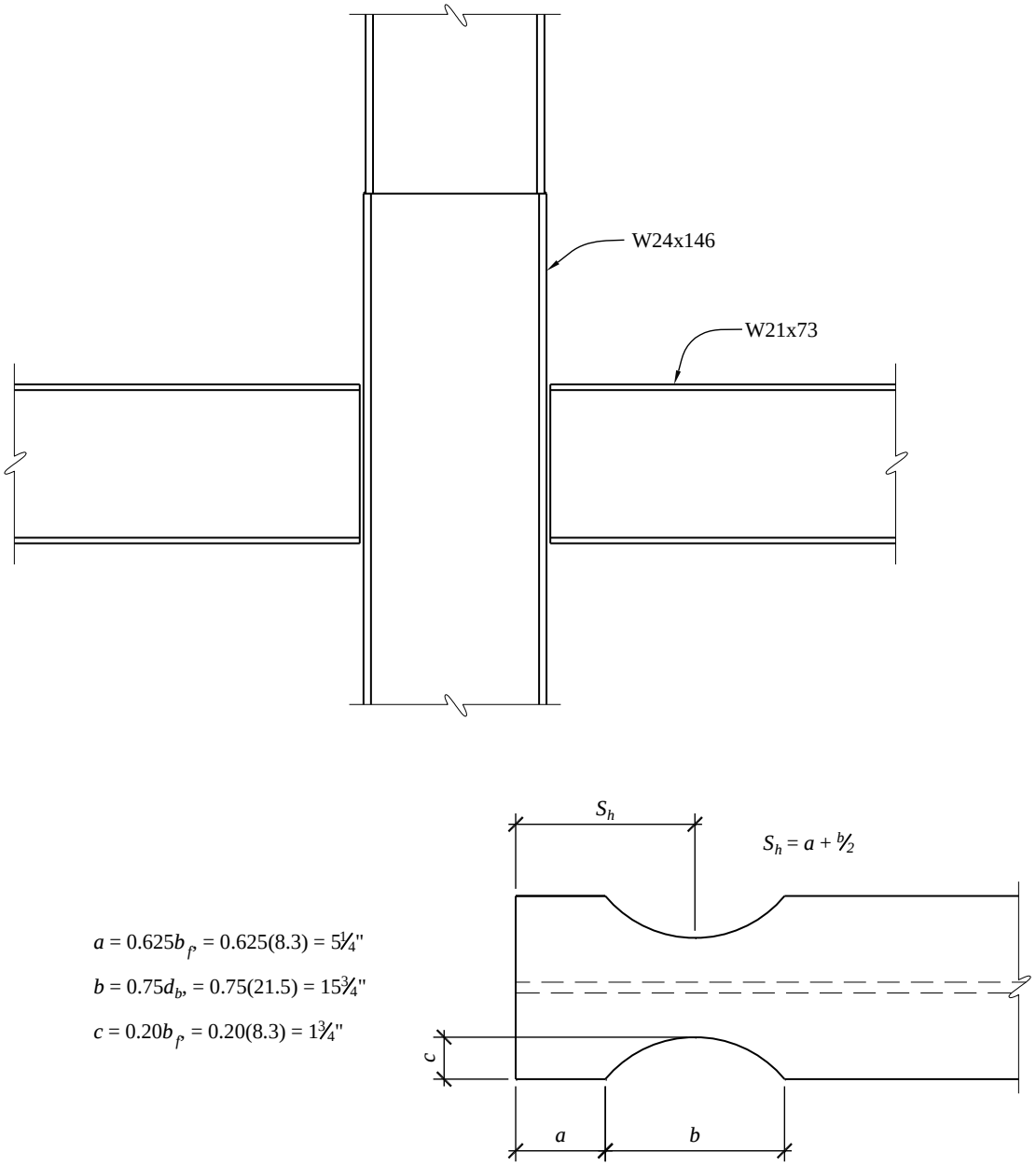

Figure 6.2-9 Reduced beam section dimensions
(1.0 in. = 25.4 mm)

Therefore:

$$V_e = 2M_{pr} / L' = 2(7361\text{in-kips}) / (248.8\text{in.}) = 59.2\text{kips}$$

$$V_g = w_u L' / 2 = (2.42\text{klf})(1/12)(248.8\text{ in.}) / 2 = 25.1\text{ kips}$$

$$V_p = 59.2\,\text{kips} + 25.1\,\text{kips} = 84.3\,\text{kips}$$

For the beam on the right, with gravity moments adding to seismic:

$$M^{\bullet}_{pb,r} = M_{pr} + V_e\left(S_h + \frac{d_c}{2}\right) + V_g\left(S_h + \frac{d_c}{2}\right)$$
$$= (7{,}361) + (59.2)\left((13.2) + \frac{(24.74)}{2}\right) + (25.1)\left((13.2) + \frac{(24.74)}{2}\right) = 9{,}517 \text{ in.-kips}$$

For the beam on the left, with gravity moments subtracting from seismic:

$$M^{\bullet}_{pb,r} = M_{pr} + V_e\left(S_h + \frac{d_c}{2}\right) - V_g\left(S_h + \frac{d_c}{2}\right)$$
$$= (7{,}361) + (59.2)\left((13.2) + \frac{(24.74)}{2}\right) - (25.1)\left((13.2) + \frac{(24.74)}{2}\right) = 8{,}233 \text{ in.-kips}$$

$$\sum M^{\bullet}_{pb} = M^{\bullet}_{pb,r} + M^{\bullet}_{pb,l} = 9{,}517 + 8{,}233 = 17{,}749 \text{ in.-kips}$$

Note that in most cases, the gravity moments cancel out and can be ignored for this check.

For the columns, the sum of the moments at the top and bottom flanges of the beam is:

$$\sum M_{BF} = \sum Z_c\left(F_{yc} - \frac{P_{uc}}{A_g}\right)$$

$$\sum M_{BF} = 2\left[418 \text{ in.}^3\left(50 \text{ ksi} - \frac{228 \text{ kips}}{43 \text{ in.}^2}\right)\right] = 37{,}367 \text{ in.-kips}$$

where:

M_{BF} = column moment at beam flange elevation

Referring to Figure 6.2-6, the moment at the beam centerline is:

$$\sum M^{\bullet}_{pc} = \sum M_{BF} + V^{\bullet}_c \frac{d_b}{2}$$

where:

$V^{\bullet}_c$ = $\left[M_{BF_i} + M_{BF_{i+1}}\right]/h_c$, based on the expected yielding of the spliced column assuming an inflection point at column mid-height (e.g., a portal frame) and not the expected shear when the mechanism forms, which is:

$$V_c = \left[\frac{1}{2}\sum M^{\cdot}_{pb_i} + \frac{1}{2}\sum M^{\cdot}_{pb_{i+1}}\right] / h$$, where h is the story height

h_c = clear column height between beams = (13.33 ft)(12 in./ft) – 21.24 in. = 139 in.

$$V^{\cdot}_c = \frac{(18{,}683 \text{ in.-kips}) + (7{,}964 \text{ in.-kips})}{(139 \text{ in.})} = 192 \text{ kips}$$

$$V_c = \left[\frac{1}{2}\sum M^{\cdot}_{pb_i} + \frac{1}{2}\sum M^{\cdot}_{pb_{i+1}}\right] / h = \left[\frac{1}{2}(17749) + \frac{1}{2}(14976)\right] / \left[(13.33)(12)\right]$$

=102 kips

Thus:

$$\sum M^{\cdot}_{pc} = 37{,}367 \text{ in.-kips} + (192 \text{ kips})\frac{(21.24 \text{ in.})}{2} = 39{,}400 \text{ in.-kips}$$

The ratio of column moment strengths to beam moment strengths is computed as:

$$\text{Ratio} = \frac{\sum M^{\cdot}_{pc}}{\sum M^{\cdot}_{pb}} = \frac{39{,}400 \text{ in.-kips}}{17{,}749 \text{ in.-kips}} = 2.22 > 1$$ OK

Since the ratio is greater than 2, bracing is only required at the top flange per AISC 341 Section 9.7a.

4. Check the Beam Strength: Per AISC 358 Equation 5.8-4, the beam strength at the reduced section is:

$$\phi M_{pr} = \phi F_y Z_e = (0.9)(50 \text{ksi})(122 \text{ in.}^3) = 5{,}490 \text{ in.-kips}$$

From analysis, M_u = 4072 in-kips. Therefore, $\phi M_{pr} \geq M_u$; the beam has adequate strength.

The moment at the column face is:

$$M_f = M_{pr} + V_e S_h \pm V_g S_h$$

$$M_{f,r} = 7{,}361 \text{ in.-kips} + (59.2 \text{ kips})(13.2 \text{ in.}) + (25.1 \text{ kips})(13.2 \text{ in.}) = 8{,}474 \text{ in.-kips}$$

$$M_{f,r} = 8{,}474 \text{ in.-kips} \leq \phi_d R_y F_y Z_x = (1.0)(1.1)(50)(172) = 9{,}460 \text{ in.-kips}$$ OK

To check the shear in the beam, first the appropriate equation must be selected:

$$2.24\sqrt{\frac{E}{F_{yw}}} = 2.24\sqrt{\frac{(29{,}000 \text{ ksi})}{(50 \text{ ksi})}} = 53.9$$

$$h/t_w = 46.6 \le 53.9$$

Therefore:

$$V_n = 0.6F_yA_wC_v$$

where C_v = 1.0.

$$V_n = 0.6(50\,\text{ksi})(21.2\,\text{in.})(0.455\,\text{in.})(1.0) = 289\ \text{kips}$$

Comparing this to V_p:

$$\phi V_n = 289 \ge 84.3 = V_p$$ OK

Check the beam lateral bracing. Per AISC 341 Section 9.8, the maximum spacing of the lateral bracing is:

$$L_b \le 0.086 r_y E / F_y = 0.086(1.81\,\text{in.})(29{,}000\,\text{ksi}) / (50\,\text{ksi}) = 90\,\text{in.} = 7'\text{-}6''$$

The braces near the plastic hinges are required to have a minimum strength of:

$$P_{br} = \frac{0.06M_u}{h_o}$$

$$= \frac{0.06(1.1)(50\,\text{ksi})(172\,\text{in.}^3)}{21.24\,\text{in.}^2 - 0.74\,\text{in.}^2} = 27.7\ \text{kips}$$

where:

$M_u = R_yF_yZ$

h_o = the distance between flange centroids

The required brace stiffness is:

$$\beta_{br} = \frac{10M_uC_d}{\phi L_b h_o}$$

$$= \frac{10(1.1)(50\,\text{ksi})(172\,\text{in.}^3)(1.0)}{0.75(6.39\,\text{ft})(12\,\text{in./ft})(21.24\,\text{in.}^2 - 0.74\,\text{in.}^2)} = 80.2\ \text{kips/in.}$$

L_b is taken as L_p. These values are for the typical lateral braces. No supplemental braces are required at the reduced section per AISC 358 Section 5.3.1.

5. Check Connection Design:

Check the need for continuity plates. Continuity plates are required per AISC 358 Section 2.4.4 unless:

$$t_{cf} \geq 0.4\sqrt{1.8 b_{bf} t_{bf} \left(\frac{F_{yb} R_{yb}}{F_{yc} R_{yc}} \right)}$$

$$\geq 0.4\sqrt{1.8(8.30 \text{ in.})(0.74 \text{ in.})\left(\frac{(50 \text{ ksi})(1.1)}{(50 \text{ ksi})(1.1)} \right)} = 1.33 \text{ in.}$$

And:

$$t_{cf} \geq \frac{b_{bf}}{6} = \frac{8.30 \text{ in.}}{6} = 1.38 \text{ in.}$$

Since t_{cf} = 1.09 inches, continuity plates are required. See below for the design of the plates.

Checking web crippling per AISC 360 Section J10.3:

$$R_u = \frac{M_{f,r}}{d_b - t_f} = \frac{8{,}474 \text{ in.-kips}}{(21.24 \text{ in.}) - (0.74 \text{ in.})} = 413 \text{ kips}$$

$$R_n = 0.40 t_w^2 \left[1 + 3\left(\frac{N}{d} \right)\left(\frac{t_w}{t_f} \right)^{1.5} \right] \sqrt{\frac{E F_{yw} t_f}{t_w}}$$

$$R_n = 0.80(0.65)^2 \left[1 + 3\left(\frac{(0.74 + 5/16)}{(24.74)} \right)\left(\frac{(0.65)}{(1.09)} \right)^{1.5} \right] \sqrt{\frac{(29{,}000)(50)(1.09)}{(0.65)}} = 558 \text{ kips}$$

$$\phi R_n = 0.75(558 \text{ kips}) = 419 \text{ kips} \geq 413 \text{ kips} = R_u \qquad \text{OK}$$

Checking web local yielding per *Specification* Section J10.2:

$$R_u = 413 \text{ kips}$$

$$\phi R_n = \phi(5k + N) F_{yw} t_w$$

$$\phi R_n = (1.00)\left(5(1.59 \text{ in.}) + (0.74 \text{ in.} + \tfrac{5}{16} \text{ in.})\right)(50 \text{ ksi})(0.65 \text{ in.}) = 293 \text{ kips}$$

Therefore, since $\phi R_n \leq R_u$, as well as due to the check above, continuity plates are required. The force that the continuity plates must take is 413 - 293 = 120 kips. Therefore, each plate takes 60 kips. The minimum thickness of the plates is the thickness of the beam flanges, 0.74 inch. The minimum width of the plates per AISC 341 Section 7.4 is:

$$b_{pl} = b_{f,b} - 2(k_{1,b} + \tfrac{1}{2}\text{ in.})$$

$$= 8.31\text{ in.} - 2\left(0.875\text{ in.} + 0.5\text{ in.}\right) = 5.56\text{ in.}$$

Checking the strength of the plate with minimum dimensions:

$$\phi R_n = \phi t_{pl} b_{pl} F_y$$

$$= \left(1.0\right)\left(0.74\text{ in.}\right)\left(5.56\text{ in.}\right)\left(50\text{ ksi}\right) = 206\text{ kips}$$

Therefore, since ϕR_n = 206 kips > 60 kips, the minimum continuity plates have adequate strength. Alternatively, a W24x192 section will work in lieu of adding continuity plates.

6. Check Panel Zone: The *Standard* defers to AISC 341 for the panel zone shear calculation.

   The panel zone shear calculation for Story 2 of the frame in the E-W direction at Grid C (column: W24x176; beam: W21x73) is from AISC 360 Section J10.6. Check the shear requirement at the panel zone in accordance with AISC 341 Section 9.3. The factored shear R_u is determined from the flexural strength of the beams connected to the column. This depends on the style of connection. In its simplest form, the shear in the panel zone (R_u) is as follows for W21x73 beams framing into each side of a W24x146 column (such as Level 2 at Grid C):

$$R_u = \sum \frac{M_f}{d_b - t_{fb}} = \frac{16,285}{21.24 - 0.74} = 794\text{ kips}$$

   M_f is the moment at the column face determined by projecting the expected moment at the plastic hinge points to the column faces (see Figure 6.2-5):

$$M_f = M_{pr} + V_e S_h \pm V_g S_h$$

$$M_{f,r} = 7,361\text{ in.-kips} + \left(59.2\text{ kips}\right)\left(13.2\text{ in.}\right) + \left(25.1\text{ kips}\right)(13.2\text{ in.}) = 8,474\text{ in.-kips}$$

$$M_{f,l} = 7361\text{in}^{-}\text{kips} + \left(59.2\,\text{kips}\right)\left(13.2\text{ in.}\right) - \left(25.1\text{kips}\right)(13.2\text{ in.}) = 7811\text{in}^{-}\text{kips}$$

   Note that in most cases, the gravity moments cancel out and can be ignored for this check. The total moment at the column face is:

$$\sum M_f = M_{f,r} + M_{f,l} = 8,474\text{ in.-kips} + 7,811\text{ in.-kips} = 16,285\text{ in.-kips}$$

   The shear transmitted to the joint from the story above, V_c, opposes the direction of R_u and may be used to reduce the demand. Previously calculated, this is 102 kips at this location. Thus the frame R_u = 794 - 102 = 692 kips.

   The column axial force (Load Combination: $1.2D + 0.5L + \Omega_o E$) is P_r = 228 kips.

$$0.75P_c = 0.75F_yA_g = 0.75(50\text{ ksi})(43\text{ in.}^2) = 1{,}613\text{ kips}$$

Since $P_r \le 0.75\ P_c$, using AISC 360 Equation J10-11:

$$R_n = 0.60F_y d_c t_w \left(1 + \frac{3b_{cf}t_{cf}^2}{d_b d_c t_w}\right)$$

$$R_n = 0.60(50)(24.74)(0.65)\left(1 + \frac{3(12.90)(1.09)^2}{(21.24)(24.74)(0.65)}\right) = 547\text{ kips}$$

Since ϕ_v is 1, $\phi_v R_n$ = 547 kips.

$$\phi_v R_n = 547\text{ kips} < 692\text{ kips} = R_u$$

Therefore, doubler plates are required. The required additional strength from the doubler plates is 692 - 547 = 145 kips. The strength of the doubler plates is:

$$\phi_v R_n = 0.6t_{doub}d_c F_y$$

Therefore, to satisfy the demand the doubler plate must be at least 1/4 inch thick. Plug welds are required as:

$$t = 0.25\text{ in.} < (d_z + w_z)/90 = [21.24 + 24.74 - 2(1.09)]/90 = 0.49\text{ in.}$$

Use four plug welds spaced 12 inches apart. Alternatively, the use of a W24x192 column will not require doubler plates ($\phi_v R_n$ = 737 kips).

6.2.5 Analysis and Design of Alternative B: SCBF

6.2.5.1 Modal Response Spectrum Analysis. As with the SMF, find the approximate building period (T_a) using *Standard* Equation 12.8-7:

$$T_a = C_t h_n^x = (0.02)(102.3)^{0.75} = 0.64\text{ sec}$$

C_uT_a, the upper limit on the building period, is determined per *Standard* Table 12.8-1:

$$T = C_uT_a = (1.4)(0.64) = 0.896\text{ sec}$$

It is assumed that the calculated period will exceed C_uT_a; this is verified after member selection. The seismic response coefficient (C_s) is determined from *Standard* Equation 12.8-2 as follows:

$$C_s = \frac{S_{DS}}{R/I} = \frac{1}{6/1} = 0.167$$

However, *Standard* Equation 12.8-3 indicates that the value for C_s need not exceed:

$$C_s = \frac{S_{D1}}{T(R/I)} = \frac{0.6}{(0.896\,\text{sec})(6/1)} = 0.112$$

and the minimum value for C_s per *Standard* Equation 12.8-5 is:

$$C_s = 0.044 I S_{DS} \geq 0.01 = (0.044)(1)(1) = 0.044$$

Use C_s = 0.112.

Seismic base shear is computed using *Standard* Equation 12.8-1 as:

$$V = C_S W = (0.112)(13{,}156\,\text{kips}) = 1{,}473\ \text{kips}$$

where *W* is the seismic mass of the building as determined above.

In evaluating the building in ETABS, twelve modes are analyzed, resulting in a total modal mass participation of 99 percent. The *Standard* Sec. 12.9.1 requires at least 90 percent participation. As before with Alternative A, strength is scaled to 85 percent of the equivalent lateral force base shear and drift is scaled by $gC_d/(R/I)$.

6.2.5.2 Size members. The method used to size members is as follows:

1. Select brace sizes based on strength
2. Select column sizes based on special seismic load combinations (*Standard* Sec. 12.4.3.2)
3. Select beam sizes based on the load imparted by the expected strength of the braces
4. Check drift (*Standard* Sec. 12.12)
5. Design the connection

Reproportion member sizes as necessary after each check. After the weight and stiffness have been modified by changing member sizes, the response spectrum must be rescaled. Torsional amplification is a significant consideration in this alternate.

1. Select Preliminary Member Sizes and Check Strength: The preliminary member sizes are shown for the braced frame in the E-W direction (seven bays) in Figure 6.2-10 and in the N-S direction (five bays) in Figures 6.2-11 and 6.2-12.

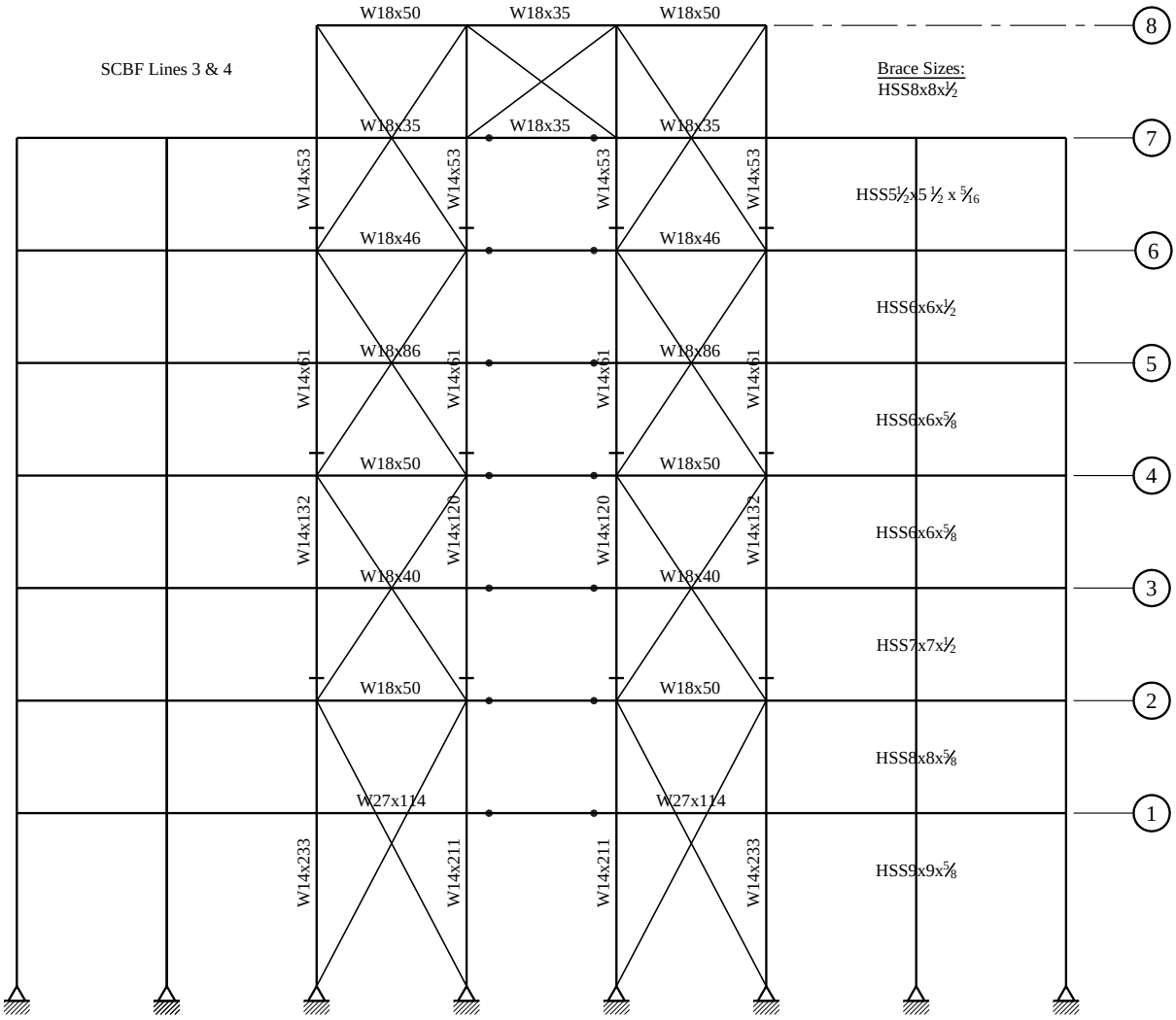

Figure 6.2-10 Braced frame in E-W direction

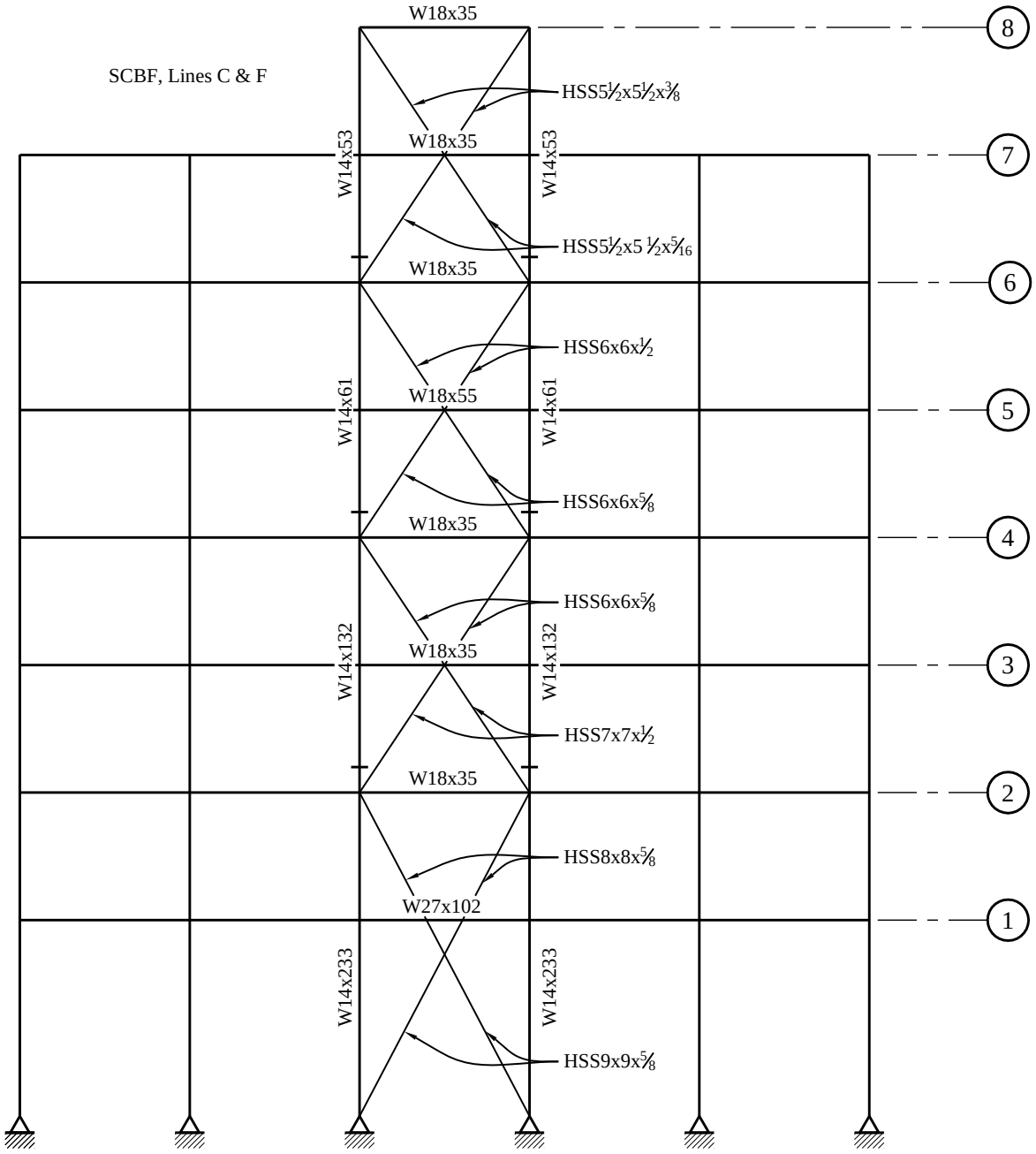

Figure 6.2-11 Braced frame in N-S direction on Gridlines C and F

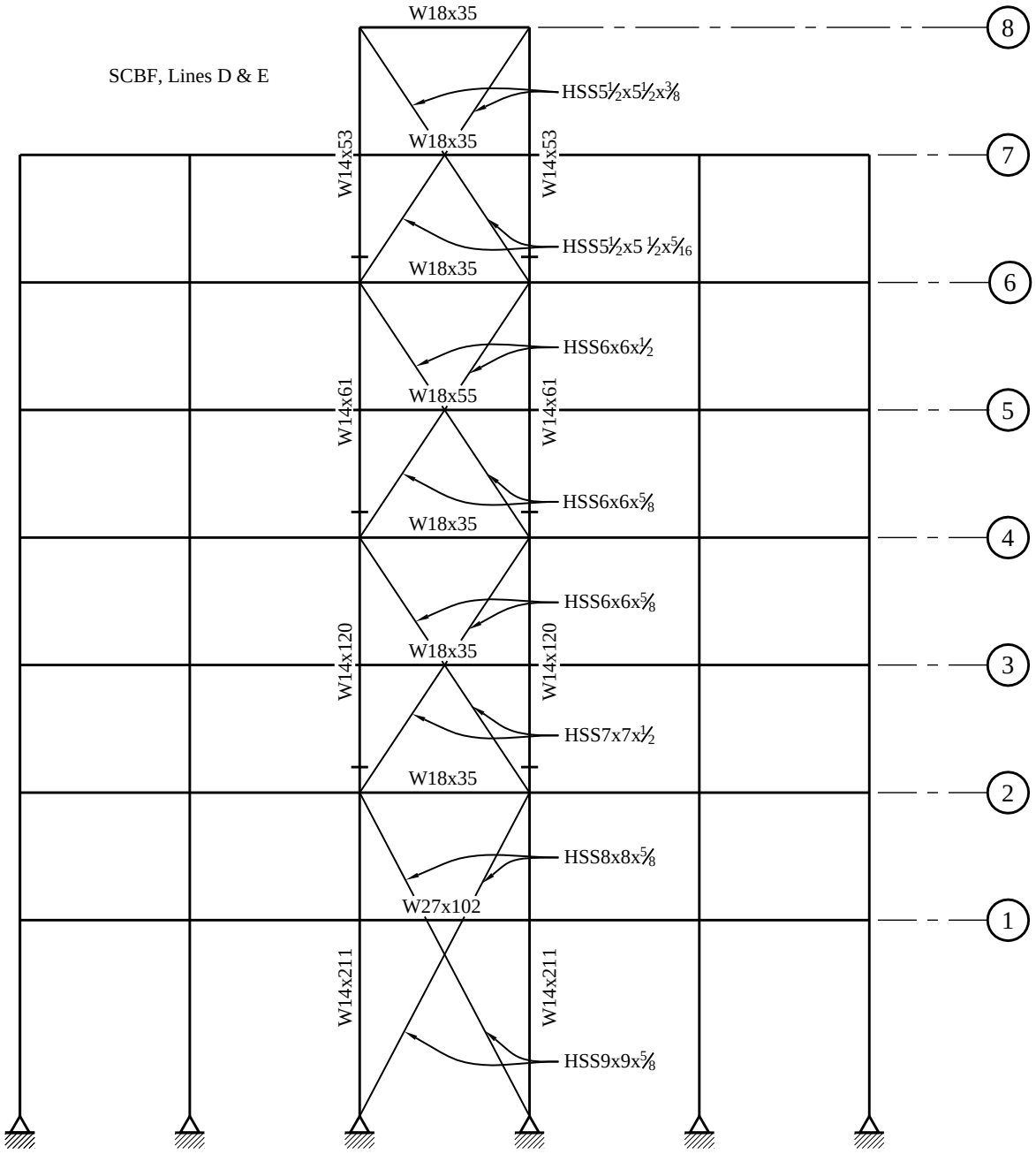

Figure 6.2-12 Braced frame in N-S direction on Gridlines D and E

Check slenderness and width-to-thickness ratios—the geometrical requirements for local stability. In accordance with AISC 341 Section C13.2a, bracing members must satisfy the following:

$$\frac{kl}{r} \le 200$$

All members are seismically compact for SCBF per AISC SDM Table 1-2, thus satisfying slenderness requirements.

Columns: Wide flange members must comply with the width-to-thickness ratios contained in AISC 341 Table I-8-1. Flanges must satisfy the following:

$$\frac{b}{t} \le 0.30\sqrt{E / F_y} = 7.23$$

Webs in combined flexural and axial compression (where $P_u/\phi_b P_y = 0.385 > 0.125$) must satisfy the following:

$$\frac{h_c}{t_w} \le 1.12\sqrt{E / F_y}\left(2.33 - \frac{P_u}{\phi_b P_y}\right) = 52.5$$

Braces: Rectangular HSS members must satisfy the following:

$$\frac{b}{t} \le 0.64\sqrt{E / F_y} = 16.1$$

Using a redundancy factor of 1.3 on the earthquake loads, the braces are checked for strength using ETABS and found to be satisfactory.

2. Select Column Sizes: Columns are checked using special seismic load combinations; ρ does not apply in these combinations (see *Standard* Sec. 12.3.4.1 Item 6). The columns are then checked for strength using ETABS and found to be satisfactory.

3. Select Beam Sizes: The beams are sized to be able to resist the expected plastic and post-buckling capacity of the braces. In the computer model, the braces are removed and replaced with forces representing their capacities. These loads are applied for four cases reflecting earthquake loads applied both left and right in the two orthogonal directions (T_{1x}, T_{2x}, T_{1y}, T_{2y}). For instance, in T_{1x}, the earthquake load is imagined to act left to right; the diagonal braces expected to be in tension under this loading are replaced with the force $R_y F_y A_g$ and the braces expected to be in compression are replaced with the force $0.3P_n$. For T_{2x}, the tension braces are now in compression and vice versa. T_{1y} and T_{2y} apply in the other orthogonal direction.

   The load cases applied are as follows:

   $\left(1.2 + 0.2S_{DS}\right)D + 0.5L + T$ (four combinations; use all four T's)

   $\left(0.9 - 0.2S_{DS}\right)D + T$ (four combinations; use all four T's)

   Beam strength is checked for each of these eight load combinations using ETABS and found to be satisfactory.

4. Check Story Drift: After designing the members for strength, the ETABS model is used to determine the design story drift. The results are summarized in Table 6.2-2.

Table 6.2-2 Alternative B Story Drifts under Seismic Load

	Elastic Displacement at Building Corner, From Analysis		Expected Displacement ($=\delta_e C_d$)		Design Story Drift Ratio		Allowable Story Drift Ratio
Level	δ_eE-W (in.)	δ_eN-S (in.)	δ E-W (in.)	δ N-S (in.)	Δ E-W/h (%)	Δ N-S/h (%)	Δ/h (%)
Level 7	1.63	1.75	8.14	8.76	0.72	0.93	2.0
Level 6	1.41	1.48	7.07	7.38	0.74	0.94	2.0
Level 5	1.19	1.20	5.97	5.99	0.76	0.84	2.0
Level 4	0.96	0.94	4.80	4.72	0.81	0.85	2.0
Level 3	0.71	0.69	3.56	3.43	0.72	0.71	2.0
Level 2	0.49	0.47	2.44	2.33	0.60	0.59	2.0
Level 1	0.30	0.28	1.49	1.40	0.56	0.52	2.0

1.0 in. = 25.4 mm.

All story drifts are within the allowable story drift limit of $0.020h_{sx}$ in accordance with ***Standard*** Section 12.12 and the allowable deflections for this building from Section 6.2.3.6 above. As shown in the table above, the drift is far from being the governing design consideration.

5. Design the Connection: Figure 6.2-13 illustrates a typical connection design at a column per AISC 341 Section 13.

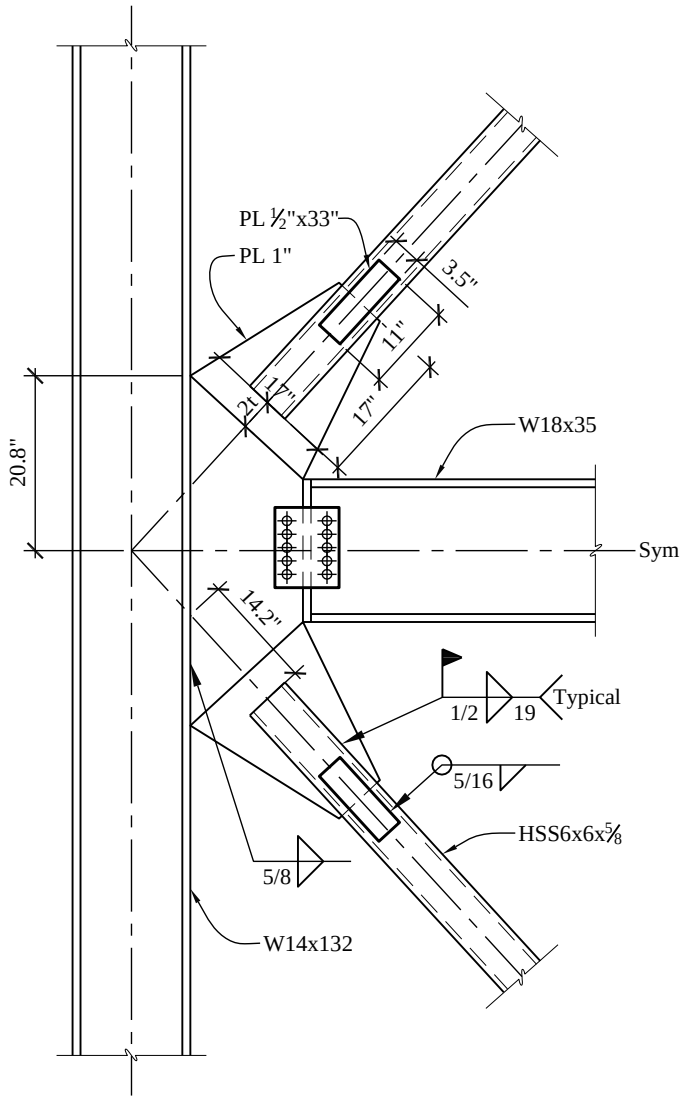

Figure 6.2-13 Bracing connection detail (1.0 in. = 25.4 mm, 1.0 ft = 0.3048 m)

The connection designed in this example is at the fourth floor on Gridline C. The required strength of the connection is to be the nominal axial tensile strength of the bracing member. For an HSS6x6x5/8, the expected axial tensile strength is computed using AISC 341 Section 13.3a:

$$R_u = R_y F_y A_g = (1.4)(46 \text{ ksi})(11.7 \text{ in.}^2) = 753 \text{ kips}$$

The area of the gusset is determined using the plate thickness and section width (based on geometry). See Figure 6.2-13 for the determination of this dimension. The thickness of the gusset is chosen to be 1 inch.

For tension yielding of the gusset plate:

$$\phi T_n = \phi F_y A_g = (0.90)(50 \text{ ksi})(1 \text{ in.} \times 17 \text{ in.}) = 765 \text{ kips} > 753 \text{ kips} \qquad \text{OK}$$

For fracture in the net section:

$\phi T_n = \phi F_u A_n = (0.75)(65 \text{ ksi})(1 \text{ in.} \times 17 \text{ in.}) = 829 \text{ kips} > 753 \text{ kips}$ OK

For a tube slotted to fit over a connection plate, there will be four welds. The demand in each weld will be 753 kips/4 = 188 kips. The design strength for a fillet weld per AISC 360 Table J2.5 is:

$\phi F_w = \phi(0.6F_{exx}) = (0.75)(0.6)(70 \text{ ksi}) = 31.5 \text{ ksi}$

For a 1/2-inch fillet weld, the required length of weld is determined to be:

$$L_w = \frac{188}{(0.707)(0.5 \text{ in.})(31.5 \text{ ksi})} = 16.9 \text{ in.}$$

Therefore, use 17 inches of weld.

In accordance with the exception of AISC 341 Section 13.3b, the design of brace connections need not consider flexure if the gusset can accommodate the inelastic rotation associated with brace post-buckling deformations. This is typically done by providing a “hinge zone"; the gusset plate is detailed such that it can form a plastic hinge over a distance of 2*t* (where *t* = thickness of the gusset plate) from the end of the brace. The gusset plate must be permitted to flex about this hinge, unrestrained by any other structural member. See also AISC 341 Section C13.3b. With such a pinned-end condition, the compression brace tends to buckle out-of-plane. During an earthquake, there will be alternating cycles of compression and tension in a single bracing member and its connections. Proper detailing is imperative so that tears or fractures in the steel do not initiate during the cyclic loading.

While the gusset is permitted to hinge, it must not buckle. To prevent buckling, the gusset compression strength must exceed the expected brace strength in compression per AISC 341 Section 13.3c. Determine the nominal compressive strength of the brace member. The effective brace length (*kL*) is the distance between the hinge zones on the gusset plates at each end of the brace member. This length is somewhat dependent on the gusset design. For the brace being considered, *kL* = 161 inches the expected compressive strength is determined using expected (not specified minimum) material properties per AISC 360 Section E3:

$$P_n = F_{cr} A_g$$

where:

A_g = gross area of the brace

F_{cr} = flexural buckling stress, determined as follows

When:

$$\frac{kL}{r} \le 5.18\sqrt{E / R_y F_y} = 119$$

$$F_{cr} \le \left[0.692^{\frac{R_y F_y}{F_e}} \right] R_y F_y$$

Otherwise,

$$F_{cr} \le F_e$$

where:

$$F_e = \frac{\pi^2 E}{\left(\frac{kL}{r}\right)^2}$$

The equations have been recalibrated to use the expected stress rather than the specified minimum yield stress. Note that the 0.877 factor, which represents out-of-straightness, is not used here in order to calculate an upper bound brace strength and thereby ensure adequate gusset compression strength. Here, kL/r = (1)(161)/(2.17) = 74.2, thus:

$$F_e = \frac{\pi^2 (29{,}000 \text{ ksi})}{(74.2)^2} = 52.0 \text{ ksi}$$

$$F_{cr} = \left[0.692^{\frac{(1.4)(46 \text{ ksi})}{(52 \text{ ksi})}} \right] (1.4)(46 \text{ ksi}) = 40.8 \text{ ksi}$$

$$P_n = (40.8 \text{ ksi})(11.7 \text{ in.}^2) = 478 \text{ kips}$$

Now, using the expected compressive load from the brace of 449 kips, check the buckling capacity of the gusset plate using the section above. By this method, illustrated by Figure 6.2-13, the compressive force per unit length of gusset plate is (478 kips/23.5 in.) = 20.3 kips/in.

Try a plate thickness of 1 inch:

$f_a = P/A$ = 20.3 kips/(1 in. × 1 in.) = 20.3 ksi

The gusset plate is modeled as a 1-inch-wide by 1-inch-deep rectangular section, fixed at both ends. The length, from geometry, is 17.2 inches. The effective length factor, k, for this "column" is 1.2 per AISC 360 Table C-C2.2. The radius of gyration, r, for a plate is $t / \sqrt{12}$.

Per AISC 360 Section E3:

$$\frac{kL}{r} = \frac{(1.2)(17.2 \text{ in.})}{(0.29 \text{ in.})} = 71.2$$

$$F_e = \frac{\pi^2 (29{,}000 \text{ ksi})}{(71.2)^2} = 56.5 \text{ ksi}$$

$$F_{cr} = \left[0.658^{\frac{(50 \text{ ksi})}{(56.5 \text{ ksi})}} \right] (50 \text{ ksi}) = 34.5 \text{ ksi}$$

$$F_{cr} = 34.5 \text{ksi} > 20.3 \text{ksi} = f_a$$ OK

Next, check the reduced section of the tube, which has a 1-1/8-inch-wide slot for the gusset plate (the thickness of the gusset plus an extra 1/8 inch for ease of construction). The reduction in HSS6x6x5/8 section due to the slot is (0.581 in. × 1.125 in. × 2) = 1.31 in.^{2} the net section, A_{net} = (11.7 - 1.31) = 10.4 in.^{2}

To ensure gross section yielding governs, reinforcement is added over the area of the slot. The shear lag factor is computed per AISC 360 Table D3.1:

$$U = 1 - \bar{x} / l$$

where:

$$\bar{x} = \frac{B^2 + 2BH}{4(B+H)} = \frac{(6 \text{ in.})^2 + 2(6 \text{ in.})(6 \text{ in.})}{4(6 \text{ in.} + 6 \text{ in.})} = 2.25 \text{ in.}$$

and l is the length of the weld as determined above.

$$U = 1 - \frac{(2.25 \text{ in.})}{(17 \text{ in.})} = 0.867$$

Thus, the effective area of the section is:

$$A_e = UA_{net} = (0.867)(10.4 \text{ in.}^2) = 9.02 \text{ in.}^2$$

Try a reinforcing plate 1/2 inch thick and 3-1/2 inches wide on each side of the brace. (The necessary width can be computed from the effective area, but that calculation is not performed here.) Grade 50 material is used in order to match or exceed the brace material strength, thus allowing for treatment of the material as homogenous. The area of the section is (2 × 0.5 in. × 3.5 in.) = 3.5 in.^{2}. The distance of its center of gravity from the center of gravity of the slotted brace is:

$$\bar{x} = \frac{B}{2} + \frac{t_{reinf}}{2} = \frac{(6 \text{ in.})}{2} + \frac{(0.5 \text{ in.})}{2} = 3.25 \text{ in.}$$

Thus, the area of the reinforced section is:

$$A = A_n + A_{reinf} = 10.4 \text{ in.}^2 + 3.5 \text{ in.}^2 = 13.9 \text{ in.}^2$$

The weighted average of the *x*'s is 2.53 inches. Thus, the shear lag factor for the reinforced section is:

$$U = 1 - \frac{(2.53 \text{ in.})}{(16.9 \text{ in.})} = 0.850$$

Thus, the effective area of the section is:

$$A_e = UA_{net} = (0.850)\left(13.9 \text{in.}^2\right) = 11.8 \text{ in.}^2$$

Now, check the effective area of the reinforced section against the original section of the brace per AISC 341 Section 13.2b:

$$\frac{A_g}{A_e} = \frac{(11.7 \text{ in.}^2)}{(11.8 \text{ in.}^2)} = 0.99 \le 1 \qquad \text{OK}$$

The reinforcement is attached to the brace such that its expected yield strength is developed.

$$R_u = A_{reinf} R_y F_y = 3.5 \text{ in.}^2 (1.1)(50 \text{ ksi}) = 193 \text{ kips}$$

The plate will be developed with two 5/16-inch fillet welds, 14 inches long:

$$R_n = 2\phi 0.6 F_{exx} \sqrt{2}/2 \, sL = 2(0.75)(0.6)(70 \text{ ksi}) \sqrt{2}/2 \, (5/16 \text{ in.})(14 \text{ in.}) = 195 \text{ kips}$$

The force must be developed into the plate, carried past the reduced section developed out of the plate. To accomplish this, the reinforcement plate will be 33 inches: 14 inches on each side of the reduced section, 2 inches of anticipated over slot, plus 1 inch to provide erection tolerance.

The complete connection design includes the following checks (which are not demonstrated here):

- Attachment of reinforcement to brace
- Brace shear rupture
- Brace shear yield
- Gusset block shear
- Gusset yield, tension rupture, shear rupture weld at both the column and the beam
- Web crippling and yielding for both the column and the beam
- Gusset edge buckling
- Beam-to-column connection

6.2.6 Cost Comparison

For each case, the total structural steel was estimated. The takeoffs are based on all members, but do not include an allowance for plates and bolts at connections. The result of the material takeoffs are as follows:

- Alternative A, Special Steel Moment Resisting Frame: 640 tons
- Alternative B, Special Steel Concentrically Braced Frame: 646 tons

The higher weight of the systems with bracing is primarily due to the placement of the bracing in the core, where resistance to torsion is poor. Torsional amplification and drift limitations both increased the weight of steel in the bracing. The weight of the moment-resisting frame is controlled by drift and the strong column rule.

6.3 TEN-STORY HOSPITAL, SEATTLE, WASHINGTON

This example features a buckling-restrained braced frame (BRBF) building. The example covers:

- Analysis issues specific to buckling-restrained braced frames
- Proportioning of buckling-restrained braces
- Capacity design principles
- Nonlinear response history analysis
- Buckling-restrained brace connections

6.3.1 Building Description

This ten-story hospital includes a two-story podium structure beneath an eight-story tower, as shown in Figures 6.3-1 and 6.3-2. The podium is 211.3 feet by 121.3 feet in plan, while the tower's floorplate is square with 91.3-foot sides. Story heights are 18 feet in the podium and reduce to 15 feet throughout the tower, bringing the total building height to 156 feet. As the tower is centered horizontally on the podium below, the entire building is symmetric about a single axis. Both the podium and the tower have large roof superimposed dead loads due to heavy HVAC equipment located there.

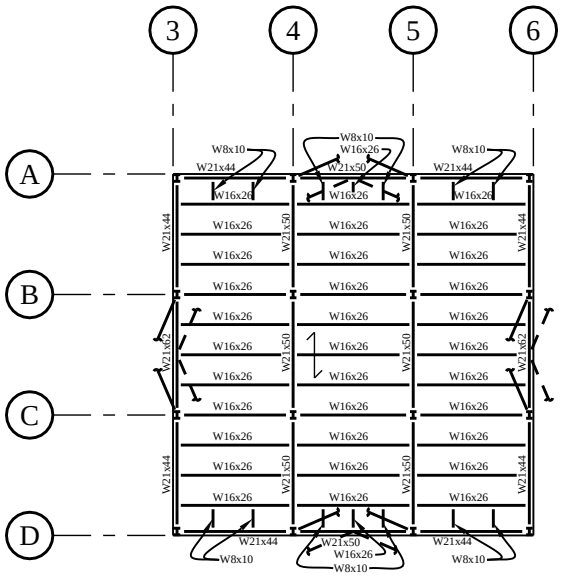

Figure 6.3-1 Typical tower plan

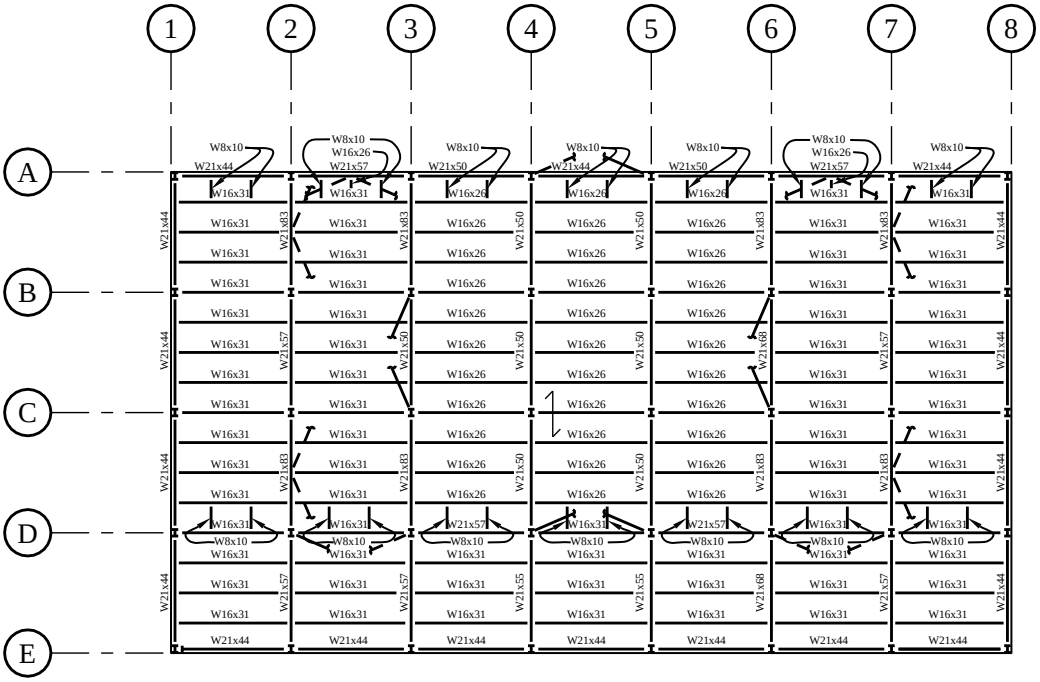

Figure 6.3-2 Level 3 podium plan

The structure exemplifies a common situation for hospital facilities. The combination of a stiff podium structure beneath a more flexible tower results in significant force transfer at the floor level between them.

The vertical-load-carrying system consists of lightweight concrete fill on steel deck floors supported by steel beams and girders that span to steel columns. The bay spacing is 30 feet each way. There are three floor beams per bay. All beams and girders are composite.

BRBFs have been selected for this building because they provide high stiffness paired with a high degree of ductility and stable hysteretic properties. The building has a thick mat foundation. The foundation soil is representative of Site Class C conditions identical to those discussed in Section 3.2. The design of foundations is not included here.

6.3.1.1 Design method. Seismic forces, rather than wind forces, govern the building's lateral design (in part due to the mass of the thick concrete-filled decks). The lateral force-resisting system throughout the tower consists of BRBFs in the middle bay along each side of the perimeter—Gridlines 3, 6, A D, as can be seen in the representative elevation of Figure 6.3-3. These BRBFs deliver lateral loads to the collectors and diaphragm at the third floor where both in-plane and out-of-plane discontinuities exist. This transfer occurs in-plane along Gridlines A and D to two braced bays nearer the ends of the podium and out-of-plane from a single braced bay in the tower along Gridlines 3 and 6 to braces in the two adjacent bays along Gridlines 2 and 7 in the podium below. The podium bracing configuration is illustrated in Figure 6.3-2. A typical bracing elevation in the transverse direction of the podium (illustrating the out-of-plane offset) is shown in Figure 6.3-4.

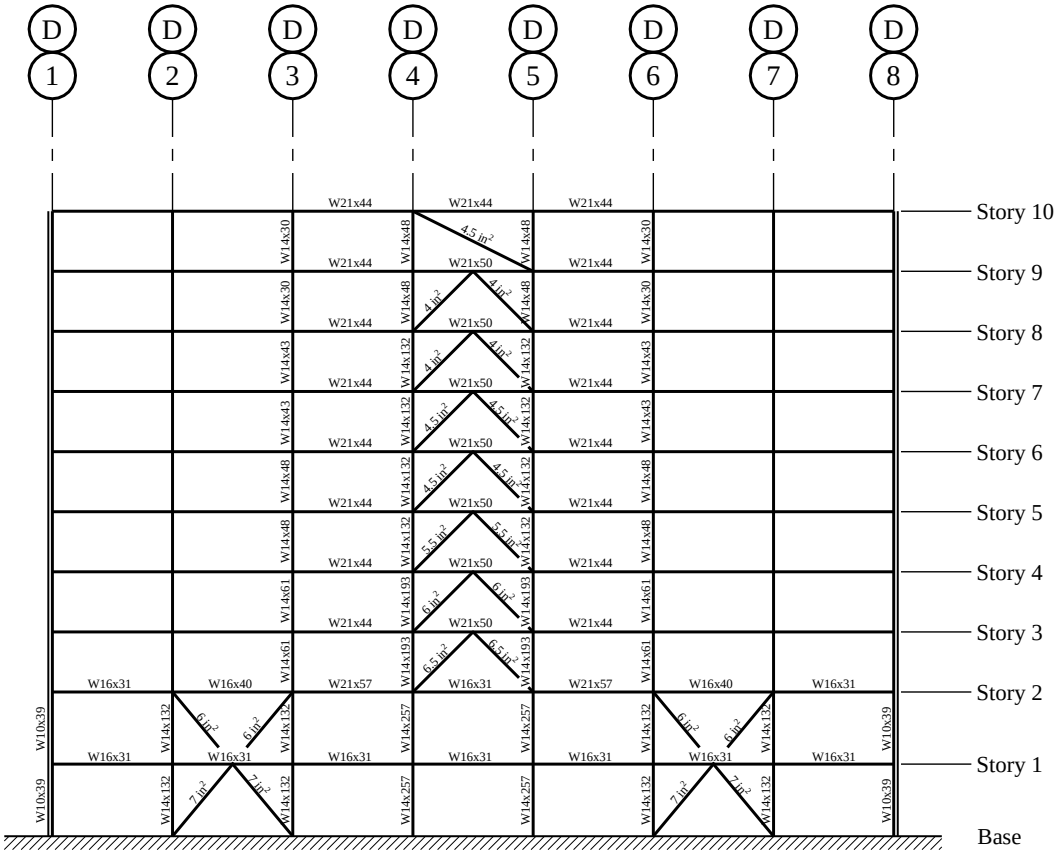

Figure 6.3-3 Longitudinal elevation at Gridline D

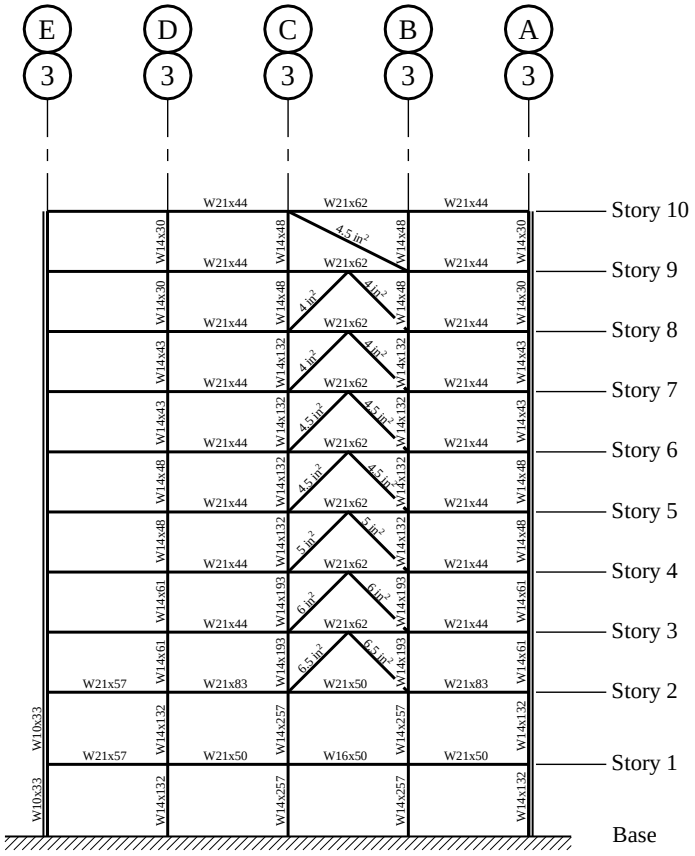

Gridlines 3 & 5

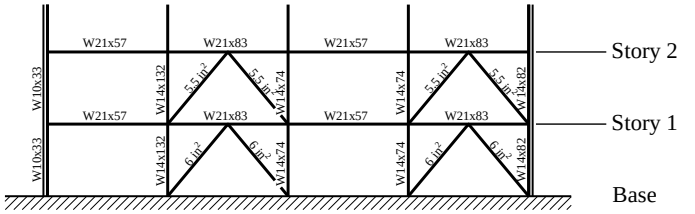

Gridlines 2 & 6

Figure 6.3-4 Transverse elevations

An ELF analysis is first performed to scale the base shear for the subsequent MRSA used for strength design of the buckling-restrained braces (BRB). Each BRB is designed for its share of 100 percent of the horizontal component of the earthquake lateral load without considering additional tributary vertical loads. This is done to encourage distributed yielding of braces up the height of the structure and is justified because the braces will shed any gravity load upon first yield and transfer it to the connecting beams and columns, which are designed to accommodate gravity loads without support provided by the braces. Beams, columns collectors are preliminarily sized using capacity design principles considering plastic mechanisms that develop based on the brace sizes determined using elastic MRSA. Finally, a

nonlinear response history analysis (NRHA) is executed to verify BRB strains remain at acceptable levels, check that story drifts do not exceed allowable limits possibly reduce column sizes from what the plastic mechanism analyses require. The details of this design procedure are summarized in Table 6.3-1.

Table 6.3-1 Design Philosophy

Element	Action	Analysis Method	Software	Acceptance Criteria
BRBs	Strength	MRSA	ETABS	AISC 341
	Deformation	NRHA	PERFORM	ASCE 41
Columns	Strength	NRHA	PERFORM	AISC 360
	Rotation	NRHA	PERFORM	ASCE 41
Diaphragms	Story Drift	NRHA	PERFORM	ASCE 7
Collector beams, braced-bay beams, etc.	Strength	MRSA	ETABS	AISC 360

6.3.2 Basic Requirements

6.3.2.1 *Provisions* parameters. Section 3.2 illustrates the determination of design ground motion parameters for this example. They are as follows:

- S_{DS} = 0.859
- S_{D1} = 0.433
- Occupancy Category IV
- Seismic Design Category D

For BRBFs (*Standard* Table 12.2-1):

- R = 8
- Ω_o = 2.5
- C_d = 5

These values are representative of a seismic force-resisting system that is a unification of two previously different BRBF system classifications: those with non-moment-resisting beam-column connections and those with moment-resisting beam-column connections. Modifications to Section 15.7 of AISC 341 now require the beam-to-column connections for a building frame system either to meet the requirements for fully restrained (FR) moment connections as specified in AISC 341 Section 11.2a or to possess sufficient rotation capacity to accommodate the rotation required to achieve a story drift of 2.5 percent. The later compliance path is selected for this design example. This requirement effectively amounts to a braced frame with simple beam-to-column connections per AISC 360 Section B3.6a with rotation specified at 2.5 percent. A standard detail illustrating this connection is presented in Figure 6.3-5.

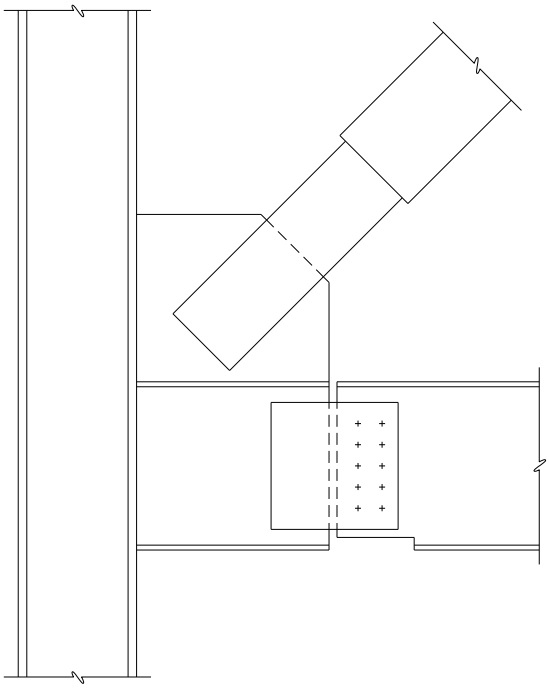

Figure 6.3-5 "Pinned" beam-to-column connection

6.3.2.2 Loads.

- Roof live load, L_r: 25 psf
- Roof dead load, *D:* 135 psf
- Exterior wall cladding: 300 plf of spandrel beams
- Floor live load, *L:* 60 psf
- Partitions: 10 psf
- Floor dead load, *D:* 104 psf
- Floor live load reductions: per the IBC

Roof dead load includes roofing, insulation, lightweight concrete-filled metal deck, concrete ponding allowance, framing, mechanical and electrical equipment, ceiling fireproofing. Floor dead load includes lightweight concrete-filled metal deck, ponding allowance, framing, mechanical and electrical equipment, ceiling and fireproofing. Due to potential for rearrangement, partition loads are considered live loads per *Standard* Section 4.2.2 but are also included in the effective seismic weight in accordance with *Standard* Section 12.7.2. Therefore, the seismic weight of a typical tower floor, whose footprint is a square 8,342 ft^2 in area, is 104 + 10 + 300(30)(3)(4)/8,342 = 127 psf.

6.3.2.3 Materials

- Concrete for drilled piers: f_c' = 5 ksi, normal weight (NW)
- Concrete for floors: f_c' = 3 ksi, lightweight (LW)
- All other concrete: f_c' = 4 ksi, NW
- Structural steel:
  Wide flange sections: ASTM A992, Grade 50
  Plates: ASTM A36

6.3.3 Structural Design Criteria

6.3.3.1 Building configuration. The hospital building does not possess any stiffness, strength, or weight irregularities despite the relatively tall height of the podium stories. At the podium levels, the two braced bays corresponding to each line of single-bay chevron bracing in the tower above provide more than enough additional strength to compensate for the slight increase in floor-to-floor height. The story drift ratio increases up the full height of the structure, meeting the exception of *Standard* Section 12.3.2.2 for assessing vertical stiffness and weight irregularities. However, the structure does possess both a vertical geometric irregularity (Type 3) and an in-plane discontinuity in vertical lateral force-resisting element irregularity (Type 4) since the lateral force-resisting system transitions from a single chevron braced bay in the tower to two chevron braced bays at the podium levels. The two chevron braced bays in the podium occur two bays away from the tower braced bay in the longitudinal direction. The Type 4 vertical irregularity triggers an increase in certain design forces per *Standard* Sections 12.3.3.3 and 12.3.3.4. Together, the Type 3 and Type 4 vertical irregularities preclude the use of an equivalent lateral force analysis as defined in *Standard* Section 12.8 based on the permissions in *Standard* Table 12.6-1. Note that this analysis prohibition is also triggered by the flexibility of the structure, as its fundamental period (see Sec. 6.3.4.1) exceeds $3.5T_s = 3.5(S_{D1}/S_{DS})$ seconds = 3.5 × (0.433/ 0.859) seconds = 1.76 seconds. Nevertheless, the design base shear still must be determined using the equivalent lateral force analysis procedures to ensure that the design base shear for a modal response spectrum analysis meets the requirements of *Standard* Section 12.9.4.

Due to the building's symmetry and the strong torsional resistance provided by the layout of the vertical lateral force-resisting elements, numerous plan irregularities are not expected. Analysis reveals that the structure is torsionally regular the only horizontal structural irregularity present is an out-of-plane offset irregularity (Type 4) triggered by the shift in the vertical lateral force-resisting system from Gridlines 3 and 6 in the tower to Gridlines 2 and 7 in the podium structure below. The only additional provisions triggered by the Type 4 horizontal structural irregularity relate to three-dimensional modeling requirements.

6.3.3.2 Redundancy. The limited number of braced bays in each direction of the tower require the redundancy factor (ρ) to be taken as 1.3 per *Standard* Section 12.3.4.2 Item a and Table 12.3-3. Because there are only two BRBF chevrons in each direction throughout the tower, removal of a single brace would dramatically increase flexural demands in the beam at that location and would certainly result in at least a 33 percent reduction in story strength even if the resulting system does not have an extreme torsional irregularity. The 1.3 redundancy factor (ρ) is incorporated as a load factor on the seismic loads used in the design of the braces.

6.3.3.3 Orthogonal load effects. *Standard* Section 12.5.4 stipulates a combination of 100 percent of the seismic forces in one direction plus 30 percent of the seismic forces in the orthogonal direction, at a minimum, for structures in Seismic Design Category D. However, it has been shown (Wilson, 2004) that use of the 100/30 percentage combination rule can result in member designs that are not equally resistant to earthquake ground motions originating from different directions. Instead, a SRSS combination of seismic forces from two full-magnitude response spectra analyses conducted along each principal axis of the building is performed to ensure the design forces remain independent of the selected reference coordinate system (in this case, the building's main orthogonal axes).

In the context of NRHA, orthogonal pairs of ground motion acceleration histories are applied simultaneously in accordance with the requirements of *Standard* Section 12.5.4 for structures in Seismic Design Category D.

6.3.3.4 Structural component load effects. The effect of seismic load as defined by *Standard* Section 12.4.2 is as follows:

$$E = \rho Q_E \pm 0.2 S_{DS} D$$

In this example, $S_{DS} = 0.859$. The seismic load is combined with the gravity loads in elastic analyses as shown in *Standard* Section 12.4.3.2, resulting in the following load combinations:

$$1.37D + 0.5L + 0.2S + \rho Q_E$$

$$0.73D + 1.6\mathrm{H} + \rho Q_E$$

The 0.5 coefficient on L is permitted for all occupancies in which L_o in *Standard* Table 4.1 is less than or equal to 100 psf per Exception 1 to *Standard* Section 2.3.2. The braces are designed without considering additional tributary vertical loads to encourage distributed yielding up the height of the structure. However, the surrounding beams and columns that are part of the lateral force-resisting system are designed for the above gravity loads in conjunction with the earthquake effect as specified in AISC 341 Section 16.5b. Again, the redundancy factor, ρ, is taken as 1.3 for design of the braces themselves.

In a NRHA, the structure is analyzed for the effects of the scaled pairs of ground motions simultaneously with the effects of dead load and 25 percent of the required live loads per *Standard* Section 16.2.3.

6.3.3.5 Drift limits. For a building assigned to Occupancy Category IV, the allowable story drift (*Standard* Sec. 12.12.1 and Table 12.12-1) is $\Delta_a = 0.010 h_{sx}$.

The allowable story drift for a typical podium floor is Δ_a = (0.01)(18 ft)(12 in./ft) = 2.16 in.

The allowable story drift for a typical tower floor is Δ_a = (0.01)(15 ft)(12 in./ft) = 1.80 in.

The calculated design story drifts are amplified by the appropriate C_d factor from *Standard* Table 12.2-1 in elastic analysis procedures that employ seismic response coefficients reduced by the appropriate response modification factor, R.

Standard Section 16.2.4.3 permits the allowable story drift obtained from a nonlinear response history analysis to be increased by 25 percent relative to the drift limit specified in Section 12.12.1.

The maximum allowable value of story drifts summed to the roof of the ten-story hospital building (156 feet) obtained from an elastic analysis is 18.72 inches. This same figure extracted from a nonlinear response history analysis cannot exceed 1.25(18.72 in.) = 23.40 in.

6.3.3.6 Seismic weight. The area of the tower floorplate is approximately equal to [(3)(30 ft) + (2)(8 in.)(1 ft/12 in.)]^2 = 8,342 ft^2, while the area of the podium floorplate is approximately [(7)(30 ft) + (2)(8 in.)(1 ft/12 in.)] × [(4)(30 ft) + (2)(8 in.)(1 ft/12 in.)] = 25,642 ft^2. Thus, the weights that contribute to seismic forces are as follows:

- Tower roof:

Roof *D* = (0.135)(8,342)	= 1,126 kips
Cladding = (4)(3)(30)(0.300)	= 108 kips
Total	= 1,234 kips

- Tower floor:

Floor *D* = (0.104)(8,342)	= 868 kips
Partitions = (0.010)(8,342)	= 83 kips
Cladding = (4)(3)(30)(0.300)	= 108 kips
Total	= 1,059 kips

- Podium roof:

Roof *D* = (0.135)(25,642 - 8,342)	= 2,336 kips
Floor *D* = (0.104)(8,342)	= 868 kips
Partitions = (0.010)(8,342)	= 83 kips
Cladding = (2)(11)(30)(0.300)	= 198 kips
Total	= 3,485 kips

- Podium floor:

Floor *D* = (0.104)(25,642)	= 2,667 kips
Partitions = (0.010)(25,642)	= 256 kips
Cladding = (2)(11)(30)(0.300)	= 198 kips
Total	= 3,121 kips

Total effective seismic weight of building = 1,234 + 7(1,059) + 3,485 + 3,121 = 15,253 kips

6.3.4 Elastic Analysis

The base shear is determined using an ELF analysis; the base shear so computed is needed later when evaluating the scaling of the base shears obtained from the modal response spectrum analysis.

In a subsequent section (Section 6.3.6.3.3), columns are designed using forces obtained from nonlinear response history analyses that are intended to represent the maximum force that can develop in these elements per the exception to *Standard* Section 12.4.3.1. Compliance with story drift limits is also evaluated using the results of the nonlinear response history analyses.

6.3.4.1 Equivalent Lateral Force procedure. First, the ELF base shear will be determined, followed by its vertical distribution up the height of the building.

6.3.4.1.1 ELF base shear. Compute the approximate building period, T_a, using *Standard* Equation 12.8-7:

$$T_a = C_t h_n^x = (0.03)\left(156^{0.75}\right) = 1.32 \text{ sec}$$

In accordance with *Standard* Section 12.8.2, the building period used to determine the design base shear must not exceed the following:

$$T_{max} = C_u T_a = (1.4)(1.32) = 1.85 \text{ sec}$$

The subsequent three-dimensional modal analysis finds the computed period to be approximately 2.30 seconds in each principal direction. Thus the upper limit on the fundamental period T_{max} applies.

The seismic response coefficient, C_s, is computed in accordance with *Standard* Section 12.8.1.1. Equation 12.8-2 provides the value of C_s that generally governs at short periods:

$$C_s = \frac{S_{DS}}{R/I} = \frac{0.859}{8/1.5} = 0.161$$

However, *Standard* Equation 12.8-3 indicates that the value for C_s need not exceed the following:

$$C_s = \frac{S_{D1}}{T(R/I)} = \frac{0.433}{(1.85)(8/1.5)} = 0.044$$

and the minimum value for C_s per *Standard* Equation 12.8-5 is:

$$C_s = 0.044 I S_{DS} \geq 0.01 = (0.044)(1.5)(0.859) = 0.057$$

Therefore, use C_s = 0.057.

The seismic base shear is computed per *Standard* Equation 12.8-1 as follows:

$$V = C_s W = (0.057)(15,253) = 865 \text{ kips}$$

The redundancy factor (ρ) is accounted for by setting the coefficient on the horizontal seismic load effect to 1.3 in all earthquake load combinations used for strength design of the BRBs. The redundancy factor is not applicable to the determination of deflections.

6.3.4.1.2 Vertical distribution of ELF seismic forces. *Standard* Section 12.8.3 prescribes the vertical distribution of lateral force in a multilevel structure. The floor force, F_x, is calculated using *Standard* Equation 12.8-11 as:

$$F_x = C_{vx} V$$

where (per *Standard* Eq. 12.8-12):

$$C_{vx} = \frac{w_x h_x^k}{\sum_{i=1}^{n} w_i h_i^k}$$

Using the data in Section 6.3.3.5 of this example and interpolating the exponent k as 1.68 for the period of 1.85 seconds, the vertical distribution of forces for the ELF analysis is shown in Table 6.3-2. The seismic design shear in any story is computed as follows (per *Standard* Eq. 12.8-13):

$$V_x = \sum_{i=x}^{n} F_i$$

Table 6.3-2 ELF Vertical Seismic Load Distribution

Level	Weight (w_x)	Height (h_x)	$w_x h_x^k$	C_{vx}	F_x	V_x
Roof	1,234 kips	156 ft	5,818,337	0.24	210 kips	210 kips
Story 10	1,059 kips	141 ft	4,215,392	0.18	152 kips	362 kips
Story 9	1,059 kips	126 ft	3,491,537	0.15	126 kips	488 kips
Story 8	1,059 kips	111 ft	2,823,657	0.12	102 kips	590 kips
Story 7	1,059 kips	96 ft	2,214,116	0.09	80 kips	670 kips
Story 6	1,059 kips	81 ft	1,665,744	0.07	60 kips	730 kips
Story 5	1,059 kips	66 ft	1,182,040	0.05	43 kips	772 kips
Story 4	1,059 kips	51 ft	767,496	0.03	28 kips	800 kips
Story 3	3,485 kips	36 ft	1,409,320	0.06	51 kips	851 kips
Story 2	3,121 kips	18 ft	395,253	0.02	14 kips	865 kips
Total	15,253 kips		23,982,891	1.00	865 kips	

1.0 kip = 4.45 kN
1.0 ft = 30.5 cm

All floor decks, including the roofs, are constructed of 3¾ in. lightweight concrete over 3 in. metal deck. *Standard* Sec. 12.3.1.2 allows for such diaphragms to be modeled as rigid as long as their span-to-depth ratios do not exceed three. Since the floor span-to-depth ratio is a maximum of 1.75 at the podium levels, the hospital diaphragms meet these conditions. However, *Standard* Sec. 12.3.1.2 also requires the structure to have no horizontal irregularities for its diaphragms to be modeled as rigid. Due to the out-of-plane offsets irregularity (Type 4) in the transverse lateral frames at the podium-to-tower interface, the hospital does not meet this restriction. As such, the effect on the vertical lateral force distribution of explicitly considering the stiffness of the diaphragm at the podium roof level was examined in a three-dimensional computer model of the structure and found to be insignificant (i.e., results closely matching a model with rigid diaphragms) due to the stiff nature of the thick concrete floor. Thus, it was deemed acceptable to model all diaphragms as rigid for subsequent analyses. The rigid diaphragm assumption is especially helpful in the context of nonlinear response history analysis, where the additional degrees of freedom needed to model diaphragm stiffness explicitly can render analysis times prohibitive.

Assessment of load transfer in the level 3 diaphragm would require a separate, explicit analysis. Another reasonable approach to the primary model would be to include the level 3 diaphragm explicitly and model all other diaphragms as rigid.

6.3.4.2 Three-dimensional static and Modal Response Spectrum Analysis. The three-dimensional analysis is performed for this example to accurately account for the following:

- The different centers of mass for the podium and tower levels
- The varying stiffness of the braced frames as they transition from their wide configuration at the podium levels to a single-bay arrangement throughout the tower
- The effects of bi-directional frame interaction on the columns engaged by orthogonal braced frames in the podium
- The ability of the braced frames to control torsion

The braced frames and diaphragm chords and collectors, together with all gravity system beams and columns, are explicitly modeled using three-dimensional beam-column elements. The floor diaphragms are modeled as rigid.

As mentioned previously, the ELF analysis procedure of *Standard* Section 12.8 is not admissible for this structure due to the restrictions on fundamental period in *Standard* Table 12.6-1. However, the ELF analysis of the three-dimensional model is still useful in assessing whether torsional irregularities are present. The ELF seismic forces derived in Table 6.3-2 above are applied to each diaphragm at 5 percent eccentricity orthogonal to the direction of loading. The maximum and average story drifts along an edge transverse to the direction of loading for the critical direction of eccentricity at each level are then compared. This ratio of $\delta_{max}/\delta_{avg}$ never exceeds 1.11, which is below the 1.2 limit that defines torsional irregularity. For this torsionally regular structure, the accidental torsion amplification factor, A_x, is equal to 1.0.

A three-dimensional modal response spectrum analysis is performed per *Standard* Section 12.9 using the three-dimensional computer model. The design response spectrum is based on *Standard* Section 11.4.5 and is shown in Figure 6.3-6.

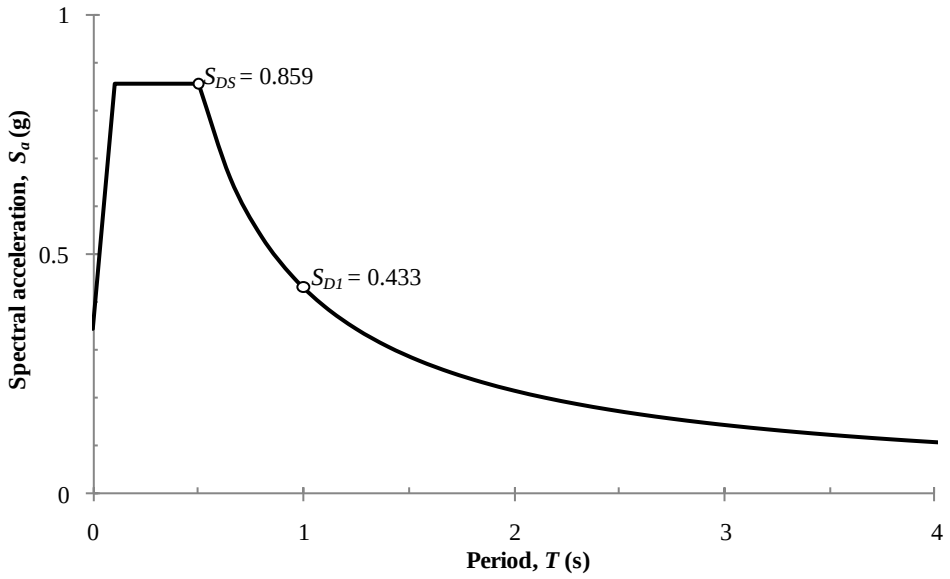

Figure 6.3-6 Design response spectrum, 5 percent damped

Within this model, the first twelve modes of vibration and the corresponding mode shapes of the structure were determined. Twelve modes provide more than enough participation to capture 90 percent of the actual mass in each direction of response as required by *Standard* Section 12.9.1.

The design value for modal base shear, V_t, is determined by combining the individual modal values for base shear after dividing the design response spectrum by the quantity R/I = 8/1.5 = 5.33 as prescribed by *Standard* Section 12.9.2. The complete quadratic combination (CQC) modal combination rule was selected for this task to account for coupling of closely-spaced modes that are likely present in symmetrical structures. Five percent modal damping in all modes is specified for the response spectrum analysis to match the assumption used in deriving the design response spectrum of Figure 6.3-6. Base shears thus obtained from the model having an effective seismic weight of 15,253 kips are as follows:

- Longitudinal: V_t = 627 kips
- Transverse: V_t = 637 kips

In accordance with *Standard* Section 12.9.4, the design values of modal base shear are compared to the base shear determined by the ELF method. If the design value for modal base shear is less than 85 percent of the ELF base shear calculated using a period of C_uT_a (see Sec. 6.3.4.1.1 above), a factor greater than unity must be applied to the design forces to raise the modal base shear up to this minimum ELF comparison value. Accordingly:

- Multiplier: 0.85 (V/V_t)
- Longitudinal multiplier: 0.85 (865 kips / 627 kips) = 1.17
- Transverse multiplier: 0.85 (865 kips / 637 kips) = 1.15

In a typical elastic analysis, it is recommended to examine lateral displacements early in the design process, as seismic (or wind) drift often controls the design of taller structures. For this building,

compliance with drift limits will ultimately be checked using a nonlinear response history analysis. However, lateral displacements are still examined in the elastic analysis to ensure they remain reasonably close to the limits derived in Section 6.3.3.5 (that is, in order to prevent wasting analysis effort on a design that is unlikely to meet the drift limits). This check is illustrated in Section 6.3.4.3 below.

To obtain elastic design forces for the BRBs, the results from the two orthogonal MRSAs in the three-dimensional model are combined via SRSS, exceeding the requirements of *Standard* Section 12.5.4.

6.3.4.3 Preliminary drift assessment. Seismic drift is examined in accordance with *Standard* Section 12.12.1. The design story drift in each translational direction was extracted from the three-dimensional ETABS model corresponding to the response spectrum case, including 5 percent accidental torsion, exciting that same direction. Although only strictly required for structures possessing torsional irregularities as defined by *Standard* Table 12.3-1, story drift was nonetheless examined at the building corners rather than the centers of mass for this structure because the location of cladding attachment is the most critical location for this check.

The lateral deflections obtained from the response spectrum analysis must be multiplied by $C_d/I(I/R) = C_d//R = 5/8 = 0.625$ to find the design story drift. However, the response spectrum used in the analysis has already been scaled twice. The spectrum was first scaled by $R/I = 8 / 1.5 = 5.33$ to obtain design-level forces; thus the resulting displacements can be amplified by $C_d/I = 5 / 1.5 = 3.33$ to obtain expected drifts. The second scaling was by a factor (in each direction) to ensure that the design base shear forces in each direction to meet the minimum 85 percent of ELF base shear. This latter scaling does not apply to drifts, per *Standard* Section 12.9.4. Thus, the 1.17 and 1.15 scale factors applied in the longitudinal and transverse directions, respectively, must be divided back out of the drifts extracted from the model used to obtain design forces for the braces. The resulting scale factors applied to the results of the scaled spectra are 3.33/1.17 = 2.85 and 3.33/1.15 = 2.90 applied in the longitudinal and transverse directions, respectively. (It would also be possible to simply perform an additional response spectrum analysis with the design spectrum multiplied by 0.625 and use the resulting story drifts directly.)

Story drifts in all ten stories of the hospital building are within the allowable story drift limit of $0.010h_{sx}$ per *Standard* Section 12.12.1 and Section 6.3.5.5 of this chapter. Although story drifts calculated using MRSA reach a maximum value at the roof level that is just 89 percent of the $0.010h_{sx}$ limit (and hence acceptable), a nonlinear response history analysis is nevertheless used to confirm that all story drifts indeed remain within prescribed limits.

A comparison of story drift ratios also confirms that no story drift ratio is more than 130 percent of that for the story above, as required to prove certain vertical irregularities are not present in the structure via the exception to *Standard* Section 12.3.2.2.

6.3.4.4 Second-order (P-delta) effects. AISC 360 requires consideration of second order effects. Such effects were investigated by conducting a three-dimensional P-delta analysis, which determined that secondary P-delta effects on the frame accounted for less than 10 percent of the primary demand. Furthermore, *Standard* Section 12.8.7 gives a different means of determining the significance of P-delta effects through the stability coefficient, θ, defined in *Standard* Equation 12.8-6. In either case, P-delta effects were found to be insignificant for this particular braced frame structure.

6.3.4.5 Brace design force summary. The maximum axial forces in each level's individual BRBs caused by horizontal earthquake loads are listed in Table 6.3-3. Again, each brace is designed for its share of 100 percent of the horizontal earthquake load effect times the redundancy factor (ρ) of 1.3 without considering additional vertical loads to encourage distributed yielding of braces up the height of

the structure. Nonetheless, the braces are also checked to ensure they do not yield under maximum live load (i.e., the load combination of $1.2D + 1.6L + 0.5L_r$).

Because the length of the yielding segment of a BRB is significantly less than its workpoint-to-workpoint length (see Sec. 6.5.3.1.1 below), the axial stiffness of the brace elements in the three-dimensional elastic analysis model must be adjusted to account for the non-prismatic nature of these elements. The modulus of elasticity of the steel in the brace elements was increased by a factor of 1.51 for single-diagonal and chevron bracing throughout the tower and 1.45 for chevron or V bracing configurations in the podium to match the true elastic stiffness of these elements as they are defined in the nonlinear response history analysis.

The sizes of the BRBF members are controlled by seismic loads, always bi-directional and with eccentricity, rather than wind loads. *Standard* Section 12.8.4.2 only requires that the 5 percent displacement of the center of mass associated with accidental torsion be applied in the direction that generates the greater effect when earthquake forces are applied simultaneously in two orthogonal directions. However, due to the intricacies of SRSS directional combination of response spectra in ETABS, the 5 percent offset is applied in both orthogonal directions at the same time, which is slightly conservative for torsional response (and is not a significant penalty for this particular building due to its regular nature in plan). The design of connections will be governed by the seismic requirements of AISC 341.

Table 6.3-3 Design Axial Forces[a] in Buckling-Restrained Bracing Members[b]

Location	Gridline A (kips)	Gridline D (kips)	Gridline 2, 3, 6, or 7 (kips)
Roof[c]	139	144	142
Story 10	117	127	126
Story 9	135	136	133
Story 8	142	141	141
Story 7	152	151	151
Story 6	167	175	170
Story 5	193	195	197
Story 4	212	214	210
Story 3	152	197[d]	187
Story 2	162	233	195

[a]Individual maxima are not necessarily on the same frame; values are maximum for any frame.
[b]All braces are oriented in the chevron configuration except for single diagonal[c] or V[d].
1.0 kip = 4.45 kN

6.3.5 Initial Proportioning and Details

The BRBFs occur on Gridlines 3, 6, A D in the tower and transfer their loads at the third floor to two BRBFs per line on Gridlines 2, 7, A D in the podium. These frames are shown schematically in plan in Figures 6.3-1 and 6.3-2 and in elevation in Figures 6.3-3 and 6.3-4. Using the horizontal component of the seismic load (amplified by the redundancy factor) as determined by response spectrum analysis and the loads from Table 6.3-3, the proportions of the braces are checked for adequacy. Then, initial sizes for

the lateral columns, beams collectors are determined from the three-dimensional elastic analysis model using capacity design principles and relevant plastic mechanism analyses. In the preliminary elastic design stage, generic BRB properties are used to derive expected brace strengths. This allows for a specific BRB supplier to be selected further downstream in the project schedule, as is usually done in traditional project delivery methods. Design forces for columns are obtained from a summation of the vertical component of the adjusted brace strengths above the level of interest, while those for horizontal elements are derived from two different plastic mechanisms, always using adjusted brace strengths in tension and compression as required by AISC 341 Section 16.5b. All lateral columns are then subject to resizing according to the force and displacement demands determined using nonlinear response history analysis.

6.3.5.1 Buckling-Restrained Brace sizes

6.3.5.1.1 Buckling-Restrained Brace mechanics. The mechanics of BRBs are such that compression buckling need not be considered in their selection. Their required strength is controlled by yielding of the steel core material only. A BRB consists of a steel core that resists imposed axial stresses together with a mortar-filled sleeve that resists buckling. The steel core has both a yielding portion and two non-yielding portions at its ends where the cross-section enlarges to facilitate connection to a gusset plate. A de-bonding agent, often proprietary, decouples the axial behavior of the core from the buckling behavior of the sleeve. In compression, a BRB acts as a sleeved column—the steel core is able to achieve the full magnitude of its squash load while, at the same time, the sleeve can provide its full Euler buckling resistance without taking on any axial load. From a performance standpoint, such a component produces very desirable balanced hysteretic behavior that exhibits both isotropic and kinematic (cyclic) strain-hardening. Unlike conventional bracing, BRB behavior is much more symmetric with respect to tension and compression and is not subject to strength and stiffness degradation.

6.3.5.1.2 Steel core area. According to AISC 341 Section 16.2a, the steel core must resist the entire axial force in the brace. This force is tabulated in Table 6.3-3. The brace design axial strength, ϕP_{ysc}, in either tension or compression, as controlled by the limit state of yielding, is equal to the following:

$$\phi P_{ysc} = \phi F_{ysc} A_{sc}$$

where:

ϕ = 0.90

F_{ysc} = specified minimum yield stress (or actual from coupon test) of the steel core

A_{sc} = net area of steel core

Setting ϕP_{ysc} equal to the P_u values in Table 6.3-3 and rearranging terms, the required net area of steel core can be expressed as follows:

$$A_{sc} = \frac{P_u}{\phi F_{ysc}}$$

This required area, together with the actual steel core area provided, is shown for each brace in Table 6.3-4. Rarely do designers know the actual yield stress of the steel core during the design phase;

hence, a minimum yield stress (F_{ysc}) of the steel core equal to 38 ksi is assumed for this example. This minimum yield stress value would be specified on the design drawings.

Table 6.3-4 Steel Core Areas for Buckling-Restrained Bracing Members[a]

Location	Gridline A (kips)		Gridline D (kips)		Gridline 2, 3, 6, or 7 (kips)	
	A_{sc} req'd (in.^{2})	A_{sc} (in.^{2})	A_{sc} req'd (in.^{2})	A_{sc} (in.^{2})	A_{sc} req'd (in.^{2})	A_{sc} (in.^{2})
Roof[b]	4.06	**4.5**	4.21	**4.5**	4.15	**4.5**
Story 10	3.42	**3.5**	3.71	**4.0**	3.68	**4.0**
Story 9	3.95	**4.0**	3.98	**4.0**	3.89	**4.0**
Story 8	4.15	**4.5**	4.12	**4.5**	4.12	**4.5**
Story 7	4.44	**4.5**	4.42	**4.5**	4.42	**4.5**
Story 6	4.88	**5.0**	5.12	**5.5**	4.97	**5.0**
Story 5	5.64	**6.0**	5.70	**6.0**	5.76	**6.0**
Story 4	6.20	**6.5**	6.26	**6.5**	6.14	**6.5**
Story 3	4.44	**4.5**	5.76[c]	**6.0**[c]	5.47	**5.5**
Story 2	4.74	**5.0**	6.81	**7.0**	5.70	**6.0**

[a]All braces are oriented in the chevron configuration except for single diagonal[b] or V[c]
1.0 in = 25.4 mm

6.3.5.2 Lateral force-resisting columns. To design the frame containing the BRBs, unless using a nonlinear analysis, the designer should assume a plastic mechanism in which all BRBs are yielding in tension or compression and have reached their strain-hardened adjusted strengths, including all sources of overstrength. These adjusted brace strengths per AISC 341 Section 16.2d are as follows:

- Compression: $\beta\omega R_y F_{ysc} A_{sc}$
- Tension: $\omega R_y F_{ysc} A_{sc}$

The adjusted brace strength values represent the yield strength of the steel core adjusted for material overstrength (R_y), strain-hardening (ω) compression overstrength (β). Whereas conventional bracing usually buckles in compression well before reaching its yield strength, BRBs are often slightly stronger in compression than in tension. The strain-hardening (ω) and compression overstrength (β) factors traditionally are provided by BRB manufacturers and are calculated from cyclic sub-assemblage testing to a brace deformation equivalent to twice the design story drift per AISC 341 Appendix T.

For the initial proportioning of braced-frame columns and beams using the three-dimensional elastic analysis model, generic values of $\beta = 1.05$, $\omega = 1.36$ $R_y = 1.21$ are assumed. A material overstrength factor, R_y, of 1.21 is selected to bring the design yield strength of the steel core, $F_{ysc} = 38$ ksi, up to the typical maximum specified steel core yield strength of 46 ksi. Note that all of these values are subject to revision for use in the nonlinear response history analysis once the BRB calibration has been performed in Section 6.3.6.2.

This capacity design methodology can easily be implemented to design lateral columns in a BRBF once the three-dimensional analysis model is constructed. The designer simply needs to generate an axial force in each brace corresponding to its adjusted brace strength as defined above, either by deleting the braces from the model and replacing them with their associated forces directly or by some other method that achieves the same result (for example, hand calculations or spreadsheets). Two different load cases must be examined for each principal direction: one with all braces in either tension or compression based on lateral load originating from one side of the frame a second with the brace forces determined by lateral load originating from the other side of the frame.

Appropriate consideration should be given to bi-directional combination of the resulting brace loads on columns engaged by two orthogonal frames. While AISC 341 is unwavering in its requirement to design columns for the full adjusted brace strengths, the displacement corresponding to the adjusted brace strength should remain constant in any direction. Thus, such a displacement imposed at 45 degrees to the principal building axes will cause yielding of all braced frames, but not full strain hardening. This reduction factor for bi-directional loading is dependent on the brace's post-yield behavior and will not be much less than one for a ductile system such as a BRBF. The 100%/30% orthogonal combination procedure defined in *Standard* Section 12.5.3 is not applicable in the context of capacity design as mandated for columns by AISC 341 Section 16.5b.

To complete the preliminary column design, the column axial loads resulting from the maximum expected brace forces defined above are substituted for the earthquake load effect and combined with vertical loads as specified in Section 5.3.3.4. The translation and twist of all diaphragms should be locked when performing the column design for stability of the model. This will ensure each column is designed for the axial force equal to the summation of the vertical components of the adjusted brace strengths of all braces above it. Column flexural forces are not considered in their design, consistent with AISC 341 Section 8.3 (1). Such an approximation is valid because localized flexural yielding of a column at locations where it receives a brace is deemed acceptable from a performance standpoint. The preliminary column designs can be seen in Figures 6.3-3 and 6.3-4.

To illustrate this process, a detailed calculation of the column design forces for the column at D4 can be seen in Table 6.3-5. Because column strengths are governed by compression buckling rather than yielding, brace actions that induce compression on the columns are considered critical. For the uppermost column below the tower roof, the 228-kip design force is equal to the sum of the design load due to gravity/vertical earthquake effect of 102 kips and the vertical component of the adjusted brace strength in tension at that level, equal to 126 kips. The adjusted brace strength in tension is used here because tension in the single diagonal brace at the roof will impose compressive forces on the column below, as can be seen in the elevation of Figure 6.3-3. At lower levels with chevron bracing, the design axial load in the column is calculated as follows:

1. Start with the vertical component of the roof brace in tension (126 kips).

2. Add the associated design gravity and vertical earthquake effect loading at that level.

3. Add the sum of the vertical components of the adjusted brace strengths in compression of all chevron bracing at levels above.

4. Subtract half of the sum of the unbalanced vertical loads (difference in vertical components of adjusted brace strengths in compression and tension) on the beams intersecting all chevron bracing at that level and above.

This procedure recognizes that for levels with chevron bracing, the adjusted brace strength in compression will always control over that in tension and will enter the column below at the base of that level. Additionally, the unbalanced vertical load from the chevron transmits shear to the beam above and ultimately the column that works to alleviate the downward gravity and brace compression forces.

Table 6.3-5 Determination of Column Design Forces for Column at Gridline D4

Level	Brace[a] Area	$(1.2+0.2S_{DS})D$ + $0.5L$ + $0.2S$	Brace Angle α[b]	Vertical Component of Adjusted Brace Strengths		Column Required Strength P_u
				Tension[c]	Compression[d]	
Roof	4.5 in^2	102 kips	26.6°	126 kips	132 kips	228 kips
Story 10	4.0 in^2	196 kips	45°	177 kips	186 kips	318 kips
Story 9	4.0 in^2	293 kips	45°	177 kips	186 kips	596 kips
Story 8	4.5 in^2	390 kips	45°	199 kips	209 kips	873 kips
Story 7	4.5 in^2	486 kips	45°	199 kips	209 kips	1174 kips
Story 6	5.5 in^2	583 kips	45°	243 kips	255 kips	1474 kips
Story 5	6.0 in^2	681 kips	45°	265 kips	279 kips	1821 kips
Story 4	6.5 in^2	780 kips	45°	288 kips	302 kips	2191 kips
Story 3	none	947 kips	-	-	-	2660 kips
Story 2	none	1106 kips	-	-	-	2819 kips

[a]All braces are oriented in the chevron configuration except for single diagonal at the roof level.
[b]Measured from the horizontal.
[c]$\omega R_y F_{ysc} A_{sc} \sin\alpha$
[d]$\beta\omega R_y F_{ysc} A_{sc} \sin\alpha$
1.0 kip = 4.45 kN
1.0 in = 25.4 mm

Columns are spliced at every other level to simplify erection. Column sizes are subject to revision due to results from nonlinear response history analysis. While tension forces in the columns may not control their design, tension demands can certainly affect the design of base plates, anchor rods drilled piers. The design tension force at the base of this same column calculated in a similar manner (using the appropriate load combination) is equal to 1,222 kips.

6.3.5.3 Lateral force-resisting beams. The braced frame beams were designed for gravity loads corresponding to $1.37D + 0.5L + 0.2S$, without accounting for any mid-span support provided by chevron bracing, together with earthquake loads extracted from two different plastic mechanism analyses. The first of these mechanisms assumes both the brace(s) above and below the beam of interest have reached their full adjusted brace strengths. The beam is then designed for its share (depending on its location along the line of framing) of the horizontal component of the resulting story force together with the largest drag force from the brace(s) above. In the second mechanism, the brace(s) below the beam of interest is assumed to have reached their full adjusted brace strengths at the same time the diaphragm reaches its design force (this mechanism requires a rough diaphragm analysis to derive collector forces). The beam must resist the same share of the horizontal component of the diaphragm force at that line of framing plus the largest drag force from the brace(s) above, determined by the difference between the force in the brace(s) below minus the diaphragm force at that line of framing. In either mechanism, the

braced frame beam is also designed for any unbalanced upward component of the BRBs that would arise in a chevron or V-bracing configuration. These mechanisms and their associated forces are illustrated in Figure 6.3-7.

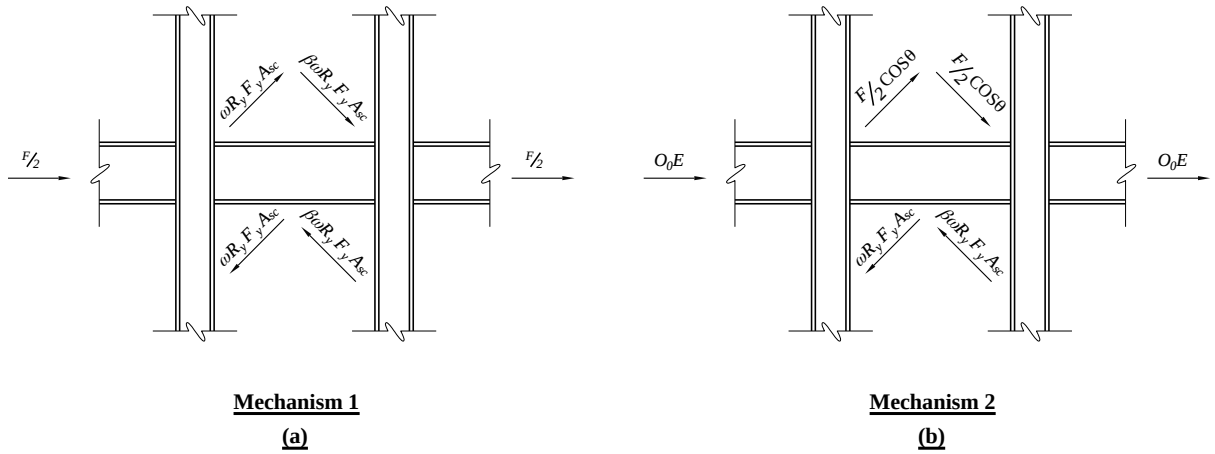

Figure 6.3-7 BRB plastic mechanism

As an example, consider the beam engaged in a chevron bracing configuration along Gridline D above the ninth story. The shear and moment in the beam corresponding to the load combination of $1.37D + 0.5L + 0.2S$, calculated by neglecting the mid-span support provided by the chevron bracing below, are equal to 18 kips and 128 kip-ft, respectively. The brace above is a 4.5 in^2 single diagonal while two 4 $in.^2$ braces frame into the midpoint of the beam from below in a chevron configuration. Hence the upward force at midspan resulting from the unbalanced upward component of the chevron braces below reaching their adjusted strengths is given by the following:

$$\omega R_y F_{ysc} A_{sc} (\beta - 1)\sin\alpha = (1.36)(1.21)(38)(4)(1.05 - 1)(\sin 45°) = 9 \text{ kips}$$

This unbalanced upward component reduces the shear demand in the beam by $P/2 = 9/2 = 5$ kips and the moment by $PL/4 = (9)(30)/4 = 66$ kip-ft. Hence the moment demand that will eventually be combined with the critical axial demand determined by plastic mechanism analysis is:

128 kip-ft - 66 kip-ft = 62 kip-ft

The first plastic mechanism shown in Figure 6.3-7 considers both the brace(s) above and below the beam of interest to have reached their adjusted strengths. Hence, the plastic story shear below the tenth floor is equal to:

$$\omega R_y F_{ysc} A_{sc} (1 + \beta)\cos\alpha = (1.36)(1.21)(38)(4)(1 + 1.05)(\cos 45°) = 363 \text{ kips}$$

The plastic story shear above the tenth floor is:

$$\beta\omega R_y F_{ysc} A_{sc} \cos\alpha = (1.05)\ (1.36)(1.21)(38)(4.5)(\cos 26.6°) = 264 \text{ kips}$$

(The brace at the tenth story is a single-diagonal.)

The story force corresponding to this yielding mechanism is equal to the difference between these two values, or 99 kips. Since the chevron braces below the tenth floor beam receive the lateral force at the midpoint of the associated line of framing, half of this story force (attributed to inertial mass) is presumed to come from each half of the braced frame beam, or approximately 50 kips. This 50-kip force is added to the 264-kip horizontal component from the yielding single-diagonal brace above that must be dragged through the braced frame beam to the chevron braces below, resulting in a design axial force of 314 kips for the first plastic mechanism.

The second plastic mechanism illustrated in Figure 6.3-7 requires estimation of the force entering the braced frame beam from the diaphragm at that floor in accordance with *Standard* Section 12.10. As shown in Figure 6.3-7 this is a collector force thus the value of F_{px} calculated using *Standard* Equation 12.10-1 requires amplification by the overstrength value, Ω_0, of 2.5; this gives 2.5 × 142 kips = 355 kips. This value cannot be taken as less than the minimum of $0.2S_{DS}Iw_{px}$, which gives a value of 270 kips. (Note that the overstrength factor does not apply to this minimum, even for collectors.) Thus, the 355 kips governs the corresponding frame force can be taken as 55 percent of this force (that is taking 1/2 adding 10 percent to account for accidental eccentricity): 195 kips. The chevron braces below the tenth-floor braced frame beam are still assumed to have reached their yield strength, resulting in the same 363-kip frame shear at that level. Hence the statically consistent force in the (now elastic) single-diagonal brace above the tenth floor is equal to the difference between these two values, or 168 kips. Just as is done in the calculation of the design axial force resulting from the first plastic mechanism, half of the 195-kip story force (the maximum from the diaphragm) is added to the 168-kip horizontal component from the single-diagonal brace above that must be dragged through the braced frame beam to the chevron braces below, resulting in a design axial force of 265 kips for the second plastic mechanism.

The 314 kips obtained from the first plastic mechanism (both braces above and below the beam at their adjusted strengths) controls. Thus, the braced frame beam along Gridline D above the ninth story must be designed for a 62 kip-ft moment in combination with a 314 kip axial force. The axial strength is typically determined without accounting for the benefits of composite action with the concrete-filled deck above. Although some minor benefit can be obtained from considering the composite contribution to flexural strength, this is often neglected for simplicity; flexural forces due to brace unbalanced loading are typically small in the inverted-V configuration they oppose gravity forces. The axial capacity of braced frame beams is often controlled by flexural-torsional buckling (as opposed to buckling about the weak axis).

6.3.5.4 Third floor/low roof collector forces. Collector elements that transfer forces between the single bay of chevron bracing in the tower to the multiple, offset bays of chevron bracing in the podium are sized in a manner identical to the lateral force-resisting beams. The same two plastic mechanisms—one involving braces above and below the level of interest reaching their full adjusted strengths the second involving the braces below the level of interest reaching their full adjusted strengths in conjunction with the diaphragm delivering its maximum force to the framing in line with the braces—are assumed the forces are traced from the single bays of chevron bracing above through the collector lines to the chevron bracing below. Story forces accumulate in the collectors and braced frame beams based on the fraction of the full length of the line of framing represented by the particular beam section of interest. In the case of the out-of-plane offset that occurs between Gridlines 2 and 3 (and 6 and 7), the horizontal component of the adjusted chevron brace strengths above the third floor must be distributed into the diaphragm via the adjacent collector elements, then collected by collector elements along the outer line of framing (at Gridlines 2 or 7) to be channeled to the chevron braces in the podium levels below. As with the braced frame beams, the axial capacity of these collector elements is based on that of the bare steel section and usually is governed by flexural-torsional buckling. It is acceptable to calculate the flexural capacity of the collector elements considering composite action with the concrete-filled deck above.

6.3.5.5 Connection design. According to AISC 341 Section 16.3, gussets and beam-column connections must be designed for $1.1 \times C_{max}$, where C_{max} is the adjusted brace strength in compression as defined in AISC 341 Section 16.2d. Connection design is not illustrated here since this topic is more thoroughly treated elsewhere and is not unique to BRBF systems. The connection of the 4.5 in.^{2} single diagonal brace to the frame beam below it at the tenth floor would need to be designed for $1.1\beta\omega R_y F_{ysc} A_{sc}$ = 1.1(1.05)(1.36)(1.21)(38)(4.5) = 325 kips in tension and compression based the full expected and strain-hardened brace capacity. However, it should be mentioned that a designer might consider using NRHA to design for potentially reduced connection force demands; such a reduction would likely be limited to establishing a lower value for the strain-hardening factor ω for each brace.

6.3.6 Nonlinear Response History Analysis

After completing a preliminary design using three-dimensional modal response spectrum analysis, nonlinear response history analysis is performed to:

- Establish brace deformation demands (and verify the adequacy of specified braces for the application)
- Determine expected drifts
- Re-examine the required strength of column members in the BRBF

The braced frames and diaphragm chords and collectors, together with all primary gravity system beams and columns, are explicitly modeled using three-dimensional beam-column elements. Secondary gravity framing is omitted from the nonlinear model for simplicity. The floor diaphragms are still modeled as rigid.

The specific goals of the nonlinear response history analysis are threefold. First, even though the original elastic design is found to comply with the drift limitations of *Standard* Section 12.12.1, the nonlinear response history analysis can more accurately predict results such as story drift. Hence, the acceptability of the design in satisfying story drift requirements is evaluated using the procedures of *Standard* Section 16.2.4. Second, the ability of the BRBs to perform at the Immediate Occupancy (IO) performance level in a design basis earthquake (DBE) event will be verified explicitly. Third, the required strength of column elements in the BRBF system is re-evaluated according to the "maximum force that can be developed by the system" as permitted by AISC 341-05 Section 16.5b. The use of a nonlinear response history analysis to determine this maximum force for individual elements is justified in the provisions of *Standard* Section 12.4.3.1. Specifically, the exception to this section permits the determination of "the maximum force that can develop in the element … by a rational, plastic mechanism analysis or nonlinear response analysis utilizing realistic expected values of material strengths." *Standard* Section 16.2 then defines the requirements for nonlinear response history analysis. In this design example, only the columns in the BRBF system are examined. This is due to the limited savings potential of economizing the relatively small number of BRBF beam and collector elements in the structure that have already been reasonably sized (attributable to the absence of large BRB elements) using a rational plastic mechanism analysis. The designer of a taller building with bulky BRB elements should probably consider using the same procedure to potentially reduce design force demands on the BRBF beams and collectors as well as the columns.

A second, separate three-dimensional building model is assembled in the PERFORM program its similarity to the ETABS model used for the elastic design is confirmed by comparing fundamental periods and loads.

6.3.6.1 Design ground motions. In Chapter 3, risk-targeted maximum considered earthquake (MCE) response spectra are determined in accordance with *Standard* Section 11.4 using NGA attenuation relations. Seven pairs of time histories are selected and scaled to be consistent with the event magnitudes, fault distances source mechanisms controlling the MCE spectrum for the Seattle, Washington, hospital site. The base ground motions in the suite are scaled to the MCE response spectrum so as to satisfy the requirements of *Standard* Section 16.1.3.2 for periods between 0.18 and 4.95 seconds. The translational structural periods for the hospital facility are found to be approximately 2.3 seconds, so the period range of interest is from $0.2 \times 2.3 = 0.46$ seconds to $1.5 \times 2.3 = 3.45$ seconds, which is narrower than the preliminary range used in the ground motion selection and scaling. Design-level ground motions are obtained by multiplying MCE motions by 2/3 per *Standard* Section 16.2.3.

6.3.6.2 Basis of nonlinear design. In keeping with the intent of the building code to protect essential facilities in a seismic event, the hospital should perform at the IO performance level under ground shaking corresponding to the DBE. As is traditionally the case in elastic designs, an explicit performance check at the MCE is not done here. The building is assumed to meet Life Safety (LS) performance objectives at the MCE if it meets IO performance criteria at the DBE.

At the present time, there are three international providers of BRBs: CoreBrace and StarSeismic in the United States Nippon Steel in Japan. In the preliminary design stage, it is often the case that any one of these three brace manufacturers may ultimately be chosen as the supplier. Thus, generic BRB properties may be assumed until the later stages of a project. However, a specific BRB supplier must be selected to accurately model actual brace behavior in the PERFORM NRHA model.

BRBs in the NRHA are modeled using expected properties based on test results provided by CoreBrace; acceptance criteria are based on Section 2.8.3 of ASCE 41 for deformation-controlled elements. There are three different types of brace-to-gusset connections used for BRBs: bolted, welded pinned. However, generic “ACME” braces are used throughout the structure hence the nature of the brace-to-gusset connection is not considered. All other structural elements are modeled using expected properties. Because the lateral beams and columns are connected by simple pin connections in this example (see Section 6.3.2.1), the beams will not require consideration of inelastic behavior. Unless some column element sizes are reduced based on NRHA results, inelastic column actions are not likely, although it is possible that uneven (or higher-mode) story drifts will result in inelastic flexural demands.

The initial gravity load condition is $1.0D + 0.25L$ per *Standard* Section 16.2.3.

6.3.6.3 Buckling-Restrained Brace calibration. In order to capture the nonlinear BRB behavior as accurately as possible in the NRHA computer model, brace properties are calibrated to match test results provided by CoreBrace. Typically, a number of calibrations are performed on a range of different brace sizes. Critical modeling parameters are then interpolated between (or extrapolated from) those established for a brace or braces of similar size. For illustration purposes, one calibration is shown and modeling parameters are matched to corresponding values for the flat core plate test specimen. (Note that the specific series of BRBs tested possess a post-yield modulus of elasticity that is unusually stiff.)

Data to which critical brace parameters are calibrated is obtained from a standard cyclic testing protocol that is in line with the requirements of AISC 341 Appendix T and ASCE 41 Section 2.8.3. Elastic displacement components in both the connection region and the non-yielding brace segments (the larger “elastic bar” segment in PERFORM) of the BRB specimens are subtracted out of measured displacements

in the test data. As a result, the inelastic core plate's force-displacement behavior is isolated to facilitate calibration. The result of the calibration is a backbone curve that reasonably envelopes the observed cyclic test hysteretic behavior.

BRB elements typically are modeled in nonlinear computer analysis software as three components in series: a stiff connection region, an elastic bar segment an inelastic yielding segment. The workpoint-to-workpoint length of the BRB element in the three-dimensional computer model must be divided reasonably into these three components. Thus, the stiff connection zone size and relative stiffness are determined by a rough gusset plate design based on a representative brace size and geometry in the building. The elastic bar segment's length and cross-sectional area are set such that their proportions relative to the inelastic yielding segment remain identical to those of the test specimen. The remainder of this section is devoting to developing modeling parameters for the inelastic yielding portion of the BRB element.

One key modeling parameter for the inelastic portion of the BRB elements is its initial elastic stiffness, K_o. This value is simply set to equal $A_{sc}E / L_y$, where L_y is the length of the yielding segment set to equal the same proportion of the brace length outside the connection region as the test specimen. Next, the designer must select a post-yield stiffness, K_f, for the inelastic portion of the backbone curve. This value is chosen such that the post-yield slope of the hysteresis loops obtained from the computer model is similar to that in the test data is typically a percentage of the initial stiffness, K_o. For the hospital building in this example, K_f = 1.5 percent of K_o to match the observed hysteretic behavior of the test specimen.

Other key modeling inputs are the strain-hardening and compression overstrength factors that define the ultimate strength of the BRB elements. Each brace in the hospital computer analysis model is assigned strain-hardening (ω) and compression overstrength (β) factors equal to 1.63 and 1.05, respectively. These values are selected to match the full hardened strength of the test specimen in tension and compression and are different from the generic values assumed earlier for the plastic mechanism analysis used to design beams in columns in the BRBF. Because the compression overstrength factor does not equal 1.0, the BRB behavior is not symmetric in tension and compression. The material strength of the braces in the model is set to equal the minimum specified strength for this project (i.e., R_yF_y = 38 ksi). Alternatively, one could use the actual material strength as determined by coupon test of BRB specimens tested specifically for that particular project.

All nonlinear analysis software programs require an ultimate deformation or strain value corresponding to the BRB having reached its fully-hardened strength as an input in the inelastic BRB component's properties. This figure was set such that the strain matched that observed in the test at full compression hardening. Additionally, the program requires information about the rate of isotropic hardening between cycles. In the nonlinear analysis software used for this design example, the rate of isotropic hardening is captured by inputting the maximum brace deformation corresponding to the average of the initial BRB yield strength and its strength after full hardening (this cyclic hardening parameter can also be defined in terms of accumulated deformations but is not done so here). To match the vertical progression of hysteretic behavior (i.e., hardening between progressive loading cycles) observed in the test specimen, this hardening parameter was set to 2/3 of the deformation from initial yield to fully-hardened strength. Finally, the software must know at what point the deformation in the nonlinear BRB component has exceeded its capacity. Since the BRBs in this example are expected to perform well below their capacity and this value was never reached during the standard testing protocol, an artificially high number was selected for this input individual brace performance was subject to review as outlined in Section 6.3.6.3.1.

The above parameters are sufficient to define a bilinear elastic-plastic backbone curve for the BRB elements in the computer analysis model. The hysteretic behavior of the BRB component matching the test specimen extracted from the computer model is compared with the experimental test data in

Figure 6.3-8. One can see that the backbone curve modeling parameters accurately capture the observed experimental hysteresis properties for this size component. With some additional effort, a trilinear backbone curve can also be calibrated to the test data to better capture the "rounding" of the actual BRB hysteretic loops. The trilinear curve considers a higher component stiffness value just after yield before the ultimate post-yield stiffness value, K_f, prevails. This third stiffness value, together with the force-deformation point at which the ultimate post-yield stiffness (K_f) "takes over," must be calibrated to the test data as well. Figure 6.3-9 shows the inelastic BRB component's hysteretic behavior as modeled using the trilinear backbone curve together with the experimental test data to which it is calibrated. Subsequent analysis results are based on BRB inelastic components modeled using the trilinear backbone curve because the additional accuracy of the tri-linear backbone curve can be realized without causing excessive analysis run times for this example building.

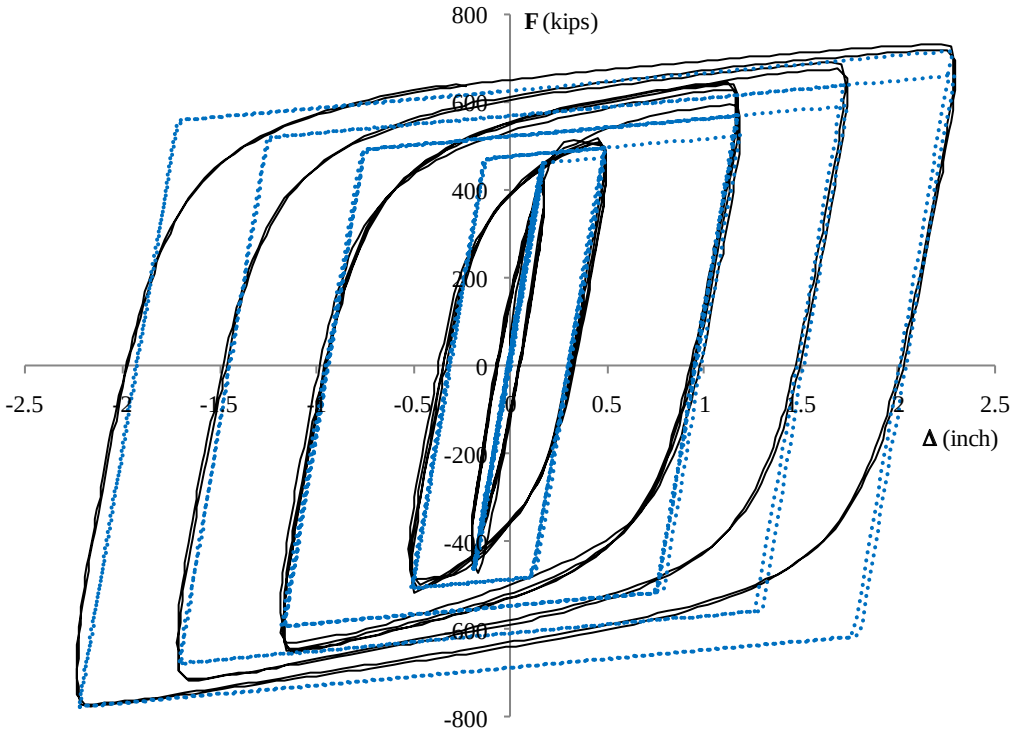

Figure 6.3-8 Bilinear BRB calibration (A_{sc} = 12 in^2)
(1.0 in. = 25.4 mm; 1.0 kip = 4.45 kN)

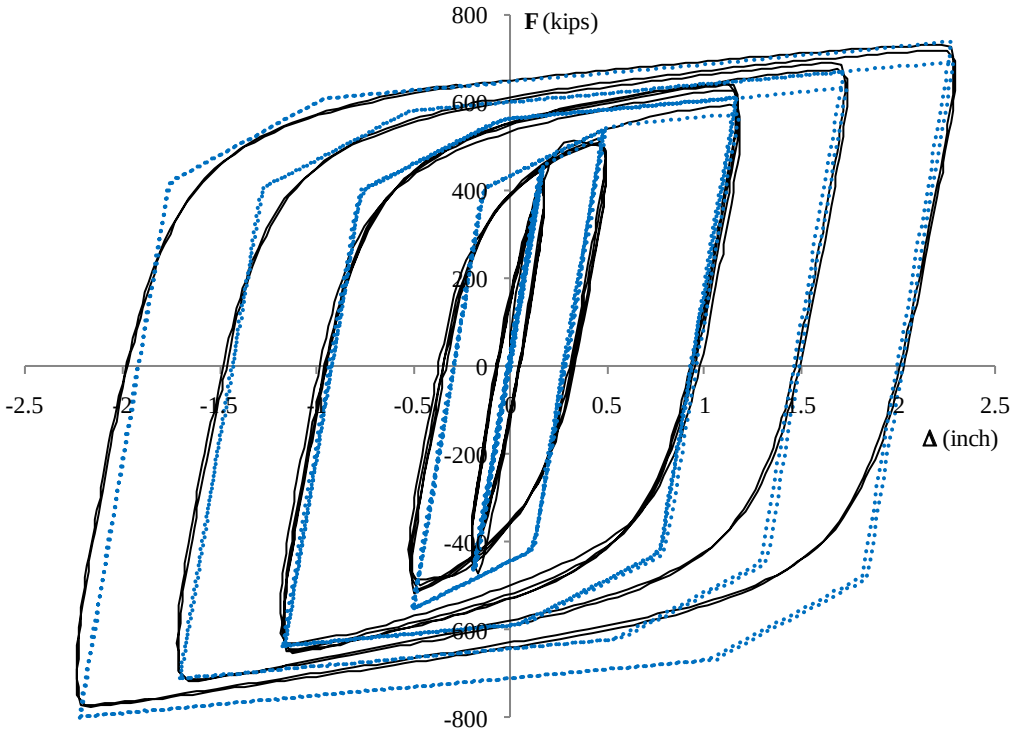

Figure 6.3-9 Trilinear BRB calibration (A_{sc} = 12 in^2)
(1.0 in. = 25.4 mm; 1.0 kip = 4.45 kN)

6.3.6.4 Results.

6.3.6.4.1 BRB strains. One goal of the NRHA is to confirm the ability of the BRBs to perform at the IO performance level in a DBE event. The acceptance criteria for BRB strain, as dictated by ASCE 41 Section 2.8.3, can be seen in Figure 6.3-10 (overlaid on the corresponding test results). No permanent, visible damage was observed during the standard experimental testing protocol used to calibrate the BRB elements the test was terminated at or near Point 2 as defined in the Type 1 and Type 2 component force versus deformation curves for deformation-controlled actions in ASCE 41 Section 2.4.4.3. Consequently, the IO, LS Collapse Prevention (CP) acceptance criteria are equal to 0.67 × 0.75, 0.75 1.0 times the deformation at Point 2 on the component force versus deformation curves, respectively. Observe that the limiting BRB strains for IO performance in tension and compression are $6.64\Delta_y / L_y = 6.64 \times 0.00131 = 0.008704$ and $6.47\Delta_y / L_y = 6.47 \times 0.00131 = 0.008482$, in turn.

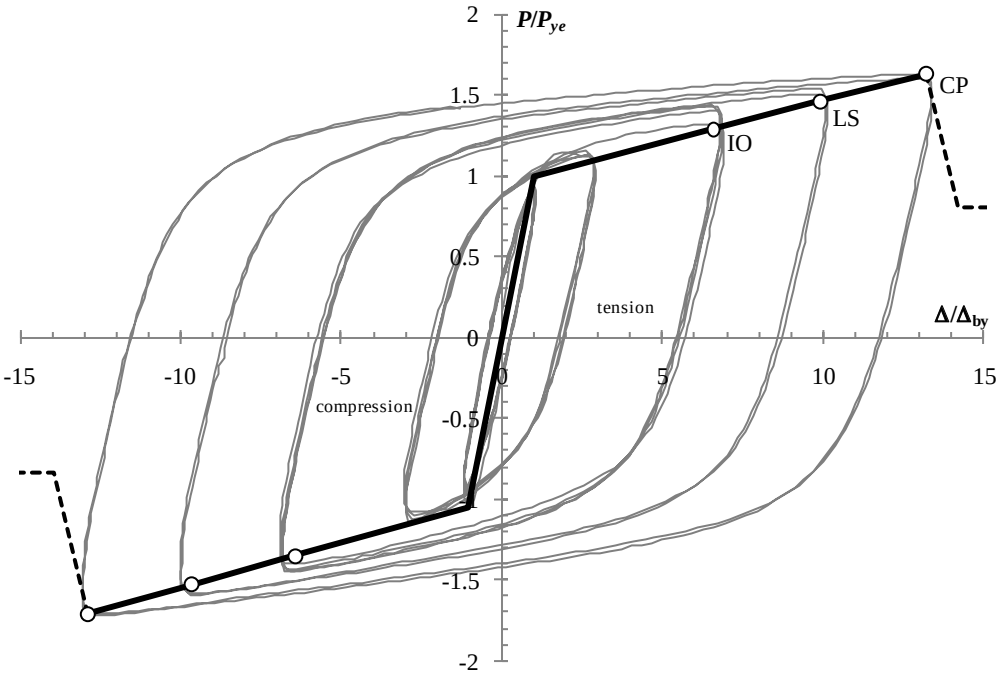

Figure 6.3-10 BRB strain acceptance criteria

The ratio of maximum inelastic deformation demand $\Psi = \Delta/\Delta_y$ observed along a subset of the 92 total BRB elements during each of the seven ground motion time histories to the relevant IO performance point in tension or compression is shown in Table 6.3-6. Braces for which results are presented are chosen to represent BRB elements in all ten levels of the structure. As permitted by ***Standard*** Section 16.2.4 for analyses including at least seven ground motion pairs, the average BRB Ψ_{max}/Ψ_{IO} value across the seven earthquake records is calculated for each brace. In assessing the performance of the entire structure, the maximum of these 92 average BRB inelastic deformation demand values is extracted and compared with the relevant IO performance point in tension or compression. Table 6.3-6 shows that this critical Ψ_{max}/Ψ_{IO} value for the hospital structure is equal to 0.566, indicating acceptable performance of the BRB elements in the DBE event according to the methodology set forth in ***Standard*** Section 16.2.4. The procedure set forth in the ***Standard*** may lead to designs that fail a criterion in some element or measure for every ground motion but still pass the criteria on average.

Table 6.3-6 Ratio of Maximum BRB Inelastic Deformation Demand Ψ to Immediate Occupancy (IO) Performance Limit (Ψ_{max}/Ψ_{IO})

BRB ID	Record ID							Average
	1	2	3	4	5	6	7	
1	0.245	0.350	0.173	0.159	0.125	0.250	0.486	0.255
2	0.331	0.472	0.179	0.267	0.201	0.282	0.732	0.351
.	.	.	.	.	.	.	.	.
.	.	.	.	.	.	.	.	.
.	.	.	.	.	.	.	.	.
16	0.187[a]	0.189[a]	0.154	0.185	0.266	0.294	0.215	0.212

Table 6.3-6 Ratio of Maximum BRB Inelastic Deformation Demand Ψ to Immediate Occupancy (IO) Performance Limit (Ψ_{max}/Ψ_{IO})

BRB ID	Record ID							Average
	1	2	3	4	5	6	7	
17	0.574	0.258	0.319	0.251	0.350	0.450	0.314	0.359
18	0.770	0.314	0.321	0.217	0.313	0.369	0.316	0.374
19	0.956	0.537	0.542	0.245	0.343	0.615	0.373	0.515
20	1.082	0.532	0.588	0.268	0.329	0.753	0.310	0.551
21	1.001	0.392	0.574	0.351	0.231	0.609	0.465	0.518
22	0.875	0.402	0.520	0.264	0.357	0.718	0.534	0.524
23	0.545	0.414	0.371	0.258	0.399	0.644	0.455	0.440
.	.	.	.	.	.	.	.	.
.	.	.	.	.	.	.	.	.
.	.	.	.	.	.	.	.	.
89	0.642	1.064[a]	0.572[a]	0.254[a]	0.695	0.478	0.263	**0.566**[b]
90	0.605	0.959[a]	0.328[a]	0.180	0.425	0.262	0.215	0.424
91	0.518	0.592[a]	0.382	0.371	0.347	0.212	0.181	0.372
92	0.241	0.366	0.364	0.631	0.368	0.248	0.410	0.375
Max	1.086	1.286	0.834	0.631	0.857	0.759	0.792	**0.566**[b]

[a] All Ψ_{max}/Ψ_{IO} values for the individual braces are controlled by the compression strain limit except those denoted by the superscript [a] (for which the tension strain limit controls).

[b] Note that the 0.566 structure "usage ratio" is equal to the maximum of the average Ψ_{max}/Ψ_{IO} values across the seven ground motion pairs for each BRB element, **not** the average of the maximum Ψ_{max}/Ψ_{IO} values for each of the seven ground motion pairs across all 92 BRB elements.

6.3.6.4.2 Drift assessment. Although seismic drift was preliminarily examined in Section 6.3.4.3 to ensure the design possessed reasonable stiffness before modeling its nonlinear behavior, conformance with story drift limits is assessed using the procedures of *Standard* Section 16.2. The maximum story drift ratio in each translational direction was extracted from the three-dimensional PERFORM model for each of the seven ground motion pairs. As before, story drift was examined at the building corners rather than the center of mass.

Once the maximum story drift ratio at every story and corner of the floorplate is identified in each of the seven time histories, the resulting seven values for each story are averaged (as allowed by *Standard* Section 16.2.4) the maximum average story drift ratio is identified to assess compliance with the allowable story drift, which *Standard* Section 16.2.4.3 permits to be increased by 25 percent relative to the drift limit specified in Section 12.12.1 in the context of nonlinear response history analysis. Thus, the relevant story drift limit for nonlinear response history analysis is $(1 + 0.25)(0.010h_{sx}) = 0.0125h_{sx}$. Figure 6.3-11 shows, for each story, the story drift ratios in the longitudinal direction for each time history, the average of all seven the allowable story drift ratio. (Also shown are the analysis results and drift limit for MRSA, which are discussed below.) The controlling story drift for the NRHA occurs in the seventh story, where it is about 93 percent of the allowable story drift. Table 6.3-7 illustrates how this value is calculated using drift ratios at the critical corner of the floorplate. Drifts in the transverse direction are somewhat smaller.

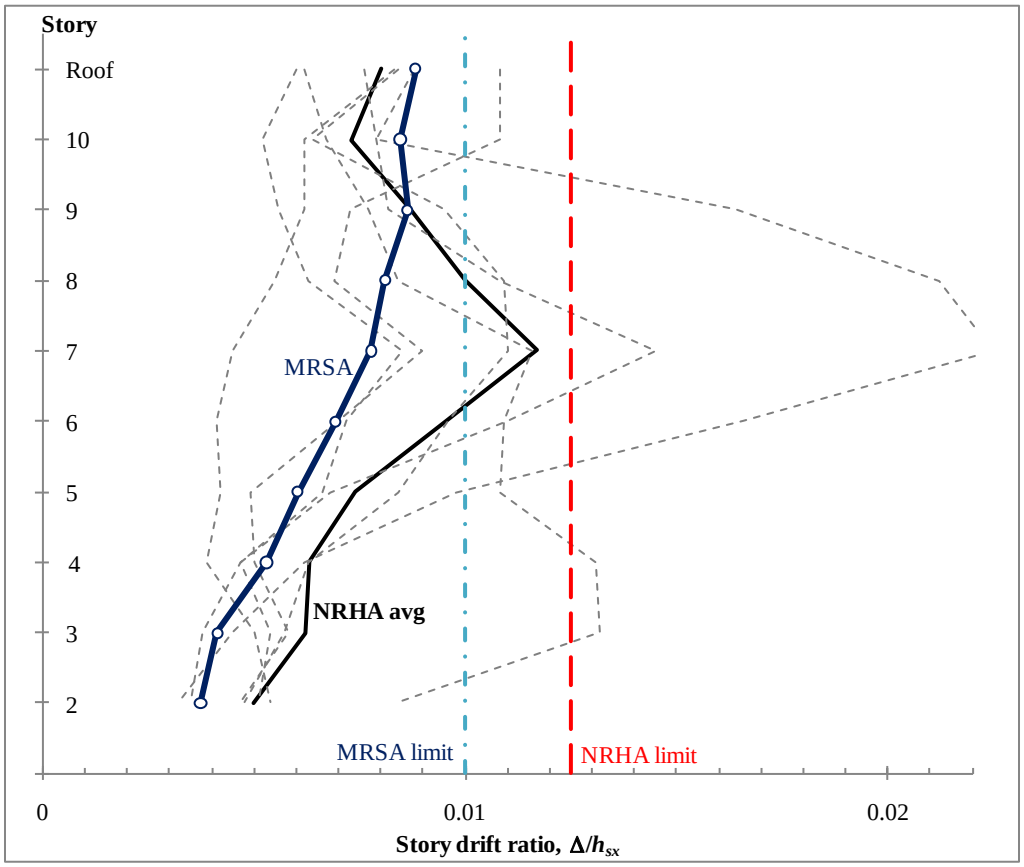

Figure 6.3-11 Longitudinal story drift ratios (and drift limits)

Table 6.3-7 Maximum Longitudinal Story Drift Ratio at Critical Corner of Building Floorplate

Level	Record ID							Average
	1	2	3	4	5	6	7	
Roof	0.0084	0.0088	0.0076	0.0108	0.0062	0.0060	0.0083	0.0080
Story 10	0.0064	0.0079	0.0079	0.0108	0.0067	0.0052	0.0062	0.0073
Story 9	0.0095	0.0164	0.0082	0.0073	0.0077	0.0056	0.0062	0.0087
Story 8	0.0109	0.0212	0.0108	0.0069	0.0084	0.0063	0.0055	0.0100
Story 7	0.0110	0.0225	0.0145	0.0090	0.0116	0.0085	0.0045	**0.0117**[a]
Story 6	0.0096	0.0166	0.0110	0.0070	0.0109	0.0072	0.0041	0.0095
Story 5	0.0084	0.0098	0.0068	0.0049	0.0108	0.0066	0.0042	0.0074
Story 4	0.0063	0.0062	0.0047	0.0050	0.0131	0.0047	0.0039	0.0063

Table 6.3-7 Maximum Longitudinal Story Drift Ratio at Critical Corner of Building Floorplate

Level	Record ID							Average
	1	2	3	4	5	6	7	
Story 3	0.0057	0.0045	0.0054	0.0058	0.0132	0.0038	0.0050	0.0062
Story 2	0.0048	0.0032	0.0051	0.0047	0.0084	0.0035	0.0054	0.0050

[a] Note that the 0.0117 structure story drift ratio is equal to the maximum of the average story drift ratio values across the seven ground motion pairs for each story, **not** the average of the maximum story drift ratio values for each of the seven ground motion pairs across all ten stories.

The maximum story drift calculated earlier using MRSA reached a maximum value at the roof level equal to 89 percent of the $0.010h_{sx}$ limit prescribed in *Standard* Section 12.12.1. The magnitude of this maximum was similar in both principal building axes. The design story drifts obtained from the MRSA were also found to increase from story to story up the height of the structure. Contrast the preliminary elastic MRSA drift results with those just presented from the NRHA. First, the maximum story drift no longer always occurs at the uppermost level of the building; the specific location of the maximum varies depending on the ground motion. Second, the maximum story drift is no longer consistent between the two primary structural axes. This is an important point and is a direct result of the way the ground motion pairs were applied to the structure. While not required by the *Standard*, some engineers elect to re-analyze the structure with the ground motions rotated, in order to investigate sensitivity to ground-motion orientation; this results in a total of 14 analyses, with a corresponding increase in effort. However, a detailed discussion of this and other ground motion issues is beyond the scope of this design example. Finally perhaps most importantly, the maximum story drift from the NRHA, $0.0117h_{sx}$, is 31 percent higher than that from the MRSA, $0.89 \times 0.010h_{sx} = 0.0089h_{sx}$.

The results in this section highlight an important misconception of NRHA in general. There is no guarantee of economizing a design with respect to the required strength or stiffness of a frame simply by performing a NRHA. Rather, when executed correctly, a NRHA simply assures a more accurate representation of actual structural performance in a particular seismic event. This increase in the accuracy of seismic response parameters can actually increase the required frame strength or stiffness in some instances.

6.3.6.4.3 Column design forces. All BRBF columns were initially designed in Section 6.3.5.2 to resist the vertical component of the adjusted strengths of any braces above, using capacity design principles and generic values of the brace material overstrength (R_y), strain-hardening (ω) compression overstrength (β) parameters. Thus, the lateral columns are expected to remain nominally elastic in the DBE event. More realistic expected BRB behavior specific to a particular BRB product line and supplier is modeled in Section 6.3.6.2 based on experimental test data. The required strengths of the columns in the BRBF as specified in AISC 341 Section 16.5b are subject to revision based on results from the NRHA, as is permitted in the exception to *Standard* Section 12.4.3.1. To this end, Table 6.3-8 shows the maximum compressive axial force attained at every story in the BRBF column at Gridline D/4 during each of the seven time history analyses. This force represents the summation of the gravity load prescribed in *Standard* Section 16.2.3 ($1.0D + 0.25L$) plus the additional force imposed by the relevant earthquake time history pair. As above, compression forces are the most critical for column design because column strengths are governed by compression buckling rather than yielding.

The model included column potential hinges with axial-moment interaction relationships determined from ASCE 41. Inelastic rotations were limited to IO values per that standard. However, virtually no inelastic rotation was recorded in the analyses.

Table 6.3-8 also identifies the overall maximum compression force in the column at every story across all seven ground motion pairs, together with the column design force determined by plastic mechanism analysis in Section 6.3.5.2. While *Standard* Section 16.2.4 permits the use of average member forces in determining design values with at least seven ground motions, maximum member force values are selected for design of the columns due to their critical role in sustaining the vertical load-carrying capacity of the structure. Even when using maximum values of member forces extracted from the time histories, substantial savings in column design forces and hence steel tonnage are facilitated by NRHA in this example.

Table 6.3-8 Comparison of Column Design Forces from NRHA and Plastic Analysis for Column at Gridline D/4

Level	Maximum Compression Force (kips) Record ID							Design Axial Force Q_E (kips)		Percent Reduction in Design Force[c]
	1	2	3	4	5	6	7	NRHA[a]	Plastic[b]	
Roof	152	154	152	156	148	155	168	168	228	26%
Story 10	214	216	216	219	211	217	231	231	318	27%
Story 9	404	412	393	393	382	397	416	416	596	30%
Story 8	603	616	589	567	571	578	590	616	873	29%
Story 7	812	842	800	743	774	768	781	842	1174	28%
Story 6	986	1068	1018	948	996	948	972	1068	1474	28%
Story 5	1198	1320	1264	1183	1214	1113	1145	1320	1821	28%
Story 4	1414	1566	1504	1430	1421	1276	1264	1566	2191	29%
Story 3	1750	1851	1780	1707	1651	1486	1421	1851	2660	30%
Story 2	1861	1965	1894	1818	1764	1598	1535	1965	2819	30%

[a]Maximum of individual maxima from the seven time histories.
[b]As determined in Table 6.3-5.
[c]Relative to that determined using plastic analysis.
1.0 kip = 4.45 kN1.0 in = 25.4 mm

In addition to these significant reductions in column design forces, the same procedure reveals a design tension uplift force at this same column of 336 kips, which is just 28 percent of the comparable 1,222-kip force obtained from plastic analysis. This force reduction enables tremendous savings in the design of foundation elements such as base plates, anchor rods drilled piers.

With the possible exception of the foundation elements just mentioned, despite the fact that the column design forces have been sharply reduced relative to those obtained from the plastic mechanism analysis in Section 6.3.5.2, none of the column sizes are actually reduced in this example. This is because the structure is currently very close to the allowable story drift limit. In other words, the NRHA reveals that stiffness, not strength, governs the design of the BRBF examined here. A prudent designer might consider enlarging select braces in conjunction with reducing column sizes as allowed by the NRHA

design forces in Table 6.3-8 to increase cost savings on the project, depending on the relative prices of BRBs and structural steel. However, the tradeoff between BRB and column stiffness would have to preserve the overall stiffness of the frame in order to ensure the allowable drift limit is still satisfied. In particular, it may be possible to increase the brace size in Story 7 (and possibly Stories 6 and 8) while reducing the column size considerably.

6.3.6.4.4 Brace-to-gusset connection design. As mentioned earlier, brace-to-gusset connections for BRBs take on three different forms: bolted, welded pinned. The specific nature of this connection is not considered in this design example. However, the possible additional benefit of economizing on material by using NRHA to determine connection design forces will be demonstrated. As shown in Section 6.3.5.5, the connection of the single diagonal brace below the roof to its gusset would need to be designed for 325 kips in tension and compression. Using the maximum BRB force results from NRHA (obtained in the same manner that column design forces were determined), this design value can be reduced to 210 kips in tension and 213 kips in compression, representing a reduction of approximately 35 percent in both cases. This corresponds to utilizing a lower strain-hardening factor, ω, corresponding to a more refined method of establishing deformation demands. It should be noted that this reduction is not explicitly allowed by AISC 341; therefore, it would constitute "alternate means and methods" and be subject to approval by the building official.

6.3.6.4.5 Summary of NRHA goals. Before concluding, the exact extent to which NRHA was used in this design example merits emphasis one last time. Based on the fundamental period of the structure, the minimum level of sophistication required for its seismic lateral analysis is an elastic MRSA. Thus, in keeping with code requirements, a three-dimensional model of the structure was created the BRBs were designed to accommodate force demands determined by MRSA. BRBF beams, columns collectors were then designed using a rational plastic mechanism analysis with the assumption that any earthquake load effect is determined from the full adjusted brace strengths in tension and compression. This example then goes beyond elastic analysis and relies on a NRHA for three additional aspects of the design. First, NRHA is used to verify that the strains in the BRBs designed to MRSA forces indeed satisfy the IO performance requirements in DBE-level shaking using the methodology in ASCE 41 Section 2.8.3. Second, compliance with the allowable story drift limit was evaluated in the context of NRHA and the provisions of *Standard* Section 16.2.4. Finally, as a demonstration, NRHA was used to establish reduced design axial forces for the BRBF columns using the exception to *Standard* Section 12.4.3.1 to justify the use of NRHA in determining their required strength as stipulated in AISC 341 Section 16.5b. However, because the structure was found to be at the allowable drift limit as designed using plastic mechanism analysis, the potential savings offered by these reduced column design forces went unrealized.

Designers could elect to place an even greater emphasis on NRHA during the design of such a structure. For example, design forces for BRBF beams and collectors might also be set using NRHA, as was illustrated for the columns, rather than by plastic mechanism analysis. Depending on the relative prices of BRBs and structural steel, designers could economize the design by enlarging select BRB elements (relative to what MRSA finds is necessary) in order to reduce some column sizes. Justifying such a design would require iterative NRHA runs to ensure the structure's overall stiffness is such that allowable drift limits are not exceeded. Finally, the entire structure might be designed using NRHA exclusively. BRB sizes would be established not by MRSA but instead by NRHA and hence a different force distribution that takes into account the building's inelastic characteristics.

7

Reinforced Concrete

By Peter W. Somers, S.E.

Originally developed by Finley A. Charney, PhD, P.E.

Contents

7.1 SEISMIC DESIGN REQUIREMENTS 7
7.1.1 Seismic Response Parameters 7
7.1.2 Seismic Design Category 8
7.1.3 Structural Systems 8
7.1.4 Structural Configuration 9
7.1.5 Load Combinations 9
7.1.6 Material Properties 10
7.2 DETERMINATION OF SEISMIC FORCES 11
7.2.1 Modeling Criteria 11
7.2.2 Building Mass 12
7.2.3 Analysis Procedures 13
7.2.4 Development of Equivalent Lateral Forces 13
7.2.5 Direction of Loading 19
7.2.6 Modal Analysis Procedure 20
7.3 DRIFT AND P-DELTA EFFECTS 21
7.3.1 Torsion Irregularity Check for the Berkeley Building 21
7.3.2 Drift Check for the Berkeley Building 23
7.3.3 P-delta Check for the Berkeley Building 27
7.3.4 Torsion Irregularity Check for the Honolulu Building 29
7.3.5 Drift Check for the Honolulu Building 29
7.3.6 P-Delta Check for the Honolulu Building 31
7.4 STRUCTURAL DESIGN OF THE BERKELEY BUILDING 32
7.4.1 Analysis of Frame-Only Structure for 25 Percent of Lateral Load 33
7.4.2 Design of Moment Frame Members for the Berkeley Building 37
7.4.3 Design of Frame 3 Shear Wall 60

7.5 STRUCTURAL DESIGN OF THE HONOLULU BUILDING 66
7.5.1 Compare Seismic Versus Wind Loading 66
7.5.2 Design and Detailing of Members of Frame 1 69

In this chapter, a 12-story reinforced concrete office building with some retail shops on the first floor is designed for both high and moderate seismic loading. For the more extreme loading, it is assumed that the structure will be located in Berkeley, California and for the moderate loading, in Honolulu, Hawaii.

The basic structural configuration for both locations is shown in Figures 7-1 and 7-2, which show a typical floor plan and building section, respectively. The building has 12 stories above grade and one basement level. The typical bays are 30 feet long in the north-south (N-S) direction and either 40 or 20 feet long in the east-west (E-W) direction.

The main gravity framing system consists of seven continuous 30-foot spans of pan joists. These joists are spaced at 36 inches on center and have an average web thickness of 6 inches and a depth below slab of 16 inches. Due to fire code requirements, a 4-inch-thick floor slab is used, giving the joists a total depth of 20 inches. The joists are supported by concrete beams running in the E-W direction. The building is constructed of normal-weight concrete.

Concrete walls are located around the entire perimeter of the basement level.

For both locations, the seismic force-resisting system in the N-S direction consists of four 7-bay moment-resisting frames. At the Berkeley location, these frames are detailed as special moment-resisting frames. Due to the lower seismicity and lower demand for system ductility, the frames of the Honolulu building are detailed as intermediate moment-resisting frames as permitted by ASCE 7.

In the E-W direction, the seismic force-resisting system for the Berkeley building is a dual system composed of a combination of moment frames and frame-walls (walls integrated into a moment-resisting frame). Along Grids 1 and 8, the frames have five 20-foot bays. Along Grids 2 and 7, the frames consist of two exterior 40-foot bays and one 20-foot interior bay. At Grids 3, 4, 5 and 6, the interior bay consists of shear walls infilled between the interior columns. The exterior bays of these frames are similar to Grids 2 and 7. For the Honolulu building, the structural walls are not necessary, so E-W seismic resistance is supplied by the moment frames along Grids 1 through 8. The frames on Grids 1 and 8 are five-bay frames and those on Grids 2 through 7 are three-bay frames with the exterior bays having a 40-foot span and the interior bay having a 20-foot span. Hereafter, frames are referred to by their gridline designation (e.g., Frame 1 is located on Grid 1).

The foundation system is not considered in this example, but it is assumed that the structure for both the Berkeley and Honolulu locations is founded on very dense soil (shear wave velocity of approximately 2,000 feet per second).

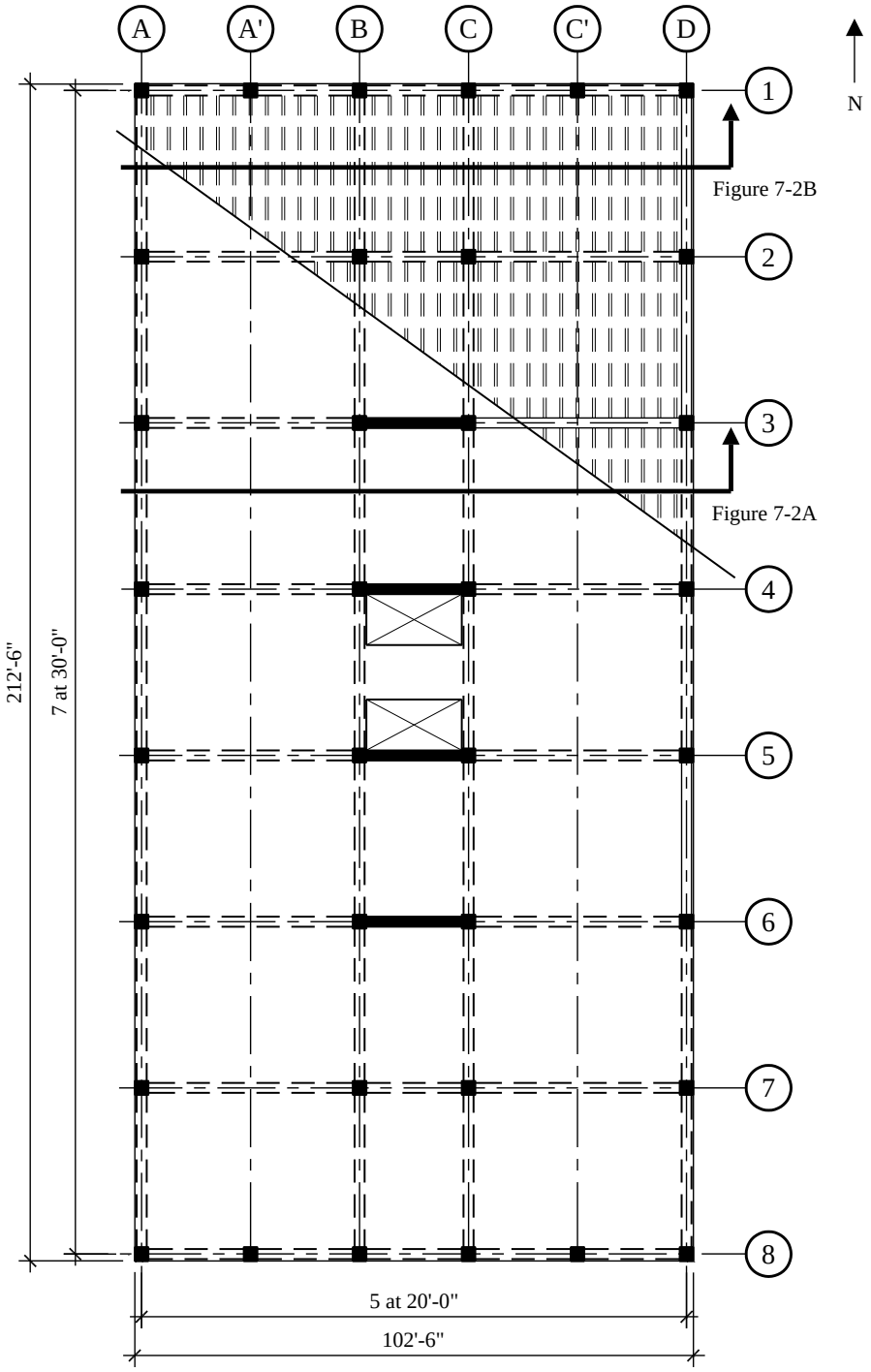

Figure 7-1 Typical floor plan of the Berkeley building; the Honolulu building is similar but without structural walls (1.0 ft = 0.3048 m)

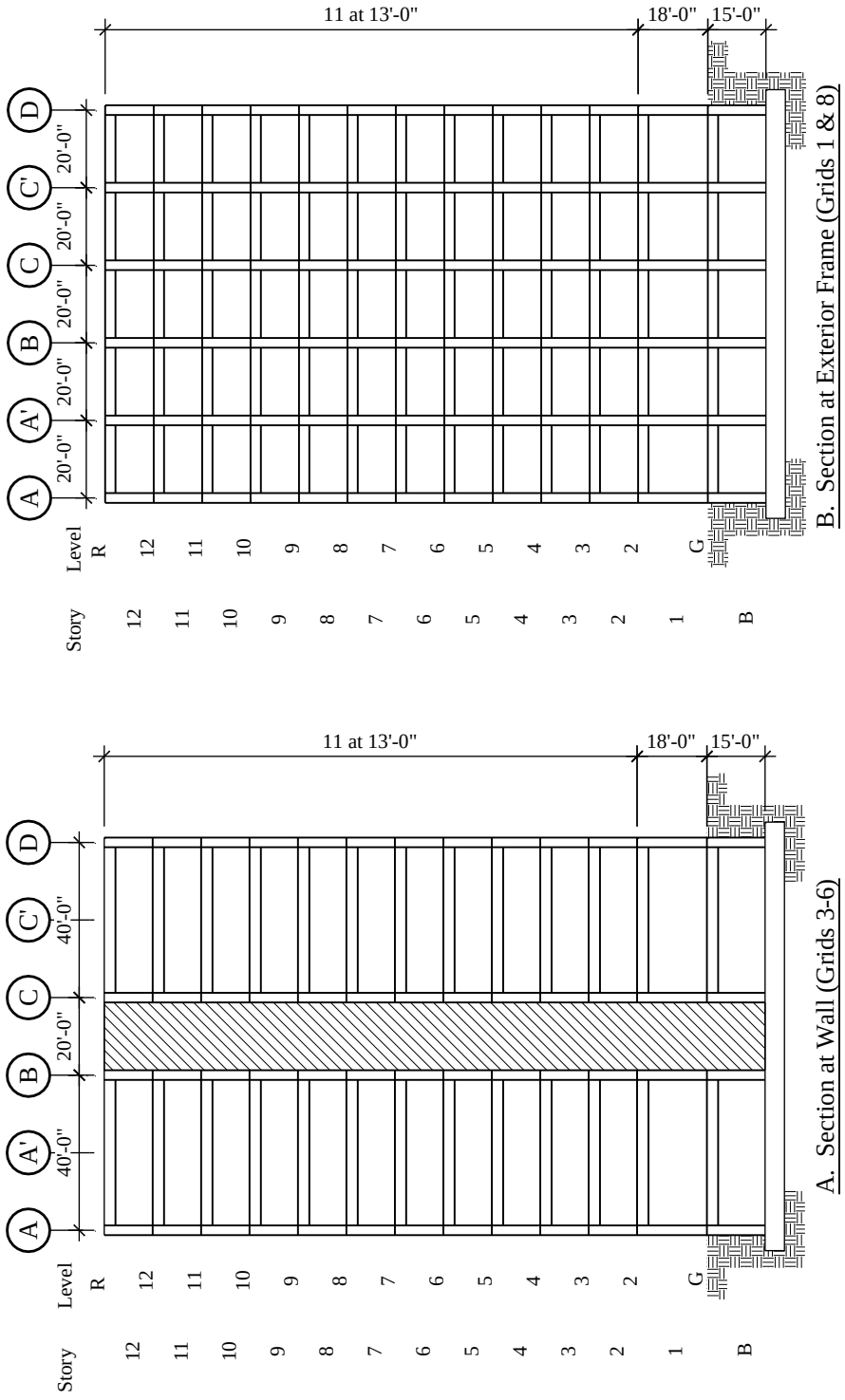

Figure 7-2 Typical elevations of the Berkeley building; the Honolulu building is similar but without structural walls (1.0 ft = 0.3048 m)

The calculations herein are intended to provide a reference for the direct application of the design requirements presented in the 2009 *NEHRP Recommended Provisions* (hereafter, the *Provisions*) and its primary reference document ASCE 7-05 *Minimum Design Loads for Buildings and Other Structures* (hereafter, the *Standard*) and to assist the reader in developing a better understanding of the principles behind the *Provisions* and ASCE 7.

Because a single building configuration is designed for both high and moderate levels of seismicity, two different sets of calculations are required. Instead of providing one full set of calculations for the Berkeley building and then another for the Honolulu building, portions of the calculations are presented in parallel. For example, the development of seismic forces for the Berkeley and Honolulu buildings are presented before structural design is considered for either building. The design or representative elements then is given for the Berkeley building followed by the design of the Honolulu building. Each major section (development of forces, structural design, etc.) is followed by discussion. In this context, the following portions of the design process are presented in varying amounts of detail for each structure:

1. Seismic design criteria

2. Development and computation of seismic forces

3. Structural analysis and drift checks

4. Design of structural members including typical beams, columns and beam-column joints in Frame 1; and for the Berkeley building only, the design of the shear wall on Grid 3

In addition to the *Provisions* and the *Standard*, ACI 318-08 is the other main reference in this example. Except for very minor exceptions, the seismic force-resisting system design requirements of ACI 318 have been adopted in their entirety by the *Provisions*. Cases where requirements of the *Provisions*, the *Standard* and ACI 318 differ are pointed out as they occur. In addition to serving as a reference standard for seismic design, the *Standard* is also cited where discussions involve gravity loads, live load reduction, wind loads and load combinations.

The following are referenced in this chapter:

ACI 318 American Concrete Institute. 2008. *Building Code Requirements and Commentary for Structural Concrete*.

ASCE 7 American Society of Civil Engineers. 2005. *Minimum Design Loads for Buildings and Other Structures*.

ASCE 41 American Society of Civil Engineers. 2006. *Seismic Rehabilitation of Existing Buildings*, including Supplement #1.

Moehle Moehle, Jack P., Hooper, John D and Lubke, Chris D. 2008. "Seismic design of reinforced concrete special moment frames: a guide for practicing engineers," *NEHRP Seismic Design Technical Brief No. 1*, produced by the NEHRP Consultants Joint Venture, a partnership of the Applied Technology Council and the Consortium of Universities for Research in Earthquake Engineering, for the National Institute of Standards and Technology, Gaithersburg, MD., NIST GCR 8-917-1

The structural analysis for this chapter was carried out using the ETABS Building Analysis Program, version 9.5, developed by Computers and Structures, Inc., Berkeley, California. Axial-flexural interaction for column and shear wall design was performed using the PCA Column program, version 3.5, created and developed by the Portland Cement Association.

7.1 SEISMIC DESIGN REQUIREMENTS

7.1.1 Seismic Response Parameters

For Berkeley, California, the short period and one-second period spectral response acceleration parameters S_S and S_1 are 1.65 and 0.68, respectively. For the very dense soil conditions, Site Class C is appropriate as described in *Standard* Section 20.3. Using S_S = 1.65 and Site Class C, *Standard* Table 11.4-1 lists a short period site coefficient, F_a, of 1.0. For S_1 > 0.5 and Site Class C, *Standard* Table 11.4-2 gives a velocity based site coefficient, F_v, of 1.3. Using *Standard* Equation 11.4-1 and 11.4-2, the adjusted maximum considered spectral response acceleration parameters for the Berkeley building are:

$$S_{MS} = F_a S_S = 1.0(1.65) = 1.65$$

$$S_{M1} = F_v S_1 = 1.3(0.68) = 0.884$$

The design spectral response acceleration parameters are given by *Standard* Equation 11.4-3 and 11.4-4:

$$S_{DS} = 2/3\ S_{MS} = 2/3\ (1.65) = 1.10$$

$$S_{D1} = 2/3\ S_{M1} = 2/3\ (0.884) = 0.589$$

The transition period, T_s, for the Berkeley response spectrum is:

$$T_s = \frac{S_{D1}}{S_{DS}} = \frac{0.589}{1.10} = 0.535 \text{ sec}$$

T_s is the period where the horizontal (constant acceleration) portion of the design response spectrum intersects the descending (constant velocity or acceleration inversely proportional to T) portion of the spectrum. It is used later in this example as a parameter in determining the type of analysis that is required for final design.

For Honolulu, the short-period and one-second period spectral response acceleration parameters are 0.61 and 0.18, respectively. For Site Class C soils and interpolating from *Standard* Table 11.4-1, the F_a is 1.16 and from *Standard* Table 11.4-1, the interpolated value for F_v is 1.62. The adjusted maximum considered spectral response acceleration parameters for the Honolulu building are:

$$S_{MS} = F_a S_S = 1.16(0.61) = 0.708$$

$$S_{M1} = F_v S_1 = 1.62(0.178) = 0.288$$

and the design spectral response acceleration parameters are:

$$S_{DS} = 2/3\ S_{MS} = 2/3\ (0.708) = 0.472$$

$$S_{D1} = 2/3\ S_{M1} = 2/3\ (0.288) = 0.192$$

The transition period, T_s, for the Honolulu response spectrum is:

$$T_s = \frac{S_{D1}}{S_{DS}} = \frac{0.192}{0.472} = 0.407 \text{ sec}$$

7.1.2 Seismic Design Category

According to *Standard* Section 1.5, both the Berkeley and the Honolulu buildings are classified as Occupancy Category II. *Standard* Table 11.5-1 assigns an occupancy importance factor, *I*, of 1.0 to all Occupancy Category II buildings.

According to *Standard* Tables 11.6-1 and 11.6-2, the Berkeley building is assigned to Seismic Design Category D and the Honolulu building is assigned to Seismic Design Category C.

7.1.3 Structural Systems

The seismic force-resisting systems for both the Berkeley and the Honolulu buildings consist of moment-resisting frames in the N-S direction. E-W loading is resisted by a dual frame-wall system in the Berkeley building and by a set of moment-resisting frames in the Honolulu building. For the Berkeley building, assigned to Seismic Design Category D, *Standard* Table 12.2-1 requires that all concrete moment-resisting frames be designed and detailed as special moment frames. Similarly, *Standard* Table 12.2-1 requires shear walls in dual systems to be detailed as special reinforced concrete shear walls. For the Honolulu building assigned to Seismic Design Category C, *Standard* Table 12.2-1 permits the use of intermediate moment frames for all building heights.

Standard Table 12.2-1 provides values for the response modification coefficient, *R*, the system overstrength factor, Ω_0 and the deflection amplification factor, C_d, for each structural system type. The values determined for the Berkeley and Honolulu buildings are summarized in Table 7-1.

Table 7-1 Response Modification, Overstrength and Deflection Amplification Coefficients for Structural Systems Used

Location	Response Direction	Building Frame Type	*R*	Ω_0	C_d
Berkeley	N-S	Special moment frame	8	3	5.5
	E-W	Dual system incorporating special moment frame and special shear wall	7	2.5	5.5
Honolulu	N-S	Intermediate moment frame	5	3	4.5
	E-W	Intermediate moment frame	5	3	4.5

For the Berkeley building dual system, *Standard* Section 12.2.5.1 requires that the moment frame portion of the system be designed to resist at least 25 percent of the total seismic force. As discussed below, this requires that a separate analysis of a frame-only system be carried out for loading in the E-W direction.

7.1.4 Structural Configuration

Based on the plan view of the building shown in Figure 7-1, the only potential horizontal irregularity is a Type 1a or 1b torsional irregularity (*Standard* Table 12.3-1). While the actual presence of such an irregularity cannot be determined without analysis, it appears unlikely for both the Berkeley and the Honolulu buildings because the lateral force-resisting elements of both buildings are distributed evenly over the floor. However, this will be determined later.

As for the vertical irregularities listed in *Standard* Table 12.3-2, the presence of a soft or weak story cannot be determined without analysis. In this case, however, the first story is suspect, because its height of 18 feet is well in excess of the 13-foot height of the story above. However, it is assumed (but verified later) that a vertical irregularity does not exist.

7.1.5 Load Combinations

The combinations of loads including earthquake effects are provided in *Standard* Section 12.4. Load combinations for other loading conditions are in *Standard* Chapter 2.

For the Berkeley structure, the basic strength design load combinations that must be considered are:

$1.2D + 1.6L$ (or $1.6L_r$)

$1.2D + 0.5L \pm 1.0E$

$0.9D \pm 1.0E$

In addition to the combinations listed above, for the Honolulu building wind loads govern the design of a portion of the building (as determined later), so the following strength design load combinations should also be considered:

$1.2D + 0.5L \pm 1.6W$

$0.9D \pm 1.6W$

The load combination including only 1.4 times dead load will not control for any condition in these buildings.

In accordance with *Standard* Section 12.4.2 the earthquake load effect, E, be defined as:

$$E = \rho Q_E + 0.2 S_{DS} D$$

where gravity and seismic load effects are additive and

$$E = \rho Q_E - 0.2 S_{DS} D$$

where the effects of seismic load counteract gravity.

The earthquake load effect requires the determination of the redundancy factor, ρ, in accordance with *Standard* Section 12.3.4. For the Honolulu building (Seismic Design Category C), $\rho = 1.0$ per *Standard* Section 12.3.4.1.

For the Berkeley building, ρ must be determined in accordance with *Standard* Section 12.3.4.2. For the purpose of the example, the method in *Standard* Section 12.3.4.2, Method b, will be utilized. Based on the preliminary design, it is assumed that $\rho = 1.0$ because the structure has a perimeter moment frame and is assumed to be regular based on the plan layout. As discussed in the previous section, this will be verified later.

For the Berkeley building, substituting E and with ρ taken as 1.0, the following load combinations must be used for seismic design:

$(1.2 + 0.2S_{DS})D + 0.5L \pm Q_E$

$(0.9 - 0.2\ S_{DS})D \pm Q_E$

Finally, substituting 1.10 for S_{DS}, the following load combinations must be used:

$1.42D + 0.5L \pm Q_E$

$0.68D \pm Q_E$

For the Honolulu building, substituting E and with ρ taken as 1.0, the following load combinations must be used for seismic design:

$(1.2 + 0.2S_{DS})D + 0.5L \pm Q_E$

$(0.9 - 0.2S_{DS})D \pm Q_E$

Finally, substituting 0.472 for S_{DS}, the following load combinations must be used:

$1.30D + 0.5L \pm Q_E$

$0.80D \pm Q_E$

The seismic load combinations with overstrength given in *Standard* Section 12.4.3.2 are not utilized for this example because there are no discontinuous elements supporting stiffer elements above them and collector elements are not addressed.

7.1.6 Material Properties

For the Berkeley building, normal-weight concrete of 5,000 psi strength is used everywhere (except as revised for the lower floor shear walls as determined later). All reinforcement has a specified yield strength of 60 ksi. As required by ACI 318 Section 21.1.5.2, the longitudinal reinforcement in the moment frames and shear walls either must conform to ASTM A706 or be ASTM A615 reinforcement, if the actual yield strength of the steel does not exceed the specified strength by more than 18 ksi and the ratio of actual ultimate tensile stress to actual tensile yield stress is greater than 1.25.

The Honolulu building also uses 5,000 psi concrete and ASTM A615 Grade 60 reinforcing steel. ASTM 706 reinforcing is not required for an intermediate moment frame.

7.2 DETERMINATION OF SEISMIC FORCES

The determination of seismic forces requires an understanding of the magnitude and distribution of structural mass and the stiffness properties of the structural system. Both of these aspects of design are addressed in the mathematical modeling of the structure.

7.2.1 Modeling Criteria

Both the Berkeley and Honolulu buildings will be analyzed with a three-dimensional mathematical model using the ETABS software. Modeling criteria for the seismic analysis is covered in *Standard* Section 12.7. This section covers how to determine the effective seismic weight (addressed in the next section) and provides guidelines for the modeling of the building. Of most significance in a concrete building is modeling realistic stiffness properties of the structural elements considering cracked sections in accordance with *Standard* Section 12.7.3, Item a. Neither the *Standard* nor ACI 318 provides requirements for modeling cracked sections for seismic analysis, but the typical practice is to use a reduced moment of inertia for the beams, columns and walls based on the expected level of cracking. This example utilizes the following effective moment of inertia, I_{eff}, for both buildings:

- Beams: $I_{eff} = 0.3I_{gross}$
- Columns: $I_{eff} = 0.5I_{gross}$
- Walls: $I_{eff} = 0.5I_{gross}$

The effective stiffness of the moment frame elements is based on the recommendations in Moehle and ASCE 41 and account for the expected axial loads and reinforcement levels in the members. The value for the shear walls is based on the recommendations in ASCE 41 for cracked concrete shear walls.

The following are other significant aspects of the mathematical model that should be noted:

1. The structure is modeled with 12 levels above grade and one level below grade. The perimeter basement walls are modeled as shear panels as are the main structural walls at the Berkeley building. The walls are assumed to be fixed at their base, which is at the basement level.

2. All floor diaphragms are modeled as infinitely rigid in plane and infinitely flexible out-of-plane, consistent with common practice for a regular-shaped concrete diaphragm (see *Standard* Section 12.3.1.2).

3. Beams, columns and structural wall boundary members are represented by two-dimensional frame elements. The beams are modeled as T-beams using the effective slab width per ACI 318 Section 8.10, as recommended by Moehle.

4. The structural walls of the Berkeley building are modeled as a combination of boundary columns and shear panels with composite stiffness.

5. Beam-column joints are modeled in accordance with Moehle, which references the procedure in ASCE 41. Both the beams and columns are modeled with end offsets based on the geometry, but the beam offset is modeled as 0 percent rigid, while the column offset is modeled as 100 percent rigid. This provides effective stiffness for beam-column joints consistent with the expected behavior of the

joint: strong column-weak beam condition. (While the recommendations in Moehle are intended for special moment frames, the same joint rigidities are used for Honolulu for consistency.)

6. P-delta effects are neglected in the analysis for simplicity. This assumption is verified later in this example.

7. While the base of the model is located at the basement level, the seismic base for determination of forces is assumed to be at the first floor, which is at the exterior grade.

7.2.2 Building Mass

Before the building mass can be determined, the approximate size of the different members of the seismic force-resisting system must be established. For special moment frames, limitations on beam-column joint shear and reinforcement development length usually control. An additional consideration is the amount of vertical reinforcement in the columns. ACI 318 Section 21.4.3.1 limits the vertical steel reinforcing ratio to 6 percent for special moment frame columns; however, 3 to 4 percent vertical steel is a more practical upper-bound limit.

Based on a series of preliminary calculations (not shown here), it is assumed that for the Berkeley building all columns and structural wall boundary elements are 30 inches by 30 inches, beams are 24 inches wide by 32 inches deep and the panel of the structural wall is 16 inches thick. It has already been established that pan joists are spaced at 36 inches on center, have an average web thickness of 6 inches and, including a 4-inch-thick slab, are 20 inches deep. For the Berkeley building, these member sizes probably are close to the final sizes. For the Honolulu building (which does not have the weight of concrete walls and ends up with slightly smaller frame elements: 28- by 28-inch columns and 20- by 30-inch beams), the masses computed from the Berkeley member sizes are slightly high but are used for consistency.

In addition to the building structural weight, the following superimposed dead loads are assumed:

- Roofing = 10 psf
- Partition = 10 psf (see *Standard* Section 12.7.2, Item 2)
- Ceiling and M/E/P = 10 psf
- Curtain wall cladding = 10 psf (on vertical surface area)

Based on the above member sizes and superimposed dead load, the individual story weights and masses are listed in Table 7-2. These masses are used for the analysis of both the Berkeley and the Honolulu buildings. Note from Table 7-2 that the roof and lowest floor have masses slightly different from the typical floors. It is also interesting to note that the average density of this building is 12.4 pcf, which is in the range of typical concrete buildings with relatively high floor-to-floor heights.

Table 7-2 Story Weights and Masses

Level	Weight (kips)	Mass (kips-sec^2/in.)
Roof	3,352	8.675
12	3,675	9.551
11	3,675	9.551
10	3,675	9.551
9	3,675	9.551
8	3,675	9.551
7	3,675	9.551
6	3,675	9.551
5	3,675	9.551
4	3,675	9.551
3	3,675	9.551
2	3,817	9.879
Total	43,919	113.736

(1.0 kip = 4.45 kN, 1.0 in. = 25.4 mm)

In the ETABS model, these masses are applied as uniform distributed masses across the extent of the floor diaphragms in order to provide a realistic distribution of mass in the dynamic model as described below. The structural framing is modeled utilizing massless elements since their mass is included with the floor mass. Note that for relatively heavy cladding systems, it would be more appropriate to model the cladding mass linearly along the perimeter in order to more correctly model the mass moment of inertia. This has little impact in relatively light cladding systems as is the case here, so the cladding masses are distributed across the floor diaphragms for convenience.

7.2.3 Analysis Procedures

The selection of analysis procedures is in accordance with *Standard* Table 12.6-1. Based on the initial review, it appears that the Equivalent Lateral Force (ELF) procedure is permitted for both the Berkeley and Honolulu buildings. However, as we shall see, the analysis demonstrates that the Berkeley building is torsionally irregular, meaning that the Model Response Spectrum Analysis (MRSA) procedure is required. Regardless of irregularities, it is common practice to use the MRSA for buildings in regions of high seismic hazard since the more rigorous analysis method tends to provide lower seismic forces and therefore more economical designs. For the Honolulu building, located in a region of lower seismic hazard and with wind governing in some cases, the ELF will be used. However, a dynamic model of the Honolulu building is used for determining the structural periods.

It should be noted that even though the Berkeley building utilizes the MRSA, the ELF must be used for at least determining base shear for scaling of results as discussed below.

7.2.4 Development of Equivalent Lateral Forces

This section covers the ELF procedure for both the Berkeley and Honolulu buildings. Since the final analysis of the Berkeley building utilizes the MRSA procedure, the ELF is illustrated for determining base shear only. The complete ELF procedure is illustrated for the Honolulu building.

7.2.4.1 Period Determination. Requirements for the computation of building period are given in *Standard* Section 12.8.2. For the preliminary design using the ELF procedure, the approximate period, T_a, computed in accordance with *Standard* Equation 12.8.7 can be used:

$$T_a = C_t h_n^x$$

The method for determining approximate period will generally result in periods that are lower (hence, more conservative for use in predicting base shear) than those computed from a more rigorous mathematical model. If a more rigorous analysis is carried out, the resulting period may be too high due to a variety of possible modeling simplifications and assumptions. Consequently, the *Standard* places an upper limit on the period that can be used for design. The upper limit is $T = C_u T_a$ where C_u is provided in *Standard* Table 12.8-1.

For the N-S direction of the Berkeley building, the structure is a reinforced concrete moment-resisting frame and the approximate period is calculated according to *Standard* Equation 12.8-7 using $C_t = 0.016$ and $x = 0.9$ per *Standard* Table 12.8-2. For $h_n = 161$ feet, $T_a = 1.55$ seconds and $S_{D1} > 0.40$ for the Berkeley building, $C_u = 1.4$ and the upper limit on the analytical period is $T = 1.4(1.55) = 2.17$ seconds.

For E-W seismic activity in Berkeley, the structure is a dual system, so $C_t = 0.020$ and $x = 0.75$ for "other structures." The approximate period, $T_a = 0.90$ second and the upper limit on the analytical period is $1.4(0.90) = 1.27$ seconds.

For the Honolulu building, the $T_a = 1.55$ second period computed above for concrete moment frames is applicable in both the N-S and E-W directions. For Honolulu, S_{D1} is 0.192 and, from *Standard* Table 12.8-1, C_u can be taken as 1.52. The upper limit on the analytical period is $T = 1.52(1.55) = 2.35$ seconds.

For the detailed period determination at both the Berkeley and Honolulu buildings, computer models were developed based on the criteria in Section 7.2.1.

A summary of the Berkeley analysis is presented in Section 7.2.6, but the fundamental periods are presented here. The computed N-S period of vibration is 2.02 seconds. This is between the approximate period, $T_a = 1.55$ seconds and $C_u T_a = 2.17$ seconds. In the E-W direction, the computed period is 1.42 seconds, which is greater than both $T_a = 0.90$ second and $C_u T_a = 1.27$ seconds. Therefore, the periods used for the ELF procedure are 2.02 seconds in the N-S direction and 1.27 seconds in the E-W direction.

For the Honolulu building, the computed periods in the N-S and E-W directions are 2.40 seconds and 2.33 seconds, respectively. The N-S period is similar to the Berkeley building because there are no walls in the N-S direction of either building, but the Honolulu period is higher due to the smaller framing member sizes. In the E-W direction, the increase in period from 1.42 seconds at the Berkeley building to 2.33 seconds indicates a significant reduction in stiffness due to the lack of the walls in the Honolulu building. For both the E-W and the N-S directions, T_a for the Honolulu building is 1.55 seconds and $C_u T_a$ is 2.35 seconds. Therefore, for the purpose of computing ELF forces, the periods are 2.35 seconds and 2.33 seconds in the N-S and E-W directions, respectively.

A summary of the approximate and computed periods is given in Table 7-3.

Table 7-3 Comparison of Approximate and Computed Periods (in seconds)

Method of Period Computation	Berkeley		Honolulu	
	N-S	E-W	N-S	E-W
Approximate T_a	1.55	0.90	1.55	1.55
Approximate × C_u	2.17	**1.27**	**2.35**	2.35
ETABS	**2.02**	1.42	2.40	**2.33**

*Bold values should be used in the ELF analysis.

7.2.4.2 Seismic Base Shear. For the ELF procedure, seismic base shear is determined using the short period and 1-second period response acceleration parameters, the computed structural period and the system response modification factor (*R)*.

Using *Standard* Equation 12.8-1, the design base shear for the structure is:

$$V = C_s W$$

where W is the total effective seismic weight of the building and C_s is the seismic response coefficient computed in accordance with *Standard* Section 12.8.1.1.

The seismic design base shear for the Berkeley is computed as follows:

For the moment frame system in the N-S direction with W = 43,919 kips (see Table 7-2), S_{DS} = 1.10, S_{D1} = 0.589, R = 8, I = 1 and T = 2.02 seconds:

$$C_{s,max} = \frac{S_{DS}}{R/I} = \frac{1.10}{8/1} = 0.1375$$

$$C_s = \frac{S_{D1}}{T(R/I)} = \frac{0.589}{2.02(8/1)} = 0.0364$$

$$C_{s,min} = 0.044 S_{DS} I = 0.044(1.1)(1) = 0.0484$$

$$C_{s,min} = 0.01$$

$C_{s,min}$ = 0.0484 controls and the design base shear in the N-S direction is V = 0.0484 (43,919) = 2,126 kips.

In the E-W direction with the dual system, $C_{s,max}$ and $C_{s,min}$ are as before, T = 1.27 seconds and

$$C_s = \frac{S_{D1}}{T(R/I)} = \frac{0.589}{1.27(7/1)} = 0.0670$$

In this case, C_s = 0.0670 controls and V = 0.0670 (43,919) = 2,922 kips.

For the Honolulu building, base shears are computed in a similar manner and are nearly the same for the N-S and the E-W directions. With W = 43,919 kips, S_{DS} = 0.474, S_{D1} = 0.192, R = 5, I = 1 and T = 2.35 seconds in the N-S direction:

$$C_{s,max} = \frac{S_{DS}}{R/I} = \frac{0.472}{5/1} = 0.0944$$

$$C_s = \frac{S_{D1}}{T(R/I)} = \frac{0.192}{2.35(5/1)} = 0.0163$$

$$C_{s,min} = 0.044 S_{DS} I = 0.044(0.472)(1.0) = 0.0207$$

$$C_{s,min} = 0.01$$

C_s = 0.0207 controls and V = 0.0207 (43,919) = 908 kips.

Due to rounding, the E-W base shear is also 908 kips. A summary of the Berkeley and Honolulu seismic design parameters are provided in Table 7-4.

Table 7-4 Comparison of Periods, Seismic Shears Coefficients and Base Shears for the Berkeley and Honolulu Buildings

Location	Response Direction	Building Frame Type	T (sec)	C_s	V (kips)
Berkeley	N-S	Special moment frame	2.02	0.0485	2,126
	E-W	Dual system incorporating special moment frame and structural wall	1.27	0.0670	2,922
Honolulu	N-S	Intermediate moment frame	2.35	0.0207	908
	E-W	Intermediate moment frame	2.33	0.0207	908

(1.0 kip = 4.45 kN)

7.2.4.3 Vertical Distribution of Seismic Forces. The vertical distribution of seismic forces for the ELF is computed from *Standard* Equations 12.8-11 and 12.8-12.:

$$F_x = C_{vx} V$$

$$C_{vx} = \frac{w_x h_x^k}{\sum_{i=1}^{n} w_i h_i^k}$$

where:

k = 1.0 for T < 0.5 second

k = 2.0 for T > 2.5 seconds

k = 0.75 + 0.5T for 1.0 < T < 2.5 seconds

Based on the equations above, the seismic story forces, shears and overturning moments are easily computed using a spreadsheet. Since the analysis of the Berkeley building utilizes the MRSA procedure, the vertical force distribution for the ELF procedure will not be used for the design and are not shown here. The vertical force distribution computations for the Honolulu building are shown in Table 7-5. The table is presented with as many significant digits to the left of the decimal as the spreadsheet generates but that should not be interpreted as real accuracy; it is just the simplest approach.

Table 7-5 Vertical Distribution of N-S and E-W Seismic Forces for the Honolulu Building*

Level	Height h (ft)	Weight W (kips)	Wh^k	Wh^k/Σ	Force F_x (kips)	Story Shear V_x (kips)	Overturning Moment M_x (ft-k)
R	161.00	3,352	59,048,176	0.196	177.8	177.8	
12	148.00	3,675	55,053,755	0.183	165.8	343.6	2,312
11	135.00	3,675	46,128,207	0.153	138.9	482.5	6,779
10	122.00	3,675	37,963,112	0.126	114.3	596.9	13,052
9	109.00	3,675	30,564,359	0.101	92.0	688.9	20,811
8	96.00	3,675	23,938,555	0.079	72.1	761.0	29,767
7	83.00	3,675	18,093,222	0.060	54.5	815.5	39,660
6	70.00	3,675	13,037,074	0.043	39.3	854.8	50,262
5	57.00	3,675	8,780,453	0.029	26.4	881.2	61,374
4	44.00	3,675	5,336,045	0.018	16.1	897.3	72,830
3	31.00	3,675	2,720,196	0.009	8.2	905.5	84,494
2	18.00	3,817	992,774	0.003	3.0	908.5	96,265
Total		43,919	301,655,927	1.000	908		112,617

*Table based on T = 2.35 sec and k = 1.92.
(1.0 ft = 0.3048 m, 1.0 kip = 4.45 kN, 1.0 ft-kip = 1.36 kN-m)

The computed seismic story shears for the Honolulu buildings are shown graphically in Figure 7-3. Also shown in this figure are the wind load story shears determined in accordance with the *Standard* based on a 3-second gust of 105 mph and Exposure Category B. The wind shears have been multiplied by the 1.6 load factor to make them comparable to the strength design seismic loads (with a 1.0 load factor).

As can be seen, the N-S seismic shears are significantly greater than the corresponding wind shears, but the E-W seismic and wind shears are closer. In the lower stories of the building, wind controls the strength demands and, in the upper levels, seismic forces control the strength demands. (A somewhat more detailed comparison is given later when the Honolulu building is designed.) With regards to detailing the Honolulu building, *all* of the elements must be detailed for inelastic deformation capacity as required by ACI 318 for intermediate moment frames.

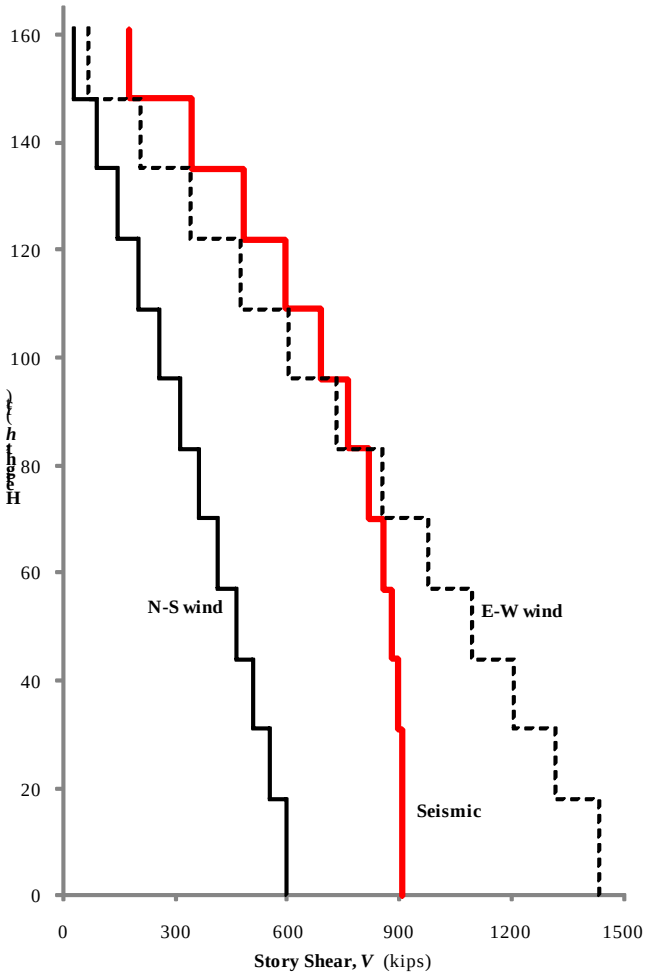

Figure 7-3 Comparison of wind and seismic story shears for the Honolulu building (1.0 ft = 0.3048 m, 1.0 kip = 4.45 kN)

As expected, wind loads do not control the design of the Berkeley building based on calculations not presented here. (Note that the comparison between wind and seismic forces should be based on more than just the base shear values. For buildings where the wind and seismic loads are somewhat similar, it is possible that overturning moment for wind could govern even where the seismic base shear is greater, in which case a more detailed analysis of specific member forces would need to be performed to determine the controlling load case.)

7.2.4.4 Horizontal Force Distribution and Torsion. The story forces are distributed to the various vertical elements of the seismic force-resisting system based on relative rigidity using the ETABS model. As described previously, the buildings are modeled using rigid diaphragms at each floor. Since the structures are symmetric in both directions and the distribution of mass is assumed to be uniform, there is no inherent torsion (*Standard* Section 12.8.4.1) at either building. However, accidental torsion needs to be considered in accordance with *Standard* Section 12.8.4.2.

For this example, accidental torsion is applied to each level as a moment equal to the story shear multiplied by 5 percent of the story width perpendicular to the direction of loading. The applied moment is based on the ELF forces for both the Berkeley building (analyzed using the MRSA) and Honolulu building (ELF). The computation of the accidental torsion moments for the Honolulu building is shown in Table 7-6.

Table 7-6 Accidental Torsion for the Honolulu Building

Level	Force F_x (kips)	N-S Building Width (ft)	N-S Torsion (ft-kips)	E-W Building Width (ft)	E-W Torsion (ft-kips)
R	177.8	103	911	216	1,915
12	165.8	103	850	216	1,787
11	138.9	103	712	216	1,499
10	114.3	103	586	216	1,234
9	92.0	103	472	216	995
8	72.1	103	369	216	780
7	54.5	103	279	216	590
6	39.3	103	201	216	426
5	26.4	103	136	216	287
4	16.1	103	82	216	175
3	8.2	103	42	216	90
2	3.0	103	15	216	33

(1.0 kip = 4.45 kN, 1.0 ft-kip = 1.36 kN-m)

Amplification of accidental torsion, which needs to be considered for buildings with torsional irregularities in accordance with *Standard* Section 12.8.4.3, will be addressed if required after the irregularities are determined.

7.2.5 Direction of Loading

For the initial analysis, the seismic loading is applied in two directions independently as permitted by *Standard* Section 12.5. This assumption at the Berkeley building will need to be verified later since *Standard* Section 12.5.4 requires consideration of multi-directional loading (the 100 percent-30 percent procedure) for columns that form part of two intersection systems and have a high seismic axial load.

Note that rather than checking whether or not multi-directional loading needs to be considered, some designers apply the seismic forces using the 100 percent-30 percent rule (or an SRSS combination of the two directions) as common practice when intersecting systems are utilized since today's computer analysis programs can make the application of multi-directional loading easier than checking each specific element. Since multi-directional loading is not a requirement of the *Standard*, the Berkeley building will not be analyzed in this manner unless required for specific columns.

The Honolulu building, in Seismic Design Category C, does not require consideration of multi-directional loading since it does not contain the nonparallel system irregularity (*Standard* Section 12.5.3).

7.2.6 Modal Analysis Procedure

The Berkeley building will be analyzed using the MRSA procedure of *Standard* Section 12.9 and the ETABS software. The building is modeled based on the criteria discussed in Section 7.2.1 and analyzed using a response spectrum generated by ETABS based on the seismic response parameters presented in Section 7.1.1. The modal parameters were combined using the complete quadratic combination (CQC) method per *Standard* Section 12.9.3.

The computed periods and the modal response characteristics of the Berkeley building are presented in Table 7-7. In order to capture higher mode effects, 12 modes were selected for the analysis and with 12 modes, the accumulated modal mass in each direction is more than 90 percent of the total mass as required by *Standard* Section 12.9.1.

Table 7-7 Periods and Modal Response Characteristics for the Berkeley Building

Mode	Period (sec)	% of Effective Mass Represented by Mode*		Description
		N-S	E-W	
1	2.02	83.62 (83.62)	0.00 (0.00)	First Mode N-S
2	1.46	0.00 (83.62)	0.00 (0.00)	First Mode Torsion
3	1.42	0.00 (83.62)	74.05 (74.05)	First Mode E-W
4	0.66	9.12 (92.74)	0.00 (74.05)	Second Mode N-S
5	0.38	2.98 (95.72)	0.00 (74.05)	Third Mode N-S
6	0.35	0.00 (95.72)	16.02 (90.07)	Second Mode E-W
7	0.25	1.36 (97.08)	0.00 (90.07)	Fourth Mode N-S
8	0.18	0.86 (97.94)	0.00 (90.07)	Fifth Mode N-S
9	0.17	0.00 (97.94)	0.09 (90.16)	Second Mode Torsion
10	0.15	0.00 (97.94)	5.28 (95.44)	Third Mode E-W
11	0.10	0.59 (98.53)	0.00 (95.44)	Sixth Mode N-S
12	0.08	0.00 (98.53)	3.14 (98.58)	Fourth Mode E-W

*Accumulated modal mass in parentheses.

One of the most important aspects of the MRSA procedure is the scaling requirement. In accordance with *Standard* Section 12.9.4, the results of the MRSA cannot be less than 85 percent of the results of the ELF. This is commonly accomplished by running the MRSA to determine the modal base shear. If the modal base shear is more than 85 percent of the ELF base shear in each direction, then no scaling is required. However, if the model base shear is less than the ELF base shear, then the response spectrum is scaled upward so that the modal base shear is equal to 85 percent of the ELF base shear. This is illustrated in Table 7-8.

Table 7-8 Scaling of MRSA results for the Berkeley Building

Direction	V_{ELF} (kips)	$0.85V_{ELF}$ (kips)	V_{MRSA} (kips)	Scale Factor
N-S	2,126	1,807	1,462	1.24
E-W	2,922	2,483	2,296	1.08

(1.0 kip = 4.45 kN)

Therefore, the response spectrum functions for the Berkeley analysis will be scaled by 1.24 and 1.08 in the N-S and E-W directions, respectively, which will result in the modal base shears being equal to 85 percent of the static base shears.

As discussed previously, the accidental torsion requirement for the model analysis will be satisfied by applying the torsional moments computed for the ELF procedure as a static load case that will be combined with the dynamic load case for the MRSA forces.

7.3 DRIFT AND P-DELTA EFFECTS

The checks of story drift and P-delta effect are contained in this section, but first, deflection-related configuration checks are performed for each building. As discussed previously, these structures could contain torsional or soft-story irregularities. The output from the drift analysis will be used to determine if either of these irregularities is present in the buildings. However, the presence of a soft story irregularity impacts only the analysis procedure limitations for the Berkeley building and has no impact on the design procedures for the Honolulu building.

7.3.1 Torsion Irregularity Check for the Berkeley Building

In Section 7.1.4 it was mentioned that torsional irregularities are unlikely for the Berkeley building because the elements of the seismic force-resisting system were well distributed over the floor area. This will now be verified by comparing the story drifts at each end of the building in accordance with *Standard* Table 12.3-1. For this check, drifts are computed using the ETABS program using the ELF procedure (to avoid having to obtain modal combinations of drifts at multiple points) and including accidental torsion with $A_x = 1.0$. Note that since this check is only for relative drifts, the C_d factor is not included.

The drift computations and torsion check for the E-W direction are shown in Table 7-9. The drift values are shown only for one direction of accidental torsion (positive torsion moment) since the other direction is the opposite due to symmetry.

Table 7-9 Torsion Check for Berkeley Building Loaded in the E-W Direction

Story	Story Drift North End (in)	Story Drift South End(in)	Average Story Drift (in)	Max Drift / Average Drift
Roof	0.180	0.230	0.205	1.12
12	0.184	0.246	0.215	1.14
11	0.188	0.261	0.225	1.16
10	0.192	0.276	0.234	1.18
9	0.193	0.288	0.241	1.20
8	0.192	0.296	0.244	1.21
7	0.188	0.298	0.243	1.23
6	0.178	0.292	0.235	1.24
5	0.164	0.278	0.221	1.26
4	0.144	0.254	0.199	1.28
3	0.117	0.218	0.167	1.30
2	0.119	0.229	0.174	1.32

(1.0 in = 25.4 mm)

As can be seen from the table, a torsional irregularity (Type 1a) does exist at Story 8 and below because the ratio of maximum to average drift exceeds 1.2. This is counterintuitive for a symmetric building but can happen for a building in which the lateral elements are located towards the center of a relatively long floor plate, as occurs here. This configuration results in a relatively large accidental torsion load but relatively low torsional resistance.

For loading in the N-S direction, similar computations (not shown here) demonstrate that the structure is torsionally regular.

The presence of the torsional irregularity in the E-W direction has several implications for the design:

- The qualitative determination for using the redundancy factor, ρ, equal to 1.0 is not applicable per *Standard* Section 12.3.4.2, Item b, as previously assumed in Section 7.1.5. For the purposes of this example, we will assume $\rho = 1.0$ based on *Standard* Section 12.3.4.2, Item a. Due to the number of shear walls and moment frames in the E-W direction, the loss of individual wall or frame elements would still satisfy the criteria of *Standard* Table 12.3-3. This would have to be verified independently and if those criteria were not met, then analysis would have to be revised with $\rho = 1.3$.

- The ELF procedure is not permitted per *Standard* Table 12.6-1. This does not change the analysis since we are utilizing the MRSA procedure.

- The amplification of accidental torsion needs to be considered per *Standard* Section 12.8.4.3. The A_x factor is computed for each floor in this direction and the analysis is revised. See below.

- Story drifts need to be checked at both ends of the building rather than at the floor centroid, per *Standard* Section 12.12.1. This is covered in Section 7.3.2 below.

The initial determination of accidental torsion was based on $A_x = 1.0$. Due to the torsional irregularity, accidental torsion for the E-W direction of loading needs to be computed again with the amplification factor. This is shown in Table 7-10. Note that while the determination of the torsional irregularity is based on story drifts, the computation of the torsional amplification factor is based on story displacements.

Table 7-10 Accidental Torsion for the Berkeley Building

Level	Force F_x (kips)	E-W Building Width (ft)	E-W Torsion (ft-k)	Max Displ (in)	Ave Displ (in)	A_x	E-W Torsion, $A_x M_{ta}$ (ft-k)
Roof	474.8	213	5,045	3.17	2.60	1.03	5,186
12	463.3	213	4,923	2.94	2.40	1.04	5,128
11	408.0	213	4,335	2.69	2.18	1.06	4,575
10	354.7	213	3,769	2.43	1.96	1.07	4,029
9	303.5	213	3,225	2.15	1.72	1.08	3,493
8	254.6	213	2,706	1.87	1.48	1.10	2,970
7	208.2	213	2,213	1.57	1.24	1.11	2,463
6	164.5	213	1,748	1.27	1.00	1.13	1,976
5	123.8	213	1,316	0.98	0.76	1.15	1,511
4	86.6	213	920	0.70	0.54	1.17	1,075
3	53.3	213	567	0.45	0.34	1.19	674
2	26.1	213	278	0.23	0.17	1.20	333

(1.0 kip = 4.45 kN, .0 ft = 0.3048 m, 1.0 ft-kip = 1.36 kN-m)

With the revised accidental torsion values for the E-W direction of loading, the ETABS model is rerun for the drift checks and member design in subsequent sections.

7.3.2 Drift Check for the Berkeley Building

Story drifts are computed in accordance with *Standard* Section 12.9.2 and then checked for acceptance based on *Standard* Section 12.12.1. According to *Standard* Table 12.12-1, the story drift limit for this Occupancy Category II building is $0.020h_{sx}$, where h_{sx} is the height of story x. This limit may be thought of as 2 percent of the story height. Quantitative results of the drift analysis for the N-S and E-W directions are shown in Tables 7-11a and 7-11b, respectively. The story drifts are taken directly from the modal combinations in ETABS. Due to the torsional irregularity in the E-W direction, drifts are checked at both ends of the structure, while N-S drifts are checked at the building centroid.

In neither case does the computed drift ratio (amplified story drift divided by h_{sx}) exceed 2 percent of the story height. Therefore, the story drift requirement is satisfied. A plot of the total deflection in both the N-S and E-W directions is shown in Figure 7-4 and a plot of story drifts is in Figure 7-5.

An example calculation for drift in Story 5 loaded in the N-S direction is given below. Note that the relevant row is highlighted in Table 7-11a.

Story drift = Δ_{5e} = 0.208 inch
Deflection amplification factor, C_d = 5.5
Importance factor, I = 1.0
Amplified story drift = $\Delta_5 = C_d \Delta_{5e}/I$ = 5.5(0.208)/1.0 = 1.14 inches
Amplified drift ratio = Δ_5/h_5 = (1.14/156) = 0.00733 = 0.733% < 2.0% OK

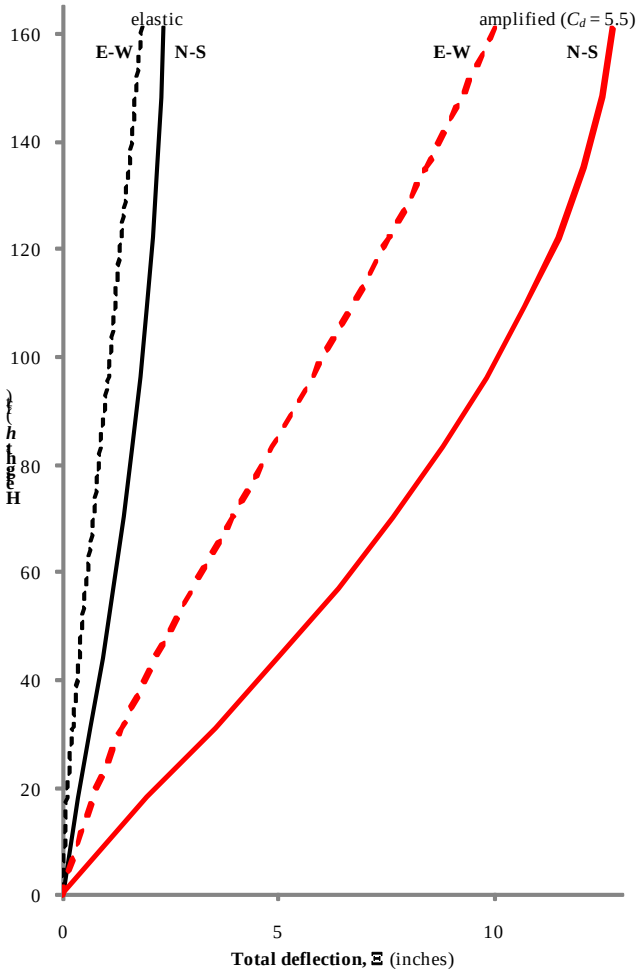

Figure 7-4 Deflected shape for Berkeley building
(1.0 ft = 0.3048 m, 1.0 in = 25.4 mm)

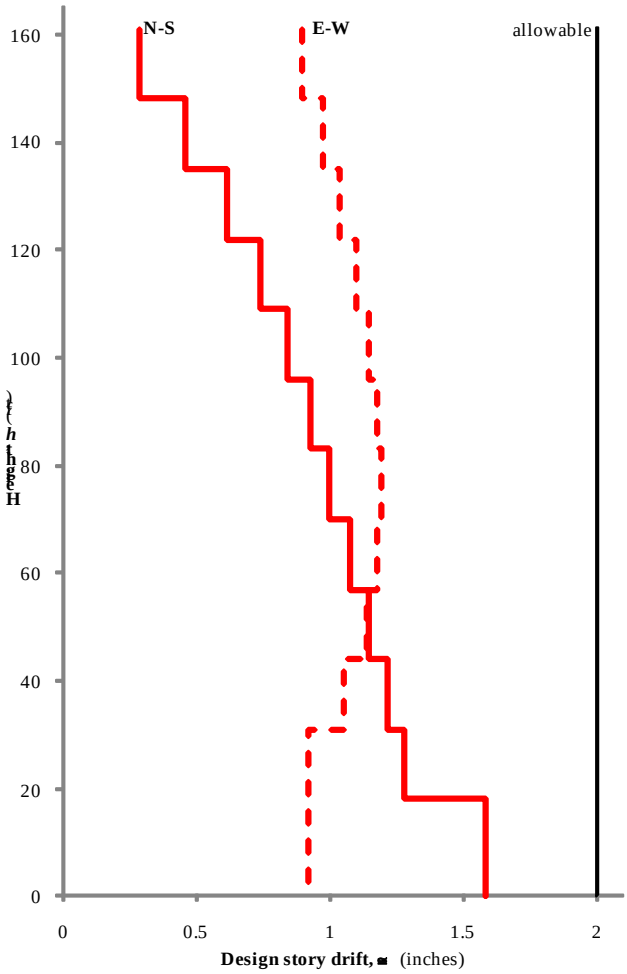

Figure 7-5 Drift profile for Berkeley building
(1.0 ft = 0.3048 m)

Table 7-11a Drift Computations for the Berkeley Building Loaded in the N-S Direction

Story	Story Drift (in)	Story Drift × C_d [*] (in)	Drift Ratio[**] (%)
Roof	0.052	0.29	0.184
12	0.083	0.46	0.293
11	0.112	0.61	0.393
10	0.134	0.74	0.474
9	0.153	0.84	0.540
8	0.168	0.93	0.593
7	0.182	1.00	0.641
6	0.195	1.07	0.688
5	**0.208**	**1.14**	**0.733**
4	0.221	1.21	0.778
3	0.232	1.28	0.819
2	0.287	1.58	0.732

[*] C_d = 5.5 for loading in this direction.
[**] Story height = 156 inches for Stories 3 through roof and 216 inches for Story 2.
(1.0 in = 25.4 mm)

Table 7-11b Drift Computations for the Berkeley Building Loaded in the E-W Direction

Story	Story Drift North End (in)	Story Drift South End (in)	Max Story Drift × C_d [*] (in)	Max Drift Ratio[**] (%)
Roof	0.163	0.163	0.90	0.576
12	0.177	0.177	0.97	0.623
11	0.188	0.188	1.03	0.663
10	0.199	0.199	1.10	0.702
9	0.208	0.208	1.14	0.734
8	0.214	0.214	1.18	0.755
7	0.217	0.217	1.19	0.763
6	0.215	0.215	1.18	0.756
5	0.207	0.207	1.14	0.729
4	0.192	0.192	1.05	0.675
3	0.167	0.168	0.92	0.591
2	0.167	0.167	0.92	0.425

[*] C_d = 5.5 for loading in this direction.
[**] Story height = 156 inches for Stories 3 through roof and 216 inches for Story 2.
(1.0 in = 25.4 mm)

The story deflection information will be used to determine whether or not a soft story irregularity exists. As indicated previously, a soft story irregularity (Vertical Irregularity Type 1a) would not impact the design since we are utilizing the MRSA. However, an extreme soft story irregularity (vertical irregularity Type 1b) is prohibited in Seismic Design Category D building per *Standard* Section 12.3.3.1.

However, *Standard* Section 12.3.2.2 lists an exception:

> Structural irregularities of Types 1a, 1b, or 2 in Table 12.3-2 do not apply where no story drift ratio under design lateral load is less than or equal to 130 percent of the story drift ratio of the next story above…. The story drift ratios of the top two stories of the structure are not required to be evaluated.

To determine whether the exception applies to the Berkeley building, the ratio of the drift ratios are reported in Table 7-11c.

Table 7-11c Drift Ratio Comparisons for Stiffness Irregularity Check

Story	North-South Drift Ratio	Ratio to Story Above	East-West Drift Ratio	Ratio to Story Above
Roof	0.184	-	0.184	-
12	0.293	1.59	0.293	1.09
11	0.393	**1.34**	0.393	1.06
10	0.474	1.21	0.474	1.06
9	0.540	1.14	0.540	1.05
8	0.593	1.10	0.593	1.03
7	0.641	1.08	0.641	1.01
6	0.688	1.07	0.688	0.99
5	0.733	1.07	0.733	0.96
4	0.778	1.06	0.778	0.93
3	0.819	1.05	0.819	0.88
2	0.732	0.89	0.732	0.72

As can be seen the vertical irregularity does not apply in the E-W direction since the ratio is less than 1.3 at all stories. In the N-S direction, however, the ratio exceeds 1.3 at the two upper stories. While the top stories are excluded from this check, the ratio of 1.34 at Story 11 means that the story stiffness's need to be evaluated to determine whether there is a stiffness irregularity based on *Standard* Table 12.3-2.

Since this controlling ratio of drift ratios is at an upper floor and just exceeds the 1.3 limit, it could be reasonable to conclude that a stiffness irregularity does not exist. For the purposes of this example, as long as an extreme stiffness irregularity is not present (which seems highly unlikely given the relative drift ratios), the presence of a non-extreme stiffness irregularity does not have a substantive impact on the design since this example utilizes the MRSA procedure anyway. In accordance with *Standard* Table 12.6-1, the ELF procedure would not be permitted if there were to be a stiffness irregularity. Therefore, the required stiffness checks for the N-S direction are not shown in this example.

7.3.3 P-delta Check for the Berkeley Building

In accordance with *Standard* Section 12.8.7 (as referenced by *Standard* Section 12.9.6 for the MRSA), P-delta effects need not be considered in the analysis if the stability coefficient, θ, is less than 0.10 for each story. However, the *Standard* also limits θ to a maximum value determined by *Standard* Equation 12.8-17 as:

$$\theta_{\max} = \frac{0.5}{\beta C_d} \leq 0.25$$

Taking β as 1.0 (see *Standard* Section 12.8.7), the limit on stability coefficient for both directions is 0.5/(1.0)5.5 = 0.091.

The P-delta analysis for each direction of loading is shown in Tables 7-12a and 7-12b. For this P-delta analysis a story live load of 20 psf (50 psf for office occupancy reduced to 40 percent per *Standard* Section 4.8.1) was included in the total story load calculations. Deflections and story shears are based on the MRSA with no upper limit on period in accordance with *Standard* Sections 12.9.6 and 12.8.6.2. As can be seen in the last column of each table, θ does not exceed the maximum permitted value computed above and P-delta effects can be neglected for both drift and strength analyses.

An example P-delta calculation for the Story 5 under N-S loading is shown below. Note that the relevant row is highlighted in Table 7-12a.

Amplified story drift = Δ_5 = 1.144 inches
Story shear = V_5 = 1,240 kips
Accumulated story weight P_5 = 36,532 kips
Story height = h_{s5}= 156 inches
I = 1.0
C_d = 5.5
$\theta = (P_5 I \Delta_5/(V_5 h_{s5} C_d) = (36{,}532)(1.0)(1.144)/(6.5)(1{,}240)(156) = 0.0393 < 0.091$ OK

Table 7-12a P-Delta Computations for the Berkeley Building Loaded in the N-S Direction

Story	Story Drift (in)	Story Shear (kips)	Story Dead Load (kips)	Story Live Load (kips)	Total Story Load (kips)	Accum. Story Load (kips)	Stability Coeff, θ
Roof	0.287	261	3,352	420	3,772	3,772	0.0048
12	0.457	495	3,675	420	4,095	7,867	0.0085
11	0.613	672	3,675	420	4,095	11,962	0.0127
10	0.740	807	3,675	420	4,095	16,057	0.0172
9	0.842	914	3,675	420	4,095	20,152	0.0216
8	0.926	1,003	3,675	420	4,095	24,247	0.0261
7	1.000	1,083	3,675	420	4,095	28,342	0.0305
6	1.073	1,161	3,675	420	4,095	32,437	0.0349
5	**1.144**	**1,240**	**3,675**	**420**	**4,095**	**36,532**	**0.0393**
4	1.214	1,322	3,675	420	4,095	40,627	0.0435
3	1.278	1,400	3,675	420	4,095	44,722	0.0476
2	1.581	1,462	3,817	420	4,237	48,959	0.0446

(1.0 in = 25.4 mm, 1.0 kip = 4.45 kN)

Table 7-12b P-Delta Computations for the Berkeley Building Loaded in the E-W Direction

Story	Story Drift (in)	Story Shear (kips)	Story Dead Load (kips)	Story Live Load (kips)	Total Story Load (kips)	Accum. Story Load (kips)	Stability Coeff, θ
Roof	0.899	463	3,352	420	3,772	3,772	0.0085
12	0.972	843	3,675	420	4,095	7,867	0.0106
11	1.035	1,104	3,675	420	4,095	11,962	0.0131
10	1.096	1,275	3,675	420	4,095	16,057	0.0161
9	1.145	1,396	3,675	420	4,095	20,152	0.0193
8	1.177	1,512	3,675	420	4,095	24,247	0.0220
7	1.191	1,645	3,675	420	4,095	28,342	0.0239
6	1.180	1,787	3,675	420	4,095	32,437	0.0250
5	1.137	1,927	3,675	420	4,095	36,532	0.0251
4	1.054	2,073	3,675	420	4,095	40,627	0.0241
3	0.921	2,215	3,675	420	4,095	44,722	0.0217
2	0.918	2,296	3,817	420	4,237	48,959	0.0165

(1.0 in = 25.4 mm, 1.0 kip = 4.45 kN)

7.3.4 Torsion Irregularity Check for the Honolulu Building

A test for torsional irregularity for the Honolulu building can be performed in a manner similar to that for the Berkeley building. Based on computations not shown here, the Honolulu building is not torsionally irregular. This is the case because the walls, which draw the torsional resistance towards the center of the Berkeley building, do not exist in the Honolulu building. Therefore, the torsional amplification factor, A_x = 1.0 for all levels and the accidental torsion moments used for the analysis do not need to be revised.

7.3.5 Drift Check for the Honolulu Building

The story drift computations for the Honolulu building deforming under the N-S and E-W seismic loading are shown in Tables 7-13a and 7-13b.

These tables show that the story drift at all stories is less than the allowable story drift of $0.020h_{sx}$ (*Standard* Table 12.12-1). Even though it is not pertinent for Seismic Design Category C buildings, a soft first story does not exist for the Honolulu building because the ratio of first story drift to second story drift does not exceed 1.3.

Table 7-13a Drift Computations for the Honolulu Building Loaded in the N-S Direction

Story	Total Drift (in)	Story Drift (in)	Story Drift × C_d* (in)	Drift Ratio (%)
Roof	1.938	0.057	0.259	0.166
12	1.880	0.087	0.391	0.251
11	1.793	0.115	0.517	0.331
10	1.678	0.138	0.623	0.399
9	1.540	0.157	0.708	0.454
8	1.382	0.172	0.773	0.496
7	1.210	0.182	0.821	0.526
6	1.028	0.190	0.854	0.547
5	0.838	0.194	0.873	0.559
4	0.644	0.195	0.881	0.565
3	0.449	0.198	0.889	0.570
2	0.251	0.247	1.113	0.515

*C_d = 4.5 for loading in this direction; total drift is at top of story, story height = 156 inches for Stories 3 through roof and 216 inches for Story 2.
(1.0 in. = 25.4 mm)

Table 7-13b Drift Computations for the Honolulu Building Loaded in the E-W Direction

Story	Total Drift (in)	Story Drift (in)	Story Drift × C_d* (in)	Drift Ratio (%)
Roof	2.034	0.051	0.230	0.147
12	1.983	0.083	0.376	0.241
11	1.899	0.115	0.518	0.332
10	1.784	0.142	0.639	0.410
9	1.642	0.164	0.736	0.473
8	1.478	0.181	0.814	0.522
7	1.297	0.194	0.874	0.559
6	1.103	0.203	0.915	0.586
5	**0.900**	**0.209**	**0.942**	**0.604**
4	0.691	0.213	0.958	0.614
3	0.478	0.216	0.970	0.622
2	0.262	0.261	1.173	0.543

C_d = 4.5 for loading in this direction; total drift is at top of story, story height = 156 inches for Levels 2 through roof and 216 inches for Level 1.
(1.0 in = 25.4 mm)

A sample calculation for Story 5 of Table 7-13b (highlighted in the table) is as follows:

Deflection at top of story = δ_{5e} =0.900 inches
Deflection at bottom of story = δ_{4e} = 0.691 inch
Story drift = $\Delta_{5e} = \delta_{5e} - \delta_{4e}$ = 0.900 - 0.0691 = 0.209 inch
Deflection amplification factor, C_d = 4.5
Importance factor, I = 1.0
Amplified story drift = $\Delta_5 = C_d \Delta_{5e}/I$ = 4.5(0.209)/1.0 = 0.942 inch
Amplified drift ratio = Δ_5 / h_5 = (0.942/156) = 0.00604 = 0.604% < 2.0% OK

Therefore, story drift satisfies the drift requirements.

7.3.6 P-Delta Check for the Honolulu Building

Calculations for P-delta effects are shown in Tables 7-14a and 7-14b for N-S and E-W loading, respectively.

Table 7-14a P-Delta Computations for the Honolulu Building Loaded in the N-S Direction

Story	Story Drift (in)	Story Shear (kips)	Story Dead Load (kips)	Story Live Load (kips)	Total Story Load (kips)	Accum. Story Load (kips)	Stability Coeff, θ
Roof	0.259	177.8	3,352	420	3,772	3,772	0.0069
12	0.391	343.6	3,675	420	4,095	7,867	0.0123
11	0.517	482.5	3,675	420	4,095	11,962	0.0183
10	0.623	596.9	3,675	420	4,095	16,057	0.0245
9	0.708	688.9	3,675	420	4,095	20,152	0.0307
8	0.773	761.0	3,675	420	4,095	24,247	0.0370
7	0.821	815.5	3,675	420	4,095	28,342	0.0432
6	0.854	854.8	3,675	420	4,095	32,437	0.0494
5	0.873	881.2	3,675	420	4,095	36,532	0.0556
4	0.881	897.3	3,675	420	4,095	40,627	0.0618
3	0.889	905.5	3,675	420	4,095	44,722	0.0682
2	1.113	908.5	3,817	420	4,237	48,959	0.0650

(1.0 in = 25.4 mm, 1.0 kip = 4.45 kN)

Table 7-14b P-Delta Computations for the Honolulu Building Loaded in the E-W Direction

Story	Story Drift (in)	Story Shear (kips)	Story Dead Load (kips)	Story Live Load (kips)	Total Story Load (kips)	Accum. Story Load (kips)	Stability Coeff, θ
Roof	0.230	177.8	3,352	420	3,772	3,772	0.0079
12	0.376	343.6	3,675	420	4,095	7,867	0.0128
11	0.518	482.5	3,675	420	4,095	11,962	0.0183
10	0.639	596.9	3,675	420	4,095	16,057	0.0239
9	0.736	688.9	3,675	420	4,095	20,152	0.0296
8	0.814	761.0	3,675	420	4,095	24,247	0.0351
7	0.874	815.5	3,675	420	4,095	28,342	0.0407
6	0.915	854.8	3,675	420	4,095	32,437	0.0462
5	**0.942**	**881.2**	**3,675**	**420**	**4,095**	**36,532**	**0.0515**
4	0.958	897.3	3,675	420	4,095	40,627	0.0568
3	0.970	905.5	3,675	420	4,095	44,722	0.0626
2	1.173	908.5	3,817	420	4,237	48,959	0.0617

(1.0 in = 25.4 mm, 1.0 kip = 4.45 kN)

The stability ratio at Story 5 from Table 7-14b is computed as follows:

Amplified story drift = Δ_5 = 0.942 inch
Story shear = V_5 = 881.2 = kips
Accumulated story weight P_5 = 36,532 kips
Story height = h_{s5} = 156 inches
C_d = 4.5
$\theta = [P_5 (\Delta_5/C_d)]/(V_5 h_{s5}) = 36{,}532(0.942/4.5)/(881.2)(156) = 0.0515$

The requirements for maximum stability ratio ($0.5/C_d = 0.5/4.5 = 0.111$) are satisfied. Because the stability ratio is less than 0.10 at all floors, P-delta effects need not be considered (*Standard* Section 12.8.7).

7.4 STRUCTURAL DESIGN OF THE BERKELEY BUILDING

Frame-wall interaction plays an important role in the behavior of the structure loaded in the E-W direction. This behavior has the following attributes:

1. For frames without walls (Frames 1, 2, 7 and 8), the shears developed in the beams (except for the first story) do not differ greatly from story to story. This allows for uniformity in the design of the beams.

2. For frames containing structural walls (Frames 3 through 6), the overturning moments in the structural walls are reduced as a result of interaction with the remaining frames (Frames 1, 2, 7 and 8).

3. For the frames containing structural walls, the 40-foot-long girders act as outriggers further reducing the overturning moment resisted by the structural walls.

4. A significant load reversal occurs at the top of frames with structural walls. This happens because the structural wall pulls back on (supports) the top of Frame 1. The deflected shape of the structure loaded in the E-W direction also shows the effect of frame-wall interaction because the shape is neither a cantilever mode (wall alone) nor a shear mode (frame alone). It is the "straightening out" of the deflected shape of the structure that causes the story shears in the frames without walls to be relatively equal.

Some of these attributes are shown graphically in Figure 7-6, which illustrates the total story force resisted by Frames 1, 2 and 3.

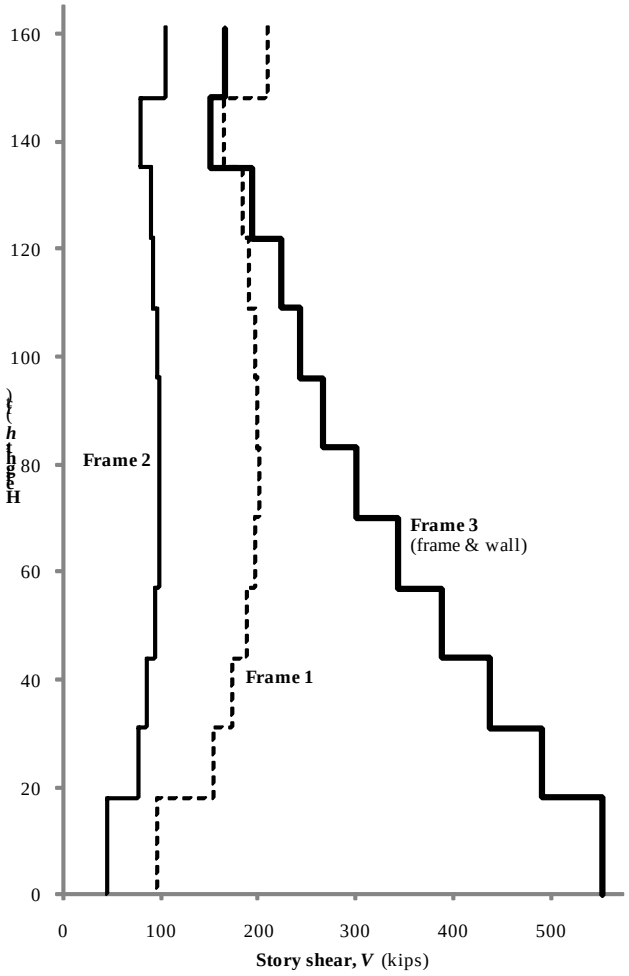

Figure 7-6 Story shears in the E-W direction
(1.0 ft = 0.3048 m, 1.0 kip = 4.45 kN)

7.4.1 Analysis of Frame-Only Structure for 25 Percent of Lateral Load

Where a dual system is utilized, *Standard* Section 12.2.5.1 requires that the moment frames themselves are designed to resist at least 25 percent of the total base shear. This provision ensures that the dual system has sufficient redundancy to justify the increase from $R = 6$ for a special reinforced concrete

structural wall to $R = 7$ for a dual system (see *Standard* Table 12-2). This 25 percent analysis was carried out using the ETABS program with the mathematical model of the building being identical to the previous version except that the panels of the structural walls were removed. The boundary elements of the walls were retained in the model so that behavior of the interior frames (Frames 3, 4, 5 and 6) would be analyzed in a rational way. (It could be argued that keeping the boundary columns in the 25 percent model violates the intent of the provision since they are an integral part of the shear walls. However, in this condition, the columns are needed for the moment frames adjacent to the walls and those in longitudinal direction (which resist a small amount of torsion). Since these eight boundary columns resist only a small portion (just over 15 percent) the total base shear for the 25 percent model, the intent of the dual system requirements is judged to be satisfied. It should be noted that it is not the intent of the *Standard* to allow dual systems of co-planar and integral moment frames and shear walls.)

The seismic demands for this frame-only analysis were scaled such that the spectra base shear is equal to 25 percent of the design base shear for the dual system. In this case, the response spectrum was scaled such that the frame-only base shear is equal to $(0.25)(0.85)V_{ELF}$. While this may not result in story forces exactly equal to 25 percent of the story forces from the MRSA of the dual system, the method used is assumed to meet the intent of this provision of the *Standard.*

The results of the analysis are shown in Figures 7-7, 7-8 and 7-9 for the frames on Grids 1, 2 and 3, respectively. The frames on Grids 6, 7 and 8 are similar by symmetry and Grids 4 and 5 are similar to Grid 3. In these figures, the original analysis (structural wall included) is shown by a heavy line and the 25 percent (frame-only) analysis is shown by a light, dashed line. As can be seen, the 25 percent rule controls only at the lower level of the building. Therefore, for the design of the beams and columns at the lower two levels (not part of this example), the greater of the dual system and frame-only analysis should be used. For the purposes of this example, which includes representative designs for the framing at a middle level, design forces from the dual system analysis will satisfy the 25 percent requirement.

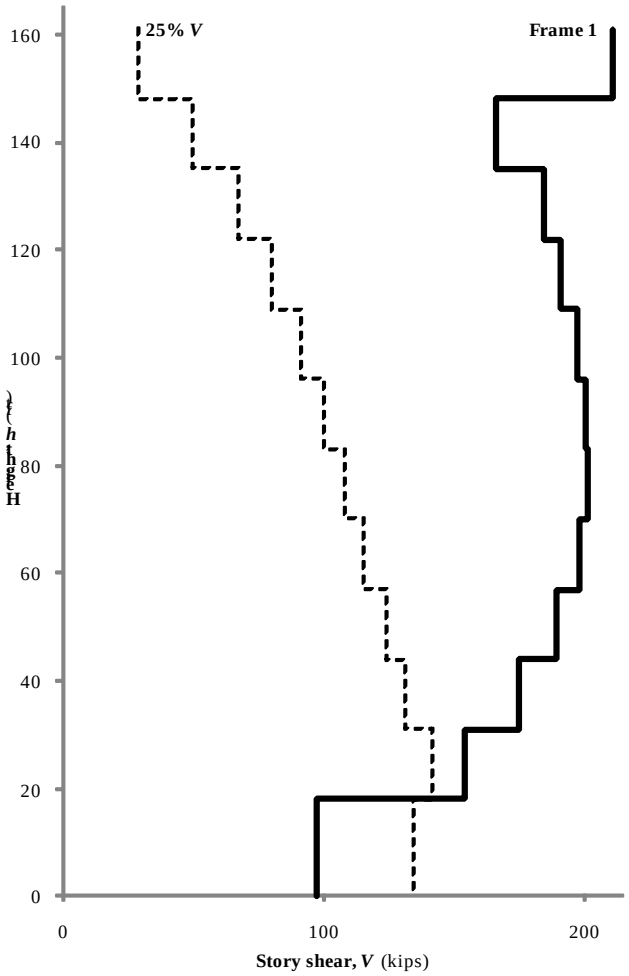

Figure 7-7 25 percent story shears, Frame 1 E-W direction
(1.0 ft = 0.3048 m, 1.0 kip = 4.45 kN)

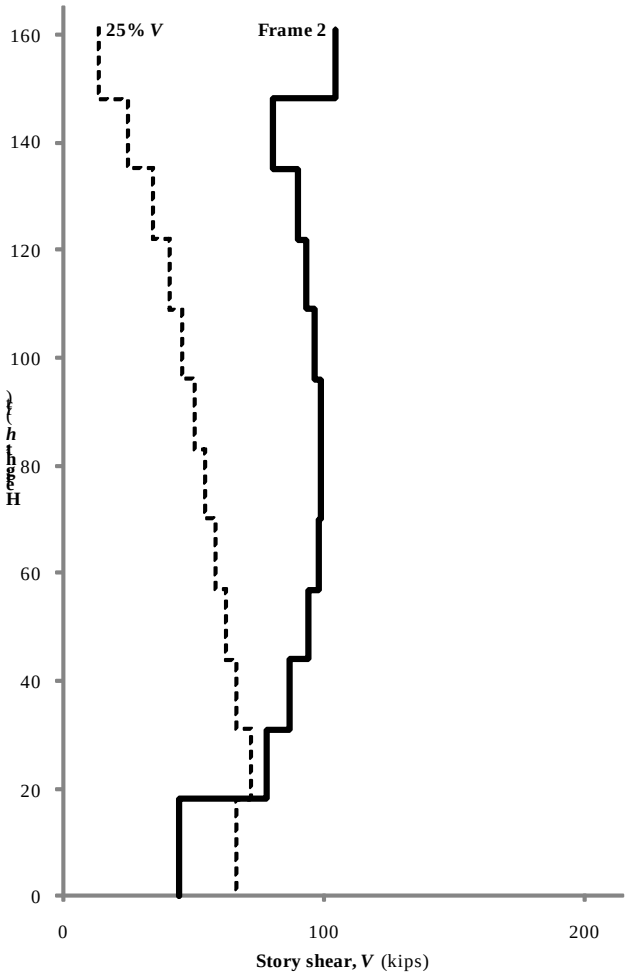

Figure 7-8 25 percent story shears, Frame 2 E-W direction
(1.0 ft = 0.3048 m, 1.0 kip = 4.45 kN)

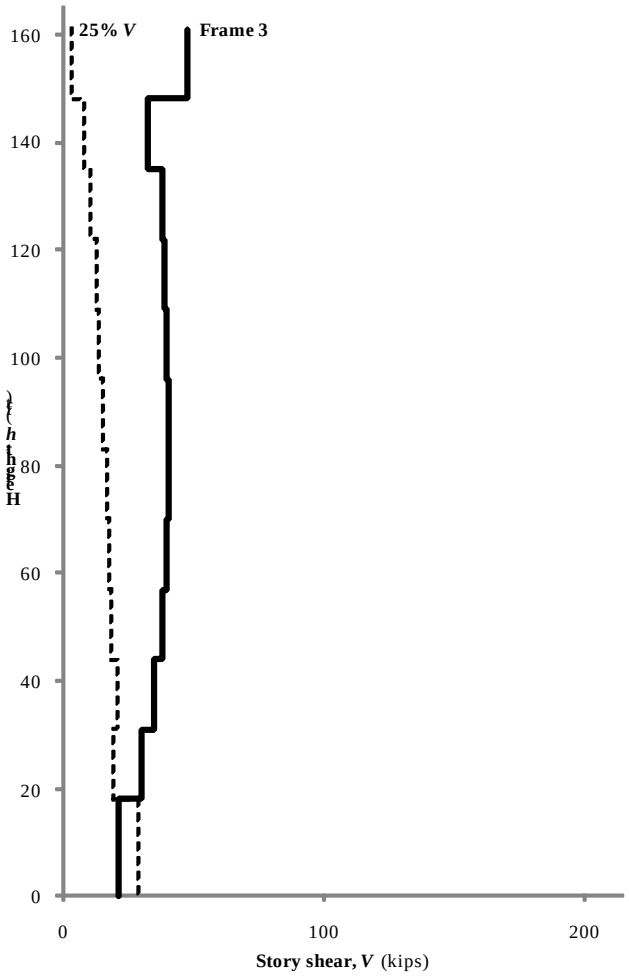

Figure 7-9 25 percent story shear, Frame 3 E-W direction
(1.0 ft = 0.3048 m, 1.0 kip = 4.45 kN)

7.4.2 Design of Moment Frame Members for the Berkeley Building

For this part of the example, the design and detailing of five beams and one interior column along Grid 1 on Level 5 are presented in varying amounts of detail. The beams are designed first because the flexural capacity of the as-designed beams is a factor in the design and detailing of the column and the beam-column joint.

Before continuing with the example, it should be mentioned that the design of ductile reinforced concrete moment frame members is controlled by the flexural reinforcement in the beams. The percentage and placement of beam flexural reinforcement governs the flexural rebar cutoff locations, the size and spacing of beam shear reinforcement, the cross-sectional characteristics of the column, the column flexural reinforcement and the column shear reinforcement. The beam reinforcement is critical because the basic concept of ductile frame design is to force most of the energy-dissipating deformation to occur through inelastic rotation in plastic hinges at the ends of the beams.

In carrying out the design calculations, three different flexural strengths are used for the beams. These capacities are based on the following:

- Design strength: ϕ = 0.9, tensile stress in reinforcement at 1.00 f_y
- Nominal strength: ϕ = 1.0, tensile stress in reinforcement at 1.00 f_y
- Probable strength: ϕ = 1.0, tensile stress in reinforcement at 1.25 f_y

Various aspects of the design of the beams and other members depend on the above capacities are as follows:

- Beam rebar cutoffs: Design strength
- Beam shear reinforcement: Probable strength of beam
- Beam-column joint strength: Probable strength of beam
- Column flexural strength: 6/5 × nominal strength of beam
- Column shear strength: Probable strength of column or beam

In addition, beams in ductile frames will always have top and bottom longitudinal reinforcement throughout their length. In computing flexural capacities, only the tension steel will be considered. This is a valid design assumption because reinforcement ratios are quite low, yielding a depth to the neutral axis similar to the depth of the compression reinforcement.

Finally, a sign convention for bending moments is required in flexural design. In this example, where the steel at the top of a beam section is in tension, the moment is designated as a negative moment. Where the steel at the bottom is in tension, the moment is designated as a positive moment. All moment diagrams are drawn using the reinforced concrete or tension-side convention. For beams, this means negative moments are plotted on the top and positive moments are plotted on the bottom. For columns, moments are drawn on the tension side of the member.

7.4.2.1 Preliminary Calculations. Before the quantity and placement of reinforcement is determined, it is useful to establish, in an overall sense, how the reinforcement will be distributed. The preliminary design established that the moment frame beams would be 24 inches wide by 32 inches deep and the columns would be 30 inches by 30 inches. Note that the beam widths were selected to consider the beam-column joints "confined" per ACI 318 Section 21.7.4.1, which requires beam widths of at least 75 percent of the column width.

In order to determine the effective depth used for the design of the beams, it is necessary to estimate the size and placement of the reinforcement that will be used. In establishing this depth, it is assumed that #8 bars will be used for longitudinal reinforcement and that hoops and stirrups will be constructed from #4 bars. In all cases, clear cover of 1.5 inches is assumed. Since this structure has beams spanning in two orthogonal directions, it is necessary to layer the flexural reinforcement as shown in Figure 7-10. The reinforcement for the E-W spanning beams was placed in the upper and lower layers because the strength demand for these members is somewhat greater than that for the N-S beams.

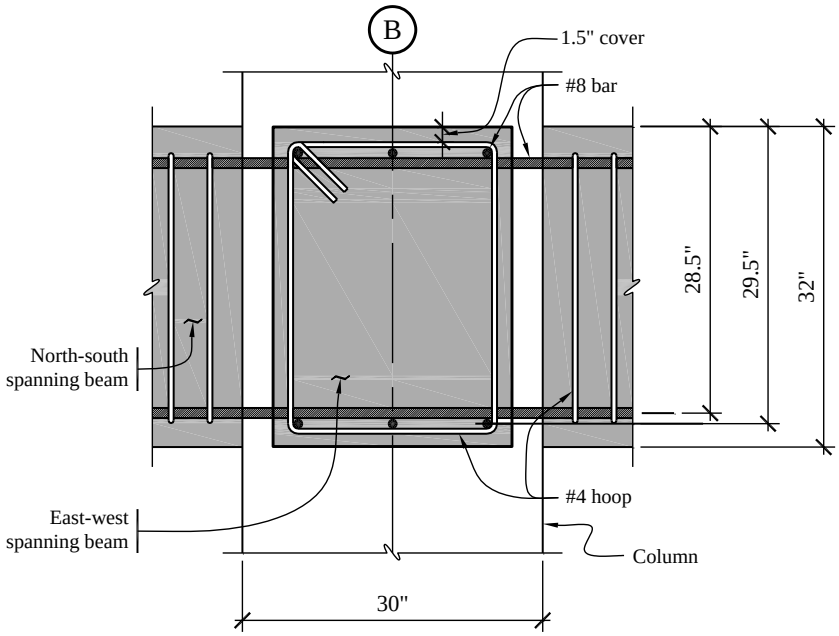

Figure 7-10 Layout for beam reinforcement
(1.0 ft = 0.3048 m, 1.0 in. = 25.4 mm)

Given Figure 7-10, compute the effective depth for both positive and negative moment as follows:

Beams spanning in the E-W direction, d = 32 - 1.5 - 0.5 - 1.00/2 = 29.5 inches

Beams spanning in the N-S direction, d = 32 - 1.5 - 0.5 - 1.0 - 1.00/2 = 28.5 inches

For negative moment bending, the effective width is 24 inches for all beams. For positive moment, the slab is in compression and the effective T-beam width varies according to ACI 318 Section 8.12. The effective widths for positive moment are as follows (with the parameter controlling effective width shown in parentheses):

20-foot beams in Frames 1 and 8: b = 24 + 20(12)/12 = 44 inches (span length)

20-foot beams in Frames 2 and 7: b = 20(12)/4 = 60 inches (span length)

40-foot beams in Frames 2 through 7: b = 24 + 2[8(4)] = 88 inches (slab thickness)

30-foot beams in Frames A and D: b = 24 + [6(4)] = 48 inches (slab thickness)

30-foot beams in Frames B and C: b = 24 + 2[8(4)] = 88 inches (slab thickness)

ACI 318 Section 21.5.2 controls the longitudinal reinforcement requirements for beams. The minimum reinforcement to be provided at the top and bottom of any section is as follows:

$$A_{s,min} = \frac{200 b_w d}{f_y} = \frac{200(24)(29.5)}{60,000} = 2.36 \text{ in}^2$$

This amount of reinforcement can be supplied by three #8 bars with $A_s = 2.37$ in^2. Since the three #8 bars will be provided continuously top and bottom, reinforcement required for strength will include these #8 bars.

Before getting too far into member design, it is useful to check the required tension development length for hooked bars since the required length may control the dimensions of the exterior columns and the boundary elements of the structural walls.

From Equation 21-6 of ACI 318 Section 21.7.5.1, the required development length is as follows:

$$l_{dh} = \frac{f_y d_b}{65\sqrt{f_c'}}$$

For normal-weight (NW) concrete, the computed length cannot be less than 6 inches or $8d_b$.

For straight typical bars, $l_d = 2.5l_{dh}$ and for straight "top" bars, $l_d = 3.25l_{dh}$ (ACI 318 Sec. 21.7.5.2). These values are applicable only where the bars are anchored in well-confined concrete (e.g., column cores and plastic hinge regions with confining reinforcement). The development length for the portion of the bar extending into unconfined concrete must be increased by a factor of 1.6 per ACI 318 Section 12.7.5.3. Development length requirements for hooked and straight bars are summarized in Table 7-15.

Where hooked bars are used, the hook must be 90 degrees and be located within the confined core of the column or boundary element. For bars hooked into 30-inch-square columns with 1.5 inches of cover and #4 ties, the available development length is 30 - 1.50 - 0.5 = 28.0 inches. With this amount of available length, there will be no problem developing hooked bars in the columns.

Table 7-15 is applicable to bars anchored in joint regions only. For development of bars outside of joint regions, ACI 318 Chapter 12 should be used.

Table 7-15 Tension Development Length Requirements for Hooked Bars and Straight Bars in 5,000 psi NW Concrete

Bar Size	d_b (in)	l_{dh} hook (in)	l_d typ (in)	l_d top (in)
#4	0.500	6.5	16.3	21.2
#5	0.625	8.2	20.4	26.5
#6	0.750	9.8	24.5	31.8
#7	0.875	11.4	28.6	37.1
#8	1.000	13.1	32.6	42.4
#9	1.128	14.7	36.8	47.9
#10	1.270	16.6	41.4	53.9
#11	1.410	18.4	46.0	59.8

(1.0 in = 25.4 mm)

Another requirement to consider prior to establishing column sizes is ACI 381 Section 21.7.2.3 which sets a minimum ratio of 20 for the column width to the diameter of the largest longitudinal beam bar passing through the joint. This requirement is easily satisfied for the 30-inch columns in this example.

7.4.2.2 Design of Representative Frame 1 Beams. The preliminary design of the beams of Frame 1 was based on members with a depth of 32 inches and a width of 24 inches. The effective depth for positive and negative bending is 29.5 inches and the effective widths for positive and negative bending are 44 and 24 inches, respectively. This assumes the stress block in compression is less than the 4.0-inch flange thickness.

The layout of the geometry and gravity loading on the three eastern-most spans of Level 7 of Frame 1 as well as the unfactored gravity and seismic moments are illustrated in Figure 7-11. The seismic and gravity moments are taken directly from the ETABS program output. The seismic forces are from the E-W spectral load case plus the controlling accidental torsion case (the torsional moment where translation and torsion are additive). Note that all negative moments are given at the face of the column and that seismic moments are considerably greater than those due to gravity.

Factored bending moment envelopes for all five spans are shown in Figure 7-11. Negative moment at the supports is controlled by the 1.42*D* + 0.5*L* + 1.0*E* load combination and positive moment at the support is controlled by 0.68*D* - 1.0*E*. Mid-span positive moments are based on the load combination 1.2*D* + 1.6*L*.

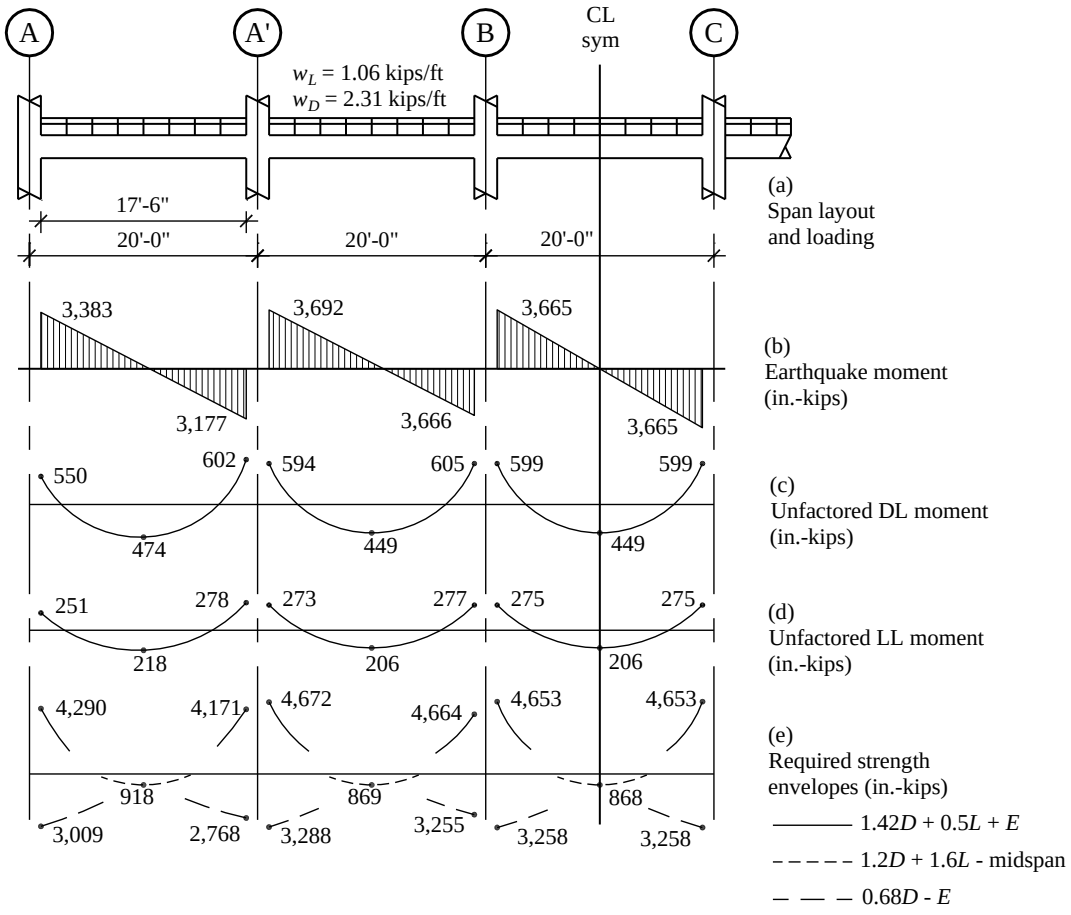

Figure 7-11 Bending moments for Frame 1
(1.0 ft = 0.3048 m, 1.0 in-kip = 0.113 kN-m)

7.4.2.2.1 Longitudinal Reinforcement. The design process for determining longitudinal reinforcement is illustrated as follows for Span A-A'.

1. Design for Negative Moment at the Face of the Exterior Support (Grid A):

   M_u = 1.42(-550) + 0.5(-251) + 1.0(-3,383) = -4,290 inch-kips

   Try one #8 bar in addition to the three #8 bars required for minimum steel:

   A_s = 4(0.79) = 3.16 in^2
   f_c' = 5,000 psi
   f_y = 60 ksi
   Width b for negative moment = 24 inches
   d = 29.5 in.
   Depth of compression block, $a = A_s f_y / 0.85 f_c' b$
   a = 3.16 (60)/[0.85 (5) 24] = 1.86 inches
   Design strength, $\phi \quad M_n = \phi \quad A_s f_y (d - a/2)$
   $\phi \quad M_n$ = 0.9(3.16)60(29.5 – 1.86/2) = 4,875 inch-kips > 4,290 inch-kips OK

2. Design for Positive Moment at Face of Exterior Support (Grid A):

   M_u = [-0.68(550)] + [1.0(3,383)] = 3,008 inch-kips

   Try the three #8 bars required for minimum steel:

   A_s = [3(0.79)] = 2.37 in ^{2}
   Width b for positive moment = 44 inches
   d = 29.5 inches
   a = [2.37(60)]/[0.85(5)44] = 0.76 inch
   $\phi \quad M_n$ = 0.9(2.37) 60(29.5 – 0.76/2) = 3,727 inch-kips > 3,008 inch-kips OK

3. Positive Moment at Midspan:

   M_u = [1.2(474)] + [1.6(218)] = 918.1 inch-kips

   Minimum reinforcement (three #8 bars) controls by inspection.

4. Design for Negative Moment at the Face of the Interior Support (Grid A'):

   M_u = 1.42(-602) + 0.5(-278) + 1.0(-3,177) = -4,172 inch-kips

   Try one #8 bars in addition to the three #8 bars required for minimum steel:

   $\phi \quad M_n$ = 4,875 inch-kips > 4,172 inch-kips OK

5. Design for Positive Moment at Face of Interior Support (Grid A'):

   M_u = [-0.68(602)] + [1.0(3,177)] = 2,767 inch-kips

   Three #8 bars similar to the exterior support location are adequate by inspection.

Similar calculations can be made for the Spans A'-B and B-C and then the remaining two spans are acceptable via symmetry. A summary of the preliminary flexural reinforcing is shown in Table 7-16.

In addition to the computed strength requirements and minimum reinforcement ratios cited above, the final layout of reinforcing steel also must satisfy the following from ACI 318 Section 21.5.2:

Minimum of two bars continuous top and bottom	OK (three #8 bars continuous top and bottom)
Positive moment strength greater than 50 percent negative moment strength at a joint	OK (at all joints)
Minimum strength along member greater than 0.25 maximum strength	OK (A_s provided = three #8 bars is more than 25 percent of reinforcement provided at joints)

The preliminary layout of reinforcement is shown in Figure 7-12. The arrangement of bars is based on the above computations and Table 7-16 summary of the other spans. Note that a slightly smaller amount of reinforcing could be used at the top of the exterior spans, but #8 bars are selected for consistency. In addition, the designer could opt to use four #8 bars continuous throughout the span for uniformity and ease of placement.

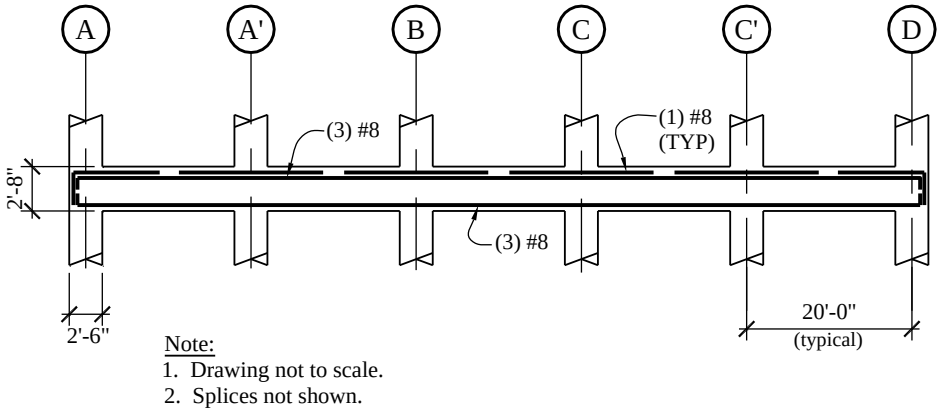

Figure 7-12 Preliminary rebar layout for Frame 1
(1.0 ft = 03.048 m)

As mentioned above, later phases of the frame design will require computation of the design strength and the maximum probable strength at each support. The results of these calculations are shown in Table 7-16.

Table 7-16 Design and Maximum Probable Flexural Strength For Beams in Frame 1

	Item	Location*					
		A	A'	B	C	C'	D
Negative Moment	Moment Demand (inch-kips)	4,290	4,672	4,664	4,664	4,672	4,290
	Reinforcement	four #8	four #8	four #8	four #8	four #8	four #8
	Design Strength (inch-kips)	4,875	4,875	4,875	4,875	4,875	4,875
	Probable Strength (inch-kips)	7,042	7,042	7,042	7,042	7,042	7,042
Positive Moment	Moment Demand (inch-kips)	3,009	3,288	3,255	3,255	3,289	3,009
	Reinforcement	three #8	three #8	three #8	three #8	three #8	three #8
	Design Strength (inch-kips)	3,727	3,727	3,727	3,727	3,727	3,727
	Probable Strength (inch-kips)	5,159	5,159	5,159	5,159	5,159	5,159

*Moment demand is taken as the larger of the beam moments on each side of the column.
(1.0 in-kip = 0.113 kN-m)

As an example of computation of probable strength, consider the case of four #8 top bars plus the portion of slab reinforcing within the effective beam flange width computed above, which is assumed to be 0.002(4 inches)(44-24)=0.16 square inches. (The slab reinforcing, which is not part of this example, is assumed to be 0.002 for minimum steel.)

A_s = 4(0.79) + 0.16 = 3.32 in^2
Width b for negative moment = 24 inches
d = 29.5 inches
Depth of compression block, $a = A_s(1.25f_y)/0.85f_c'b$
a = 3.32(1.25)60/[0.85(4)24] = 2.44 inches
$M_{pr} = 1.0A_s(1.25f_y)(d - a/2)$
M_{pr} = 1.0(3.32)1.25(60)(29.6 – 2.44/2) = 7,042 inch-kips

For the case of three #8 bottom bars:

A_s = 3(0.79) = 2.37 in^2
Width b for positive moment = 44 inches
d = 29.5 inches
a = 2.37(1.25)60/[0.85(5)44] = 0.95 inch
M_{pr} = 1.0(2.37)1.25(60)(29.5 – 0.95/2) = 5,159 inch-kips

At this point in the design process, the layout of reinforcement has been considered preliminary because the quantity of reinforcement placed in the beams has a direct impact on the magnitude of the stresses developed in the beam-column joint. If the computed joint stresses are too high, the only remedies are increasing the concrete strength, increasing the column area, changing the reinforcement layout, or

increasing the beam depth. The complete check of the beam-column joint is illustrated in Section 7.4.2.3 below, but preliminary calculations indicate that the joint is adequate, so the design can progress based on the reinforcing provided.

Because the arrangement of steel is acceptable from a joint strength perspective, the cutoff locations of the various bars may be determined (see Figure 7-12 for a schematic of the arrangement of reinforcement). The three #8 bars (top and bottom) required for minimum reinforcement are supplied in one length that runs continuously across the two end spans and are spliced in the center span. An additional #8 top bar is placed at each column.

To determine where added top bars should be cut off in each span, it is assumed that theoretical cutoff locations correspond to the point where the continuous top bars develop their design flexural strength. Cutoff locations are based on the members developing their design flexural capacities (f_y = 60 ksi and ϕ = 0.9). Using calculations similar to those above, it has been determined that the design flexural strength supplied by a section with only three #8 bars is 3,686 inch-kips for negative moment.

Sample cutoff calculations are given for Span B-C. To determine the cutoff location for negative moment, both the additive and counteractive load combinations must be checked to determine the maximum required cutoff length. In this case, the $1.42D + 0.5L \pm Q_E$ load combination governs. Loading diagrams for determining cutoff locations are shown in Figure 7-13.

For negative moment cutoff locations, refer to Figure 7-14, which is a free body diagram of the left end of the member in Figure 7-13. Since the goal is to develop a negative moment capacity of 3,686 inch-kips in the continuous #8 bars, summing moments about Point A in Figure 7-14 can be used to determine the location of this moment demand. The moment summation is as follows:

$$4{,}653 + \frac{0.318x^2}{2} - 68.2x = 3{,}686$$

In the above equation, 4,653 (inch-kips) is the negative moment demand at the face of column, 0.318 (kips/inch) is the factored gravity load, 68.2 kips is the end shear and 3,686 inch-kips is the design strength of the section with three #8 bars. Solving the quadratic equation results in x = 14.7 inches. ACI 318 Section 12.10.3 requires an additional length equal to the effective depth of the member or 12 bar diameters (whichever is larger). Consequently, the total length of the bar beyond the face of the support is 14.7 + 29.5 = 44.2 inches and a 3'-9" extension beyond the face of the column could be used at this location. Similar calculations should be made for the other beam ends.

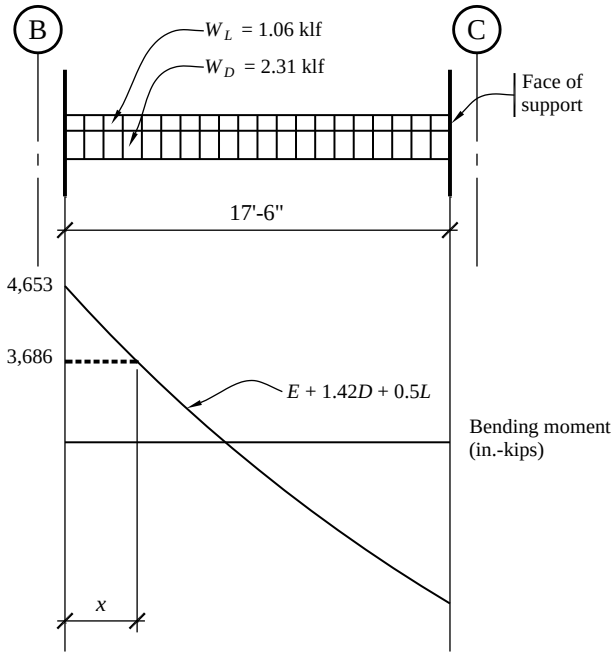

Figure 7-13 Loading for determination of rebar cutoffs
(1.0 ft = 0.3048 m, 1.0 klf = 14.6 kN/m, 1.0 in-kip = 0.113 kN-m)

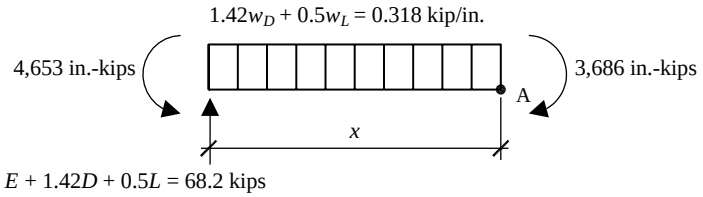

Figure 7-14 Free body diagram
(1.0 kip = 4.45kN, 1.0 klf = 14.6 kN/m, 1.0 in-kip = 0.113 kN-m)

As shown in Figure 7-15, another requirement in setting cutoff length is that the bar being cut off must have sufficient length to develop the strength required in the adjacent span. From Table 7-15, the required development length of the #8 top bars in tension is 42.4 inches if the bar is anchored in a confined joint region. The confined length in which the bar is developed is shown in Figure 7-15 and consists of the column depth plus twice the depth of the beam (the length for beam hoops per ACI 318 Section 21.5.3.1). This length is 30 + 32 + 32 = 94 inches, which is greater than the 42.4 inches required. The column and beam are considered confined because of the presence of closed hoop reinforcement as required by ACI 318 Sections 21.5.3 and 21.6.4.

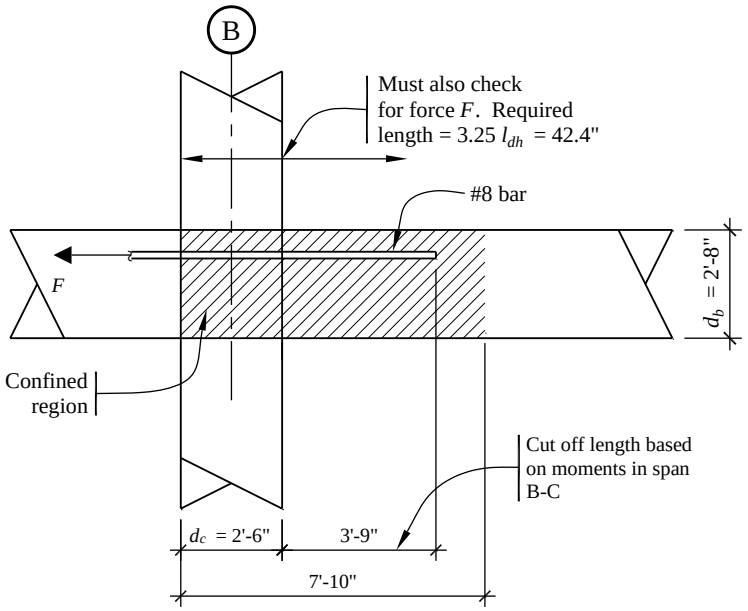

Figure 7-15 Development length for top bars
(1.0 ft = 0.3048 m, 1.0 in. = 25.4 mm)

The continuous top bars are spliced at the center of Span B-C and the bottom bars at Spans A'-B and C-C' as shown in Figure 7-16. The splice length is taken as Class B splice length for #8 bars. These splice locations satisfy the requirements of ACI 318 Section 21.5.2.3 for permitted splice locations.

The splice length is determined in accordance with ACI 318 Section 12.15, which indicates that the splice length is 1.3 times the development length. From ACI 318 Section 12.2.2, the development length, l_d, is computed as:

$$l_d = \left(\frac{3}{40} \frac{f_y}{\lambda \sqrt{f_c'}} \frac{\psi_t \psi_e \psi_s}{\left(\frac{c_b + K_{tr}}{d_b} \right)} \right) d_b$$

using ψ_t = 1.3 (top bar), ψ_e =1.0 (uncoated), ψ_s = 1.0 (#8 bar), λ = 1.0 (NW concrete) and taking ($c + K_{tr}$) / d_b as 2.5 (based on clear cover and confinement), the development length for one #8 top bar is:

$$l_d = \left(\frac{3}{40} \left(\frac{60{,}000}{(1.0)\sqrt{5{,}000}} \right) \frac{(1.3)(1.0)(1.0)}{(2.5)} \right) (1.0) = 33.1 \text{ inches}$$

The splice length = 1.3(33.1) = 43 inches. Therefore, use a 43-inch contact splice for the top bars. Computed in a similar manner, the required splice length for the #8 bottom bars is 34 inches. According to ACI 318 Section 21.5.2.3, the entire region of the splice must be confined by closed hoops spaced at the smaller of d/4 or 4 inches.

The final bar placement and cutoff locations for all five spans are shown in Figure 7-16.

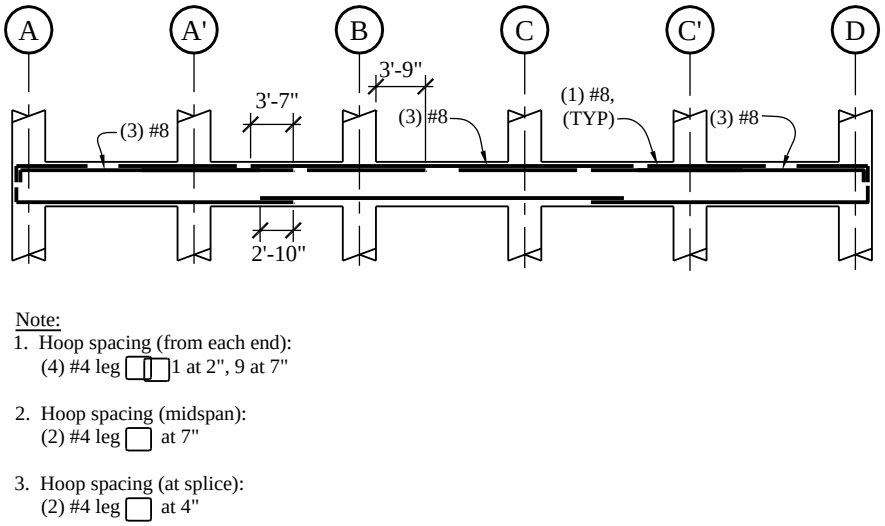

Figure 7-16 Final bar arrangement
(1.0 ft = 0.3048 m, 1.0 in. = 25.4 mm)

7.4.2.2.2 Transverse Reinforcement. The requirements for transverse reinforcement in special moment frame beams, include shear strength requirements (ACI 318 Sec. 21.5.4) covered here first and then detailing requirements (ACI 318 Sec. 21.5.3).

To avoid nonductile shear failures, the shear strength demand is computed as the sum of the factored gravity shear plus the maximum earthquake shear. The maximum earthquake shear is computed based on the maximum probable beam moments described and computed previously. The probable moment strength at each support is shown in Table 7-16.

Figure 7-17 illustrates the development of the design shear strength envelopes for Spans A-A', A'-B and B-C. In Figure 7-17a, the maximum probable earthquake moments are shown for seismic forces acting to the east (solid lines) and to the west (dashed lines). The moments shown occur at the face of the supports.

The earthquake shears produced by the maximum probable moments are shown in Figure 7-17b. For Span B-C, the values shown in the figure are:

$$V_E = \frac{M_{pr}^{-} + M_{pr}^{+}}{l_{clear}}$$

where l_{clear} = 17 feet-6 inches = 210 inches

Note that the magnitude of the earthquake shear can vary with direction (if the beam moment capacities are different at each end). However, in this case the shears are the same in both directions and are computed as:

V_E = (7,042 + 5,159) / 210 = 58.1 kips

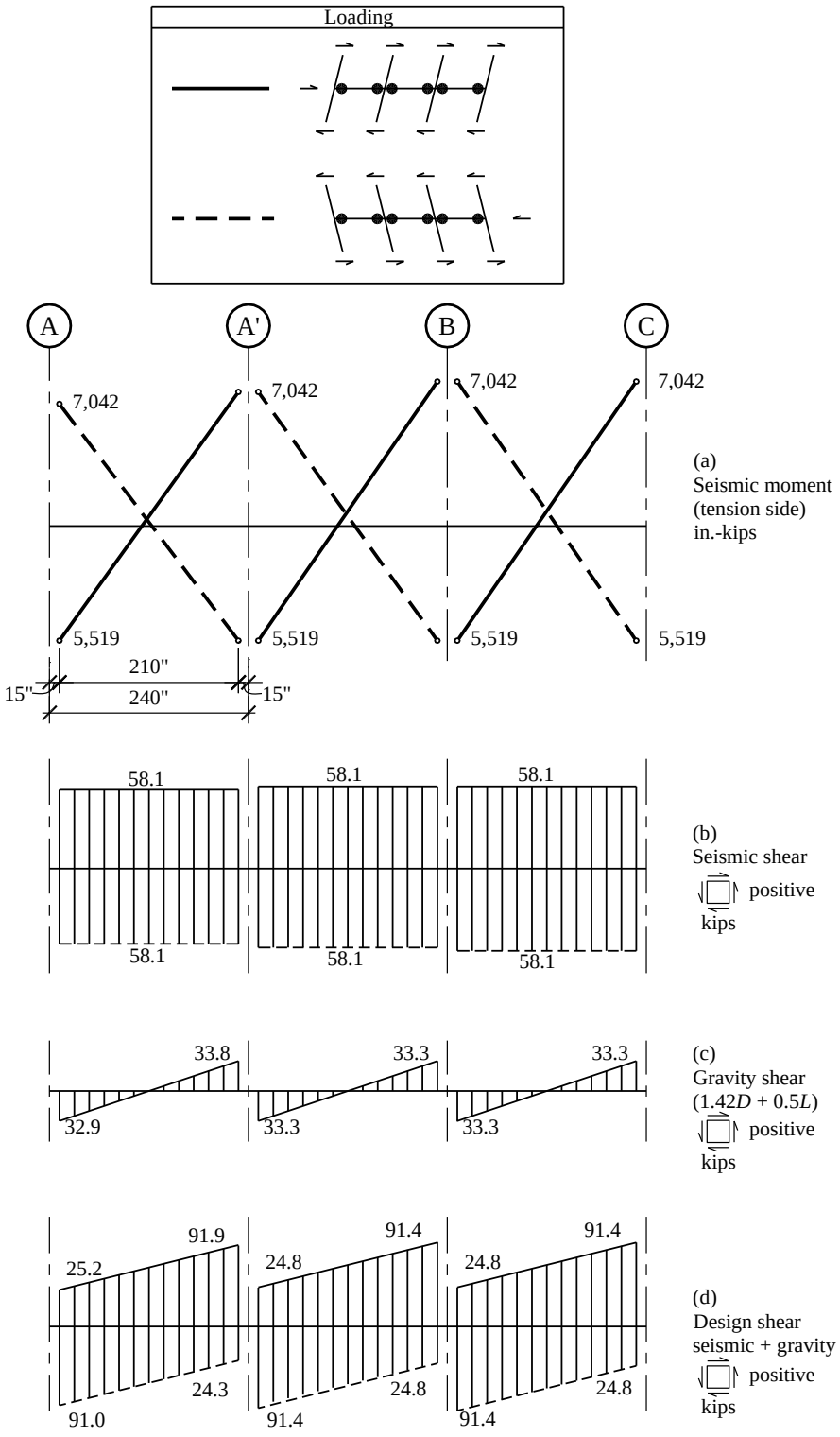

Figure 7-17 Shear forces for transverse reinforcement
(1.0 in. = 25.4 mm, 1.0 kip = 4.45kN, 1.0 in-kip = 0.113 kN-m)

The gravity shears shown in Figure 7-17c are taken from the ETABS model:

Factored gravity shear = $V_G = 1.42V_{dead} + 0.5V_{live}$
V_{dead} = 20.2 kips
V_{live} = 9.3 kips
$V_G = 1.42(20.2) + 0.5(9.3) = 33.3$ kips

Total design shears for each span are shown in Figure 7-17d. The strength envelope for Span B-C is shown in detail in Figure 7-18, which indicates that the maximum design shears is 58.1 + 33.3 = 91.4 kips. While this shear acts at one end, a shear of 58.1 – 33.3 = 24.8 kips acts at the opposite end of the member. In the figure the sloping lines indicate the shear demands along the beam and the horizontal lines indicate the shear capacities at the end and center locations.

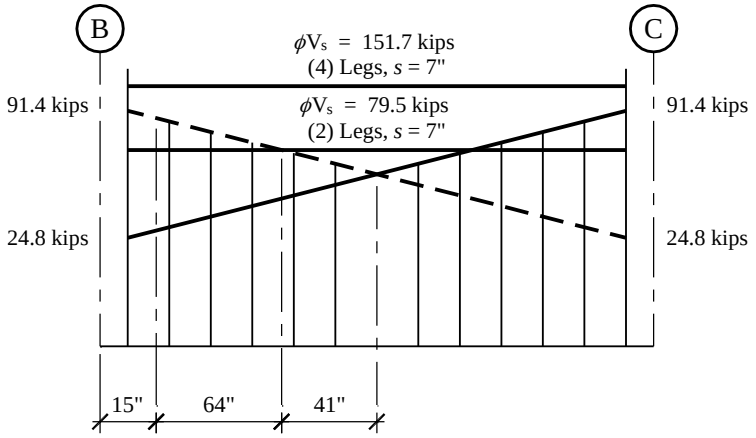

Figure 7-18 Detailed shear force envelope in Span B-C
(1.0 in. = 25.4 mm, 1.0 kip = 4.45kN)

In designing shear reinforcement, the shear strength can consist of contributions from concrete and from steel hoops or stirrups. However, according to ACI 318 Section 21.5.4.2, the design shear strength of the concrete must be taken as zero where the axial force is small ($P_u/A_g f'_c < 0.05$) and the ratio V_E/V_u is greater than 0.5. From Figure 7-17, this ratio is $V_E/V_u = 58.1/91.4 = 0.64$, so concrete shear strength must be taken as zero.

Compute the required shear strength provided by reinforcing steel at the face of the support:

$V_u = \phi \quad V_s = 91.4$ kips
$V_s = A_v f_y d/s$

For reasons discussed below, assume four #4 vertical legs ($A_v = 0.8$ in^2), $f_y = 60$ ksi and $d = 29.5$ inches and compute the required spacing as follows:

$s = \phi \quad A_v f_y d/V_u = 0.75[4(0.2)](60)(29.5/91.4) = 11.6$ inches

At midspan, the design shear V_u = (91.4 + 24.8)/2 = 58.1 kips, which is the same as the earthquake shear since gravity shear is nominally zero. Compute the required spacing assuming two #4 vertical legs:

s = 0.75[2(0.2)](60)(29.5/58.1) = 9.13 inches

In terms of detailing requirements, ACI 318 Section 21.5.3.1 states that closed hoops at a tighter spacing are required over a distance of twice the member depth from the face of the support and ACI 318 Section 21.5.3.4 indicates that stirrups are permitted away from the ends.

Therefore, the shear strength requirements at this transition point should be computed. At a point equal to twice the beam depth, or 64 inches from the support, the shear is computed as:

V_u = 91.4 - (64/210)(91.4 – 24.8) = 71.1 kips

Compute the required spacing assuming two #4 vertical legs:

s = 0.75[2(0.2)](60)(29.5/71.1) = 7.4 inches

Before the final layout can be determined, the detailing requirements need to be considered. The first hoop must be placed 2 inches from the face of the support and the maximum hoop spacing at the beam ends is per ACI 318 Section 21.5.3.2 as follows:

d/4 = 29.5/4 = 7.4 inches
$8d_b$ = 8(1.0) = 8.0 inches
$24d_h$ = 24(0.5) = 12.0 inches

Outside of the region at the beam ends, ACI 318 Section 21.5.3.4 permits stirrups with seismic hooks to be spaced at a maximum of d/2.

Therefore, at the beam ends, overlapped close hoops with four legs will be spaced at 7 inches and in the middle, closed hoops with two legs will be spaced at 7 inches. This satisfies both the strength and detailing requirements and results in a fairly simple pattern. Note that hoops are being used along the entire member length. This is being done because the earthquake shear is a large portion of the total shear, the beam is relatively short and the economic premium is negligible.

This arrangement of hoops will be used for Spans A-A', B-C and C'-D. In Spans A'-B and C-C', the bottom flexural reinforcement is spliced and hoops must be placed over the splice region at d/4 or a maximum of 4 inches on center per ACI 318 Section 21.5.2.3.

One additional requirement at the beam ends is that where hoops are required (the first 64 inches from the face of support), longitudinal reinforcing bars must be supported as specified in ACI 318 Section 7.10.5.3 as required by ACI 318 Section 21.5.3.3. Hoops should be arranged such that every corner and alternate longitudinal bar is supported by a corner of the hoop assembly and no bar should be more than 6 inches clear from such a supported bar. This will require overlapping hoops with four vertical legs as assumed previously. Details of the transverse reinforcement layout for all spans of Level 5 of Frame 1 are shown in Figure 7-16.

7.4.2.3 Check Beam-Column Joint at Frame 1. Prior to this point in the design process, preliminary calculations were used to check the beam-column joint, since the shear force developed in the beam-column joint is a direct function of the beam longitudinal reinforcement. These calculations are often done early in the design process because if the computed joint shear is too high, the only remedies are

increasing the concrete strength, increasing the column area, changing the reinforcement layout, or increasing the beam depth. At this point in the design, the joint shear is checked for the final layout of beam reinforcing.

The design of the beam-column joint is based on the requirements of ACI 318 Section 21.7. While ACI 318 provides requirements for joint shear strength, it does not specify how to determine the joint shear demand, other than to indicate that the joint forces are computed using the probable moment strength of the beam (ACI 318 Sec. 21.7.2.1). This example utilizes the procedure for determining joint shear demand contained in Moehle. The shear in the joint is a function of the shear in the column and the tension/compression couple contributed by the beam moments. The method for determining column shear is illustrated in Figure 7-19. In this free-body diagram, the column shear, V_{col}, is determined from equilibrium as follows:

$$V_{col} = \frac{\left[\left(M_{pr,L} + M_{pr,R}\right) + \left(V_{e,L} + V_{e,R}\right)\frac{h}{2}\right]}{l_c}$$

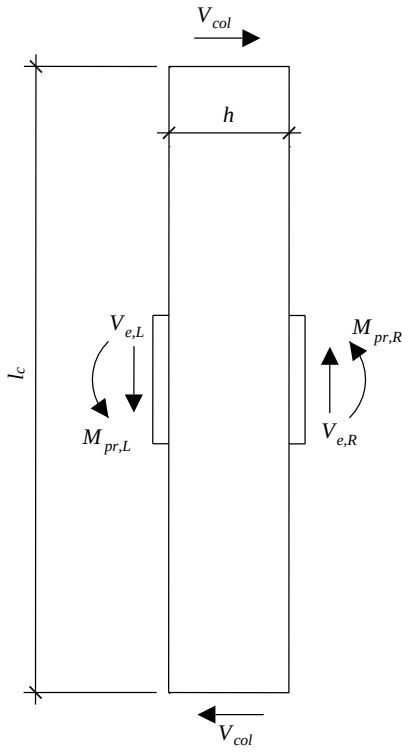

Figure 7-19 Column shear free body diagram

The determination of the forces in the joint of the column on Grid C of Frame 1 is based on Figure 7-16a, which shows how plastic moments are developed in the various spans for equivalent lateral forces acting to the east. An isolated sub-assemblage from the frame showing moments is shown in Figures 7-20b. The beam shears shown in Figure 7-20c are based on the probable moment strengths shown in Table 7-16.

For forces acting from west to east, compute the earthquake shear in Span B-C as follows:

$V_E = (M_{pr}^- + M_{pr}^+)/l_{clear} = (7{,}042 + 5{,}159)/(240 - 30) = 58.1$ kips

For Span C-C', the earthquake shear is the same since the probable moments are equal and opposite.

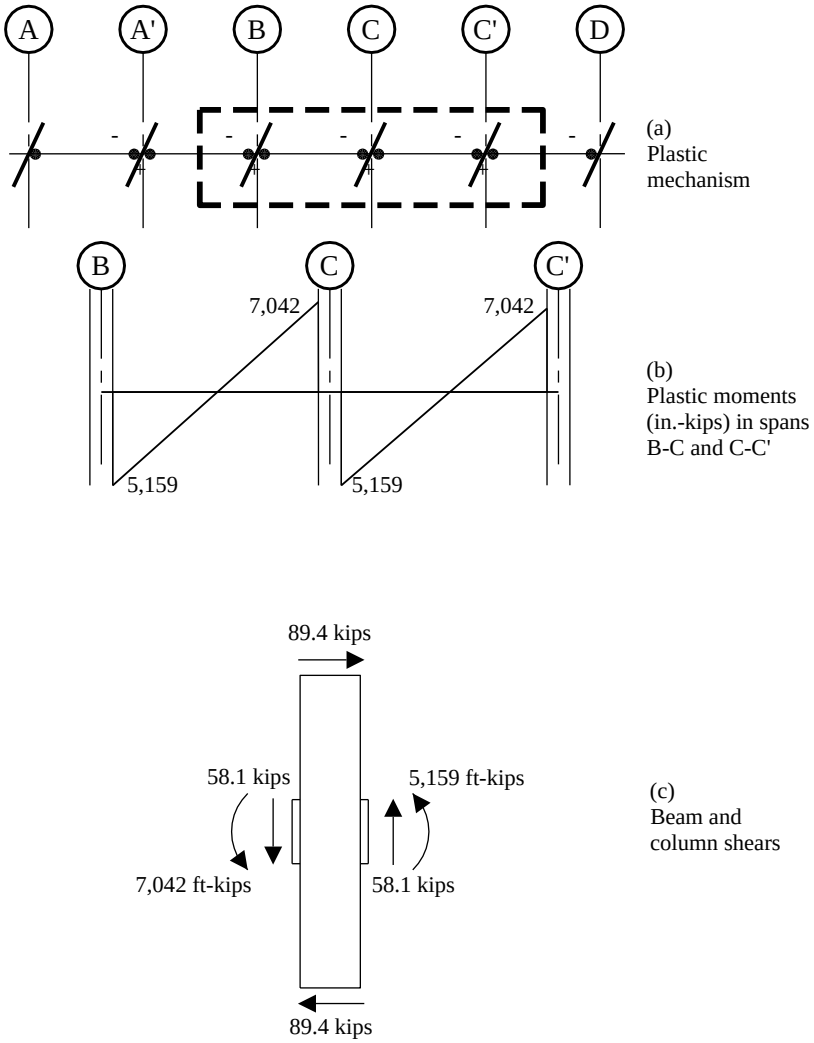

Figure 7-20 Diagram for computing column shears
(1.0 ft = 0.3048 m, 1.0 kip = 4.45kN, 1.0 in-kip = 0.113 kN-m)

With h = 30 inches and l_c = 156 inches, the column shear is computed as follows:

$$V_{col} = \frac{\left[(7{,}042 + 5{,}159) + (58.1 + 58.1)\frac{30}{2}\right]}{156} = 89.4 \text{ kips}$$

With equal spans, gravity loads do not produce significant column shears, except at the end column, where the seismic shear is much less. Therefore, gravity loads are not included in this computation.

The forces in the beam reinforcement for negative moment are based on four #8 bars at 1.25 f_y:

$T = C = 1.25(60)[(4(0.79)] = 237.0$ kips

For positive moment, three #8 bars also are used, assuming $C = T$, C = 177.8 kips.

As illustrated in Figure 7-21, the joint shear force V_j is computed as follows:

$V_j = T + C - V_{col}$
$= 237.0 + 177.8 - 89.4$
$= 325.4$ kips

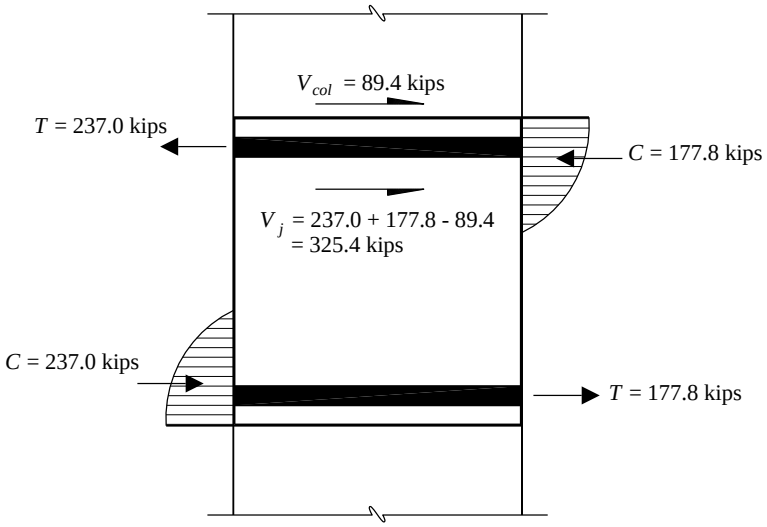

Figure 7-21 Computing joint shear stress (1.0 kip = 4.45kN)

For joints confined on three faces or on two opposite faces, the nominal shear strength is based on ACI 318 Section 21.7.4 as follows:

$$V_n = 15\sqrt{f_c'}A_j = 15\sqrt{5{,}000}(30)^2 = 954.6 \text{ kips}$$

For joints of special moment frames, ACI 318 Section 9.3.4 permits ϕ = 0.85, so ϕV_n = 0.85(954.6 kips) = 811.4 kips, which exceeds the computed joint shear, so the joint is acceptable. Joint stresses would be checked for the other columns in a similar manner.

ACI 318 Section 21.7.3.1 specifies the amount of transverse reinforcement required in the joint. Since the joint is not confined on all four sides by a beam, the total amount of transverse reinforcement required by ACI 318 Section 21.6.4.4 will be placed within the depth of the joint. As shown later, this reinforcement consists of four-leg #4 hoops at 4 inches on center.

7.4.2.4 Design of a Typical Interior Column of Frame 1. This section illustrates the design of a typical interior column on Gridline A'. The column, which supports Level 7 of Frame 1, is 30 inches square and is constructed from 5,000 psi concrete and 60 ksi reinforcing steel. An isolated view of the column is shown in Figure 7-22. The flexural reinforcement in the beams framing into the column is shown in Figure 7-16. Using simple tributary area calculations (not shown), the column supports an unfactored axial dead load of 367 kips and an unfactored axial reduced live load of 78 kips. The ETABS analysis indicates that the maximum axial earthquake force is 33.7 kips, tension or compression. The load combination used to compute this force consists of the full earthquake force in the E-W direction plus amplified accidental torsion. Since this column is not part of a N-S moment frame, orthogonal effects need not be considered per *Standard* Section 12.5.4. Hence, the column is designed for axial force plus uniaxial bending.

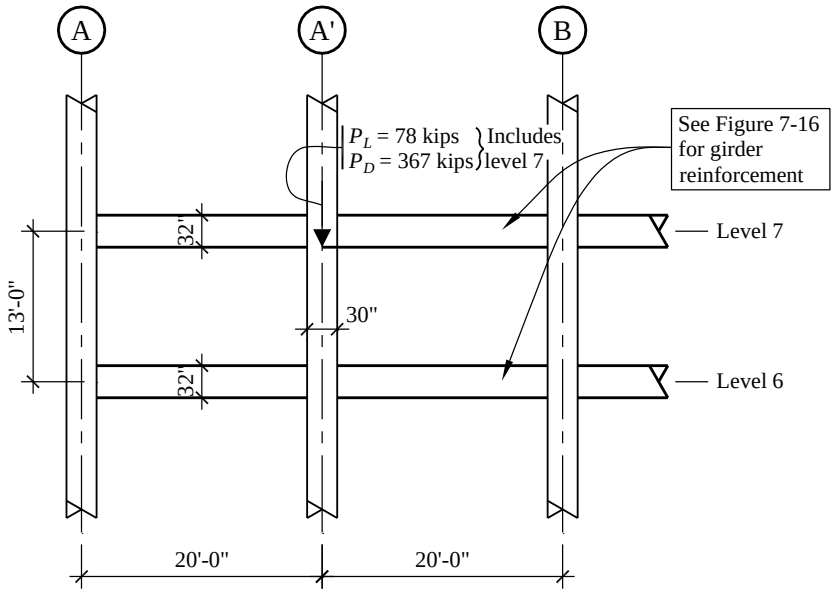

Figure 7-22 Layout and loads on column of Frame A'
(1.0 ft = 0.3048 m, 1.0 in. = 25.4 mm, 1.0 kip = 4.45kN)

7.4.5.3.1 Longitudinal Reinforcement. To determine the axial design loads, use the controlling basic load combinations:

1.42*D* + 0.5*L* + 1.0E

0.68*D* - 1.0*E*

The combination that results in maximum compression is:

P_u = 1.42(367.2) + 0.5(78.0) + 1.0(33.7) = 595 kips (compression)

The combination for minimum compression (or tension) is:

P_u = 0.68(367.2) - 1.0(33.7) = 216 kips (compression)

The maximum axial compression force of 595 kips is greater than $0.1f_c'A_g = 0.1(5)(30^2) = 450$ kips, so the design is based on ACI 318 Section 21.6 for columns (see ACI 318 Sec. 21.6.1). According to ACI 318 Section 21.6.2, the sum of nominal column flexural strengths at the joint must be at least 6/5 of the sum of nominal flexural strength of the beams framing into the column. Beam moments at the face of the support are used for this computation. These capacities are provided in Table 7-16.

Nominal (negative) moment strength at end A' of Span A-A' = 4,875/0.9 = 5,417 inch-kips

Nominal (positive) moment strength at end A' of Span A' B = 3,727/0.9 = 4,141 inch-kips

Sum of beam moment at the joint = 5,417 + 4,141 = 9,558 inch-kips

Required sum of column design moments = 6/5 × 9,558 = 11,469 inch-kips.

Individual column design moment = 11,469/2 = 5,735 inch-kips

Knowing the factored axial load and the required design flexural strength, a column with adequate capacity must be selected. Figure 7-23 shows a P-M interaction curve for a 30- by 30-inch column with longitudinal reinforcing consisting of twelve #8 bars (1.05 percent steel). Computed using PCA Column, the curve is based on a ϕ factor of 1.0 as required for nominal strength. At axial forces of 595 kips and 216 kips, solid horizontal lines are drawn. The dots on the lines represent the required average nominal flexural strength (5,735 inch-kips) at each axial load level. These dots must lie to the left of the curve representing the nominal column strengths. Since the dots are within the capacity curve for both design and nominal moments strengths at both the minimum and maximum axial forces, this column design is clearly adequate.

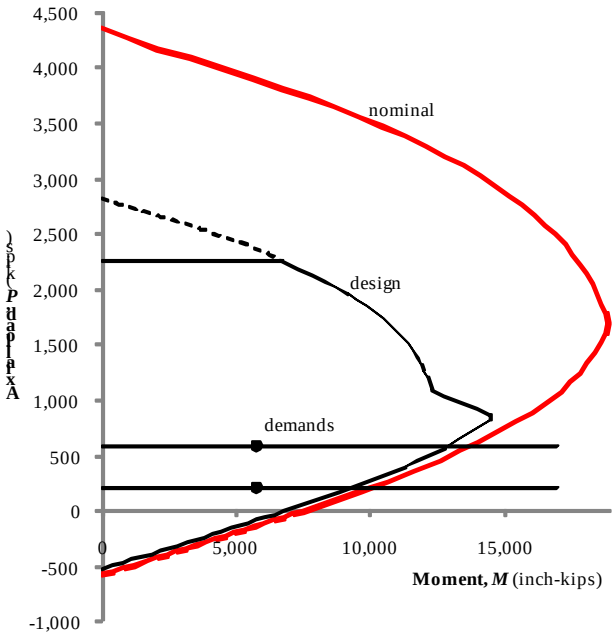

Figure 7-23 Design interaction diagram for column on Gridline A'
(1.0 kip = 4.45kN, 1.0 ft-kip = 1.36 kN-m)

7.4.2.4.2 Transverse Reinforcement. The design of transverse reinforcement for columns of special moment frames must consider confinement requirements (ACI 318 Sec. 21.6.4) and shear strength requirements (ACI 318 Sec. 21.6.5). The confinement requirements are typically determined first.

Based on ACI 318 Section 21.6.4.1, tighter spacing of confinement is generally required at the ends of the columns, over a distance, l_o, equal to the larger of the following:

Column depth = 30 inches
One-sixth of the clear span = (156-32)/6 = 20.7 inches
18 inches

There are both spacing and quantity requirements for the reinforcement. ACI 318 Section 21.6.4.3 specifies the spacing as the minimum of the following:

One-fourth the minimum column dimension = 30/4=7.5 inches

Six longitudinal bar diameters = 6(1.0) = 6.0 inches

Dimension $s_o = 4 + (14 - h_x) / 3$, where s_o is between 4 inches and 6 inches and h_x is the maximum horizontal spacing of hoops or cross ties.

For the column with twelve #8 bars and #4 hoops and cross ties, $h_x = 8.833$ inches and $s_o = 5.72$ inches, which controls the spacing requirement.

ACI 318 Section 21.6.4.4 gives the requirements for minimum transverse reinforcement in terms of cross sectional area. For rectangular sections with hoops, ACI 318 Equations 21-4 and 21-5 are applicable:

$$A_{sh} = 0.3\left(\frac{sb_c f'_c}{f_{yt}}\right)\left(\frac{A_g}{A_{ch}} - 1\right)$$

$$A_{sh} = 0.09\left(\frac{sb_c f'_c}{f_{yt}}\right)$$

The first of these equations controls when $A_g/A_{ch} > 1.3$. For the 30- by 30-inch columns:

$A_{ch} = (30 - 1.5 - 1.5)^2 = 729$ in^2
$A_g = 30\ (30) = 900$ in^2
$A_g/A_{ch} = 900/729 = 1.24$

Therefore, ACI 318 Equation 21-5 controls. Try hoops with four #4 legs:

$b_c = 30 - 1.5 - 1.5 = 27.0$ inches
$s = [4\ (0.2)(60{,}000)]/[0.09\ (27.0)(5{,}000)] = 3.95$ inches

This spacing controls the design, so hoops consisting of four #4 bars spaced at 4 inches will be considered acceptable.

ACI 318 Section 21.6.4.5 specifies the maximum spacing of transverse reinforcement in the region beyond the l_o zones. The maximum spacing is the smaller of 6.0 inches or $6d_b$, which for #8 bars is also 6 inches. Hoops and crossties with the same details as those placed in the critical regions of the column will be used.

7.4.2.4.3 Check Column Shear Strength. The amount of transverse reinforcement computed in the previous section is the minimum required for confinement. The column also must be checked for shear strength in based on ACI 318 Sec. 21.6.5.1. According to that section, the column shear is based on the probable moment strength of the columns, but need not be more than what can be developed into the column by the beams framing into the joint. However, the design shear cannot be less than the factored shear determined from the analysis.

The shears computed based on the probable moment strength of the column can be conservative since the actual column moments are limited by the moments that can be delivered by the beams. For this example, however, the shear from the column probable moments will be checked first and then a determination will be made if a more detailed limit state analysis should be used.

As determined from PCA Column, the maximum probable moment of the column in the range of factored axial load is 14,940 in.-kips. With a clear height of 124 inches, the column shear can be determined as 2(14,940)/124 = 241 kips. This shear will be compared to the capacity provided by the 4-leg #4 hoops spaced at 6 inches on center. If this capacity is in excess of the demand, the columns will be acceptable for shear.

For the design of column shear capacity, the concrete contribution to shear strength may be considered because the minimum $P_u > A_g f'_c/20$. The design shear strength contributed by concrete and reinforcing steel are as follows:

$$V_c = 2\sqrt{f'_c}bd = 2\sqrt{5{,}000}(30)(27.5) = 116.7 \text{ kips}$$

$$V_s = A_v f_y d / s = (4)(0.2)(60)(27.5)/6 = 220.0 \text{ kips}$$

$\phi \quad V_n = \phi \quad (V_c + V_s) = 0.75(116.7 + 220.0) = 252.5 \text{ kips} > 241 \text{ kips}$ OK

The column with the minimum transverse steel is therefore adequate for shear. The final column detail with both longitudinal and transverse reinforcement is given in Figure 7-24. The spacing of reinforcement through the joint has been reduced to 4 inches on center. This is done for practical reasons only. Column bar splices, where required, should be located in the center half of the column and must be proportioned as Class B tension splices.

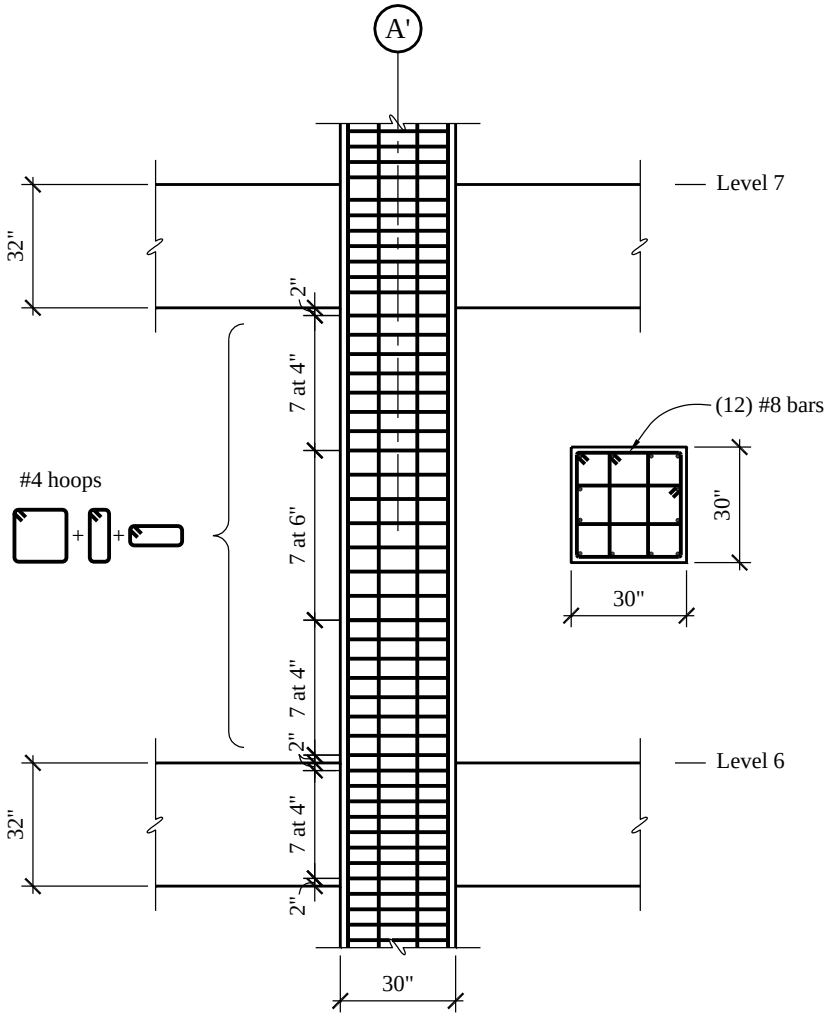

Figure 7-24 Details of reinforcement for column
(1.0 in. = 25.4 mm)

7.4.3 Design of Frame 3 Shear Wall

This section addresses the design of a representative shear wall. The shear wall includes the 16-inch wall panel in between two 30- by 30-inch columns. The design includes shear, flexure-axial interaction and boundary elements.

The factored forces acting on the structural wall of Frame 3 are summarized in Table 7-17. The axial compressive forces are based on the self-weight of the wall, a tributary area of 1,800 square feet of floor area for the entire wall (includes column self-weight), an unfactored floor dead load of 139 psf and an unfactored (reduced) floor live load of 20 psf. Based on the assumed 16-inch wall thickness, the wall between columns weighs (1.33 feet)(17.5 feet)(13 feet)(150 pcf) = 45.4 kips per floor. The total axial force for a typical floor is:

$P_u = 1.42D + 0.5L = 1.42[1{,}800(0.139) + 45{,}400] + 0.5[1{,}800(0.02)] = 456$ kips for maximum compression

$P_u = 0.68D = 0.68[1{,}800(0.139) + 45{,}400] = 201$ kips for minimum compression

The bending moments come from the ETABS analysis, using a section cut to combine forces in the wall panel and end columns.

Note that the gravity moments and the earthquake axial loads on the shear wall are assumed to be negligible given the symmetry of the system, so neither of these load effects are considered in the shear wall design.

Table 7-17 Design Forces for Grid 3 Shear Wall

Supporting Level	Axial Compressive Force P_u (kips)		Shear V_u (kips)	Moment M_u (inch-kips)
	$1.42D + 0.5L$	$0.68D$		
R	420	201	173.2	35,375
12	876	402	133.9	50,312
11	1,332	603	156.7	63,337
10	1,788	804	195.7	73,993
9	2,243	1,005	221.8	81,646
8	2,699	1,206	252.4	86,298
7	3,155	1,408	294.6	90,678
6	3,611	1,609	344.9	102,405
5	4,067	1,810	400.7	132,941
4	4,523	2,011	467.5	178,321
3	4,979	2,212	546.0	241,021
2	5,435	2,413	663.3	366,136
1	5,891	2,614	580.3 (use 663.3)	258,851

(1.0 kip = 4.45 kN, 1.0 inch-kip = 0.113 kN-m)

7.4.3.1 Design for Shear Loads. First determine the required shear reinforcement in the wall panel and then design the wall for combined bending and axial force. The nominal shear strength of the wall is given by ACI 318 Equation 21-7:

$$V_n = A_{cv}(\alpha_c \lambda \sqrt{f_c'} + \rho_t f_y)$$

where α_c = 2.0 because h_w/l_w = 161/22.5 = 7.15 > 2.0, where the 161 feet is the wall height and 22.5 feet is the overall wall length from the edges of the 30-inch boundary columns.

Using f_c' = 5,000 psi, f_y = 60 ksi, λ = 1.0, A_{cv} = (22.5)(12)(16) = 4,320 in^2, the required amount of shear reinforcement, ρ_t , can be determined by setting $\phi V_n = V_u$. In accordance with ACI 318 Section 9.3.4, the ϕ factor for shear is 0.60 for special structural walls unless the wall is specifically designed to be governed by flexure yielding. If the walls were designed to be flexure-critical, then the ϕ factor for shear would be 0.75, consistent with typical shear design. Unlike special moment frames, shear-critical special shear walls are permitted (with the reduced ϕ), although it should be noted that in areas of high seismic hazard many practitioners recommend avoiding shear-critical shear walls where practical. In this case, ϕ = 0.60 will be used for design.

The required reinforcement ratio for strength is determined as:

$$\rho_t = \frac{\left(\frac{663{,}300}{0.60}\right) - \left(2\sqrt{5{,}000}(4{,}320\right)}{4{,}320(60{,}000)} = 0.0019$$

Since this is less than the minimum ratio of 0.0025 required by ACI 318 Section 21.9.2.1, that minimum will apply to all levels of the wall. (This is a good indication that the actual wall thickness can be reduced, but this example will proceed with the 16-inch wall thickness.) Assuming two curtains of #5 bars spaced at 15 inches on center, ρ_t = 0.0026 and ϕV_n = 768 kips, which exceeds the required shear capacity at all levels.

Vertical reinforcing will be the same as the horizontal reinforcing based on the minimum reinforcing ratio requirements of ACI 318 Section 21.9.2.1

7.4.3.2 Design for Flexural and Axial Loads. The flexural and axial design of special shear walls includes two parts: design of the wall for flexural and axial loads and the design of boundary elements where required. This section covers the design loads and the following section covers the boundary elements.

The wall analysis was performed using PCA Column and considers the wall panel plus the boundary columns. For axial and flexural loads, ϕ = 0.65 and 0.90, respectively. Figure 7-25 shows the interaction diagram for the wall section below Level 2, considering the range of possible factored axial loads. The wall panel is 16 inches thick and has two curtains of #5 bars at 15 inches on center. The boundary columns are 30 by 30 inches with twelve #9 bars at this location. The section is clearly adequate because the interaction curve fully envelopes the design values.

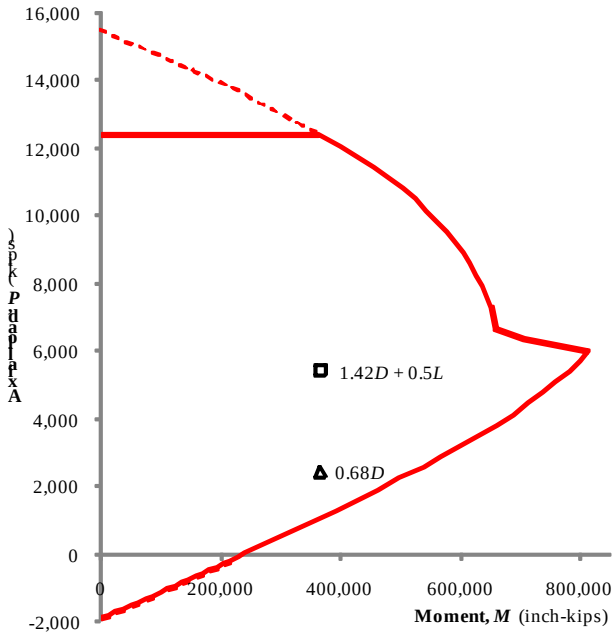

Figure 7-25 Interaction diagram for structural wall
(1.0 kip = 4.45kN, 1.0 in-kip = 0.113 kN-m)

7.4.3.3 Design of Boundary Elements. An important consideration in the ductility of special reinforced concrete shear walls is the determination of where boundary elements are required and the design of them where they are required. ACI 318 provides two methods for this. The first approach, specified in ACI 318 Section 21.9.6.2, uses a displacement based procedure. The second approach, described in ACI 318 Section 21.9.6.3 uses a stress-based procedure and will be illustrated for this example.

In accordance with ACI 318 Section 21.9.6.3, special boundary elements are required where the maximum extreme fiber compressive stress exceeds $0.2f'_c$ and they can be terminated where the stress is less than $0.15f'_c$. The stresses are determined based on the factored axial and flexure loads as shown in Table 7-18. The stresses are determined using a wall area of 5,160 in^2, a section modulus of 284,444 in^3 and f'_c = 5,000 psi.

Table 7-18 Grid 3 Shear Wall Boundary Element Check

Supporting Level	Axial Force P_u (kips)	Moment M_u (inch-kips)	Maximum stress		Boundary Element Required?
			(ksi)	(× f_c')	
R	420	35,375	0.206	0.04	No
12	876	50,312	0.347	0.07	No
11	1,332	63,337	0.481	0.10	No
10	1,788	73,993	0.607	0.12	No
9	2,243	81,646	0.722	0.14	No
8	2,699	86,298	0.827	0.17	Yes
7	3,155	90,678	0.930	0.19	Yes
6	3,611	102,405	1.060	0.21	Yes
5	4,067	132,941	1.256	0.25	Yes
4	4,523	178,321	1.503	0.30	Yes
3	4,979	241,021	1.812	0.36	Yes
2	5,435	366,136	2.340	0.47	Yes
1	5,891	258,851	2.052	0.41	Yes

(1.0 kip = 4.45 kN, 1.0 in-kip = 0.113 kN-m)

As can be seen, special boundary elements are required at the base of the wall and can be terminated above Level 8.

Where they are required, the detailing of the special boundary element is based on ACI 318 Section 21.9.6.4.

According to ACI 318 Section 21.9.6.4 Item (a), the special boundary elements must have a minimum plan length equal to the greater of c - 0.1l_w, or c/2, where c is the neutral axis depth and l_w is the wall length. The neutral axis depth is a function of the factored axial load and the nominal (ϕ = 1.0) flexural capacity of the wall section. This value is obtained from the PCA Column analysis for the wall section and range of axial loads. For the Level 2 wall with twelve #9 vertical bars at each boundary column and two curtains of #5 bars at 15 inches at vertical bars, the computed neutral axis depths are 32.4 inches and 75.3 inches for axial loads of 5,434 and 2,513 kips, respectively. For the governing case of 75.3 inches and a wall length of 270 inches, the boundary element length is the greater of 75.3 - 0.1(270) = 48.3 inches and the second is 75.3/2 = 37.7 inches.

It is clear, therefore, that the special boundary element needs to extend beyond the 30-inch edge columns at least at the lower levels. For the wall below Level 5 where the maximum factored axial load is 4,067 kips, c = 53.6 inches and the required length is 27 inches, which fits within the boundary column. For the walls from the basement to below Level 4, the boundary element can be detailed to extend into the wall panel, or the concrete strength could be increased. Based on the desire to simply the reinforcing, the wall concrete could be increased to f_c' = 7,000 psi and the required boundary element length below Level 2 is 26.9 inches. Figure 7-26 illustrates the variation in neutral axis depth based on factored axial load and concrete strength. Although there is a cost premium for the higher strength concrete, this is still in the range of commonly supplied concrete and will save costs by allowing the column rebar cage to serve as the boundary element and have only distributed reinforcing in the wall panel itself. The use of 7,000 psi concrete at the lower levels will impact the calculations for maximum extreme fiber stress per

Table 7-18, but since the 7,000 psi concrete extends up to Level 4, not Level 8, the vertical extent of the boundary elements is unchanged.

It is expected that the increase in concrete strength (and thus the modulus of elasticity) at the lower floors will have a slight impact on the overall building stiffness, but this will not impact the overall design. However, this should be verified.

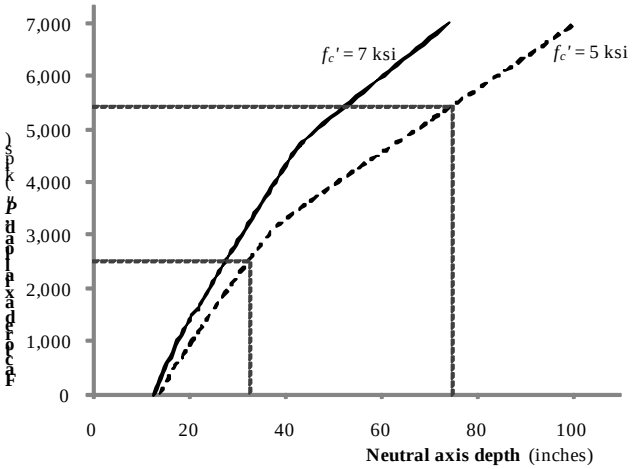

Figure 7-26 Variations of neutral axis depth
(1.0 in. = 25.4 mm, 1.0 kip = 4.45 kN)

Where special boundary elements are required, transverse reinforcement must conform to ACI 318 Section 21.9.6.4(c), which refers to ACI 318 Sections 21.6.4.2 through 21.6.4.4. In addition, this section indicates that ACI 318 Equation 21-4 need not apply and the transverse reinforcing spacing limit of ACI 318 Section 21.6.4.3(a) can be one-third of the least dimension of the element. Similar to columns of special moment frames, there are requirements for spacing and total area of transverse reinforcing.

The spacing is determined as follows:

One-third of least dimension = 30/3 = 10 inches

Six longitudinal bar diameters = 6(1.125) = 6.75 inches

Dimension $s_o = 4 + (14 - h_x) / 3$, where s_o is between 4 inches and 6 inches and h_x is the maximum horizontal spacing of hoops or cross ties.

Where hoops are used, the transverse reinforcement must satisfy ACI 318 Equation 21-5:

$$A_{sh} = 0.09\left(\frac{sb_c f_c'}{f_{yt}}\right)$$

If #4 hoops with two crossties in each direction are used similar to the moment frame columns, $A_{sh} = 0.80$ in^2 and $b_c = 27$ inches. For $f_c' = 7{,}000$ psi and $f_{yt} = 60$ ksi,

$s = [(0.8)(60{,}000)]/[0.09(27.0)(7{,}000)] = 2.82$ inches

which is impractical. Therefore, use #5 hoops and cross ties for the 7,000 psi concrete below Level 4, so $A_{sh} = 4(0.31) = 1.24$ in^2 and $s = 4.4$ inches.

Where the concrete strength is 5,000 psi above Level 4, use #4 hoops and cross ties and the spacing, s = 3.95 inches.

Therefore, for the special boundary elements, use hoops with two cross ties spaced at 4 inches. The hoops and cross ties are #5 below Level 4 and #4 above Level 4. ACI 318 Section 21.9.6.4(d) also requires that the boundary element transverse reinforcement be extended beyond the base of the wall a distance equal to the tension development length of the longitudinal reinforcement in the boundary elements unless there is a mat or footing, in which case the transverse reinforcement extends down at least 12 inches.

Details of the boundary element and wall panel reinforcement are shown in Figures 7-27 and 7-28, respectively. The vertical reinforcement in the boundary elements will be spliced as required using either Class B lap splices or Type 2 mechanical splices at all locations. According to Table 7-15 (prepared for 5,000 psi concrete), there should be no difficulty in developing the horizontal wall panel steel into the 30- by 30-inch boundary elements.

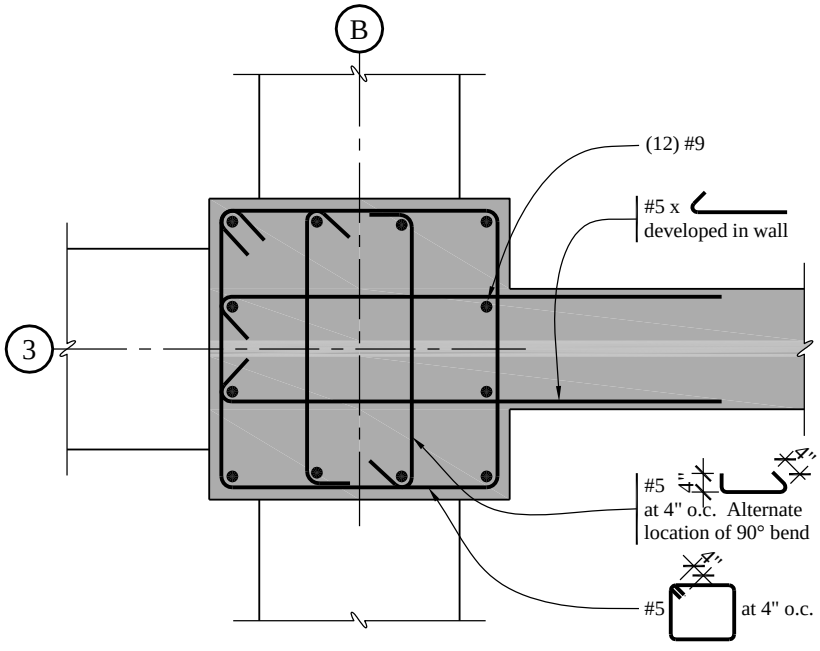

Figure 7-27 Details of structural wall boundary element
(1.0 in. = 25.4 mm)

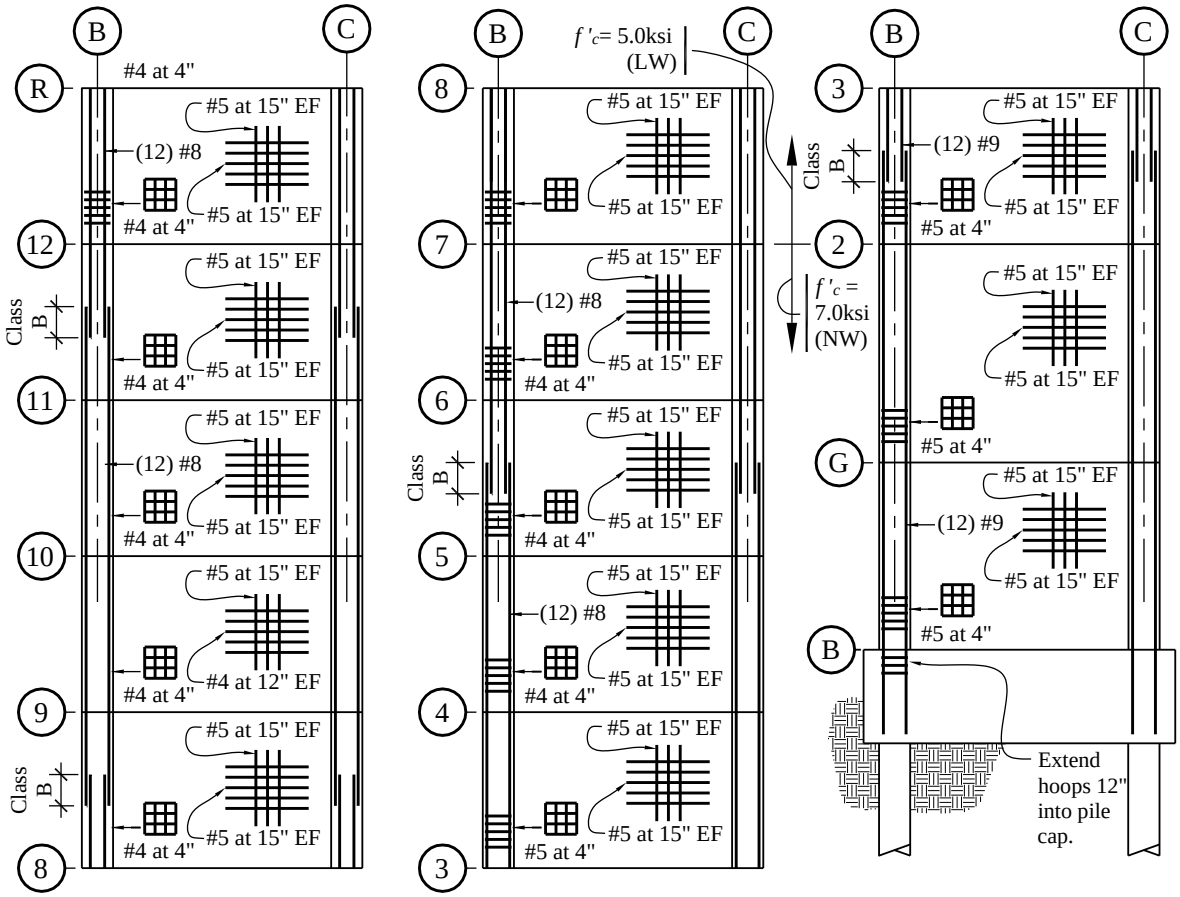

Figure 7-28 Overall details of structural wall
(1.0 in. = 25.4 mm)

7.5 STRUCTURAL DESIGN OF THE HONOLULU BUILDING

The structure illustrated in Figures 7-1 and 7-2 is now designed and detailed for the Honolulu building. Because of the relatively moderate level of seismicity, the lateral load-resisting system will consist of a series of intermediate moment-resisting frames in both the E-W and N-S directions. This is permitted for Seismic Design Category C buildings in accordance with *Standard* Table 12.2-1. Design guidelines for the reinforced concrete framing members are provided in ACI 318 Section 21.3.

As noted previously, the beams are assumed to be 30 inches deep by 20 inches wide and the columns are 28 inches by 28 inches. These are slightly smaller than the Berkeley building, reflecting the lower seismicity.

7.5.1 Compare Seismic Versus Wind Loading

As has been discussed and as illustrated in Figure 7-3, wind forces appear to govern the strength requirements of the structure at the lower floors and seismic forces control at the upper floors. The seismic and wind shears, however, are so close at the middle levels of the structure that a careful

evaluation must be made to determine which load governs for strength. This determination requires consideration of several load cases for both wind and seismic loads.

Because the Honolulu building is in Seismic Design Category C and does not have a Type 5 horizontal irregularity (*Standard* Table 12.3-1); orthogonal loading effects need not be considered per *Standard* Section 12.5.3. However, as required by *Standard* Section 12.8.4.2, accidental torsion must be considered. Torsional amplification is not required per *Provisions* Section 12.8.4.3 because the building does not have a torsional irregularity as determined previously.

For wind, the *Standard* requires that buildings over 60 feet in height be checked for four loading cases under the Method 2 Analytical Procedure of *Standard* Section 6.5. The required load cases are shown in Figure 7-29, which is reproduced directly from *Standard* Figure 6-9. In Cases 1 and 2, load is applied separately in the two orthogonal directions, but Case 2 adds a torsional component. Cases 3 and 4 involve wind loads in two directions simultaneously and Case 4 adds a torsional component.

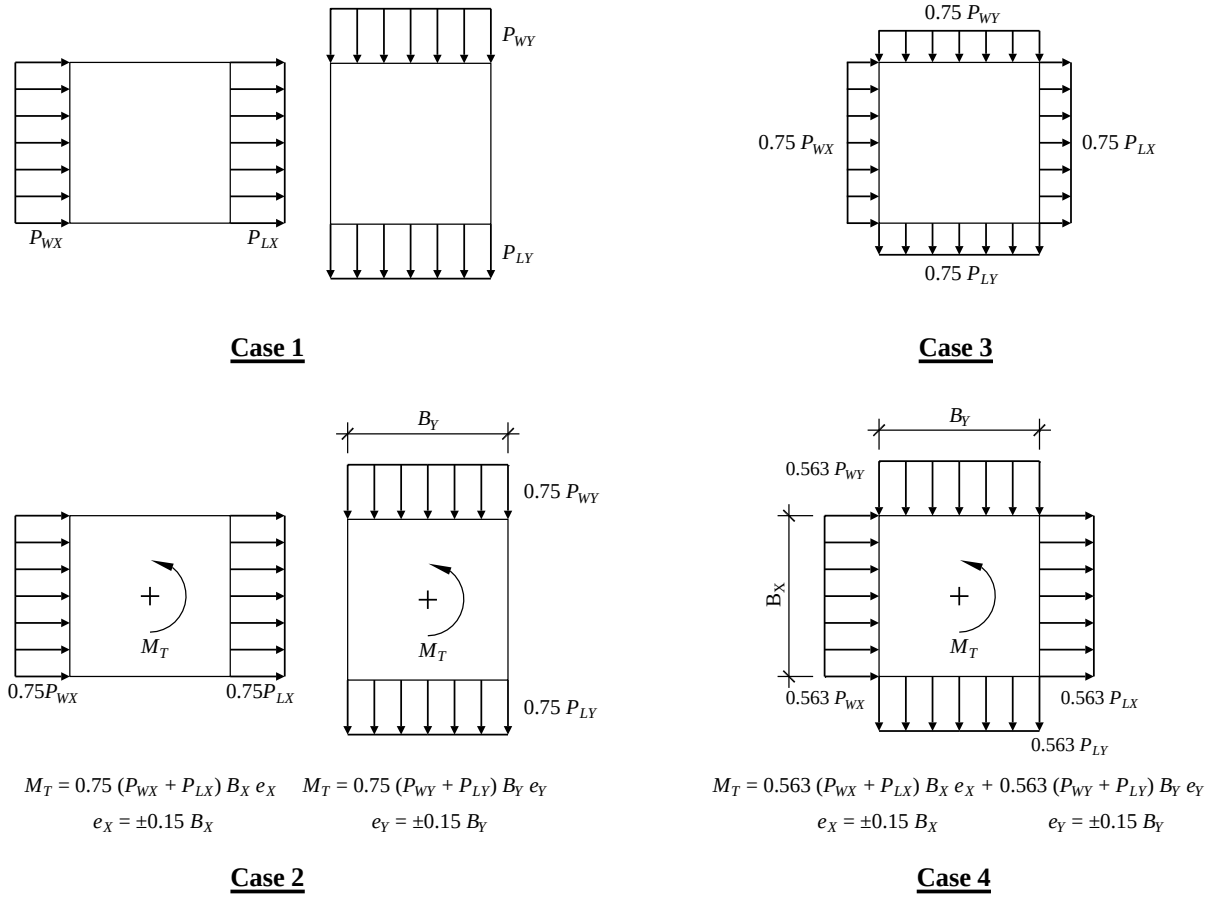

Figure 7-29 Wind loading requirements from ASCE 7

In this example, only loading in the E-W direction is considered. Hence, the following lateral load conditions are applied to the ETABS model:

E-W seismic with accidental torsion

Wind Case 1 applied in E-W direction only

Wind Case 2 applied in E-W direction only

Wind Case 3

Wind Case 4

All cases with torsion are applied in such a manner as to maximize the shears in the elements of Frame 1, for whose members the design is illustrated in the following section.

A simple method for determining which load case is likely to govern is to compare the beam shears for each story. For the five load cases indicated above, the beam shears produced from seismic effects control at the sixth level, with the next largest forces coming from direct E-W wind Case 1. This is shown graphically in Figure 7-30, where the beam shears at the center bay of Frame 1 are plotted versus story height. Note that this comparison is based on 1.0 times seismic loads and 1.6 times wind loads consistent with the strength design load combinations. Wind controls load at the lower four stories and seismic controls for all other stories. This is somewhat different from that shown in Figure 7-3, wherein the total story shears are plotted and where wind controlled for the lower five stories. A basic difference between Figures 7-3 and 7-30 is that Figure 7-30 includes torsion effects.

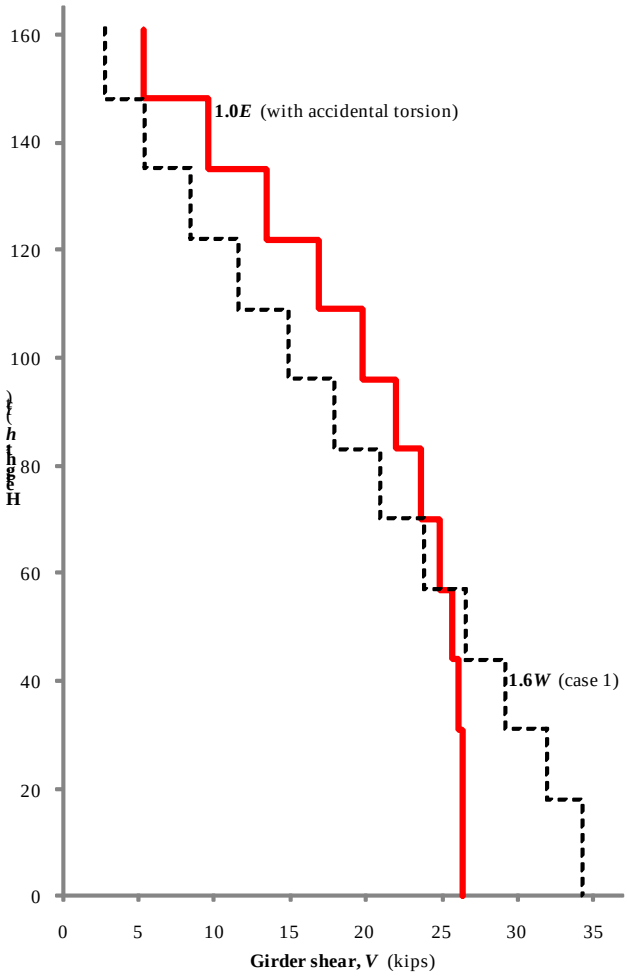

Figure 7-30 Wind versus seismic shears in center bay of Frame 1
(1.0 ft = 0.3048 m, 1.0 kip = 4.45kN)

7.5.2 Design and Detailing of Members of Frame 1

In this section, the beams and a typical interior column of Level 6 of Frame 1 are designed and detailed.

7.5.2.1 Initial Calculations. The girders of Frame 1 are 30 inches deep and 20 inches wide. For positive moment bending, the effective width of the compression flange is taken as 20 + 20(12)/12 = 40.0 inches. Assuming 1.5-inch cover, #4 stirrups and #9 longitudinal reinforcement, the effective depth for computing flexural and shear strength is 30 - 1.5 - 0.5 - 1.125 / 2 = 27.4 inches.

7.5.2.2 Design of Representative Beams. ACI 318 Section 21.3.4 provides the minimum requirements for longitudinal and transverse reinforcement in the beams of intermediate moment frames. The requirements for longitudinal steel are as follows:

1. The positive moment strength at the face of a joint shall be at least one-third of the negative moment strength at the same joint.

2. Neither the positive nor the negative moment strength at any section along the length of the member shall be less than one-fifth of the maximum moment strength supplied at the face of either joint.

The second requirement has the effect of requiring top and bottom reinforcement along the full length of the member. The minimum reinforcement ratio at any section is taken from ACI 318 Section 10.5.1 as $200/f_y$ or 0.0033 for f_y = 60 ksi. However, according to ACI 318 Section 10.5.3, the minimum reinforcement provided need not exceed 1.33 times the amount of reinforcement required for strength.

The gravity loads and design moments for the first three spans of Frame 1 are shown in Figure 7-31. The seismic and gravity moments are determined from ETABS analysis, similar to the Berkeley building. All moments are given at the face of the support. The gravity moments shown in Figures 7-31c and 7-31d are slightly different from those shown for the Berkeley building (Figure 7-11) because the beam self-weight is less and the clear span is longer due to the reduction in column size.

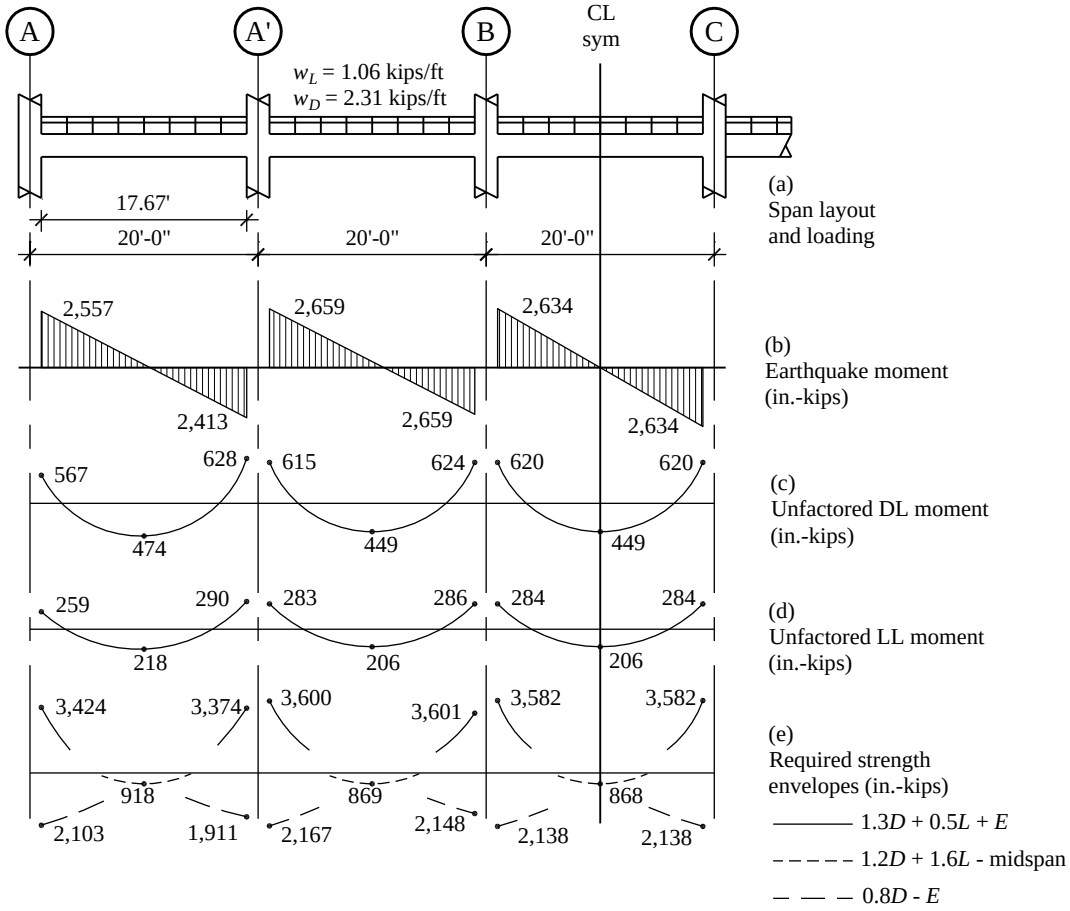

Figure 7-31 Bending moment envelopes at Level 6 of Frame 1
(1.0 ft = 0.3048 m, 1.0 kip/ft = 14.6 kN/m, 1.0 in-kip = 0.113 kN-m)

7.5.2.2.1 Longitudinal Reinforcement. Based on a minimum amount of longitudinal reinforcing of $0.0033b_w d = 0.0033(20)(27.4)=1.83$ in^2, provide two #9 bars continuous top and bottom as a starting point and provide additional reinforcing as required.

1. Design for Negative Moment at the Face of the Exterior Support (Grid A)

M_u = -1.3 (567) - 0.5 (259) - 1.0 (2,557) = -3,423 inch-kips

Try two #9 bars plus one #7 bar.

A_s = 2 (1.00) + 0.60 = 2.60 in^2
Depth of compression block, a = [2.6 (60)]/[0.85 (5) 20] = 1.83 inches
Nominal strength, M_n = [2.60 (60)] [27.4 - 1.83/2] = 4,131 inch-kips
Design strength, ϕM_n = 0.9 (4,131) = 3,718 inch-kips > 3,423 inch-kips OK

This reinforcement also will work for negative moment at all other supports.

2. Design for Positive Moment at the Face of the Exterior Support (Grid A)

M_u = -0.8 (567) + 1.0 (2,557) = 2,114 inch-kips

Try the minimum of two #9 bars.

A_s = 2 (1.00) = 2.00 in^2
a = 2.00 (60)/[0.85 (5) 40] = 0.71 inch
M_n = [2.00 (60)] [27.4 – 0.71/2] = 3,246 inch-kips
ϕM_n = 0.9 (3,246) = 2,921 inch-kips > 2,114 inch-kips OK

This reinforcement also will work for positive moment at all other supports.

The layout of flexural reinforcement layout is shown in Figure 7-32. The top short bars are cut off 5 feet-0 inch from the face of the support. The bottom bars are spliced in Spans A'-B and C-C' with a Class B lap length of 37 inches. Unlike special moment frames, there are no requirements that the spliced region of the bars in intermediate moment frames be confined by hoops over the length of the splice. Note that the steel clearly satisfies the detailing requirements of ACI 318 Section 21.3.4.1.

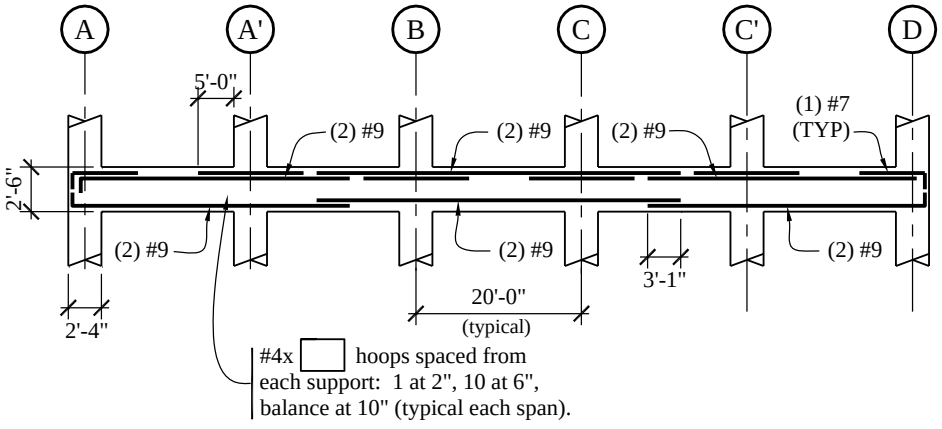

Figure 7-32 Longitudinal reinforcement layout for Level 6 of Frame 1
(1.0 in. = 25.4 mm, 1.0 ft = 0.3048 m)

7.5.2.2.2 Transverse Reinforcement. The requirements for transverse reinforcement in intermediate moment frames are somewhat different from those in special moment frames, both in terms of detailing and shear design. The shear strength requirements will be covered first, followed by the detailing requirements.

In accordance with ACI 318 Section 21.3.3, the design earthquake shear for the design of intermediate moment frame beams must be larger than the smaller of the following:

a. The sum of the shears associated with the nominal moment strength at the ends of the members. Nominal moment strengths are computed with a flexural reinforcement tensile strength of $1.0f_y$ and a flexural ϕ factor of 1.0.

b. Two times the factored earthquake shear force determined from the structural analysis.

In either case, the earthquake shears are combined with the factored gravity shears to determine the total design shear.

Consider the end span between Grids A and A'. For determining earthquake shears per Item a above, the nominal strengths at the ends of the beam were computed earlier as 3,246 inch-kips for positive moment at Support A' and 4,131 inch-kips for negative moment at Support A. Compute the design earthquake shear V_E:

$$V_E = \frac{3{,}246 + 4{,}131}{212} = 34.8 \text{ kips}$$

where 212 inches is the clear span of the member. The shear is the same for earthquake forces acting in the other direction.

For determining earthquake shears per Item b above, the shear is taken from the ETABS analysis as 23.4 kips. The design earthquake shear for this method is 2(23.4 kips) = 46.8 kips.

Since the design shear using Item a is the smaller value, it is used for computing the design shear.

The gravity load shears are taken from the ETABS model. Since the gravity shears at Grid A' are similar but slightly larger than those at Grid A, Grid A' will be used for the design. From the ETABS analysis, V_D = 20.7 kips and V_L = 9.5 kips.

The factored design shear V_u = 1.3(20.7) + 0.5(9.5) + 1.0(46.8) = 66.5 kips. This shear force applies for earthquake forces coming from either direction as shown in the shear strength design envelope in Figure 7-33.

The design shear force is resisted by a concrete component, V_c and a steel component, V_s. Note that the concrete component may be used regardless of the ratio of earthquake shear to total shear. The required design strength is:

$$V_u \leq \phi \quad V_c + \phi \quad V_s$$

where ϕ = 0.75 for shear.

$$V_c = \frac{2\sqrt{5{,}000}(20)(27.4)}{1{,}000} = 77.5 \text{ kips}$$

The shear to be resisted by reinforcing steel, assuming two #4 vertical legs ($A_v = 0.4$) and $f_y = 60$ ksi is:

$$V_s = \frac{V_u - \phi V_c}{\phi} = \frac{66.5 - 0.75(77.5)}{0.75} = 11.2 \text{ kips}$$

Using $V_s = A_v f_y d/s$:

$$s = \frac{(0.4)(60)(27.4)}{11.2} = 58.7 \text{ inches}$$

Minimum transverse steel requirements are given in ACI 318 Section 21.3.4.2. At the ends of the beam, hoops are required. The first hoop must be placed 2 inches from the face of the support and within a distance 2*h* from the face of the support, the spacing should be not greater than *d*/4, eight times the smallest longitudinal bar diameter, 24 times the hip bar diameter, or 12 inches. For the beam under consideration *d*/4 controls minimum transverse steel, with the maximum spacing being 27.4/4 = 6.8 inches, which is less than what is required for shear strength.

In the remainder of the span, stirrups are permitted and must be placed at a maximum of *d*/2 (ACI 318 Sec. 21.3.4.3).

Because the earthquake shear (at midspan where the gravity shear is essentially zero) is greater than 50 percent of the shear strength provided by concrete alone, the minimum requirements of ACI 318 Section 11.4.6.1 must be checked:

$$s_{\max} = \frac{A_v f_{yt}}{0.75\sqrt{f_c'} b_w} = \frac{0.4(60{,}000)}{0.75\sqrt{5{,}000}(20)} = 20.8 \text{ inches}$$

This spacing does not control over the *d*/2 requirement. The layout of transverse reinforcement for the beam is shown in Figure 7-32. This spacing is used for all other spans as well.

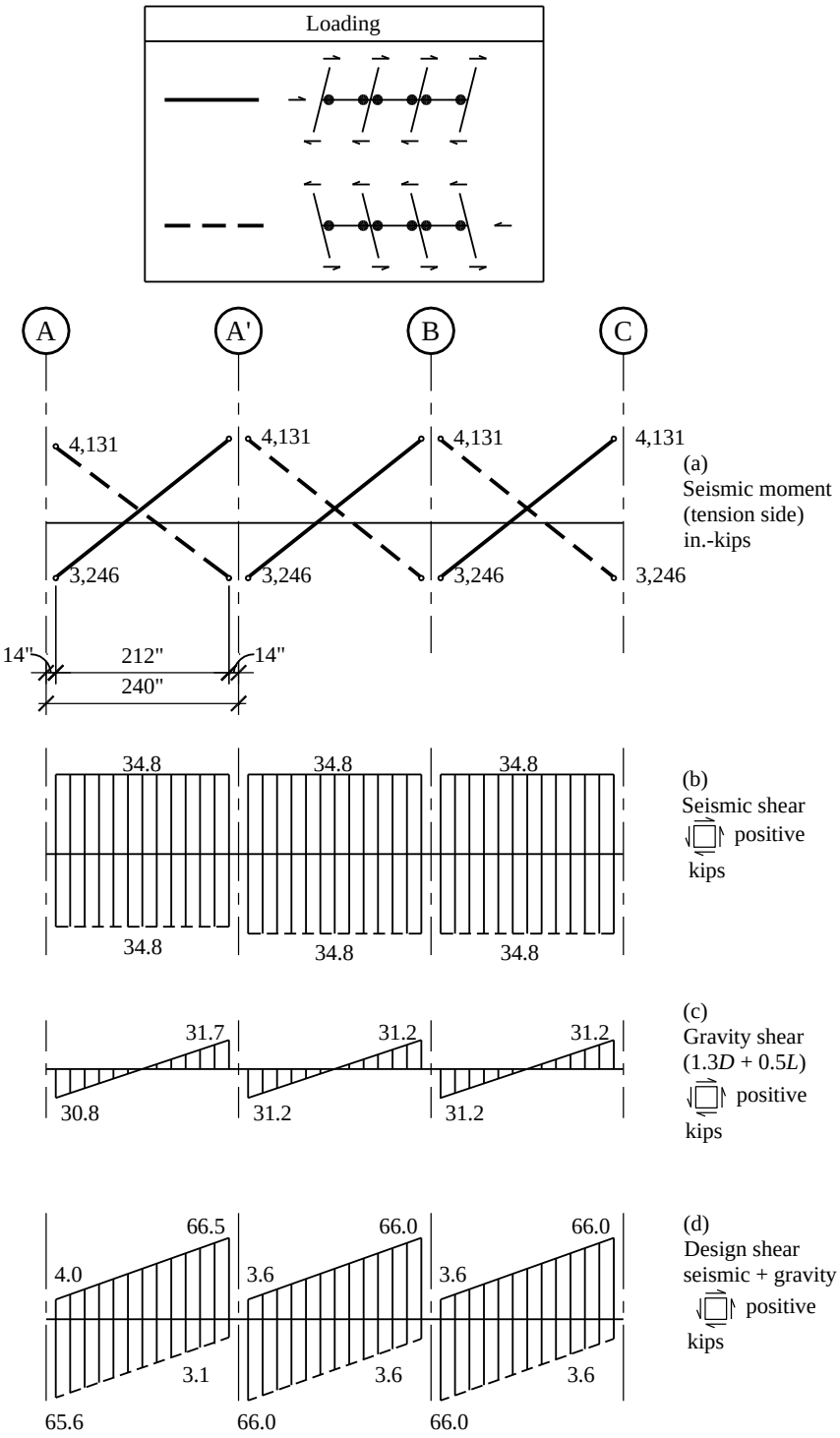

Figure 7-33 Shear strength envelopes for Span A-A' of Frame 1
(1.0 in. = 25.4 mm, 1.0 kip = 4.45kN, 1.0 in-kip = 0.113 kN-m)

7.5.2.3 Design of Representative Column of Frame 1. This section illustrates the design of a typical interior column on Gridline A'. The column, which supports Level 6 of Frame 1, is 28 inches square and is constructed from 5,000 psi concrete and 60 ksi reinforcement. An isolated view of the column is shown in Figure 7-34.

The column supports an unfactored axial dead load of 506 kips and an unfactored axial live load (reduced) of 117 kips. The ETABS analysis indicates that the axial earthquake force is ±19.9 kips, the earthquake shear force is ±37.7 kips and the earthquake moments at the top and the bottom of the column are ±2,408 and ±2,340 inch-kips, respectively. Moments and shears due to gravity loads are assumed to be negligible.

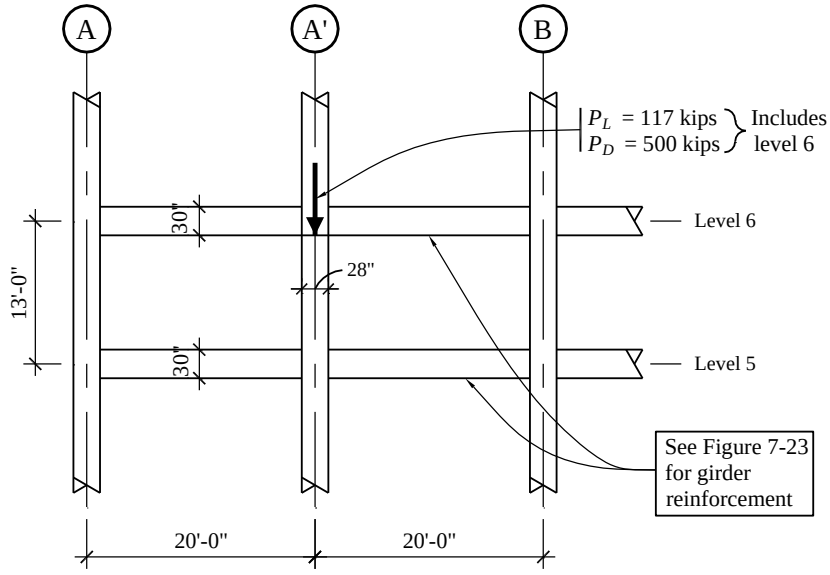

Figure 7-34 Isolated view of Column A'
(1.0 ft = 0.3048 m, 1.0 kip = 4.45kN)

7.5.2.3.1 Longitudinal Reinforcement. The factored gravity force for maximum compression (without earthquake) is:

$P_u = 1.2(506) + 1.6(117) = 794$ kips

This force acts with no significant gravity moment.

The factored gravity force for maximum compression (including earthquake) is:

$P_u = 1.3(506) + 0.5(117) + 19.9 = 736$ kips

The factored gravity force for minimum compression (including earthquake) is:

$P_u = 0.8(506) – 19.9 = 385$ kips

Before proceeding with the flexural strength calculations, first determine whether or not slenderness effects need to be considered. For a frame that is unbraced against sideway, ACI 318 Section 10.10.1 allows slenderness effects to be neglected where $kl_u/r < 22$. For a 28- by 28-inch column with a clear unbraced length, l_u = 126 inches, r = 0.3(28) = 8.4 inches (ACI 318 Sec. 10.10.1.2) and l_u/r = 126/8.4 = 15.0. Therefore, as long as the effective length factor k for this column is less than 22/15.0 = 1.47, then slenderness effects can be ignored. It is reasonable to assume that k is less than 1.47 and this can be confirmed using the commentary to ACI 318 Section 10.10.1.

Continuing with the design, an axial-flexural interaction diagram for a 28- by 28-inch column with 12 #8 bars (ρ = 0.0121) is shown in Figure 7-35. The column clearly has the strength to support the applied loads (represented as solid dots in the figure).

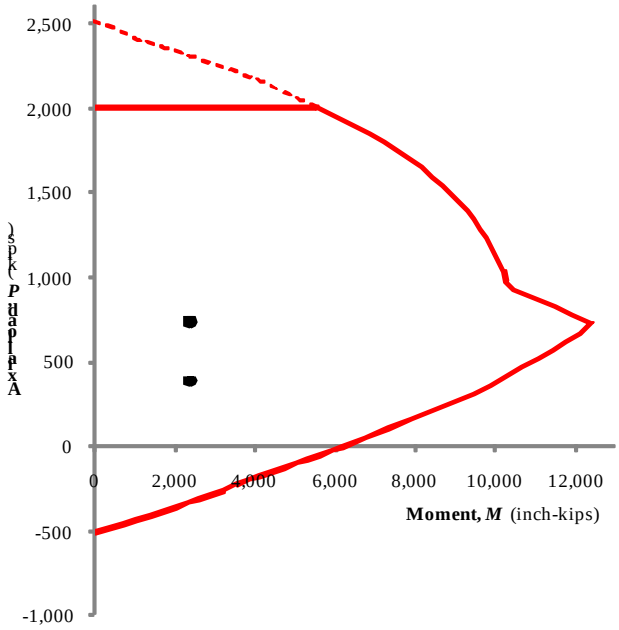

Figure 7-35 Interaction diagram for column
(1.0 kip = 4.45kN, 1.0 ft-kip = 1.36 kN-m)

7.5.2.3.2 Transverse Reinforcement. The design earthquake shear for columns in determined in the same manner as for beams in accordance with ACI 318 Section 21.3.3 as described in Section 7.5.2.2.2. Assuming two times the shear from analysis will produce the smaller design shear, the ETABS analysis indicates that the shear force is 37.7 kips and the design shear is 2.0(37.7) = 75.4 kips.

The concrete supplies a capacity of:

$$\phi V_c = 0.75(2\sqrt{5{,}000}(28)(25.6)) = 76.0 \text{ kips} > 75.4 \text{ kips} \qquad \text{OK}$$

Therefore, steel reinforcement is not required for strength, but shear reinforcement is required per ACI 318 Section 11.4.6.1 since the design shear exceeds one-half of the design capacity of the concrete alone. First, however, determine the detailing requirements for transverse reinforcement in intermediate moment frame columns in accordance ACI 318 Section 21.3.5.

Within a region l_o from the face of the support, the tie spacing must not exceed:

$8d_b = 8(1.0) = 8.0$ inches (using #8 longitudinal bars)
$24d_{tie} = 24\ (0.5) = 12.0$ inches (using #4 ties)
1/2 the smallest dimension of the frame member = 28/2 = 14 inches
12 inches

The 8-inch maximum spacing controls. Ties at this spacing are required over a length l_o of:

1/6 clearspan of column = 126/6 = 21 inches
Maximum cross section dimension = 28 inches
18 inches

Given the above, a four-legged #4 tie spaced at 8 inches over a depth of 28 inches will be used. The top and bottom ties will be provided at 4 inches from the beam soffit and floor slab.

Beyond the end regions, ACI 318 Section 21.3.5.4 requires that tie spacing satisfy ACI 318 Sections 7.10 and 11.4.5.1, but the minimum shear reinforcing requirement of ACI 318 Section 11.4.6.1 also applies.

Of the above requirements, ACI 318 Section 11.4.5.1, which requires ties at $d/2$ maximum spacing, governs. Therefore, use a 12-inch tie spacing in the middle region of the column.

The layout of the transverse reinforcing for the subject column is shown in Figure 7-36

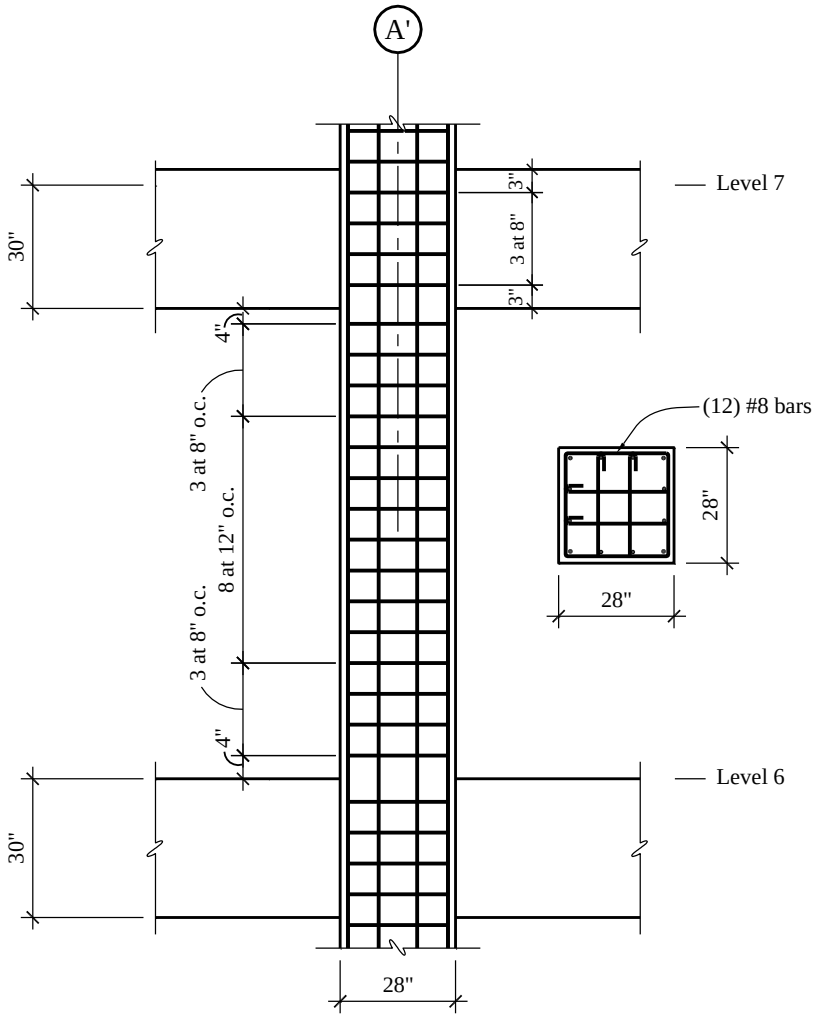

Figure 7-36 Column reinforcement
(1.0 in. = 25.4 mm)

7.5.2.4 Design of Beam-Column Joint. Joint reinforcement for intermediate moment frames is addressed in ACI 318 Section 21.3.5.5, which refers to ACI 318 Section 11.10. ACI 318 Section 11.10 requires that all beam-column connections have a minimum amount of transverse reinforcement through the beam-column joints. The only exception is in non-seismic frames where the column is confined on all four sides by beams framing into the column. The amount of reinforcement required is given by ACI 318 Equation 11-13:

$$A_{v,\min} = 0.75\sqrt{f_c'}\frac{b_w s}{f_{yt}}$$

This is the same equation used to proportion minimum transverse reinforcement in beams. Assuming A_v is supplied by four #4 ties and f_y = 60 ksi:

$$s = \frac{4(0.2)(60{,}000)}{0.75\sqrt{5{,}000}(28)} = 32.4 \text{ inches}$$

This essentially permits no ties to be located in the joint. Since it is good practice to provide transverse reinforcing in moment frame joints, ties will be provided at the same 8-inch spacing as at the ends of the columns. The arrangement of ties within the beam-column joint is shown in Figure 7-36.

8

Precast Concrete Design

Suzanne Dow Nakaki, S.E.

Originally developed by
Gene R. Stevens, P.E. and James Robert Harris, P.E., PhD

Contents

8.1 HORIZONTAL DIAPHRAGMS 4

8.1.1 Untopped Precast Concrete Units for Five-Story Masonry Buildings Located in Birmingham, Alabama and New York, New York 4

8.1.2 Topped Precast Concrete Units for Five-Story Masonry Building Located in Los Angeles, California (see Sec. 10.2) 18

8.2 THREE-STORY OFFICE BUILDING WITH INTERMEDIATE PRECAST CONCRETE SHEAR WALLS 26

8.2.1 Building Description 27

8.2.2 Design Requirements 28

8.2.3 Load Combinations 29

8.2.4 Seismic Force Analysis 30

8.2.5 Proportioning and Detailing 33

8.3 ONE-STORY PRECAST SHEAR WALL BUILDING 45

8.3.1 Building Description 45

8.3.2 Design Requirements 48

8.3.3 Load Combinations 49

8.3.4 Seismic Force Analysis 50

8.3.5 Proportioning and Detailing 52

8.4 SPECIAL MOMENT FRAMES CONSTRUCTED USING PRECAST CONCRETE 65

8.4.1 Ductile Connections 65

8.4.2 Strong Connections 67

This chapter illustrates the seismic design of precast concrete members using the *NEHRP Recommended Provisions* (referred to herein as the *Provisions*) for buildings in several different seismic design categories. Over the past several years there has been a concerted effort to coordinate the requirements in the *Provisions* with those in ACI 318, so that now there are very few differences between the two. Very briefly, the *Provisions* set forth the following requirements for precast concrete structural systems.

- Precast seismic systems used in structures assigned to Seismic Design Category C must be intermediate or special moment frames, or intermediate precast or special structural walls.

- Precast seismic systems used in structures assigned to Seismic Design Category D must be special moment frames, or intermediate precast (up to 40 feet) or special structural walls.

- Precast seismic systems used in structures assigned to Seismic Design Category E or F must be special moment frames or special structural walls.

- Prestress provided by prestressing steel resisting earthquake-induced flexural and axial loads in frame members must be limited to 700 psi or $f'_c/6$ in plastic hinge regions. These values are different from the ACI 318 limitations, which are 500 psi or $f'_c/10$.

- An ordinary precast structural wall is defined as one that satisfies ACI 318 Chapters 1-18.

- An intermediate precast structural wall must meet additional requirements for its connections beyond those defined in ACI 318 Section 21.4. These include requirements for the design of wall piers that amplify the design shear forces and prescribe wall pier detailing and requirements for explicit consideration of the ductility capacity of yielding connections.

- A special structural wall constructed using precast concrete must satisfy the acceptance criteria defined in *Provisions* Section 9.6 if it doesn't meet the requirements for special structural walls constructed using precast concrete contained in ACI 318 Section 21.10.2.

Examples are provided for the following concepts:

- The example in Section 8.1 illustrates the design of untopped and topped precast concrete floor and roof diaphragms of the five-story masonry buildings described in Section 10.2 of this volume of design examples. The two untopped precast concrete diaphragms of Section 8.1.1 show the requirements for Seismic Design Categories B and C using 8-inch-thick hollow core precast, prestressed concrete planks. Section 8.1.2 shows the same precast plank with a 2-1/2-inch-thick composite lightweight concrete topping for the five-story masonry building in Seismic Design Category D described in Section 10.2. Although untopped diaphragms are commonly used in regions of low seismic hazard, their design is not specifically addressed in the *Provisions*, the *Standard*, or ACI 318.

- The example in Section 8.2 illustrates the design of an intermediate precast concrete shear wall building in a region of low or moderate seismicity, which is where many precast concrete seismic force-resisting systems are constructed. The precast concrete walls in this example resist the seismic forces for a three-story office building located in southern New England (Seismic Design Category B). The *Provisions* have a few requirements beyond those in ACI 318 and these requirements are identified in this example. Specifically, ACI 318 requires that in connections that are expected to yield, the yielding be restricted to steel elements or reinforcement. The *Provisions* also require that the deformation capacity of the connection be compared to the deformation demand on the connection unless Type 2 mechanical splices are used. There are

additional requirements for intermediate precast structural walls relating to wall piers; however, due to the geometry of the walls used in this design example, this concept is not described in the example.

- The example in Section 8.3 illustrates the design of a special precast concrete shear wall for a single-story industrial warehouse building in Los Angeles. For buildings assigned to Seismic Design Category D, the *Provisions* require that the precast seismic force-resisting system be designed and detailed to meet the requirements for either an intermediate or special precast concrete structural wall. The detailed requirements in the *Provisions* regarding explicit calculation of the deformation capacity of the yielding element are shown here.

- The example in Section 8.4 shows a partial example for the design of a special moment frame constructed using precast concrete per ACI 318 Section 21.8. Concepts for ductile and strong connections are presented and a detailed description of the calculations for a strong connection located at the beam-column interface is presented.

Tilt-up concrete wall buildings in all seismic zones have long been designed using the precast wall panels as concrete shear walls for the seismic force-resisting system. Such designs usually have been performed using design force coefficients and strength limits as if the precast walls emulated the performance of cast-in-place reinforced concrete shear walls, which they usually do not. Tilt-up buildings assigned to Seismic Design Category C or higher should be designed and detailed as intermediate or special precast structural wall systems as defined in ACI 318.

In addition to the *Provisions*, the following documents are either referred to directly or are useful design aids for precast concrete construction:

ACI 318	American Concrete Institute. 2008. *Building Code Requirements for Structural Concrete*.
AISC 360	American Institute of Steel Construction. 2005. *Specification for Structural Steel Buildings*.
AISC Manual	American Institute of Steel Construction. 2005. *Manual of Steel Construction,* Thirteen Edition.
Moustafa	Moustafa, Saad E. 1981 and 1982. "Effectiveness of Shear-Friction Reinforcement in Shear Diaphragm Capacity of Hollow-Core Slabs." *PCI Journal*, Vol. 26, No. 1 (Jan.-Feb. 1981) and the discussion contained in *PCI Journal*, Vol. 27, No. 3 (May-June 1982).
PCI Handbook	Precast/Prestressed Concrete Institute. 2004. *PCI Design Handbook,* Sixth Edition.
PCI Details	Precast/Prestressed Concrete Institute. 1988. *Design and Typical Details of Connections for Precast and Prestressed Concrete,* Second Edition.
SEAA Hollow Core	Structural Engineers Association of Arizona, Central Chapter. *Design and Detailing of Untopped Hollow-Core Slab Systems for Diaphragm Shear*.

The following style is used when referring to a section of ACI 318 for which a change or insertion is proposed by the *Provisions*: *Provisions* Section xxx (ACI 318 Sec. yyy) where "xxx" is the section in the *Provisions* and "yyy" is the section proposed for insertion into ACI 318.

8.1 HORIZONTAL DIAPHRAGMS

Structural diaphragms are horizontal or nearly horizontal elements, such as floors and roofs, that transfer seismic inertial forces to the vertical seismic force-resisting members. Precast concrete diaphragms may be constructed using topped or untopped precast elements depending on the Seismic Design Category. Reinforced concrete diaphragms constructed using untopped precast concrete elements are not addressed specifically in the *Standard*, in the *Provisions*, or in ACI 318. Topped precast concrete elements, which act compositely or noncompositely for gravity loads, are designed using the requirements of ACI 318 Section 21.11.

8.1.1 Untopped Precast Concrete Units for Five-Story Masonry Buildings Located in Birmingham, Alabama and New York, New York

This example illustrates floor and roof diaphragm design for five-story masonry buildings located in Birmingham, Alabama, on soft rock (Seismic Design Category B) and in New York, New York (Seismic Design Category C). The example in Section 10.2 provides design parameters used in this example. The floors and roofs of these buildings are to be untopped 8-inch-thick hollow core precast, prestressed concrete plank. Figure 10.2-1 shows the typical floor plan of the diaphragms.

8.1.1.1 General Design Requirements. In accordance with ACI 318, untopped precast diaphragms are permitted only in Seismic Design Categories A through C. Static rational models are used to determine shears and moments on joints as well as shear and tension/compression forces on connections. Dynamic modeling of seismic response is not required. Per ACI 318 Section 21.1.1.6, diaphragms in Seismic Design Categories D through F are required to meet ACI 318 Section 21.11, which does not allow untopped diaphragms. In previous versions of the *Provisions*, an appendix was presented that provided a framework for the design of untopped diaphragms in higher Seismic Design Categories in which diaphragms with untopped precast elements were designed to remain elastic and connections designed for limited ductility. However, in the 2009 *Provisions*, that appendix has been removed. Instead, a white paper describing emerging procedures for the design of such diaphragms has been included in Part 3 of the *Provisions*.

The design method used here is that proposed by Moustafa. This method makes use of the shear friction provisions of ACI 318 with the friction coefficient, μ, being equal to 1.0. To use $\mu = 1.0$, ACI 318 requires grout or concrete placed against hardened concrete to have clean, laitance free and intentionally roughened surfaces with a total amplitude of approximately 1/4 inch (peak to valley). Roughness for formed edges is provided either by sawtooth keys along the length of the plank or by hand roughening with chipping hammers. Details from the SEAA Hollow Core reference are used to develop the connection details. Note that grouted joints with edges not intentionally roughened can be used with $\mu = 0.6$.

The terminology used is defined in ACI 318 Section 2.2.

8.1.1.2 General In-Plane Seismic Design Forces for Untopped Diaphragms. For Seismic Design Categories B through F, *Standard* Section 12.10.1.1 defines a minimum diaphragm seismic design force.

For Seismic Design Categories C through F, *Standard* Section 12.10.2.1 requires that collector elements, collector splices and collector connections to the vertical seismic force-resisting members be designed in accordance with *Standard* Section 14.4.3.2, which amplifies design forces by means of the overstrength factor, Ω_o.

For Seismic Design Categories D, E and F, *Standard* Section 12.10.1.1 requires that the redundancy factor, ρ, be used on transfer forces only where the vertical seismic force-resisting system is offset and the diaphragm is required to transfer forces between the elements above and below, but need not be applied to inertial forces defined in *Standard* Equation 12.10-1.

Parameters from the example in Section 10.2 used to calculate in-plane seismic design forces for the diaphragms are provided in Table 8.1-1.

Table 8.1-1 Design Parameters from Example 10.2

Design Parameter	Birmingham 1	New York City
ρ	1.0	1.0
Ω_o	2.5	2.5
C_s	0.12	0.156
w_i (roof)	861 kips	869 kips
w_i (floor)	963 kips	978 kips
S_{DS}	0.24	0.39
I	1.0	1.0

1.0 kip = 4.45 kN.

8.1.1.3 Diaphragm Forces for Birmingham Building 1. The weight tributary to the roof and floor diaphragms (w_{px}) is the total story weight (w_i) at Level *i* minus the weight of the walls parallel to the direction of loading.

Compute diaphragm weight (w_{px}) for the roof and floor as follows:

- Roof:

Total weight	= 861 kips
Walls parallel to force = (45 psf)(277 ft)(8.67 ft / 2)	= -54 kips
w_{px}	= 807 kips

- Floors:

Total weight	= 963 kips
Walls parallel to force = (45 psf)(277 ft)(8.67 ft)	= -108 kips
w_{px}	= 855 kips

Compute diaphragm demands in accordance with *Standard* Equation 12.10-1:

$$F_{px} = \frac{\sum_{i=x}^{n} F_i}{\sum_{i=x}^{n} w_i} w_{px}$$

Calculations for F_{px} are provided in Table 8.1-2.

Table 8.1-2 Birmingham 1 F_{px} Calculations

Level	w_i (kips)	$\sum_{i=x}^{n} w_i$ (kips)	F_i (kips)	$\sum_{i=x}^{n} F_i = V_i$ (kips)	w_{px} (kips)	F_{px} (kips)
Roof	861	861	175	175	807	164
4	963	1,824	156	331	855	155
3	963	2,787	117	448	855	137
2	963	3,750	78	526	855	120
1	963	4,713	39	565	855	103

1.0 kip = 4.45 kN.

The values for F_i and V_i used in Table 8.1-2 are listed in Table 10.2-2.

The minimum value of $F_{px} = 0.2S_{DS}Iw_{px}$ = 0.2(0.24)1.0(807 kips) = 38.7 kips (roof)
= 0.2(0.24)1.0(855 kips) = 41.0 kips (floors)

The maximum value of $F_{px} = 0.4S_{DS}Iw_{px}$ = 2(38.7 kips) = 77.5 kips (roof)
= 2(41.0 kips) = 82.1 kips (floors)

Note that the calculated F_{px} in Table 8.1-2 is substantially larger than the specified maximum limit value of F_{px}. This is generally true at upper levels if the R factor is less than 5.

To simplify the design, the diaphragm design force used for all levels will be the maximum force at any level, 82 kips.

8.1.1.4 Diaphragm Forces for New York Building. The weight tributary to the roof and floor diaphragms (w_{px}) is the total story weight (w_i) at Level i minus the weight of the walls parallel to the force.

Compute diaphragm weight (w_{px}) for the roof and floor as follows:

- Roof:

Total weight	=	870 kips
Walls parallel to force = (48 psf)(277 ft)(8.67 ft / 2)	=	-58 kips
w_{px}	=	812 kips

- Floors:

Total weight	=	978 kips
Walls parallel to force = (48 psf)(277 ft)(8.67 ft)	=	-115 kips
w_{px}	=	863 kips

Calculations for F_{px} are provided in Table 8.1-3.

Table 8.1-3 New York F_{px} Calculations

Level	w_i (kips)	$\sum_{i=x}^{n} w_i$ (kips)	F_i (kips)	$\sum_{i=x}^{n} F_i = V_i$ (kips)	w_{px} (kips)	F_{px} (kips)
Roof	870	870	229	229	812	214
4	978	1,848	207	436	863	204
3	978	2,826	155	591	863	180
2	978	3,804	103	694	863	157
1	978	4,782	52	746	863	135

1.0 kip = 4.45 kN.

The values for F_i and V_i used in Table 8.1-3 are listed in Table 10.2-7.

The minimum value of $F_{px} = 0.2S_{DS}Iw_{px}$	= 0.2(0.39)1.0(870 kips)	= 67.9 kips (roof)
	= 0.2(0.39)1.0(978 kips)	= 76.3 kips (floors)
The maximum value of $F_{px} = 0.4S_{DS}Iw_{px}$	= 2(67.9 kips)	= 135.8 kips (roof)
	= 2(76.3 kips)	= 152.6 kips (floors)

As for the Birmingham example, note that the calculated F_{px} given in Table 8.1-3 is substantially larger than the specified maximum limit value of F_{px}.

To simplify the design, the diaphragm design force used for all levels will be the maximum force at any level, 153 kips.

8.1.1.5 Static Analysis of Diaphragms. The balance of this example will use the controlling diaphragm seismic design force of 153 kips for the New York building. In the transverse direction, the loads will be distributed as shown in Figure 8.1-1.

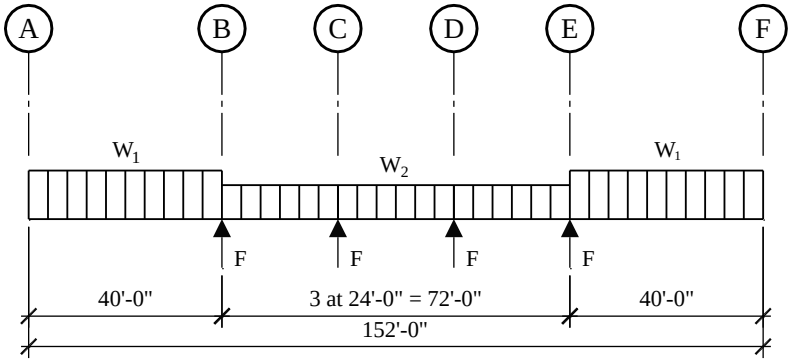

Figure 8.1-1 Diaphragm force distribution and analytical model
(1.0 ft = 0.3048 m)

The *Standard* requires that structural analysis consider the relative stiffness of the diaphragms and the vertical elements of the seismic force-resisting system. Since a pretopped precast diaphragm doesn't satisfy the conditions of either the flexible or rigid diaphragm conditions identified in the *Standard*, maximum in-plane deflections of the diaphragm must be evaluated. However, that analysis is beyond the scope of this document. Therefore, with a rigid diaphragm assumption, assuming the four shear walls have the same stiffness and ignoring torsion, the diaphragm reactions at the transverse shear walls (*F* as shown in Figure 8.1-1) are computed as follows:

F = 153 kips/4 = 38.3 kips

The uniform diaphragm demands are proportional to the distributed weights of the diaphragm in different areas (see Figure 8.1-1).

W_1 = [67 psf (72 ft) + 48 psf (8.67 ft)4](153 kips / 863 kips) = 1,150 lb/ft

W_2 = [67 psf (72 ft)](153 kips / 863 kips) = 855 lb/ft

Figure 8.1-2 identifies critical regions of the diaphragm to be considered in this design. These regions are:

- Joint 1: Maximum transverse shear parallel to the panels at panel-to-panel joints
- Joint 2: Maximum transverse shear parallel to the panels at the panel-to-wall joint
- Joint 3: Maximum transverse moment and chord force
- Joint 4: Maximum longitudinal shear perpendicular to the panels at the panel-to-wall connection (exterior longitudinal walls) and anchorage of exterior masonry wall to the diaphragm for out-of-plane forces
- Joint 5: Collector element and shear for the interior longitudinal walls

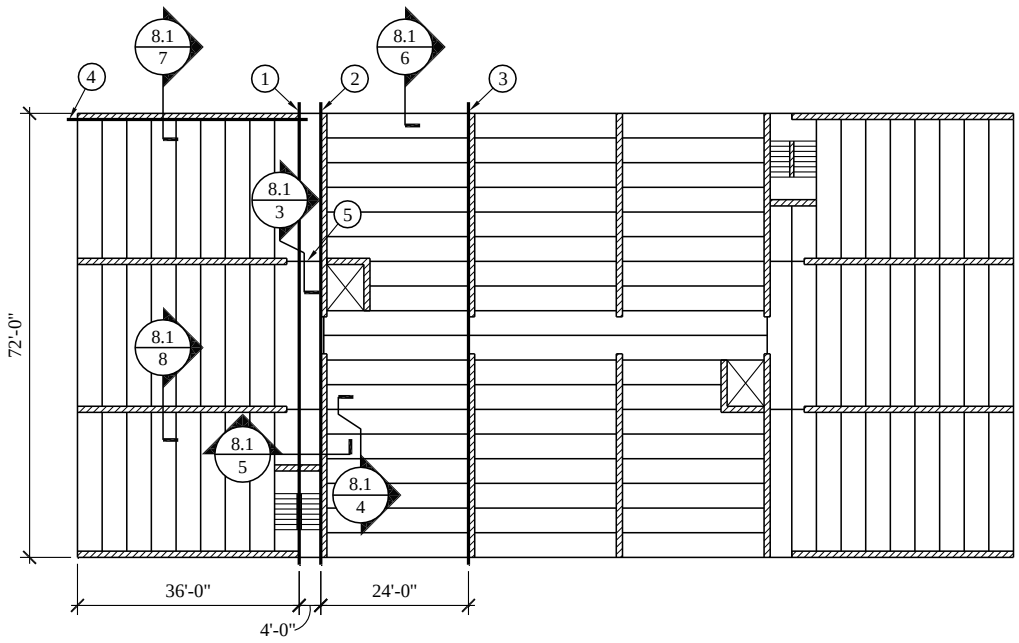

Figure 8.1-2 Diaphragm plan and critical design regions
(1.0 ft = 0.3048 m)

Joint forces are as follows:

- Joint 1 – Transverse forces:

  Shear, V_{u1} = 1.15 kips/ft (36 ft) = 41.4 kips
  Moment, M_{u1} = 41.4 kips (36 ft / 2) = 745 ft-kips
  Chord tension force, $T_{u1} = M/d$ = 745 ft-kips / 71 ft = 10.5 kips

- Joint 2 – Transverse forces:

  Shear, V_{u2} = 1.15 kips/ft (40 ft) = 46 kips
  Moment, M_{u2} = 46 kips (40 ft / 2) = 920 ft-kips
  Chord tension force, $T_{u2} = M/d$ = 920 ft-kips / 71 ft = 13.0 kips

- Joint 3 – Transverse forces:

  Shear, V_{u3} = 46 kips + 0.86 kips/ft (24 ft) – 38.3 kips = 28.3 kips
  Moment, M_{u3} = 46 kips (44 ft) + 20.6 kips (12 ft) - 38.3 kips (24 ft) = 1,352 ft-kips
  Chord tension force, $T_{u3} = M/d$ = 1,352 ft-kips / 71 ft = 19.0 kips

- Joint 4 – Longitudinal forces:

  Wall force, F = 153 kips / 8 = 19.1 kips
  Wall shear along wall length, V_{u4} = 19.1 kips (36 ft)/(152 ft / 2) = 9.0 kips
  Collector force at wall end, $T_{u4} = C_{u4}$ = 19.1 kips - 9.0 kips = 10.1 kips

- Joint 4 – Out-of-plane forces:

The ***Standard*** has several requirements for out-of-plane forces. None are unique to precast diaphragms and all are less than the requirements in ACI 318 for precast construction regardless of seismic considerations. Assuming the planks are similar to beams and comply with the minimum requirements of ***Standard*** Section 12.14 (Seismic Design Category B and greater), the required out-of-plane horizontal force is:

$0.05(D+L)_{plank} = 0.05(67 \text{ psf} + 40 \text{ psf})(24 \text{ ft} / 2) = 64.2 \text{ plf}$

According to ***Standard*** Section 12.11.2 (Seismic Design Category B and greater), the minimum anchorage for masonry walls is:

$400(S_{DS})(I) = 400(0.39)1.0 = 156 \text{ plf}$

According to ***Standard*** Section 12.11.1 (Seismic Design Category B and greater), bearing wall anchorage must be designed for a force computed as:

$0.4(S_{DS})(W_{wall}) = 0.4(0.39)(48 \text{ psf})(8.67 \text{ ft}) = 64.9 \text{ plf}$

Standard Section 12.11.2.1 (Seismic Design Category C and greater) requires masonry wall anchorage to flexible diaphragms to be designed for a larger force. Due to its geometry, this diaphragm is likely to be classified as rigid. However, the relative deformations of the wall and diaphragm must be checked in accordance with ***Standard*** Section 12.3.1.3 to validate this assumption.

$F_p = 0.85(S_{DS})(I)(W_{wall}) = 0.85(0.39)1.0[(48 \text{ psf})(8.67 \text{ ft})] = 138 \text{ plf}$

(Note that since this diaphragm is not flexible, this load is not used in the following calculations.)

The force requirements in ACI 318 Section 16.5 will be described later.

- Joint 5 – Longitudinal forces:

Wall force, $F = 153 \text{ kips} / 8 = 19.1 \text{ kips}$
Wall shear along each side of wall, $V_{u5} = 19.1 \text{ kips } [2(36 \text{ ft}) / 152 \text{ ft}]/2 = 4.5 \text{ kips}$
Collector force at wall end, $T_{u5} = C_{u5} = 19.1 \text{ kips} - 2(4.5 \text{ kips}) = 10.1 \text{ kips}$

- Joint 5 – Shear flow due to transverse forces:

Shear at Joint 2, $V_{u2} = 46 \text{ kips}$
$Q = A\,d$
$A = (0.67 \text{ ft})(24 \text{ ft}) = 16 \text{ ft}^2$
$d = 24 \text{ ft}$
$Q = (16 \text{ ft}^2)(24 \text{ ft}) = 384 \text{ ft}^3$
$I = (0.67 \text{ ft})(72 \text{ ft})^3 / 12 = 20{,}840 \text{ ft}^4$
$V_{u2}Q/I = (46 \text{ kip})(384 \text{ ft}^3) / 20{,}840 \text{ ft}^4 = 0.847 \text{ kip/ft}$ maximum shear flow
Joint 5 length = 40 ft
Total transverse shear in joint 5, $V_{u5} = 0.847 \text{ kip/ft})(40 \text{ ft})/2 = 17 \text{ kips}$

ACI 318 Section 16.5 also has minimum connection force requirements for structural integrity of precast concrete bearing wall building construction. For buildings over two stories tall, there are force

requirements for horizontal and vertical members. This building has no vertical precast members. However, ACI 318 Section 16.5.1 specifies that the strengths "... for structural integrity shall apply to all precast concrete structures." This is interpreted to apply to the precast elements of this masonry bearing wall structure. The horizontal tie force requirements for a precast bearing wall structure three or more stories in height are:

- 1,500 pounds per foot parallel and perpendicular to the span of the floor members. The maximum spacing of ties parallel to the span is 10 feet. The maximum spacing of ties perpendicular to the span is the distance between supporting walls or beams.

- 16,000 pounds parallel to the perimeter of a floor or roof located within 4 feet of the edge at all edges.

ACI's tie forces are far greater than the minimum tie forces given in the ***Standard*** for beam supports and anchorage of masonry walls. They do control some of the reinforcement provided, but most of the reinforcement is controlled by the computed connections for diaphragm action.

8.1.1.6 Diaphragm Design and Details. The phi factors used for this example are as follows:

- Tension control (bending and ties): $\phi = 0.90$

- Shear: $\phi = 0.75$

- Compression control in tied members: $\phi = 0.65$

The minimum tie force requirements given in ACI 318 Section 16.5 are specified as nominal values, meaning that $\phi = 1.00$ for those forces.

Note that although buildings assigned to Seismic Design Category C are not required to meet ACI 318 Section 21.11, some of the requirements contained therein are applied below as good practice but shown as optional.

8.1.1.6.1 Joint 1 Design and Detailing. The design must provide sufficient reinforcement for chord forces as well as shear friction connection forces, as follows:

- Chord reinforcement, $A_{s1} = T_{u1}/\phi f_y$ = (10.5 kips)/[0.9(60 ksi)] = 0.19 in^2 (The collector force from the Joint 4 calculations at 10.1 kips is not directly additive.)

- Shear friction reinforcement, $A_{vf1} = V_{u1}/\phi\mu f_y$ = (41.4 kips)/[(0.75)(1.0)(60 ksi)] = 0.92 in^2

- Total reinforcement required = 2(0.19 in^2) + 0.92 in^2 = 1.30 in^2

- ACI tie force = (1.5 kips/ft)(72 ft) = 108 kips; reinforcement = (108 kips)/(60 ksi) = 1.80 in^2

Provide four #5 bars (two at each of the outside edges) plus four #4 bars (two each at the interior joint at the ends of the plank) for a total area of reinforcement of 4(0.31 in^2) + 4(0.2 in^2) = 2.04 in^2.

Because the interior joint reinforcement acts as the collector reinforcement in the longitudinal direction for the interior longitudinal walls, the cover and spacing of the two #4 bars in the interior joints will be provided to meet the requirements of ACI 318 Section 21.11.7.6 (optional):

- Minimum cover = 2.5(4/8) = 1.25 in., but not less than 2.00 in.
- Minimum spacing = 3(4/8) = 1.50 in., but not less than 1.50 in.

Figure 8.1-3 shows the reinforcement in the interior joints at the ends of the plank, which is also the collector reinforcement for the interior longitudinal walls (Joint 5). The two #4 bars extend along the length of the interior longitudinal walls as shown in Figure 8.1-3.

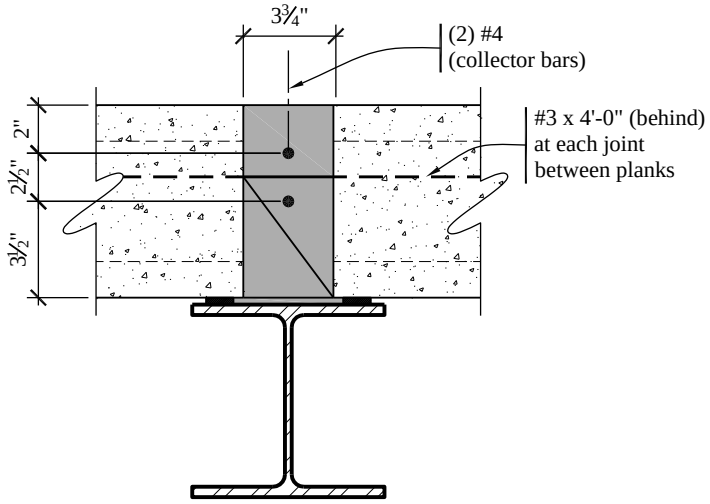

Figure 8.1-3 Interior joint reinforcement at the ends of plank and collector reinforcement at the end of the interior longitudinal walls - Joints 1 and 5
(1.0 in. = 25.4 mm)

Figure 8.1-4 shows the extension of the two #4 bars of Figure 8.1-3 into the region where the plank is parallel to the bars (see section cut on Figure 8.1-2). The bars will need to be extended the full length of the diaphragm unless supplemental plank reinforcement is provided. This detail makes use of this supplement plank reinforcement (two #4 bars or an equal area of strand) and shows the bars anchored at each end of the plank. The anchorage length of the #4 bars is calculated using ACI 318 Chapter 12:

$$l_d = \left(\frac{f_y \psi_t \psi_e}{25\lambda\sqrt{f_c'}} \right) d_b = \left(\frac{60{,}000\,\text{psi}\,(1.0)(1.0)}{25(1.0)\sqrt{4{,}000}\,\text{psi}} \right) d_b = 37.9 d_b$$

Using #4 bars, the required l_d = 37.9(0.5 in.) = 18.9 in. Therefore, use l_d = 4 ft, which is the width of the plank.

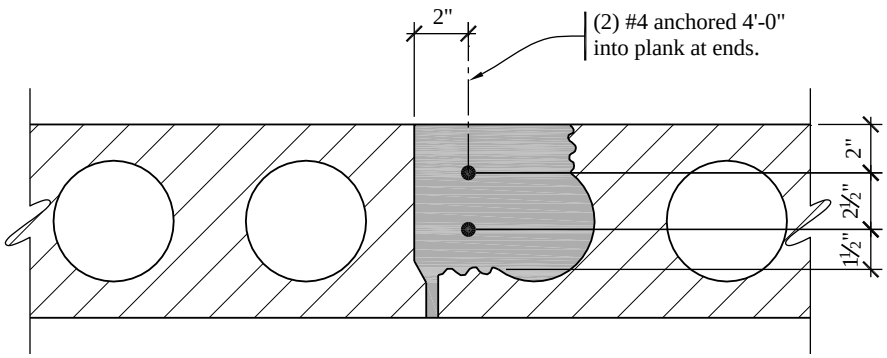

Figure 8.1-4 Anchorage region of shear reinforcement for Joint 1 and collector reinforcement for Joint 5
(1.0 in. = 25.4 mm)

8.1.1.6.2 Joint 2 Design and Detailing. The chord design is similar to the previous calculations:

- Chord reinforcement, $A_{s2} = T_{u2}/\phi f_y$ = (13.0 kips)/[0.9(60 ksi)] = 0.24 in^2

The shear force may be reduced along Joint 2 by the shear friction resistance provided by the supplemental chord reinforcement ($2A_{chord} - A_{s2}$) and by the four #4 bars projecting from the interior longitudinal walls across this joint. The supplemental chord bars, which are located at the end of the walls, are conservatively excluded here. The shear force along the outer joint of the wall where the plank is parallel to the wall is modified as follows:

$$V_{u2}^{Mod} = V_{u2} - \left[\phi f_y \mu \left(A_{4\#4}\right)\right] = 46 - \left[0.75\left(60\,\text{ksi}\right)\left(1.0\right)\left(4 \times 0.2\,\text{in}^2\right)\right] = 36.0 \text{ kips}$$

This force must be transferred from the planks to the wall. Using the arrangement shown in Figure 8.1-5, the required shear friction reinforcement (A_{vf2}) is computed as:

$$A_{vf\,2} = \frac{V_{u2}^{Mod}}{\phi f_y \left(\mu \sin\alpha_f + \cos\alpha_f\right)} = \frac{36.0\,\text{kips}}{0.75\left(1.0\sin 26.6° + \cos 26.6°\right)} = 0.60\,\text{in}^2$$

Use two #3 bars placed at 26.6 degrees (2-to-1 slope) across the joint at 6 feet from the ends of the plank (two sets per plank). The angle (α_f) used above provides development of the #3 bars while limiting the grouting to the outside core of the plank. The total shear reinforcement provided is 6(0.11 in^2) = 0.66 in^2. Note that the spacing of these connectors will have to be adjusted at the stair location.

The shear force between the other face of this wall and the diaphragm is:

V_{u2}-F = 46-38.3 = 7.7 kips

The shear friction resistance provided by #3 bars in the grout key between each plank (provided for the 1.5 klf requirement of ACI 318) is computed as:

$\phi A_{vf} f_y \mu$ = (0.75)(10 bars)(0.11 in^2)(60 ksi)(1.0) = 49.5 kips

The development length of the #3 bars will now be checked. For the 180 degree standard hook, use ACI 318 Section 12.5, l_{dh} times the factors of ACI 318 Section 12.5.3, but not less than $8d_b$ or 6 inches. Side cover exceeds 2-1/2 inches and cover on the bar extension beyond the hook is provided by the grout and the planks, which is close enough to 2 inches to apply the 0.7 factor of ACI 318 Section 12.5.3. For the #3 hook:

$$l_{dh} = 0.7\left(\frac{0.02\psi_e f_y}{\sqrt{f_c'}}\right)d_b = 0.7\left(\frac{0.02(1.0)(60{,}000\,\text{psi})}{\sqrt{4{,}000}\,\text{psi}}\right)0.375 = 4.98 \text{ in. } (\leq 6 \text{ in. minimum})$$

The available distance for the perpendicular hook is approximately 5-1/2 inches. The bar will not be fully developed at the end of the plank because of the 6-inch minimum requirement. The full strength is not required for shear transfer. By inspection, the diagonal #3 hook will be developed in the wall as required for the computed diaphragm-to-shear-wall transfer. The straight end of the #3 bar will now be checked. The standard development length of ACI 318 Section 12.2 is used for l_d.

$$l_d = \frac{f_y d_b}{25\sqrt{f_c'}} = \frac{60{,}000(0.375)}{25\sqrt{4{,}000}} = 14.2 \text{ in.}$$

Figure 8.1-5 shows the reinforcement along each side of the wall on Joint 2.

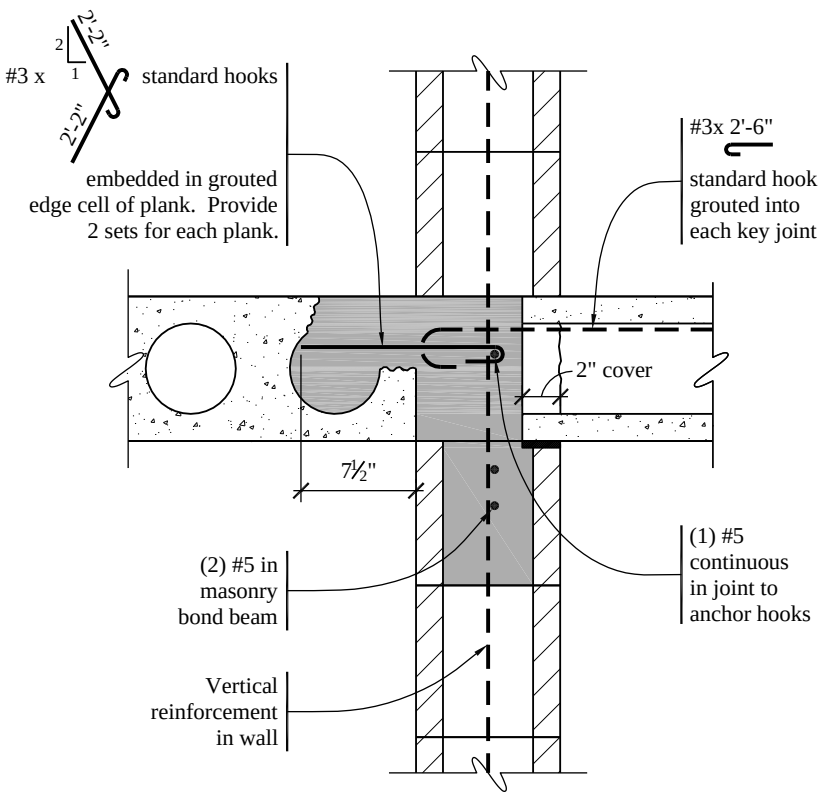

Figure 8.1-5 Joint 2 transverse wall joint reinforcement
(1.0 in. = 25.4 mm, 1.0 ft = 0.3048 m)

8.1.1.6.3 Design and Detailing at Joint 3. Compute the required amount of chord reinforcement at Joint 3 as:

$$A_{s3} = T_{u3}/\phi f_y = (19.0 \text{ kips})/[0.9(60 \text{ ksi})] = 0.35 \text{ in}^2$$

Use two #4 bars, $A_s = 2(0.20) = 0.40$ in^2 along the exterior edges (top and bottom of the plan in Figure 8.1-2). Require cover for chord bars and spacing between bars at splices and anchorage zones per ACI 318 Section 21.11.7.6 (optional).

- Minimum cover = 2.5(4/8) = 1.25 in., but not less than 2.00 in.
- Minimum spacing = 3(4/8) = 1.50 in., but not less than 1.50 in.

Figure 8.1-6 shows the chord element at the exterior edges of the diaphragm. The chord bars extend along the length of the exterior longitudinal walls and act as collectors for these walls in the longitudinal direction (see the Joint 4 collector reinforcement calculations and Figure 8.1-7).

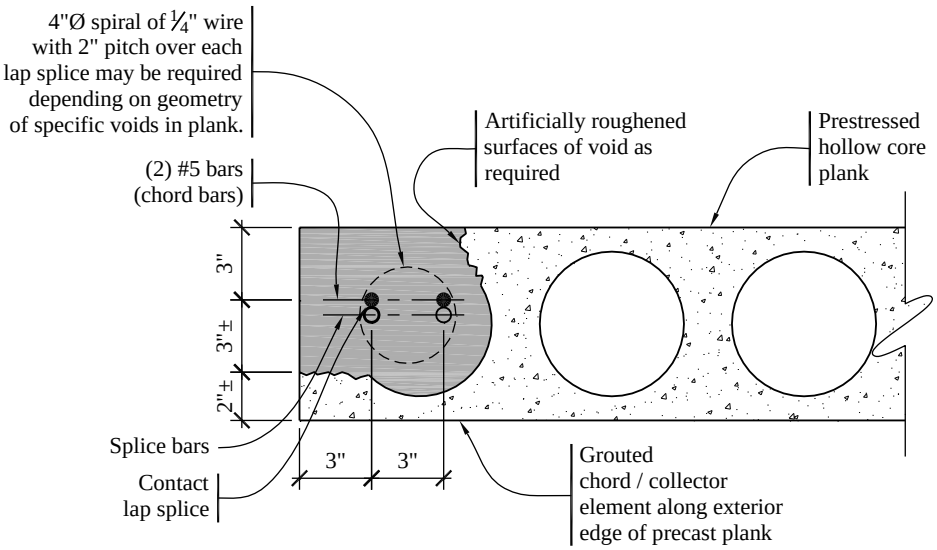

Figure 8.1-6 Joint 3 chord reinforcement at the exterior edge (1.0 in. = 25.4 mm)

Joint 3 must also be checked for the minimum ACI tie forces. The chord reinforcement obviously exceeds the 16 kip perimeter force requirement. To satisfy the 1.5 kips per foot requirement, a 6 kip tie is needed at each joint between the planks, which is satisfied with a #3 bar in each joint (0.11 in^2 at 60 ksi = 6.6 kips). This bar is required at all bearing walls and is shown in subsequent details.

8.1.1.6.4 Joint 4 Design and Detailing. The required shear friction reinforcement along the wall length is computed as:

$$A_{vf4} = V_{u4}/\phi\mu f_y = (9.0 \text{ kips})/[(0.75)(1.0)(60 \text{ ksi})] = 0.20 \text{ in}^2$$

Based upon the ACI tie requirement, provide #3 bars at each plank-to-plank joint. For eight bars total, the area of reinforcement is 8(0.11) = 0.88 in^2, which is more than sufficient even considering the marginal development length, which is less favorable at Joint 2. The bars are extended 2 feet into the grout key, which is more than the development length and equal to half the width of the plank.

The required collector reinforcement is computed as:

$$A_{s4} = T_{u4}/\phi f_y = (10.1 \text{ kips})/[0.9(60 \text{ ksi})] = 0.19 \text{ in}^2$$

The two #4 bars, which are an extension of the transverse chord reinforcement, provide an area of reinforcement of 0.40 in^2.

The reinforcement required by the *Standard* for out-of-plane force (156 plf) is far less than the ACI 318 requirement.

Figure 8.1-7 shows this joint along the wall.

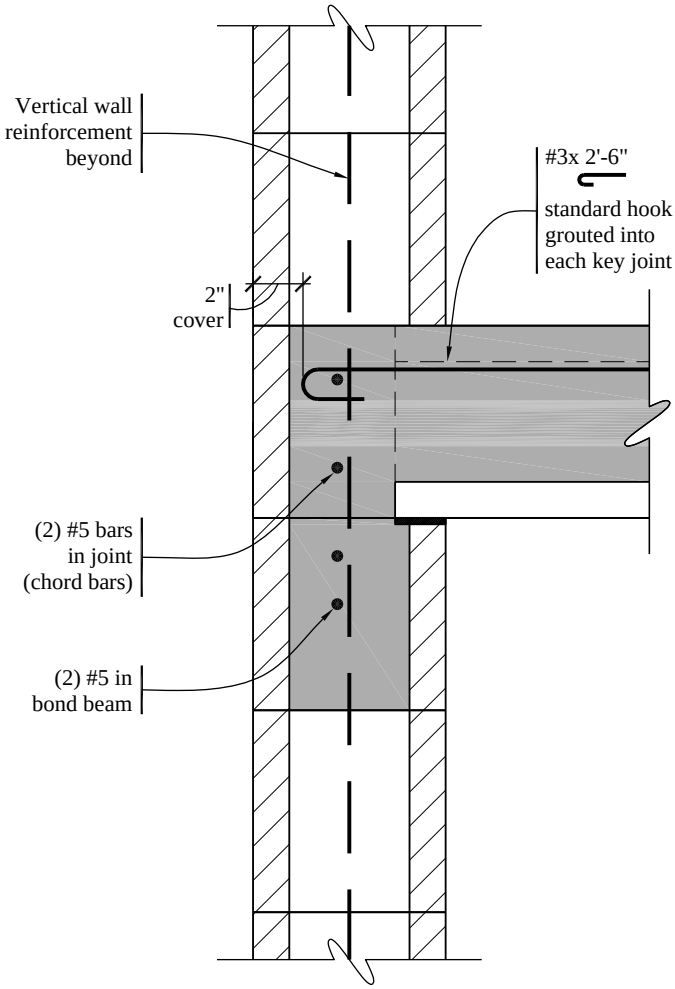

Figure 8.1-7 Joint 4 exterior longitudinal walls to diaphragm reinforcement and out-of-plane anchorage
(1.0 in. = 25.4 mm, 1.0 ft = 0.3048 m)

8.1.1.6.5 Joint 5 Design and Detailing. The required shear friction reinforcement along the wall length is computed as:

$$A_{vf5} = V_{u5}/\phi\mu f_y = (16.9 \text{ kips})/[(0.75)(1.0)(0.85)(60 \text{ ksi})] = 0.44 \text{ in}^2$$

Provide #3 bars at each plank-to-plank joint for a total of 8 bars.

The required collector reinforcement is computed as:

$$A_{s5} = T_{u5}/\phi f_y = (10.1 \text{ kips})/[0.9(60 \text{ ksi})] = 0.19 \text{ in}^2$$

Two #4 bars specified for the design of Joint 1 above provide an area of reinforcement of 0.40 in^2. Figure 8.1-8 shows this joint along the wall.

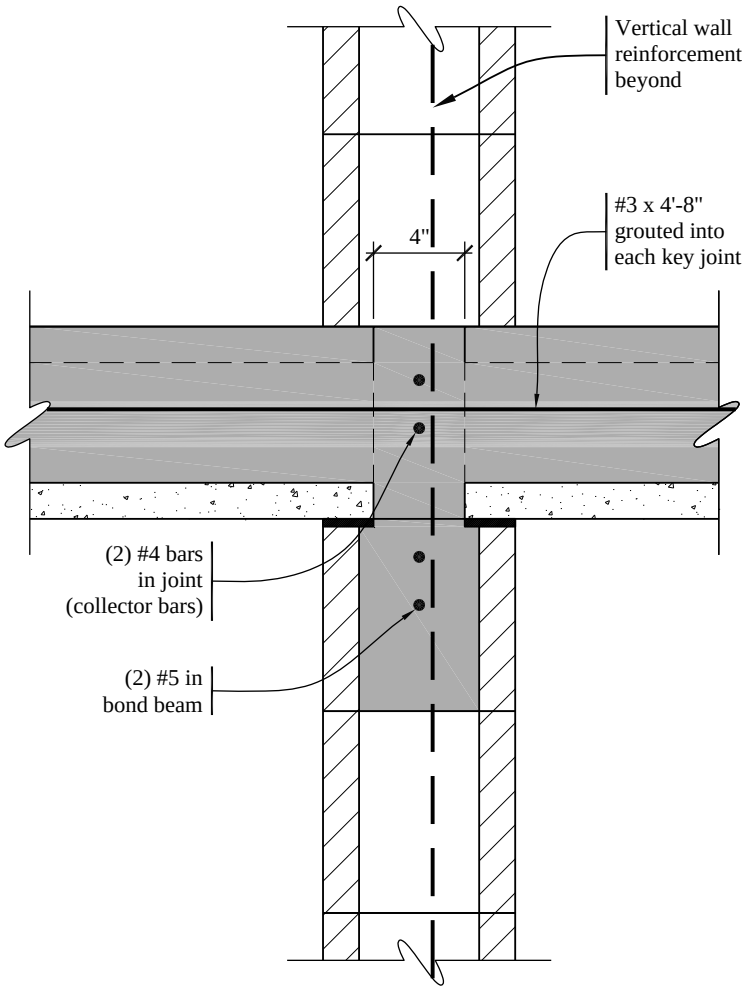

Figure 8.1-8 Wall-to-diaphragm reinforcement along interior longitudinal walls - Joint 5
(1.0 in. = 25.4 mm, 1.0 ft = 0.3048 m)

8.1.2 Topped Precast Concrete Units for Five-Story Masonry Building Located in Los Angeles, California (see Sec. 10.2)

This design shows the floor and roof diaphragms using topped precast units in the five-story masonry building in Los Angeles, California. The topping thickness exceeds the minimum thickness of 2 inches as required for composite topping slabs by ACI 318 Section 21.11.6. The topping is lightweight concrete (weight = 115 pcf) with a 28-day compressive strength (f'_c) of 4,000 psi and is to act compositely with the 8-inch-thick hollow-core precast, prestressed concrete plank. Design parameters are provided in Section 10.2. Figure 10.2-1 shows the typical floor and roof plan.

8.1.2.1 General Design Requirements. Topped diaphragms may be used in any Seismic Design Category. ACI 318 Section 21.11 provides design provisions for topped precast concrete diaphragms. *Standard* Section 12.10 specifies the forces to be used in designing the diaphragms.

8.1.2.2 General In-Plane Seismic Design Forces for Topped Diaphragms. The in-plane diaphragm seismic design force (F_{px}) is calculated using *Standard* Equation 12.10-1 but must not be less than $0.2S_{DS}Iw_{px}$ and need not be more than $0.4S_{DS}Iw_{px}$. V_x must be added to F_{px} calculated using Equation 12.10-1 where:

S_{DS} = the spectral response acceleration parameter at short periods

I = occupancy importance factor

w_{px} = the weight tributary to the diaphragm at Level x

V_x = the portion of the seismic shear force required to be transferred to the components of the vertical seismic force-resisting system due to offsets or changes in stiffness of the vertical resisting member at the diaphragm being designed

For Seismic Design Category C and higher, *Standard* Section 12.10.2.1 requires that collector elements, collector splices and collector connections to the vertical seismic force-resisting members be designed in accordance with *Standard* Section 12.4.3.2, which combines the diaphragm forces times the overstrength factor (Ω_0) and the effects of gravity forces. The parameters from the example in Section 10.2 used to calculate in-plane seismic design forces for the diaphragms are provided in Table 8.1-4.

Table 8.1-4 Design Parameters from Section 10.2

Design Parameter	Value
Ω_o	2.5
w_i (roof)	1,166 kips
w_i (floor)	1,302 kips
S_{DS}	1.0
I	1.0
Seismic Design Category	D

1.0 kip = 4.45 kN.

8.1.2.3 Diaphragm Forces. As indicated previously, the weight tributary to the roof and floor diaphragms (w_{px}) is the total story weight (w_i) at Level i minus the weight of the walls parallel to the force.

Compute diaphragm weight (w_{px}) for the roof and floor as follows:

- Roof:

Total weight	= 1,166 kips
Walls parallel to force = (60 psf)(277 ft)(8.67 ft / 2)	= -72 kips
w_{px}	= 1,094 kips

- Floors:

Total weight	= 1,302 kips
Walls parallel to force = (60 psf)(277 ft)(8.67 ft)	= -144 kips
w_{px}	= 1,158 kips

Compute diaphragm demands in accordance with *Standard* Equation 12.10-1:

$$F_{px} = \frac{\sum_{i=x}^{n} F_i}{\sum_{i=x}^{n} w_i} w_{px}$$

Calculations for F_{px} are provided in Table 8.1-5. The values for F_i and V_i are listed in Table 10.2-17.

Table 8.1-5 F_{px} Calculations from Section 10.2

Level	w_i (kips)	$\sum_{i=x}^{n} w_i$ (kips)	F_i (kips)	$\sum_{i=x}^{n} F_i = V_i$ (kips)	w_{px} (kips)	F_{px} (kips)
Roof	1,166	1,166	564	564	1,094	529
4	1,302	2,468	504	1,068	1,158	501
3	1,302	3,770	378	1,446	1,158	444
2	1,302	5,072	252	1,698	1,158	387
1	1,302	6,374	126	1,824	1,158	331

1.0 kip = 4.45 kN.

The minimum value of $F_{px} = 0.2S_{DS}Iw_{px}$	= 0.2(1.0)1.0(1,094 kips)	= 219 kips (roof)
	= 0.2(1.0)1.0(1,158 kips)	= 232 kips (floors)
The maximum value of $F_{px} = 0.4S_{DS}Iw_{px}$	= 2(219 kips)	= 438 kips (roof)
	= 2(232 kips)	= 463 kips (floors)

The value of F_{px} used for design of the diaphragms is 463 kips, except for collector elements where forces will be computed below.

8.1.2.4 Static Analysis of Diaphragms. The seismic design force of 463 kips is distributed as in Section 8.1.1.6 (Figure 8.1-1 shows the distribution). The force is three times higher than that used to design the untopped diaphragm for the New York design due to the higher seismic demand. Figure 8.1-2 shows critical regions of the diaphragm to be considered in this design. Collector elements will be designed for 2.5 times the diaphragm force based on the overstrength factor (Ω_0).

Joint forces taken from Section 8.1.1.5 times 3.0 are as follows:

- Joint 1 – Transverse forces:

  Shear, V_{u1} = 41.4 kips × 3.0 = 124 kips
  Moment, M_{u1} = 745 ft-kips × 3.0 = 2,235 ft-kips
  Chord tension force, $T_{u1} = M/d$ = 2,235 ft-kips / 71 ft = 31.5 kips

- Joint 2 – Transverse forces:

  Shear, V_{u2} = 46 kips × 3.0 = 138 kips
  Moment, M_{u2} = 920 ft-kips × 3.0 = 2,760 ft-kips
  Chord tension force, $T_{u2} = M/d$ = 2,760 ft-kips / 71 ft = 38.9 kips

- Joint 3 – Transverse forces:

  Shear, V_{u3} = 28.3 kips × 3.0 = 84.9 kips
  Moment, M_{u2} = 1,352 ft-kips × 3.0 = 4,056 ft-kips
  Chord tension force, $T_{u3} = M/d$ = 4,056 ft-kips / 71 ft = 57.1 kips

- Joint 4 – Longitudinal forces:

  Wall force, F = 19.1 kips × 3.0 = 57.3 kips
  Wall shear along wall length, V_{u4} = 9 kips × 3.0 = 27.0 kips
  Collector force at wall end, $\Omega_0 T_{u4}$ = 2.5(10.1 kips)(3.0) = 75.8 kips

- Joint 4 – Out-of-plane forces:

  Just as with the untopped diaphragm, the out-of-plane forces are controlled by ACI 318 Section 16.5, which requires horizontal ties of 1.5 kips per foot from floor to walls.

- Joint 5 – Longitudinal forces:

  Wall force, F = 463 kips / 8 walls = 57.9 kips
  Wall shear along each side of wall, V_{u4} = 4.5 kips × 3.0 = 13.5 kips
  Collector force at wall end, $\Omega_0 T_{u4}$ = 2.5(10.1 kips)(3.0) = 75.8 kips

- Joint 5 – Shear flow due to transverse forces:

  Shear at Joint 2, V_{u2} = 138 kips
  $Q = A\,d$
  A = (0.67 ft) (24 ft) = 16 ft^2
  d = 24 ft
  Q = (16 ft^2) (24 ft) = 384 ft^3
  I = (0.67 ft) (72 ft)^3 / 12 = 20,840 ft^4
  $V_{u2}Q/I$ = (138 kip) (384 ft^3) / 20,840 ft^4 = 2.54 kips/ft maximum shear flow
  Joint 5 length = 40 ft
  Total transverse shear in joint 5, V_{u5} = 2.54 kips/ft) (40 ft)/2 = 50.8 kips

8.1.2.5 Diaphragm Design and Details

8.1.2.5.1 Minimum Reinforcement for 2.5-inch Topping. ACI 318 Section 21.11.7.1 references ACI 318 Section 7.12, which requires a minimum $A_s = 0.0018bd$ for grade 60 welded wire reinforcement. For a 2.5-inch topping, the required $A_s = 0.054$ in^2/ft. WWR 10×10 - W4.5×W4.5 provides 0.054 in^2/ft. The minimum spacing of wires is 10 inches and the maximum spacing is 18 inches. Note that the ACI 318 Section 7.12 limit on spacing of five times thickness is interpreted such that the topping thickness is not the pertinent thickness.

8.1.2.5.2 Boundary Members. Joint 3 has the maximum bending moment and is used to determine the boundary member reinforcement of the chord along the exterior edge. The need for transverse boundary member reinforcement is reviewed using ACI 318 Section 21.11.7.5. Calculate the compressive stress in the chord with the ultimate moment using a linear elastic model and gross section properties of the topping. It is conservative to ignore the precast units, but this is not necessary since the joints between precast units are grouted. As developed previously, the chord compressive stress is:

$$6M_{u3}/td^2 = 6(4{,}056\times12)/(2.5)(72\times12)^2 = 157 \text{ psi}$$

The chord compressive stress is less than $0.2f'_c = 0.2(4{,}000) = 800$ psi. Transverse reinforcement in the boundary member is not required.

The required chord reinforcement is:

$$A_{s3} = T_{u3}/\phi f_y = (57.1 \text{ kips})/[0.9(60 \text{ ksi})] = 1.06 \text{ in}^2$$

8.1.2.5.3 Collectors. The design for Joint 4 collector reinforcement at the end of the exterior longitudinal walls and for Joint 5 at the interior longitudinal walls is the same.

$$A_{s4} = A_{s5} = \Omega_0 T_{u4}/\phi f_y = (75.8 \text{ kips})/[0.9(60 \text{ ksi})] = 1.40 \text{ in}^2$$

Use two #8 bars ($A_s = 2 \times 0.79 = 1.58$ in^2) along the exterior edges, along the length of the exterior longitudinal walls and along the length of the interior longitudinal walls. Provide cover for chord and collector bars and spacing between bars per ACI 318 Section 21.11.7.6.

- Minimum cover = 2.5(8/8) = 2.5 in., but not less than 2.0 in.
- Minimum spacing = 3(8/8) = 3.0 in., but not less than 1.5 in.

Figure 8.1-9 shows the diaphragm plan and section cuts of the details and Figure 8.1-10 shows the boundary member and chord/collector reinforcement along the edge. Given the close margin on cover, the transverse reinforcement at lap splices also is shown.

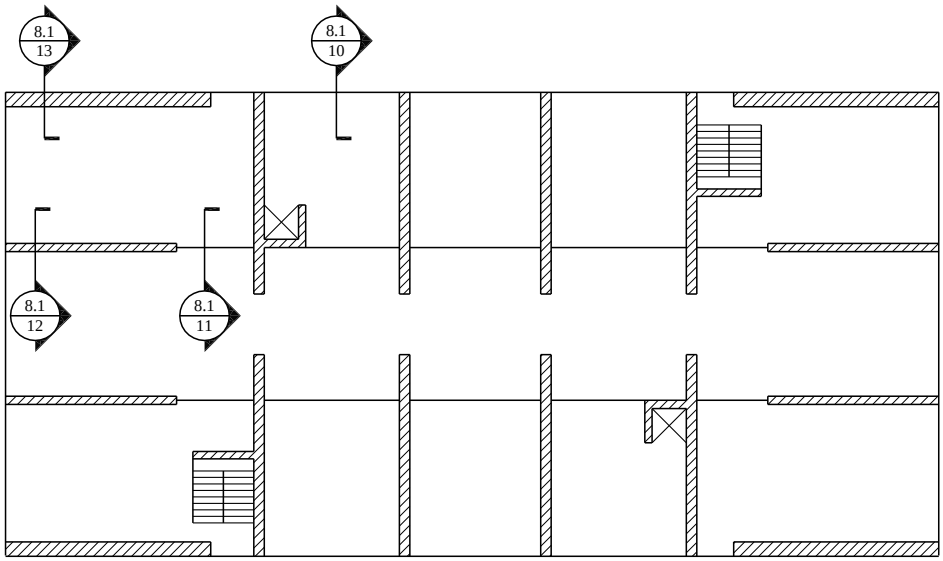

Figure 8.1-9 Diaphragm plan and section cuts

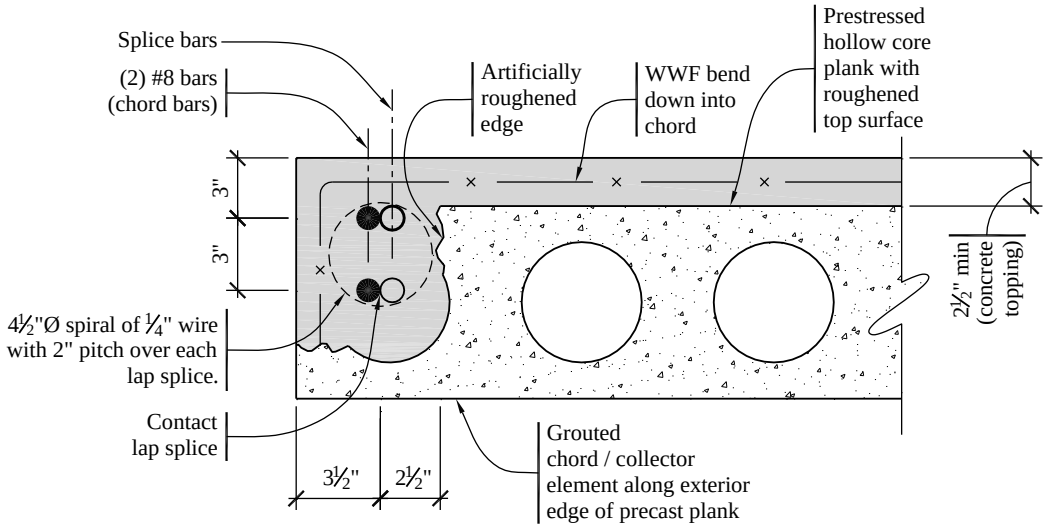

Figure 8.1-10 Boundary member and chord and collector reinforcement
(1.0 in. = 25.4 mm)

Figure 8.1-11 shows the collector reinforcement for the interior longitudinal walls. The side cover of 2-1/2 inches is provided by casting the topping into the cores and by the stems of the plank. A minimum space of 1 inch is provided between the plank stems and the sides of the bars.

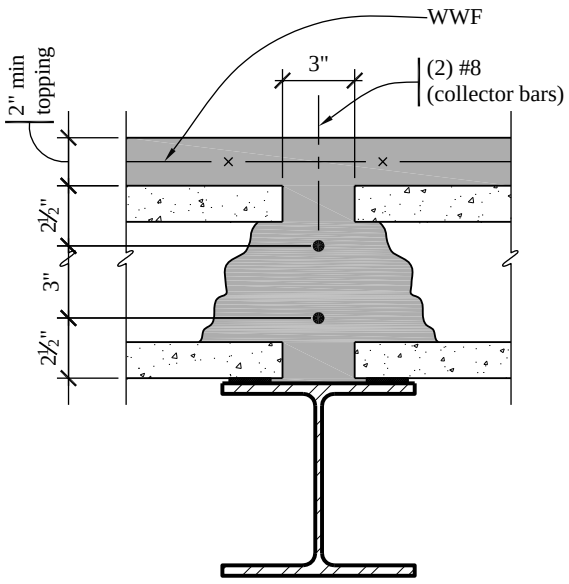

Figure 8.1-11 Collector reinforcement at the end of the interior longitudinal walls - Joint 5
(1.0 in. = 25.4 mm, 1.0 ft = 0.3048 m)

8.1.2.5.4 Shear Resistance. In thin composite and noncomposite topping slabs on precast floor and roof members, joints typically are tooled during construction, resulting in cracks forming at the joint between precast members. Therefore, the shear resistance of the topping slab is limited to the shear friction strength of the reinforcing crossing the joint.

ACI 318 Section 21.11.9.1 provides an equation for the shear strength of the diaphragm, which includes both concrete and reinforcing components. However, for noncomposite topping slabs on precast floors and roofs where the only reinforcing crossing the joints is the field reinforcing in the topping slab, the shear friction capacity at the joint will always control the design. ACI 318 Section 21.11.9.3 defines the shear strength at the joint as follows:

$\phi V_n = \phi A_{vf} f_y \mu = 0.75(0.054 \text{ in}^2/\text{ft})(60 \text{ ksi})(1.0)(0.85) = 2.07 \text{ kips/ft}$

Note that $\mu = 1.0\lambda$ is used since the joint is assumed to be pre-cracked.

The shear resistance in the transverse direction is:

2.07 kips/ft (72 ft) = 149 kips

which is greater than the Joint 1 shear (maximum transverse shear) of 124 kips.

At the plank adjacent to Joint 2, the shear strength of the diaphragm in accordance with ACI 318 Section 21.11.9.1 is:

$$\phi V_n = \phi A_{cv}\left(2\lambda\sqrt{f_c'} + \rho_t f_y\right) = 0.75\left(2.5\times 72\times 12\right)\left(2\left(1.0\right)\sqrt{4{,}000} + 0.0018\times 60{,}000\right) = 348 \text{ kips}$$

Number 3 dowels are used to provide continuity of the topping slab welded wire reinforcement across the masonry walls. The topping is to be cast into the masonry walls as shown in Figure 8.1-12 and the spacing of the #3 bars is set to be modular with the CMU.

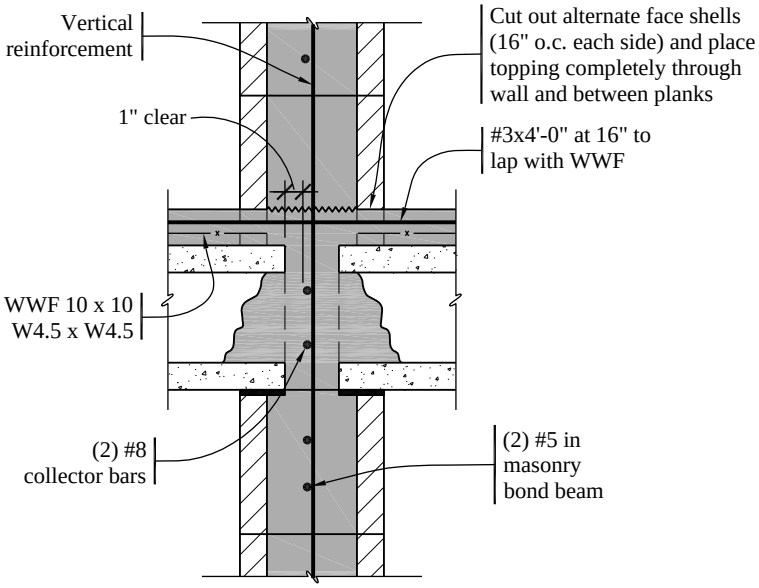

Figure 8.1-12 Wall-to-diaphragm reinforcement along interior longitudinal walls - Joint 5
(1.0 in. = 25.4 mm, 1.0 ft = 0.3048 m)

The required shear reinforcement along the exterior longitudinal wall (Joint 4) is:

$A_{vf4} = V_{u4}/\phi\mu f_y$ = (27.0 kips)/[(0.75)(1.0)(0.85)(60 ksi)] = 0.71 in^2

The required shear reinforcement along the interior longitudinal wall (Joint 5) is:

$A_{vf5} = V_{u5}/\phi\mu f_y$ = (50.8 kips)/[(0.75)(1.0)(0.85)(60 ksi)] = 1.32 in^2

Number 3 dowels spaced at 16” o.c. provide

A_v = (0.11 in^2) (40 ft x 12 in/ft) / 16 in = 3.30 in^2

8.1.2.5.5 Check of Out-of-Plane Forces. At Joint 4, the out-of-plane forces are checked as follows:

$F_p = 0.85\ S_{DS}\ I\ W_{wall}$ = 0.85(1.0)(1.0)(60 psf)(8.67 ft) = 442 plf

With bars at 4 feet on center, F_p = 4 ft (442 plf) = 1.77 kips.

The required reinforcement, A_s = 1.77 kips/(0.9)(60ksi) = 0.032 in^2. Provide #3 bars at 4 feet on center, which provides a nominal strength of 0.11×60/4 = 1.7 klf. This detail satisfies the ACI 318 Section 16.5

required tie force of 1.5 klf. The development length was checked in the prior example. Using #3 bars at 4 feet on center will be adequate and the detail is shown in Figure 8.1-13. The detail at Joint 2 is similar.

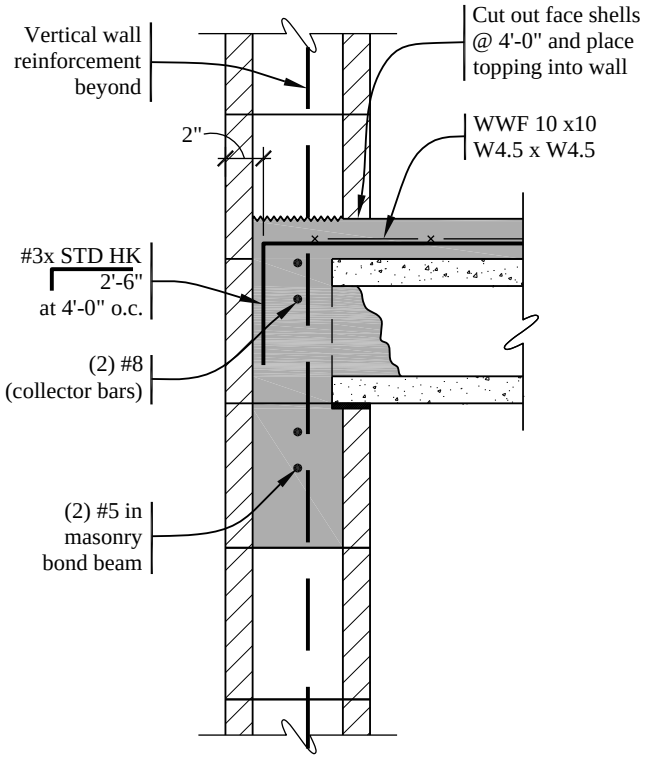

Figure 8.1-13 Exterior longitudinal wall-to-diaphragm reinforcement and out-of-plane anchorage - Joint 4
(1.0 in. = 25.4 mm, 1.0 ft = 0.3048 m).

8.2 THREE-STORY OFFICE BUILDING WITH INTERMEDIATE PRECAST CONCRETE SHEAR WALLS

This example illustrates the seismic design of intermediate precast concrete shear walls. These walls can be used up to any height in Seismic Design Categories B and C but are limited to 40 feet for Seismic Design Categories D, E and F.

ACI 318 Section 21.4.2 requires that yielding between wall panels or between wall panels and the foundation be restricted to steel elements. However, the *Provisions* are more specific in their means to accomplish the objective of providing reliable post-elastic performance. *Provisions* Section 21.4.3 (ACI 318 Sec. 21.4.4) requires that connections that are designed to yield be capable of maintaining 80 percent of their design strength at the deformation induced by the design displacement. Alternatively, they can use Type 2 mechanical splices.

Additional requirements are contained in the *Provisions* for intermediate precast walls with wall piers (*Provisions* Sec. 14.2.2.4 [ACI 318 Sec. 21.4.5]); however, these requirements do not apply to the solid wall panels used for this example.

8.2.1 Building Description

This precast concrete building is a three-story office building (Occupancy Category II) in southern New England on Site Class D soils. The structure utilizes 10-foot-wide by 18-inch-deep prestressed double tees (DTs) spanning 40 feet to prestressed inverted tee beams for the floors and the roof. The DTs are to be constructed using lightweight concrete. Each of the above-grade floors and the roof are covered with a 2-inch-thick (minimum), normal-weight cast-in-place concrete topping. The vertical seismic force-resisting system is to be constructed entirely of precast concrete walls located around the stairs and elevator/mechanical shafts. The only features illustrated in this example are the rational selection of the seismic design parameters and the design of the reinforcement and connections of the precast concrete shear walls. The diaphragm design is not illustrated.

As shown in Figure 8.2-1, the building has a regular plan. The precast shear walls are continuous from the ground level to 12 feet above the roof. The walls of the elevator/mechanical pits are cast-in-place below grade. The building has no vertical irregularities. The story height is 12 feet.

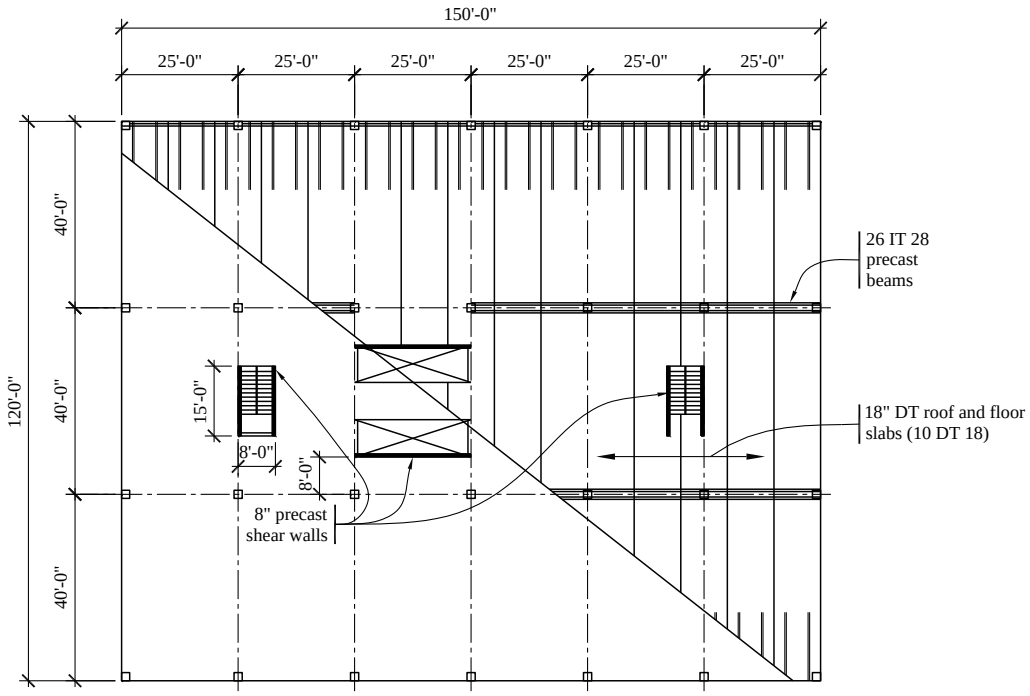

Figure 8.2-1 Three-story building plan
(1.0 in. = 25.4 mm, 1.0 ft = 0.3048 m)

The precast walls are estimated to be 8 inches thick for building mass calculations. These walls are normal-weight concrete with a 28-day compressive strength, f'_c, of 5,000 psi. Reinforcing bars used at the ends of the walls and in welded connectors are ASTM A706 (60 ksi yield strength). The concrete for the foundations and below-grade walls has a 28-day compressive strength, f'_c, of 4,000 psi.

8.2.2 Design Requirements

8.2.2.1 Seismic Parameters. The basic parameters affecting the design and detailing of the building are shown in Table 8.2-1.

Table 8.2-1 Design Parameters

Design Parameter	Value
Occupancy Category II	I = 1.0
S_S	0.266
S_1	0.08
Site Class	D
F_a	1.59
F_v	2.4
$S_{MS} = F_a S_S$	0.425
$S_{M1} = F_v S_1$	0.192
S_{DS} = 2/3 S_{MS}	0.283
S_{D1} = 2/3 S_{M1}	0.128
Seismic Design Category	B
Basic Seismic Force-Resisting System	Bearing Wall System
Wall Type	Intermediate Precast Shear Walls
R	4
Ω_0	2.5
C_d	4

A Bearing Wall System is defined in the *Standard* as "a structural system with bearing walls providing support for all or major portions of the vertical loads." In the 2006 International Building Code, this requirement is clarified by defining a concrete Load Bearing Wall as one which "supports more than 200 pounds per linear foot of vertical load in addition to its own weight." While the IBC definition is much more stringent, this interpretation is used in this example. Note that if a Building Frame Intermediate Precast Shear Wall system were used, the design would be based on R=5, Ω_o=2 ½ and C_d=4½.

Note that in Seismic Design Category B an ordinary precast shear wall could be used to resist seismic forces. However, the design forces would be 33 percent higher since they would be based on R = 3, Ω_o = 2.5 and C_d = 3. Ordinary precast structural walls need not satisfy any provisions in ACI 318 Chapter 21.

8.2.2.2 Structural Design Considerations

8.2.2.2.1 Precast Shear Wall System. This system is designed to yield in bending at the base of the precast shear walls without shear slip at any of the joints. The remaining connections (shear connectors

and flexural connectors away from the base) are then made strong enough to ensure that the inelastic action is forced to the intended location.

Although it would be desirable to force yielding to occur in a significant portion of the connections, it frequently is not possible to do so with common configurations of precast elements and connections. The connections are often unavoidable weak links. Careful attention to detail is required to assure adequate ductility in the location of first yield and to preclude premature yielding of other connections. For this particular example, the vertical bars at the ends of the shear walls (see Figure 8.2-6) act as flexural reinforcement for the walls and are selected as the location of first yield. The yielding will not propagate far into the wall vertically due to the unavoidable increase in flexural strength provided by unspliced reinforcement within the panel. The issue of most significant concern is the performance of the shear connections (see Figure 8.2-7) at the same joint. The connections are designed to provide the necessary shear resistance and avoid slip without providing increased flexural strength at the connection since such an increase would also increase the maximum shear force on the joint. At the base of the panel, welded steel angles are designed to be flexible for uplift but stiff for in-plane shear.

8.2.2.2.2 Building System. No height limits are imposed (*Standard* Table 12.2-1).

For structural design, the floors are assumed to act as rigid horizontal diaphragms to distribute seismic inertial forces to the walls parallel to the motion. The building is regular both in plan and elevation, for which, according to *Standard* Table 12.6-1, use of the Equivalent Lateral Force (ELF) procedure (*Standard* Sec. 12.8) is permitted.

Orthogonal load combinations are not required for this building (*Standard* Sec. 12.5.2).

Ties, continuity and anchorage must be considered explicitly when detailing connections between the floors and roof and the walls and columns.

This example does not include consideration of nonstructural elements.

Collector elements are required due to the short length of shear walls as compared to the diaphragm dimensions, but they are not designed in this example.

Diaphragms need to be designed for the required forces (*Standard* Sec. 12.10), but that design is not illustrated here.

The bearing walls must be designed for a force perpendicular to their plane (*Standard* Sec. 12.11), but design for that requirement is not shown for this building.

The drift limit is $0.025h_{sx}$ (*Standard* Table 12.12-1), but drift is not computed here.

ACI 318 Section 16.5 requires minimum strengths for connections between elements of precast building structures. The horizontal forces were described in Section 8.1; the vertical forces will be described in this example.

8.2.3 Load Combinations

The basic load combinations require that seismic forces and gravity loads be combined in accordance with the factored load combinations presented in *Standard* Section 12.4.2.3. Vertical seismic load effects are described in *Standard* Section 12.4.2.2.

According to *Standard* Section 12.3.4.1, $\rho = 1.0$ for structures in Seismic Design Categories A, B and C, even though this seismic force-resisting system is not particularly redundant.

The relevant load combinations from ASCE 7 are as follows:

$(1.2 + 0.2S_{DS})D \pm \rho Q_E + 0.5L$

$(0.9 - 0.2S_{DS})D \pm \rho Q_E$

Into each of these load combinations, substitute S_{DS} as determined above:

$1.26D + Q_E + 0.5L$

$0.843D - Q_E$

These load combinations are for loading in the plane of the shear walls.

8.2.4 Seismic Force Analysis

8.2.4.1 Weight Calculations. For the roof and two floors:

18-inch double tees (32 psf) + 2-inch topping (24 psf)	= 56.0 psf
Precast beams at 40 feet	= 12.5 psf
16-inch square columns	= 4.5 psf
Ceiling, mechanical, miscellaneous	= 4.0 psf
Exterior cladding (per floor area)	= 5.0 psf
Partitions	= 10.0 psf
Total	= 92.0 psf

Note that since the design snow load is 30 psf, it can be ignored in calculating the seismic weight (*Standard* Sec. 12.7.2). The weight of each floor including the precast shear walls is:

(120 ft)(150 ft)(92 psf / 1,000) + [(15 ft)4 + (25 ft)2](12 ft)(0.10 ksf) = 1,788 kips

Considering the roof to be the same weight as a floor, the total building weight is $W = 3(1{,}788 \text{ kips}) = 5{,}364$ kips.

8.2.4.2 Base Shear. The seismic response coefficient, C_s, is computed using *Standard* Equation 12.8-2:

$$C_S = \frac{S_{DS}}{R/I} = \frac{0.283}{4/1} = 0.0708$$

except that it need not exceed the value from *Standard* Equation 12.8-3 computed as:

$$C_S = \frac{S_{D1}}{T(R/I)} = \frac{0.128}{0.29(4/1)} = 0.110$$

where *T* is the fundamental period of the building computed using the approximate method of *Standard* Equation 12.8-7:

$$T_a = C_r h_n^x = (0.02)(36)^{0.75} = 0.29 \text{ sec}$$

Therefore, use $C_s = 0.0708$, which is larger than the minimum specified in *Standard* Equation 12.8-5:

$$C_s = 0.044(S_{DS})(I) \geq 0.01 = 0.044(0.283)(1.0) = 0.012$$

The total seismic base shear is then calculated using *Standard* Equation 12.8-1 as:

$$V = C_s W = (0.0708)(5{,}364) = 380 \text{ kips}$$

Note that this force is substantially larger than a design wind would be. If a nominal 20 psf were applied to the long face and then amplified by a load factor of 1.6, the result would be less than half this seismic force already reduced by an *R* factor of 4.

8.2.4.3 Vertical Distribution of Seismic Forces. The seismic lateral force ,F_x, at any level is determined in accordance with *Standard* Section 12.8.3:

$$F_x = C_{vx} V$$

where:

$$C_{vx} = \frac{w_x h_x^k}{\sum_{i=1}^{n} w_i h_i^k}$$

Since the period, *T*, is less than 0.5 seconds, k = l in both building directions. With equal weights at each floor level, the resulting values of C_{vx} and F_x are as follows:

- Roof: $C_{vr} = 0.50$; $F_r = 190$ kips
- Third Floor: $C_{v3} = 0.333$; $F_3 = 127$ kips
- Second Floor: $C_{v2} = 0.167$; $F_2 = 63$ kips

8.2.4.4 Horizontal Shear Distribution and Torsion

8.2.4.4.1 Longitudinal Direction. Design each of the 25-foot-long walls at the elevator/mechanical shafts for half the total shear. Since the longitudinal walls are very close to the center of rigidity, assume that torsion will be resisted by the 15-foot-long stairwell walls in the transverse direction. The forces for each of the longitudinal walls are shown in Figure 8.2-2.

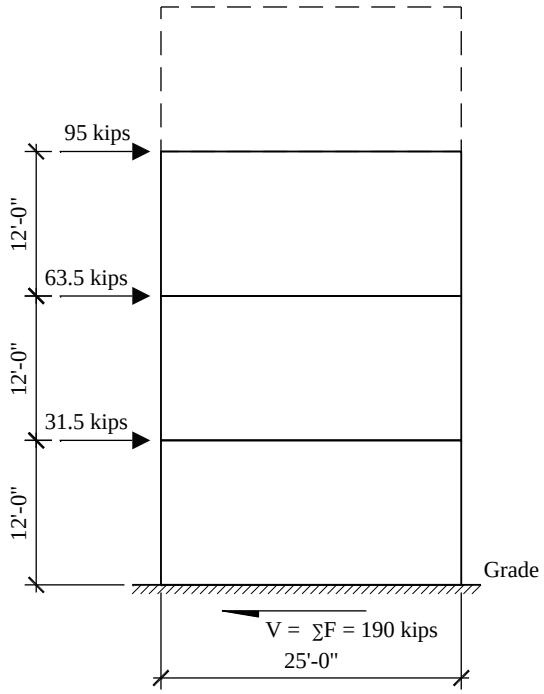

Figure 8.2-2 Forces on the longitudinal walls
(1.0 kip = 4.45 kN, 1.0 ft = 0.3048 m)

8.2.4.4.2 Transverse Direction. Design the four 15-foot-long stairwell walls for the total shear including 5 percent accidental torsion (*Standard* Sec. 12.8.4.2). A rough approximation is used in place of a more rigorous analysis considering all of the walls. The maximum force on the walls is computed as follows:

V = 380/4 + 380(0.05)(150)/[(100 ft moment arm) × (2 walls in each set)] = 109 kips

Thus:

F_r = 109(0.50) = 54.5 kips

F_3 = 109(0.333) = 36.3 kips

F_2 = 109(0.167) = 18.2 kips

Seismic forces on the transverse walls of the stairwells are shown in Figure 8.2-3.

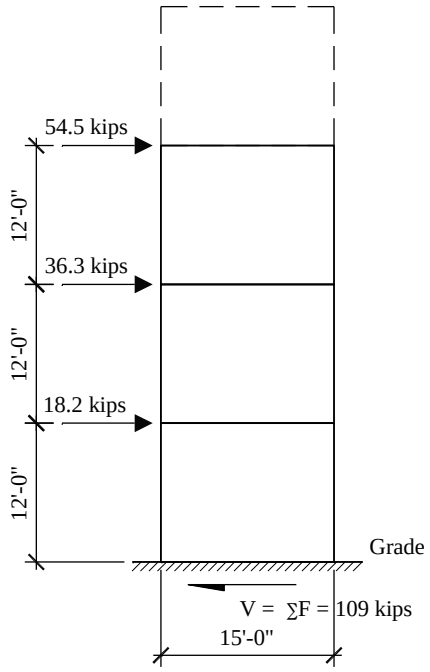

Figure 8.2-3 Forces on the transverse walls
(1.0 kip = 4.45 kN, 1.0 ft = 0.3048 m)

8.2.5 Proportioning and Detailing

The strength of members and components is determined using the strengths permitted and required in ACI 318 Chapters 1 through 19, plus Sections 21.1.2 and 21.4.

8.2.5.1 Overturning Moment and End Reinforcement. Design shear panels to resist overturning by means of reinforcing bars at each end with a direct tension coupler at the joints. A commonly used alternative is a threaded post-tensioning (PT) bar inserted through the stack of panels, but the behavior is different than assumed by ACI 318 Section 21.4 since the PT bars don't yield. If PT bars are used, the system should be designed as an Ordinary Precast Shear Wall (allowed in SDC B.) For a building in a higher seismic design category, a post tensioned wall would need to be qualified as a Special Precast Structural Wall Based on Validation Testing per 14.2.4.

8.2.5.1.1 Longitudinal Direction. The free-body diagram for the longitudinal walls is shown in Figure 8.2-4. The tension connection at the base of the precast panel to the below-grade wall is governed by the seismic overturning moment and the dead loads of the panel and supported floors and roof. In this example, the weights for an elevator penthouse, with a floor and equipment load at 180 psf between the shafts and a roof load at 20 psf, are included. The weight for the floors includes double tees, ceiling and partitions (total load of 70 psf) but not beams and columns. Floor live load is 50 psf, except 100 psf is used in the elevator lobby. Roof snow load is 30 psf. (The elevator penthouse is so small that it was ignored in computing the gross seismic forces on the building, but it is not ignored in the following calculations.)

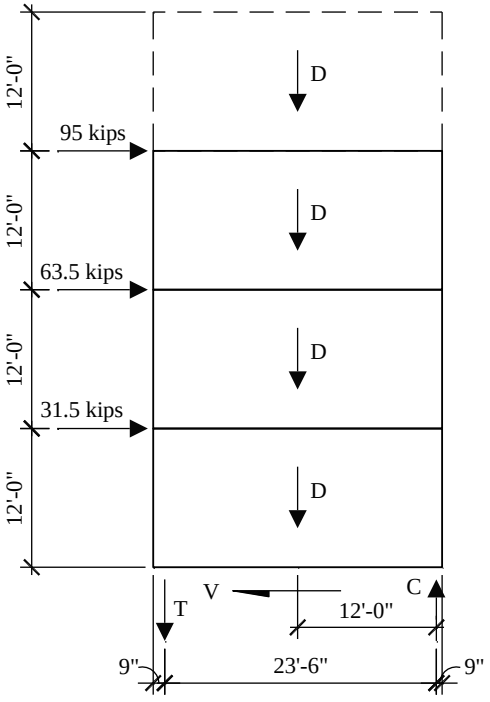

Figure 8.2-4 Free-body diagram for longitudinal walls
(1.0 kip = 4.45 kN, 1.0 ft = 0.3048 m)

At the base:

M_E = (95 kips)(36 ft) + (63.5 kips)(24 ft) + (31.5 kips)(12 ft) = 5,320 ft-kips

$\sum D$ = wall + exterior floors/roof + lobby floors + penthouse floor + penthouse roof
= (25 ft)(48 ft)(0.1 ksf) + (25 ft)(48 ft / 2)(0.070 ksf)(3) + (25 ft)(8 ft / 2)(0.070 ksf)(2)
+ (25 ft)(8 ft / 2)(0.18 ksf) + (25ft)(24 ft / 2)(0.02 ksf)
= 120 + 126 + 14 + 18 + 6 = 284 kips

$\sum L$ = (25 ft)(48 ft / 2)(0.05 ksf)(2) + (25 ft)(8 ft / 2)(0.1 ksf) = 60 + 10 = 70 kips

$\sum S$ = (25ft)(48 ft + 24 ft)(0.03 ksf)/2 = 27 kips

Using the load combinations described above, the vertical loads for combining with the overturning moment are computed as:

$P_{max} = 1.26D + 0.5L + 0.2S$ = 397 kips

$P_{min} = 0.843D$ = 239 kips

The axial load is quite small for the wall panel. The average compression P_{max}/A_g = 0.165 ksi (3.3 percent of f'_c). Therefore, the tension reinforcement can easily be found from the simple couple shown in Figure 8.2-4.

The effective moment arm is:

jd = 25 - 1.5 = 23.5 ft

and the net tension on the uplift side is:

$$T_u = \frac{M}{jd} - \frac{P_{\min}}{2} = \frac{5,320}{23.5} - \frac{239}{2} = 107 \text{ kips}$$

The required reinforcement is:

$A_s = T_u/\phi f_y$ = (107 kips)/[0.9(60 ksi)] = 1.98 in^2

Use two #9 bars (A_s = 2.0 in^2) at each end with Type 2 couplers for each bar at each panel joint. Since the flexural reinforcement must extend a minimum distance, d, (the flexural depth) beyond where it is no longer required, use both #9 bars at each end of the panel at all three levels for simplicity. Note that if it is desired to reduce the bar size up the wall, the design check of ACI 318 Section 21.4.3 must be applied to the flexural strength calculation at the upper wall panel joints.

At this point a check per ACI 318 Section 16.5 will be made. Bearing walls must have vertical ties with a nominal strength exceeding 3 kips per foot and there must be at least two ties per panel. With one tie at each end of a 25-foot panel, the demand on the tie is:

T_u = (3 kip/ft)(25 ft)/2 = 37.5 kips

The two #9 bars are more than adequate for the ACI requirement.

Although no check for confinement of the compression boundary is required for intermediate precast shear walls, it is shown here for interest. Using the check from ACI 318 Section 21.9.6, the depth to the neutral axis is:

- Total compression force, $A_s f_y + P_{max}$ = (2.0)(60) + 397 = 517 kips
- Compression block, a = (517 kips)/[(0.85)(5 ksi)(8 in. width)] = 15.2 in.
- Neutral axis depth, $c = a/(0.80)$ = 19.0 in.

The maximum depth (c) with no boundary member per ACI 318 Equation 21-8 is:

$$c \le \frac{l}{600\left(\delta_u / h_w\right)}$$

where the term (δ_u/h_w) shall not be taken as less than 0.007.

Once the base joint yields, it is unlikely that there will be any flexural cracking in the wall more than a few feet above the base. An analysis of the wall for the design lateral forces using 50 percent of the gross moment of inertia, ignoring the effect of axial loads and applying the C_d factor of 4 to the results gives a ratio (δ_u/h_w) far less than 0.007. Therefore, applying the 0.007 in the equation results in a distance, c, of 71 inches, far in excess of the 19 inches required. Thus, ACI 318 would not require transverse

reinforcement of the boundary even if this wall were designed as a special reinforced concrete shear wall. For those used to checking the compression stress as an index:

$$\sigma = \frac{P}{A} + \frac{M}{S} = \frac{389}{8(25)12} + \frac{6(5{,}320)}{8(25)^2(12)} = 694 \text{ psi}$$

The limiting stress is $0.2f'_c$, which is 1,000 psi, so no transverse reinforcement is required at the ends of the longitudinal walls.

8.2.5.1.2 Transverse Direction. The free-body diagram of the transverse walls is shown in Figure 8.2-5. The weight of the precast concrete stairs is 100 psf and of the roof over the stairs is 70 psf.

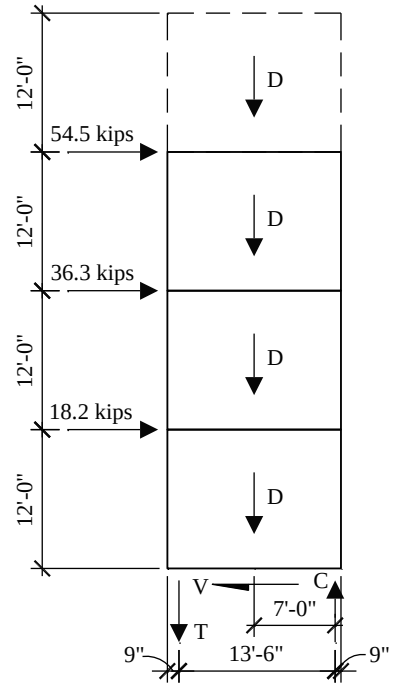

Figure 8.2-5 Free-body diagram of the transverse walls
(1.0 kip = 4.45 kN, 1.0 ft = 0.3048 m)

The transverse wall is similar to the longitudinal wall.

At the base:

M_E = (54.5 kips)(36 ft) + (36.3 kips)(24 ft) + (18.2 kips)(12 ft) = 3,052 ft-kips

$\sum D$ = (15 ft)(48 ft)(0.1 ksf) + 2(12.5 ft / 2)(10 ft / 2)(0.07 ksf)(3) + (15 ft)(8 ft / 2)[(0.1 ksf)(3) + (0.07 ksf)]
= 72 + 13 + 18 + 4 = 107 kips

$\sum L$ = 2(12.5 ft / 2)(10 ft / 2)(0.05 ksf)(2) + (15 ft)(8 ft / 2)(0.1 ksf)(3)
= 6 + 18 = 24 kips

$\sum S$ = [2(12.5 ft / 2)(10 ft / 2) + (15 ft)(8 ft / 2)](0.03 ksf) = 3.7 kips

P_{max} = 1.26(107) + 0.5(24) + 0.2(4) = 148 kips

P_{min} = 0.843(107) = 90.5 kips

jd = 15 - 1.5 = 13.5 ft

$T_u = (M_{net}/jd) - P_{min}/2$ = (3,052/13.5) - 90.5/2 = 181 kips

$A_s = T_u/\phi f_y$ = (181 kips)/[0.9(60 ksi)] = 3.35 in^2

Use two #10 and one #9 bars (A_s = 3.54 in^2) at each end of each wall with a Type 2 coupler at each bar for each panel joint. All three bars at each end of the panel will also extend up through all three levels for simplicity. Following the same method for boundary member check as on the longitudinal walls:

- Total compression force, $A_s f_y + P_{max}$ = (3.54)(60) + 148 = 360 kips
- Compression block, a = (360 kips)/[(0.85)(5 ksi)(8 in. width)] = 10.6 in.
- Neutral axis depth, $c = a/(0.80)$ = 13.3 in.

Even though this wall is more flexible and the lateral loads will induce more flexural cracking, the computed deflections are still small and the minimum value of 0.007 is used for the ratio (δ_u/h_w). This yields a maximum value of c = 42.9 inches, thus confinement of the boundary would not be required. The check of compression stress as an index gives:

$$\sigma = \frac{P}{A} + \frac{M}{S} = \frac{140}{8(15)12} + \frac{6(2{,}930)}{8(15)^2(12)} = 951 \text{ psi}$$

Since σ < 1,000 psi, no transverse reinforcement is required at the ends of the transverse walls. Note how much closer to the criterion this transverse wall is by the compression stress check.

The overturning reinforcement and connection are shown in Figure 8.2-6.

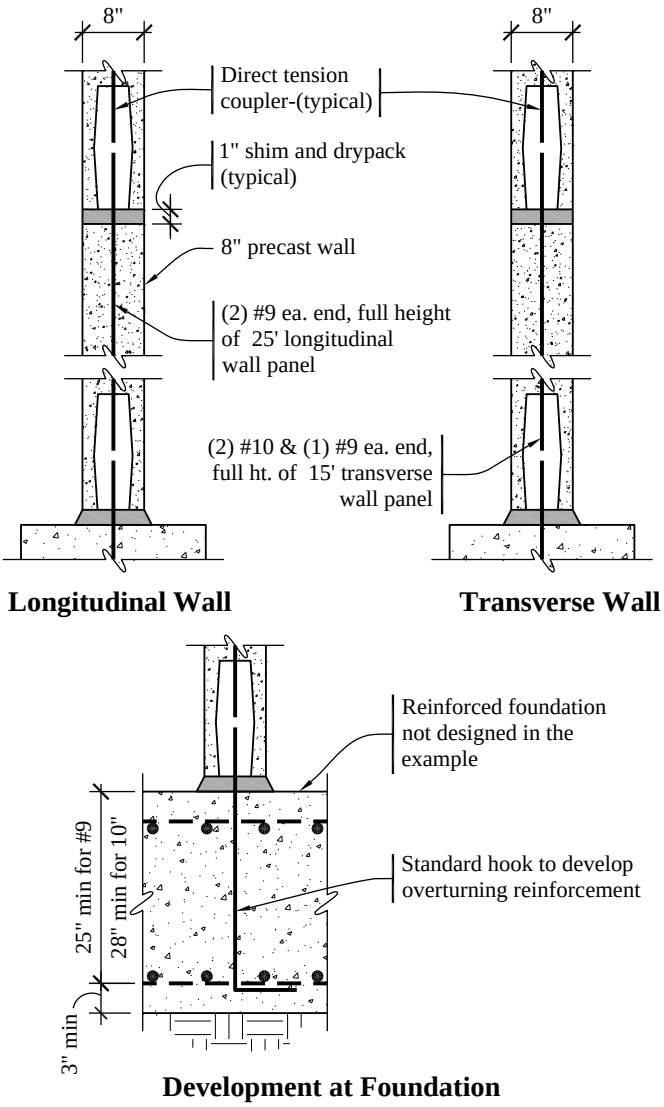

Figure 8.2-6 Overturning connection detail at the base of the walls
(1.0 in = 25.4 mm, 1.0 ft = 0.3048 m)

ACI 318 Section 21.4.3 requires that elements of the connection that are not designed to yield develop at least $1.5S_y$. This requirement applies to the anchorage of the coupled bars.

The bar in the panel is made continuous to the roof; therefore, no calculation of development length is necessary in the panel. The dowel from the foundation will be hooked; otherwise the depth of the foundation would be more than required for structural reasons. The size of the foundation will provide adequate cover to allow the 0.7 factor on ACI's standard development length for hooked bars. For the #9 bar:

$$1.5l_{dh} = \frac{1.5(0.7)(1,200)d_b}{\sqrt{f_c'}} = \frac{1,260(1.128)}{\sqrt{4,000}} = 22.5 \text{ in.}$$

Similarly, for the #10 bar, the length is 25.3 inches.

Like many shear wall designs, this design does concentrate a demand for overturning resistance on the foundation. In this instance the resistance may be provided by a large footing (on the order of 20 feet by 28 feet by 3 feet thick) under the entire stairwell or by deep piers or piles with an appropriate cap for load transfer. Refer to Chapter 4 for examples of design of each type of foundation, although not for this particular example. Note that the *Standard* permits the overturning effects at the soil-foundation interface to be reduced under certain conditions.

8.2.5.2 Shear Connections and Reinforcement. Panel joints often are designed to resist the shear force by means of shear friction, but that technique is not used for this example because the joint at the foundation will open due to flexural yielding. This opening would concentrate the shear stress on the small area of the dry-packed joint that remains in compression. This distribution can be affected by the shims used in construction. With care taken to detail the grouted joint, shear friction can provide a reliable mechanism to resist this shear. Alternatively, the joint can be designed with direct shear connectors that will prevent slip along the joint. That concept is developed here.

8.2.5.2.1 Longitudinal Direction. The design shear force is based on the yield strength of the flexural connection. The flexural strength of the connection can be approximated as follows:

$$\frac{M_y}{M_u} = \frac{A_s f_y jd + P_{max}(jd/2)}{M_E} = \frac{\left(2.0\text{in}^2\right)\left(60\text{ ksi}\right)\left(23.5\text{ ft}\right)+\left(397\text{ kip}\right)(23.5\text{ ft}/2)}{5{,}320\text{ ft-kips}} = 1.41$$

Therefore, the design shear, V_u, at the base is 1.5(1.41)(190 kips) = 402 kips.

The base shear connection is shown in Figure 8.2-7 and is to be flexible vertically but stiff horizontally in the plane of the panel. The vertical flexibility is intended to minimize the contribution of these connections to overturning resistance, which would simply increase the shear demand.

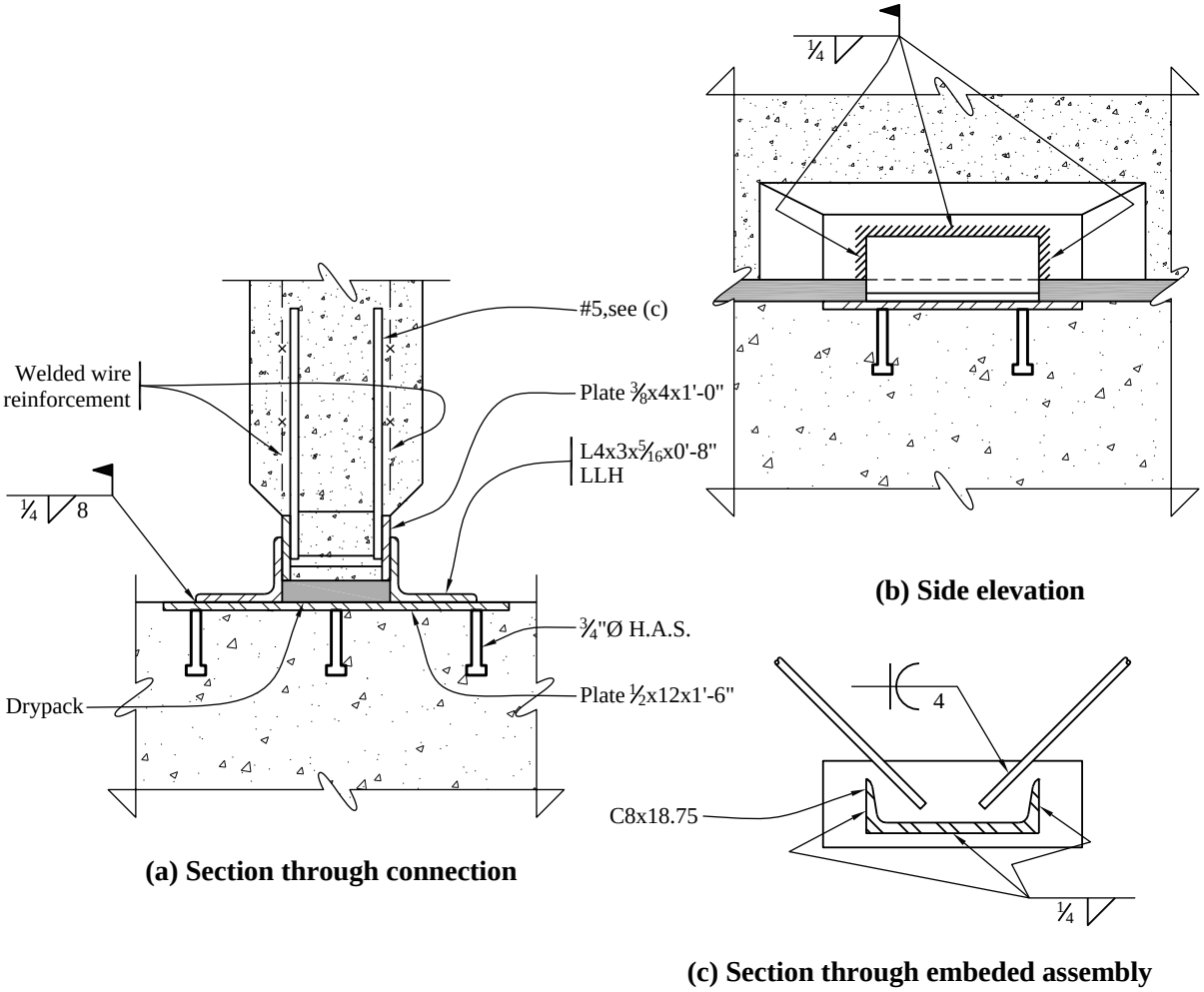

Figure 8.2-7 Shear connection at base
(1.0 in = 25.4 mm, 1.0 ft = 0.3048 m)

In the panel, provide an assembly with two face plates measuring 3/8" × 4" × 12" connected by a C8x18.75 and with diagonal #5 bars as shown in the figure. In the foundation, provide an embedded plate 1/2" × 12" × 1'-6" with six 3/4-inch-diameter headed anchor studs as shown. In the field, weld an L4×3×5/16 × 0'-8", long leg horizontal, on each face. The shear capacity of this connection is checked as follows:

- Shear in the two loose angles:

  $\phi V_n = \phi(0.6F_u)tl(2) = (0.75)(0.6)(58\text{ ksi})(0.3125\text{ in.})(8\text{ in.})(2) = 130.5\text{ kip}$

- Weld at toe of loose angles:

  $\phi V_n = \phi(0.6F_u)t_e l(2) = (0.75)(0.6)(70\text{ ksi})(0.25\text{ in.} / \sqrt{2})(8\text{ in.})(2) = 89.1\text{ kip}$

- Weld at face plates, using Table 8-8 in AISC Manual (13th edition):

  $\phi V_n = \phi C C_1 D l$ (2 sides)
  ϕ =0.75
  C_1 = 1.0 for E70 electrodes
  L = 8 in.
  D = 4 (sixteenths of an inch)
  K = 2 in. / 8 in. = 0.25
  a = eccentricity, summed vectorally: horizontal component is 4 in.; vertical component is 2.67 in.; thus, al = 4.80 in. and a = 4.8 in. / 8 in. = 0.6 from the table. By interpolation, C = 1.73
  ϕV_n = 0.75(1.73)(1.0)(4)(8)(2) = 83.0 kip

  Weld from channel to plate has at least as much capacity, but less demand.

- Bearing of concrete at steel channel:

  $f_c = \phi(0.85 f'_c) = 0.65(0.85)(5 \text{ ksi}) = 2.76$ ksi

  The C8 has the following properties:

  t_w = 0.487 in.
  b_f = 2.53 in.
  t_f = 0.39 in. (average)

  The bearing will be controlled by bending in the web (because of the tapered flange, the critical flange thickness is greater than the web thickness). Conservatively ignoring the concrete's resistance to vertical deformation of the flange, compute the width (b) of flange loaded at 2.76 ksi that develops the plastic moment in the web:

  $M_p = \phi F_y t_w^2/4 = (0.9)(50 \text{ ksi})(0.487^2 \text{ in}^2)/4 = 2.67$ in-kip/in.

  $M_u = f_c[(b\text{-}t_w)^2/2 - (t_w/2)^2/2] = 2.76[(b - 0.243 \text{ in.})^2 - (0.243 \text{ in.})^2]/2$

  setting the two equal results in b = 1.65 inches.

  Therefore, bearing on the channel is:

  $\phi V_c = f_c(2 - t_w)(l) = (2.76 \text{ ksi})[(2(1.65) - 0.487 \text{ in.}](6 \text{ in.}) = 46.6$ kip

To the bearing capacity on the channel is added the four #5 diagonal bars, which are effective in tension and compression; ϕ = 0.75 for shear is used here:

$\phi V_s = \phi f_y A_s \cos\alpha = (0.75)(60 \text{ ksi})(4)(0.31 \text{ in}^2)(\cos 45°) = 39.5$ kip

Thus, the total capacity for transfer to concrete is:

$\phi V_n = \phi V_c + \phi V_s = 46.6 + 39.6 = 86.1$ kip

The capacity of the plate in the foundation is governed by the headed anchor studs. ACI 318 Appendix D has detailed information on calculating the strength of headed anchor studs. ACI 318 Section D3.3 has additional requirements for anchors resisting seismic forces in Seismic Design Categories C through F. Capacity in shear for anchors located far from an edge of concrete, such as these and with sufficient embedment to avoid the pryout failure mode is governed by the capacity of the steel, which is required by ACI 318 Section D3.3.4:

$\phi V_{sa} = \phi\, n\, A_{se}\, f_{uta}$ = (0.65)(6 studs)(0.44 in^2 per stud)(60 ksi) = 103 kip

In summary, the various shear capacities of the connection are as follows:

- Shear in the two loose angles: 130.5 kip
- Weld at toe of loose angles: 89.1 kip
- Weld at face plates: 83.0 kip
- Transfer to concrete: 86.1 kip
- Headed anchor studs at foundation: 103 kip

The number of embedded plates (n) required for a panel is:

n =402/83.0 = 4.8

Use five connection assemblies, equally spaced along each side (4'-0" on center works well to avoid the end reinforcement). The plates are recessed to position the #5 bars within the thickness of the panel and within the reinforcement of the panel.

It is instructive to consider how much moment capacity is added by the resistance of these connections to vertical lift at the joint. The vertical force at the tip of the angle that will create the plastic moment in the leg of the angle is:

$T = M_p/x = F_y l t^2/4 / (l\text{-}k)$ = (36 ksi)(8 in.)(0.3125^2 in^2)/4]/(4 in. - 0.69 in.) = 2.12 kips

There are five assemblies with two loose angles each, giving a total vertical force of 21 kips. The moment resistance is this force times half the length of the panel, which yields 265 ft-kips. The total demand moment, for which the entire system is proportioned, is 5,320 ft-kips. Thus, these connections will add approximately 5 percent to the resistance and ignoring this contribution is reasonable. If a straight plate measuring 1/4 inch by 8 inches (which would be sufficient) were used and if the welds and foundation embedment did not fail first, the tensile capacity would be 72 kips each, a factor of 42 increase over the angles and the shear connections would have the unintended effect of more than doubling the flexural resistance, which would require a much higher shear force to develop a plastic hinge at the wall base.

Using ACI 318 Section 11.10, check the shear strength of the precast panel at the first floor:

$$\phi V_c = \phi 2 A_{cv} \sqrt{f_c'}\, hd = 0.75(2)\sqrt{5{,}000}\,(8)(23.5)(12) = 239 \text{ kips}$$

Because $\phi V_c \geq V_u$ = 190 kips, the wall is adequate for shear without even considering the reinforcement. Note that the shear strength of the wall itself is not governed by the overstrength required for the connection. However, since $V_u \geq 0.5\phi V_c$ = 120 kips, ACI 318 Section 11.9.8 requires minimum wall reinforcement in accordance with ACI 318 Section 11.9.9 rather than Chapters 14 or 16. For the minimum required ρ_h = 0.0025, the required reinforcement is:

$A_v = 0.0025(8)(12) = 0.24$ in^2/ft

As before, use two layers of welded wire reinforcement, WWF 4×4 - W4.0×W4.0, one on each face. The shear reinforcement provided is:

$A_v = 0.12(2) = 0.24$ in^2/ft

Next, compute the required connection capacity at Level 2. Even though the end reinforcing at the base extends to the top of the shear wall, the connection still needs to be checked for flexure in accordance with *Provisions* Section 21.4.3 (ACI 318 Sec. 21.4.4). At Level 2:

M_E = (95 kips)(24 ft) + (63.5 kips)(12 ft) = 3,042 ft-kips

There are two possible approaches to the design of the joint at Level 2.

First, if Type 2 couplers are used at the Level 2 flexural connection, then the connection can be considered to have been "designed to yield," and no overstrength is required for the design of the flexural connection. In this case, the bars are designed for the moment demand at the Level 2 joint.

Alternately, if a non-yielding connection is used at the Level 2 connection, then to meet the requirements of *Provisions* Section 21.4.4 (ACI 318 Sec. 21.4.3), the flexural strength of the connection at Level 2 must be $1.5S_y$ or:

$M_u = 1.5(1.41)M_E = 1.5(1.41)(3{,}042$ ft-kips$) = 6{,}433$ ft-kips

At Level 2, the gravity loads on the wall are:

$\sum D$ = wall + exterior floors/roof + lobby floors + penthouse floor + penthouse roof
= (25 ft)(36 ft)(0.1 ksf) + (25 ft)(48 ft / 2)(0.070 ksf)(2) + (25 ft)(8 ft / 2)(0.070 ksf)(1) +
(25 ft)(8 ft / 2)(0.18 ksf) + (25 ft)(24 ft / 2)(0.02 ksf)
= 90 + 84 + 7 + 18 + 6 = 205 kips

$\sum L$ = (25 ft)(48 ft / 2)(0.05 ksf)(1) + (25 ft)(8 ft / 2)(0.1 ksf) = 30 + 10 = 40 kips

$\sum S$ = (25ft)(48 ft + 24 ft)(0.03 ksf)/2 = 27 kips

P_{max} = 1.26(205) + 0.5(40) + 0.2(27) = 285 kips

P_{min} = 0.843(205) = 173 kips

Note that since the maximum axial load was used to determine the maximum yield strength of the base moment connection, the maximum axial load is used here to determine the nominal strength of the Level 2 connection. For completeness, the base moment overstrength provided should be checked using the minimum axial load as well and compared to the moment strength at Level 2 using the minimum axial load.

$$\phi M_n = 0.9\left[A_s f_y jd + P_{max}(jd/2)\right] = 0.9\left[\left(2.0\text{ in}^2\right)\left(60\text{ ksi}\right)\left(23.5\text{ ft}\right)+\left(285\text{ kips}\right)(23.5\text{ ft}/2)\right]$$
$$= 5{,}552\text{ ft-kips}$$

Therefore, the non-yielding flexural connection at Level 2 must be strengthened.

Provide:

$$T_u = \frac{M_u}{jd} - \frac{P_{min}}{2} = \frac{6{,}433}{23.5} - \frac{285}{2} = 131\text{ kips}$$

The required reinforcement is:

$A_s = T_u/\phi f_y$ = (131 kips)/[0.9(60 ksi)] = 2.43 in^2

In addition to the two #9 bars that extend to the roof, provide one #6 bar developed into the wall panel above and below the joint. Note that no increase on the development length for the #6 bar is required for this connection since the connection itself has been designed for the loads to promote base yielding per *Provisions* Section 21.4.4 (ACI 318 Sec. 21.4.3).

Since the Level 2 connection is prevented from yielding, shear friction can reasonably be used to resist shear sliding at this location. Also, because of the lack of flexural yield at the joint, it is not necessary to make the shear connection flexible with respect to vertical movement should an embedded plate detail be desired.

The design shear for this location is:

$V_{u,Level\ 2}$ = 1.5(1.41)(95+63.5) = 335 kips

Using the same recessed embedded plate assemblies in the panel as at the base, but welded with a straight plate, the number of plates, *n, is* 335/83.0 = 4.04. Use four plates, equally spaced along each side.

Figure 8.2-8 shows the shear connection at the second and third floors of the longitudinal precast concrete shear wall panels.

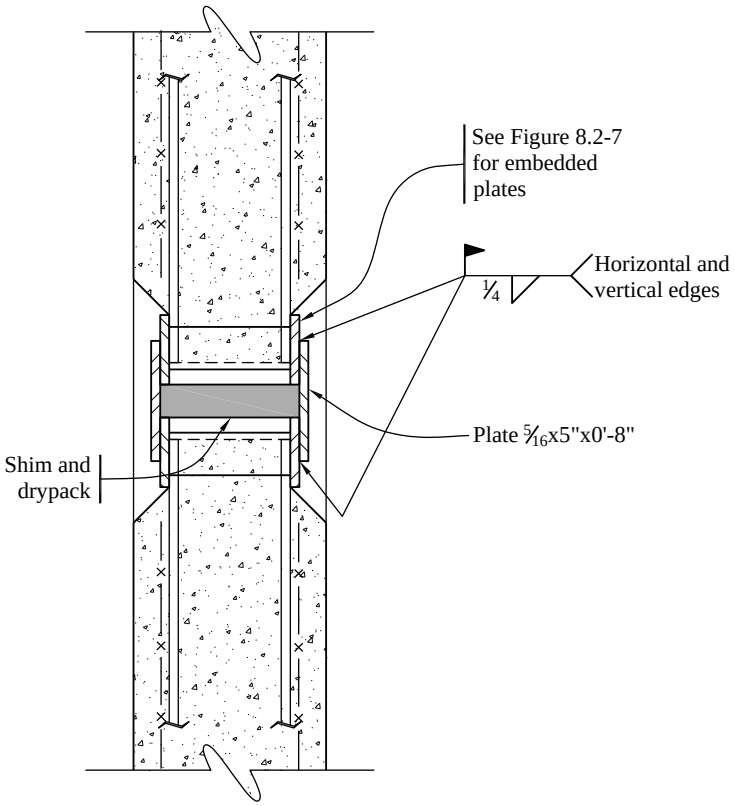

Figure 8.2-8 Shear connections on each side of the wall at the second and third floors (1.0 in = 25.4 mm)

8.3 ONE-STORY PRECAST SHEAR WALL BUILDING

This example illustrates the design of a precast concrete shear wall for a single-story building in a region of high seismicity. For buildings assigned to Seismic Design Category D, ACI 318 Section 21.10 requires that special structural walls constructed of precast concrete meet the requirements of ACI 318 Section 21.9, in addition to the requirements for intermediate precast structural walls. Alternately, special structural walls constructed using precast concrete are allowed if they satisfy the requirements of ACI ITG-5.1, *Acceptance Criteria for Special Unbonded Post-Tensioned Precast Structural Walls Based on Validation Testing (ACI ITG 5.1-07)*. Design requirements for one such type of wall have been developed by ACI ITG 5 and have been published by ACI as *Requirements for Design of a Special Unbonded Post-Tensioned Precast Shear Wall Satisfying ACI ITG-5.1 (ACI ITG 5.2-09)*. ITG 5.1 and ITG 5.2 describe requirements for precast walls for which a self-centering mechanism is provided by post-tensioning located concentrically within the wall. More general requirements for special precast walls are contained in *Provisions* Section 14.2.4. Section 14.2.4 is an updated version of Section 9.6 of the 2003 *Provisions*, which formed the basis for ITG 5.1 and ITG 5.2.

8.3.1 Building Description

The precast concrete building is a single-story industrial warehouse building (Occupancy Category II) located in the Los Angeles area on Site Class C soils. The structure has 8-foot-wide by 12.5-inch-deep

prestressed double tee (DT) wall panels. The roof is light gage metal decking spanning to bar joists that are spaced at 4 feet on center to match the location of the DT legs. The center supports for the joists are joist girders spanning 40 feet to steel tube columns. The vertical seismic force-resisting system is the precast/prestressed DT wall panels located around the perimeter of the building. The average roof height is 20 feet and there is a 3-foot parapet. Figure 8.3-1 shows the plan of the building, which is regular.

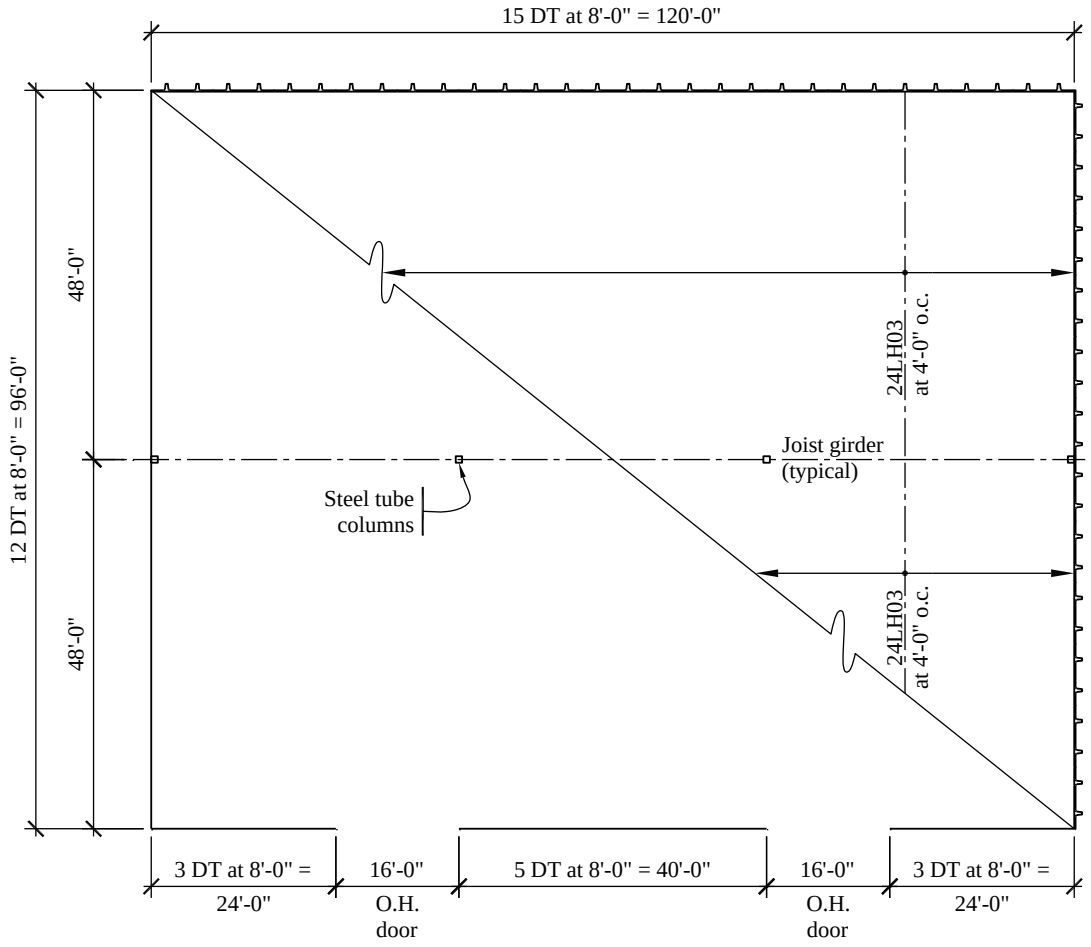

Figure 8.3-1 Single-story industrial warehouse building plan
(1.0 ft = 0.3048 m)

The precast wall panels used in this building are typical DT wall panels commonly found in many locations but not normally used in southern California. For these wall panels, an extra 1/2 inch has been added to the thickness of the deck (flange). This extra thickness is intended to reduce cracking of the flanges and provide cover for the bars used in the deck at the base. The use of thicker flanges is addressed later.

The wall panels are normal-weight concrete with a 28-day compressive strength of $f'c$ = 5,000 psi. Reinforcing bars used in the welded connections of the panels and footings are ASTM A706 (60 ksi). The concrete for the foundations has a 28-day compressive strength of $f'c$ = 4,000 psi.

In *Standard* Table 12.2-1 the values for special reinforced concrete shear walls are for both cast-in-place and precast walls. In Section 2.2, ACI 318 defines a special structural wall as "a cast-in-place or precast wall complying with the requirements of 21.1.3 through 21.1.7, 21.9 and 21.10, as applicable, in addition to the requirements for ordinary reinforced concrete structural walls." ACI 318 Section 21.10 defines requirements for special structural walls constructed using precast concrete, including that the wall must satisfy all of the requirements of ACI 318 Section 21.9.

Unfortunately, several of the requirements of ACI 318 Section 21.9 are problematic for a shear wall system constructed using DT wall panels. These include the following:

1. ACI 318 Section 21.9.2.1 requires reinforcement to be spaced no more than 18 inches on center and be continuous. This would require splices to the foundation along the DT flange.

2. ACI 318 Section 21.9.2.2 requires two curtains of reinforcement for walls with shear stress greater than $2\lambda\sqrt{f'c}$. For low loads, this might not be a problem, but for high shear stresses, placing two layers of reinforcing in a DT flange would be a challenge.

3. While ACI 318 Section 21.1.5.3 allows prestressing steel to be used in precast walls, ACI 318 Commentary R21.1.5 states that the "capability of a structural member to develop inelastic rotation capacity is a function of the length of the yield region along the axis of the member. In interpreting experimental results, the length of the yield region has been related to the relative magnitudes of nominal and yield moments." Since prestressing steel does not have a defined yield plateau, the ratio of nominal to yield moment is undefined. This limits the ability of the structural member to develop inelastic rotation capacity—a key assumption in the definition of the *R* value for a special reinforced concrete wall system.

Therefore, these walls will be designed using the ACI category of intermediate precast structural walls.

8.3.2 Design Requirements

8.3.2.1 Seismic Parameters of the *Provisions*. The basic parameters affecting the design and detailing of the building are shown in Table 8.3-1.

Table 8.3-1 Design Parameters

Design Parameter	Value
Occupancy Category II	$I = 1.0$
S_S	1.5
S_1	0.60
Site Class	C
F_a	1.0
F_v	1.3
$S_{MS} = F_a S_S$	1.5
$S_{M1} = F_v S_1$	0.78
$S_{DS} = 2/3\ S_{MS}$	1.0
$S_{D1} = 2/3\ S_{M1}$	0.52
Seismic Design Category	D
Basic Seismic Force-Resisting System	Bearing Wall System
Wall Type	Intermediate Precast Structural Wall
R	4
Ω_0	2.5
C_d	4

8.3.2.2 Structural Design Considerations

8.3.2.2.1 Intermediate Precast Structural Walls Constructed Using Precast Concrete. The intent of the intermediate precast structural wall requirements is to provide yielding in a dry connection for bending at the base of each precast shear wall panel while maintaining significant shear resistance in the connection. The flexural connection for a wall panel at the base is located in one DT leg while the connection at the other leg is used for compression. Per ACI 318 Section 21.4, these connections must yield only in steel elements or reinforcement and all other elements of the connection (including shear resistance) must be designed for 1.5 times the force associated with the flexural yield strength of the connection.

Yielding will develop in the dry connection at the base by bending in the horizontal leg of the steel angle welded between the embedded plates of the DT and footing. The horizontal leg of this angle is designed in a manner to resist the seismic tension of the shear wall due to overturning and then yield and deform inelastically. The connections on the two legs of the DT are each designed to resist 50 percent of the shear. The anchorage of the connection into the concrete is designed to satisfy the $1.5S_y$ requirements of ACI 318 Section 21.4.3. Careful attention to structural details of these connections is required to ensure

tension ductility and resistance to large shear forces that are applied to the embedded plates in the DT and footing.

8.3.2.2.2 Building System. The height limit in Seismic Design Category D (*Standard* Table 12.2-1) is 40 feet.

The metal deck roof acts as a flexible horizontal diaphragm to distribute seismic inertia forces to the walls parallel to the earthquake motion *(Standard* Sec. 12.3.1.1).

The building is regular both in plan and elevation.

The redundancy factor, ρ, is determined in accordance with *Standard* Section 12.3.4.2. For this structure, which is regular and has more than two perimeter wall panels (bays) on each side in each direction, $\rho = 1.0$.

The structural analysis to be used is the ELF procedure (*Standard* Sec. 12.8) as permitted by *Standard* Table 12.6-1.

Orthogonal load combinations are not required for flexible diaphragms in Seismic Design Category D (*Standard* Sec. 12.5.4).

This example does not include design of the foundation system, the metal deck diaphragm, or the nonstructural elements.

Ties, continuity and anchorage (*Standard* 12.11) must be considered explicitly when detailing connections between the roof and the wall panels. This example does not include the design of those connections, but sketches of details are provided to guide the design engineer.

There are no drift limits for single-story buildings as long as they are designed to accommodate predicted lateral displacements (*Standard* Table 12.12-1, Footnote c).

8.3.3 Load Combinations

The basic load combinations (*Standard* Sec. 12.4.2.3) require that seismic forces and gravity loads be combined in accordance with the following factored load combinations:

$$(1.2 + 0.2S_{DS})D \pm \rho Q_E + 0.5L + 0.2S$$

$$(0.9 - 0.2S_{DS})D \pm \rho Q_E + 1.6H$$

At this flat site, both S and H equal 0. Note that roof live load need not be combined with seismic loads, so the live load term, L, can be omitted from the equation. Therefore:

$$1.4D + \rho Q_E$$

$$0.7D - \rho Q_E$$

These load combinations are for the in-plane direction of the shear walls.

8.3.4 Seismic Force Analysis

8.3.4.1 Weight Calculations. Compute the weight tributary to the roof diaphragm:

Roofing	= 2.0 psf
Metal decking	= 1.8 psf
Insulation	= 1.5 psf
Lights, mechanical, sprinkler system, etc.	= 3.2 psf
Bar joists	= 2.7 psf
Joist girder and columns	= 0.8 psf
Total	= 12.0 psf

The total weight of the roof is computed as:

(120 ft × 96 ft)(12 psf / 1,000) = 138 kips

The exterior DT wall weight tributary to the roof is:

(20 ft / 2 + 3 ft)[42 psf / 1,000](120 ft + 96 ft)2 = 236 kips

Total building weight for seismic lateral load, W = 138+236 = 374 kips

8.3.4.2 Base Shear. The seismic response coefficient (C_s) is computed using *Standard* Equation 12.8-2 as:

$$C_S = \frac{S_{DS}}{R/I} = \frac{1.0}{4/I} = 0.25$$

except that it need not exceed the value from *Standard* Equation 12.8-3, as follows:

$$C_S = \frac{S_{D1}}{T(R/I)} = \frac{0.52}{0.189(4/1)} = 0.69$$

where T is the fundamental period of the building computed using the approximate method of *Standard* Equation 12.8-7:

$$T_a = C_r h_n^x = (0.02)\left(20.0\right)^{0.75} = 0.189 \text{ sec}$$

Therefore, use C_s = 0.25, which is larger than the minimum specified in *Standard* Equation 12.8-5:

$C_s = 0.044(S_{DS})(I) \geq 0.01 = 0.044(1.0)(1.0) = 0.044$

The total seismic base shear is then calculated using *Standard* Equation 12.8-1, as:

$V = C_s W = (0.25)(374) = 93.5$ kips

8.3.4.3 Horizontal Shear Distribution and Torsion. Torsion is not considered in the shear distribution in buildings with flexible diaphragms. The shear along each side of the building will be equal, based on a tributary area force distribution.

8.3.4.3.1 Longitudinal Direction. The total shear along each side of the building is $V/2$ = 46.75 kips. The maximum shear on longitudinal panels (at the side with the openings) is:

V_{lu} = 46.75/11 = 4.25 kips

On each side, each longitudinal wall panel resists the same shear force as shown in the free-body diagram of Figure 8.3-2, where D_1 represents roof joist reactions and D_2 is the panel weight.

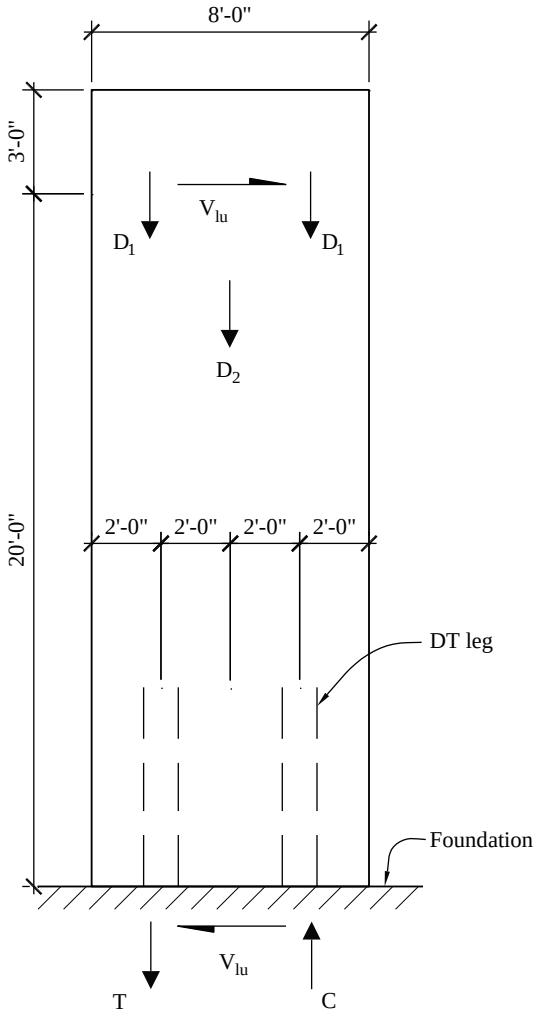

Figure 8.3-2 Free-body diagram of a panel in the longitudinal direction
(1.0 ft = 0.3048 m)

8.3.4.3.2 Transverse Direction. Seismic forces on the transverse wall panels are all equal and are:

V_{tu} = 46.75/12 = 3.90 kips

Figure 8.3-3 shows the transverse wall panel free-body diagram.

Note the assumption of uniform distribution to the wall panels in a line requires that the roof diaphragm be provided with a collector element along its edge. The chord designed for diaphragm action in the perpendicular direction will normally be capable of fulfilling this function, but an explicit check should be made in the design.

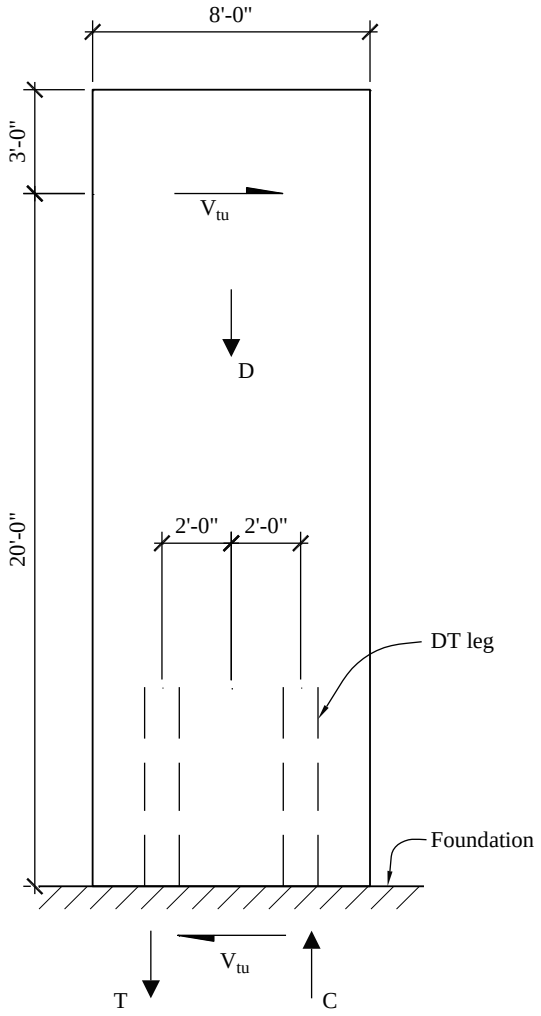

Figure 8.3-3 Free-body diagram of a panel in the transverse direction
(1.0 ft = 0.3048 m)

8.3.5 Proportioning and Detailing

The strength of members and components is determined using the strengths permitted and required in ACI 318 including Chapter 21.

8.3.5.1 Tension and Shear Forces at the Panel Base. Design each precast shear panel to resist the seismic overturning moment by means of a ductile tension connector at the base of the panel. A steel angle connector will be provided at the connection of each leg of the DT panel to the concrete footing. The horizontal leg of the angle is designed to yield in bending as needed in an earthquake. ACI 318

Section 21.4 requires that dry connections at locations of nonlinear action comply with applicable requirements of monolithic concrete construction and satisfy both of the following:

1. Where the moment action on the connection is assumed equal to $1.5M_y$, the co-existing forces on all other components of the connection other than the yielding element shall not exceed their design strength.

2. The nominal shear strength for the connection shall not be less than the shear associated with the development of $1.5M_y$ at the connection.

8.3.5.1.1 Longitudinal Direction. Use the free-body diagram shown in Figure 8.3-2. The maximum tension for the connection at the base of the precast panel to the concrete footing is governed by the seismic overturning moment and the dead loads of the panel and the roof. The weight for the roof is 11.2 psf, which excludes the joist girders and columns.

- At the base:

  M_E = (4.25 kips)(20 ft) = 85.0 ft-kips

- Dead loads:

  $$D_1 = (11.2/1{,}000)\left(\frac{48}{2}\right)4 = 1.08 \text{ kips}$$

  D_2 = 0.042(23)(8) = 7.73 kips

  ΣD = 2(1.08) + 7.73 = 9.89 kips

  1.4D = 13.8 kips

  0.7D = 6.92 kips

Compute the tension force due to net overturning based on an effective moment arm, d, of 4.0 feet (the distance between the DT legs). The maximum is found when combined with 0.7D:

$T_u = M_E/d$ - 0.7D/2 = 85.0/4 - 6.92/2 = 17.8 kips

8.3.5.1.2 Transverse Direction. For the transverse direction, use the free-body diagram of Figure 8.3-3. The maximum tension for connection at the base of the precast panel to the concrete footing is governed by the seismic overturning moment and the dead loads of just the panel. No load from the roof is included, since it is negligible.

At the base:

M_E = (3.90 kips)(20 ft) = 78.0 ft-kips

The dead load of the panel (as computed above) is D_2 = 7.73 kips and 0.7D = 5.41.

The tension force is computed as above for d = 4.0 feet (the distance between the DT legs):

T_u = 78.0/4 - 5.41/2 = 16.8 kips

This tension force is less than that at the longitudinal wall panels. Use the tension force of the longitudinal wall panels for the design of the angle connections.

8.3.5.2 Size the Yielding Angle. The angle, which is the ductile element of the connection, is welded between the plates embedded in the DT leg and the footing. This angle is an L5×3-1/2×3/4 × 0'-6-1/2" with the long leg vertical. The steel for the angle and embedded plates will be ASTM A572, Grade 50. The horizontal leg of the angle needs to be long enough to provide significant displacement at the roof, although this is not stated as a requirement in either the *Provisions* or ACI 318. This will be examined briefly here. The angle and its welds are shown in Figure 8.3-4.

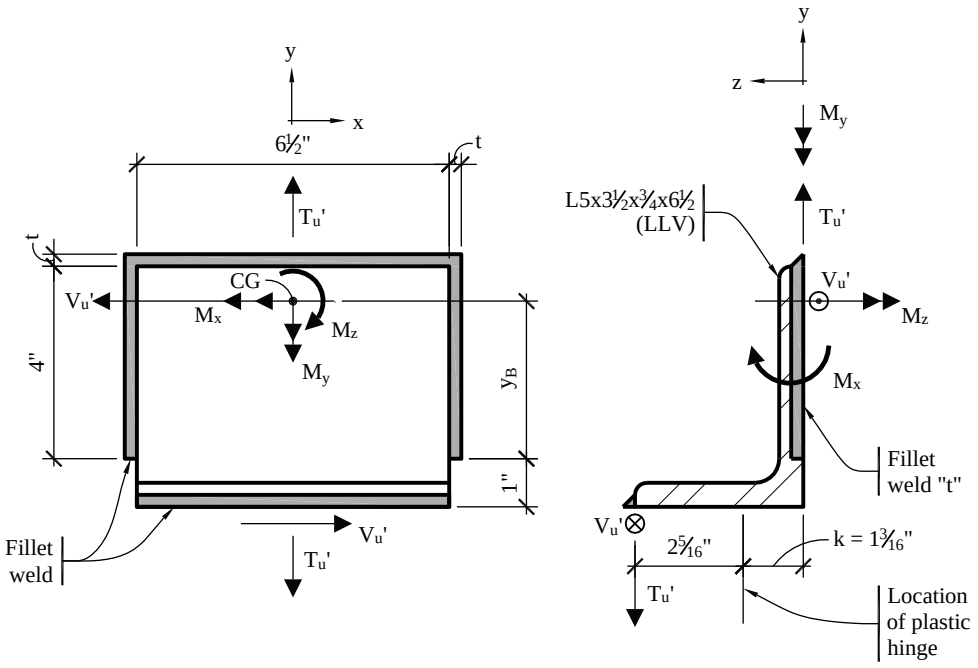

Figure 8.3-4 Free-body of the angle and the fillet weld connecting the embedded plates in the DT and the footing (elevation and section)
(1.0 in = 25.4 mm)

The location of the plastic hinge in the angle is at the toe of the fillet (at a distance, *k*, from the heel of the angle.) The bending moment at this location is:

$M_u = T_u(3.5 - k) = 17.8(3.5 - 1.1875) = 41.2$ in.-kips

$$\phi_b M_n = 0.9 F_y Z = 0.9(50)\left[\frac{6.5(0.75)^2}{4}\right] = 41.1 \text{ in-kips}$$

Providing a stronger angle (e.g., a shorter horizontal leg) will simply increase the demands on the remainder of the assembly. Using ACI 318 Section 21.4.3, the tension force for the remainder of this

connection and the balance of the wall design are based upon a probable strength equal to 150 percent of the yield strength. Thus:

$$T_{pr} = \frac{M_n(1.5)}{3.5 - k} = \frac{(50)(6.5)(0.75)^2 / 4}{0.9(3.5 - 1.1875)} \times 1.5 = 27.0 \text{ kips}$$

The amplifier, required for the design of the balance of the connection, is:

$$\frac{T_{pr}}{T_u} = \frac{27.0}{17.8} = 1.52$$

The shear on the connection associated with this force in the angle is:

$$V_{pr} = V_E \frac{T_{pr}}{T_u} = 4.25 \times 1.52 = 6.46 \text{ kips}$$

Check the welds for the tension force of 27.0 kips and a shear force 6.46 kips.

The *Provisions* Section 21.4.4 (ACI 318 21.4.3) requires that connections that are designed to yield be capable of maintaining 80 percent of their design strength at the deformation induced by the design displacement. For yielding of a flat bar (angle leg), this can be checked by calculating the ductility capacity of the bar and comparing it to C_d. Note that the element ductility demand (to be calculated below for the yielding angle) and the system ductility, C_d, are only equal if the balance of the system is rigid. This is a reasonable assumption for the intermediate precast structural wall system described in this example.

The idealized yield deformation of the angle can be calculated as follows:

$$P_y = \frac{M_n}{L} = \frac{50(6.5)(0.75^2) / 4}{2.25} = 19.8 \text{ kips}$$

$$\Delta_{y,idealized} = \frac{P_y L^3}{3EI} = \frac{19.83(2.31^3)}{3(29,000)(6.5 \times 0.75^3 / 12)} = 0.012 \text{ in.}$$

It is conservative to limit the maximum strain in the bar to $\varepsilon_{sh} = 15\varepsilon_y$. At this strain, a flat bar would be expected to retain all its strength and thus meet the requirement of maintaining 80 percent of its strength.

Assuming a plastic hinge length equal to the section thickness:

$$\phi_p = \frac{15\varepsilon_y}{d/2} = \frac{15(50/29,000)}{0.75/2} = 0.06897$$

$$\Delta_{sh} = \phi_p L_p \left(L - \frac{L_p}{2}\right) + \Delta_y = 0.06897(0.75)\left(2.31 - \frac{0.75}{2}\right) + 0.012 = 0.112 \text{ in.}$$

Since the ductility capacity at strain hardening is 0.112/0.012 = 9.3 is larger than C_d = 4 for this system, the requirement of *Provision* Section 21.4.4 (ACI 318 Sec. 21.4.3) is met.

8.3.5.3 Welds to Connection Angle. Welds will be fillet welds using E70 electrodes.

- For the base metal, $\phi R_n = \phi(F_y)A_{BM}$.

  For which the limiting stress is ϕF_y = 0.9(50) = 45.0 ksi.

- For the weld metal, $\phi R_n = \phi(F_y)A_w$ = 0.75(0.6)70(0.707)A_w.

  For which the limiting stress is 22.3 ksi.

Size a fillet weld, 6.5 inches long at the angle to the embedded plate in the footing. Using an elastic approach:

Resultant force = $\sqrt{V_{pr}^2 + T_{pr}^2} = \sqrt{6.46^2 + 27.0^2}$ = 27.8 kips

A_w = 27.8/22.3 = 1.24 in^2

$t = A_w/l$ =1.24 in^2 / 6.5 in. = 0.19 in.

For a 3/4 inch angle leg, use a 5/16 inch fillet weld. Given the importance of this weld, increasing the size to 3/8 inch would be a reasonable step. With ordinary quality control to avoid flaws, increasing the strength of this weld by such an amount should not have a detrimental effect elsewhere in the connection.

Now size the weld to the plate in the DT. Continue to use the conservative elastic method to calculate weld stresses. Try a fillet weld 6.5 inches long across the top and 4 inches long on each vertical leg of the angle. Using the free-body diagram of Figure 8.3-4 for tension and Figure 8.3-5 for shear, the weld moments and stresses are:

$M_x = T_{pr}(3.5)$ = 27.0(3.5) = 94.5 in-kips
$M_y = V_{pr}(3.5)$ = (6.46)(3.5) = 22.6 in-kips
$M_z = V_{pr}(y_b + 1.0)$
= 6.46(2.77 + 1.0) = 24.4 in-kips

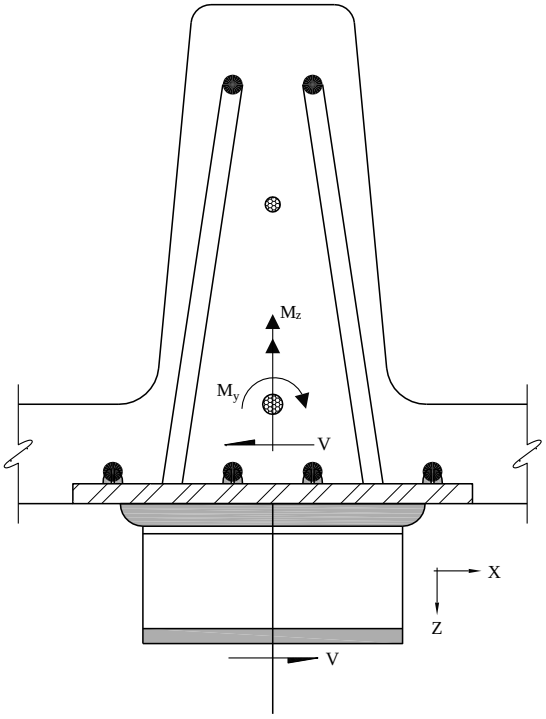

Figure 8.3-5 Free-body of angle with welds, top view, showing only shear forces and resisting moments

For the weld between the angle and the embedded plate in the DT as shown in Figure 8.3-5, the section properties for a weld leg (t) are:

$A = 14.5t$ in^2

$I_x = 25.0t$ in^4

$I_y = 107.4t$ in^4

$I_p = I_x + I_y = 132.4t$ in^4

$y_b = 2.90$ in.

$x_L = 3.25$ in.

To check the weld, stresses are computed at all four ends (and corners). The maximum stress is at the lower right end of the inverted "U" shown in Figure 8.3-4.

$$\sigma_x = \frac{V_{pr}}{A} + \frac{M_z y_b}{I_p} = \frac{6.46}{14.5t} + \frac{(24.4)(2.90)}{132.4t} = \frac{0.98}{t} \text{ ksi}$$

$$\sigma_y = -\frac{T_{pr}}{A} + \frac{M_z x_L}{I_p} = -\frac{27.0}{14.5t} + \frac{(24.4)(3.25)}{132.4t} = \frac{-1.26}{t} \text{ ksi}$$

$$\sigma_z = -\frac{M_y x_L}{A} - \frac{M_z y_b}{I_p} = -\frac{(22.6)(3.25)}{107.4t} - \frac{(94.5)(2.90)}{25.0t} = \frac{-11.8}{t} \text{ ksi}$$

$$\sigma_R = \sqrt{\sigma_x^2 + \sigma_y^2 + \sigma_z^2} = \frac{1}{t}\sqrt{0.98^2 + 1.26^2 + 11.8^2} = \frac{11.9}{t} \text{ ksi}$$

Thus, t = 11.9/22.3 = 0.53 inch, which can be taken as 9/16 inch. Field welds are conservatively sized with the elastic method for simplicity and to minimize construction issues.

8.3.5.4 Panel Reinforcement. Check the maximum compressive stress in the DT leg. Note that for an intermediate precast structural wall, ACI 318 Section 21.9.6 does not apply and transverse boundary element reinforcing is not required. However, the cross section must be designed for the loads associated with 1.5 times the moment that yields the base connectors.

Figure 8.3-6 shows the cross section used. The section is limited by the area of dry-pack under the DT at the footing.

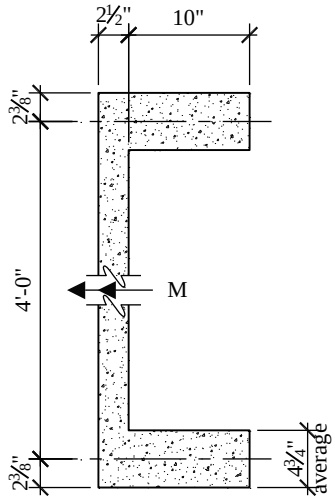

Figure 8.3-6 Cross section of the DT dry-packed at the footing
(1.0 in = 25.4 mm, 1.0 ft = 0.3048 m)

The reason to limit the area of dry-pack at the footing is to locate the boundary elements in the legs of the DT, at least at the bottom of the panel. The flange between the legs of the DT is not as susceptible to cracking during transportation as are the corners of DT flanges outside the confines of the legs. The compressive stress due to the overturning moment at the top of the footing and dead load is:

A = 227 in^2

S = 3240 in^3

$$\sigma_z = \frac{P}{A} + \frac{M_E}{S} = \frac{13{,}800}{227} + \frac{1.52\left(85{,}000 \times 12\right)}{3{,}240} = 539 \text{ ksi}$$

Roof live loads need not be included as a factored axial load in the compressive stress check, but the force from the prestress steel will be added to the compression stress above because the prestress force will be effective a few feet above the base and will add compression to the DT leg. Each leg of the DT will be reinforced with one 1/2-inch-diameter strand and one 3/8-inch-diameter strand. Figure 8.3-7 shows the location of these prestressed strands.

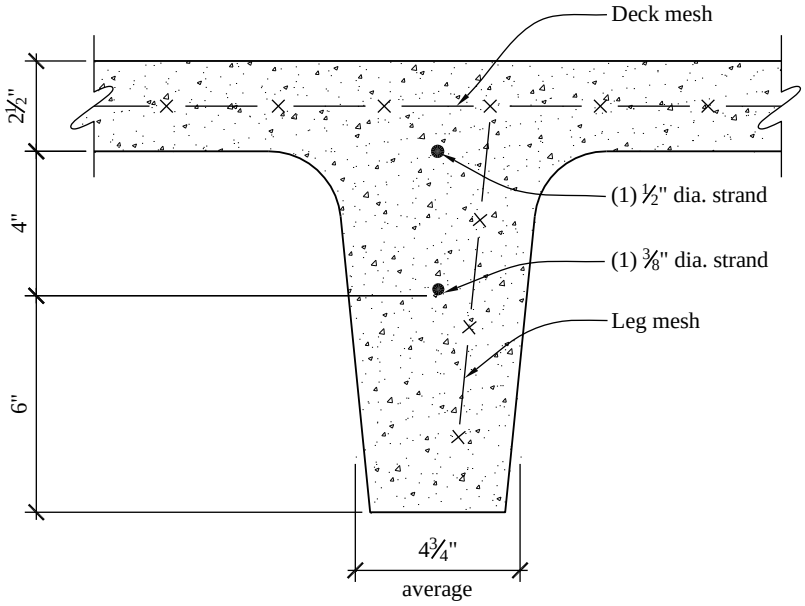

Figure 8.3-7 Cross section of one DT leg showing the location of the bonded prestressing tendons or strand
(1.0 in = 25.4 mm, 1.0 ft = 0.3048 m)

Next, compute the compressive stress resulting from these strands. Note that the moment at the height of strand development above the footing, about 26 inches for the effective stress (f_{se}), is less than at the top of footing. This reduces the compressive stress by:

$$\frac{\left(4.25\right)(26)}{3{,}240} \times 1{,}000 = 34 \text{ psi}$$

In each leg, use:

$P = 0.58 f_{pu} A_{ps} = 0.58(270 \text{ ksi})[0.153 + 0.085] = 37.3$ kips

$A = 168$ in^2

$e = y_b - CG_{Strand} = 9.48 - 8.57 = 0.91$ in.

S_b = 189 in^3

$$\sigma = \frac{P}{A} + \frac{Pe}{S} = \frac{37{,}300}{168} + \frac{0.91(37{,}300)}{189} = 402 \text{ psi}$$

Therefore, the total compressive stress is approximately 539 + 402 - 34 = 907 psi.

Since yielding is restricted to the steel angle and the DT is designed to be 1.5 times stronger than the yield force in the steel angle, the full strength of the strand can be used to resist axial forces in the DT stem, without concern for yielding in the strand.

D_2 = (0.042)(20.83)(8) = 7.0 kips

P_{min} = 0.7(7.0 + 2(1.08)) = 6.41 kips

M_E = (1.52)(4.25)(17.83) = 115.2 ft-kips

$T_{u,stem} = M_E/d - P_{min}/2$= 25.5 kips

The area of tension reinforcement required is:

$A_{ps} = T_{u,stem}/\phi f_{py}$ = (25.5 kips)/[0.9(270 ksi)] = 0.10 in^2

The area of one 1/2-inch-diameter strand and one 3/8-inch-diameter strand is 0.153 in^2 + 0.085 in^2 = 0.236 in^2. The mesh in the legs is available for tension resistance but is not required in this check.

To determine the nominal shear strength of the concrete for the connection design, complete the shear calculation for the panel in accordance with ACI 318 Section 11.9. The demand on each panel is:

$V_u = V_{pr}$ = 6.46 kips

Only the deck between the DT legs is used to resist the in-plane shear (the legs act like flanges, meaning that the area effective for shear is the deck between the legs). First, determine the minimum required shear reinforcement based on ACI 318 Section 11.9.

$$\phi V_c = \phi 2\lambda\sqrt{f_c'}hd = 0.75(2)(1.0)\sqrt{5{,}000}(2.5)(48) = 12.7 \text{ kips}$$

Since V_u of 6.46 kips exceeds $\phi V_u/2$ of 6.36 kips, provide minimum reinforcement per ACI 318 Section 11.9.9.2. Using welded wire reinforcement, the required areas of reinforcement are:

$A_v = A_{vh}$ = (0.0025)(2.5)(12) = 0.075 in^2/ft

Provide 6×6 – W4.0×W4.0 welded wire reinforcement.

$A_{sv} = A_{sh}$ = 0.08 in^2/ft

The prestress force and the area of the DT legs are excluded from the calculation of the nominal shear strength of the DT wall panel. The prestress force is not effective at the base, where the connection is and the legs are like the flanges of a channel, which are not effective in shear.

8.3.5.5 Tension and Shear at the Footing Embedment. Reinforcement to anchor the embedded plates is sized for the same tension and shear. Reinforcement in the DT leg and in the footing will be welded to embedded plates as shown in Figure 8.3-8.

The welded reinforcement is sloped to provide concrete cover and to embed the bars in the central region of the DT leg and footing. The tension reinforcement area required in the footing is:

$$A_{s,Sloped} = \frac{T_{u,stem}}{\phi f_y \cos\theta} = \frac{27.0}{(0.9)(60)\cos 26.5°} = 0.56 \text{ in}^2$$

Use two #5 bars (A_s = 0.62 in^2) at each embedded plate in the footing.

The shear bars in the footing will be two #4 bars placed on an angle of two-to-one. The resultant shear resistance is:

ϕV_n = 0.75(0.2)(2)(60)(cos26.5°) = 16.1 kips

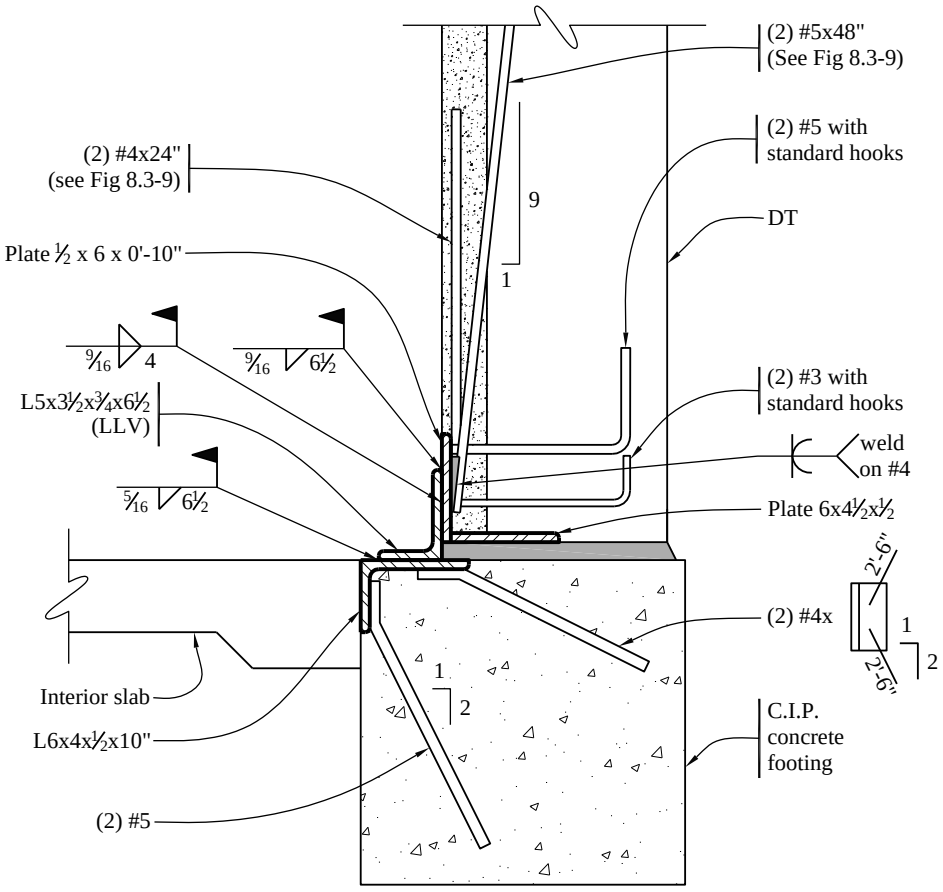

Figure 8.3-8 Section at the connection of the precast/prestressed shear wall panel and the footing
(1.0 in = 25.4 mm)

8.3.5.6 Tension and Shear at the DT Embedment. The area of reinforcement for the welded bars of the embedded plate in the DT, which develops tension as the angle bends through cycles, is:

$$A_s = \frac{T_{u,stem}}{\phi f_y \cos\theta} = \frac{27.0}{(0.9)(60)\cos 6.3°} = 0.503 \text{ in}^2$$

Two #5 bars are adequate. Note that the bars in the DT leg are required to extend upward the development length of the bar, which would be 22 inches. In this case, they will be extended 22 inches past the point of development of the effective stress in the strand, which totals approximately 48 inches.

The same embedded plate used for tension will also be used to resist one-half the nominal shear. This shear force is 6.46 kips. The transfer of direct shear to the concrete is easily accomplished with bearing on the sides of the reinforcing bars welded to the plate. Two #5 and two #4 bars (explained later) are welded to the plate. The available bearing area is approximately A_{br} = 4(0.5 in.)(5 in.[available]) = 10 in^2 and the bearing capacity of the concrete is ϕV_n = (0.65)(0.85)(5 ksi)(10 in^2) = 27.6 kips, which is greater than the 6.46 kip demand.

The weld of these bars to the plate must develop both the tensile demand and this shear force. The weld is a flare bevel weld, with an effective throat of 0.2 times the bar diameter along each side of the bar. (Refer to the PCI Handbook.) Using the weld capacity for the #5 bar:

ϕV_n = (0.75)(0.6)(70 ksi)(0.2)(0.625 in.)(2) = 7.9 kips/in

The shear demand is prorated among the four bars as (6.46 kip)/4 = 1.6 kips. The tension demand is $T_{u,stem}$/2(13.5 kips). The vectorial sum of shear and tension demand is 13.6 kips. Thus, the minimum length of weld is 13.6/7.9 = 1.7 inches.

8.3.5.7 Resolution of Eccentricities at the DT Embedment. Check the twisting of the embedded plate in the DT for M_z. Use M_z = 24.4 in-kips.

$$A_s = \frac{M_z}{\phi f_y (jd)} = \frac{24.4}{0.9(60)(9.0)} = 0.05 \text{ in}^2$$

Use one #4 bar on each side of the vertical embedded plate in the DT as shown in Figure 8.3-9. This is the same bar used to transfer direct shear in bearing.

Check the DT embedded plate for M_y (equal to 22.6 in-kips) and M_x (equal to 94.5 in-kips) using the two #4 bars welded to the back side of the plate near the corners of the weld on the loose angle and the two #3 bars welded to the back side of the plate near the bottom of the DT leg (as shown in Figure 8.3-9). It is relatively straightforward to compute the resultant moment magnitude and direction, assume a triangular compression block in the concrete and then compute the resisting moment. It is quicker to make a reasonable assumption as to the bars that are effective and then compute resisting moments about the X and Y axes. That approximate method is demonstrated here. The #5 bars are effective in resisting M_x and one each of the #3 and #5 bars are effective in resisting M_y. For M_y assume that the effective depth extends 1 inch beyond the edge of the angle (equal to twice the thickness of the plate). Begin by assigning one-half of the "corner" #5 bar to each component.

With A_{sx} = 0.31 + 0.31/2 = 0.47 in^2:

$\phi M_{nx} = \phi A_s f_y jd$ = (0.9)(0.47 in^2)(60 ksi)(0.95)(5 in.) = 120 in-kips (> 94.5 in-kips)

With A_{sy} = 0.11 + 0.31/2 = 0.27 in^2:

$\phi M_{ny} = \phi A_s f_y jd$ = (0.9)(0.27 in^2)(60 ksi)(0.95)(5 in.) = 69 in-kips (> 22.6 in-kips)

Each component is strong enough, so the proposed bars are satisfactory.

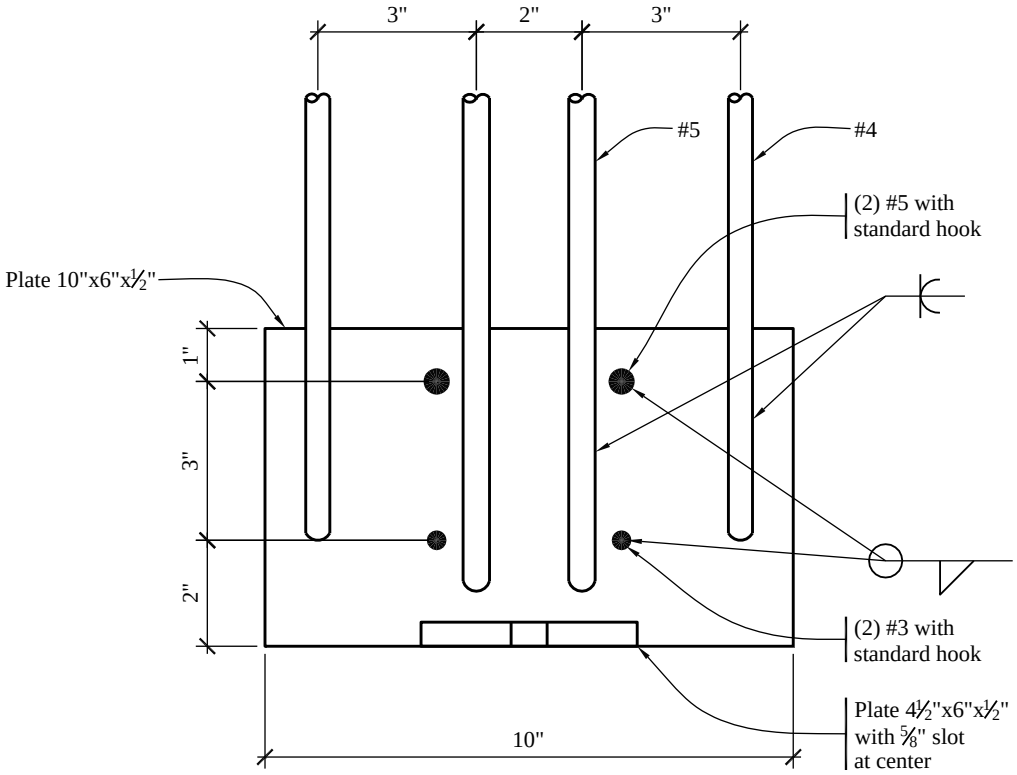

Figure 8.3-9 Details of the embedded plate in the DT at the base
(1.0 in = 25.4 mm)

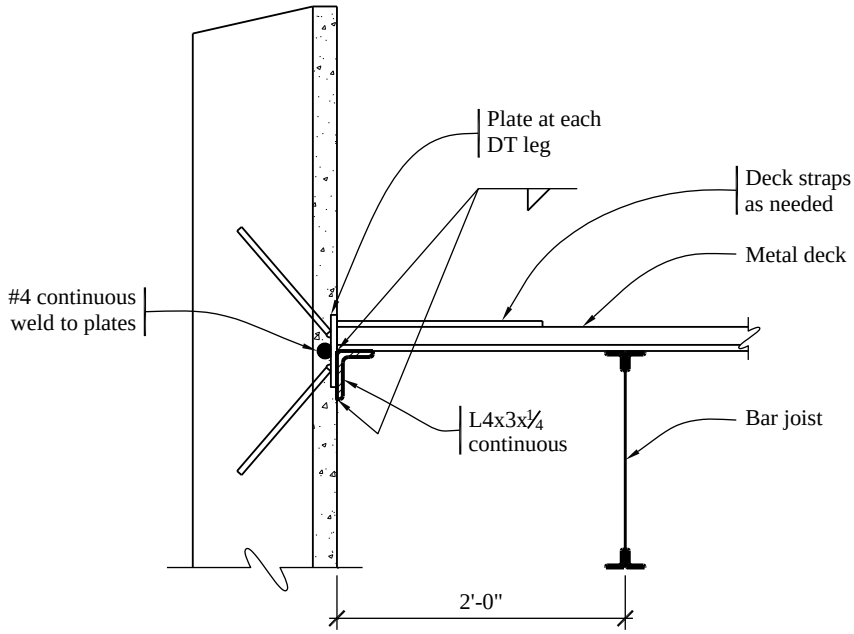

Figure 8.3-10 Sketch of connection of non-load-bearing DT wall panel at the roof
(1.0 in = 25.4 mm, 1.0 ft = 0.3048 m)

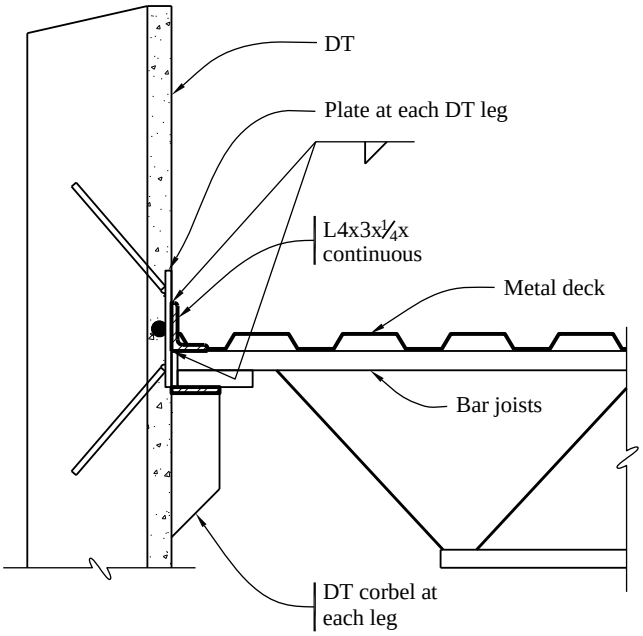

Figure 8.3-11 Sketch of connection of load-bearing DT wall panel at the roof
(1.0 in = 25.4 mm)

8.3.5.8 Other Connections. This design assumes that there is no in-plane shear transmitted from panel to panel. Therefore, if connections are installed along the vertical joints between DT panels to control the

out-of-plane alignment, they should not constrain relative movement in-plane. In a practical sense, this means the chord for the roof diaphragm should not be a part of the panels. Figures 8.3-10 and 8.3-11 show the connections at the roof and DT wall panels. These connections are not designed here. Note that the continuous steel angle would be expected to undergo vertical deformations as the panels deform laterally.

Because the diaphragm supports concrete walls out of their plane, *Standard* Section 12.11.2.1 requires specific force minimums for the connection and requires continuous ties across the diaphragm. Also, it specifically prohibits use of the metal deck as the ties in the direction perpendicular to the deck span. In that direction, the designer may wish to use the top chord of the bar joists, with an appropriate connection at the joist girder, as the continuous cross ties. In the direction parallel to the deck span, the deck may be used, but the laps should be detailed accordingly.

In precast DT shear wall panels with flanges thicker than 2-1/2 inches, consideration may be given to using vertical connections between the wall panels to transfer vertical forces resulting from overturning moments and thereby reduce the overturning moment demand. These types of connections are not considered here, since the uplift force is small relative to the shear force and cyclic loading of bars in thin concrete flanges is not always reliable in earthquakes.

8.4 SPECIAL MOMENT FRAMES CONSTRUCTED USING PRECAST CONCRETE

As for special concrete walls, the *Standard* does not distinguish between a cast-in-place and a precast concrete special moment frame in Table 12.2-1. However, ACI 318 Section 21.8 provides requirements for special moment frames constructed using precast concrete. That section provides requirements for designing special precast concrete frame systems using either ductile connections (ACI 318 Sec. 21.8.2) or strong connections (ACI 318 Sec. 21.8.3.) ACI 318 Section 21.8.4 also explicitly allows precast moment frame systems that meet the requirements of ACI 374.1, *Acceptance Criteria for Moment Frames based on Structural Testing*.

8.4.1 Ductile Connections

For moment frames constructed using ductile connections, ACI 318 requires that plastic hinges be able to form in the connection region. All of the requirements for special moment frames must still be met, plus there is an increased factor that must be used in developing the shear demand at the joint.

It is interesting to note that while Type 2 connectors can be used anywhere (including in a plastic hinge region) in a cast-in-place frame, these same connectors cannot be used closer than $h/2$ from the joint face in a ductile connection. The rationale behind this requirement is that in a jointed system, a concentrated crack occurs at the joint between precast elements in a ductile connection. Thus the rotation is concentrated at this location. Type 2 connectors are actually strong connections, relative to the bar, as they are designed to develop the tensile strength of the bar. The objective of Type 2 connectors is that they relocate the yielding away from the connector, into the bar itself.

If a Type 2 connector is used at the face of a column as shown in Figure 8.4-1 and the bar size is the same in both the column and the beam, yielding will occur at the joint at the face of the column but not be able to spread into the beam to develop a plastic hinge, due to the strength of the connector. This concentrates the yielding in the bar to the left of the connector and likely will fracture the bar when significant rotation is imposed on the beam.

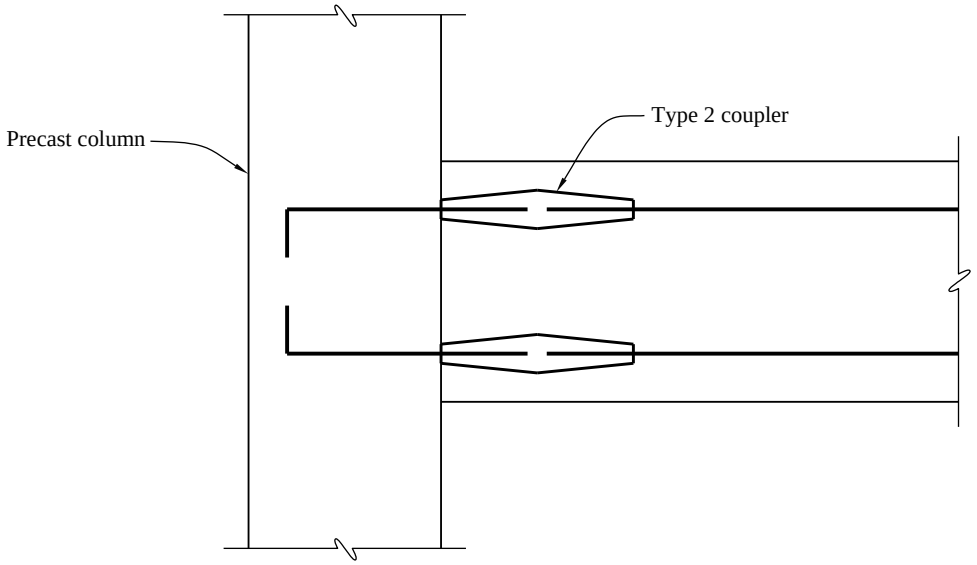

Figure 8.4-1 Type 2 coupler location in a strong connection
(1.0 in = 25.4 mm, 1.0 ft = 0.3048 m)

In a ductile connection, frame yielding takes place at the connection. This is most easily accomplished by extending the reinforcement out of the precast column element and coupling this rebar at the end of the precast beam. Since the couplers have to be located a minimum distance of $h/2$ from the joint face (i.e., column face) the resulting gap between the precast beam and precast column is filled with cast-in-place concrete as shown in Figure 8.4-2.

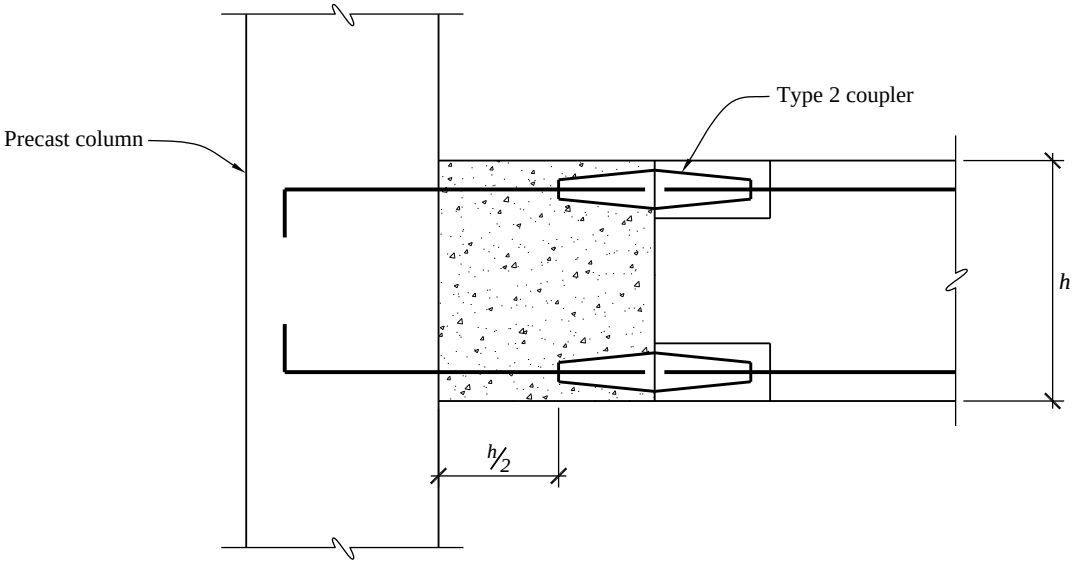

Figure 8.4-2 Type 2 coupler location in a ductile connection
(1.0 in = 25.4 mm, 1.0 ft = 0.3048 m)

8.4.2 Strong Connections

ACI 318 also provides design rules for strong connections used in special moment frames. The concept is to provide connections that are strong enough to remain elastic when a plastic hinge forms in the beam. Thus the frame behavior is the same as would occur if the connection were monolithic.

Using the frame in Figure 8.4-3 (ignoring gravity forces for simplicity), design forces for the plastic hinge region and the associated forces on the precast connection are computed. Assuming inflection points at mid-height of the columns and a seismic shear force of V_{col} on each column:

$$V_b = V_{col} \frac{H_c}{L_b}$$

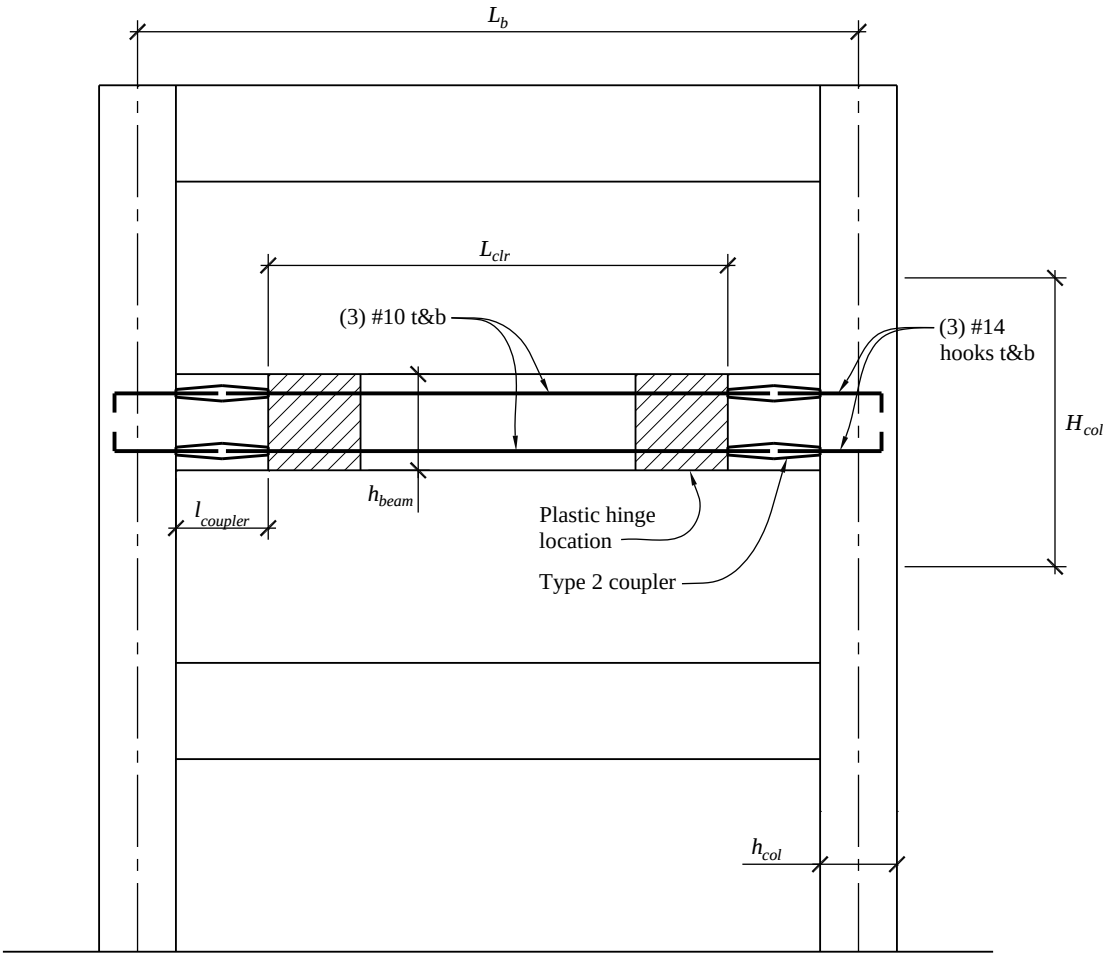

Figure 8.4-3 Moment frame geometry
(1.0 in = 25.4 mm, 1.0 ft = 0.3048 m)

Under seismic loads alone, the shear is constant along the beam length. Therefore, the moment at the joint between the end of the beam and the column is:

$$M_{joint} = V_b \frac{L_b - h_{col}}{2}$$

The plastic hinge, however, will be relocated to the side of the Type 2 coupler away from the column. With a coupler length of $l_{coupler}$, the moment at the end of the coupler is:

$$M_b = M_{joint} - V_b l_{coupler}$$

In order to ensure that the hinge forms at the intended location (away from the precast connection), the connection needs to be designed to be stronger than the moment associated with the development of the plastic hinge. This is done by upsizing the bar that is anchored into the column.

8.4.2.1 Strong Connection Example. In the following numerical example, a single-bay frame is designed to meet the requirements of a precast frame using strong connections at the beam-column interface. Using Figure 8.4-3 and the following geometry:

H_{col} = 12 ft

h_{col} = 36 in.

L_b = 30 ft (column centerline to column centerline)

$l_{coupler}$ = 18 in.

$L_{clr} = L_b - h_{col} - 2l_{coupler}$ = 24 ft (distance between plastic hinge locations)

h_{beam} = 42 in.

Reinforcing the beam with three #10 bars top and bottom, the nominal moment strength of the beam is:

$$a = \frac{A_s F_y}{0.85 f_c' b} = \frac{3(1.27)(60)}{0.85(5)(18)} = 3.0 \text{ in.}$$

$$\phi M_n = \phi A_s F_y \left(d - \frac{a}{2} \right) = 0.9(3)(1.27)(60)\left(33 - \frac{3.0}{2} \right) / 12 = 540 \text{ ft-kips}$$

This is the moment strength at the plastic hinge location. The strong precast connection must be designed for the loads that occur at the connection when the beam at the plastic hinge location develops its probable strength.

Therefore, the moment strength at the beam-column interface (which also is the precast joint location) must be at least:

$$M_{u,joint} = M_{pr} \frac{L_b - h_{col}}{L_{clr}}$$

Where:

$$M_{pr} = \phi M_n \frac{1.25}{\phi} = 540\frac{1.25}{0.9} = 750 \text{ ft-kips}$$

Therefore, the design strength of the connection must be at least:

$$M_{u,\,joint} = 750\frac{30 - 36/12}{24} = 843 \text{ ft-kips}$$

Using #14 bars in the column side of the Type 2 coupler:

$$a = \frac{A_s F_y}{0.85 f_c' b} = \frac{3(2.25)(60)}{0.85(5)(18)} = 5.3 \text{ in.}$$

$$\phi M_n = \phi A_s F_y \left(d - \frac{a}{2}\right) = 0.9(3)(2.25)(60)\left(33 - \frac{5.3}{2}\right)/12 = 921 \text{ ft-kips}$$

which is greater than the load at the connection (843 ft-kips) when the plastic hinge develops.

If column-to-column connections are required, ACI 318 Section 21.8.3(d) requires a 1.4 amplification factor, in addition to loads associated with the development of the plastic hinge in the beam. Locating the column splice near the point of inflection, while difficult for construction, can help to make these forces manageable.

The beam shear, when the plastic hinge location reaches its nominal strength, is:

$$V_{beam} = \frac{\phi M_n}{L_{clr}/2} = \frac{540}{24/2} = 20 \text{ kips}$$

Assuming inflection points at the mid-span of the beam and mid-height of the column, the column shear is:

$$V_{col} = V_{beam}\frac{L_b}{H_{col}} = 20\frac{30}{12} = 50 \text{ kips}$$

However, the column shear must be amplified to account for the development of the plastic hinge.

$$V_u = V_{col}\frac{M_{pr}}{\phi M_n} = 50\frac{750}{540} = 69 \text{ kips}$$

The column design moment is:

$$M_u = V_u \frac{(H_{col} - h_{beam})}{2} = 69\frac{12 - 42/12}{2} = 293 \text{ ft-kips}$$

At the connection, this moment is amplified by 1.4 for a strong connection design moment of 410 ft-kips. This moment must be combined with the axial load on the connection from both gravity loads and amplified seismic forces.

The balance of the design is the same as for a cast-in-place special moment frame.

9

Composite Steel and Concrete

Clinton O. Rex, P.E., PhD

Originally developed by
James Robert Harris, P.E., PhD and Frederick R. Rutz, P.E., PhD

Contents

9.1 BUILDING DESCRIPTION 3
9.2 PARTIALLY RESTRAINED COMPOSITE CONNECTIONS 7
9.2.1 Connection Details 7
9.2.2 Connection Moment-Rotation Curves 10
9.2.3 Connection Design 13
9.3 LOADS AND LOAD COMBINATIONS 17
9.3.1 Gravity Loads and Seismic Weight 17
9.3.2 Seismic Loads 18
9.3.3 Wind Loads 19
9.3.4 Notional Loads 19
9.3.5 Load Combinations 20
9.4 DESIGN OF C-PRMF SYSTEM 21
9.4.1 Preliminary Design 21
9.4.2 Application of Loading 22
9.4.3 Beam and Column Moment of Inertia 23
9.4.4 Connection Behavior Modeling 24
9.4.5 Building Drift and P-delta Checks 24
9.4.6 Beam Design 26
9.4.7 Column Design 27
9.4.8 Connection Design 28
9.4.9 Column Splices 29
9.4.10 Column Base Design 29

The 2009 *NEHRP Recommended Provisions* for the design of a composite building using a "Composite Partially Restrained Moment Frame" (C-PRMF) as the lateral force-resisting system is illustrated in this chapter by means of an example design. The C-PRMF lateral force-resisting system is recognized in *Standard* Section 12.2 and in AISC 341 Part II Section 8; and it is an appropriate choice for buildings in low to moderate Seismic Design Categories (SDC A to D). There are other composite lateral force-resisting systems recognized by the *Standard* and AISC 341; however, the C-PRMF is the only one illustrated in this set of design examples.

The design of a C-PRMF is different from the design of a more traditional steel moment frame in three important ways. First, the design of a Partially Restrained Composite Connection (PRCC) differs in that the connection itself is not designed to be stronger than the beam it is connecting. Consequently, the lateral system typically will hinge within the connections and not within the associated beams or columns. Second, because the connections are neither simple nor rigid, their stiffness must be accounted for in the frame analysis. Third, because the connections are weaker than fully restrained moment connections, the lateral force-resisting system requires more frames with more connections, resulting in a highly redundant system.

In addition to the 2009 *NEHRP Recommended Provisions* (referred to herein as the *Provisions*), the following documents are referenced throughout the example:

ACI 318	American Concrete Institute. 2008. *Building Code Requirements for Structural Concrete*.
AISC 341	American Institute of Steel Construction. 2005. *Seismic Provisions for Structural Steel Buildings*, including Supplement No. 1.
AISC 360	American Institute of Steel Construction. 2005. *Specification for Structural Steel Buildings*.
AISC Manual	American Institute of Steel Construction. 2005. *Steel Construction Manual*. Thirteenth Edition.
AISC SDGS-8	American Institute of Steel Construction. 1996. *Partially Restrained Composite Connections*, Steel Design Guide Series 8. Chicago: AISC.
AISC SDM	American Institute of Steel Construction. 2006. *Seismic Design Manual.* First Edition.
Arum (1996)	Mayangarum, Arum, 12-5-1996. Design, Analysis and Application of Bolted Semi-Rigid Connections for Moment Resisting Frames, MS Thesis, Lehigh University.
ASCE TC	American Society of Civil Engineers Task Committee on Design Criteria for Composite Structures in Steel and Concrete. October 1998. "Design Guide for Partially Restrained Composite Connections," *Journal of Structural Engineering* 124(10).
RCSC	Research Council on Structural Connections. 2004. *Specification for Structural Joints Using ASTM A325 or A490 Bolts.*
Standard	American Society of Civil Engineers, 2005, ASCE/SEI 7-05 Minimum Design Loads for Buildings and other Structures

Yura (2006) Yura, Joseph A and Helwig, Todd A. (2-8-2006) Notes from SSRC/AISC Short Course 2 on “Beam Buckling and Bracing”The short-form designations presented above for each citation are used throughout.

The PRCC used in the example has been subjected to extensive laboratory testing, resulting in the recommendations of AISC SDGS-8 and ASCE TC. ASCE TC is the newest of the two guidance documents and is referenced here more often; however, AISC SDGS-8 provides information not in ASCE TC, which is still pertinent to the design of this type of frame. While both of these documents provide guidance for design of PRCC, the method presented in this design example deviates from that guidance based on more recent code requirements for stability and on years of experience in designing C-PRMF systems.

The structure is analyzed using three-dimensional, static, nonlinear methods. The SAP 2000 analysis program, v. 14.0 (Computers and Structures, Inc., Berkeley, California) is used in the example.

The symbols used in this chapter are from Chapter 2 of the *Standard* or the above referenced documents, or are as defined in the text. U.S. Customary units are used.

9.1 BUILDING DESCRIPTION

The example building is a four-story steel framed medical office building located in Denver, Colorado (see Figures 9.1-1 through 9.1-3). The building is free of plan and vertical irregularities. Floor and roof slabs are 4.5-inch normal-weight reinforced concrete on 0.6-inch form deck (total slab depth of 4.5 inches.). Typically slabs are supported by open web steel joists which are supported by composite steel girders. Composite steel beams replace the joists at the spandrel locations to help control cladding deflections. The lateral load-resisting system is a C-PRMF in accordance with *Standard* Table 12.2-1 and AISC 341 Part II Section 8. The C-PRMF uses PRCCs at almost all beam-to-column connections. A conceptual detail of a PRCC is presented in Figure 9.1-4. The key advantage of this type of moment connection is that it requires no welding. The lack of field welding results in erection that is quicker and easier than that for more traditional moment connections with CJP welding and the associated inspections.

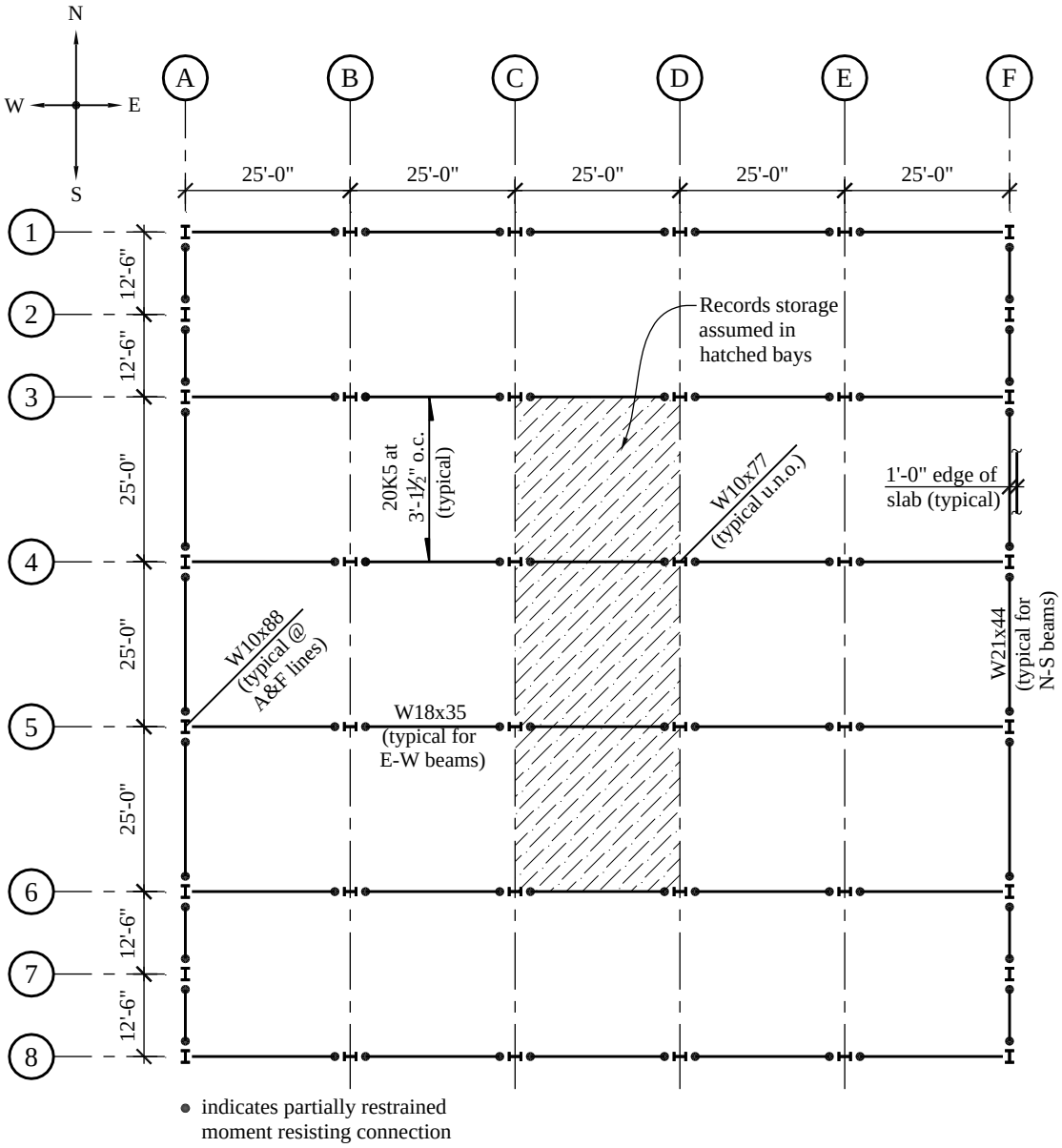

Figure 9.1-1 Typical floor and roof plan

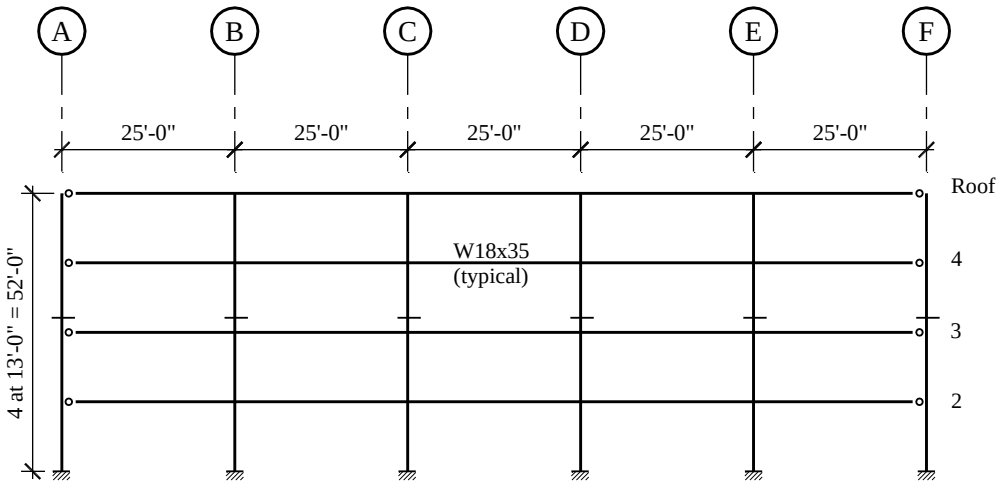

Figure 9.1-2 Building end elevation

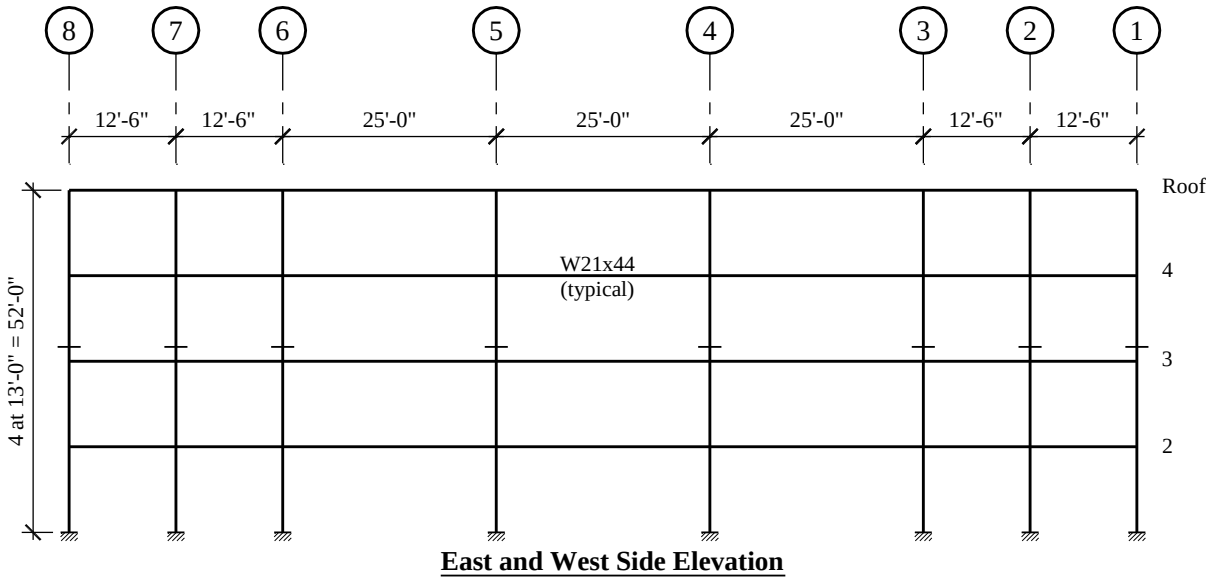

Figure 9.1-3 Building side elevation

The building is located in a relatively low seismic hazard region, but localized internal storage loading and Site Class E are used in this example to provide somewhat higher seismic design forces for purposes of illustration and to push the example building into Seismic Design Category C.

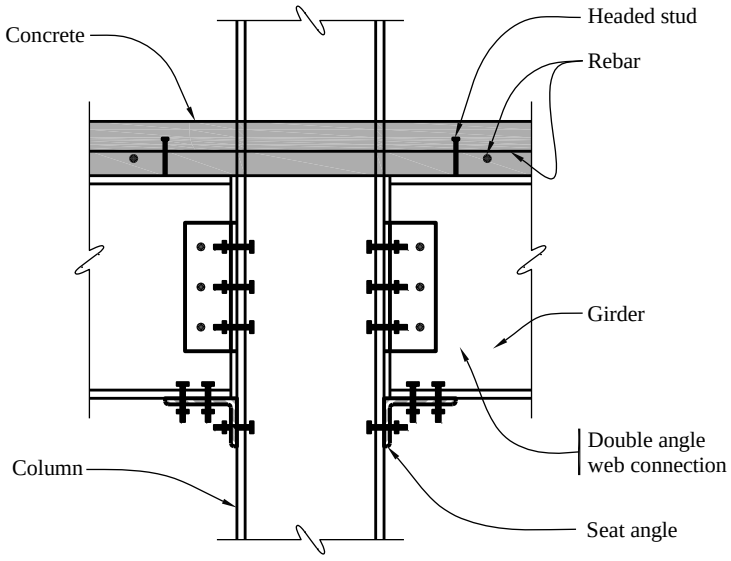

Figure 9.1-4 Conceptual partially restrained composite connection (PRCC)

There are no foundations designed in this example. For this location and system, the typical foundation would be a drilled pier and voided grade beam system, which would provide flexural restraint for the strong axis of the columns at their base (very similar to the foundation for a conventional steel moment frame). The main purpose here is to illustrate the procedures for the PRCCs. The floor and roof slabs serve as horizontal diaphragms distributing the seismic forces and by inspection they are stiff enough to be considered as rigid.

The typical bay spacing is 25 feet. Architectural considerations allowed an extra column at the end bay of each side in the north-south direction, which is useful in what is the naturally weaker direction. The exterior frames in the north-south direction have moment-resisting connections at all columns. The frames in each bay in the east-west direction have moment-resisting connections at all columns except the end columns. Composite connections to the weak axis of the column are feasible, but they are not used for this design. The PRCC connection locations are illustrated in Figure 9.1-1.

Material properties in this example are as follows:

- Structural steel beams and columns (ASTM A992): F_y = 50 ksi
- Structural steel connection angles and plates (ASTM A36): F_y = 36 ksi
- Concrete slab (4.5 inches thick on form deck, normal weight): f_c' = 3,000 psi
- Steel reinforcing bars (ASTM A615): F_y = 60 ksi

9.2 PARTIALLY RESTRAINED COMPOSITE CONNECTIONS

9.2.1 Connection Details

The type of PRCC used for this example building consists of a reinforced composite slab, a double-angle bolted web connection and a bolted seat angle. In real partially restrained building design, it is advantageous to select and design the complete PRCC simply based on beam depth and element capacities. Generally it is impractical to "tune" connections to beam plastic moment capacities and/or lateral load demands. This allows the designer to develop an in-house suite of PRCC details and associated behavior curves for each nominal beam depth ahead of time. Slight adjustments can be made later to account for real versus nominal beam depth.

It is considered good practice (particularly for capacity-based seismic design) to provide substantial rotation capacity at connections while avoiding non-ductile failure modes. This requirement for ductile rotation capacity is expressed in AISC 341 Part II Section 8.4 as a requirement for story drift of 0.04 radians. Because much of the drift in a partially restrained building comes from connection rotation, this story drift requirement implies a connection rotation ductility requirement. In short, connections must be detailed to allow ductile modes to dominate over non-ductile failure modes.

Practical detailing is limited by commonly available components. For instance, the largest angle leg commonly available is 8 inches, which can reasonably accommodate four 1-inch-diameter bolts. As a result, the maximum shear that can be delivered from the beam flange to the seat angle is limited by shear in four A490-X bolts. Bolt shear failure is generally considered to be non-ductile, so the rest of the connection design and detailing aims to maximize moment capacity of the connection while avoiding this limit state.

The connection details chosen for this example are illustrated in Figures 9.2-1, 9.2-2, 9.2-3 and 9.2-4.

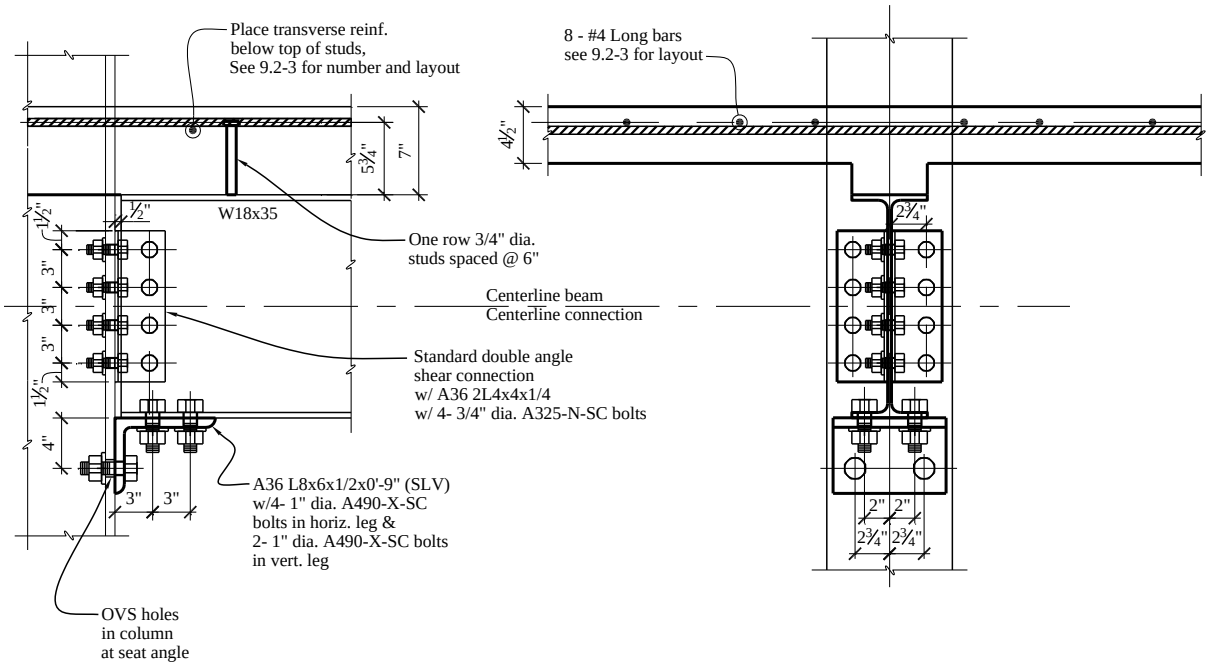

Figure 9.2-1 Typical interior W18x35 PRCC

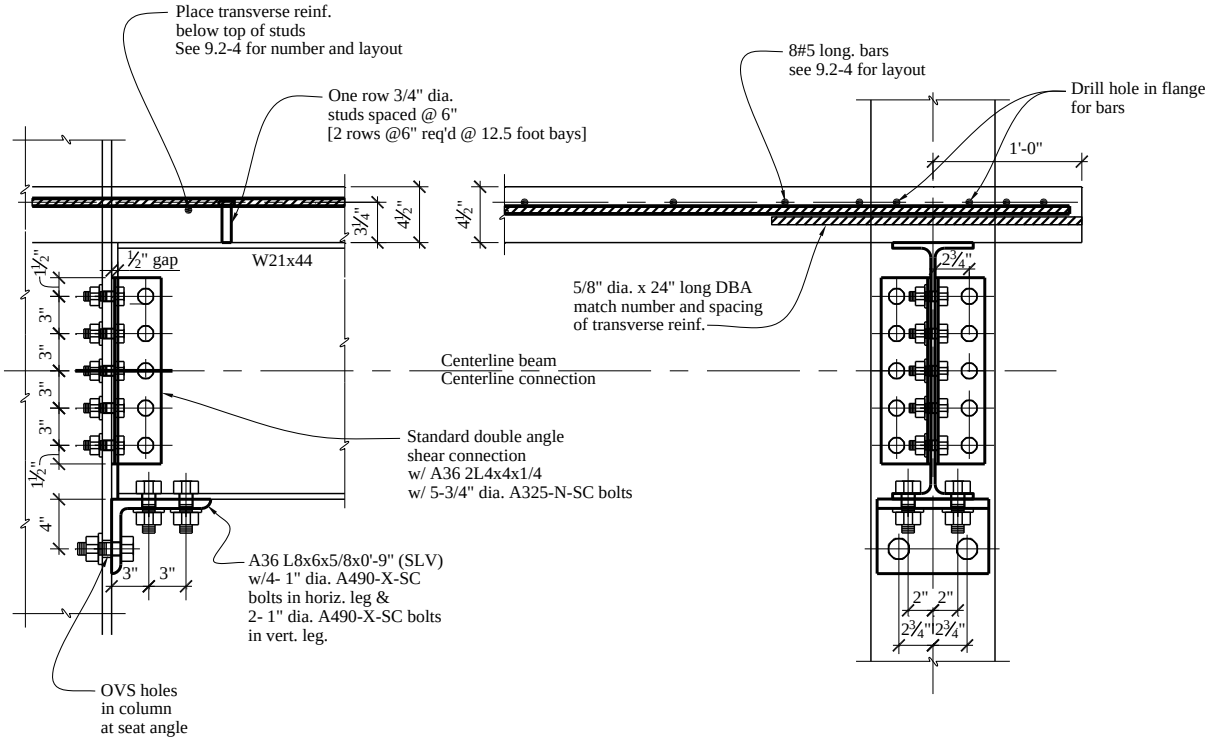

Figure 9.2-2 Typical spandrel W21x44 PRCC

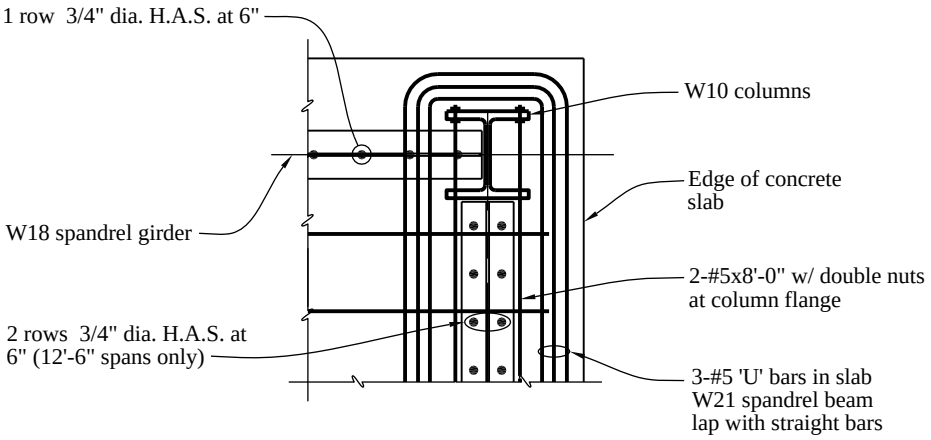

Figure 9.2-3 Typical corner PRCC

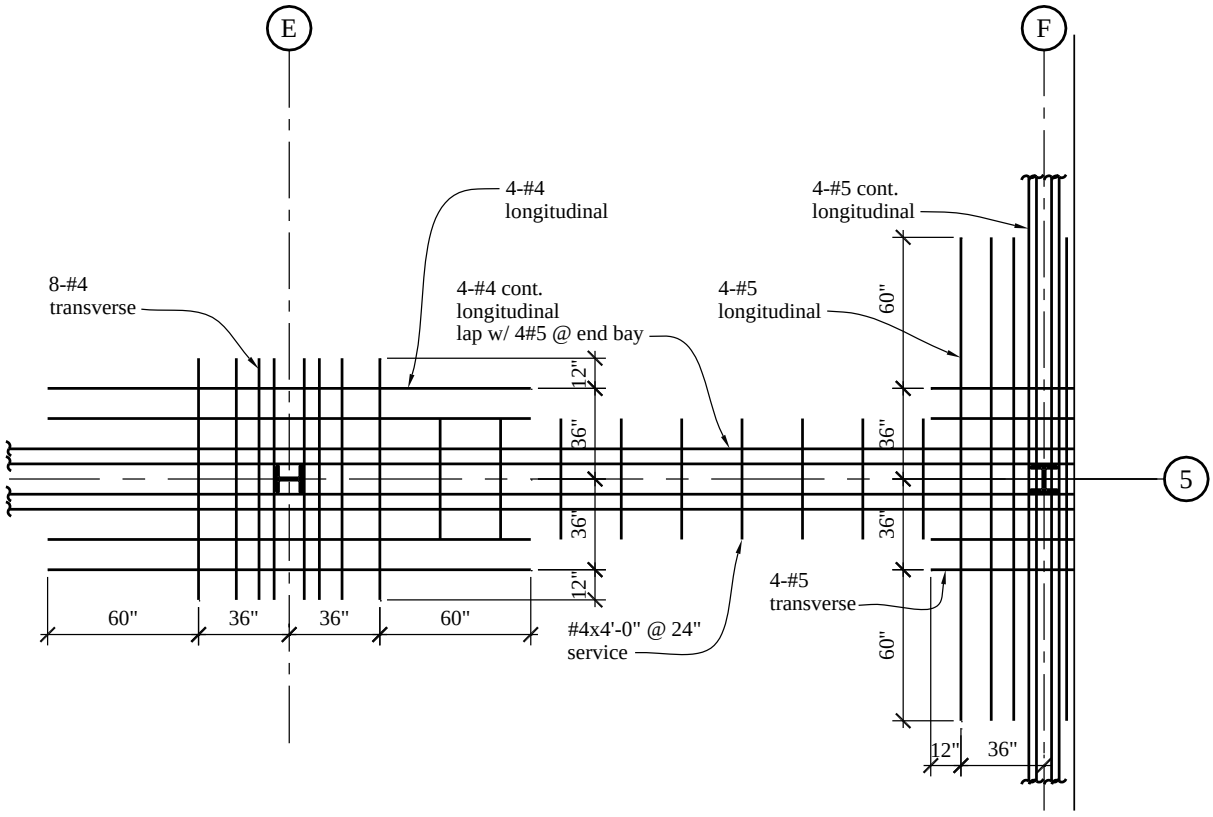

Figure 9.2-4 Typical PRCC reinforcing plan

9.2.2 Connection Moment-Rotation Curves

Two connection moment-rotation curves are required for the design of partially restrained buildings: the nominal moment-rotation curve and the modified moment-rotation curve.

The nominal moment-rotation curve, obtained from connection test data or from published moment-rotation prediction models, is used for service-level load design. For this example, the published moment-rotation prediction model given in ASCE TC is used to define the moment-rotation curve for the PRCC.

Negative moment-rotation behavior (slab in tension):

$$M_c^- = C_1\left(1 - e^{-C_2\theta}\right) + C_3\theta \qquad \text{(ASCE TC, Eq. 4)}$$

Where:

C_1 = 0.18(4 × $A_{rb}F_{yrb}$ + 0.857$A_{sa}F_{ya}$)(d + Y_3), kip-in.
C_2 = 0.775
C_3 = 0.007(A_{sa} + A_{wa})F_{ya} (d + Y_3), kip-in.
θ = connection rotation (mrad = radians × 1,000)
d = beam depth, in.
Y_3 = distance from top of beam to the centroid of the longitudinal slab reinforcement, in.
A_{rb} = area of longitudinal slab reinforcement, in^2
A_{sa} = gross area of seat angle leg, in^2
(For use in these equations, A_{sa} is limited to a maximum of 1.5A_{rb})
A_{wa} = gross area of double web angles for shear calculations, in^2
(For use in these equations, A_{wa} is limited to a maximum of 2.0A_{sa})
F_{yrb} = yield stress of reinforcing, ksi
F_{ya} = yield stress of seat and web angles, ksi

Positive moment-rotation behavior (slab in compression):

$$M_c^+ = C_1\left(1 - e^{-C_2\theta}\right) + (C_3 + C_4)\theta \qquad \text{(ASCE TC, Eq. 3)}$$

Where:

C_1 = 0.2400[(0.48A_{wa}) + A_{sa}](d + Y_3)F_{ya}, kip-in.
C_2 = 0.0210(d + Y_3/2)
C_3 = 0.0100(A_{wL} + A_L)(d + Y_3)F_{ya}, kip-in.
C_4 = 0.0065 A_{wL}(d + Y_3)F_{ya}, kip-in.

The modified moment-rotation curve is used for strength level load design. The Direct Analysis Method requires two modifications to the nominal moment-rotation curve: an elastic stiffness reduction and a strength reduction. AISC 360 Section 7.3(3) requires an elastic stiffness reduction of 0.8, which is accomplished by translating the connection rotation by an elastic stiffness reduction offset. This translation can be shown as follows:

$$\theta_{cDAM} = \theta_c + \frac{M_c}{4 \times K_{ci}}$$

Where:

M_c = connection moment from the nominal moment-rotation curve, kip-in.
K_{ci} = connection initial stiffness, kip-in./mrad; because the moment-rotation curve is nonlinear, it is necessary to define how the initial stiffness will be measured. For this example, the initial stiffness will be taken as the secant stiffness to the moment-rotation curve at θ = 2.5 mrad as suggested in ASCE TC. Note that this will be different values for the positive and negative moment-rotation portions of the connection behavior.

$$K_{ci} = \frac{M_{c@2.5\,mrad}}{2.5\,mrad}$$

The second modification to the nominal moment-rotation curve is a strength reduction associated with ϕ. ASCE TC recommends using ϕ equal to 0.85. The associated connection strength is given by:

$M_{cDAM} = 0.85\ M_c$

From these equations, curves for M-θ can be developed for a particular connection. The moment-rotation curves for the typical connections associated with the W18x35 girder and the W21x44 spandrel beam are presented in Figures 9.2-5 and 9.2-6, respectively.

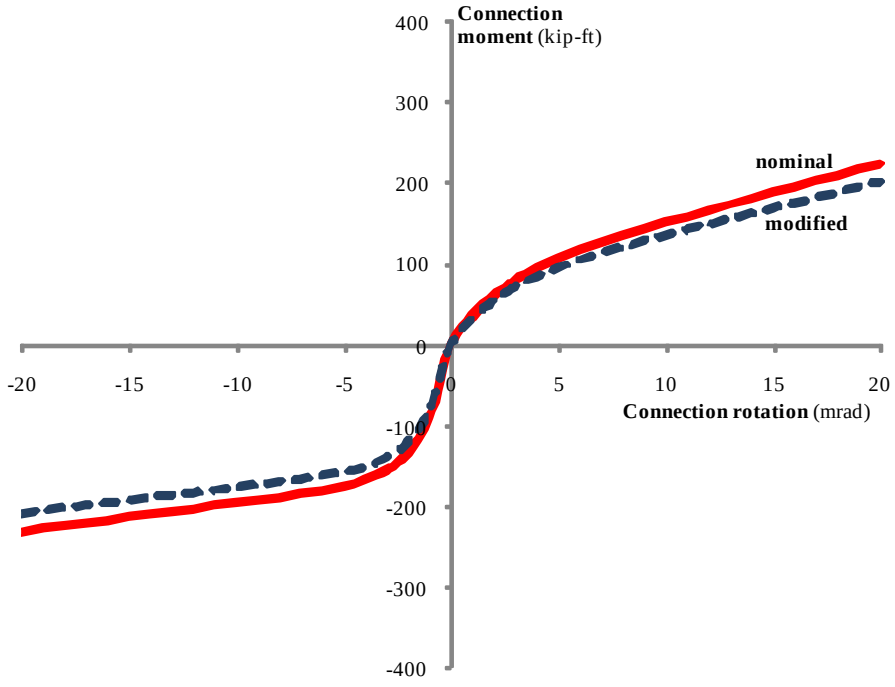

Figure 9.2-5 Typical interior W18x35 PRCC M-θ curves

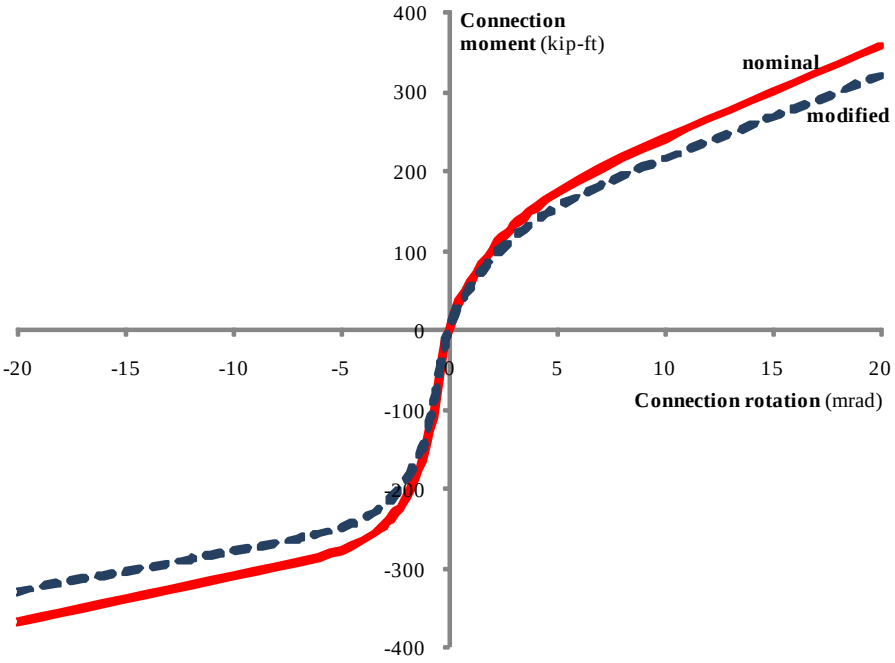

Figure 9.2-6 Typical spandrel W21x44 PRCC *M*-θ curves

Important key values from the above connection curves are summarized in Table 9.2-1 for reference in later parts of the example design.

Table 9.2-1 Key Connection Values From Moment-Rotation Curves

	W18x35 PRCC	W21x44 PRCC
K_{ci}^- (kip-in/rad) (nominal)	704,497	1,115,253
K_{ci}^+ (kip-in/rad) (nominal)	338,910	554,498
M_c^- @ 20 mrad (kip-ft) (nominal/modified)	232/206	367/326
M_c^+ @ 10 mrad (kip-ft) (nominal/modified)	151/127	240/202

These curves and the corresponding equations do not reproduce the results of any single test. Rather, they are averages fitted to real test data using numerical methods and they smear out the slip of bolts into bearing. Articles in the *AISC Engineering Journal* (Vol. 24, No.2; Vol. 24, No.4; Vol. 27, No.1; Vol. 27, No. 2; and Vol. 31, No. 2) describe actual test results. Those tests demonstrate clearly the ability of the connection to satisfy the rotation requirements of AISC 341 Part II Section 8.4.

9.2.3 Connection Design

This section illustrates the detailed design decisions and checks associated with the typical W21x44 spandrel beam connection. A complete design would require similar checks for each different connection type in the building. Design typically involves iteration on some of the chosen details until all the design checks are within acceptable limits.

9.2.3.1 Longitudinal Reinforcing Steel. The primary negative moment resistance derives from tensile yielding of slab reinforcing steel. Since ductile response of the connection requires that the reinforcing steel yield and elongate prior to failure of other connection components, providing too much reinforcing is not a good thing. The following recommendations are from ASCE TC.

A minimum of six bars (three bars each side of column), #6 or smaller, should be used (eight #5 bars have been used in this example). The bars should be distributed symmetrically within a total effective width of seven column flange widths (36 inches at each side of the column has been used in this example). For edge beams, the steel should be distributed as symmetrically as possible, with at least one-third (minimum three bars) of the total reinforcing on the exterior side of the column. Bars should extend a minimum of one-fourth of the beam length or 24 bar diameters past the assumed inflection point at each side of the column. For seismic design a minimum of 50 percent of the reinforcing steel should be detailed continuously. Continuous reinforcing should be spliced with a Class B tension lap splice and minimum cover should be in accordance with ACI 318.

9.2.3.2 Transverse Reinforcing Steel. The purpose of the transverse reinforcing steel is to help promote the force transfer from the tension reinforcing to the column and to prevent potential shear splitting of the slab over the beams, thus allowing the beam studs to transfer the reinforcing tension force into the beam. ASCE TC recommends the following.

Provide transverse reinforcement, consistent with a strut-and-tie model as shown in Figure 9.2-7. In the limit (maximum), this amount will be equal to the longitudinal reinforcement. The transverse reinforcing should be placed below the top of the studs to prevent a cone-type failure over the studs. The transverse bars should extend at least 12 bar diameters or 12 inches, whichever is larger, on either side of the outside longitudinal bars.

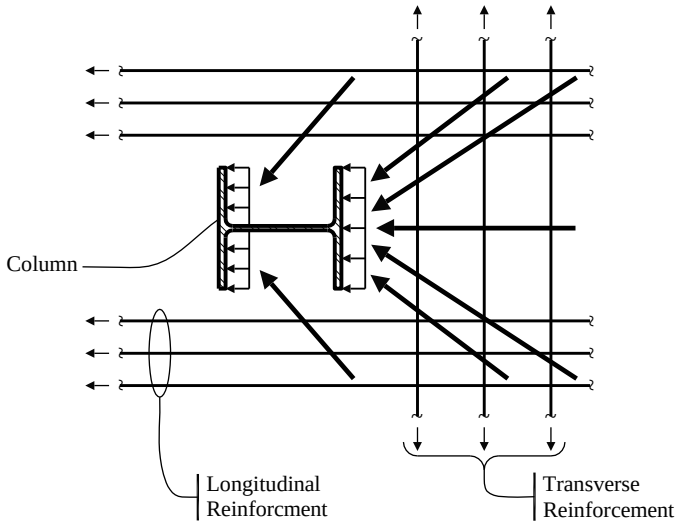

Figure 9.2-7 Force transfer mechanism from slab to column

Concrete bearing stresses on the column flange should be limited to $1.8f_c'$ per the ASCE TC recommendations. For the W21x44 PRCC, the sum of the positive and negative moment capacity is 607 kip-ft. The moment arm is approximately 22.95 inches (20.7 + 4.5/2). So the maximum possible transfer of force from the slab to the column, if each connection is at maximum and opposite strengths on each side of the column, is 607 ft-kip/22.95 inches = 317 kips. A W10x88 column has a 10.3-inch-wide flange. Assuming uniform bearing of the concrete on each flange, the bearing stress would be 317 kips / 2 flanges / 4.5-inch-thick slab / 10.3-inch-wide flange = 3.42 ksi, which is less than the recommended limit of $1.8f_c'$. It is also necessary to check this force against the flange local bending and web local yielding limit states given in Chapter J of AISC 360. It is important to have concrete filling the gap between column flanges; otherwise, the force must be transferred by a single column flange.

9.2.3.3 Connection Moment Capacity Limits. AISC 341 Part II Section 8.4 requires that the PRCC have a nominal strength that is at least equal to 50 percent of the nominal M_p for the connected beam ignoring composite action. ASCE TC recommends 75 percent as a good target, with 50 percent as a lower limit and 100 percent as an upper limit. ASCE TC also recommends using the moment capacity at 20 mrad for negative moment and 10 mrad for positive moment to determine the nominal connection moment capacity. From the W21x44 PRCC connection curve, the negative moment capacity at 20 mrad is 367 kip-ft and the positive moment capacity at 10 mrad is 240 kip-ft. With M_p of the beam being 398 kip-ft, the ratio of connection-to-beam moment capacity is 0.922 and 0.603 for negative and positive moments, respectively.

9.2.3.4 Seat Angle. The typical gage for the bolts attaching the seat angle to the column is 5.5 inches to allow sufficient room for bolt tightening on the inside of the column. For a 1-inch bolt diameter and a 1.75-inch minimum edge distance to a sheared edge, the minimum angle length is 9 inches. Per ASCE TC, the minimum area of the outstanding angle leg should be:

$$A_{samin} = 1.33 \times F_{yrd} \times A_{rb} / F_{ya} = 5.497 \text{ in}^2$$

A 5/8-inch thick angle with the 9-inch angle length results in A_{sa} equal to 5.625 in^2.

The outstanding angle dimension is controlled by the number of bolts attaching the angle to the beam flange. As previously discussed, a minimum 8-inch dimension is desired here to allow room for four 1-inch-diameter bolts.

The vertical angle dimension has to be sufficient both to allow room for bolts to the column flange and to permit yielding when the seat angle is in tension. The ductility of the connection, when in positive bending, is derived from angle hinging, as shown in Figure 9.2-8.

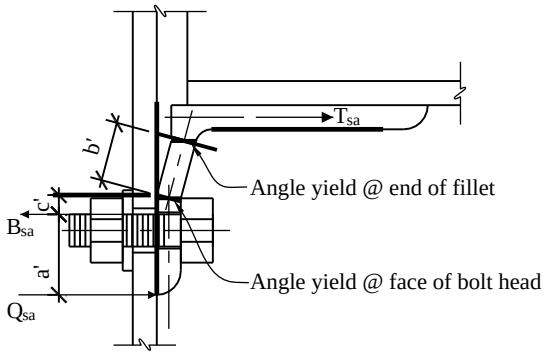

Figure 9.2-8 Typical angle tension hinging mechanism

This mechanism is based on research by Arum (1996). The following equations can be used to determine the associated angle tension, prying forces and bolt forces associated with the angle hinging mechanism.

$a' = L_{vsa} - g_{sa} + d_{bsa} / 2 = 2.500$ in.

$c' = (W_{sa} - d_{bsa}) / 2 = 0.313$ in.

$b' = L_{vsa} - a' - c' - k_{sa} = 2.062$ in.

$M_{psa} = F_{ya} \times t_{sa}^2 \times L_{sa} / 4 = 31.641$ kip-in

$T_{sa} = 2 \times M_{psa} / b' = 30.682$ kips

$Q_{sa} = M_{psa} / a' \times (1 + 2 \times c' / b') = 16.491$ kips

$B_{sa} = T_{sa} + Q_{sa} = 47.173$ kips

The above equations were derived in the same fashion as the prying action equations currently given in Section 9 of the AISC Manual with the same limitations applied to a'. The nomenclature in the above equations is shown in Figure 9.2-9.

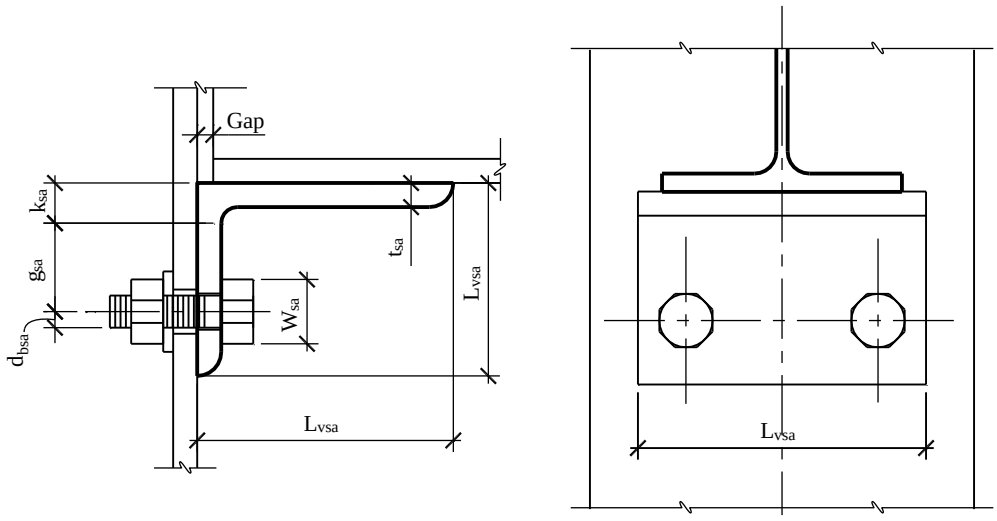

Figure 9.2-9 Seat angle nomenclature

The author recommends that the ratio of t_{sa}/b' be limited to no more than 0.5, so that the angle can properly develop the assumed hinges. For the example detail, the ratio is 0.303.

9.2.3.5 Bolts in Vertical Seat Angle Leg. The bolts in the vertical seat angle leg are designed primarily to resist tension in the case of connection positive moment. To protect against premature tension failure, the bolt force calculated in the previous section should be magnified by R_y from AISC 341 Table I-6-1.

$R_y \times B_{sa} = 1.5 \times 47.173 \text{ kips} = 70.76 \text{ kips}$

The tension capacity for two 1-inch-diameter A490 bolts is 133 kips.

9.2.3.6 Bolts in Outstanding Seat Angle Leg. The bolts in the outstanding leg of the seat angle must be designed for the shear transfer between the beam flange and the seat angle. For positive moments, this force is limited by tension hinging of the seat angle as calculated previously. For negative moments, this force is the sum of tension from the reinforcing steel and tension developed from hinging of the web angles. In general, the later will be significantly more than the former. The tension hinging capacity of the web angles, T_{wa}, is calculated in the same way as the tension hinging of the seat angle. Again, to protect against premature shear failure of bolts, the tension capacity of the web angle and the reinforcing steel is magnified by an appropriate R_y. ASCE TC recommends $R_y = 1.25$ for the reinforcing steel.

$R_y \times T_{wa} + R_y \times F_{yrd} \times A_{rb} = 1.5 \times 22.5 \text{ kips} + 1.25 \times 60 \text{ ksi} \times 2.48 \text{ in}^2 = 220 \text{ kips}$

The published shear capacity for four 1-inch-diameter A490-X bolts is 177 kips; however, this capacity includes a 0.8 reduction to account for joint lengths up to 50 inches per the RCSC. The RCSC further states that this reduction does not apply in cases where the distribution of force is essentially uniform along the joint. When one increases the published shear capacity by 1/0.8, the revised shear capacity is 221 kips. Bolt bearing at the beam flange and at the seat angle should also be checked.

9.2.3.7 Double Angle Web Connection. The primary purpose of the double angle web connection is to resist shear. Therefore, it can be selected directly from the AISC Manual; the specific design limits will not be addressed here. The required shear force is determined by adding the seismic demand to the

gravity demand. The seismic demand for the W21x44 PRCC is the sum of the positive and negative moment capacity (607 kip-ft) divided by the appropriate beam length. For the typical 25-foot beam length, the seismic shear is approximately 25 kips.

9.3 LOADS AND LOAD COMBINATIONS

9.3.1 Gravity Loads and Seismic Weight

The design gravity loads and the associated seismic weights for the example building are summarized in Table 9.3-1. The seismic weight of the storage live load is taken as 50 percent of the design gravity load (a minimum of 25 percent is required by *Standard* Section 12.7.2). To simplify this design example, the roof design is assumed to be the same as the floor design and floor loads are used rather than considering special roof and snow loads.

Table 9.3-1 Gravity Load and Seismic Weight

	Gravity Load	Seismic Weight
Non-Composite Dead Loads (D_{nc})		
4.5-in. Slab on 0.6-in. Form Deck (4.5-in. total thickness) plus Concrete Ponding	58 psf	58 psf
Joist and Beam Framing	6 psf	6 psf
Columns	2 psf	2 psf
Total:	66 psf	66 psf
Composite Dead Loads (D_c)		
Fire Insulation	4 psf	4 psf
Mechanical and Electrical	6 psf	6 psf
Ceiling	2 psf	2 psf
Total:	12 psf	12 psf
Precast Cladding System	800 plf	800 plf
Live Loads (L)		
Typical Area Live and Partitions (Reducible)	70 psf	10 psf
Records Storage Area Live (Non-Reducible)	200 psf	100 psf

The reason for categorizing dead loads as non-composite and composite is explained in Section 9.4.2.

Live loads are applied to beams in the analytical model, with corresponding live load reductions appropriate for beam design. Column live loads are adjusted to account for different live load reduction factors, including the 20 percent reduction on storage loads for columns supporting two or more floors per *Standard* Section 4.8.2.

9.3.2 Seismic Loads

The basic seismic design parameters are summarized in Table 9.3-2

Table 9.3-2 Seismic Design Parameters

Parameter	Value
S_s	0.20
S_1	0.06
Site Class	E
F_a	2.5
F_v	3.5
$S_{MS} = F_a S_s$	0.50
$S_{M1} = F_v S_1$	0.21
$S_{DS} = 2/3 S_{MS}$	0.33
$S_{D1} = 2/3 S_{M1}$	0.14
Occupancy Category	II
Importance Factor	1.0
Seismic Design Category (SDC)	C
Frame Type per *Standard* Table 12.2-1	Composite Partially Restrained Moment Frame
R	6
Ω_0	3
C_d	5.5

For Seismic Design Category C, the height limit is 160 feet, so the selected system is permitted for this 52-foot-tall example building. The building is regular in both plan and elevation; consequently, the Equivalent Lateral Force Procedure of Section 12.8 is permitted in accordance with *Standard* Table 12.6-1. The seismic weight, W, totals 7,978 kips. The approximate period is determined to be 0.66 seconds using Equation 12.8-7 and the steel moment-resisting frame parameters of Table 12.8-2. The coefficient for upper limit on calculated period, C_u, from Table 12.8-1 is 1.62, resulting in T_{max} of 1.07 seconds for purposes of determining strength-level seismic forces.

A specific value for PRCC stiffness must be selected in order to conduct a dynamic analysis to determine the building period. It is recommended that the designer use K_{ci} of the negative moment-rotation behavior given in Section 9.2.2 above for this analysis. This should result in the shortest possible analytical building period and thus the largest seismic design forces. For the example building, the computed periods of vibration in the first modes are 2.13 and 1.95 seconds in the north-south and east-west directions, respectively. These values exceed T_{max}, so strength-level seismic forces must be computed using T_{max} for the period. The seismic response coefficient is then given by:

$$C_s = \frac{S_{D1}}{T\left(\frac{R}{I}\right)} = \frac{0.14}{1.07\left(\frac{6}{1.0}\right)} = 0.022$$

The total seismic forces or base shear is then calculated as:

$V = C_s W = (0.022)(7{,}978) = 174$ kips (*Standard* Eq. 12.8-1)

The distribution of the base shear to each floor (by methods similar to those used elsewhere in this volume of design examples) is:

Roof (Level 4):	77 kips
Story 4 (Level 3):	53 kips
Story 3 (Level 2):	31 kips
Story 2 (Level 1):	13 kips
Σ:	174 kips

For Seismic Design Category C, the value of ρ is permitted to be taken as 1.0 per *Standard* Section 12.3.4.1, so the above story shears are applied as E_h without any additional magnification.

9.3.3 Wind Loads

From calculations not illustrated here, the gross service-level wind force following ASCE 7 is 83 kips (assuming 90 mph, 3-second-gust wind speed). Including the directionality effect and the strength load factor, the design wind force is less than the design seismic base shear. The wind force is not distributed in the same fashion as the seismic force, thus the story shears and the overturning moments for wind are considerably less than for seismic. The distribution of the wind base shear to each floor is:

Roof (Level 4):	13 kips
Story 4 (Level 3):	25 kips
Story 3 (Level 2):	23 kips
Story 2 (Level 1):	22 kips
Σ:	83 kips

Because the wind loads are substantially below the seismic loads, they are not considered in subsequent strength design calculations; however, wind drift is considered in the design.

9.3.4 Notional Loads

AISC 360 now requires that notional loads be included in the building analysis. As shown later, the example building qualifies for application of notional loads to gravity-only load combinations. The notional load at level i is $N_i = 0.002Y_i$, where Y_i is the gravity load applied at level i. For our example building, these values are as follows:

ND_{nc} = 4,258 kips × 0.002 = 8.516 kips / 4 floors = 2.13 kips/floor

ND_c = 2,393 kips × 0.002 = 4.786 kips / 4 floors = 1.20 kips/floor

NL = 4,469 kips × 0.002 = 8.938 kips / 4 floors = 2.23 kips/floor

The notional loads are applied in the same manner as the seismic and wind loads in each orthogonal direction of the building and they are factored by the same load factors that are applied to their corresponding source (such as 1.2 or 1.4 for dead loads). It is important to note that, in general, notional loads should be determined, at a minimum, on a column-by-column basis rather than for an entire floor as done above. This will allow the design to capture the effect of gravity loads that are not symmetric about

the center of the building. The example building happens to have gravity loads that are concentric with the center of the building, so it does not matter in this case.

9.3.5 Load Combinations

Three load combinations (from *Standard* Section 2.3.2) are considered in this design example.

- Load Combination 2: $1.2D + 1.6L$
- Load Combination 5: $1.2D + 0.5L + 1.0E$
- Load Combination 7: $0.9D + 1.0E$

Expanding the combinations for vertical and horizontal earthquake effects, breaking D into D_{nc} and D_c (defined in Section 9.3.1) and including notional loads, results in:

- Load Combination 2: $1.2(D_{nc} + ND_{nc}) + 1.2(D_c + ND_c) + 1.6(L + NL)$
- Load Combination 5: $1.2D_{nc} + 1.2D_c + 0.5L + 1.0E_h + 1.0E_v$
  $E_v = 0.2S_{DS}(D_{nc} + D_c) = 0.2(0.33)(D_{nc} + D_c) = 0.067(D_{nc} + D_c)$
  $1.267D_{nc} + 1.267D_c + 0.5L + 1.0E_h$
- Load Combination 7: $0.9\,D_{nc} + 0.9\,D_c + 1.0\,E_h - 1.0\,E_v$
  $0.833\,D_{nc} + 0.833\,D_c + 1.0\,E_h$

D_{nc} has to be applied separately to the columns and beams because of the two-stage connection behavior (discussed later). D_{ncc} is for column loading and D_{ncb} is for beam loading. This breakout of the loading results in the following combinations:

- Stage 1 Analysis:

  Load Combinations 2 and 5: $1.2\,D_{ncb}$

  Load Combination 7: $0.9\,D_{ncb}$

- Stage 2 Analysis:

  Load Combination 2: $1.2(D_{ncc} + ND_{nc}) + 1.2(D_c + ND_c) + 1.6(L + NL)$

  Load Combination 5: $1.2D_{ncc} + 0.067D_{ncb} + 1.267D_c + 0.5L + 1.0E_h$

  Load Combination 7: $0.9D_{ncc} - 0.067D_{ncb} + 0.833D_c + 1.0E_h$

The columns are designed from the Stage 2 Analysis and the beams are designed from the linear combination of the Stage 1 and Stage 2 Analyses.

Because partially restrained connection behavior is nonlinear, seismic and wind drift analyses must be carried out for each complete load combination, rather than for horizontal loads by themselves. Note that *Standard* Section 12.8.6.2 allows drifts to be checked using seismic loads based on the analytical building period.

- Seismic Drift: $1.0D_{ncc} + 0.067D_{ncb} + 1.0D_c + 0.5L + 1.0E_h$
- Wind Drift: $1.0D_{ncc} + 1.0D_c + 0.5L + 1.0W$

The typical permeations of the above combinations have to be generated for each orthogonal direction of the building; however, orthogonal effects need not be considered for Seismic Design Category C provided the structure does not have a horizontal structural irregularity (*Standard* Sec. 12.5.3).

9.4 DESIGN OF C-PRMF SYSTEM

9.4.1 Preliminary Design

The goal of an efficient partially restrained building design is to have a sufficient number of beams, columns and connections participating in the lateral system so that the forces developed in any of these elements from lateral loads is relatively small compared to the gravity design. In other words, design for gravity as if the connections are pinned; add the connections and check to see if any beams or columns must be upsized to handle the lateral loads. The author cautions designers against trying to reduce beam sizes below the initial gravity sizes unless a full inelastic, path-dependent analysis accounting for potential shakedown of the connections is conducted. At this time, such an analysis typically is relegated to academic study and is not applied in real building design. The analysis methods described below do not go to that level of detail.

Once the building has been designed for gravity, a preliminary lateral analysis can be made to assess whether the proposed steel framing sizes may be suitable for lateral loads in combination with gravity loads. Typically this is done assuming all the PRCCs are rigid connections. Two basic checks can be based on this preliminary analysis. First, review connection moments that come from the lateral load cases alone (earthquake moments and wind moments) without gravity. If these moments (at strength levels) exceed approximately 75 percent of the negative moment capacity of the PRCC then either additional beams, columns and connections need to be added to the lateral system or existing beams need to be upsized to provide larger PRCCs with higher capacities. Second, perform a preliminary assessment of the building drift. While there is no simple, reliable relationship between rigid frame drift and C-PRMF drift, the author typically assumes that the partially restrained system will drift approximately twice as much as a fully rigid analysis indicates. Keep in mind that these preliminary checks are made to establish basic system proportions before extensive modeling efforts are made to include the real partially restrained behavior of the building.

Using this preliminary design method, initial floor framing was selected. In accordance with the ASCE TC, the beams are designed to be 100 percent composite; no partial composite design is used.

The W18x35 typical interior girder is determined from a simple beam design. This typical size would work for all locations with the exception of the girders that support storage load on both sides (Grids 4 and 5 between Grids C and D). For simplicity, the example design was not further refined. The W18x35 size would also work as the Grid Line A and F spandrel beams; however, a W21x44 spandrel beam is used to help control drift in the north-south direction and help equalize the building periods in both directions. Note that the W21x44 improves drift more due to the increase in beam depth, which increases PRCC moment-rotation stiffness, rather than because of the increase in the moment of inertia of the steel beam section.

9.4.2 Application of Loading

PRCC do not develop substantial beam end restraint until after the concrete has hardened (since the reinforcing steel cannot be mobilized without the concrete). At the time of concrete casting, the bare steel elements of the connection are all that are present to resist rotation at the beam ends. The degree of restraint provided by the bare steel connection varies depending on the details; however, for purposes of design, the connection stiffness prior to concrete hardening typically is assumed to be zero (a pinned beam end). Consequently, the connection actually has two stages of behavior that need to be accounted for in the analysis. These two stages are the pre-composite stage, when the connection is assumed to behave as a pin and the post-composite stage, when the connection is assumed to have the full moment-rotation behavior determined in Section 9.2.2. In a building where the complete lateral system is provided by PRCCs, temporary bracing may be required to provide lateral stability prior to concrete hardening.

The above two-stage connection behavior requires separation of dead load into portions consistent with each stage. This is why the dead loads in Section 9.3.1 are separated into D_{nc} and D_c. The D_{nc} load is placed on the beams during the Stage 1 analysis (when the connections are pins) but is not placed on the beams (other than the seismic fraction) during the Stage 2 analysis (when the connections have PRCC stiffness). In Stage 2 analysis, the D_{nc} loads are placed directly on the columns so that their destabilizing effects are accounted for properly in the nonlinear P-delta analysis. That is why D_{nc} loads are further broken down into D_{ncc} and D_{ncb}. The Stage 2 load combinations are presented graphically in Figures 9.4-1 and 9.4-2.

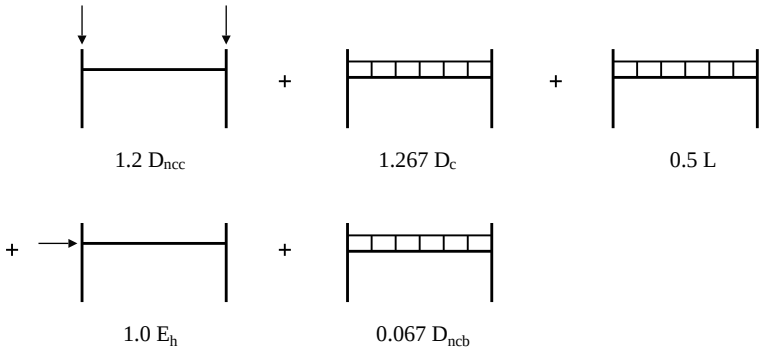

Figure 9.4-1 Stage 2 Load Combination 5

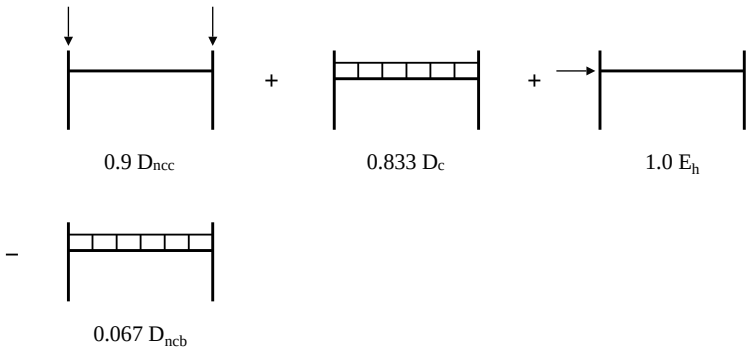

Figure 9.4-2 Stage 2 Load Combination 7

9.4.3 Beam and Column Moment of Inertia

ASCE TC recommends that the beam moment of inertia used for frame analysis be increased to account for the stiffening effect that the composite slab has on the beam moment of inertia. The use of the increased moment of inertia is also required by AISC 341 Part II Section 8.3. The following equivalent moment of inertia is recommended:

$$I_{eq} = 0.6I_{LB+} + 0.4I_{LB-} \qquad \text{(Eq. 5, ASCE TC)}$$

I_{LB+} and I_{LB-} are the lower bound moments of inertia in positive and negative bending, respectively. I_{LB+} can be determined from Table 3-20 in the AISC Manual as 1,594 in^4 for the W18x35 interior girder and 1,570 in^4 for the W21x44 spandrel beam once composite beam design values are known. Note that the W21x44 spandrel 100 percent composite design is limited by the effective slab capacity, which is why its composite moment of inertia is so close to that of the W18x35 interior girder. I_{LB-} can be assumed as the bare steel moment of inertia, as 510 in^4 for the W18x35 interior girder and 843 in^4 for the W21x44 spandrel beam. It is permitted to account for the transformed area of the reinforcing steel in calculating I_{LB-}, but the bare steel beam property has been used in this example. The equivalent moment of inertia is then calculated as:

- W18x35 Interior Girder: $I_{eq} = 0.6(1{,}594) + 0.4(510) = 1{,}160$ in^4
- W21x44 Spandrel Beam: $I_{eq} = 0.6(1{,}570) + 0.4(843) = 1{,}279$ in^4

The bare steel moment of inertia values in the building analysis are revised to these values, which are suitable for service-level limit state checks. Use of a 0.8 reduction factor on the beam moment of inertia is required by AISC 360 Section 7.3(3) for strength-level checks from direct analysis.

The bare steel moment of inertia for the columns is appropriate for service-level checks. For strength-level checks, the same 0.8 reduction factor on the moment of inertia used on beams would apply to the columns. A further reduction on the column moment of inertia for strength-level checks is required if P_r/P_y exceeds 0.5. A quick scan of the column loads from the building analysis results indicates that the only columns that exceed this value are the first-story columns at Grids C-4, C-5, D-4 and D-5 for Load Combination 2 only. The adjustment factor is calculated to be:

$$\tau_b = 4[P_r/P_y(1-P_r/P_y)] = 4[612 \text{ kips}/1130 \text{ kips } (1- 612 \text{ kips}/1130 \text{ kips})] = 0.99$$

In the author's judgment, the above reduction on so few columns will have little or no effect on the building analysis results and it is ignored for this example.

9.4.4 Connection Behavior Modeling

For each connection type (such as W18 PRCC or W21 PRCC), there are four different connection behavior models used, as developed in Section 9.2.2. First, the connection is modeled as a linear spring with nominal stiffness K_{ci}. This is done for the dynamic analysis of the building needed to determine the building period. Second, a service-level analysis is conducted using the full nonlinear nominal service moment-rotation behavior. Third, a connection Stage 1 building analysis is done with the connections having no moment resistance (analytical pins) so the beam pre-composite loads can be applied. Finally, a Stage 2 building strength analysis under factored loads is performed with the full modified nonlinear moment-rotation behavior.

The multi-linear elastic link option provided in SAP2000 is used to model the connection springs for all stages. This nonlinear spring model allows user-defined behavior for two types of analysis, linear and nonlinear, for each spring type. This is helpful to handle the various connection behaviors because the dynamic analysis and the Stage 1 pre-composite beam load analysis can both be linear analysis which automatically switches the connection spring to the defined linear behavior. Another important point is that this particular spring model stays on the defined connection curve in a nonlinear-elastic manner. That is, the analysis simply rides up and down always converging at moment-rotation points on the connection backbone curve. This allows what is known as a path independent analysis; the order of the loading does not matter. This is in contrast with a spring model with different connection unloading behavior, such as might be used to model the full hysteric connection behavior. If the connection unloading behavior is considered, the analysis is no longer path independent because the answer will depend on the sequence of loads that are applied. This path-dependent analysis is more accurate and allows consideration of connection shakedown to be captured in the model; however, it is also much more complicated when compared to the path-independent analysis. Since the simpler, path-independent connection modeling approach does not capture connection shakedown behavior, the author does not recommend reducing beam sizes from the pure simple pinned gravity design discussed in Section 9.4.1.

9.4.5 Building Drift and P-delta Checks

Drifts should be checked using the service moment-rotation curves along with the full moment of inertias for the beams and columns (no 0.8 reduction). Because of the nonlinear connection behavior, the analysis is nonlinear. Though optional, the author recommends including P-delta effects in the service drift checks for partially restrained building designs. Drifts are computed for the nonlinear load combinations developed in Section 9.3.5.

9.4.5.1 Torsional Irregularity Check. *Standard* Table 12.3-1 defines torsional irregularities. The story drift values at the each end of the example building and their average story drift values including *P*-delta are presented in Table 9.4-1. Since the ratio of maximum drift to average drift does not exceed 1.2, no torsional irregularity exists, accidental torsion need not be amplified and drift may be checked at the center of the building (rather than at the corners).

Table 9.4-1 Torsional Irregularity and Seismic Drift Checks

Story	North-south Direction (in.)						East-west Direction (in.)					
	Displacement		Story Drift				Displacement		Story Drift			
	A-1	F-1	A-1	F-1	avg	max/avg	F-1	F-8	F-1	F-8	avg	max/avg
1	0.40	0.45	0.40	0.45	0.43	1.06	0.31	0.37	0.31	0.37	0.34	1.08
2	0.91	1.03	0.51	0.58	0.55	1.06	0.72	0.84	0.41	0.47	0.44	1.07
3	1.32	1.49	0.41	0.46	0.43	1.06	1.05	1.22	0.33	0.38	0.35	1.08
4	1.55	1.76	0.23	0.27	0.25	1.06	1.23	1.44	0.19	0.22	0.20	1.08

9.4.5.2 Seismic Drift and P-delta Effect. The allowable seismic story drift is taken from *Standard* Table 12.12-1 as $0.025h_{sx}$ = (0.025)(13 ft × 12 in./ft) = 3.9 in. With C_d of 5.5 and I of 1.0, this corresponds to a story drift limit of 0.71 inch under the equivalent elastic forces (see *Standard* Section 12.8.6 for story drift determination). Review of the average drift values in Table 9.4-1 shows that all drifts are within the 0.71-inch limit.

Table 9.4-2 P-delta Effect Checks

Story	North-south Direction (in.)						East-west Direction (in.)					
	Displacement		Story Drift				Displacement		Story Drift			
	w/o P-Δ	w/ P-Δ	w/o P-Δ	w/ P-Δ	$P\Delta_{amp}$	θ	w/o P-Δ	w/ P-Δ	w/o P-Δ	w/ P-Δ	P-Δ_{amp}	θ
1	0.38	0.43	0.38	0.43	1.14	0.12	0.30	0.34	0.30	0.34	1.12	0.10
2	0.86	0.97	0.48	0.55	1.14	0.12	0.70	0.78	0.40	0.44	1.12	0.10
3	1.25	1.41	0.39	0.43	1.10	0.09	1.02	1.13	0.32	0.35	1.09	0.08
4	1.48	1.66	0.24	0.25	1.06	0.06	1.22	1.33	0.19	0.20	1.05	0.04

Separate analyses are conducted to determine seismic drifts with and without P-delta effects. Due to the nonlinear connection behavior, all of the analyses are nonlinear. The ratio of these two drifts (P-Δ_{amp}) is compared to the 1.5 limit for ratio of second-order drift to first-order drift set forth in AISC 360 Section 7.3(2). Because the ratios are all below the 1.5 limit, it is permissible to apply the notional loads as a minimum lateral load for the gravity-only combination and not in combination with other lateral loads. The results of these analyses are given in Table 9.4-2.

Provisions Section 12.8.7 now defines the stability coefficient (θ) as follows:

$$\theta = \frac{P_x \Delta I}{V_x h_{sx} C_d}$$

The story drift (Δ) is defined in *Standard* Section 12.8.6 as:

$$\Delta = \frac{C_d \delta_{xe}}{I}$$

Replacing Δ in the stability coefficient equation results in:

$$\theta = \frac{P_x \delta_{xe}}{V_x h_{sx}}$$

This value of θ can also be calculated from the P-delta amplifier presented in Table 9.4-2 by the following:

$$\theta = 1 - \frac{1}{P\Delta_{amp}}$$

The stability coefficients presented in Table 9.4-2 were calculated in this manner. Review of the values shows that θ varies from 0.04 to 0.12. *Provisions* Section 12.8.7 now requires that θ not exceed 0.10 unless the building satisfies certain criteria when subjected to either nonlinear static (pushover) analysis or nonlinear response history analysis. Because θ for the building in the north-south direction exceeds 0.10 in the lower stories, the designer would have to either increase the building stiffness in that direction or conduct an approved nonlinear analysis. Such nonlinear analysis is beyond the scope of this example.

9.4.5.3 Wind Drift. A wind drift limit of h_{sx}/400 was chosen based on typical office practice for this type of building. This gives a story drift limit of 13 × 12 / 400 = 0.39 inch. The wind drift values presented in Table 9.4-3 were determined for the 50-year return interval wind loads previously determined in Section 9.3.3 above. Review of the drift values indicates that all drifts are within the 0.39-inch limit.

Table 9.4-3 Wind Drift Results

	North-south Direction (in.)		East-west Direction (in.)	
Story	Displacement	Story Drift	Displacement	Story Drift
1	0.19	0.19	0.15	0.15
2	0.39	0.20	0.32	0.17
3	0.52	0.13	0.42	0.11
4	0.57	0.05	0.47	0.04

9.4.6 Beam Design

AISC 341 Part II Section 8.3 requires that composite beams be designed in accordance with AISC 360 Chapter I. The beams are designed for 100 percent composite action and sufficient shear studs to develop 100 percent composite action are provided between the end and midspan. They do not develop 100 percent composite action between the column and the inflection point, but it may be easily demonstrated that they are more than capable of developing the full force in the reinforcing steel within that distance. Composite beam design is not unique to this example; however, composite beams acting as part of the lateral load-resisting system is unique and deserves further attention.

As a result of connection restraint, negative moments will develop at beam ends. These moments must be considered when checking beam strength. The inflection point cannot be counted on as a brace point, so it may be necessary to consider the full beam length as unbraced for checking lateral-torsional buckling and comparing that capacity to the negative end moments. Note that there are C_b equations in the

literature that do a better job (as compared to the standard C_b equation in AISC 360) of predicting the lateral-torsional buckling strength of beams that are continuously attached to a composite slab floor system (Yura, 2006)

AISC 341 Part II Section 8 does not specifically address compactness criteria for beams; however, given that the beams are not being required to develop M_p, other than possibly under gravity loads, it is unlikely they would need to be seismically compact. The author recommends that they meet the compactness criteria of AISC 360. A quick check in Table 1-1 of the AISC Manual indicates that both W18x35 and W21x44 are compact for flexure.

9.4.7 Column Design

Requirements for column design are found in AISC 341 and AISC 360. AISC 341 Part II Section 8.2 requires that columns meet the requirements of AISC 341 Part I Sections 6 and 8. W10 columns of A992 steel meet all Section 6 material requirements.

AISC 341 Part I Section 8.3 requires a special load combination if $P_u/\phi_c P_n$ exceeds 0.4 for a column in a seismic load combination. The only columns that exceed this limit are the interior columns on Grid Lines C and D under the storage load. Because they are so close to the center of the building, the seismic axial force in these columns is very small. Consequently, including the overstrength factor of 3.0 on the seismic axial portion of the column load will not have a meaningful effect on the column loads and can be ignored in this example.

The nominal strength of the columns is determined using $K = 1.0$ in accordance with AISC 360 Section 7.1. The associated column strength unity checks are presented in Table 9.4-4. The unity checks presented are for the first story of the center four columns in the building.

Table 9.4-4 Column Strength Check for W10x77

	Seismic Load Combination	Gravity Load Combination
Axial force, P_u	370 kip	612 kip
Moment, M_u	55 ft-kip	35 ft-kip
Interaction	0.606	0.866

Part II Section 8 does not specifically address the required compactness criteria; however, given the high R value for the lateral load-resisting system, the author has assumed that the columns would need to meet the seismically compact criteria given in Part I Table I-9-1. A W10x77 column from the lower level of an interior bay with storage load is illustrated (the axial load from the seismic load combination is used):

- Column Flange:

$$\lambda_{ps} = 0.3\sqrt{\frac{E}{F_y}} = 0.3\sqrt{\frac{29{,}000}{50}} = 7.22$$

$$\frac{b_f}{2t_f} = 5.86 \text{ (AISC Manual)} < 7.22$$

- Column Web:

$$C_a = \frac{P_u}{\phi_b P_y} = \frac{370 \text{ kips}}{0.9(50)22.6} = 0.364 > 0.125$$

$$\lambda_{ps} = 1.12\sqrt{\frac{E}{F_y}}\left(2.33 - C_a\right) \geq 1.49\sqrt{\frac{E}{F_y}}$$

$$\lambda_{ps} = 1.12\sqrt{\frac{29{,}000}{50}}\left(2.33 - 0.364\right) = 53.03 \;\geq\; 1.49\sqrt{\frac{29{,}000}{50}} = 35.88$$

$$\frac{h}{t_w} = 14.8 \text{ (AISC Manual)} < 53.03$$

As an alternative to calculating the compactness criteria by hand, the designer can use the AISC SDM Table 1-2. A quick review of this table indicates that the W10x77 is compact for flexure (beam) and for axial loads (column). The dash in the table indicates that applied axial loads as large as P_y still result in the column meeting the seismically compact criteria.

The equivalent of the weak-beam–strong-column concept for the C-PRMF lateral system is a weak connection-strong column. This is not specifically addressed in AISC 341; however, ASCE TC recommends the following check:

$$\sum M_{p,col}\left(1 - \frac{P_u}{P_y}\right) \geq 1.25\left(M_{cu}^{-} + M_{cu}^{+}\right)$$

For the same lower level interior W10x77 one gets:

$$2 \times 50 \times 97.6\left(1 - \frac{370 \text{ kips}}{50 \times 22.6}\right) = 547 \text{ ft-kips} \geq 1.25(232 + 151) = 479 \text{ ft-kips}$$

9.4.8 Connection Design

There is really little to do with the connection design at this stage because the full nonlinear connection behavior is being used in the analysis. This means that the connection moments will never exceed the connection capacity during the analysis. This is in contrast to any analysis method that models the connections with linear behavior. When the connections are modeled with linear behavior, it is up to the designer to confirm that the final connection results are consistent with the expected connection behavior. This might be very easy for building designs where connection moments are small; however, when the connections are being pushed close to their capacity, that sort of independent connection check by the designer can be problematic.

Although not entirely necessary, it is useful to check where the connections are along the expected behavior curves for any given analysis so one can see just how hard the connections are being pushed. The connection moment demand versus design capacities (including ϕ) are presented in Table 9.4-5. The demand values are from different load combinations. A quick check of this table indicates that this

building design is not being pushed particularly hard and that there is likely significant reserve capacity in the lateral system.

Table 9.4-5 Connection Moment Demand vs. Capacity (kip-ft)

	W21 PRCC		W18 PRCC	
	(-) M-θ	(+) M-θ	(-) M-θ	(+) M-θ
Demand	136	87.0	126	37.0
Capacity	312	204	197	128
Ratio	0.44	0.43	0.64	0.29

9.4.9 Column Splices

Column splice design would be in accordance with AISC 341 Part I Section 8.4 but is not illustrated in this example.

9.4.10 Column Base Design

Column base design would be in accordance with AISC 341 Part I Section 8.5 but is not illustrated in this example.

10

Masonry

James Robert Harris, PE, PhD and
Frederick R. Rutz, PE, PhD

Contents

10.1 WAREHOUSE WITH MASONRY WALLS AND WOOD ROOF, LOS ANGELES, CALIFORNIA 3
10.1.1 Building Description 3
10.1.2 Design Requirements 4
10.1.3 Load Combinations 6
10.1.4 Seismic Forces 8
10.1.5 Side Walls 9
10.1.6 End Walls 25
10.1.7 In-Plane Deflection – End Walls 44
10.1.8 Bond Beam – Side Walls (and End Walls) 45
10.2 FIVE-STORY MASONRY RESIDENTIAL BUILDINGS IN BIRMINGHAM, ALABAMA; ALBUQUERQUE, NEW MEXICO; AND SAN RAFAEL, CALIFORNIA 45
10.2.1 Building Description 45
10.2.2 Design Requirements 48
10.2.3 Load Combinations 50
10.2.4 Seismic Design for Birmingham 1 51
10.2.5 Seismic Design for Albuquerque 69
10.2.6 Birmingham 2 Seismic Design 81
10.2.7 Seismic Design for San Rafael 89
10.2.8 Summary of Wall D Design for All Four Locations 101

This chapter illustrates application of the 2009 *NEHRP Recommended Provisions* (the *Provisions*) to the design of a variety of reinforced masonry structures in regions with different levels of seismicity. Example 10.1 features a single-story masonry warehouse building with tall, slender walls, and Example 10.2 presents a five-story masonry hotel building with a bearing wall system designed in areas with different seismicities. Selected portions of each building are designed to demonstrate specific aspects of the design provisions.

Masonry is a discontinuous and heterogeneous material. The design philosophy of reinforced grouted masonry approaches that of reinforced concrete; however, there are significant differences between masonry and concrete in terms of restrictions on the placement of reinforcement and the effects of the joints. These physical differences create significant differences in the design criteria.

All structures were analyzed using two-dimensional (2D) static methods using the RISA 2D program, V.5.5 (Risa Technologies, Foothill Ranch, California). Example 10.2 also uses the SAP 2000 program, V6.11 (Computers and Structures, Berkeley, California) for dynamic analyses to determine the structural periods.

All examples are for buildings of concrete masonry units (CMU); neither prestressed masonry shear walls nor autoclaved aerated concrete masonry shear walls are included.

In addition to the *Provisions* and the *Standard*, the following documents are referenced in this chapter:

ACI 318 — American Concrete Institute. 2008. *Building Code Requirements for Structural Concrete*.

TMS 402 — The Masonry Society. 2008. *Building Code Requirements for Masonry Structures*, TMS 402/ACI 530/ASCE 5.

IBC — International Code Council. 2009. *International Building Code*.

NCMA — National Concrete Masonry Association. *A Manual of Facts on Concrete Masonry*, NCMA-TEK is an information series from the National Concrete Masonry Association, various dates. NCMA-TEK 14-1BA, *Section Properties of Concrete Masonry Walls* and NCMA-TEK 14-11B, *Strength Design of Concrete Masonry Walls for Axial Load & Flexure*, are referenced here.

USGS — United States Geological Survey. *Seismic Design Maps* web application.

The short form designations for each citation are used throughout. The citation to the IBC is because one of the designs employees a tall, slender wall that is partially governed by wind loads and the IBC provisions are used for that design.

Regarding TMS 402:

- The 2005 edition of the *Standard*, in its Supplement 1, refers to the 2005 edition of TMS 402.
- The 2010 edition of the *Standard* refers to the 2008 edition of TMS 402.
- The examples herein are prepared according to the 2008 edition of TMS 402.

10.1 WAREHOUSE WITH MASONRY WALLS AND WOOD ROOF, LOS ANGELES, CALIFORNIA

This example features a one-story building with reinforced masonry bearing walls and shear walls.

10.1.1 Building Description

This simple rectangular warehouse is 100 feet by 200 feet in plan (Figure 10.1-1). The masonry walls are 30 feet high on all sides, with the upper 2 feet being a parapet. The wood roof structure slopes slightly higher towards the center of the building for drainage. The walls are 8 inches thick on the long side of the building, for which the slender wall design method is adopted, and 12 inches thick on both ends. The masonry is grouted in the cells containing reinforcement, but it is not grouted solid. The specified strength of masonry is 2,000 psi. Normal-weight CMU with Type S mortar are assumed.

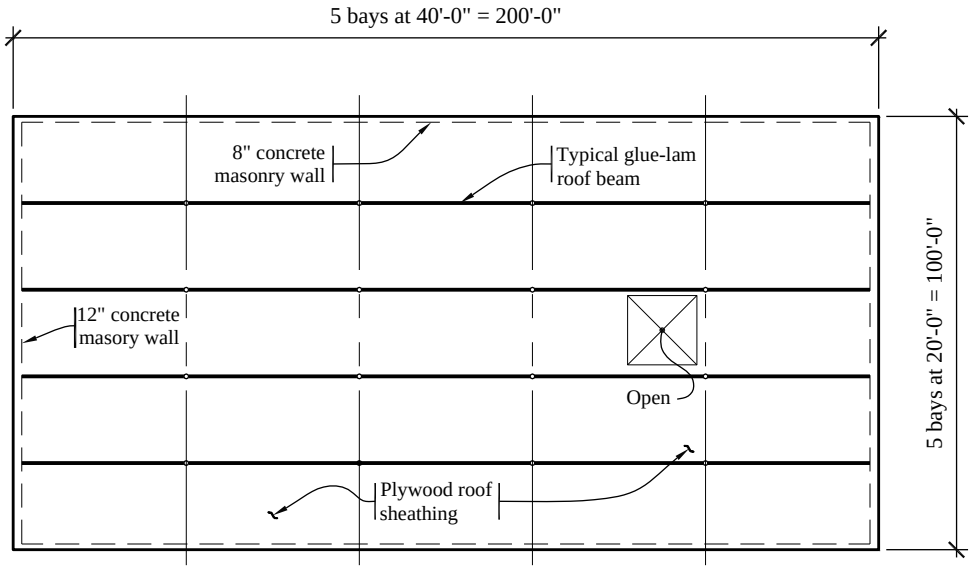

Figure 10.1-1 Roof plan
(1.0 in. = 25.4 mm, 1.0 ft = 0.3048 m)

The long side walls are solid (no openings). The end walls are penetrated by several large doors, which results in more highly stressed piers between the doors (Figure 9.1-2); thus, the greater thickness for the end walls.

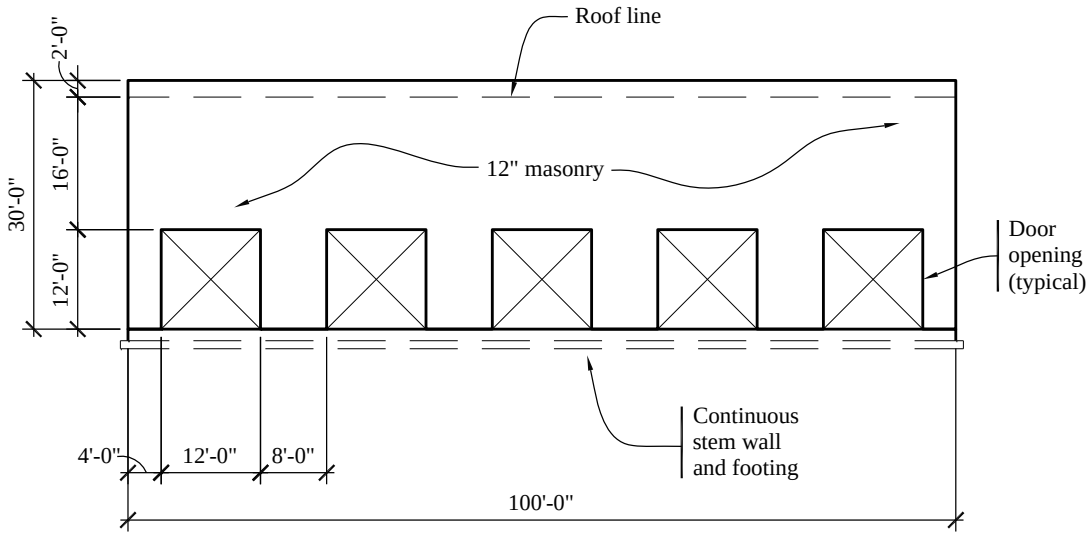

Figure 10.1-2 End wall elevation
(1.0 in. = 25.4 mm, 1.0 ft = 0.3048 m)

The floor is concrete slab-on-grade construction. Conventional spread footings are used to support the interior steel columns. The soil at the site is a dense, gravelly sand.

The roof structure is wood and acts as a diaphragm to carry lateral loads in its plane from and to the exterior walls. The roofing is ballasted, yielding a total roof dead load of 20 psf. There are no interior walls for seismic resistance. This design results in a highly stressed diaphragm with large calculated deflections. The design of the wood roof diaphragm and the masonry wall-to-diaphragm connections is illustrated in Sec. 11.2.

In this example, the following aspects of the structural design are considered:

- Design of reinforced masonry walls for seismic loads
- Computation of *P-delta* effects.

10.1.2 Design Requirements

This building could qualify for the simplified approach in *Standard* Section 12.14, although the "long" method per *Standard* Section 11.4-11.6 has been followed.

10.1.2.1 Seismic parameters. The ground motion response coefficients are found from USGS based upon latitude and longitude. The site class is taken from a site-specific geotechnical report and is typical for dense sands and gravels. The warehouse is not designated for hazardous materials and does not house any essential facility, thus the occupancy category is "all other".

Site Class = C

S_S = 2.14

S_1 = 0.74

Occupancy Category (*Standard* Sec. 1.5.1) = II

The remaining basic parameters depend on the ground motion adjusted for site conditions.

10.1.2.2 Response parameter determination. The mapped spectral response factors must be adjusted for site class in accordance with *Standard* Section 11.4.3. The adjusted spectral response acceleration parameters are computed according to *Standard* Equations 11.4-1 and 11.4-2 for the short period and one-second period, respectively, as follows:

$S_{MS} = F_a S_S = 1.0(2.14) = 2.14$

$S_{M1} = F_v S_1 = 1.3(0.74) = 0.96$

Where F_a and F_v are site coefficients defined in *Standard* Tables 11.4-1 and 11.4-2, respectively. The design spectral response acceleration parameters (*Standard* Sec. 11.4.4) are determined in accordance with *Standard* Equations 11.4-3 and 11.4-4 for the short-period and one-second period, respectively:

$$S_{DS} = \frac{2}{3} S_{MS} = \frac{2}{3}(2.14) = 1.43$$

$$S_{D1} = \frac{2}{3} S_{M1} = \frac{2}{3}(0.96) = 0.64$$

The Seismic Design Category may be determined by the design spectral acceleration parameters combined with the Occupancy Category. For buildings assigned to Seismic Design Category D, masonry shear walls must satisfy the requirements for special reinforced masonry shear walls in accordance with *Standard* Section 12.2. A summary of the seismic design parameters follows:

- Seismic Design Category (*Standard* Sec. 11.6): D
- Seismic Force-Resisting System (*Standard* Table 12.2-1): Special Reinforced Masonry Shear Wall
- Response Modification Factor, *R:* 5
- Deflection Amplification Factor, C_d*:* 3.5
- System Overstrength Factor, Ω_0*:* 2.5
- Redundancy Factor, ρ (*Standard* Sec. 12.3.4.2): 1.0

(Determination of ρ is discussed in Section 10.1.3 below.)

10.1.2.3 Structural design considerations. With respect to the lateral load path, the roof diaphragm supports approximately the upper 16 feet of the masonry walls (half the clear span plus the parapet) in the out-of-plane direction, transferring the lateral force to in-plane masonry shear walls. This is more precisely calculated in Section 10.1.4.1.

Soil structure interaction is not considered.

The building is of bearing wall construction.

Other than the opening in the roof, the building is symmetric about both principal axes, and the vertical elements of the seismic force-resisting system are arrayed entirely at the perimeter. The opening is not large enough to be considered an irregularity (per *Standard* Table 12.3-1); thus, the building is regular, both horizontally and vertically. *Standard* Table 12.6-1 permits several analytical procedures to be used; the equivalent lateral force (ELF) procedure (*Standard* Sec. 12.8) is selected for use in this example. The direction of loading requirements of *Standard* Section 12.5 are for walls that act in both principal directions, which is not the case for this structure, as will be discussed in more detail.

There is no inherent torsion because the building is symmetric. The effects of accidental torsion and its potential amplification, need not be included because the roof diaphragm is flexible (*Standard* Sec. 12.8.4.2).

The masonry bearing walls also must be designed for forces perpendicular to their plane (*Standard* Sec. 12.11.1).

For in-plane loading, the walls are treated as cantilevered shear walls. For out-of-plane loading, the walls are treated as simply supported at top and bottom. The assumption of a pinned connection at the base is deemed appropriate because the foundation is shallow and narrow, which permits rotation near the base of the wall.

10.1.3 Load Combinations

The basic load combinations are the same as specified in *Standard* Section 2.3.2. The seismic load effect, E, is defined by *Standard* Equations 12.4-1, 12.4-3 and 12.4-4, as follows:

$$E = E_h + E_v = \rho Q_E \pm 0.2 S_{DS} D = (1.0) Q_E \pm 0.2(1.43) D = Q_E \pm 0.286 D$$

This assumes $\rho = 1.0$ as will be confirmed in the following section.

10.1.3.1 Redundancy Factor. In accordance with *Standard* Section 12.3.4.2, the redundancy factor, ρ, applies to the in-plane load direction.

In order to achieve $\rho = 1.0$, the two conditions in *Standard* Section 12.3.4.2 must be met. In the long direction there are no walls with height-to length ratios exceeding 1.0; thus $\rho = 1.0$ in the long direction. In the short direction the pier heights do exceed the length; thus their conditions must be checked. For our case, both are met.

Although the calculation is not shown here, note that a single 8-foot-long pier carries approximately 23 percent (determined by considering the relative rigidities of the piers) of the in-plane load for each end wall. Thus, failure of a single pier results in less than 33 percent reduction in base shear resistance.

Loss of a single pier will not result in extreme torsional irregularity because the diaphragm is flexible.

Even if the diaphragm were rigid, an extreme torsional irregularity would not be created. The lateral deflection of end wall with all piers in place is approximately 0.018 inch (determined by RISA analysis). Lateral deflection of end wall with one pier removed is 0.024 inch. The larger deflection divided by the average of both deflections is less than 1.4:

$$\frac{0.024}{\left(\frac{0.018+0.024}{2}\right)} = 1.14 < 1.4$$

Therefore, even if the diaphragm were rigid, there is no extreme torsional irregularity as per *Standard* Table 12.3-1.

10.1.3.2 Combination of load effects. Load combinations for the in-plane loading direction from *Standard* Section 2.3.2 are:

$1.2D + 1.0E + 0.5L + 0.2S$

and

$0.9D + 1.0E + 1.6H$

L, S and H do not apply for this example (roof live load, L_r, is not floor live load, L) so the load combinations become:

$1.2D + 1.0E$

and

$0.9D + 1.0E$

For this case, $E = E_h \pm E_v = \rho Q_E \pm 0.2\, S_{DS} D = (1.0)Q_E \pm (0.2)(1.43)D = Q_E \pm 0.286D$

Where the effect of the earthquake determined above, $1.2D + 1.0(Q_E \pm 0.2D)$, is inserted in each of the load combinations, the controlling cases are $1.486D + Q_E$ when gravity and seismic are additive and $0.614D - Q_E$ when gravity and seismic counteract.

These load combinations are for the in-plane direction of loading. Load combinations for the out-of-plane direction of loading are similar except that the redundancy factor, ρ, is not applicable. Thus, for this example (where $\rho = 1.0$), the load combinations for both the in-plane and the out-of-plane directions are $1.486D + Q_E$ and $0.614D - Q_E$.

The combination of earthquake motion (and corresponding loading) in two orthogonal directions as per *Standard* Section 12.5.3.a need not be considered. *Standard* Section 12.5.4 for Seismic Design Category D refers to Section 12.5.3 for Category C, which requires consideration of direction to produce maximum effect where horizontal irregularity Type 5 exists ("non-parallel systems"); this building does not have that irregularity. *Standard* Section 12.5.4 also requires consideration of direction for maximum effect for elements that are part of intersecting systems *if* those elements receive an axial load from seismic action that exceeds 20 percent of their axial strength; axial loads are less than that for this building.

If a masonry control joint is provided at the corner, there are no elements acting in two directions. The short pier at the corner can be designed as an "L" shaped element, which means that it does participate in both directions. The vertical seismic force in that pier, generated by frame action, is small and easily less than 20 percent of its capacity. Therefore, no element of the seismic force-resisting system is required to

be checked for the direction of load that produces the maximum effect. Although it is not required, the typical pier in the end wall will be checked using the method of *Standard* Section 12.5.3.a. to illustrate the *Standard's* method for design to account for orthogonal effects.

10.1.4 Seismic Forces

Seismic base shear, diaphragm force and wall forces are discussed below.

10.1.4.1 Base Shear. Base shear is computed using the parameters determined previously. The *Standard* does not recognize the effect of long, flexible diaphragms on the fundamental period of vibration. The approximate period equations, which limit the computed period, are based only on the height. Since the structure is relatively short and stiff, short-period response will govern the design equations. According to *Standard* Section 12.8 (for short-period structures):

$$V = C_s W = \left[\frac{S_{DS}}{R/I}\right] W = \left[\frac{1.43}{5/1}\right] W = 0.286\ W$$

The seismic weight for forces in the long direction is as follows:

Roof = (20 psf)(100 ft)(200 ft)	= 400 kips
End walls = (103 psf) (2 walls)[(30 ft)(100 ft) – (5)(12 ft)(12 ft)](17.8 ft/28 ft)*	= 299 kips
Side walls = (65 psf) (30ft)(200ft)(2 walls)	= 780 kips
Total	= 1,479 kips

*Only the portion of the end walls that is distributed to the roof contributes to seismic weight in the long direction.

(The initial estimates of 65 psf for 8-inch CMU and 103 psf for 12-inch CMU are slightly higher than normal-weight CMU with grouted cells at 24 inches on center. However, grouted bond beams at 4 feet on center will be included, as will certain additional grouted cells.)

Note that the centroid of the end walls is determined to be 17.8 feet above the base, so the portion of the weight distributed to the roof is approximately the total weight multiplied by 17.8 feet/28 feet (weights and section properties of the walls are described subsequently).

Therefore, the base shear to each of the long walls is as follows:

V_u = (0.286)(1,479 kips)/2 = 211 kips

The seismic weight for forces in the short direction is:

Roof = (20 psf)(100 ft)(200 ft)	= 400 kips
Side walls = (65 psf)(2 walls)(30ft)(200ft)(15ft/28ft)*	= 418 kips
End walls = (103 psf)(2 walls)[(30ft)(100ft)-5(12ft)(12ft)]	= 470 kips
Total	= 1,288 kips

*Only the portion of the side walls that is distributed to the roof contributes to seismic weight in the short direction.

The base shear to each of the short walls is as follows:

V_u = (0.286)(1,288 kips)/2 = 184 kips

10.1.4.2 Diaphragm force. See Section 11.2 for diaphragm forces and design.

10.1.4.3 Wall forces. Because the diaphragm is flexible with respect to the walls, shear is distributed to the walls on the basis of beam theory, ignoring walls perpendicular to the motion (this is the "tributary" basis).

The building is symmetric. Given the previously explained assumption that accidental torsion need not be applied, the force to each wall becomes half the force on the diaphragm.

All exterior walls are bearing walls and, according to *Standard* Section 12.11.1, must be designed for a normal (out-of-plane) force of $0.4S_{DS}IW_w$ where W_w = weight of wall. The out-of-plane design is shown in Section 10.1.5.2.

10.1.5 Side Walls

The total base shear is the design force. *Standard* Section 14.4, which cites TMS 402, is the reference for design strengths. The compressive strength of the masonry, f_m', is 2,000 psi. TMS 402 Section 1.8.2.2 gives $E_m = 900f_m'$ = (900)(2 ksi) = 1,800 ksi.

For 8-inch-thick CMU with vertical cells grouted at 24 inches on center and horizontal bond beams at 48 inches on center, the weight is conservatively taken as 65 psf (recall the CMU are normal weight) and the net bedded area is 51.3 in.^{2}/ft based on tabulations in NCMA-TEK 14-1B.

10.1.5.1 Horizontal reinforcement – side walls. As determined in Section 10.1.4.1, the design base shear tributary to each longitudinal wall is 211 kips. Based on TMS 402 Section 1.17.3.6.2.1, the design shear strength must exceed either the shear corresponding to the development of 1.25 times the nominal flexure strength of the wall (which is very unlikely in this example due to the length of wall) or 2.5 times V_u , which in this case is 2.5(211) = 528 kips.

From TMS 402 Section 3.3.4.1.2.1, the masonry component of the shear strength capacity for reinforced masonry is as follows:

$$V_{nm} = \left[4.0 - 1.75\left(\frac{M_u}{V_u d_v}\right)\right] A_n \sqrt{f_m'} + 0.25\, P_u$$

For a single-story cantilever wall, $M_u/V_u d_v = h/d$, which is (28/200) = 0.14 for this case. For the long walls and conservatively treating P as 0.614 times the weight of the wall only, without considering the roof weight contribution:

$$V_{nm} = [4.0 - 1.75(0.14)](51.3)(200)\sqrt{2{,}000} + 0.25\left[(0.614)(390)\right] = 1{,}783 \text{ kips}$$

and

ϕV_m = 0.8(1,783) = 1,426 kips > 528 kips OK

where ϕ = 0.8 is the strength reduction factor for shear from TMS 402 Section 3.1.4.3.

Horizontal reinforcement therefore is not required for shear strength but is required if the wall is to qualify as a Special Reinforced Masonry Wall (TMS 402 Sec. 1.17.3.2.6.b). *Standard* Table 12.2-1 does not permit lower quality masonry walls in Seismic Design Category D.

According to TMS 402 Section 1.17.3.2.6.c, minimum horizontal reinforcement is $0.0007A_g$ = (0.0007)(7.625 in.)(8 in.) = 0.043 in.^{2} per course, but the authors believe it prudent to use more horizontal reinforcement for shrinkage in this very long wall and then use minimum reinforcement in the vertical direction [this concept applies even though this wall requires far more than the minimum reinforcement (also $0.0007A_g$) in the vertical direction due to its large height-to-thickness ratio]. Two #5 bars at 48 inches on center provide 0.103 in.^{2} per course. This amounts to 0.4 percent of the area of masonry plus the grout in the bond beams. The actual shrinkage properties of the masonry and the grout as well as local experience should be considered in deciding how much reinforcement to provide. For long walls that have no control joints, as in this example, providing more than minimum horizontal reinforcement is appropriate.

10.1.5.2 Out-of-plane flexure – side walls. The design demand for seismic out-of-plane flexure is $0.4S_{DS}Iw_w$ (*Standard* Sec. 12.11.1). For a wall weight of 65 psf for the 8-inch-thick CMU side walls, this demand is 0.4(1.43)(1)(65 psf) = 37 psf.

Calculations for out-of-plane flexure become somewhat involved and include the following:

1. Select a trial design.

2. Investigate to ensure ductility (i.e., check maximum reinforcement limit).

3. Make sure the trial design is suitable for wind (or other nonseismic) lateral loadings using the wind provisions of the *Standard* (which satisfies the IBC). (This is not illustrated in this example).

4. Calculate mid-height deflection due to wind by TMS 402. (Not illustrated in this example). (Note that while the *Standard* has story drift requirements, it does not impose a mid-height deflection limit for walls).

5. Calculate seismic demand. This computation requires consideration of *P-delta* effects because of the wall slenderness. (Seismic demand is greater than wind for this wall.)

6. Determine seismic resistance and compare to the demand determined in Step 5.

Proceed with these steps as follows:

10.1.5.2.1 Trial design. A trial design of #7 bars at 24 inches on center is selected. See Figure 10.1-3.

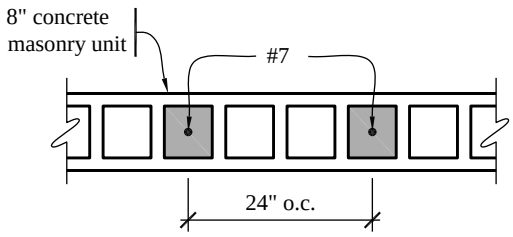

Figure 10.1-3 Trial design for 8-inch-thick CMU wall
(1.0 in. = 25.4 mm)

10.1.5.2.2 Investigate to ensure ductility. The critical strain condition corresponds to a strain in the extreme tension reinforcement (which is a single #7 centered in the wall in this example) equal to α times the strain at yield stress. α is the tension reinforcement strain factor (equal to 1.5 for out-of-plane flexure due to wind; see TMS 402 Commentary 3.3.3.5).

Based on TMS 402 Section 3.3.3.5.1.a and Commentary 3.3.3.5 (where α is defined) for this case:

t = 7.63 in.

$d = t/2$ = 3.81 in.

ε_m = 0.0025

$\varepsilon_s = 1.5\varepsilon_y = 1.5(f_y/E_s)$ = 1.5(60 ksi / 29,000 ksi) = 0.0031

$$c = \left[\frac{\varepsilon_m}{\left(\varepsilon_m + \varepsilon_s\right)}\right] d = 1.70 \text{ in.}$$

$a = 0.8c$ = 1.36 in.

The Whitney compression stress block, a = 1.36 inches for this strain distribution, is greater than the 1.25-inch face shell width. Thus, the compression stress block is broken into two components: one for full compression against solid masonry (the face shell), and another for compression against the webs and grouted cells but accounting for the open cells. These are shown as C_1 and C_2 in Figure 10.1-4:

$C_1 = 0.80 f_m'$ (1.25 in.)b = (0.80)(2 ksi)(1.25)(24) = 48 kips (for a 24-inch length)

$C_2 = 0.80\ f_m'$ (a-1.25 in.)(8 in.) = (0.80)(2 ksi)(1.36-1.25)(8) = 1.41 kips (for a 24-inch length)

The 8-inch dimension in the C_2 calculation is for the combined width of the grouted cell and the adjacent mortared webs over a 24-inch length of wall. The actual width of one cell plus the two adjacent webs will vary with various block manufacturers and may be larger or smaller than 8 inches. The 8-inch value has the benefit of simplicity (and is correct for solidly grouted walls).

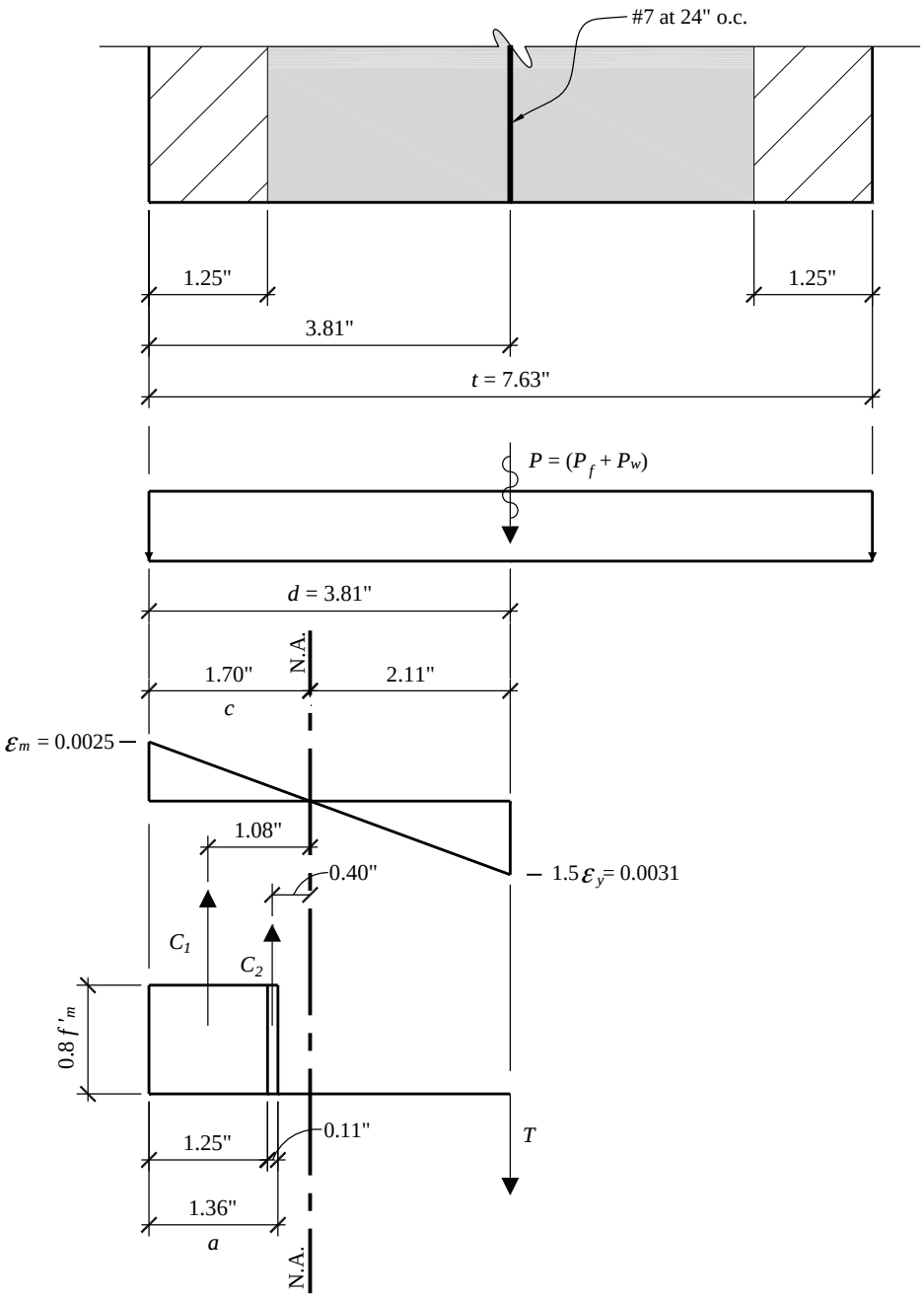

Figure 10.1-4 Investigation of out-of-plane ductility for the 8-inch-thick CMU side walls (1.0 in. = 25.4 mm)

T is based on $F_y A_s$ (TMS 402 Sec. 3.3.3.5.1.c):

$T = F_y A_s = (1.0)(60 \text{ ksi})(0.60 \text{ in.}^2) = 36$ kips (for a 24-inch length)

P is based on the load combination of $D + 0.75L + 0.525Q_E$ (TMS 402 Sec. 3.3.3.5.1.d).

Q_E is the effect of horizontal seismic motions, and P is a vertical force. Q_E produces overturning forces, but because this is such a long wall, the vertical force due to horizontal seismic motion is not significant, so the net total vertical force is taken as zero here. Therefore Q_E is zero in determining P for this wall.

Conservatively neglecting the roof weight:

$$Q_E = F_p = 0.2 S_{DS} D = (0.2)(1.43)\left[(65 \text{ psf})\left(\frac{28 \text{ ft}}{2} + 2 \text{ ft}\right)\left(\frac{24 \text{ in}}{12 \text{ in}}\right)\right] = 595 \text{ lb/24 in. length}$$

$$P = (65 \text{ psf})\left(\frac{28 \text{ ft}}{2} + 2 \text{ ft}\right)\left(\frac{24 \text{ ft}}{12 \text{ in}}\right) + (0.75)(0) \pm (0.525)(0 \text{ lb}) = 2.08 \text{ kips/24 in. length}$$

Check $C_1 + C_2 > T + P$ (all for 24-inch length):

$T + P = 36 + 2.08 = 38.1$ kips

$C_1 + C_2 = 49.4$ kips > 38.1 kips OK

The compression capacity is greater than the tension capacity; therefore, the ductile failure mode criterion is satisfied.

10.1.5.2.3 Check for wind load. The wind design check is beyond the scope of this seismic example, so it is not presented here. Both strength and deflection need to be ascertained in accordance with a building code; most are based on the *Standard*, which we are using. For our example, a check on strength to resist wind was found to conform to the *Standard* and is not shown here.

10.1.5.2.4 Calculate mid-height deflection due to wind by *Standard.* Deflection due to wind was found to conform to the *Standard* and is not shown here.

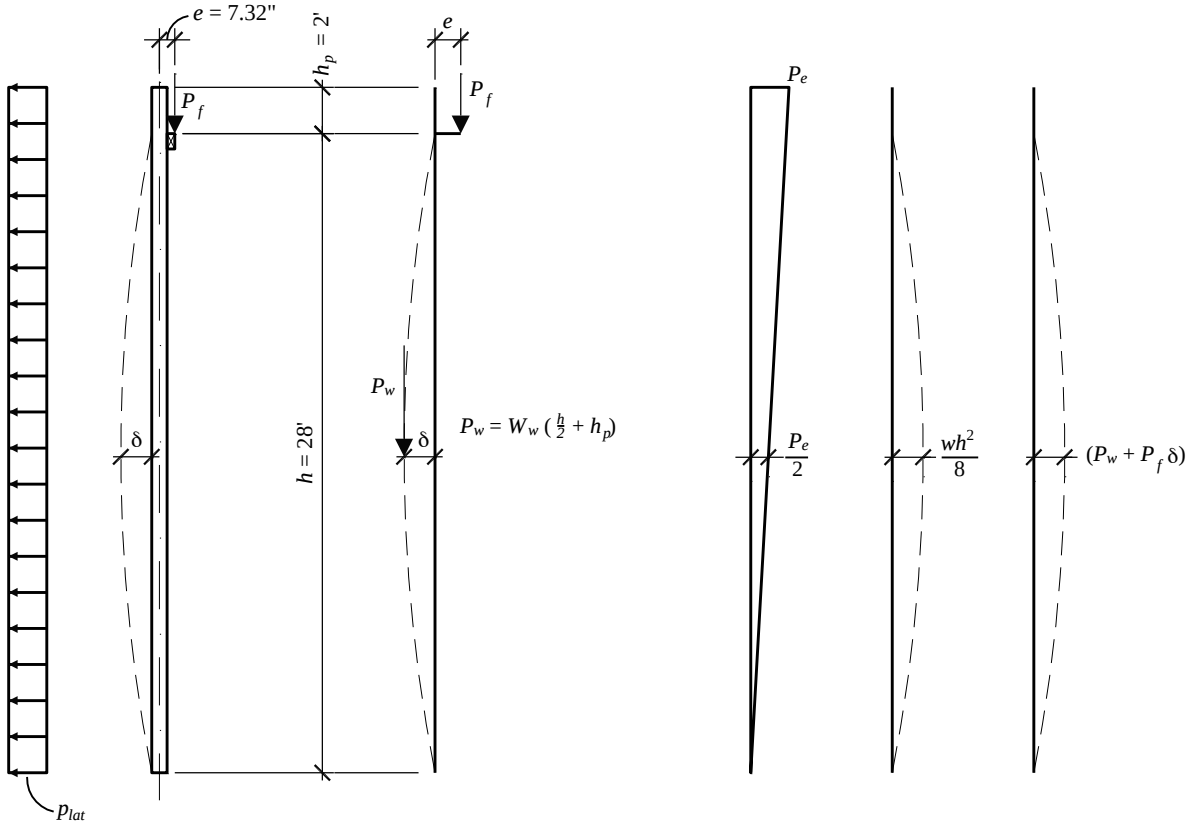

Figure 10.1-5 Basis for out-of-plane deflection calculation

10.1.5.2.5 Calculate seismic demand. For this case, the two load factors for dead load apply: 0.614*D* and 1.486*D*. Conventional wisdom holds that the lower dead load will result in lower moment-resisting capacity of the wall, so the 0.614*D* load factor would be expected to govern. However, the lower dead load also results in lower *P-delta*, so both cases should be checked. (As it turns out, the higher factor of 1.486*D* controls).

w_u = 37 psf (from Sec. 10.1.5.3)

Check moment capacity for 0.614*D*: TMS 402 Section 3.3.5.3 requires consideration of the secondary moment from the axial force acting through the deflection. TMS 402 Section 3.3.5.4 gives an equation that is essentially bilinear (two straight lines joined at the point of cracking). NCMA TEK 14-1B illustrates that determining the final moment by this method requires iteration.

Roof load, P_f = (20 psf)(10 ft) = 200 plf

Wall load (at mid-height), P_w = (65 psf)(16 ft) = 1,040 plf

$P = P_f + P_w$ = 1,240 plf

P_{uf} = (0.614)(200 plf) = 123 plf

P_{uw} = (0.614)(1,040 plf) = 638 plf

$P_u = P_{uf} + P_{uw} = 761$ plf

Eccentricity, $e = 7.32$ in. (distance from wall centerline to roof reaction centerline)

Modulus of elasticity, $E_m = 1{,}800{,}000$ psi

$f_m' = 2000$ psi

Modular ratio, $n = \frac{E_s}{E_m} = 16.1$

The modulus of rupture, f_r, is found from TMS 402 Table 3.1.8.2. The values given in the table are for either hollow CMU or fully grouted CMU. Values for partially grouted CMU are not given; Footnote a indicates that interpolation between these values must be performed. As illustrated in Figure 9.1-6, and shown below, the interpolated value for this example is based on relative areas of hollow and grouted cells:

$$f_r = 63 + (163 - 63)\left[\frac{(103 - 60)}{(183 - 60)}\right] = 98 \text{ psi}$$

Another method for making the interpolation, while approximate, is simpler. It is based on 2/3 of the cells being hollow and 1/3 of the cells being grouted for the case of grouted cells at 24 inches on center:

$$f_r = 63\left(\frac{2}{3}\right) + 163\left(\frac{1}{3}\right) = 96 \text{ psi}$$

For this example, the value of $f_r = 98$ psi will be used.

From mechanics:

$I_g = 443$ in.^{4}/ft

$S_g = 116$ in.^{3}/ft

From NCMA TEK 14-1B:

$I_n = 355$ in.^{4}/ft

$S_n = 93.2$ in.^{3}/ft

$A_n = 51.3$ in.^{2}/ft

$M_{cr} = S_n(f_r + P/A_n) = 93.2(98 + 1240/51.3) = 11{,}386$ in-lb/ft. Use $M_{cr} = 11{,}400$ in.-lb/ft. Note: this equation for M_{cr} is not in TMS 402; however, it is valid based on mechanics.

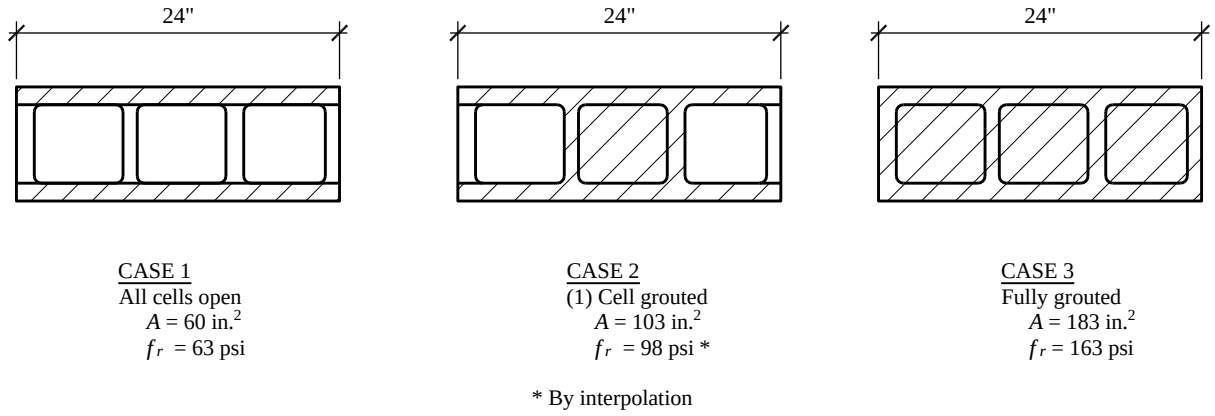

Figure 10.1-6 Basis for interpolation of modulus of rupture, f_r (1.0 in. = 25.4 mm, 1.0 psi = 6.89 kPa).

Refer to Figure 10.1-7 for determining I_{cr}. The neutral axis shown on the figure is not the conventional neutral axis by linear analysis; instead, it is the plastic centroid, which is simpler to locate, especially where the neutral axis position results in a T beam cross-section. (For this wall, the neutral axis does not produce a T section, but for the end wall in this building, a T section does result.) Cracked moments of inertia computed by this procedure are less than those computed by linear analysis but generally not so much less that the difference is significant. (This is the method used for computing the cracked section moment of inertia for slender walls in the standard for concrete structures, ACI 318.) Axial load does enter the computation of the plastic neutral axis and the effective area of reinforcement. Thus:

T = (0.60 in.^{2}/ 2 ft)(60 ksi) = 18.0 klf

$C = T + P$ = 19.24 klf

$a = C/(0.8\, f'_m b)$ = (19.24 klf)/(0.8(2.0 ksi)(12 in./ft) = 1.002 in.

$c = a/0.8$ = 1.25 in.

$A_{se} = A_s + P/f_y$ = 0.30 in.^{2}/ft + 1.240 klf/60 ksi = 0.32 in.^{2}/ft

Note: TMS 402 uses the term A_s to mean the same thing as effective area of reinforcement (TMS 402 Sec. 1.5 and Commentary 3.3.5.4). A_{se} is used here to distinguish effective area from actual area, A_s.

$I_{cr} = nA_{se}(d\text{-}c)^2 + bc^3/3$

= 16.1(0.32 in.^{2}/ft)(3.81 in. - 1.25 in.)^2 + (12 in./ft)(1.25 in.)^3/3

= 42.1 in.^{4}/ft

Note that I_{cr} could be recomputed for $P_u = 0.614D$ and $P_u = 1.486D$, but that refinement is not pursued in this example. In the opinion of the authors, the most correct method for computing the cracked section properties is to use P_u. This will necessitate two sets of cracked section properties for this example. For purposes of illustration, one set of cracked section properties, with $P = 1.0D$, is computed.

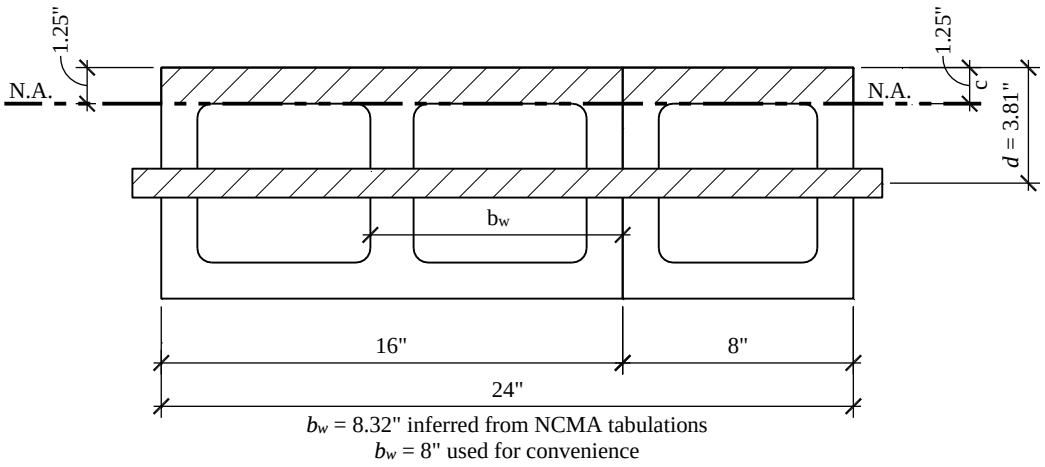

Figure 10.1-7 Cracked moment of inertia (I_{cr}) for 8-inch-thick CMU side walls (1.0 in. = 25.4 mm)

The computation of the secondary moment in an iterative fashion is shown below:

First iteration:

$$M_{u1} = w_u h^2 / 8 + P_{uf} e_u + (P_{uf} + P_{uw})\delta_u$$

$$M_{u1} = \frac{(37 \text{ psf}/12)(336 \text{ in.})^2}{8} + (123 \text{ plf})\left(\frac{7.32 \text{ in.}}{2}\right) + (761 \text{ plf})(0)$$

M_{u1} = 43,512 + 450 + 0 = 43,962 in.-lb/ft > M_{cr} = 11,400 in.-lb/ft

$$\delta_{s1} = \frac{5M_{cr}h^2}{48EI_g} + \frac{5(M_{u1} - M_{cr})h^2}{48EI_{cr}}$$

$$\delta_{s1} = \frac{5(11,400)(336)^2}{48(1,800,000)(443)} + \frac{5(44,962 - 11,400)(336)^2}{48(1,800,000)(42.1)} = 0.168 + 5.05 = 5.07 \text{ in.}$$

Second iteration:

$$M_{u2} = 43,512 + 450 + (761)(5.07) = 47,820 \text{ in.-lb}$$

$$\delta_{s2} = 0.165 + \frac{5(47,820 - 11,400)(336)^2}{48(1,800,000)(42.1)} = 0.165 + 5.652 = 5.82 \text{ in.}$$

Third iteration

M_{u3} = 43,512 + 450 + (761)(5.82) = 48,391 in.-lb/ft

$$\delta_{s3} = 0.165 + \frac{5\left(48{,}391 - 11{,}400\right)(336)^2}{48(1{,}800{,}000)(42.1)} = 0.165 + 5.74 = 5.91 \text{ in.}$$

Convergence check:

$$\frac{5.91 - 5.82}{5.82} = 1.5\% < 5\%$$

M_u = 48,391 in.-lb/ft (for the 0.614*D* load case)

Using the same procedure, find M_u for the 1.486*D* load case. The results are summarized below:

First iteration:

P_u = 1.486 (P_f + P_w) = 1.486(200 + 1,040) =297 + 1,545 = 1,843 plf

M_{u1} = 44,811 in.-lb/ft

δ_{u1} = 5.39 in.

Second iteration:

M_{u2} = 54,739 in.-lb/ft

δ_{u2} = 6.93 in.

Third iteration:

M_{u3} = 57,579 in.-lb/ft

δ_3 = 7.37 in.

Fourth iteration:

M_{u4} = 58,392 in.-lb/ft

δ_{u4} = 7.50 in.

Check convergence:

$$\frac{7.50 - 7.37}{7.50} = 1.7\% < 5\%$$

M_u = 58,392 in.-lb/ft (for the 1.486*D* load case)

The iterative method described above is consistent with NCMA TEK 14-11B. The authors note that ACI 318, the standard for concrete structures, includes provisions for the design of slender walls that are somewhat different. For the computation of deflection at nominal strength, 75 percent of the cracked stiffness is used. The 0.75 factor represents a margin for safety, because the required strength, M_u, depends on the computed deflection. The absence of the bilinear relation is much closer to deflection computations by other methods, such as given in TMS 402, Section 1.13.3.2. The absence of bilinear relations allows direct computation of the final deflection and moment, rather than iteration. For illustration, the method that predicts the secondary moment directly and upon which the ACI 318 slender wall direct calculation is based, is shown here:

$$M_u = M_{u1}\left(\frac{1}{1-\frac{P_u}{P_e}}\right)$$

Where:

$$P_e = \frac{\pi^2 EI_{cr}}{h^2} = \frac{\pi^2 (1{,}800 \text{ ksi})(42.1 \text{ in.}^2)}{(28 \text{ ft x } 12)^2} = 6.62 \text{ k/ft}$$

Therefore, for the 1.486*D* case:

$$M_u = 44.8 \text{ in.-k/ft}\left(\frac{1}{1-\frac{1.84 \text{ k/ft}}{6.62 \text{ k/ft}}}\right) = 62.0 \text{ in.-k/ft}$$

which is approximately 6 percent larger than M_u = 58.4 in.-k/ft by the iterative method above. In this calculation, the 0.75 factor on P_e used in ACI 318 has not been included.

10.1.5.2.6 Determine flexural strength of wall. Refer to Figure 10.1-8. As in the case for the ductility check, a strain diagram is drawn. Unlike the ductility check, the strain in the steel is not predetermined. Instead, as in conventional strength design of reinforced concrete, a rectangular stress block is computed first and then the flexural capacity is checked.

$T = A_s f_y$ = (0.30 in.^{2}/ft)60 ksi = 18.0 klf

The results for the two axial load cases are shown in Table 10.1-2 below.

Table 10.1-2 Flexural Strength of Side Wall

Load Case	0.614*D* + *E*	1.486*D* + *E*
P_u, klf	0.761	1.843
$C = T + P_u$, klf	18.76	19.84
$a = C / (0.8f'_m b)$, in.	0.978	1.03
$M_n = C\,(d - a/2)$, in.-kip/ft	62.3	65.35
$\phi M_n = 0.9M_n$, in.-kip/ft	56.1	58.8

Table 10.1-2 Flexural Strength of Side Wall

M_u, in.-kip/ft	48.4	58.4*
Acceptance	OK	OK

*The M_u from the alternative direct computation is approximately 5% higher than the design strength.

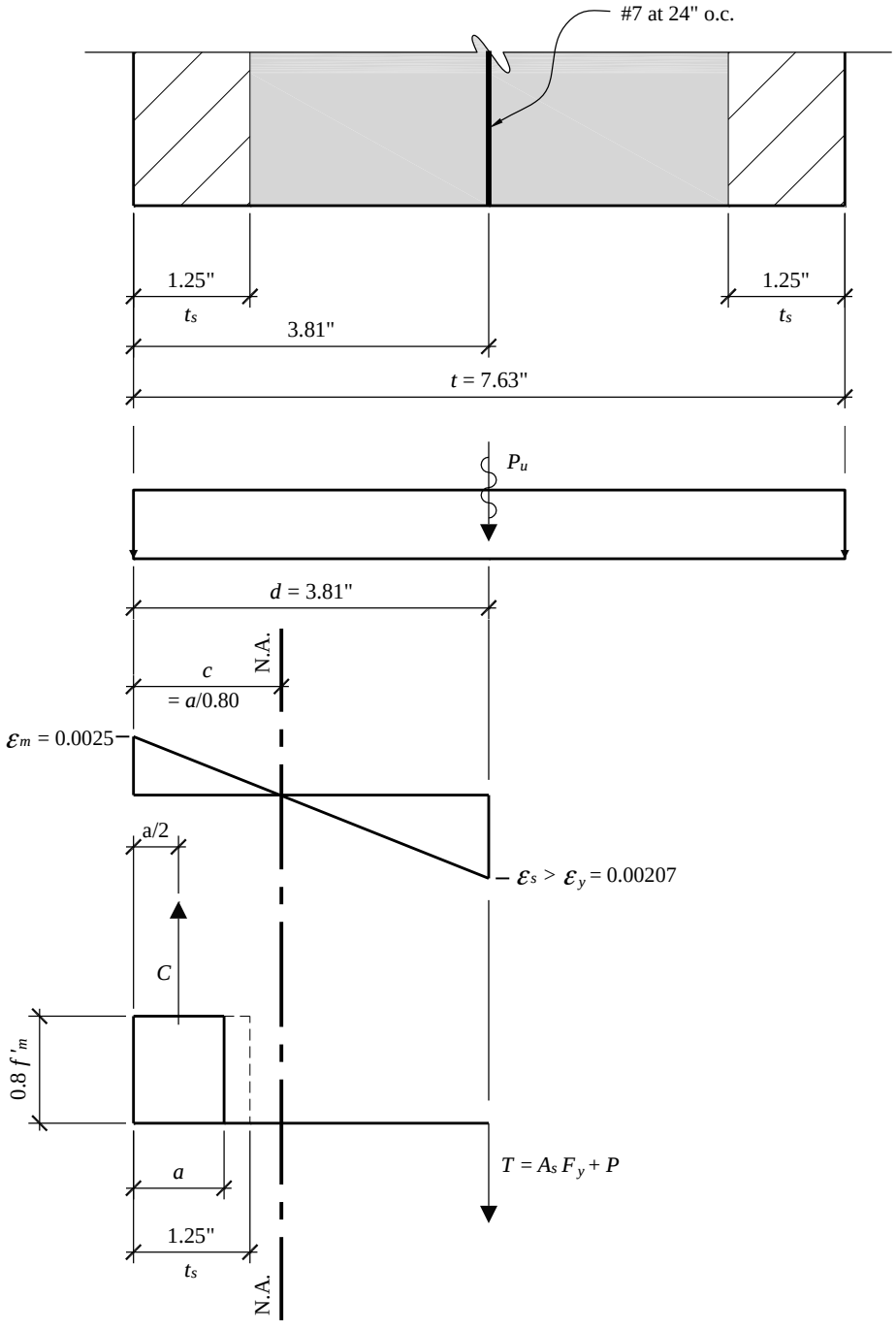

Figure 10.1-8 Out-of-plane strength for 8-inch-thick CMU walls

(1.0 in. = 25.4 mm)

Note that either wind or earthquake may control the stiffness and strength out-of-plane; earthquake controls for this example. A careful reading of *Standard* Section 12.5 should be made to see if the orthogonal loading combination will be called for; as discussed earlier, the orthogonal combination is not required for this example (although an orthogonal combination check will be made for illustration purposes later).

10.1.5.3 In-plane flexure – side walls. In-plane calculations for flexure in masonry walls include two items per the *Provisions*:

- Ductility check
- Strength check

It is recognized that this wall is very strong and stiff in the in-plane direction. Many engineers would not even consider these checks as necessary in ordinary design. The ductility check is illustrated here to show a method of implementing the requirement.

10.1.5.3.1 Ductility check. For this case, with $M_u/V_u d_v < 1$ and $R > 5$, TMS 402 Section 3.3.3.5.4 refers to Section 3.3.3.5.1, which stipulates that the critical strain condition corresponds to a strain in the extreme tension reinforcement equal to 1.5 times the strain associated with F_y. This calculation uses unfactored gravity loads. (See Figure 10.1-9.)

$$c = \left(\frac{\varepsilon_m}{\varepsilon_m + \varepsilon_s}\right) d = \left(\frac{0.0025}{0.0025 + 0.0031}\right) 200 \text{ ft} = 89.29 \text{ ft}$$

$a = 0.8c = 71.43$ ft

$C_m = 0.8 f'_m a b_{avg} = (0.8)\ (2 \text{ ksi})(71.43 \text{ ft})(51.3 \text{ in.}^2/\text{lf}) = 5{,}862$ kips

Where b_{avg} is taken from the average area used earlier, 51.3 in.^{2}/ft results; see Figure 10.1-9 for locations of tension steel and compression steel (the rebar in the compression zone will act as compression steel). From this it can be seen that:

$$T_{s1} = f_y \left(\frac{73.80}{(2)(2 \text{ ft o.c.})}\right)(0.60) = 664 \text{ kips}$$

$$T_{s2} = f_y \left(\frac{36.91}{2 \text{ ft}}\right)(0.60) = 664 \text{ kips}$$

$$C_{s1} = f_y \left(\frac{15.42}{2 \text{ ft o.c.}}\right)(0.60) = 278 \text{ kips}$$

$$C_{s2} = (f_y)\left(\frac{73.87}{(2)(2\text{ ft})}\right)(0.60) = 665 \text{ kips}$$

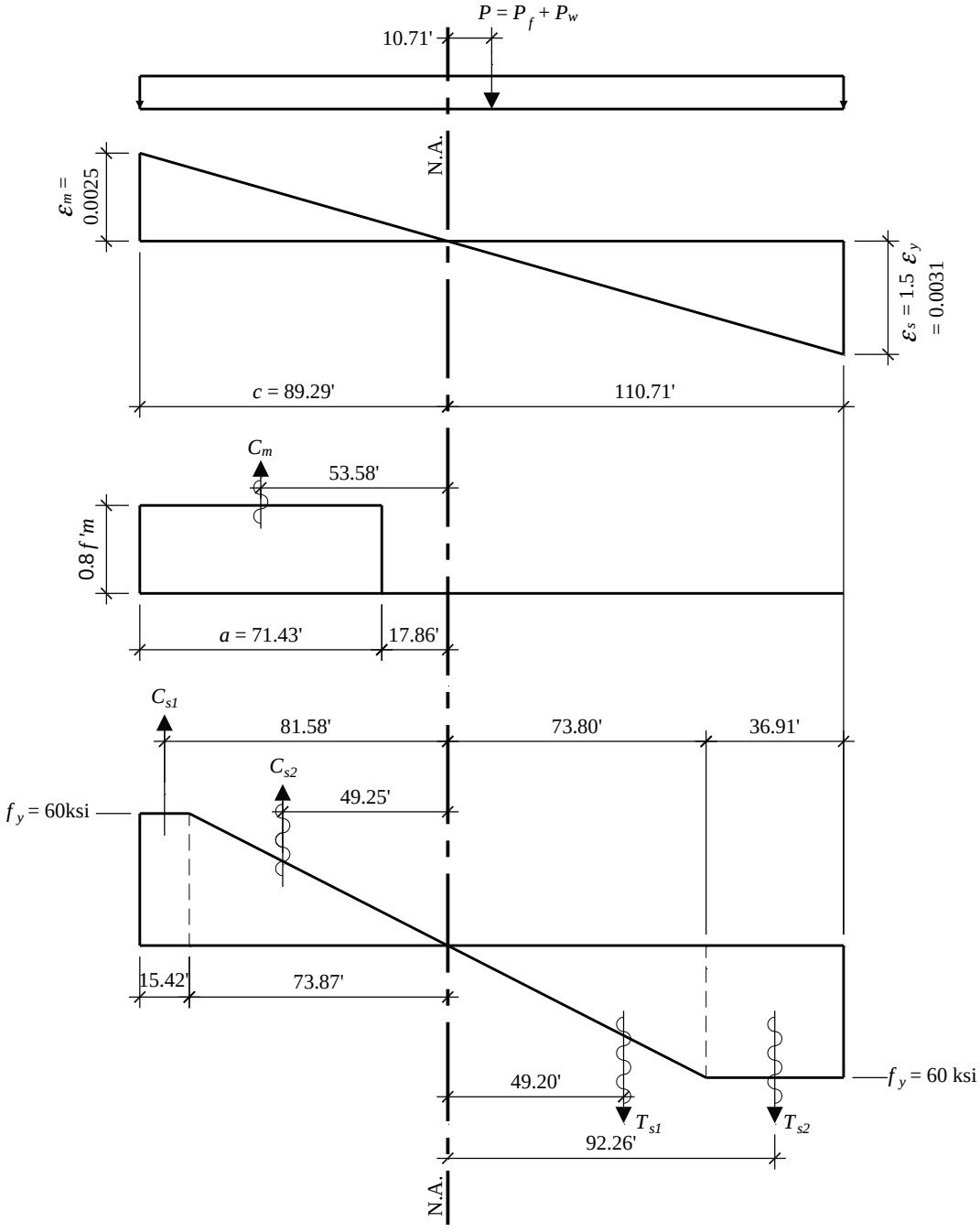

Figure 10.1-9 In-plane ductility check for side walls
(1.0 in. = 25.4 mm, 1.0 ksi = 6.89 MPa)

Some authorities would not consider the compression resistance of reinforcing steel that is not confined within ties. In one location (Section 3.1.8.3) TMS 402 clearly requires transverse reinforcement (ties) for any steel used in compression, while in another place (Section 3.3.3.5.1.e) it explicitly permits inclusion of compression reinforcement with or without lateral restraining reinforcement for checks on maximum flexural tensile reinforcement (i.e., ductility checks). TMS 402 Commentary 3.3.3.5 explains that confinement reinforcement is not required because the maximum masonry compressive strain will be less than ultimate values. This inconsistency does not usually have a significant effect on computed results. The authors have taken credit for unconfined compression reinforcement for strength and included it in ductility checks (but there is no objection to the practice of neglecting unconfined compression reinforcement used by some engineers).

In the authors' opinion, there are two approaches to the determination of *P*, one following TMS 402 and the other following the ***Standard***:

P is at the base of the wall rather than at the mid-height:

- TMS 402 Section 3.3.3.5.1.d:

  $D + 0.75L + 0.525\ Q_E$

  Since Q_E represents the effect of horizontal seismic forces, which equals zero for our case, and roof live load is not combined with seismic loads, this reduces to *D*:

  $P = P_w + P_f$ = [(0.065 ksf) (30 ft) + (0.02 ksf)(10 ft)](200 ft) = 430 kips

- ***Standard*** Section 12.4.2.3:

  $(1.2 + 0.2\ S_{DS})D + \rho Q_E + L + 0.2S$

  which reduces to:

  $[1.2 + (0.2)(1.43)]D + 0 + 0 + 0$

  $P_u = (1.486)(P_f + P_w)$ = (1.486)(480 kips) = 713 kips

Continuing with the in-plane ductility check:

$\Sigma C > P + \Sigma T$

$C_m + C_{s1} + C_{s2} > P + T_{s1} + T_{s2}$

And conservatively using the higher of the two values for *P*,

5,862 + 278 + 665 > 713 + 664 + 664 6,805 > 2,041 OK

Therefore, there is enough compression capacity to ensure ductile failure. Note that either of the two values for *P* brings us to the same conclusion for this case.

It should also be noted that even if the compression reinforcement were neglected, there would still be enough compression capacity to ensure ductile failure.

In the opinion of the authors, flexural yield is feasible for walls with $M_u/V_u d_v$ in excess of 1.0; this criterion limits the compressive strain in the masonry, which leads to good performance in strong ground shaking. For walls with $M_u/V_u d_v$ substantially less than 1.0, the wall will fail in shear before a flexural yield is possible. Therefore, the criterion does not affect performance. Well distributed and well developed reinforcement to control the shear cracks is the most important ductility attribute for such walls.

10.1.5.4.2 Strength check. The wall is so long with respect to its height that in-plane strength for flexure is acceptable by inspection.

10.1.5.5 Shear – side walls.

10.1.5.5.1 Out-of-plane shear in side walls. Compute out-of-plane shear at the base of a wall in accordance with *Standard* Section 12.11.1:

$F_p = 0.4 S_{DS} I w_w$ = (0.4)(1.43)(1.0)(65 psf)(28 ft/2) = (37 psf)(14 ft) = 521 plf.

The "capacity design" requirement in TMS 402 Section 1.17.3.2.6.1 applies to behavior in-plane, not out-of-plane.

The capacity computed per TMS 402 Section 3.3.4.1.2.1 is as follows:

$$V_m = \left[4.0 - 1.75\left(\frac{M_u}{V_u d_v}\right)\right] A_n \sqrt{f'_m} + 0.25\, P_u$$

$M_u/V_u d_v$ need not be taken larger than 1.0 (and $M_u/V_u d_v$ does exceed 1.0 for a short distance above the base). A_n, as determined earlier, is taken as 51.3 in.^{2}/ft. Note: If the dimensions from Figure 109.7 are used, A_n is taken as $b_w d$ = (8.32 in.)(3.81 in.) + (24 - 8.32 in.)(1.25 in.) = 51.3 in.^{2}/ft, a similar value.

The authors note that traditional practice in reinforced masonry has been to compute shear stress on the basis of areas equaling width times depth to reinforcement *(bd)*. For the in-plane shear strength, the difference between *bd* and A_n is not too great, but for the out-of-plane shear strength of walls with one layer of reinforcement in their centers, the difference is very substantial. Therefore, the authors have substituted $b_w d$ (= 8 in. × 3.81in. = 30.5 in.^{2} ; see Figure 10.1-7) for A_n in the equation below.

Because shear exists at both the bottom and the top of the wall, conservatively neglect the effect of *P*:

$V_m = [4.0 - 1.75(1.0)](30.5 \text{in.}^2/\text{ft})\sqrt{2{,}000} + 0 = 3.07$ kips/24" = 1.53 klf

ϕV_m = (0.8)(1.53) = 1.23 klf > 0.52 klf OK

10.1.5.5.2 In-plane shear in side walls. As indicated in Sections 10.1.4.1 and 10.1.5.1, the in-plane demand at the base of the wall, V_u = 2.5(211 kips) = 528 kips and the shear capacity, ϕV_m, is larger than (4.13 klf)(200 ft) = 826 kips.

For the purpose of understanding likely behavior of the building somewhat better, V_n is estimated more accurately than simply limiting $M_u/V_u d_v$ to 1 for these long walls:

$M_u/V_u d_v = h/l$ = 28/200 = 0.14

$P_u = 0.614D = (0.614)(430 \text{ kips}) = 264 \text{ kips}$

$V_m = [4.0 - 1.75(0.14)][200(51.3)](0.045) + 0.25(264) = 1{,}733 + 66 = 1{,}799 \text{ kips}$

$V_{ns} = 0.5(A_v/s)f_y d = 0.5(0.62/4.0)(60)(200) = 930 \text{ kips}$ (for 2-#5 in bond beams at 4 ft o.c.)

$V_n = 1{,}799 + 930 = 2{,}729 \text{ kips}$

Maximum $V_n = 6\sqrt{f'_m}A_n = 6(0.045 \text{ ksi})(10{,}260 \text{ in.}^2) = 2{,}770 > 2{,}729 \text{ kips}$

$\phi V_n = 0.8(2{,}729) = 2{,}183 \text{ kip} > 528 \text{ kips} = V_u$

The calculated seismic force, $V_E = 211$kips (from Sec. 10.1.4.1)

$\phi V_n/V_E = 10.3 >> R$ used in design

In other words, it is unlikely that the long masonry walls will yield in either in-plane shear or flexure at the design seismic ground motion. The walls will likely yield in out-of-plane response, and the roof diaphragm may also yield. The roof diaphragm for this building is illustrated in Section 11.2.

10.1.6 End Walls

The transverse walls are designed in a manner similar to the longitudinal walls. Complicating the design of the transverse walls are the door openings, which leave a series of masonry piers between the doors.

10.1.6.1 Horizontal reinforcement – end walls. The minimum reinforcement, per TMS 402 Section 1.17.3.2.6, is $0.0007A_g = (0.0007)(11.625 \text{ in.})(8 \text{ in.}) = 0.065 \text{ in.}^2$ per course. The maximum spacing of horizontal reinforcement is 48 inches, for which the minimum reinforcement is 0.39 in.^{2}. Two #4 in bond beams at 48 inches on center would satisfy the requirement. The large amount of vertical reinforcement would combine to satisfy the minimum total reinforcement requirement. However, given the 100-foot length of the wall, a larger amount is desired for control of restrained shrinkage as discussed in Section 10.1.5.1. Two #5 at 48 inches on center will be used.

10.1.6.2 Vertical reinforcement – end walls. The area for each bay subject to out-of-plane wind is 20 feet wide by 30 feet high because wind load applied to the doors is transferred to the masonry piers. However, the area per bay subject to both in-plane and out-of-plane seismic forces is reduced by the area of the doors. This is because the doors are relatively light compared to the masonry. See Figures 10.1-11 and 10.1-12.

10.1.6.3 Out-of-plane flexure – end walls. Out-of-plane flexure is considered in a manner similar to that illustrated in Section 10.1.5.2. The design of this wall must account for the effect of door openings between a row of piers. The steps are the same as identified previously and are summarized here for convenience:

1. Select a trial design.

2. Investigate to ensure ductility.

3. Make sure the trial design is suitable for wind (or other non-seismic) lateral loadings using the wind provisions of the *Standard.*

4. If wind controls over seismic (it does not in this example), then calculate the mid-height deflection due to wind by TMS 402.

5. Calculate the seismic demand.

6. Determine the seismic resistance and compare to the demand determined in Step 5.

10.1.6.3.1 Trial design. A trial design of 12-inch-thick CMU reinforced with two #6 bars at 24 inches on center is selected. The self-weight of the wall, accounting for horizontal bond beams at 4 feet on center, is taken as 103 psf. Adjacent to each door jamb, the vertical reinforcement is placed into two cells. See Figure 10.1-10.

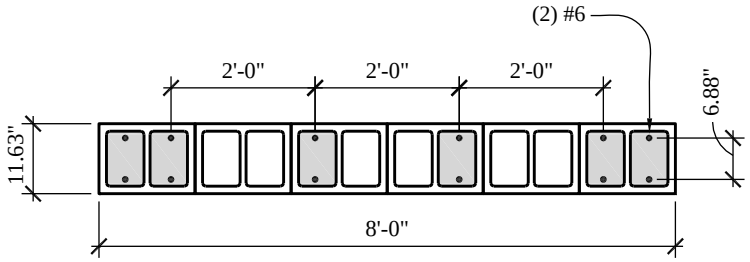

Figure 10.1-10 Trial design for piers on end walls
(1.0 in. = 25.4 mm, 1.0 ft = 0.3048 m)

Next, determine the design load locations. The centroid for seismic loads, out-of-plane, is the centroid of the mass of the wall and, accounting for the door openings, is determined to be 17.8 feet above the base. See Figures 10.1-11 and 10.1-12.

10.1.6.3.2 Investigate to ensure ductility. The critical strain condition corresponds to a strain in the extreme tension reinforcement (which is a pair of #6 bars in the end cell in this example) equal to α times the strain at yield stress. As for the side walls, $\alpha = 1.5$ for out-of-plane flexure due to wind (TMS 402 Section 3.3.3.5 and Commentary 3.3.3.5). See Figure 10.1-13.

For this case:

t = 11.63 in.

d = 11.63 - 2.38 = 9.25 in.

ε_m = 0.0025 (TMS Sec. 402 3.3.2.c)

$\varepsilon_s = 1.5\ \varepsilon_y = 1.5\ (f_y/E_s) = 1.5$ (60 ksi /29,000 ksi) = 0.0031 (TMS 402 Sec. 3.3.3.5.1.a and Commentary 3.3.3.5)

$$c = \left[\frac{\varepsilon_m}{(\varepsilon_m + \varepsilon_s)}\right] d = 4.13 \text{ in.}$$

$a = 0.8c = 3.30$ in. (TMS 402 Sec. 3.3.3.5.1.b)

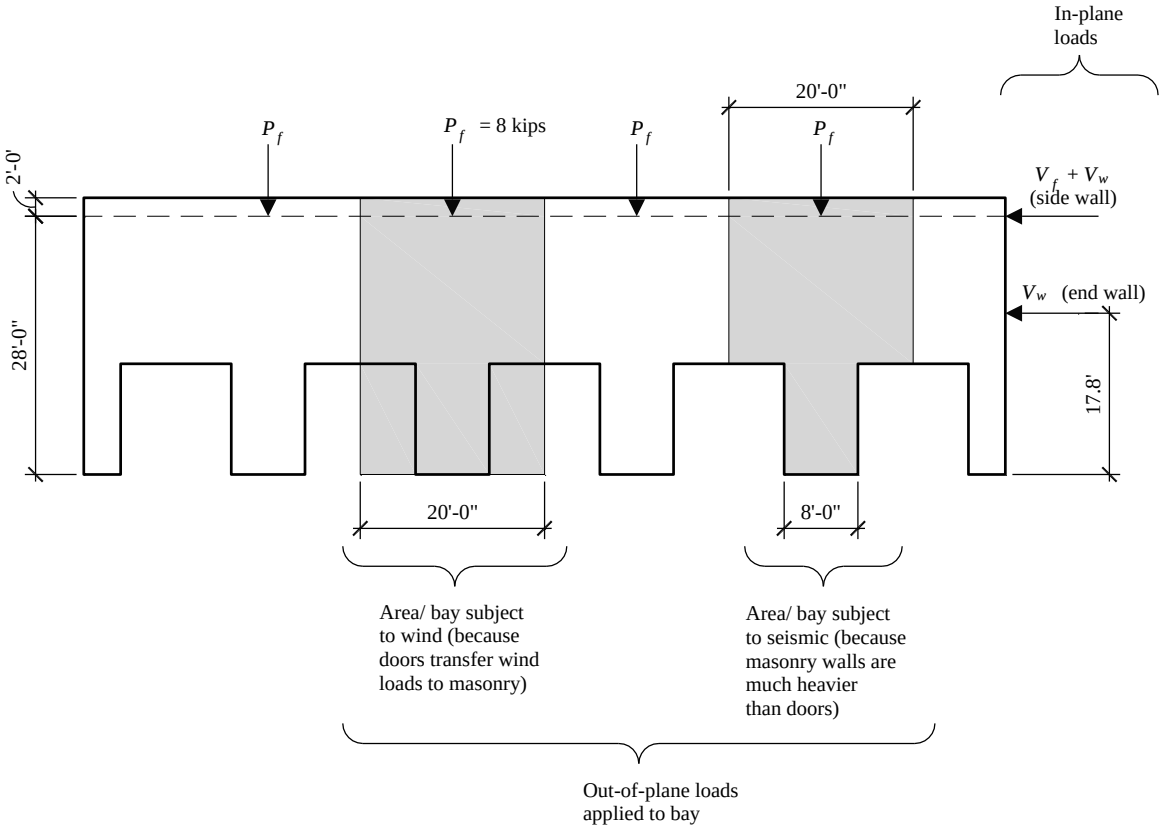

Figure 10.1-11 In-plane loads on end walls
(1.0 ft = 0.3048 m)

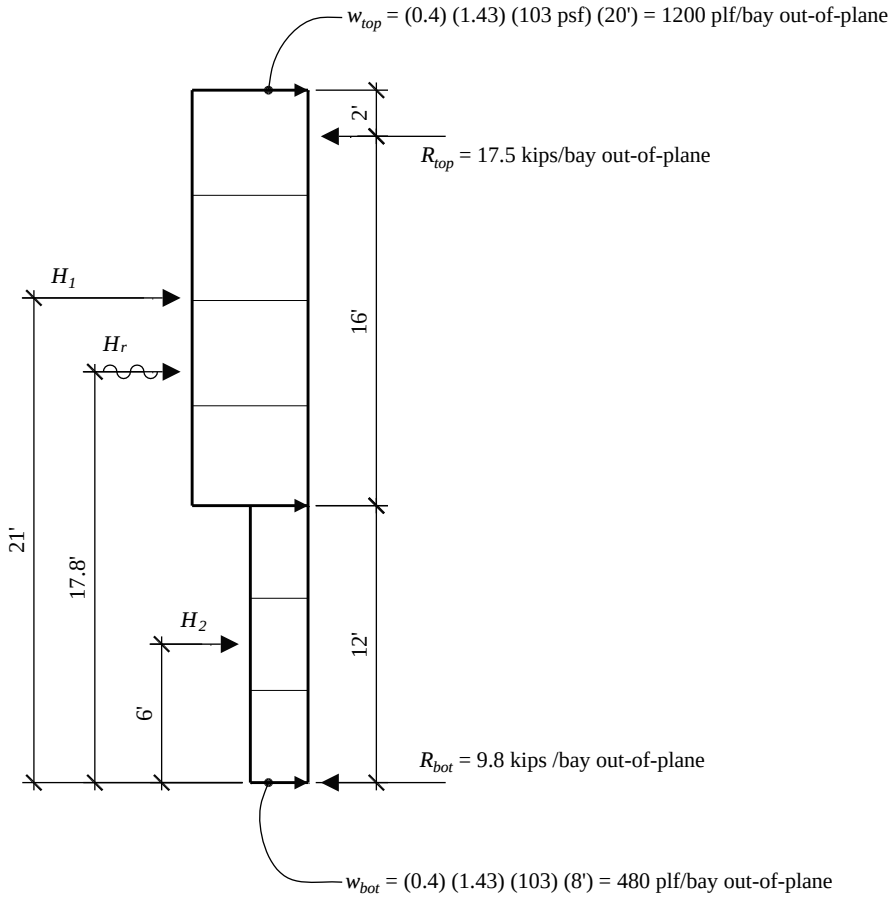

Figure 10.1-12 Out-of-plane load diagram and resultant of lateral loads (1.0 ft = 0.3048 m, 1.0 lb = 4.45 N, 1.0 kip = 4.45 kN)

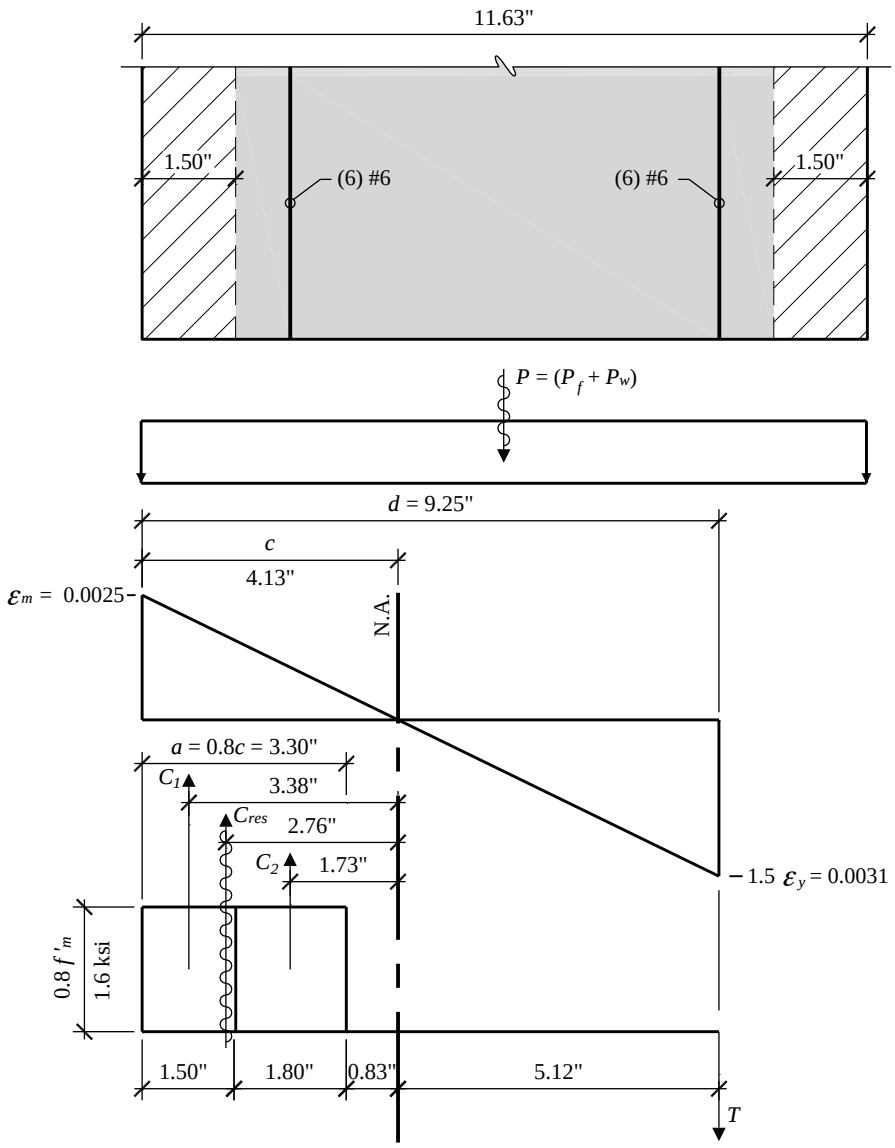

Figure 10.1-13 Investigation of out-of-plane ductility for end wall
(1.0 in. = 25.4 mm, 1.0 ksi = 6.89 MPa)

Note that the Whitney compression stress block, a = 3.30 inches deep, is greater than the 1.50-inch face shell thickness. Thus, the compression stress block is broken into two components: one for full compression against solid masonry (the face shell) and another for compression against the webs and grouted cells but accounting for the open cells. These are shown as C_1 and C_2 in Figure 10.1-14. The values are computed using TMS 402 Section 3.3.2.g:

$C_1 = 0.80f_m'$ (1.50 in.)b = (0.80)(2 ksi)(1.50)(96) = 230 kips (for full length of pier)

$C_2 = 0.80f_m'$ (a - 1.50 in.)(6(8 in.)) = (0.80)(2 ksi)(3.30 - 1.50)(48) = 138 kips

The 48-inch dimension in the C_2 calculation is the combined width of grouted cell and adjacent mortared webs over the 96-inch length of the pier.

$T = F_y A_s$ = (60 ksi)(6 × 0.44 in.^{2}) = 158 kips/pier

P is computed at the head of the doors. The dead load component of P is:

$P = (P_f + P_w)$ = (0.020 ksf)(20 ft)(20 ft) + (0.103 ksf)(18 ft)(20 ft) = 8.0 + 37.1

P = 45.1 kips/pier

From TMS 402 Section 3.3.3.5.1.d, axial forces are taken from the load combination of the following:

$P = D + 0.75L + 0.525Q_E$ with $Q_E = F_p = 0.2S_{DS}D$ = (0.2)(1.43)(45.1) = 12.9 kips/pier

P = 45.1 kips/pier + (0.75)(0) + (0.525)(12.9 kips/pier)

P = 51.9 kips/pier

$C_1 + C_2 > P + T$

368 kip > 210 kips

The compression capacity is greater than the tension capacity, so the ductility criterion is satisfied.

10.1.6.3.3 Check for wind loading. Wind pressure per bay is over the full 20-foot-wide by 30-foot-high bay, as discussed above, and is based on the *Standard*. While both strength and deflection need to be ascertained per a building code (the IBC was used), the calculations are not presented here.

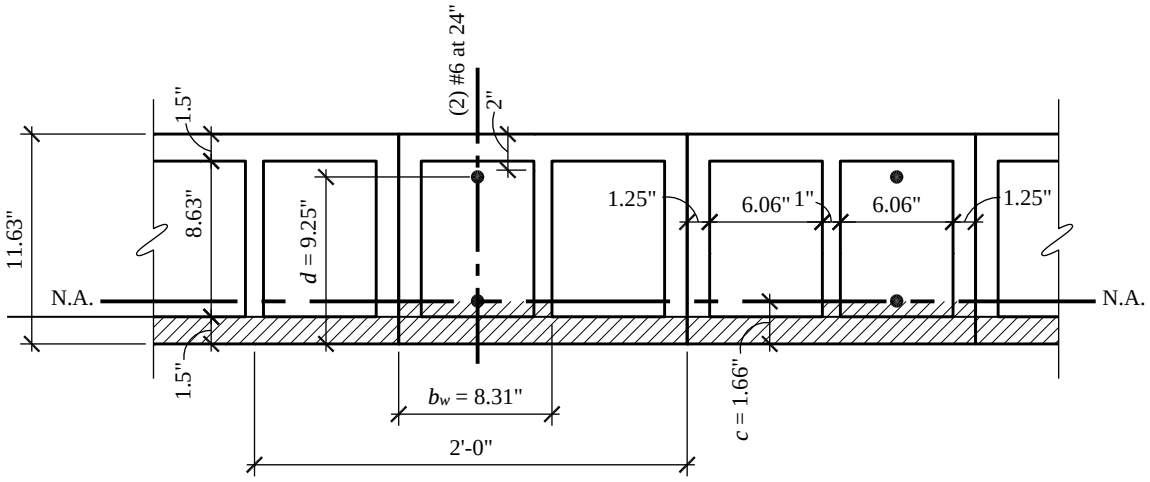

Figure 10.1-14 Cracked moment of inertia (I_{cr}) for end walls.
Dimension "c" depends on calculations shown for Figure 10.1-16.
(1.0 in. = 25.4 mm, 1.0 ft = 0.3048 m)

10.1.6.3.4 Calculate out-of-plane seismic demand. For this example, the load combination 0.614*D* has been used, and for this calculation, forces and moments over a single pier (width = 96 in.) are used. This does not violate the $b > 6t$ rule (TMS 402 Sec. 3.3.4.3.3.d) because the pier is reinforced at 24 inches on center. The use of the full width of the pier instead of a 24-inch width is simply for calculation convenience.

For this example, a *P-delta* analysis using RISA-2D was run, resulting in the following:

Maximum moment, M_u = 95.6 ft-kips/bay = 95.6/20 ft = 4.78 klf (does not control)

Moment at top of pier, M_u = 89.3 ft-kips/pier = 89.3 / 8 ft = 11.2 klf (controls)

Shear at bottom of pier, V_u = 9.61 kips/pier

Reaction at roof, V_u = 17.5 kips/bay

Axial force at base, R_u = 31.2 kips/pier (includes load factor on *D* of 0.614)

10.1.6.3.6 Determine moment resistance at the top of the pier. See Figure 10.1-15.

A_s = 6-#6 = 2.64 in.^{2}/pier

d = 9.25 in.

T = 2.64(60) = 158.4 kip/pier

$C = T + P$ = 184.1 kip/pier (P is based on D of (0.614)(37.1 + 8 kip) = 27.7 kip/pier at top of pier)

$a = C / (0.8f'_m b)$ = 184.1 / [(0.8)(2)96] = 1.20 in.

Because a is less than the face shell thickness (1.50 in.), compute as for a rectangular beam. Moments are computed about the centerline of the wall.

$M_n = C\,(t/2 - a/2) + P\,(0) + T\,(d - t/2)$

$= 184.1(5.81 - 1.20/2) + 158.4(9.25\text{-}5.81) = 1{,}504$ in.-kip = 125.4 ft-kip

$\varphi M_n = 0.9(125.4) = 112.8$ ft-kip

Because moment capacity at the top of the pier, ϕM_n = 112.8 ft-kips, exceeds the maximum moment demand at top of pier, M_u = 89.3ft-kips, the condition is acceptable.

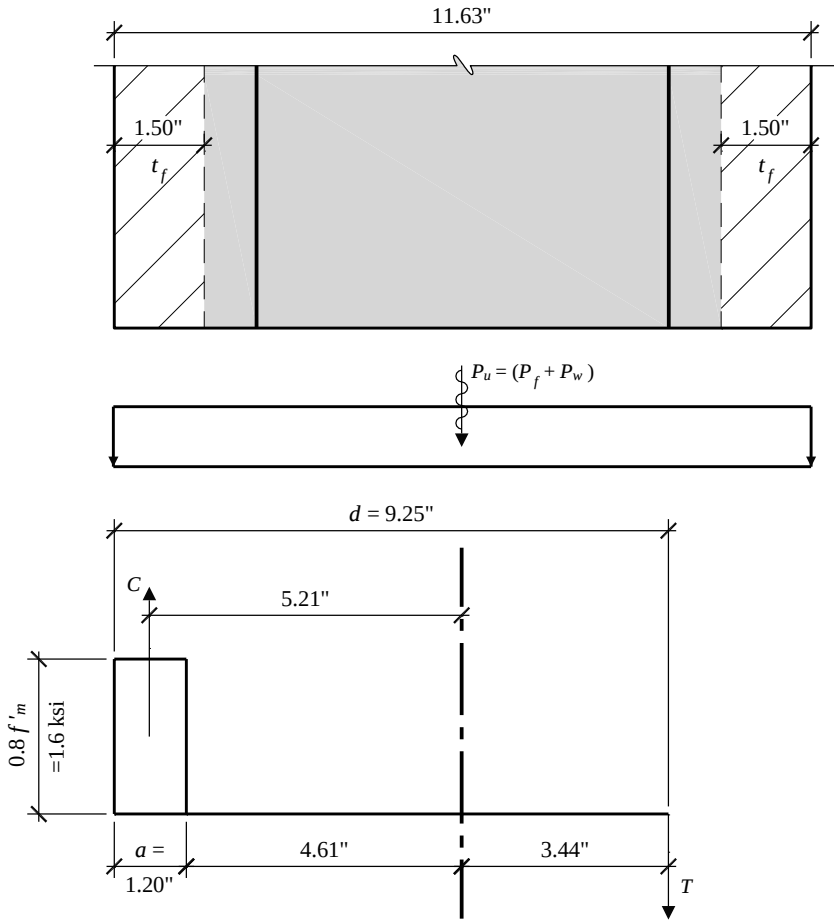

Figure 10.1-15 Out-of-plane seismic strength of pier on end wall
(1.0 in. = 25.4 mm, 1.0 ksi = 6.89 MPa)

10.1.6.4 In-plane flexure – end walls. There are several possible methods to compute the shears and moments in the individual piers of the end wall. For this example, the end wall was modeled using RISA-2D. The horizontal beam was modeled at the top of the opening, rather than at its mid-height. The in-plane lateral loads (see Figure 10.1-11) were applied at the 12-foot elevation and combined with joint moments representing transfer of the horizontal forces from their point of action down to the 12-foot elevation. Vertical load due to roof beams and the self-weight of the end wall were included. The input loads are shown in Figure 10.1-16. For this example:

w = (18 ft)(103 psf) + (20 ft)(20 psf) = 2.254 klf

H = (184 kip)/5 = 36.8 kip

$M = C_s[(V_{f\,long} + V_{w\,long})h_{long} + (V_{w\,short})(h_{short})]$ (refer to Fig. 10.1-11).

M = 0.286[(400 + 418)(28 ft – 12 ft) + 470(17.8 ft – 12 ft)] = 452 ft-kip

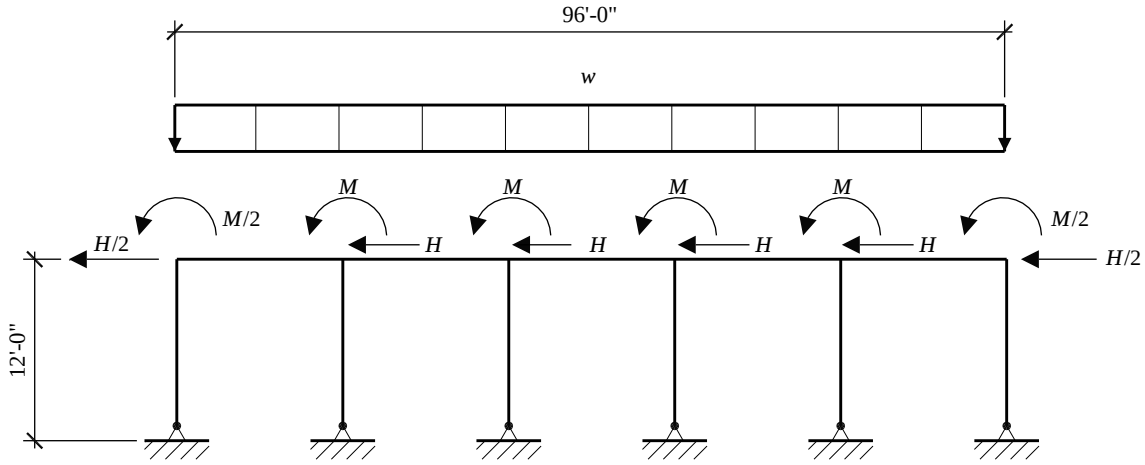

Figure 10.1-16 Input loads for in-plane end wall analysis
(1.0 ft = 0.3048 m)

The input forces at the end wall are distributed over all the piers to simulate actual conditions. The RISA-2D frame analysis accounts for the relative stiffnesses of the 4-foot- and 8-foot-wide piers (continuity of the 4-foot-wide piers at the corners was not considered). The final distribution of forces, shears and moments for an interior pier is shown on Figure 10.1-17.

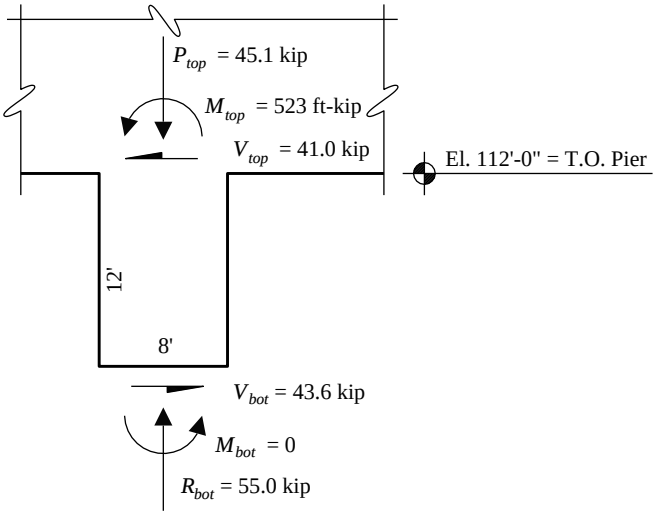

Figure 10.1-17 In-plane design condition for 8-foot-wide pier
(1.0 ft = 0.3048 m)

Continuing with the trial design for in-plane pier design, use two #6 bars at 24 inches on center supplemented by adding two #6 bars in the cells adjacent to the door jambs (see Figures 10.1-10 and 10.1-18).

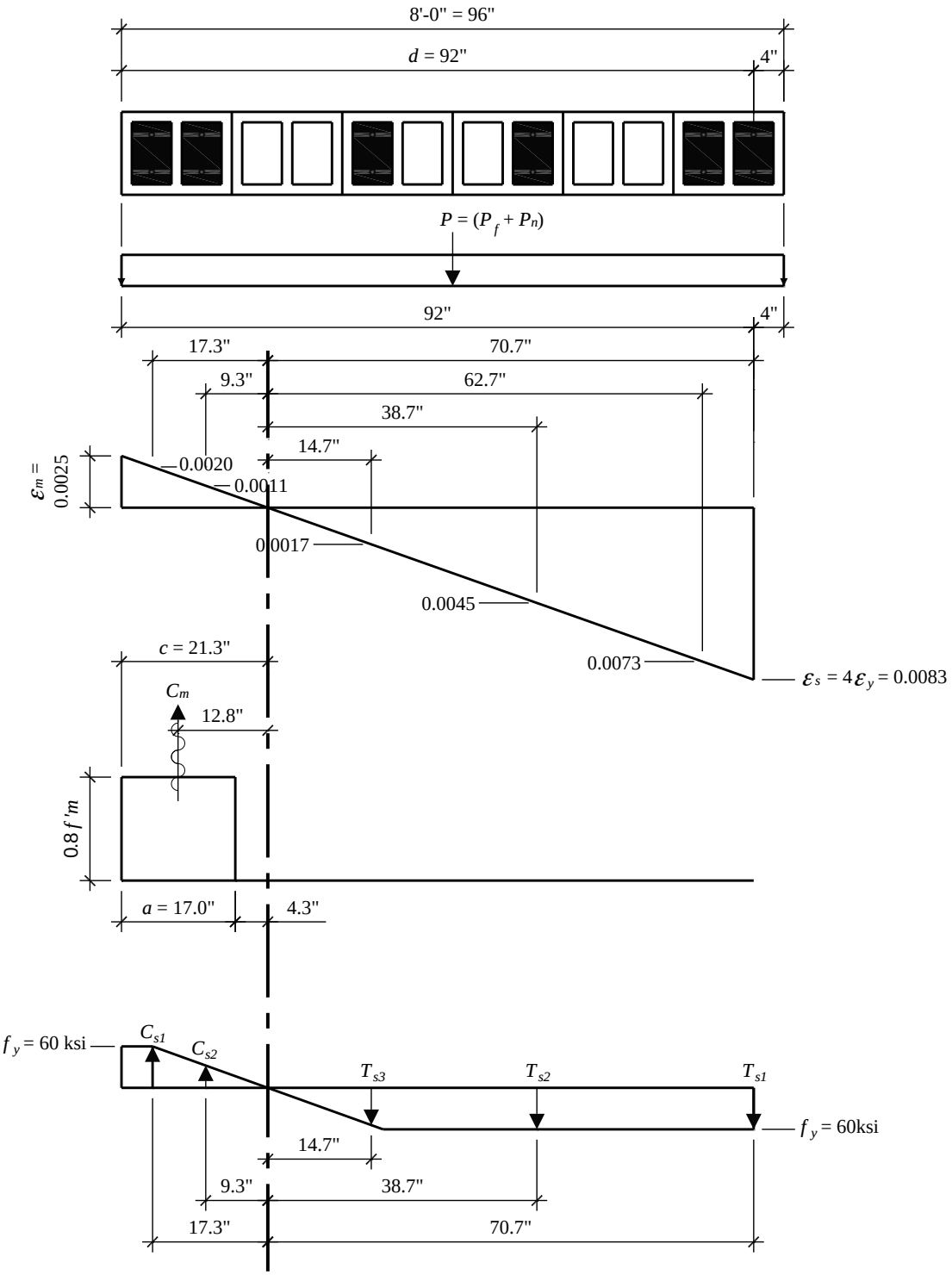

Figure 10.1-18 In-plane ductility check for 8-foot-wide pier
(1.0 in. = 25.4 mm, 1.0 ksi = 6.89 MPa)

The design values for in-plane design at the top of the pier are:

Table 10.1-3 In-plane Design Values at Pier Top

Unfactored	$0.614D + 1.0E$	$1.486D + 1.0E$
P = 45.1 kips	P_u = 41.2 kips	P_u = 67.0 kips
V = 43.6 kips	V_u = 43.6 kips	V_u = 43.6 kips
M = 523 ft-kips	M_u = 523 ft-kips	M_u = 523 ft-kips
$M_u/V_u d_v$	1.50	1.50

The ductility check is illustrated in Figure 10.1-18. Because $M_u/V_u d_v > 1$for this special reinforced masonry shear wall subject to in-plane loads, $\alpha = 4$:

$\varepsilon_m = 0.0025$

$\varepsilon_s = 4\varepsilon_y = (4\ )(60/29{,}000) = 0.0083$

d = 92 in.

From the strain diagram (Fig. 10.1-18), the strains at the rebar locations from left to right are:

$\varepsilon = 0.0020$
$\varepsilon = 0.0011$
$\varepsilon = 0.0017$
$\varepsilon = 0.0045$
$\varepsilon = 0.0073$
$\varepsilon = 0.0083$

To check ductility, use unfactored loads (from Section 10.1.6.3.2):

$P = P_f + P_w$ = 8 kips + 37.1 kips = 45.1 kips

$a = 0.8c$ = 17.0 in.

$C_m = (0.8f_m')ab$ = (1.6 ksi)(17.0 in.)(11.63 in.) = 315.5 kips

$T_{s1} = T_{s2} = F_y A_s$ = (60 ksi)(2 × 0.44 in.^{2}) = 52.8 kips

$T_{s3} = \varepsilon E A_s$ = (0.0017)(29,000 ksi)(2 × 0.44 in.^{2}) = 43.4 kip

$C_{s1} = \varepsilon E A_s$ = (0.0021)(29,000 ksi)(2 × 0.44 in.^{2}) = 53.6 kip

$C_{s2} = \varepsilon E A_s$ = (0.0011)(29,000 ksi)(2 × 0.44 in.^{2}) = 28.1 kip

$\Sigma C > \Sigma T + P$

$C_m + C_{s1} + C_{s2} > T_{s1} + T_{s2} + T_{s3} + P$

315.5 + 53.6 + 28.1 > 52.8 + 52.8 + 43.4 + 45.1

397 kips > 194 kips OK

Because compression capacity exceeds tension capacity, the requirement for ductile behavior is OK.

Note that maximum P for the wall to remain ductile is $P_{max} = \Sigma C - \Sigma T = 248$ kips. Thus, $\phi P_{max} = 223$ kips in order to assure ductility.

For the strength check, see Figure 10.1-19.

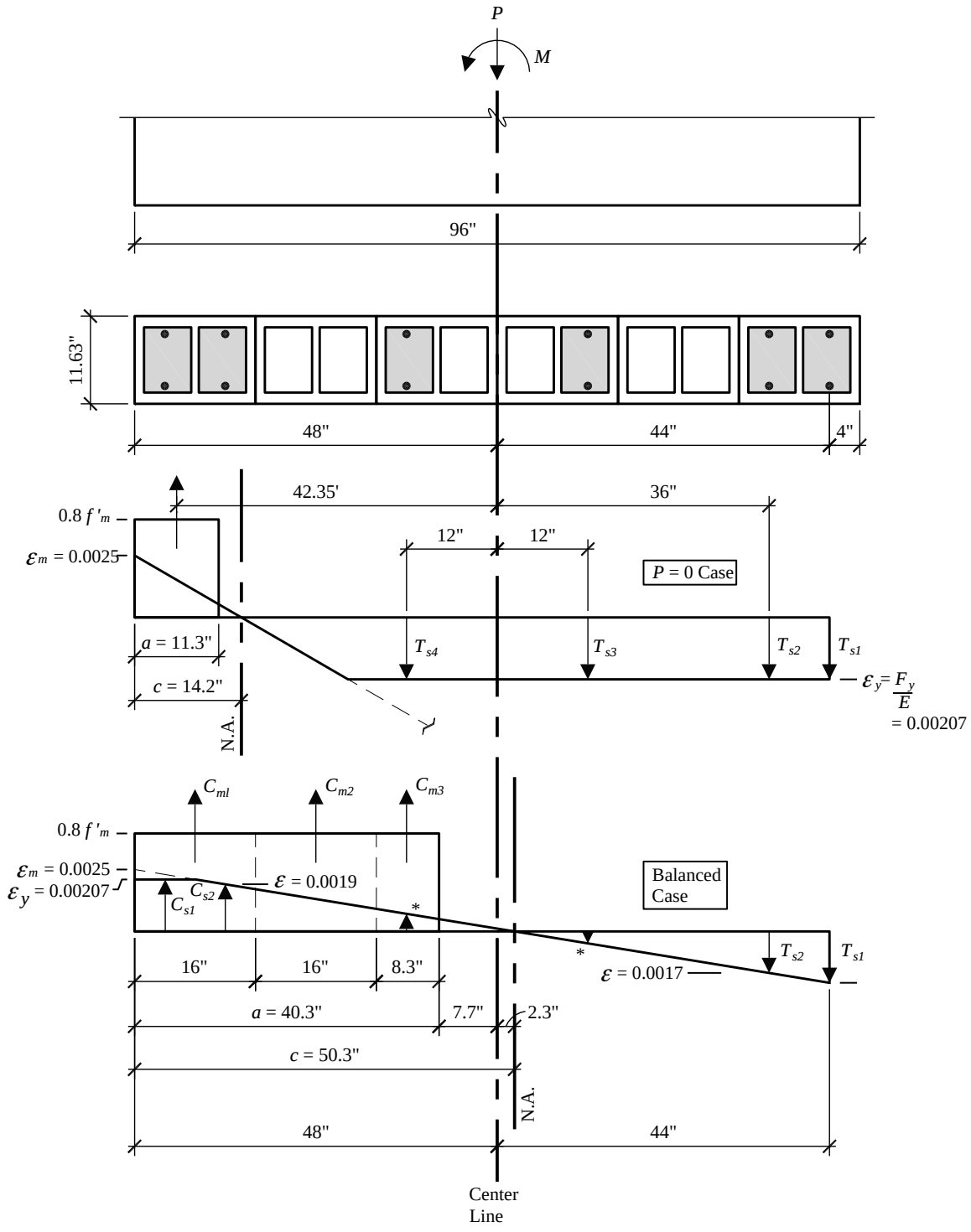

Figure 10.1-19 In-plane seismic strength of pier.
Strain diagram superimposed on strength diagram for both cases.
Note that locations with low force in reinforcement, marked by *, are neglected.
(1.0 in. = 25.4 mm)

To ascertain the strength of the pier, a ϕP_n - ϕM_n curve is developed. Only the portion below the "balance point" is examined since that portion is sufficient for the purposes of this example. (Ductile failures occur only at points on the curve that are below the balance point, so this is consistent with the overall approach).

For the P = 0 case, assume all bars in tension reach their yield stress and neglect compression steel (a conservative assumption):

$T_{s1} = T_{s2} = T_{s3} = T_{s4} = (2)(0.44 \text{ in.}^2)(60 \text{ ksi}) = 52.8$ kips

$C_m = \Sigma T_s = (4)(52.8) = 211.2$ kips

$C_m = 0.8f'_m ab = (0.8)(2 \text{ ksi})a(11.63 \text{ in.}) = 18.6a$

Thus, a = 11.3 inches and $c = a/0.8$ = 11.3 / 0.8 = 14.2 inches.

$\Sigma M_{cl} = 0$

$M_n = 42.35\ C_m + 44T_{s1} + 36T_{s2} + 12T_{s3} - 12T_{s4} = 13{,}168$ in.-kips

$\phi M_n = (0.9)(13{,}168) = 11{,}851$ in.-kips = 988 ft-kips

For the balanced case:

d = 92 in.

$\varepsilon = 0.0025$

$\varepsilon_y = 60/29{,}000 = 0.00207$

$$c = \left(\frac{\varepsilon_m}{\varepsilon_m + \varepsilon_y} \right) d = 50.3 \text{ in.}$$

$a = 0.8c = 40.3$ in.

Compression values are determined from the Whitney compression block adjusted for fully grouted cells or ungrouted cells:

$C_{m1} = (1.6 \text{ ksi})(16 \text{ in.})(11.63 \text{ in.}) = 297.8$ kips

$C_{m2} = (1.6 \text{ ksi})(16 \text{ in.})(2 \times 1.50 \text{ in.}) = 76.8$ kips

$C_{m3} = (1.6 \text{ ksi})(8.3 \text{ in.})(11.63 \text{ in.}) = 154.4$ kips

$C_{s1} = (0.88 \text{ in.}^2)(60 \text{ ksi}) = 52.8$ kips

$C_{s2} = (0.88 \text{ in.}^2)(60 \text{ ksi})(0.0019 / 0.00207) = 48.5$ kips

T_{s1} = (0.88 in.^{2})(60 ksi) = 52.8 kips

T_{s2} = (0.88 in.^{2})(60 ksi)(0.0017 / 0.00207) = 43.4 kips

$\Sigma F_y = 0$:

$P_n = \Sigma C - \Sigma T$ = 297.8 + 76.8 + 154.4 + 52.8 + 48.5 -52.8 - 43.4 = 534 kips

ϕP_n = (0.9)(534) = 481 kips

$\Sigma M_{cl} = 0$:

$M_n = 40C_{m1} + 24C_{m2} + 11.85C_{m3} + 44C_{s1} + 36C_{s2} + 44T_{s1} + 36T_{s2}$ = 23,540 in.-kips

ϕM_n = (0.9)(23,540) = 21,186 in.-kips = 1,765 ft-kips

The two cases are plotted in Figure 10.1-20 to develop the ϕP_n - ϕM_n curve on the pier. The demand (P_u, - M_u) also is plotted. As can be seen, the pier design is acceptable because the demand is within the ϕP_n - ϕM_n curve. (See the Birmingham 1 example in Section 10.2 for additional discussion of ϕP_n - ϕM_n curves.) By linear interpolation, ϕM_n at the minimum axial load is 1,096 ft- kip.

The authors note that the use of ϕ = 0.9 on P_n at the balance point is consistent with TMS 402, but, because of the ductility requirement, the balance point will never be reached. The maximum P_n for this pier, as per the ductility requirement (from Sec. 10.1.6.4), would be (397 kips - 149 kips) = 248 kips (as discussed above), well below the 481 kips at P_b. To illustrate the point, this maximum expressed as $\phi P_{n\max}$ = 223 kips, is illustrated in Figure 10.1-20.

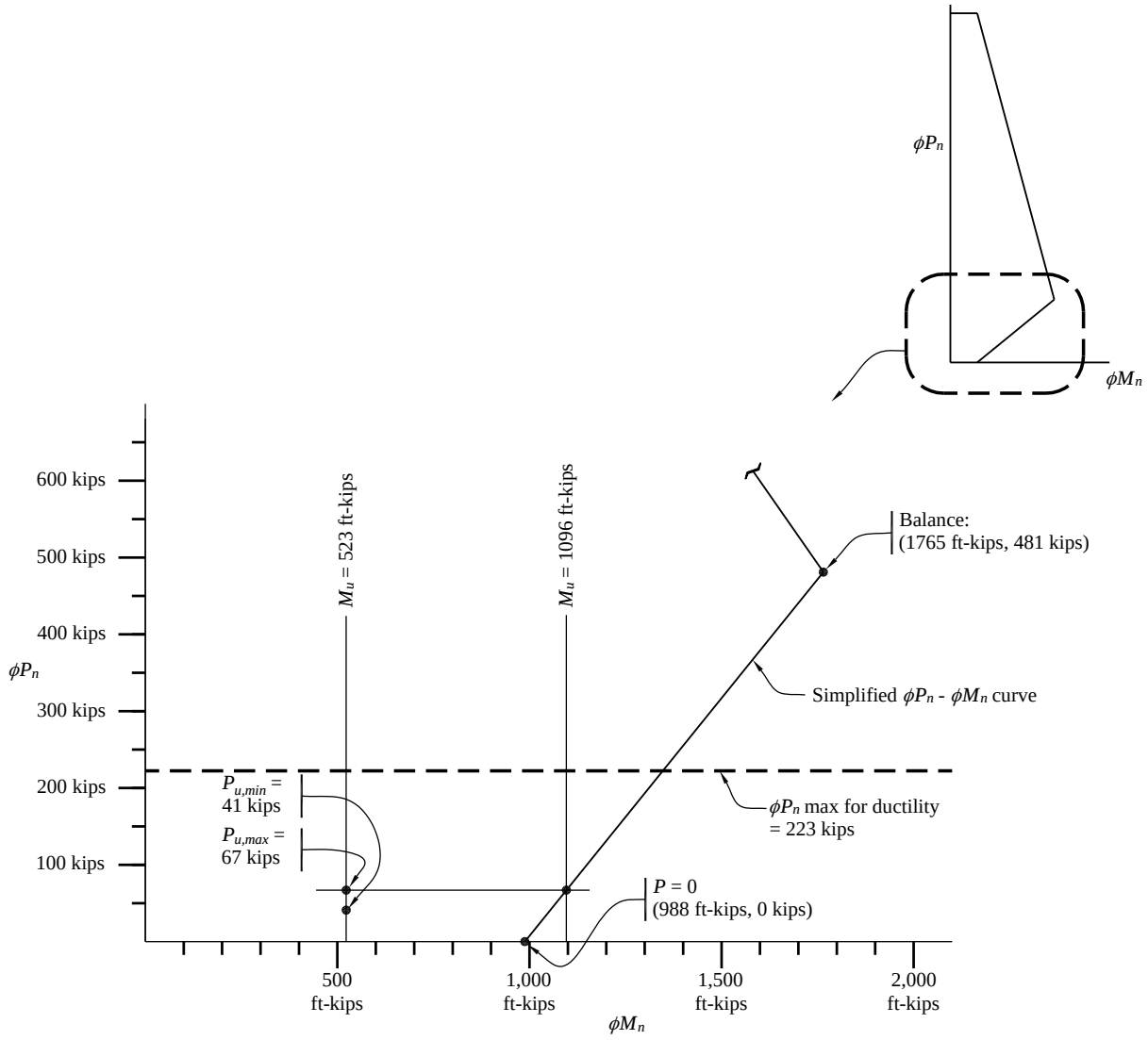

Figure 10.1-20 In-plane ϕP_n - ϕM_n diagram for pier
(1.0 kip = 4.45 kN, 1.0 ft-kip = 1.36 kN-m)

10.1.6.5 Combined loads. Although it is not required by the *Standard*, it is educational to illustrate the orthogonal combination of seismic loads for this pier (as if *Standard* Section 12.5.3.a were required), shown in Table 10.1-4:

Table 10.1-4 Combined Loads for Flexure in End Wall Pier

0.614D	Out-of-Plane		In-Plane		Total	
Case 1	1.0(87.7/112.8)	+	0.3(523/1026)	=	0.93 < 1.00	OK
Case 2	0.3(87.7/112.8)	+	1.0(523/1026)	=	0.74 < 1.00	OK

Values are in kips; 1.0 kip = 4.45 kN.

10.1.6.6 Shear – end walls.

10.1.6.6.1 In-plane shear at end wall piers. The in-plane shear at the base of the pier is 43.6 kips per bay. At the head of the opening where the moment demand is highest, the in-plane shear is slightly less (based on the weight of the pier). There, V = 43.6 kips - (0.286)(8 ft)(12 ft)(0.103 ksf) = 40.8 kips. Per TMS 402 Section 1.17.3.2.6.1.1, the design shear strength, ϕV_n, must exceed the shear corresponding to the development of 1.25 times the nominal flexural strength, M_n, or 2.5V_u, whichever is smaller. Using the results in Figure 10.1-20, the 125 percent implies a factor on shear by analysis of:

$$1.25\left(\frac{\phi M_n}{M_u}\right)\left(\frac{1}{\phi}\right)(V_u) = 1.25\left(\frac{1096}{523}\right)\left(\frac{1}{0.9}\right)V_u = 2.91\ V_u$$

But 2.91V_u > 2.5V_u; therefore, 2.5V_u controls (TMS 402 Sec. 1.17.3.2.6.1.1).

Therefore, the required shear capacities at the base and head of the pier are (2.5)(43.6 kips) = 109 kips and (2.5)(40.8) = 102 kips, respectively.

The in-plane shear capacity is computed as follows where the net area, A_n, of the pier is the area of face shells plus the area of grouted cells and adjacent webs:

$$V_m = \left[4.0 - 1.75\left(\frac{M_u}{V_u d_v}\right)\right] A_n \sqrt{f'_m} + 0.25 P_u$$

As discussed previously, $M_u/V_u d_v$ need not exceed 1.0 in the above equation.

A_n = (96 in. × 1.50 in. × 2) + (6 cells × 8 in. × 8.63 in.) = 702 in.^{2} / bay

Recall that horizontal reinforcement is 2-#5 at 48 inches in bond beams:

$$V_{ns} = 0.5\left(\frac{A_v}{s}\right) f_y d_v$$
$$= 0.5\left(\frac{0.62 \text{ in.}^2}{48 \text{ in.}}\right)(60 \text{ ksi})(96 \text{ in.})$$
$$= 37.2 \text{ kips/bay}$$

At the base of the pier:

V_m = [4.0 - 1.75(0)](702 in.^{2})(0.0447 ksi) + (0.25)(0.614 × 55.0 kips)

V_m = 79.0 kips/bay

ϕV_n = (0.8)(79.0 + 37.2) = 116.2 kips/bay > 109 kips/bay = 2.5 V_u OK

At the head of the pier:

V_m = [4.0 - 1.75(1.0)](702 in.^{2})(0.0447 ksi) + (0.25)(0.614 × 45.1 kips) = 77.5 kips/bay

ϕV_n = (0.8)(77.5 + 37.2) = 91.8 kips/bay < 102 kips/bay = 2.5 V_u N.G.

This non-ductile situation can be addressed by increasing the compression capacity. For this case, the other cells in the pier will be grouted, resulting in $A_n = b_w d$ = (11.63 in.)(92 in.) = 1070 in.^{2}. (Note that while TMS 402 permits $A_n = b_w d_v$, the authors have elected to use the slightly more conservative $b_w d$ in the determination of area.) This results in V_m = 114.5 kips and ϕV_n = 121 kips > 102 kips = 2.5 V_u which is OK.

Note: The design of the piers in the end walls of this example will remain the same without iteration to reflect the additional grouted cells. Note also that there is no additional vertical reinforcement; only grout has been added to the cells.

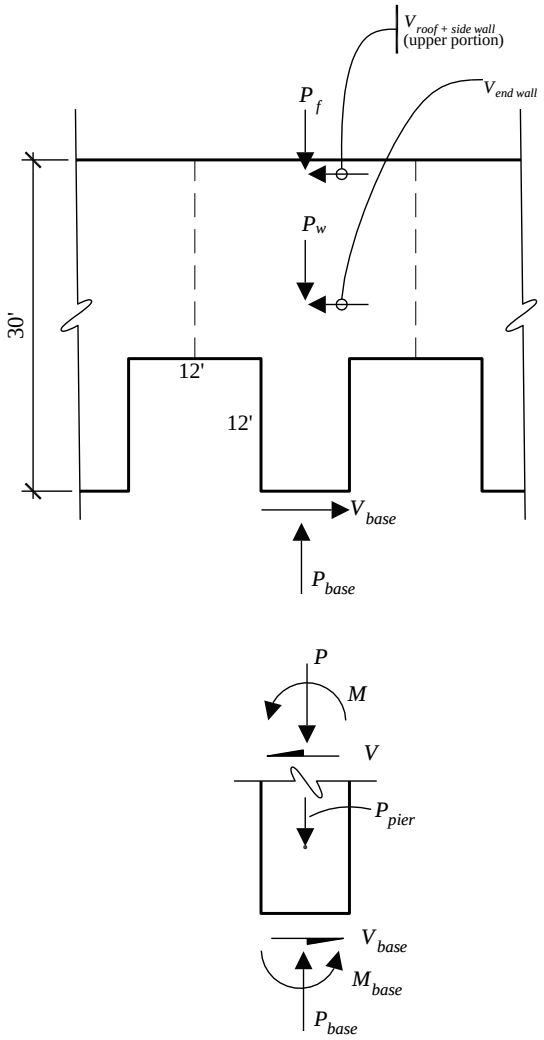

Figure 10.1-21 In-plane shear at end wall

10.1.6.6.1 Out-of-Plane Shear at End Wall Piers. For out-of-plane shear, see Figure 10.1-12. Shear at the top of wall is 15.3 kips/bay, and shear at the base of the pier is 10.3 kips/bay. From the RISA-2D analysis, which included *P-delta*, the shear at the head of the opening is 4.57 kips. The same multiplier of 2.5 for development of 125 percent of flexural capacity will be applied to out-of-plane shear resulting in 38.25 kips at the top of the wall, 11.4 kips at the head of the opening (top of pier) and 25.8 kips at the base of the pier.

Out-of-plane shear capacity is computed using the same equation. $\Sigma b_w d$ is taken as the net area A_n. Note that $M_u/V_u d_v$ is zero at the support because the moment is assumed to be zero; however, a few inches into the vertical span, $M_u/V_u d_v$ will exceed 1.0, so the limiting value of 1.0 is used here. This is typically the case where considering out-of-plane loads on a wall.

For computing shear capacity at the top of the wall:

$A_n = b_w d$ = ((8 in./2 ft) × 20 ft)(9.25 in.) = 740 in.^{2}

V_m = [4.0 - 1.75(1)](740 in.^{2})(0.0447 ksi) + (0.25)(0.614 × 8.0) = 75.7 kips/bay

ϕV_m = (0.8)(75.7) = 60.5 kips/bay

For computing shear capacity in the pier:

A_n = (8 in./cell)(12 cells)(9.25 in.) = 888 in.^{2}

V_m = [4.0 - 1.75(1)](888 in.^{2})(0.0447 ksi) + (0.25)(0.614 × 41.67) = 95.7 kips/bay

ϕV_m = (0.8)(95.7) = 76.6 kips/bay

At the top of wall:

$\phi V_n = \phi V_m$ = 60.5 kips/bay > 15.3 kips/bay = V_u OK

At the pier:

$\phi V_n = \phi V_m$ = 76.6 kips/bay > 10.3 kips/bay = V_u OK

10.1.7 In-Plane Deflection – End Walls

Deflection of the end wall (short wall) has two components as illustrated in Figure 10.1-22.

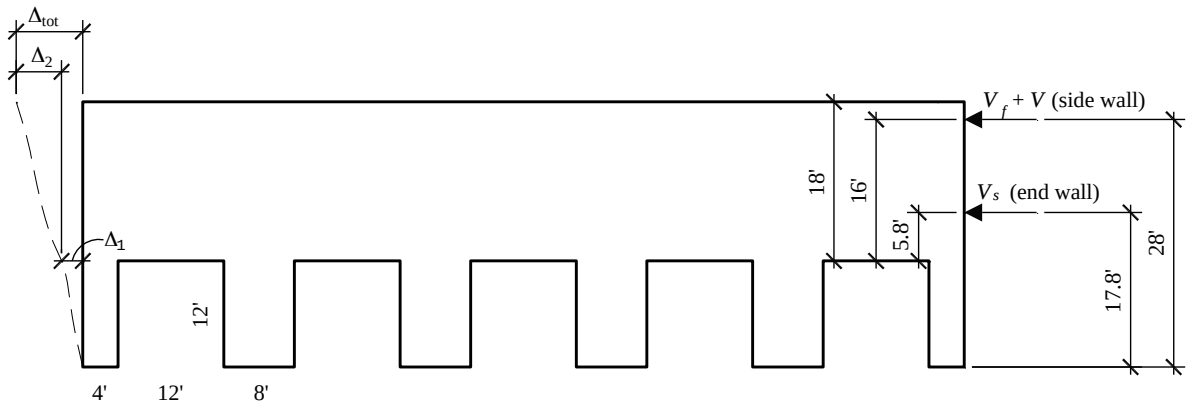

Figure 10.1-22 In-plane deflection of end wall
(1.0 ft = 0.3048 m)

As obtained from the RISA-2D analysis of the piers, $\Delta_1 = 0.047$ in.:

$$\Delta_2 = \sum \frac{\alpha VL}{AG}$$

where α is the form factor equal to 6/5 and:

$G = E_m/2(1 + \mu) = 1{,}800 \text{ ksi} / 2(1 + 0.15) = 782 \text{ ksi}$

$A = A_n$ = area of face shells + area of grouted cells

$= (100 \text{ ft} \times 12 \text{ in./ft} \times 2 \times 1.50 \text{ in.}^2) + (50)(8 \text{ in.})(8.63 \text{ in.}) = 7{,}050 \text{ in.}^2$

Note: Contribution to base shear of end walls (above the doors) is C_s (end wall weight) = (0.286)[(470 kips/2) - (103 psf)(5)(8 ft)(12 ft)] = 53 kips. Contribution to base shear of long walls plus roof is C_s (long wall + roof weight) = (0.286)[(400+418)/2] = 117 kips.

Therefore:

$$\Delta_2 = \left(\frac{6}{5}\right)\frac{(53)(5.8\times12)}{(7{,}050)(782)} + \left(\frac{6}{5}\right)\frac{(117)(16\times12)}{(7{,}050)(782)} = 0.0008 + 0.0049 = 0.006 \text{ in.}$$

and

$\Delta_{total} = C_d(0.047 + 0.006) = 3.5(0.053 \text{ in.}) = 0.19 \text{ in.} < 2.35 \text{ in.}$ OK

where $(2.35 = 0.007h_n = 0.01h_{sx})$ (TMS 402 Sec. 3.3.5.4).

Note that the drift limits for masonry structures are smaller than for other types of structure. It is possible to interpret *Standards* Table 12.12-1 to give a limit of $0.007h_n$ for this structure, but that limit also is easily satisfied. The real displacement in this structure is in the roof diaphragm; see Sec. 11.2.4.2.3.

10.1.8 Bond Beam – Side Walls (and End Walls)

Reinforcement for the bond beam located at the elevation of the roof diaphragm can be used for the diaphragm chord. The uniform lateral load for the design of the chord is the lateral load from the long wall plus the lateral load from the roof and is equal to 1.17 klf. The maximum tension in rebar is equal to the maximum moment divided by the diaphragm depth:

$$M = \frac{(1.17 \text{ klf})(200\text{ft})^2}{8} = 5{,}850 \text{ ft-kips}$$

M/d = 5,850 ft-kips/100 ft = 58.5 kips

The seismic load factor is 1.0. The required reinforcement is:

$A_{reqd} = T/\phi F_y$ = 58.5/(0.9)(60) = 1.081 in.^{2}

This will be satisfied by two #7 bars, A_s = (2 × 0.60 in.^{2}) = 1.20 in.^{2}

In Sec. 11.2.4.2.2, the diaphragm chord is designed as a wood member utilizing the wood ledger member. Using either the wood ledger or the bond beam is considered acceptable.

10.2 FIVE-STORY MASONRY RESIDENTIAL BUILDINGS IN BIRMINGHAM, ALABAMA; ALBUQUERQUE, NEW MEXICO; AND SAN RAFAEL, CALIFORNIA

10.2.1 Building Description

In plan, this five-story residential building has bearing walls at 24 feet on center (see Figures 10.2-1 and 10.2-2). All structural walls are of 8-inch-thick concrete masonry units (CMU). The floor is of 8-inch-thick hollow core precast, prestressed concrete planks. To demonstrate the incremental seismic requirements for masonry structures, the building is partially designed for four locations: two sites in Birmingham, Alabama; a site in Albuquerque, New Mexico; and a site in San Rafael, California. The two sites in Birmingham have been selected to illustrate the influence of different soil profiles at the same location. The building is designed for Site Classes C and E in Birmingham.

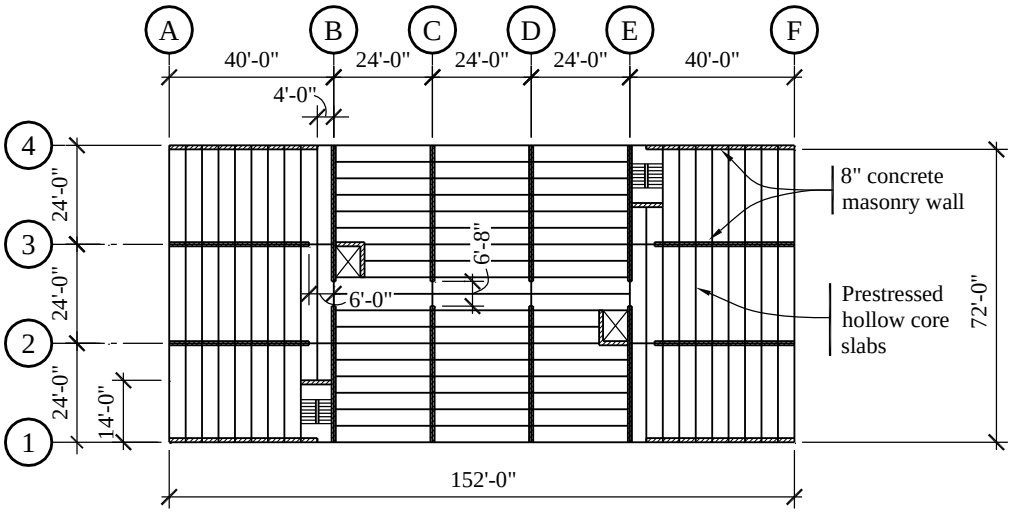

Figure 10.2-1 Typical floor plan
(1.0 in. = 25.4 mm, 1.0 ft = 0.3048 m)

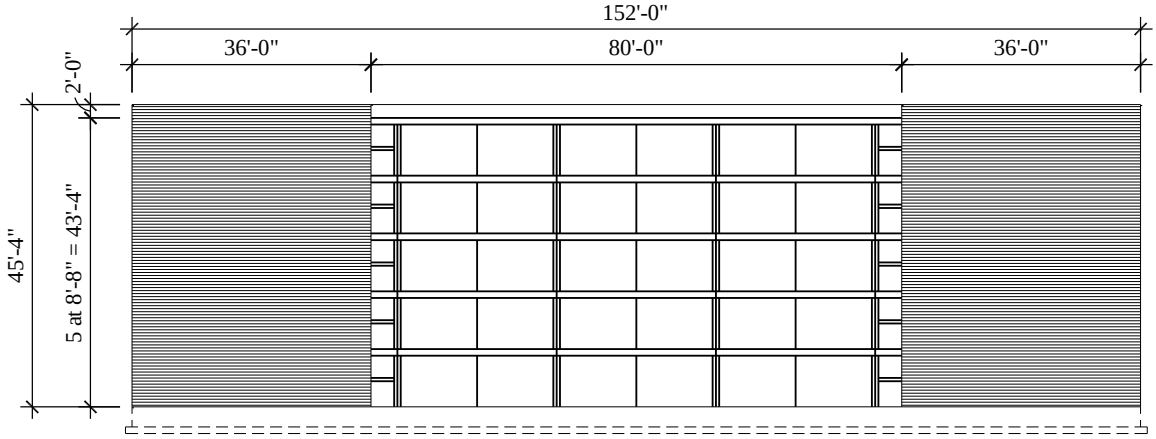

Figure 10.2-2 Building elevation
(1.0 in. = 25.4 mm, 1.0 ft = 0.3048 m)

For the Albuquerque and both Birmingham sites, it is assumed that shear friction reinforcement in the joints of the diaphragm planks is sufficient to resist seismic forces, so no topping is used. For the San Rafael site, a cast-in-place 2½-inch-thick reinforced lightweight concrete topping is applied to all floors. The structure is free of irregularities both in plan and elevation. ACI 318, Sections 21.1.1.6 and 21.11.1, require reinforced cast-in-place toppings as diaphragms in Seismic Design Category D and higher. Thus, the Birmingham example in Site Class E / Seismic Design Category D would require a topping, although that is not included in this example.

The design of an untopped diaphragm (for Seismic Design Categories A, B and C) is not addressed explicitly in ACI 318. The designs of both untopped and topped diaphragms for these buildings are

described in Chapter 8 of this volume using ACI 318 for the topped diaphragm in the San Rafael building. The *Provisions* provide guidance for the design of untopped precast plank diaphragms in Part 3, RP10.

For the purpose of determining the site class coefficient (*Standard* Sec. 11.4.2 and 20.3), a stiff soil profile with standard penetration test results of $15 < N < 50$ is assumed for the San Rafael site resulting in a Site Class D for this location. The Birmingham 1 and Albuquerque sites have soft rock with $N > 50$, resulting in Site Class C. The Birmingham 2 site has soft clay with $N < 15$, which results in Site Class E. The two Birmingham sites are presented to illustrate how different soil conditions at the same location (same seismicity) can result in different Seismic Design Categories. No foundations are designed in this example. The foundation systems are assumed to be able to carry the superstructure loads including the overturning moments.

The masonry walls in two perpendicular directions act as bearing and shear walls with different levels of axial loads. The geometry of the building in plan and elevation results in nearly equal lateral resistance in both directions. The walls are constructed of CMU and typically are minimally reinforced in all locations. Figure 10.2-3 illustrates the wall layout.

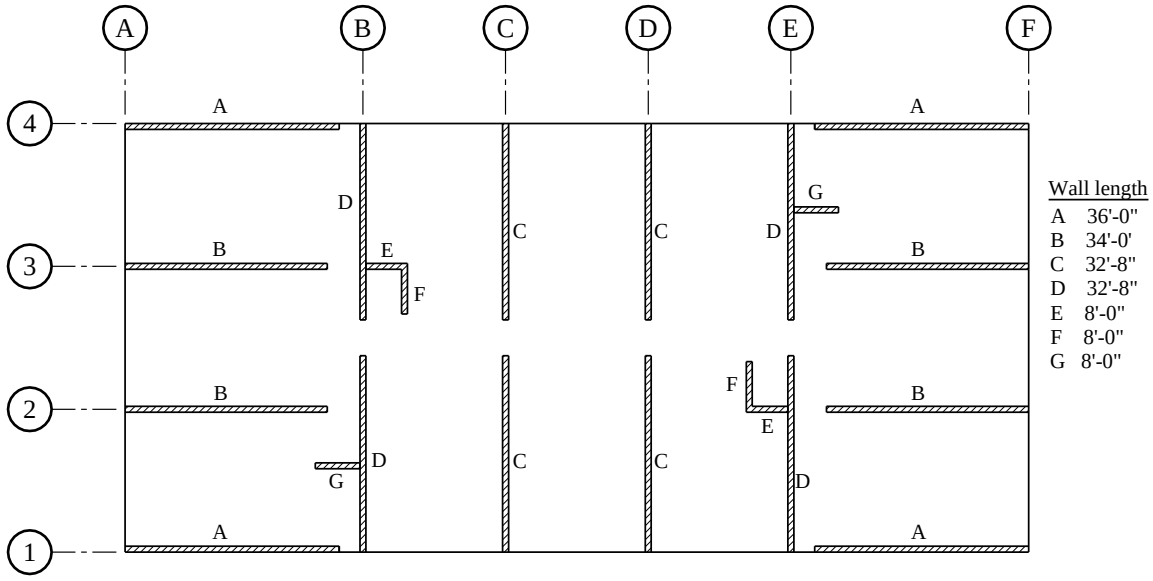

Figure 10.2-3 Plan of walls
(1.0 ft = 0.3048 m)

The floors serve as horizontal diaphragms distributing the seismic forces to the walls and are assumed to be stiff enough to be considered rigid. There is little information about the stiffness of untopped precast diaphragms. The design procedure in Section RP10 of Part 3 of the *Provisions* results in a diaphragm intended to remain below the elastic limit until the walls reach an upper bound estimate of strength; therefore, it appears that the assumption is reasonable.

Material properties are as follows:

- The compressive strength of masonry, f'_m, is taken as 2,000 psi, and the steel reinforcement has a yield limit of 60 ksi.

- The design snow load (on an exposed flat roof) is less than the roof live load for all locations.

This example covers the following aspects of a seismic design:

- Determining the equivalent lateral forces
- Design of selected masonry shear walls for their in-plane loads
- Computation of drifts

The story heights are small enough that the design of the masonry walls for out-of-plane forces is nearly trivial. In-plane response governs both the reinforcement in the wall and the connections to the diaphragms.

10.2.2 Design Requirements

10.2.2.1 Seismic parameters. The basic parameters affecting the design and detailing of the buildings are shown in Table 10.2-1. The Seismic Design Category for Birmingham 2 deserves special comment. The value of S_{DS} would imply a Seismic Design Category of C, while the value of S_{D1} would imply Seismic Design Category D, per Tables 11.6-1 and 11.6-2 of the *Standard*, where in Section 11.6 a provision permits the use of Table 11.6-1 alone if $T < 0.8\ S_{D1}/S_{DS}$ and the floor diaphragm is considered rigid or has a span of less than 40 feet. As will be shown for this building, $T_a = 0.338$ seconds and $0.8\ S_{D1}/S_{DS} = 0.446$. In the author's opinion, the untopped diaphragm may not be sufficiently rigid and thus Table 11.6-2 is considered, resulting in Seismic Design Category D.

10.2.2.2 Structural design considerations. The floors act as horizontal diaphragms, and the walls parallel to the motion act as shear walls for all four buildings.

The system is categorized as a bearing wall system (*Standard* Sec. 12.2). For Seismic Design Category D, the bearing wall system has a height limit of 160 feet and must comply with the requirements for special reinforced masonry shear walls. Note that the structural system is one of uncoupled shear walls. Crossing beams over the interior doorways (their design is not included in this example) will need to continue to support the gravity loads from the deck slabs above during the earthquake, but are not designed to provide coupling between the shear walls.

The building is symmetric and appears to be regular both in plan and elevation. It will be shown, however, that the building is torsionally irregular. *Standard* Table 12.6-1 permits use of the ELF procedure in accordance with *Standard* Section 12.8 for Birmingham 1 and Albuquerque (Seismic Design Categories B and C). By the same table, the Seismic Design Category D buildings (Birmingham 2 and San Rafael) must use a dynamic analysis for design. A careful reading of *Standard* Table 12.6-1 for Seismic Design Category D reveals that all of the rows do not apply to our building except the last, "all other structures"; thus, ELF analysis is not permitted, but modal analysis is permitted. For this particular building arrangement, it will be shown that the modal response spectrum analysis does not identify any particular effect of the horizontal torsional irregularity, as will be illustrated; thus it is the authors' opinion that ELF analysis would be sufficient.

Table 10.2-1 Design Parameters

Design Parameter	Value for Birmingham 1	Value for Birmingham 2	Value for Albuquerque	Value for San Rafael
S_s (Map 1)	0.266	0.266	0.456	1.5
S_1 (Map 2)	0.105	0.105	0.137	0.6
Site Class	C	E	C	D
F_a	1.2	2.45	1.2	1
F_v	1.7	3.49	1.66	1.5
$S_{MS} = F_a S_s$	0.32	0.65	0.55	1.5
$S_{M1} = F_v S_1$	0.18	0.37	0.23	0.9
$S_{DS} = 2/3\ S_{MS}$	0.21	0.43	0.37	1
$S_{D1} = 2/3\ S_{M1}$	0.12	0.24	0.15	0.6
Seismic Design Category	B	D	C	D
Diaphragm Topping req'd per ACI 318?	No	Yes*	No	Yes
Masonry Wall Type	Ordinary Reinforced	Special Reinforced	Intermediate Reinforced	Special Reinforced
Standard Design Coefficients (Table 12.2-1)				
R	2.0	5	3.5	5
Ω_0	2.5	2.5	2.5	2.5
C_d	1.75	3.5	2.25	3.5

*For this masonry example, Birmingham 2 is designed without topping on the precast planks. It is assumed that the precast planks at floors and roof have connections sufficiently rigid to permit the idealization of rigid horizontal diaphragms.

The type of masonry shear wall is selected to illustrate the various requirements as well as to satisfy Table 12.2-1 of the *Standard*. Note that "Ordinary Reinforced Masonry Shear Walls" could be used for Seismic Design Category C at this height.

The orthogonal direction of loading combination requirement (*Standard* Sec. 12.5) needs to be considered for structures assigned to Seismic Design Category D. However, the arrangement of this building is not particularly susceptible to orthogonal effects; the walls are not subject to axial force from horizontal seismic motions, only bending and shear.

The walls are all solid, and there are no significant discontinuities, as defined by *Standard* Section 12.3.2.2, in the vertical elements of the seismic force-resisting system.

Ignoring the short walls at stairs and elevators, there are eight shear walls in each direction; therefore, the system appears to have adequate redundancy (*Standard* Sec. 12.3.4.2). The redundancy factor, however, will be computed.

Tie and continuity requirements (*Standard* Sec. 12.11) must be addressed when detailing connections between floors and walls (see Chapter 8 of this volume).

Nonstructural elements (*Standard* Chapter 13) are not considered in this example.

Collector elements are required in the diaphragm for longitudinal response (*Standard* Sec. 12.10). Rebar in the longitudinal direction, spliced into bond beams, is used for this purpose (see Chapter 8 of this volume).

Diaphragms must be designed for the required forces (*Standard* Sec. 12.10 and *Provisions* Part 3, Sec. RP10).

The structural walls must be designed for the required out-of-plane seismic forces (*Standard* Sec. 12.11) in addition to out-of-plane wind on exterior walls and 5 psf differential air pressure on interior walls.

Each wall acts as a vertical cantilever in resisting in-plane forces. The walls are classified as masonry cantilever shear wall structures in *Standard* Table 12.12-1, which limits story drift to 0.01 times the story height.

10.2.3 Load Combinations

The basic load combinations are those in *Standard* Section 2.3.2. The seismic load effect, E, is defined by *Standard* Section 12.4, as follows:

$$E = E_h + E_v = \rho Q_E \pm 0.2 S_{DS} D$$

10.2.3.1 Redundancy Factor. The Redundancy Factor, ρ, is a multiplier on design force effects and applies only to the in-plane direction of the shear walls. For structures in Seismic Design Categories A, B and C, $\rho = 1.0$ (*Standard* Sec. 12.3.4.1). For structures in Seismic Design Category D, ρ is determined per *Standard* Section 12.3.4.2.

For a shear wall building assigned to Seismic Design Category D, $\rho = 1.0$ as long as it can be shown that failure of a shear wall or pier with a height-to-length ratio greater than 1.0 would not result in more than a 33 percent reduction in story strength or create an extreme torsional irregularity. The intent is that the aspect ratio is based on story height, not total height.

$$\frac{\text{height}}{\text{length}} = \frac{8'}{32.67'} = 0.24 < 1.0$$

Because no walls have a ratio exceeding 1.0, none have to be removed to check for redundancy and $\rho = 1.0$. If one were to consider the removal of one shear wall in either direction, 1/8 or 12.5 percent resistance would be removed. 12.5% < 33%, so $\rho = 1.0$. Therefore, for this example, the redundancy factor is 1.0 for the buildings assigned to Seismic Design Category D.

10.2.3.2 Combination of load effects. The seismic load effect, E, determined for each of the buildings is as follows:

Birmingham 1: $E = (1.0)Q_E \pm (0.2)(0.21)D = Q_E \pm 0.04D$

Birmingham 2: $E = (1.0)Q_E \pm (0.2)(0.43)D = Q_E \pm 0.09D$

Albuquerque: $E = (1.0)Q_E \pm (0.2)(0.37)D = Q_E \pm 0.07D$

San Rafael: $E = (1.0)Q_E \pm (0.2)(1.00)D = Q_E \pm 0.20D$

The applicable load combinations from *Standard* Sections 2.3.2 and 12.4.2.3 are:

$1.2D + 1.0E + 0.5L + 0.2S$

where the effects of gravity and seismic loads are additive, and

$0.9D + 1.0E + 1.6H$

where the effects of gravity and seismic loads are counteractive. H is the effect of lateral pressures of soil and water in soil. The 0.5 factor on L is because $L_0 < 100$ psf for these residential buildings. Per the *Standard,* corridors are "same as occupancy served", except for the first floor.

Load effect H does not apply for this design, and the snow load effect, S, does not exceed the minimum roof live load at any of the buildings. Consideration of snow loads is not required in the effective seismic weight, W, of the structure where the design snow load does not exceed 30 psf (*Standard* Sec. 12.7.2).

The basic load combinations are combined with E as determined above, and the load combinations representing the extreme cases are as follows:

Birmingham 1: $1.24D + Q_E + 0.5L$
$0.86D - Q_E$

Birmingham 2: $1.29D + Q_E + 0.5L$
$0.81D - Q_E$

Albuquerque: $1.27D + Q_E + 0.5L + 0.2S$
$0.83D - Q_E$

San Rafael: $1.40D + Q_E + 0.5L$
$0.70D - Q_E$

These combinations are for the in-plane direction. Load combinations for the out-of-plane direction are similar except that the redundancy factor (1.0 in all cases for in-plane loading) is not applicable.

10.2.4 Seismic Design for Birmingham 1

10.2.4.1 Birmingham 1 weights. This site is assigned to Seismic Design Category B, and the walls are designed as ordinary reinforced masonry shear walls (*Standard* Table 12.2-1), which stipulates that the minimum reinforcement requirements of TMS 402 Section 1.17.3.2.3.1 be followed. Given the length of the walls, vertical reinforcement of #4 bars at 8 feet on center works well for detailing reasons and will be used here (10 feet is the maximum spacing per TMS 402). For this example, 45 psf will be used for the 8-inch-thick lightweight CMU walls. The 45 psf value includes grouted cells, as well as bond beams in the course just below the floor planks.

67 psf is used for 8-inch-thick, normal-weight hollow core plank plus the non-masonry partitions. 67 psf is also used for the roof plank plus roofing.

Story weight, w_i, is computed as follows.

For the roof:

Roof slab (plus roofing) = (67 psf) (152 ft)(72 ft) = 733 kips

Walls = (45 psf)(589 ft)(8.67 ft/2) + (45 psf)(4)(36 ft)(2 ft) = 128 kips

Total = 861 kips

Note that there is a 2-foot-high masonry parapet on four walls and the total length of masonry wall, including the short walls not used in the seismic force-resisting system, is 589 feet.

For a typical floor:

Slab (plus partitions) = 733 kips

Walls = (45 psf)(589 ft)(8.67 ft) = 230 kips

Total = 963 kips

Total effective seismic weight, W = 861 + (4)(963) = 4,713 kips.

This total excludes the lower half of the first story walls, which do not contribute to seismic loads that are imposed on CMU shear walls.

10.2.4.2 Birmingham 1 base shear calculation. The seismic response coefficient, C_s, is computed using *Standard* Section 12.8.

Per *Standard* Equation 12.8-2:

$$C_s = \frac{S_{DS}}{R/I} = \frac{0.21}{2/1} = 0.105$$

The value of C_s need not be greater than *Standard* Equation 12.8-3:

$$C_s = \frac{S_{D1}}{T(R/I)} = \frac{0.12}{0.338\left(2/1\right)} = 0.178$$

where T is the fundamental period of the building approximated per *Standard* Equation 12.8-7 as follows:

$$T_a = C_t h_n^x = (0.02)(43.33^{0.75}) = 0.338 \text{ sec}$$

where C_t = 0.02 and x = 0.75 are from *Standard* Table 12.8-2 (the approximate period, based on building system and building height, is the same for all locations).

The value for C_s is taken as 0.105 (the lesser of the two computed values). This value is larger than the minimum specified in *Standard* Equation 12.8-5 (Sup. 2):

$$C_s = 0.044 I S_{DS} \geq 0.010$$

$$= (0.044)(1.0)(0.21) = 0.00924 = 0.010 \qquad \text{(0.105 controls)}$$

The total seismic base shear is then calculated using *Standard* Equation 12.8-1 as follows:

$V = C_s W = (0.105)(4{,}713) = 495$ kips

10.2.4.3 Birmingham 1 vertical distribution of seismic forces. *Standard* Section 12.8.3 stipulates the procedure for determining the portion of the total seismic load assigned to each floor level. The story force, F_x, is calculated using *Standard* Equations 12.8-11 and 12.8-12 as follows:

$$F_x = C_{vx} V$$

and

$$C_{vx} = \frac{w_x h_x^k}{\sum_{i=1}^{n} w_i h_i^k}$$

where C_{vx} is a vertical distribution factor which has the effect of distributing more of the base shear to the upper levels to mimic the dynamic response of the structure.

For $T = 0.338$ sec < 0.5 sec, $k = 1.0$.

The seismic design shear in any story is determined from *Standard* Equation 12.8-13:

$$V_x = \sum_{i=x}^{n} F_i$$

Although not specified in the *Standard* or used in design, story overturning moment may be computed using the following equation:

$$M_x = \sum_{i=x}^{n} F_i (h_i - h_x)$$

The application of these equations for this building is shown in Table 10.2-2.

Table 10.2-2 Birmingham 1 Seismic Forces and Moments (i.e., Seismic Demand) by Level

Level x	w_x (kips)	h_x (ft)	$w_x h_x^k$ (ft-kips)	C_{vx}	F_x (kips)	V_x (kips)	$M_{(x-1)}$ (ft-kips)
5	861	43.34	37,310	0.3089	153	153	1,326
4	963	34.67	33,384	0.2764	137	290	3,840
3	963	26.00	25,038	0.2073	103	393	7,245
2	963	17.33	16,692	0.1382	68	461	11,240
1	963	8.67	8,346	0.0691	34	495	15,530
$\sum$	4,715		120,770	1.0000	495		

1.0 kips = 4.45 kN, 1.0 ft = 0.3048 m.

Note that F_x, V_x and M_x are all factored loads.

A note regarding locations of V and M: the vertical weight at the roof (fifth level), which includes the upper half of the wall above the fifth floor (fourth level), produces an inertial force that contributes to the shear, V, the walls supporting the fifth level. That shear in turn generates a moment that increases towards the level below (fourth level). Resisting this moment is the rebar in the wall combined with the wall weight above the fourth level. The story overturning moment is tabulated for the level below the level that receives the story force. This is illustrated in Figure 10.2-4.

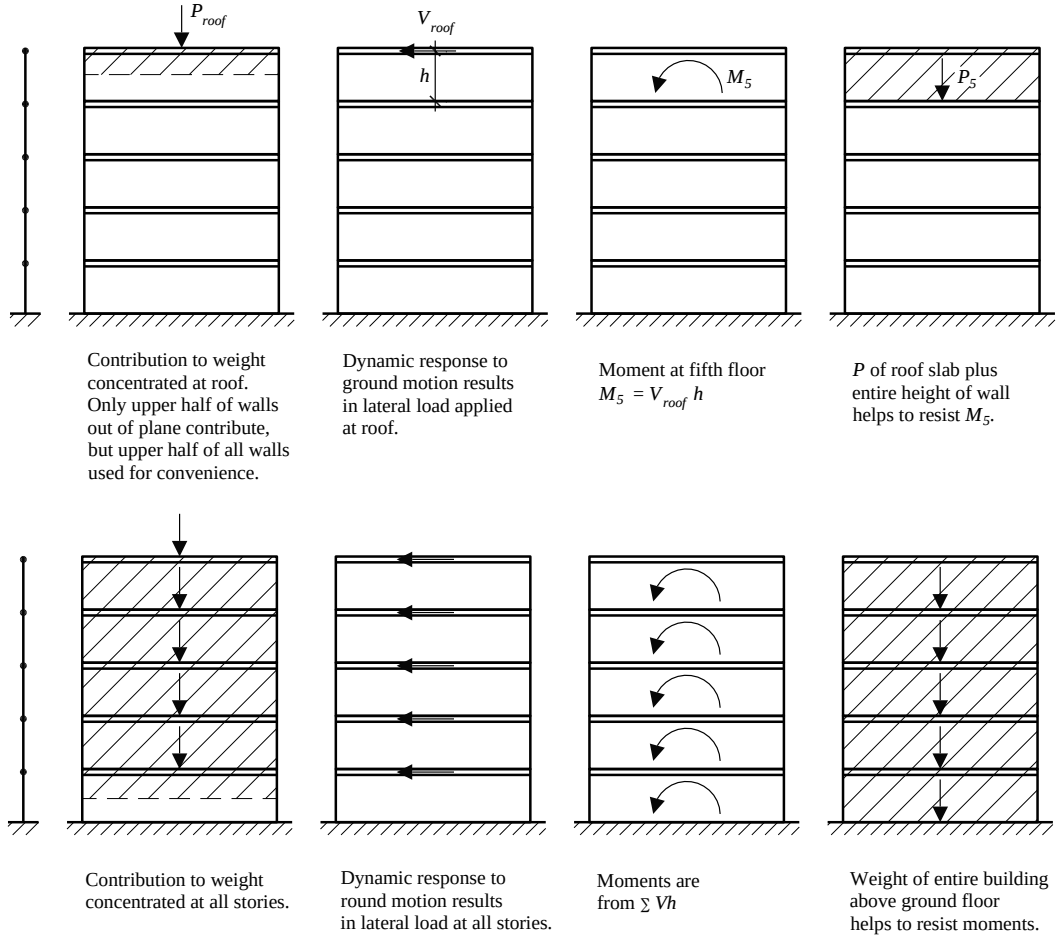

Figure 10.2-4 Location of moments due to story shears

10.2.4.4 Birmingham 1 horizontal distribution of forces. The wall lengths are shown in Figure 10.2-3. The initial grouting pattern is essentially the same for Walls A, B, C and D. Because of a low relative stiffness, the effects Walls E, F and G are ignored in this analysis. Walls A, B, C and D are so nearly the same length that their stiffnesses are assumed to be the same for this example.

Torsion is considered according to *Standard* Section 12.8.4. For a symmetric plan, as in this example, the only torsion to be considered is the accidental torsion, M_{ta}, caused by an assumed eccentricity of the mass each way from its actual location by a distance equal to 5 percent of the dimension of the structure perpendicular to the direction of the applied loads.

Dynamic amplification of the torsion need not be considered for Seismic Design Category B per *Standard* Section 12.8.4.3.

For this example, the building is analyzed in the transverse direction only. The evaluation of Wall D is selected for this example. The rigid diaphragm distributes the lateral forces into walls in both directions. Two components of force must be considered: direct shear and shear induced by torsion.

The direct shear force carried by each Wall D is one-eighth of the total story shear (eight equal walls). The torsional moment per *Standard* Section 12.8.4.2 is as follows:

$$M_{ta} = 0.05bV_x = (0.05)(152 \text{ ft})V_x = 7.6V_x$$

The torsional force per wall, V_t, is:

$$V_t = \frac{M_t Kd}{\sum Kd^2}$$

where K is the stiffness (rigidity) of each wall. Note that all the walls in both directions are included.

Because all the walls in this example are assumed to be equally long, then they are equally stiff:

$$V_t = M_t \left[\frac{d}{\sum d^2} \right]$$

where d is the distance from each wall to the center of twisting.

$$\sum d^2 = 4(36)^2 + 4(12)^2 + 4(36)^2 + 4(12)^2 = 11{,}520 \text{ ft}^2$$

The maximum torsional shear force in Wall D, therefore, is:

$$V_t = \frac{(7.6V)(36 \text{ ft})}{11{,}520 \text{ ft}^2} = 0.0238V$$

The total shear in Wall D is:

$$V_{tot} = 0.125V + 0.0238V = 0.149V$$

The total story shear and overturning moment may now be distributed to Wall D and the wall proportions checked. The wall capacity is checked before considering deflections.

10.2.4.5 Birmingham 1 transverse wall (Wall D). The *Provisions* and the *Standard* define the seismic load as a strength or limit state design level effect. TMS 402 Chapter 3 defines strength design for

masonry. Strength design of masonry, as defined in TMS 402, is illustrated here. It is also permissible to use the allowable stress design method of TMS 402 by factoring the seismic load effects, but that will not be illustrated here.

The required strength is derived from the load combinations defined previously.

10.2.4.5.1 Birmingham 1 shear strength. TMS 402 Section 3.1.3 states that the design strength must be greater than the required strength. The design strength is equal to the nominal strength times a strength-reduction factor:

$$V_u \leq \phi V_n$$

The strength reduction factor, ϕ, is 0.8 (TMS 402 Sec. 3.1.4.3).

The nominal shear strength, V_n, is:

$$V_n = V_{nm} + V_{ns}$$

Likewise:

$$\phi V_n = \phi(V_{nm} + V_{ns})$$

The shear strength provided by masonry (TMS 402 Sec. 3.3.4.1.2.1) is as follows:

$$V_{nm} = \left[4.0 - 1.75\left(\frac{M_u}{V_u d_v}\right)\right] A_n \sqrt{f'_m} + 0.25\, P_u$$

For grouted cells at 8 feet on center:

A_n = (2 × 1.25 in. × 32.67 ft × 12 in./ft) + (8 in. × 5.13 in. × 5 cells) = 1,185 in.^{2}

The shear strength provided by reinforcement (given by TMS 402 Sec. 3.3.4.1.2.3) is as follows:

$$V_{ns} = 0.5\left(\frac{A_v}{s}\right) F_y d_v$$

The wall will have a bond beam with two #4 bars at each story to bear the precast floor planks and wire joint reinforcement at alternating courses. Common joint reinforcement with 9-gauge wires at each face shell will be used; each wire has a cross-sectional area of 0.017 in.^{2}. With six courses of joint reinforcement and two #4 bars, the total area per story is 0.60 in.^{2} or 0.07 in.^{2}/ft. Given that the story height is less than half the wall length, the authors believe that it is acceptable to treat the distribution of horizontal reinforcement as if being uniformly distributed for shear resistance.

V_{ns} = 0.5(0.07 in.^{2}/ft)(60 ksi)(32.67 ft) = 68.3 kips

The maximum nominal shear strength of the member (Wall D in this case) for $M/Vd_v > 1.00$ is given by TMS 402 Section 3.3.4.1.2.1:

$$V_n(\max) = 4A_n\sqrt{f'_m}$$

The coefficient 4 becomes 6 for $M/Vd_v < 0.25$ (TMS 402 Sec. 3.3.4.1.2a). Interpolation between yields the following:

$$V_n\ (\max) = \left(6.67 - 2.67\left(\frac{M_u}{V_u d_v}\right)\right)A_n\sqrt{f'_m}$$

The shear strength of Wall D, based on the equations listed above, is summarized in Table 10.2-3. Note that V_x and M_x in this table are values from Table 10.2-2 multiplied by 0.149 (which represents the portion of direct and torsional shear assigned to Wall D). P_u is the dead load of the roof or floor times the tributary area for Wall D, taken as 0.86*D* for the minimum (conservative) P_u. (Note that there is a small load from the floor plank parallel to the wall.)

Table 10.2-3 Shear Strength Calculations for Birmingham 1 Wall D

Story	V_x (kips)	M_x (ft-kips)	$M_x/V_x d_v$	$V_u = V_x$ (kips)	P_u (kips)	V_{nm} (kips)	V_{ns} (kips)	V_n (kips)	V_n (*max*) (kips)	ϕV_n (kips)
5	22.8	198	0.266	22.8	35.3	196	68	**264**	316	211
4	43.2	572	0.405	43.2	76.5	193	68	**261**	296	209
3	58.6	1080	0.564	58.6	118	189	68	**257**	274	206
2	68.7	1675	0.746	68.7	158	182	68	250	**248**	198
1	73.8	2314	0.960	73.8	200	173	68	241	**218**	174

1.0 kip = 4.45 kN, 1.0 ft-kip = 1.36 kN-m.

Values shown in **bold** are the controlling values for V_n

For all levels, $\phi V_n > V_u$, so it is OK for this Ordinary Reinforced Masonry Shear Wall.

10.2.4.5.2 Birmingham 1 axial and flexural strength. All the walls in this example are bearing shear walls since they support vertical loads as well as lateral forces. In-plane calculations include:

- Strength check
- Ductility check

10.2.4.5.2.1 Strength check. The wall demands, using the load combinations determined previously, are presented in Table 9.2-4 for Wall D. In the table, Load Combination 1 is 1.245*D* + Q_E + 0.5*L* and Load Combination 2 is 0.86D + Q_E.

Table 10.2-4 Demands for Birmingham 1 Wall D

Story	P_D (kips)	P_L (kips)	Load Combination 1		Load Combination 2	
			P_u (kips)	M_u (ft-kips)	P_u (kips)	M_u (ft-kips)
5	49	0	61	198	42	198
4	98	15	129	572	84	572
3	147	25	195	1,080	126	1,080
2	196	34	260	1,675	168	1,675
1	245	41	324	2,314	210	2,314

1.0 kip = 4.45 kN, 1.0 ft-kip = 1.36 kN-m.

P_D and P_L are based on floor tributary area of 540 ft^2. P_L has been reduced per *Standard* Section 4.8 using $K_{LL} = 2$.

Strength at the bottom story (where P, V and M are the greatest) is examined here. (For a real design, all levels should be examined). As will be shown, Load Combination 2 from Table 10.2-4 is the controlling case because it has the same lateral load as Load Combination 1, but with lower values of axial force.

For the base of the shear walls:

$P_{u_{min}} = 210$ kips

$P_{u_{max}} = 324$ kips

$M_u = 2{,}314$ ft-kips

Try one #4 bar in each end cell and a #4 bar at 8 feet on center for the interior cells. A curve of ϕP_n - ϕM_n , representing the wall strength envelope, are developed and used to evaluate P_u and M_u determined above. Three cases are analyzed and their results are used in plotting the ϕP_n - ϕM_n curve.

In accordance with TMS 402 Section 3.3.2, the strength of the section is reached as the compressive strains in masonry reach their maximum usable value of 0.0025 for CMU. The force equilibrium in the section is attained by assuming an equivalent rectangular stress block of $0.8f'_m$ over an effective depth of $0.8c$, where c is the distance of the neutral axis from the fibers of maximum compressive strain. Stress in all steel bars is taken into account. The strains in the bars are proportional to their distance from the neutral axis. For strains above yield, the stress is independent of strain and is taken as equal to the specified yield strength, F_y. See Figure 10.2-5 for strains and stresses for all three cases selected.

Case 1 ($P = 0$)

Assume all tension bars yield (which can be verified later):

$T_{s1} = (0.20 \text{ in.}^2)(60 \text{ ksi}) = 12.0$ kips

$T_{s2} = (0.20 \text{ in.}^2)(60 \text{ ksi}) = 12.0$ kips each

Because the neutral axis is close to the compression end of the wall, compression steel, C_{s1}, is neglected (it would make little difference anyway) for Case 1:

$\Sigma F_y = 0$:

$C_m = \Sigma T$

$C_m = (4)(12.0) = 48.0$ kips

The compression block is entirely within the first grouted cell:

$C_m = 0.8\, f'_m ab$

$48.0 = (0.8)(2.0 \text{ ksi})a(7.625 \text{ in})$

$a = 3.9$ in. $= 0.33$ ft

$c = a/0.8 = 0.33/0.8 = 0.41$ ft

Thus, the neutral axis is determined to be 0.41 feet from the compression end on the wall, which is within the first grouted cell:

$\Sigma M_{cl} = 0$: (The math is a little easier if moments are taken about the wall centerline.)

$M_n = (16.33\text{-}0.33/2 \text{ ft})C_m + (16.00 \text{ ft})T_{s1} + (0.00 \text{ ft})\Sigma T_{s2} + (0.00 \text{ ft})P_n$

$M_n = (16.17)(48.0) + (16.00)(12) + 0 + 0 = 968$ ft-kips

$\phi M_n = (0.9)(968) = 871$ ft-kips

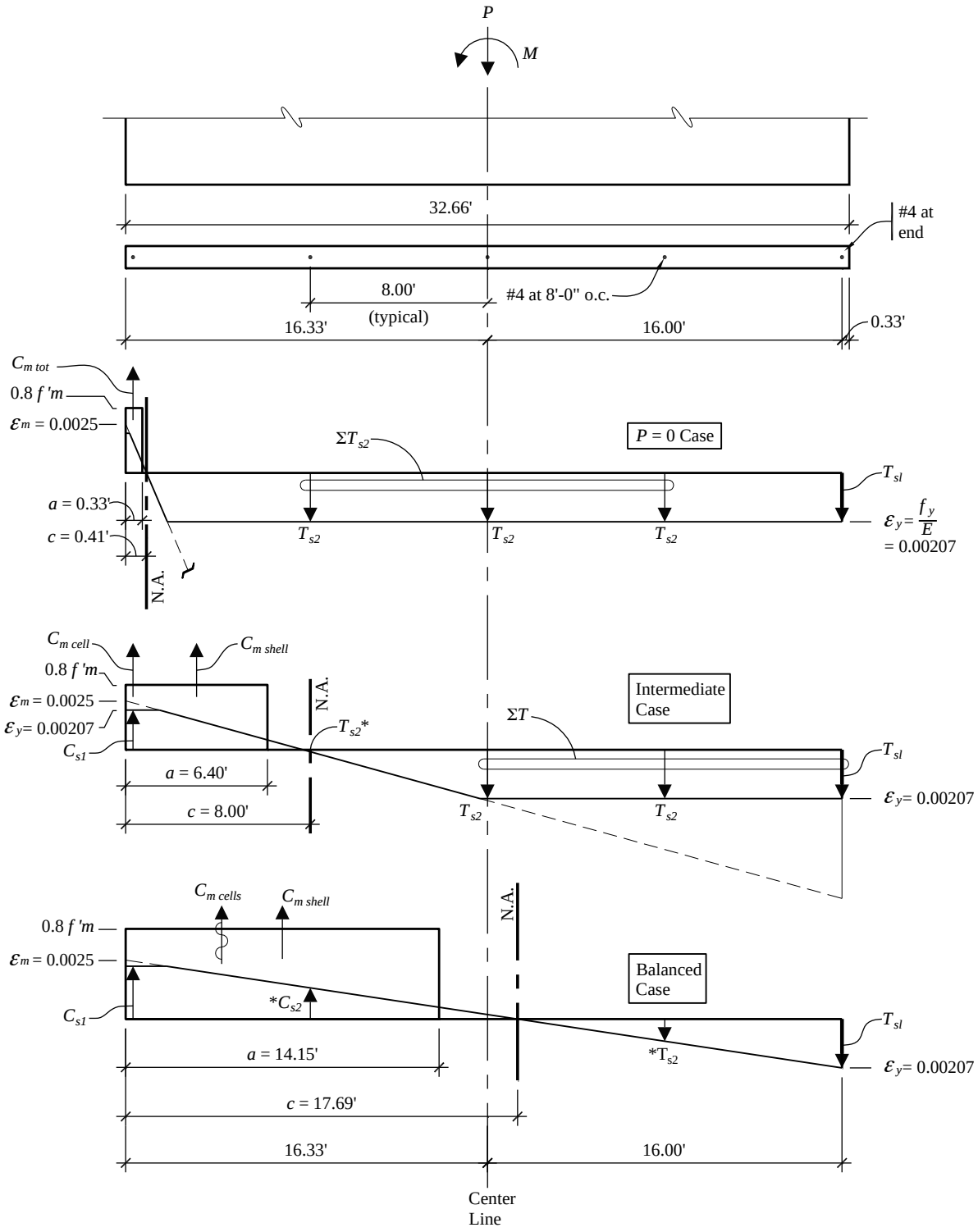

Figure 10.2-5 Strength of Birmingham 1 Wall D.
Strain diagram superimposed on strength diagram for the three cases.
*The low force in the selected reinforcement is neglected in the calculations.
(1.0 ft = 0.3048 m)

To summarize, Case 1:

ϕP_n = 0 kips

ϕM_n = 871 ft-kips

Case 2 (Intermediate case between P = 0 and P_{bal})

Let c = 8.00 feet (this is an arbitrary selection). Thus, the neutral axis is defined at 8 feet from the compression end of the wall:

$a = 0.8c = (0.8)(8.00) = 6.40$ ft

$C_{m\ shells} = 0.8f'_m(2\text{ shells})(1.25\text{ in. / shell})(6.40\text{ ft }(12\text{ in./ft}) = 307.2$ kips

$C_{m\ cells} = 0.8\ f'_m(41\text{ in.}^2) = 65.6$ kips

$C_{m\ tot} = C_{m\ shells} + C_{m\ cells} = 307.2 + 65.6 = 373$ kips

$C_{s1} = (0.20\text{ in.}^2)(60\text{ ksi}) = 12$ kips (Compression steel is included in this case.)

$T_{s1} = (0.20\text{ in.}^2)(60\text{ ksi}) = 12$ kips

$T_{s2} = (0.20\text{ in.}^2)(60\text{ ksi}) = 12$ kips each

Some authorities would interpret TMS 402 Section 3.1.8.3 to mean the compression resistance of reinforcing steel that is not enclosed within ties be neglected. The TMS 402 Commentary 3.3.3.5 allows inclusion of compression in the reinforcement where the maximum amount of reinforcement is limited to promote flexural ductility. The authors have chosen to follow the more specific example of the commentary. The difference in flexural resistance is not significant, but the difference for the maximum reinforcement requirement (i.e., ductility requirement) can be significant.

$\Sigma F_y = 0$:

$C_{m\ tot} + C_{s1} = P_n + T_{s1} + \Sigma T_{s2}$

$373 + 12 = P_n + (3)(12.0)$

$P_n = 349$ kips

$\phi P_n = (0.9)(349) = 314$ kips

$\Sigma M_{cl} = 0$:

$M_n = (13.13\text{ ft})C_{m\ shell} + (16.00\text{ ft})(C_{m\ cell} + C_{s1}) + (16.00\text{ ft})T_{s1} + (8.00\text{ ft})T_{s2}$

$M_n = (13.13)(307.2) + (16.00)(65.6 + 12) + (16.00)(12.0) + (8.00\text{ ft})(12.0) = 5{,}563$ ft-kips

ϕM_n = (0.9)(5,563) = 5,007 ft-kips

To summarize Case 2:

ϕP_n = 314 kips

ϕM_n = 5,007 ft-kips

Case 3 (Balanced case)

In this case, T_{s1} just reaches its yield stress:

$$c = \left[\frac{0.0025}{(0.0025 + 0.00207)}\right](32.33 \text{ ft}) = 17.69 \text{ ft}$$

$a = 0.8c$ = (0.8)(17.69) = 14.15 ft

$C_{m\ shells} = 0.8f'_m$(2 shells)(1.25 in./shell)(14.15 ft) (12 in./ft) = 679.2 kips

$C_{m\ cells} = 0.8f'_m$(2 cells)(41 in.^{2}/cell) = 131.2 kips

$C_{m\ tot} = C_{m\ shells} + C_{m\ cells}$ = 810.4 kips

C_{s1} = (0.20 in.^{2})(60 ksi) = 12.0 kips

T_{s1} = (0.20 in.^{2})(60 ksi) = 12.0 kips

C_{s2} and T_{s2} are neglected because they are small.

$\Sigma F_y = 0$:

$P_n = \Sigma C - \Sigma T$

$P_n = C_{m\ tot} + C_{s1} - T_{s1}$ = 810.4 + 12.0 - 12.0 = 810.4 kips

ϕP_n = (0.9)(810.4) = 729 kips

$\Sigma M_{cl} = 0$:

$M_n = 9.26\ C_{m\ shells} + ((16 + 8)/2)\ C_{m\ cells} + 16\ C_{s1} + 16\ T_{s1}$

M_n = (9.26)(679.2) + (12.0)(131.2) + (16.00)(12.0) + (16.0)(12.0) = 8,248 kips

ϕM_n = (0.9)(8,248) = 7,423 ft-kips

To summarize Case 3:

ϕP_n = 729 kips

ϕM_n = 7,423 ft-kips

Using the results from the three cases above, the ϕP_n - ϕM_n curve shown in Figure 10.2-6 is plotted. Although the portion of the ϕP_n - ϕM_n curve above the balanced failure point could be determined, it is not necessary here. Thus, only the portion of the curve below the balance point is examined. This is the region of high moment capacity.

Similar to reinforced concrete beam-columns, in-plane compression failure of the cantilevered shear wall will occur if $P_u > P_{bal}$ and yield of tension steel will occur first if $P_u < P_{bal}$. A ductile failure mode is essential to the design, so the portion of the curve above the "balance point" is not useable. In fact, the ductility (maximum reinforcement) requirement prevents P_u from approaching P_{bal}.

As can be seen, the points for ($P_{u\ min}$, M_u) and ($P_{u\ max}$, M_u) are within the ϕP_n - ϕM_n envelope; thus, the strength design is acceptable with the minimum reinforcement. Figure 10.2-6 shows two schemes for determining the design flexural resistance for a given axial load. One interpolates along the straight line between pure bending and the balanced load. The second makes use of intermediate points for interpolation. This particular example illustrates that there can be a significant difference in the interpolated moment capacity between the two schemes for axial loads midway between the balanced load and pure bending.

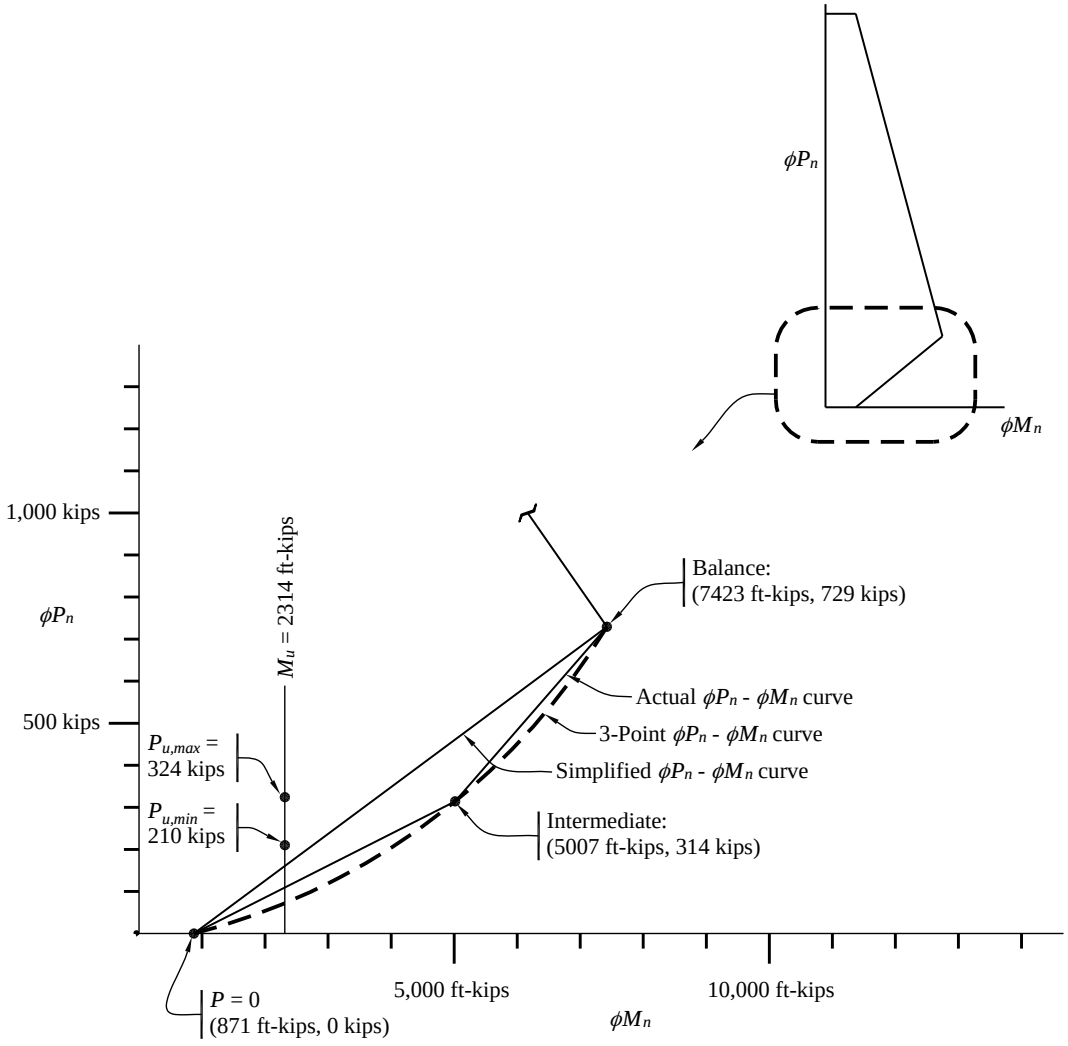

Figure 10.2-6 ϕP_n - ϕM_n Diagram for Birmingham 1 Wall D
(1.0 kip = 4.45 kN, 1.0 ft-kip = 1.36 kN-m)

10.2.4.5.3 Ductility check. For this case, with $M_u/V_u d_v < 1$ and $R > 1.5$, TMS 402 Section 3.3.3.5.4 refers to Section 3.3.3.5.1, which stipulates that the critical strain condition correspond to a strain in the extreme tension reinforcement equal to 1.5 times the strain associated with F_y. This calculation uses unfactored gravity loads. Refer to Figure 10.2-7 and the following calculations which illustrate this use of loads at the bottom story (highest axial loads). Calculations for other stories are not presented in this example.

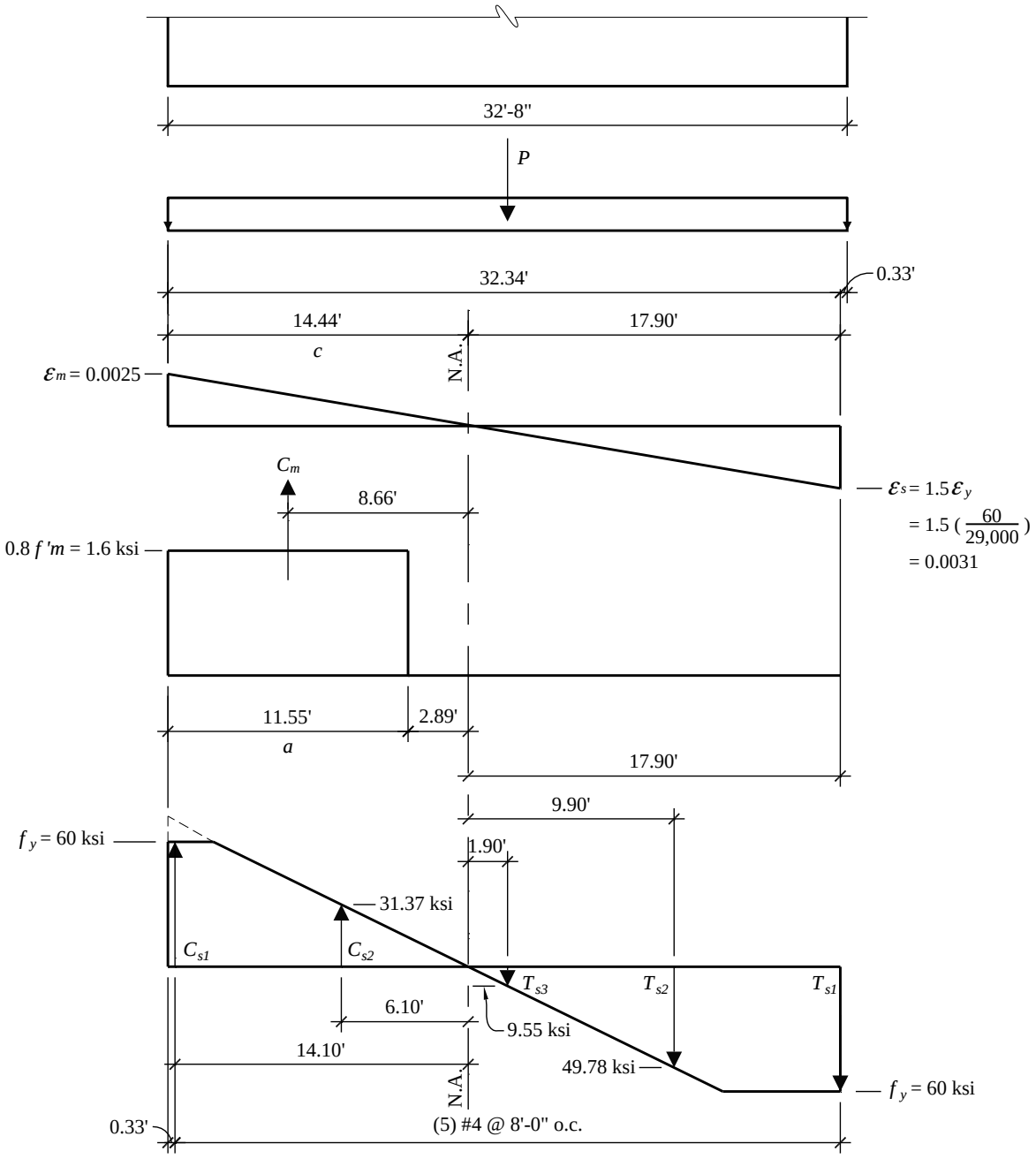

Figure 10.2-7 Ductility check for Birmingham 1 Wall D
(1.0 ft = 0.3048 m, 1.0 ksi = 6.89 MPa)

For Level 1 (bottom story), the unfactored axial loads are:

P = 245 kips

Refer to Figure 10.2-7:

$C_m = 0.8\ f'_m(ab + 2A_{cell}) = (1.6\text{ ksi})[(0.8 \times 14.44\text{ ft} \times 12\text{ in./ft})(2)(1.25\text{ in.}) + (2)(41\text{ in.}^2)] = 686\text{ kips}$

$C_{s1} = F_y A_s = (60\text{ ksi})(0.20\text{ in.}^2) = 12.0\text{ kips}$

$C_{s2} = (31.37\text{ ksi})(0.20\text{ in.}^2) = 6.3\text{ kips}$

$T_{s1} = (60\text{ ksi})(0.20\text{ in.}^2) = 12.0\text{ kips}$

$T_{s2} = (49.78\text{ ksi})(0.20\text{ in.}^2) = 10.0\text{ kips}$

$T_{s3} = (9.55\text{ ksi})(0.20\text{ in.}^2) = 1.9\text{ kips.}$

$\sum C > \sum P + T$

$C_m + C_{s1} + C_{s21} > P + T_{s1} + T_{s2} + T_{s3}$

$686 + 12.0 + 6.3 > 245.0 + 12.0 + 10.0 + 1.9$

$704\text{ kips} > 269\text{ kips}$ OK

There is more compression capacity than required, so the ductile failure condition controls.

10.2.4.6 Birmingham 1 deflections. The calculations for deflection involve many variables and assumptions, and it must be recognized that any calculation of deflection is approximate at best.

The *Standard* requires that deflections be calculated and compared with the prescribed limits set forth by *Standard* Table 12.12-1. Furthermore, *Standard* Section 12.7.3 requires that the effect of cracking be considered in establishing the elastic stiffness of masonry elements. In contrast, TMS 402 has two provisions that contradict the *Standard*: Section 1.17.2.4 effectively dismisses the drift requirement for all masonry shear walls except Special Reinforced Masonry Shear Walls, and Section 1.9.2 permits the use of uncracked stiffness. This example follows the requirements of the *Standard*. Elastic deflections are calculated considering cracking and then increased by C_d to account for non-linear response during the design earthquake. Recognizing that *P-delta* effects are minor for the in-plane direction, we solve for $\delta_{total} = \delta_{flexural} + \delta_{shear}$ for elastic and increase that value by C_d. The story drift, Δ, is the difference between δ_{total} for adjacent stories.

The following procedure is used for calculating deflections:

1. For purpose of illustration, moments and cracking moments in each story are computed and are shown in Table 10.2-5.

2. Cracking moment is determined from $M_{cr} = S(f_r + P_{u\ min} / A_n)$.

3. Compute deflection for each level.

While I_{cr} can be determined from principles of mechanics, the authors prefer to consider the following:

- $I_{cr} < I_g$
- For walls with no compression, the calculation for I_{cr} is straightforward.

- For walls with compression, one can adjust A_s to account for the effect of compression, resulting in A_{se}.
- ACI 318 permits $I_{cr} = 0.35I_g$ for cracked, reinforced concrete walls (ACI 318 Sec. 10.10.4.1).
- Alternatively, a (complicated) equation for I can be used (ACI 318 Eq. 10-8).
- TMS 402 Section 3.1.5.2 permits up to one-half of gross section properties for use in deflection calculations when considering effects of cracking on reinforced masonry members.

For this example, the effect of cracking is recognized by taking I_{eff} as 35 percent of the gross moment of inertia, as recommended for reinforced concrete walls in ACI 318. Other approximations can be used. In the authors' opinion, the approximations pale in uncertainty in comparison to the approximation of nonlinear deformation using C_d.

For the Birmingham 1 building:

b_e = effective masonry wall width, averaged over the entire wall length

b_e = [(2 × 1.25 in.)(32.67 ft × 12) + (5 cells)(41 in.^{2}/cell)]/(32.67 ft × 12) = 3.02 in.

$S = b_e\, l^2/6$ = (3.02)(32.67 × 12)^2/6 = 77,434 in.^{3}

f_r = (0.063 ksi)(11 cells/12 cells) + (0.163 ksi) (1 cell/12 cells) = 0.071 ksi
(for CMU with every 12th cell grouted)

$A_n = b_e\, l$ = (3.02 in.)(32.67 ft × 12) = 1,185 in.^{2}

P_u is calculated using 1.00D (see Table 10.2-4). 1.00D is considered to be a reasonable value for axial load for this admittedly approximate analysis. If greater conservatism is desired, P_u could be calculated using 0.86D. (Recall that the 0.86 factor accounts for E_v in the upward direction [i.e., 0.9 - 0.2 S_{DS}], leading to a lower bound on P_u).

The results are shown in Table 10.2-5.

Table 10.2-5 Birmingham 1 Cracked Wall Determination

Level	$P_{u_{min}}$ (kips)	M_{cr} (ft-kips)	M_u (ft-kips)	Status
5	49	725	198	Uncracked
4	98	992	572	Uncracked
3	147	1,259	1,080	Uncracked
2	196	1,525	1,675	Cracked
1	245	1,792	2,314	Cracked

1.0 kip = 4.45 kN, 1.0 ft-kip = 1.36 kN-m.

For uncracked walls:

$In. = I_g = bl^3/12 = (3.02 \text{ in.})(32.67 \times 12)^3 /12 = 1.52 \times 10^6 \text{ in.}^4$

$I_{eff} = 0.35\ I_g = 0.532 \times 106 \text{ in.}^4$

The calculation of δ considers flexural and shear deflections. For the final determination of deflection, a RISA-2D analysis is made. The result is summarized Table 10.2-6 below. Figure 10.2-8 illustrates the deflected shape of the wall.

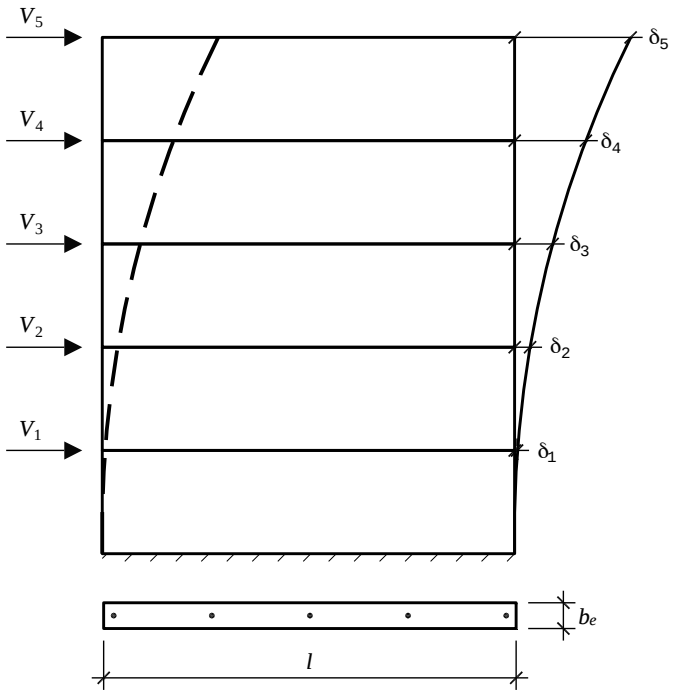

Figure 10.2-8 Shear wall deflections

Table 10.2-6 Deflections, Birmingham 1

Level	F (kips)	I_{eff} (in.^{4})	$\delta_{flexural}$ (in.)	δ_{shear} (in.)	δ_{total} (in.)	$C_d\,\delta_{total}$ (in.)	Δ (in.)
5	22.8	1.52×10^7	0.201	0.032	0.233	0.408	0.096
4	20.4	1.52×10^7	0.150	0.028	0.178	0.312	0.097
3	15.3	1.52×10^7	0.099	0.024	0.123	0.215	0.096
2	10.1	0.053×10^7	0.051	0.017	0.068	0.119	0.079
1	5.1	0.053×10^7	0.014	0.009	0.023	0.040	0.040

1.0 kip = 4.45 kN, 1.0 in. = 25.4 mm.
$F = 0.149F_x$, for F_x from Table 10.2-2.
Δ = story drift.

The maximum story drift occurs at Levels 3 and 4 (*Standard* Table 12.12-1):

Δ_{max} = 0.097 in.

The drift limit = 0.01h_n (TMS 402 Sec. 1.17.2.4 and *Standard* Table 12.12-1).

Δ_{max} = 0.097 in. < 1.04 in. = 0.01h_n OK

10.2.4.7 Birmingham 1 out-of-plane forces. The *Standard* Section 12.11.1 requires that the bearing walls be designed for out-of-plane loads determined as follows:

$w = 0.40 S_{DS} I W_w \geq 0.1 W_w$

w = (0.40)(0.24)(1)(45 psf) = 4.3 psf < 4.5 psf = 0.1W_w

where:

W_w = weight of wall

The calculated seismic load, w = 4.5 psf, is much less than wind pressure for exterior walls and is also less than the 5 psf required by the IBC for interior walls. Thus, seismic loads do not control the design of any of the walls for loading in the out-of-plane direction.

10.2.4.8 Birmingham 1 orthogonal effects. Orthogonal effects do not have to be considered for Seismic Design Category B (*Standard* Section 12.5.2).

This completes the design of Transverse Wall D.

10.2.4.9 Summary of Design for Birmingham 1 Wall D.

- 8-inch CMU
- f'$_m$ = 2,000 psi
- Reinforcement:

  One vertical #4 bar at wall end cells.

  Vertical #4 bars at 8 feet on center at intermediate cells throughout.

  Bond beam with two #4 bars at each story just below the floor and roof slabs.

  Horizontal joint reinforcement at 16 inches.

- Grout at cells with reinforcement and at bond beams.

10.2.5 Seismic Design for Albuquerque

This example focuses on differences from the design for the Birmingham 1 site. The walls are designed as Intermediate Reinforced Masonry Shear Walls even though the *Standard* would permit Ordinary Masonry Shear Walls. While the maximum reinforcement, and thus the grout, is increased, the change in *R* factor is advantageous in that the required strength is less.

This site is assigned to Seismic Design Category C, and the walls will be designed as intermediate reinforced masonry shear walls (*Standard* Table 12.2-1. Intermediate reinforced masonry shear walls have a minimum of #4 bars at 4 feet on center (TMS 402 Sec. 1.17.3.2.5).

10.2.5.1 Albuquerque Weights

As before, use 67 psf for 8-inch-thick normal-weight hollow core plank plus the non-masonry partitions. For this example, 48 psf will be assumed for the 8-inch CMU walls. The 48 psf value includes grouted cells as well as bond beams in the course just below the floor planks. It will be shown that this symmetric building, with a seemingly well distributed lateral force-resisting system, has "extreme torsional irregularity" by the *Standard.*

Story weight, w_i:

- Roof:

  Roof slab (plus roofing) = (67 psf) (152 ft)(72 ft) = 733 kips
  Walls = (48 psf)(589 ft)(8.67 ft/2) + (48 psf)(4)(36 ft)(2 ft) = 136 kips
  Total = 869 kips

  There is a 2-foot-high masonry parapet on four walls, and the total length of masonry wall is 589 feet.

- Typical floor:

  Slab (plus partitions) = 733 kips
  Walls = (48 psf)(589 ft)(8.67 ft) = 245 kips
  Total = 978 kips

Total effective seismic weight, W = 869 + (4)(978) = 4,781 kips.

This total excludes the lower half of the first-story walls, which do not contribute to seismic loads that are imposed on CMU shear walls.

10.2.5.2 Albuquerque base shear calculation.

The seismic response coefficient, C_s, is computed from *Standard* Section 12.8:

$$C_s = \frac{S_{DS}}{R/I} = \frac{0.37}{3.5/1} = 0.106$$

The value of C_s need not be greater than:

$$C_s = \frac{S_{D1}}{T(R/I)} = \frac{0.15}{0.338\left(3.5/1\right)} = 0.127$$

where T is the same as found in Section 10.2.4.2.

The value for C_s is taken as 0.106 (the lesser of the two computed values). This value is still larger than the minimum specified in *Standard* Equation 12.8-5 (Sup. 2):

$$C_s = 0.044 I S_{DS} \geq 0.01$$

$$= 0.044(1.0)(0.37) = 0.0163 \geq 0.01 \qquad \text{(0.106 controls)}$$

Note that this is essentially the same as the value for Birmingham 1, even though S_{DS} is 71 percent larger. This is because we are using a system with an R factor that is 75 percent larger. We continue with this example because we will find an unexpected result arising from a requirement which applies in Seismic Design Category C but not in Seismic Design Category B.

The total seismic base shear is then calculated using *Standard* Equation 12.8-1:

$V = C_s W = (0.106)(4{,}781) = 507$ kips

10.2.5.3 Albuquerque vertical distribution of seismic forces

The vertical distribution of seismic forces is determined in accordance with *Standard* Section 12.8.3, which was described in Section 10.2.4.3. Note that for the *Standard*, $k = 1.0$ because T is less than 0.5 seconds (similar to the Birmingham 1 building).

The application of the *Standard* equations for this building is shown in Table 10.2-7:

Table 10.2-7 Albuquerque Seismic Forces and Moments by Level

Level x	w_x (kips)	h_x (ft)	$w_x h_x^k$ (ft-kips)	C_{vx}	F_x (kips)	V_X (kips)	M_x (ft-kips)
5	869	43.34	37,657	0.3076	156	156	1,350
4	978	34.67	33,904	0.2770	141	297	3,930
3	978	26.00	25,428	0.2077	105	402	7,410
2	978	17.33	16,949	0.1385	70	472	11,500
1	978	8.67	8,476	0.0692	35	507	15,900
$\sum$	4,781		122,414	1.0000	507		

1.0 kip = 4.45 kN, 1.0 ft = 0.3048 m, 1.0 ft-kip = 1.36 kN-m.

10.2.5.4 Albuquerque horizontal distribution of forces

The initial distribution is the same as Birmingham 1. See Section 10.2.4.4 and Figure 10.2-3 for wall designations.

Total shear in Wall D:

$$V_{tot} = 0.125V + 0.0238V = 0.149V$$

For Seismic Design Category C structures, *Standard* Section 12.8.4.3 requires a check of torsional irregularity using the ratio of maximum displacement at the end of the structure, including accidental torsion, to the average displacement of the two ends of the building. For this simple and symmetric structure, the actual displacements do not have to be computed to find the ratio. Relying on symmetry and the assumption of rigid diaphragm behavior used to distribute the forces, the ratio of the maximum

displacement of Wall D to the average displacement of the floor will be the same as the ratio of the wall shears with and without accidental torsion:

$$\frac{F_{max}}{F_{ave}} = \frac{0.149V}{0.125V} = 1.190$$

This can be extrapolated to the end of the rigid diaphragm:

$$\frac{\delta_{max}}{\delta_{ave}} = 1 + 0.190\left(\frac{152/2}{36}\right) = 1.402$$

Standard Table 12.3-1 defines a building as having a "Torsional Irregularity" if this ratio exceeds 1.2 and as having an "Extreme Torsional Irregularity" if this ratio exceeds 1.4. Thus, an important result of the Seismic Design Category C classification is that the total torsion must be amplified by the factor (*Standard* Eq. 12.8-14):

$$A_x = \left(\frac{\delta_{max}}{1.2\delta_{ave}}\right)^2 = \left(\frac{1.402}{1.2}\right)^2 = 1.365$$

Therefore, the portion of the base shear for design of Wall D is increased to:

$$V_{tot} = 0.125V + 1.365(0.0238V) = 0.158V$$

which is a 6 percent increase from the fraction before considering torsional irregularity.

The total story shear and overturning moment may now be distributed to Wall D and the wall proportions checked. The wall capacity will be checked before considering deflections.

10.2.5.5 Albuquerque Transverse Wall D

The strength or limit state design concept is used in TMS 402 Chapter 3.

10.2.5.5.1 Albuquerque shear strength. Similar to the design for Birmingham 1, the shear wall design is governed by the following:

$$V_u \le \phi V_n$$

$$V_n = V_{nm} + V_{ns}$$

$$V_{n\,\max} = (4 \text{ to } 6) A_n \sqrt{f'_m} \quad \text{depending on } M_u/V_u d_v$$

$$V_{nm} = \left[4\text{-}1.75\left(\frac{M_u}{V_u d_v}\right)\right] A_n \sqrt{f'_m} + 0.25\, P_u$$

$$V_{ns} = 0.5\left(\frac{A_v}{s}\right) f_y d_v$$

where:

A_n = (2 × 1.25 in. × 32.67 ft × 12 in.) + (41 in.^{2} × 9 cells) = 1,349 in.^{2}

The shear strength of each Wall D, based on the aforementioned formulas and the strength reduction factor of $\phi = 0.8$ for shear from TMS 402 Section 3.3.2, is summarized in Table 10.2-8. Note that V_x and M_x in this table are values from Table 10.2-7 multiplied by 0.158 (representing the portion of direct and indirect shear assigned to Wall D), and P_u is the dead load of the roof or floor times the tributary area for Wall D.

Table 10.2-8 Albuquerque Shear Strength Calculation for Wall D

Story	V_x (kips)	M_x (ft-kips)	$M_x/V_x d_v$	2.5 V_x (kips)	P_u (kips)	V_{nm} (kips)	V_{ns} (kips)	V_n (kips)	V_n (max) (kips)	ϕV_n (kips)
5	24.6	213	0.266	24.6	35	222	68	**290**	359	232
4	46.9	621	0.405	47.0	75	217	68	**285**	337	228
3	63.5	1,171	0.564	63.5	115	211	68	**279**	312	223
2	74.6	1,817	0.746	74.6	156	202	68	**270**	282	216
1	80.1	2,512	0.960	80.1	196	189	68	257	**248**	198

1.0 kip = 4.45 kN, 1.0 ft-kip = 1.36 kN-m.

Values shown in **bold** are the controlling values for V_n

For all levels, $\phi V_n > V_{u,}$, so this Intermediate Reinforced Masonry shear wall is OK.

10.2.5.5.2 Albuquerque axial and flexural strength. The walls in this example are all load-bearing shear walls because they support vertical loads as well as lateral forces. In-plane calculations include the following:

- Strength check
- Ductility check

10.2.5.5.2.1 Strength check. Wall demands, using load combinations determined previously, are presented in Table 9.2-9 for Wall D. In the table, Load Combination 1 is $1.27D + Q_E + 0.5L$ and Load Combination 2 is $0.83D + Q_E$.

Table 10.2-9 Demands for Albuquerque Wall D

Level	P_D (kips)	P_L (kips)	Load Combination 1		Load Combination 2	
			P_u (kips)	M_u (ft-kips)	P_u (kips)	M_u (ft-kips)
5	50	0	64	213	42	213
4	100	15	135	621	83	612
3	149	25	202	1,171	124	1,171
2	199	34	270	1,817	165	1,817

Table 10.2-9 Demands for Albuquerque Wall D

Level	P_D (kips)	P_L (kips)	Load Combination 1		Load Combination 2	
			P_u (kips)	M_u (ft-kips)	P_u (kips)	M_u (ft-kips)
1	249	41	337	2,512	207	2,512

1.0 kip = 4.45 kN, 1.0 ft-kip = 1.36 kN-m.

As in Section 10.2.4.5.2, the strength at the bottom story (where *P*, *V* and *M* are the greatest) is examined. The strength design considers Load Combination 2 from Table 10.2-9 to be the governing case because it has the same lateral load as Load Combination 1 but with lower values of axial force. Refer to Figure 10.2-9 for notation and dimensions.

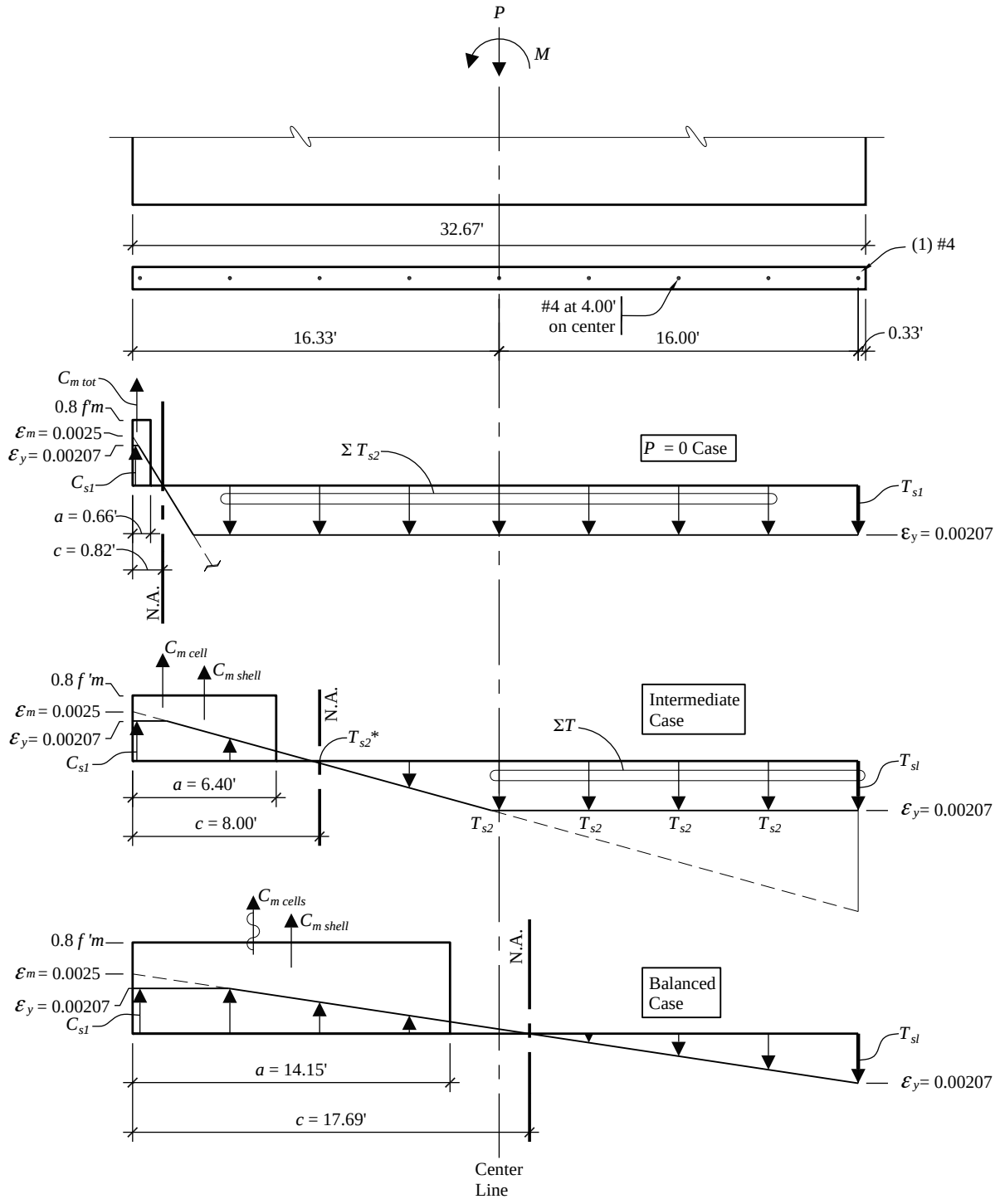

Figure 10.2-9 Strength of Albuquerque Wall D
Strain diagram superimposed on strength diagram for the three cases.
Low forces in the reinforcement are neglected in the calculations.
(1.0 ft = 0.3048 m)

Examine the strength of Wall D at Level 1:

$P_{u\ min.}$ = 207 kips

$P_{u\ max}$ = 337 kips

M_u = 2,512 ft-kips

Because intermediate reinforced masonry shear walls are used (Seismic Design Category C), vertical reinforcement is required at 4 feet on center in accordance with TMS 402 Section 1.17.3.2.5. Therefore, try one #4 bar in each end cell and #4 bars at 4 feet on center at all intermediate cells.

The calculation procedure is similar to that for the Birmingham 1 building presented in Section 10.2.4.5.2. The results of the calculations (not shown) for the Albuquerque building are summarized below and shown in Figure 10.2-9.

- P = 0 case:

  ϕP_n = 0

  ϕM_n = 1,562 ft-kips

- Intermediate case:

  c = 8.0 ft

  ϕP_n = 349 kips

  ϕM_n = 5,929 ft-kips

- Balanced case:

  ϕP_n = 854

  ϕM_n = 8,697 ft-kips

With the intermediate case, it is simple to use the three points to make two straight lines on the interaction diagram. Use the simplified ϕP_n - ϕM_n curve shown in Figure 10.2-10. The straight line from pure bending to the balanced point is conservative and can easily be used where the design is not as close to the criterion. It is the nature of lightly reinforced and lightly loaded masonry walls that the intermediate point is frequently useful.

Use one #4 bar in each end cell and one #4 bar at 4 feet on center throughout the remainder of the wall.

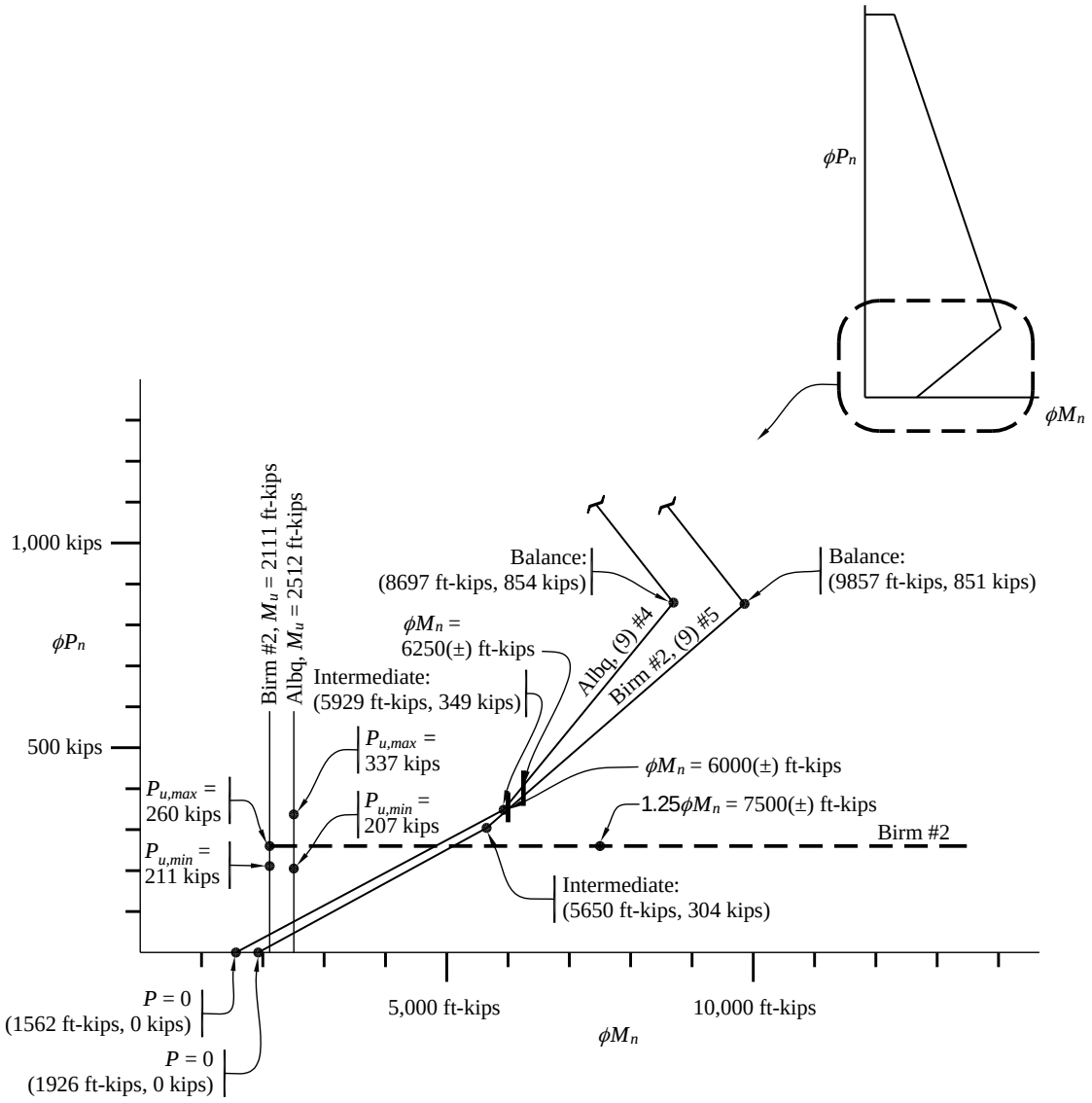

Figure 10.2-10 ϕP_n - ϕM_n Diagram for Albuquerque and Birmingham 2 Wall D
(1.0 kip = 4.45 kN, 1.0 ft-kip = 1.36 kN-m)

While Birmingham 2 has a lesser demand than Albuquerque, more robust reinforcement is required prescriptively because it is Seismic Design Category D. The greater flexural resistance will also necessitate a design to resist greater shear, a requirement that applies to special reinforced masonry shear walls (TMS 402, Sec. 1.17.3.2.6.1), which are required for Seismic Design Category D.

10.2.5.5.2.2 Ductility check. Refer to Section 10.2.4.5.2, Item 2, for explanation. The strain distribution is shown in Figure 10.2-11. If *M/Vd* equals or exceeds 1.0, the multiplier on steel yield strain for intermediated reinforced masonry walls (TMS 402 Sec. 333.5.2) is 3.0, not 1.5. For this design *M/Vd* = 0.96. For Level 1 (bottom story), the unfactored loads are as follows:

P = 249 kips

$C_m = 0.8\ f_m'\ [(a)(b) + A_{cells}]$
where b = face shells = (2 × 1.25 in.) and A_{cell} = 41 in.^{2}

C_m = (1.6 ksi)[(11.55 ft × 12)(2.5 in.) + (3)(41)] = 751 kips

$C_{s1} = F_y A_s$ = (60 ksi)(0.20 in.^{2}) = 12 kips

C_{s2} = (51.9 ksi)(0.20 in.^{2}) = 10.4 kips

C_{s3} = (31.4 ksi)(0.20 in.^{2}) = 6.3 kips

C_{s4} and T_{s5} are small, so are neglected

$T_{s1} = T_{s2}$ = = (60 ksi)(0.20 in.^{2}) = 12 kips

T_{s3} = (49.8 ksi)(0.20 in.^{2}) = 10.0 kips

T_{s4}= (29.7 ksi)(0.20 sq. in.) = 5.9 kips

$\sum C > \sum P + T$

$C_m + C_{s1} + C_{s2} + C_{s3} > P + T_{s1} + T_{s2} + T_{s3} + T_{s4}$

751 + 12 + 10.4 > 249 + 12 + 12 + 10.0 + 5.9

773 kips > 289 kips OK

There is more compression capacity than required, so a ductile failure condition controls.

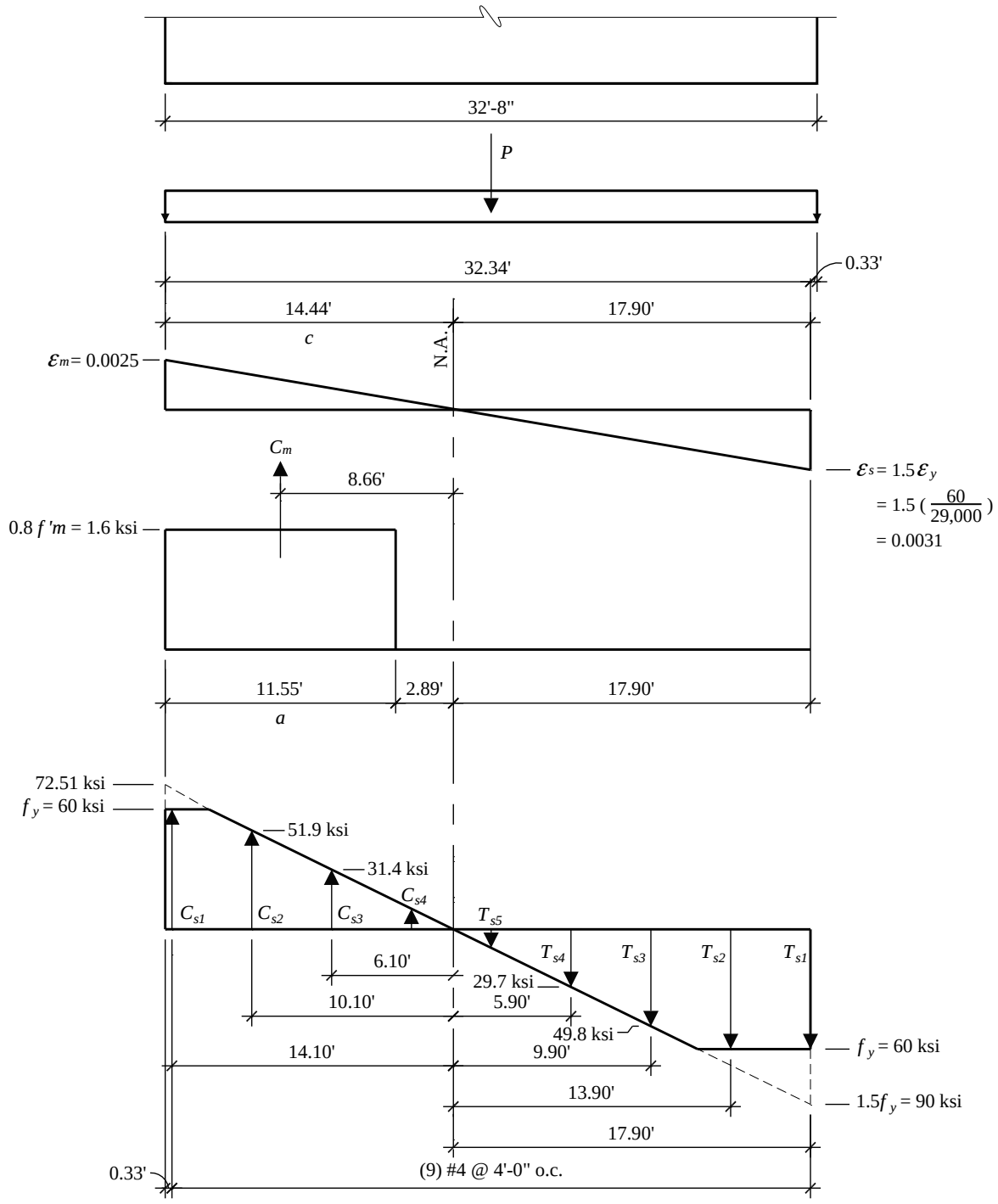

Figure 10.2-11 Ductility check for Albuquerque
(1.0 kip = 4.45 kN, 1.0 ft-kip = 1.36 kN-m)

10.2.5.6 Albuquerque deflections. Refer to Section 10.2.4.6 for more explanation. For the Albuquerque building, the determination of whether the walls will be cracked is as follows:

b_e = effective masonry wall width

b_e = [(2 × 1.25 in.)(32.67 ft × 12) + (9 cells)(41 in.^{2}/cell)]/(32.67 ft × 12) = 3.44 in.

$A_n = b_e\, l$ = (3.44 in.)(32.67 × 12) = 1,349 in.^{2}

$S = b_e\, l^2/6$ = (3.44)(32.67 × 12)^2 /6 = 88,100 in.^{3}

f_r = (0.063 ksi)(5 cells/6 cells) + (0.163 ksi)(1 cell/6 cells) = 0.080 ksi

P_u is calculated using 1.00D (see Table 10.2-9 for values and refer to Sec. 10.2.4.6 for discussion). Table 10.2-10 summarizes these calculations.

Table 10.2-10 Albuquerque Cracked Wall Determination

Level	P_u (kips)	M_{cr} (ft-kips)	M_x (ft-kips)	Status
5	50	859	213	Uncracked
4	100	1,132	621	Uncracked
3	149	1,398	1,171	Uncracked
2	199	1,610	1,817	Cracked
1	249	1,952	2,512	Cracked

1.0 kip = 4.45 kN, 1.0 ft-kip = 1.36 kN-m.

For the uncracked walls:

$I_n = I_g = bl^3/12$ = (3.44 in.)(32.67 × 12)^3/12 = 1.73 × 10^7 in.^{4}

For the cracked wall:

I_{eff} = 0.35 I_g = 0.606 × 10^7 in.^{4}

The calculation of δ should consider shear deflection in addition to flexural deflection. This example uses a RISA 2D analysis. The results are summarized in Table 10.2-11.

Table 10.2-11 Albuquerque Deflections

Level	F (kips)	I_{eff} (in.^{4})	$\delta_{flexural}$ (in.)	δ_{shear} (in.)	δ_{total} (in.)	$C_d\,\delta_{total}$ (in.)	Δ (in.)
5	23.2	1.73 × 10^7	0.181	0.032	0.213	0.479	0.110
4	21.0	1.73 × 10^7	1.134	0.030	0.164	0.369	0.115
3	15.6	1.73 × 10^7	0.089	0.024	0.113	0.254	0.112
2	10.4	0.61 × 10^7	0.046	0.017	0.063	0.142	0.092
1	5.2	0.61 × 10^7	0.013	0.009	0.022	0.050	0.052

1.0 kip = 4.45 kN, 1.0 in. = 25.4 mm.
F = 0.149 F_x , for F_x from Table 10.2-7.
Δ = story drift.

The maximum story drift occurs between Levels 4 and 3:

Δ_4 = 0.115 in. < 1.04 in. = 0.01 h_n (*Standard* Table 12.2-1) OK

10.2.5.7 Albuquerque out-of-plane forces. *Standard* Section 512.11.1 requires that bearing walls be designed for out-of-plane loads, determined as follows:

$w = 0.40\ S_{DS}\ I W_w \geq 0.1 W_w$

$w = (0.40)(0.37)(1)(48\text{ psf}) = 7.1\text{ psf} > 4.8\text{ psf} = 0.1 W_w$,

So the equivalent normal pressure due to the design earthquake is 7.1 psf. This is greater than the design differential air pressure of 5 psf. However, the lateral pressure is sufficiently low for this short wall that the authors consider it acceptable by inspection, without further calculation. So, seismic loads do not govern the design of Wall D for loading in the out-of-plane direction.

10.2.5.8 Albuquerque orthogonal effects. According to *Standard* Section 12.5.3, orthogonal interaction effects have to be considered for Seismic Design Category C where the ELF procedure is used (as it is here). However, the out-of-plane component of only 30 percent of 7.1 psf on the wall does not produce a significant effect where combined with the in-plane direction of loads, so no further calculation is made.

This completes the design of the transverse Wall D for the Albuquerque building.

10.2.5.9 Summary of Albuquerque Wall D design

- 8-inch CMU
- f'_m = 2,000 psi
- Reinforcement:

  Vertical #4 bars at 4 feet on center throughout the wall.

  Bond beam with two #4 at each story just below the floor or roof slabs.

  Horizontal joint reinforcement at alternate courses.

10.2.6 Birmingham 2 Seismic Design

The emphasis here is on differences from the previous two locations for the same building. *Standard* Table 12.6-1 requires that design of a Seismic Design Category D building with torsional irregularity be based on a dynamic analysis. Although it is not explicitly stated, the implication is that the analytical model should be three-dimensional in order to capture the torsional response. This example compares both the ELF procedure and the modal response spectrum analysis procedure and demonstrates that, as long as the torsional effects are accounted for, the static analysis (ELF method) could be considered adequate for design.

10.2.6.1 Birmingham 2 weights

The floor weight for this example uses the same 67 psf for 8-inch-thick, normal-weight hollow core plank plus roofing and the nonmasonry partitions as used in the prior examples (see Sec. 10.2.1). This site is assigned to Seismic Design Category D, and the walls are designed as special reinforced masonry shear walls (*Standard* Table 12.2-1). Special reinforced masonry shear walls have a maximum spacing of rebar at 4 feet on center both horizontally and vertically (TMS 402 Sec. 1.17.3.2.6). Also, the total area of horizontal and vertical reinforcement must exceed 0.002 times the gross area of the wall and neither direction may have a ratio of less than 0.0007. The vertical #4 bars at 48 inches used for the Albuquerque design yield a ratio of 0.00055, so it must be increased. #5 bars at 48 inches (yielding 0.00085) is selected. The latter is chosen in order to avoid unnecessarily increasing the shear demand. Therefore, the horizontal reinforcement must be (0.0020 - 0.00085)(7.625 in.)(12 in./ft) = 0.105 in.^{2}/ft Two #5 bars in bond beams at 48 inches on center will be adequate. For this example, 56 psf weight for the 8-inch-thick CMU walls will be assumed. The 56 psf value includes grouted cells and bond beams.

Story weight, w_i:

- Roof:

  Roof slab (plus roofing) = (67 psf) (152 ft)(72 ft) = 733 kips
  Walls = (56 psf)(589 ft)(8.67 ft/2) + (56 psf)(4)(36 ft)(2 ft) = 159 kips
  Total = 892 kips

  There is a 2-foot-high masonry parapet on four walls, and the total length of masonry wall is 589 feet.

- Typical floor:

  Slab (plus partitions) = 733 kips
  Walls = (56 psf)(589 ft)(8.67 ft) = 286 kips
  Total = 1,019 kips

Total effective seismic weight, W = 892 + (4)(1,019) = 4,968 kips.

This total excludes the lower half of the first story walls, which do not contribute to seismic loads that are imposed on CMU shear walls.

10.2.6.2 Birmingham 2 base shear calculation.

The ELF analysis proceeds as described for the previous locations. The seismic response coefficient, C_s, is computed using *Standard* Section 12.8:

$$C_s = \frac{S_{DS}}{R/I} = \frac{0.43}{5/1} = 0.086 \quad \text{(Controls)}$$

$$C_s = \frac{S_{D1}}{T(R/I)} = \frac{0.24}{0.338\left(5/1\right)} = 0.142$$

The fundamental period of the building, based on *Standard* Equation 12.8-7 is approximately 0.338 seconds as computed previously (the approximate period, based on building system and building

height, is the same for all locations). The value for C_s is taken as 0.086 (the lesser of the two values). This value is still larger than the minimum specified in *Standard* (Sup. 2) Equation 12.8-5, which is:

$$C_s = 0.044 S_{D1} I = (0.044)(0.24)(1) = 0.011$$

The total seismic base shear is calculated using *Standard* Equation 12.8-1:

$$V = C_s W = (0.086)(4{,}968) = 427 \text{ kips}$$

This is somewhat less than the 507 kips computed for the Albuquerque design, due to the larger *R* factor.

A three-dimensional (3D) model is created in SAP2000 for the modal response spectrum analysis. The masonry walls are modeled as shell bending elements, and the floors are modeled as an assembly of beams and shell membrane elements. The beams have very little mass and a large flexural moment of inertia to avoid consideration of modes of vertical vibration of the floors. The flexural stiffness of the beams is released at the bearing walls in order to avoid a wall-slab frame that would inadvertently increase the torsional resistance. The mass of the floors is captured by the shell membrane elements. Table 10.2-12 shows data on the modes of vibration used in the analysis.

Standard Section 11.4.5 is used to create the response spectrum for the modal analysis. The key points that define the spectrum are as follows:

$T_S = S_{D1}/S_{DS} = 0.21/0.43 = 0.56$ sec

$T_0 = 0.2\ T_S = 0.11$ sec

at $T = 0$, $S_a = 0.4\ S_{DS}/R = 0.034\ g$

from $T = T_0$ to T_S, $S_a = S_{DS}/R = 0.086\ g$

for $T > T_S$, $S_a = S_{D1}/(RT) = 0.042/T$

The computed fundamental period is less than the approximate period. The transverse direction base shear from the SRSS combination of the modes is 293 kips, which is considerably less than that obtained using the ELF method.

Standard Section 12.8.2 requires that the modal base shear be compared with the ELF base shear computed using a period no larger than $C_u T_a$. As shown in Section 10.2.4.2, $T_a = 0.338$ seconds. Per *Standard* Table 12.8-1, $C_u = 1.46$. Thus, $C_u T_a = 0.49$ seconds. However, the computed period, *T*, is only 0.2467 seconds (as shown in Table 10.2-12), which is less than $C_u T_a$ so the ELF base shear must be computed at that period. Since *T* is less that T_S/S_{DS}., the ELF base shear for comparison is 427 kips as just computed. Because 85 percent of 427 kips = 363 kips, *Standard* Section 12.9.4 dictates that all the results of the modal analysis be multiplied by the following:

$$\frac{0.85 V_{ELF}}{V_{Modal}} = \frac{363}{293} = 1.24$$

Both analyses are carried forward as discussed in the subsequent sections.

Table 10.2-12 Birmingham 2 Periods, Mass Participation Factors and Modal Base Shears in the Transverse Direction for Modes Used in Analysis

Mode Number	Period, (seconds)	Individual Mode (percent)			Cumulative Sum (percent)			Trans. Base Shear
		Long.	Trans.	Vert.	Long.	Trans.	Vert.	
1	0.2467	0.00	0.00	0.00	0.00	0.00	0.00	0.0
2	0.1919	0.00	70.18	0.00	0.00	70.18	0.00	288.7
3	0.1915	70.55	0.00	0.00	70.55	70.18	0.00	0.0
4	0.0579	0.00	18.20	0.00	70.55	88.39	0.00	47.3
5	0.0574	17.86	0.00	0.00	88.41	88.39	0.00	0.0
6	0.0535	0.00	4.09	0.00	88.41	92.48	0.00	10.3
7	0.0532	4.17	0.00	0.00	92.58	92.48	0.00	0.0
8	0.0413	0.00	0.01	0.00	92.58	92.48	0.00	0.0
9	0.0332	1.50	0.24	0.00	94.08	92.72	0.00	0.5
10	0.0329	0.30	2.07	0.00	94.38	94.79	0.00	4.5
11	0.0310	1.28	0.22	0.00	95.66	95.01	0.00	0.5
12	0.0295	0.22	1.13	0.00	95.89	96.14	0.00	2.4
13	0.0253	1.97	0.53	0.00	97.86	96.67	0.00	1.1
14	0.0244	0.53	1.85	0.00	98.39	98.52	0.00	3.8
15	0.0190	1.05	0.36	0.00	99.44	98.89	0.00	0.7
16	0.0179	0.33	0.94	0.00	99.77	99.82	0.00	1.8
17	0.0128	0.19	0.07	0.00	99.95	99.90	0.00	0.1
18	0.0105	0.03	0.10	0.00	99.99	99.99	0.00	0.2

1 kip = 4.45 kN.

10.2.6.3 Birmingham 2 vertical distribution of seismic forces. The dynamic analysis is revisited for the horizontal distribution of forces in the next section but, as demonstrated there, the ELF procedure is considered adequate to account for the torsional behavior in this example; the dynamic analysis certainly can be used to deduce the vertical distribution of forces. The purpose of this analysis is to study amplification of accidental torsion. Note that Mode 1 has no net base force in the longitudinal, transverse, or vertical directions. The mode shape confirms that it is purely torsional.

The vertical distribution of seismic forces for the ELF analysis is determined in accordance with *Standard* Section 12.8.3, which was described in Section 10.2.4.3, in which $k = 1.0$ because $T < 0.5$ seconds (similar to the Birmingham 1 and Albuquerque buildings). It should be noted that the response spectrum analysis (modal analysis) may result in moments that are less than those calculated using the ELF method; however, because of its relative simplicity, the ELF is used in this example.

Application of the *Standard* equations for this building is shown in Table 10.2-13:

Table 10.2-13 Birmingham 2 Seismic Forces and Moments by Level

Level x	w_x (kips)	h_x (ft)	$w_x h_x$ (ft-kips)	C_{vx}	F_x (kips)	V_x (kips)	M_x (ft-kips)

5	892	43.34	38,659	0.3045	130	130	1,130
4	1,019	34.67	35,329	0.2782	119	249	3,290
3	1,019	26.00	26,494	0.2086	89	338	6,220
2	1,019	17.33	17,659	0.1391	59	397	9,660
1	1,019	8.67	8,835	0.0695	30	427	13,360
∑	4,968		126,976	1.000	427		

1.0 kip = 4.45 kN, 1.0 ft = 0.3048 m, 1.0 ft-kip = 1.36 kN-m.

10.2.6.4 Birmingham 2 horizontal distribution of forces. The ELF analysis for Birmingham 2 is the same as that for the Albuquerque location; see Section 10.2.5.4.

Total shear in Wall D:

$$V_{tot} = 0.125V + 1.365(0.0238)V = 0.158V = 67.4 \text{ kips}$$

The fact that the fundamental mode is torsional does confirm, to an extent, that the structure is torsionally sensitive. This modal analysis does not show any significant effect of the torsion, however, because of the symmetry. The pure symmetry of this structure is somewhat idealistic. Real structures usually have some real eccentricity between mass and stiffness and dynamic analysis then yields coupled modes, which contribute to computed forces.

The *Standard* does not require that the accidental eccentricity be analyzed dynamically. For illustration, however, this is approximated by adjusting the mass of the floor elements to generate an eccentricity of 5 percent of the 152-foot length of the building. Table 10.2-14 shows the results of such an analysis. (Accidental torsion could also be considered using a linear combination of the dynamic results and a statically applied moment equal to the accidental torsional moment.)

The transverse direction base shear from the SRSS combination of the modes with dynamic torsion is 258.4 kips, less than the 293 kips for the symmetric model. The amplification factor for this base shear is 363/258 = 1.41. This smaller base shear from modal analysis of a model with an artificially introduced eccentricity is normal for two primary reasons: First, the mass participates in more modes. The participation in the largest mode generally is less, and the combined result is dominated by the largest single mode. Second, the period for the fundamental mode generally increases, because there is more flexibility between the mass and the foundation. The increase in period will reduce the spectral response except for structures with short periods (such as this one).

In order to demonstrate that the ELF method for addressing torsional effects per the *Standard* produces a conservative result, let us consider torsional effects based on modal analysis in greater detail than required by the *Standard*: The base shear in Wall D is computed by adding the in-plane reactions. For the symmetric model the result is 36.6 kips, which is 12.5 percent of the total of 293 kips, as would be expected. Amplifying this by the 1.24 factor (to bring the modal result to 85 percent of the ELF result) yields 45 kips Application of a static horizontal torsion equal to the 5 percent eccentricity times a base shear of 363 kips adds 8 kips, for a total of 53 kips. If the static horizontal torsion is amplified by 1.365, as found in the analysis for the Albuquerque location, the total becomes 56 kips, which is less than the 64 kips (0.149*V*) or 67 kips (0.158*V*) computed in the ELF analysis without and with, respectively, the amplification of accidental torsion. The Wall D base shear from the modal analysis with the eccentric model was 42 kips (SRSS); with the amplification of base shear equal to 1.41 (to reach 85 percent of the ELF), this becomes 59 kips. Note that this value is less than the shear from the ELF model including amplified static torsion (67 kips). The conclusion is that more careful consideration of torsional effects

than actually required by the *Standard* does not indicate any more penalty than already given by the procedures for the ELF in the *Standard*. Therefore the remainder of the example designs for this building are completed using the ELF.

Table 10.2-14 Birmingham 2 Periods, Mass Participation Factors and Modal Base Shears in the Transverse Direction for Modes Used in Approximate Accidental Torsion Analysis

Mode	Period	Individual Mode (percent)			Cumulative Sum (percent)			Trans.
Number	(sec)	Long.	Trans.	Vert.	Long.	Trans.	Vert.	Base Shear
1	0.2507	0.0	8.8	0.0	0.0	8.8	0.0	36.0
2	0.1915	70.5	0.0	0.1	70.5	8.8	0.1	0.0
3	0.1867	0.0	61.4	0.0	70.5	70.2	0.1	252.7
4	0.0698	0.0	2.9	0.0	70.5	73.1	0.1	8.1
5	0.0613	1.1	0.0	23.0	71.6	73.1	23.1	0.0
6	0.0575	19.2	0.0	0.0	90.9	73.1	23.2	0.0
7	0.0570	0.0	13.7	0.0	90.9	86.8	23.2	35.5
8	0.0533	0.0	5.6	0.0	90.9	92.4	23.2	14.1
9	0.0480	1.2	0.0	12.8	92.0	92.4	35.9	0.0
10	0.0380	1.4	0.0	0.0	93.5	92.4	35.9	0.0
11	0.0374	0.0	0.4	0.0	93.5	92.8	35.9	0.8
12	0.0327	1.7	0.0	0.2	95.2	92.8	36.1	0.0
13	0.0322	0.0	3.1	0.0	95.2	95.9	36.1	6.7
14	0.0263	2.8	0.0	0.1	98.0	95.9	36.2	0.0
15	0.0243	0.0	3.0	0.0	98.0	98.8	36.2	6.1
16	0.0201	1.6	0.0	0.1	99.6	98.8	36.3	0.0
17	0.0164	0.0	1.1	0.0	99.6	100.0	36.3	2.2
18	0.0141	0.4	0.0	0.1	100.0	100.0	36.3	0.0

The "extreme torsional irregularity" has an additional consequence for Seismic Design Category D: *Standard* Section 12.3.3.4 requires that the design forces for connections between diaphragms, collectors and vertical elements (walls) be increased by 25 percent. For this example, the diaphragm of precast elements is designed using the different requirements of the *Provisions*, Part 3, RP10.

10.2.6.5 Birmingham 2 transverse wall (Wall D). The total story shear and overturning moment (from the ELF analysis) may now be distributed to Wall D and the wall proportions checked. The wall capacity is checked before considering deflections.

The design demands are slightly smaller than for the Albuquerque design, largely due to an R of 5 instead of 3.5, yet there is more reinforcement, both vertical and horizontal in the walls, because of the prescriptive detailing requirements for Seismic Design Category D. This illustration will focus on those items where the additional reinforcement has special significance.

10.2.6.5.1 Birmingham 2 shear strength. Refer to Section 10.2.5.5.1 for most quantities. Compared to Albuquerque, the additional horizontal reinforcement raises V_s *and* the additional grouted cells raises A_n and therefore both V_{nm} and V_n(max).

$A_v/s = (4)(0.31 \text{ in.}^2)/(8.67 \text{ ft}) = 0.1431 \text{ in.}^2/\text{ft}$

V_{ns} = 0.5(0.1431)(60 ksi)(32.67 ft) = 140.2 kips

A_n = (2 × 1.25 in. × 32.67 ft × 12 in.) + (41 in.^{2} × 9 cells) = 1,349 in.^{2}

The shear strength of Wall D is summarized in Table 10.2-15 below. (V_x and M_x in this table are values from Table 10.2-13 multiplied by 0.158, the portion of direct and torsional shear assigned to the wall.) Clearly, the dynamic analysis would make it possible to design this wall for smaller forces, but the minimum configuration suffices. Note also that the format of Table 10.2-15 differs from that of its counterparts for Birmingham 1 and Albuquerque: a column for $2.5V_x$ is included here because, for special reinforced masonry shear walls, TMS 402 Section 1.17.3.2.6.1.1 requires the shear capacity to exceed the lesser of the shear corresponding to $1.25M_n$ or $2.5V_x$. The intent is to require response controlled by flexure in most cases, but to permit non-ductile shear response if the shear capacity is 2.5 times the demand from analysis.

Table 10.2-15 Birmingham 2 Shear Strength Calculation for Wall D

Story	V_x (kips)	M_x (ft-kips)	M_x/V_xd_v	$2.5V_x$ (kips)	P_u (kips)	V_{nm} (kips)	V_{ns} (kips)	V_n (kips)	V_n(max) (kips)	ϕV_n (kips)
5	20.5	178	0.265	51.2	42	224	140	364	**361**	289
4	39.3	520	0.405	98.3	84	220	140	360	**337**	270
3	53.4	983	0.563	134	126	213	140	353	**312**	249
2	62.7	1,526	0.745	157	168	205	140	345	**282**	226
1	67.5	2,111	0.957	169	210	193	140	333	**248**	199

1.0 kip = 4.45 kN, 1.0 ft-kip = 1.36 kN-m.
Values shown in **bold** are the controlling values for V_n

V_n(max) is less than V_n at all levels, so it controls in the determination of ϕV_n. $\phi V_n > 2.5V_x$ for all levels, so the design is satisfactory for shear (without needing to check whether ϕV_n is greater than the shear corresponding to $1.25M_n$).

10.2.6.5.2 Birmingham 2 axial and flexural strength. Once again, the similarities to the design for the Albuquerque location are exploited. The in-plane calculations include the following:

- Strength check
- Ductility check

10.2.6.5.2.1 Strength check. The wall demands, using the load combinations determined previously, are presented in Table 10.2-16 for Wall D. In the table, Load Combination 1 is $1.29D + Q_E + 0.5L$ and Load Combination 2 is $0.81D + Q_E$.

Table 10.2-16 Birmingham 2 Demands for Wall D

Level	P_D (kips)	P_L (kips)	Load Combination 1		Load Combination 2	
			P_u (kips)	M_u (ft-kips)	P_u (kips)	M_u (ft-kips)
5	53	0	68	178	43	178

Table 10.2-16 Birmingham 2 Demands for Wall D

Level	P_D (kips)	P_L (kips)	Load Combination 1		Load Combination 2	
			P_u (kips)	M_u (ft-kips)	P_u (kips)	M_u (ft-kips)
4	104	15	134	520	84	520
3	156	25	201	983	126	983
2	208	34	268	1526	168	1526
1	260	41	335	2111	211	2111

1.0 kip = 4.45 kN, 1.0 ft-kip = 1.36 kN-m.

Strength at the bottom story (where P, V and M are the greatest) is less than required for the Albuquerque design. The demands for Birmingham 2 are plotted on Figure 10.2-10 along with those for Albuquerque (showing that the design for Albuquerque has sufficient axial and flexural capacity for this Birmingham 2 location).

10.2.6.5.2.2 Ductility check. The requirements for ductility are described in Sections 10.2.4.5.3 and 10.2.5.5.3. Because the wall reinforcement and loads are so similar to those for the Albuquerque building, the computations are not repeated here. A brief review of the Albuquerque ductility calculations (Sec. 10.2.5.5.3) reveals that the Birmingham 2 reinforcement satisfies the ductility provisions.

10.2.6.6 Birmingham 2 deflections. The calculations for deflection would be similar to that for the Albuquerque location. The calculation is not repeated here; refer to Sections 10.2.4.6 and 10.2.5.6. While the C_d factor is larger, 3.5 versus. 2.25, the resulting maximum story drift is still less than the 0.01 h_n allowable and therefore is OK.

10.2.6.7 Birmingham 2 out-of-plane forces. *Standard* Section 12.11 requires that the bearing walls be designed for out-of-plane loads, determined as follows:

$$w = 0.40\, S_{DS}\, I W_w \geq 0.1 W_w$$

$$w = (0.40)(0.43)(1)(56 \text{ psf}) = 9.6 \text{ psf} \geq 0.1 W_w$$

The calculated seismic load, w = 9.6 psf, is less than wind pressure for exterior walls. This is larger than the design differential pressure of 5 psf across an interior wall (per the IBC). Given the story height for either interior or exterior walls, the out-of-plane seismic force is sufficiently low that it is considered acceptable by inspection without further calculation.

10.2.6.8 Birmingham 2 orthogonal effects. According to *Standard* Section 12.5.3, orthogonal interaction effects should be considered for Seismic Design Category D where the ELF procedure is used (as it is here). However, the out-of-plane component of only 30 percent of 9.6 psf on the wall does not produce a significant effect where combined with the in-plane direction of loads, so no further calculation is made.

This completes the design of Transverse Wall D.

10.2.6.9 Summary of Birmingham 2 Wall D

- 8-inch CMU
- f'_m = 2,000 psi

- Reinforcement:

  9 vertical #5 bars per wall at 4’-0” on center.

  Two bond beams with two #5 at each story, at bearing for the planks and at 4 feet above each floor.

  Horizontal joint reinforcement at alternate courses is recommended, but not required.

10.2.7 Seismic Design for San Rafael

Once again, the differences from the designs for the other locations are emphasized. As explained for the Birmingham 2 building, the *Standard* would require a dynamic analysis for the design of this building. For the reasons explained in Section 10.2.6.4, this design is illustrated using the ELF procedure.

10.2.7.1 San Rafael weights

Use 91 psf for 8-inch-thick, normal-weight hollow core plank, 2.5-inch lightweight concrete topping (115 pcf), plus the non-masonry partitions. This building is in Seismic Design Category D, and the walls will be designed as special reinforced masonry shear walls (*Standard* Table 12.2-1), which requires prescriptive seismic reinforcement (TMS 402 Section 1.17.3.2.6). Special reinforced masonry shear walls have a minimum spacing of vertical reinforcement of 4 feet on center. The demand is considerably larger than that for the other Seismic Design Category D building (Birmingham 2), so more reinforcement is required. Trial reinforcement is selected as nine #7 bars at 4’-0” on center. For this example, a 60 psf weight for the 8-inch CMU walls is assumed. The 60 psf value includes grouted cells and bond beams in the course just below the floor planks and in the course 4 feet above the floors. (Note that the wall is 43.33 feet high, not 8 feet high, for purpose of determining the maximum spacing of vertical and horizontal reinforcement.)

A typical wall section is shown in Figure 9.2-12.

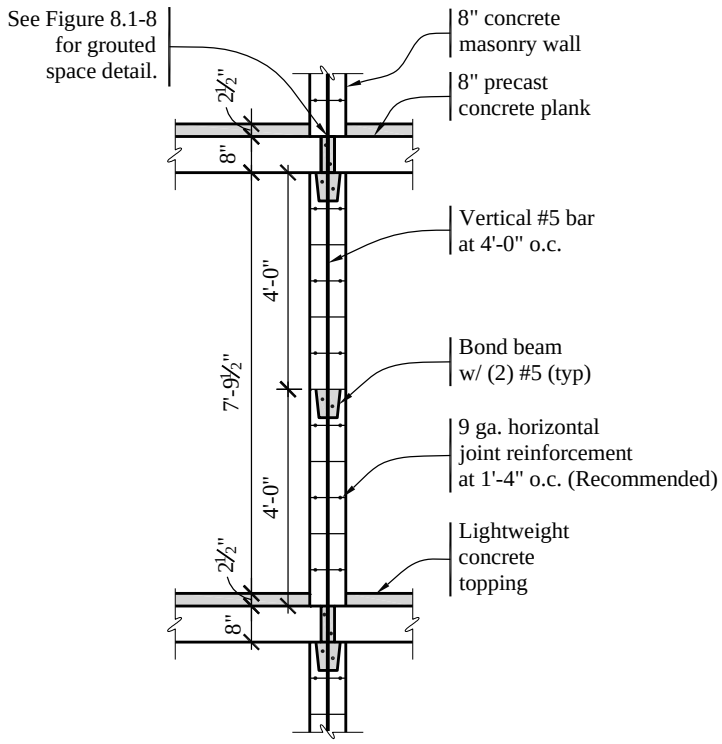

Figure 9.2-12 Typical wall section for the San Rafael location
(1.0 in. = 25.4 mm, 1.0 ft = 0.3048 m)

Story weight ,w_i:

- Roof weight:

  Roof slab (plus roofing) = (91 psf) (152 ft)(72 ft) = 996 kips
  Walls = (60 psf)(589 ft)(8.67 ft/2) + (60 psf)(4)(36 ft)(2 ft) = 170 kips
  Total = 1,166 kips

  There is a 2-foot-high masonry parapet on four walls, and the total length of masonry wall is 589 feet.

- Typical floor:

  Slab (plus partitions) = 996 kips
  Walls = (60 psf)(589 ft)(8.67 ft) =306 kips
  Total = 1,302 kips

Total effective seismic weight, W = 1,166 + (4)(1,302) = 6,374 kips.

This total excludes the lower half of the first story walls, which do not contribute to the seismic loads that are not imposed on the CMU shear walls.

10.2.7.2 San Rafael base shear calculation. The seismic response coefficient, C_s, is computed using *Standard* Section 12.8:

$$C_s = \frac{S_{DS}}{R/I} = \frac{1.00}{5/1} = 0.20 \qquad \text{(Controls)}$$

$$C_s = \frac{S_{D1}}{T(R/I)} = \frac{0.60}{0.338(5/1)} = 0.355$$

where T is the fundamental period of the building, which is 0.338 seconds as computed previously. The value for C_s is taken as 0.20 (the lesser of these two). This value is still larger than the minimum specified in *Standard*, Section 12.8-5, which is:

$C_s = 0.044 S_{D1} I = (0.044)(0.60)(1) = 0.026$

The total seismic base shear is then calculated using *Standard* Equation 12.8-1:

$V = C_s W = (0.20)(6{,}374) = 1{,}275$ kips

10.2.7.3 San Rafael vertical distribution of seismic forces. The vertical distribution of seismic forces is determined in accordance with *Standard* Section 12.8.3, which is described in Section 10.2.4.3. Note that for the *Standard*, $k = 1.0$ because $T = 0.338$ seconds, which is less than 0.5 seconds (similar to the previous example buildings).

The application of the *Provisions* equations for this building is shown in Table 10.2-17:

Table 10.2-17 San Rafael Seismic Forces and Moments by Level

Level x	w_x (kips)	h_x (ft)	$w_x h_x^k$ (ft-kips)	C_{vx}	F_x (kips)	V_x (kips)	M_x (ft-kips)
5	1,166	43.34	50,534	0.309	394	394	3,420
4	1,302	34.67	45,140	0.276	353	747	9,890
3	1,302	26.00	33,852	0.207	264	1,011	18,660
2	1,302	17.33	22,564	0.138	176	1,187	28,950
1	1,302	8.67	11,288	0.069	88	1,275	40,000
$\sum$	6,374		163,378	1.000	1,275		

1.0 kip = 4.45 kN, 1.0 ft = 0.3048 m, 1.0 ft-kip = 1.36 kN-m

10.2.7.4 San Rafael horizontal distribution of forces

This is the same as for the Birmingham 2 design; see Section 10.2.6.4.

Total shear in Wall D:

$V_{tot} = 0.125V + 1.365(0.0238)V = 0.158V = 201.5$ kips

10.2.7.5 San Rafael Transverse Wall D.

10.2.7.5.1 Shear strength. This design continues to illustrate ELF analysis and, as explained for the Birmingham 2 design, smaller demands could be derived from dynamic analysis. All other parameters are similar to those for Birmingham 2 except the following:

A_n = (2 × 1.25 in. × 32.67 ft × 12 in.) + (41 in.^{2} × 9 cells) = 1,349 in.^{2}

The shear strength of each Wall D, based on the aforementioned formulas and data, are summarized in Table 10.2-18.

Table 10.2-18 San Rafael Shear Strength Calculations for Wall D

Story	V_x (kips)	M_x (ft-kips)	M_x/V_xd_v	$2.5V_x$ (kips)	P_u (kips)	V_{nm} (kips)	V_{ns} (kips)	V_n (kips)	V_n (max) (kips)	ϕV_n (kips)
5	62.3	540	0.265	156	46.3	225	163	388	**360**	288
4	118	1,563	0.405	295	92.6	222	163	385	**337**	270
3	160	2,948	0.564	400	161	222	163	385	**311**	249
2	188	4,574	0.745	470	185	209	163	372	**282**	226
1	201	6,320	0.962	503	231	197	163	360	**247**	198

1.0 kip = 4.45 kN, 1.0 ft-kip = 1.36 kN-m.

The maximum on V_n controls over the sum of V_m and V_s at all stories. Since ϕV_n does not exceed $2.5V_x$ except at the top story it is necessary to check the shear corresponding to $1.25\phi M_n$, (as discussed below in Section 10.2.7.5.3). It will be learned, once ϕM_n is determined below, that an increase in shear capacity is required. However, as we are not there yet, let us proceed in a sequence similar to a real design and continue with the flexural design.

10.2.7.5.2 Axial and flexural strength. The basics of flexural design are demonstrated for the previous locations. The demand is much higher at this location, which introduces issues about the amount and distribution of reinforcement in excess of the minimum requirements. Therefore, both strength and ductility checks are examined.

10.2.7.5.2.1 Strength check. Load combinations, using factored loads, are presented in Table 10.2-19 for Wall D. In the table, Load Combination 1 is $1.4D + Q_E + 0.5L$ and Load Combination 2 is $0.7D + Q_E$.

Table 10.2-19 San Rafael Load Combinations for Wall D

Level x	P_D (kips)	P_L (kips)	Load Combination 1		Load Combination 2	
			P_u (kips)	M_u (ft-kips)	P_u (kips)	M_u (ft-kips)
5	66	0	92	540	46	540
4	132	15	185	1563	92	1563
3	198	25	277	2948	139	2948
2	265	34	371	4574	186	4574
1	331	41	463	6320	232	6320

1.0 kip = 4.45 kN, 1.0 ft-kip = 1.36 kN-m.

Strength at the bottom story (where P, V and M are the greatest) is examined. This example considers Load Combination 2 from Table 10.2.19 to be the governing case, because it has the same lateral load as Load Combination 1 but lower values of axial force.

Refer to Figure 10.2-13 for notation and dimensions.

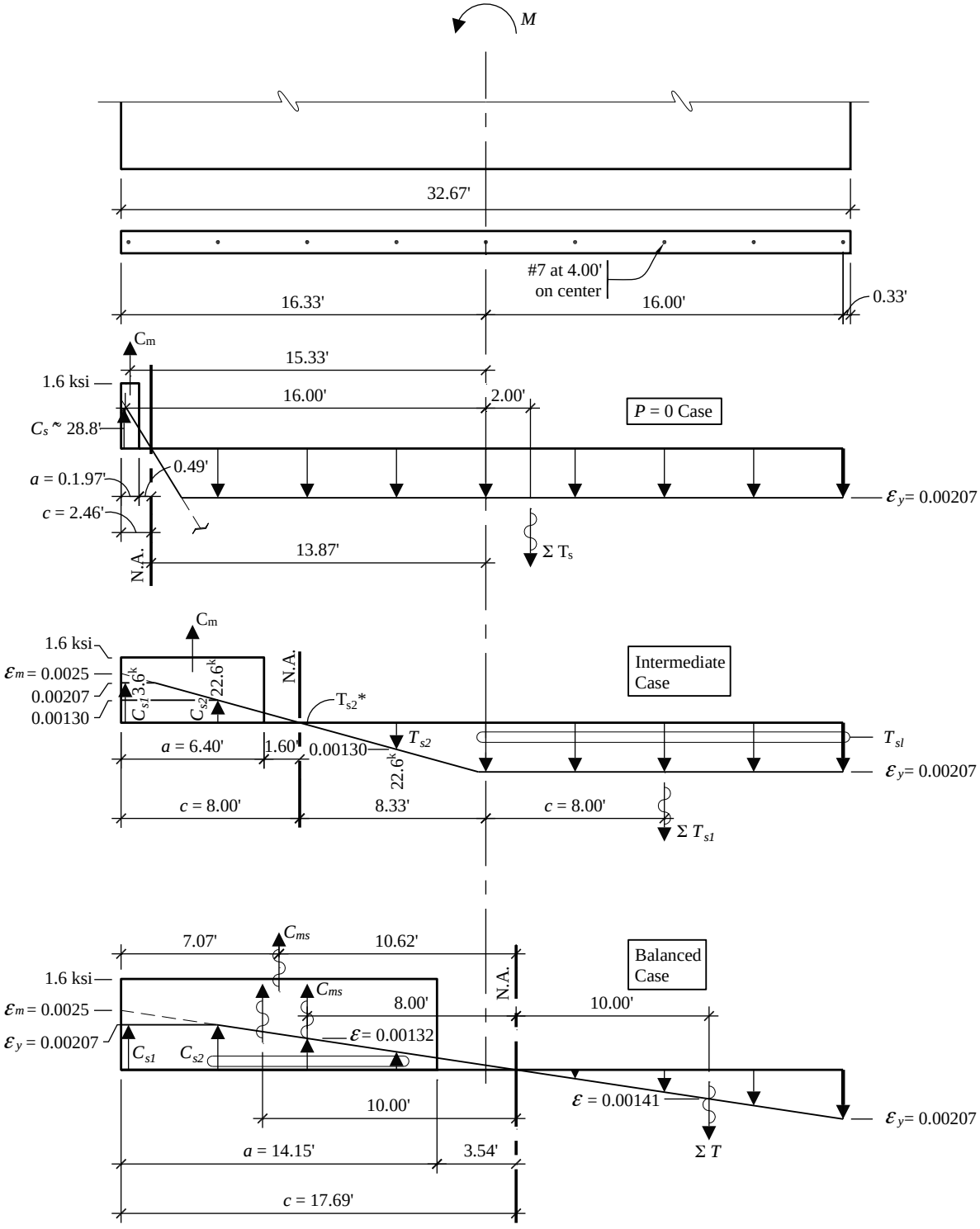

Figure 10.2-13 San Rafael: Strength of Wall D
Strength diagrams superimposed on strain diagrams for the three cases.
(1.0 ft = 0.3048 m)

Examine the strength of Wall D at Level 1:

- $P_{u_{min}}$ = 232 kips
- $P_{u_{max}}$ = 463 kips
- M_u = 6,320 ft-kips

Because special reinforced masonry shear walls are used (Seismic Design Category D), vertical reinforcement at 4 feet on center and horizontal bond beams at 4 feet on center are prescribed (TMS 402, Sec. 1.14.2.2.5). For this bending moment, the #5 bars at 4'-0" on center used at Birmingham 2 will not suffice (refer to the ϕP_n - ϕM_n diagram for Birmingham 2 in Figure 10.2-10). It is desirable to keep the reinforcement to as small an amount as necessary in order to keep ϕM_n relatively low, in order to keep the required shear capacity down when the check for shear corresponding to $1.25\phi M_n$ is made.

The calculation procedure is similar to that presented in Section 10.2.4.5.2. The strain and stress diagrams are shown in Figure 10.2-14 and the results are as follows:

- P = 0 case:

  ϕP_n = 0

  ϕM_n = 4,492 ft-kips

- Intermediate case (setting c = 8.0 ft):

  ϕP_n = 265 kips

  ϕM_n = 7,261 ft-kips

- Balanced case:

  ϕP_n = 852 kips

  ϕM_n = 10,364 ft-kips

The simplified ϕP_n - ϕM_n curve is shown in Figure 10.2-14 and indicates that the design with nine #7 bars is satisfactory.

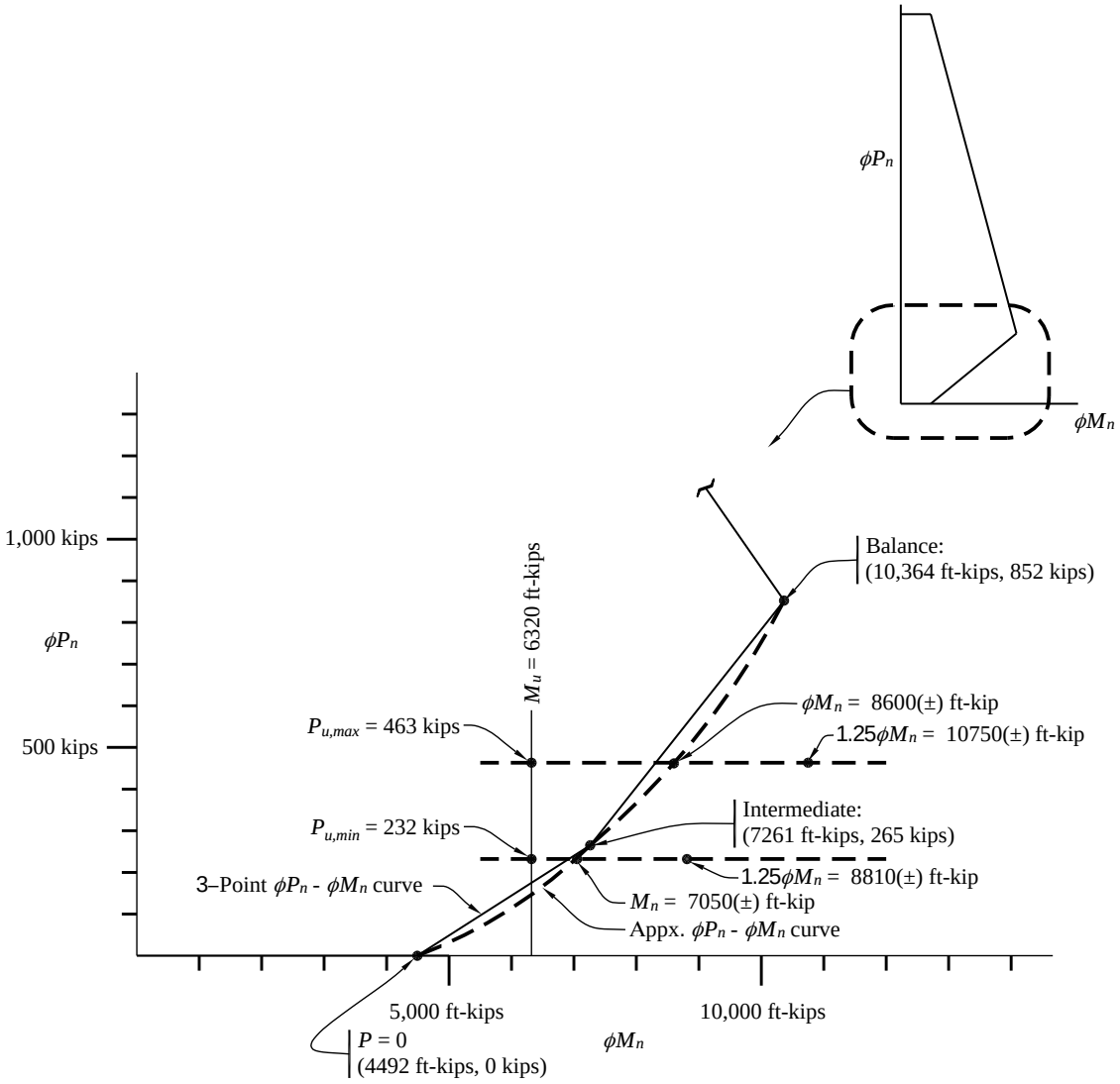

Figure 10.2-14 ϕP_n - ϕM_n Diagram for San Rafael Wall D
(1.0 kip = 4.45 kN, 1.0 kip-ft = 1.36 kN-m)

10.2.7.5.2.2 Ductility check. TMS 402 Section 3.3.3.5.4 is illustrated in the prior designs. Recall that this calculation uses factored gravity axial loads (based on the *Standard*) to result in the minimum P_u value instead of load combination $D + 0.75L + 0.525Q_E$ per TMS 402 Section 3.3.3.5.1.d. Refer to Figure 10.2-15 and the following calculations which illustrate this using loads at the bottom story (highest axial loads). The extra grout required for shear is also ignored here. More grout gives higher compression capacity, which is conservative.

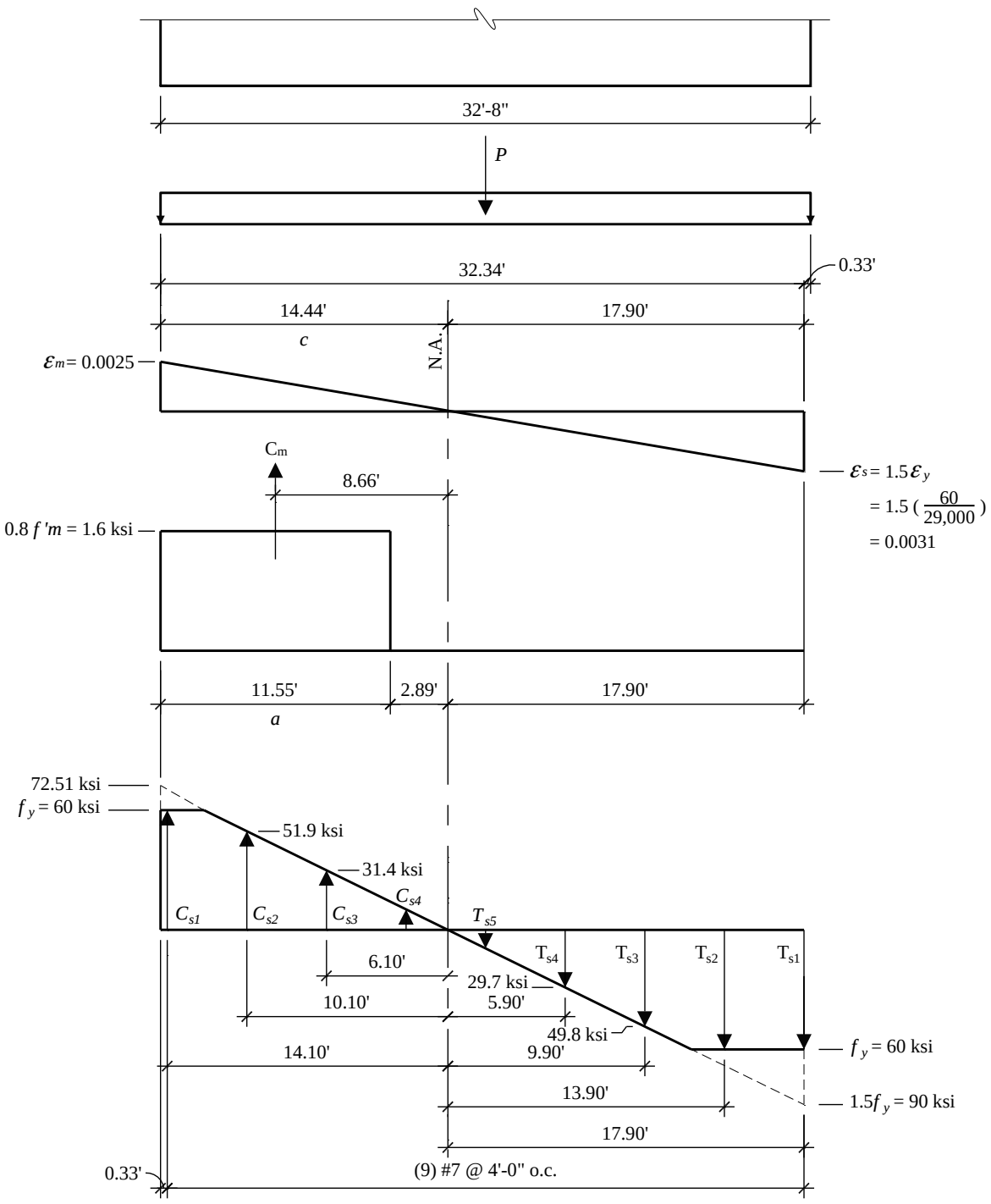

Figure 10.2-15 Ductility Check for San Rafael Wall D
(1.0 ft = 0.3048 m, 1.0 ksi = 6.89 MPa)

For Level 1 (the bottom story), the unfactored loads are as follows:

P = 331 kips

$C_m = 0.8f'_m[(2.5 \text{ in.})(11.55 \text{ ft})(12) + (3 \text{ cells})(41 \text{ in.}^2)] = 751$ kips

$C_{s1} = (0.60 \text{ in.}^2)(60 \text{ ksi}) = 36$ kips

$C_{s2} = (0.60 \text{ in.}^2)(51.9 \text{ ksi}) = 31$ kips

$C_{s3} = (0.60 \text{ in.}^2)(31.4 \text{ ksi}) = 19$ kips

C_{s4} is neglected.

$\sum C = 837$ kips

$T_{s1} = T_{s2} = (0.60 \text{ in.}^2)(60 \text{ ksi}) = 36$ kips

$T_{s3} = (0.60 \text{ in.}^2)(49.8 \text{ ksi}) = 30$ kips

$T_{s4} = (0.60 \text{ in.}^2)(18 \text{ ksi}) = 18$ kips

T_{s5} is neglected.

$\sum T = 120$ kips

$\sum C > \sum P + T$

837 kips > 451kips OK

The compression capacity is larger than the tension capacity, so ductile failure is assured. The maximum area of flexural tensile reinforcement requirement of TMS 402 Section 3.3.3.5 is satisfied.

10.2.7.5.3 Check for Shear Corresponding to $1.25\phi M_n$. From Figure 10.2-14, values for $1.25\phi M_n$ can be obtained:

- Load Combination 1:

  P_u max = 463 kips

  $1.25\phi M_n = 10{,}750$ ft-kips

- Load Combination 2:

  P_u min = 232 kips

  $1.25\phi M_n = 8{,}810$ ft-kips

Both cases need to be checked. As our example focuses on Load Combination 2, only that case is discussed below.

$$1.25\left(\frac{M_n}{M_u}\right) = 1.25\frac{\left(\frac{8810}{0.9}\right)}{6320} = 1.94$$, which is less than the 2.5 upper bound.

Therefore, the shear demand is 1.94 times the value from analysis. Referring to Table 10.2-18, V_u = (1.94)(201 kips) = 390 kips > 198 kips = ϕV_n. There is more shear demand than allowed; this can be addressed by adding grouted cells.

$$\text{Additional grouted cells} = \left(\frac{390 - 198}{(1.6 \text{ ksi})(41 \text{ in.}^2/\text{cell})}\right) = 2.9 \text{ cells}$$

If the two cells adjacent to the end cells of the wall are grouted (for a total of four additional grouted cells), the shear requirement is satisfied. The additional grout will add to the building weight slightly. The authors recommend that another design iteration be performed to address significant increases in building weight; however, another iteration is not presented here. Note that the above shear check is just for Load Combination 2. Load Combination 1 also needs to be checked; it may necessitate even more grouted cells.

10.2.7.6 San Rafael deflections. Recall the assertion that the calculations for deflection involve many variables and assumptions and that any calculation of deflection is approximate at best. The requirements and procedures for computing deflection are provided in Section 10.2.4.6.

For the San Rafael building, the determination of whether the walls will be cracked is as follows:

b_e = effective masonry wall width

b_e = [(2 × 1.25 in.)(32.67 ft × 12) + (13 cells)(41 in.^{2}/cell)]/32.67 ft × 12) = 3.86 in.

$A_n = b_e\, l$ = (3.86 in.)(32.67 × 12) = 1513 in.^{2}

$S = b_e\, l^2/6$ = (3.86)(32.67 × 12)^2/6 = 98,877 in.^{3}

f_r = 0.063(36 cells/49 cells) + 1.63(13 cells/49 cells) = 0.090 ksi

P_u is calculated using 1.00D (see Table 10.2-19 for values and refer to Section 10.2.4.6 for discussion). Table 10.2-20 provides a summary of these calculations. (The extra grout required for shear strength is also not considered here; the revision would reduce slightly the computed deflections by raising the cracking moment.)

Table 10.2-20 San Rafael Cracked Wall Determination

Level	$P_{u_{min}}$ (kips)	M_{cr} (ft-kips)	M_x (ft-kips)	Status
5	66	1101	540	Uncracked
4	132	1460	1563	Cracked
3	198	1820	2948	Cracked
2	265	2185	4574	Cracked
1	331	2544	6320	Cracked

1.0 kip = 4.45 kN, 1.0 ft-kip = 1.36 kN-m.

For the uncracked wall:

$In. = I_g = b_e l^3/12 = (3.86 \text{ in.})(32.67 \times 12)^3/12 = 1.94 \times 10^7 \text{ in.}^4$

As in the three previous examples, I_{cr} will be taken as $0.35I_g$ for the wall deflection calculation.

For this example, the deflection computation instead will use the cracked moment of inertia in the lower two stories and the gross moment of inertia in the upper three stories. The results from a RISA 2D analysis, in which both flexural and shear deflections are included, are shown in Table 10.2-21 and are approximately 50 percent higher than the use of I_{eff} over the full height.

Table 10.2-21 San Rafael Deflections

Level	F (kips)	I_{eff} (in.^{4})	$\delta_{flexural}$ (in.)	δ_{shear} (in.)	δ_{total} (in.)	$C_d\,\delta_{total}$ (in.)	Δ (in.)
5	62.3	1.94×10^7	0.431	0.067	0.498	1.743	0.406
4	55.8	0.679×10^7	0.321	0.062	0.382	1.337	0.420
3	41.7	0.679×10^7	0.212	0.050	0.262	0.917	0.409
2	27.8	0.679×10^7	0.110	0.035	0.145	0.508	0.336
1	13.9	0.679×10^7	0.030	0.019	0.049	0.172	0.172

kip = 4.45 kN, 1.0 in. = 25.4 mm.

$F = F_x$ for level (from Table 10.2-17) × 0.158

The maximum drift occurs at Level 4; per *Provisions* Table 5.2.8 it is:

$\Delta = 0.420 \text{ in.} < 1.04 \text{ in.} = 0.01h_n$ (*Standard* Table 12.12-1**)** OK

10.2.7.7 San Rafael out-of-plane forces

Standard Section 12.11 requires that bearing walls be designed for out-of-plane loads determined as follows:

$w = 0.40\, S_{DS}\, I W_w \geq 0.1 W_w$

$w = (0.40)(1.00)(1)(60 \text{ psf}) = 24\text{psf} \geq 6.0 \text{ psf} = 0.1W_w$

The out-of-plane bending moment, using the strength design method for masonry, for the pressure w =24 psf and considering the *P*-delta effect, is computed to be 2,232 in.-lb/ft. This compares to a computed strength of the wall of 30,000 in.-lb/ft, considering the #7 bars at 4 feet on center. Thus, the wall is loaded to approximately 7 percent of its capacity in flexure in the out-of-plane direction. (See Section 10.1.5.2.5 for a more detailed discussion of strength design of masonry walls, including the *P-delta* effect.)

10.2.7.8 San Rafael orthogonal effects According to *Standard* Section 12.5.3, orthogonal interaction effects have to be considered for Seismic Design Category D where the ELF procedure is used (as it is here).

The out-of-plane effect is 7 percent of capacity, as discussed in Section 10.2.7.7. Where considering the 0.3 combination factor, the out-of-plane action adds approximately 2 percent overall to the interaction effect. For the lowest story of the wall, this could conceivably require a slight increase in capacity for in-plane actions. In the authors' opinion, this is on the fringe of requiring real consideration (in contrast to the end walls of Example 10.1).

This completes the design of the transverse Wall D.

10.2.7.9 Summary of San Rafael Wall D

- 8-inch CMU
- f'_m = 2,000 psi
- Reinforcement:

  Vertical #7 bars at 4 feet on center at intermediate cells.

  Two bond beams with two #5 bars at each story, at floor bearing and at 4 feet above each floor.

  Horizontal joint reinforcement at alternate courses recommended but not required.

- Grout:

  All cells with reinforcement and bond beams, plus grout at four additional cells.

10.2.8 Summary of Wall D Design for All Four Locations

Table 10.2-22 compares the reinforcement and grout for Wall D designed for each of the four locations.

Table 10.2-22 Variation in Reinforcement and Grout by Location for Wall D

	Birmingham 1	Albuquerque	Birmingham 2	San Rafael
Vertical bars	5 - #4	9 - #4	9 - #5	9 - #7
Horizontal bars	10 - #4 + jt. reinf.	10 - #4 + jt. reinf.	20 - #5	20 - #5
Grout (cu. ft)	91	122	152	162

1 cu. ft = 0.0283 m^3.

11

Wood Design

Peter W. Somers, P.E., S.E.

Contents

11.1 THREE-STORY WOOD APARTMENT BUILDING, SEATTLE, WASHINGTON 3
11.1.1 Building Description.....3
11.1.2 Basic Requirements 6
11.1.3 Seismic Force Analysis.....9
11.1.4 Basic Proportioning 11
11.2 WAREHOUSE WITH MASONRY WALLS AND WOOD ROOF, LOS ANGELES, CALIFORNIA.....30
11.2.1 Building Description.....30
11.2.2 Basic Requirements 31
11.2.3 Seismic Force Analysis.....33
11.2.4 Basic Proportioning of Diaphragm Elements 34

This chapter examines the design of a variety of wood building elements. Section 11.1 features a three-story, wood-frame apartment building. Section 11.2 illustrates the design of the roof diaphragm and wall-to-roof anchorage for the masonry building featured in Section 10.1. In both cases, only those portions of the designs necessary to illustrate specific points are included.

Typically, the weak link in wood systems is the wood strength at the connections, but the desired ductility must be developed by means of these connections. Wood members have some ductility in compression (particularly perpendicular to grain) but little in tension. Nailed plywood shear panels develop considerable ductility through yielding of nails and crushing of wood adjacent to nails. Because wood structures are composed of many elements that must act as a whole, the connections must be considered carefully to ensure that the load path is complete. Tying the structure together is essential to good earthquake-resistant construction.

Wood elements often are used in low-rise masonry and concrete buildings. The same basic principles apply to the design of wood elements, but certain aspects of the design (for example, wall-to-diaphragm anchorage) are more critical in mixed systems than in all-wood construction.

Wood structural panel sheathing is referred to as "plywood" in this chapter. However, sheathing can include plywood and other products, such as oriented-strand board (OSB), that conform to the appropriate materials standards.

The calculations herein are intended to provide a reference for the direct application of the design requirements presented in the 2009 *NEHRP Recommended Provisions* (hereafter, the *Provisions*) and its primary reference document, ASCE 7-05 *Minimum Design Loads for Buildings and Other Structures* (hereafter, the *Standard*) and to assist the reader in developing a better understanding of the principles behind the *Provisions* and the *Standard*.

In addition to the *Provisions*, the documents below are referenced in this chapter. Although the *Standard* references the 2005 edition of the AF&PA SDPWS, this chapter utilizes the 2008 edition, which is the more recent, updated version. Note that the 2005 editions of the AF&PA NDS and AF&PA NDS Supplement are the latest versions.

ACI 318	American Concrete Institute. 2008. *Building Code Requirements and Commentary for Structural Concrete.*
ACI 530	American Concrete Institute. 2005. *Building Code Requirements for Masonry Structures.*
ANSI/AITC A190.1	American Institute of Timber Construction. 2002. *Structural Glued-Laminated Timber.*
ASCE 7	American Society of Civil Engineers. 2005. *Minimum Design Loads for Buildings and Other Structures.*
AF&PA Guideline	American Forest & Paper Association 1996. *Manual for Engineered Wood Construction (LRFD), Pre-Engineered Metal Connectors Guideline.*
AF&PA NDS	American Forest & Paper Association. 2005. *National Design Specification.*

AF&PA NDS	American Forest & Paper Association. 2005. *National Supplement Design Specification, Design Values for Wood Construction.*
AF&PA SDPWS	American Forest & Paper Association. 2008. *Special Design Provisions for Wind and Seismic.*
WWPA Rules	Western Wood Products Association. 2005. *Western Lumber Grading Rules.*

11.1 THREE-STORY WOOD APARTMENT BUILDING, SEATTLE, WASHINGTON

This example features a wood-frame building with plywood diaphragms and shear walls.

11.1.1 Building Description

This three-story wood-frame apartment building has a double-loaded central corridor. The building is typical stick-frame construction consisting of wood joists and stud bearing walls supported by a concrete foundation wall and strip footing system. The seismic force-resisting system consists of plywood floor and roof diaphragms and plywood shear walls. Figure 11.1-1 shows a typical floor plan and Figure 11.1-2 shows a longitudinal section and elevation. The building is located in a residential neighborhood a few miles north of downtown Seattle.

The shear walls in the longitudinal direction are located on the exterior faces of the building and along the corridor. The entire solid (non-glazed) area of the exterior walls has plywood sheathing, but only a portion of the corridor walls will require sheathing. In the transverse direction, the end walls and one line of interior shear walls provide lateral resistance. It should be noted that while plywood sheathing generally is used at the exterior walls for reasons beyond just lateral load resistance, the interior longitudinal (corridor) and transverse shear walls could be designed using gypsum wallboard as permitted by AF&PA SDPWS Section 4.3.7.5. However, the corridor shear walls are not included in this example and the interior transverse walls are designed using plywood sheathing, largely due to the required shear capacity.

The floor and roof systems consist of wood joists supported on bearing walls at the perimeter of the building, the corridor lines, plus one post-and-beam line running through each bank of apartments. Exterior walls are framed with 2×6 studs for the full height of the building to accommodate insulation. Interior bearing walls require 2×6 or 3×4 studs on the corridor line up to the second floor and 2×4 studs above the second floor. Apartment party walls are not load-bearing; however, they are double walls and are constructed of staggered 2×4 studs at 16 inches on center. Surfaced, dry (seasoned) lumber is used for all framing to minimize shrinkage. Floor framing members are assumed to be composed of Douglas Fir-Larch material and wall framing is Hem-Fir No. 2, as graded by the WWPA Rules. The material and grading of other framing members associated with the lateral design is as indicated in the example. The lightweight concrete floor fill is for sound isolation and is interrupted by the party walls, corridor walls and bearing walls.

The building is founded on interior footing pads, continuous strip footings and concrete foundation walls (Figure 11.1-3). The depth of the footings and the height of the walls are sufficient to provide crawlspace clearance beneath the first floor.

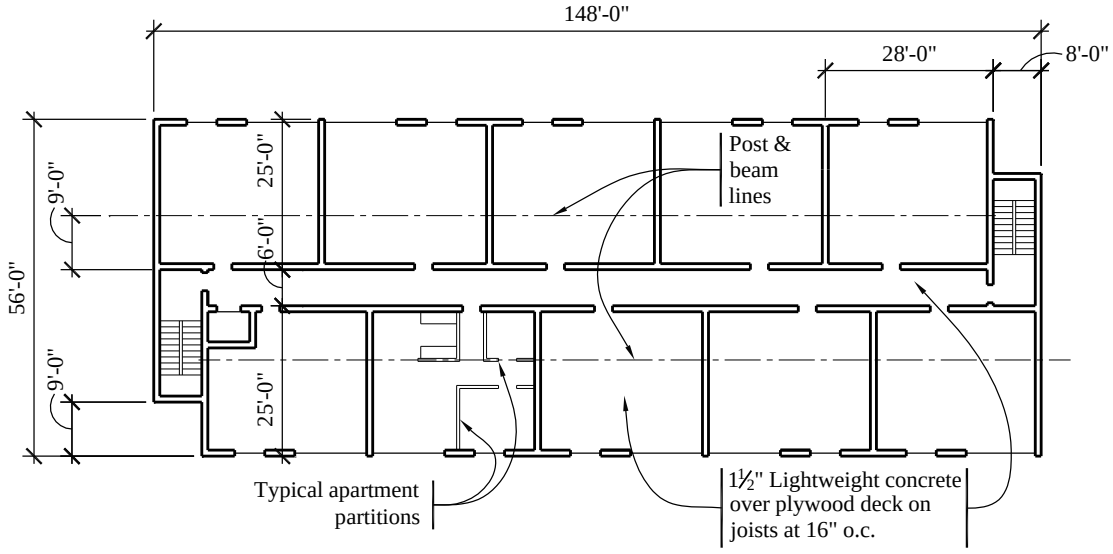

Figure 11.1-1 Typical floor plan
(1.0 ft = 0.3048 m)

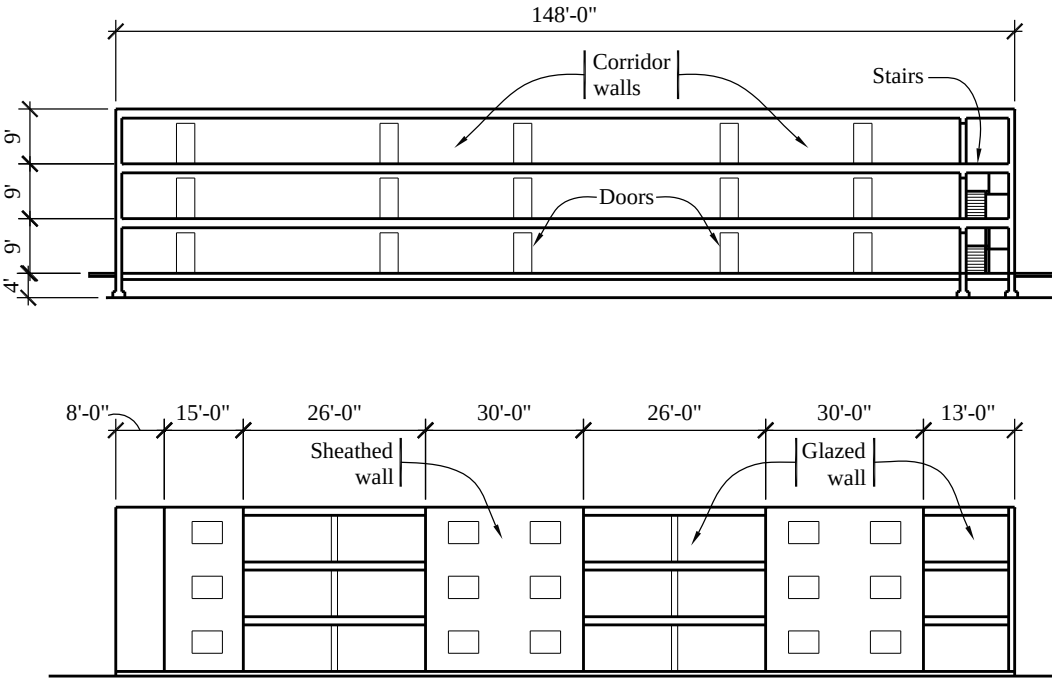

Figure 11.1-2 Longitudinal section and elevation
(1.0 ft = 0.3048 m)

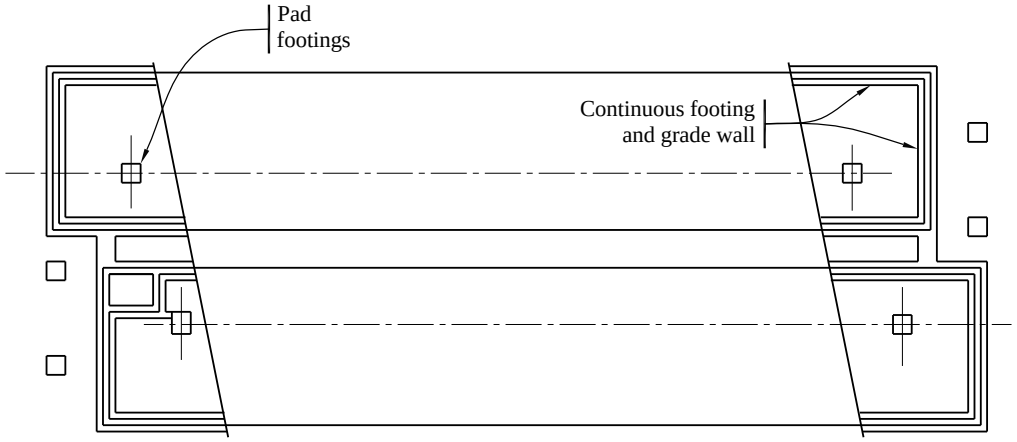

Figure 11.1-3 Foundation plan

11.1.1.1 Scope. In this example, the structure is designed and detailed for forces acting in the transverse and longitudinal directions, including the following:

- Development of seismic loads using the Simplified Alternative Structural Design Criteria (herein referred to as the "simplified procedure") contained in Standard Section 12.14.
- Design and detailing of transverse plywood walls for shear and overturning moment.
- Design and detailing of plywood floor and roof diaphragms.
- Design and detailing of wall and diaphragm chord members.
- Design and detailing of longitudinal plywood walls using the requirements for perforated shear walls.

The simplified procedure, new to the 2005 edition of the *Standard*, is permitted for relatively short, simple and regular structures utilizing shear walls or braced frames. The seismic analysis and design procedure is much less involved than a building utilizing a seismic force resisting system listed in *Standard* Section 12.2 and analyzed using one of the procedures listed in *Standard* Section 12.6. See Section 11.1.2.2 for a more detailed discussion of what is and is not required for the seismic design. In accordance with *Standard* Section 12.14.1.1, the subject building qualifies for the simplified procedure because of the following attributes:

- Residential occupancy
- Three stories in height
- Bearing wall lateral system
- At least two lines of lateral force-resisting elements in both directions, at least one on each side of the center of mass
- No cantilevered diaphragms or structural irregularities

11.1.2 Basic Requirements

11.1.2.1 Seismic Parameters

Table 11.1-1 Seismic Parameters

Design Parameter	Value
Occupancy Category (*Standard* Sec. 1.5.1)	II
Short-Period Response, S_S	1.34
Site Class (*Standard* Sec. 11.4.2)	D
Seismic Design Category (*Standard* Sec. 11.6)	D
Seismic Force-Resisting System (*Standard* Table 12.14-1)	Wood Structural Panel Shear Walls
Response Modification Coefficient, *R*	6.5

11.1.2.2 Structural Design Criteria

11.1.2.2.1 Ground Motion Parameter. Unlike the typical design procedures in *Standard* Chapter 12, the simplified procedure requires consideration of just one spectral response parameter, S_{DS}. This is because the behavior of short, stiff buildings for which the simplified procedure is permitted will always be governed by short-period response. In accordance with *Standard* Section 12.14.8.1:

$$S_{DS} = 2/3F_aS_S$$

The site coefficient, F_a, can be determined using *Standard* Section 12.14.8.1 with simple default values based on soil type or using *Standard* Table 11.4-1 if the site class is known. Since *Standard* Table 11.4-1 generally will result in more favorable value, that method is used for this example. Using $S_S = 1.34$ and Site Class D, *Standard* Table 11.4-1 lists a short-period site coefficient, F_a, of 1.0. Therefore, in accordance with *Standard* Equation:

$$S_{DS} = 2/3(1.0)(1.34) = 0.89$$

11.1.2.2.2 Seismic Design Category (Standard Sec. 11.6). Where the simplified procedure is used, *Standard* Section 11.6 permits the Seismic Design Category to be determined based on *Standard* Table 11.6-1 only. Based on the Occupancy Category and the design spectral response acceleration parameter, the subject building is assigned to Seismic Design Category D.

11.1.2.2.3 Seismic Force-Resisting Systems (Standard Sec. 12.14.4). See Figure 11.1-4. For both directions, the load path for seismic loading consists of plywood floor and roof diaphragms and plywood shear walls. Because the lightweight concrete floor topping is discontinuous at each partition and wall, it is not considered to be a structural diaphragm. In accordance with *Standard* Table 12.14-1, building has a bearing wall system comprised of light-framed walls sheathed with wood structural panels. The response modification factor, *R*, is 6.5 for both directions.

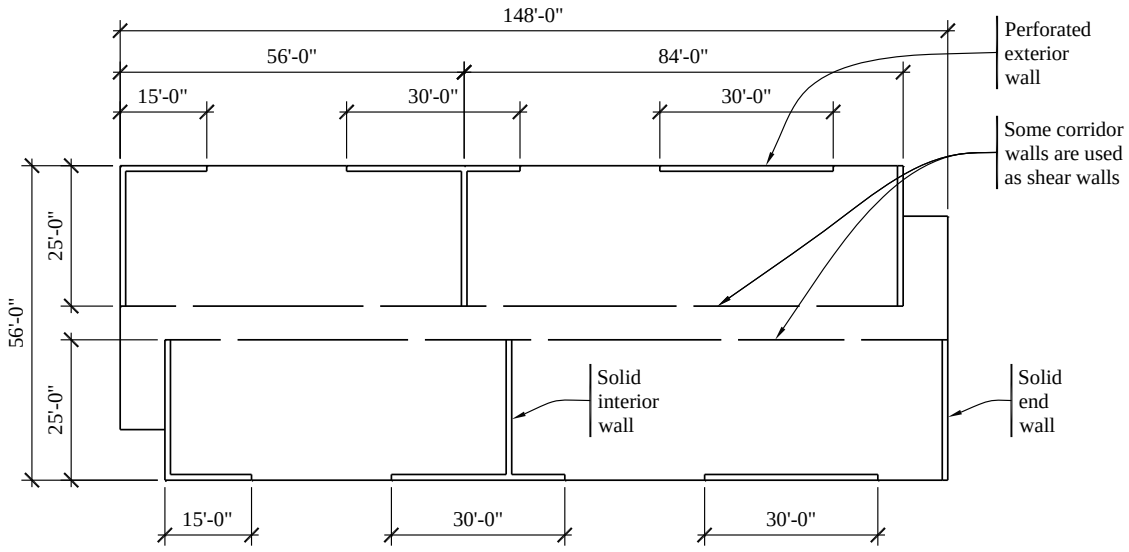

Figure 11.1-4 Load path and shear walls
(1.0 ft = 0.3048 m)

11.1.2.2.4 Diaphragm Flexibility (Standard Sec. 12.14.5). *Standard* Section 12.14.5 defines a diaphragm comprised of wood structural panels as flexible. Because the lightweight concrete floor topping is discontinuous at each partition and wall, it is not considered to be a structural diaphragm.

11.1.2.2.5 Application of Loading (Standard Sec. 12.14.6). For the simplified procedure, seismic loads are permitted to be applied independently in two orthogonal directions.

11.1.2.2.6 Design and Detailing Requirements (Standard Sec. 12.14.7). The plywood diaphragms are designed for the forces prescribed in *Standard* Section 12.14.7.4. The design of foundations is per *Standard* Section 12.13 and wood design requirements are based on *Standard* Section 14.4 as discussed in greater detail below. This example does not require any collector elements (*Standard* Sec. 12.14.7.3).

11.1.2.2.7 Analysis Procedure (Standard Sec. 12.14.8). For the simplified procedure, only one analysis procedure is specified and it is described in greater detail in Section 11.1.3.1 below.

11.1.2.2.8 Drift Limits (Standard Sec. 12.14.8.5). Where the simplified procedure is used, there are not any specific drift limitations because the types of structures for which the simplified procedure is applicable are generally not drift-sensitive. As specified in *Standard* Section 12.14.8.5, if a determination of expected drift is required (for the design of cladding for example), then drift is permitted to be computed as 1 percent of the building height unless a more detailed analysis is performed.

11.1.2.2.9 Combination of Load Effects (Standard Sec. 12.14.3). The basic design load combinations are as stipulated in *Standard* Chapter 2 as modified by the *Standard* Sec. 12.14.3.1.3. Seismic load effects according to the *Standard* Equations 12.14-5 and 12.14-6 are as follows:

$$E = Q_E + 0.2S_{DS}D$$

$$E = Q_E - 0.2S_{DS}D$$

where seismic and gravity are additive and counteractive, respectively.

For S_{DS} = 0.89, the design load combinations are as follows:

$(1.2 + 0.2S_{DS})D + 1.0Q_E + 0.5L + 0.2S = 1.38D + 1.0Q_E + 0.5L + 0.2S$

$(0.9 - 0.2S_{DS})D - 1.0Q_E = 0.72D - 1.0Q_E$

Note that there is no redundancy factor for the simplified procedure.

11.1.2.3 Basic Gravity Loads

- Roof:

Table 11.1-2 Roof Gravity Loads

Load Type	Value
Live/Snow Load (in Seattle, snow load governs over roof live load; in other areas this may not be the case)	25 psf
Dead Load (including roofing, sheathing, joists, insulation and gypsum ceiling)	15 psf

- Floor:

Table 11.1-3 Floor Gravity Loads

Load Type	Value
Live Load	40 psf
Dead Load (1-1/2-in. lightweight concrete, sheathing, joists and gypsum ceiling. At first floor, omit ceiling but add insulation.)	20 psf
Interior Partitions and Corridor Walls (8 ft high at 11 psf)	7 psf distributed floor load
Exterior Frame Walls (wood siding, plywood sheathing, 2×6 studs, batt insulation and 5/8-in. gypsum wallboard)	15 psf of wall surface
Exterior Double Glazed Window Wall	9 psf of wall surface
Party Walls (double-stud sound barrier)	15 psf of wall surface
Stairways	20 psf

Typical Footing (10 in. by 1 ft-6 in.) and Stem Wall (10 in. by 4 ft-0 in.)	690 plf
Applicable Seismic Weights at Each Level	
W_{roof} = Area (roof dead load + interior partitions + party walls) + End Walls + Longitudinal Walls	182.8 kips
$W_3 = W_2$ = Area (floor dead load + interior partitions + party walls) + End Walls + Longitudinal Walls	284.2 kips
Effective Total Building Weight, W	751 kips

For modeling the structure, the first floor is assumed to be the seismic base, because the short crawlspace with concrete foundation walls is stiff compared to the superstructure.

11.1.3 Seismic Force Analysis

The analysis is performed manually following a step-by-step procedure for determining the base shear (*Standard* Sec. 12.14.8.1), vertical distribution of forces (*Standard* Sec. 12.14.8.2) and horizontal distribution of forces (*Standard* Sec. 12.14.8.3). For a building with flexible diaphragms, *Standard* Section 12.14.8.3.1 allows the horizontal distribution of forces to be based on tributary areas and accidental torsion need not be considered for the simplified procedure.

11.1.3.1 Base Shear Determination. According to *Standard* Equation 12.14-11:

$$V = \frac{FS_{DS}}{R}W$$

Where F = 1.2 for a three-story building, R = 6.5 and W = 751 kips as determined previously. Therefore, the base shear is computed as follows:

$$V = \frac{(1.2)(0.89)}{6.5}(751) = 123.4 \text{ kips (both directions)}$$

11.1.3.2 Vertical Distribution of Forces. Forces are distributed as shown in Figure 11.1-5, where the story forces are calculated according to *Standard* Equation 12.14-12 as follows:

$$F_x = \frac{w_x}{W}V$$

This results in a uniform vertical distribution of forces, where the story force is based on the relative seismic weight of the story with all stories at the same seismic acceleration (as opposed to the triangular or parabolic vertical distribution used in the Equivalent Lateral Force procedure of *Standard* Sec. 12.8)

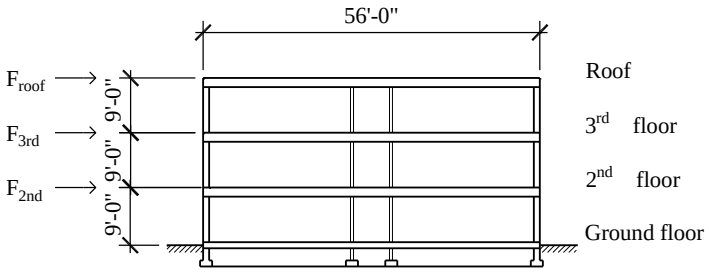

Figure 11.1-5 Vertical shear distribution
(1.0 ft = 0.3048 m)

The story force at each floor is computed as:

F_{roof} = [182.8/751](123.4)	= 30.0 kips
F_{3rd} = [284.2/751](123.4)	= 46.7 kips
F_{2nd} = [284.2/751](123.4)	= 46.7 kips
Σ	= 123.4 kips

11.1.3.3 Horizontal Distribution of Shear Forces to Walls. Since the diaphragms are defined as flexible by *Standard* Section 12.14.5, the horizontal distribution of forces is based on tributary area to the individual shear walls in accordance with *Standard* Section 12.14.8.3.1. For this example, forces are distributed as described below.

11.1.3.3.1 Longitudinal Direction. In this direction, there are four lines of resistance, but only the exterior walls are considered in this example. The total story force tributary to the exterior wall is determined as follows:

$(25/2)/56F_x = 0.223F_x$

The distribution to each individual shear wall segment along this exterior line is discussed in Section 11.1.4.7 below.

11.1.3.3.2 Transverse Direction. Again, based on the flexible diaphragm assumption, force is to be distributed based on tributary area. As shown in Figure 11.1-4, there are three sets of two shear walls, each offset in plan by 8 feet. For the purposes of this example, each set of walls is assumed to be in alignment, resisting the same tributary width. The result is that the building is modeled with a diaphragm consisting of two simple spans, which provides a more reasonable horizontal distribution of force than a pure tributary area distribution.

For a two-span, flexible diaphragm, the central walls will resist one-half of the total load, or $0.50F_x$. The other walls resist story forces in proportion to the width of diaphragm between them and the central walls. The left set of walls in Figure 11.1-4 resists $(60/2)/148F_x = 0.203F_x$ and the right set resists $(88/2)/148F_x = 0.297F_x$, where 60 feet and 88 feet represent the dimension from the ends of the building to the centroid of the two central walls. Note that this does not exactly match the existing diaphragm spans, but is a reasonable simplification to account for the three sets of offset shear walls at the ends and middle of the building.

11.1.3.4 Diaphragm Design Forces. As specified in *Standard* Section 12.14.7.4, the design forces for floor and roof diaphragms are the same forces as computed for the vertical distribution in Section 11.1.3.2 above plus any force due to offset walls (not applicable for this example).

The weight tributary to the diaphragm, w_{px}, need not include the weight of walls parallel to the force. For this example, however, since the shear walls in both directions are relatively light compared to the total tributary diaphragm weight, the diaphragm force is computed based on the total story weight, for convenience. Therefore, the diaphragm forces are exactly the same as the story forces shown above.

11.1.4 Basic Proportioning

Designing a plywood diaphragm and plywood shear wall building principally involves the determination of sheathing thicknesses and nailing patterns to accommodate the applied loads. This is especially the case where the simplified procedure is utilized, since there are not any deflection checks and possible subsequent design iterations.

In addition to the wall and diaphragm design, this design example features framing member and connection design for elements including shear wall end posts and hold-downs, foundation anchorage and diaphragm chords.

Nailing patterns in diaphragms and shear walls have been established on the basis of tabulated requirements included in the AF&PA SDPWS. It is important to consider the framing requirements for a given nailing pattern and capacity as indicated in the notes following the tables. In addition to strength requirements, AF&PA SDPWS Section 4.2.4 places aspect ratio limits on plywood diaphragms (length/width must not exceed 4/1 for blocked diaphragms) and AF&PA SDPWS Section 4.3.4 places similar limits on shear walls (height/width must not exceed 2/1 for full design capacities).

11.1.4.1 Strength of Members and Connections. The *Standard* references the AF&PA NDS and AF&PA SDPWS for engineered wood structures. These reference standards support both Allowable Stress Design (ASD) and Load and Resistance Factor Design (LRFD) as permitted by the *Standard*. For this example, LRFD is utilized. The AF&PA NDS and AF&PA Supplement contains the material design values for framing members and connections, while the AF&PA SDPWS contains the diaphragm and shear wall tables as well as detailing requirements for shear wall and diaphragm systems.

Throughout this example, the resistance of members and connections subjected to seismic forces, acting alone or in combination with other prescribed loads, is determined in accordance with the AF&PA NDS and AF&PA SDPWS. The methodology is somewhat different between the AF&PA NDS for framing members and connections and the AF&PA SDPWS for shear walls and diaphragms.

For framing members and connections, the AF&PA NDS incorporates the notation F_b, F_t, Z, etc., for reference design values, which are then modified using standard wood adjustment factors, C_M, C_r, C_F, etc. (used for both ASD and LRFD) and then for LRFD are modified by a format conversion factor, K_F, a resistance factor, ϕ and a time effect factor, λ, to compute an adjusted design resistance, F_b', F_t', Z'. These factors are defined in AF&PA NDS Appendix N.

For shear walls and diaphragms, the AF&PA SDPWS contains tabulated unit shear values, v_s, which are multiplied by a resistance factor, ϕ_D, equal to 0.8. This is the only modification to the tabulated design values since this building utilizes Douglas Fir Larch framing. Additional modification would be required for other species in accordance with the footnotes to the tabular values in the AF&PA SDPWS.

For pre-engineered connection elements, the AF&PA NDS does not contain a procedure for converting the manufacturer's cataloged values (typically as ASD values) to LRFD. However, such a procedure is contained in a guideline published with the 1996 edition of the LRFD wood standard (AF&PA Guideline). The AF&PA Guideline contains a method for converting allowable stress design values for cataloged metal connection hardware (for example, tie-down anchors) into ultimate capacities for use with strength design. The procedure, which is used for this example, can generally be described as taking the catalog ASD value, multiplying by 2.88 and dividing the by the load duration factor on which the cataloged value is based (typically 1.33 or 1.60 for pre-engineered connection hardware often used for wind or seismic design).

11.1.4.2 Transverse Shear Walls. The design will focus on the more highly loaded interior walls; the end walls would be designed in a similar manner.

11.1.4.2.1 Load to Interior Transverse Walls. As computed in Section 11.1.3.3.2, the total story force resisted by the central walls is $0.50F_x$. Since the both walls are the same length and material, each individual wall will resist one-half of the total or $0.25F_x$. Therefore:

F_{roof} = 0.25(30.0)	= 7.50 kips
F_{3rd} = 0.25(46.7)	= 11.68 kips
F_{2nd} = 0.25(26.7)	= 11.68 kips
Σ	= 30.86 kips

The story forces and story shears resisted by the individual wall segment is illustrated in Figure 11.1-6.

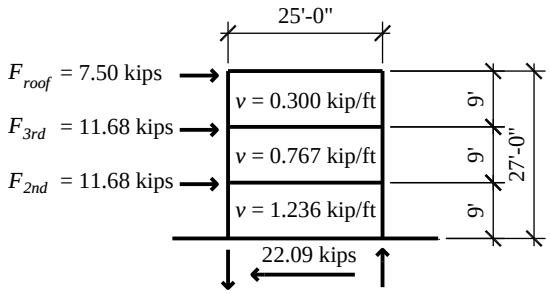

Figure 11.1-6 Transverse section: end wall
(1.0 ft = 0.3048 m, 1.0 kip = 4.45 kN, 1.0 kip/ft = 14.6 kN/m)

11.1.4.2.2 Roof to Third Floor

V = 7.50 kips

v = 7.50/25 = 0.300 klf

Try a 1/2-inch (15/32) plywood rated sheathing (not Structural I) on blocked 2× Hem-Fir members at 16 inches on center with 8d common nails at 6 inches on center at panel edges and 12 inches on center at intermediate framing members. From AF&PA SDPWS Table 4.3A, this shear wall assembly has a nominal unit shear capacity, v_s, of 0.520 klf. However, according to Note 3 of AF&PA SDPWS Table 4.3A, the design shear resistance values are for Douglas Fir-Larch or Southern Pine and must be adjusted for Hem-Fir wall framing. The specific gravity adjustment factor equals 1-(0.5-SG) where SG is

the specific gravity of the framing lumber. From AF&PA NDS Table 11.3.2A, the SG for Hem-Fir is 0.43. Therefore, the adjustment factor is 1-(0.5-0.43) = 0.93. The adjusted shear capacity is computed as follows:

$0.93\phi_D v_s = 0.93(0.8)(0.520) = 0.387$ klf > 0.300 klf OK

While 3/8- or 7/16-inch plywood could be used at this level, 1/2-inch is used for consistency with the lower floors.

11.1.4.2.3 Third Floor to Second Floor

$V = 7.50 + 11.68 = 19.18$ kips

$v = 19.18/25 = 0.767$ klf

Try 1/2-inch (15/32) plywood rated sheathing (not Structural I) on blocked 2× Hem-Fir members at 16 inches on center with 10d nails at 3 inches on center at panel edges and at 12 inches on center at intermediate framing members. From AF&PA SDPWS Table 4.3A, this shear wall assembly has a nominal unit shear capacity, v_s, of 1.200 klf. The adjusted shear capacity is computed as follows:

$0.93\phi_D v_s = 0.93(0.8)(1.200) = 0.893$ klf > 0.767 klf OK

For this shear wall assembly, the width of framing at panel edges needs to be checked relative to AF&PA SDPWS Section 4.3.7.1. In accordance with Item 4 of that section, 3× framing is required at adjoining panel edges since the wall has 10d nails spaced at 3 inches or less and because the unit shear capacity exceeds 0.700 klf for a building assigned to Seismic Design Category D.

However, an exception to this section permits double 2× framing to be substituted for the 3× member, provided that the 2× framing is adequately stitched together. Since the double 2× framing is often preferred over the 3× member, this procedure will be utilized for this example. The exception requires the double 2× members to be connected to "transfer the induced shear between members." For the purposes of this example, the induced shear along the vertical plane between adjacent panels will assumed to be equal to the adjusted design shear of 0.893 klf.

Using 16d common wire nails and 2× Hem-Fir framing, AF&PA NDS Table 11N specifies a lateral design value, *Z*, of 0.122 kips per nail. The adjusted design capacity is:

$Z' = ZK_F\phi\lambda = (0.122)(2.16/0.65)(0.65) = 0.264$ kips per nail

and the number of nails per foot is 0.893/0.264 = 3.4, so provide 4 nails per foot. Therefore, use double 2× framing at panel edges fastened with 16d at 3 inches on center and staggered (as required by the exception where the nail spacing is less than 4 inches).

11.1.4.2.4 Second Floor to First Floor

19.18 + 11.68 = 30.86 kips

$v = 30.86/25 = 1.236$ klf

Try 5/8-inch (19/32) plywood rated sheathing (not Structural I) on blocked 2-inch Hem-Fir members at 16 inches on center with 10d common nails at 2 inches on center at panel edges and 12 inches on center at

intermediate framing members. From AF&PA SDPWS Table 4.3A, this shear wall assembly has a nominal unit shear capacity, v_s, of 1.740 klf. The adjusted shear capacity is computed as follows:

$0.93\phi_D v_s = 0.93(0.8)(1.740) = 1.294 \text{ klf} > 1.236 \text{ klf}$ OK

This shear wall assembly also requires 3× or stitched double 2× framing at panel edges. In this case, 3× framing is recommended, since the tight nail spacing required to stitch the double 2× members could lead to splitting and bolts or lag screws would not be economical.

Rather than increasing the plywood thickness at this level, adequate capacity could be achieved by using Douglas Fir-Larch framing members or using 1/2-inch plywood on both sides of the shear wall framing.

11.1.4.3 Transverse Shear Wall Anchorage. AF&PA SDPWS Section 4.3.6.4.2 requires tie-down (hold-down) anchorage at the ends of shear walls where net uplift is induced. Net uplift is computed as the combination of the seismic overturning moment and the dead load counter-balancing moment using the load combination $0.72D - 1.0Q_E$.

The design requirements for the shear wall end posts and tie-downs have evolved over the past several code cycles. The 2008 AF&PA SDPWS requires the tie-down devices (Sec. 4.3.6.4.2) and end posts (Sec. 4.3.6.1.1) to be designed for a tension or compression force equal to the induced unit shear multiplied by the shear wall height. It can be inferred from AF&PA SDPWS Figure 4E, that the shear wall height, h, refers to the sheathing height and not the story height, since the end post load is a function of the length of shear wall sheathing that engages the end post.

11.1.4.3.1 Tie-down Anchors at Third Floor. For the typical 25-foot interior wall segment, the overturning moment at the third floor is:

$M_0 = 9(7.50) = 67.5 \text{ ft-kip} = Q_E$

For the counter-balancing moment, it is assumed that the interior transverse walls will engage a certain length of exterior and corridor bearing wall for uplift resistance. The width of floor is taken as the length of solid wall panel at the exterior, or 10 feet. See Figures 11.1-1 and 11.1-13. For convenience, the same length is used for the longitudinal walls. The designer should take care to assume a reasonable amount of tributary dead loads that can be engaged considering the connections and stiffness of the cross wall elements. In this situation, considering that the exterior and corridor walls are plywood-sheathed shear walls, the assumption noted above is considered reasonable.

The weight of interior wall, 11 psf, is used for both conditions.

Shear wall self weight = (9 ft)(25 ft)(11 psf)/1,000	= 2.47 kips
Tributary floor = (10 ft)(25 ft)(15 psf)/1,000	= 3.75 kips
Tributary longitudinal walls = (9 ft)(10 ft)(11 psf)(2)/1,000	= 1.98 kips
Σ	= 8.20 kips

$0.72Q_D = 0.72(8.20)(12.5) = 73.8 \text{ ft-kip}$

Since the dead load stabilizing moment exceeds the overturning moment, uplift anchorage is not required at the third floor. An end post for shear wall boundary compression is required, but since the design is similar to the second floor end post, it is not illustrated here.

11.1.4.3.2 Tie-down Anchors at Second Floor

The overturning moment at the second floor is:

M_0 = 18(7.50) + 9(11.68) = 240 ft-kip

The counter-balancing moment is computed using the same assumptions as for the third floor.

Shear wall self weight = (18 ft)(25 ft)(11 psf)/1,000	= 4.95 kips
Tributary floor = (10 ft)(25 ft)(15 psf)(2)/1,000	= 7.50 kips
Tributary longitudinal walls = (18 ft)(10 ft)(11 psf)(2)/1,000	= 3.96 kips
Σ	= 16.41 kips

$0.72Q_D$ = 0.72(16.41)(12.5) = 148 ft-kips

M_0 (net) = 240 - 148 = 92 ft-kips

As would be expected, uplift anchorage is required.

As described above, the design uplift force is computed using a unit shear demand of 0.768 klf at the second floor and a net length of wall height equal to 8 feet. Note that 8 feet is appropriate for this calculation given the detailing for this structure. As shown in Figure 11.1-10, the plywood sheathing is not detailed as continuous across the floor framing, which results in a net sheathing height of approximately 8 feet. If the sheathing were detailed across the floor framing, then 9 feet would be the appropriate wall height for use in computing tie-down demands. Since there is no net uplift force at the third floor, the third floor load need not be considered. Therefore, the design uplift force at the second floor is:

T = 0.768 klf (8 ft) = 6.14 kips

Note that this uplift force exceeds the forces determined using the net overturning moment, which would be equal to 92 ft-kips / 25 ft = 3.68 kips, thus providing the intended added level of conservatism for the end posts and tie-downs.

Use a double tie-down anchor to connect the end posts. For ease of construction, select a tie-down device that screws to the end post. See Figure 11.1-7. A tie-down with a 5/8-inch threaded rod and fourteen 1/4-inch screws has a cataloged ASD capacity of 5.645 kips for Douglas Fir-Larch framing based on a load duration factor of 1.6. Using the AF&PA Guideline procedure for pre-engineered connections described in Section 11.1.4.1 (K_F = 2.88/1.60), the LRFD capacity is determined as follows:

$ZK_F\phi\lambda$ = (5.645)(2.88/1.60)(0.65)(1.0) = 6.60 kips > 6.14 kips OK

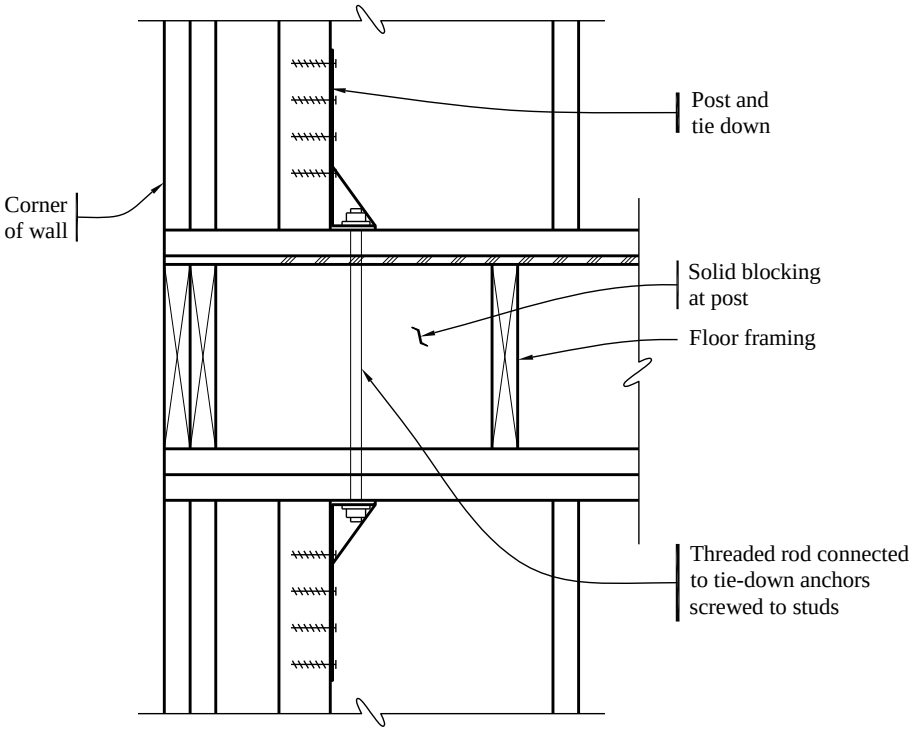

Figure 11.1-7 Shear wall tie down at suspended floor framing

11.1.4.3.3 Tie-down Anchors at First Floor. The overturning moment at the first floor is:

$M_0 = 27(7.50) + 18(11.68) + 9(11.68) = 517$ ft-kip $= Q_E$

The counter-balancing moment is computed using the same assumptions as for the second floor.

Shear wall self weight = (27 ft)(25 ft)(11 psf)/1,000	= 7.42 kips
Tributary floor = (10 ft)(25 ft)(15 psf)(3)/1,000	= 11.25 kips
Tributary longitudinal walls = (27 ft)(10 ft)(11 psf)(2)/1,000	= 5.94 kips
Σ	= 24.61 kips

$0.72Q_D = 0.72(24.61)12.5 = 222$ ft-kip

M_0 (net) = 517-222 = 295 ft-kip

As expected, uplift anchorage is required. The design uplift force is computed using a unit shear force of 1.236 klf at the first floor and a net wall height of 8 feet. Combined with the uplift force at the second floor, the total design uplift force at the first floor is:

$T = 6.14$ kips + 1.236 klf (8 ft) = 16.0 kips

Use a double tie-down anchor that extends down into the foundation with an anchor bolt. Tie-downs with a 7/8-inch threaded rod anchor and three 1-inch bolts through a 6×6 Douglas Fir-Larch end post have a

cataloged capacity of 12.1 kips based on a load duration factor of 1.6. The LRFD capacity of two tie downs is computed as follows:

$2ZK_F\phi\lambda$ = 2(12.1)(2.88/1.60)(0.65)(1.0) = 28.3 kips > 16.0 kips OK

Next, check the LRFD capacity of the bolts in double shear. For the three bolts, the AF&PA NDS gives the following equation:

$3ZK_F\phi\lambda$ = 3(5.50)(2.16/0.65)(0.65)(1.0) = 35.6 kips > 16.0 kips OK

The strength of the end post, based on failure across the net section, must also be checked. A reasonable approach to preclude net tension failure from being a limit state would be to provide an end post whose nominal resistance exceeds the nominal strength of the tie-down device. The nominal strength of the first-floor double tie-down is 28.3/0.65 = 43.5 kips. Therefore, the nominal tension capacity at the net section should be greater than 43.5 kips.

Try a 6×6 Douglas Fir-Larch No. 1 end post. Accounting for 1-1/16-inch bolt holes, the net area of the post is 24.4 in^2. Using ϕ = 1.0 for nominal strength, according to the AF&PA NDS Supplement:

$F_t' = F_tK_F\phi\lambda$ = (0.825)(2.16/0.8)(1.0)(1.0) = 2.228 ksi

$T' = F_t'A$ = 2.228(24.4) = 44.5 kips > 54.4 kips OK

Not shown here but for a group of bolts, the row and/or group tear-out capacity must be checked for all bolted connections with multiple fasteners. Refer to AF&PA NDS Section 10.1.2 and Appendix E.

For the maximum compressive load at the end post, combine the maximum gravity load plus the seismic overturning load. However, since the exterior and interior longitudinal walls are load-bearing stud walls, the gravity load demand on the shear wall end post is minimal.

Therefore, without any significant gravity load, the compression force on the end post is the same as the tension force per AF&PA SDPWS Section 4.3.6.1.1 and equal to 16.0 kips at the first floor.

Due to the relatively short clear height of the post, the governing condition is bearing perpendicular to the grain on the bottom plate. Check the bearing of the 6×6 end post on a 3×6 Douglas Fir-Larch No. 2 plate, per the AF&PA NDS Supplement:

$F'_{c\perp} = F_{c\perp}K_F\phi\lambda$ = (0.625)(1.875/0.9)(0.9)(1.0) = 1.17 ksi

$C' = F'_{c\perp}A$ = 1.17(5.5)(5.5) = 35.4 kips > 16.0 kips OK

11.1.4.3.4 Check Overturning at the Soil Interface. A summary of the overturning forces is shown in Figure 11.1-8. To compute the overturning at the soil interface, the overturning moment must be increased for the 4-foot foundation height:

M_0 = 517 + 30.9(4.0) = 640 ft-kip

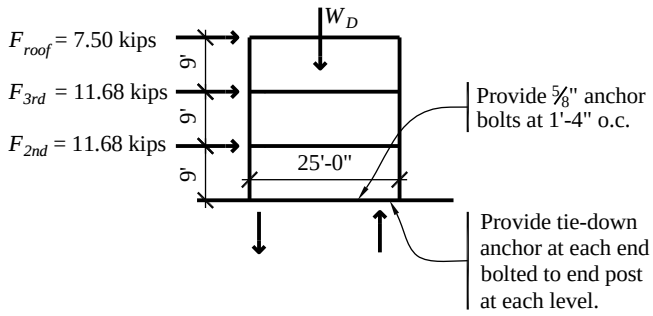

Figure 11.1-8 Transverse wall: overturning
(1.0 ft = 0.3048 m, 1.0 in. = 25.4 mm, 1.0 kip = 4.45 kN)

However, it then may be reduced in accordance with *Standard* Section 12.14.8.4:

$M_0 = 0.75(640) = 480$ ft-kip

To determine the total resistance, combine the weight above with the dead load of the first floor and foundation.

Load from first floor = (25 ft) (10 ft) (20-4+1) psf / 1,000 = 4.25 kips

where 4 psf is the weight reduction due to the absence of a ceiling and 1 psf is the weight of insulation.

The length of the longitudinal foundation wall included is a conservative approximation of the amount that can be engaged assuming minimum nominal reinforcement in the foundation.

Foundation weight = (690 plf [10 ft +10 ft + 25 ft])/1,000	= 31.05 kips
First floor	= 4.25 kips
Structure above	= 24.61 kips
Σ	= 59.91 kips

Therefore, $0.72D - 1.0Q_E = 0.72(59.91)(12.5 \text{ ft}) - 1.0(480) = 59.2$ ft-kips, which is greater than zero, so the overturning check is acceptable.

11.1.4.3.5 Anchor Bolts for Shear. At the first floor, the unit shear demand, *v*, is 1.236 klf.

Try 5/8-inch bolts in a 3×6 Douglas Fir-Larch sill plate, in single shear, parallel to the grain. In accordance with the AF&PA NDS:

$ZK_F\phi\lambda = (1.11)(2.16/0.65)(0.65)(1.0) = 2.40$ kips per bolt

The required bolt spacing is 2.4/(1.236/12) = 23.3 in. Therefore, provide 5/8-inch bolts at 16 inches on center to match the joist layout.

AF&PA SDPWS Section 4.3.6.4.3 requires plate washers at all shear wall anchor bolts and where the nominal unit shear capacity exceeds 400 plf, the plate washer needs to extend within 1/2 inch of the edge of the plate on the side with the sheathing, so provide 4.5-inch-square plate washers.

Note that in addition to the capacity of the bolt in the wood sill, the bolt capacity in the concrete foundation wall should be checked based on ACI 318 Appendix D.

11.1.4.6 Remarks on Shear Wall Connection Details. In typical platform frame construction, details must be developed that will transfer the lateral loads through the floor system and, at the same time, accommodate normal material sizes and the cross-grain shrinkage in the floor system. The connections for wall overturning in Section 11.1.4.5 are an example of one of the necessary force transfers. The transfer of diaphragm shear to supporting shear walls is another important transfer, as is the transfer from a shear wall on one level to the level below.

The floor-to-floor height is 9 feet with approximately 1 foot occupied by the floor framing. Using standard 8-foot-long plywood sheets for the shear walls, a gap occurs over the depth of the floor framing. It is common to use the floor framing to transfer the lateral shear force. Figures 11.1-9 and 11.1-10 depict this accomplished by nailing the plywood to the bottom plate of the shear wall, which is nailed through the floor plywood to the double 2×12 chord in the floor system.

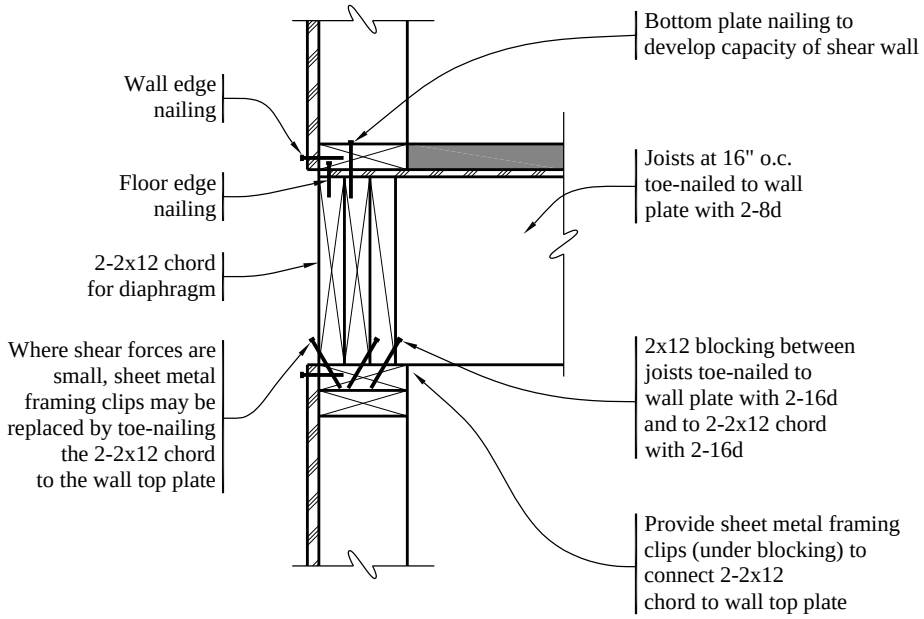

Figure 11.1-9 Bearing wall
(1.0 in = 25.4 mm)

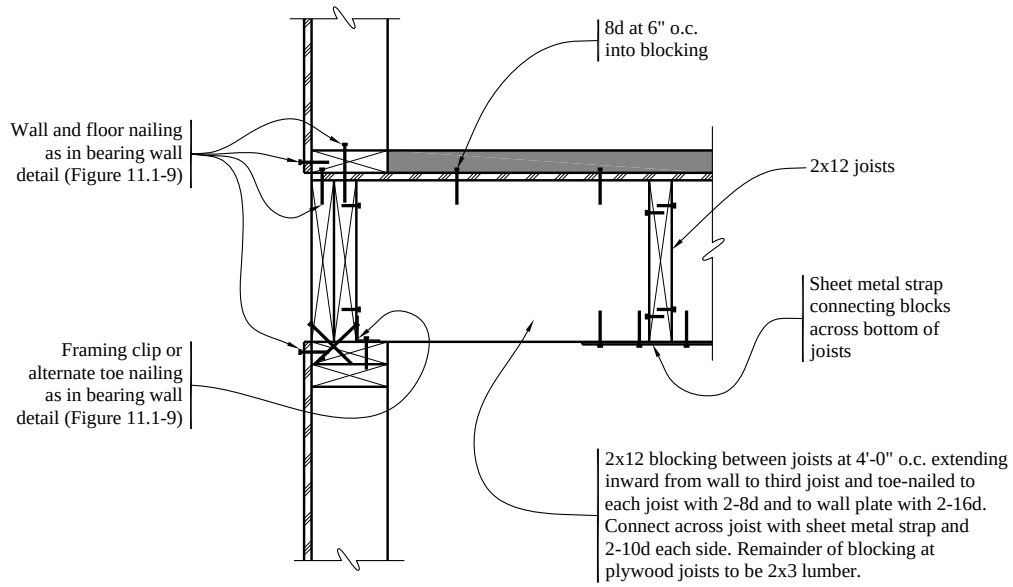

Figure 11.1-10 Nonbearing wall
(1.0 in. = 25.4 mm)

The top plate of the lower shear wall also is connected to the double 2×12 by means of sheet metal framing clips to the double 2×12 to transfer the force back out to the lower plywood. (Where the forces are small, toe nails between the double 2×12 and the top plate may be used for this connection.) This technique leaves the floor framing free for cross-grain shrinkage.

The floor plywood is nailed directly to the framing at the edge of the floor, before the plate for the upper wall is placed. Also, the floor diaphragm is connected directly to framing that spans over the openings between shear walls. The axial strength and the connections of the double 2×12 chords, allows them to function as collectors to move the force from the full length of the diaphragm to the discrete shear walls. (According to *Standard* Sec. 12.14.7.3, the design of collector elements in wood shear wall buildings need not consider increased seismic demands due to overstrength.)

The floor joist is toe nailed to the wall below for forces normal to the wall. Likewise, full-depth blocking is provided adjacent to walls that are parallel to the floor joists, as shown in Figure 11.1-10. (Elsewhere, the blocking for the floor diaphragm only need be small pieces, flat 2×4s for example.) The connections at the foundation are similar (see Figure 11.1-11).

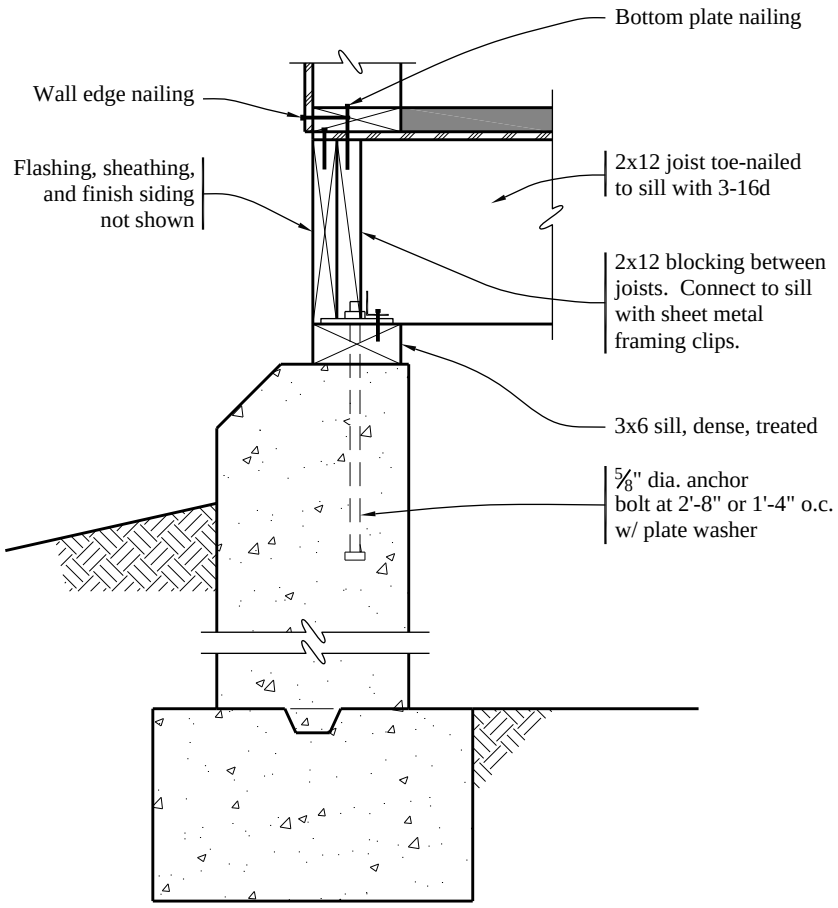

Figure 11.1-11 Foundation wall detail
(1.0 in. = 25.4 mm)

The particular combinations of nails and bent steel framing clips shown in Figures 11.1-9, 11.1-10 and 11.1-11 to accomplish the necessary force transfers are not the only possible solutions. A great amount of leeway exists for individual preference, as long as the load path has no gaps. Common carpentry practices often will provide most of the necessary transfers, but careful attention to detailing and inspection is an absolute necessity to ensure a complete load path.

11.1.4.5 Roof Diaphragm. While it has been common practice to design plywood diaphragms as simply supported beams spanning between shear walls, the diaphragm design for this example will consider some continuity at the central shear walls. The design will be based on the shears associated with the tributary area distribution of force to the shear walls and will account for moments at the diaphragm midspan as well as the central shear walls. (Note that this diaphragm assumption would result in a slightly different distribution of lateral loads to the shear walls, which is not accounted for in this example.)

From Section 11.1.3.4, the diaphragm design force at the roof is the same as the roof story force, so $F_{P,roof}$ = 30.0 kips.

As discussed previously, the design force computed in this example includes the internal force due to the weight of the walls parallel to the motion. Particularly for one-story buildings, it is common practice to remove that portion of the design force. It is conservative to include it, as is done here.

11.1.4.5.1 Diaphragm Nailing. Idealizing the building as a two-span diaphragm with three sets of walls as described previously, the maximum diaphragm shear occurs at the ends of the 88-foot diaphragm span. Assuming a uniform distribution of the diaphragm force across the building, the maximum shear over the entire diaphragm width is computed as follows:

V = (30.0)(88/148)/2 = 8.93 kips

v = 8.93 / 56 ft = 0.160 klf

Try 1/2-inch (15/32) plywood rated sheathing (not Structural I) on blocked 2-inch Douglas Fir-Larch members at 16 inch on center, with 8d nails at 6 inches on center at all boundaries and panel edges and 12 inches on center at intermediate framing members. From AF&PA SDPWS Table 4.2A, this diaphragm assembly has a nominal unit shear capacity, v_s, of 0.540 klf. The adjusted shear capacity is computed as follows:

$\phi_D v_s$ = 0.8(0.540) = 0.432 klf > 0.160 klf OK

11.1.4.5.2 Chord and Splice Connection. Diaphragm continuity is an important factor in the design of the chords. The design must consider the tension/compression forces, due to positive moment at the middle of the span as well as negative moment at the interior shear wall. It is reasonable (and conservative) to design the chord for the positive moment assuming a simply supported beam and for the negative moment accounting for continuity. The positive moment is $wl^2/8$, where w is the unit diaphragm force and l is the length of the governing diaphragm span. For a continuous beam of two unequal spans, under a uniform load, the maximum negative moment is:

$$M^- = \frac{wl_1^3 + wl_2^3}{8(l_1 + l_2)}$$

where w is the unit diaphragm force and l_1 and l_2 are the lengths of the two diaphragm spans. For w = 30.0 kips / 148 ft = 0.203 klf, the maximum positive moment is:

$0.203(88)^2 / 8$ = 197 ft-kip

and the maximum negative moment is:

$$\frac{0.203(88)^3 + 0.203(60)^3}{8(88+60)} = 154 \text{ ft-kips}$$

The positive moment controls and the design chord force is 197/56 = 3.51 kips. Try a double 2×12 Douglas Fir-Larch No. 2 chord. Due to staggered splices, compute the tension capacity based on a single 2×12, with an area of A_n = 16.88 in^2. According to the AF&PA NDS Supplement:

$F_t' = F_t K_F \phi \lambda$ = (0.575)(2.16/0.8)(0.8)(1.0) = 1.537 ksi

$T' = F_t' A$ = 1.537(16.88) = 25.9 kips > 3.51 kips OK

For chord splices, use 16d nails in the staggered chord members. According to the AF&PA NDS, the capacity of one 16d common wire nail in single shear with two 2× Douglas Fir-Larch members is 0.141 kips. The adjusted strength per nail is:

$Z' = ZK_F\phi\lambda = (0.141)(2.16/0.65)(0.65)(1.0) = 0.305$ kips

The number of required nails at the splice is 3.51/0.305 = 11.5, so use twelve 16d nails. Assuming a 4-foot splice length, provide two rows of six 16d nails at 8 inches on center. A typical chord splice connection is shown in Figure 11.1-12.

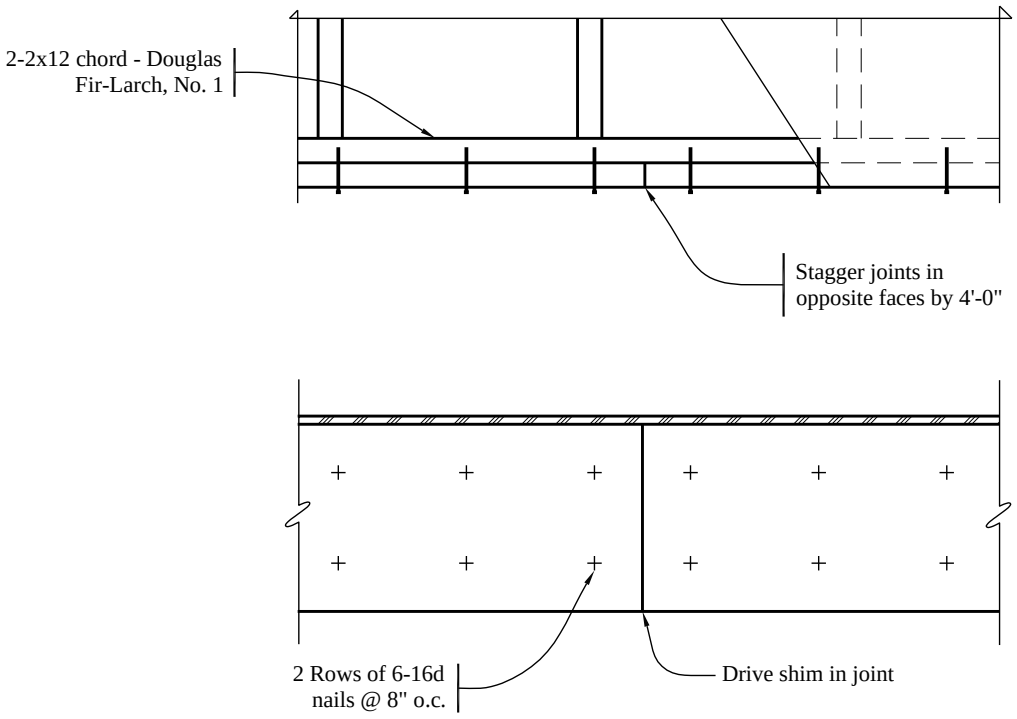

Figure 11.1-12 Diaphragm chord splice
(1.0 ft = 0.3048 m, 1.0 in. = 25.4 mm)

11.1.4.6 Second- and Third-Floor Diaphragm. The design of the second- and third-floor diaphragms follows the same procedure as for the roof diaphragm. From Section 10.1.3.4, the diaphragm design force for both floors is $F_{p,3rd} = F_{p,2nd} = 46.7$ kips.

11.1.4.6.1 Diaphragm Nailing. The maximum diaphragm shear is computed as follows:

$V = (46.7)(88/148)/2 = 13.88$ kips

$v = 13.88 / 56$ ft $= 0.248$ klf

With an adjusted capacity of 0.432 klf, the same diaphragm as at the roof also works for the floors.

11.1.4.6.2 Chord and Splice Connection. Computed as described above for the roof diaphragm, the maximum positive moment is 306 ft-kips and the design chord force is 5.48 kips.

By inspection, a double 2×12 chord spliced with 16d nails similar to the roof level is adequate. The number of nails at the floors is 5.48/0.305 = 18 nails, so for the 4-foot splice length, provide two rows of nine 16d nails at 5 inches on center on each side of the splice joint.

11.1.4.7 Longitudinal Direction. Only one exterior shear wall section will be designed here. The design of the corridor shear walls would be similar to that of the transverse walls. For loads in the longitudinal direction, diaphragm stresses are negligible and the nailing provided for the transverse direction is more than adequate.

The design of the exterior wall utilizes the provisions for perforated shear walls as defined in AF&PA SDPWS Sections 4.3.4.1 and 4.3.5.3. The procedure for perforated shear walls applies to walls with openings that have not been specifically designed and detailed for force transfer around the openings. Essentially, a perforated wall is treated in its entirety rather than as a series of discrete wall piers. The use of this design procedure is limited by several conditions as specified in AF&PA SDPWS Section 4.3.5.3.

The main aspects of the perforated shear wall design procedure are as follows. The design shear capacity of the shear wall is the sum of the capacities of each segment (all segments must have the same sheathing and nailing) reduced by an adjustment factor that accounts for the geometry of the openings. Uplift anchorage (tie-down) is required only at the ends of the wall (not at the ends of all wall segments), but all wall segments must resist a specified tension force (using anchor bolts at the foundation and strapping or other means at upper floors). Requirements for shear anchorage and collectors (drag struts) across the openings are also specified. It should be taken into account that the design capacity of a perforated shear wall is less than that of a standard segmented wall with all segments restrained against overturning. However, the procedure is useful in eliminating interior hold downs for specific conditions and thus is illustrated in this example.

The portion of the story force resisted by each exterior wall was computed previously as $0.223F_x$. The exterior shear walls are composed of three separate perforated shear wall segments (two at 30 feet long and one at 15 feet long, all with the same relative length of full-height sheathing), as shown in Figure 11.1-2. This section will focus on the design of a 30-foot section. Assuming that load is distributed to the wall sections based on relative length of the shear panel, then the total story force to the 30-foot section is $(30/75)0.223F_x = 0.089F_x$ per floor. The load per floor is:

$F_{roof} = 0.089(30.0) = 2.67$ kips
$F_{3rd} = 0.089(46.7) = 4.16$ kips
$F_{2nd} = 0.089(46.7) = 4.16$ kips
$\Sigma = 10.99$ kips

11.1.4.7.1 Perforated Shear Wall Resistance. The design shear capacity for perforated shear walls is computed as the factored shear resistance for the sum of the wall segments, multiplied by an adjustment factor that accounts for the percentage of full-height (solid) sheathing and the ratio of the maximum opening to the story height as described in AF&PA SDPWS Section 4.3.3.5. At each level, the design shear capacity, V_{wall}, is:

$$V_{wall} = (vC_0)\Sigma L_i$$

where:

v = factored shear resistance (AF&PA SDPWS Table 4.3A)
C_0 = shear capacity adjustment factor (AF&PA SDPWS Table 4.3.3.5)
ΣL_i = sum of shear wall segment lengths

For the subject wall, the widths of perforated shear wall segments are 4+10+4 = 18 feet, the percent of full-height sheathing is 18/30 = 0.60 and the maximum opening height is 4 feet. Therefore, per AF&PA SDPWS Table 4.3.3.5, C_0 = 0.83.

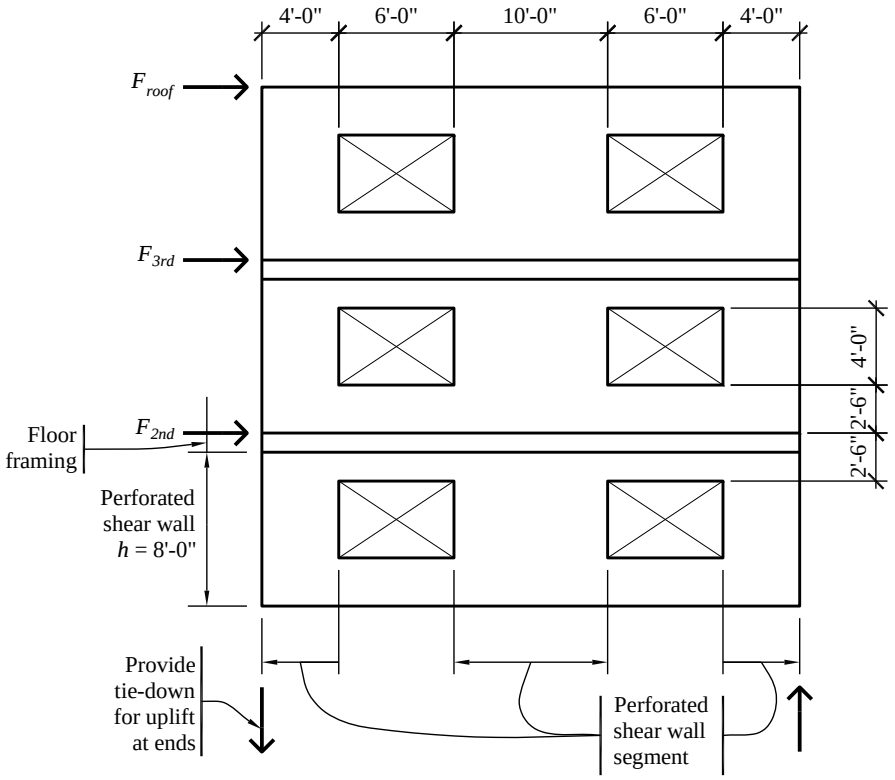

Figure 11.1-13 Perforated shear wall at exterior
(1.0 ft = 0.3048 m, 1.0 in. = 25.4 mm)

The wall geometry (and thus the adjustment factor and total length of wall segments) is the same at all three levels, as shown in Figure 11.1-13. Perforated shear wall plywood and nailing are determined below.

- Roof to third floor:

  V = 2.67 kips

  Required v = 2.67/0.83/18 = 0.179 klf

  Try 1/2-inch (15/32) plywood rated sheathing (not Structural I) on blocked 2× Hem-Fir members at 16 inches on center with 8d nails at 6 inches on center at panel edges and at 12 inches on center at

intermediate framing members. From AF&PA SDPWS Table 4.3A, this shear wall assembly has a nominal unit shear capacity, v_s, of 0.520 klf. Adjusting for framing material, the shear capacity is computed as follows:

$0.93\phi_D v_s = 0.93(0.8)(0.520) = 0.387 \text{ klf} > 0.179 \text{ klf}$ OK

- Third floor to second floor:

  $V = 2.67+4.16 = 6.83$ kips

  Required $v = 6.83/0.83/18 = 0.457$ klf

Try 1/2-inch (15/32) plywood rated sheathing (not Structural I) on blocked 2× Hem-Fir members at 16 inches on center with 8d nails at 4 inches on center at panel edges and at 12 inches on center at intermediate framing members. From AF&PA SDPWS Table 4.3A, this shear wall assembly has a nominal unit shear capacity, v_s, of 0.760 klf. Adjusting for framing material, the shear capacity is computed as follows:

$0.93\phi_D v_s = 0.93(0.8)(0.760) = 0.565 \text{ klf} > 0.457 \text{ klf}$ OK

- Second floor to first floor:

  $V = 6.83+4.16 = 10.99$ kips
  Required $v = 10.99/0.83/18 = 0.735$ klf

Try 1/2-inch (15/32) plywood rated sheathing (not Structural I) on blocked 2× Hem-Fir members at 16 inches on center with 10d nails at 3 inch on center at panel edges and at 12 inch on center at intermediate framing members. From AF&PA SDPWS Table 4.3A, this shear wall assembly has a nominal unit shear capacity, v_s, of 1.200 klf. Adjusting for framing material, the shear capacity is computed as follows:

$0.93\phi_D v_s = 0.93(0.8)(1.200) = 0.893 \text{ klf} > 0.735 \text{ klf}$ OK

Note that the nominal unit shear capacity of 1.200 klf is less than the maximum permitted nominal shear capacity of 1.740 klf in accordance with AF&PA SDPWS Section 4.3.5.3, Item 3.

11.1.4.7.2 Perforated Shear Wall Tension Chord. According to AF&PA SDPWS Section 4.3.6.1.2, tension and compression chords and associated anchorage must be evaluated at the ends of the wall only. Uplift anchorage at each wall segment is treated separately as described later. The tension and compression forces at the wall ends are determined per AF&PA SDPWS Equation 4.3-8 as follows:

$$T = C = \frac{Vh}{C_0 \sum L_i}$$

where:

V = design shear force in the shear wall
h = shear wall height (per floor)
C_0 = shear capacity adjustment factor
ΣL_i = sum of widths of perforated shear wall segments

For this example, the tension chord and tie-down will be designed at the first floor only; the other floors would be computed similarly and tie-down devices, as shown in Figure 11.1-7, would be used. For h = 8 ft, C_0 = 0.83 and ΣL_i = 18 ft, the tension force is computed as follows:

Third floor: T = 2.67(8)/(0.83×18)	= 1.42 kips
Second floor: T = (2.67 + 4.16)(8)/(0.83×18)	= 3.66 kips
First floor: T = (2.67 + 4.16 + 4.16)(8)/(0.83×18)	= 6.42 kips
Σ	= 11.50 kips

For the dead load to resist the tension chord uplift, assume a tributary floor width equal to the half the span of the window header at the end wall segment. The tributary width is 6.5 feet and the tributary joist span is 8 feet. The tributary weight is computed as follows:

Exterior wall weight = (27 ft)(6.5 ft)(9 psf)/1,000	= 1.58 kips
Tributary roof = (8 ft)(6.5 ft)(15 psf)/1,000	= 0.78 kips
Tributary floor = (8 ft)(6.5 ft)(20 psf)(2)/1,000	= 2.08 kips
Σ	= 4.44 kips

The net uplift is computed as follows:

$0.72D - 1.0E = 0.72(4.44) - 11.5 = 8.30$ kips

Therefore, uplift anchorage is required per AF&PA SDPWS Section 4.3.6.4.2. Since the chord member resists the perforated shear wall compression load and supports the window header as well, use a 6×6 Douglas Fir-Larch No. 1, similar to the transverse walls. The post has ample tension capacity. For the anchorage, try a tie-down device with a 7/8-inch anchor bolt and twenty 1/4-inch screws into the post. Using the method described above for computing the strength of a pre-engineered tie-down, the capacity is computed as follows:

$ZK_F\phi\lambda = (7.87)(2.88/1.60)(0.65)(1.0) = 9.2$ kips > 8.3 kips OK

The design of the tie-downs at the second and third floors is similar.

11.1.4.7.3 Perforated Shear Wall Compression Chord. The force in the compression chord is the same as the tension chord equal to 11.5 kips at the first floor. Again, just the chord at the first floor will be designed here; the design at the upper floors would be similar. Although not explicitly required by AF&PA SDPWS Section 4.3.6.1.2, it is rational to combine the chord compression with gravity loading, using the load combination $1.4D + 1.0Q_E + 0.5L + 0.2S$, in order to design the chord member. The dead load is as computed above and the live load and snow load are 4.16 kips and 1.30 kips, respectively. Therefore, the design compression force is as follows:

$1.38(4.44) + 1.0(11.5) + 0.5(4.16) + 0.2(1.30) = 20.0$ kips

The bearing capacity on the bottom plate was computed previously as 35.4 kips, which is greater than 20.0 kips. Note that where end posts are loaded in both directions, orthogonal effects must be considered in accordance with *Standard* Section 12.5.

11.1.4.7.4 Anchorage at Shear Wall Segments. The anchorage at the base of a shear wall segment (bottom plate to floor framing or foundation wall) is designed per AF&PA SDPWS Section 4.3.6.4. This section requires two types of anchorage: in-plane shear anchorage (AF&PA SDPWS Sec. 4.3.6.4.1.1)

and distributed uplift anchorage (AF&PA SDPWS Sec. 4.3.6.4.1.2). While both types of anchorage need only be provided at the full-height sheathing, the shear anchorage is usually extended at least over the entire length of the perforated shear wall to simplify the detailing and reduce the possibility of construction errors.

The in-plane shear anchorage is required to resist the following:

$$v = \frac{V}{C_0 \sum L_i}$$

where:

V = design shear force in the shear wall
C_0 = shear capacity adjustment factor
ΣL_i = sum of widths of perforated shear wall segments

This equation is the same as was previously used to compute unit shear demand on the wall segments. Therefore, the in-plane anchorage will be designed to meet the following unit, in-plane shear forces:

- Third floor: v = 0.179 klf
- Second floor: v = 0.457 klf
- First floor: v = 0.735 klf

The required distributed uplift force, t, is equal to the in-plane shear force, v. Per AF&PA SDPWS Section 4.3.6.4, this uplift force must be provided with a complete load path to the foundation. That is, the uplift force at each level must be combined with the uplift forces at the levels above (similar to the way overturning moments are accumulated down the building).

At the foundation level, the unit in-plane shear force, v and the unit uplift force, t, are combined for the design of the bottom plate anchorage to the foundation wall. The design unit forces are as follows:

- Shear: v = 0.735 klf
- Tension: t = 0.179+0.457+0.735 = 1.371 klf

Assuming that stresses on the wood bottom plate govern the design of the anchor bolts, the anchorage is designed for shear (single shear, wood-to-concrete connection) and tension (plate washer bearing on bottom plate). The interaction between shear and tension need not be considered in the wood design for this configuration of loading.

Try a 5/8-inch bolt at 32 inches on center with a 4.5-inch square plate washer (AF&PA SDPWS Section 4.3.6.4.3 requires plate washer to extend within 1/2 inch of the 5.5-inch-wide bottom plate). As computed previously, the shear capacity of a 5/8-inch bolt in a 3×6 Douglas Fir-Larch sill plate is 2.40 kips. The demand per bolt is 0.735 klf (32/12) = 1.96 kips, so the 32-inch spacing is adequate for shear.

For anchor bolts at 32 inches on center, the tension demand per bolt is 1.371 klf (32/12) = 3.66 kips. Bearing capacity of the plate washer (using a Douglas Fir No. 2 bottom plate) is computed per AF&PA NDS Supplement as follows:

$F'_{c\perp} = F_{c\perp} K_F \phi \lambda = (0.625)(1.875/0.9)(0.9)(1.0) = 1.17$ ksi

$C' = F'_{c\perp} A = 1.17(4.5)(4.5) = 23.7$ kips > 3.66 kips OK

The anchor bolts themselves must be designed for combined shear and tension in accordance with ACI 318-08.

In addition to designing the anchor bolts for uplift, a positive load path must be provided to transfer the uplift forces into the bottom plate. One method for providing this load path continuity is to use metal straps nailed to the studs and lapped around the bottom plate, as shown in Figure 11.1-14. Attaching the studs directly to the foundation wall (using embedded metal straps) for uplift and using the anchor bolts for shear only is an alternative approach.

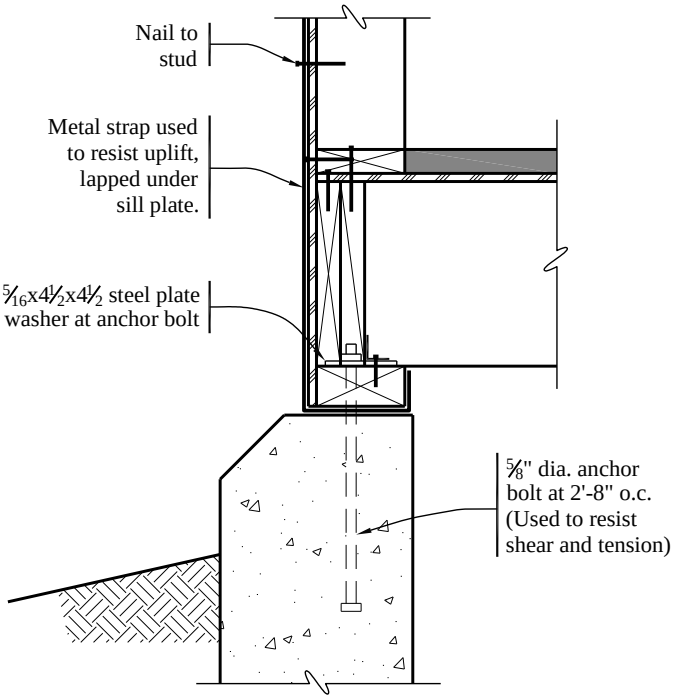

Figure 11.1-14 Perforated shear wall detail at foundation
(1.0 ft = 0.3048 m, 1.0 in. = 25.4 mm)

At the upper floors, the load transfer for in-plane shear is accomplished by using nailing or framing clips between the bottom plates, rim joists and top plates in a manner similar to that for standard shear walls. The uniform uplift force can be resisted either by using the nails in withdrawal (for small uplift demand) or by providing vertical metal strapping between studs above and below the level considered. This type of connection is shown in Figure 11.1-15. For this type of connection (and the one shown in

Figure 11.1-14) to be effective, shrinkage of the floor framing must be minimized using dry or manufactured lumber.

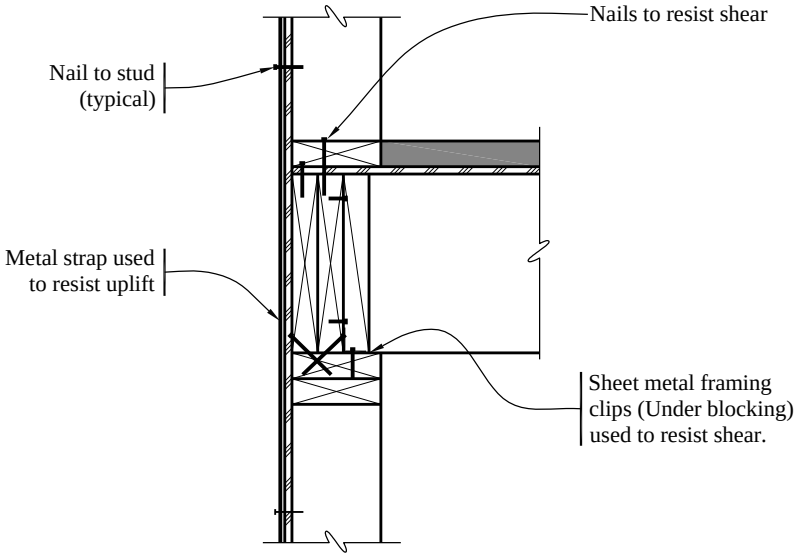

Figure 11.1-15 Perforated shear wall detail at floor framing

For example, consider the second floor. The required uniform uplift force, t = 0.244+0.496 = 0.740 klf. Place straps at every other stud, so the required strap force is 0.740(32/12) = 1.97 kips. Provide an 18-gauge strap with twelve 10d nails at each end.

11.2 WAREHOUSE WITH MASONRY WALLS AND WOOD ROOF, LOS ANGELES, CALIFORNIA

This example features the design of the wood roof diaphragm and wall-to-diaphragm anchorage for the one-story masonry building described in Section 10.1 of this volume of design examples. Refer to that example for more detailed building information and the design of the masonry walls.

11.2.1 Building Description

This is a very simple rectangular warehouse, 100 feet by 200 feet in plan (see Figure 11.2-1), with a roof height of 28 feet. The wood roof structure slopes slightly, but it is nominally flat. The long walls (side walls) are 8 inches thick and solid and the shorter end walls are 12 inches thick and penetrated by several large openings.

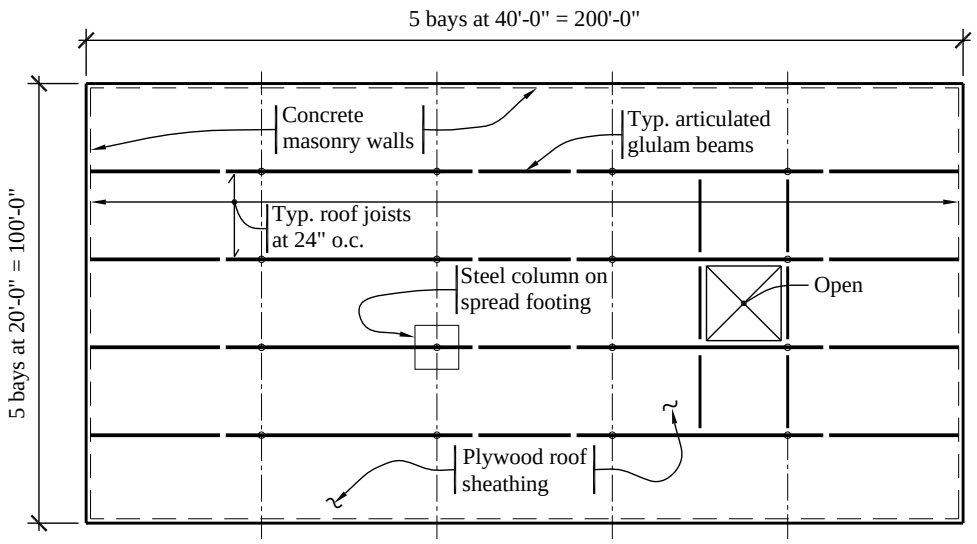

Figure 11.2-1 Building plan
(1.0 ft = 0.3048 m, 1.0 in. = 25.4 mm)

Based on gravity loading requirements, the roof structure consists of wood joists, supported by 8-3/4-inch-wide by 24-inch-deep glued-laminated timber beams on steel columns. The joists span 20 feet and the beams span 40 feet, as an articulated system. Typical roof framing is assumed to be Douglas Fir-Larch No 1 as graded by the WWPA Rules. The glued-laminated timber beams meet the requirements of Combination 24F-V4 per AITC A190.1.

The plywood roof deck acts as a diaphragm to carry lateral loads to the exterior walls. There are no interior walls for seismic resistance. The roof contains a large opening that interrupts the diaphragm continuity. The diaphragm contains continuous cross ties in both principal directions that serve as part of the wall anchorage system.

The following aspects of the structural design are considered in this example:

- Development of diaphragm forces based on the Equivalent Lateral-Force Procedure used for the masonry wall design (Sec. 10.1)
- Design and detailing of a plywood roof diaphragm with a significant opening
- Computation of drift and P-delta effects
- Anchorage of diaphragm and roof joists to masonry walls
- Design of cross ties and subdiaphragms

11.2.2 Basic Requirements

11.2.2.1 Seismic Parameters

Table 11.2-1 Seismic Parameters

Design Parameter	Value
S_S	1.50
S_1	0.60
Site Class (*Standard* Sec. 11.4.2)	C
Occupancy Category (*Standard* Sec. 1.5.1)	II
Seismic Design Category (*Standard* Sec. 11.6)	D
Seismic Force-Resisting System (*Standard* Table 12.2-1)	Special Reinforced Masonry Shear Walls
Response Modification Factor, R	5
System Overstrength Factor, Ω_0	2.5
Deflection Amplification Factor, C_d	3.5

11.2.2.2 Structural Design Criteria. A complete discussion on the criteria for ground motion, seismic design category, load path, structural configuration, redundancy, analysis procedure and shear wall design is included in Section 10.1 of this volume of design examples.

11.2.2.2.1 Design and Detailing Requirements. Since this building has a wood structural panel diaphragm with masonry shear walls, the diaphragm can be considered flexible in accordance with *Standard* Section 12.3.1.1. There are not any irregularities (*Standard* Sec. 12.3.2) that would impact the diaphragm design and the diaphragm and wall anchorage system is permitted to be designed with the redundancy factor equal to 1.0 per *Standard* Section 12.3.4.1.

The design of the diaphragm is based on *Standard* Section 12.10. The large opening in the diaphragm must be fitted with edge reinforcement (*Standard* Sec. 12.10.1). However, the diaphragm does not require any collector elements that would have to be designed for the special load combinations (*Standard* Sec. 12.10.2.1).

The requirements for anchorage of masonry walls to flexible diaphragms (*Standard* Sec. 12.11.2) are of great significance in this example.

11.2.2.2.2 Seismic Load Effects and Combinations. The basic design load combinations for the seismic design, as stipulated in *Standard* Section 12.4.2.3, were computed in Section 10.1 of this volume of design examples, as follows:

$$1.4D + 1.0Q_E$$

where gravity and earthquake are additive and

$$0.7D - 1.0Q_E$$

where gravity and earthquake counteract.

The roof live load, L_r, is not combined with seismic loads (see *Standard* Chapter 2) and the design snow load is zero for this Los Angeles location.

11.2.2.2.3 Deflection and Drift Limits. In-plane deflection and drift limits for the masonry shear walls are considered in Section 10.1.

As illustrated below, the diaphragm deflection is much greater than the shear wall deflection. According to *Standard* Section 12.12.2, in-plane diaphragm deflection must not exceed the permissible deflection of the attached elements. Because the walls are essentially pinned at the base and simply supported at the roof, they are capable of accommodating large deflections at the roof diaphragm.

For illustrative purposes, story drift is determined and compared to the requirements of *Standard* Table 12.12-1. However, according to this table, there is essentially no drift limit for a single-story structure as long as the architectural elements can accommodate the drift (assumed to be likely in a warehouse structure with no interior partitions). As a further check on the deflection, P-delta effects (*Standard* Sec. 12.8.7) are evaluated.

11.2.3 Seismic Force Analysis

Building weights and base shears are as computed in Section 10.1. (The building weights used in this example are based on a preliminary version of Example 10.1 and thus minor numerical differences may exist between the two examples). *Standard* Section 12.10.1.1 specifies that floor and roof diaphragms be designed to resist a force, F_{px}, computed in accordance with *Standard* Equation 12.10-1 as follows:

$$F_{px} = \frac{\sum_{i=x}^{n} F_i}{\sum_{i=x}^{n} w_i} w_{px}$$

plus any force due to offset walls (not applicable for this example). For one-story buildings, the first term of this equation will be equal to the seismic response coefficient, C_s, which is 0.286. The effective diaphragm weight, w_{px}, is equal to the weight of the roof plus the tributary weight of the walls perpendicular to the direction of the motion. The tributary weights are as follows:

- Roof = 20(100)(200) = 400 kips
- Side walls = 2(65)(28/2+2)(200) = 416 kips
- End walls = 2(103)(28/2+2)(100) = 330 kips

The diaphragm design force is computed as:

- Transverse: $F_{p,roof}$ = 0.286(400+416) = 233 kips
- Longitudinal: $F_{p,roof}$ = 0.286(400+330) = 209 kips

These forces exceed the minimum diaphragm design forces given in *Standard* Section 12.10.1.1, because C_s exceeds the minimum factor of $0.2S_{DS}$.

11.2.4 Basic Proportioning of Diaphragm Elements

The design of plywood diaphragms primarily involves the determination of sheathing sizes and nailing patterns to accommodate the applied loads. Large openings in the diaphragm and wall anchorage requirements, however, can place special requirements on the diaphragm capacity. Diaphragm deflection is also a consideration.

Nailing patterns for diaphragms are established on the basis of tabulated requirements included in the AF&PA SDPWS. It is important to consider the framing requirements for a given nailing pattern and capacity as indicated in the notes following the tables. In addition to strength requirements, AF&PA SDPWS Section 4.2.4 places aspect ratio limits on plywood diaphragms (length-to-width must not exceed 4/1 for blocked diaphragms). However, it should be taken into consideration that compliance with this aspect ratio does not guarantee that drift limits will be satisfied.

While there is no specific limitation on deflection for this example, the diaphragm has been analyzed for deflection as well as for shear capacity.

In the calculation of diaphragm deflections, the chord splice slip factor can result in large additions to the total deflection. This chord splice slip, however, is often negligible where the diaphragm is continuously anchored to a bond beam in a masonry wall. Therefore, chord splice slip is assumed to be zero in this example.

11.2.4.1 Strength of Members and Connections. As described in more detail in Section 11.1.4.1, the *Standard* references the AF&PA NDS and AF&PA SDPWS for engineered wood structures. Diaphragm design is based on AF&PA SDPWS Section 4.2, which provides design criteria for both ASD and LRFD methods. This example utilizes LRFD as the design basis, so the diaphragm design is based on the tabulated unit shear values, v_s, which are multiplied by a resistance factor, ϕ_D, equal to 0.80.

Refer to Section 11.1.4.1 for a summary of the design methodology in the AF&PA NDS for framing members and connections.

11.2.4.2 Roof Diaphragm Design for Transverse Direction

11.2.4.2.1 Plywood and Nailing. The diaphragm design force is $F_{p,roof}$ = 233 kips and the maximum end shear is $0.5F_{p,roof}$ = 116.5 kips. This corresponds to a unit shear force of v = (116.5/100) = 1.165 klf. (Note that per *Standard* Sec. 12.8.4.2, accidental torsion need not be considered for flexible diaphragms.)

Due to the relatively high diaphragm shears, closely spaced nailing will be required, so in accordance with AF&PA SDPWS Section 4.2.7.1.1, Item 3, 3-inch nominal framing will be provided. Assuming 3-inch nominal framing, try blocked 1/2-inch (15/32) Structural I plywood rated sheathing with 10d common nails at 2 inches on center at diaphragm boundaries and continuous panel edges and at 3 inches on center at other panel edges. The use of 2×4 flat blocking at continuous panel edges satisfies the requirements for blocked diaphragms. From AF&PA SDPWS Table 4.2A:

$\phi_D v_s$ = 0.80(1.640) = 1.31 klf > 1.165 klf OK

Because the diaphragm shear decreases towards the midspan of the diaphragm, the diaphragm capacity may be reduced towards the center of the building. A reasonable configuration for the interior of the building utilizes 2-inch nominal framing and 1/2-inch (15/32) Structural I plywood rated sheathing plywood with 10d at 4 inches on center at diaphragm boundaries and continuous panels edges and

6 inches on center nailing at other panel edges. Determine the distance, *X*, from the end wall where the transition can be made, as follows:

- $\phi_D v_s$ = 0.80(0.850) = 0.68 klf (AF&PA SDPWS Table 4.2A)
- Shear capacity = 0.68(100) = 68.0 kips
- Uniform diaphragm demand = 233/200 = 1.165 klf
- *X* = (117-68)/1.165 = 42.1 ft (assumed as 50 ft from the diaphragm edge)

In a building of this size, it may be beneficial to further reduce the diaphragm nailing towards the middle of the roof. However, due to the requirements for subdiaphragms (see below) and diaphragm capacity in the longitudinal direction and for simplicity of design, no additional nailing pattern is used.

Table 11.2-1 contains a summary of the diaphragm framing and nailing requirements (all nails are 10d common). See Figure 11.2-2 for designation of framing and nailing zones and Figure 11.2-3 for typical plywood layout.

Table 11.2-2 Roof Diaphragm Framing and Nailing Requirements

Zone*	Framing	Structural 1 Plywood	Nail Spacing (in.)			Capacity (kip/ft)
			Boundaries and Cont. Panel Edges	Other Panel Edges	Intermediate Framing Members	
A	3×12	15/32 in.	2	3	12	1.31
B	2×12	15/32 in.	4	6	12	0.68

1.0 in. = 25.4 mm, 1.0 kip/ft = 14.6 kN/m.

* Refer to Figure 11.2-2 for zone designation.

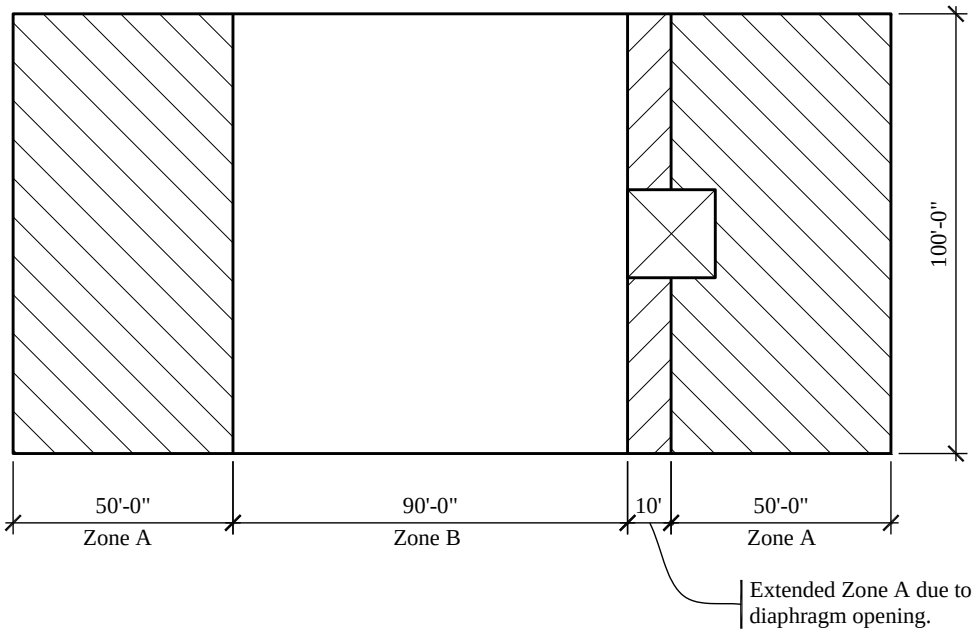

Figure 11.2-2 Diaphragm framing and nailing layout
(1.0 ft = 0.3048 m)

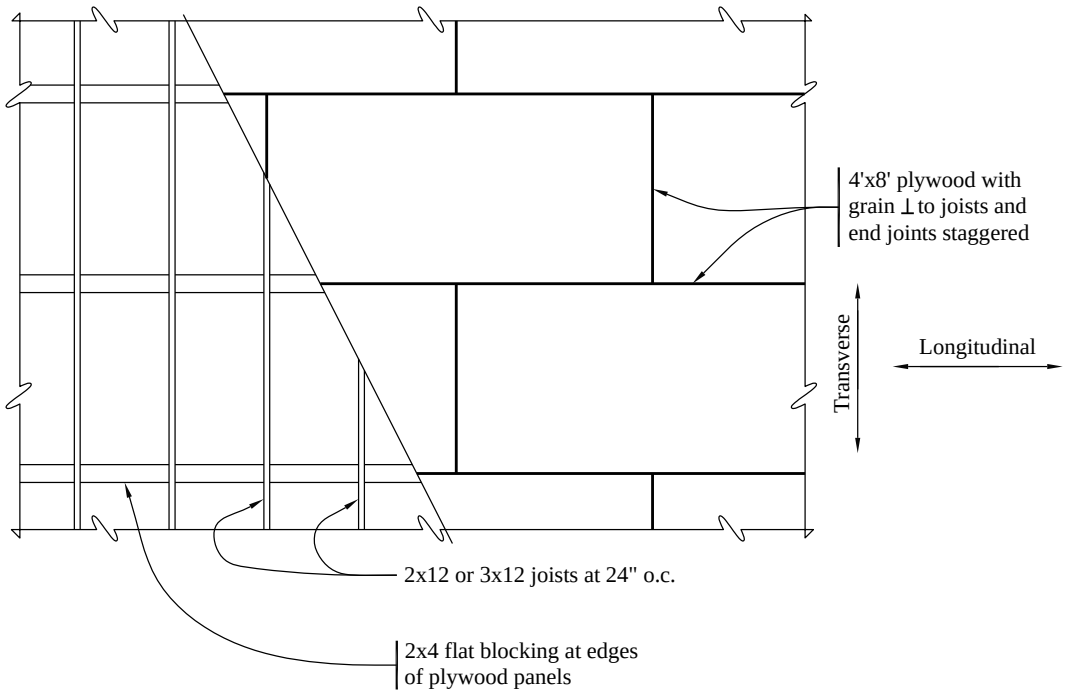

Figure 11.2-3 Typical diaphragm plywood layout
(1.0 ft = 0.3048 m, 1.0 in = 25.4mm)

11.2.4.2.2 Chord Design. Although the bond beam at the masonry wall could be used as a diaphragm chord, this example illustrates the design of the wood ledger member as a chord. Chord forces are computed using a simply supported beam analogy, where the design force is the maximum moment divided by the diaphragm depth.

- Diaphragm moment, $M = wL^2/8 = F_{p,roof}L/8 = 233(200/8) = 5{,}825$ ft-kips
- Chord force, $T = C = 5{,}825/(100 - 16/12) = 59.0$ kips

Try a select structural Douglas Fir-Larch 4×12 for the chord. Assuming two 1-1/16-inch bolt holes (for 1-inch bolts) at splice locations, the net chord area is 31.9 in^2. Tension strength (parallel to wood grain), per the AF&PA NDS, is as follows:

$F_t' = F_t C_F K_F \phi \lambda = (1{,}000 \text{ psi})(1.0)(2.16/0.8)(0.8)(1.0) = 2{,}160$ psi

$T' = F_t' A = 2{,}160(31.9)/1000 = 68.9 \text{ kips} > 59.0 \text{ kips}$ OK

Design the splice for the maximum chord force of 59.0 kips. Try bolts with steel side plates using 1-inch A307 bolts, with a 3-1/2-inch length in the main member. The capacity, according to the AF&PA NDS, is as follows:

$Z' = Z K_F \phi \lambda = (4.90)(2.16/0.65)(0.65)(1.0) = 10.6$ kips per bolt

The number of bolts required (at each side of the splice joint) is 59.0/10.6 = 5.6.

Use two rows of three bolts. The edge distance, end distance and spacing meet the AF&PA NDS requirements to avoid capacity reductions and the reduction for multiple bolts (group action factor) is negligible. The net area of the 4×12 chord with two rows of 1-1/16-inch holes is 31.9 in^2 as assumed above. Therefore, use six 1-inch A307 bolts on each side of the chord splice (see Figure 11.2-4).

In addition to the bolt checks, the steel splice plates would need to be check for tension. Although it is shown for illustration, this type of chord splice may not be the preferred splice against a masonry wall since the bolts and side plate, would have to be recessed into the wall.

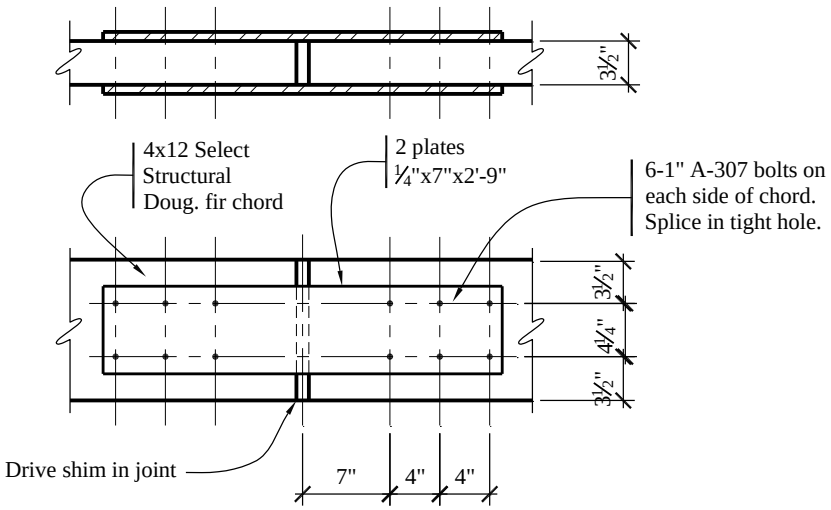

Figure 11.2-4 Chord splice detail
(1.0 ft = 0.3048 m, 1.0 in. = 25.4 mm)

11.2.4.2.3 Diaphragm Deflection and P-delta Check. Based on the procedure for contained in AF&PA SDPWS Section 4.2.2, diaphragm deflection is computed as follows:

$$\delta_{dia} = \frac{5vL^3}{8EAW} + \frac{0.25vL}{1000G_a} + \frac{\sum\left(x\Delta_c\right)}{2W}$$

The equation produces the midspan diaphragm displacement in inches and the individual variables *must* be entered in the force or length units as described below. A small increase in diaphragm deflection due to the large opening is neglected and the effects of the variable nail spacing are neglected for simplicity. The chord slip deflection is assumed to be zero because the chord is connected to the continuous bond beam at the top of the masonry wall.

The variables above and associated units used for computations are as follows:

v = (233/2)/100 = 1,165 plf (shear per foot at boundary)

L = 200 ft (diaphragm length)

W = 100 ft (diaphragm width)

A = effective area of 4×12 chord and two-#6 bars assumed to be in the bond beam
= 39.38 in^2 + 2(0.44)(29,000,000/1,900,000) = 52.81 in^2

E = 1,900,000 psi (for Douglas Fir-Larch select structural chord)

G_a = 1.2(18) = 21.6 kips/in. (apparent diaphragm shear stiffness from AF&PA SDPWS Table 4.2A accounting for nail slip and panel shear deformation, based on sheathing and nailing at the outer zone and increased by 1.2 per Footnote 3, assuming four-ply minimum sheathing)

Bending deflection = $5vL^3/8EAW$ = 0.58 in.

Shear/nail slip deflection = $0.25vL/1000G_a$ = 2.71 in.

Deflection due to chord slip at splices = $\Sigma(x\Delta_c)/2W \approx$ 0.00 in. (as noted above)

Total for diaphragm:

δ_{dia} = 0.58+2.71+0.00 = 3.29 in.

End wall deflection = 0.037 in. (see Sec. 10.1 of this volume of design examples)

Therefore, the total elastic deflection δ_{xe} = 3.29+0.037 = 3.29 in.

Total deflection, $\delta_x = C_d\,\delta_{xe}/I$ = 3.5(3.29)/1.0 = 11.53 in.

The drift ratio at the center of the diaphragm = δ_x/h_{sx} = 11.53/[28(12)] = 0.034.

This exceeds the maximum drift ratio of 0.025 permitted for most low-rise buildings in Occupancy Category II (*Standard* Table 12.12-1). However, for one-story buildings, *Standard* Table 12.12-1, Footnote c permits unlimited drift, provided that the structural elements and finishes can accommodate the drift. The limit for masonry cantilever shear wall structures (0.007) should only be applied to the in-plane movement of the end walls (0.13/h = 0.0004 < 0.007). The construction of the out-of-plane walls allows them to accommodate very large drifts. It is further expected that the building does not contain interior elements that are sensitive to drift.

P-delta effects are computed according to *Provisions* Section 12.8.7, which modifies *Standard* Section 12.8.7 for determining the stability coefficient, θ, per *Provisions* Equation 12.8-16:

$$\theta = \frac{P_x \Delta I}{V_x h_{sx} C_d}$$

(Note that the *Provisions* adds the importance factor, *I*, that was missing in the *Standard* equation.) Because the midspan diaphragm deflection is substantially greater than the deflection at the top of the masonry end walls, it would be overly conservative to consider the entire design load at the maximum deflection. Therefore, the stability coefficient is computed by splitting the P-delta product into two terms: one for the diaphragm and one for the end walls.

For the diaphragm, consider the weight of the roof and side walls at the maximum displacement. (This overestimates the P-delta effect. The computation could consider the average displacement of the total weight, which would lead to a reduced effective delta. Also, the roof live load need not be included.)

P = 400+416 = 816 kips

Δ= 11.53 in.

V = 233 kips (diaphragm force)

For the end walls, consider the weight of the end walls at the wall displacement:

P = 330 kips

Δ = (3.5)(0.037) = 0.13 in.

V = 264 kips (additional base shear for wall design)

For story height, h = 28 feet, the stability coefficient is:

$$\theta = \left(\frac{P\Delta}{V} + \frac{P\Delta}{V} \right) \Big/ hC_d = \left(\frac{816(11.53)}{233} + \frac{330(0.13)}{264} \right) \Big/ (28)(12)(3.5) = 0.034$$

For θ < 0.10, P-delta effects need not be considered based on *Provisions* Section 12.8.7.

Since the P-delta effects are not significant for this structure and the *Standard* does not impose drift limitations for this type of structure, the computed diaphragm deflections appear acceptable.

11.2.4.2.4 Detail at Opening. Consider diaphragm strength at the roof opening as required by *Standard* Section 12.10.1. The diaphragm nailing must be checked for the reduced total width of diaphragm sheathing and the chords must be checked for bending forces at the opening.

Check diaphragm nailing for the shear in the diaphragm at edge of opening. The maximum shear at the exterior-side edge of the opening is computed as follows:

Shear = 116.5 - [40(1.165)] = 69.9 kips

v = 69.9/(100-20) = 0.874 klf

Because the opening is centered in the width of the diaphragm, half the force to the diaphragm must be distributed on each side of the opening.

Diaphragm capacity in this area is 0.680 klf as computed previously (see Table 11.2-1 and Figure 11.2-2). Because the diaphragm demand at the reduced section exceeds the capacity, the extent of the Zone A nailing and framing should be increased. For simplicity, extend the Zone A nailing to the interior edge of the opening (60 feet from the end wall). The diaphragm strength is now adequate for the reduced overall width at the opening.

11.2.4.2.5 Framing around Opening. The opening is located 40 feet from one end of the building and is centered in the other direction (Figure 11.2-5). This does not create any panels with very high aspect ratios.

In order to develop the chord forces, continuity will be required across the glued-laminated beams in one direction and across the roof joists in the other direction.

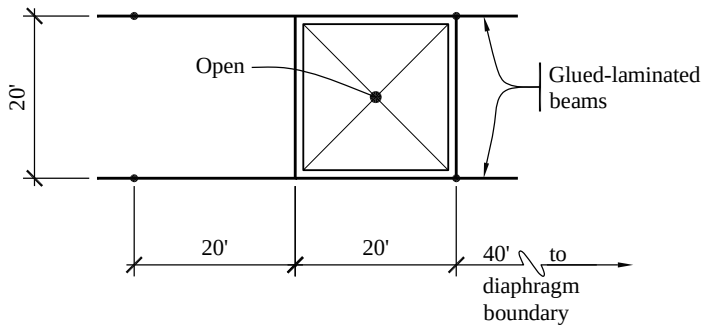

Figure 11.2-5 Diaphragm at roof opening
(1.0 ft = 0.3048 m)

11.2.4.2.6 Chord Forces at Opening. To determine the chord forces on the edge joists, split the diaphragm into smaller free-body sections, assume the inflection points will be at the midpoint of the elements (Figure 11.2-6) and compute the forces at the opening using a uniformly distributed diaphragm demand of 233/200 = 1.165 klf.

For Element 1 (shown in Figure 11.2-7):

w_1 = 1.165/2 = 0.582 kips/ft (assuming half the diaphragm load on each side of the opening)

V_{1B} = 0.5[116.5-(40)(1.165)] = 35.0 kips (based on diaphragm unit shear on right side of opening)

V_{1A} = 35.0-20(0.582) = 23.3 kips (based on diaphragm unit shear on left side of opening)

M_1 = (1/2)[35.0(10) + 23.3(10)] = 291 ft-kips (assuming equal moments at each edge of the section)

The chord force due to M_1 = 291/40 = 7.28 kips. This is only 35 psi on the glued-laminated beam on the edge of the opening. This member is adequate by inspection. On the other side of this diaphragm element, the chord force is much less than the maximum global chord force (59.0 kips), so the ledger and ledger splice are adequate.

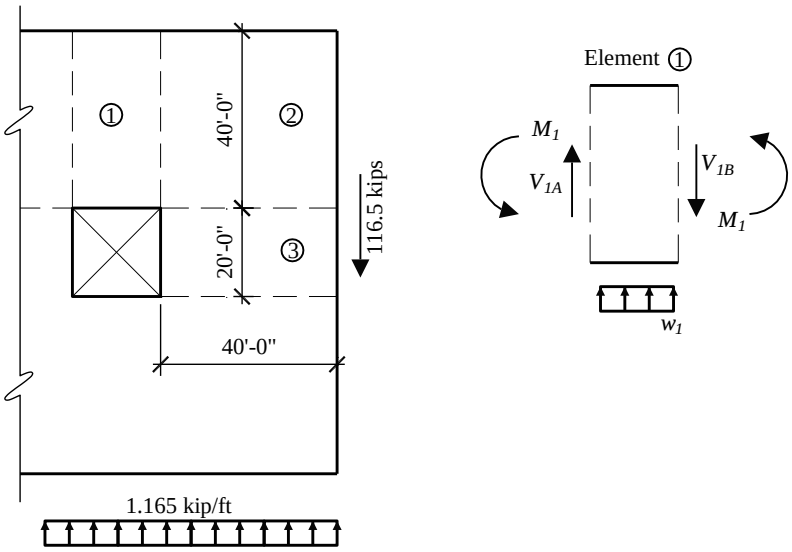

Figure 11.2-6 Chord forces and Element 1 free-body diagram
(1.0 ft = 0.3048 m, 1.0 kip = 4.45 kN, 1.0 kip/ft = 14.6 kN/m)

For Element 3, analyze Element 2 (shown in Figure 11.2-7) in the same manner as Element 1:

w_2 = 1.165(40/100) = 0.466 kips/ft

V_3 = 116.5(40/100) = 46.6 kips

V_{1B} = 35.0 kips

M_1 = 291 ft-kips.

T_{1B} is the chord force due to moment on the total diaphragm:

M = 116.5(40) - 1.165(40^2/2) = 3,728 ft-kips

T_{1B} = 3,728/100 = 37.3 kips

ΣM_0:M_3 = M_1 + 40V_3 - 40T_{1B} - $w_2 40^2/2$ = 291 ft-kips

Therefore, the chord force on the roof joist = 291/40 = 7.26 kips

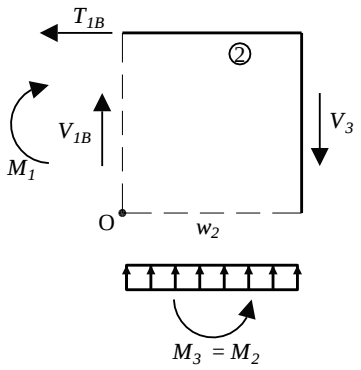

Figure 11.2-7 Free-body diagram for Element 2

Alternatively, the chord design should consider the wall anchorage force interrupted by the opening. As described in Section 11.2.4.4.1, the edge members on each side of the opening are used as continuous cross-ties, with maximum cross-tie force of 16.6 kips. Therefore, the cross-tie will adequately serve as a chord at the opening.

11.2.4.3 Roof Diaphragm Design for Longitudinal Direction

Force = 209 kips

Maximum end shear = 0.50(209) = 104.5 kips

Diaphragm unit shear, v = 104.5/200 = 0.523 klf

For this direction, the plywood layout is Case 3 in AF&PA SDPWS Table 4.2A. Using 1/2-inch Structural I plywood rated sheathing, blocked, with 10d common nails at 4 inches on center at diaphragm boundaries and continuous panel edges parallel to the load (ignoring the capacity of the extra nails in the outer zones), per AF&PA SDPWS Table 4.2A:

$\phi_D v_s$ = 0.80(0.850) = 0.68 klf > 0.523 klf OK

Therefore, use the same nailing designed for the transverse direction. Compared with the transverse direction, the diaphragm deflection and P-delta effects will be satisfactory.

11.2.4.4 Masonry Wall Anchorage to Roof Diaphragm. As stipulated in *Standard* Section 12.11.2.1, masonry walls must be anchored to flexible diaphragms to resist out-of-plane forces computed per *Standard* Equation 12.11-1 as follows:

$F_P = 0.8 S_{DS} I W_p = 0.8(1.0)(1.0) W_p = 0.8\ W_p$

Side walls, F_P = 0.8(65psf)(2+28/2)/1,000 = 0.83 klf

End walls, F_P = 0.8(103psf)(2 + 28/2)/1,000 = 1.32 klf

11.2.4.4.1 Anchoring Joists Perpendicular to Walls (Side Walls). The roof joists are spaced at 2 feet on center, so as a preliminary design, consider a connection at every other joist that will develop 4(0.83) =

3.32 kip/joist. Note that 4 feet is the maximum anchor spacing allowed without having to check the walls for resistance to bending between anchors (*Standard* Sec. 12.11.2).

A common connection for this application is a metal tension tie-down or hold-down device that is anchored to the masonry wall with an embedded bolt and is either nailed, screwed, or bolted to the roof joist. Other types of anchors include metal straps that are embedded in the wall and nailed to the top of the joist. The ledger is not used for this force transfer because the eccentricity between the anchor bolt and the plywood creates tension perpendicular to the grain in the ledger (cross-grain bending), which is prohibited. Also, using the edge nails to resist tension perpendicular to the edge of the plywood is not permitted.

Try a tension tie with a 3/4-inch headed anchor bolt, embedded in the bond beam and with 18 10d nails into the side of the joist (Figure 11.2-8). The cataloged ASD tension capacity of this connector is 3.61 kips based on a load duration factor of 1.60. Modifying the allowable values using the procedure in Section 11.1.4.5 results in a design LRFD capacity of:

$Z'K_F\phi\lambda$ = (3.61)(2.88/1.60)(0.65)(1.0) = 4.22 kips per anchor > 3.32 kips OK

The joists anchored to the masonry wall must also be adequately connected to the diaphragm sheathing. Determine the adequacy of the typical nailing for intermediate framing members. The nail spacing is 12 inches and the joist length is 20 feet, so there are 20 nails per joist. From the AF&PA NDS, the LRFD capacity of a single 10d common nail in 1/2-inch plywood is:

$Z'K_F\phi\lambda$ = (0.090)(2.16/0.65)(0.65) = 0.194 kips per nail

20(0.194) = 3.88 kips > 3.32 kips OK

The embedded anchor bolt also serves as the ledger connection, for both gravity loading and in-plane shear transfer at the diaphragm. Therefore, the strength of the anchorage to masonry and the strength of the bolt in the wood ledger must be checked.

For the anchorage to masonry, check the combined tension and shear resulting from the out-of-plane seismic loading (3.32 kips per bolt) and the vertical gravity loading. Assuming 20 psf dead load (roof live load need not be combined with seismic loads), a 10-foot tributary roof width and ledger bolts at 2 feet on center (at tension ties and in between) the vertical load per bolt = (20 psf)(10 ft)(2 ft)/1,000 = 0.40 kip. Using the load combinations described previously, the design horizontal tension and vertical shear on the bolt are as follows:

$b_{af} = 1.0Q_E$ = 3.32 kips

b_{vf} = 1.4D = 1.4(0.40) = 0.56 kip

The anchor bolts in masonry are designed according to ACI 530 as adopted by the *Standard* (Sec. 14.4) and as modified by *Standard* Sections 14.4.7.6 and 14.4.7.7. *Standard* Section 14.4.7.6 requires the strength of the anchorage connecting diaphragms to other parts of the seismic force-resisting system to be governed by steel tensile or shear yielding unless the anchorage is designed for 2.5 times the required forces. For this example, the anchorage is proportioned such that the steel governs the capacity. *Standard* Section 14.4.7.7 modifies the shear strength requirements for anchorage, requiring that the shear capacity is not more than 2 times the strength due to masonry pry-out.

Using 3/4-inch headed anchor bolts with an effective embedment depth of 6 inches, both tensile strength, B_{an} and shear strength, B_{vn}, will be computed assuming the masonry strength, f'_m, is 2,000 psi and the steel strength, f_y, is 36,000 psi. Tensile strength per ACI 530 Section 3.1.6.2 is taken as the lesser of the following:

$$B_{an} = A_b f_y = 0.44(36) = 15.8 \text{ kips}$$

$$B_{an} = 4A_{pt}\sqrt{f'_m} = 4(113)\sqrt{2{,}000} = 20.2 \text{ kips}$$

where A_{pt} is the projected area of the right cone and is equal to $\pi(l_b)^2$, where l_b is the effective embedment depth. Therefore, $A_{pt} = \pi(6)^2 = 113$ in^2.

Since the steel strength governs, *Standard* Section 14.4.7.6 is met and $\phi = 0.9$. Therefore the design strength in tension is 0.9(15.8) = 14.2 kips.

Shear strength per ACI 530 Section 3.1.6.3 is taken as the lesser of the following:

$$B_{av} = 0.6A_b f_y = 0.6(0.44)(36) = 9.50 \text{ kips}$$

$$B_{av} = 4A_{pv}\sqrt{f'_m} = 4(56.5)\sqrt{2{,}000} = 10.1 \text{ kips}$$

where A_{pv} is one half of the projected area of the right cone and is equal to 113/2 = 56.5 in^2. Since the steel strength governs, *Standard* Section 14.4.7.6 is met for shear and $\phi = 0.9$. Therefore, the design strength in shear is 0.9(9.50) = 8.55 kips.

Shear and tension are combined per ACI 530 Section 3.1.6.4 as:

$$\frac{b_{an}}{\varphi B_{an}} + \frac{b_{av}}{\varphi B_{av}} = \frac{3.32}{14.2} + \frac{0.56}{8.55} = 0.30 < 1.0$$

OK

Figure 11.2-8 summarizes the details of the connection. In-plane seismic shear transfer (combined with gravity) and orthogonal effects are considered in a subsequent section.

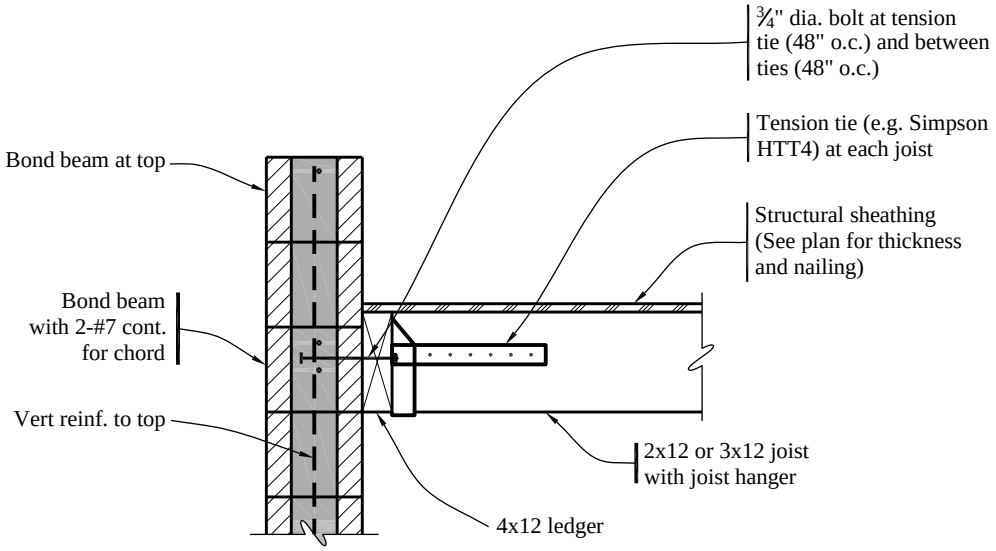

Figure 11.2-8 Anchorage of masonry wall perpendicular to joists
(1.0 in. = 25.4 mm)

According to *Standard* Section 12.11.2.2.1, diaphragms must have continuous cross-ties to distribute the anchorage forces into the diaphragms. Although the *Standard* does not specify a maximum spacing, 20 feet is common practice for this type of construction and seismic design category.

For cross-ties at 20 feet on center, the wall anchorage force per cross-tie is:

(0.83 klf)(20 ft) = 16.6 kips

Try a 3×12 Douglas Fir-Larch No. 1 as a cross-tie. Assuming one row of 1-1/8-inch bolt holes, the net area of the section is 25.3 in^2. Tension strength (parallel to wood grain) per the AF&PA NDS Supplement is:

$F'_T = F_t K_F \phi \lambda$ = (0.675)(2.16/0.8)(0.8) = 1.46 ksi

$T' = F'_t A$ = (1.46)(25.3) = 36.9 kips > 16.6 kips OK

However, the cross-tie must be checked for combined gravity and lateral loads. The governing case for combined loads is midspan where the maximum gravity moment is combined with seismic tension. The 3×12 cross-tie has the following properties:

A = 28.1 in^2

S = 52.7 in^3

F'_t = 1.46 ksi

$F'_b = F_b C_r K_F \phi \lambda$ = (1.000)(1.15)(2.16/0.85)(0.85) = 2.48 kips

The factored dead load moment is computed using the load combinations described above as:

M_u = 1.4(20 psf)(2 ft)(20 ft)^2/8 = 2.80 ft-kips

The factored stresses are computed as:

f_t = 16.6/28.1 = 0.591 ksi

f_b = (2.80)(12)/52.7 = 0.638 ksi

Combined stresses are checked in accordance with AF&PA NDS Section 3.9.1 as follows:

$$\frac{f_t}{F_t^{'}} + \frac{f_b}{F_b^t} = \frac{0.591}{1.46} + \frac{0.638}{2.48} = 0.66 < 1.0$$

OK

At the splices, try a double tie-down device with three 1-inch bolts in double shear through the 3×12 member (Figure 11.2-9). Product catalogs provide design capacities for single tie-downs only; the design of double hold-downs requires two checks. First, consider twice the capacity of one tie-down and, second, consider the capacity of the bolts in double shear.

For the double tie-down, use the procedure in Section 11.1.4.5 to modify the allowable values:

$2ZK_F\phi\lambda$ = 2(8.81)(2.88/1.60)(0.65)(1.0) = 20.6 kips > 16.6 kips OK

For the four bolts, the AF&PA NDS gives:

$4ZK_F\phi\lambda$ = 4(3.50)(2.16/0.65)(0.65)(1.0) = 30.2 kips > 16.6 kips OK

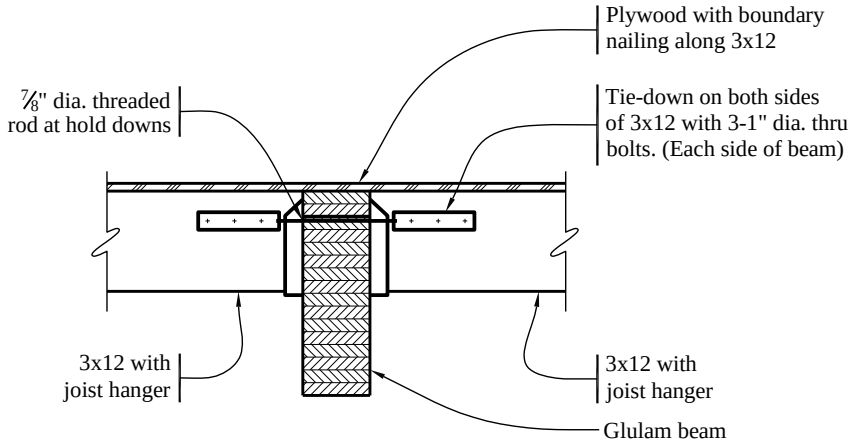

Figure 11.2-9 Chord tie at roof opening
(1.0 in. = 25.4 mm)

In order to transfer the wall anchorage forces into the cross-ties, the subdiaphragms between these ties must be checked per ***Standard*** Section 12.11.2.2.1. There are several ways to perform these

subdiaphragm calculations. One method is illustrated in Figure 11.2-10. The subdiaphragm spans between cross-ties and utilizes the glued-laminated beam and ledger as its chords. The 1-to-1 aspect ratio meets the requirement of 2.5 to 1 for subdiaphragms per ***Standard*** Section 12.11.2.2.1.

For the typical subdiaphragm (Figure 11.2-10):

F_p = 0.83 klf

v = (0.83)(20/2)/20 = 0.415 klf.

The subdiaphragm demand is less than the minimum diaphragm capacity (0.68 klf along the center of the side walls). In order to develop the subdiaphragm strength and boundary nailing must be provided along the cross-tie beams.

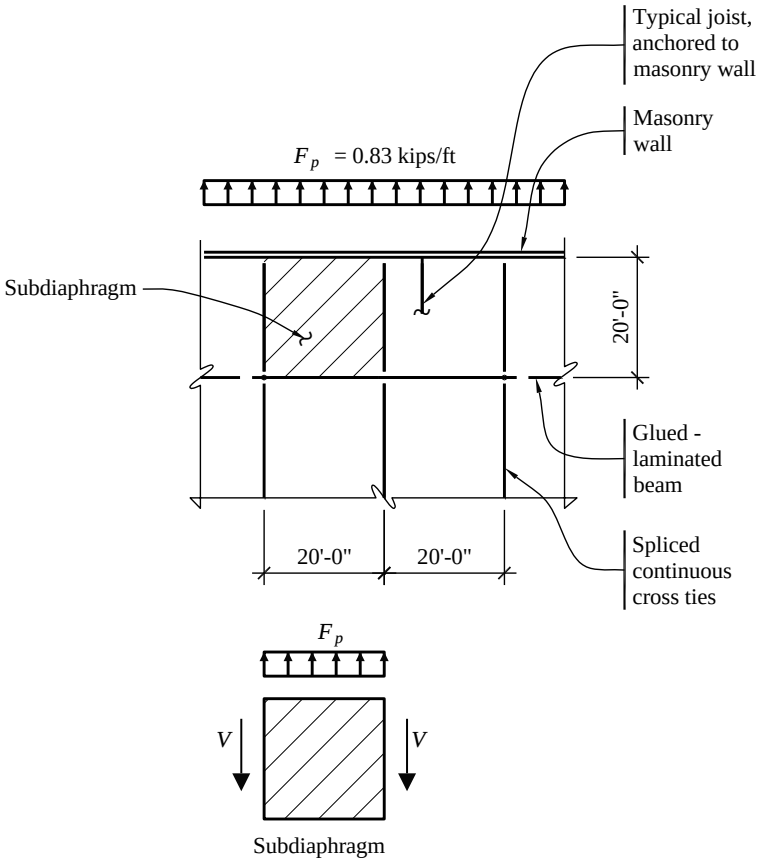

Figure 11.2-10 Cross tie plan layout and subdiaphragm free-body diagram for side walls (1.0 ft = 0.3048 m, 1.0 kip/ft = 14.6 kN/m)

11.2.4.4.2 Anchorage at Joists Parallel to Walls (End Walls). Where the joists are parallel to the walls, tied elements must transfer the forces into the main body of the diaphragm, which can be accomplished by using either metal strapping and blocking or metal rods and blocking. This example uses threaded rods that are inserted through the joists and coupled to the anchor bolt (Figure 11.2-11). Blocking is

added on both sides of the rod to transfer the force into the plywood sheathing. The tension force in the rod causes a compression force on the blocking through the nut and on the bearing plate at the innermost joist.

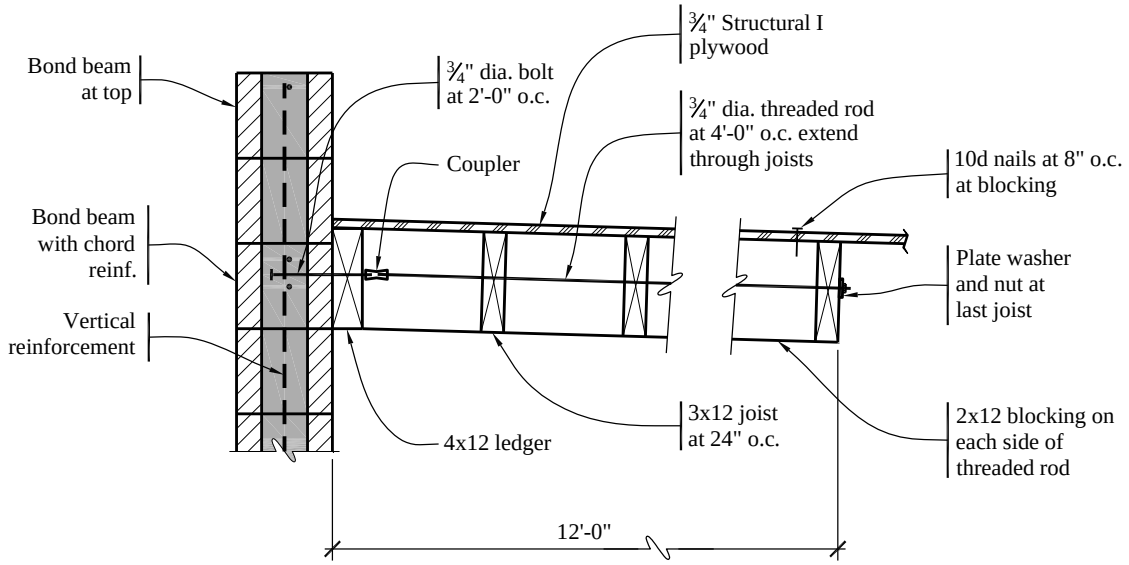

Figure 11.2-11 Anchorage of masonry wall parallel to joists
(1.0 ft = 0.3048 m, 1.0 in. = 25.4 mm)

The anchorage force at the end walls is 1.32 klf. Space the connections at 4 feet on center so that the wall need not be designed for flexure. Thus, the anchorage force is 5.28 kips per anchor.

Try a 3/4-inch headed anchor bolt, embedded into the masonry. In this case, gravity loading on the ledger is negligible and can be ignored and the anchor can be designed for tension only. (In-plane shear transfer and orthogonal effects are considered later.)

As computed for 3/4-inch headed anchor bolts (with 6 inch embedment), the design axial strength is ϕB_{an} = 14.2 kips > 5.28 kips. Therefore, the bolt is acceptable.

Using couplers rated for 125 percent of the strength of the rod material, the threaded rods are then coupled to the anchor bolts and extend six joist spaces (12 feet) into the roof framing. (This length of 12 feet is required for the subdiaphragm force transfer discussed below.)

Nailing the blocking to the plywood sheathing is determined using nail capacities from the AF&PA NDS. As computed previously, the LRFD capacity of a single 10d common nail, $Z'K_F\phi\lambda$ = 0.194 kips per nail. Thus, 28 nails are required (5.28/0.194). This corresponds to a nail spacing of approximately 10 inches for two 12-foot rows of blocking. Space nails at 8 inches for convenience.

Use the glued-laminated timber beams (at 20 feet on center) to provide continuous cross-ties and check the subdiaphragms between the beams to provide adequate load transfer to the beams per *Standard* Section 12.11.2.2.1:

Design tension force on beam = (1.32 klf)(20 ft) = 26.4 kips

The stress on the beam is f_t = 26,400/[8.75(24)] = 126 psi, which is small. The beam is adequate for combined moment due to gravity loading and axial tension.

At the beam splices, try 3/4-inch bolts with steel side plates. Per the AF&PA NDS:

$ZK_F\phi\lambda$ = (3.34)(2.16/0.65)(0.65)(1.0) = 7.21 kips per bolt

The number of bolts required (on each side of the splice joint) is 26.4/7.21 = 3.7.

Use four bolts in a single row at mid-height of the beam, with 1/4-inch by 4-inch steel side plates. The reduction (group action factor) for multiple bolts is negligible. Although not included in this example, the steel side plates should be checked for tension capacity on the gross and net sections. There are pre-engineered hinged connectors for glued-laminated beams that could provide sufficient tension capacity for the splices.

In order to transfer the wall anchorage forces into the cross-ties, the subdiaphragms between these ties must be checked per *Provisions* Section 12.11.2.2.1. The procedure is similar to that used for the side walls as described previously. The end wall condition is illustrated in Figure 11.2-12. The subdiaphragm spans between beams and utilizes a roof joist as its chord. In order to adequately engage the subdiaphragm, the wall anchorage ties must extend back to this chord. Since the maximum aspect ratio for subdiaphragms is 2.5 to 1, the minimum depth is 20/2.5 = 8 feet.

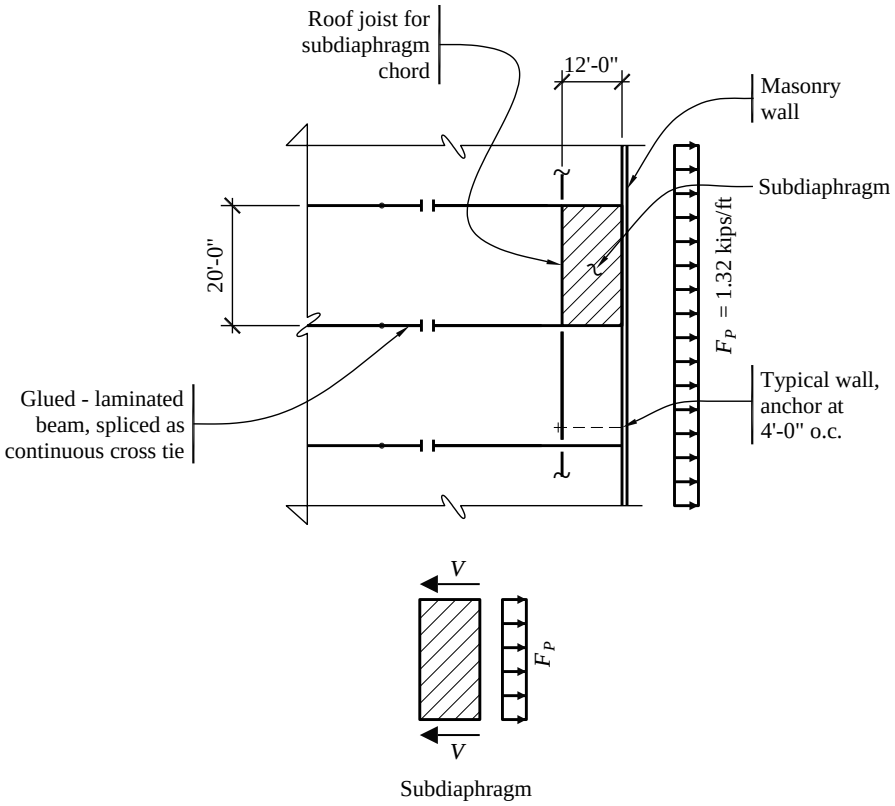

Figure 11.2-12 Cross tie plan layout and subdiaphragm free-body diagram for end walls (1.0 ft = 0.3048 m, 1.0 kip/ft = 14.6 kN/m)

For the typical subdiaphragm (Figure 11.2-12):

F_p = 1.32 klf

v = (1.32)(20/2)/8 = 1.65 klf

As computed previously (see Table 11.2-1 and Figure 11.2.2), the diaphragm strength in this area is 1.17 klf < 1.65 klf. Therefore, increase the subdiaphragm depth to 12 feet (six joist spaces):

v = (1.32)(20/2)/12 = 1.10 klf > 1.17 klf OK

In order to develop the subdiaphragm strength, boundary nailing must be provided along the cross-tie beams. There are methods of refining this analysis using multiple subdiaphragms so that all of the tension anchors need not extend 12 feet into the building.

11.2.4.4.3 Transfer of Shear Wall Forces. The in-plane diaphragm shear must be transferred to the masonry wall by the ledger, parallel to the wood grain. The connection must have sufficient capacity for the diaphragm demands as follows:

- Side walls: 0.523 klf

- End walls: 1.165 klf

For each case, the capacity of the bolted wood ledger and the capacity of the anchor bolts embedded into masonry must be checked. Because the wall connections provide a load path for both in-plane shear transfer and out-of-plane wall forces, the bolts must be checked for orthogonal load effects in accordance with *Standard* Section 12.5. That is, the combined demand must be checked for 100 percent of the lateral load effect in one direction (e.g., shear) and 30 percent of the lateral load effect in the other direction (e.g., tension).

At the side walls, the wood ledger with 3/4-inch bolts (Figure 11.2-8) must be designed for gravity loading (0.56 kip per bolt as computed above) as well as seismic shear transfer. The seismic load per bolt (at 2 feet on center) is 0.523(2) = 1.05 kips.

Combining gravity shear and seismic shear produces a resultant force of 1.19 kips at an angle of 28 degrees from the axis of the wood grain. The bolt capacity in the wood ledger can be determined using the formulas for bolts at an angle to the grain per the AF&PA NDS (either adjusting for dowel bearing strength per Section 11.3.3 or adjusting the tabulated bolt values per Appendix J). The resulting design value, Z = 1.41 kips and the LRFD capacity is determined as follows:

$ZK_F\phi\lambda$ = (1.41)(2.16/0.65)(0.65)(1.0) = 3.05 kips > 1.19 kips OK

This bolt spacing also satisfies the load combination for gravity loading (dead and roof live) only.

For the check of the embedded anchor bolts, the factored demand on a single bolt is 1.05 kips in horizontal shear (in-plane shear transfer), 3.32 kips in tension (out-of-plane wall anchorage) and 0.56 kip in vertical shear (gravity). Orthogonal effects are checked, using the following two equations:

$$\frac{0.3(3.32)}{8.75} + \frac{\sqrt{1.05^2 + 0.56^2}}{2.66} = 0.56$$

and

$$\frac{3.32}{8.75} + \frac{\sqrt{(0.3\times 1.05)^2 + 0.56^2}}{2.66} = 0.62 \text{ (controls)} < 1.0 \quad \text{OK}$$

At the end walls, the ledger with 3/4-inch bolts (Figure 11.2-11) need only be checked for in-plane seismic shear because gravity loading is negligible. For bolts spaced at 4 feet on center, the demand per bolt is 1.165(4) = 4.66 kips parallel to the grain of the wood. Per the AF&PA NDS:

$ZK_F\phi\lambda$ = (1.61)(2.16/0.65)(0.65)(1.0) = 3.48 kips < 4.66 kips NG

Therefore, add 3/4-inch headed bolts evenly spaced between the tension ties such that the bolt spacing is 2 feet on center and the demand per bolt is 1.165(2) = 2.33 kips. These added bolts are used for in-plane shear only and do not have coupled tension tie rods.

For the check of the embedded bolts, the factored demand on a single bolt is 2.33 kips in horizontal shear (in-plane shear transfer), 5.28 kips in tension (out-of-plane wall anchorage), 0 kip in vertical shear (gravity is negligible). Orthogonal effects are checked using the following two equations:

$$\frac{0.3(5.28)}{8.75} + \frac{2.33}{2.66} = 1.06 \text{ (controls)} > 1.0 \qquad \text{NG}$$

$$\frac{5.28}{8.75} + \frac{0.3(2.33)}{2.66} = 0.86$$

Since one of the equations is slightly more than unity, the bolt capacity can be increased by using a larger bolt or more embedment depth, or more bolts can be added. With this minor revision, the wall connections satisfy the requirements for combined gravity and seismic loading, including orthogonal effects.

12

Seismically Isolated Structures

Charles A. Kircher, P.E., Ph.D.

Contents

12.1 BACKGROUND AND BASIC CONCEPTS 4
12.1.1 Types of Isolation Systems 4
12.1.2 Definition of Elements of an Isolated Structure 5
12.1.3 Design Approach 6
12.1.4 Effective Stiffness and Effective Damping 7
12.2 CRITERIA SELECTION 7
12.3 EQUIVALENT LATERAL FORCE PROCEDURE 9
12.3.1 Isolation System Displacement 9
12.3.2 Design Forces 11
12.4 DYNAMIC LATERAL RESPONSE PROCEDURE 15
12.4.1 Minimum Design Criteria 15
12.4.2 Modeling Requirements 16
12.4.3 Response Spectrum Analysis 18
12.4.4 Response History Analysis 18
12.5 EMERGENCY OPERATIONS CENTER USING DOUBLE-CONCAVE FRICTION PENDULUM BEARINGS, OAKLAND, CALIFORNIA 21
12.5.1 System Description 22
12.5.2 Basic Requirements 25
12.5.3 Seismic Force Analysis 34
12.5.4 Preliminary Design Based on the ELF Procedure 36
12.5.5 Design Verification Using Nonlinear Response History Analysis 51
12.5.6 Design and Testing Criteria for Isolator Units 61

Chapter 17 of ASCE/SEI 7-05 (the ***Standard***) addresses the design of buildings that incorporate a seismic isolation system. It defines load, design and testing requirements specific to the isolation system and interfaces with the other chapters of the ***Standard*** for design of the structure above the isolation system and of the foundation and structural elements below.

The 2009 ***NEHRP Recommended Provisions*** (the ***Provisions***) incorporates changes to ground motion criteria that significantly affect the analysis of isolated structures. Isolated structures typically are used for important or essential facilities that have functional performance objectives beyond life safety. Accordingly, more advanced methods of analysis are required for design of these structures. Site-specific hazard analysis is common and dynamic (response history) analysis is routine for design, or design verification, of isolated structures.

The ***Standard*** uses the notation MCE for "maximum considered earthquake" ground motions. The ***Provisions*** have modified the definition and designation of MCE to MCE_R, which is defined as "risk-targeted maximum considered earthquake" ground motions. In the corresponding text of the ***Standard*** where maximum considered earthquake (MCE) is stated the intent of the ***Provisions*** is that risk-targeted maximum considered earthquake (MCE_R) ground motions be used. Consistent with the ***Provisions***, ASCE/SEI 7-10 replaced maximum considered earthquake (MCE) by risk-targeted maximum considered earthquake (MCE_R) ground motions.

A discussion of background, basic concepts and analysis methods is followed by an example that illustrates the application of the ***Standard*** to the structural design of a building with an isolation system. The example building is a three-story emergency operations center (EOC) with a steel concentrically braced frame above the isolation system. The isolation system utilizes sliding friction pendulum bearings, a type of bearing commonly used for seismic isolation of buildings. Although the facility is hypothetical, it is of comparable size and configuration to actual base-isolated EOCs and is generally representative of base-isolated buildings. The example comprehensively describes the EOC's configuration, defines appropriate criteria and design parameters and develops a preliminary design using the equivalent lateral force (ELF) procedure. It also includes a check of the preliminary design using dynamic analysis as required by the ***Standard*** and a discussion of isolation system design and testing criteria.

The example EOC is assumed to be located in Oakland, California, a region of very high seismicity subject to particularly strong ground motions. Large seismic demands pose a challenge for the design of base-isolated structures in terms of the displacement capacity of the isolation system and the configuration of the structure above the isolation system. The isolation system will need to accommodate large lateral displacements, often in excess of 2 feet. The structure above the isolation system should be configured to resist lateral forces without developing large overturning loads that could cause excessive uplift displacement of isolators. The example addresses these issues and illustrates that isolated structures can be designed to meet the requirements of the ***Standard***, even in regions of very high seismicity. Designing an isolated structure in a region of lower seismicity would follow the same approach. The isolation system displacement, overturning forces and so forth, would all be reduced; and therefore easier to accommodate using available isolation system devices.

The isolation system of the building in the example uses a type of friction pendulum system (FPS) bearing that has a double concave configuration. These bearings are composed of large top and bottom concave plates with an articulated slider in between that permits lateral displacement of the plates with gravity acting as a restoring force. FPS bearings have been used for a number of building projects, including the 2010 Mills-Peninsula hospital in Burlingame, California. Using FPS bearings in this example should not be taken as an endorsement of this particular type of isolator to the exclusion of others. The requirements of the ***Standard*** apply to all types of isolations systems and other types of

isolators (and supplementary damping devices) could have been used equally well in the example. Other common types of isolators include high-damping rubber (HDR) and lead-rubber (LR) bearings.

In addition to the *Standard* and the *Provisions*, the following documents are either referenced directly, provide background, or are useful aids for the analysis and design of seismically isolated structures.

- ATC 1996 — Applied Technology Council. 1996. *Seismic Evaluation and Retrofit of Buildings*, ATC40.
- Constantinou — Constantinou, M. C., P. Tsopelas, A. Kasalanati and E. D. Wolff. 1999. *Property Modification Factors for Seismic Isolation Bearings*, Technical Report MCEER-99-0012. State University of New York.
- Sarlis — Sarlis, A. A. S. and M. C. Constantinou. 2010. "Modeling Triple Friction Pendulum Isolators in Program SAP2000," State University of New York, Buffalo, New York, June 27, 2010.
- ETABS — Computers and Structures, Inc. (CSI). 2009. *ETABS Linear and Nonlinear Static and Dynamic Analysis and Design of Building Systems*. CSI, Berkeley, California.
- ASCE 41 — American Society of Civil Engineers (ASCE). 2006. *Seismic Rehabilitation of Existing Buildings*, ASCE 41-06, ASCE, Washington, D.C.
- FEMA 222A — Federal Emergency Management Agency (FEMA). 1995. *NEHRP Recommended Provisions for Seismic Regulations for New Buildings*, FEMA 222A.
- FEMA P-695 — Federal Emergency Management Agency (FEMA). 2009. Quantification of Building Seismic Performance Factors, FEMA P-695, Washington, D.C.
- 1991 UBC — International Conference of Building Officials. 1991. *Uniform Building Code*.
- 1994 UBC — International Conference of Building Officials. 1994. *Uniform Building Code*.
- 2006 IBC — International Code Conference. 2006. *International Building Code*.
- Kircher — Kircher, C. A., G. C. Hart and K. M. Romstad. 1989. "Development of Design Requirements for Seismically Isolated Structures" in *Seismic Engineering and Practice*, Proceedings of the ASCE Structures Congress, American Society of Civil Engineers, May 1989.
- PEER 2006 — Pacific Earthquake Engineering Research (PEER) Center. 2006. *PEER NGA Database*, PEER, University of California, Berkeley, California, http://peer.berkeley.edu/nga/
- SEAOC 1999 — Seismology Committee, Structural Engineers Association of California. 1999. *Recommended Lateral Force Requirements and Commentary*, 7th Ed.
- SEAONC Isolation — Structural Engineers Association of Northern California. 1986. *Tentative Seismic Isolation Design Requirements*.

- USGS 2009 http://earthquake.usgs.gov/design maps/usapp/

12.1 BACKGROUND AND BASIC CONCEPTS

Seismic isolation, commonly referred to as base isolation, is a design concept that presumes a structure can be substantially decoupled from potentially damaging earthquake ground motions. By decoupling the structure from ground shaking, isolation reduces response in the structure that would otherwise occur in a conventional, fixed-base building. Alternatively, base-isolated buildings may be designed for reduced earthquake response to produce the same degree of seismic protection. Isolation decouples the structure from ground shaking by making the fundamental period of the isolated structure several times greater than the period of the structure above the isolation system.

The potential advantages of seismic isolation and the advancements in isolation system products led to the design and construction of a number of isolated buildings and bridges in the early 1980s. This activity, in turn, identified a need to supplement existing seismic codes with design requirements developed specifically for such structures. These requirements assure the public that isolated buildings are safe and they provide engineers with a basis for preparing designs and building officials with minimum standards for regulating construction.

Initial efforts to develop design requirements for base-isolated buildings began with ad hoc groups of the Structural Engineers Association of California (SEAOC), whose Seismology Committee has a long history of contributing to codes. The northern section of SEAOC was the first to develop guidelines for the use of elastomeric bearings in hospitals. These guidelines were adopted in the late 1980s by the California Office of Statewide Health Planning and Development (OSHPD) and were used to regulate the first base-isolated hospital in California. Efforts to develop general requirements to govern the design of base-isolated buildings resulted in the publication of SEAONC Isolation and appendix in the 1991 UBC and an appendix in FEMA 222A. While technical changes have been made subsequently, most of the basic concepts for the design of seismically isolated structures found in the *Standard* can be traced back to the initial work by the northern section of SEAOC. Additional background may be found in the commentary to the SEAOC 1999 *Blue Book*.

The isolation system requirements in ASCE Standard 41, *Seismic Rehabilitation of Existing Buildings*, are comparable to those for new buildings.

12.1.1 Types of Isolation Systems

The *Standard* requirements are intentionally broad, accommodating all types of acceptable isolation systems. To be acceptable, the *Standard* requires the isolation system to:

- Remain stable for maximum earthquake displacements.
- Provide increasing resistance with increasing displacement.
- Have limited degradation under repeated cycles of earthquake load.
- Have well-established and repeatable engineering properties (effective stiffness and damping).

The *Standard* recognizes that the engineering properties of an isolation system, such as effective stiffness and damping, can change during repeated cycles of earthquake response (or otherwise have a range of

values). Such changes or variability of design parameters are acceptable provided that the design is based on analyses that conservatively bound (limit) the range of possible values of design parameters.

The first seismic isolation systems used in buildings in the United States were composed of either high-damping rubber (HDR) or lead-rubber (LR) elastomeric bearings. Other types of isolation systems now include sliding systems, such as the friction pendulum system, or some combination of elastomeric and sliding isolators. Some applications at sites with very strong ground shaking use supplementary fluid-viscous dampers in parallel with either sliding or elastomeric isolators to control displacement. While generally applicable to all types of systems, certain requirements of the *Standard* (in particular, prototype testing criteria) were developed primarily for isolation systems with elastomeric bearings.

Isolation systems typically provide only horizontal isolation and are rigid or semi-rigid in the vertical direction. An example of a rare exception to this rule is the full (horizontal and vertical) isolation of a building in southern California, isolated by large helical coil springs and viscous dampers. While the basic concepts of the *Standard* can be extended to full isolation systems, the requirements are only for horizontal isolation systems. The design of a full isolation system requires special analyses that explicitly include vertical ground shaking and the potential for rocking response.

Seismic isolation is commonly referred to as base isolation because the most common location of the isolation system is at or near the base of the structure. The *Standard* does not restrict the plane of isolation to the base of the structure but does require the foundation and other structural elements below the isolation system to be designed for unreduced (R_I = 1.0) earthquake forces.

12.1.2 Definition of Elements of an Isolated Structure

The design requirements of the *Standard* distinguish between structural elements that are either components of the isolation system or part of the structure below the isolation system (e.g., foundation) and elements of the structure above the isolation system. The isolation system is defined by Chapter 17 of the *Standard* as follows:

> The collection of structural elements includes all individual isolator units, all structural elements that transfer force between elements of the isolation system and all connections to other structural elements. The isolation system also includes the wind-restraint system, energy-dissipation devices and/or the displacement restraint system if such systems and devices are used to meet the design requirements of this chapter.

Figure 12.1-1 illustrates this definition and shows that the isolation system consists not only of the isolator units but also of the entire collection of structural elements required for the system to function properly. The isolation system typically includes segments of columns and connecting girders just above the isolator units because such elements resist moments (due to isolation system displacement) and their yielding or failure could adversely affect the stability of isolator units.

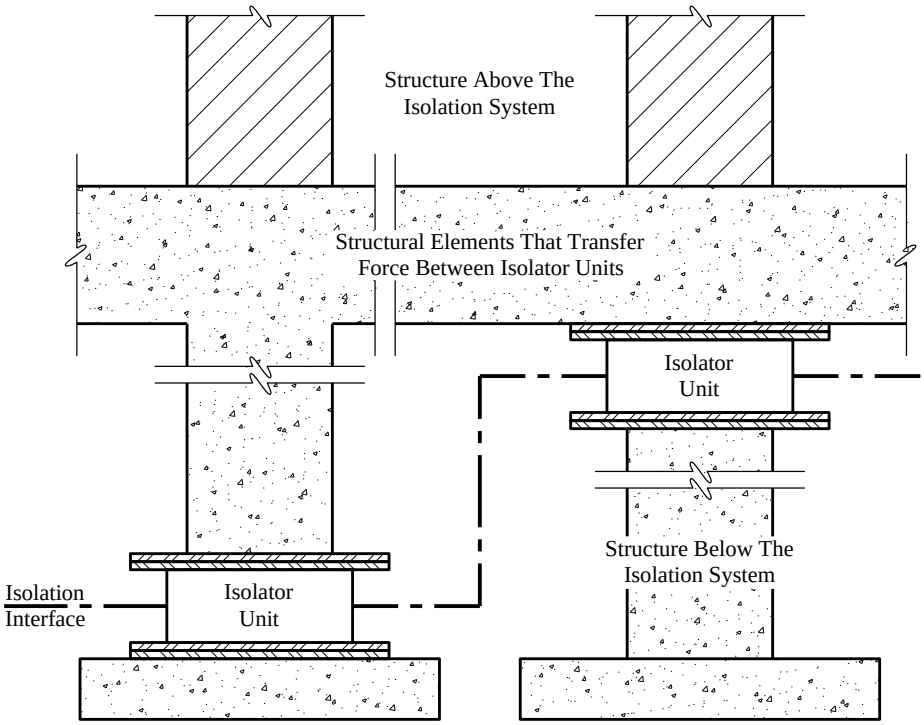

Figure 12.1-1 Isolation system terminology

The isolation interface is an imaginary boundary between the upper portion of the structure, which is isolated and the lower portion of the structure, which is assumed to move rigidly with the ground. Typically, the isolation interface is a horizontal plane, but it may be staggered in elevation in certain applications. The isolation interface is important for design of nonstructural components, including components of electrical and mechanical systems that cross the interface and must accommodate large relative displacements.

The wind-restraint system is typically an integral part of isolator units. Elastomeric isolator units are very stiff at very low strains and usually satisfy drift criteria for wind loads and the static (breakaway) friction force of sliding isolator units is usually greater than the wind force.

12.1.3 Design Approach

The design of isolated structures using the *Standard* has two objectives: achieving life safety in a major earthquake and limiting damage due to ground shaking. To meet the first performance objective, the isolation system must be stable and capable of sustaining forces and displacements associated with maximum considered earthquake (MCE_R) ground motions and the structure above the isolation system must remain essentially elastic when subjected to design earthquake (DE) ground motions. Limited ductility demand is considered necessary for proper functioning of the isolation system. If significant inelastic response were permitted in the structure above the isolation system, unacceptably large drifts could result due to the nature of long-period vibration. Limiting ductility demand on the superstructure has the additional benefit of meeting the second performance objective of damage control.

The *Standard* addresses the performance objectives by requiring the following:

- Design of the superstructure for forces associated with the design earthquake, reduced by only a fraction of the factor permitted for design of conventional, fixed-base buildings ($R_I = 3/8R \leq 2.0$).
- Design of the isolation system and elements of the structure below the isolation system (i.e., the foundation) for unreduced design earthquake forces ($R_I = 1.0$).
- Design and prototype testing of isolator units for forces (including effects of overturning) and displacements associated with the MCE_R.
- Provision of sufficient separation between the isolated structure and surrounding retaining walls and other fixed obstructions to allow unrestricted movement during the MCE_R.

12.1.4 Effective Stiffness and Effective Damping

The *Standard* utilizes the concepts of effective stiffness and effective damping to define key parameters of inherently nonlinear, inelastic isolation systems in terms of amplitude-dependent linear properties. Effective stiffness is the secant stiffness of the isolation system at the amplitude of interest. Effective damping is the amount of equivalent viscous damping described by the hysteresis loop at the amplitude of interest. Figure 12.1-2 shows the application of these concepts to both hysteretic isolator units (e.g., friction or yielding devices) and viscous isolator units and shows the *Standard* equations used to determine effective stiffness and effective damping from tests of prototypes.

Ideally, the effective damping of velocity-dependent devices (including viscous isolator units) should be based on the area of hysteresis loops measured during cyclic testing of the isolation system at full-scale earthquake velocities. Tests of prototypes are usually performed at lower velocities (due to test facility limitations), resulting in hysteresis loops with less area for systems with viscous damping, which produce lower (conservative) estimates of effective damping. Conversely, testing at lower velocities can overestimate effective damping for certain systems (e.g., sliding systems with a coefficient of friction that decreases for repeated cycles of earthquake load).

12.2 CRITERIA SELECTION

As specified in the *Standard,* the design of isolated structures must be based on the results of the ELF procedure, response spectrum analysis, or (nonlinear) response history analysis. Because isolation systems typically are nonlinear, linear methods (ELF procedure and response spectrum analysis) use effective stiffness and damping properties to model nonlinear isolation system components.

The ELF procedure is intended primarily to prescribe minimum design criteria and may be used for design of a very limited class of isolated structures (without confirmatory dynamic analyses). The simple equations of the ELF procedure are useful tools for preliminary design and provide a means of expeditious review and checking of more complex calculations. The *Standard* also uses these equations to establish lower-bound limits on results of dynamic analysis that may be used for design. Table 12.2-1 summarizes site conditions and structure configuration criteria that influence the selection of an acceptable method of analysis for designing of isolated structures. Where none of the conditions in Table 12.2-1 applies, all three methods are permitted.

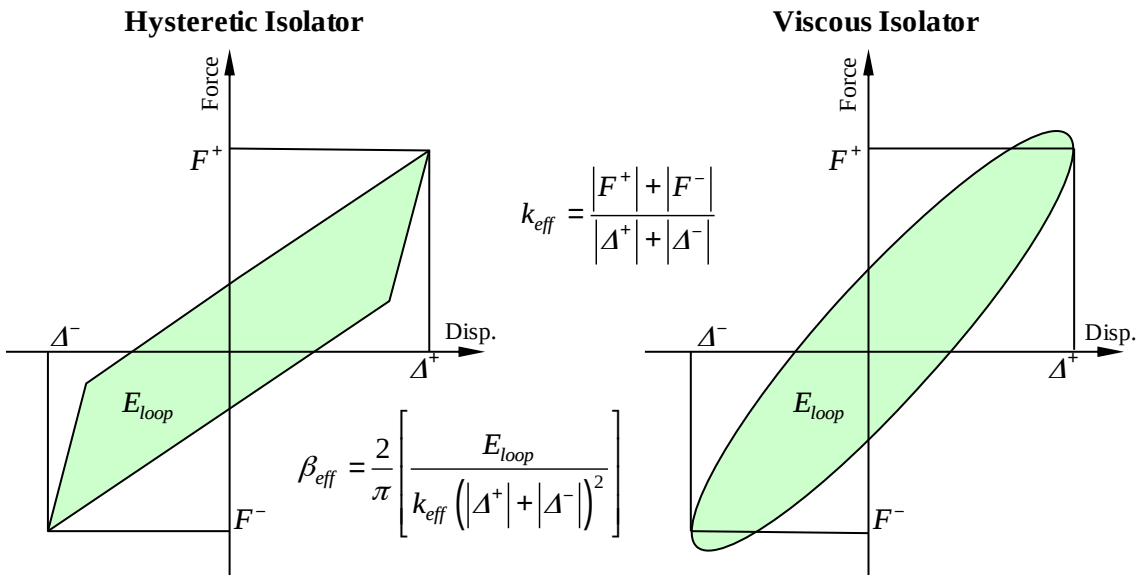

Figure 12.2-1 Effective stiffness and effective damping

Table 12.2-1 Acceptable Methods of Analysis*

Site Condition or Structure Configuration Criteria	ELF Procedure	Modal Response Spectrum Analysis	Seismic Response History Analysis
Site Conditions			
Near-source ($S_1 \geq 0.6$)	NP	P	P
Soft soil (Site Class E or F)	NP	NP	P
Superstructure Configuration			
Flexible or irregular superstructure (height > 4 stories, height > 65 ft, or $T_M > 3.0$ sec., or $T_D \leq 3T$)**	NP	P	P
Nonlinear superstructure (requiring explicit modeling of nonlinear elements; *Standard* Sec. 17.6.2.2.1)	NP	NP	P
Isolation System Configuration			
Highly nonlinear isolation system or system that otherwise does not meet the criteria of *Standard* Sec. 17.4.1, Item 7	NP	NP	P

* P indicates permitted and NP indicates not permitted by the *Standard*.

** T is the elastic, fixed-base period of the structure above the isolation system.

Seismic criteria are based on the same site and seismic coefficients as conventional, fixed-base structures (e.g., mapped value of S_1 as defined in *Standard* Chapter 11). Additionally, site-specific design criteria

are required for isolated structures located on soft soil (Site Class E or F) or near an active source such that S_1 is greater than or equal to 0.6, or when nonlinear response history analysis is used for design.

12.3 EQUIVALENT LATERAL FORCE PROCEDURE

The ELF procedure is a displacement-based method that uses simple equations to determine isolated structure response. The equations are based on ground shaking defined by 1-second spectral acceleration and the assumption that the shape of the design response spectrum at long periods is inversely proportional to period as shown in *Standard* Figure 11.4-1. There is also a $1/T^2$ portion of the spectrum at periods greater than T_L. However, in most parts of the Unites States T_L is longer than the period of typical isolated structures. Although the ELF procedure is considered a linear method of analysis, the equations incorporate amplitude-dependent values of effective stiffness and damping to account implicitly for the nonlinear properties of the isolation system. The equations are consistent with the nonlinear static procedure of ASCE 41 assuming the superstructure is rigid and lateral displacements occur primarily in the isolation system.

12.3.1 Isolation System Displacement

The isolation system displacement for the design earthquake is determined using *Standard* Equation 17.5-1:

$$D_D = \left(\frac{g}{4\pi^2} \right) \frac{S_{D1} T_D}{B_D}$$

where the damping factor, B_D, is based on effective damping, β_D, using *Standard* Table 17.5-1. This equation describes the peak (spectral) displacement of a single-degree-of-freedom (SDOF) system with period, T_D and damping, β_D, for the design earthquake spectrum defined by the seismic coefficient, S_{D1}. S_{D1} corresponds to 5 percent damped spectral response at a period of 1 second. B_D, converts 5 percent damped response to the level of damping of the isolation system. B_D is 1.0 when effective damping, β_D, is 5 percent of critical. Figure 12.3-1 illustrates the underlying concepts of *Standard* Equation 17.5-1 and the amplitude-dependent equations of the *Standard* for effective period, T_D and effective damping, β_D.

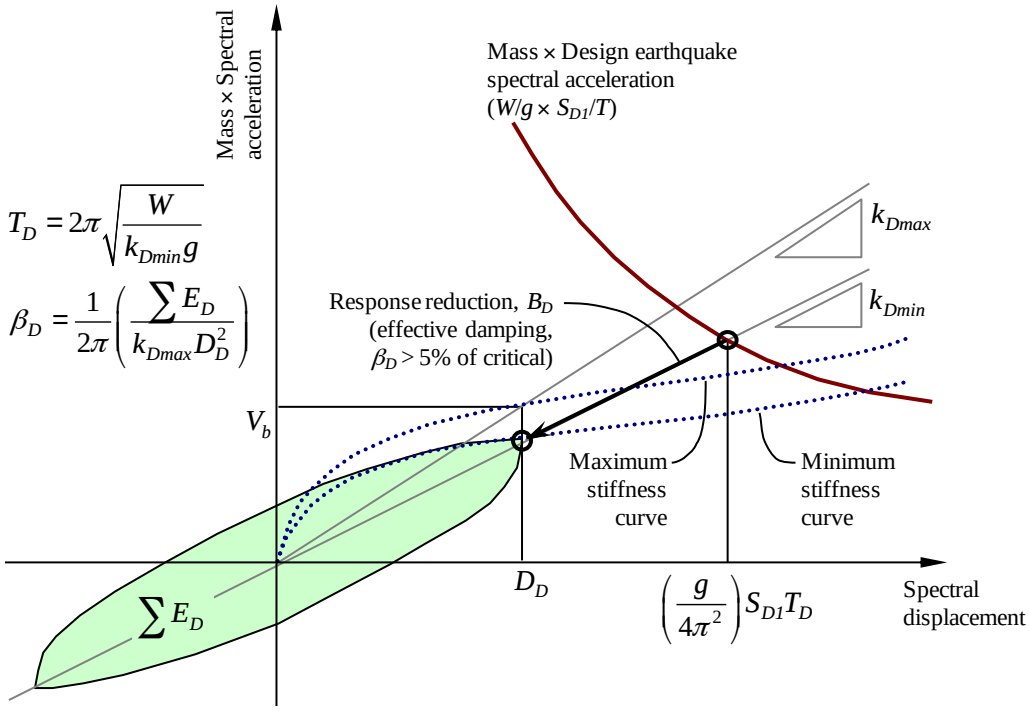

Figure 12.3-1 Isolation system capacity and earthquake demand

The equations for maximum displacement, D_M and design displacement, D_D, reflect differences due to the corresponding levels of ground shaking. The maximum displacement is associated with MCE_R ground motions (characterized by S_{M1}) whereas the design displacement corresponds to design earthquake ground motions (characterized by S_{D1}). In general, the effective period and the damping factor (T_M and B_M, respectively) used to calculate the maximum displacement are different from those used to calculate the design displacement (T_D and B_D) because the effective period tends to shift and effective damping may change with the increase in the level of ground shaking.

As shown in Figure 12.3-1, the calculation of effective period, T_D, is based on the minimum effective stiffness of the isolation system, k_{Dmin}, as determined by prototype testing of individual isolator units. Similarly, the calculation of effective damping is based on the minimum loop area, E_D, as determined by prototype testing. Use of minimum effective stiffness and damping produces larger estimates of effective period and peak displacement of the isolation system.

The design displacement, D_D and maximum displacement, D_M, represent peak earthquake displacements at the center of mass of the building without the additional displacement that can occur at other locations due to actual or accidental mass eccentricity. Equations for determining total displacement, including the effects of mass eccentricity as an increase in the displacement at the center of mass, are based on the plan dimensions of the building and the underlying assumption that building mass and isolation stiffness have a similar distribution in plan. The increase in displacement at corners for 5 percent mass eccentricity is approximately 15 percent if the building is square in plan and as much as 30 percent if the building is long in plan. Figure 12.3-2 illustrates design displacement, D_D and maximum displacement, D_M, at the center of mass of the building and total maximum displacement, D_{TM}, at the corners of an isolated building.

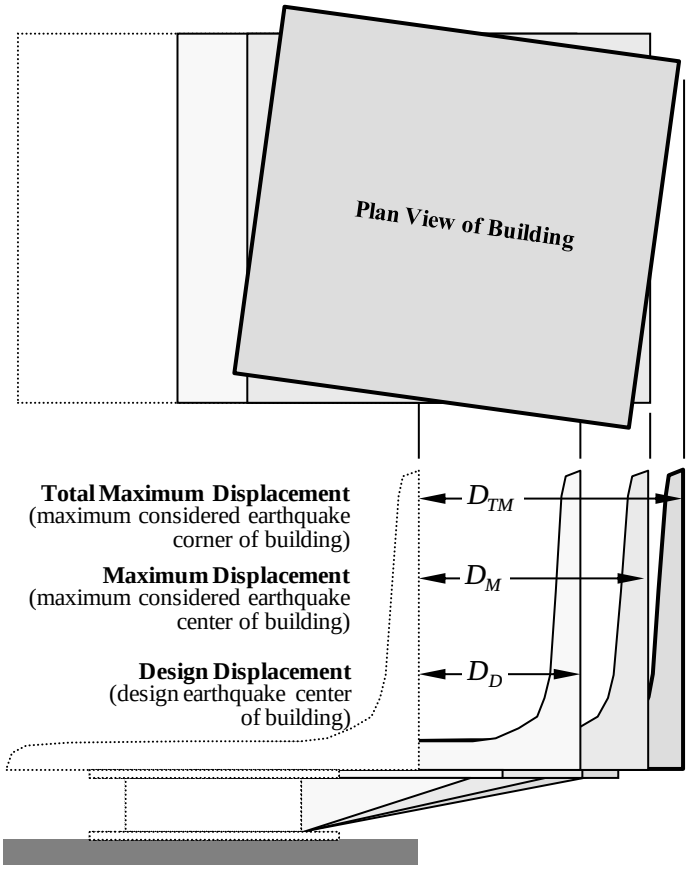

Figure 12.3-2 Design, maximum and total maximum displacement

12.3.2 Design Forces

Forces required by the *Standard* for design of isolated structures are different for design of the superstructure and design of the isolation system and other elements of the structure below the isolation system (i.e., the foundation). In both cases, however, use of the maximum effective stiffness of the isolation system is required to determine a conservative value of design force.

In order to provide appropriate overstrength, peak design earthquake response (without reduction) is used directly for design of the isolation system and the structure below. Design for unreduced design earthquake forces is considered sufficient to avoid inelastic response or failure of connections and other elements for ground shaking as strong as that associated with the MCE_R (i.e., shaking as much as 1.5 times that of the design earthquake). The design earthquake base shear, V_b, is given by *Standard* Equation 17.5-7:

$$V_b = k_{Dmax} D_D$$

where k_{Dmax} is the maximum effective stiffness of the isolation system at the design displacement, D_D. Because the design displacement is conservatively based on minimum effective stiffness, *Standard* Equation 17.5-7 implicitly induces an additional conservatism of a worst-case combination mixing maximum and minimum effective stiffness in the same equation. Rigorous modeling of the isolation

system for dynamic analyses precludes mixing of maximum and minimum stiffness in the same analysis (although separate analyses typically are required to determine bounding values of both displacement and force).

Design earthquake response is reduced by a modest factor for design of the superstructure above the isolation interface, as given by *Standard* Equation 17.5-8:

$$V_s = \frac{V_b}{R_I} = \frac{k_{D\max} D_D}{R_I}$$

The reduction factor, R_I, is defined as three-eighths of the R factor for the seismic force-resisting system of the superstructure, as specified in *Standard* Table 12.2-1, with an upper-bound value of 2.0. A relatively small R_I factor is intended to keep the superstructure essentially elastic for the design earthquake (i.e., keeping earthquake forces at or below the true strength of the seismic force-resisting system). The *Standard* also imposes three limits on design forces that require the value of V_s to be at least as large as each of the following:

1. The shear force required for design of a conventional, fixed-base structure of the same effective seismic weight (and seismic force-resisting system) and period T_D.

2. The shear force required for wind design.

3. A factor of 1.5 times the shear force required for activation of the isolation system.

The first two limits seldom govern design but do reflect principles of good design. The third often governs design of very long period systems with substantial effective damping (e.g., the example EOC in Sec. 12.5) and is included in the *Standard* to ensure that the isolation system displaces significantly before lateral forces reach the strength of the seismic force-resisting system.

For designs using the ELF procedure, the lateral forces, F_x, must be distributed to each story over the height of the structure, assuming an inverted triangular pattern of lateral load (*Standard* Eq. 17.5-9):

$$F_x = \frac{V_s w_x h_x}{\sum_{i=n}^{n} w_i h_i}$$

Because the lateral displacement of the isolated structure is dominated by isolation system displacement, the actual pattern of lateral force in the isolated mode of response is distributed almost uniformly over height. Nevertheless, the *Standard* requires an inverted triangular pattern of lateral load to capture possible higher-mode effects that might be missed by not modeling superstructure flexibility and explicitly considering isolation system nonlinearity. Response history analysis that models superstructure flexibility and nonlinear properties of isolators would directly incorporate higher mode effects in the results.

The ELF formulas may be used to construct plots of design displacement and base shear as a function of effective period, T_D or T_M, of the isolation system. For example, design displacement (D_D), total maximum displacement (D_{TM}) and design forces for the isolation system (V_b) and the superstructure (V_s) are shown in Figure 12.3-3 for a steel special concentrically braced frame (SCBF) superstructure and in

Figure 12.3-4 for a steel ordinary concentrically braced frame (OCBF) superstructure as functions of the effective period of the isolation system.

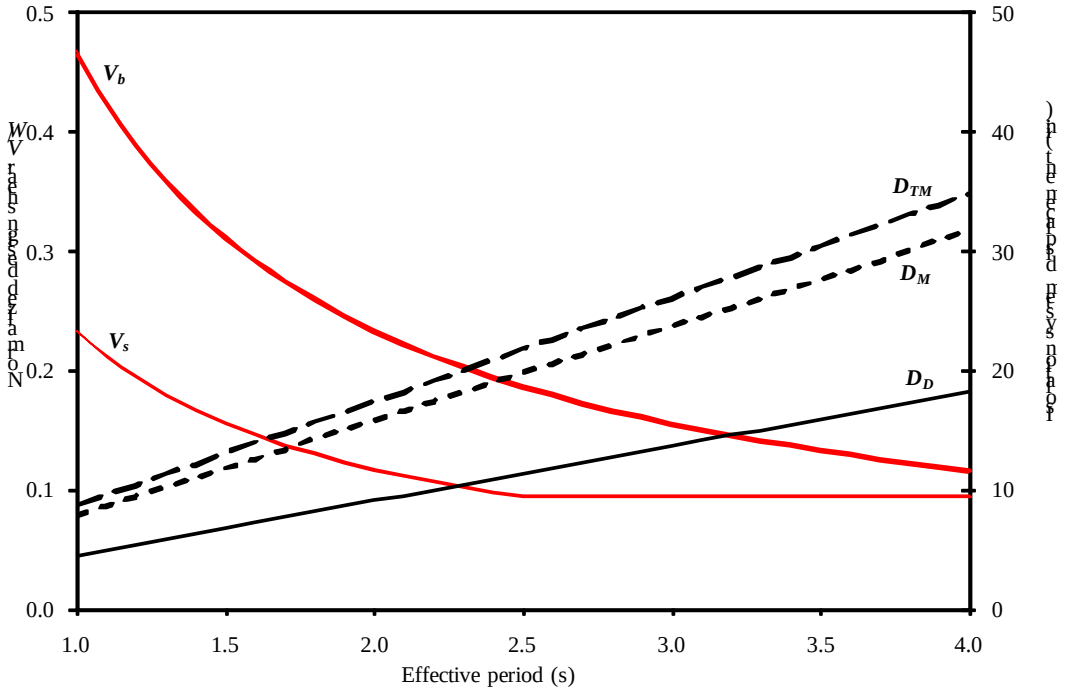

Figure 12.3-3 Isolation system displacement and shear force (SCBF)
(R/I = 6.0/1.5, R_I = 2.0) (1.0 in. = 25.4 mm)

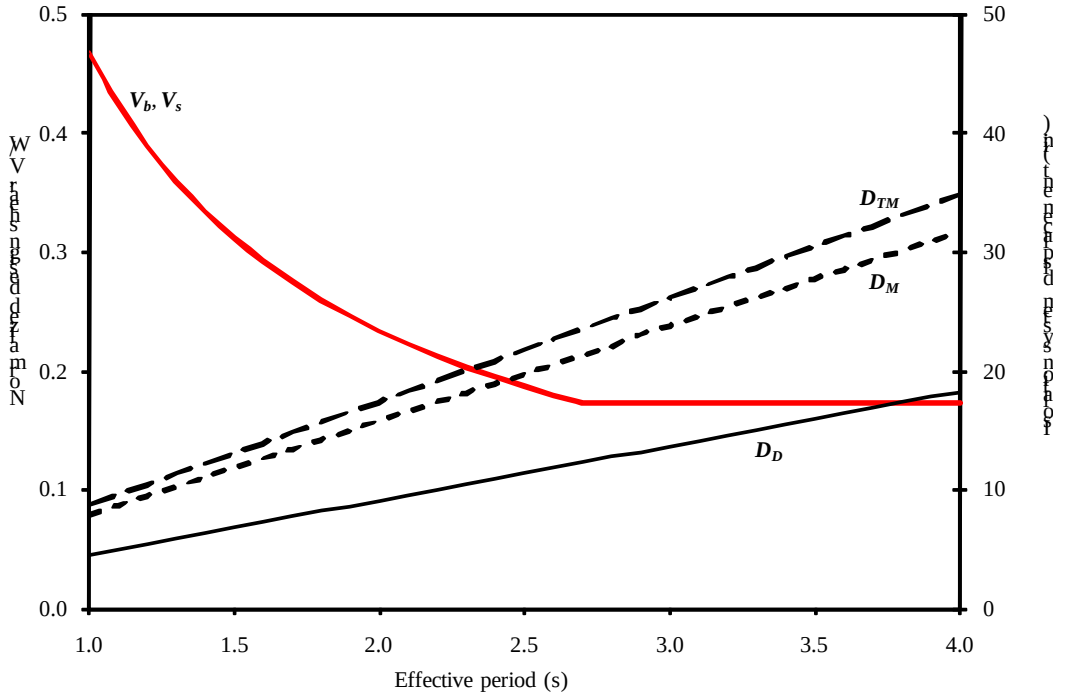

Figure 12.3-4 Isolation system displacement and shear force (OCBF)
(R/I = 3.25/1.5, R_I = 1.0) (1.0 in. = 25.4 mm)

Figures 12.3-3 and 12.3-4 illustrate design properties for a building located in a region of high seismicity, relatively close to an active fault, with a 1-second spectral acceleration parameter, S_1, equal to 0.75 and site conditions corresponding to the C-D boundary (Site Class CD). Note: Seismic hazard and site conditions (and effective damping of the isolation system) were selected to be the same as those of the example EOC facility (Sec. 12.5). Table 12.3-1 summarizes the key response and design parameters that are used with various ELF formulas to construct the plots shown Figures 12.3-3 and 12.3-4.

Table 12.3-1 Summary of Key Response and Design Parameters Used to Construct Illustrative Plots of Design Displacements and Forces as a Function of Effective Period in Figures 12.3-3 and 12.3-4

Key Response or Design Parameter			
Symbol	Description	Value	
	Ground Motion and Site Amplification Parameters		
S_1	1-Second Spectral Acceleration (g)	0.75	
S_s	Short Period Spectral Acceleration (g)	1.25	
F_v	1-Second Site Coefficient (Site Class C-D)	1.4	
F_a	Short-Period Site Coefficient (Site Class C-D)	1.0	
	Isolation System Design Parameters		
β_D	Effective Damping - Design Level Response	20%	
B_D	Damping Factor - Design Level Response	1.5	
β_M	Effective Damping - MCE_R Level Response	13%	
B_M	Damping Factor - MCE_R Level Response	1.3	
D_{TM}/D_M	Torsional Response Amplification	1.1	
	Superstructure Design Parameters	SCBF	OCBF
R	Response Modification Factor - Fixed-Base Structure	6.0	3.25
I	Importance Factor - Fixed-Base Structure	1.5	1.5
R_I	Response Modification Factor - Isolated Structure	2.0	1.0
I	Importance Factor - Isolated Structure	1.0	1.0

* Chapter 17 of the *Standard* does not require use of occupancy importance factor to determine design loads on the superstructure of an isolated building (I = 1.0).

The plots in Figures 12.3-3 and 12.3-4 illustrate the fundamental trade-off between displacement and force as a function of isolation system displacement. As the period is increased, design forces decrease and design displacements increase linearly. Plots like those shown in Figures 12.3-3 and 12.3-4 can be constructed during conceptual design once site seismicity and soil conditions are known (or are assumed) to investigate trial values of effective stiffness and damping of the isolation system. In this particular example, an isolation system with an effective period of approximately 3.5 to 4.0 seconds would require approximately 30 inches of total maximum displacement capacity, which is near the practical limit of moat covers, flexible utility connections, etc., that must accommodate isolation system displacement. Design force, V_s, on the superstructure would be approximately 10 percent of the building weight for a steel SCBF system and approximately 17 percent for a steel OCBF superstructure (subject to other limits on V_s per *Standard* Section 17.5.4.3).

The *Standard* does not permit use of steel OCBFs as the superstructure of an isolated building that is an Essential Facility located in a region of high seismicity (close to an active fault). In contrast, Section 1613.6.2 of the 2006 *International Building Code* (IBC) permits steel OCBFs and ordinary moment frames (OMFs) to be used for structures assigned to Seismic Design Category D, E or F, provided that the following conditions are satisfied:

- The value of R_I is taken as 1.0
- Steel OMFs and OCBFs are designed in accordance with AISC 341.

The underlying concept of Section 1613.6.2 of the 2006 IBC is to trade the higher strength of steel OCBFs designed using R_I = 1.0 for the larger inelastic response capacity of steel SCBFs. This trade-off is not unreasonable provided that the isolation system and surrounding structure are configured to not restrict displacement of the isolated structure in a manner that could cause large inelastic demands to occur in the superstructure. If an isolated building is designed with a superstructure system not permitted by the *Standard* (e.g., steel OCBFs), then the stability of the superstructure should be verified for MCE_R ground motions using the response history procedure with explicit modeling of the stiffening effects of isolators at very large displacements (e.g., due to high rubber strains in an elastomeric bearing, or engagement of the articulated slider with the concave plates of a friction pendulum bearing) and the effects of nearby structures (e.g., possible impact with moat walls).

12.4 DYNAMIC LATERAL RESPONSE PROCEDURE

While the ELF procedure equations are useful tools for preliminary design of the isolations system, the *Standard* requires a dynamic analysis for most isolated structures. Even where not strictly required by the *Standard*, the use of dynamic analysis (usually response history analysis) to verify the design is common.

12.4.1 Minimum Design Criteria

The *Standard* encourages the use of dynamic analysis but recognizes that along with the benefits of more complex models and analyses also comes an increased chance of design error. To avoid possible under-design, the *Standard* establishes lower-bound limits on results of dynamic analysis used for design. The limits distinguish between response spectrum analysis (a linear, dynamic method) and response history analysis (a nonlinear, dynamic method). In all cases, the lower-bound limit on dynamic analysis is established as a percentage of the corresponding design parameter calculated using the ELF procedure equations. Table 12.4-1 summarizes the percentages that define lower-bound limits on dynamic analysis.

Table 12.4-1 Summary of Minimum Design Criteria for Dynamic Analysis

Design Parameter	Response Spectrum Procedure	Response History Procedure
Total design displacement, D_{TD}	90% D_{TD}	90% D_{TD}
Total maximum displacement, D_{TM}	80% D_{TM}	80% D_{TM}
Design force on isolation system, V_b	90% V_b	90% V_b
Design force on irregular superstructure, V_s	100% V_s	80% V_s
Design force on regular superstructure, V_s	80% V_s	60% V_s

The *Standard* permits more liberal drift limits where the design of the superstructure is based on dynamic analysis. The ELF procedure drift limits of $0.010h_{sx}$ are increased to $0.015h_{sx}$ for response spectrum analysis and to $0.020h_{sx}$ for response history analysis (where h_{sx} is the story height at level x). Usually a stiff system (e.g., braced frames) is selected for the superstructure (to limit damage to nonstructural components sensitive to drift) and drift demand typically is less than approximately $0.005h_{sx}$. *Standard* Section 17.6.4.4 requires an explicit check of superstructure stability at the MCE_R displacement if the design earthquake story drift ratio exceeds $0.010/R_I$.

12.4.2 Modeling Requirements

As for the ELF procedure, the *Standard* requires the isolation system to be modeled for dynamic analysis using stiffness and damping properties that are based on tests of prototype isolator units. Additionally, dynamic analysis models are required to account for the following:

- Spatial distribution of individual isolator units.
- Effects of actual and accidental mass eccentricity.
- Overturning forces and uplift of individual isolator units.
- Variability of isolation system properties (due to rate of loading, etc.).

The *Standard* requires explicit nonlinear modeling of elements if response history analysis is used to justify design loads less than those permitted for ELF or response spectrum analysis. This option is seldom exercised and the superstructure typically is modeled using linear elements and conventional methods. Special modeling concerns for isolated structures include two important and related issues: uplift of isolator units and P-delta effects on the isolated structure. Typically, isolator units have little or no ability to resist tension forces and can uplift when earthquake overturning (upward) loads exceed factored gravity (downward) loads. Local uplift of individual elements is permitted (*Standard* Sec. 17.2.4.7), provided the resulting deflections do not cause overstress or instability of the isolated structure. To calculate uplift effects, gap elements may be used in nonlinear models or tension may be released manually in linear models.

The effects of P-delta loads on the isolation system and adjacent elements of the structure can be quite significant. The compression load, P, can be large due to earthquake overturning (and factored gravity loads) at the same time that large displacements occur in the isolation system. Computer analysis programs (most of which are based on small-displacement theory) may not correctly calculate P-delta moments at the isolator level in the structure above or in the foundation below. Figure 12.4-1 illustrates moments due to P-delta effects (and horizontal shear loads) for an elastomeric bearing isolation system and three configurations of a sliding isolation system. For the elastomeric system, the P-delta moment is split one-half up and one-half down. For the flat and single-dish sliding systems, the full P-delta moment is applied to the foundation below (due to the orientation of the sliding surface). A reverse (upside down) orientation of the flat and single-sided sliding systems would apply the full P-delta moment on the structure above. For the double-dish sliding system, P-delta moments are split one-half up and one-half down, in a manner similar to an elastomeric bearing, provided that the friction (and curvature) properties of the top and bottom concave dishes are the same.

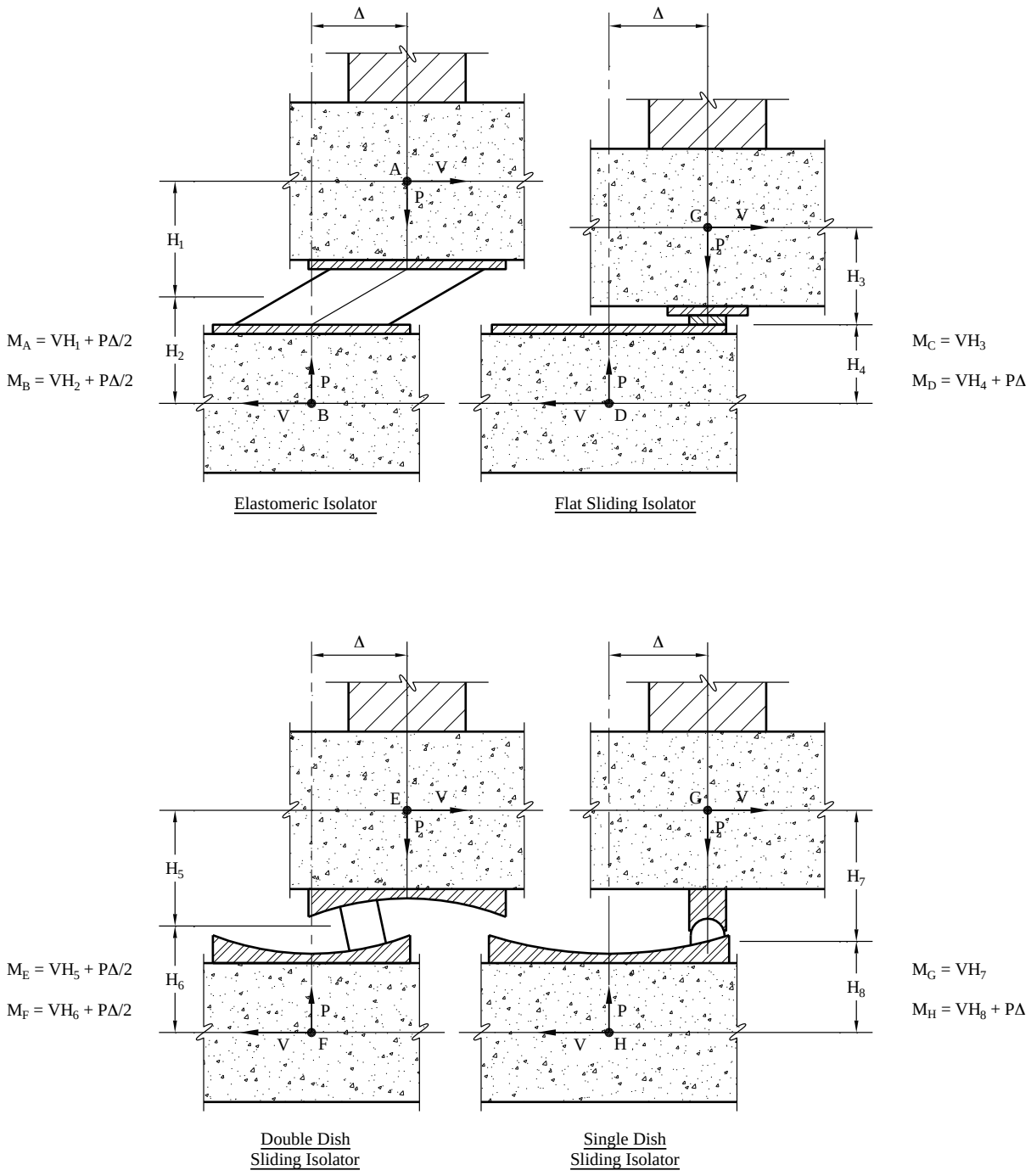

Figure 12.4-1 Moments due to horizontal shear and P-delta effects

12.4.3 Response Spectrum Analysis

Response spectrum analysis methods require that isolator units be modeled using amplitude-dependent values of effective stiffness and damping that are essentially the same as those of the ELF procedure, subject to the limitation that the effective damping of the isolated modes of response not exceed 30 percent of critical. Higher modes of response usually are assumed to have 2 to 5 percent damping, a value of damping appropriate for a superstructure that remains essentially elastic. As previously noted, maximum and minimum values of effective stiffness of the isolation system are used to calculate separately maximum displacement of the isolation system (using minimum effective stiffness) and maximum forces in the superstructure (using maximum effective stiffness). The *Standard* requires horizontal loads to be applied in two orthogonal directions and peak response of the isolation system and other structural elements is determined using the 100 percent plus 30 percent combination method.

The *Provisions* now define ground motions in terms of *maximum* spectral response in the horizontal plane (where previous editions used *average* horizontal response). Consequently, at a given period of interest (for instance, the effective period of the isolation system), it may be overly conservative to combine 30 percent of the maximum spectral response load applied in the orthogonal direction with 100 percent of the maximum spectral response load applied in the horizontal direction of interest to determine peak spectral response of the isolation system and other structural elements. In the opinion of the author, it would be reasonable to not apply 30 percent of spectral response load at the fundamental (isolated) mode in the orthogonal direction when applying 100 percent of the maximum spectral response load in the horizontal direction of interest. However, the 100 percent plus 30 percent combination method would still be appropriate for all higher modes, since spectral response at higher-mode periods is, in general, independent of fundamental (isolated) mode spectral response.

The design shear at any story, determined by RSA, cannot be taken as less than the story shear resulting from application of the ELF distribution of force over height (*Standard* Equation 17.5-9) where anchored to a value of base shear, V_s, determined by RSA in the direction of interest. This limit is intended to avoid underestimation of higher-mode response when isolators are modeled using effective stiffness and damping properties, rather than actual nonlinear properties. The value of V_s determined by RSA is typically less than the value of V_s prescribed by ELF using *Standard* Equation 17.5-8, which combines maximum effective stiffness, k_{Dmax}, with design displacement, D_D, based on minimum effective stiffness, although the difference generally is small and the values of design shear determined by RSA are similar to those required by the ELF procedure.

Standard Section 17.6.3.4 does not explicitly require the value of base shear, V_s, determined by RSA to comply with the *Standard* Section 17.5.4.2 limits on V_s. In the opinion of the author, the *Standard* Section 17.5.4.3 limits on base shear apply to all methods of analysis and should be complied with when RSA is used as the basis for design. It may be noted that *Standard* Section 17.6.4.2 requires V_s to comply with the *Standard* Section 17.5.4.3 limits on V_s when the design is based on the response history analysis procedure, which otherwise has more liberal design shear requirements than either the RSA or ELF procedure. As previously discussed (Sec. 12.3.2), the third limit of *Standard* Section 17.5.4.3 is included in the *Standard* to ensure that the isolation system displaces significantly before lateral forces reach the strength of the seismic force-resisting system.

12.4.4 Response History Analysis

For response history analysis, nonlinear force-deflection characteristics of isolator units are modeled explicitly (rather than using effective stiffness and damping). For most types of isolators, force-deflection properties can be approximated by bilinear, hysteretic curves that can be modeled using commercially available nonlinear structural analysis programs. Such bilinear hysteretic curves should have

approximately the same effective stiffness and damping at amplitudes of interest as the true force-deflection characteristics of isolator units (as determined by prototype testing). More sophisticated nonlinear models may be necessary to represent accurately response of isolators with complex configurations or properties (e.g., "triple pendulum" sliding bearings), to capture stiffening effects at very large displacements (e.g., of elastomeric bearings), or to model rate-dependent effects explicitly (Sarlis 2010).

Figure 12.4-2 shows a bilinear idealization of the response of a typical nonlinear isolator unit. Figure 12.4-2 also includes simple equations defining the yield point (D_y, F_y) and end point (D, F) of a bilinear approximation that has the same effective stiffness and damping as the true curve (at displacement, D).

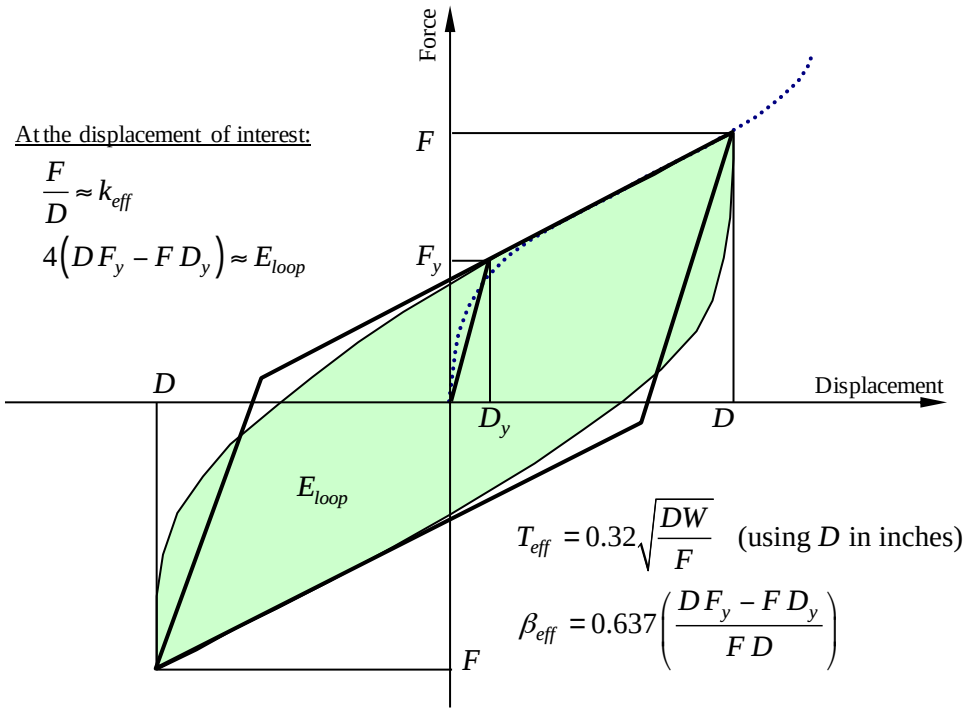

Figure 12.4-2 Bilinear idealization of isolator unit behavior

Response history analysis with explicit modeling of nonlinear isolator units is commonly used for the evaluation of isolated structures. Where at least seven pairs of ground motion acceleration components are employed, the values used in design for each response parameter of interest may be the average of the corresponding analysis maxima. Where fewer pairs are used (with three pairs of ground motion acceleration components being the minimum number permitted), the maximum value of each parameter of interest must be used for design.

The response history method is not a particularly useful design tool due to the complexity of results, the number of analyses required (to account for different locations of eccentric mass), the need to combine different types of response at each point in time, etc. It should be noted that while *Standard* Chapter 16 does not require consideration of accidental torsion for either the linear or nonlinear response history procedures, Chapter 17 does require explicit consideration of accidental torsion, regardless of the analysis method employed. Response history analysis is most useful when used to verify a design by checking a

few key design parameters, such as isolation displacement, overturning loads and uplift and story shear force.

The *Provisions* (Sections 17.3.2 and 16.1.3.2) now require ground motions to be scaled to match maximum spectral response in the horizontal plane (where previous editions defined spectral response in terms of average horizontal response). In concept, at a given period of interest, maximum spectral response of scaled records should, on average, be the same as that defined by the design spectrum of interest (DE or MCE_R).

Neither the *Standard* nor the *Provisions* specify how the two scaled components of each record should be applied to a three-dimensional model (i.e., how the two components of each record should be oriented with respect to the axes of the model). This lack of guidance has sometimes caused users to perform an unnecessarily large number of response history analyses for design verification of an isolated structure. In the author's opinion, the following steps describe an acceptable approach for scaling, orienting and applying ground motion components to a three-dimensional model of an isolated structure (when based on the new maximum definition of the ground motions).

- Step 1 - Selection and Scaling of Records. Select and scale ground motion records as required by *Provisions* Section 17.3.2. The records would necessarily be scaled differently to match the DE spectrum and the MCE_R spectrum, respectively. While the *Provisions* permits as few as three records for response history analysis (with design/verification based the most critical of the three), a set of at least seven records is recommended such that the average value of the response parameter of interest may be used for design or design verification.

- Step 2 - Grouping of Stronger Components. Group the horizontal components of each record in terms of stronger and weaker components. The stronger component of each record is the component that has the larger spectral response at periods of interest. For isolated structures, periods of interest are approximately from T_D to T_M. The records may require rotation of horizontal axes before grouping to better distinguish between stronger and weaker components at the period of interest. Orient stronger horizontal components such that peak response occurs in the same (positive or negative) direction. In general, the same grouping of components can be used for both DE and MCE_R analyses (just scaled by a different factor), since T_D and T_M are typically about the same and response spectra do not vary greatly from period to period at long periods.

- Step 3 - Verification of Component Grouping. Verify that the average spectral response of the set of stronger components is comparable to the design spectrum of interest (e.g., DE or MCE_R spectrum) at periods of interest (i.e., T_M, if checking MCE_R displacement). If the average spectrum of stronger components is not adequate, then the scaling factor should be increased accordingly. Note: Increasing ground motions to match average spectral response of stronger components with the design spectrum of interest is not required by *Provisions* Section 17.3.2 but is consistent with the "maximum" definition of ground motions.

- Step 4 - Application of Scaled Records. In general, apply the set of scaled records to the three-dimensional model of the isolated structure in four basic orientations with respect to the primary (orthogonal) horizontal axes of the superstructure:

    1. Apply the set of scaled records with stronger components aligned in the positive direction of the first horizontal axis of the model.

2. Apply the set of scaled records with stronger components aligned in the positive direction of the second horizontal axis of the model.

3. Apply the set of scaled records with stronger components aligned in the negative direction of the first horizontal axis of the model.

4. Apply the set of scaled records with stronger components aligned in the negative direction of the second horizontal axis of the model.

For each of the four sets of analyses, find the average value of the response parameter of interest (if the set of ground motion contains at least seven records) or the maximum value of the response parameter (if the set of ground motions contains less than seven records). The more critical response of the four sets of analyses should be used for design or design verification.

The four orientations of ground motions of Step 4 are required, in general, for design of elements, since the most critical positive or negative direction of peak response typically is not known for individual elements. However, for design verification of key global response parameters that are relatively insensitive to positive/negative orientation of ground motion components (e.g., maximum isolation system displacement, peak story shear, peak story displacement), only the first two sets of analyses are necessary. Although the above steps require some "homework" by the engineer to develop an appropriate set of scaled records, only two sets of response history analyses are typically required to verify the design of most isolated structures.

The above response history analysis recommendations apply to each model of the structure, which necessarily include at least two models whose properties represent upper-bound and lower-bound force-deflection properties of the isolation system, respectively. Different models could also be used to explicitly evaluate various locations of accidental mass eccentricity, as required by *Standard* Section 17.6.2.1.b. However, this approach would require multiple additional models to consider "the most disadvantageous location of accidental eccentric mass." In the opinion of the author, these additional response history analyses are unnecessary and the effects of accidental mass eccentricity can be calculated by factoring the results of response history analyses (of a model that does not explicitly include accidental mass eccentricity). The amount by which the response parameter of interest should be factored may be determined by assuming that accidental torsion increases response in proportion to the increase in isolation system displacement, as prescribed by the ELF requirements of *Standard* Section 17.5.3.5.

12.5 EMERGENCY OPERATIONS CENTER USING DOUBLE-CONCAVE FRICTION PENDULUM BEARINGS, OAKLAND, CALIFORNIA

This example features the seismic isolation of a hypothetical EOC, assumed to be located in Oakland, California, approximately 6 kilometers from the Hayward fault. The isolation system incorporates double-concave friction pendulum sliding bearings, although other types of isolators could have been used in this example. Isolation is an appropriate design strategy for EOCs and other buildings where the goal is to limit earthquake damage and protect facility function. The example illustrates the following design topics:

- Determination of seismic design parameters.
- Preliminary design of superstructure and isolation systems (using the ELF procedure).
- Dynamic analysis of a seismically isolated structure.

- Specification of isolation system design and testing criteria.

While the example includes development of the entire structural system, the primary focus is on the design and analysis of the isolation system. Examples in other chapters have more in-depth descriptions of the provisions governing detailed design of the superstructure above and the foundation below.

12.5.1 System Description

This EOC is a three-story, steel-braced frame structure with a large, centrally located mechanical penthouse. Story heights are 14 feet at the first floor to accommodate computer access flooring and other architectural and mechanical systems and 12 feet at the second and third floors (and penthouse). The roof and penthouse roof decks are designed for significant live load to accommodate a helicopter landing pad and to meet other functional requirements of the EOC. Figure 12.5-1 shows the three-dimensional model of the structural system.

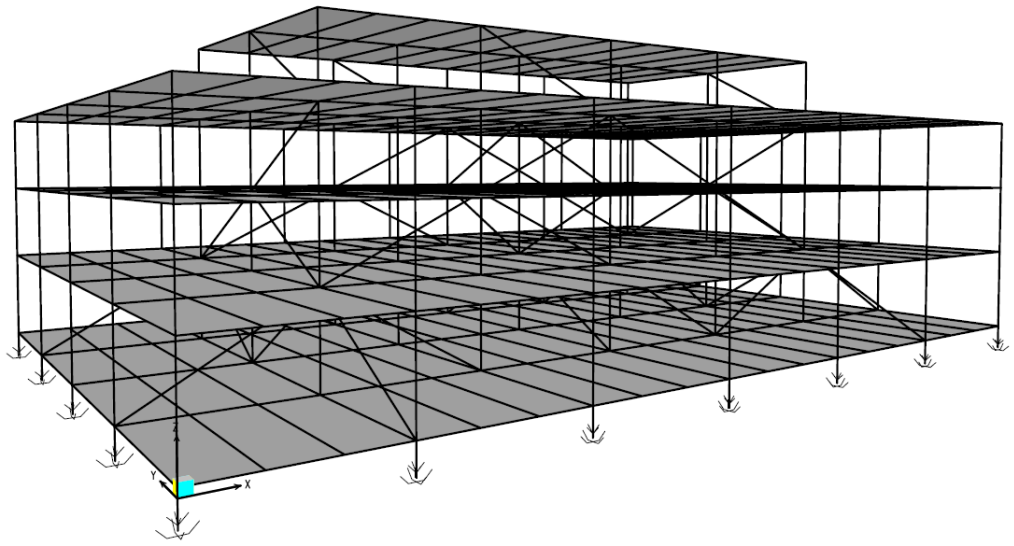

Figure 12.5-1 Three-dimensional model of the structural system

The structure (which is regular in configuration) has plan dimensions of 100 feet by 150 feet at all floors except for the penthouse, which is approximately 50 feet by 100 feet in plan. Columns are spaced at 25 feet in both directions. Figures 12.5-2 and 12.5-3 are framing plans for the typical floor levels (1, 2, 3 and roof) and the penthouse roof.

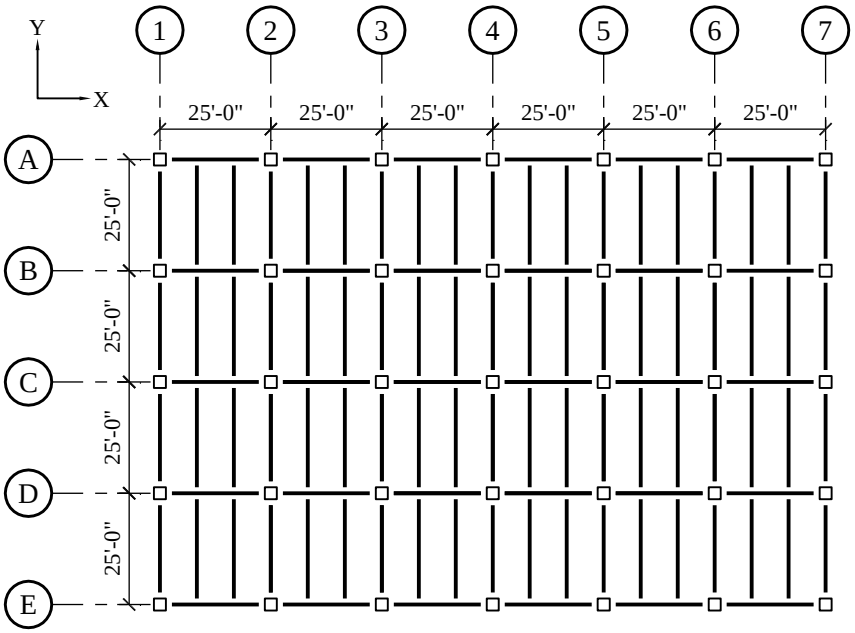

Figure 12.5-2 Typical floor framing plan (1.0 ft = 0.3048 m)

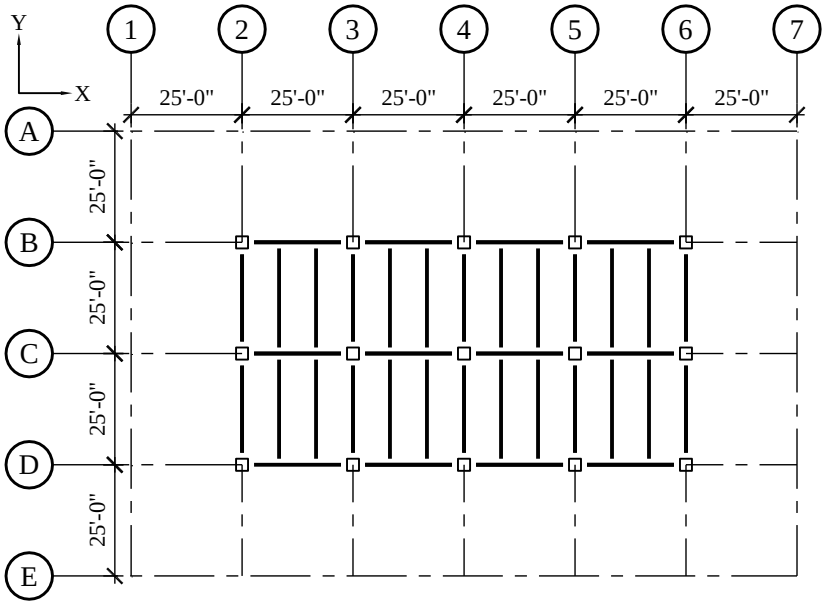

Figure 12.5-3 Penthouse roof framing plan (1.0 ft = 0.3048 m)

The vertical load-carrying system consists of concrete fill on steel deck floors, supported by steel beams at 8.3 feet on center and steel girders at column lines. Isolator units support the columns below the first floor. The foundation is a heavy mat (although spread footings or piles could be used depending on the soil type, depth to the water table and other site conditions).

The lateral system consists of a roughly symmetrical pattern of concentrically braced frames. These frames are located on Column Lines B and D in the longitudinal direction and on Column Lines 2, 4 and 6 in the transverse direction. Figures 12.5-4 and 12.5-5 show the longitudinal and transverse elevations, respectively. Braces are specifically configured to reduce the concentration of earthquake overturning and uplift loads on isolator units by:

- Increasing the number of bays with bracing at lower stories.
- Locating braces at interior (rather than perimeter) column lines (providing more hold-down weight).
- Avoiding common end columns for transverse and longitudinal bays with braces.

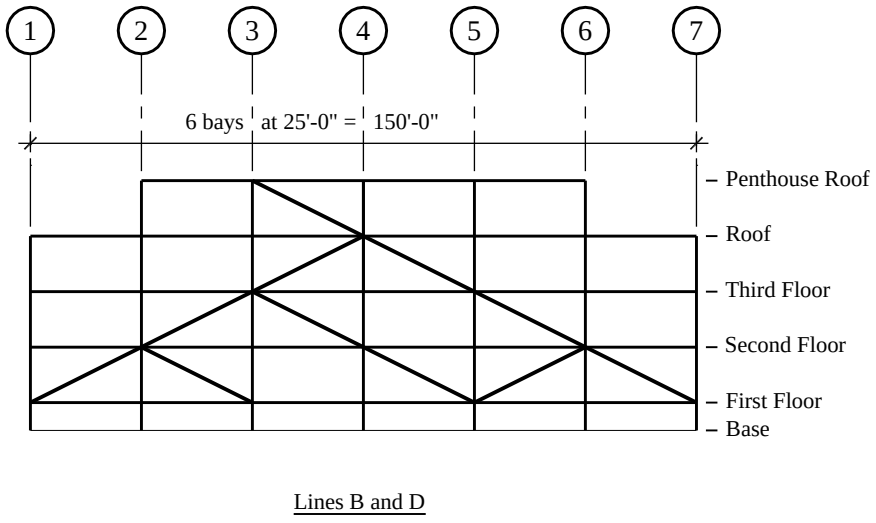

Figure 12.5-4 Longitudinal bracing elevation (Column Lines B and D)

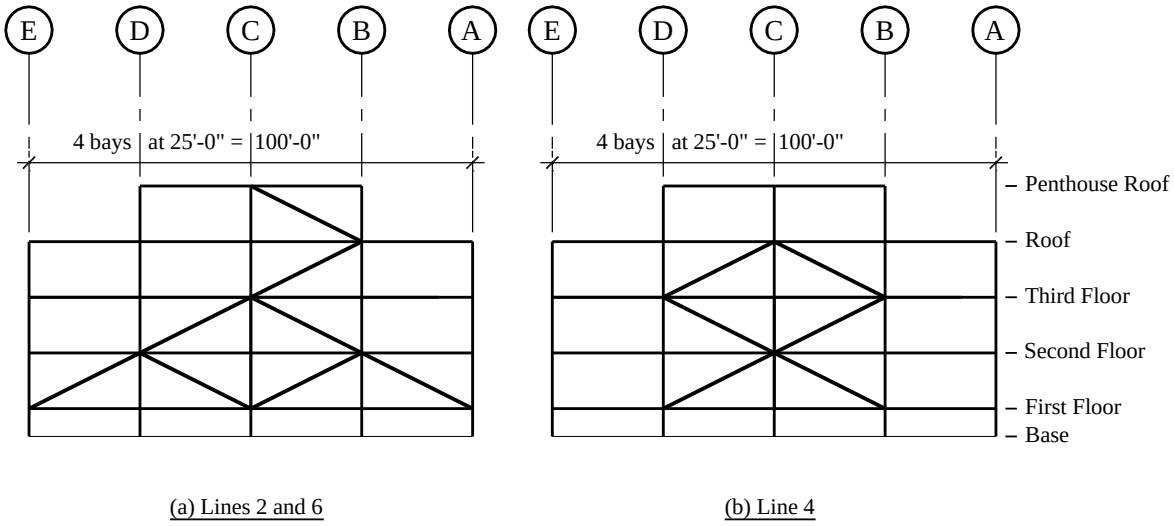

Figure 12.5-5 Transverse bracing elevations:
(a) on Column Lines 2 and 6 and (b) on Column Line 4

The isolation system has 35 identical elastomeric isolator units, located below columns. The first floor is just above grade and the isolator units are approximately 3 feet below grade to provide clearance below the first floor for construction and maintenance personnel. A short retaining wall borders the perimeter of the facility and provides approximately 3 feet of "moat" clearance for lateral displacement of the isolated structure. Access to the EOC is provided at the entrances by segments of the first floor slab, which cantilever over the moat.

Girders at the first-floor column lines are much heavier than the girders at other floor levels and have moment-resisting connections to columns. These girders stabilize the isolator units by resisting moments due to vertical (P-delta effect) and horizontal (shear) loads. Column extensions from the first floor to the top plates of the isolator units are stiffened in both horizontal directions, to resist these moments and to serve as stabilizing haunches for the beam-column moment connections.

12.5.2 Basic Requirements

12.5.2.1 Specifications.

- General: ASCE Standard ASCE 7-05 (*Standard*)
- Seismic Loads: 2009 NEHRP Recommended Provisions (Provisions)
- Other Loads and Load Combinations: 2006 *International Building Code* (2006 IBC)

12.5.2.2 Materials.

- Concrete:

  Strength (floor slabs): f'_c = 3 ksi

Strength (foundations below isolators): f'_c = 5 ksi

Weight (normal): 150 pcf

- Steel:

  Columns: F_y = 50 ksi

  Primary first-floor girders (at column lines): F_y = 50 ksi

  Other girders and floor beams: F_y = 36 ksi

  Braces: F_y = 46 ksi

- Steel deck: 3-inch-deep, 20-gauge deck

12.5.2.3 Gravity loads.

- Dead Loads:

  Main structural elements (slab, deck and framing): self weight

  Miscellaneous structural elements (and slab allowance): 10 psf

  Architectural facades (all exterior walls): 20 psf

  Roof parapets: 20 psf

  Partitions (all enclosed areas): 20 psf

  Suspended MEP/ceiling systems and supported flooring: 15 psf

  Mechanical equipment (penthouse floor): 50 psf

  Roofing: 10 psf

- Reducible live loads:

  Floors (1-3): 100 psf

  Roof decks and penthouse floor: 50 psf

- Live load reduction: 2006 IBC Section 1607.9 permits area-based live load reduction of not more than 50 percent for elements with live loads from a single story (girders) and not more than 60 percent for elements with live loads from multiple stories (axial component of live load on columns at lower levels and isolator units).

- EOC weight (dead load) and live load (from ETABS model, *Guide* Sec. 12.5.3.1):

Penthouse roof	W_{PR}	= 794 kips
Roof (penthouse floor)	W_R	= 2,251 kips

Third floor	W_3 = 1,947 kips
Second floor	W_2 = 1,922 kips
First floor	W_1 = 2,186 kips
Total EOC weight (updated guess - k)	W = 9,100 kips
Live load (L) without reduction	L = 5,476 kips
Reduced live load (L) on isolation system	L = 2,241 kips

Table 12.5-1 Summary of dead load (D) and reduced live load (L) on isolator units in kips (from ETABS model, *Guide* Sec. 12.5.3.1)* (D/L)

Column line	1	2	3	4
A	138 / 34	251 / 58	206 / 44	204 / 43
B	253 / 58	290 / 77	323 / 86	342 / 92
C	206 / 43	323 / 86	367 / 99	334 / 90

1.0 kip = 4.45 kN.

*Loads at Column Lines 5, 6 and 7 (not shown) are similar to those at Column Lines 3, 2 and 1, respectively; loads at Column Lines D and E (not shown) are similar to those at Column Lines B and A, respectively.

12.5.2.4 Seismic design parameters.

12.5.2.4.1 Performance criteria (Standard Sec. 1.5.1).

- Designated Emergency Operation Center: Occupancy Category IV
- Occupancy Importance Factor: I = 1.5 (conventional)
- Occupancy Importance Factor (*Standard* Chapter 17): I = 1.0 (isolated)

  Note: *Standard* Chapter 17 does not require use of the occupancy importance factor to determine the design loads on the structural system of an isolated building (i.e., I = 1.0). However, the component importance factor is still required by Chapter 13 to determine seismic forces on nonstructural components of isolated structures (I_p = 1.5 for Occupancy Category IV facilities).
- Seismic Design Category (*Standard* Section 11.6): Seismic Design Category F

12.5.2.4.2 Ground motions for Oakland EOC site (*Provisions* Chapters 11 and 21).

- Site Location, Hazard and Soil Conditions (assumed):

  Site latitude and longitude: 37.80°, -122.25°

  Source (fault) controlling hazard at the Oakland site: Hayward

  Maximum moment magnitude earthquake on controlling source: M7.3

Closest distance from site to Hayward Fault (Joyner-Boore distance): 5.9 km

Site soil type (assumed for preliminary design): Site Class C-D

Site shear wave velocity (assumed for response history analysis): $v_{s,30}$ = 450 m/s

- Short-Period Design Parameters (USGS web site):

  Short-period MCE_R spectral acceleration (USGS 2009): S_S = 1.24

  Site coefficient (*Standard* Table 11.4-1): F_a = 1.0

  Short-period MCE_R spectral acceleration adjusted for site class ($F_a S_S$): S_{MS} = 1.24

  DE spectral acceleration ($2/3 S_{MS}$): S_{DS} = 0.83

- 1-Second Design Parameters (USGS web site):

  1-Second MCE_R spectral acceleration: S_1 = 0.75

  Site coefficient (*Standard* Table 11.4-2): F_v = 1.4

  1-Second MCE_R spectral acceleration adjusted for site class ($F_v S_1$): S_{M1} = 1.05

  DE spectral acceleration ($2/3 S_{M1}$): S_{D1} = 0.7

12.5.2.4.3 Design spectra (*Provisions* Section 11.4). Figure 12.5-6 plots DE and MCE_R response spectra as constructed in accordance with the procedure of *Provisions* Section 11.4 using the spectrum shape defined by *Provisions* Figure 11.4-1. *Standard* Section 17.3.1 requires a site-specific ground motion hazard analysis to be performed in accordance with Chapter 21 for sites with S_1 greater than 0.6 (e.g., sites near active sources). Subject to other limitations of *Provisions* Section 21.4, the resulting site-specific DE and MCE_R spectra may be taken as less than 100 percent but not less than 80 percent of the default design spectrum of *Standard* Figure 11.4-1.

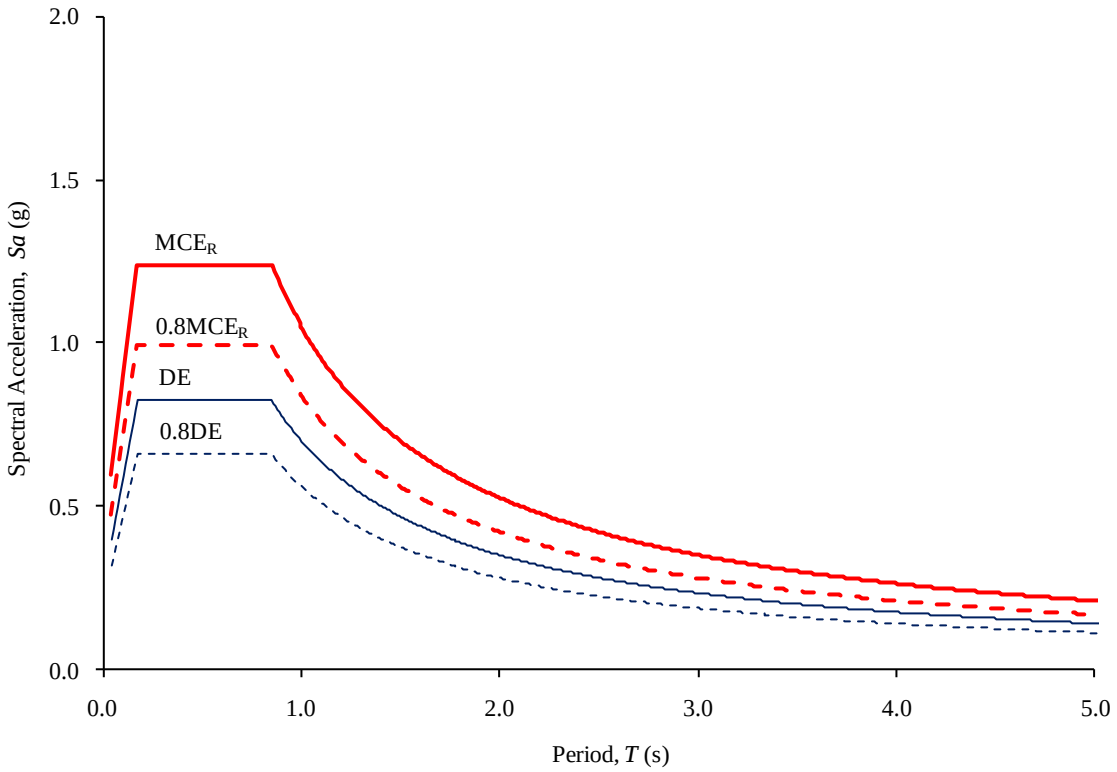

Figure 12.5-6 DE and MCE_R spectra and 80 percent limits

For this example, site-specific spectra for the design earthquake and the maximum considered earthquake were assumed to be 100 percent of the respective spectra shown in Figure 12.5-6. In general, site-specific spectra for regions of high seismicity, with well defined fault systems (like the Hayward fault), would be expected to be similar to the default design spectra of *Standard* Figure 11.4-1.

12.5.2.4.4 DE and MCE_R ground motion records (*Standard* Sec. 17.3.2). For response history analysis, *Standard* Section 17.6.3.4 requires at least three pairs of horizontal ground motion acceleration components to be selected from actual earthquake records and scaled to match either the DE or the MCE_R spectrum and at least seven pairs if the average value of the response parameter of interest is used for design (which is typically the case). Selection and scaling of appropriate ground motions should be performed by a ground motion expert experienced in earthquake hazard of the region, considering site conditions, earthquake magnitudes, fault distances and source mechanisms that influence ground motion hazard at the building site.

For this example, a set of seven ground motion records are selected from the near-field (NF) and far-field (FF) record sets of FEMA P-695. FEMA P-695 is a convenient source of the 50 strongest ground motion records of large magnitude earthquakes available from the Pacific Earthquake Engineering Research Center (PEER) NGA database (PEER 2006), the records most suitable for response history evaluation of structures in regions of high seismicity. The seven records selected from the FEMA P-695 ground motion sets have fault source and site characteristics that best match those of the example EOC, that is, records of magnitude M7.0 or greater earthquakes recorded close to fault rupture at soil sites (Site Class C or D). Table 12.5-2 lists these seven earthquake records and summarizes key properties. As shown in this table, the average magnitude (M7.37), the average site-source distance (5.2 km) and the average shear wave

velocity (446 m/s) closely match the maximum magnitude of the Hayward fault (M7.3), the closest distance from the Hayward fault to the Oakland site (5.9 km) and the Oakland site conditions (Site Class C-D), respectively, as required by record selection requirements of *Standard* Section 17.3.2.

Table 12.5-2 Seven Earthquake Records Selected for Response History Analysis of Example Base-Isolated EOC Facility

FEMA P-695 Record ID No.	Earthquake			Source Characteristics				Site Conditions	
	Year	Name	Record Station	Mag. (M_W)	Distance, D_f (km)		Fault Mechanism	Site Class	$v_{S,30}$ (m/s)
					JB	Rupture			
NF-8	1992	Landers	Lucerne	7.3	2.2	15.4	Strike-slip	C	685
FF-10	1999	Kocaeli	Arcelik	7.5	10.6	13.5	Strike-slip	C	523
NF-25	1999	Kocaeli	Yarimca	7.5	1.4	5.3	Strike-slip	D	297
FF-3	1999	Duzce	Bolu	7.1	12.0	12.0	Strike-slip	D	326
NF-14	1999	Duzce	Duzce	7.1	0.0	6.6	Strike-slip	D	276
FF-4	1999	Hector Mine	Hector	7.1	10.4	11.7	Strike-slip	C	685
NF-28	2002	Denali	TAPS PS#10	7.9	0.2	3.8	Strike-slip	D	329
Mean Property of Seven Records				7.37	5.2	9.8			446

Standard Section 17.3.2 provides criteria for scaling earthquake records to match a target spectrum over the period range of interest, defined as $0.5T_D$ to $1.25T_M$. In this example, T_D and T_M are 3.5 and 3.9 seconds, respectively, so the period range of interest is from 1.75 to 4.9 seconds. For each period in this range, the average of the square-root-of-the-sum-of-the-squares (SRSS) combination of each pair of horizontal components of scaled ground motion should be equal to or greater than the target spectrum. The target spectrum is defined as 1.0 times the design spectrum of interest (either the DE or the MCE_R spectrum).

Table 12.5-3 summarizes the factors used to scale the seven records to mach either the DE or MCE_R spectrum, in accordance with *Standard* Section 17.3.2. The seven records were first "normalized" by their respective values of PGV_{PEER} to reduce inappropriate amounts of record-to-record variability using the procedures of Section A.8 of FEMA P-695. As shown in Table 12.5-3, PGV normalization tends to increase the intensity of those records of smaller than average magnitude events or from sites farther than average from the source and to decrease the intensity of those records of larger than average magnitude events or from sites closer than average to the source, but has no net effect on the overall intensity of the record set (i.e., median value of normalization factors is 1.0 for the record set).

Scaling factors were developed such that the average value of the response spectra of normalized records equals or exceeds the spectrum of interest (either the DE or MCE_R spectrum) over the period range of interest, 1.75 to 4.9 seconds. These scaling factors are given in Table 12.5-3 and reflect the total amount that each as-recorded ground motion is scaled for response history analysis. Table 12.5-3 shows that a median scaling factor of 1.04 is required to envelop the DE spectrum (records are increased slightly, on average, to match the DE spectrum) and a median scaling factor of 1.56 is required to envelop the MCE_R spectrum over the period range of interest.

Table 12.5-3 Summary of Factors Used to Scale Each of the Seven Records to Match the DE or MCE_R Spectrum

FEMA P-695 Record ID No.	Earthquake			Normalization and Scaling Factors			
	Year	Name	Record Station	PGV_{PEER} (cm/s)	PGV Normal Factor	Oakland Site	
						DE	MCE_R
NF-8	1992	Landers	Lucerne	97.2	0.60	0.62	0.94
FF-10	1999	Kocaeli	Arcelik	27.4	2.13	2.21	3.32
NF-25	1999	Kocaeli	Yarimca	62.4	0.93	0.97	1.46
FF-3	1999	Duzce	Bolu	59.2	0.99	1.02	1.54
NF-14	1999	Duzce	Duzce	69.6	0.84	0.87	1.31
FF-4	1999	Hector Mine	Hector	34.1	1.71	1.78	2.67
NF-28	2002	Denali	TAPS PS#10	98.5	0.59	0.62	0.92
Mean Property of Seven Records				58.3	1.00	1.04	1.56

Figure 12.5-7 compares the MCE_R spectrum for the Oakland site with the average spectrum of the SRSS combination, the average spectrum of stronger components and the average spectrum of other (orthogonal) components of the seven scaled records. This figure shows:

- The average spectrum of the SRSS combination of scaled record to envelop the MCE_R spectrum from 1.75 seconds ($0.5T_D$) to 4.9 seconds ($1.25T_M$), as required by ***Standard*** Section 17.3.2.

- The average spectrum of larger scaled components comparable to the MCE_R spectrum at response periods of interest (e.g., 3.9 seconds for MCE_R analysis).

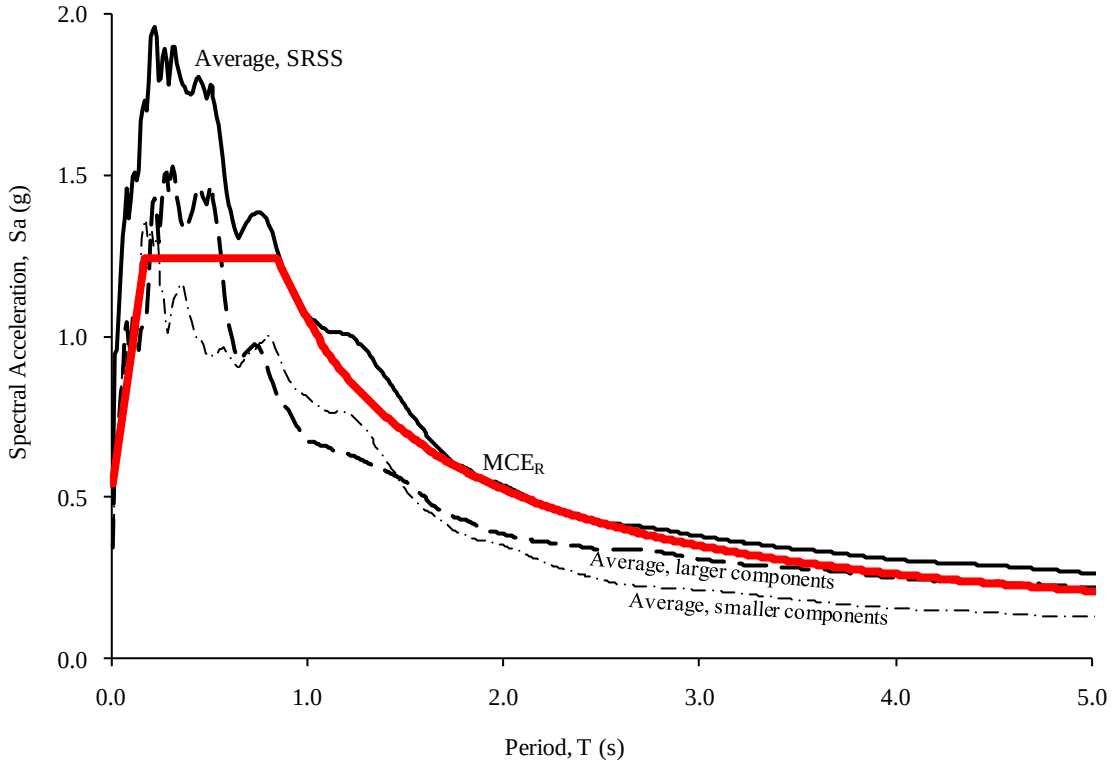

Figure 12.5-7 Comparison of the MCE_R spectrum with the average spectrum of the SRSS combination of the seven scaled records, the average spectrum of the seven larger components of the seven scaled records and the average spectrum of the other orthogonal components of the seven scaled records listed in Table 12.5-3

12.5.2.5 Structural design criteria.

12.5.2.5.1 Design basis.

- Seismic force-resisting system: Special steel concentrically braced frames (height < 100 feet)
- Response modification factor, R (*Standard* Table 12.2-1): $R = 6$ (conventional)
- Response modification factor for design of the superstructure, R_I (*Standard* Sec. 17.5.4.2, $3/8R \leq 2$): $R_I = 2$ (isolated)
- Plan irregularity (of superstructure) (*Standard* Table 12.3-1): None
- Vertical irregularity (of superstructure) (*Standard* Table 12.3-2): None
- Lateral response procedure (*Standard* Sec. 17.4.1, $S_1 > 0.6$): Dynamic analysis
- Redundancy factor (*Standard* Sec. 12.3.4): $\rho \geq 1.0$ (conventional); $\rho = 1.0$ (isolated)

Standard Section 12.3.4 requires the use of a calculated ρ value, which could be greater than 1.0 for a conventional structure with a brace configuration similar to the superstructure of the base-isolated EOC.

However, in the author's opinion, the use of R_I equal to 2.0 (rather than R equal to 6) as required by *Standard* Section 17.5.4.2 precludes the need to further increase superstructure design forces for redundancy.

12.5.2.5.2 Horizontal earthquake loads and effects (*Standard* Chapters 12 and 17).

- Design earthquake (acting in either the X or Y direction): DE (site specific)
- Maximum considered earthquake (acting in either the X or Y direction): MCE (site specific)
- Mass eccentricity - actual plus accidental: $0.05b$ = 5 ft (X direction); $0.05d$ = 7.5 ft (Y direction)

The superstructure is essentially symmetric about both primary horizontal axes, however, the placement of the braced frames results in a ratio of maximum corner displacement to average displacement of 1.25 including accidental eccentricity, exceeding the threshold of 1.2 per the definition of the *Standard*. If the building were not on isolators, the accidental torsional eccentricity would need to be increased from 5 percent to 5.4 percent of the building dimension. The input to the superstructure is controlled by the isolation system and it is the author's opinion that the amplification of accidental torsion is not necessary for such otherwise regular structures. Future editions of the *Standard* should address this issue. Also refer to the discussion of analytical modeling of accidental eccentricities in *Guide* Chapter 4.

- Superstructure design (reduced DE response): $Q_E = Q_{DE/2}$ = DE/2.0
- Isolation system and foundation design (unreduced DE response): $Q_E = Q_{DE}$ = DE/1.0
- Check of isolation system stability (unreduced MCE response): $Q_E = Q_{MCE}$ = MCE/1.0

12.5.2.5.3 Combination of horizontal earthquake load effects. Response due earthquake loading in the X and Y directions is as follows:

Q_E = Max ($1.0Q_{EX}+0.3Q_{EY}$, $0.3Q_{EX}+1.0Q_{EY}$)

In general, the horizontal earthquake load effect, Q_E, on the response parameter of interest is influenced by only one direction of horizontal earthquake load and $Q_E = Q_{EX}$ or $Q_E = Q_{EY}$. Exceptions include vertical load on isolator units due to earthquake overturning forces.

12.5.2.5.4 Combination of horizontal and vertical earthquake load effects.

- Design earthquake ($Q_E \pm 0.2S_{DS}D$): $E = Q_E \pm 0.17D$
- Maximum considered earthquake ($Q_E \pm 0.2S_{MS}D$): $E = Q_E \pm 0.25D$

12.5.2.5.5 Superstructure design load combinations (2006 IBC, Sec. 1605.2.1, using $R_I = 2$).

- Gravity loads (dead load and reduced live load): $1.2D + 1.6L$
- Gravity and earthquake loads ($1.2D + 0.5L + 1.0E$): $1.37D + 0.5L + Q_{DE/2}$
- Gravity and earthquake loads ($0.9D - 1.0E$): $0.73D - Q_{DE/2}$

12.5.2.5.6 Isolation system and foundation design load combinations (2006 IBC, Sec. 1605.2.1).

- Gravity loads (for example, long term load on isolator units): $1.2D + 1.6L$
- Gravity and earthquake loads ($1.2D + 0.5L + 1.0E$): $1.37D + 0.5L + Q_{DE}$
- Gravity and earthquake loads ($0.9D - 1.0E$): $0.73D - Q_{DE}$

12.5.2.5.7 Isolation system stability load combinations (*Standard* Sec. 17.2.4.6).

- Maximum short term load on isolator units ($1.2D + 1.0L + |E|$): $1.45D + 1.0L + Q_{MCE}$
- Minimum short term load on isolator units ($0.8D - |E|$): $0.8D - Q_{MCE}$

Note that in the above combinations, the vertical earthquake load ($0.2S_{MS}D$) component of $|E|$ is included in the maximum (downward) load combination but excluded from the minimum (uplift) load combination. It is the author's opinion that vertical earthquake ground shaking is of a dynamic nature, changing direction too rapidly to affect appreciably uplift of isolator units and need not be used with the load combinations of *Standard* Section 17.2.4.6 for determining minimum (uplift) vertical loads on isolator units due to the MCE_R.

12.5.3 Seismic Force Analysis

12.5.3.1 Basic approach to modeling. To expedite calculation of loads on isolator units and other elements of the seismic-force-resisting system, a three-dimensional model of the EOC is developed and analyzed using the ETABS computer program (CSI, 2009). While there are a number of commercially available programs to choose from, ETABS is selected for this example since it permits the automated release of tension in isolator units subject to uplift and has built-in elements for modeling other nonlinear properties of isolator units. Arguably, all of the analyses performed by the ETABS program could be done by hand or by spreadsheet calculation (except for confirmatory response history analyses).

The ETABS model is used to perform the following types of analyses and calculations:

- Gravity Load Evaluation. Calculate maximum long-term load ($1.2D + 1.6L$) on isolator units (*Guide* Table 12.5-1).
- ELF Procedure (and RSA). Calculate gravity and reduced design earthquake load response for design of the superstructure (ignoring uplift of isolator units).
- Nonlinear Static Analysis (with ELF loads). Calculate gravity and unreduced design earthquake load response for design of the isolation system and foundation (considering uplift of isolator units).
- Nonlinear Static Analysis (with ELF loads). Calculate gravity and unreduced design earthquake load response to determine maximum short-term load (downward force) on isolator units (*Guide* Table 12.5-5) and minimum short-term load (downward force) of isolator units (*Guide* Table 12.5-6).
- Nonlinear Static Analysis (with ELF loads). Calculate gravity and unreduced MCE_R load response to determine maximum short-term load (downward force) on isolator units (*Guide*

Table 12.5-7) and minimum short-term load (uplift displacement) of isolator units (*Guide* Table 12.5-8)

- Nonlinear Response History Analysis. Calculate gravity and scaled design earthquake or MCE_R ground motion response (average of seven records) for key response parameters:

  1. Design earthquake and MCE_R displacement (including uplift) of isolator units (*Guide* Table 12.5-12).

  2. Design earthquake and MCE_R peak story shears (*Guide* Table 12.5-14).

  3. MCE_R short-term load (downward force) on isolator units (*Guide* Table 12.5-15).

The *Standard* requires modal response spectrum analysis or seismic response history analysis for the EOC (see *Guide* Table 12.2-1). In general, the modal response spectrum method of dynamic analysis is considered sufficient for facilities that are located at a stiff soil site, which have an isolation system meeting the criteria of *Standard* Section 17.4.1, Item 7. However, nonlinear static analysis is used for the design of the EOC, in lieu of modal response spectrum analysis, to permit explicit modeling of potential uplift of isolator units. For similar reasons, nonlinear seismic response history analysis is used to verify design parameters with explicit modeling of potential uplift of isolator units.

Chapter 17 of the *Standard* does not define methods for nonlinear static analysis of base-isolated structures. For this example, nonlinear static loads are applied in one orthogonal direction at a time and the more critical value of the response of the parameter of interest is used for design. In the author's opinion, uni-directional application of earthquake load (in lieu of a 100 percent, 30 percent combination) is considered appropriate for static loads which are based on the maximum direction of response (the new ground motion criterion of the *Provisions*) when used with a conservative distribution of force over height (i.e., ELF distribution of force as described by *Standard* Eq. 17.5-9).

12.5.3.2 Detailed modeling considerations. Rather than a complete description of the ETABS model, key assumptions and methods used to model elements of the isolation system and superstructure are described below.

12.5.3.2.1 Mass eccentricity. *Standard* Section 17.6.2.1 requires consideration of mass eccentricity. Because the building in the example is doubly symmetric, there is no actual eccentricity of building mass (but such would be modeled if the building were not symmetric). Modeling of accidental mass eccentricity would require several analyses, each with the building mass located at different eccentric locations (for example, four quadrant locations in plan). This is problematic, particularly for dynamic analysis using multiple ground motion inputs. In this example, only a single (actual) location of mass eccentricity is considered and calculated demands are increased moderately for the design of the seismic force-resisting system and isolation system to account for accidental eccentricity (e.g., peak displacements calculated by dynamic analysis are increased by 10 percent for design of the isolation system).

12.5.3.2.2 P-delta effects. P-delta moments in the foundation and the first-floor girders just above isolator units due to the large lateral displacement of the superstructure are modeled explicitly. For this example which uses a "double dish" isolator configuration, the model distributes half of the P-delta moment to the structure above and half of the P-delta moment to the foundation below the isolator units. ETABS permits explicit modeling of the P-delta moment, but certain computer programs may not. In such cases, the designer must separately calculate these moments and add them to other forces for the

design of affected elements. The P-delta moments are quite significant, particularly at isolator units that resist large earthquake overturning loads along lines of lateral bracing.

12.5.3.2.3 Isolator unit uplift. *Standard* Section 17.2.4.7 permits local uplift of isolator units, provided the resulting deflections do not cause overstress of isolator units or other structural elements. Uplift of some isolator units is possible (for unreduced earthquake loads) due to the high seismic demand associated with the site. Accordingly, isolator units are modeled with gap elements that permit uplift when there is a net tension load on an isolator unit.

12.5.3.2.4 Bounding values of bilinear stiffness of isolator units. The design of elements of the seismic force-resisting system is usually based on a linear, elastic model of the superstructure. When such models are used, *Standard* Section 17.6.2.2.1 requires that the stiffness properties of nonlinear isolation system components be based on the maximum effective stiffness of the isolation system (since this assumption produces larger earthquake forces in the superstructure). Conversely, the *Standard* requires that calculation of isolation system displacements be based on the minimum effective stiffness of the isolation system (since this assumption produces larger isolation system displacements).

The concept of bounding values, as discussed above, applies to all analysis methods. For the ELF procedure (and RSA), values of maximum effective stiffness, k_{Dmax} and k_{Mmax}, are used for calculating design forces and minimum values of effective stiffness, k_{Dmin} and k_{Dmax}, are used for calculating design displacements. Where (nonlinear) response history analysis is used, isolators are explicitly modeled as bilinear hysteretic elements with upper- or lower-bound stiffness curves, respectively. Upper-bound stiffness curves are used to verify the forces used for the design of the superstructure and lower-bound stiffness curves are used to verify design displacements of the isolation system.

12.5.4 Preliminary Design Based on the ELF Procedure

12.5.4.1 Design of the isolation system. Preliminary design of the isolation system begins with determination of isolation system properties (e.g., effective period and damping of the isolation system), which depend on the type and size of isolation bearings (e.g., friction pendulum or elastomeric bearings) and the type and size of supplementary dampers if such are also incorporated into the isolation system. The size of bearings is related to the amount of vertical load that must be supported and the maximum amount of lateral earthquake displacement that must be accommodated. Maximum earthquake displacement is a function of both the MCE_R ground motions at the building site and the effective period and damping of the isolation system. Thus, preliminary design tends to be an iterative process that involves selecting a bearing type and size that can adequately support vertical loads while accommodating maximum earthquake displacement. While some projects "fine tune" the isolation system by using bearings of different types and sizes (due to large variations in vertical load on bearings), this example uses a single bearing type and size for each of the 35 bearing locations.

Vertical loads on bearings include load combinations representing both long-term gravity loads, factored dead and live load ($1.2D + 1.6L$) and short-term loads that include both gravity and seismic load effects. Seismic loads on bearings due to overturning are not known initially (they must be calculated using models of the superstructure). For the example EOC building, a trial size of bearings is based on a conservative estimate of gravity loads. The most heavily loaded column (Column C3, *Guide* Table 12.5-1) has a long-term load of approximately 600 kips and the rated capacity of bearings should be at least 600 kips.

The size of bearings (the maximum lateral displacement capacity) depends on the type of system and products available, but informed choices regarding an appropriate value of effective period can be made

by constructing plots (based on ELF design formulas) such as those shown in Figure 12.3-3 for a steel SCBF superstructure. Consider, first, values of superstructure design shear, V_s. Figure 12.3-3 shows that values of superstructure design shear will be the same for all isolation systems that have an effective period, T_D, of approximately 2.5 seconds or greater. Longer effective periods reduce lateral forces (and overturning loads), but superstructure strength will be governed by minimum base shear requirements. An effective period, T_D, of approximately 2.5 seconds (and effective period, T_M, of not more than approximately 3.0 seconds) would be appropriate for isolation system with elastomeric bearings that have inherent limits on rubber stiffness and strain capacity. Friction systems can have somewhat longer periods that would not reduce the level of force required for lateral design of the superstructure but would reduce overturning loads on columns, isolators and foundations. Longer effective periods reduce forces at the expense of increased displacement, which may be infeasible or could increase the cost of other structural elements (such as a moat wall), flexible utility connections and other nonstructural components that cross the isolation interface. The differing conditions and criteria of each project must be considered in selecting appropriate (optimal) properties for the isolation system.

For this example, which incorporates friction pendulum bearings, the trial bearing size and properties (such as the curvature of the concave plates) are selected from products that are available from a specific manufacturer (EPS), which have a relatively long effective period, T_M. A long effective period will minimize loads on the superstructure but could require MCE_R displacement capacity beyond practical limits. As shown in Figure 12.3-3, an effective period of 4 seconds (or greater) would require over 36 inches of displacement and the moat clearance would need to be at least 36 inches, which would be infeasible for most projects. The design shear and displacement plots in Figure 12.3-3 are constructed with values of effective damping that closely match friction pendulum bearing properties at the response amplitudes of interest; they are valid for this type and size of bearing but not necessarily other bearing types or sizes.

Based on the preceding discussions, the double-concave friction pendulum bearing (FPT8844/12-12/8-6) shown in Figure 12.5-8 is selected for the EOC example. This bearing has concave plate radii, r_P, of 88 inches (for both top and bottom concave plates), which produces an effective period in the range of 3.5 to 4.0 seconds. Articulated slider dimensions are shown in Figure 12.5-8. The inside diameter of the concave plates (44 in.) provides approximately 33 inches of displacement capacity before the articulated slider engages the boundary of the concave plates (44 inches [dish diameter] minus 12 inches [slider diameter] plus approximately 1 inch [due to slider articulation]).

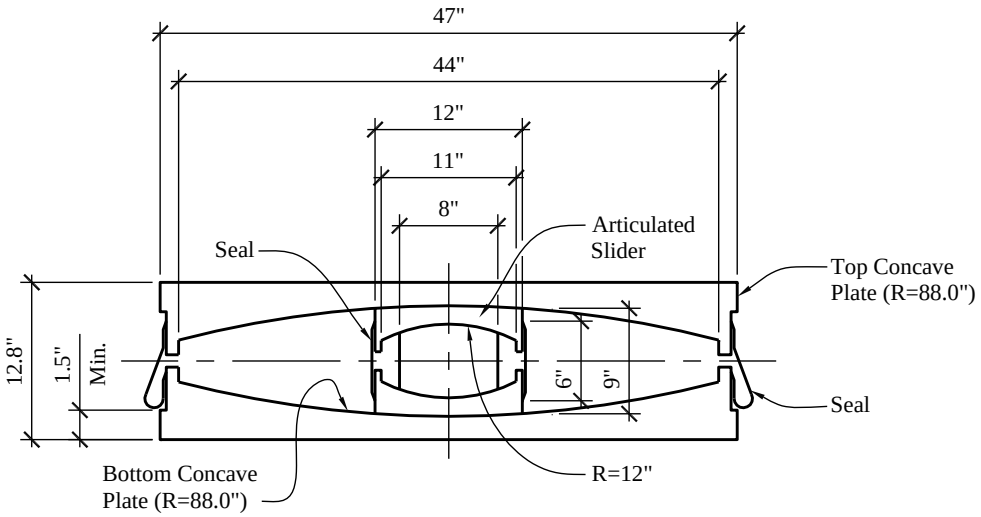

Figure 12.5-8 Section view of the double-concave friction pendulum bearing (FPT8844/12-12/8-6)

The friction pendulum bearing (FPT8844/12-12/8-6) has a rated vertical load capacity of 800 kips, which can adequately support long-term loads ($1.2D + 1.6L$) which are summarized in *Guide* Table 12.5-1 (the maximum long-term load is approximately 600 kips). The rated capacity of the bearing should also exceed short-term isolation system design loads ($1.37D + 0.5L + Q_{DE}$), the values of which are calculated later in this section (see *Guide* Table 12.5-5). The friction pendulum bearing does not resist uplift and may not function properly should uplift occur. For this example, uplift is not permitted for short-term isolation system design loads ($0.73D - Q_{DE}$), which is shown to be the case later in this section (see *Guide* Table 12.5-6). *Standard* Section 17.2.4.6 requires bearings (and other elements of the isolation system) to remain stable for the total maximum displacement of the isolation system and short-term MCE_R loads ($1.45D + 1.0L + Q_{MCE}$ and $0.80D - Q_{MCE}$). Bearing stability must be verified by prototype testing for both maximum downward loads ($1.45D + 1.0L + Q_{MCE}$), which are calculated later in this section (see *Guide* Table 12.5-7) and maximum uplift displacements (due to $0.80D - Q_{MCE}$), which are also calculated later in this section (See *Guide* Table 12.5-8).

In addition to basic configuration and curvature, key properties of the friction pendulum bearings include the amount of dynamic (sliding) friction and the level of static (breakaway) friction of the sliding surfaces. For double-concave bearings, sliding surfaces include (1) the surface between the top of the articulated slider and the top concave plate and (2) the surface between the bottom of the articulated slider and the bottom concave plate (and to a lesser degree, friction surfaces inside the articulated slider). For this example, bearing friction is taken to be nominally the same value for the top and bottom sliding surfaces.

The sliding friction (based on the friction coefficient) is influenced by several factors, including the following:

- Vertical load (pressure on sliding surfaces): In general, the greater the vertical-load pressure, the lower the value of the friction coefficient.

- Rate of lateral load (bearing velocity): In general, the greater the velocity, the higher the value of the friction coefficient (although the friction coefficient tends to be fairly constant at moderate and high earthquake velocities).

- Bearing temperature (surface temperature of sliding surfaces): In general, the hotter the bearing, the lower the value of the friction coefficient. Bearings get hot due to repeated cycles of earthquake load. Bearing temperature is a function of the duration of earthquake shaking (the number of cycles of dynamic load) and the friction force on the sliding surface. The greater the number of cycles of dynamic load, the hotter the bearing. The greater the friction force (due to larger vertical load or friction coefficient), the hotter the bearing.

Other factors influencing friction and sliding bearing performance include manufacturing tolerances (not all bearings can be made exactly the same) and the effects of aging and possible contamination of sliding surfaces (which should be minimal for bearings with protective seals and not exposed to the environment).

For the preliminary design of the isolation system (and subsequent analyses of the isolation system), nominal and bounding values of the siding friction coefficient are used to construct hysteresis loops that define effective stiffness, effective period and the effective damping of the isolations system (i.e., all 35 bearings acting together) as a function of isolation system displacement. For this example, the nominal value of the friction coefficient of top and bottom concave plates is $\mu_{p,nom} = 0.06$, with a lower-bound value of $\mu_{p,min} = 0.04$ and an upper-bound value of $\mu_{p,max} = 0.08$ and the friction coefficient of the articulated slider (internal surfaces) is $\mu_s = 0.02$. Static breakaway friction is assumed to be less than or equal to $\mu_{p,max}$. A relatively large variation in the friction coefficient, a factor of 2, is used to bound all sources of friction coefficient variability, described above, including possible change in properties over the life of the bearing. As discussed later in *Guide* Section 12.5.6, isolation system properties based on assumed values must be verified by testing of isolator prototypes.

The effective stiffness (normalized by building weight), $k_{eff,D}/W$, may be calculated approximately as a function of bearing displacement, D, in inches for the double-concave friction pendulum bearing, as follows:

$$k_{eff,D}/W = \mu_P + \left(\frac{1}{2r_P - h_s + 2r_s - h_c}\right)D$$

where the term, μ_P, represents nominal, upper-bound or lower-bound value of the sliding friction coefficient, r_p is the radius of the concave plates, h_s is the height of the articulated slider, r_s is the radius of the articulated slider and h_c is the height of the core of the articulated slider. Similarly, the bi-linear concepts shown in *Guide* Figure 12.1-2 are used to calculate effective period, $T_{eff,D}$ and effective damping, $\beta_{eff,D}$, as a function of bearing displacement, D, in inches for the double concave friction pendulum bearing, as follows:

$$T_{eff,D} = 0.32\sqrt{\frac{D}{k_{eff,D}/W}}$$

$$\beta_{eff,D} = 0.637\left(\frac{DF_y - D_y k_{eff,D}/W}{Dk_{eff,D}/W}\right)$$

where:

$$D_y = 2\left(\mu_P - \mu_S\right) d_S$$

$$A_y = \mu_P + \left(\frac{1}{2r_P - h_s + 2r_s - h_c}\right) D_y$$

Figures 12.5-9, 12.5-10 and 12.5-11 are plots of effective stiffness, effective period and effective damping, respectively, based on the above formulas and the geometric and sliding friction properties of the double-concave friction pendulum bearing. These curves are useful design aids that are referred to in subsequent sections when determining amplitude-dependent properties of the isolation system.

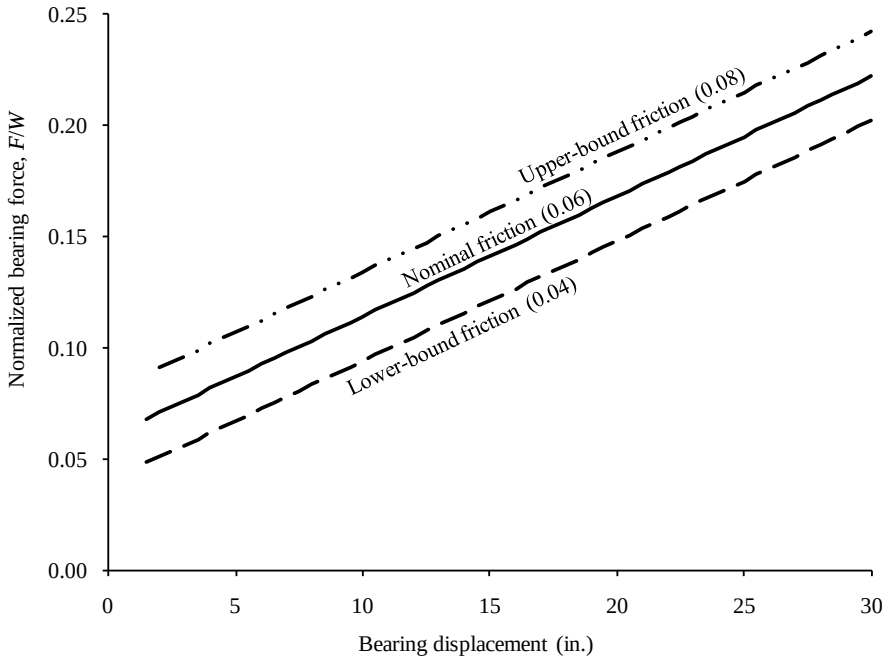

Figure 12.5-9 Effective stiffness as a function of the displacement of the double-concave friction pendulum bearing (FPT8844/12-12/8-6)

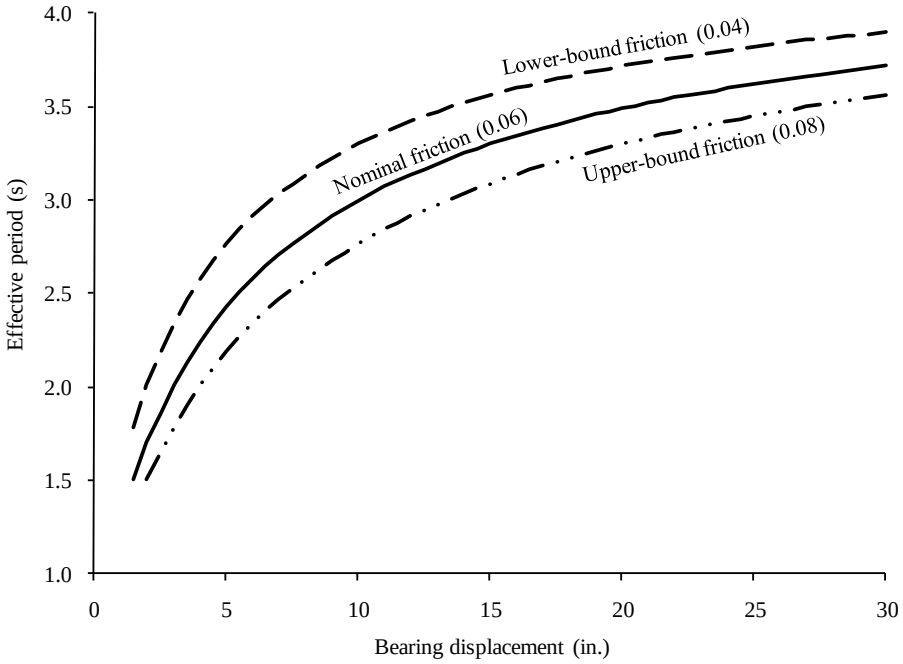

Figure 12.5-10 Effective period as a function of the displacement of the double-concave friction pendulum bearing (FPT8844/12-12/8-6)

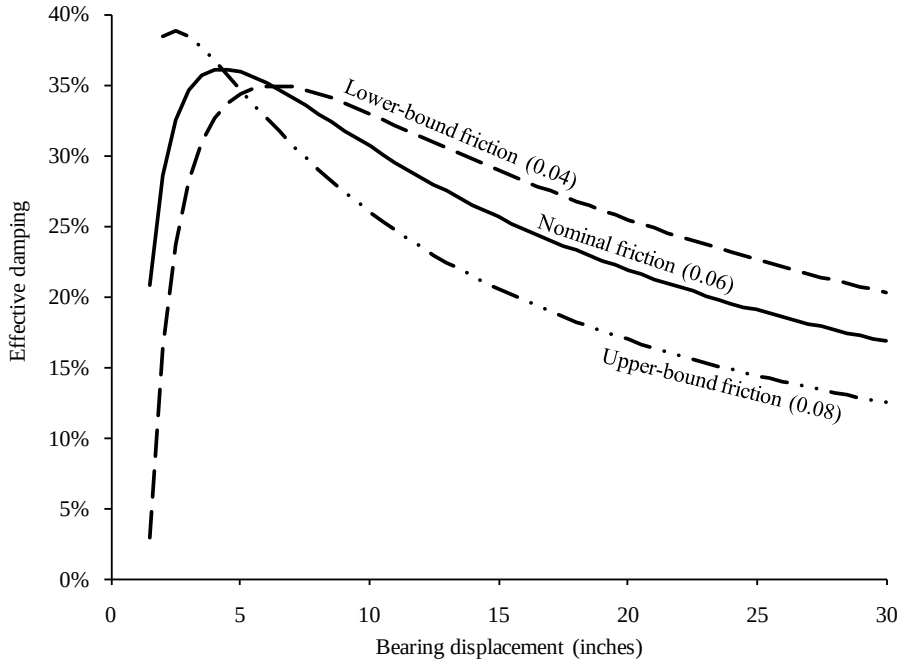

Figure 12.5-11 Effective damping as a function of the displacement of the double-concave friction pendulum bearing (FPT8844/12-12/8-6)

12.5.4.2 Calculation of design values.

12.5.4.2.1 Design displacements. Preliminary design begins with the engineer's selection of the effective period (and effective damping) of the isolated structure and the calculation of the design displacements. This process is necessarily iterative, since the effective period (and effective damping) is amplitude dependent. In this example, the effective DE period of the EOC facility (i.e., effective period at design earthquake displacement) is estimated using lower-bound properties of *Guide* Figure 12.5-10 to be approximately T_D = 3.5 seconds at a design displacement of D_D = 16.0 inches, calculated using *Standard* Equation 17.5-1 as follows:

$$D_D = \left(\frac{g}{4\pi^2}\right)\frac{S_{D1}T_D}{B_D} = (9.8)\frac{0.7(3.5)}{1.5} = 16.0 \text{ in.}$$

The 1.5 value of the damping coefficient, B_D, is given in *Standard* Table 17.5-1 assuming 20 percent effective damping at 16.0 inches of isolation system displacement, which is consistent with lower-bound effective damping shown in *Guide* Figure 12.5-11.

The same approach is used to estimate the MCE_R period, in this case T_M = 3.9 seconds at a maximum displacement of approximately D_M = 30 inches, calculated using *Standard* Equation 17.5-3 as follows:

$$D_M = \left(\frac{g}{4\pi^2}\right)\frac{S_{M1}T_M}{B_M} = (9.8)\frac{1.05(3.9)}{1.3} = 30.9 \text{ in.}$$

The 1.3 value of the damping coefficient, B_M, is given in *Standard* Table 17.5-1 assuming 13 percent effective damping at approximately 30 inches of isolation system displacement, which is consistent with lower-bound effective damping shown in *Guide* Figure 12.5-11. It may be noted from this figure that the effective damping of the isolation system and related benefits of reduced response decrease significantly with response amplitude at large displacements.

The total displacement of specific isolator units (considering the effects of torsion) is calculated based on the plan dimensions of the building, the total torsion (due to actual, plus accidental eccentricity) and the distance from the center of resistance of the building to the isolator unit of interest. Using *Standard* Equations 17.5-5 and 17.5-6, the total design displacement, D_{TD} and the total maximum displacement, D_{TM}, of isolator units located on Column Lines 1 and 7 are calculated for the critical (transverse) direction of earthquake load to be approximately 20 percent greater than D_D and D_M, respectively. *Standard* Equations 17.5-5 and 17.5-6 assume that mass is distributed in plan in proportion to isolation system stiffness, offset by 5 percent, providing no special resistance to rotation of the building above the isolation system. These assumptions are reasonable, in general, but are not appropriate for isolation systems that have inherent resistance to torsion. For example, systems which have less load on bearings at the perimeter (as is the case of most buildings) and/or more stiffness at the perimeter (due to stiffer bearings) would not experience this amount of additional response due to torsion.

For sliding systems, friction forces are roughly proportional to applied load and the center of resistance would tend to move with any change in the actual center of mass, such as that associated with accidental mass eccentricity. Accordingly, additional displacement due to accidental mass eccentricity is taken as 10 percent, the minimum value of additional displacement permitted by *Standard* Section 17.5.3.3. Applying a 10 percent increase to the design and maximum displacement values produces total design and maximum displacement (i.e., at building corners) values of D_{TD} = 17.6 inches (1.1 × 16.0) and

D_{TM} = 34.0 inches (1.1 × 30.9), respectively, the latter of which is about the displacement capacity of the bearing.

12.5.4.2.2 Minimum and maximum effective stiffness. *Standard* Equation 17.5-2 expresses the effective period at the design displacement in terms of building weight (dead load) and the minimum effective stiffness of the isolation system, k_{Dmin}. Rearranging terms and solving for minimum effective stiffness results in the following:

$$k_{D\min} = \left(\frac{4\pi^2}{g}\right)\frac{W}{T_D^2} = \left(\frac{1}{9.8}\right)\frac{9{,}100}{3.5^2} = 75.8 \text{ kips/in.}$$

Similarly, the minimum effective stiffness at the maximum displacement is calculated as follows:

$$k_{M\min} = \left(\frac{4\pi^2}{g}\right)\frac{W}{T_D^2} = \left(\frac{1}{9.8}\right)\frac{9{,}100}{3.9^2} = 61.1 \text{ kips/in.}$$

Estimates of the maximum effective stiffness at the design displacement, D_D = 16.0 inches and maximum displacement, D_M = 30.9 inches, can be made using *Guide* Figure 12.5-9, which shows the upper-bound effective stiffness to be approximately 20 percent greater than the lower-bound effective stiffness at 16.0 inches and the upper-bound effective stiffness to be approximately 15 percent greater than lower-bound effective stiffness at 30.9 inches of displacement:

$$k_{D\max} = 1.2(75.8) = 91.0 \text{ kips / in.}$$

$$k_{M\max} = 1.15(61.1) = 70.3 \text{ kips / in.}$$

As noted earlier, the range of effective stiffness illustrated in *Guide* Figure 12.5-9 represents the isolation system as a whole rather than the range of effective stiffness associated with individual bearings and is intended to address a number of factors that influence potential variation in bearing properties, including the effects of aging and contamination, etc. A report, *Property Modification Factors for Seismic Isolation Bearings* (Constantinou, 1999), provides guidance for establishing a range of effective stiffness (and effective damping) properties that captures various sources of the variation over the design life of the isolator units. The range of effective stiffness of the isolation system has a corresponding range of effective periods (with different levels of spectral demand). As discussed in *Guide* Section 12.3, the longest effective period (corresponding to the minimum effective stiffness) of the range is used to define isolation system design displacement and the shortest effective period (corresponding to the maximum effective stiffness) of the range is used to define the design forces on the superstructure.

12.5.4.2.3 Lateral design forces. The lateral force required for the design of the isolation system, foundation and other structural elements below the isolation system is given by *Standard* Equation 17.5-7:

$$V_b = k_{Dmax} D_D = 91.0(16.0) = 1{,}456 \text{ kips}$$

The lateral force required for checking stability and ultimate capacity of elements of the isolation system may be calculated as follows:

$$V_{MCE} = k_{Mmax} D_M = 70.3(30.9) = 2{,}172 \text{ kips}$$

The (unreduced) base shear of the design earthquake is approximately 16 percent of the weight of the EOC and the (unreduced) base shear of the MCE is approximately 24 percent of the weight. Subject to the limits of *Standard* Section 17.5.4.3, the design earthquake base shear, V_s, is reduced by the R_I factor in accordance with *Standard* Equation 17.5-8:

$$V_s = \frac{k_{D\max} D_D}{R_I} = \frac{91.0(16.0)}{2.0} = 728 \text{ kips}$$

This force is only approximately 8 percent of the dead load weight of the EOC, which is less than the limits of Item 3 of Section 17.5.4.3 that require a minimum base shear of at least 1.5 times the "break-away friction level of a sliding system." In this example, breakaway friction is assumed to be less than or equal to the maximum value of sliding friction, $\mu_{P,max}$ = 0.08, such that the minimum design earthquake base shear, V_s, is calculated as follows:

$$V_s = 1.5\mu_{P,\max} W = 1.5(0.08)9{,}100 = 1{,}092 \text{ kips}$$

which is substantially less than the lateral force that would be required for the design of a conventional, fixed-base, EOC building of the same size and height, seismic force-resisting system and site seismic conditions. Story shear forces on the superstructure are distributed vertically over the height of the structure in accordance with *Standard* Equation 17.5-9, as shown in Table 12.5-4.

Table 12.5-4 Vertical Distribution of Reduced Design Earthquake Forces (V_s = 1,092 kips)

Floor level, x (Story)	Floor weight, w_x (kips)	Cumulative weight (kips)	Height above isolation system, h_x (ft)	Story force, F_x, (kips) (*Standard* Eq. 17.5-9)	Cumulative story force (kips)	Cum. force divided by cumulative weight
PH Roof	794		54			
(Penthouse)		794		196	196	25%
Roof	2,251		42			
(Third)		3,045		432	628	21%
Third Floor	1,947		30			
(Second)		4,992		267	895	18%
Second Floor	1,922		18			
(First)		6,914		158	1,053	15%
First Floor	2,186		4			
(Isolation)		9,100		40	1,092	12%

1.0 ft = 0.3048 m, 1.0 kip = 4.45 kN.

Standard Equation 17.5-9 distributes lateral seismic design forces (V_s = 1.092 kips) over the height of the building's superstructure in an inverted triangular pattern, effectively doubling shear force at the roof level, as indicated by values of cumulative story force divided by weight above shown in Table 12.5-4. Because the superstructure is much stiffer laterally than the isolation system, it tends to move as a rigid

body, rather than in the first mode, with a pattern of lateral seismic forces that is typically more uniformly distributed over the height of the building. The use of a triangular load pattern for design is intended to account for higher-mode response that may be excited by superstructure flexibility and isolation system nonlinearity. *Standard* Equation 17.5-9 is also used to distribute forces over the height of the building for unreduced DE and MCE_R forces, as summarized in Table 12.5-5. Unreduced forces are required for design of isolator units.

Table 12.5-5 Vertical Distribution of Unreduced Design Earthquake and MCE_R Forces

Story	Design Earthquake Forces			MCE_R Forces		
	Story force, F_x (kips) (*Standard* Eq. 17.5-9)	Cumulative story force (kips)	Cum. force divided by cumulative weight	Story force, F_x (kips) (*Standard* Eq. 17.5-9)	Cumulative story force (kips)	Cum. force divided by cumulative weight
Penthouse	261	261	33%	389	389	49%
Third	576	837	27%	859	1,248	41%
Second	356	1,192	24%	530	1,778	35%
First	211	1,403	20%	315	2,093	30%
Isolation	53	1,456	16%	79	2,172	24%

12.5.4.2.4 Design earthquake forces for isolator units. Tables 12.5-6 and 12.5-7 show the maximum and minimum downward forces for design of the isolator units. These forces result from the simultaneous application of gravity loads and unreduced design earthquake story forces, summarized in Table 12.5-5, to the ETABS model of the EOC. (See *Guide* Sec. 12.5.2.5 for the design load combinations.) As described in *Guide* Section 12.5.2.5, loads are applied separately in the two horizontal directions and results for both directions are reported in these tables (i.e., x direction / y direction). All values in Table 12.5-7 are positive, indicating that uplift does not occur at any bearing location for unreduced DE loads.

Table 12.5-6 Maximum Downward Force (kips) for Isolator Design $(1.37D + 0.5L + Q_{DE})^*$

Line	Maximum downward force (kips)			
	1	2	3	4
A	225 / 225	383 / 498	334 / 356	336 / 359
B	480 / 389	590 / 668	674 / 700	633 / 812
C	349 / 328	641 / 709	632 / 631	586 / 570

1.0 kip = 4.45 kN

* Forces at Column Lines 5, 6 and 7 (not shown) are similar to those at Column Lines 3, 2 and 1, respectively; loads at Column Lines D and E (not shown) are similar to those at Column Lines B and A, respectively.

Table 12.5-7 Minimum Downward Force (kips) for Isolator Design ($0.73D - Q_{DE}$)*

	Maximum downward force (kips)			
Line	1	2	3	4
A	84 / 85	160 / 65	149 / 128	150 / 135
B	67 / 146	144 / 58	197 / 199	224 / 56
C	125 / 146	235 / 160	269 / 265	234 / 223

1.0 kip = 4.45 kN

* Forces at Column Lines 5, 6 and 7 (not shown) are similar to those at Column Lines 3, 2 and 1, respectively; loads at Column Lines D and E (not shown) are similar to those at Column Lines B and A, respectively.

12.5.4.2.5 MCE_R forces and displacements for isolator units. Simultaneous application of gravity loads and unreduced MCE_R story forces, as summarized in Table 12.5-5, to the ETABS model of the EOC results in the maximum downward forces on isolator units shown in *Guide* Table 12.5-8 and the maximum uplift displacements shown in Table 12.5-9. The load orientations and MCE_R load combinations are described in *Guide* Section 12.5.2.5. Table 12.5-9 shows that uplift did not occur at most bearing locations and was very small at the few locations where MCE_R overturning forces exceeded factored gravity loads.

Table 12.5-8 Maximum (MCE_R) Downward Force (kips) on Isolator Units ($1.45D + 1.0L + Q_{MCE}$)*

	Maximum downward force (kips)			
Line	1	2	3	4
A	269 / 270	467 / 644	404 / 439	406 / 445
B	616 / 476	754 / 869	845 / 883	793 / **1,063**
C	430 / 395	804 / 905	785 / 783	732 / 705

1.0 kip = 4.45 kN.

*Forces at Column Lines 5, 6 and 7 (not shown) are similar to those at Column Lines 3, 2 and 1, respectively; loads at Column Lines D and E (not shown) are similar to those at Column Lines B and A, respectively.

Table 12.5-9 Maximum (MCE_R) Uplift Displacement (in.) of Isolator Units ($0.8D - Q_{MCE}$)*

	Maximum uplift displacement (in.)			
Line	1	2	3	4
A	No Uplift	No Uplift	No Uplift	No Uplift
B	No Uplift	0 / 0.007	No Uplift	0 / 0.011
C	No Uplift	No Uplift	No Uplift	No Uplift

1.0 in. = 25.4 mm.

* Displacements at Column Lines 5, 6 and 7 (not shown) are similar to those at Column Lines 3, 2 and 1, respectively; displacements at Column Lines D and E (not shown) are similar to those at Column Lines B and A, respectively.

12.5.4.2.6 Limits on dynamic analysis. The displacements and forces determined by the ELF procedure provide a basis for expeditious assessment of size and capacity of isolator units and the required strength of the superstructure. The results of the ELF procedure also establish limits on design parameters when dynamic analysis is used as the basis for design. Specifically, the total design displacement, D_{TD} and the total maximum displacement of the isolation system, D_{TM}, determined by dynamic analysis cannot be less than 90 percent and 80 percent, respectively, of the corresponding ELF procedure values:

$D_{TD,\,dynamic} \geq 0.9D_{TD,\,\mathrm{ELF}} = 0.9(17.6) = 15.8$ in.

$D_{TM,\,dynamic} \geq 0.8D_{TM,\,\mathrm{ELF}} = 0.8(34.0) = 27.2$ in.

Similarly, the lateral force, V_b, required for design of the isolation system, foundation and all structural elements below the isolation system and the lateral force, V_s, required for design of the superstructure determined by dynamic analysis are limited to 90 percent and 80 percent, respectively, of the ELF procedure values:

$V_{b,\,dynamic} \geq 0.9V_{b,\,\mathrm{ELF}} = 0.9(1{,}456) = 1{,}310$ kips $(= 0.144W)$

$V_{s,\,dynamic} \geq 0.8V_{s,\,\mathrm{ELF}} = 0.8(1{,}092) = 874$ kips $(= 0.096W)$

As an exception to the above, lateral forces less than 80 percent of the ELF results are permitted for design of superstructures of regular configuration, if justified by response history analysis (which is seldom, if ever, the case). However, $V_{s,dynamic}$ is also subject to the limits of Section 17.5.4.3 for response history analysis (and also, by inference, for response spectrum analysis) which govern the value of $V_{s,ELF}$ in this example and thus govern the minimum value of design base shear (regardless of the analysis method used for design):

$V_{s,\,dynamic} \geq V_{s,\,\mathrm{ELF}} = 1.0(1{,}092) = 1{,}092$ kips $(= 0.12W)$

12.5.4.3 Preliminary design of the superstructure. The lateral forces, developed in the previous section, in combination with gravity loads, provide a basis for preliminary design of the superstructure, using methods similar to those used for a conventional building. In this example, selection of member sizes was made based on the results of ETABS model calculations. Detailed descriptions of the design calculations are omitted, since the focus of this section is on design aspects unique to isolated structures (i.e., the design of the isolation system, which is described in the next section).

Figures 12.5-12 and 12.5-13 are elevation views at Column Lines 2 and B, respectively. Figure 12.5-14 is a plan view of the building that shows the framing at the first floor level.

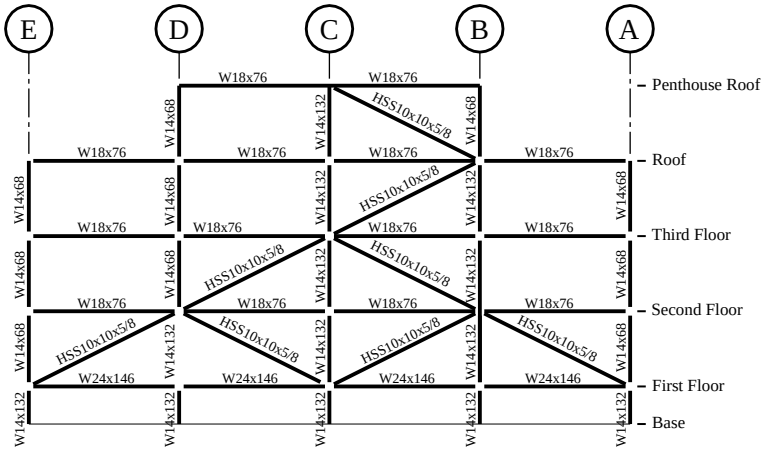

a) Lines 2 and 6

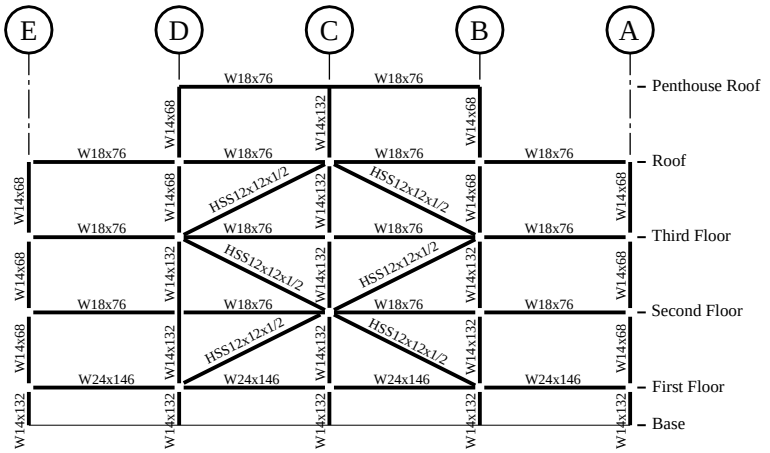

b) Line 4

Figure 12.5-12 Elevation of framing on Column Lines 2 ,4 and 6

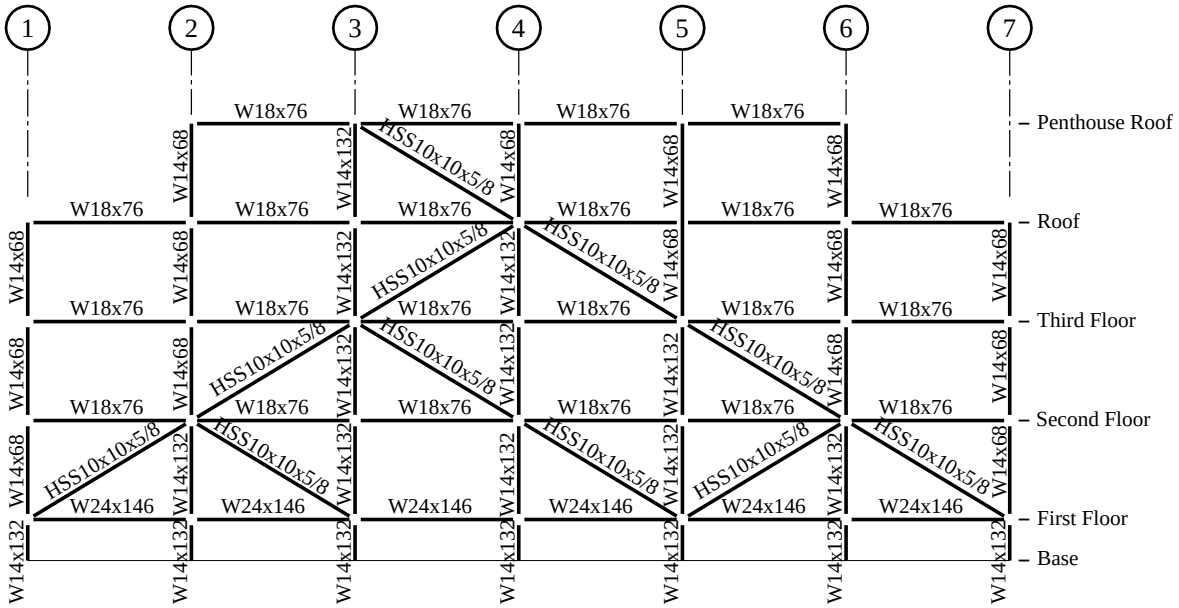

Figure 12.5-13 Elevation of framing on Column Lines B and D

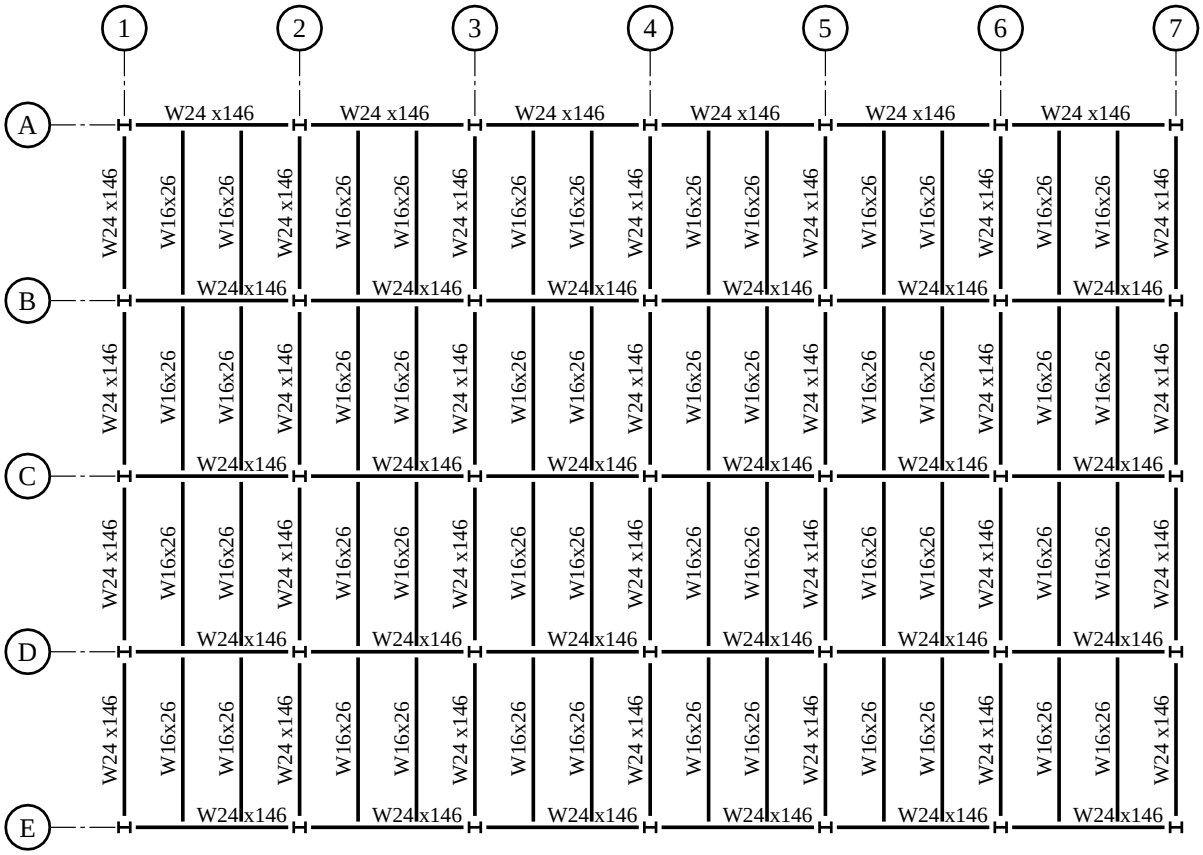

Figure 12.5-14 First floor framing plan

As shown in the elevations (Figures 12.5-12 and 12.5-13), relatively large (HSS 10×10×5/8) tubes are conservatively used throughout the structure for diagonal bracing. A quick check of these braces indicates that stresses will be at or below yield for earthquake loads. For example, the four braces at the third story, on Lines 2, 4 and 6 (critical floor and direction of bracing) resist a reduced design earthquake force of approximately 175 kips (628 kips / 4 braces × cos[25°]), on average. The corresponding average brace stress is only approximately 8 ksi (for reduced design earthquake forces) and only approximately 11 ksi and 16 ksi for unreduced DE and MCE_R earthquake forces, respectively, indicating that the structure is expected to remain elastic even for MCE_R demand.

As shown in Figure 12.5-14, the first-floor framing has relatively heavy, W24×146 girders along lines of bracing (Lines B, D, 2, 4 and 6). These girders resist P-delta moments as well as other forces. A quick check of these girders indicates that only limited yielding is likely, even for the MCE_R loads (and approximately 3 feet of MCE_R displacement). Girders on Line 2 that frame into the column at Line B (critical columns and direction of framing) resist a P-delta moment due to the MCE_R force of approximately 800 kip-ft (1,063 kips / 2 girders × 3 feet / 2). Additional moment in these girders due to MCE_R shear force in isolators is approximately 500 kip-ft (1,063 kips × 0.24 × 4 feet / 2 girders). Thus, total moment is approximately 1,300 kips due to gravity and MCE_R loads (and 3 feet of MCE_R displacement), which is conservatively less than the plastic capacity of these girders (i.e., $\phi_b M_p$ = 1,570 kip-ft).

12.5.4.4 Isolator connection detail. The isolation system has a similar detail at each column for the example EOC, as shown in Figure 12.5-15. The column has a large, stiffened base plate that bears directly on the top of the isolator unit. The column base plate is circular, with a diameter comparable to that of the top plate of the isolator unit. Heavy, first-floor girders frame into and are moment connected to the columns (moment connections are required at this floor only). The columns and base plates are strengthened by plates that run in both horizontal directions, from the bottom flange of the girder to the base. Girders are stiffened above the seat plates and at temporary jacking locations. The top plate of the isolator unit is bolted to the column base plate and the bottom plate of the isolator unit is bolted to the foundation. The foundation (and grout) directly below the isolator must have sufficient strength to support concentrated bearing loads from the concave plate and articulated slider above (for all possible lateral displacements of the isolator). Similarly, the column base plate and structure just above the isolator must have sufficient strength to transfer concentrated bearing loads to the concave plate and articulated slider below.

The foundation connection accommodates the removal and replacement of isolator units, as required by *Standard* Section 17.2.4.8. Anchor bolts pass through holes in this plate and connect to threaded couplers that are attached to deeply embedded rods. Figure 12.5-15 illustrates connection details typical of isolated structures; other details could be developed that work just as well and certainly details would be different for structures that have a different configuration or material.

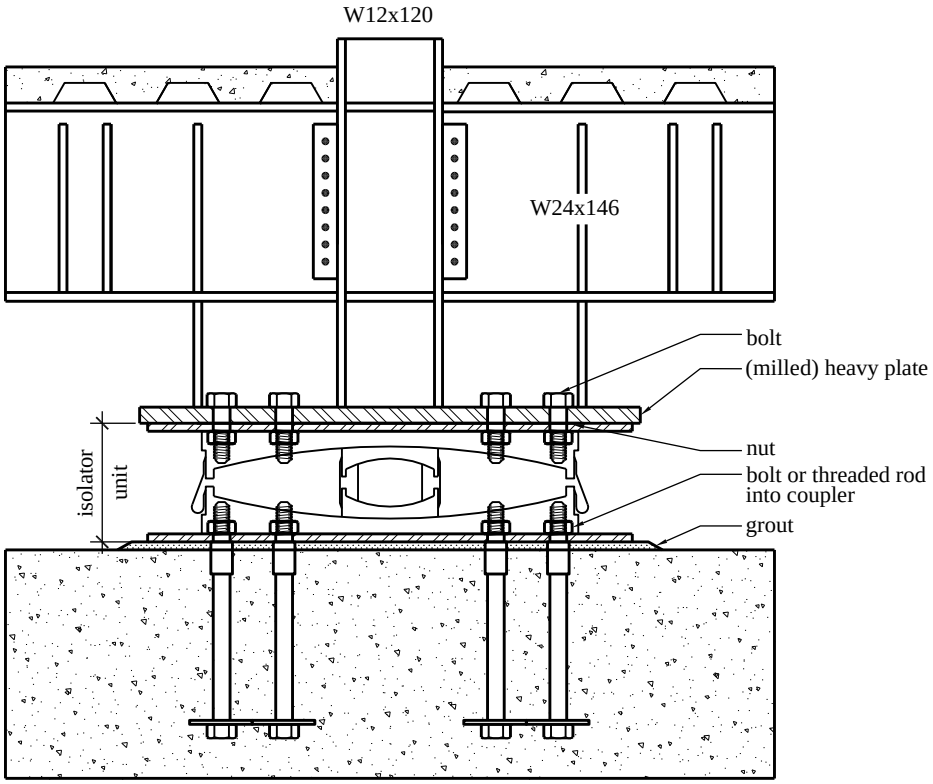

Figure 12.5-15 Typical detail of the isolation system at columns
(for clarity, some elements are not shown)

With the exception of the portion of the column above the first-floor slab, each element shown in Figure 12.5-11 is an integral part of the isolation system (or foundation) and is designed for the gravity and unreduced design earthquake loads. In particular, the first-floor girder, the connection of the girder to the column and the connection of the column to the base plate are designed for gravity loads and forces caused by horizontal shear and P-delta effects due to the unreduced design earthquake loads (as shown earlier in *Guide* Figure 12.4-1).

12.5.5 Design Verification Using Nonlinear Response History Analysis

The *Standard* requires dynamic analysis for design of isolated buildings like the example EOC that are located at sites with 1-second spectral acceleration, S_1, greater than or equal to 0.6g (see *Guide* Table 12.2-1). The *Standard* also requires that the dynamic analysis requirement be satisfied using response history analysis (RHA) for isolated buildings like the example EOC that have an isolation systems that does not fully comply with the criteria of Item 7 of *Standard* Section 17.4.1. In practice it is common to use the RHA procedure to verify the design of structures with sliding or high-damping isolation systems.

This example uses RHA to determine final design displacements of the isolation system and to confirm that ELF-based forces used for preliminary design of the superstructure and isolation system are valid. While results of RHA could be used to refine the preliminary design of the superstructure (e.g., reduce size of lateral bracing, etc.), this example uses RHA primarily for “design verification” of key global

response parameters (i.e., confirmation of ELF-based story shear force). If the RHA procedure were used as the primary basis for superstructure design, then response results would be required for design of individual elements, rather than for checking a limited number of global response parameters.

12.5.5.1 Ground motion records. The RHA procedure evaluates DE and MCE_R response of the example EOC using the set of seven ground motion records previously described in *Guide* Section 12.5.4.4. Seven records are used for RHA so that the average value of the response parameter of interest can be used for design (or design verification).

Each record has two horizontal components, one of which is identified as the "larger" component in terms of spectral acceleration at the effective period of the isolation system (i.e., 3.9 seconds). The ground motion records are grouped (oriented) in terms of the larger component (Step 2) and are applied to the analytical model (Step 4) in accordance with procedure recommended in *Guide* Sec. 12.4.4.

Guide Table 12.5-2 summarizes key source and site properties used as the basis for record selection and *Guide* Table 12.5-3 summarizes factors used to scale each record to match design earthquake and MCE_R response spectra, respectively. *Guide* Figure 12.5-7 compares the average spectra of the seven scaled records (for the SRSS combination of components and the larger component, respectively) with the MCE_R response spectrum demonstrating compliance with scaling requirements of *Standard* Section 17.3.2 and the recommendations of *Guide* Section 12.4.4 (Step 3).

12.5.5.2 ETABS models. The ETABS computer program is used for RHA of analytical models of the isolated structure, as previously discussed in *Guide* Section 12.5.3. Two basic ETABS models are developed for RHA analysis, both having the same superstructure but representing lower-bound and upper-bound stiffness properties of isolators (FP bearings), respectively.

Elements of the superstructure and isolation system (other than the isolators) are modeled as linear elastic elements based on member sizes developed by preliminary design (*Guide* Section 12.5.4.3). Elements are not expected to yield significantly, even for MCE_R response and the assumption of linear elastic behavior is quite reasonable. For RHA, ETABS internally calculates modal damping based on the hysteretic properties of the nonlinear elements (isolators) and an additional amount of user-specified modal damping. For the EOC example, additional damping is limited to 2 percent of critical for all modes, since the steel superstructure remains essentially linear elastic.

Two types of isolator nonlinearity are modeled explicitly. First, gap elements, just above each isolator, model potential uplift of the isolation system. The gap elements transmit downward (compressive) forces but release and permit upward displacement of the structure, if upward (tension) forces occur. The purpose of the gap elements is to check for possible uplift due to overturning loads exceeding factored gravity loads and to calculate the maximum amount of vertical displacement, should uplift occur. The second type of isolator nonlinearity is that associated with horizontal force-deflection properties of isolators.

For this example, nonlinear force-deflection properties of the isolator units are modeled using the ETABS nonlinear "Isolator2" element. This element was originally developed for FP bearing with a single concave plate and requires the user to input the initial stiffness (effective stiffness before the articulated slider displaces on the concave plate), the friction coefficient properties and the radius of the concave plate. For the double concave FP bearing of this example, an "effective" radius, r_{eff}, is used to account for simultaneous sliding of the articulated slider on the two concave plates. The effective radius, r_{eff}, of the two dishes is 185 inches, based on the radius of each concave plate (r_p = 88 inches), the height of the articulated slider (h_s = 9 inches), the radius of the articulated slider (r_s = 12 inches) and the height of the internal core (h_c = 6 inches):

$r_{eff} = 2r_p - h_s + 2r_s - h_c = 2 \times 88$ in. - 9 in. + 2×12 in. - 6 in. = 185 inches

The Isolator2 element simulates bilinear, hysteretic behavior commonly used to model the nonlinear properties of friction-pendulum bearings, although the double-concave configuration generally requires more sophisticated representation of bearing properties. For example, very complex models of this bearing have been developed and implemented in 3D-BASIS (Constantinou, et al.) and SAP2000 (CSI). Use of these more sophisticated models would be required for double-concave friction pendulum bearings configured to have different friction coefficients for the surfaces of top and bottom concave plates, respectively, or for projects which explicitly model the stiffening effects of articulated slider engagement with the boundary of concave plates. Such modeling is not required for the EOC example and the bilinear curve of the Isolator2 element (available in ETABS) is used for design verification.

The Isolator2 element requires the user to input three sliding friction parameters: (1) the "fast" value of the sliding coefficient of friction, (2) the "slow" value of the sliding coefficient of friction and (3)a "rate" parameter that essentially governs transition between slow and fast properties (e.g., when the bearing reaches peak displacement and reverses direction of travel). For the Isolator2 element, "fast" represents velocities in excess of approximately 1 to 2 inches per second. Typically, during strong ground motions, such as those of this example, sliding velocities are well in excess of 2 inches per second and isolation system response is dominated by "fast" sliding friction properties.

Lower-bound and upper-bound values of sliding friction coefficient are used to represent lower-bound and upper-bound values FP bearing of "stiffness," as previously discussed in *Guide* Section 12.5.4.1. Lower-bound and upper-bound values of sliding friction coefficient, 4 percent and 8 percent respectively, are used to model "fast" sliding friction properties of the FP bearings. One-half of these values, 2 percent and 4 percent respectively, are used to model "slow" sliding friction properties. These values are consistent with observed behavior ("slow" properties are approximately one-half of "fast" properties) and have little influence on peak dynamic response.

Figure 12.5-16 illustrates hysteresis loops based on upper-bound and lower-bound stiffness properties of FP bearings, normalized by vertical load (P). The slope of these loops is proportional to the inverse of the effective radius (185 inches) and the thickness (vertical height) of these loops is twice the value of the sliding friction coefficient. The upper-bound loop, plotted to D_D = 16 inches, is based on 8 percent sliding friction and the lower-bound loop, plotted to D_M = 30.9 inches, is based on 4 percent sliding friction. The hysteresis loops shown in Figure 12.5-16 could be modeled using appropriate values of bilinear element.

While the bearings of this example all have identical properties, stiffness varies as a function of vertical load (since friction force is a function of vertical load). Thus, values of the initial stiffness (a required parameter of the Isolator2 element of ETABS) are a function of vertical load. While technically different for each bearing, the same value of initial stiffness is assumed for bearings that have similar amounts of vertical load. Table 12.5-10 provides values of initial FP bearing stiffness for three bearing load groups (regions): Region A: bearings at interior column locations with heavier loads (15 locations), Region B: bearings at perimeter column locations, except corners (16 locations) and Region C: bearings at corner columns with lighter loads (4 locations). Similarly, Table 12.5-11 shows values of effective isolator stiffness, corresponding to 16 inches of peak design earthquake and 30.9 inches of peak MCE_R response, respectively. Values of effective stiffness shown in Table 12.5-11 are not required for response history analysis but would be required (along with corresponding values of the damping coefficient) for response spectrum analysis using ETABS.

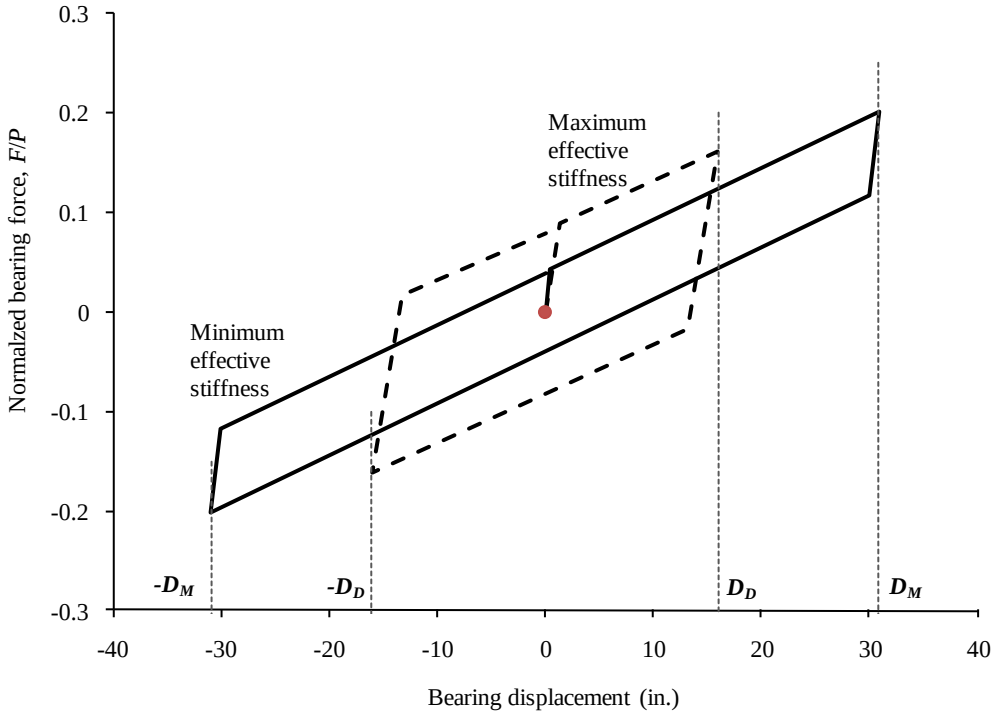

Figure 12.5-16 Example hysteresis loops used to model EOC bearings (1.0 in. = 25.4 mm)

Table 12.5-10 Summary of Initial Stiffness Properties of FP Bearings Used in ETABS Response History Analysis of the Example EOC

Region	Bearing Load Group			Bearing Initial Stiffness (kips/in.)	
	Column Location	Number of Bearings	Average Load (kips)	Lower-Bound (4% Friction)	Upper-Bound (8% Friction)
A	Interior	15	325	13.5	9.0
B	Perimeter	16	230	9.6	6.4
C	Corner	4	135	5.6	3.8
All	All	35	260	10.8	7.2

Table 12.5-11 Summary of Effective Stiffness Properties of FP Bearings of the Example EOC Building (Appropriate for Response Spectrum Analysis)

Bearing Load Group	Bearing Effective Stiffness (kips/in.)			
	Design Earthquake Response (at D_D = 16.0 in.)		MCE_R Response (at D_M = 30.9 in.)	
Region	Lower-Bound (4% Friction)	Upper-Bound (8% Friction)	Lower-Bound (4% Friction)	Upper-Bound (8% Friction)
A	2.57	3.38	2.18	2.60
B	1.82	2.39	1.54	1.84
C	1.07	1.40	0.90	1.08
All	2.06	2.71	1.74	2.08

For isolators with known properties, parameters defining bilinear stiffness may be based on test data provided by the manufacturer. For example, Figure 12.5-17 compares hysteresis loops based on upper-bound and lower-bound stiffness properties (normalized by weight) with actual hysteresis loops of cyclic load tests of a prototype of the double-concave friction pendulum bearing. In this case, design loops are constructed for the same peak displacement (approximately 30 inches) as that of the prototype test. Test results indicate an average effective stiffness (normalized by vertical load) of k_{eff}/P = 0.0074 kip/in./kip at 30 inches of peak displacement that is well bounded by maximum and minimum values of effective stiffness k_{Mmin} = 0.0067 kip/in./kip (1.74 kips/in. / 260 kips) to k_{Mmax} = 0.0080 kip/in./kip (2.08 kips/in. / 260 kips), respectively. Test results also indicate an average effective damping of approximately 18 percent for the three cycles of prototype testing, which supports the use of an effective damping value, β_M = 15 percent, for calculating MCE_R response (ELF procedure).

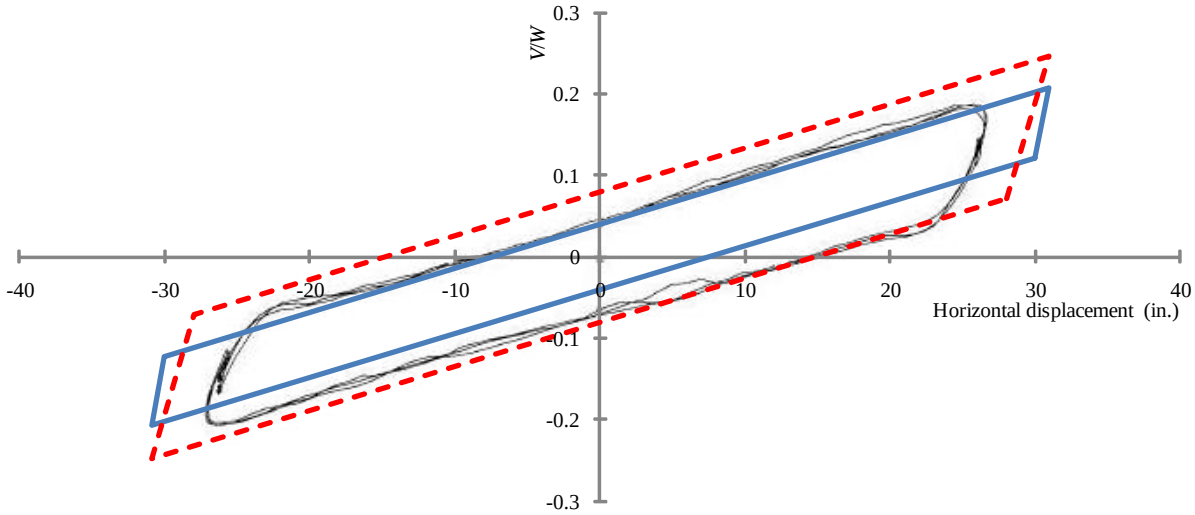

Figure 12.5-17 Comparison of modeled and tested hysteresis loops for EOC bearings (1.0 in. = 25.4 mm, 1.0 kip/in. = 0.175 kN/mm)

12.5.5.3 Analysis process. The two primary ETABS models, incorporating lower-bound (4 percent sliding friction) and upper-bound (8 percent sliding friction) properties are analyzed for the set of seven ground motion records applied to the models in each of four orientations of the larger component of

records with respect to the primary horizontal axes of the model: (1) positive X-axis direction, (2) negative X-axis direction, (3) positive Y-axis direction and (4) negative Y-axis direction, respectively.

The average value of the parameter of interest is calculated for each of four record set orientations and the more critical value of positive and negative orientations of the record set is used for design verification in the (x or y) direction of interest (e.g., story shear in the x direction). The more critical value of each of the four record set orientations is used for design verification when the response parameter of interest is not direction dependent (e.g., peak isolation system displacement). This process is repeated for ground motion records scaled to DE and MCE_R spectral accelerations.

Although a large number of data are generated by these analyses, only limited number of response parameters is required for design verification. Response parameters of interest include the following:

- Design Earthquake:
    1. Peak isolation system displacement
    2. Peak story shear forces (envelope over building height)
- Maximum Considered Earthquake:
    1. Peak isolation system displacement
    2. Peak downward load on any isolator unit ($1.45D + 1.0L + Q_{MCE}$)
    3. Peak uplift displacement of any isolator unit ($0.8D - Q_{MCE}$).

12.5.5.4 Summary of results of response history analyses. RHA results are generally consistent with and support design values based on ELF formulas. The ETABS model with lower-bound stiffness properties (4 percent sliding friction) governs peak isolation system displacements. The lower-bound stiffness model also governs peak uplift displacement of isolators. The ETABS model with upper-bound stiffness properties (8 percent sliding friction) governs peak story shear forces and peak downward loads on isolators, although the value of the response parameters typically are similar for the two ETABS models. Specific results are summarized and compared to ELF values in the following sections.

12.5.5.4.1 Peak isolation system displacement. Table 12.5-12 summarizes peak isolation system displacements calculated by RHA for DE and MCE_R ground motions (average displacement of seven records). RHA results show the larger value of peak displacements in the X-axis and Y-axis directions and the peak displacement in the X-Y plane. Total displacement (at corners due to rotation) is based on the minimum 10 percent increase due to accidental mass eccentricity for both ELF and RHA results. Results of the evaluation of uplift are also included in Table 12.5-12.

Table 12.5-12 Summary of Peak DE and MCE_R Displacements of the Isolation System Calculated Using RHA (Average Displacement of Seven Records) and Comparison with DE and MCE_R Displacements Calculated Using ELF Formulas

Response Parameter	Method of Analysis		
	ELF Formulas	RHA - Average of Seven Records	
		Maximum (X, Y)	X-Y Plane
Design Earthquake - Isolation System Displacement (inches)			
Design (Center)	16.0	15.0	15.9
Total (Corner)	17.6	16.5	17.5
Uplift	NA	No uplift (all records)	
MCE_R - Isolation System Displacement (inches)			
MCE_R (Center)	30.9	28.2	29.6
Total (Corner)	34.0	31.1	32.5
Uplift	NA	Less than 0.01 in. (2/7 records)	

The average value of peak DE displacement in the X-Y plane is 15.9 inches, as compared to 16.0 inches calculated using ELF formulas. The average value of peak MCE_R displacement is 29.6 inches, as compared to 30.8 inches calculated using ELF formulas. The total DE displacement is found to be 17.5 inches and the total MCE_R displacement is found to be 32.5 inches (including a 10 percent increase in displacement to account for the effects of accidental mass eccentricity not explicitly modeled in the RHA analysis).

Peak isolation system displacements calculated using RHA are slightly less than the corresponding values determined by ELF formulas, but within the RHA limits (minimum) based on ELF formulas (see *Guide* Section 12.5.4.2.6). The total MCE_R displacement of 32.6 inches is just less than the 33-inch displacement capacity of the FP bearing (displacement at which the articulated slider would engage the restraining edge of concave plates).

Uplift did not occur at bearing locations for the DE ground motions. A very small amount of uplift occurred during two of the seven MCE_R ground motion records, which is less than but consistent with the amount of uplift previously determined by nonlinear static (pushover) analysis (see *Guide* Table 12.5-8).

The *Standard* does not require the response of individual records to be used for design, or design verification, where seven or more records are used for RHA. Nonetheless, it is prudent to consider the implications of the results of individual record analyses and it is helpful to use ELF formulas to evaluate RHA results (serving as a sanity check on results). Table 12.5-12 summarizes peak displacements calculated by RHA for individual records scaled to DE and MCE_R ground motions. The results in this table are based on an application of records with the larger components aligned with the X-axis direction of the model. RHA results show values of peak displacement in the X-axis and Y-axis directions and in the X-Y plane. A couple of observations may be made. First, the peak displacement in the direction of the larger component is almost the same, on average, as the peak response in the X-Y plane. The second observation that may be made is that the displacement response varies greatly between records and that this variation is correlated directly with the variation of spectral response at long periods.

For example, peak design earthquake displacement of Record Number NF-25 (the Yarmica record from the 1999 Kocaeli earthquake) is 30.7 inches in the X-Y plane (30.5 inches in the X-axis direction), which is less than the unrestrained displacement capacity of the FP bearing, but approximately twice the average

displacement of the seven records. As shown in *Guide* Table 12.5-12, this record was scaled by 0.97 for DE analysis of the ETABS model (i.e., the as-recorded ground motions are actually slightly stronger than the scaled record). Large displacements (e.g., in excess of 30 inches) are realistic for long-period systems near active sources.

Review of the response spectra of the scaled records shows that the Yarmica record also has the largest values of response spectral acceleration and displacement at long periods. Table 12.5-13 summarizes values of response spectral acceleration and displacement at the effective DE period, T_D = 3.5 seconds, for records scaled to the design earthquake and at the effective MCE_R period, T_M = 3.9 seconds, for records scaled to the MCE_R. Using the same concepts as those of the ELF formulas (e.g., reducing response based on the effective damping of the isolation system), peak isolation displacements are calculated directly from the response spectra of individual records and the results are summarized in Table 12.5-13. The very close agreement between displacements calculated using RHA and ELF methods (applied to response spectra of individual records) illustrates the usefulness of ELF methods and the related concepts of effective period and damping, to provide a "sanity check" of RHA results.

Table 12.5-13 Summary of Peak DE and MCE_R Displacements of the Isolation System Calculated Using RHA and Comparison with DE and MCE_R Displacements Calculated Using ELF Methods Applied to the Response Spectra Of Individual Records

Response Parameter	Seven Scaled Earthquake Ground Motion Records (FEMA P-695 ID No.)							Average Value
	NF-8	FF-10	NF-25	FF-3	NF-14	FF-4	NF-28	
RHA - Peak Isolation System Displacement - Design Earthquake (in.)								
X Direction	14.9	18.3	30.5	7.5	14.2	5.8	13.6	15.0
Y Direction	3.2	4.9	11.3	7.1	9.5	5.6	7.7	7.1
X-Y Direction	15.0	18.8	30.7	8.9	14.9	7.4	15.8	15.9
ELF Estimate of Peak Isolation System Displacement - Design Earthquake (in.) - T_D = 3.5 sec.								
S_{aD} [T_D] (g)	0.182	0.124	0.305	0.106	0.186	0.096	0.133	0.187
S_{dD} [T_D] (in.)	21.9	14.9	36.6	12.7	22.3	11.5	16.0	22.4
$D_D = S_{dM}/B_D$	14.6	9.9	24.4	8.5	14.9	7.7	10.6	15.0
RHA - Peak Isolation System Displacement - MCE_R (in.)								
X Direction	28.6	36.5	58.1	11.4	27.3	13.0	22.7	28.2
Y Direction	4.5	9.7	21.8	10.3	18.8	9.0	13.2	12.5
X-Y Direction	28.7	38.1	58.5	13.6	28.6	13.6	26.0	29.6
ELF Estimate of Peak Isolation System Displacement - MCE_R (in.) – T_M = 3.9 sec.								
S_{aM} [T_M] (g)	0.310	0.295	0.536	0.118	0.225	0.150	0.159	0.256
S_{dM} [T_M] (in.)	46.2	43.9	79.9	17.6	33.6	22.4	23.8	38.2
$D_M = S_{dM}/B_D$	35.5	33.8	61.5	13.5	25.8	17.2	18.3	29.4

Table 12.5-13 shows that the peak MCE_R displacement for two scaled records (Yarmica and Arcelik) exceeds the 33-inch displacement capacity of the FP bearing—that is, the articulated slider will engage and be restrained by the concave plates. Such engagement would reduce displacement of the isolation system but also increase story shear force and overturning loads and increase the possibility of damage to the isolation system and the superstructure. It should be expected that displacements calculated for one or two records of a set of seven records scaled to match an MCE_R response spectrum for a site close to an active fault will exceed the average displacement of the set, even by as much as by a factor of two. The *Standard* requires design for the average and therefore tacitly accepts that displacements calculated for some records will be larger than the average displacement required for design of the isolation system.

It would be prudent, however, for designers to consider the consequences of the very unlikely event that the MCE_R displacement is exceeded in an actual earthquake. In the case of the example EOC, displacements larger than MCE_R displacement would be expected to cause damage to the bearings, but not catastrophic failure of the isolation system or superstructure. The concave plates (and surrounding moat) would limit displacement of the isolation system (i.e., the isolation system would not displace laterally to failure). As the bearings (and surrounding moat) limit displacement, forces would increase significantly in the seismic force-resisting system of the structure above, comparable to peak response of a conventional (fixed-base) building. Yielding and inelastic response would likely occur, but the *Standard* requirement that special framing (e.g., SCBF) be used for the superstructure provides the requisite ductility to inelastically resist the response due to impact restraint of isolators (and the surrounding moat).

12.5.5.4.2 Peak story shear force. Table 12.5-14 summarizes story shear force results in the X-axis and Y-axis directions and compares these values with story shear forces calculated by ELF formulas for unreduced design earthquake loads. Figure 12.5-17 shows story shears calculated by ELF formulas and by RHA methods.

Table 12.5-14 and Figure 12.5-18 show the inherent (and intentional) conservatism of the ELF formulas, which assume an inverted triangular pattern of lateral loads to account for potential higher-mode effects. The example EOC has minimal contribution from higher modes, as reflected in the lower values of story shear at upper floor and roof elevations. For the example EOC, design story shear forces are based on the limits of *Standard* Section 17.5.4.3 ($V_s = 1.5 \times 0.08W = 0.12W$, where $0.08W$ represents the "breakaway" friction level of a sliding system), which apply to all methods of analysis, including RHA.

Table 12.5-14 Summary of Peak Design Story Shear Forces and Comparison with Design Earthquake Story Shear Values Calculated Using ELF Methods

Response Parameter	Method of Analysis		
	ELF Formulas	Peak RHA Result	
		X-axis Direction	Y-axis Direction
Design Earthquake - Story Shear (kips)			
Penthouse	261	150	147
Third Story	837	546	531
Second Story	1,192	874	855
First Story	1,403	1,183	1,173
V_b (Isolators)	1,456	1,440	1,449

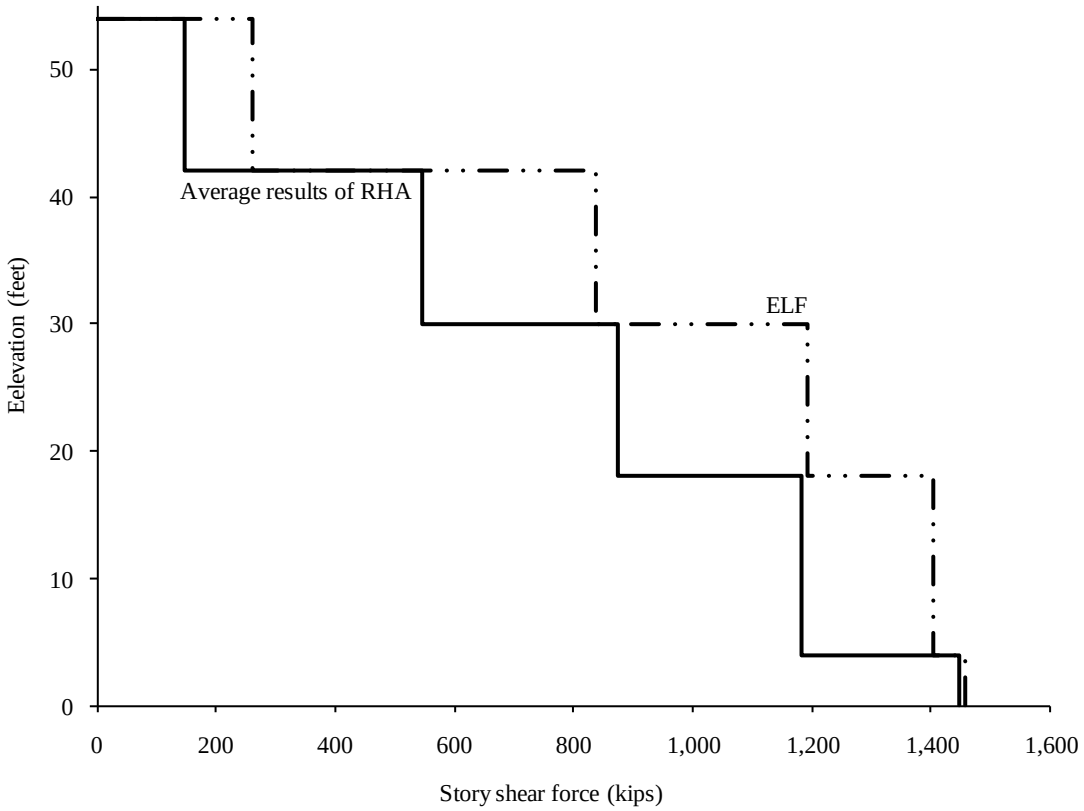

Figure 12.5-18 Comparison of story shear force based on RSA and ELF procedures

12.5.5.4.3 Peak downward loads on isolators. Table 12.5-15 summarizes maximum downward forces on isolator units determined from the MCE_R response history analyses. This table reports the two values for each isolator location representing both the X-axis and Y-axis orientations of the larger component of shaking of the ground motion record.

Table 12.5-15 Maximum Downward Force (kips) on Isolator Units ($1.45D + 1.0L + Q_{MCE}$)*

	Maximum downward force (kips)			
Line	1	2	3	4
A	247 / 245	512 / 532	376 / 383	378 / 385
B	534 / 512	639 / 637	753 / 764	796 / **825**
C	380 / 371	718 / 726	707 / 707	620 / 620

1.0 kip = 4.45 kN.

* Forces at Column Lines 5, 6 and 7 (not shown) are similar to those at Column Lines 3, 2 and 1, respectively; loads at Column Lines D and E (not shown) are similar to those at Column Lines B and A, respectively.

Table 12.5-15 indicates a maximum downward force of 825 kips (at Column B4), which is somewhat less than the maximum value of downward force predicted using the ELF (pushover) methods (1,063 kips in *Guide* Table 12.5-7). The difference between RHA and ELF results reflects differences in overturning loads and patterns of story shear forces shown in the previous section. For this example, RHA results are used to verify ELF (pushover) values, but they could play a more meaningful role in reducing overturning loads for projects with a more challenging configuration of the superstructure.

12.5.6 Design and Testing Criteria for Isolator Units

Detailed design of the isolator units typically is the responsibility of the manufacturer subject to the design and testing (performance) criteria included in the construction documents (drawings and/or specifications). Performance criteria typically include a basic description and size(s) of isolator units; design life, durability, environmental loads and fire-resistance criteria; quality assurance and quality control requirements (including QC testing of production units); design criteria (loads, displacements, effective stiffness and damping); and prototype testing requirements. This section summarizes the design criteria and prototype testing requirements for the isolator units (FP bearings) of the example EOC.

12.5.6.1 Bearing design loads.

- Maximum Long-Term Load (from Table 12.5-1, Col. C3): $1.2D + 1.6L = 600$ kips
- Maximum Short-Term Load (from Tables 12.5-8/12.5-15, Col. B4): $1.45D + 1.0L + |E| =$ 1,000 kips
- Minimum Short-Term Load (from Table 12.5-9, Col. B4): $0.8D - |E| = 0$ kips (less than 0.1 inch of uplift)
- For Cyclic-Load Testing (*Standard* Sec. 17.8.2.2):

  Typical Load (Table 12.5-1, average all bearings): $1.0D + 0.5L = 290$ kips

  Upper-Bound Load (Table 12.5-6, average all bearings): $1.37D + 0.5L + Q_{DE} = 500$ kips

  Lower-Bound Load (Table 12.5-7, average all bearings): $0.73D - Q_{DE} = 150$ kips

Item 2 of *Standard* Section 17.8.2.2 requires that cyclic tests at different displacement amplitudes be performed for typical vertical load ($1.0D + 0.5L$) and for upper-bound and lower-bound values of vertical load (for load-bearing isolators) where upper-bound and lower-bound loads are based on the load combinations of *Standard* Section 17.2.4.6 (vertical load stability). The load combinations of *Standard* Section 17.2.4 define "worst case" MCE_R loading conditions for checking isolator stability. In the opinion of the author, these load combinations are, in general, too extreme for cyclic load testing to verify isolator response properties (at lower levels of response). For the EOC example, upper-bound and lower-bound values of vertical load are based (roughly) on average bearing load at peak design earthquake response, as defined by the loads in Tables 12.5-6 and 12.5-7, respectively. The range of vertical load, from 150 kips to 500 kips, addresses the intent of the cyclic testing requirements (i.e., to measure possible variation in effective stiffness and damping properties).

12.5.6.2 Bearing design displacements (Table 12.5-12).

- Design earthquake displacement: $D_D = 16$ in.

- Total design earthquake displacement: D_{TD} = 17.5 in.
- Maximum considered earthquake displacement: D_M = 30 in.
- Total maximum considered earthquake displacement: D_{TM} = 32.5 in.

12.5.6.3 Bearing effective stiffness and damping criteria.

- Minimum effective stiffness normalized by load (typical vertical load):

  Design earthquake displacement: $k_{Dmin} \geq$ 0.0079 kips/in./kip

  Maximum considered earthquake displacement: $k_{Mmin} \geq$ 0.0067 kips/in./kip

- Maximum effective stiffness normalized by weight (typical vertical load):

  Design earthquake displacement: $k_{Dmax} \leq$ 0.0104 kips/in./kip

  Maximum considered earthquake displacement: $k_{Mmax} \leq$ 0.0080 kips/in./kip

The k_{Dmin}, k_{Dmax}, k_{Mmin} and k_{Mmax} criteria are properties of the isolation system as a whole (calculated from the properties of individual isolator units using *Standard* Equations 17.8-3 through 17.8-6). The above limits on effective stiffness of the isolation system include changes in isolator properties over the life of the structure (due to contamination, aging, etc.), as well as other effects that may not be addressed by prototype testing (e.g., changes in properties under repeated cycles of dynamic load). Ideally, prototype bearings would have properties near the center of the specified range of effective stiffness.

Effective damping (typical vertical load):

- Design earthquake displacement: $\beta_D \geq$ 20 percent
- Maximum considered earthquake displacement: $\beta_M \geq$ 13 percent

12.5.6.4 Prototype bearing testing criteria. *Standard* Section 17.8 prescribes a series of prototype tests to establish and validate design properties used for design of the isolation system and defines "generic" acceptance criteria (Sec. 17.8.2) with respect to force-deflection properties of test specimens. Table 12.5-16 summarizes the sequence and cycles of prototype testing found in *Standard* Section 17.8.2, applicable to the FP bearing of the example EOC.

Table 12.5-16 Prototype Test Requirements

No. of Cycles	*Standard* Criteria		Example EOC Criteria	
	Vertical Load	Lateral Load	Vertical Load	Lateral Load
Cyclic Load Tests to Establish Effective Stiffness and Damping (*Standard* Sec. 17.8.2.2, w/o Item 1)				
3 cycles	Typical	$0.25D_D$	290 kips	4 in.
3 cycles	Upper-bound	$0.25D_D$	500 kips	4 in.
3 cycles	Lower-bound	$0.25D_D$	150 kips	4 in.
3 cycles	Typical	$0.5D_D$	290 kips	8 in.
3 cycles	Upper-bound	$0.5D_D$	500 kips	8 in.
3 cycles	Lower-bound	$0.5D_D$	150 kips	8 in.
3 cycles	Typical	$1.0D_D$	290 kips	16 in.
3 cycles	Upper-bound	$1.0D_D$	500 kips	16 in.
3 cycles	Lower-bound	$1.0D_D$	150 kips	16 in.
3 cycles	Typical	$1.0D_M$	290 kips	30 in.
3 cycles	Upper-bound	$1.0D_M$	500 kips	30 in.
3 cycles	Lower-bound	$1.0D_M$	150 kips	30 in.
3 cycles	Typical	$1.0D_{TM}$	290 kips	32.5 in.
Cyclic Load Tests to Check Durability (*Standard* Sec. 17.8.2.2)				
17 cycles*	Typical	$1.0D_{TD}$	290 kips	17.5 in.
Static Load Test of Isolator Stability (*Standard* Sec. 17.8.2.5)				
N/A	Maximum	$1.0D_{TM}$	1,000 kips	32.5 in.
N/A	Minimum	$1.0D_{TM}$	0.1 in. of uplift	32.5 in.

1.0 in. = 25.4 mm, 1.0 kip = 4.45 kN.
* 17 cycles = $30S_{D1}/S_{DS}B_D$ (may be performed in 3 sets of tests (6 cycles each), if tests are dynamic.

13

Nonbuilding Structure Design

By J. G. (Greg) Soules, P.E., S.E.

Originally developed by Harold O. Sprague, Jr., P.E.

Contents

13.1 NONBUILDING STRUCTURES VERSUS NONSTRUCTURAL COMPONENTS 4
13.1.1 Nonbuilding Structure 5
13.1.2 Nonstructural Component 6
13.2 PIPE RACK, OXFORD, MISSISSIPPI 6
13.2.1 Description 7
13.2.2 *Provisions* Parameters 7
13.2.3 Design in the Transverse Direction 8
13.2.4 Design in the Longitudinal Direction 11
13.3 STEEL STORAGE RACK, OXFORD, MISSISSIPPI 13
13.3.1 Description 13
13.3.2 *Provisions* Parameters 14
13.3.3 Design of the System 15
13.4 ELECTRIC GENERATING POWER PLANT, MERNA, WYOMING 17
13.4.1 Description 17
13.4.2 *Provisions* Parameters 19
13.4.3 Design in the North-South Direction 20
13.4.4 Design in the East-West Direction 21
13.5 PIER/WHARF DESIGN, LONG BEACH, CALIFORNIA 21
13.5.1 Description 21
13.5.2 *Provisions* Parameters 22
13.5.3 Design of the System 23
13.6 TANKS AND VESSELS, EVERETT, WASHINGTON 24
13.6.1 Flat-Bottom Water Storage Tank 25
13.6.2 Flat-Bottom Gasoline Tank 28

13.7 VERTICAL VESSEL, ASHPORT, TENNESSEE 31
13.7.1 Description 31
13.7.2 *Provisions* Parameters 32
13.7.3 Design of the System 33

Chapter 15 of the *Standard* is devoted to nonbuilding structures. Nonbuilding structures comprise a myriad of structures constructed of all types of materials with markedly different dynamic characteristics and a wide range of performance requirements.

Nonbuilding structures are a general category of structure distinct from buildings. Key features that differentiate nonbuilding structures from buildings include human occupancy, function, dynamic response and risk to society. Human occupancy, which is incidental in most nonbuilding structures, is the primary purpose of most buildings. The primary purpose and function of nonbuilding structures can be incidental to society, or the purpose and function can be critical for society.

In the past, many nonbuilding structures were designed for seismic resistance using building code provisions developed specifically for buildings. These code provisions were inadequate to address the performance requirements and expectations that are unique to nonbuilding structures. For example, consider secondary containment for a vertical vessel containing hazardous materials. Nonlinear performance and collapse prevention, which are performance expectations for buildings, are insufficient for a secondary containment structure, which must not leak.

Seismic design requirements specific to nonbuilding structures were first introduced in the 2000 *Provisions*. Before the introduction of the 2000 *Provisions*, the seismic design of nonbuilding structures depended on the various trade organizations and standards development organizations that were not connected with the building codes.

This chapter develops examples specifically to help clarify Chapter 15 of the *Standard*. The solutions developed are not intended to be comprehensive but instead focus on correct interpretation of the requirements. Complete solutions to the examples cited are beyond the scope of this chapter.

In addition to the *Provisions* and *Commentary*, the following publications are referenced in this chapter:

API 650	American Petroleum Institute, *Welded Steel Tanks for Oil Storage*, 10th edition, Addendum 4, 2005.
ASCE	American Society of Civil Engineers, *Guidelines for Seismic Evaluation and Design of Petrochemical Facilities*, 1997.
ASME BPVC	American Society of Mechanical Engineers, *Section VIII, Division 2, Alternate Rules, Rules for Construction of Pressure Vessels*, 2007 Edition, 2008 Addenda.
AWWA D100	American Water Works Association, *Welded Steel Tanks for Water Storage*, 2005.
Bachman and Dowty	Bachman, Robert and Dowty, Susan, "Nonstructural Component or Nonbuilding Structure?", Building Safety Journal, International Code Council, April-May 2008.
Jacobsen	Jacobsen, L.S., "Impulsive Hydrodynamics of Fluid Inside a Cylindrical Tank and of Fluid Surrounding a Cylindrical Pier," Bulletin of the Seismological Society of America, 39(3), 189-204, 1949.
Morison	Morison, J.R., O'Brien, J.W. and Sohaaf, S.A., "The Forces Exerted by Surface Waves on Piles," Petroleum Transactions, AIME, Vol. 189; 1950.

RMI — Rack Manufacturers Institute, *Specification for the Design, Testing and Utilization of Industrial Steel Storage Racks*, MH16.1, 2008

Soules — Soules, J. G., "The Seismic Provisions of the 2006 IBC – Nonbuilding Structure Criteria," Proceedings of 8th National Conference on Earthquake Engineering, San Francisco, CA, April 18, 2006.

13.1 NONBUILDING STRUCTURES VERSUS NONSTRUCTURAL COMPONENTS

Many industrial structures are classified as either nonbuilding structures or nonstructural components. This distinction is necessary to determine how the practicing engineer designs the structure. The intent of the *Standard* is to provide a clear and consistent design methodology for engineers to follow regardless of whether the structure is a nonbuilding structure or a nonstructural component. Central to the methodology is how to determine which classification is appropriate. Table 13-1 provides a simple method to determine the appropriate classification. Additional discussion on this topic can be found in Bachman and Dowty (2008).

The design methodology contained in Chapter 13 of the *Standard* focuses on nonstructural component design. As such, the amplification by the supporting structure of the earthquake-induced accelerations is critical to the design of the component and its supports and attachments. The design methodology contained in Chapter 15 of the *Standard* focuses on the direct effects of earthquake ground motion on the nonbuilding structure.

Table 13-1 Applicability of the Chapters of the *Standard*

Supporting Structure	Supported Item	
	Nonstructural Component	Nonbuilding Structure
Building	Chapter 12 for supporting structure; Chapter 13 for supported item	Chapter 12 for supporting structure; Chapter 15 for supported item
Nonbuilding	Chapter 15 for supporting structure; Chapter 13 for supported item	Chapter 15 for both supporting structure and supported item

The example shown in Figure 13-1 is a combustion turbine, electric-power-generating facility with four bays. Each bay contains a combustion turbine and supports an inlet filter on the roof. The uniform seismic dead load of the supporting roof structure is 30 psf. Each filter weighs 34 kips.

The following two examples illustrate the difference between nonbuilding structures that are treated as nonstructural components, using *Standard* Chapter 13 and those which are designed in accordance with *Standard* Chapter 15. In many instances, the weight of the supported nonbuilding structure is relatively small compared to the weight of the supporting structure (less than 25 percent of the combined weight) such that the supported nonbuilding structure will have a relatively small effect on the overall nonlinear earthquake response of the primary structure during design-level ground motions. It is permitted to treat such structures as nonstructural components and use the requirements of *Standard* Chapter 13 for their design. Where the weight of the supported structure is relatively large (greater than or equal to 25 percent of the combined weight) compared to the weight of the supporting structure, the overall response can be affected significantly. In such cases it is intended that seismic design loads and detailing requirements be

determined following the procedures of *Standard* Chapter 15. Where there are multiple large nonbuilding structures, such as vessels supported on a primary nonbuilding structure and the weight of an individual supported nonbuilding structure does not exceed the 25 percent limit but the combined weight of the supported nonbuilding structures does, it is recommended that the combined analysis and design approach of *Standard* Chapter 15 be used.

This difference in design approach is explored in the following example.

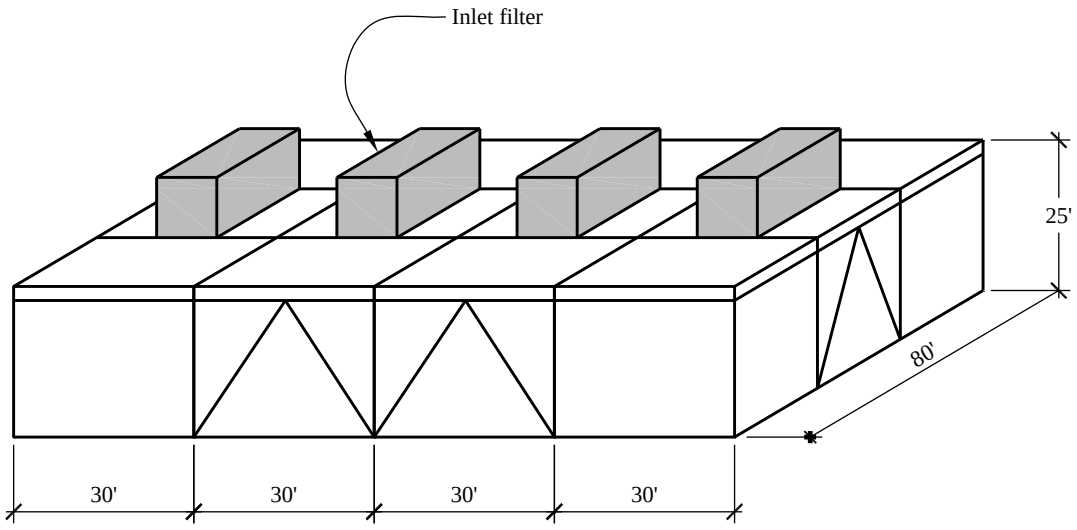

Figure 13-1 Combustion turbine building (1.0 ft = 0.3048 m)

13.1.1 Nonbuilding Structure

For the purpose of illustration, assume that the four filter units are connected in a fashion that couples their dynamic response through a rigid diaphragm. Therefore, it is appropriate to combine the masses of the four filter units for both the transverse and longitudinal direction responses.

13.1.1.1 Calculation of seismic weights.

All four inlet filters = W_{IF} = 4(34 kips) = 136 kips

Support structure = W_{SS} = 4(30 ft)(80 ft)(30 psf) = 288 kips

The combined weight of the nonbuilding structure (inlet filters) and the supporting structural system is:

$W_{combined}$ = 136 kips + 288 kips = 424 kips

13.1.1.2 Selection of design method. The ratio of the supported weight to the total weight is:

$$\frac{W_{IF}}{W_{Combined}} = \frac{136}{424} = 0.321 > 25\%$$

Because the weight of the inlet filters is 25 percent or more of the combined weight of the nonbuilding structure and the supporting structure (*Standard* Sec. 15.3.2), the inlet filters are classified as "nonbuilding structures" and the seismic design forces must be determined from analysis of the combined seismic-resistant structural systems. This would require modeling the filters, the structural components of the filters and the structural components of the combustion turbine supporting structure to determine accurately the seismic forces on the structural elements as opposed to modeling the filters as lumped masses.

13.1.2 Nonstructural Component

For the purpose of illustration, assume that the inlet filters are independent structures, although each is supported on the same basic structure. Unlike the previous example where the filter units were connected to each other through a rigid diaphragm, the four filter units are not connected in a fashion that couples their dynamic response. In other words, the four independent structures do not significantly affect the response of the support structure. In this instance, one filter is the nonbuilding structure. The question is whether it is heavy enough to significantly change the response of the combined system.

13.1.2.1 Calculation of seismic weights.

One inlet filter = W_{IF} = 34 kips

Support structure = W_{SS} = 4(30 ft)(80 ft)(30 psf) = 288 kips

The combined weight of the nonbuilding structures (all four inlet filters) and the supporting structural system is:

$$W_{combined} = 4(34 \text{ kips}) + 288 \text{ kips} = 424 \text{ kips}$$

13.1.2.2 Selection of design method. The ratio of the supported weight to the total weight is:

$$\frac{W_{IF}}{W_{Combined}} = \frac{34}{424} = 0.08 < 25\%$$

Because the weight of an inlet filter is less than 25 percent of the combined weight of the nonbuilding structures and the supporting structure (*Standard* Sec. 15.3.1), the inlet filters are classified as "nonstructural components" and the seismic design forces must be determined in accordance with *Standard* Chapter 13. In this example, the filters could be modeled as lumped masses. The filters and the filter supports could then be designed as nonstructural components.

13.2 PIPE RACK, OXFORD, MISSISSIPPI

This example illustrates the calculation of design base shears and maximum inelastic displacements for a pipe rack using the equivalent lateral force (ELF) procedure. The pipe rack in this example is supported at grade and is considered a nonbuilding structure.

13.2.1 Description

A two-tier, 12-bay pipe rack in a petrochemical facility has concentrically braced frames in the longitudinal direction and ordinary moment frames in the transverse direction. The pipe rack supports four runs of 12-inch-diameter pipe carrying naphtha on the top tier and four runs of 8-inch-diameter pipe carrying water for fire suppression on the bottom tier. The minimum seismic dead load for piping is 35 psf on each tier to allow for future piping loads. The seismic dead load for the steel support structure is 10 psf on each tier.

Pipe supports connect the pipe to the structural steel frame and are designed to support the gravity load and resist the seismic and wind forces perpendicular to the pipe. The typical pipe support allows the pipe to move in the longitudinal direction of the pipe to avoid restraining thermal movement. The pipe support near the center of the run is designed to resist longitudinal and transverse pipe movement as well as provide gravity support; such supports are generally referred to as fixed supports.

Pipes themselves must be designed to resist gravity, wind, seismic and thermally induced forces, spanning from support to support.

If the pipe run is continuous for hundreds of feet, thermal/seismic loops are provided to avoid a cumulative thermal growth effect. The longitudinal runs of pipe in this example are broken up into sections by providing thermal/seismic loops at spaced intervals as shown in Figure 13-2. In Figure 13-2, it is assumed thermal/seismic loops are provided at each end of the pipe run.

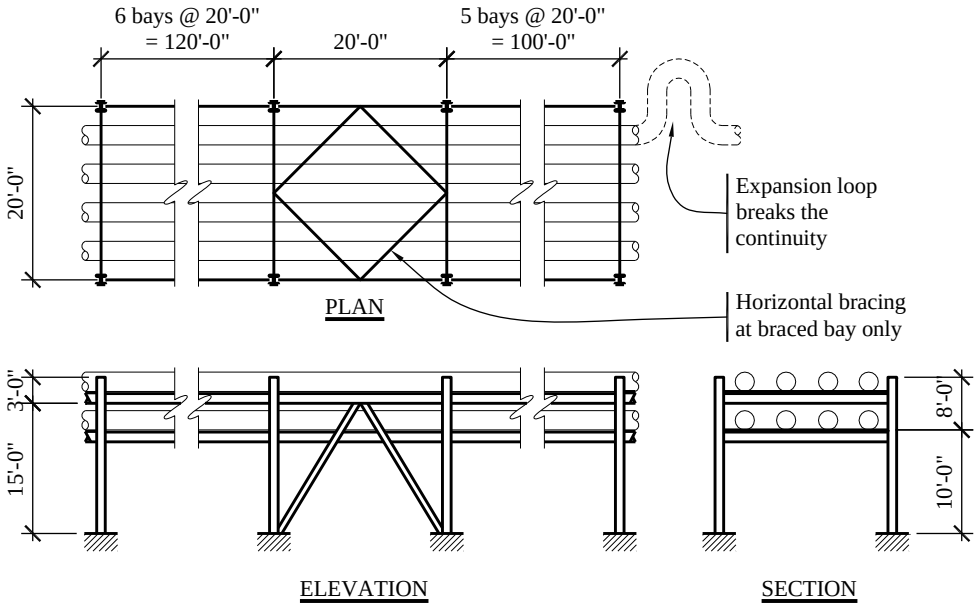

Figure 13-2 Pipe rack (1.0 ft = 0.3048 m)

13.2.2 *Provisions* Parameters

13.2.2.1 Ground motion. See Section 3.2 for an example illustrating the determination of design ground motion parameters. For this example, the parameters are as follows:

S_{DS} = 0.40
S_{D1} = 0.18

13.2.2.2 Occupancy category and importance factor. The upper piping carries a toxic material (naphtha) (Occupancy Category III – *Standard* Table 1-1) and the lower piping is required for fire suppression (Occupancy Category IV – *Standard* Table 1-1). The naphtha piping and the fire water piping are included in *Standard* Section 1.5.1; therefore, the pipe rack is assigned to Occupancy Category IV based on the more severe category.

Standard Section 15.4.1.1 directs the user to use the largest value of *I* based on the applicable reference document listed in *Standard* Chapter 23, the largest value selected from *Standard* Table 11.5-1, or as specified elsewhere in *Standard* Chapter 15. It is important to be aware of the requirements of *Standard* Section 15.4.1.1. While the importance factor for most structures will be determined based on *Standard* Table 11.5-1, there are reference documents that define importance factors greater than those found in *Standard* Table 11.5-1. Additionally, *Standard* Section 15.5.3 requires that steel storage racks in structures open to the public be assigned an importance factor of 1.5. This additional requirement for steel storage racks addresses a risk to the public that is not addressed by *Standard* Table 11.5-1 and *Standard* Table1-1. For this example, *Standard* Table 11.5-1 governs the choice of importance factor. According to *Standard* Section 11.5.1, the importance factor, *I*, is 1.5 based on Occupancy Category IV.

13.2.2.3 Seismic design category. For this structure assigned to Occupancy Category IV with S_{DS} = 0.40 and S_{D1} = 0.18, the Seismic Design Category is D according to *Standard* Section 11.6.

13.2.3 Design in the Transverse Direction

13.2.3.1 Design coefficients. According to *Standard* Section 15.4-1, either *Standard* Table 12.2-1 or *Standard* Table 15.4-1 may be used to determine the seismic parameters, although mixing and matching of values and requirements from the tables is not allowed. In *Standard* Chapter 15, selected nonbuilding structures similar to buildings are provided an option where both lower *R* values and less restrictive height limits are specified. This option permits selected types of nonbuilding structures which have performed well in past earthquakes to be constructed with fewer restrictions in Seismic Design Categories D, E and F provided seismic detailing is used and design force levels are considerably higher. The *R* value-height limit trade-off recognizes that the size of some nonbuilding structures is determined by factors other than traditional loadings and result in structures that are much stronger than required for seismic loadings (Soules, 2006). Therefore, the structure's ductility demand is generally much lower than a corresponding building. The *R* value-height trade-off also attempts to obtain the same structural performance at the increased heights. The user will find that the option of reduced *R* value with less restricted height will prove to be the economical choice in most situations due to the relative cost of materials and construction labor. It must be emphasized that the *R* value-height limit trade-off of *Standard* Table 15.4-1 applies only to nonbuilding structures similar to buildings and cannot be applied to building structures.

In *Standard* Table 12.2-1, ordinary steel moment frames are not permitted in Seismic Design Category D (with some exceptions) and cannot be used in this example. There are several options for ordinary steel moment frames found in *Standard* Table 15.4-1. These options are as follows:

1. *Standard* Table 15.4-1, Ordinary moment frames of steel, R = 3.5, Ω_o = 3, C_d = 3. According to Note c in *Standard* Table 15.4-1, this system is allowed for pipe racks up to 65 feet high using bolted end plate moment connections and per Note d this system is allowed for pipe racks up to 35 feet without limitations on the connection type. This option requires the use of the AISC 341.

2. *Standard* Table 15.4-1, Ordinary moment frames of steel with permitted height increase, R = 2.5, Ω_0 = 2, C_d = 2.5. This option is intended for pipe racks with height greater than 65 feet and limited to 100 feet. This option is not applicable for this example.

3. *Standard* Table 15.4-1, Ordinary moment frames of steel with unlimited height, R=1, Ω_0 = 1, C_d = 1. This option does not require the use of the AISC 341.

For this example, Option 1 above is chosen. Using *Standard* Table 15.4-1, the parameters for this ordinary steel moment frame are:

R = 3.5
Ω_0 = 3
C_d = 3

Ordinary steel moment frames are retained for use in nonbuilding structures such as pipe racks because they allow greater flexibility for accommodating process piping and are easier to design and construct than special steel moment frames.

13.2.3.2 Seismic response coefficient. Using *Standard* Equation 12.8-2:

$$C_s = \frac{S_{DS}}{R/I} = \frac{0.4}{3.5/1.5} = 0.171$$

From analysis, T = 0.42 second. For nonbuilding structures, the fundamental period is generally approximated for the first iteration and must be verified with final calculations. *Standard* Section 15.4.4 makes clear that the approximate period equations of *Standard* Section 12.8.2 do not apply to nonbuilding structures.

Using *Standard* Equation 12.8-3 for $T \leq T_L$, C_s does not need to exceed

$$C_s = \frac{S_{D1}}{T(R/I)} = \frac{0.18}{0.42(3.5/1.5)} = 0.184$$

Using *Standard* Equation 12.8-5, C_s must not be less than

$C_s = 0.044IS_{DS} \geq 0.01 = 0.044(1.5)(0.4) = 0.0264$

Standard Equation 12.8-2 controls; C_s = 0.171.

13.2.3.3 Seismic weight.

The seismic weight resisted by the moment frame in the transverse direction is shown below based on two levels of piping, a 20 ft bent spacing, a bent width (perpendicular with the piping) of 20 ft, piping dead weight of 35 psf and structure dead weight of 10 psf.

W = 2(20 ft)(20 ft)(35 psf + 10 psf) = 36 kips

13.2.3.4 Base shear. Using *Standard* Equation 12.8-1:

$V = C_s W$ = 0.171(36 kips) = 6.2 kips

13.2.3.5 Drift. Although not shown here, drift of the pipe rack in the transverse direction was calculated by elastic analysis using the design forces calculated above. The calculated lateral drift, δ_{xe} = 0.328 inch. Using *Standard* Equation 12.8-15:

$$\delta_x = \frac{C_d \delta_{xe}}{I} = \frac{3(0.328)}{1.5} = 0.656 \text{ in.}$$

The lateral drift must be checked with regard to acceptable limits. The acceptable limits for nonbuilding structures are not found in codes. Rather, the limits are what is acceptable for the performance of the piping. In general, piping can safely accommodate the amount of lateral drift calculated in this example. P-delta effects must also be considered and checked as required in *Standard* Section 15.4.5.

13.2.3.6 Redundancy factor. Some nonbuilding structures are designed with parameters from *Standard* Table 12.2-1 or 15.4-1 if they are termed "nonbuilding structures similar to buildings". For such structures (assigned to Seismic Design Category D, E, or F) the redundancy factor applies. Pipe racks, being fairly simple moment frames or braced frames, are in the category similar to buildings. Because this structure is assigned to Seismic Design Category D, *Standard* Section 12.3.4.2 applies.

Considering the transverse direction, the seismic force-resisting system is an ordinary moment resisting frame with only two columns in a single frame. The frames repeat in an identical pattern. Loss of moment resistance at the beam-to-column connections at both ends results in a loss of more than 33 percent in story strength. Therefore, *Standard* Section 12.3.4.2, Condition (a) is not met. The moment frame as described above consists only of a single bay. Therefore, *Standard* Section 12.3.4.2, Condition b is not met. The value of ρ in the transverse direction is therefore 1.3.

13.2.3.7 Determining *E*. In *Standard* Section 12.4.2, E is defined to include the effects of horizontal and vertical ground motions and can be summarized as follows:

$E = \rho Q_E \pm 0.2 S_{DS} D$

where Q_E is the effect of the horizontal earthquake ground motions, which is determined primarily by the base shear just computed and D is the effect of dead load. By putting a simple multiplier on the effect of dead load, the last term is an approximation of the effect of vertical ground motion. For the moment frame, the joint moment is influenced by both terms. E with the "+" on the second term where combined with dead and live loads will generally produce the largest negative moment at the joints, while E with the "-" on the second term where combined with the minimum dead load (0.6D) will produce the largest positive joint moments.

The *Standard* also requires the consideration of an overstrength factor, Ω_0, on the effect of horizontal motions in defining E_m for components susceptible to brittle failure. *Standard* Section 12.4.3 defines E_m and this definition can be summarized as follows:

$$E_m = \Omega_0 Q_E \pm 0.2 S_{DS} D$$

The moment frame portion of the pipe rack does not have components that require such consideration.

13.2.4 Design in the Longitudinal Direction

13.2.4.1 Design coefficients. In *Standard* Section 15.4-1, either *Standard* Table 12.2-1 or *Standard* Table 15.4-1 may be used to determine the seismic parameters. In *Standard* Table 12.2-1, ordinary steel concentrically braced frames are not permitted for Seismic Design Category D (with some exceptions) and cannot be used for this example. There are several options for ordinary steel concentrically braced frames found in *Standard* Table 15.4-1. These options are as follows:

1. *Standard* Table 15.4-1, Ordinary steel concentrically braced frame, $R = 3.25$, $\Omega_0 = 2$, $C_d = 3.25$. According to Note b in *Standard* Table 15.4-1, this system is allowed for pipe racks up to 65 feet high. This option requires the use of AISC 341.

2. *Standard* Table 15.4-1, Ordinary steel concentrically braced frames with permitted height increase, $R = 2.5$, $\Omega_0 = 2$, $C_d = 2.5$. This option is intended for pipe racks with height greater than 65 feet and limited to 160 feet. This option is not applicable for this example.

3. *Standard* Table 15.4-1, Ordinary steel concentrically braced frames with unlimited height, $R = 1.5$, $\Omega_0 = 1$, $C_d = 1.5$. This option does not require the use of AISC 341.

For this example, Option 1 above is chosen. Using *Standard* Table 15.4-1, the parameters for this ordinary steel concentrically braced frame are:

$R = 3.25$
$\Omega_0 = 2$
$C_d = 3.25$

13.2.4.2 Seismic response coefficient. Using *Standard* Equation 12.8-2:

$$C_s = \frac{S_{DS}}{R/I} = \frac{0.4}{3.25/1.5} = 0.185$$

From analysis, $T = 0.24$ second. The fundamental period for nonbuilding structures is generally approximated for the first iteration and must be verified with final calculations.

Using *Standard* Equation 12.8-3, C_s does not need to exceed:

$$C_s = \frac{S_{D1}}{T(R/I)} = \frac{0.18}{0.24(3.25/1.5)} = 0.346$$

Using *Standard* Equation 12.8-5, C_s must not be less than:

$C_s = 0.044IS_{DS} \geq 0.01 = 0.044(1.5)(0.4) = 0.0264$

Standard Equation 12.8-2 controls; $C_s = 0.185$.

13.2.4.3 Seismic weight.

$W = 2(240 \text{ ft})(20 \text{ ft})(35 \text{ psf} + 10 \text{ psf}) = 432 \text{ kips}$

13.2.4.4 Base shear. Using *Standard* Equation 12.8-1:

$V = C_sW = 0.185(432 \text{ kips}) = 79.9 \text{ kips}$

13.2.4.5 Redundancy factor. The pipe rack in this example does not meet either of the two redundancy conditions specified in *Standard* Section 12.3.4.2. Condition a is not met because only one set of bracing is provided on each side, so removal of one brace would result in a reduction of greater than 33 percent in story strength. Condition b is not met because two bays of seismic force-resisting perimeter framing are not provided in each orthogonal direction. Therefore, the redundancy factor, ρ, is 1.3. If two bays of bracing were provided on each side of the pipe rack in the longitudinal direction, the pipe rack would meet Condition (a) and qualify for a redundancy factor, ρ, of 1.0 in that direction.

13.2.4.6 Determine *E*. In *Standard* Section 12.4.2, *E* is defined to include the effects of horizontal and vertical ground motions and can be summarized as follows:

$E = \rho Q_E \pm 0.2\, S_{DS}\, D$

where Q_E is the effect of the horizontal earthquake ground motions, which is determined primarily by the base shear just computed and *D* is the effect of dead load. By putting a simple multiplier on the effect of dead load, the last term is an approximation of the effect of vertical ground motion.

The *Standard* also requires the consideration of an overstrength factor, Ω_0, on the effect of horizontal motions in defining E_m for components susceptible to brittle failure. *Standard* Section 12.4.3 defines E_m and this definition can be summarized as follows:

$E_m = \Omega_0\, Q_E \pm 0.2\, S_{DS}\, D$

The ordinary steel concentrically braced frame portion of the pipe rack does have components that require such consideration. The beams connecting each moment frame in the longitudinal direction act as collectors and, as required by *Standard* Section 12.10.2.1, must be designed for the seismic load effect including overstrength factor.

13.2.4.7 Orthogonal loads. Because the pipe rack in this example is assigned to Seismic Design Category D, *Standard* Section 12.5.4 requires that the braced sections of the pipe rack be evaluated using the orthogonal combination rule of *Standard* Section 12.5.3a. Two cases must be checked: 100 percent

transverse seismic force plus 30 percent longitudinal seismic force and 100 percent longitudinal seismic force plus 30 percent transverse seismic force. The vertical seismic force represented by $0.2S_{DS}D$ is only applied once in each load case. Do not include the vertical seismic force in with both horizontal seismic load combinations. In this pipe rack example, due to the bracing configuration, the foundation and column anchorage would be the only components impacted by the orthogonal load combinations.

13.3 STEEL STORAGE RACK, OXFORD, MISSISSIPPI

This example uses the ELF procedure to calculate the seismic base shear in the east-west direction for a steel storage rack.

13.3.1 Description

A four-tier, five-bay steel storage rack is located in a retail discount warehouse. There are concentrically braced frames in the north-south and east-west directions. The general public has direct access to the aisles and merchandise is stored on the upper racks. The rack is supported on a slab on grade. The design operating load for the rack contents is 125 psf on each tier. The weight of the steel support structure is assumed to be 5 psf on each tier.

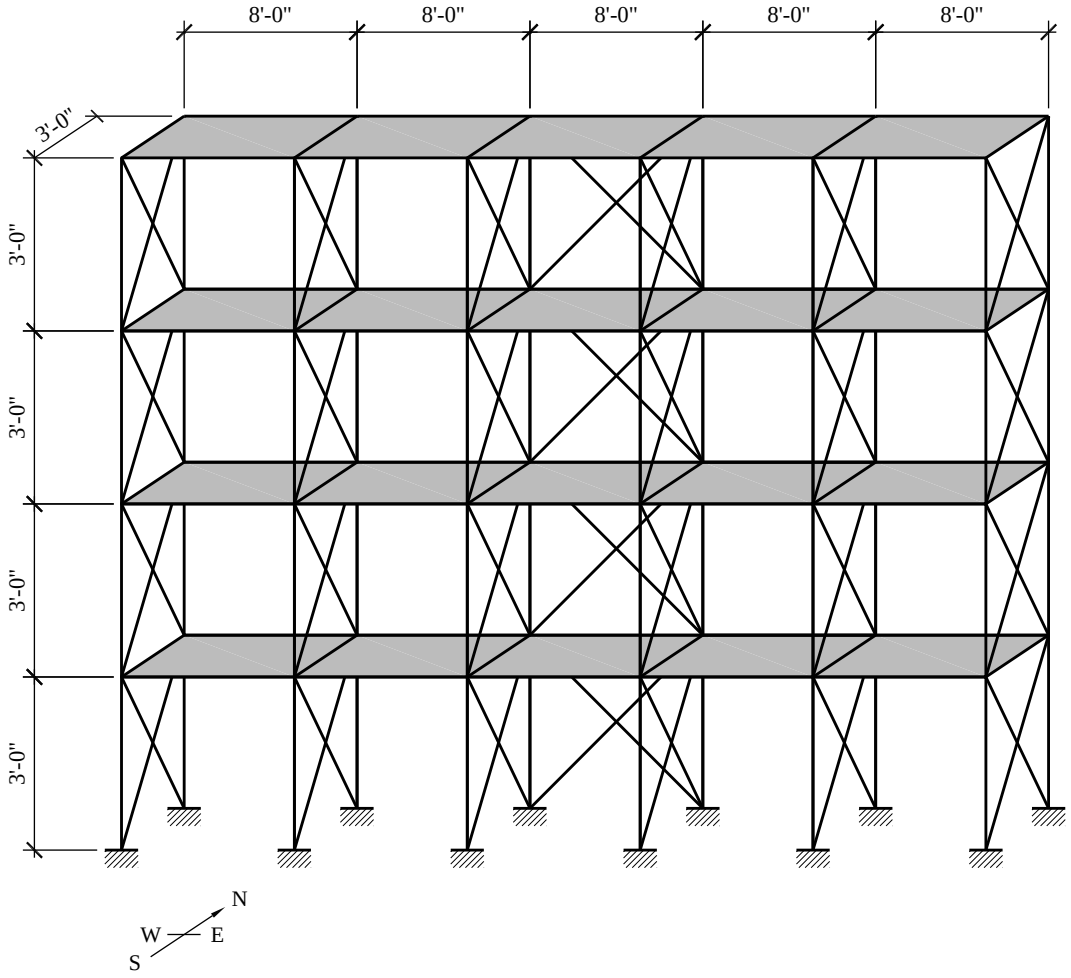

Figure 13-3 Steel storage rack (1.0 ft = 0.3048 m)

13.3.2 *Provisions* Parameters

13.3.2.1 Ground motion. The spectral response acceleration coefficients at the site are as follows:

S_{DS} = 0.40
S_{D1} = 0.18

13.3.2.2 Occupancy category and importance factor. Use *Standard* Section 1.5.1. The storage rack is in a retail facility. Therefore, the storage rack is assigned to Occupancy Category II. According to *Standard* Section 15.5.3 (item 2), $I = I_p = 1.5$ because the rack is in an area open to the general public.

13.3.2.3 Seismic design category. Use *Standard* Tables 11.6-1 and 11.6-2. Given Occupancy Category II, S_{DS} = 0.40 and S_{D1} = 0.18, the Seismic Design Category is C.

13.3.2.4 Design coefficients. According to *Standard* Table 15.4-1, the design coefficients for this steel storage rack are as follows:

$R = 4$
$\Omega_0 = 2$
$C_d = 3½$

13.3.3 Design of the System

13.3.3.1 Seismic response coefficient. *Standard* Section 15.5.3 allows designers some latitude in selecting the seismic design methodology. Designers may use the Rack Manufacturer's Institute specification (MH16.1-2008) to design steel storage racks. In other words, racks designed using the RMI method of Section 15.5.3 are deemed to comply. As an alternate, designers may use the requirements of *Standard* Sections 15.5.3.1 through 15.5.3.4. The RMI approach will be used in this example.

Using RMI Section 2.6.3, from analysis, $T = 0.24$ seconds. For this particular example, the short period spectral value controls the design. The period for taller racks, however, may be significant and will be a function of the operating weight. As shown in the calculations that follow, in the RMI method the importance factor appears in the equation for V rather than in the equation for C_s. The seismic response coefficient from RMI is:

$$C_s = \frac{S_{D1}}{T(R)} = \frac{0.18}{0.24(4)} = 0.188$$

But need not be greater than:

$$C_s = \frac{S_{DS}}{R} = \frac{0.4}{4} = 0.10$$

Nor less than:

$$C_s = 0.044 S_{DS} = 0.044(0.4) = 0.0176$$

The governing value of $C_s = 0.10$. From RMI Section 2.6.2, the seismic base shear is calculated as follows:

$$V = C_s I_p W_s = 0.1(1.5) W_s = 0.15 W_s$$

13.3.3.2 Condition 1 (each rack loaded).

13.3.3.2.1 Seismic weight. In accordance with RMI Section 2.6.8, Item 1:

W_s = 4(5)(8 ft)(3 ft)[0.67(125 psf)+5 psf] = 42.6 kips

13.3.3.2.2 Design forces and moments. Using RMI Section 2.6.2, the design base shear for Condition 1 is calculated as follows:

$V = C_s I_p W_s$ = 0.15(42.6 kips) = 6.39 kips

In order to calculate the design forces, shears and overturning moments at each level, seismic forces must be distributed vertically in accordance with RMI Section 2.6.6. The calculations are shown in Table 13.3-1.

Table 13.3-1 Seismic Forces, Shears and Overturning Moment

Level x	W_x (kips)	h_x (ft)	$w_x h_x^k$ (k = 1)	$\frac{w_x h_x^k}{\sum_{i=1}^{n} w_i h_i}$	F_x (kips)	V_x (kips)	M_x (ft-kips)
5	10.65	12	127.80	0.40	2.56		
						2.56	7.68
4	10.65	9	95.85	0.30	1.92		
						4.48	21.1
3	10.65	6	63.90	0.20	1.28		
						5.76	38.4
2	10.65	3	31.95	0.10	0.63		
						6.39	57.6
Σ	42.6		319.5				

1.0 ft = 0.3048 m, 1.0 kip = 4.45 kN, 1.0 ft-kip = 1.36 kN-m.

13.3.3.2.3 Resisting moment at the base.

$M_{OT,\ resisting} = W_s$ (1.5 ft) = 42.6(1.5 ft) = 63.9 ft-kips

13.3.3.3 Condition 2 (only top rack loaded).

13.3.3.3.1 Seismic weight. In accordance with RMI Section 2.6.2, Item 2:

W_s = 1(5)(8 ft)(3 ft)(125 psf) + 4(5)(8 ft)(3 ft)(5 psf) = 17.4 kips

12.3.3.3.2 Base shear. Using RMI Section 2.6.2, the design base shear for Condition 2 is calculated as follows:

$V = C_s I_p W_s$ = 0.15(17.4 kips) = 2.61 kips

13.3.3.3.3 Overturning moment at the base. Although the forces could be distributed as shown above for Condition 1, a simpler, conservative approach for Condition 2 is to assume that a seismic force equal to the entire base shear is applied at the top level. Using that simplifying assumption,

$M_{OT} = V_b$ (12 ft) = 2.61 kip (12 ft) = 31.3 ft-kips

13.3.3.3.4 Resisting moment at the base.

$M_{OT,\ resisting} = W_s$ (1.5 ft) = 17.4(1.5 ft) = 26.1 ft-kips

13.3.3.4 Controlling conditions. Condition 1 controls shear demands at all but the top level. Although the overturning moment is larger under Condition 1, the resisting moment is larger than the overturning moment. Under Condition 2 the resistance to overturning is less than the applied overturning moment. Therefore, the rack anchors must be designed to resist the uplift induced by the base shear for Condition 2.

13.3.3.5 Torsion. It should be noted that the distribution of east-west seismic shear will induce torsion in the rack system because the east-west brace is only on the back of the storage rack. The torsion should be resisted by the north-south braces at each end of the bay where the east-west braces are placed. If the torsion were to be distributed to each end of the storage rack, the engineer would be required to calculate the transfer of torsional forces in diaphragm action in the shelving, which may be impractical. Therefore, north-south braces are provided in each bay.

13.4 ELECTRIC GENERATING POWER PLANT, MERNA, WYOMING

This example highlights some of the differences between the design of nonbuilding structures and the design of building structures. The boiler building in this example illustrates a solution using the ELF procedure. Due to mass irregularities, the boiler building would probably also require a modal analysis. For brevity, the modal analysis is not illustrated.

13.4.1 Description

Large boilers in coal-fired electric power plants generally are suspended from the supporting steel near the roof level. Additional lateral supports (called buck stays) are provided near the bottom of the boiler. The buck stays resist lateral forces but allow the boiler to move vertically. Lateral seismic forces are resisted at the roof and at the buck stay level. Close coordination with the boiler manufacturer is required in order to determine the proper distribution of seismic forces.

In this example, a boiler building for a 950 MW coal-fired electric power generating plant is braced laterally with ordinary concentrically braced frames in both the north-south and east-west directions. The facility is part of a grid and is not for emergency backup of an Occupancy Category IV facility.

The dead load of the structure, equipment and piping, W_{DL}, is 16,700 kips.

The weight of the boiler in service, W_{Boiler}, is 31,600 kips.

The natural period of the structure (determined from analysis) is as follows:

North-South, T_{NS} = 1.90 seconds

East-West, T_{EW} = 2.60 seconds

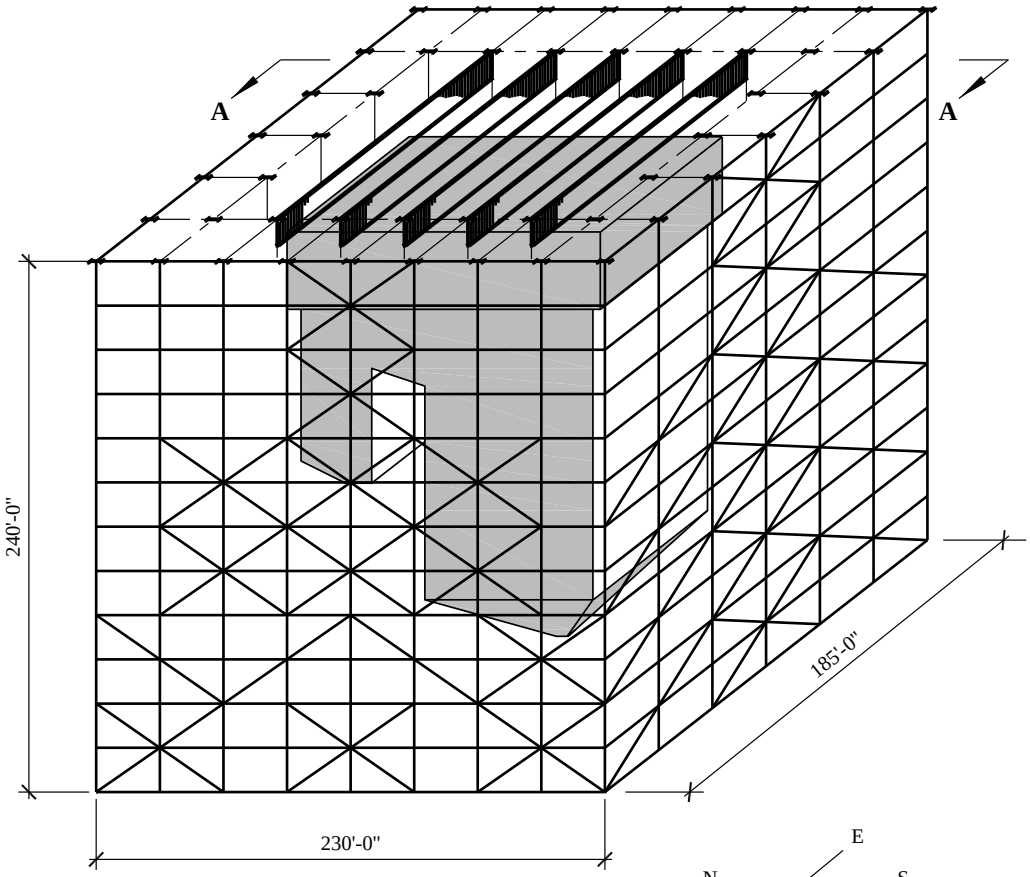

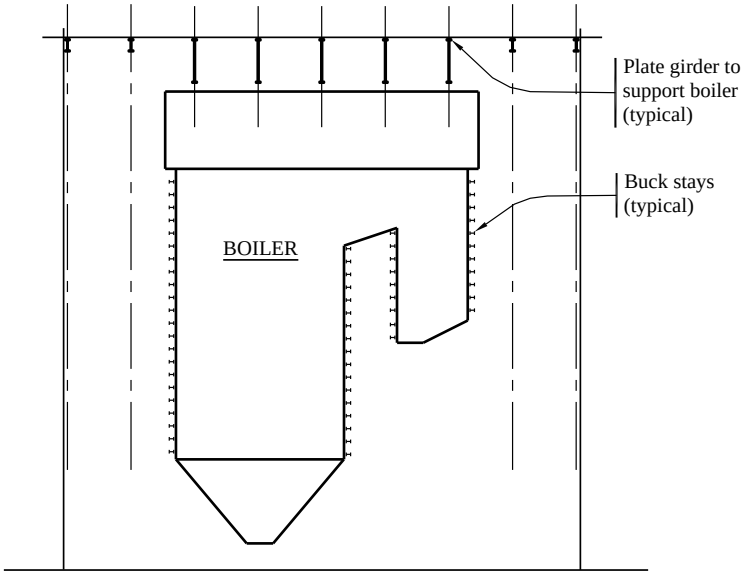

Section A-A

Figure 13-4 Boiler building (1.0 ft = 0.3048 m)

13.4.2 *Provisions* Parameters

Occupancy Category (*Standard* Sec. 1.5.1) (for continuous operation, but not for emergency backup of an Occupancy Category IV facility)	=	III
Occupancy Importance Factor, I (*Standard* Sec. 11.5.1)	=	1.25
Short-period Response, S_S	=	0.864
One-second Period Response, S_1	=	0.261
Site Class (*Standard* Sec. 11.4.2)	=	D (default)
Short-period Site Coefficient, F_a (*Standard* Table 11.4-1)	=	1.155
Long-period Site Coefficient, F_v (*Standard* Table 11.4-2)	=	1.877
Design Spectral Acceleration Response Parameters		
$S_{DS} = (2/3)S_{MS} = (2/3)F_aS_S = (2/3)(1.155)(0.864)$	=	0.665
$S_{D1} = (2/3)S_{M1} = (2/3)F_vS_1 = (2/3)(1.877)(0.261)$	=	0.327
Seismic Design Category (*Standard* Sec. 11.6)	=	D
Seismic Force-resisting System (*Standard* Table 15.4-1)	=	Ordinary steel concentrically braced frame with unlimited height
Response Modification Coefficient, R	=	1.5
System Overstrength Factor, Ω_0	=	1
Deflection Amplification Factor, C_d	=	1.5
Height Limit (*Standard* Table 15.4-1)	=	Unlimited

According to *Standard* Section 15.4-1, either *Standard* Table 12.2-1 or *Standard* Table 15.4-1 may be used to determine the seismic parameters, although mixing and matching of values and requirements from the tables is not allowed. If the structure were classified as a "building," its height would be limited to 35 feet for a Seismic Design Category D ordinary steel concentrically braced frame, according to *Standard* Table 12.2-1. A review of *Standard* Table 12.2-1 shows that three steel high ductility braced frame systems (two eccentrically braced systems and the special concentrically braced system) and two special moment frame systems can be used at a height of 240 feet. In most of these cases, the additional requirements of *Standard* Section 12.2.5.4 must be met to qualify the system at a height of 240 feet. Boiler buildings normally are constructed using ordinary concentrically braced frames.

As discussed in Section 13.2.3.1 above, Chapter 15 of the *Standard* presents options to increase height limits for design of some nonbuilding structures similar to buildings where *R* factors are reduced. For this example, an ordinary steel concentrically braced frame with unlimited height is chosen from *Standard* Table 15.4-1. By using a significantly reduced *R* value, the seismic design and detailing requirements of AISC 341 need not be applied.

13.4.3 Design in the North-South Direction

13.4.3.1 Seismic response coefficient. Using *Standard* Equation 12.8-2:

$$C_s = \frac{S_{DS}}{R/I} = \frac{0.665}{1.5/1.25} = 0.554$$

From analysis, T = 1.90 seconds. Using *Standard* Equation 12.8-3, C_S does not need to exceed

$$C_s = \frac{S_{D1}}{T(R/I)} = \frac{0.327}{1.90(1.5/1.25)} = 0.143$$

but using *Standard* Equation 12.8-5, C_s must not be less than:

$C_s = 0.044IS_{DS} \geq 0.01 = 0.044(1.25)(0.665) = 0.0366$

Standard Equation 12.8-3 controls; C_s = 0.143.

13.4.3.2 Seismic weight. Calculate the total seismic weight, W, as follows:

$W = W_{DL} + W_{Boiler}$ = 16,700 kips + 31,600 kips = 48,300 kips

13.4.3.3 Base shear. Using *Standard* Equation 12.8-1:

$V = C_sW$ = 0.143(48,300 kips) = 6,907 kips

13.4.3.4 Redundancy factor. The structure in this example meets the requirements of Condition b specified in *Standard* Section 12.3.4.2, because two bays of seismic force-resisting perimeter framing are provided in each orthogonal direction. Therefore, the redundancy factor, ρ, is 1.0.

It is important to note that each story resists more than 35 percent of the base shear because the boiler is hung from the top of the structure. Therefore, each story must comply with the requirements of Condition b. If a story resisted less than 35 percent of the base shear, the requirements of *Standard* Section 12.3.4.2 would not apply and that story would not be considered in establishing the redundancy factor.

13.4.3.5 Determining *E*. *E* is defined to include the effects of horizontal and vertical ground motions as follows:

$E = \rho Q_E \pm 0.2\, S_{DS}\, D$

where Q_E is the effect of the horizontal earthquake ground motions, which is determined primarily by the base shear just computed and D is the effect of dead load. By putting a simple multiplier on the effect of dead load, the last term is an approximation of the effect of vertical ground motion.

The *Standard* also requires the consideration of an overstrength factor, Ω_0, on the effect of horizontal motions in defining E for components susceptible to brittle failure.

$$E = \Omega_0 Q_E \pm 0.2 S_{DS} D$$

The ordinary steel concentrically braced frames have components that require such consideration. The beams transferring shear from one set of braces to another act as collectors and, as required by *Standard* Section 12.10.2.1, must be designed for the seismic load effect including overstrength factor.

13.4.4 Design in the East-West Direction

13.4.4.1 Seismic response coefficient. Using *Standard* Equation 12.8-2:

$$C_s = \frac{S_{DS}}{R/I} = \frac{0.665}{1.5/1.25} = 0.554$$

From analysis, T = 2.60 seconds. Using *Standard* Equation 12.8-3, C_s does not need to exceed:

$$C_s = \frac{S_{D1}}{T(R/I)} = \frac{0.327}{2.60(1.5/1.25)} = 0.105$$

Using *Standard* Equation 12.8-5, C_s must not be less than:

$$C_s = 0.044 I S_{DS} \geq 0.01 = 0.044(1.25)(0.665) = 0.0366$$

Standard Equation 12.8-3 controls; C_s = 0.105.

13.4.4.2 Seismic weight. Calculate the total seismic weight, W, as follows:

$$W = W_{DL} + W_{Boiler} = 16{,}700 \text{ kips} + 31{,}600 \text{ kips} = 48{,}300 \text{ kips}$$

13.4.4.3 Base shear. Using *Standard* Equation 12.8-1:

$$V = C_s W = 0.105(48{,}300 \text{ kips}) = 5072 \text{ kips}$$

13.5 PIER/WHARF DESIGN, LONG BEACH, CALIFORNIA

This example illustrates the calculation of the seismic base shear in the east-west direction for the pier using the ELF procedure. Piers and wharves are covered in *Standard* Section 15.5.6.

13.5.1 Description

A cruise ship company is developing a pier in Long Beach, California, to service ocean liners. The pier contains a large warehouse owned by the cruise ship company. In the north-south direction, the pier is tied directly to an abutment structure supported on grade. In the east-west direction, the pier resists

seismic forces using moment frames. Calculations for the abutment are not included in this example, but it is assumed to be much stiffer than the moment frames.

The design live load for warehouse storage is 1,000 psf.

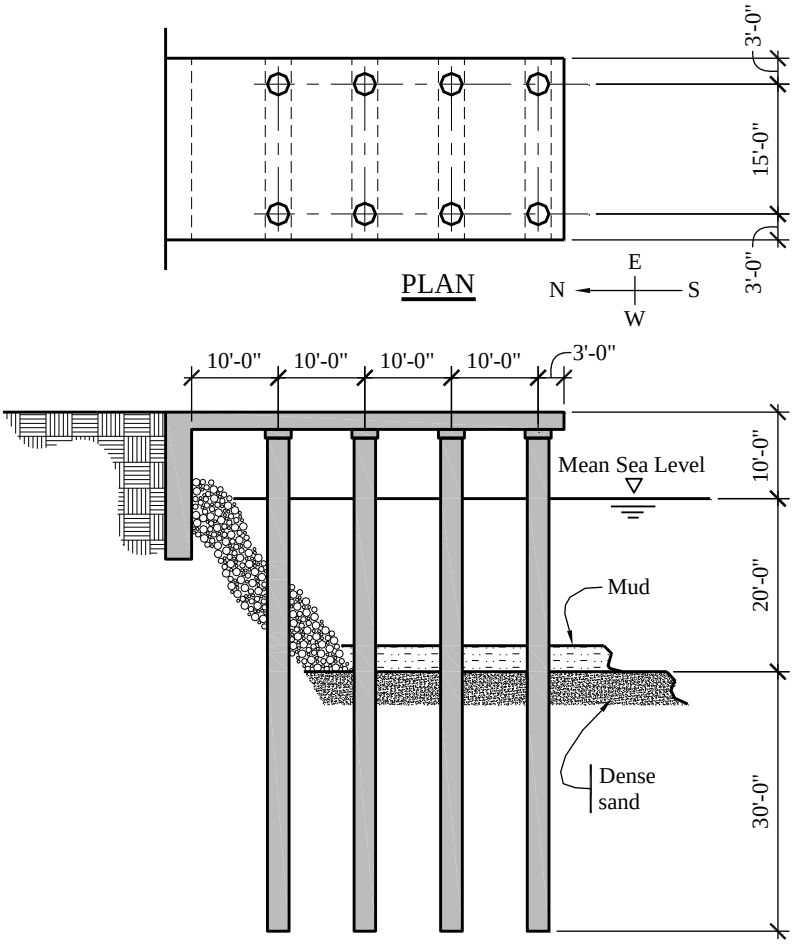

Figure 13-5 Pier plan and elevation (1.0 ft = 0.3048 m)

13.5.2 *Provisions* Parameters

Occupancy Category (*Standard* Sec. 1.5.1) (The pier serves cruise ships that carry no hazardous materials.)	=	II
Importance Factor, I (*Standard* Sec. 11.5.1)	=	1.0
Short-period Response, S_S	=	1.75

One-second Period Response, S_1	=	0.60
Site Class (*Standard* Chapter 20)	=	D (dense sand)
Short-period Site Coefficient, F_a (*Standard* Table 11.4-1)	=	1.0
Long-period Site Coefficient, F_v (*Standard* Table 11.4-2)	=	1.5
Design Spectral Acceleration Response Parameters		
$S_{DS} = (2/3)S_{MS} = (2/3)F_aS_S = (2/3)(1.0)(1.75)$	=	1.167
$S_{D1} = (2/3)S_{M1} = (2/3)F_vS_1 = (2/3)(1.5)(0.60)$	=	0.60
Seismic Design Category (*Standard* Sec. 11.6)	=	D
Seismic Force-resisting System (*Standard* Table 15.4-1)	=	Intermediate concrete moment frame with permitted height increase
Response Modification Coefficient, R	=	3
System Overstrength Factor, Ω_0	=	2
Deflection Amplification Factor, C_d	=	2.5
Height Limit (*Standard* Table 15.4-1)	=	50 ft

If the structure were classified as a building, an intermediate reinforced concrete moment frame would not be permitted in Seismic Design Category D.

13.5.3 Design of the System

13.5.3.1 Seismic response coefficient. Using *Standard* Equation 12.8-2:

$$C_s = \frac{S_{DS}}{R/I} = \frac{1.167}{3/1.0} = 0.389$$

From analysis, T = 0.596 seconds. Using *Standard* Equation 12.8-3, C_s does not need to exceed:

$$C_s = \frac{S_{D1}}{T\left(R/I\right)} = \frac{0.60}{0.596\left(3/1.0\right)} = 0.336$$

Using *Standard* Equation 12.8-5, C_s must not be less than:

$C_s = 0.044IS_{DS} \geq 0.01 = 0.044(1.0)(1.167) = 0.0513$

Standard Equation 12.8-3 controls; C_s = 0.336.

13.5.3.2 Seismic weight. In accordance with *Standard* Section 12.7.2, calculate the dead load due to the deck, beams and support piers, as follows:

W_{Deck} = 1.0(43 ft)(21 ft)(0.150 kip/ft^3) = 135.5 kips

W_{Beam} = 4(2 ft)(2 ft)(21 ft)(0.150 kip/ft^3) = 50.4 kips

W_{Pier} = 8[π(1.25 ft)^2][(10 ft - 3 ft) + (20 ft)/2](0.150 kip/ft^3) = 100.1 kips

$W_{DL} = W_{Deck} + W_{Beams} + W_{Piers}$ = 135.5 + 50.4 + 100.1 = 286.0 kips

Calculate 25 percent of the storage live load, as follows:

$W_{1/4\ LL}$ = 0.25(1,000 psf)(43 ft)(21 ft) = 225.8 kips

Standard Section 15.5.6.2 requires that all applicable marine loading combinations be considered (such as those for mooring, berthing, wave and current on piers and wharves). For this example, additional seismic loads from water flowing around the piles will be considered. A "virtual" mass (Jacobsen, 1959) of water equal to a column of water of identical dimensions of the circular pile is to be considered in the effective seismic mass. This additional weight is calculated as follows:

$W_{Virtual\ Mass}$ = 8[π(1.25 ft)^2][(20 ft)/2](64 pcf) = 25.1 kips

Therefore, the total seismic weight is

$W = W_{DL} + W_{1/4LL} + W_{Virtual\ Mass}$ = 286.0 + 225.8 + 25.1 = 536.9 kips

Additional seismic forces from the water due to wave action may also act on the piles. These additional forces are highly dependent on the acceleration and velocity of the waves and are heavily dependent on the geometry of the body of water. These forces can be calculated using the Morison Equation (Morison, 1950). The determination of these forces is beyond the scope of this example.

13.5.3.3 Base shear. Using *Standard* Equation 12.8-1:

$V = C_s W$ = 0.336(536.9 kips) = 180.4 kips

13.5.3.4 Redundancy factor. The pier in this example has a sufficient number of moment frames that loss of moment resistance at both ends of a single beam would not result in more than a 33 percent reduction in story strength. However, the direct tie to a much stiffer abutment at the north end likely would cause an extreme torsional irregularity for east-west motion, so that Condition (a) would not be met. Condition (b) is not met because two bays of seismic force-resisting perimeter framing are not provided in each orthogonal direction. Therefore, the redundancy factor, ρ, is taken to be 1.3.

13.6 TANKS AND VESSELS, EVERETT, WASHINGTON

The seismic response of tanks and vessels can be significantly different from that of buildings. For a structure composed of interconnected solid elements, it is not difficult to recognize how ground motions accelerate the structure and cause inertial forces within the structure. Tanks and vessels, where empty, respond in a similar manner.

Where there is liquid in the tank, the response is much more complicated. As earthquake ground motions accelerate the tank shell, the shell applies lateral forces to the liquid. The response of the liquid to those lateral forces may be amplified significantly if the period content of the earthquake ground motion is similar to the natural sloshing period of the liquid.

Earthquake-induced impulsive fluid forces are those calculated assuming that the liquid is a solid mass. Convective fluid forces are those that result from sloshing in the tank. It is important to account for convective forces on columns and appurtenances inside the tank, because they are affected by sloshing in the same way that waves affect a pier in the ocean.

Freeboard considerations are critical. Oftentimes, the roof acts as a structural diaphragm. If a tank does not have sufficient freeboard, the sloshing wave can rip the roof from the wall of the tank. This could result in failure of the wall and loss of the liquid within.

Seismic design for liquid-containing tanks and vessels is complicated. The fluid mass that is effective for impulsive and convective seismic forces is discussed in AWWA D100 and API 650.

13.6.1 Flat-Bottom Water Storage Tank

13.6.1.1 Description. This example illustrates the calculation of the design base shear and the required freeboard using the procedure outlined in AWWA D100 for a steel water storage tank used to store potable water for fire protection within a chemical plant (Figure 13-6). According to *Standard* Section 15.7.7.1, the governing reference document for this tank is AWWA D100. *Standard* Chapter 15 makes no modifications to this document for the seismic design of flat-bottom water storage tanks. AWWA D100 is written in terms of allowable stress design (ASD) while the seismic requirements of the *Standard* are written in terms of strength design. AWWA D100 translates the force equations from the *Standard* by substituting 1.4*R* for *R*. For the purposes of this example, all loads are calculated in terms of strength design. Where appropriate, AWWA D100 equations are referenced for the determination of impulsive and convective (sloshing) masses.

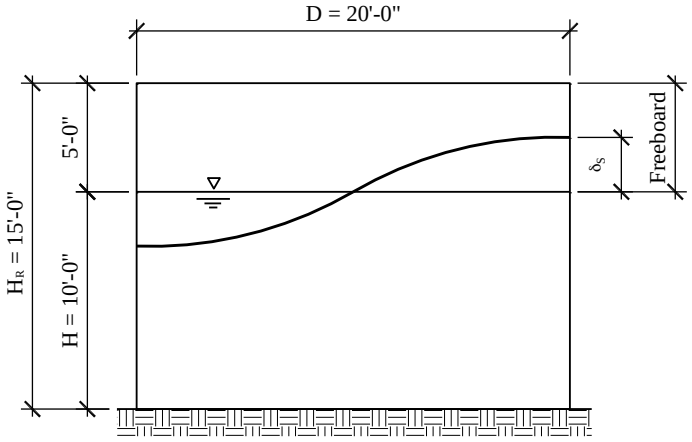

Figure 13-6 Storage tank section (1.0 ft = 0.3048 m)

The weight of the tank shell, roof, bottom and equipment is 15,400 pounds.

13.6.1.2 Seismic design parameters.

Occupancy Category (*Standard* Sec. 1.5.1)	=	IV
Importance Factor, I (*Standard* Sec. 11.5.1)	=	1.5
Short-period Response, S_S	=	1.236
One-second Period Response, S_1	=	0.406
Long-period Transition Period, T_L	=	6 seconds
Site Class (*Standard* Chapter 20)	=	C (per geotech)
Short-period Site Coefficient, F_a (*Standard* Table 11.4-1)	=	1.0
Long-period Site Coefficient, F_v (*Standard* Table 11.4-2)	=	1.39
Design Spectral Acceleration Response Parameters		
$S_{DS} = (2/3)S_{MS} = (2/3)F_aS_S = (2/3)(1.0)(1.236)$	=	0.824
$S_{D1} = (2/3)S_{M1} = (2/3)F_vS_1 = (2/3)(1.39)(0.406)$	=	0.376
Seismic Force-resisting System (*Standard* Table 15.4-2)	=	Flat-bottom, ground-supported, mechanically anchored steel tank
Response Modification Coefficient, R	=	3
System Overstrength Factor, Ω_0	=	2
Deflection Amplification Factor, C_d	=	2.5

13.6.1.3 Calculations for impulsive response.

13.6.1.3.1 Natural period for the first mode of vibration. AWWA D100 Section 13.5.1 does not require the computation of the natural period for the first mode of vibration. The impulsive acceleration is assumed to be equal to S_{DS}.

13.6.1.3.2 Spectral acceleration. Based on AWWA D100 Section 13.5.1, the impulsive acceleration is set equal to S_{DS}.

$S_{ai} = S_{DS} = 0.824$

13.6.1.3.3 Seismic (impulsive) weight.

$W_{tank} = 15.4$ kips

$W_{iwater} = \pi(10 \text{ ft})^2(10 \text{ ft})(0.0624 \text{ kip/ft}^3)\ (W_i/W_T) = 196.0\ (0.542)$ kips $= 106.2$ kips

The ratio W_i/W_T (= 0.542) was determined from Equation 13-24 (only valid for $D/H \geq 1.333$) of AWWA D100 for a diameter-to-liquid height ratio of 2.0 as shown below:

$$\frac{W_i}{W_T} = \frac{\tanh\left(0.866\frac{D}{H}\right)}{0.866\frac{D}{H}} = \frac{\tanh\left(0.866\frac{20}{10}\right)}{0.866\frac{20}{10}} = 0.542$$

$W_i = W_{tank} + W_{iwater} = 15.4 + 106.2 = 121.6$ kips

13.6.1.3.4 Base Shear.

According to *Standard* Equation 15.7-5:

$$V_i = \frac{S_{ai}W_i}{R/I} = \frac{0.824(121.6)}{3/1.5} = 50.1\,\text{kips}$$

13.6.1.4 Calculations for convective response natural period for the first mode of sloshing.

13.6.1.4.1 Natural period for the first mode of sloshing. Using *Standard* Equation 15.7-12:

$$T_c = 2\pi\sqrt{\frac{D}{3.68g\tanh\left(\frac{3.68H}{D}\right)}} = 2\pi\sqrt{\frac{20\text{ ft}}{3.68\left(32.174\ \frac{\text{ft}}{s^2}\right)\tanh\left(\frac{3.68(10\text{ ft})}{20\text{ ft}}\right)}} = 2.65\text{ s}$$

13.6.1.4.2 Spectral acceleration. Using *Standard* Equation 15.7-10 with $T_c < T_L = 6$ seconds:

$$S_{ac} = \frac{1.5S_{D1}}{T_c} = \frac{1.5(0.376)}{2.65} = 0.212$$

13.6.1.4.3 Seismic (convective) weight.

$W_c = W_{water}$ (W_c/W_T) = 196 (0.437) = 85.7 kips

The ratio W_c/W_T (= 0.437) was determined from Equation 13-26 (valid for all D/H) of AWWA D100 for a diameter-to-liquid height ratio of 2.0 as shown below:

$$\frac{W_c}{W_T} = 0.230\left(\frac{D}{H}\right)\tanh\left(3.67\frac{H}{D}\right) = 0.230\left(\frac{20}{10}\right)\tanh\left(3.67\frac{10}{20}\right) = 0.437$$

13.6.1.4.4 Base shear. According to *Standard* Equation 15.7-6:

$$V_c = \frac{S_{ac}I}{1.5}W_c = \frac{0.212(1.5)}{1.5}(85.7) = 18.2\,\text{kips}$$

13.6.1.5 Design base shear. Item b of *Standard* Section 15.7.2 indicates that impulsive and convective components may, in general, be combined using the SRSS method. *Standard* Equation 15.7-4 requires that the direct sum be used for ground-supported storage tanks for liquids. Note b under *Standard* Section 15.7.6.1 allows the use of the SRSS method in lieu of using *Standard* Equation 15.7-4. Therefore, the base shear is computed as follows:

$$V = \sqrt{V_i^2 + V_c^2} = \sqrt{50.1^2 + 18.2^2} = 53.3 \text{ kips}$$

13.6.1.6 Minimum freeboard. Because the tank is assigned to Occupancy Category IV, the full value of the theoretical wave height must be provided for freeboard. For the case of Occupancy Category IV tanks, the wave height is calculated based on the convective acceleration using the actual value of T_L and an importance factor of 1.0. *Standard* Table 15.7-3 indicates that a minimum freeboard equal to δ_s is required for this tank. Using *Standard* Equation 15.7-13 and Note c (sets I = 1.0 for Occupancy Category IV for wave height determination) from *Standard* Section 15.7.6.1:

$$\delta_s = 0.5 D_i I S_{ac} = 0.5(20 \text{ ft})(1.0)(0.212) = 2.12 \text{ ft}$$

The 5 feet of freeboard provided is adequate.

13.6.2 Flat-Bottom Gasoline Tank

13.6.2.1 Description. This example illustrates the calculation of the base shear and the required freeboard using the procedure outlined in API 650 for a petrochemical storage tank in a refinery tank farm (Figure 13-7). An impoundment dike is not provided to control liquid spills. According to Standard Section 15.7.8.1, the governing reference document for this tank is API 650. API 650 is written in terms of allowable stress design (ASD) while the seismic requirements of the *Standard* are written in terms of strength design. API 650 translates the force equations from the *Standard* by substituting R_w for R, where R_w is equal to 1.4R. For the purposes of this example, all loads are calculated in terms of strength design. Where appropriate, API 650 equations are referenced for the determination of impulsive and convective (sloshing) masses.

The tank is a flat-bottom, ground-supported, self-anchored, welded steel tank constructed in accordance with API 650. The weight of the tank shell, roof, bottom and equipment is 490,000 pounds.

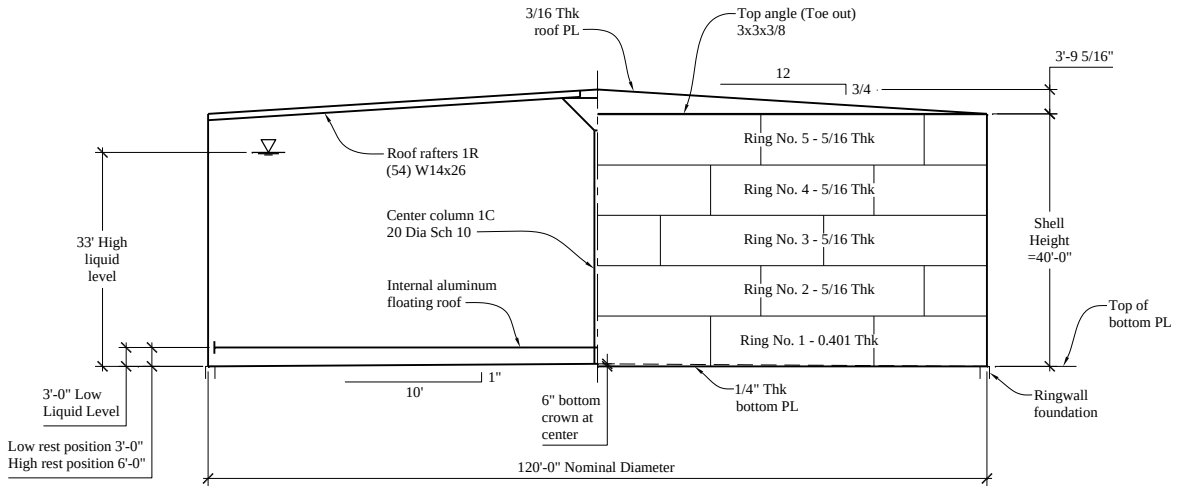

Figure 13-7 Storage tank section (1.0 ft = 0.3048 m)

13.6.2.2 Seismic design parameters.

Occupancy Category (*Standard* Sec. 1.5.1) (The tank is used for storage of toxic or explosive material.)	=	III
Importance Factor, I (*Standard* Sec. 11.5.1)	=	1.25
Design Spectral Acceleration Response Parameters (Using the same site as in Section 13.6.1)		
$S_{DS} = (2/3)S_{MS} = (2/3)F_aS_S = (2/3)(1.0)(1.236)$	=	0.824
$S_{D1} = (2/3)S_{M1} = (2/3)F_vS_1 = (2/3)(1.39)(0.406)$	=	0.376
Seismic Force-Resisting System (*Standard* Table 15.4-2)	=	Flat-bottom, ground-supported, self- anchored steel tank
Response Modification Coefficient, R	=	2.5
System Overstrength Factor, Ω_0	=	2
Deflection Amplification Factor, C_d	=	2

13.6.2.3 Calculations for impulsive response.

13.6.2.3.1 Natural period for the first mode of vibration. API 650 Section E.4.8.1 does not require the computation of the natural period for the first mode of vibration. The impulsive acceleration is assumed to be equal to S_{DS}.

13.6.2.3.2 Spectral acceleration. Based on API 650 Section 13.5.1, the impulsive acceleration is set equal to S_{DS}.

$S_{ai} = S_{DS} = 0.824$

13.6.2.3.3 Seismic (impulsive) weight.

$W_{tank} = 490.0$ kips

$W_{Gas} = \pi(60 \text{ ft})^2(33 \text{ ft})(0.0474 \text{ kip/ft}^3)(W_i/W_p) = 17{,}691 \text{ kips } (0.316) = 5{,}590 \text{ kips}$

The ratio W_i/W_p (= 0.316) was determined from Equation E-13 (only valid for $D/H \geq 1.333$) of API 650 for a diameter-to-liquid height ratio of 3.636 as shown below:

$$\frac{W_i}{W_p} = \frac{\tanh\left(0.866\frac{D}{H}\right)}{0.866\frac{D}{H}} = \frac{\tanh\left(0.866\frac{120}{33}\right)}{0.866\frac{120}{33}} = 0.316$$

$W_i = W_{tank} + W_{Gas} = 490 + 5590 = 6{,}080$ kips

13.6.2.3.4 Base shear. According to *Standard* Equation 15.7-5:

$$V_i = \frac{S_{ai}W_i}{R/I} = \frac{0.824(6080)}{2.5/1.25} = 2{,}505 \text{ kips}$$

13.6.2.4 Calculations for convective response.

13.6.2.4.1 Natural period for the first mode of sloshing. Using *Standard* Equation 15.7-12:

$$T_c = 2\pi\sqrt{\frac{D}{3.68g\tanh\left(\frac{3.68H}{D}\right)}} = 2\pi\sqrt{\frac{120 \text{ ft}}{3.68\left(32.174\ \frac{\text{ft}}{s^2}\right)\tanh\left(\frac{3.68(33 \text{ ft})}{120 \text{ ft}}\right)}} = 7.22 \text{ s}$$

13.6.2.4.2 Spectral acceleration. Using *Standard* Equation 15.7-11 with $T_c > T_L = 6$ seconds:

$$S_{ac} = \frac{1.5S_{D1}T_L}{T_c^2} = \frac{1.5(0.376)(6)}{7.22^2} = 0.0649$$

13.6.2.4.3 Seismic (convective) weight.

$W_c = W_{GAS}\,(W_c/W_p) = 17691\ (0.640) = 11{,}322$ kips

The ratio W_c/W_p (= 0.640) was determined from Equation E-15 (valid for all D/H) of API 650 for a diameter-to-liquid height ratio of 3.636 as shown below:

$$\frac{W_c}{W_T} = 0.230\left(\frac{D}{H}\right)\tanh\left(3.67\frac{H}{D}\right) = 0.230\left(\frac{120}{33}\right)\tanh\left(3.67\frac{33}{120}\right) = 0.640$$

13.6.2.4.4 Base shear. According to *Standard* Equation 15.7-6:

$$V_c = \frac{S_{ac}I}{1.5}W_c = \frac{0.0649(1.5)}{1.5}(11{,}322) = 735 \text{ kips}$$

13.6.2.5 Design base shear. Item (b) of *Standard* Section 15.7.2 indicates that impulsive and convective components may, in general, be combined using the SRSS method. *Standard* Equation 15.7-4 requires that the direct sum be used for ground-supported storage tanks for liquids. Note b under *Standard* Section 15.7.6.1 allows the use of the SRSS method in lieu of using *Standard* Equation 15.7-4. Therefore, the base shear is computed as follows:

$$V = \sqrt{V_i^2 + V_c^2} = \sqrt{2505^2 + 735^2} = 2{,}611 \text{ kips}$$

13.6.2.6 Minimum freeboard. Because the tank is assigned to Occupancy Category III and S_{DS} is greater than 0.50, the freeboard provided must be at least 70 percent of the full value of the theoretical wave height (based on T_L = 4 s). For the case of Occupancy Category III tanks, the wave height is calculated based on the convective acceleration using a value of T_L equal to 4 seconds and an importance factor of 1.25 according to *Standard* Section 15.7.6.1, Note (d). *Standard* Table 15.7-3 indicates that a minimum freeboard equal to $0.7\delta_s$ is required for this tank. Using *Standard* Equation 15.7-13 and Note (d) (sets I = 1.25 and T_L to 4 seconds for Occupancy Category III for wave height determination) from *Standard* Section 15.7.6.1:

$\delta_s = 0.5D_iIS_{ac} = 0.5(120 \text{ ft})(1.25)(0.0433) = 3.25 \text{ ft}$

$$S_{ac} = \frac{1.5S_{D1}T_L}{T_c^2} = \frac{1.5(0.376)4}{7.22^2} = 0.0433$$

$0.7\ \delta_s = 2.27 \text{ ft}$

The 7 feet of freeboard provided also includes a 3-foot allowance for an aluminum internal floating roof and the roof framing. The seismic freeboard must be sufficient to avoid forcing the floating roof into the fixed roof framing. The freeboard provided is adequate. The reduced freeboard requirement recognizes that providing seismic freeboard for Occupancy Category I, II, or III tanks is an economic decision (reducing damage) and not a life-safety issue. Because of this, a reduced freeboard is allowed. If secondary containment were provided, no freeboard would be required based on *Standard* Table 15.7-3, Footnote (b).

13.7 VERTICAL VESSEL, ASHPORT, TENNESSEE

13.7.1 Description

This example illustrates the calculation of the base shear using the ELF procedure for a flexible vertical vessel (Figure 13-8). The vertical vessel contains highly toxic material (Occupancy Category IV).

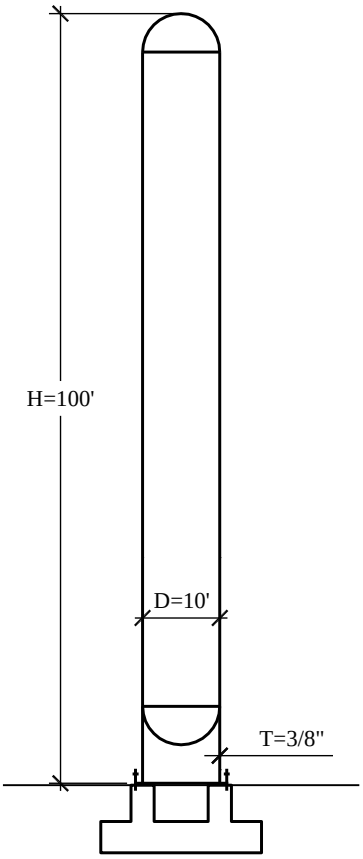

Figure 13-8 Vertical vessel (1.0 ft = 0.3048 m)

The weight of the vertical vessel plus contents is 300,000 pounds.

Standard Section 15.4.4 allows the fundamental period of a nonbuilding structure to be determined using a properly substantiated analysis. The period of the vertical vessel is calculated using the equation for a uniform vertical cylindrical steel vessel as found in Appendix 4.A of ASCE (1997). The period of the vessel is calculated as follows:

$$T = \frac{7.78}{10^6}\left(\frac{H}{D}\right)^2\sqrt{\frac{12WD}{t}} = \frac{7.78}{10^6}\left(\frac{100}{10}\right)^2\sqrt{\frac{12(300000/100)10}{0.375}} = 0.762\text{s}$$

where: T = period (s)
W = weight (lb/ft)
H = height (ft)
D = diameter (ft)
T = shell thickness (in.)

13.7.2 *Provisions* Parameters

13.7.2.1 Ground motion. The design response spectral accelerations are defined as follows:

S_{DS} = 1.86
S_{D1} = 0.79

13.7.2.2 Importance factor. The vertical vessel contains highly toxic material. Therefore, it is assigned to Occupancy Category IV, as required by *Standard* Section 1.5.1. Using *Standard* Table 11.5.1, the importance factor, *I*, is equal to 1.5.

13.7.2.3 Seismic coefficients. The vertical vessel used in this example is a skirt-supported distributed mass cantilevered structure. There are three possible entries in *Standard* Table 15.4-2 that describe the vessel in question:

1. Elevated tanks, vessels, bins, or hoppers: Single pedestal or skirt supported – welded steel.

2. Elevated tanks, vessels, bins, or hoppers: Single pedestal or skirt supported – welded steel with special detailing.

3. All other steel and reinforced concrete distributed mass cantilever structures not covered herein including stacks, chimneys, silos and skirt-supported vertical vessels that are not similar to buildings.

All three options are keyed to the detailing requirements of *Standard* Section 15.7.10. Two of the options specifically require that Items (a) and (b) of *Standard* Section 15.7.10 be met. The intent of *Standard* Section 15.7.10 and *Standard* Table 15.4-2 is that skirt-supported vessels be checked for seismic loads based on R/I = 1.0 if the structure is assigned to Occupancy Category IV or if an *R* factor of 3.0 is used in the design of the vessel. Skirt-supported vessels fail in buckling, which is not a ductile failure mode, so a more conservative design approach is required. The R/I = 1.0 check typically will govern the design of the skirt over using loads determined with an *R* factor of 3 in a moderate to high area of seismic activity. The only benefit of using an *R* factor of 3 in this case is in the design of the foundation. The foundation is not required to be designed for the R/I = 1.0 load. For the R/I = 1.0 load, the skirt can be designed based on critical buckling (factor of safety of 1.0). The critical buckling strength of a skirt can be determined using a number of published sources. The two most common methods for determining the critical buckling strength of a skirt are ASME BVPC Section VIII, Division 2, Paragraph 4.4 using a factor of safety of 1.0 and AWWA D100 Section 13.4.3.4. Calculating the critical buckling strength of a skirt is beyond the scope of this example.

For this example, the skirt-supported vertical vessel will be treated as "all other steel and reinforced concrete distributed mass cantilever structures not covered herein including stacks, chimneys, silos and skirt-supported vertical vessels that are not similar to buildings" from *Standard* Table 15.4-2. The seismic design parameters for this structure are as follows:

Response Modification Coefficient, *R*	=	3
System Overstrength Factor, Ω_0	=	2
Deflection Amplification Factor, C_d	=	2.5

13.7.3 Design of the System

13.7.3.1 Seismic response coefficient. Using *Standard* Equation 12.8-2:

$$C_s = \frac{S_{DS}}{R/I} = \frac{1.86}{3/1.5} = 0.930$$

Using *Standard* Equation 12.8-3, C_s does not need to exceed:

$$C_s = \frac{S_{D1}}{T(R/I)} = \frac{0.79}{0.762(3/1.5)} = 0.518$$

Using *Standard* Equation 15.4-1, C_s must not be less than:

$C_s = 0.044IS_{DS} \geq 0.03 = 0.044(1.5)(1.86) = 0.123$

Standard Equation 12.8-3 controls; $C_s = 0.518$.

13.7.3.2 Base shear. Using *Standard* Equation 12.8-1:

$V = C_sW = 0.518(300 \text{ kips}) = 155.4 \text{ kips}$

13.7.3.3 Vertical distribution of seismic forces. *Standard* Section 12.8.3 defines the vertical distribution of seismic forces in terms of an exponent, *k*, related to structural period. If the structural period is less than or equal to 0.5 second, $k = 1$ and results in an inverted triangular distribution of forces. If the structural period is greater than or equal to 2.5 seconds, $k = 2$ and results in a parabolic distribution of forces. For periods between 0.5 second and 2.5 seconds, the value of *k* is determined by linear interpolation between 1 and 2. The significance of the distribution requirements of *Standard* Section 12.8.3 is that the height of the centroid to the horizontal seismic force increases (thus increasing the overturning moment) as the period increases above 0.5 second (Figure 13-9).

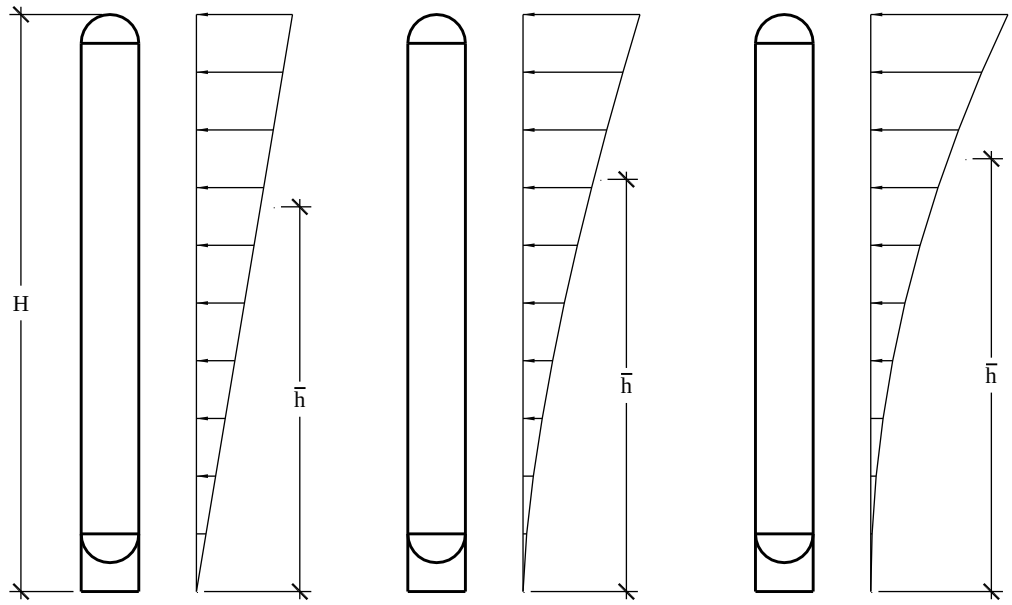

Figure 13-9 Vertical distribution of seismic forces

Once *k* is determined, the height to the centroid, $\bar{h}$, of the horizontal seismic force is equal to:

$$\bar{h} = \frac{(k+1)}{(k+2)}H$$

where *H* is the vertical height of the vertical vessel.

For the vessel period of $T = 0.762$ second,

$$k = 1 + \frac{0.762 - 0.5}{2.5 - 0.5} = 1.131$$

The value of $\bar{h}$ is then calculated as:

$$\bar{h} = \frac{(1.131+1)}{(1.131+2)}(100) = 0.681(100) = 68.1\text{ft}$$

The overturning moment is then calculated as $M = V\bar{h}$ = 155.4(68.1) = 10,583 ft-kips.

14

Design for Nonstructural Components

Robert Bachman, S.E., John Gillengerten, S.E. and Susan Dowty, S.E.

Contents

14.1 DEVELOPMENT AND BACKGROUND OF THE REQUIREMENTS FOR NONSTRUCTURAL COMPONENTS 3
14.1.1 Approach to Nonstructural Components 3
14.1.2 Force Equations 4
14.1.3 Load Combinations and Acceptance Criteria 5
14.1.4 Component Amplification Factor 6
14.1.5 Seismic Coefficient at Grade 7
14.1.6 Relative Location Factor 7
14.1.7 Component Response Modification Factor 7
14.1.8 Component Importance Factor 7
14.1.9 Accommodation of Seismic Relative Displacements 8
14.1.10 Component Anchorage Factors and Acceptance Criteria 9
14.1.11 Construction Documents 9
14.2 ARCHITECTURAL CONCRETE WALL PANEL 10
14.2.1 Example Description 10
14.2.2 Design Requirements 12
14.2.3 Spandrel Panel 12
14.2.4 Column Cover 19
14.2.5 Additional Design Considerations 20
14.3 HVAC FAN UNIT SUPPORT 21
14.3.1 Example Description 21
14.3.2 Design Requirements 22
14.3.3 Direct Attachment to Structure 23
14.3.4 Support on Vibration Isolation Springs 26

14.3.5 Additional Considerations for Support on Vibration Isolators....31
14.4 ANALYSIS OF PIPING SYSTEMS....33
14.4.1 ASME Code Allowable Stress Approach....33
14.4.2 Allowable Stress Load Combinations....34
14.4.3 Application of the *Standard*....36
14.5 PIPING SYSTEM SEISMIC DESIGN....38
14.5.1 Example Description....38
14.5.2 Design Requirements....43
14.5.3 Piping System Design....45
14.5.4 Pipe Supports and Bracing....48
14.5.5 Design for Displacements....53
14.6 ELEVATED VESSEL SEISMIC DESIGN....55
14.6.1 Example Description....55
14.6.2 Design Requirements....58
14.6.3 Load Combinations....60
14.6.4 Forces in Vessel Supports....60
14.6.5 Vessel Support and Attachment....62
14.6.6 Supporting Frame....65
14.6.7 Design Considerations for the Vertical Load-Carrying System....69

Chapter 13 of the *Standard* addresses architectural, mechanical and electrical components of buildings. The examples presented here illustrate many of the requirements and procedures. Design and anchorage are illustrated for exterior precast concrete cladding and for a roof-mounted HVAC unit. The rooftop unit is examined in two common installations: directly attached and isolated with snubbers. This chapter also contains an explanation of the fundamental aspects of the *Standard* and an explanation of how piping, designed according to the ASME Power Piping code, is checked for the force and displacement requirements of the *Standard*. Examples are also provided that illustrate how to treat non-ASME piping located within a healthcare facility and a platform-supported vessel located on an upper floor within a building.

The variety of materials and industries involved with nonstructural components is large and numerous documents define and describe methods of design, construction, manufacture, installation, attachment, etc. Some of the documents address seismic issues, but many do not. *Standard* Chapter 23 contains a listing of approved standards for various nonstructural components.

In addition to the *Standard*, the following are referenced in this chapter:

- ACI 318 — American Concrete Institute. 2008. Building Code Requirements for Structural Concrete.
- ASHRAE APP IP — American Society of Heating, Refrigeration and Air-Conditioning Engineers (ASHRAE). 1999. *Seismic and Wind Restraint Design*, Chapter 53.
- ASME B31.1 — American Society of Mechanical Engineers. 2001. *Power Piping Code*.
- IBC — International Code Council. 2006. *International Building Code*.

The symbols used in this chapter are drawn from Chapter 11 of the *Standard* or reflect common engineering usage. The examples are presented in U.S. customary units.

14.1 DEVELOPMENT AND BACKGROUND OF THE REQUIREMENTS FOR NONSTRUCTURAL COMPONENTS

14.1.1 Approach to Nonstructural Components

The *Standard* requires that nonstructural components be checked for two fundamentally different demands placed upon them by the response of the structure to earthquake ground motion: resistance to inertial forces and accommodation of imposed displacements. Building codes have long had requirements for resistance to inertial forces. Most such requirements apply to the component mass and acceleration that vary with the basic ground motion parameter and a few broad categories of components. These broad categories are intended to distinguish between components whose dynamic response couples with that of the supporting structure in such a fashion as to cause the component response accelerations to be amplified above the accelerations of the structure and those components that are rigid enough with respect to the structure so that the component response is not amplified over the structural response. In recent years, a coefficient based on the function of the building or of the component has been introduced as another multiplier for components important to life safety or essential facilities.

The *Standard* includes an equation to compute the inertial force that involves two additional concepts: variation of acceleration with relative height within the structure and reduction in design force based upon

available ductility in the component or its attachment. The *Standard* also includes a quantitative measure for the deformation imposed upon nonstructural components. The inertial force demands tend to control the seismic design for isolated or heavy components, whereas the imposed deformations are important for the seismic design for elements that are continuous through multiple levels of a structure or across expansion joints between adjacent structures, such as cladding or piping.

The remaining portions of this section describe the sequence of steps and decisions prescribed by the *Standard* to check these two seismic demands on nonstructural components.

14.1.2 Force Equations

The following seismic force equations are prescribed for nonstructural components (*Standard* Eq. 13.3-1 through 13.3-3):

$$F_p = \frac{0.4 a_p S_{DS} W_p}{R_p / I_p}\left(1 + 2\frac{z}{h}\right)$$

$$F_{p_{max}} = 1.6 S_{DS} I_p W_p$$

$$F_{p_{min}} = 0.3 S_{DS} I_p W_p$$

where:

F_p = horizontal equivalent static seismic design force centered at the component's center of gravity and distributed relative to the component's mass distribution

a_p = component amplification factor (between 1.0 and 2.5) as tabulated in *Standard* Table 13.5-1 for architectural components and *Standard* Table 13.6-1 for mechanical and electrical components

S_{DS} = five percent damped spectral response acceleration parameter at short period as defined in *Standard* Section 11.4.4

W_p = component operating weight

R_p = component response modification factor (between 1.0 to 12.0) as tabulated in *Standard* Table 15.5-1 for architectural components and *Standard* Table 13.6-1 for mechanical and electrical components

I_p = component importance factor (either 1.0 or 1.5) as indicated in *Standard* Section 13.1.3

z = elevation in structure of component point of attachment relative to the base

h = roof elevation of the structure or elevation of highest point of the seismic force-resisting system of the structure relative to the base

The seismic design force, F_p, is to be applied independently in the longitudinal and transverse directions. F_p should be applied in both the positive and negative directions if higher demands will result. The

effects of these loads on the component are combined with the effects of static loads. *Standard* Equations 13.3-2 and 13.3-3 provide maximum and minimum limits for the seismic design force.

For each point of attachment, a force, F_p, should be determined based on *Standard* Equation 13.3-1. The minima and maxima determined from *Standard* Equations 13.3-2 and 13.3-3 must be considered in determining each F_p. The weight, W_p, used to determine each F_p should be based on the tributary weight of the component associated with the point of attachment. For designing the component, the attachment force, F_p, should be distributed relative to the component's mass distribution over the area used to establish the tributary weight. With the exception of structural walls, which are covered by *Standard* Section 12.11.1 and anchorage of concrete or masonry structural walls, which is covered by *Standard* Section 12.11.2, each anchorage force should be based on simple statics determined by using all the distributed loads applied to the complete component. Cantilever parapets that are part of a continuous element should be checked separately for parapet forces.

14.1.3 Load Combinations and Acceptance Criteria

Load combinations for use in determining the overall demand on an item are defined in *Standard* Section 2.3. Earthquakes cause loads on structures and nonstructural components in both the horizontal and vertical directions. Where these loads are applied to structural and nonstructural systems, the results (forces, stresses, displacements, etc.) are called "effects". In *Standard* Section 12.4.2, seismic load effects are defined. The effects resulting from horizontally applied loads are termed horizontal load effects, E_h and the effects resulting from vertically applied loads are termed vertical load effects, E_v. The E_v term is simply a constant $0.2S_{DS}$ multiplied by the dead load.

Because the load combinations defined in *Standard* Section 2.3 provide a single term, E, to define the earthquake, the horizontal and vertical load effects were sometimes misapplied by casual users of the *Standard and* the effects E_h and E_v were simply added as if they were applied in the same direction. To eliminate this confusion, when the *Standard* was reorganized as part of the development of its 2005 edition, a new Section 12.4 was added to separate the horizontal and vertical components of the seismic load and provide a reconstituted version of the load combinations provided in Section 2.3 of the *Standard*. The seismic load combinations substituted the vertical coefficient term, $0.2S_{DS}$ (representing E_v) directly into the load combinations. These are not alternate versions of Section 2.3 but instead present expanded versions of the load combinations of Section 2.3. It was intended by the ASCE 7 Seismic Task Committee that unless otherwise noted or excepted, the load combinations provided in Section 12.4 of the *Standard* be used for the design of all structures and nonstructural components.

The 2006 IBC has its own set of load combinations that are very similar to those provided in ASCE 7-05. In general, 2006 IBC load combinations take precedence over those of ASCE 7-05 where they are in conflict. However, for the remainder of the discussion and examples provided herein, the load combinations of *Standard* Section 12.4 are used.

14.1.3.1 Seismic load effects. From Section 12.4.2, the horizontal seismic load effect E_h and vertical seismic load effect E_v are determined by applying the horizontal component load F_p and the vertical dead load D, respectively, in the structural analysis as indicated below.

$$E_h = \rho Q_E \qquad \text{(}\textit{Standard}\text{ Eq. 12.4-3)}$$

$$E_v = 0.2S_{DS}D \qquad \text{(}\textit{Standard}\text{ Eq. 12.4-4)}$$

where:

Q_E = effect of horizontal seismic forces (due to application of F_p for nonstructural components) (*Standard* Sec. 12.4.2-1)

ρ = redundancy factor = 1.0 for nonstructural components (*Standard* Sec 13.3.1)

D = dead load effect (due to vertical load application)

Where the effects of vertical gravity loads and horizontal earthquake loads are additive,

$$E = \rho Q_E + 0.2 S_{DS} D$$

And where the effects of vertical gravity load counteract those of horizontal earthquake loads,

$$E = \rho Q_E - 0.2 S_{DS} D$$

where:

E = effect of horizontal and vertical earthquake-induced forces

14.1.3.2 Strength load combinations. The *Standard* provides load combinations that are to be used to determine design member forces, stresses and displacements in *Standard* Sections 2.3 and 2.4. In *Standard* Section 2.3, load combinations are provided for Strength Design and in *Standard* Section 2.4, load combinations are provided for Allowable Stress Design. For purposes of the Chapter 13 examples, only the Strength Load Combinations are used.

For Strength Load Combinations involving seismic loads, the terms defined above in Section 14.1.3.1 are substituted for E in the Basic Load Combinations for Strength Design of *Standard* Section 2.3.2 to determine the design member and connection forces to be used in conjunction with seismic loads. Once the substitutions have been made, the strength load combinations of Section 2.3.2 are presented in *Standard* Section 12.4.2.3, as follows:

$(1.2 + 0.2 S_{DS})\, D + \rho Q_E + L + 0.2 S$ (*Standard* Basic Load Combination 5)

$(0.9 - 0.2 S_{DS})\, D + \rho Q_E + 1.6 H$ (*Standard* Basic Load Combination 7)

For nonstructural components, the terms L, S and H typically are zero and load combinations with overstrength generally are not applicable.

14.1.4 Component Amplification Factor

The component amplification factor, a_p, found in *Standard* Equation 13.3-1 represents the dynamic amplification of the component relative to the maximum acceleration of the component support point(s). Typically, this amplification is a function of the fundamental period of the component, T_p and the fundamental period of the support structure, T. When components are designed or selected, the effective fundamental period of the structure, T, is not always available. Also, for most nonstructural components, the component fundamental period, T_p, can be obtained accurately only by expensive shake-table or pullback tests. As a result, the determination of a component's fundamental period by dynamic analysis, considering T/T_p ratios, is not always practicable. For this reason, acceptable values of a_p are provided in the *Standard* tables. Therefore, component amplification factors from either these tables or a dynamic

analysis may be used. Values for a_p are tabulated for each component based on the expectation that the component will behave in either a rigid or a flexible manner. For simplicity, a step function increase based on input motion amplifications is provided to help distinguish between rigid and flexible behavior. If the fundamental period of the component is less than 0.06 second, no dynamic amplification is expected and a_p may be taken to equal 1.0. If the fundamental period of the component is greater than 0.06 second, dynamic amplification is expected and a_p is taken to equal 2.5. In addition, a rational analysis determination of a_p is permitted if reasonable values of both T and T_p are available. Acceptable procedures for determining a_p are provided in *Commentary* Chapter 13.

14.1.5 Seismic Coefficient at Grade

The short-period design spectral acceleration, S_{DS}, considers the site seismicity and local soil conditions. The site seismicity is obtained from the design value maps (or software) and S_{DS} is determined in accordance with *Standard* Section 11.4.4. The coefficient S_{DS} is the used to design the structure. The *Standard* approximates the effective peak ground acceleration as $0.4S_{DS}$, which is why 0.4 appears in *Standard* Equation 13.3-1.

14.1.6 Relative Location Factor

The relative location factor, $\left(1+2\frac{z}{h}\right)$, scales the seismic coefficient at grade, resulting in values varying linearly from 1.0 at grade to 3.0 at roof level. This factor approximates the dynamic amplification of ground acceleration by the supporting structure.

14.1.7 Component Response Modification Factor

The component response modification factor, R_p, represents the energy absorption capability of the component's construction and attachments. In the absence of applicable research, these factors are based on judgment with respect to the following benchmark values:

- R_p = 1.0 or 1.5: brittle or buckling failure mode is expected
- R_p = 2.5: some minimal level of energy dissipation capacity
- R_p = 3.5: ductile materials and detailing
- R_p = 4.5: non-ASME B31 conforming piping and tubing with threaded joints and/or mechanical couplings
- R_p = 6.0: ASME 31 conforming piping and tubing with thread joints and/mechanical couplings
- R_p = 9.0 or 12.0: highly ductile piping and tubing joined with brazing or butt welding

14.1.8 Component Importance Factor

The component importance factor, I_p, represents the greater of the life safety importance and the hazard exposure importance of the component. The factor indirectly accounts for the functionality of the component or structure by requiring design for a lesser amount of inelastic behavior (or higher force

level). It is assumed that a lesser amount of inelastic behavior will result in a component that will have a higher likelihood of functioning after a major earthquake.

14.1.9 Accommodation of Seismic Relative Displacements

The *Standard* requires that seismic relative displacements, D_p, be determined in accordance with several equations. For two connection points on Structure A (or on the same structural system), one at Level *x* and the other at Level *y*, D_p is determined from *Standard* Equation 13.3-5 as follows:

$$D_p = \delta_{xA} - \delta_{yA}$$

Because the computed displacements frequently are not available to the designer of nonstructural components, one may use the maximum permissible structural displacements per *Standard* Equation 13.3-6:

$$D_p = \frac{\left(h_x - h_y\right)}{h_{sx}} \Delta_{aA}$$

For two connection points on Structures A and B (or on two separate structural systems), one at Level *x* *and* the other at Level *y*, D_P is determined from *Standard* Equations 13.3-7 and 13.3-8 as follows:

$$D_p = \left|\delta_{xA}\right| + \left|\delta_{yB}\right|$$

$$D_p = \frac{h_x \Delta_{aA}}{h_{sx}} + \frac{h_y \Delta_{aB}}{h_{sx}}$$

where:

D_p = seismic relative displacement that the component must be designed to accommodate.

δ_{xA} = deflection of building Level *x* of Structure A, determined by an elastic analysis as defined in *Standard* Section 12.8.6 including being multiplied by the C_d factor.

δ_{yA} = deflection of building Level *y* of Structure A, determined in the same fashion as δ_{xA}.

h_x = height of upper support attachment at Level *x* as measured from the base.

h_y = height of lower support attachment at Level *y* as measured from the base.

Δ_{aA} = allowable story drift for Structure A as defined in *Standard* Table 12.2-1.

h_{sx} = story height used in the definition of the allowable drift, Δ_a, in *Standard* Table 12.2-1.

δ_{yB} = deflection of building Level *y* of Structure B, determined in the same fashion as δ_{xA}.

Δ_{aB} = allowable story drift for Structure B as defined in *Standard* Table 12.2-1. Note that Δ_{aA}/h_{sx} = the drift index.

The effects of seismic relative displacements must be considered in combination with displacements caused by other loads as appropriate. Specific methods for evaluating seismic relative displacement effects of components and associated acceptance criteria are not specified in the *Standard*. However, the intention is to satisfy the purpose of the *Standard*. Therefore, for nonessential facilities, nonstructural components can experience serious damage during the design-level earthquake provided they do not constitute a serious life-safety hazard. For essential facilities, nonstructural components can experience some damage or inelastic deformation during the design-level earthquake provided they do not significantly impair the function of the facility.

14.1.10 Component Anchorage Factors and Acceptance Criteria

Design seismic forces in the connected parts, F_p, are prescribed in *Standard* Section 13.4.

Anchors embedded in concrete or masonry are proportioned to carry the least of the following:

- 1.3 times the prescribed seismic design force, or
- The maximum force that can be transferred to the anchor by the component or its support.

The value of R_p used in Section 13.3.1 to determine the forces in the connected part (i.e., the anchor) shall not exceed 1.5 unless at least one of the following conditions is satisfied:

- The component anchorage is designed to be governed by the strength of a ductile steel element.
- The anchorage design of post-installed anchors is tested for seismic application in accordance with the procedures of ACI 355.2 and has a design capacity determined in accordance with ACI 318 Appendix D.
- The anchor is designed in accordance with *Standard* Section 14.2.2.14.

Determination of design seismic forces in anchors must consider installation eccentricities, prying effects, multiple anchor effects and the stiffness of the connected system.

Use of power actuated fasteners is not permitted for seismic design tension forces in Seismic Design Categories D, E and F unless approved for such loading. It should be noted that the term used in previous editions of the *Standard* was “powder” actuated instead of “power” actuated. The term was changed to cover a broader range of fastener types than is implied by “powder-driven”.

Per *Standard* Sections 14.2.2.17 and 14.2.2.18, the design strength of anchors in concrete is to be determined in accordance with ACI 318 Appendix D as modified by these *Standard* Sections.

14.1.11 Construction Documents

Construction documents must be prepared by a registered design professional and must include sufficient detail for use by the owner, building officials, contractors and special inspectors; *Standard* Section 13.2.7 includes specific requirements.

14.2 ARCHITECTURAL CONCRETE WALL PANEL

14.2.1 Example Description

In this example, the architectural components are a 4.5-inch-thick precast normal-weight concrete spandrel panel and a column cover supported by the structural steel frame of a five-story building, as shown in Figures 14.2-1 and 14.2-2.

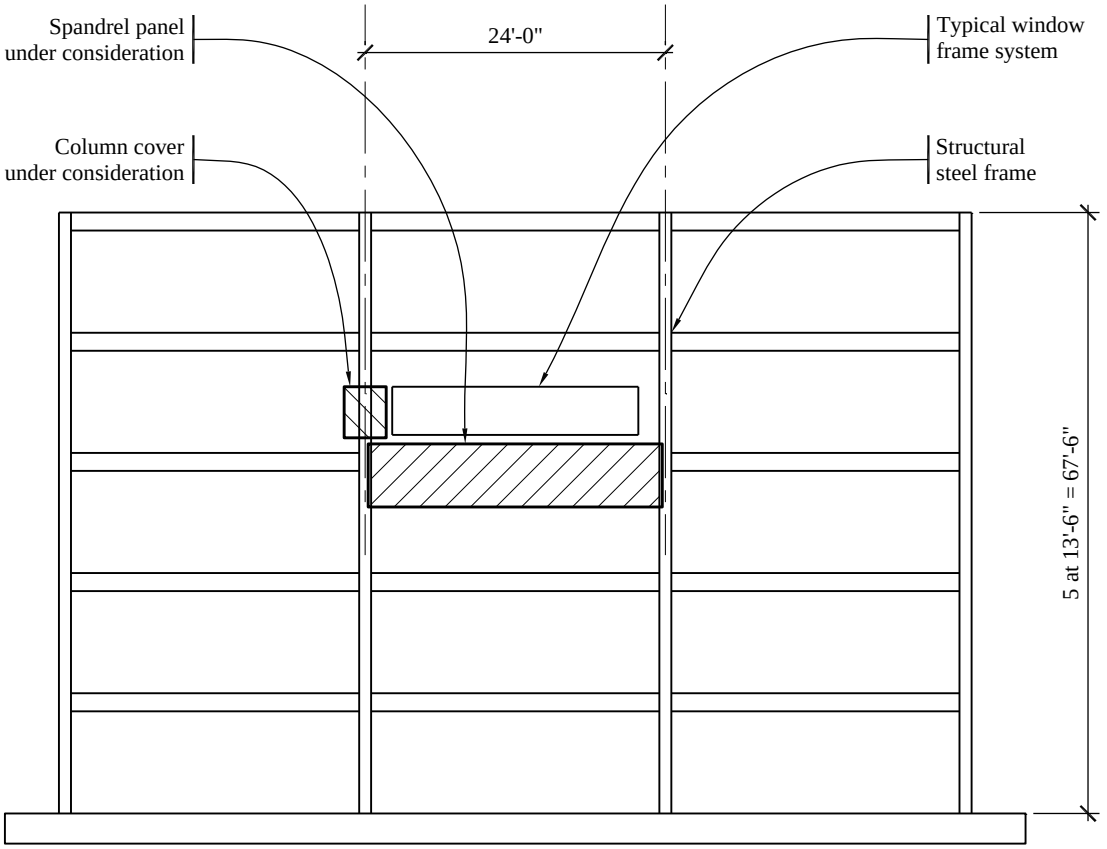

Figure 14.2-1 Five-story building elevation showing panel location
(1.0 ft = 0.3048 m)

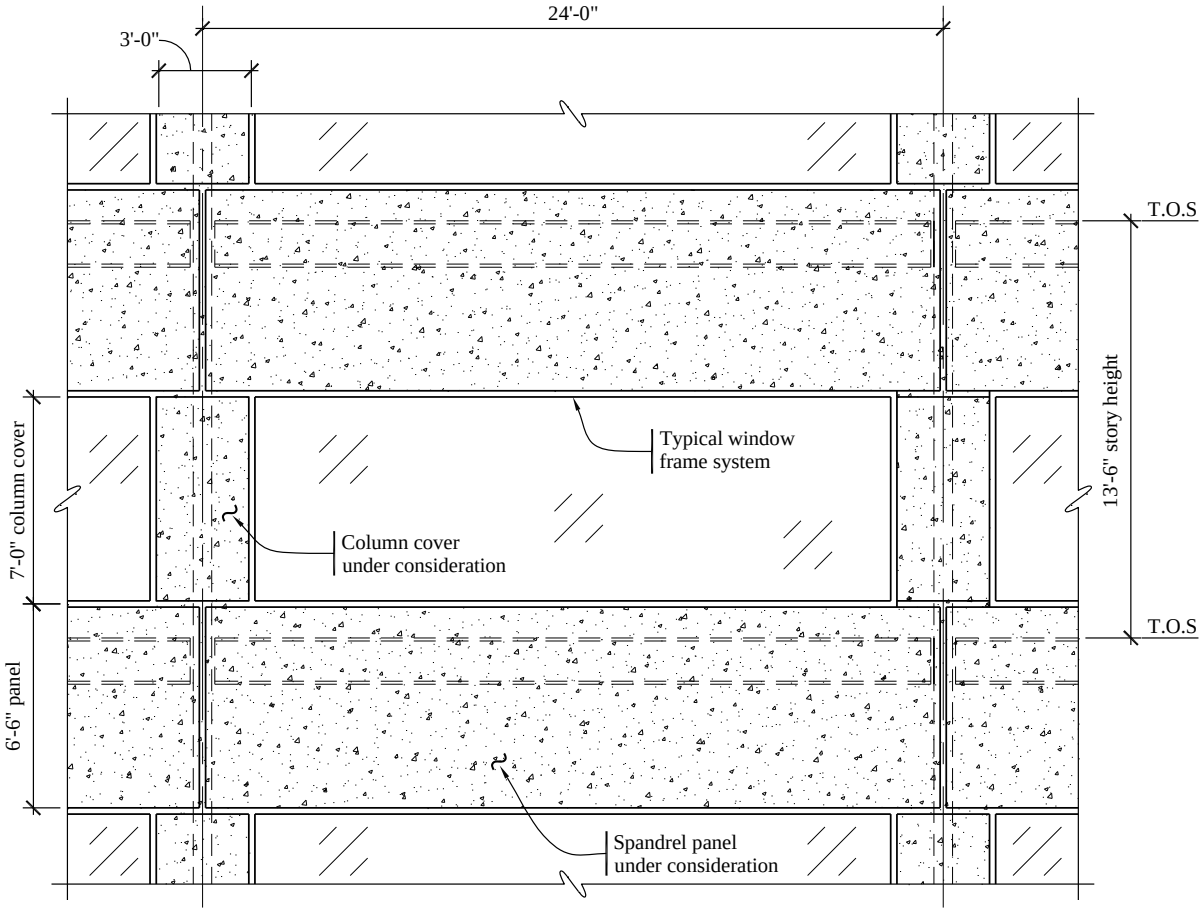

Figure 14.2-2 Detailed building elevation
(1.0 ft = 0.3048 m)

The columns at the third level of the five-story office building support the spandrel panel under consideration. The columns between the third and fourth levels of the building support the column cover under consideration. The building, located near a significant active fault in Los Angeles, California, is assigned to Occupancy Category II. Wind pressures normal to the building are 17 psf, determined in accordance with the *Standard*. The spandrel panel supports glass windows weighing 10 psf.

This example develops prescribed seismic forces for the selected spandrel panel and prescribed seismic displacements for the selected column cover.

It should be noted that details of precast connections vary according to the preferences and local practices of the precast panel supplier. In addition, some connections may involve patented designs. As a result, this example will concentrate on quantifying the prescribed seismic forces and displacements. After the prescribed seismic forces and displacements are determined, the connections can be detailed and designed according to the appropriate AISC and ACI codes and the recommendations of the Precast/Prestressed Concrete Institute (PCI).

14.2.2 Design Requirements

14.2.2.1 *Provisions* parameters and coefficients

a_p = 1.0 for wall panels (*Standard* Table 13.5-1)

a_p = 1.25 for fasteners of the connecting system (*Standard* Table 13.5-1)

S_{DS} = 1.487 (for the selected location and site class) (given)

Seismic Design Category = D (*Standard* Table 11.6-1)

Spandrel panel W_p = (150 lb/ft^3)(24 ft)(6.5 ft)(0.375 ft) = 8,775 lb

Glass W_p = (10 lb/ft^2)(21 ft)(7 ft) = 1,470 lb (supported by spandrel panel)

Column cover W_p = (150 lb/ft^3)(3 ft)(7 ft)(0.375 ft) = 1,181 lb

R_p = 2.5 for wall panels (*Standard* Table 13.5-1)

R_p = 1.0 for fasteners of the connecting system (*Standard* Table 13.5-1)

I_p = 1.0 (*Standard* Sec. 13.1.3)

$$\frac{z}{h} = \frac{40.5 \text{ ft}}{67.5 \text{ ft}} = 0.6$$ (at third floor)

According to *Standard* Section 13.3.1 (and repeated in Section 12.3.4.1 Item 3), the redundancy factor, ρ, does not apply to the design of nonstructural components and therefore may be taken as 1.0 in load combinations where it appears.

14.2.2.2 Performance criteria. Component failure must not cause failure of an essential architectural, mechanical, or electrical component (*Standard* Sec. 13.2.3).

Component seismic attachments must be bolted, welded, or otherwise positively fastened without considering the frictional resistance produced by the effects of gravity (*Standard* Sec. 13.4).

The effects of seismic relative displacements must be considered in combination with displacements caused by other loads as appropriate (*Standard* Sec. 13.3.2).

Exterior nonstructural wall panels that are attached to or enclose the structure must be designed to resist the forces in accordance with *Standard* Section 13.3.1 and must be able to accommodate movements of the structure resulting from response to the design basis ground motion, D_p, or temperature changes (*Standard* Sec. 13.5.3).

14.2.3 Spandrel Panel

14.2.3.1 Connection details. Figure 14.2-3 shows the types and locations of connections that support one spandrel panel.

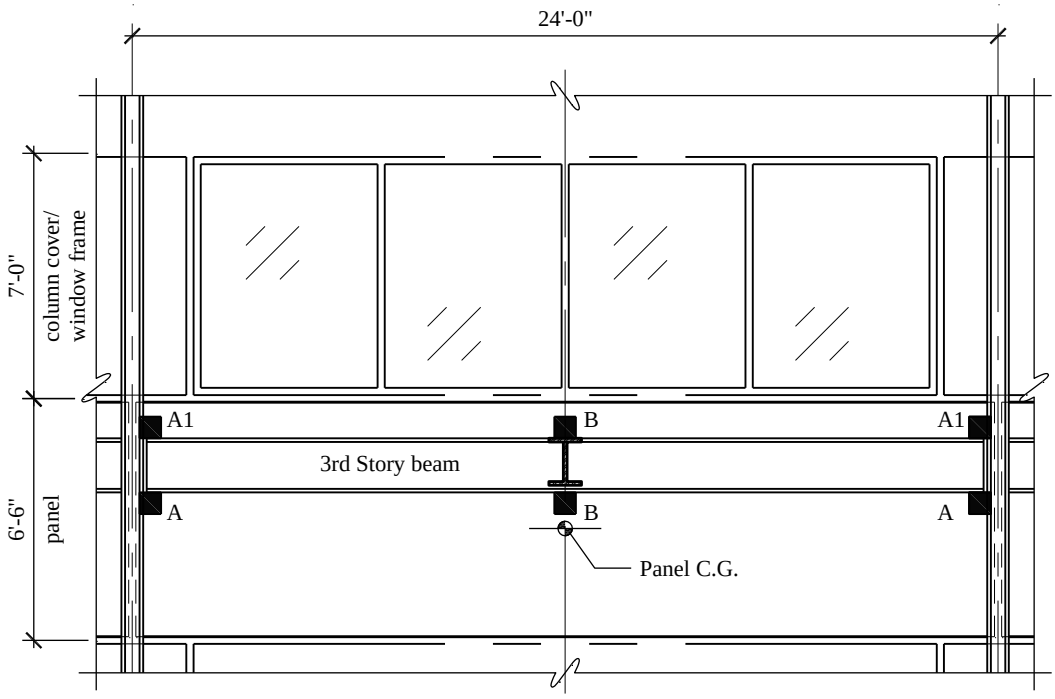

Figure 14.2-3 Spandrel panel connection layout from interior
(1.0 ft = 0.3048 m)

The connection system must resist the weight of the panel and supported construction including the eccentricity between that load and the supports as well as inertial forces generated by response to the seismic motions in all three dimensions. Furthermore, the connection system must not create undue interaction between the structural frame and the panel, such as restraint of the natural shrinkage of the panel or the transfer of floor live load from the beam to the panel. The panels are usually very stiff compared to the frame and this requires careful release of potential constraints at connections. PCI's *Architectural Precast Concrete* (Third Edition, 1989) provides an extended discussion of important design concepts for such panels.

For this example, the basic gravity load and vertical accelerations are resisted at the two points identified as A, which provide the recommended simple and statically determinant system for the main gravity weight. The eccentricity of vertical loads is resisted by a force couple at the two pairs of A1 and A connections. Horizontal loads parallel to the panel are resisted by the A connections. Horizontal loads perpendicular to the panel are resisted by two pairs of A and A1 connections and the pair of midspan B connections. The A connections, therefore, restrain movement in three dimensions while the A1 and B connections restrain movement in only one dimension, perpendicular to the panel. Connection components can be designed to resolve some eccentricities by bending of the element; for example, the eccentricity of the horizontal in-plane force with the structural frame can be resisted by bending the A connection.

The practice of resisting the horizontal in-plane force at two points varies with seismic demand and local industry practice. The option is to resist all of the in-plane horizontal force at one connection in order to avoid restraint of panel shrinkage. The choice made here depends on local experience indicating that

precast panels of this length have been restrained at the two ends without undue shrinkage restraint problems.

The A and A1 connections are often designed to take the loads directly to the columns, particularly on steel moment frames where attachments to the flexural hinging regions of beams are difficult to accomplish. The lower B connection often requires an intersecting beam to provide sufficient stiffness and strength to resist the loads.

The column cover is supported both vertically and horizontally by the column, transfers no loads to the spandrel panel and provides no support for the window frame.

The window frame is supported both vertically and horizontally along the length of the spandrel panel and transfers no loads to the column covers.

14.2.3.2 Prescribed seismic forces. Lateral forces on the wall panels and connection fasteners include seismic loads and wind loads. Design for wind forces is not illustrated here.

14.2.3.2.1 Panels.

$D = W_p$ = 8,775 lb + 1,470 lb = 10,245 lb (vertical gravity effect)

$$F_p = \frac{0.4(1.0)(1.487)(10,245\text{ lb})}{\left(2.5/1.0\right)}\left(1+2(0.6)\right) = 5,362\text{ lb}$$ (*Standard* Eq. 13.3-1)

$$F_{p_{max}} = 1.6(1.487)(1.0)(10,245\text{ lb}) = 24,375\text{ lb}$$ (*Standard* Eq. 13.3-2)

$$F_{p_{min}} = 0.3(1.487)(1.0)(10,245\text{ lb}) = 4,570\text{ lb}$$ (*Standard* Eq. 13.3-3)

$E_h = \rho Q_E$ (*Standard* Eq. 12.4-3)

$E_v = 0.2 S_{DS} D$ (*Standard* Eq. 12.4-4)

where:

Q_E (due to horizontal application of F_p) = 5,362 lb (*Standard* Sec. 12.4.2-1)

ρ = 1.0 (because panels are nonstructural components) (*Standard* Sec 13.3.1)

D = dead load effect (due to vertical load application)

Substituting, the following is obtained:

$E_h = \rho Q_E$ = (1.0)(5,362 lb) = 5,362 lb (horizontal earthquake effect)

$E_v = 0.2 S_{DS} D = 0.2 S_{DS} D$ = (0.2)(1.487)(10,245 lb) = 3,047 lb (vertical earthquake effect)

The above terms are then substituted into the following Basic Load Combinations for Strength Design from Section 12.4.2.3 to determine the design member and connection forces to be used in conjunction with seismic loads.

$(1.2 + 0.2S_{DS})\ D + \rho Q_E + L + 0.2S$ (*Standard* Basic Load Combination 5)

$(0.9 - 0.2S_{DS})\ D + \rho Q_E + 1.6H$ (*Standard* Basic Load Combination 7)

For nonstructural components, the terms *L*, *S* and *H* typically are zero and load combinations with overstrength generally are not applicable.

14.2.3.2.2 Connection fasteners. The *Standard* specifies a reduced R_p and an increased a_p for "fasteners" with the intention of preventing premature failure in those elements of connections that are inherently brittle, such as embedments that depend on concrete breakout strength, or are simply too small to adequately dissipate energy inelastically, such as welds or bolts. The net effect more than triples the design seismic force.

$$F_p = \frac{0.4(1.25)(1.487)(10,245\text{ lb})}{\left(1.0/1.0\right)}\left(1+2\left(0.6\right)\right) = 16,757\text{ lb}$$ (*Standard* Eq. 13.3-1)

$$F_{p_{max}} = 1.6(1.487)(1.0)(10,245\text{ lb}) = 24,375\text{ lb}$$ (*Standard* Eq. 13.3-2)

$$F_{p_{min}} = 0.3(1.487)(1.0)(10,245\text{ lb}) = 4,570\text{ lb}$$ (*Standard* Eq. 13.3-3)

$E_h = \rho Q_E$ (*Standard* Eq. 12.4-3)

$E_v = 0.2S_{DS}D$ (*Standard* Eq. 12.4-4)

where:

Q_E (due to horizontal application of F_p) = 16,757 lb (*Standard* Sec. 12.4.2-1)

ρ = 1.0 (because panels are nonstructural components) (*Standard* Sec 13.3.1)

D = dead load effect (due to vertical load application)

Substituting, the following is obtained:

$E_h = \rho Q_E = (1.0)(16,757\text{ lb}) = 16,757\text{ lb}$ (horizontal earthquake effect)

$E_v = 0.2S_{DS}D = 0.2S_{DS}D = (0.2)(1.487)(10,245\text{ lb}) = 3,047\text{ lb}$ (vertical earthquake effect)

The above terms are then substituted into the following Basic Load Combinations for Strength Design from Section 12.4.2.3 to determine the design member and connection forces to be used in conjunction with seismic loads.

$(1.2 + 0.2S_{DS})\ D + \rho Q_E + L + 0.2S$ (*Standard* Basic Load Combination 5)

$(0.9 - 0.2S_{DS})\ D + \rho Q_E + 1.6H$ (*Standard* Basic Load Combination 7)

For precast panels, the terms *L, S and H* typically are zero. Load combinations with overstrength generally are not applicable to nonstructural components.

14.2.3.3 Proportioning and design.

14.2.3.3.1 Panels. The wall panels should be designed for the following loads in accordance with ACI 318. The design of the reinforced concrete panel is standard and is not illustrated in this example. Spandrel panel moments are shown in Figure 14.2-4. Reaction shears (V_u), forces (H_u) and moments (M_u) are calculated for applicable strength load combinations.

For this example, the values of *F*, *L*, *S and H* are assumed to be zero.

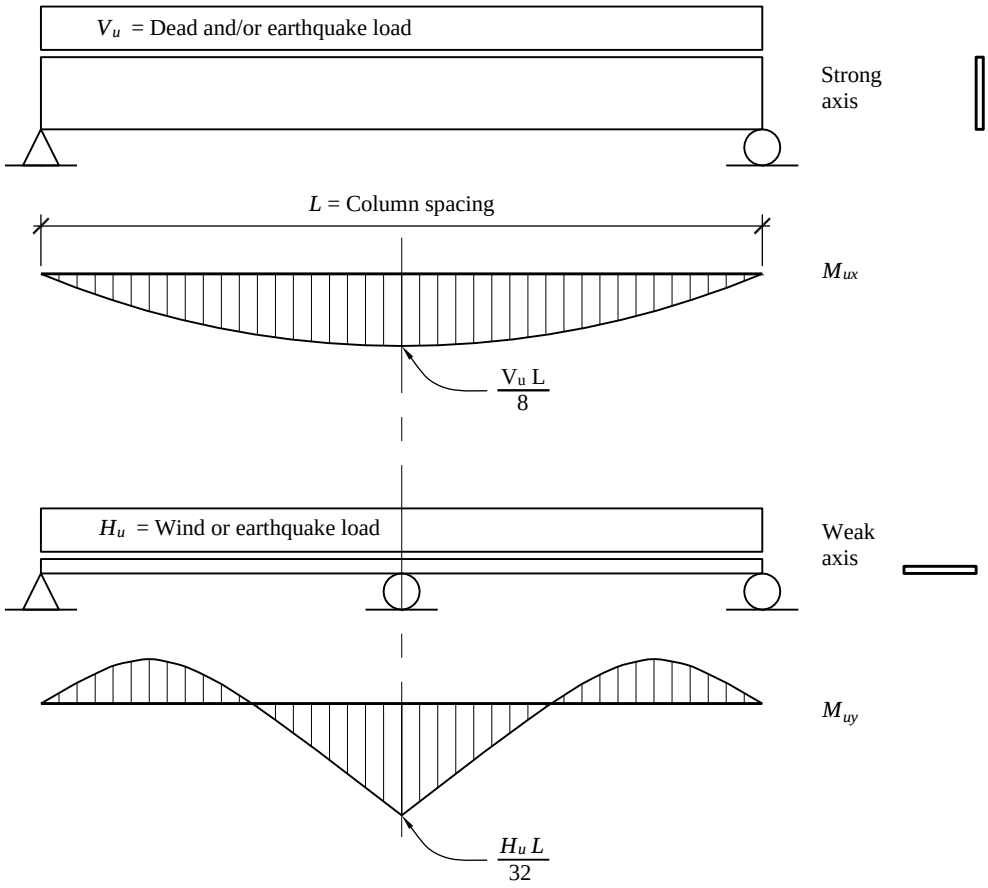

Figure 14.2-4 Spandrel panel moments

Standard Basic Load Combination 1: $1.4(D + F)$ (from *Standard* Sec. 2.3.2)

$V_u = 1.4(10{,}245 \text{ lb}) = 14{,}343 \text{ lb}$ (vertical load downward)

$$M_{ux} = \frac{(14{,}343 \text{ lb})(24 \text{ ft})}{8} = 43{,}029 \text{ ft-lb}$$ (strong axis moment)

Standard Basic Load Combination 5: $(1.2 + 0.2S_{DS})\,D + \rho Q_E + L + 0.2S$

V_{umax} = [1.2 + 0.2(1.487)] (10,245 lb) = 15,341 lb (vertical load downward)

$\Leftrightarrow H_u = 1.0(5{,}362 \text{ lbs}) = 5{,}362$ lb (horizontal load parallel to panel)

$\perp H_u = 1.0(5{,}362 \text{ lbs}) = 5{,}362$ lb (horizontal load perpendicular to panel)

$$M_{ux_{max}} = \frac{(15{,}341 \text{ lb})(24 \text{ ft})}{8} = 46{,}023 \text{ ft-lb}$$ (strong axis moment)

$$M_{uy} = \frac{(5{,}362 \text{ lb})(24 \text{ ft})}{32} = 4{,}022 \text{ ft-lb}$$ (weak axis moment)

Standard Basic Load Combination 7: $(0.9 - 0.2S_{DS})\,D + \rho Q_E + 1.6H$

V_{umin} = [1.2 – 0.2(1.487)] (10,245 lb) = 6,174 lb (vertical load downward)

$\Leftrightarrow H_u = 1.0(5{,}362 \text{ lb}) = 5{,}362$ lb (horizontal load parallel to panel)

$\perp H_u = 1.0(5{,}362 \text{ lb}) = 5{,}362$ lb (horizontal load perpendicular to panel)

$$M_{ux_{min}} = \frac{(6{,}174 \text{ lb})(24 \text{ ft})}{8} = 18{,}522 \text{ ft-lb}$$ (strong axis moment)

$$M_{uy} = \frac{(5{,}362 \text{ lb})(24 \text{ ft})}{32} = 4{,}022 \text{ ft-lb}$$ (weak axis moment)

14.2.3.3.2 Connection fasteners. The connection fasteners should be designed for the following loads in accordance with ACI 318 (Appendix D) and the AISC specification. There are special reduction factors for anchorage in high seismic demand locations and those reduction factors would apply to this example. The design of the connection fasteners is not illustrated in this example. Spandrel panel connection forces are shown in Figure 14.2-5. Reaction shears (V_u), forces (H_u) and moments (M_u) are calculated for applicable strength load combinations.

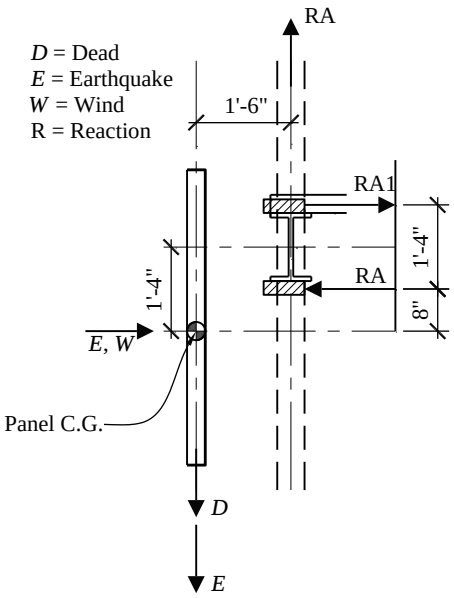

Figure 14.2-5 Spandrel panel connection forces

Standard Basic Load Combination 1: $1.4(D + F)$ (from *Standard* Section 2.3.2)

$$V_{uA} = \frac{1.4(10,245 \text{ lb})}{2} = 7,172 \text{ lb}$$ (vertical load downward at Points A and A1)

M_{uA} = (7,172 lb)(1.5 ft) = 10,758 ft-lb (moment resisted by paired Points A and A1)

Horizontal couple from moment at A and A1 = 10758 / 1.33 = 8071 lb

Standard Basic Load Combination 5: $(1.2 + 0.2S_{DS})\,D + \rho Q_E + L + 0.2S$

$$V_{uA\max} = \frac{[1.2 + 0.2(1.487)]\ (10,245 \text{ lb})}{2} = 7,671 \text{ lb}$$ (vertical load downward at Point A)

$$\perp H_{uA} = 1.0(16,757 \text{ lb})\frac{3}{16} = 3,142 \text{ lb}$$ (horizontal load perpendicular to panel at Points A and A1)

H_{Ain} = (7,671 lb)(1.5 ft) / (1.33 ft) + (3142 lb)(2.0 ft) / (1.33 ft) = 13366 lb (inward force at Point A)

H_{A1out} = (7671 lb)(1.5 ft) / (1.33 ft) + (3,142 lb)(0.67) / (1.33 ft) = 10222 lb(outward force at Point A1)

$$\Leftrightarrow H_{uA} = \frac{1.0(16,757 \text{ lb})}{2} = 8,378 \text{ lb}$$ (horizontal load parallel to panel at Point A)

M_{u2A} = (8,378 lb)(1.5 ft) = 12,568 ft-lb (flexural moment at Point A)

$$\perp H_{uB} = 1.0(16{,}757 \text{ lb})\frac{5}{8} = 10{,}473 \text{ lb}$$ (horizontal load perpendicular to panel at Points B and B1)

H_B = (10,743 lb)(2.0 ft) / (1.33 ft) = 15,714 lb (inward or outward force at Point B)

H_{B1} = (10,473 lb)(0.67 ft) / (1.33 ft) = 5,237 lb (inward or outward force at Point B1)

Standard Basic Load Combination 7: $(0.9 - 0.2S_{DS})\,D + \rho Q_E + 1.6H$

$$V_{uA\min} = \frac{\left[1.2 - 0.2\left(1.487\right)\right]\left(10{,}245 \text{ lb}\right)}{2} = 3{,}086 \text{ lb}$$ (vertical load downward at Point A)

Horizontal forces are the same as combination $1.2D + 1.0E$. No uplift occurs; the net reaction at Point A is downward. Maximum forces are controlled by prior combination. It is important to realize that inward and outward acting horizontal forces generate different demands where the connections are eccentric to the center of mass, as in this example. Only the maximum reactions are computed above.

14.2.3.4 Prescribed seismic displacements. Prescribed seismic displacements are not applicable to the building panel because all connections are at essentially the same elevation.

14.2.4 Column Cover

14.2.4.1 Connection details. Figure 14.2-6 shows the key to the types of forces resisted at each column cover connection.

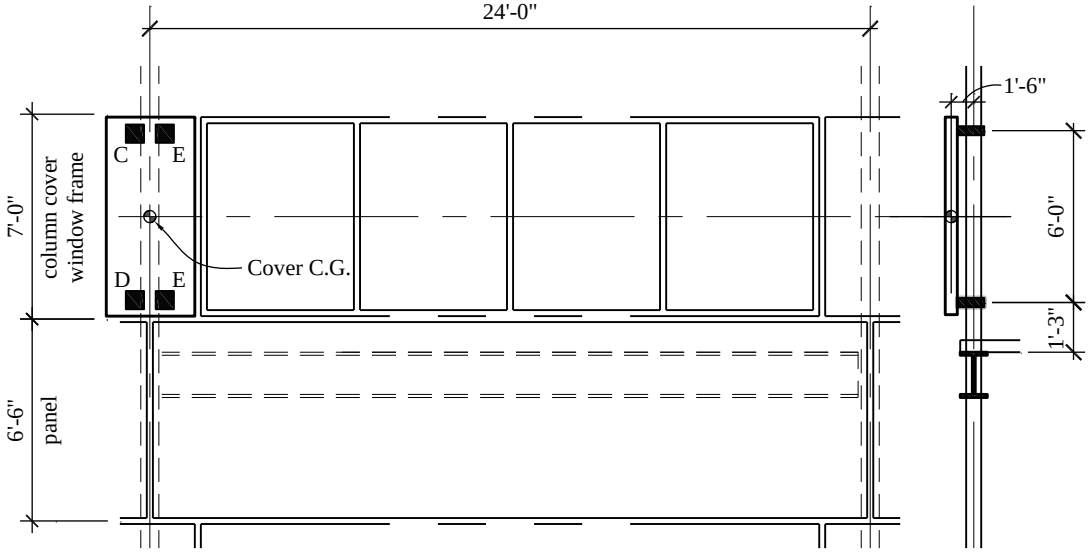

Figure 14.2-6 Column cover connection layout
(1.0 ft = 0.3048 m)

Vertical loads, horizontal loads parallel to the panel and horizontal loads perpendicular to the panel are resisted at Point C. The eccentricity of vertical loads is resisted by a force couple at Points C and D. The horizontal load parallel to the panel eccentricity between the panel and the support is resisted in flexure of the connection. The connection is designed to take the loads directly to the columns.

Horizontal loads parallel to the panel are all resisted at Point D. The vertical load eccentricity between the panel and the support is resisted by a force couple of Points C and D. The eccentricity of horizontal loads parallel to the panel is resisted by flexure at the connection. The connection is designed to not restrict vertical movement of the panel due to thermal effects or seismic input. The connection is designed to take the loads directly to the columns.

Horizontal loads perpendicular to the panel are resisted equally at Points C and D and the two points identified as E. The connections are designed to take the loads directly to the columns.

There is no load eccentricity associated with the horizontal loads perpendicular to the panel.

In this example, all connections are made to the sides of the column because usually there is not enough room between the outside face of the column and the inside face of the cover to allow a feasible load-carrying connection.

14.2.4.2 Prescribed seismic forces. Calculation of prescribed seismic forces for the column cover is not shown in this example. They should be determined in the same manner as illustrated for the spandrel panels.

14.2.4.3 Prescribed seismic displacements. The results of an elastic analysis of the building structure usually are not available in time for use in the design of the precast cladding system. As a result, prescribed seismic displacements usually are calculated based on allowable story drift requirements:

h_{sx} = story height = 13’-6”

h_x = height of upper support attachment = 47’-9”

h_y = height of lower support attachment = 41’-9”

$\Delta_{aA} = 0.020 h_{sx}$ (*Standard* Table 12.12-1)

$$D_{pmax} = \frac{(h_x - h_y)\Delta_{aA}}{h_{sx}} = \frac{(72 \text{ in.})0.020 h_{sx}}{h_{sx}} = 1.44 \text{ in.}$$ (*Standard* Eq. 13.3-6)

The joints at the top and bottom of the column cover must be designed to accommodate an in-plane relative displacement of 1.44 inches. The column cover will rotate somewhat as these displacements occur, depending on the nature of the connections to the column. If the supports at one level are “fixed” to the columns while the other level is designed to “float,” then the rotation will be that of the column at the point of attachment.

14.2.5 Additional Design Considerations

14.2.5.1 Window frame system. The window frame system is supported by the spandrel panels above and below. Assuming that the spandrel panels move rigidly in-plane with each floor level, the window frame system must accommodate a prescribed seismic displacement based on the full story height.

$$D_{pmax} = \frac{(h_x - h_y)\Delta_{aA}}{h_{sx}} = \frac{(162 \text{ in.})0.020h_{sx}}{h_{sx}} = 3.24 \text{ in.} \quad \text{(Standard Eq. 13.3-6)}$$

The window frame system must be designed to accommodate an in-plane relative displacement of 3.24 inches between the supports. Normally this is accommodated by a clearance between the glass and the frame. *Standard* Section 13.5.9.1 prescribes a method of checking such a clearance. It requires that the clearance be large enough so that the glass panel will not fall out of the frame unless the relative seismic displacement at the top and bottom of the panel exceeds 125 percent of the predicted value amplified by the building importance factor. If h_p and b_p are the respective height and width of individual panes and if the horizontal and vertical clearances are designated c_1 and c_2, respectively, then the following expression applies:

$$D_{clear} = 2c_1\left(1 + \frac{h_p c_2}{b_p c_1}\right) \geq 1.25D_p \quad \text{(Standard Sec. 13.5.9.1)}$$

For h_p = 7 feet, b_p = 5 feet and D_p = 3.24 inches and setting $c_1 = c_2$, the required clearance is 0.84 inch.

14.2.5.2 Building corners. Some thought needs to be given to seismic behavior at external building corners. The preferred approach is to detail the corners with two separate panel pieces, mitered at a 45 degree angle, with high grade sealant between the sections. An alternative choice of detailing L-shaped corner pieces would introduce more seismic mass and load eccentricity into connections on both sides of the corner column.

14.2.5.3 Dimensional coordination. It is important to coordinate dimensions with the architect and structural engineer. Precast concrete panels must be located a sufficient distance from the building structural frame to allow room for the design of efficient load transfer connection pieces. However, distances must not be so large as to increase unnecessarily the load eccentricities between the panels and the frame.

14.3 HVAC FAN UNIT SUPPORT

14.3.1 Example Description

In this example, the mechanical component is a 4-foot-high, 5-foot-wide, 8-foot-long, 3,000-pound HVAC fan unit that is supported on the two long sides near each corner (Figure 14.3-1). The component is located at the roof level of a five-story office building, near a significant active fault in Los Angeles, California. The building is assigned to Occupancy Category II. Two methods of attaching the component to the 4,000 psi, normal-weight roof slab are considered, as follows:

- Direct attachment to the structure with 36 ksi, carbon steel, cast-in-place anchors.
- Support on vibration isolation springs that are attached to the slab with 36 ksi, carbon steel, post-installed expansion anchors. The nominal gap between the vibration spring seismic restraints and the base frame of the fan unit is presumed to be greater than 0.25 in.

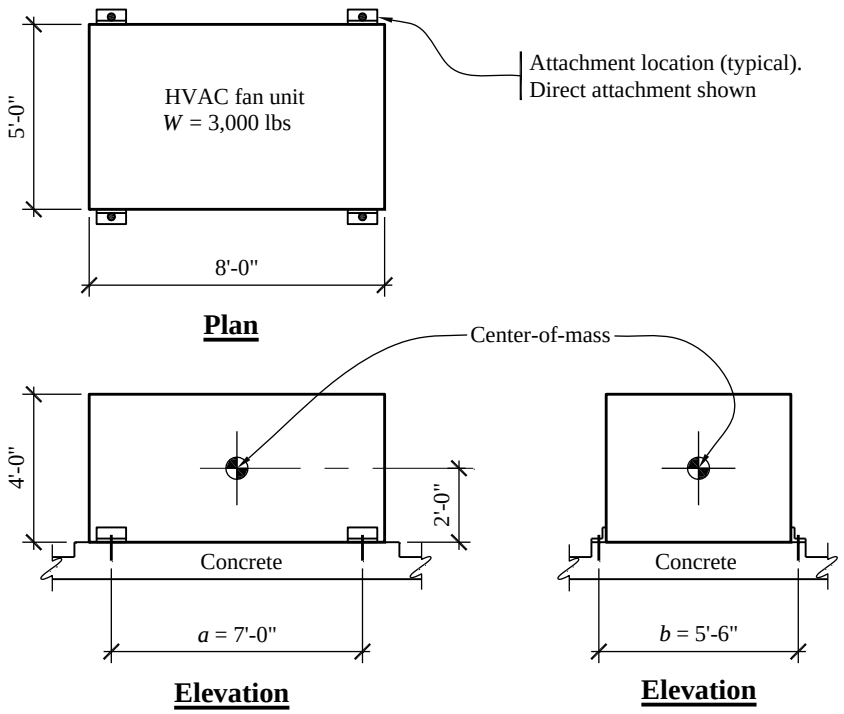

Figure 14.3-1 HVAC fan unit
(1.0 ft = 0.3048 m, 1.0 lb = 4.45 N)

14.3.2 Design Requirements

14.3.2.1 Seismic design parameters and coefficients.

a_p = 2.5 for both direct attachment and spring isolated (*Standard* Table 13.6-1)

a_p = 2.5 (*Standard* Table 13.6-1)

S_{DS} = 1.487 (for the selected location and site class) (given)

Seismic Design Category = D (*Standard* Table 11.6-1)

W_p = 3,000 lb (given)

R_p = 6.0 for HVAC fans, directly attached (not vibration isolated) (*Standard* Table 13.6-1)

R_p = 2.0 for spring isolated components with restraints (*Standard* Table 13.6-1)

R_p = 1.5 for anchors in concrete or masonry unless criteria of *Standard* Section 13.4.2 are satisfied

I_p = 1.0 (*Standard* Sec. 13.1.3)

z/h = 1.0 (for roof-mounted equipment)

14.3.2.2 Performance criteria. Component failure should not cause failure of an essential architectural, mechanical, or electrical component (*Standard* Sec. 13.2.3).

Component seismic attachments must be bolted, welded, or otherwise positively fastened without consideration of frictional resistance produced by the effects of gravity (*Standard* Sec. 13.4).

Anchors embedded in concrete or masonry must be proportioned to carry the lesser of (a) 1.3 times the force in the component and its supports due to the prescribed forces and (b) the maximum force that can be transferred to the anchor by the component and its supports (*Standard* Sec. 13.4.2).

Attachments and supports transferring seismic loads must be constructed of materials suitable for the application and must be designed and constructed in accordance with a nationally recognized structural standard (*Standard* Sec. 13.6.5).

Components mounted on vibration isolation systems must have a bumper restraint or snubber in each horizontal direction. Vertical restraints must be provided where required to resist overturning. Isolator housings and restraints must also be constructed of ductile materials. A viscoelastic pad, or similar material of appropriate thickness, must be used between the bumper and equipment item to limit the impact load (*Standard* Table 13.6-1, footnote b). Such components also must resist doubled seismic design forces if the nominal clearance (air gap) between the equipment support frame and restraints is greater than 0.25 in. (*Standard* Table 13.6-1, footnote b).

14.3.3 Direct Attachment to Structure

This section illustrates design for cast-in-place concrete anchors that satisfies the requirements of ACI 318, Appendix D, where the component anchorage embedment strength is greater than the strength capacity of the ductile steel anchorage element. Therefore, the R_p of the component (R_p = 6) can be used for the component anchorage design.

14.3.3.1 Prescribed seismic forces. See Figure 14.3-2 for a free-body diagram for seismic force analysis.

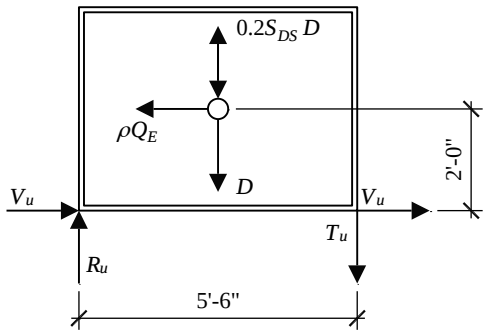

Figure 14.3-2 Free-body diagram for seismic force analysis
(1.0 ft = 0.348 m)

$$F_p = \frac{0.4(2.5)(1.487)(3{,}000\ \text{lb})}{(6.0/1.0)}\left[1 + 2(1)\right] = 2{,}231\ \text{lb} \qquad \text{(}\textit{Standard}\text{ Eq. 13.3-1)}$$

$F_{p_{max}} = 1.6(1.487)(1.0)(3{,}000 \text{ lb}) = 7{,}138 \text{ lb}$ (*Standard* Eq. 13.3-2)

$F_{p_{min}} = 0.3(1.487)(1.0)(3{,}000 \text{ lb}) = 1{,}338 \text{ lb}$ (*Standard* Eq. 13.3-3)

Since F_p is greater the F_{pmin} and less than F_{pmax}, the value determined from Equation 13.3-1 applies.

$E_h = \rho Q_E$ (*Standard* Eq. 12.4-3)

$E_v = 0.2 S_{DS} D$ (*Standard* Eq. 12.4-4)

where:

Q_E (due to horizontal application of F_p) = 2,231 lb (*Standard* Sec. 12.4.2-1)

ρ = 1.0 (HVAC units are nonstructural components) (*Standard* Sec. 13.3.1)

D = dead load effect (due to vertical load application)

Substituting, one obtains:

$E_h = \rho Q_E = (1.0)(2{,}231 \text{ lb}) = 2{,}231 \text{ lb}$ (horizontal earthquake effect)

$E_v = 0.2 S_{DS} D = 0.2 S_{DS} D = (0.2)(1.487)(3{,}000 \text{ lb}) = 892 \text{ lb}$ (vertical earthquake effect)

The above terms are then substituted into the following Basic Load Combinations for Strength Design of Section 12.4.2.3 to determine the design member and connection forces to be used in conjunction with seismic loads.

$(1.2 + 0.2 S_{DS})\, D + \rho Q_E + L + 0.2 S$ (*Standard* Basic Load Combination 5)

$(0.9 - 0.2 S_{DS})\, D + \rho Q_E + 1.6 H$ (*Standard* Basic Load Combination 7)

Based on the free-body diagram, the seismic load effects can be used to determine bolt shear, V_u and tension, T_u (where a negative value indicates tension). In the calculations below, the signs of S_{DS} and F_p have been selected to result in the largest value of T_u.

$U = (1.2 + 0.2 S_{DS})\, D + \rho Q_E$

$$V_u = \frac{1.0\ (2{,}231 \text{ lb})}{4 \text{ bolts}} = 558 \text{ lb/bolt}$$

$$T_u = \frac{\left[1.2 - 0.2\left(1.487\right)\right]\ \left(3{,}000 \text{ lb}\right)\left(2.75 \text{ ft}\right) - 1.0\ \left(2{,}231\right)\ \left(2 \text{ ft}\right)}{(5.5 \text{ ft})(2 \text{ bolts})} = 299 \text{ lb/bolt (no tension)}$$

$U = (0.9 - 0.2 S_{DS}) D + \rho Q_E$

$$V_u = \frac{1.0\ (2{,}231\ \text{lb})}{4\ \text{bolts}} = 558\ \text{lb/bolt}$$

$$T_u = \frac{\left[0.9 - 0.2\left(1.487\right)\right]\ \left(3{,}000\ \text{lb}\right)\left(2.75\ \text{ft}\right) - 1.0\ \left(2{,}231\ \text{lb}\right)\ \left(2\ \text{ft}\right)}{(5.5\ \text{ft})(2\ \text{bolts})} = 46\ \text{lb/bolt (no tension)}$$

14.3.3.2 Proportioning and design. See Figure 14.3-3 for anchor for direct attachment to structure.

Check one 1/4-inch-diameter cast-in-place anchor embedded 2 inches into the concrete slab with no transverse reinforcing engaging the anchor and extending through the failure surface. Although there is no required tension strength on these anchors, design strengths and tension/shear interaction acceptance relationships are calculated to demonstrate the use of the *Standard* equations.

Assume the following material properties have been specified for the concrete slab and anchors:

f_c' = 4,000 psi, normal weight concrete, λ = 1.0, with no supplementary anchor reinforcing provided

$A_{se,N} = A_{se,V} = 0.032\ \text{in}^2$

f_y = 36,000 psi (ductile steel)

f_{uta} = 58,000 psi

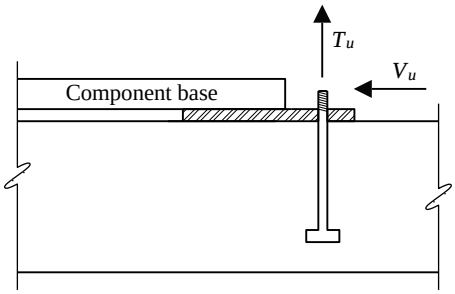

Figure 14.3-3 Anchor for direct attachment to structure

14.3.3.2.1 Design tension strength on isolated anchor in slab, away from edge, loaded concentrically.

Tension capacity of steel, ϕ = 0.75 (ductile steel element):

$$\phi N_{sa} = \phi A_{se,N} F_{uta} = 0.75(0.032\ \text{in}^2)(58{,}000\ \text{psi}) = 1{,}392\ \text{lb} \qquad \text{(ACI 318-08 Eq. D-1, D-3)}$$

Tension capacity of concrete, ϕ = 0.70 and apply an additional 0.75 factor to determine seismic concrete capacities as required by Sections D.3.3 and D.3.3.3 of ACI 318-08. Also assume configuration is such that there is no eccentricity, no pull-through and no edge or group effect:

$$0.75\phi N_b = 0.75\phi k_c \lambda \sqrt{f_c'} h_{ef}^{1.5} = 0.75(0.70)24(1.0)\sqrt{4{,}000}(2^{1.5}) = 2{,}254\ \text{lb} \qquad \text{(ACI 318-08 Eq. D-1, D-7)}$$

The steel capacity controls in tension, so Section D.3.3.4 of ACI 318-08 is satisfied, but since there is no tension demand, the point is moot.

14.3.3.2.2 Design shear strength on isolated anchor, away from edge.

Shear capacity of steel, $\phi = 0.65$ (ductile steel element):

$$\phi V_{sa} = \phi\, 0.6 A_{se,V} F_{uta} = 0.65(0.6)(0.032 \text{ in}^2)(58{,}000 \text{ psi}) = 724 \text{ lb} \qquad \text{(ACI 318-08 Eq. D-1, D-19)}$$

Shear capacity of concrete, far from edge, limited to pry-out, no supplementary reinforcing, $\phi = 0.70$:

$$\phi V_{cp} = \phi\, k_{cp} N_{cb} = \phi\, k_{cp} N_{sa} = \phi\, k_{cp} A_{se,N} f_{uta} \qquad \text{(ACI 318-08 Eq. D-1, D-4, D-30)}$$

$$\phi V_{cp} = 0.70(1.0)(0.032 \text{ in}^2)(58{,}000 \text{ psi}) = 1{,}299 \text{ lb}$$

The steel capacity controls in shear, with $\phi V_N = \phi V_{sa} = 724$ lb.

Per *Standard* Section 13.4.2, anchors embedded in concrete or masonry must be proportioned to carry at least 1.3 times the force in the connected part due to the prescribed forces. Thus, $V_u = 1.3(558) =$ 725 pounds, so the anchor is inadequate (mathematically), but would be deemed acceptable given the practical precision of engineering design.

14.3.3.2.3 Combined tension and shear. ACI 318-08 provides an equation (Eq. D-29) for the interaction of tension and shear on an anchor or a group of anchors:

$$\frac{N_u}{\phi N_N} + \frac{V_u}{\phi V_N} \le 1.2 \text{, which applies where either term exceeds 0.2}$$

Since the tension demand, N_u, is zero, by inspection, this equation is also satisfied.

14.3.3.2.3 Summary. At each corner of the component, provide one 1/4-inch-diameter cast-in-place anchor embedded 2 inches into the concrete slab. Transverse reinforcement engaging the anchor and extending through the failure surface is not necessary.

14.3.4 Support on Vibration Isolation Springs

14.3.4.1 Prescribed seismic forces. Design forces for vibration isolation springs with the seismic stop gap clearance presumed to be greater than 1/4 inch are determined by an analysis of earthquake forces applied in a diagonal horizontal direction as shown in Figure 14.3-4. Terminology and concept are taken from ASHRAE APP IP. In the equations below, $F_{pv} = E_v = 0.2 S_{DS} W_p$:

Angle of diagonal loading:

$$\theta = \tan^{-1}\left(\frac{b}{a}\right) \qquad \text{(ASHRAE APP IP Eq. 17)}$$

Tension per isolator:

$$T_u = \frac{W_p - F_{pv}}{4} - \frac{F_p h}{2}\left(\frac{\cos\theta}{b} + \frac{\sin\theta}{a}\right) \qquad \text{(ASHRAE APP IP Eq. 18)}$$

Compression per isolator:

$$C_u = \frac{W_p + F_{pv}}{4} + \frac{F_p h}{2}\left(\frac{\cos\theta}{b} + \frac{\sin\theta}{a}\right) \qquad \text{(ASHRAE APP IP Eq. 19)}$$

Shear per isolator:

$$V_u = \frac{F_p}{4} \qquad \text{(ASHRAE APP IP Eq. 20)}$$

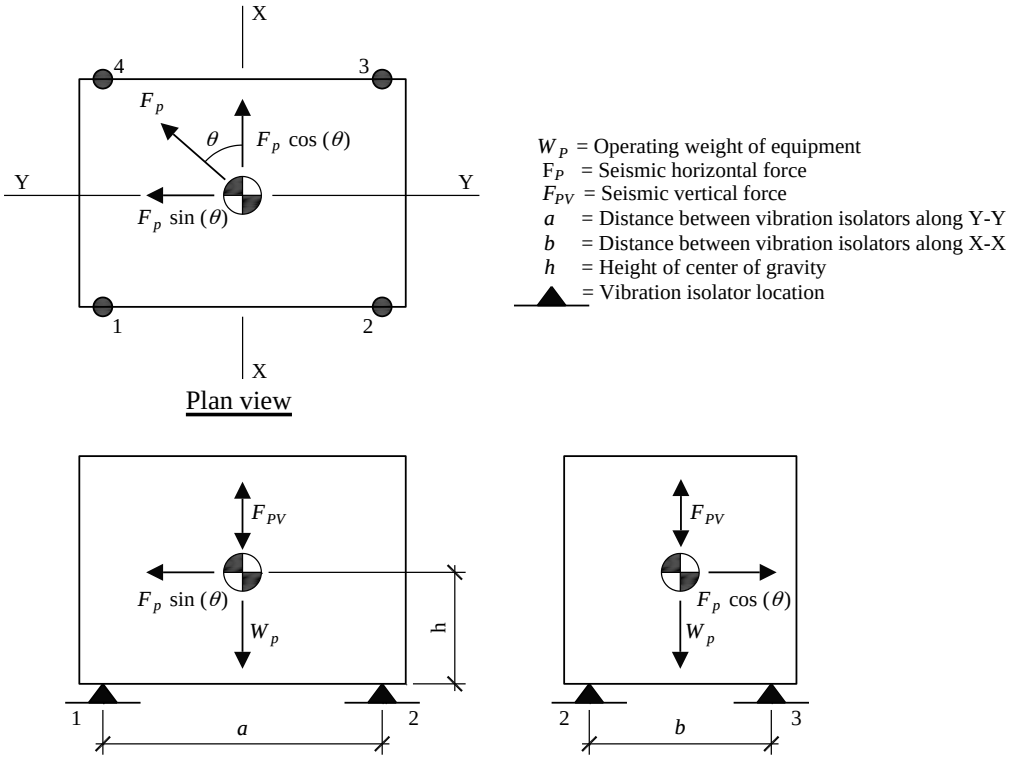

Figure 14.3-4 ASHRAE diagonal seismic force analysis for vibration isolation springs

Select the worst-case assumption. Design for post-installed expansion anchors, requiring the use of R_p = 2.0 and nominal clearance between equipment and restraint greater than 1/4 inch.

$$F_p = \frac{0.4(2.5)(1.487)\left(3{,}000 \text{ lb}\right)}{(2.0/1.0)}\left(1 + 2(1)\right) = 6{,}692 \text{ lb} \qquad \text{(}\textit{Standard}\text{ Eq. 13.3-1)}$$

$F_{p_{max}} = 1.6(1.487)(1.0)(3{,}000 \text{ lb}) = 7{,}138 \text{ lb}$ (*Standard* Eq.13.3-2)

$F_{p_{min}} = 0.3(1.487)(1.0)(3{,}000 \text{ lb}) = 1{,}338 \text{ lb}$ (*Standard* Eq. 13.3-3)

Components mounted on vibration isolation systems must have a bumper restraint or snubber in each horizontal direction. Per *Standard* Table 13.6-1, footnote b, the design force must be taken as $2F_p$ if nominal clearance (air gap) between equipment and seismic restraint is greater than 0.25 inch.

$Q_E = 2F_p = 2(6{,}692 \text{ lb}) = 13{,}384 \text{ lb}$ (*Standard* Sec. 6.1.3)

$\rho = 1.0$ (HVAC units are nonstructural components) (*Standard* Sec. 13.3.1)

$\rho Q_E = (1.0)(13{,}384 \text{ lb}) = 13{,}384 \text{ lb}$ (horizontal earthquake effect)

$F_{pv(\text{ASHRAE})} = 0.2S_{DS}D = (0.2)(1.487)(3{,}000 \text{ lb}) = 892 \text{ lb}$ (vertical earthquake effect)

$D = W_p = 3{,}000 \text{ lb}$ (vertical gravity effect)

The above terms are then substituted into the Basic Load Combinations for Strength Design of Section 12.4.2.3 to determine the design member and connection forces to be used in conjunction with seismic loads.

$(1.2 + 0.2S_{DS})\,D + \rho Q_E + L + 0.2S$ (*Standard* Basic Load Combination 5)

$(0.9 - 0.2S_{DS})\,D + \rho Q_E + 1.6H$ (*Standard* Basic Load Combination 7)

These seismic load effects can be used to determine bolt shear, V_u and tension, T_u (where a negative value indicates tension). In the calculations below, the signs of S_{DS} and F_p have been selected to result in the largest value of T_u.

$U = (1.2 + 0.2S_{DS})D + \rho Q_E$

$$T_u = \frac{1.2(3{,}000 \text{ lb}) - (892 \text{ lb})}{4} - \frac{(13{,}384 \text{ lb})(2 \text{ ft})}{2}\left[\frac{\cos(51.8 \text{ deg})}{7 \text{ ft}} + \frac{\sin(51.8 \text{ deg})}{5.5 \text{ ft}}\right] = -2{,}405 \text{ lb}$$

$$C_u = \frac{1.2(3{,}000 \text{ lb}) + (892 \text{ lb})}{4} + \frac{(13{,}384 \text{ lb})(2 \text{ ft})}{2}\left[\frac{\cos(51.8 \text{ deg})}{7 \text{ ft}} + \frac{\sin(51.8 \text{ deg})}{5.5 \text{ ft}}\right] = 4{,}204 \text{ lb}$$

$$V_u = \frac{13{,}384 \text{ lb}}{4} = 3{,}346 \text{ lb}$$

$U = (0.9 - 0.2S_{DS})D + \rho Q_E$

$$\theta = \tan^{-1}\left(\frac{7 \text{ ft}}{5.5 \text{ ft}}\right) = 51.8^{\circ}$$

$$T_u = \frac{0.9(3{,}000\text{ lb}) - (892\text{ lb})}{4} - \frac{(13{,}384\text{ lb})(2\text{ ft})}{2}\left[\frac{\cos(51.8\text{ deg})}{7\text{ ft}} + \frac{\sin(51.8\text{ deg})}{5.5\text{ ft}}\right] = 2{,}630\text{ lb}$$

$$C_u = \frac{0.9(3{,}000\text{ lb}) + (892\text{ lb})}{4} + \frac{(13{,}384\text{ lb})(2\text{ ft})}{2}\left[\frac{\cos(51.8\text{ deg})}{7\text{ ft}} + \frac{\sin(51.8\text{ deg})}{5.5\text{ ft}}\right] = -3{,}980\text{ lb}$$

$$V_u = \frac{13{,}384\text{ lb}}{4} = 3{,}346\text{ lb}$$

Note that the above values need to be multiplied by 1.3 per Section 13.4.2 to obtain the design values to be compared with design capacities. Therefore, the following values will be used for checking against design capacities of the post-installed anchors.

Tension = 1.3(2,630 lb) = 3,419 lb

Shear = 1.3(3,980 lb) = 5,174 lb

14.3.4.2 Proportioning and details. Anchor and snubber loads for support on vibration isolation springs are shown in Figure 14.3-5.

Check the vibration isolation system within a housing anchored with one 5/8-inch-diameter post-installed wedge expansion anchors embedded 9 inches into the 10-inch-thick, 4,000 psi concrete housekeeping pad. The expansion anchors selected are specifically designed for seismic forces and have been tested for use in cracked concrete, following the procedures of ACI 355.2. Unless at least one of three conditions is satisfied, *Standard* Section 13.4.2 requires that the anchorage design forces be determined using $R_p = 1.5$. One of these conditions is that post-installed anchors be tested to verify their seismic capacity in accordance with the procedures of ACI 355.2. Since anchors selected for this example have been tested per ACI 355.2, this condition has been satisfied and anchorage design forces do not need to be modified and are those provided in Section 14.3.4.1 of this example. For the purpose of this example it is assumed that there are no edge effects or groups effects. Also, for this example the local prying effects of attachment members are assumed to be negligible. In most real cases these effects will exist and would either increase the design anchor force or reduce the capacity of the anchor.

The *Standard* refers to ACI 318 to determine the capacity of anchors, including the design strength of post-installed expansion anchors. ACI 318 refers to the testing procedures of ACI 355.2-01 for verifying the seismic capacities of post-installed anchors. The ICC Evaluation Service provides testing procedures and acceptance criteria for post-installed anchors for both non-seismic and seismic applications. For nonstructural components, non-seismic post-installed anchors are permitted but are severely penalized. This example uses seismic anchors, which have been tested for use in cracked concrete and have ICC-ES reports approving their used for seismic applications consistent with the requirements of ACI 318 Appendix D and ACI 355.2.

Assume the following material properties have been specified for the concrete slab and anchors:

f_c' = 4,000 psi, normal weight concrete, $\lambda = 1.0$, with no supplementary anchor reinforcing provided

For post-installed anchors, assume sleeves extend through shear plane

$A_{se,N} = A_{se,V} = 0.17\text{ in}^2$

f_y = 84,800 psi (ductile steel)

f_{uta} = 106,000 psi

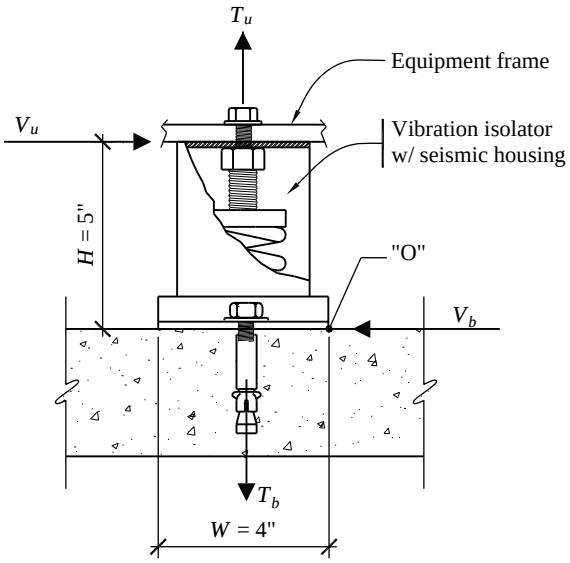

Figure 14.3-5 Anchor and snubber loads for support on vibration isolation springs (1.0 in. = 25.4 mm)

14.3.4.2.1 Tension strength of an isolated anchor in slab, away from edge, with no group effects.

Tension capacity of steel, ϕ = 0.75 (ductile steel element):

$\phi N_{sa} = \phi A_{se,N} F_{uta}$ = 0.75(0.17 in^2)(106,000 psi) = 13,515 lb (ACI 318-08 Eq. D-1, D-3)

Tension capacity of concrete, ϕ = 0.65 and apply an additional 0.75 factor to determine seismic concrete capacities as required by Sections D.3.3 and D.3.3.3 of ACI 318-08. Also assume configuration is such that there is no eccentricity, no pull-through and no edge or group effect:

$$0.75\phi N_b = 0.75\phi k_c \lambda \sqrt{f_c'} h_{ef}^{1.5} = 0.75(0.65)17(1.0)\sqrt{4{,}000}(9^{1.5}) = 14{,}151 \text{ lb}$$ (ACI 318-08 Eq. D-1, D-7)

The steel capacity controls in tension, so Section D.3.3.4 of ACI 318-08 is satisfied. Therefore, $\phi N_n = \phi N_{sa}$ = 13,515 lb, so tension alone is okay since capacity is greater than demand.

14.3.4.2.2 Design shear strength on isolated anchor in slab, away from edge. Allowable stress shear values are obtained from ICC Evaluation Service ESR-2251, ITW Trubolt Wedge anchors. Similar certified allowable values are expected with anchors from other manufacturers.

Anchor diameter = 5/8 in.

Anchor depth = 9 in.

f_c' = 4,000 psi

Shear capacity of steel, ϕ = 0.65:

$\phi V_{sa} = \phi\, 0.60 A_{se,V} f_{uta} = 0.65(0.60)(0.17 \text{ in}^2)(106{,}000 \text{ psi}) = 7{,}030 \text{ lb}$ (ACI 318-08 Eq. D-1, D-19)

Shear capacity of concrete, far from edge, limited to pry-out, no supplementary reinforcing, ϕ = 0.70:

$\phi V_{cp} = \phi k_{cp} N_{cb} = \phi k_{cp} N_{sa} = \phi k_{cp} A_{se,N} f_{uta}$ (ACI 318-08 Eq. D-1, D-4, D-30)

$\phi V_{cp} = 0.70(1.0)(0.17 \text{ in}^2)(106{,}000 \text{ psi}) = 12{,}614 \text{ lb}$

The steel capacity controls in shear, with $\phi V_N = \phi V_{sa}$ = 7,030 lb

14.3.4.2.3 Combined tension and shear. ACI 318-08 provides an equation (Eq. D-32) for the interaction of tension and shear on an anchor or a group of anchors:

$\frac{N_u}{\phi N_N} + \frac{V_u}{\phi V_N} \le 1.2$, which applies where either term exceeds 0.2

Substituting the demand and capacities computed above, one obtains:

(3,419/13,515) + (5,174/7,030) = 0.99 which is less than 1.2

Therefore, the preliminary anchor design is okay.

14.3.4.2.4 Summary. At each corner of the HVAC fan unit, a proposed design provides a vibration isolation system within a housing anchored with one 5/8-inch-diameter post-installed expansion anchor embedded 9 inches into the concrete slab. When checked against the design loadings, these anchors work, but may not be practical in normal design situations. Other anchor configurations should be investigated, such as two anchors or four anchors per corner, which would reduce both the size of anchor and depth of embedment and required concrete pad thickness. Also, consideration should be given to requiring a limit of gap clearance to ¼ inch (which would require special inspection during construction to be sure it happened) to reduce design seismic forces on seismic restraints and associated anchorage.

14.3.5 Additional Considerations for Support on Vibration Isolators

Vibration isolation springs are provided for equipment to prevent vibration from being transmitted to the building structure. However, they provide virtually no resistance to horizontal seismic forces. In such cases, some type of restraint is required to resist the seismic forces. Figure 14.3-6 illustrates one concept where a bolt attached to the equipment base is allowed to slide a controlled distance (gap) in either direction along its longitudinal axis before it contacts resilient impact material.

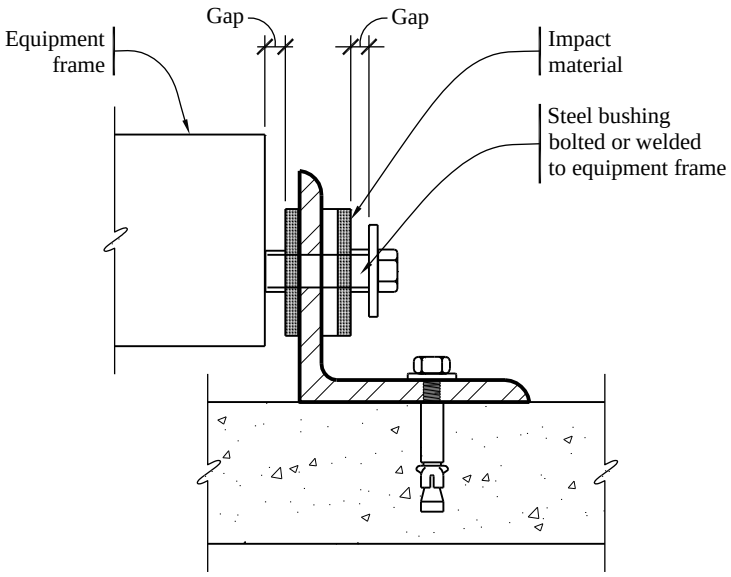

Figure 14.3-6 Lateral restraint required to resist seismic forces

Design of restraints for vibration-isolated equipment varies for different applications and for different manufacturers. In most cases, restraint design incorporates all directional capability with an air gap, a soft impact material and a ductile restraint or housing.

Restraints should have all-directional restraint capability to resist both horizontal and vertical motion. Vibration isolators have little or no resistance to overturning forces. Therefore, if there is a difference in height between the equipment's center of gravity and the support points of the springs, rocking is inevitable and vertical restraint is required.

An air gap between the restraint device and the equipment prevents vibration from transmitting to the structure during normal operation of the equipment. Air gaps generally are no greater than 1/4 inch. Dynamic tests indicate a significant increase in acceleration for air gaps larger than 1/4 inch.

A soft impact material, often an elastomer such as bridge bearing neoprene, reduces accelerations and impact loads by preventing steel-to-steel contact. The thickness of the elastomer can significantly reduce accelerations to both the equipment and the restraint device and should be addressed specifically for life-safety applications.

A ductile restraint or housing is critical to prevent catastrophic failure. Unfortunately, housed isolators made of brittle materials such as cast iron often are assumed to be capable of resisting seismic loads and continue to be installed in seismic zones.

Overturning calculations for vibration-isolated equipment must consider a worst-case scenario as illustrated in Section 14.3.4.1. However, important variations in calculation procedures merit further discussion. For equipment that is usually directly attached to the structure or mounted on housed vibration isolators, the weight can be used as a restoring force since the equipment will not transfer a tension load to the anchors until the entire equipment weight is overcome at any corner. For equipment installed on any other vibration-isolated system (such as the separate spring and snubber arrangement shown in Figure 13.3-5), the weight cannot be used as a restoring force in the overturning calculations.

As the foregoing illustrates, design of restraints for resiliently mounted equipment is a specialized topic. The *Standard* sets out only a few of the governing criteria. Some suppliers of vibration isolators in the highest seismic zones are familiar with the appropriate criteria and procedures. Consultation with these suppliers may be beneficial.

14.4 ANALYSIS OF PIPING SYSTEMS

14.4.1 ASME Code Allowable Stress Approach

Piping systems typically are designed to satisfy national standards such as ASME B31.1. Piping required to be designed to other ASME piping codes uses similar approaches with similar definition of terms.

14.4.1.1 Earthquake design requirements. ASME B31.1 Section 101.5.3 requires that the effects of earthquakes, where applicable, be considered in the design of piping, piping supports and restraints using data for the site as a guide in assessing the forces involved. However, earthquakes need not be considered as acting concurrently with wind.

14.4.1.2 Stresses due to sustained loads. The effects of pressure, weight and other sustained loads must meet the requirements of ASME B31.1 Equation 11A:

$$S_L = \frac{PD_o}{4t_n} + \frac{0.75iM_A}{Z} \le 1.0S_h$$

where:

S_L = sum of the longitudinal stresses due to pressure, weight and other sustained loads

P = internal design pressure, psig

D_o = outside diameter of pipe, in.

t_n = nominal pipe wall thickness, in.

i = stress intensification factor from ASME Piping Code Appendix D, unitless
= 1.0 for straight pipe
≥ 1.0 for fittings and connections

M_A = resultant moment loading on cross section due to weight and other sustained loads, in-lb

Z = section modulus, in^3

S_h = basic material allowable stress at maximum (hot) temperature from ASME Piping Code Appendix A

For example, ASTM A53 seamless pipe and tube, Grade B: S_h = 15.0 ksi for -20 to 650 degrees Fahrenheit.

14.4.1.3 Stresses due to occasional loads. The effects of pressure, weight and other sustained loads and occasional loads including earthquake, must meet the requirements of ASME B31.1 Equation 12A:

$$\frac{PD_o}{4t_n} + \frac{0.75iM_A}{Z} + \frac{0.75iM_B}{Z} \le kS_h$$

where:

M_B = resultant moment loading on cross-section due to occasional loads, such as from thrust loads, pressure and flow transients and earthquake. Use one-half the earthquake moment range. Effects of earthquake anchor displacements may be excluded if they are considered in Equation 13A, in-lb.

k = duration factor, unitless.
= 1.15 for occasional loads acting less than 10 percent of any 24-hour operating period.
= 1.20 for occasional loads acting less than 1 percent of any 24-hour operating period.
= 2.00 for rarely occurring earthquake loads resulting from both inertial forces and anchor movements (per ASME interpretation).

14.4.1.4 Thermal expansion stress range. The effects of thermal expansion must meet the requirements of ASME B31.1 Equation 13A:

$$S_E = \frac{iM_C}{Z} \le S_A + f\left(S_h - S_L\right)$$

where:

S_E = sum of the longitudinal stresses due to thermal expansion, ksi.

M_C = range of resultant moments due to thermal expansion. Also includes the effects of earthquake anchor displacements if not considered in Equation 12A, in-lb.

S_A = allowable stress range, ksi (per ASME B31.1 Eq. 1, $S_A = f\left(1.25S_c + 0.25S_h\right)$).

f = stress range reduction factor for cyclic conditions from the ASME Piping Code Table 102.3.2.

S_c = basic material allowable stress at minimum (cold) temperature from the ASME Piping Code Appendix A.

14.4.1.5 Summary. In the ASME B31.1 allowable stress approach, earthquake effects appear only in the M_B and M_C terms. M_B represents earthquake inertial effects and M_C represents earthquake displacement effects.

14.4.2 Allowable Stress Load Combinations

ASME B31.1 uses an allowable stress approach; therefore, allowable stress force levels and allowable stress load combinations should be used. While the *Standard* is based on strength design, Section 13.1.7 of the *Standard* permits the use of allowable stress design for nonstructural components where the reference document that is used for earthquake design of the component provides its acceptance criteria in terms of allowable stresses rather than strengths. For such cases, the allowable stress load combinations must consider dead, live, operating and earthquake loads in addition to those specified in the reference

document. The earthquake loads determined in accordance with *Standard* Section 13.3.1 are multiplied by a factor of 0.7. Also, the allowable stress load combinations of Sections 2.4 and 12.4 of the *Standard* need not be used and the allowable stress increases for load combination which include seismic loads are permitted. Where earthquake effects are not considered, load combinations should be taken from the appropriate piping system design code. Section 13.1.7 also points out that the component and system must accommodate the relative displacements specified in *Standard* Section 13.3.2.

14.4.2.1 *Standard* allowable stress load combinations. The following allowable stress load combinations, specified in *Standard* Section 12.4.3, are permitted to be used in the design of nonstructural components. The load combinations have been adjusted to apply specifically to piping by deleting the terms F and H and substituting with F_p for Q_E. Other operational loads should be added using a load factor of 1.0. No increases in allowable stress are permitted for these load combinations:

$(1.0 + 0.14S_{DS})D + 0.7F_p$

$(0.6 - 0.14S_{DS})D + 0.7F_p$

14.4.2.2 Traditional allowable stress load combinations. The following allowable stress load combinations traditionally have been used in the design of many nonstructural components, including piping. Increases in allowable stress (typically 1/3) generally have been permitted for these combinations:

$(1.0 + 0.14S_{DS})D + 0.7F_p$

$(0.9 - 0.14S_{DS})D + 0.7F_p$

14.4.2.3 Modified traditional allowable stress load combinations. It is convenient to define separate earthquake load terms to represent the separate inertial and displacement effects:

E_I = Earthquake horizontal inertial effects (M_B term)

E_Δ = Earthquake displacement effects (M_C term)

It is also convenient to use the Traditional Allowable Stress Load Combinations modified to use ASME Piping Code terminology, deleting roof load effects (L_r or S or R) and multiplying by 0.75 to account for the 1.33 allowable stress increase where W or E is included. Only modified traditional allowable stress load combinations are considered in the discussion that follows.

$0.75[(1.0 + 0.14S_{DS})D + L + S + 0.7(E_I + E_\Delta)]$

$0.75[(0.9 + 0.14S_{DS})D + 0.7(E_I + E_\Delta)]$

By replacing E_I with F_p, the following is obtained:

$0.75[(1.0 + 0.14S_{DS})D + L + S + 0.7(F_p + E_\Delta)]$

$0.75[(0.9 + 0.14S_{DS})D + 0.7(F_p + E_\Delta)]$

14.4.3 Application of the *Standard*

14.4.3.1 Overview. Piping systems are considered mechanical components. Mechanical component are exempt from the seismic requirements of *Standard* Chapter 13 under certain conditions, which are listed in Section 13.1.4. Furthermore, under certain conditions listed in Section 13.6.8, pipe supports are not required to be designed to the seismic requirements of *Standard* Chapter 13.

There are many different types of piping systems. *Standard* Section 13.6.8.1 states that pressure piping designed in accordance ASME B31 is deemed to comply with the force, relative displacement and other requirements of the *Standard* and that elevator piping must be designed to ASME 17.1. Section 13.6.8.1 requires that the force and relative displacement requirements of Section 13.3.1 be used in lieu of specific force and displacement requirements of ASME B31. Fire sprinkler systems designed and installed in accordance with NPFA 13-2007 are deemed to comply with the force and displacement requirements of the *Standard* (see *Provisions* Section 13.6.8.2). Other piping is required to satisfy *Standard* Section 13.6.11, which refers to Sections 13.4, 13.6.5.3 and 13.6.5. Section 13.6.5 requires piping supports to be designed for the forces and displacements of *Standard* Sections 13.3.1 and 13.3.2. Section 13.4 provides special requirements for the design and detailing of anchorage that supports or anchors nonstructural components including piping. *Standard* Section 13.6.3 requires that mechanical components, including piping, that are assigned an I_p greater than 1.0 themselves be designed for the forces and displacements of Sections 13.3.1 and 13.3.2. Also, where I_p is greater than 1.0, the following additional requirements are imposed.

- Provision must be made to eliminate seismic impact for components vulnerable to impact, for components constructed of nonductile materials and in cases where material ductility will be reduced (e.g., low temperature applications).

- The possibility of loads imposed on components by attached utility or service lines due to differential movement of support points on separate structures must be evaluated.

- Where piping or HVAC ductwork components are attached to structures than could displace relative to one another and for isolated structures where the components cross the isolation interface, the components must be designed to accommodate the seismic relative displacements defined in *Standard* Section 13.3.2.

14.4.3.2 Forces. *Standard* Section 13.3.1 and Table 13.6-1 provide specific guidance regarding the equivalent static forces that must be considered in the design of piping systems. Note that the piping itself need only be designed for seismic forces and displacements if required by the reference standard (i.e., ASME 17.1, ASME B31.1, or NPFA-13) or if the value of I_p assigned to the piping is greater than 1.0.

In computing the earthquake forces for piping systems, the inertial portion of the forces (noted as E_I in this example) are computed using *Standard* Equations 13.3-1, 13.3-2 and 13.3-3. Depending on the type of piping system, the value specified for R_p ranges between 3 and 12 while the value of a_p equals 2.5 for all values. For anchor points with different elevations, the average value of the F_p may be used, with minimum and maximum observed. In addition, the vertical effects should be considered, as illustrated in Section 14.4.2.

It is convenient to designate the term $\left(1 \pm \frac{0.2S_{DS}}{1.4}\right)$ by the variable β.

The vertical component of E_I can now be defined as βM_a and applied to all load combinations that include E_I.

M_B can now be defined as the resultant moment induced by the design force $0.7F_p$, where F_p is as defined by *Standard* Equations 13.3-1, 13.3-2 and 13.3-3.

14.4.3.3 Displacements. *Standard* Section 13.3.2 provides specific guidance regarding the relative displacements that must be considered. Typically piping systems are designed considering forces and displacements using elastic analysis and allowable stresses for code prescribed wind and seismic equivalent static forces in combination with operational loads.

However, no specific guidance is provided in the *Standard* except to say that the relative displacements should be "designed for". The intent of this wording was not to require that a piping system remain elastic. Indeed, many types of piping systems typically are very ductile and can accommodate large amounts of inelastic strain while still functioning quite satisfactorily. What was intended was that the relative displacements between anchor and constraining points that displace significantly relative to one another be demonstrated to be accommodated by some rational means. This accommodation can be made by demonstrating that the pipe has enough flexibility or inelastic strain capacity to accommodate the displacement by providing loops in the pipeline to permit the displacement or by adding flex lines or articulating couplings which provide free movement to accommodate the displacement. Sufficient flexibility may not exist where branch lines may be forced to move with a ceiling or where other structural systems are connected to main lines. Often this "accommodation" is done by using engineering judgment, without calculations. However, if relative displacement calculations were required for a piping system, a flexibility analysis would be required. A flexibility analysis is one in which a pipe is modeled as a finite element system with commercial pipe stress analysis programs (such as Autopipe or CAESAR II) and the points of attachment are displaced by the prescribed relative displacements. The allowable stress for such a condition may be significantly greater than the normal allowable stress for the pipe.

The internal moments resulting from support displacement may be computed by means of elastic analysis programs using the maximum computed relative displacements as described earlier and then adjusted. Adjustments should be in accordance with reference standards.

14.4.3.4 Load combinations. Combining ASME B31.1 Equations 12A and 13A with modified traditional allowable stress load combinations of Section 14.4.2.3 yields the following:

For the modified traditional equation:

$$\frac{PD_o}{4t_n} + \beta\left(\frac{0.75iM_A}{Z}\right) \pm \frac{0.75iM_B}{Z} \le kS_h$$

$$\frac{iM_C}{Z} \le S_A + f\left(S_h - S_L\right)$$

and for the modified IBC Equation 16-18:

$$\frac{PD_o}{4t_n} + 0.9\beta\left(\frac{0.75iM_A}{Z}\right) - \frac{0.75iM_B}{Z} \le kS_h$$

$$\frac{iM_C}{Z} \le S_A + f\left(S_h - S_L\right)$$

where:

β = (1.0 + 0.105S_{DS}) in the first equation and (0.9 - 0.105S_{DS}) in the second equation.

M_A = the resultant moment due to weight (including pipe contents).

M_B = the resultant moment induced by the design force 0.7F_p where F_p is as defined by *Standard* Equations 13.3-1, 13.3-2 and 13.3-3.

M_C = the resultant moment induced by the design relative seismic displacement D_p where D_p is as defined in *Standard* Sections 13.3.3 and 13.6.3.

S_{DS} and W_p, are as defined in the *Standard*.

P, D_o, t_n, I, Z, k, S_h, S_A, f and S_L are as defined in ASME B31.1.

14.5 PIPING SYSTEM SEISMIC DESIGN

14.5.1 Example Description

This example illustrates seismic design for a portion of a piping system in an acute care hospital. It illustrates determination of the seismic demands on the system, consideration of anchorage and bracing of the system and design for system displacements within the structure and between structures. The example focuses on the determination of force and displacement demands on the different components of the system. The sizing of the various elements (braces, anchor bolts, etc.) are not covered in detail.

The *Standard* provides requirements for three types of piping systems: ASME B31 pressure piping systems (Sec. 13.6.8.1), fire protection piping systems in accordance with NFPA 13 (Sec. 13.6.8.2 and 13.6.8.3) and other piping systems (Sec. 13.6.8.4). This example considers three piping runs of a chilled water piping system supported from the roof of a two-story structure. The system is not intended to meet the ASME 31 requirements and, therefore, is designed to the "other piping system" requirements of the *Standard*. The piping system is illustrated in Figures 14.5-1 and 14.5-2 and a typical trapeze-type support assembly is shown in Figures 14.5-3 and 14.5-4. One run of the piping system crosses a seismic separation joint to enter an adjacent structure. The building, located in the San Francisco Bay area of California, is assigned to Occupancy Category IV.

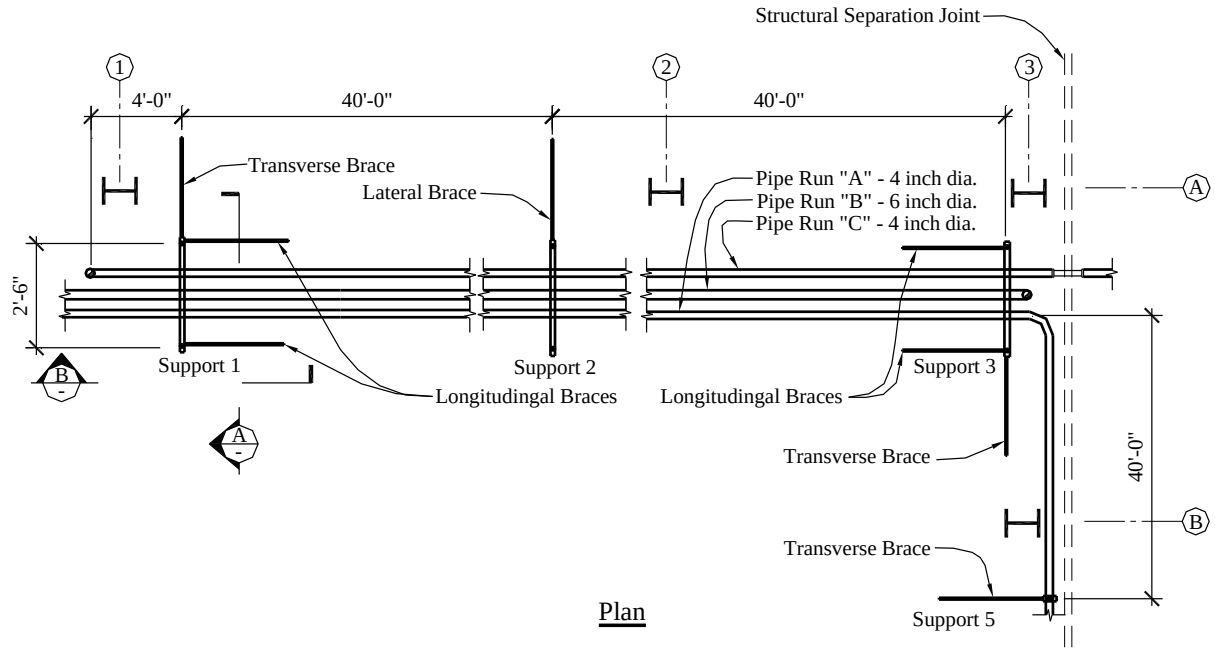

Figure 14.5-1 Piping system

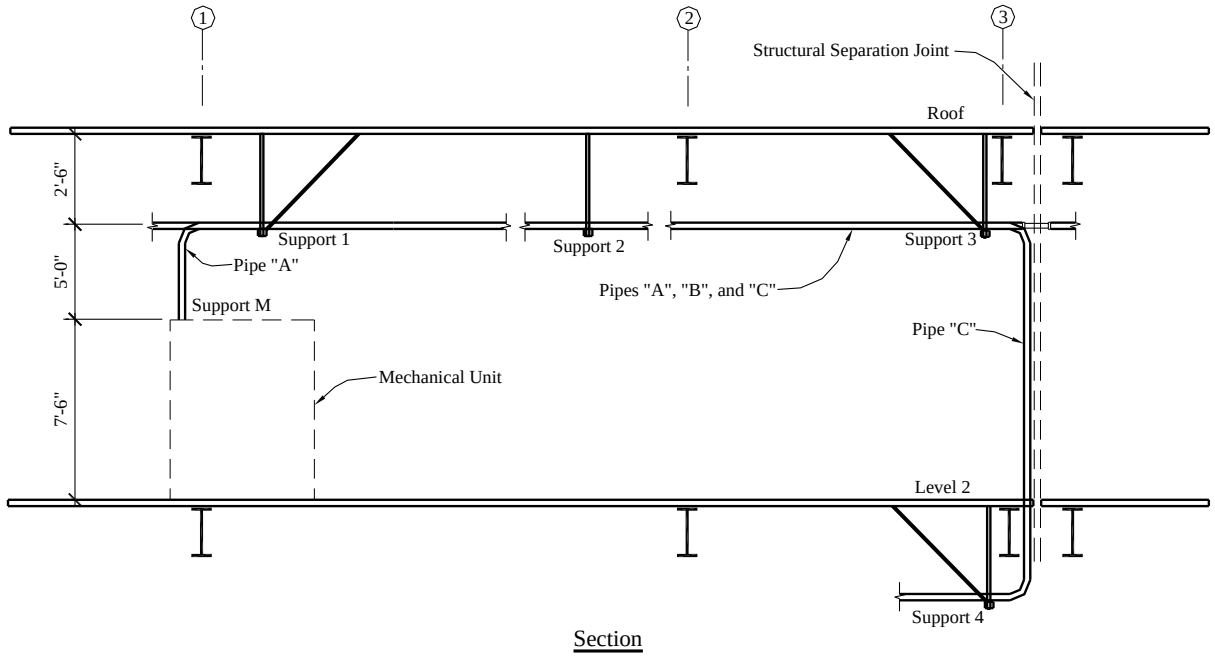

Figure 14.5-2 Piping system

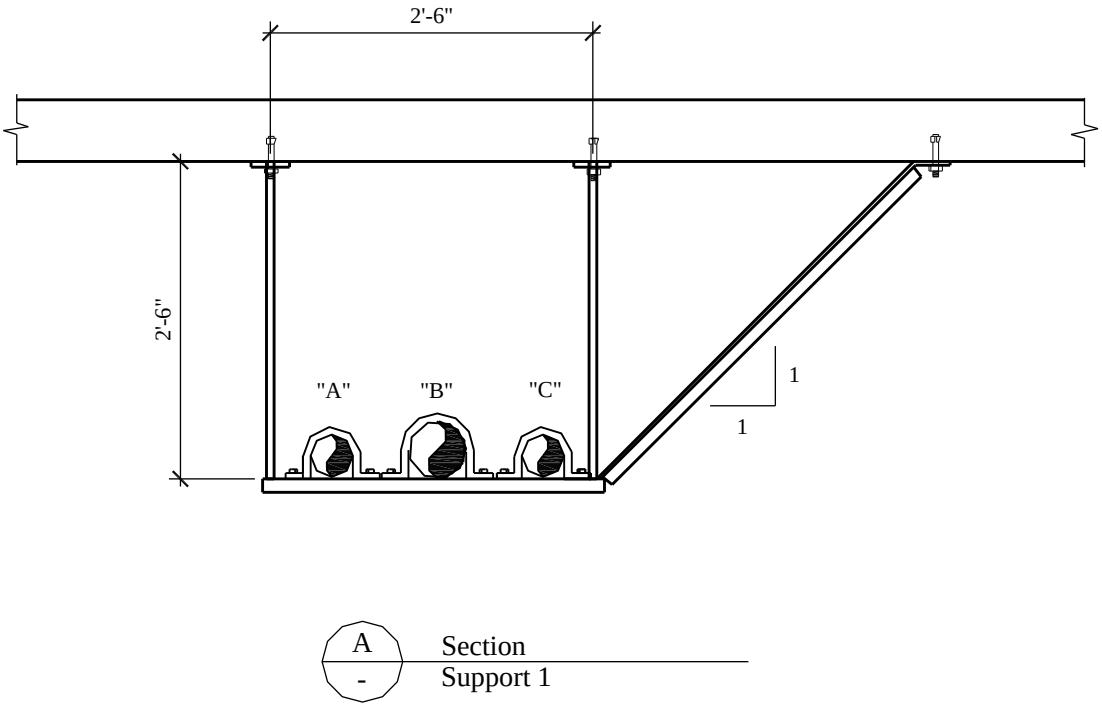

Figure 14.5-3 Typical trapeze-type support assembly

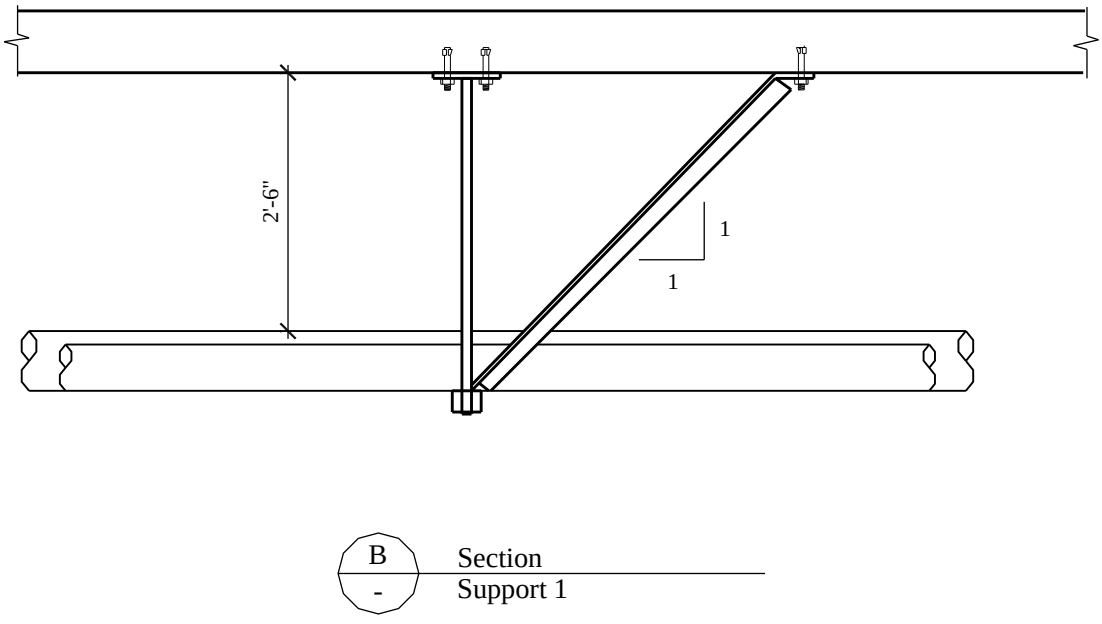

Figure 14.5-4 Typical trapeze-type support assembly

14.5.1.1 Earthquake design requirements. Earthquake design requirements for piping systems in the *Standard* depends on the system importance factor (I_p), the pipe diameter and the installation geometry. The importance factor is determined in *Standard* Section 13.1.3. Given that the structure is assigned to Occupancy Category IV, the components are assigned $I_p = 1.5$, unless it can be shown that the component is not needed for continued operation of the facility and failure of the component would not impair operations. Since failure of the piping system will result in flooding of the hospital, $I_p = 1.5$.

Some piping is exempt from some or all of the seismic requirements, provided it meets the criteria in Sections 13.1.4 or 13.6.8. The user should refer to important errata in *Standard* Section 13.1.4, which addresses exemptions. The exemptions in Section 13.1.4 apply only to components with $I_p = 1.0$ and therefore are not applicable to this example. Section 13.6.8 waives seismic support requirements for piping supported by rods less than 12 inches long and for small-diameter high-deformability piping. Our example piping meets neither condition, so seismic supports will be required.

"Other" piping systems must meet the following requirements of the *Standard*:

- Section 13.4: Nonstructural Component Anchorage
- Section 13.6.3: Mechanical Components
- Section 13.6.5: Component Supports

It is important to note that per *Standard* Section 13.6.3, where I_p is greater than 1.0, the component anchorage, bracing and the component itself (in this example, the pipe) must be designed to resist seismic forces.

14.5.1.2 System configuration. The portion of the piping system under consideration consists of three piping runs:

- Piping Run “A”, a 4-inch-diameter pipe, which connects to a large mechanical unit at Line 1 supported at the second level. It crosses a seismic separation between adjacent structures at Line 3.
- Piping Run "B", a 6-inch-diameter pipe, which has a vertical riser to the second level at Line 3.
- Piping Run "C", a 4-inch-diameter pipe, which turns 90 degrees to parallel Line 3 at Column Line 3-A.

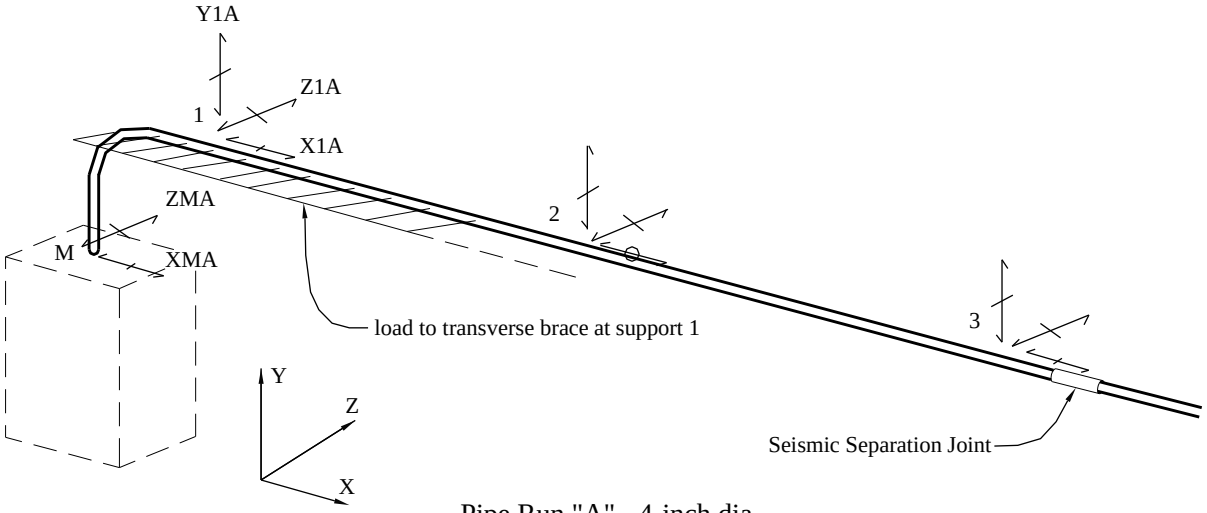

Figure 14.5-5 Piping Run A

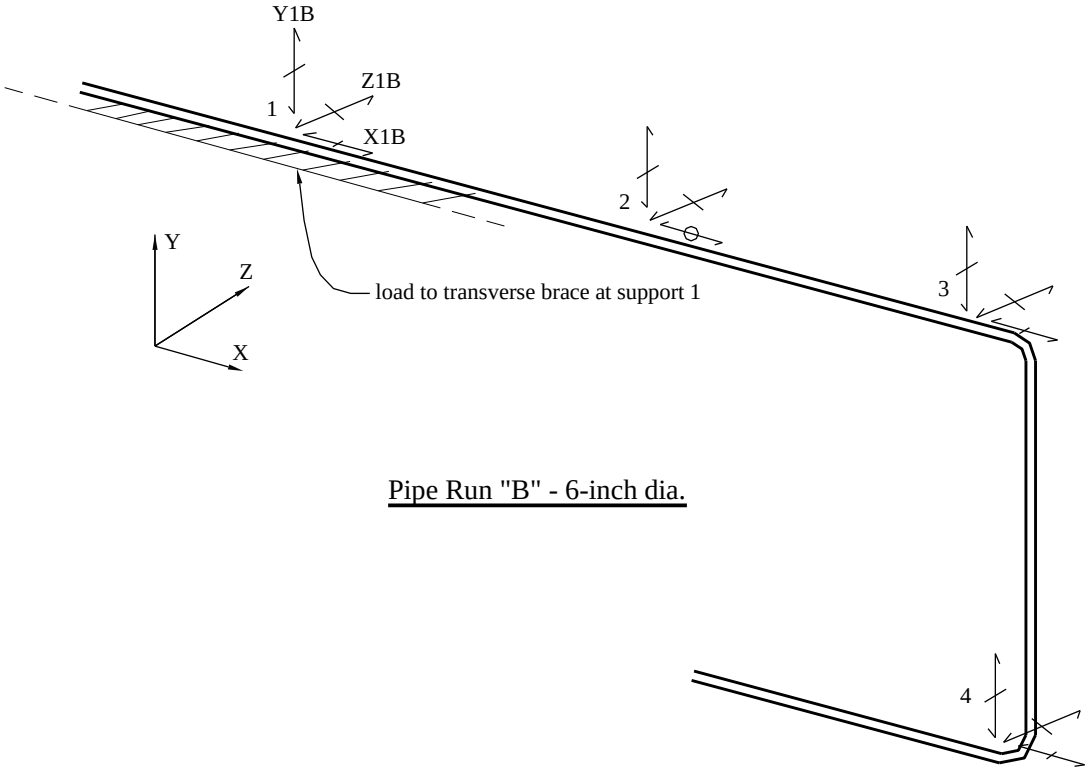

Figure 14.5-6 Piping Run B

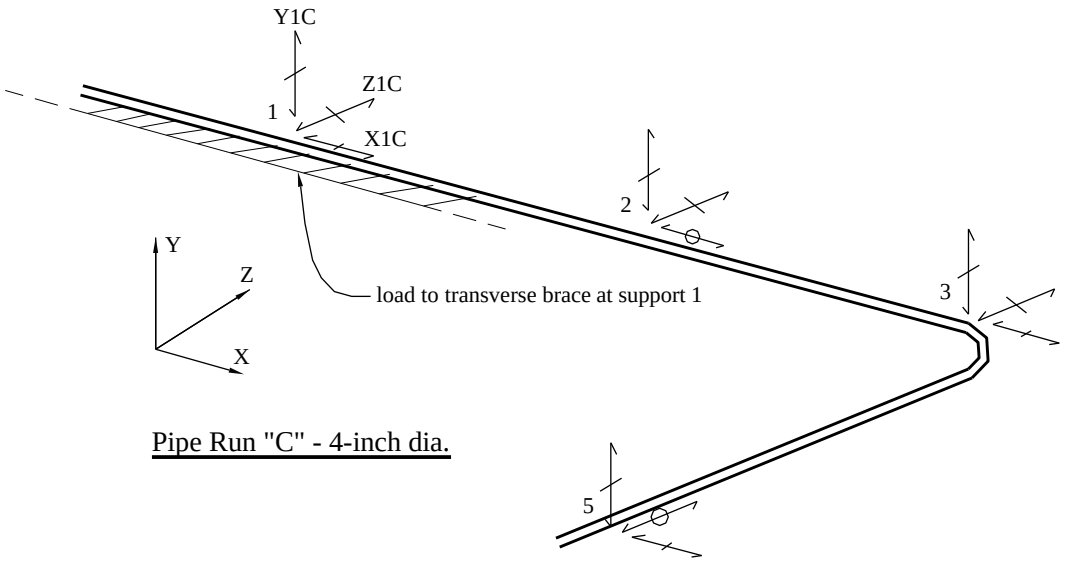

Figure 14.5-7 Piping Run C

The system consists of non-ASME B31 piping fabricated from steel Schedule 40 pipe with threaded connections. This example covers determination of the seismic forces acting on the system, a check of the seismically induced stresses in the pipes using simplifying assumptions, determination of bracing and anchorage forces and a check of the system for seismic relative displacements.

It should be noted that details of pipe bracing systems vary according to the local preferences and practices of plumbing contractors. In addition, the use of proprietary pipe hanging and bracing systems is relatively common. As a result, this example concentrates on quantifying the prescribed seismic forces and displacements and on simplified stress checks of the piping system itself. After the seismic forces and displacements are determined, the bracing and anchorage connections can be designed and detailed according to the appropriate AISC and ACI codes.

14.5.2 Design Requirements.

14.5.2.1 Seismic design parameters and coefficients.

a_p = 2.5 for piping systems (*Standard* Table 13.6-1)

R_p = 4.5 for piping not in accordance with ASME B31, constructed of high or limited deformability materials, with joints made by threading (*Standard* Table 13.6-1)

S_{DS} = 1.0 (for the selected location and site class) (given)

Seismic Design Category = D (*Standard* Table 11.6-1)

h = 30 feet (roof height) (given)

h_{sx} = 15 feet (story height) (given)

z = 30 feet (system is braced at the roof level) (given)

$$\frac{z}{h} = \frac{30.0 \text{ ft}}{30.0 \text{ ft}} = 1.0$$ (at roof)

I_p = 1.5 (*Standard* Sec. 13.1.3)

Gravity (non-seismic) supports provided every 10'-0" (given)

System working pressure *(P)* = 200 psi (given)

ASTM A53 Pipe F_y = 35 ksi, threaded connections (given)

D = Dead Load = W_p = 16.4 plf (4-inch-diameter water-filled pipe) (given)

= 31.7 plf (6-inch-diameter water-filled pipe)

Longitudinal brace spacing = 80 feet (given)

According to *Standard* Section 13.3.1 (and repeated in Sec. 12.3.4.1), the redundancy factor does not apply to the design of nonstructural components.

14.5.2.2 Seismic design forces.

$$F_p = \frac{0.4(2.5)(1.0)W_p}{4.5/1.5}(1 + 2(1)) = 1.00W_p$$ (*Standard* Eq. 13.3-1)

$$F_p = 1.6(1.0)(1.5)W_p = 2.40W_p$$ (*Standard* Eq. 13.3-2)

$$F_p = 0.3(1.0)(1.5)Wp = 0.45W_p$$ (*Standard* Eq. 13.3-3)

$$E_v = 0.2(1.0)D = 0.2D = 0.2W_p$$ (*Standard* Eq. 12.4-4)

14.5.2.3 Performance criteria. System failure must not cause failure of an essential architectural, mechanical, or electrical component (*Standard* Sec. 13.2.3).

Component seismic attachments must be bolted, welded, or otherwise positively fastened without considering the frictional resistance produced by the effects of gravity (*Standard* Sec. 13.4).

The effects of seismic relative displacements must be considered in combination with displacements caused by other loads as appropriate (*Standard* Sec. 13.3.2).

The piping system must be designed to resist the forces in accordance with *Standard* Section 13.3.1 and must be able to accommodate movements of the structure resulting from response to the design basis ground motion, D_p.

14.5.3 Piping System Design

The requirements for the design of the piping system are summarized in Table 13.2-1 of the *Standard*. The supports and attachments of all mechanical and electrical components must meet the requirements listed in Table 13.2-1. Where $I_p > 1.0$, the component itself must also meet these requirements.

14.5.3.1 Check of pipe stresses. The spacing of seismic supports is often determined by the need to limit stresses in the pipe. Therefore, the piping stress check is often performed first in order confirm the assumptions on brace spacing. For non-ASME B31 piping that is not subject to high operating temperatures or pressures, the stress check assumptions may be simplified. The pipes can be idealized as continuous beams spanning between lateral braces, while longitudinal forces can be determined using the length of pipe tributary to the longitudinal brace.

The permissible stresses in the pipe are given in *Standard* Section 13.6.11, Item 2. For piping with threaded connections, the permissible stresses are limited to 70 percent of the minimum specified yield strength.

The section properties of the Schedule 40 pipes are as follows:

4-inch diameter:

Inner diameter, d_1 = 4.026 in.

Outer diameter, d = 4.5 in.

Wall thickness, t = 0.237 in.

Plastic modulus, $Z = \frac{d^3}{6} - \frac{d_1^3}{6} = \frac{(4.5)^3}{6} - \frac{(4.026)^3}{6} = 4.31 \text{ in}^3$

Moment of inertia, $I = 0.049807(d^4 - d_1^4) = 0.049087((4.5)^4 - (4.026)^4) = 7.23 \text{ in}^4$

6-inch diameter:

Inner diameter, d_1 = 6.065 in.

Outer diameter, d = 6.625 in.

Wall thickness, t = 0.28 in.

Plastic modulus, $Z = \frac{(6.625)^3}{6} - \frac{(6.065)^3}{6} = 11.28 \text{ in}^3$

Moment of inertia, $I = 0.049087((6.625)^4 - (6.065)^4) = 28.14 \text{ in}^4$

14.5.3.1.1 Gravity and pressure loads. The longitudinal stresses due to pressure and weight may be estimated using the following equation:

$$S_L = \frac{Pd}{4t} + \frac{M_g}{Z}$$

where:

S_L = sum of the longitudinal stresses due to pressure and weight

P = internal design pressure, psig

d = outside diameter of pipe, in.

t = pipe wall thickness, in.

M_g = resultant moment loading on cross section due to weight and other sustained loads, in-lb

Z = section modulus, in^3

Vertical supports are spaced at 10-foot centers, so the moment due to gravity, M_g, may be conservatively estimated as follows:

$$M_g = \frac{Dl^2}{8} = \frac{D(10)^2}{8} = 12.5D$$

For a 4-inch-diameter pipe, where D = 16.4 plf:

$$M_g = 12.5D = 12.5(16.4) = 205 \text{ ft-lb} = 2{,}460 \text{ in-lb}$$

$$S_{L\text{-}DeadLoad} = \frac{2{,}460}{4.31} = 571 \text{ psi}$$

$$S_{L-Pressure} = \frac{200(4.5)}{4(0.237)} = 949 \text{ psi}$$

For a 6-inch-diameter pipe, where D = 31.7 plf:

$$M_g = 12.5(31.7) = 396 \text{ ft-lb} = 4{,}752 \text{ in-lb}$$

$$S_{L-DeadLoad} = \frac{4{,}752}{11.28} = 421 \text{ psi}$$

$S_{L\text{-}Pressure}$ = 1,183 psi

14.5.3.1.2 Seismic loads on Piping Runs A and C. By idealizing the piping runs as continuous beams, the maximum bending moments and reactions can be estimated readily.

Piping Runs A and C are 4-inch-diameter pipes, shown schematically in Figures 14.5-5 and 14.5-7. They are idealized as a two-span continuous beam. The design lateral load, F_p, is taken as follows:

$$F_p = 1.00W_p = 1.00(16.4) = 16.4 \text{ plf} = w$$

The maximum moment due to horizontal seismic load may be approximated as follows:

$$M_E = \frac{wl^2}{8} = \frac{16.4(40)^2}{8} = 3{,}280 \text{ ft-lb} = 39{,}360 \text{ in-lb}$$

The flexural stress associated with this moment is:

$$f_{bh} = \frac{M_E}{Z} = \frac{39{,}360}{4.31} = 9{,}132 \text{ psi}$$

The moment due to vertical seismic load, $E_v = 0.2\ W_p$, may be approximated as follows:

$$M_v = \frac{E_v l^2}{8} = \frac{0.2(16.4)(10)^2}{8} = 41 \text{ ft-lb} = 492 \text{ in-lb}$$

The flexural stress associated with this moment is:

$$f_{bv} = M_v / Z = 492 / 4.31 = 114 \text{ psi}$$

Note that for vertical seismic effects, the span of the pipe is taken as the distance between vertical supports, not the distance between lateral bracing.

The basic strength load combination including earthquake effects from *Standard* Section 12.4.2.3 (based upon *Standard* Sec. 2.3.2) that will govern is Load Combination 5:

$$U = (1.2 + 0.2S_{DS})D + 1.0\rho Q_E + 0.5L + 0.2S$$

For nonstructural components, $\rho = 1.0$ and Q_E = the forces (or stresses) resulting from applying F_p.

In this example, live load, *L and* snow load, *S*, are equal to zero. The dead load, *D*, includes bending stress due to dead load. The load factor for internal pressure is the same as that for dead load. The design stress in the pipe is therefore:

$$U = [1.2 + 0.2(1.0)](421 \text{ psi}) + 1.2(1{,}183 \text{ psi}) + 1.0(1.0)(9{,}132 \text{ psi}) = 11{,}141 \text{ psi}$$

The permissible stress from Section 13.6.11, Item 2, of the *Standard* is $0.7F_y = 0.7(35{,}000) = 24{,}500$ psi. Comparing the demand to capacity:

$$U = 11{,}141 \text{ psi} < 0.7(35{,}000 \text{ psi}) = 24{,}500 \text{ psi} \qquad \text{OK}$$

Note that a number of conservative assumptions were made for the sake of simplicity. A more precise analysis can be performed, where the piping is modeled to achieve more accurate bending moments and the effects of biaxial bending in the pipe are considered separately. Also note that at any point in the pipe

wall, the stresses caused by dead (and vertical seismic) load and by horizontal seismic load occur in different physical locations in the pipe. The peak stresses due to vertically applied load occurs at the top and bottom of the pipe, while the peak stress for horizontally applied load occurs at mid-height of the pipe. So assuming that they are both occurring in the same location and are algebraically additive is quite conservative.

14.5.3.1.3 Seismic loads on Piping Run B. Piping Run B, a 6-inch-diameter pipe, is shown schematically in Figure 14.5-6. It is idealized as a two-span continuous beam. Note that the effects of the 15-foot-high riser between Level 2 and the roof are considered separately. The design lateral load, F_p, is taken as follows:

$$F_p = 1.00W_p = 1.00(31.7) = 31.7 \text{ plf} = w$$

The maximum moment due to horizontal seismic load is approximated as follows:

$$M_E = \frac{wl^2}{8} = \frac{31.7(40)^2}{8} = 6{,}340 \text{ ft-lb} = 76{,}080 \text{ in-lb}$$

The flexural stress associated with this moment is:

$$f_{bh} = \frac{M_E}{Z} = \frac{76{,}080}{11.28} = 6{,}745 \text{ psi}$$

The moment due to the vertical seismic load, $E_v = 0.2\ W_p$, may be approximated as follows:

$$M_v = \frac{E_v l^2}{8} = \frac{0.2(31.7)(10)^2}{8} = 79.25 \text{ ft-lb} = 951 \text{ in-lb}$$

The flexural stress associated with this moment is:

$$f_{bv} = \frac{M_v}{Z} = \frac{951}{11.28} = 84 \text{ psi}$$

The design stress in the pipe is:

U = [1.2 + 0.2(1.0)](571 psi) + 1.2(941 psi) + 1.0(1.0)(6,745 psi) = 8,674 psi < 24,500 psi OK

14.5.4 Pipe Supports and Bracing

As with the design of the pipe itself, design of the vertical and lateral supports of piping systems can be simplified by making conservative assumptions. In this example, design demands on the support assembly at Support 1 (Figure 14.5-8) are determined.

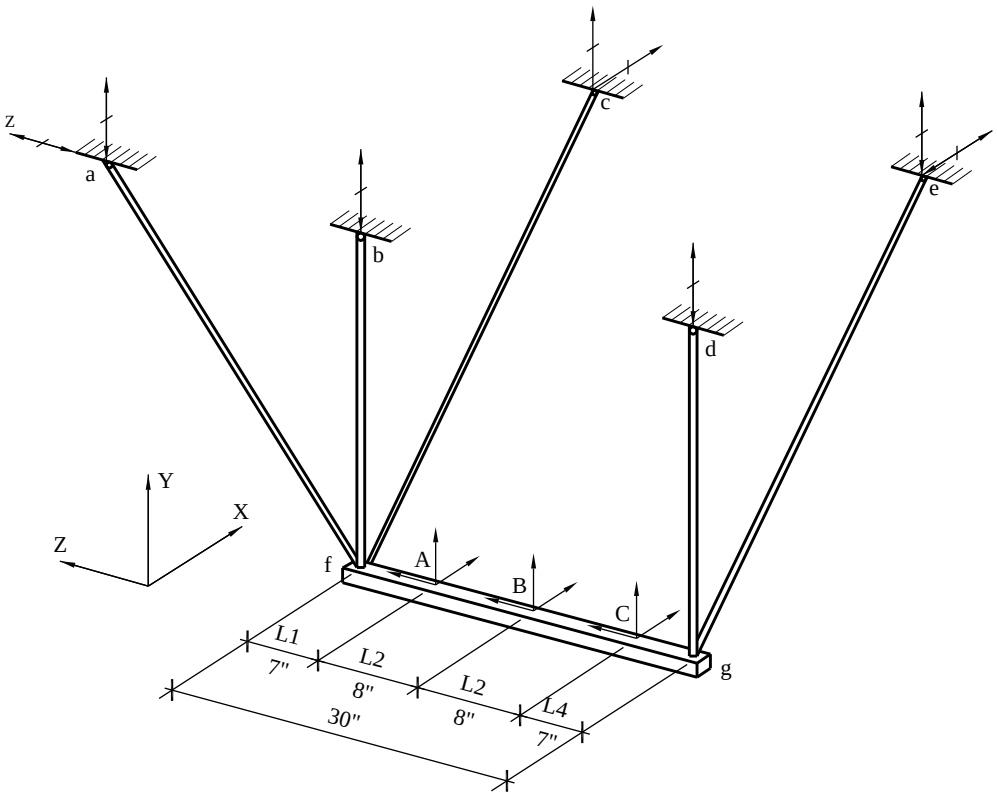

Figure 14.5-8 Design demands on piping support assembly

14.5.4.1 Vertical loads. Vertical pipe supports are often considered separately from lateral bracing. Configuration and spacing of vertical supports may be governed by plumbing codes or other standards and guidelines. Given that the vertical component of seismic force, E_v, is often low relative to other vertical loads, vertical supports proportioned for gravity and operational loads generally are adequate to resist the vertical seismic forces. However, where a support resists the vertical component of a lateral or longitudinal brace force, it should be designed explicitly to resist all applied forces. This example focuses on vertical supports associated with the lateral bracing system.

Due to the repetitious nature of the pipe gravity support system, the vertical load at the brace assembly due to gravity or vertical seismic load can be estimated based on the tributary length of pipe. Given a 10-foot spacing of vertical supports, the vertical loads due to a 4-inch-diameter pipe are as follows:

Dead load, P_{v4} = (10 ft)(16.4 plf) = 164 lb

Vertical seismic load, P_{Ev4} = 0.2(10 ft)(16.4 plf) = 33 lb

For a 6-inch diameter pipe:

Dead load, P_{v6} = (10 ft)(31.7 plf) = 317 lb

Vertical seismic load, P_{Ev6} = 0.2(10 ft)(31.7 plf) = 63 lb

14.5.4.2 Longitudinal lateral loads. Spacing of longitudinal bracing may be dictated by system geometry, thermal demands on the pipe, anchorage and brace capacities, or prescriptive limitations in standards and guidelines. In this example, we assume longitudinal braces are provided every 80 feet, which is twice the transverse brace spacing.

For Piping Run A, the total length of pipe tributary to Support 1 is approximately 40 feet (half the distance between longitudinal braces at Supports 1 and 3) plus 9 feet (length of pipe from Support 1 to Support M, the mechanical unit), or 49 feet.

The longitudinal seismic load, P_{X1A}, for the 4-inch-diameter Piping Run A is:

$$P_{X1A} = (49 \text{ ft})(F_p) = (49 \text{ ft})(16.4 \text{ plf}) = 804 \text{ lb}$$

For Piping Runs B and C, the total length of pipe tributary to Support 1 is approximately 80 feet.

The longitudinal seismic load, P_{X1B}, for the 6-inch-diameter Piping Run B is:

$$P_{X1B} = (80 \text{ ft})(F_p) = (80 \text{ ft})(31.7 \text{ plf}) = 2{,}536 \text{ lb}$$

The longitudinal seismic load, P_{X1C}, for the 4-inch-diameter Piping Run C is:

$$P_{X1C} = (80 \text{ ft})(F_p) = (80 \text{ ft})(16.4 \text{ plf}) = 1{,}312 \text{ lb}$$

14.5.4.3 Transverse lateral loads. To determine the transverse loads at support points, the pipes are idealized as continuous beams spanning between transverse braces. Assuming continuity over a minimum of two spans, the maximum reaction can be approximated conservatively as follows:

$$(2)\frac{5}{8}wl$$

where w is the distributed lateral load and l is the spacing between transverse braces.

For Piping Run A, we assume that 5/8 of the total length of pipe between the mechanical unit and the transverse brace at Support 2 is laterally supported at Support 1 (see Figure 14.5-3). The maximum transverse reaction due to Piping Run A at Support 1 may be approximated as follows:

$$P_{Z1A} = \frac{5}{8}wl = \frac{5}{8}(16.4 \text{ plf})(40 \text{ ft} + 9 \text{ ft}) = 502 \text{ lb}$$

For Piping Runs B and C, we assume that 5/8 of the total length of pipe on each side of Support 1 is laterally braced at Support 1 (see Figures 14.5-4 and 14.5-5). The maximum transverse reaction due to Piping Run B at Support 1 is then approximated as follows:

$$P_{Z1B} = (2)\frac{5}{8}wl = (2)\frac{5}{8}(31.7 \text{ plf})(40 \text{ ft}) = 1{,}585 \text{ lb}$$

The maximum transverse reaction due to Piping Run C at Support 1 is approximated as follows:

$$P_{Z1C} = (2)\frac{5}{8}wl = (2)\frac{5}{8}(16.4 \text{ plf})(40 \text{ ft}) = 820 \text{ lb}$$

14.5.4.4 Support design. The bracing system at Support 1 is shown in Figure 14.5-8. The analysis must consider design of the following bracing elements: Beam f-g, Hangers f-b and g-d, Transverse Brace a-f and Longitudinal Braces f-c and g-e. The connections at a, b, c, d and e must also be designed and are subject to special requirements.

14.5.4.4.1 Beam f-g. Beam f-g is subject to biaxial bending under vertical (Y-direction) and longitudinal (X-direction) forces. The maximum moment, which occurs at the center, is equal to:

$$M = \frac{P_A L_1}{2} + \frac{P_B L}{4} + \frac{P_C L_4}{2}$$

The factored vertical loads for the piping runs are as follows:

Piping Run A: P_A = 1.2(164 lb) + 1.0(33 lb) = 230 lb

Piping Run B: P_A = 1.2(317 lb) + 1.0(63 lb) = 443 lb

Piping Run C: P_A = 1.2(164 lb) + 1.0(33 lb) = 230 lb

The maximum moment about the x-axis of the beam due to vertical loads is:

$$M_x = \frac{230(7)}{2} + \frac{443(30)}{4} + \frac{230(7)}{2} = 4{,}933 \text{ in-lb}$$

The vertical reactions at f and g are equal to (230 + 443 +230)/2 = 452 pounds.

The factored lateral loads in the longitudinal direction determined in Section 14.5.4.2 are as follows:

Piping Run A: P_A = 804 lb

Piping Run B: P_A = 2,356 lb

Piping Run C: P_A = 1,312 lb

The maximum moment about the y-axis of the beam due to lateral loads is:

$$M_y = \frac{804(7)}{2} + \frac{2{,}356(30)}{4} + \frac{1{,}312(7)}{2} = 25{,}076 \text{ in-lb}$$

The horizontal reactions at f and g are:

$$R_f = \frac{P_A(L_2 + L_3 + L_4)}{L} + \frac{P_B}{2} + \frac{P_C L_4}{L} = \frac{804(8+8+7)}{30} + \frac{2{,}356}{2} + \frac{1{,}312(7)}{30} = 2{,}101 \text{ lb}$$

$$R_g = \frac{P_A L_1}{L} + \frac{P_B}{2} + \frac{P_C(L_1 + L_2 + L_3)}{L} = \frac{804(7)}{30} + \frac{2,356}{2} + \frac{1,312(7+8+8)}{30} = 2,371 \text{ lb}$$

Beam f-g would be designed for moments M_x and M_y acting simultaneously.

14.5.4.4.2 Brace design. By inspection, Brace g-e will govern the longitudinal brace design, since the horizontal reaction at g (2,371 lb) is larger than that at f (2,101 lb).

The horizontal load that must be resisted by the Transverse Brace a-f is the sum of the loads from the three pipes determined in Section 14.5.4.3:

R_z = 502 lb + 1,585 lb + 820 lb = 2,907 lb

Assuming the same member will be used for all braces, Brace a-f governs the design. Since the brace is installed at a 1:1 slope (45 degrees), the maximum tension or compression in the brace would be:

$$T_{max} = C_{max} + R_z\sqrt{2} = (2,907)(1.414) = 4,110 \text{ lb}$$

The brace selected must be capable of carrying C_{max} with an unbraced length of $(30 \text{ in.})\sqrt{2}$ = 42 inches. Bracing elements subject to compression should meet the slenderness ratio requirements of the appropriate material design standards.

14.5.4.4.3 Hangers. By inspection, Hanger f-b will govern the vertical element design, since the brace force in f-a governs the brace design. Since the brace is installed at a 1:1 slope (45 degrees), the maximum tension or compression due to seismic forces in the hanger is the same as the horizontal force resisted by the brace: 2,907 pounds. The vertical component of the brace force must be combined with gravity loads and the vertical seismic component.

The maximum tension force in the hanger is determined using the basic strength Load Combination 5 from *Standard* Section 12.4.3.2 (based upon *Standard* Sec. 2.3.2):

$U = (1.2 + 0.2S_{DS})D + 1.0\rho Q_E + 0.5L + 0.2S$

For nonstructural components, ρ = 1.0 and Q_E = the forces (or stresses) resulting from applying F_p.

In this example, live load, *L and* snow load, *S,* are equal to zero. The unfactored reactions at f due to the weight of the water-filled pipes is 323 pounds.

U = [1.2 + 0.2(1.0)](323 lb) + 1.0(1.0)(2,907 lb) = 3,359 lb

The maximum compression force in the hanger is determined using the basic strength Load Combination 7 from *Standard* Section 12.4.2.3 (based upon *Standard* Sec. 2.3.2):

$U = (0.9 - 0.2S_{DS})D + 1.0\,\rho Q_E + 1.6H$

Substituting the values from above and noting that the lateral earth pressure load, *H,* is not applicable:

U =[0.9 - 0.2(1.0)](323 lb) - 1.0(1.0)(2,907 lb) = -2,681 lb (tension)

F_p should be applied in the direction which creates the largest value for the item being checked. A negative sign indicates compression. The hanger selected must be capable of carrying the maximum compression with an unbraced length of 30 inches. Again, bracing elements subject to compression should meet the slenderness ratio requirements of the appropriate material design standards. It is also important to note that the length of pipe that contributes dead load to counteract the vertical component of brace force is based on the spacing of the vertical hangers, not the spacing between lateral braces.

14.5.4.5 Anchorage design. *Standard* Section 13.4 covers the attachment of the hangers and braces to the structure. Component forces are those determined in Sections 13.3.1 and 13.3.2, with important exceptions. Anchors in concrete and masonry are proportioned to carry the least of the following:

- 1.3 times the prescribed seismic design force, or
- The maximum force that can be transferred to the connected part by the component structural system.

In addition, the value of R_p may not exceed 1.5 unless the anchors are prequalified for seismic loading or the component anchorage is governed by yielding of a ductile steel element. To illustrate the effects of these provisions, consider the design of the attachment to the structure at Point a in Figure 14.5-8.

The horizontal and vertical components of the seismic brace force at Point a are 2,907 pounds each. Assuming the brace capacity does not limit the force to the anchor, the minimum design forces for the anchors is 1.3 times 2,907 pounds, which equals 3,779 pounds in tension acting currently with 3,779 pounds in shear. The maximum design force for the anchors, assuming that a ductile element does not govern the anchorage capacity and the anchor is not prequalified for seismic load, would be determined using an $R_p = 1.5$.

Substituting $R_p = 1.5$ into the seismic force Equation 13.3-1, the following is obtained:

$$F_p = \frac{0.4(2.5)(1.0)W_p}{1.5/1.5}(1+2(1)) = 3.00W_p \qquad \text{(}\textit{Standard}\text{ Eq. 13.3-1)}$$

In this case, the seismic maximum force of Equation 13.3-2, $F_p = 2.40W_p$, governs. This design force compares to the force of $F_p = 1.00W_p$ obtained previously. The amplified design forces for the anchors would be 2.4/1.0 times 2,907 pounds, which equals 6,977 pounds in tension acting currently with 6,977 pounds in shear.

14.5.5 Design for Displacements

In addition to design for seismic forces, the piping system must accommodate seismic relative displacements. For the purposes of this example, we assume that the building has a 15-foot story height and has been designed for a maximum allowable story drift:

$$\Delta_a = 0.015h_{sx} = 0.015(15)(12) = 2.7 \text{ in. per floor}$$

14.5.5.1 Design for displacements within structures. Piping Run A, a 4-inch-diameter pipe, connects to a large mechanical unit at Line 1 supported at the second level. Because the mechanical unit can be assumed to behave as a rigid body and the piping system is rigidly braced to the roof structure, the entire story drift must be accommodated in the 5'-0" piping drop (see Figure 14.5-2). There are several

approaches to accommodate the drift. The first is to provide a flexible coupling (articulated connections or braided couplings, for example). A second approach is to accommodate the drift through bending in the pipe. Loops are often used to make the pipe more flexible for thermal expansion and contraction and this approach also works for seismic loads. In this example, a straight length of a pipe is assumed. For a 4-inch-diameter Schedule 40 pipe, the moment of inertia, *I*, is equal to 7.23 in^4. Assuming the pipe is fixed against rotation at both ends, the shear and moments required to deflect the pipe 2.7 inches are as follows:

$$V = 12EI\Delta_a / l^3 = 12(29{,}000{,}000)(7.23)(2.7) / ((5.0)(12))^3 = 31{,}451 \text{ lb}$$

M = (31,451 lb)(60 in.) = 1,887,060 in-lb

$$f_b = \frac{M}{Z} = \frac{1{,}887{,}060}{4.31} = 437{,}833 \text{ psi}$$

These demands far exceed the capacity of the pipe and would overload the nozzle on the mechanical unit as well. Therefore, either a flexible coupling or a loop piping layout is required to accommodate the story drift.

Piping Run B, a 6-inch-diameter pipe, drops from the roof level to the second level at Line 3. Again, the drift demand is 2.7 inches, but in this case, it may be accommodated over the full story height of 15 feet. A simplified analysis assumes that the pipe is fixed at the roof and second level. This assumption is conservative, since in reality the horizontal runs of the pipe at the roof and Level 2 provide restraint but not fixity. For a 6-inch-diameter Schedule 40 pipe, the moment of inertia, *I*, is equal to 28.14 in^4. The shear and moments required to deflect the pipe 2.7 inches are as follows:

$$V = 12EI\Delta_a / l^3 = 12(29{,}000{,}000)(28.14)(2.7) / ((15.0)(12))^3 = 4{,}534 \text{ lb}$$

$$M = Vl/2 = (4{,}534)((15.0)(12))/2 = 408{,}150 \text{ in-lb}$$

The stress in the pipe displaced Δ_a would be:

$$f_b = \frac{M}{Z} = \frac{408{,}150}{11.28} = 36{,}184 \text{ psi}$$

This exceeds the permissible stress in the pipe, but not by a wide margin. In ASME B31.3, piping allowables are increased by a factor of 3 for stresses associated with seismic anchor movement relative displacements, but no such increases are currently provided for other piping. It is expected that threaded joints would be more highly stressed and a factor of 3 may not be conservative. Other options include refining the analysis to more accurately consider the effects of the rotational restraint provided by threaded couplings in the horizontal piping runs (which will tend to reduce the rigidity of the pipe and therefore reduce the bending stress), providing loops in the piping layout, or providing flexible couplings.

14.5.5.2 Design for displacements between structures. At the roof level, Piping Run A crosses a seismic separation between adjacent two-story structures at Line 3. Assuming story heights of 15 feet and design for a maximum allowable story drift for both buildings, the deflections of the buildings are:

$$\delta_{xA} = \delta_{xB} = (2)0.015h_{sx} = (2)0.015(15)(12) = 5.4 \text{ in.}$$

The displacement demand, D_P is determined from *Standard* Equation 13.3-7 as follows:

$$D_{p_{\max}} = |\delta_{xA}| + |\delta_{yB}| = |5.4| + |5.4| = 10.8 \text{ in.}$$

In addition to motions perpendicular to the pipe, the seismic isolation joint must accommodate movement parallel to the pipe. Assuming a 12-inch seismic separation joint is provided, during an earthquake the joint could vary from 1.2 inches (if the structures move towards each other) to 22.8 inches (if the structures move away from each other). The flexible coupling, which could include articulated connections, braided couplings, or pipe loops, must be capable of accommodating this range of movements.

14.6 ELEVATED VESSEL SEISMIC DESIGN

14.6.1 Example Description

This example illustrates seismic design for a small platform-supported vessel in the upper floor of a structure. It includes determination of the seismic design forces, anchorage of the vessel to the supporting platform, design and anchorage of the platform and demands on the floor slab of the supporting structure. The example focuses on the determination of force and displacement demands on the different components of the support system. The sizing of the various elements (beams, columns, braces, connections, anchor bolts, etc.) are not covered in detail.

This example considers a vessel supported by a platform on the second floor of a three-story structure. The contents of the vessel, a compressed non-flammable gas, are not hazardous. The structure, located in the Los Angeles area of California, is assigned to Occupancy Category II.

The design approach for nonstructural components depends on the type, size and location of the component. The *Standard* provides requirements for nonstructural components in Chapter 13 and nonbuilding structures in Chapter 15. Vessels are classified as nonbuilding structures, but in this example the provisions of *Standard* Chapter 13 apply, due to the size and location of the vessel.

14.6.1.1 Earthquake design requirements. Earthquake design requirements for vessels in the *Standard* depend on the system importance factor (I_p), the mass of the vessel relative to that of the supporting structure and the installation geometry. There are special analytical requirements triggered by Section 13.1.5 where the weight of the nonstructural component exceeds 25 percent of the effective seismic weight of the structure. The example does not cover this condition. If that were the case, the component would be classified as a nonbuilding structure and the requirements of Section 15.3.2 would apply.

The importance factor is determined in accordance with *Standard* Section 13.1.3. Given that the structure is assigned to Occupancy Category II, components are assigned I_p = 1.0, unless they must function for life-safety protection or contain hazardous materials. Neither of these conditions apply, so I_p = 1.0.

14.6.1.2 System configuration. The vessel is of steel construction and supported on four legs, which are bolted to a steel frame. A plan of the second level showing the location of the vessel is shown in Figure 14.6-1. A section through the structure showing the location of the vessel is presented in Figure 14.6-2. The supporting frame system consists of ordinary braced frames (tension-only bracing). An elevation of the vessel and supporting frame is shown in Figure 14.6-3.

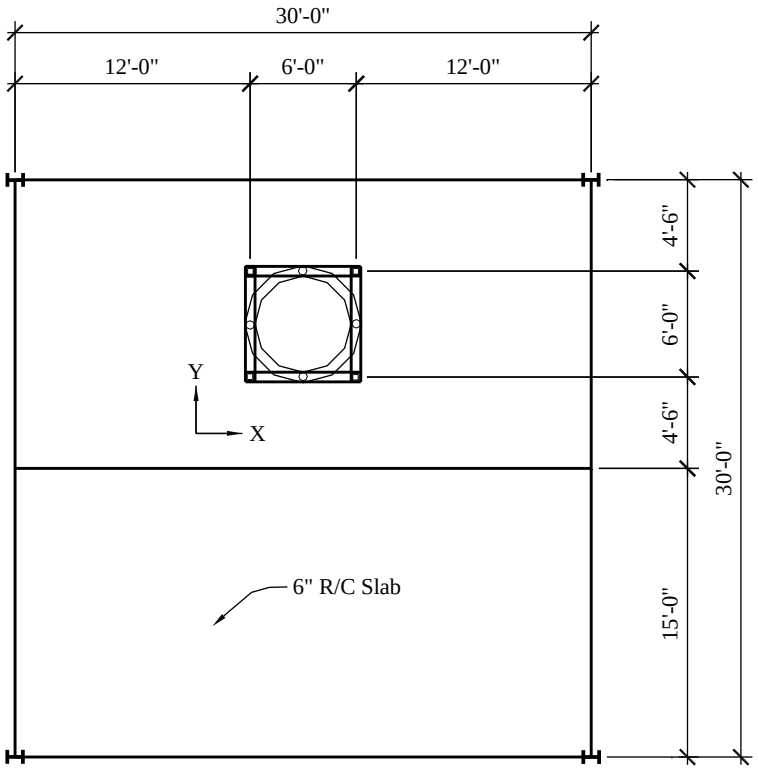

Figure 14.6-1 Elevated vessel - second-level plan

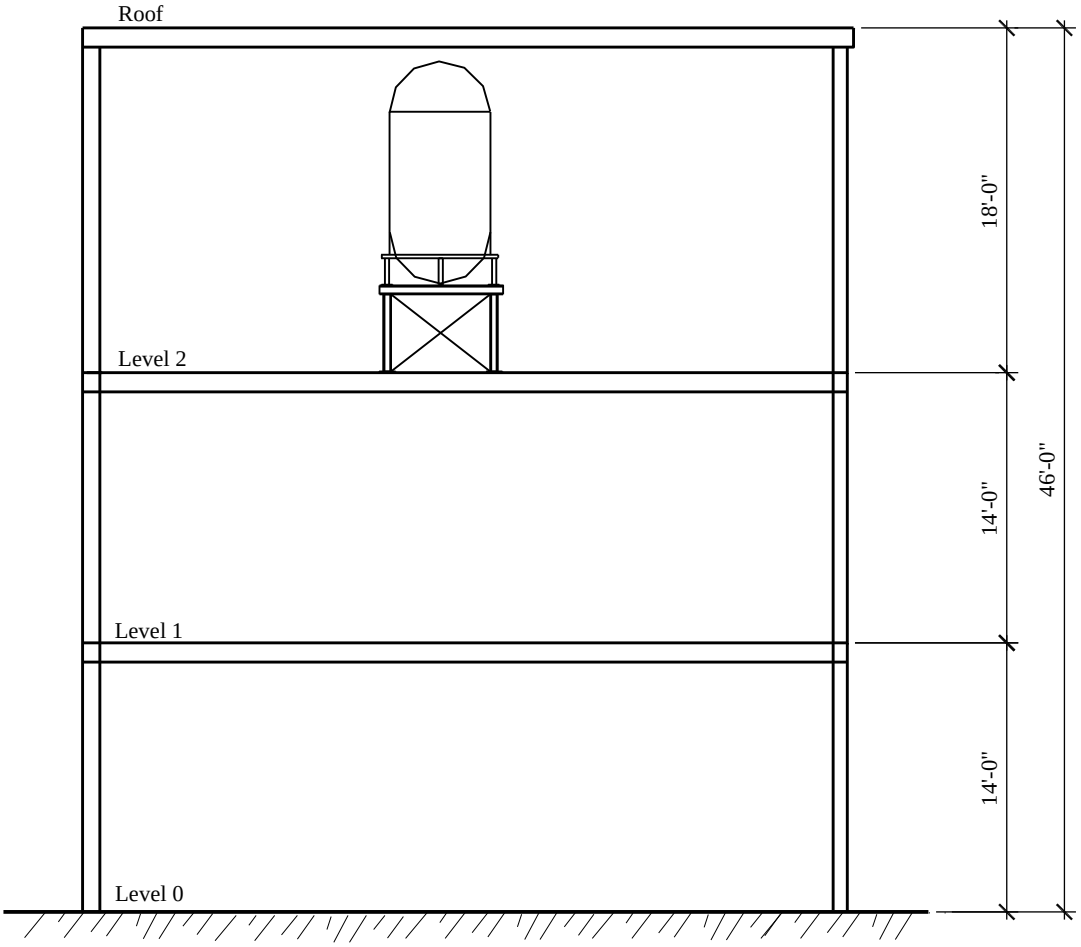

Figure 14.6-2 Elevated vessel - section

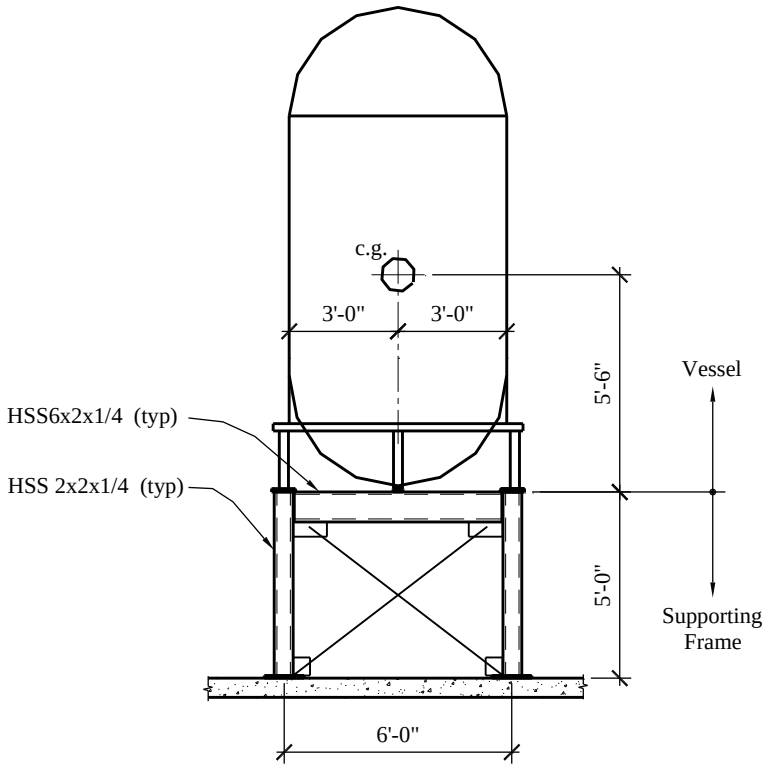

Figure 14.6-3 Elevated vessel - supporting frame system

The example covers the determination of the seismic forces in the supporting steel frame and its connection to the concrete slab at the second level and concentrates on quantifying the prescribed seismic forces for the different elements in the vessel support system. After the seismic demands are determined, the bracing and anchorage connections can be designed and detailed according to the appropriate AISC and ACI codes. Finally, methods of considering the seismic demands in the floor system due to the vessel are discussed.

14.6.2 Design Requirements

14.6.2.1 Seismic design parameters and coefficients.

a_p = 1.0 for vessels not supported on skirts and not subject to Chapter 15 (*Standard* Table 13.6-1)

R_p = 2.5 for vessels not supported on skirts and not subject to Chapter 15 (*Standard* Table 13.6-1)

S_{DS} = 1.2 (for the selected location and site class) (given)

Seismic Design Category = D (*Standard* Table 11.6-1)

h = 46 feet (roof height) (given)

z = 28 feet (system is supported at the second level) (given)

$$\frac{z}{h} = \frac{28.0 \text{ ft}}{46.0 \text{ ft}} = 0.609$$

I_p = 1.0 (*Standard* Sec. 13.1.3)

ASTM A500 Grade B steel HSS sections, F_y = 46 ksi, F_u = 58 ksi (given)

ASTM A36 steel bars and plates, F_y = 36 ksi, F_u = 58 ksi (given)

ASTM A53 Grade B pipe, F_y = 35 ksi, F_u = 60 ksi (given)

ASTM A 307 bolts and threaded rods (given)

D = Dead Load = W_p = 5,000 lb (vessel and legs) (given)

= 1,000 lb (allowance, supporting frame) (given)

According to *Standard* Section 13.3.1 (and repeated in Sec. 12.3.4.1), the redundancy factor does not apply to the design of nonstructural components.

14.6.2.2 Seismic design forces.

$$F_p = \frac{0.4(1.0)(1.2)W_p}{2.5/1.0}(1 + 2(0.609)) = 0.426W_p$$ (*Standard* Eq. 13.3-1)

Maximum $F_p = 1.6(1.2)(1.0)W_p = 1.92W_p$ (*Standard* Eq. 13.3-2)

Minimum $F_p = 0.3(1.2)(1.0)Wp = 0.36W_p$ (*Standard* Eq. 13.3-3)

$E_v = 0.2(1.2)D = 0.24D = 0.24W_p$ (*Standard* Eq. 12.4-4)

14.6.2.2.1 Vessel. The seismic forces acting on the vessel are as follows:

$F_p = 0.426W_p = 0.426(5,000)$ = 2,129 lb

$E_v = 0.24W_p = 0.24(5,000)$ = 1,200 lb

14.6.2.2.2 Supporting frame. The seismic loads due to the supporting frame self-weight are as follows:

$F_p = 0.426W_p = 0.426(1,000)$ = 426 lb

$E_v = 0.24W_p = 0.24(1,000)$ = 240 lb

14.6.2.3 Performance criteria. Component failure must not cause failure of an essential architectural, mechanical, or electrical component (*Standard* Sec. 13.2.3).

Component seismic attachments must be bolted, welded, or otherwise positively fastened without considering the frictional resistance produced by the effects of gravity (*Standard* Sec. 13.4).

The effects of seismic relative displacements must be considered in combination with displacements caused by other loads as appropriate (*Standard* Sec. 13.3.2).

The component must be designed to resist the forces in accordance with *Standard* Section 13.3.1 and must be able to accommodate movements of the structure resulting from response to the design basis ground motion, D_p.

Local elements of the structure, including connections, must be designed and constructed for the component forces where they control the design.

14.6.3 Load Combinations

The basic strength load combinations including earthquake effects from *Standard* Section 12.4.2.3 (based upon *Standard* Sec. 2.3.2) that will govern design of the vessel legs, attachments and the supporting frame are the following:

- Load Combination 5: $U = (1.2 + 0.2S_{DS})D + 1.0\rho Q_E + 0.5L + 0.2S$
- Load Combination 7: $U = (0.9 - 0.2S_{DS})D + 1.0\,\rho Q_E + 1.6H$

For nonstructural components, $\rho = 1.0$ and Q_E = the forces resulting from applying F_p. In this example, live load (*L),* snow load (*S) and* the lateral earth pressure load (*H)* are equal to zero.

14.6.4 Forces in Vessel Supports

Supports and attachments for the vessel must meet the requirements listed in *Standard* Table 13.2-1. Seismic design of the vessel itself is not required, since $I_p = 1.0$. While the vessel itself need not be checked for seismic loading, the component supports listed in *Standard* Section 13.6.5 must be designed to resist the prescribed seismic forces. The affected components include the following:

- The legs supporting the vessel
- Connection between the legs and the vessel shell
- Base plates and the welds attaching them to the legs
- Bolts connecting the base plates to the supporting frame

Standard Section 13.4.1 states that the lateral force, F_p, must be applied independently in at least two orthogonal directions. For vertically cantilevered systems, the lateral force also must be assumed to act in any horizontal direction. In this example, layout of the vessel legs is symmetric and there are two horizontal directions of interest, separated by 45 degrees. These two load cases are illustrated in Figure 14.6-4.

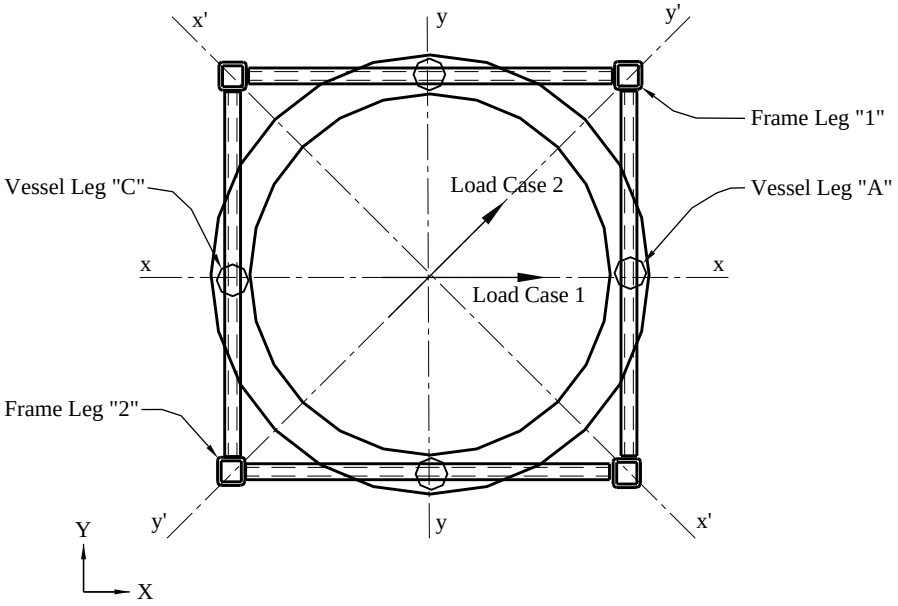

Figure 14.6-4 Elevated vessel support load cases

14.6.4.1 Case 1 - moments about the y-y axis. The height of the vessel's center-of-gravity above the bottom of the leg base plates is 5.5 feet. The moments about the bottom of these base plates are taken as follows:

$$M = (5.5)F_p = (5.5)(2{,}129) = 11{,}710 \text{ ft-lb}$$

Assuming the vessel acts as a rigid body, in Case 1 the overturning moments is resisted by the two legs along the x-x axis. The vessel is assumed to rotate about the legs on the y-y axis. The maximum tension and compression loads in the legs may be estimated as follows:

$$T = C = M / d$$

where the distance between legs A and C, d, is 6.0 feet. Therefore:

$$T = C = 11{,}710 / 6.0 = 1{,}952 \text{ lb}$$

The vertical load in each leg due to gravity is $W_p/4$ = 5,000/4 = 1,250 pounds.

The shear in each leg due to F_p is $V = F_p/4$ = 2,129/4 = 532 pounds.

14.6.4.2 Case 2 - moments about the x'-x' axis. In Case 2 the overturning moments are resisted by all four legs, two in compression and two in tension. The loads in the legs due to gravity are the same as in Case 1, as is the shear in the legs due to F_p. Under seismic load, the vessel is assumed to rotate about the x'-x axis. The maximum tension and compression loads in the legs may be estimated as follows:

$$T = C = \frac{M}{2(0.707d)}$$

where the distance between legs A and C, $0.707d$, is 4.24 feet. Therefore:

$$T = C = 11{,}710 / 2(4.24) = 1{,}380 \text{ lb}$$

14.6.5 Vessel Support and Attachment

The axial loads in the vessel legs due to seismic overturning about the y-y axis (Case 1, in Section 14.6.4.1) are substantially larger than those obtained for overturning about the x'-x' axis (Case 2, in Section 14.6.4.2) . Therefore, by inspection Case 1 governs the design of the legs.

The design compression loads on the vessel legs is governed by Load Combination 5:

U = [1.2 + 0.2(1.2)](1,250 lb) + 1.0(1.0)(1,952 lb) = 3,752 lb = C_U

The design tension load on the vessel legs is governed by Load Combination 7:

U = [0.9 – 0.2(1.2)](1,250 lb) - 1.0(1.0)(1,952 lb) = -1,127 lb = T_U

(A negative sign denotes compression.)

The design shear in each leg is U = 1.0(1.0)(532 lb) = 532 lb = V_U.

14.6.5.1 Vessel leg design. The check of the leg involves a check of the connection between the vessel and the leg and a stress check of the leg itself. The length of the leg, L, is 18 inches and the legs are fabricated from 2-inch-diameter standard pipe. The section properties of the leg are as follows:

A = 1.00 in^2

Z = 0.713 in^3

Assuming the leg is pinned at the connection to the supporting frame and fixed at the connection to the vessel, the moment and bending stress in the leg are as follows:

$M = V_U L$ = 532(18) = 9,576 in-lb

$f_b = M/Z$ = 9,756/0.713 = 13,683 psi

The maximum axial compressive stress in the leg is:

C_u/A = 3,752/1.00 = 3,752 psi

The capacities of the leg and the connection to the vessel are determined using the structural steel specifications (AISC 360). The permissible strengths are as follows:

F_a = 31,500 psi

F_{bw} = 31,500 psi

For combined loading:

$$\left|\frac{f_a}{F_a} + \frac{f_{bw}}{F_{bw}}\right| \le 1.0$$

$$\left|\frac{3,752}{31,500} + \frac{13,683}{31,500}\right| = 0.553 \le 1.0$$

14.6.5.2 Connections of the vessel leg. The connection between the vessel leg and the supporting frame is shown in Figure 14.6-5. The design of this connection involves checks of the weld between the pipe leg and the base plate, design of the base plate and design of the bolts to the supporting frame. Load Combination 7, which results in tension in the pipe leg, will govern the design of the base plates and the bolts to the supporting frame. The design of the base plate and bolts should consider the effects of prying on the tension demand in the bolts.

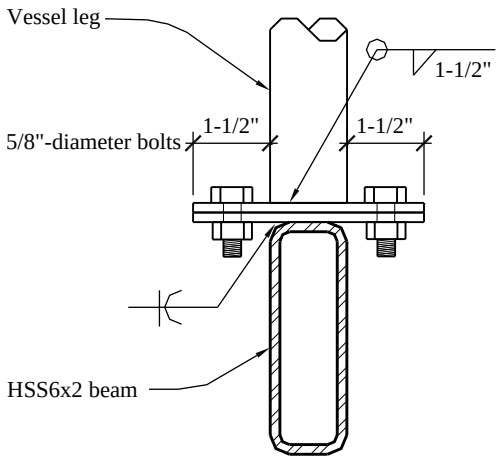

Figure 14.6-5 Elevated vessel leg connection

Each vessel leg is connected to the supporting frame by a pair of 5/8-inch-diameter bolts. The load path for this connection consists of the following elements: the weld of the leg to the connecting plate, the connecting plate acting in bending considering the effects of prying as appropriate, the bolts, the connection plate welded to the supporting frame beam and the welding of the connection plate to the supporting frame beam. Again by inspection, Case 1 (Section 14.6.4.1) governs. The factored loads in the connection are determined using Load Combinations 5 and 7 of *Standard* Section 12.4.2.3 (based upon *Standard* Sec. 2.3.2). As previously determined, the maximum compression in the connection (Load Combination 5) is:

C_U = 3,752 lb

The maximum tension in the connection (Load Combination 7) is:

$U = (0.9 - 0.2S_{DS})D + 1.0\rho Q_E + 1.6H$

U = [0.9 – 0.2(1.2)](1,250 lb) - 1.0(1.0)(1,952 lb) = -1,127 lb (tension) = T_U

The maximum shear per bolt is:

V_U = 532 lb/2 = 266 lb

The designs of the vessel leg base plate and of the connection plate at the supporting frame beams are identical. The maximum tension in each bolt is:

T_U = 1,127 lb/2 = 534 lb

The available shear and tensile strengths of the bolt are as follows:

$\phi_v r_n$ = 5,520 lb (shear)

ϕr_n = 10,400 lb (tension)

Therefore, the bolts are adequate.

The connection plates are 1/4 inch thick and 3 inches wide.

$$Z = \frac{bd^2}{4} = \frac{3(0.25)^2}{4} = 0.0469 \text{ in}^3$$

The maximum moment in the plate is:

M_U = 534 lb (1.5 in.) = 801 in-lb

The bending stress is:

$f_b = M_U / Z$ = 801/0.0469 = 17,088 psi OK

Prying action can have the effect of increasing the tensile forces in the bolts. AISC 360 permits prying action to be neglected if the plate meets minimum thickness requirements, given by:

$$t_{\min} = \sqrt{\frac{4.44Tb'}{pF_u}}$$

where p = 3 inches is the tributary length per pair of bolts

b' = (b-d_b/2) = (1.5-0.625/2) = 1.1875 in.

$$t_{\min} = \sqrt{\frac{4.44(534)(1.1875)}{3(58,000)}} = 0.13 \text{ in.}$$

This is less than the 0.25-inch thickness provided, so prying need not be considered further.

The welds of the vessel leg to the vessel body and of the leg to the upper connection plate are proportioned in a similar manner. The calculation can be simplified by assuming the weld is of unit

thickness. This yields a demand per inch of weld and an appropriate weld thickness can then be selected. The vessel leg has an outer diameter, *d,* of 2.38 inches. The weld properties for a weld of unit thickness are as follows:

$$Z = \frac{d^3}{6} = \frac{2.38^3}{6} = 2.25 \text{ in}^3$$

$A = \pi d$ =3.14(2.38) = 7.45 in.

The shear in the weld is:

v = 532 lb/7.45 in. = 714 lb/in.

The tension in the weld due to axial load is:

T = 1,127 lb/7.45 in. = 151 lb/in.

The tension to the weld due to bending (at the connection to the vessel) is:

$T = M/Z$ = 9,756/7.45 = 1,310 lb/in.

For E70 electrodes, the capacity of a fillet weld is given by:

$\phi R_n = 1.392\ Dl$ (kips/in.)

where D is the size of the weld in sixteenths of an inch and l is the weld length.

For a unit length, a 3/16-inch fillet weld has a capacity of :

$\phi R_n = 1.392(3)(1) = 4.18$ kips/in.

which will be adequate.

The same size weld is used for the vessel leg-to-vessel body joint and for the leg-to-upper connection plate joint. A similar design approach is used to proportion the weld of the lower connection plate to the HSS 6x2 beam.

14.6.6 Supporting Frame

The design of the supporting frame can be performed separately from that of the vessel. The reactions from the vessel are applied to the frame and combined with the inertial loads resulting from the supporting frame itself. The configuration of the supporting frame is shown in Figure 14.6-6.

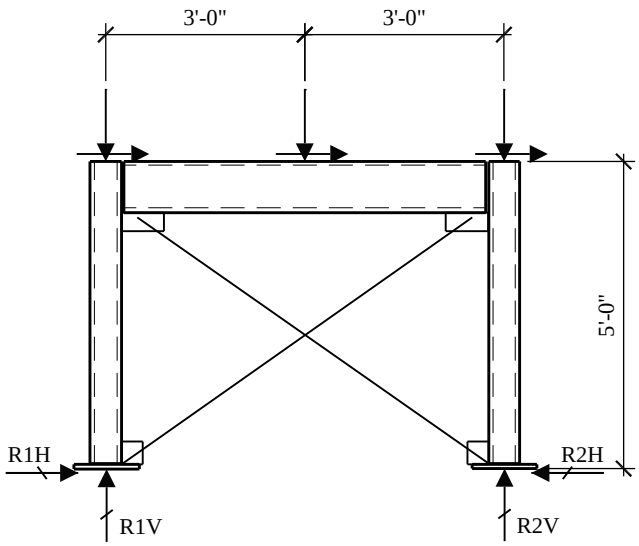

Figure 14.6-6 Elevated vessel supporting frame

The supporting frame uses Steel Ordinary Braced Frames (OBF). While the supporting frame is designed for seismic forces determined in Section 13.3, the design process for the frame itself is similar to that used for building frames or nonbuilding structures similar to buildings. In this example, seismic loads are developed for the following elements:

- Beams supporting the vessel legs
- Braces
- Columns supporting the platform and vessel
- Base plates and anchor bolts

To simplify the analysis, the self weight of the supporting frame is lumped at the vessel leg connection locations.

14.6.6.1 Support frame beams. The beams transfer vertical and horizontal loads from the vessel to the brace frames. The beams, fabricated from HSS6x2x1/4 members, are idealized as simply supported with a span of 6 feet. The reactions from the vessel legs are idealized as point loads applied at mid-span. The vertical loads applied to the beam are as follows:

P = [5,000 lb (vessel) + 10,000 lb (frame)]/4 supports = 1,500 lb

The lateral load per beam of the combined vessel and supporting frames is:

V = 0.426[5,000 lb (vessel) + 10,000 lb (frame)]/4 supports = 639 lb

The maximum load on a leg due to overturning of the vessel was computed as P = 1,952 pounds. The maximum factored vertical load, which will generate strong axis bending in the beam, is determined using Load Combination 5:

P_U = [1.2 + 0.2(1.2)](1,500 lb) + 1.0(1.0)(1,952 lb) = 4,112 lb = P_v

Acting with the horizontal load, V_U = 639 pounds.

The moment in the beams then is:

$M_{x\text{-}x} = P_U l/4$ = (4,112 lb)(6.0 ft)/4 = 6,168 ft-lb

$M_{y\text{-}y} = V_U l/4$ = (639 lb)(6.0 ft)/4 = 959 ft-lb

For an HSS6x2x1/4:

$Z_{x\text{-}x}$ = 5.84 in^3

$Z_{y\text{-}y}$ = 2.61 in^3

$$\left|\frac{f_{bx}}{F_b} + \frac{f_{by}}{F_b}\right| \le 1.0$$

$F_b = \phi F_y$ = 0.9(46,000 psi) = 41,400 psi

$$\left|\frac{f_{bx}}{F_b} + \frac{f_{by}}{F_b}\right| = \left|\frac{M_{x-x}/Z_{x-x}}{F_b} + \frac{M_{y-y}/Z_{y-y}}{F_b}\right| = \left|\frac{6{,}168(12)/5.84}{41{,}400} + \frac{959(12)/2.61}{41{,}400}\right| = 0.41 \le 1.0$$ OK

14.6.6.2 Support frame braces. The maximum brace force occurs where loads are applied in the X- or Y-direction and the loads are resisted by two frames. The horizontal force is:

V = 0.426[5,000 lb (vessel) + 10,000 lb (frame)]/2 braces = 1,278 lb

The length of the brace is:

$\sqrt{(5)^2 + (6)^2}$ = 7.81 ft

The force in the brace then is:

$$T_u = \frac{7.81}{6} 1{,}278 = 1{,}664 \text{ lb (tension)}$$

The braces consist of 5/8-inch-diameter ASTM A307 threaded rod. The nominal tensile capacity is:

ϕr_n = 10,400 lb (tension) > 1,664 lb OK

It is good practice to design the supporting frame connections to the same level as a nonbuilding structure subject to Chapter 15. In this example, the supporting frames would be treated as an ordinary braced frame. For this system, AISC 341 requires the strength of the bracing connection to be the lesser of the expected yield strength of the brace in tension, the maximum force that can be developed by the system, or the load effect based on the amplified load.

14.6.6.3 Support frame columns. The columns support the vertical loads from the vessel and frame, including the vertical component of the supporting frame brace forces. The columns are fabricated from HSS2x2x1/4 members and are idealized as pinned top and bottom with a length of 5 feet. The case where the vessel rotates about the x'-x' axis governs the design of the supporting frame columns. The overturning moment is:

$$M = (10.5)F_{p-vessel} + (5.0)F_{p-frame} = (10.5)(2{,}129) + 5.0(426) = 24{,}485 \text{ ft-lb}$$

Assuming the vessel acts as a rigid body, in Case 1 the overturning moment is resisted by the two legs along the y'-y' axis. The vessel is assumed to rotate about the legs on the x'-x' axis. The maximum tension and compression loads in the columns due to overturning may be estimated as follows:

$$T = C = M / d$$

where the distance between Frame Legs 1 and 2, $d = (6.0)\sqrt{2} = 8.48$ feet. Therefore:

$$T = C = 24{,}485 / 8.48 = 2{,}886 = 2{,}886 \text{ lb}$$

The vertical load in each leg due to gravity is $W_p/4$ = (5,000+1,000)/4 = 1,500 pounds.

The design compression load on the supporting frame columns is governed by Load Combination 5:

U = [1.2 + 0.2(1.2)](1, 500 lb) + 1.0(1.0)(2,886 lb) = 5,046 lb = C_U

The design tension load on the supporting frame columns is governed by Load Combination 7:

U = [0.9 - 0.2(1.2)](1,500 lb) - 1.0(1.0)(2,886 lb) = -1,896 lb = T_U

The capacity of the HSS2x2x1/4 column is 38,300 pounds and is therefore adequate.

14.6.6.4 Support frame connection to the floor slab. The connection of the support frame columns to the floor slab includes the following elements:

- Weld of the column and brace connection to the base plate
- Base plate
- Anchor bolts

The design of the connection of the base plate and of the base plate itself follows the typical procedures used for other structures. There are special considerations for the design of the anchor bolts to the concrete slab that are unique to nonstructural components. Anchors in concrete and masonry must be proportioned to carry the least of the following:

- 1.3 times the prescribed seismic design force, or
- The maximum force that can be transferred to the connected part by the component structural system.

The value of R_p may not exceed 1.5 unless the anchors are prequalified for seismic loading or the component anchorage is governed by yielding of a ductile steel element.

The horizontal and vertical reactions of the supporting frame columns are as follows:

C_U = 5,046 lb

T_U = -1,896 lb

V_U = 1,278 lb

Assuming that no other element of the supporting frame limits the force to the anchor, the minimum design forces for the anchors would be 1.3 times 1,896 pounds, which is 2,465 pounds in tension, acting concurrently with 1.3 times 1,278 pounds, which is 1,661 pounds in shear. The maximum design force for the anchors, assuming a ductile element does not govern the anchorage capacity and the anchor is not prequalified for seismic load, would be determined using R_p = 1.5.

Substituting R_p = 1.5 into the seismic force Equation 13.3-1 results in the following:

$$F_p = \frac{0.4(1.0)(1.2)W_p}{1.5/1.0}(1+2(0.609)) = 0.71W_p \qquad \text{(}\textit{Standard}\text{ Eq. 13.3-1)}$$

This design forces compares to $F_p = 0.426W_p$ obtained previously.

The amplified overturning moment for the design of the anchors would be:

$$M = (10.5)F_{p-vessel} + (5.0)F_{p-frame} = (10.5)(0.71)(5,000) + 5.0(0.71)(1,000) = 40{,}825 \text{ ft-lb}$$

The corresponding tension load becomes:

$$T = 40{,}825 / 8.48 = 4{,}814 \text{ lb}$$

The factored design tension is:

U = [0.9 - 0.2(1.2)](1,500 lb) - 1.0(1.0)(4,814 lb) = -3,824 lb

This is represents a 55 percent increase in the design tension. The amplified shear forces for the anchors would be (2.50/1.50)(1,278 lb), which is 2,130 pounds.

14.6.7 Design Considerations for the Vertical Load-Carrying System

This portion of the example illustrates design considerations for the floor slab supporting the nonstructural component. The floor system at Level 2 consists of a 6-inch-thick reinforced concrete flat-slab spanning between steel beams. To illustrate the effects of the vessel, the contribution of the vessel load to the overall slab demand is examined.

14.6.7.1 Slab design assumptions.

Dead load = 100 psf

Live load = 100 psf (non-reducible)

14.6.7.2 Effect of vessel loading. During design, the slab moments and shear are checked at different points along each span. In order to simply illustrate the potential effects of the vessel, this investigation will be limited to the change in the negative moments about the x-x axis over the center support. In an actual design, a complete analysis of the slab for the loads imposed by the vessel would be required. At the center support, the moments due to dead load and live load are as follows:

Maximum dead load moment, $M_{DL} = wl^2/8 = (100)(15^2)/8 = 2{,}813$ ft-lb/ft

Maximum live load moment, $M_{LL} = wl^2/8 = (100)(15^2)/8 = 2{,}813$ ft-lb/ft

The support frame columns are 6 feet apart. Assuming an additional 3 feet of slab on each side of the frame to resist loads generated by the vessel, the design moments for the strip of slab supporting the vessel are as follows:

M_{DL} = 2,813 ft-lb/ft (12 ft) = 33,756 ft-lb

M_{LL} = 2,813 ft-lb/ft (12 ft) = 33,756 ft-lb

The moments at the center support due to a point load, *P,* in one of the spans is:

$$M = \frac{Pab}{4l^2}\left(l + a\right)$$

where:

a = distance from the end support to the point load

b = distance from the point load to the center support

l = span between supports = 15 ft

The point loads due to the vessel and support frame self weight is:

P = 2(1,500 lb) = 3,000 lb

The moment in the slab due to the vessel and support frame is as follows:

$$M_{VD} = \frac{(3{,}000)(4.5)(10.5)}{4(15)^2}\left(15 + 4.5\right) + \frac{(3{,}000)(10.5)(4.5)}{4(15)^2}(15 + 10.5) = 7{,}088 \text{ ft-lb}$$

The point loads due to the vessel and support frame caused by seismic in the Y-direction are as follows:

$T = C = 24{,}485 / 6.00 = 4{,}081$ lb

The moment in the slab due to the overturning of the vessel and support frame for seismic forces in the Y-direction is:

$$M_{VD} = \frac{(4{,}081)(4.5)(10.5)}{4(15)^2}(15+4.5) + \frac{(-4{,}081)(10.5)(4.5)}{4(15)^2}(15+10.5) = \text{-1,286 ft-lb}$$

or

$$M_{VD} = \frac{(-4{,}081)(4.5)(10.5)}{4(15)^2}(15+4.5) + \frac{(4{,}081)(10.5)(4.5)}{4(15)^2}(15+10.5) = \text{1,286 ft-lb}$$

The factored moments for the slab without the vessel are:

$D + L$: $U = 1.2\ D + 1.6\ L = 1.2$ (33,756 ft-lb) + 1.6(33,756 ft-lb) = 94,517 ft-lb

The factored moments for the slab including the vessel are as follows:

$D + L$: $U = 1.2\ D + 1.6\ L = 1.2$ (33,756 ft-lb+ 7,088 ft-lb) + 1.6(33,756 ft-lb) = 103,022 ft-lb

The factored moments including seismic are as follows:

Load Combination 5:

$U = (1.2 + 0.2S_{DS})D + 1.0\rho Q_E + 0.5L + 0.2S$

$= (1.2 + 0.2(1.2))(33{,}756+7{,}088) + 1.0(1.0)(1{,}286) + 0.5(33{,}756) + 0.2(0)$

= 76,979 ft-lb

Load Combination 7:

$U = (0.9 - 0.2S_{DS})D + 1.0\ \rho Q_E + 1.6H$

$= (0.9 - 0.2(1.2))\ (33{,}756+7{,}088) + 1.0(1.0)(-1{,}286) + 1.6(0)$

= 25,671 ft-lb

In this case, the loads from the vessel do not control the design of the slab over the center support.

Appendix A

THE BUILDING SEISMIC SAFETY COUNCIL

The purpose of the Building Seismic Safety Council is to enhance the public's safety by providing a national forum to foster improved seismic safety provisions for use by the building com m unity. For the purposes of the Council, the building community is taken to include all those involved in the planning, design, construction, regulation, and utilization of buildings.

To achieve its purposes, the Council shall conduct activities and provide the leadership needed to:

1. Promote development of seismic safety provisions suitable for use throughout the United States;
2. Recommend, encourage, and promote adoption of appropriate seismic safety provisions in voluntary standards and model codes;
3. Assess implementation progress by federal, state, and local regulatory and construction agencies;
4. Identify opportunities for the improvement of seismic regulations and practices and encourage public and private organizations to effect such improvements;
5. Promote the development of training and educational courses and materials for use by design professionals, builders, building regulatory officials, elected officials, industry representatives, other members of the building community and the public.
6. Provide advice to governmental bodies on their program s of research, development, and implementation; and
7. Periodically review and evaluate research findings, practice, and experience and make recommendations for incorporation into seismic design practices.

The scope of the Council's activities encompasses seismic safety of structures with explicit consideration and assessment of the social, technical, administrative, political, legal, and economic implications of its deliberations and recommendations. Achievement of the Council's purpose is important to all in the public and private sectors. Council activities will provide an opportunity for participation by those with interest, including local, State, and Federal Government, voluntary organizations, business, industry, the design professions, the construction industry, the research com m unity and the public. Regional and local differences in the nature and magnitude of potentially hazardous earthquake events require a flexible approach adaptable to the relative risk, resources and capabilities of each com m unity. The Council recognizes that appropriate earthquake hazard reduction measures and initiatives should be adopted by existing organizations and institutions and incorporated into their legislation, regulations, practices, rules, codes, relief procedures and loan requirements, whenever possible, so that these measures and initiatives become part of established activities rather than being superposed as separate and additional.

The Council is established as a voluntary advisory, facilitative council of the National Institute of Building Sciences, a nonprofit corporation incorporated in the District of Columbia, under the authority given the Institute by the Housing and Community Development Act of 1974, (Public Law 93-383); Title V III, in furtherance of the objectives of the Earthquake Hazards Reduction Act of 1977 (Public Law 95-124); and in support of the President's National Earthquake Hazards Reduction Program, June 22, 1978.

2012-2013 BSSC Board of Direction

Chair

Jim. W. Sealy, FAIA, Architect/Consultant, *Representing: National Institute of Building Sciences*

Members

Remington B. Brown, P.E., Senior Engineering Manager, Insurance Institute for Building and Home Safety, *Representing: Insurance Institute for Building and Home Safety*

James R. Cagley, P.E., S.E. Chairman of the Board, Cagley & Associates, *Representing: Applied Technology Council*

Charles J. Carter, S.E., P.E., PhD., Vice President of Engineering and Research, American Institute of Steel Construction, *Representing: American Institute of Steel Construction*

Bradford K. Douglas, P.E., Vice President, Engineering, American Wood Council, *Representing: American Wood Council*

Jennifer Goupil, P.E., Director, Structural Engineering Institute, American Society of Civil Engineers, *Representing: American Society of Civil Engineers*

Melvyn Green, P.E., S.E., Structural Engineer, Melvyn Green & Associates, *Representing: Earthquake Engineering Research Institute*

John R. Hayes, Jr. ("Jack"), P.E., PhD., NEHRP Director, National Institute of Standards and Technology (NIST), *Representing: National Institute of Standards and Technology*

Jay W. Larson, P.E., F.ASCE, Managing Director, Construction Technical, American Iron and Steel Institute, *Representing: American Iron and Steel Institute*

Stephen S. Szoke. P.E., FACI, Director, Codes and Standards, Portland Cement Association, *Representing: Portland Cement Association*

Jason J. Thompson, Vice President of Engineering, National Concrete Masonry Association, *Representing: National Concrete Masonry Association*

BSSC Staff

Dana K. (Deke) Smith, FAIA, Executive Director, Building Seismic Safety Council
Drew N. Rowland, PMP, Program Director
Roger J. Grant, CSI, CDT, Program Director

BSSC Member Organizations

Voting Members

American Concrete Institute

American Institute of Architects

American Institute of Steel Construction

American Society of Mechanical Engineers

APA-The Engineered Wood Association

Applied Technology Council

Brick Industry Association

Building Owners & Managers Association International

California Seismic Safety Commission

Concrete Masonry Association of California and Nevada

Institute for Business and Home Safety

International Code Council, Inc.

Masonry Institute of America

National Association of Home Builders

National Fire Sprinkler Association

National Institute of Building Sciences

National Institute of Standards and Technology

PLANiT Measuring

Portland Cement Association

Rack Manufacturers Institute

Steel Deck Institute

Structural Engineers Association of San Diego

Structural Engineers Association of Washington

Affiliate Members

Architectural Testing, Inc.

Baltimore Aircoil Company

Building Technology Inc.

Collins Engineers, Inc.

BSSC Publications

For a complete list of all BSSC publications and to download copies free of charge, visit the BSSC website at www.nibs.org/bssc/publications.

BSSC Publications are also available free of charge from the Federal Emergency Management Agency at 1-800-480-2520 (by FEMA Publication Number).

For detailed information about the BSSC and its projects, visit the BSSC website at www.nibs.org/bssc or contact the Council directly at:

BSSC
1090 Vermont A venue, N .W., Suite 700, Washington, D .C . 20005;
Phone: 202-289-7800; Fax 202-289-1092
e-mail dsmith@ nibs.org

FEMA

FEMA P-751
Catalog No. 12253-1